

Kharkov  
Ukraine



Ref 7564-EE-02  
N68171-94-M-6429

DTIC  
ELECTE  
FEB 27 1995  
S G D

# MATE'94

CONFERENCE PROCEEDINGS

19950217 139

7-10 September



94

Mathematical  
Methods  
in Electromagnetic  
Theory

DISTRIBUTION STATEMENT A

Approved for public release;  
Distribution Unlimited



Dear Sirs

Research & Manufacturing Company

ISKRA

is ready to be your partner  
in  
solving various research and development  
problem  
We are waiting for your propositions

Our address:

Solyanikovsky Pereulok, 4  
Kharkov, 310004, Ukraine

tel +7-057-438022  
fax +7-0572-224309



TRADE HOUSE, Kharkov Ukraine  
Phone: (0572) 47 10 62 and 40 57 74  
Fax: (0572) 43 29 20



The two preceding International Conferences on Mathematical Methods in Electromagnetic Theory (MMET\*90 and MMET\*91) caused a great interest of the participants, both from inside and outside the Former Soviet Union. This lead us to the conclusion of the necessity of holding the MMET conference on a regular basis.

MMET\*94 is the fifth conference in this series, the first two being for domestic attendance only with Russian as working language. This time the Conference is organized by the National URSI Committee of the Ukraine, in cooperation with the URSI Commission B. It is held on September 7 to 10, 1994, in the Kharkov State University. I am grateful to Prof. L. N. Litvinenko, Vice-President of the Ukrainian NC URSI, Prof. O.A. Tretyakov, Chairman of the Commission B of NC URSI, Prof. V. A. Svich, Rector of the Kharkov State University, and Prof. A.D. Olver, Chairman of the URSI Commission B, for their great support and encouragement. The Conference Program contains 116 papers from 14 countries, including 9 Invited Papers. The covered topics are: High-Frequency Methods, Scattering and Diffraction, Transients, and Time-Domain Methods, Gratings and Rough Surfaces, Regularization Techniques, Optical Fibers, Open Waveguides and Resonators, Numerical Methods, Inverse and Synthesis Problems, Remote Sensing, Antennas, Waveguides and Discontinuities, and Nonlinear and Exotic Media.

The greatest fraction of the papers is contributed by the Young Scientists. I acknowledge the support of the URSI Commission B to the participation of 9 young scientists from ex-USSR and 3 from other countries. I hope that the Conference will be a good school for them.

I wish a success to all the participants of MMET\*94 and hope to meet all of you at the next MMET conference.

Eldar I. Veliev, General Chairman

Dist	Avail and/or Special
A-1	

General purpose of holding the MMET\*94 conference is to give a forum of ideas exchange and interaction in field of Electromagnetic Theory, between the ex-USSR and the Western electromagnetics community. The number of ex-soviet scientists able to attend international conferences is still at least two orders of magnitude less than it deserves to be. A conference held in the Ukraine, with English as the only medium of presentation, gives a unique chance to make their work available to world-wide audience.

This volume contains the contributions which have been accepted to the Program of MMET\*94. They cover all the traditional topics of the URSI Commission B activities, and demonstrate the vitality of Electromagnetics research and researchers.

I would like to express my gratitude to the effort made by the authors preparing their manuscripts in four-page manner. It was a pleasure to work with the members of TPC and LOC preparing the Conference in the time of political and economical problems in this country.

A success of the meeting is determined by the scientists who have decided to submit the papers to MMET\*94. Their participation has helped to form an exciting technical program that makes this conference a major event in Electromagnetic Theory. Thank you all.

Alexander I. Nosich, on behalf of LOC

DTIC QUALITY INSPECTED 4

**General Chairman    Prof. E. I. Veliev**

**Technical Program Committee**

Prof. L. N. Litvinenko, Co-Chairman, Academy of Sciences, Ukraine  
Prof. O.A. Tretyakov, Co-Chairman, Kharkov State University, Ukraine  
Prof. V. S. Buldyrev, St. Petersburg University, Russia  
Prof. F. Gardiol, Ecole Polytechnique Federale de Lausanne, Switzerland  
Prof. R. F. Harrington, Syracuse University, USA  
Prof. M. Hashimoto, Osaka Electro-Communications University, Japan  
Prof. M. Idemen, Istanbul Technical University, Turkey  
Prof. A. S. Ilyinsky, Moscow State University, Russia  
Prof. E. Jull, University of British Columbia, Canada  
Prof. B.Z. Katsenelenbaum, Academy of Sciences, Russia  
Prof. N. A. Khizhnyak, Academy of Sciences, Ukraine  
Prof. A.A. Kirilenko, Academy of Sciences, Ukraine  
Prof. K. Kobayashi, Chuo University, Japan  
Prof. E. Luneburg, Deutsche Aerospace, Germany  
DSc. Z.T. Nazarchuk, Academy of Sciences, Ukraine  
Prof. Y. Okuno, Kumamoto University, Japan  
Prof. A.D. Olver, University of London, United Kingdom  
Prof. H. Serbest, Cukurova University, Turkey  
Prof. S. Strom, Royal Institute of Technology, Sweden  
Prof. M Tateiba, Kyushu University, Japan  
Prof. W.-X. Zhang, Southeast University, China

**Local Organizing Committee**

Dr. V. I. Kalinichev  
Prof. V. I. Naidenko  
Prof. A. I. Nosich  
Dr. S. N. Shulga

Prof. V. A. Svich  
A. D. Ustimenko  
Dr. V.V. Veremey  
Dr. N. V. Veremey

**Secretary                    Dr. V.N. Vavilov**

**ORGANIZERS**

Ukrainian URSI Commission B in cooperation with  
Commission B of The URSI,  
European Research Office of USARDSG-UK and

**Kharkov State University**  
Institute of Radiophysics and Electronics, Ukrainian Academy of Sciences  
Institute of Radio Astronomy, Ukrainian Academy of Sciences  
ISKRA Research and Manufacturing Company  
TRIKOM Trade House

## CONTENTS

1. V. Agapov, O. Soloviev (Russia), <i>An Asymptotic 3-D Approach to the Problem of the Point Source Field Diffracted by a Localized Impedance Discontinuity</i> .....	1
2. M. Andreev, V. Borulko, O. Drobakhin (Ukraine), <i>Inversion of 1-D Reflecting Data of Multilayered Structures Using Quasi-Solutions</i> .....	7
3. A. Andrenko, S. Uckun (Turkey), <i>Green's Function Approach in the Problem of Grounded Dielectric Slab Modes Scattering by Combined Metal Screen - Dielectric Rod Discontinuities</i> .....	11
4. O.D. Anohina, G.S. Antonov, V.A. Usin, V.A. Gubar (Ukraine), <i>Solution of the Problem of Determination of Amplitude-Phase Distributions in Phased Arrays Aperture</i> .....	15
5. V.F. Apelt'cin (Russia), <i>HF Asymptotic Method to Solve the Problem of Circular Conducting Cylinder Excitation if Covered with a Thin Dielectric Layer of Variable Thickness</i> .....	18
6. A.N. Arslan (Turkey), <i>On Modeling of the Microwave Scattering and Absorption by Plant Elements</i> .....	22
7. V.V. Artemiev, S.I. Eminov (Russia), <i>The Method of the Proper Functions of the Singular Operators in the Theory of Antennas</i> .....	26
8. V.I. Babi, Z.F. Nazirov, A.A.Yantsevich (Ukraine), <i>The Modal Basis Method and Electrmagnetic Waves in Random Media</i> .....	29
9. O.V. Bagatskaya, D.O. Batrakov, S.N. Shulga, N.P. Zhuck (Ukraine), <i>Scattering of Electromagnetic Waves from an Anisotropic Inclusion Embedded in the Gyrotropic Halfspace</i> .....	30
10. M. Bakunov, S. Zhukov (Russia), <i>Transformation and Radiation of Surface Wave on a Boundary of Time-Varying Plasma</i> .....	36
11. V.A. Baranov, O.E. Den, A.L. Karpenko, A.V. Popov (Russia), <i>3-D Inverse Problems of Geometrical Optics in the Subsurface Radio Sounding</i> .....	40
12. D.O. Batrakov, N.P. Zhuck (Ukraine), <i>The Inverse Problem for a Multilayered Slab with Corrugated Bound</i> .....	44
13. S.V. Boriskina, A.G. Yarovoy (Ukraine), <i>Dielectric Slab Eigenmode Scattering from a Local Cylindrical Boundary Deformation</i> .....	50

14. I. Bubukin (Russia), <i>The Method of the Local Change of Variable During the Calculations of the Thermal Radioemission Statistical Characteristics of the Rough Sea Surface in Kirghoff's Approximation</i> .....	55
15. M. Bulahov (Russia), <i>Mathematical Methods in the Electromagnetic Wave Theory in Urban Media</i> .....	59
16. F. Capolino, S. Maci, R. Tiberio, A. Toccafondi (Italy), <i>Uniform Description of Double Diffraction Transition Regions at a Plane Angular Sector</i> .....	63
17. I. Chudinovich (Ukraine), <i>Mathematical Questions of the Boundary Equation Method in the Electrodynamics</i> .....	67
18. V.L. Danilchuk, V.N. Plotnikov, J.J. Radtsig, S.I. Eminov (Russia), <i>Theory of the Integral Equation of the Impedance Dipole</i> .....	71
19. S.G. Dmitryuk, I.V. Petrusenko (Ukraine), <i>The Numerical Analytical Method of Solving 3-D Diffraction Problems in the Complex Geometry Domain</i> .....	75
20. M. Doroshenko, R. Djobava, R. Zaridze (Georgia), <i>The Scattering of the Pulsed Electric Dipole Field by a Perfectly Conducting Bodies of Revolution</i> ....	79
21. M. Doroshenko, R. Zaridze (Georgia), <i>The Investigation of Time Responses of Dielectric Bodies of Revolution</i> .....	83
22. F.F. Dubrovka, Y.V. Petrushevsky (Ukraine), <i>Analysis of Irregular Rectangular Waveguide Structure with Arbitrary Shaped Central Septum</i> .....	87
23. A.G. Dudko, V.I. Naidenko (Ukraine), <i>H-Waveguide with Rounded Sharp Edges and Angles</i> .....	91
24. V. Dushkin, Y. Gandel, N. Morozova (Ukraine), <i>Numerical Realization for the Diffraction Problems on Multielement Gratings</i> .....	95
25. M.B. Egorov (Ukraine), <i>On the Problem of Wave Diffraction by Screens with Narrow Slots</i> .....	99
26. N. Egorova, N. Kolchigin (Ukraine), <i>Propagation of Pulse Wave Beam in the Vicinity of Underlying Surface</i> .....	103
27. N. Erokhin (Russia), <i>Mode Conversion in Inhomogeneous Chiral Medium</i>	108

28. V. Freilikher, M. Kaveh, M. Pustilnik, I. Yurkevich (Israel), A. Maradudin (USA), <i>Theory of Multiple Scattering from Systems with Bound States</i> .....	111
29. R.N. Ghose (USA), <i>Radiation Characteristics of an Electric Current Element over a High-Intrinsic-Impedance Surface</i> .....	115
30. N.N. Gorobetz, N.P. Eliseyeva (Ukraine), <i>GTD Analysis of Microstrip Antennas and Vibrator with Plane Screen</i> .....	119
31. N.N. Gorobetz, J.Y. Shavorykina, A.V. Nechosa (Ukraine), <i>Radiation of Videopulse by Finite Length Dipole Antenna</i> .....	123
32. G. Goshin, N. Lugina (Russia), <i>The Quasi-3-D Problem of Excitation of the Wire System Located on a Chiral Half-Space</i> .....	126
33. E.V. Guseva, V.I. Naidenko (Ukraine), <i>Calculation of Dispersion Characteristics of Multibeam Multistage Structures with Higher Symmetries</i> .....	130
34. E.E. Hasanov, A.S. Huseynova (Turkey), <i>Determination of the Wave Fronts by Prespecified Focal Line</i> .....	134
35. M. Hashimoto (Japan, Invited), <i>Ray Technique for Stationary Waves in Guided Wave Structures</i> .....	138
36. M.V. Isakov (Russia), <i>Effects of Bistability in the Nonlinear and Inhomogeneous 2-D Systems</i> .....	148
37. V. Kalashnikov (Russia), <i>Numerical Computation of Diffraction Coefficients for New Canonical Problem</i> .....	152
38. V. Kalinichev (Russia), <i>Surface Mode Scattering by Metal Strips on an Interface between Two Dielectric Layers</i> .....	156
39. V.Y. Karaev (Russia), <i>On the Problem of Satellite Measurements of Wind Speed</i> .....	160
40. S.K. Katenev (Ukraine), <i>Electromagnetics of Simplest H-Eigenwaves in Periodic Iris-Loaded Circular Waveguide</i> .....	164
41. V.B. Kazansky, V.A. Gridina (Ukraine), <i>Mathematical Model of Quasioptical Communication Channels with Resonant Cavities</i> .....	169
42. V.B. Kazansky, D.L. Litvinenko, L.N. Litvinenko (Ukraine), <i>Guided Wave Reflection from a Joint Between the Regular and Iris Waveguides</i> .....	172

43. E. Kerherve, P. Jarry, B. Theron, C. Trouche (France), <i>The Simplified Real-Frequency Method Applied to the Low-Noise Amplifiers Synthesis</i> .....	176
44. A.A. Kirilenko, T.I. Vassilyeva, L.A. Rud, V.I. Tkachenko (Ukraine), <i>Method of Virtual Decomposition for the Solution of 3-D Diffraction Problems</i> .....	178
45. A.I. Kleev, A.B. Manenkov (Russia), <i>Interaction of the Modes in Quasi-Optical Resonators</i> .....	182
46. V.N. Kochin, S.L. Prosvirnin, T.D. Vasilieva (Ukraine), <i>Analysis of Electromagnetic Wave Scattering by Complex Screens with Edges in Cases of Plane and Axial Symmetry</i> .....	186
47. Y.V. Kolesnichenko (Russia), <i>Modes in Multicore Optical Fibre Structures</i> .....	190
48. V.V. Konotop, M.M. Rezinkina, O.L. Rezinkin (Ukraine), <i>3-D Technique Used for the Numerical Computation of EF Created around Fractal Clusters in the Insulation</i> .....	194
49. E.V. Kuposova, S.N. Vlasov (Russia), <i>Fully Anti-Mirror Reflection from Corrugated Boundary of Dielectrics. Dielectric Echelette. Dielectric Echelette Resonators</i> .....	198
50. I. Koritzev (Turkey), <i>Recognition of Electromagnetic Fields</i> .....	202
51. S. Koshikawa, K. Kobayashi (Japan), <i>Diffraction by a Terminated, Semi-Infinite Parallel-Plate Waveguide with 3 Different Material Loading: Pt. I - The Case of E Polarization</i> .....	205
52. S. Koshikawa, K. Kobayashi (Japan), <i>Diffraction by a Terminated, Semi-Infinite Parallel-Plate Waveguide with 3 Different Material Loading: Pt. II - The Case of H Polarization</i> .....	209
53. Z. Krasinski, A. Majewsky (Poland), T. Hinata (Japan), <i>The Improved Point-Matching Method with Mathieu Function Expansion for Elliptical Fibers</i> .....	213
54. S.V. Krestyaninov, A.M. Lebedev, V.A. Permyakov (Russia), <i>Diffraction Effects at the Electromagnetic Scattering by an Inhomogeneous Plasma</i> .....	217
55. G.P. Kulemin, S.A. Velichko (Ukraine), <i>Determination of Spray Distribution over the Sea Surface by Radar</i> .....	221
56. A. Lerer, I. Donets, S. Bryzgalo (Russia), <i>The Semi-Inversion Method for Generalized Cylindrical Microwave Structures</i> .....	225



57. V.V. Lukin, V.V. Melnik, Z. Miao, N.N. Ponomarenko, A.A. Zelensky (Ukraine), <i>Expert System for Radar Image Recognition / Filtering</i> .....	229
58. E.A. Luneburg (Germany, Invited), <i>Polarimetric Radar Backscatter</i> .....	233
59. M.A. Lyalinov (Russia), <i>Asymptotics of Electromagnetic Field in the Problem of Diffraction by a Wedge with Anisotropic Face Impedances</i> .....	245
60. S. Maci, L. Borselli, C. Salvador, L. Rossi (Italy), <i>Uniform Diffraction Coefficients at Edges in a Grounded Dielectric Slab</i> .....	249
61. V.V. Meriakri, B.A. Murmuzhev, M.P. Parkhomenko (Russia), <i>Millimeter Wave Dielectric Strip Waveguides Using Ferrites and Semiconductors</i> .....	253
62. V.V. Meriakri, I.P. Nikitin, M.P. Parkhomenko (Russia), <i>Millimeter Wave Electrically and Optically Controlled Screens</i> .....	256
63. Z.T. Nazarchuk, O.I. Ovsyannikov (Ukraine), <i>The Electromagnetic Wave Scattering by Screen System in Stratified Medium</i> .....	260
64. A.G. Nerukh (Ukraine), <i>Wave Equation Green's Function for the Case of Piecewise Homogeneous and Temporally Constant Medium</i> .....	266
65. A.G. Nerukh, D.G. Scherbinin (Ukraine), <i>Stepped Function Approximation of Nonstationarity of Bounded Absorbing Dielectric</i> .....	270
66. A. Oksaoglu (Turkey), <i>Chaotic Behaviour in Varactor Circuits</i> .....	274
67. Y. Okuno (Japan), <i>A Duality Relationship between Scattered Field and Current Density Calculation in the Yasuura Method</i> .....	278
68. A. Osipov (Russia), <i>Electromagnetic Diffraction by a System of Coupled Rectangular Wedges: Efficient Solution via the Semi-Inversion Method</i> .....	282
69. L.S. Pankratov (Ukraine), <i>Application of the Homogenization Theory in Superconductivity Problems</i> .....	286
70. L.A. Pazynin (Ukraine), <i>On Wave Propagation over a Plane Surface of Variable Conductivity</i> .....	290
71. V.A. Permyakov, S.V. Krestyaninov (Russia), <i>Modified Geometrical Optics for an Inhomogeneous Isotropic Plasma</i> .....	294



72. V. A. Permyakov, A.M. Lebedev (Russia), <i>Effective Numerical Procedures for Evaluating of H and E-Wave Diffraction on the 2-D Inhomogeneous Plasma Cylinder</i> .....	298
73. R. Petit (France, Invited), <i>From Functional Analysis to the Method of Fictitious Sources in Electromagnetic Diffraction</i> .....	302
74. S. Petrov, I. Sukhoivanov (Russia), <i>Coupled Power Equation Use for Analysis of Optical Fibers with Unsteady State Power Distribution</i> .....	316
75. S.F. Pimenov (Russia), <i>Statistical Properties of Decametric Radar Signals Reflected by the Earth Surface</i> .....	319
76. S.F. Pimenov (Russia), N.A. Stepanova (Ukraine), <i>Second Order Scattering of Radio Waves by Two-Layer Medium with Rough Boundaries</i> .....	323
77. S.F. Pimenov (Russia), N.A. Stepanova (Ukraine), <i>Strong Scattering of Radio Waves by Layered Media with Rough Surface</i> .....	327
78. I.E. Pochanina, Y. K. Sirenko, N.P. Yashina (Ukraine), <i>Simulation of Particular Phenomena in Waveguide Open Cavities</i> .....	330
79. T. Popkova, A. Slepyan, G. Slepyan (Belarus), <i>Rigorous Theory of Horn Antennas: Asymptotical Computation of Backward and Broadside Radiation</i> .....	334
80. A.I. Popov (Russia), <i>Transparent Boundaries for the Parabolic Wave Equation</i> .....	338
81. S.D. Prijmenko, N.A. Khizhnyak (Ukraine), <i>Excitation of the Impedance Antenna in the Circular Waveguide</i> .....	342
82. N.I. Pyatak, O.V. Kulakov (Ukraine), <i>Electromagnetic Oscillations in a Waveguide Conjunction with Magnetized Ferrite Insertions</i> .....	346
83. P.R. Rousseau, P.H. Pathak (USA, Invited), <i>Development of Time-Domain Uniform GTD and Its Modification for Analyzing the Transient Scattering from Curved Wedge Configurations</i> .....	350
84. M. Samoilenko (Ukraine), <i>On Justification of the Method of Discrete Singularities for Some Problems of Electrodynamics</i> .....	354
85. R. Sato, H. Shirai (Japan), <i>Electromagnetic Wave Scattering by a Loaded Trough on the Ground</i> .....	358

86. S.L. Senkevich (Ukraine), <i>Spectral Approach to the Synthesis of Metal Grating Angular and Frequency Filters</i> .....	362
87. A.E. Serebryannikov, L.V. Vavriv (Ukraine), <i>Method of Trial Pulse Response in Nonstationary Electrodynamics</i> .....	366
88. V.V. Shevchenko, A.D. Skaballanovich (Russia), <i>Modes of Double Core Optical Fibres with Non-Identical Cores</i> .....	370
89. V.V. Shevchenko, S.V. Stoyanov (Russia), <i>Modes of Inhomogeneous Anisotropic Optical Fibres with Local Diagonal Tensor Permittivity of a Core</i> ..	373
90. Y.S. Shifrin, A.I. Luchaninov (Ukraine, Invited), <i>Methods of Analysis of Antennas with Nonlinear Elements</i> .....	378
91. M. Shimoda, T. Itakura (Japan, Invited), <i>Scattering of Electromagnetic Waves by Scatterers Composed of Conducting Strips</i> .....	388
92. Y.K. Sirenko, L.G. Velichko (Ukraine), <i>Inverse Boundary Value Problems in Scattering Theory: Methods, Results, Open Questions</i> .....	400
93. A.N. Sivov, A.D. Chuprin, A.D. Shatrov (Russia), <i>On Phase Characteristics of Short-Periodic Gratings</i> .....	403
94. A.N. Sivov, A.D. Chuprin, A.D. Shatrov (Russia), <i>Synthesis of Multigrad Transmission Type Converters of EM Field Polarization Structure</i> .....	406
95. D.C. Skigin, R.A. Depine (Argentina), <i>Antispecular Effects in the Electromagnetic Scattering from 1-D Rough Surfaces: Case of Oblique Incidence</i> .....	410
96. Y.G. Smirnov (Russia), <i>Vector Pseudodifferential Equations in Electromagnetic Diffraction Problem on Arbitrary Screen</i> .....	422
97. A.V. Sochilin, S.I. Eminov (Russia), <i>The Diffraction on the Thick Dipole</i> ....	426
98. A.Y. Svezhentsev (Ukraine), <i>Wave Attenuation in Rectangular-Groove Guides</i> .....	430
99. O.A. Tretyakov (Ukraine, Invited), <i>Propagation of Super-Wideband Signals through Waveguides</i> .....	434
100. Y.A. Tuchkin (Ukraine), <i>Analytical Regularization of Surface-Integral and Integro-Differential Equations in Diffraction Theory</i> .....	435

101. A. Tyzhnenko (Ukraine), <i>2-D Boundary Problem for Uniform Dielectric Structures</i> .....	440
102. E. Vasiliev, V. Solodukhov (Russia, Invited), <i>A Hybrid Approach: The Integral Equation Method and the Physical Theory of Diffraction</i> .....	443
103. C.N. Vazouras, P.G. Cottis, J.D. Kanellopoulos (Greece), <i>Application of Successive Approximations Scheme to Scattering from a Perfectly Conducting Surface, Rough in One Dimension</i> .....	455
104. N.V. Veremey, V.V. Veremey (Ukraine), <i>2-D Scattering from a Thin Screen in the Vicinity of the Interface between Two Media</i> .....	459
105. A. Vertiy, I.H. Batur, S. Aydinlik, A. Chukhlantsev, A.H. Serbest (Turkey), <i>Millimeter Wave Reflection and Transmission by Leaves</i> .....	464
106. M.V. Vesnik (Russia), <i>The Using of 2-D Solutions on 3-D Problems for Scatterers of Arbitrary Properties</i> .....	465
107. E. Vinogradova (Ukraine), <i>The Wave Scattering from Spheroidal Shells</i> ..	469
108. S.N. Vorob'ev (Ukraine), <i>Electromagnetic Wave Diffraction by Finite-Element Microstrip Structure : Comparison of Full-Wave Spectral and Approximate Methods</i> .....	472
109. V.V. Yachin, N.A. Khizhnyak (Ukraine), <i>The Scattering of Electromagnetic Waves by Periodic Metadielectric Layer</i> .....	476
110. K.P. Yatzuk, R.R. Shvelidze (Ukraine), <i>Excitation Problem of the Planar Spiral in Three Layer Dielectric</i> .....	479
111. L.V. Yurchenko (Ukraine), <i>Calculation of Electric and Magnetic Fields for the Dense Laminar Electron Beam Forming</i> .....	483
112. D. Zanevskiy, S. Nefedov, P. Petrosian (Belarus), <i>Space-Time Concentration of Wave Process</i> .....	487
113. A.A. Zvyagintsev, A.V. Strizhachenko (Ukraine), <i>High-Accuracy Method for Non-Destructive Local Parameter Microwave Measurements of Materials</i> .....	491

#### **Manuscripts received after the deadline**

114. A. Khapalyuk (Belarus), <i>The Generalized Solutions of Bessel Equation</i> ...	494
--	-----

115. D. R. Wilton (USA, Invited), *Modeling with Integral Equations in Computational Electromagnetics*.....502
116. V..F. Kravchrenko (Russia), V.A. Rvachev, V.L. Rvachev (Ukraine), *Atomic Functions Based Mathematical Methods in Signal Processing and Image Reconstruction*.....511
117. S.V. Sukhinin, N.G. Shevchenko (Russia), *Wave-Guide Properties of One-Directional Periodical 3-D Transparent and Non-Transparent Structures*.....513

# AUTHORS INDEX

Agapov, V.	1	Freilikher, V.	111
Andreev, M.	7	Gandel, Y.	95
Andrenko, A.	11	Ghose, R.N.	115
Anohina, O.D.	15	Gorobetz, N.N.	119, 123
Antonov, G.S.	15	Goshin, G.	126
Apelt'cin, V.F.	18	Gridina, V.A.	169
Arslan, A.N.	22	Gubar, V.A.	15
Artemiev, V.V.	26	Guseva, E.V.	130
Aydincik, S.	464	Hasanov, E.E.	134
Babiy, V.I.	29	Hashimoto, M.	138
Bagatskaya, O.V.	30	Hinata, T.	213
Bakunov, M.	36	Huseunova, A.S.	134
Baranov, V.A.	40	Isakov, M.V.	148
Batum, I.H.	464	Itakura, T.	388
Boriskina, S.V.	50	Jarry, P.	176
Batrakov, D.O.	30, 44	Kalashnikov, V.	152
Borselli, L.	249	Kalinichev, V.	156
Borulko, V.	7	Kanellopoulos, J.D.	455
Bryzgalo, S.	225	Karaev, V.Y.	160
Bubukin, I.	55	Karpenko, A.L.	40
Bulahov, M.	59	Katenev, S.K.	164
Capolino, F.	63	Kaveh, M.	111
Chukhlantsev, A.	464	Kazansky, V.B.	169, 172
Chudinovich, I.	67	Kerherve, E.	176
Chuprin, A.D.	403, 406	Khapalyuk, A.	494
Cottis, P.G.	455	Khizhnyak, N.A.	342, 476
Danilchuk, V.L.	71	Kirilenko, A.A.	178
Den, O.E.	40	Kleev, A.I.	182
Depine, R.A.	410	Kobayashi, K.	205, 209
Djobava, R.	79	Kochin, V.N.	186
Dmitryuk, S.G.	75	Kolchigin, N.	103
Donets, I.	225	Kolesnichenko, Y.V.	190
Doroshenko, M.	79, 83	Konotop, V.V.	194
Drobakin, O.	7	Koposova, E.V.	198
Dubrovka, F.F.	87	Koritzev, I.	202
Dudko, A.G.	91	Koshikawa, S.	205, 209
Dushkin, V.	95	Krasinski, Z.	213
Egorov, M.B.	99	Kravchenko, V.F.	511
Egorova, N.	103	Krestyaninov, S.V.	217, 294
Eliseyeva, N.P.	119	Kulemin, G.P.	221
Eminov, S.I.	26, 71, 426	Lebedev, A.M.	217, 298
Erokhin, N.	108	Lerer, A.	225
		Litvinenko, D.L.	172
		Litvinenko, L.L.	172
		Luchaninov, A.I.	378

Lugina, N.	126
Lukin, V.V.	229
Luneburg, E.	233
Lyalinov, M.A.	245
Maci, S.	63, 249
Majevsky, A.	213
Manenkov, A.B.	182
Maradudin, A.	111
Melnik, V.V.	229
Meriakri, V.V.	253, 256
Miao, Z.	229
Morozova, N.	95
Murmuzhev, B.A.	253
Naidenko, V. I.	91, 130
Nazarchuk, Z.T.	260
Nazirov, Z.F.	29
Nechosa, A.V.	123
Nefedov, S.	487
Nerukh, A.G.	266, 270
Nikitin, I.P.	256
Oksaoglu, A.	274
Okuno, Y.	278
Osipov, A.	282
Ovsyannikov, O.I.	260
Pankratov, L.S.	286
Parkhomenko, M.P.	253, 256
Pathak, P.	350
Pazynin, L.A.	290
Petit, R.	302
Petrosyan, P.	487
Petrov, S.	316
Permyakov, V.A.	217, 294, 298
Petrusenko, I.V.	75
Petrushevsky, Y.V.	87
Pimenov, S.F.	319, 323, 327,
Plotnikov, V.N.	71
Pochanina, I.E.	330
Ponomarenko, N.N.	229
Popkova, T.	334
Popov, A.I.	338
Popov, A.V.	40
Prijmenko, S.D.	342
Prosvirnin, S.L.	186
Pustilnik, M.	111
Pyatak, N.I.	346

Radtsig, J.J.	71
Rezinkin, O.L.	194
Rezinkina, M.M.	194
Rossi, L.	249
Rud, L.A.	178
Russeau, P.R.	350
Rvachev, V.A.	511
Rvachev, V.L.	511
Salvador, S.	249
Samoilenko, M.	354
Sato, R.	358
Scherbinin, D.G.	270
Senkevich, S.L.	362
Serbest, A.H.	464
Serebryannikov, A.E.	366
Shatrov, A.D.	403, 406
Shavorykina, J.Y.	123
Shevchenko, V.V.	370, 373
Shifrin, Y.S.	378
Shimoda, M.	388
Shirai, H.	358
Shulga, N.P.	30
Shvelidze, R.R.	479
Sirenko, Y.K.	330, 400
Sivov, A.N.	403, 406
Skaballanovich, A.D.	370
Skigin, D.C.	410
Slepyan, A.	334
Slepyan, G.	334
Sochilin, A.V.	426
Solodukhov, V.	443
Soloviov, O.	1
Smirnov, Y.G.	422
Stepanova, N.A.	323, 327
Stoyanov, S.V.	373
Strizhachenko, A.V.	491
Svezhentsev, A.Y.	430
Sukhoivanov, I.	316
Theron, B.	176
Tiberio, R.	63
Tkachenko, V.I.	178
Toccafondi, A.	63
Tretyakov, O.A.	434
Trouche, C.	176
Tuchkin, Y.A.	435

Tyzhnenko, A.	440
Uckun, S.	11
Usin, V.A.	15
Vasiliev, E.	443
Vasilieva, T.D.	186
Vassilyeva, T.I.	178
Vavriv, L.A.	366
Vazouras, C.N.	455
Velichko, L.G.	400
Velichko, S.A.	221
Veremey, V.V.	459
Veremey, N.V.	459
Vertiy, A.A.	464
Vesnik, M.V.	465
Vinogradova, E.D.	469
Vlasov, S.N.	198
Vorob'ev, S.N.	472
Wilton, D.	502
Yachin, V.V.	476
Yantsevich, A.A.	29
Yarovoy, A.G.	50
Yashina, N.P.	330
Yatzuk, K.P.	479
Yurchenko, L.V.	483
Yurkevich, I.	111
Zanevskiy, D.	487
Zaridze, R.	79,83
Zelensky, A.A.	229
Zhuck, N.P.	30, 44
Zhukov, S.	36
Zvyagintsev, A.A.	491



# AN ASYMPTOTIC THREE-DIMENSIONAL APPROACH TO THE PROBLEM OF THE POINT SOURCE FIELD DIFFRACTED BY LOCALIZED IMPEDANCE DISCONTINUITY

Vyacheslav Agapov and Oleg Soloviev  
Radiophysics Department, University of St. Petersburg  
St. Petersburg, Russia

## ABSTRACT

The paper presents a three-dimensional approach to obtain the point source field above a plane with impedance discontinuity of finite lateral extent. The employed asymptotic technique allows to facilitate computational procedure and, nevertheless, to retain in solution all the features of field behavior that are intrinsic to three-dimensional diffraction problems. An appropriate numerical algorithm is developed to handle modified integral equation. The proposed scheme ensures drastic reduction of CPU time. Some results of calculations are discussed.

## INTRODUCTION

This research evolves and applies an analytical-numerical method for analyzing the propagation of waves in the presence of a localized irregularity of environment. The problem to be considered is relevant to numerous practical cases (e.g. radio wave propagation over inhomogeneous Earth's surface [1, 2, 3, 4], acoustic field diffraction from inhomogeneities of the ground and noise reduction problem [5], the influence of a localized ionospheric disturbance on the electromagnetic field in the Earth-ionosphere waveguide [6, 7]).

Irrespective of the physical origin of wave process the surface impedance concept is commonly used to characterize reflective properties of environment. In this paper we are concerned primarily with the development and validation of the theory and algorithm. So, in order to avoid unnecessary cumbersome formulas, to discard the effects of guided wave propagation, and to focus on particular phenomenon of three-dimensional diffraction from localized impedance discontinuity, we restrict ourselves by the investigation of the following model: we consider the scalar field emitted by a harmonic point source in half-space bounded by piecewise homogeneous impedance plane.

There were many studies dealing with similar three-dimensional problems and there were numerous attempts to elaborate any efficient technique to solve them. First we mention so-called mixed-path approximation which was based on the one-dimensional Volterra integral

equation and totally ignored the finite lateral extent of perturbed area [1]. The two different approaches to the rigorous two-dimensional integral equation were developed: the first order perturbation technique (Born approximation) [6] and the direct numerical inversion [3, 4]. Both proved to be efficient only in the case of comparatively small irregularity because of inherent shortcomings (accuracy loss, great computational expense, etc.).

This paper is to present an asymptotic technique which allows to facilitate numerical treatment of the two-dimensional integral equation and, nevertheless, to retain in solution all the features of field behavior that are intrinsic to three-dimensional diffraction problems. An appropriate computational algorithm and some results of its implementation are discussed as well.

## STATEMENT OF THE PROBLEM

Let us consider the stationary point source (time dependence is assumed to be  $e^{-i\omega t}$ ) located at the point  $\{\rho = 0, \varphi = 0, z = z_t > 0\}$  (cylindrical coordinate system) above a plane surface  $S_c = \{z = 0\}$ . We characterize the field by scalar function  $\Phi(\rho, \varphi, z, z_t)$ , which satisfies the Helmholtz's equation and the following impedance boundary condition:

$$\frac{1}{\Phi} \frac{\partial \Phi}{\partial z} \Big|_{z=0} = -ik\delta(\rho, \varphi) \quad (1)$$

where:  $k$  - is free space wave number ( $\text{Im } k > 0$ ),  $\delta(\rho, \varphi)$  - is inhomogeneous surface impedance function  $\delta(\rho, \varphi) = \delta_c$  if  $\{\rho, \varphi, 0\} \in S_c \setminus S_p$  and  $\delta(\rho, \varphi) = \delta_p$  if  $\{\rho, \varphi, 0\} \in S_p$  ( $\text{Re } \delta_{c,p} > 0$ ), and  $S_p \subset S_c$  - is arbitrarily shaped area of inhomogeneity. We assume  $S_p$  to be of finite size (localized), so we may call it further "impedance patch" or "impedance island". The infinity condition requires  $\Phi(\rho, \varphi, z, z_t)$  to vanish if  $\rho \rightarrow \infty$ .

## METHOD

First we write out the rigorous two-dimensional integral equation for unknown function  $\Phi(\rho, \varphi, z, z_t)$  using the solution of the regular problem. Let the function  $G(\rho, z, z_t)$  satisfy the same Helmholtz's equation and the boundary condition (1) with constant  $\delta(\rho, \varphi) = \delta_c$ . Applying the second Green's formula to the functions  $G$  and  $\Phi$  one may obtain:

$$\Phi(\rho, \varphi, z, z_t) = G(\rho, z, z_t) + ik\delta \iint_{S_p} G(\rho'', 0, z) \Phi(\rho', \varphi', 0, z_t) dS'$$

where:  $\delta = \delta_p - \delta_c$  - is impedance contrast,  $\{\rho, \varphi, z\}$  - is observation point,  $\{\rho', \varphi', 0\}$  - is integration point,  $\rho'' = \sqrt{\rho^2 + \rho'^2 - 2\rho\rho' \cos(\varphi - \varphi')}$ .

Then we introduce the slowly varying attenuation functions that are ubiquitous to wave propagation theory:

$$\Phi(\rho, \varphi, z, z_t) = \frac{e^{ik\rho}}{2\pi\rho} V(\rho, \varphi, z, z_t) \quad G(\rho, z, z_t) = \frac{e^{ik\rho}}{2\pi\rho} U(\rho, z, z_t)$$

Without any loss of generality we may consider the case when both transmitter and receiver are located at the plane  $S_c$ . Hereafter, in order to simplify our expressions, we omit arguments

$z$  and  $z_t$  in the functions. The integral equation for unknown attenuation function takes a form:

$$V(\rho, \varphi) = U(\rho) + \frac{i\delta}{2\pi} k\rho e^{-ik\rho} \iint_{S_p} U(\rho'') V(\rho', \varphi') \frac{e^{ik(\rho' + \rho'')}}{\rho' \rho''} dS' \quad (2)$$

This is rigorous two-dimensional Fredholm integral equation. In the case of comparatively small inhomogeneity  $S_p < 15\lambda^2$  ( $\lambda = 2\pi/k$  - is free space wavelength) this equation was attacked with the aid of direct numerical procedures [3, 4]. For larger patch this approach seems to be awkward and we intend to develop another technique outlined by King and Wait [2] and evolved by Soloviev [7].

Introducing the elliptic coordinate system on the surface  $S_c$  [2] and substituting the variables of integration:

$$\begin{aligned} \rho' &= \frac{\rho}{2} [ch u + \cos v] & \rho'' &= \frac{\rho}{2} [ch u - \cos v] \\ -\infty < u < +\infty & & 0 \leq v \leq \pi \\ dS' &= \rho' \rho'' du dv \end{aligned}$$

we come to the equality:

$$V(\rho, \varphi) = U(\rho) + \frac{i\delta}{2\pi} k\rho \int_{v_<}^{v_>} \left( \int_{u_<(v)}^{u_>(v)} U(u, v) V(u, v) e^{ik\rho(ch u - 1)} du \right) dv \quad (3)$$

The functions  $u_<(v)$  and  $u_>(v)$  specify the boundary of the patch in elliptic coordinate system:  $\partial S_p = \{u_<(v), v_< \leq v \leq v_>\} \cup \{u_>(v), v_< \leq v \leq v_>\}$ . Then the asymptotic evaluation of integral with respect to  $u$  in (3) is carried out with the aid of stationary phase method.

We assume  $k\rho \gg 1$  to be the large parameter of the problem and, as in [7], we employ the asymptotic expansion that may be found in [8] and [9]:

$$\int_0^u f(t) e^{i\Omega(ch t - 1)} dt = \sqrt{\frac{i\pi}{2\Omega}} \operatorname{erf} \left[ -\sqrt{i\Omega} \sqrt{2sh} \frac{u}{2} \right] f(0) + \frac{i}{\Omega} e^{i\Omega(ch u - 1)} \left\{ \frac{f(0)}{2sh \frac{u}{2}} - \frac{f(u)}{sh u} \right\} + O(\Omega^{-3/2})$$

where:  $\operatorname{erf}(x) = \frac{2}{\sqrt{\pi}} \int_0^x e^{-t^2} dt$  - is the conventional error function of a complex variable [10]. It is convenient for further numerical treatment to represent the remained integral with respect to  $v$  as a contour integral along the boundary of inhomogeneous area:

$$\int_{v_<}^{v_>} F[u_>(v)] dv - \int_{v_<}^{v_>} F[u_<(v)] dv = \oint_{\partial S_p} F[u(v)] dv$$

Thus we obtain the following expression:

$$\begin{aligned} V(\rho, \varphi) &= U(\rho) + \frac{i\delta}{2} \sqrt{\frac{ik\rho}{2\pi}} \oint_{\partial S_p} \operatorname{erf} \left[ -\sqrt{ik\rho} \sqrt{2sh} \frac{u}{2} \right] U(0, v) V(0, v) dv - \\ &- \frac{\delta}{2\pi} \oint_{\partial S_p} e^{ik\rho(ch u - 1)} \left\{ \frac{U(0, v) V(0, v)}{2sh \frac{u}{2}} - \frac{U(u, v) V(u, v)}{sh u} \right\} dv + O[(k\rho)^{-3/2}] \end{aligned} \quad (4)$$

This is our general working formula. It is more accurate than that from [2] as it completely incorporates the second term of asymptotic expansion.

Let us proceed with an algorithm for handling (4). Unlike the formula (2), the asymptotic integral equation (4) contains only linear one-dimensional integrals. However, looking at it, we can infer that in order to convert (4) into the set of linear algebraic equations we have to let the observation point  $\{\rho, \varphi\}$  successively approach each point of the two-dimensional area  $S_p$ . Thus, we have to make partition of the whole patch again as in the case of the rigorous two-dimensional integral equation. So, we conclude, that the direct inversion of our general working formula will give no benefit from the performed asymptotic integration, and it is judicious to set our preference for another algorithm.

Let us note a feature: the integral operator in (4) may be represented as the sum of two items  $V = U + AV + BV$ , where  $A$  is the integral operator which acts on the function  $V(0, v)$ , and  $B$  is the integral operator which acts on the function  $V(u, v)$ . We point out that  $A$  is the Volterra integral operator and it can be easily inverted with the aid of the conventional recurrent procedure [11]. Moreover, it contains the first, dominant term of asymptotic expansion. In comparison with  $B$  its contribution to solution is expected to be as more significant as larger the value of parameter  $k\rho$ . Thus, the following combination of inversion and iteration procedures are proposed:

$$V^{(0)} = U, \quad V^{(n)} = U + AV^{(n)} + BV^{(n-1)}, \quad n = 1, 2, 3, \dots$$

where  $n$  is the iteration number. The Volterra integral operator  $A$  is inverted directly numerically during each iteration, and the Fredholm integral operator  $B$  is inverted by successive approximations.

## RESULT AND DISCUSSION

Unlike the Volterra operator from one-dimensional integral equation of Feinberg [1] the operator  $A$  contains the error function of complex variable in the kernel. Due to this feature even in the first approximation we obtain substantial three-dimensional effects, such as backward reflection and oscillating transverse diffraction pattern. Moreover, because of the presence of dominant term of asymptotic expansion in  $A$ , the convergence of our combined inversion-iteration procedure proves to be pretty rapid, though it depends upon perturbation strength and upon large parameter of the problem  $k\rho_{\min}$ , where  $\rho_{\min}$  - is the least distance between the source and the boundary of discontinuity.

We can infer that computation time required for numerical implementation of our algorithm varies as square of patch perimeter, whereas in the case of direct approach to two-dimensional integral equation it varies as square of patch surface [4].

We used the result of de Jong [3], who accomplished the direct numerical inversion of the rigorous integral equation (2), as a benchmark to test our asymptotic algorithm. In the case of the same problem as was treated in [3] (ground wave propagation over a small rectangular impedance discontinuity) our result turned to be in very good agreement with that from [3].

In order to make use of the time-consuming advantage of our algorithm we simulated the groundwave propagation in the presence of comparatively large discontinuity. The following parameters of the model were chosen:  $\delta_e = (1.4436 - 1.4436i)10^{-3}$ ,  $\delta_p = 0.2319 - 0.1468i$ . The shape of the inhomogeneity was assumed to be elliptic. The center of the ellipse was placed at the point  $\{\rho = 30\lambda, \varphi = 0\}$ , the great semi-axis  $A_p = 10\lambda$  was on the line  $\varphi = 0$ , the length of the little semi-axis  $B_p$  was varied so as to study the effect of the finite transverse dimension of the island. The figures 1 and 2 illustrate the spatial dependence of the modulus and argument

of attenuation function  $V^{(2)}$  along the line  $\varphi = 0$  (the value  $B_p = 0$  implies the absence of any irregularity).

Apart from those features of field behavior that were discussed in [3, 4], we can observe the area of longitudinal oscillations beyond the rear boundary of the patch. As it could be expected this area extends as long as the width of the first Fresnel zone remains less than the width of the discontinuity. These oscillations can not be observed if the patch is too narrow so that even just behind it the width of the first Fresnel zone exceeds the width of the patch.

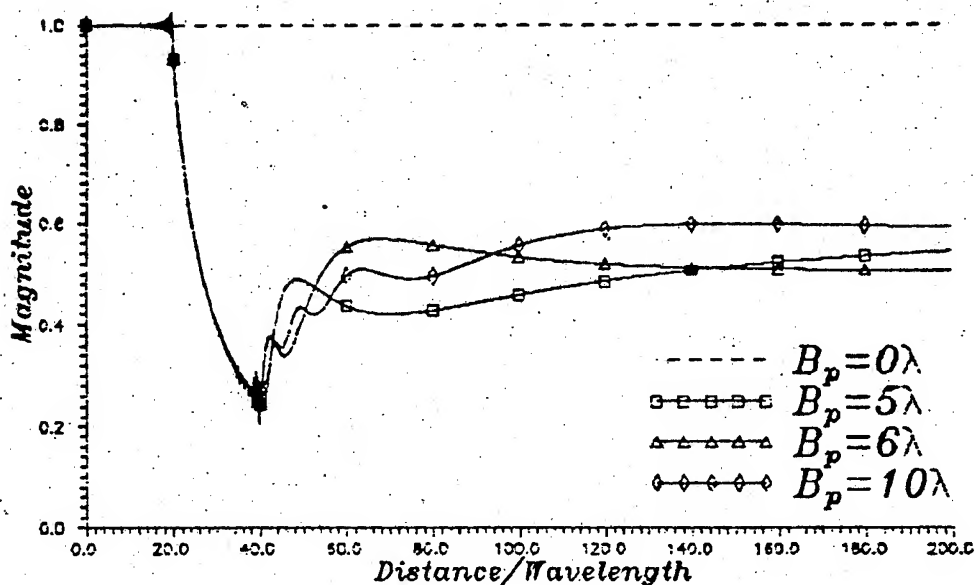


Fig.1

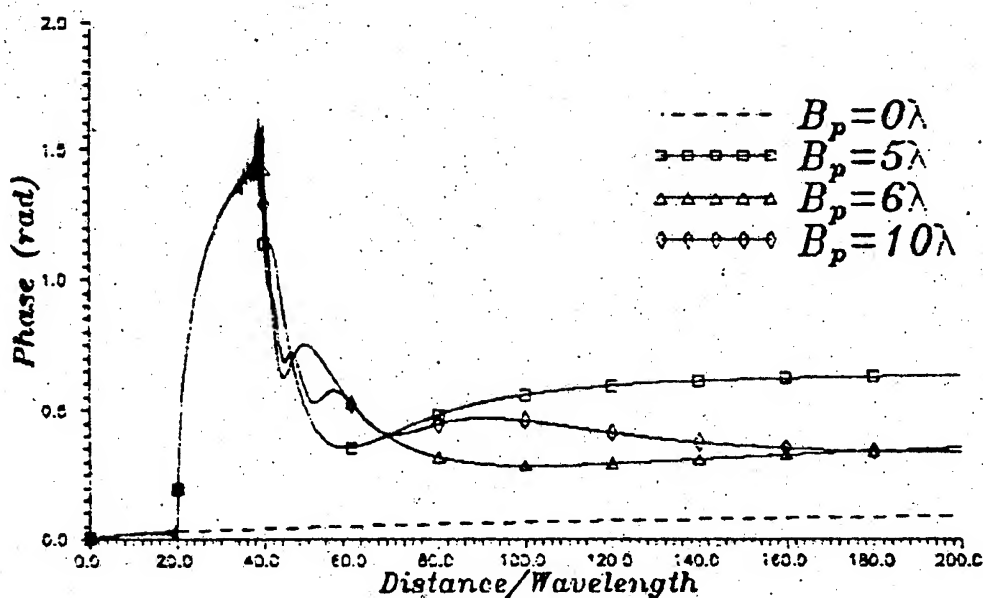


Fig.2

## References

- [1] E.L.Feinberg, *Radio Wave Propagation Along the Earth's Surface*, Nauka, Moscow, 1961.
- [2] R.J.King and J.R.Wait, in *Symposia Mathematica*, vol.18, 107-208; Istituto Nazionale di Alta Matematica, Bologna, Italy, 1976.
- [3] G.de Jong, *Radio Sci.*, 10(11), 925-933, 1975.
- [4] E.C.Field, *IEEE Trans. Antennas and Propag.*, AP-30(5), 831-836, 1982.
- [5] J.N.B.Harriott, S.N.Chandler-Wilde and D.C.Hothersall, *J. Sound and Vibration*, 148(3), 365-380, 1991.
- [6] J.R.Wait, *J. Geophys. Res.*, 69(A3), 441-445, 1964.
- [7] O.V.Soloviev, *Izv. VUZ Radiofiz.*, 33(9), 1078-1087, 1990.
- [8] V.P.Percsada, *Radiotekhnika*, 12(9), 12-19, 1957.
- [9] L.B.Felsen and N.Marcuvitz, *Radiation and Scattering of Waves*, Prentice Hall, Englewood Cliffs, N.J., 1973.
- [10] M.Abramowitz and I.Stegun, *Handbook of Mathematical Functions*, U.S. Government Printing Office, Washington, D.C. 1964.
- [11] C.Wagner, *J. Math. Phys.*, 32(4), 289-301, 1954.

*Acknowledgment.* This work was supported by the Russian Foundation for Fundamental Studies under grant 93-02-17048.

# INVERSION OF ONE-DIMENSIONAL REFLECTING DATA OF MULTILAYERED STRUCTURES USING QUASISOLUTIONS

Mikhail Andreev, Valentin Borul'ko and Oleg Drobakhin

Department of Radiophysics, Dniepropetrovsk University,  
72 Gagarin Street, Dniepropetrovsk-10, 320625, Ukraine

## ABSTRACT

An estimation of multilayered structure parameters through the frequency domain objective function minimization is examined. The finite property of frequency band and the discrete character of measurement frequencies are discussed. A numerical and real experiments results are presented.

## INTRODUCTION

There are many papers [1,2] deals with the inverse problem of multilayered structures in the general case of the plane wave excitation. But practical valuable results can be obtained only in the case of the true reflection of the experimental situation. That is why mathematical model should represent essential features not only the process of the interaction of excitation wavelet and structure but the features of measurement unit and previous processing procedure in the proper way. This fact demands to consider every concrete situation separately, because it has the unique features. The measurements in the waveband 17-40 GHz have some particular features, including the non-plane character of wave radiated from the open-end of waveguide or horn. The multifrequency method is more useful than the direct time-domain methods for this frequency range, because the former provides the more accurate results due to the calibration procedure at every frequency. Furthermore using of short time pulses demands stroboscopic techniques. It demands series of pulses, which possess discrete spectrum. Thus from spectral point of view this case equals multifrequency approach. The continuous structure of spectrum was considered [2] and an analysis of the case of discrete spectrum of data is actual.

## DIRECT PROBLEM AND PREVIOUS DATA PROCESSING

For the plane wave excitation of the plane layers dielectric structure expression similar to Lorentz transformation is usually used [1]. But it is more convenient to apply the additive representation for time-domain interpretation. Both vari-



ants are equal and take into account not only main reflections but all reverberations. It was determined experimentally that for materials with dielectric constant less 10 and distances more than 7 sm amplitudes of reverberations in single layer has values comparatively equal or less than clutter reflections of environment and level of noise.

Our experiments also show that in the case of radiating from the open end of rectangular waveguide the amplitude of time-domain peak corresponding to reflection from metal surface as function of distance can be described by the same dependence as spherical wave with the center shifted from the aperture plane. It doesn't mean that the multifrequency wavelet has spherical character, but the amplitude behavior does. This statement is true in boundaries of measurement accuracy. Using of expressions for geometrical optics provides possibility to estimate the amplitude of second surface reflection with error less 5%. According to aforementioned reasons the mathematical model was chosen as

$$R = \frac{\alpha_1}{\alpha_2 + z} R_{01} + \sum_{m=1}^M \frac{\alpha_1 \prod_{i=1}^m (1 - R_{i-1,i}^2)}{\alpha_2 + z + \sum_{i=1}^m d_i / \sqrt{\epsilon_i}} R_{m,m+1}, \quad (1)$$

where  $\alpha_1$ ,  $\alpha_2$  - some constants;  $z$  - location of front interface multilayer structure,  $M$  - number of layers;  $R_{m,m+1}$  - reflection coefficient between  $m$  and  $m+1$  media;  $d_m$  - geometrical thickness of  $m$ -th layer;  $\epsilon_m$  - dielectric constant of  $m$ -th layer.

The existence of reverberation between structure and aperture or frontier part of unit causes the additional components, which can be canceled using data for metallic plate. The connection between amplitudes of main reflection and reverberations of first and second orders in this case allows to calculate the amplitudes of reverberation for structure using scale constant which is equal to ratio of metal reflection amplitude and structure.

All aperture antennas is known to possess frequency dependence of gain. Frequency dependence of gain can be canceled by dividing structure frequency dependence on metal frequency dependence. All data must be previously processed by using time gates in time domain to pick out only informative part of signal cancelling clutter reflections from environment and reverberations with unit. The time-gate form was chosen to coincide with form of Butterworth bandpass filter. The time-gating also allows to cancel finite directivity signals in the case of director coupler using to measure reflectivity by true choice of distance

to structure.

### ALGORITHM TO SEARCH QUASISOLUTION

The parameter estimation is well-known to produce through searching the minimum of the least-square objective function for instance in time domain, but consideration was carried out for continuous case [2]. It is more convenient to construct this function in frequency domain using isometry time and frequency spaces regarding quadratic norm. To decrease number of variables the model vector was chosen in form  $f^N(\tau) = \{r \cdot \exp(jw_1\tau), r \cdot \exp(jw_2\tau), \dots, r \cdot \exp(jw_N\tau)\}$ , where  $w_1, w_2, \dots, w_N$  - series of measurement frequencies,  $\tau$  - variable time,  $r$  - complex amplitude. This approach allows to exchange complicate multivariable optimization procedure to more simple. The value  $\tau_0$  which provides minimum is quasisolution [3]. The set of vectors  $f_k^N = f^N(\tau_k)$  ( $k=1, \dots, K$ ) must be used in the case of  $K$  peaks determination. If reverberations are neglected that  $K$  is equal  $M$ . We have determined matrix  $F$  as  $(N \times M)$  matrix with columns equal  $f_k^N$ .

This problem is correct if  $\tau_0$  belongs to compact set and the measurement data projection on  $F$  (space spanned on vector  $f_k^N$ ) is unique [3]. The first demand can be simply satisfied by introduction of boundaries for  $\tau$  variations. The second demand determines rules to choose discrete series of  $w_i$ , in some simple cases it coincides with theorem of samples.

Complex values of  $r$  allow to eliminate additional oscillation of objective function through searching of the minimum of objective function as the function of  $r$  for every  $\tau$  determined as constant. The cause of oscillation for real  $r$  is the finite value of frequency band and big value of the ratio middle frequency and bandwidth. Minimization procedure for  $r$  coincides with searching of the projection of real measurements data vector on space  $F$ . The projection operator is known to equal

$$P_F = F(F^T F)^{-1} F^T \quad (2)$$

If  $\tau_k$  and  $\tau_{k+1}$  are becoming closer matrix  $F^T F$  is transforming from well conditioned to ill conditioned. Thus for generality  $P_F$  must be used expression

$$P_F = F(F^T F + \alpha I)^{-1} F^T \quad (3)$$

where  $\alpha$  - parameter of regularization. The existence of  $\alpha$  in (3) produce limit in resolution two close components.

Estimate of  $|r_k|$  allows to calculate  $\epsilon_k$  by traditional means [1], if the sign of  $r_k$  is known. The signs of  $r_k$  for  $r_1$  and  $r_M$  is known a priori. Convenient approach to determine other signs is to choose sign combination which provides proximity to

unit following expression

$$\prod_{m=1}^M (1+R_{m,m+1})/(1-R_{m,m+1})$$

The regularization procedure is to stop searching of  $r_i$  and  $\tau_i$  then absolute value  $|r_i|$  reaches the threshold, which equals the level of clutter reflections determined previously for all region of informative peaks existence.

The numerical experiment for 3-layer structure with reverberations shows the high sensitivity of estimation accuracy in the case of the equality of the each layer electrical thicknesses. The elimination of reverberations in the first and the second layers allows to decrease error from 10 % for thicknesses and 18 % for dielectric constant to 0.7 % and 1 % respectively.

A real experiment was carried out for 3-layer structure plexiglass-air-plexiglass. After previous processing of real experiment data estimates were  $\epsilon_1$ -2.6,  $\epsilon_2$ -1.2,  $\epsilon_3$ -2.8,  $d_1$ -41.2,  $d_2$ -29.6,  $d_3$ -39.0 mm ( true values for thicknesses 40.2, 30.0, 39.0 mm and  $\epsilon$  for single layer was 2.69 ).

### CONCLUSIONS

The consideration of measurement unit properties and particularities of radiated wave allow to construct the algorithm to solve inverse problem for multilayer dielectric structures not only for numerical modeling data but real experimental one.

### REFERENCES

- (1) E. Robinson: "Spectral Approach to Geophysical Inversion by Lorentz, Fourier, and Radon Transforms," Proc. IEEE, (1982) v.70, 9, pp.1039-1054.
- (2) R.G.Keys: "An Application of Marquardt's Procedure to the Seismic Inverse Problem," Proc. IEEE, (1986) v.74, 3, pp.476-486.
- (3) A.N.Tikhonov and Y.Y.Arsenin: "Solutions of Ill-Posed Problems," New York: Wiley, 1977.

**GREEN'S FUNCTION APPROACH IN THE PROBLEM  
OF GROUNDED DIELECTRIC SLAB MODES SCATTERING BY  
COMBINED METAL SCREEN-DIELECTRIC ROD INHOMOGENEITIES**

Andrey Andrenko and Savas Uckun

University of Gaziantep,  
27310, Gaziantep, Turkey

**ABSTRACT**

Scalar Green's function of grounded dielectric slab for magnetic line current source is derived analytically. The solution to the problem of slab guided modes scattering from combined inhomogeneity consisting of unclosed metal screen and dielectric rod scatterer with permittivity different from slab's one is referred to as integral equation on screen's contour with the kernel as Green's function of screen's environment and surface integral over cross-section of dielectric inhomogeneity. Therefore, such an approach allows one to consider a few problems of slab guided modes scattering for different mutual locations of metal screen and dielectric scatterer.

**INTRODUCTION**

During recent years, a great deal of effort in modern diffraction theory has been devoted to deriving solutions to scattering problems related to the location of single- and multi-element scatterers in free or homogeneous space. As it is well known, various rigorous and approximate approaches have been developed for the analysis of scattering properties of metal screens and dielectric bodies with canonical shapes of cross-section. Nevertheless, most scatterers of practical importance are usually placed in inhomogeneous medium. Although a free-space diffraction is of great value both for microwave theory and applications, the real inhomogeneous environment of the scatterers requires some new approaches for the correct investigation of the prospective electrodynamic effects.

An important class of such problems is connected with wave scattering by unclosed perfectly conducting screens and dielectric obstacles embedded into a plane-parallel layered dielectric medium. The solutions to these problems are essentially useful for the investigation of dielectric slab modes scattering and transformation from local inhomogeneities, and excitation of open slab guides. As a matter of fact, in most active and passive microwave integrated circuit devices the principle of operation is based on the modification of a guided mode field by means of discontinuities inside a regular open guide. The aim of the present paper is the further development of Green's function approach and construction of a formal solution to the problem of grounded dielectric slab natural modes scattering by combined cylindrical shaped inhomogeneity consisting of dielectric rod and unclosed metal screen. It is well known that, dielectric discontinuities can be caused by technological material defects. In addition, scatterers that are being considered have the resonant nature that is found in free-space diffraction problems. Therefore, the effects of a guided modes scattering and transformation by such inhomogeneities are expected to be used for the design of compact millimeter-wave rejective filters and mode convertors in open guides.

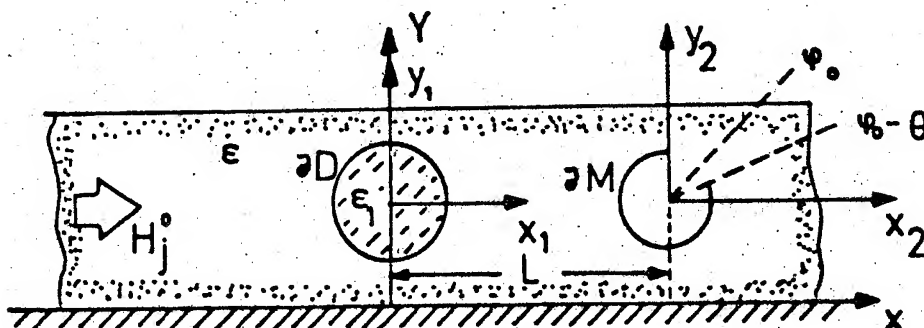


Fig.1. The geometry of combined inhomogeneity inside grounded slab guide.

# FORMULATION OF THE PROBLEM

The geometry of two-dimensional scattering problem is shown in Fig.1. The grounded dielectric slab of thickness  $d$  and permittivity  $\epsilon$  contains two local inhomogeneities separated by distance  $L$ . The first one is dielectric cylinder of radius  $R$  and permittivity  $\epsilon_1$ , while the second scatterer is unclosed, perfectly conductive cylinder of radius  $a$  having the slot of angular width  $2\theta$  positioned in  $\varphi_0$ . Assume that the distances from the centers of cylinders to ground plane are the same and equal to  $b$ . Consider the incidence of one of the even TM-guided modes (the case of H-polarized field), however a similar analysis is applicable for the odd TE-modes (the case of E-polarized field) too. As electromagnetic field of the mode has no  $E_z$  component, it can be determined in terms of  $H_z$  component as (an  $e^{-i\omega t}$  time dependence is suppressed throughout the analysis)

$$H^0(\vec{r}) = H^0_j(\vec{r}) = \begin{cases} \cos p_j y & 0 < y < d \\ \cos p_j d e^{i g_j (y-d)} & y > d \end{cases} \quad (1)$$

Define the total field through the sum

$$H(\vec{r}) = H^0(\vec{r}) + H^{sc}(\vec{r}) \quad (2)$$

where  $H^{sc}(\vec{r})$  is the field scattered by both dielectric rod and unclosed screen. The scattered field  $H^{sc}(\vec{r})$  satisfies the homogeneous Helmholtz equation

$$[\nabla^2 + k^2 \epsilon(y)] H^{sc}(\vec{r}) = 0, \quad \vec{r} \in (\partial M, \partial D, y=0, d) \quad (3)$$

where  $\epsilon(y) = \epsilon$  for  $0 < y < d$  or 1 elsewhere,  $\partial M$  is for the cross-sectional contour of the screen,  $\partial D$  is the surface of dielectric cylinder. Also, the total field has to satisfy the continuity conditions on the surface of the slab,

$$(H^0 + H^{sc})^- = (H^0 + H^{sc})^+, \quad y = d \quad (4)$$

$$\left( \frac{\partial}{\partial y} (H^0 + H^{sc}) \right)^- = \left( \frac{1}{\epsilon} \frac{\partial}{\partial y} (H^0 + H^{sc}) \right)^+, \quad y = d \quad (5)$$

boundary condition on the ground plane's surface,

$$\frac{i}{\epsilon} \frac{\partial}{\partial y} (H^0 + H^{sc}) = 0, \quad y = 0 \quad (6)$$

and continuity condition for tangential component at the surface of dielectric rod

$$(H^0 + H^{sc})^- = (H^0 + H^{sc})^+, \quad \vec{r} \in \partial D \quad (7)$$

Besides, the field must satisfy the Neumann condition at the unclosed screen

$$\frac{\partial}{\partial n} (H^0 + H^{sc}) = 0, \quad \vec{r} \in \partial M \quad (8)$$

together with the edge condition as follows

$$\int_B (k^2 \epsilon |H^{sc}|^2 + |\nabla H^{sc}|^2) d\vec{r} < \infty \quad (9)$$

for any bounded domain  $B$ , and in order to complete the formulation, a condition at infinity taking into account the discrete spectrum of slab's

guided modes as well as the field of radiation [1]. It is shown that the above formulation guaranties the uniqueness of the solution.

#### METHOD OF THE SOLUTION

For the problem of scattering from separated inhomogeneities, the scattered field can be written as the sum

$$H^{sc}(\vec{r}) = H_d^{sc}(\vec{r}) + H_s^{sc}(\vec{r}) \quad (10)$$

where  $H_d^{sc}$  is the field scattered by dielectric cylinder and  $H_s^{sc}$  is the field scattered due to the screen. Applying Green's formula to functions  $H_d^{sc}$ ,  $H_s^{sc}$  and Green's function of the slab  $G(\vec{r}, \vec{r}')$ , one obtains the following integral representation of the solution of formulated boundary-value problem

$$H_s^{sc}(\vec{r}) = \int_D \mu(\vec{r}_2') \frac{\partial}{\partial n'} G(\vec{r}, \vec{r}_2') d\vec{r}_2' \quad (11)$$

with unknown current density function  $\mu(\vec{r}')$  and

$$H_d^{sc}(\vec{r}) = k^2 (\epsilon_1 - \epsilon) \iint_D \tilde{H}(\vec{r}_1') G(\vec{r}, \vec{r}_1') dS' \quad (12)$$

a cross-sectional surface integral [2] that yields  $H(\vec{r})$  if its values over  $D$  are known. If points  $(x, y)$  are restricted inside  $D$ , (12) becomes an integral equation for the inner field in  $D$ . Here,  $G(\vec{r}, \vec{r}')$  is the scalar Green's function of unperturbed regular guide without any inhomogeneity. As scatterers that are being considered are housed inside the slab, we have to construct  $G(\vec{r}, \vec{r}')$  for magnetic-line current source location at  $\vec{r}' = (x', y')$  with  $y' < d$ . This function must satisfy nonhomogeneous Helmholtz equation, boundary conditions (4) - (6) and radiation condition. After some straightforward algebra, Green's function of grounded dielectric slab is found to be

$$G(\vec{r}_1, \vec{r}_1') = \begin{cases} \frac{i}{4} H_0^{(1)}(k\sqrt{\epsilon}|\vec{r} - \vec{r}'|) - \frac{1}{4\pi} \int_{-\infty}^{\infty} e^{ih(x-x')} ((e^{ip(d-y')} (1 - \frac{ge}{p}) + \\ \frac{1}{p} e^{ipr'} \Delta_2) (\Delta_1)^{-1} \cos py - \frac{1}{p} e^{ipr'} \sin py) dh, & 0 \leq y \leq d \\ \frac{i}{2\pi} \int_{-\infty}^{\infty} e^{ih(x-x')} e^{ig(y-d)} (\Delta_1)^{-1} \sin py' dh, & y > d \end{cases} \quad (13)$$

where  $p = (k^2 \epsilon - h^2)^{1/2}$ ,  $g = (k^2 - h^2)^{1/2}$ ,  $\Delta_1 = ig \epsilon \cos pd + p \sin pd$ ,  $\Delta_2 = ig \epsilon \sin pd - p \cos pd$  so that  $\Delta_1 = 0$  is the characteristic equation of even TM modes.

To find the scattered field, we obviously have to calculate the current density function  $\mu(\vec{r}_2')$  on the screen as well as the field  $H(\vec{r}_1')$  inside the dielectric cylinder and perform the integration in (11), (12). The corresponding Fourier-series expansions are

$$\mu(\vec{r}_2) = \frac{2}{i\pi k\sqrt{\epsilon}a} \sum_n \mu_n^j e^{in\varphi_2} \quad (14)$$

$$\tilde{H}(\vec{r}_1) = \sum_{n=-\infty}^{\infty} C_n^j J_n(k\sqrt{\epsilon}r_1) e^{in\varphi_1} \quad (15)$$

where  $(r_1, \varphi_1)$  are the local coordinates of the point inside the dielectric rod

while  $(r_2, \varphi_2)$  are the coordinates of the point at M. In order to find unknown coefficients  $\mu_n^j, C_n^j$ , conditions (7), (8) should be used. It gives the following integral equations

$$\frac{\partial}{\partial n} \int_M \mu(\vec{r}_2) \frac{\partial}{\partial n'} G(\vec{r}_1, \vec{r}_2) d\vec{r}_2' = -\frac{\partial}{\partial n} (k^2 (e_1 - e) \iint_D \bar{H}(\vec{r}_1') G(\vec{r}_1, \vec{r}_1') ds' + H^0(\vec{r})), \vec{r} \in \partial M \quad (16)$$

$$H(\vec{r}) = H^0(\vec{r}) + k^2 (e_1 - e) \iint_D \bar{H}(\vec{r}_1) G(\vec{r}, \vec{r}_1) ds' - \int_M \mu(\vec{r}_2) \frac{\partial}{\partial n'} G(\vec{r}, \vec{r}_2) d\vec{r}_2, \vec{r} \in \partial D \quad (17)$$

The treatment in (16), (17) calls for the representation of all functions in local coordinate systems connected with the scatterers that is done by applying the cylindrical functions theorem on summation. Following [1], the solution of (16) is derived by using Riemann-Hilbert Problem approach. As for (17), substituting (15) into (17) and performing all the necessary integrations [2], we obtain the system of linear algebraic equation (SLAE) for  $C_n^j$ . Omitting the details, the final result for calculation of  $\mu_n^j$  and  $C_n^j$  is given in terms of two coupled Fredholm SLAE

$$\mu_n^j = \sum_{m=-\infty}^{\infty} A_{nm} \mu_m^j + \sum_{m=-\infty}^{\infty} P_{nm} C_m^j + B_n^{(1)} \quad (18)$$

$$C_n^j = \sum_{m=-\infty}^{\infty} K_{nm} C_m^j + \sum_{m=-\infty}^{\infty} Q_{nm} \mu_m^j + B_n^{(2)} \quad (19)$$

where matrices  $A_{nm}$  and  $K_{nm}$  describe the scattering by single unclosed screen and dielectric rod, respectively, while  $P_{nm}$  and  $Q_{nm}$  correspond to the interaction between them.

#### CONCLUSION

The initial boundary-value problem is reduced to the solution of coupled Fredholm SLAE of 2<sup>nd</sup> kind type which is solvable with any described accuracy. It allows us to construct effective numerical algorithm for the calculation of mode conversion coefficients and field of radiation in the structure being considered.

#### REFERENCES

- (1) A.I.Nosich and A.S.Andrenko: "Scattering and Mode Conversion by a Screen-Like Inhomogeneity Inside a Dielectric Slab Waveguide," IEEE Trans. MTT, (1994) vol.MTT-42, 2, pp.298-307.
- (2) R.Mittra, ed.: "Computer Techniques for Electromagnetics," Pergamon, New York, 1973.
- (3) N.K.Uzunoglu and J.G.Fikioris: "Scattering from an Inhomogeneity Inside a Dielectric-Slab Waveguide," JOSA, (1982) vol.72, 5, pp.628-637.



# **SOLUTION OF THE PROBLEM OF DETERMINATIONS OF AMPLITUDE-PHASE DISTRIBUTIONS IN PHASED ARRAYS APERTURE**

O. D. Anohina, G. S. Antonov, V. A. Usin, V. A. Gubar

Kharkov Military University  
6 Svoboda Sq., Kharkov, p. o. 310006, Ukraine  
(Phone: 0572+40-41-41+2-85)

## **ABSTRACT**

The present paper gives a short characteristics of the method of determinations of amplitude-phase distributions in phased arrays aperture by means measurements of amplitude of dynamic near-field.

## **INTRODUCTION**

To determine the phased arrays characteristics by means near-field method need to know amplitude and phase distributions of near-field. For separate situations the phase measurements are rather difficult and therefore informations of phase of signals may be absent. But this informations need to treated the results of measurements and to determine antenna characteristics.

Therefore the problem determined of amplitude-phase distributions in phased arrays aperture by means amplitude measurements is highly actual.

## **DETERMINATIONS OF AMPLITUDE-PHASE DISTRIBUTIONS IN PHASED ARRAYS APERTURE**

At present the methods of near field antenna characteristics measurements and controle /1/ based on near field antenna amplitude and phase measurements and sequential recaloulation of the measurement results for far field zone (control of antenna radiation characteristics) or directly in antenna aperture (amplitude and phase distribution (APD) controle) are developed intensively.

Effective methods of APD determination in phase antenna array

(PAA) aperture require a usage of aprior information about antenna structure.

If the investigated PAA contains  $N$  radiator elements then the field excited by an antenna in a point  $\vec{r}$  is equal

$$\vec{E}_v(\vec{r}) = \sum_{i=0}^{N-1} \vec{E}_i(\vec{r}_i, \vec{\rho}_i, V), \quad (1)$$

$\vec{\rho}_i$  here is a radius-vector of  $i$ -th antenna element location,  $\{V\}$  is a fixed state of antenna elements determining APD in the array.

To find APD in the antenna array elements it is necessary to have the corresponding equation system obtained as a result of measurements of values  $\vec{E}_v$ . APD in the antenna can be found by two fundamentally different ways. The first one is connected with probe movement on a scan surface. In this case the field  $\vec{E}_v$  is measured in  $N$  different points  $\vec{r}_i$  (if the antenna contain phase shifter then it is necessary to carry out the measurement under different phasing a number of phasing must be equal a number of phase shifter states). The second way is to change the state of the antenna elements (phase shifter) under the stationary measurement probe (constant  $\vec{r}$ ) and measuring field sum  $\vec{E}_v$ . In fact, these two ways of APD obtaining in antenna elements differ only by method of formation of equation system for unknown APD. The mentioned methods require carrying out phase measurements whose realization in millimeter wave range is difficult. So why it is interesting to develop methods of APD determination based on carrying out only amplitude field measurements in near field zone. The possibility of APD determination by an amplitude measurements is based on increasing the volume of measurement information at the cost of that the field amplitude  $\vec{E}_v$  is measured not on one but on several surfaces (under the scan probe) or a signal on output of two or more stationary probes are measured.

In general case the problem of APD reconstruction by measurements of antenna radiation field in some region goes to solving an operator equation as following

$$\vec{y} = C\vec{\alpha}, \quad (2)$$

$\vec{\alpha}$  here is an element of  $A$  APD functional space;  $\vec{y}$  - is an element of functional space  $Y$  of measured field distribution;  $C$  - is an operator acting from  $A$  to  $Y$ .

Depending on type of solving problem and form of initial dataset the operator  $C$  has different structures. The simplest (from the calculation point of view) is a situation when the equation (2) connects APD in the aperture and far field of the antenna. In this case the operator  $C$  is linear and represents Fourier transformation. Correspondingly, APD can be found by reverse Fourier transformation.

More difficult is the case of amplitude measurements in near field zone when the equation (2) became nonlinear. In this paper one considers the algorithms of measurement result processing under near field measuring by mobile and stationary probes, discusses the possibility of reducing of processing time at the cost of choice of definite experiment plan and considers of using of only one stationary measuring probe.

For solution of equations of measurements applied the iteration method solution of the problem and uses "rapid" algorithm of the transform information. The method, offered author, possessing high speed of the convergence and converge to precise solution in tenth step of iterations. With availability of the measurements error the offered measurements method allowing with confidence of the amplitude and phase distributions in phased array aperture. That correctly and for case, when are on phased arrays the elements with error. Carried out numerical modelling tells about the proposed method of APD determination in PAA by amplitude measurements.

#### REFERENCE

- (1) Bahrah L. D., Kremenetski S. D., Kurochkin A. P. and other. Measurements methods of the radiating systems parameters in the near zone. Leningrad, Nauka, 1985.

# HIGH-FREQUENCY ASYMPTHOTAL METHOD TO SOLVE THE PROBLEM OF CIRCULAR CONDUCTING CYLINDER'S EXCITATION IF COVERED WITH THE THIN DIELECTRIC LAYER OF VARIABLE THICKNESS.

V.F. Apelt'cin

Lab. of Computational Electrodynamics, dep. of VMK, Moscow University,  
Lenin Hills, Moscow, Russia.

## ABSTRACT

The non complete projection method of Galiorkin's type is applied to the problem of perfectly conducting circular cylinder of radius  $a$  ( $ka \gg 1$ ) excitation if covered with a thin dielectric layer of variable thickness  $\delta(\psi)$  ( $k\delta(\psi) < 1$ ). The projection method uses as the basis the singular eigen-solutions of the radial co-ordinate  $r$  for two-dimension Helmholtz equation subjected to the Dirichlet boundary condition on the cylinder's surface  $r = a$  (the solutions of Sommerfeld type). The solutions to the ordinary differential equation's system - the unknown functions of the angular co-ordinate  $\psi$  are constructed approximately by the WKB approach on the segment  $]-\infty, +\infty[$  and satisfy the conditions of decay if  $|\psi| \rightarrow \infty$ .

## INTRODUCTION

The projection methods of Galiorkin's type if applied to the wave's diffraction problems are the generalisations to the separation of variable's method and permit to overcome the difficulties if the obstacle's boundary is noncoordinate and the separation of variable's method is not applicable. But the traditional types of Galiorkin's method using the bases of angular eigen-solutions of the Helmholtz equation ( $\exp(in\psi)$  - in two dimensions) inherit from the separation of variable's method the slow convergence of its expansions in case of high frequency:  $\max \rho(\psi) \gg \lambda$ , where  $r = \rho(\psi)$  - the scatterer's surface equation,  $\lambda$  - the wave length. The single method which permits to correct this lack is the Sommerfeld's method to solve the perfectly conducting sphere's excitation problem [1] using the singular eigen-solutions of the radial co-ordinate to the Helmholtz equation. But this method can't be applied to any other form of the obstacle's boundary. The goal of this work is to generalise the Sommerfeld's approach for the cases of non-co-ordinate boundaries of the obstacles in high-frequency case on using the projection approach to construct the solutions.

A circular perfectly conducting cylinder of radius  $a$  is excited by the field of a point source located in the point  $(r_0, \varphi_0)$ . The cylinder is covered with the layer of homogeneous dielectric the external boundary of which can be described as  $r = \rho(\psi)$ . The thickness of the layer

$(\psi) = \rho(\psi) - a$  is such one that  $\delta = \max \delta(\psi) < \lambda$ ; ( $k\delta < 1$ ), but  $ka \gg 1$ . We regard the case of E-polarization when the field is described by the wave equation

$$\Delta_{r,\psi} u(r, \psi) + k^2(r, \psi)u(r, \psi) = \frac{1}{r} \delta(r - r_0) \delta(\psi - \psi_0) \quad (1)$$

$$\text{for } r > a, \text{ where } k^2(r, \psi) = \begin{cases} k_0^2 = \epsilon_0 \omega^2; & r > \max \rho(\psi) \\ \epsilon \omega^2; & a < r \leq \rho(\psi) \end{cases}$$

$\epsilon = \epsilon_0 + \epsilon_1 = \text{const}$ , due to the usual boundary conditions on the cylinder's surface and on the boundary of the dielectric layer:

$$u(a, \psi) = 0; \quad [u]_{r=\rho(\psi)} = 0 \quad (2)$$

For  $r \rightarrow \infty$  we put usual Sommerfeld's limit conditions

$$\left( \frac{\partial u}{\partial r} - iku \right)_{r \rightarrow \infty} = O(r^{-\frac{1}{2}}).$$

Let's regard the dispersion equation

$$H_\nu^{(1)}(k_0 a) = 0 \quad (3)$$

where  $\nu = \{\nu_k\}$ ;  $k \in \mathbb{Z}$  - are the complex roots of the eq. (3):

$$\nu_k \approx k_0 a + \frac{(k_0 a)^{1/3}}{2} \left( \frac{3\pi}{4} \right)^{2/3} (4k-1)^{2/3} e^{i\pi/3} \quad [2] \quad (\text{the trigonometric approximation}).$$

The functions  $\varphi_\nu(r) = C_\nu H_\nu^{(1)}(k_0 r)$  we'll use as the basical system on constructing the approximate solution to the problem (1), (2). Here the  $C_\nu$  is the normalising coefficient.

**Statement 1** The system of functions  $\{\varphi_\nu(r)\}$  is the orthogonal system with the weight  $r^{-1}$  over the segment  $]a, \infty[$ :

$$\int_a^\infty \frac{\varphi_\nu \varphi_\mu}{r} dr = \langle \varphi_\nu, \varphi_\mu \rangle = 0 \text{ if } \nu \neq \mu.$$

The limit  $\nu \rightarrow \mu$  gives the normalising coefficient  $C_\nu^2 = \frac{\pi \nu H_\nu^{(2)}(k_0 a)}{2i \partial_\nu H_\nu^{(1)}(k_0 a)}$ .

We look for the approximate solution of the problem in the region  $a < r < \infty$ ;  $-\infty < \psi < \infty$  as the expansion

$$\tilde{u}(r, \psi) = \sum_\nu A_\nu(\psi) \varphi_\nu(r) \quad (4)$$

satisfying the conditions of decay if  $|\psi| \rightarrow \infty$ . Note that such a choice of the solution's form as (4) ensures the boundary condition's satisfaction. The validity of the representation (4) is based on the following statement

**Statement 2** If the roots of the dispersion equation (2) are simple (that is  $\partial_\nu H_\nu^{(1)}(k_0 a) \neq 0$ ), - then  $\sum_\nu \varphi_\nu(r) \varphi_\nu(r_0) = \frac{1}{r} \delta(r - r_0)$ .

The proof of the statement 2 follows the general scheme of the Watson's transformation [2] for the evident solution in case of a circular cylinder. As the solution (4) is obviously not periodical with respect to the angle  $\psi$  the solution of initial problem (1), (2) is constructed as follows:

$$u(r, \psi) = \sum_{n=-\infty}^{\infty} \tilde{u}(r, \psi + 2\pi n)$$

like the perfectly conducting circular cylinder's case without a layer [3].

On applying to the problem (1), (2) the usual Galiorkin's scheme on the segment  $r \in ]a, \infty[$  with respect to the basical system  $\{\varphi_\nu(r)\}$

$$\langle L\tilde{u}(r, \psi), \varphi_\mu(r) \rangle = \langle f, \varphi_\mu(r) \rangle$$

we obtain the ordinary differential equation's system of the following kind for the unknown functions  $A_\nu(\psi)$

$$A''_\mu(\psi) + [\mu^2 + Q_{\mu\mu}(\psi)] A_\mu(\psi) + \sum_{\nu \neq \mu} Q_{\mu\nu}(\psi) A_\nu(\psi) = \varphi_\mu(r_0) \delta(\psi - \psi_0) \quad (5)$$

where

$$Q_{\mu\nu}(\psi) = \omega^2 (\varepsilon - \varepsilon_0) C_\nu C_\mu \int_a^{\rho(\psi)} r H_\mu^{(1)}(k_0 r) H_\nu^{(1)}(k_0 r) dr.$$

The diagonal part  $\frac{d^2}{d\psi^2} + \{\mu^2 + Q_{\mu\mu}(\psi)\}$  of the differential operator of the system (5) may be inverted approximately by the WKB method [4] and we obtain the system of the following integral equations

$$A_\mu(\psi) + \int_{-\infty}^{\infty} G_\mu^{WKB}(\psi, \xi) \sum_{\nu \neq \mu} Q_{\mu\nu}(\xi) A_\nu(\xi) d\xi = \varphi_\mu(r_0) G_\mu^{WKB}(\psi, \psi_0) \quad (6)$$

Here  $G_\mu^{WKB}(\psi, \xi)$  is the WKB - approximation of the Green-function to the diagonal part of the differential equation's system satisfying the conditions of decay when  $|\psi| \rightarrow \infty$ . If we neglect the terms of the order  $O\left(\frac{(k\delta)^2}{ka}\right)$  in the WKB expansion, the corresponding approximation of the Green-function is the following

$$G_\mu^{WKB}(\psi, \xi) = \left[ 2i\mu + \frac{g(\xi)}{i\mu} \right]^{-1} \exp \left\{ i\mu |\psi - \xi| + \frac{\text{sgn}(\psi - \xi)}{2i\mu} \int_\xi^\psi g(t) dt + \frac{g(\psi) - g(\xi)}{4\mu^2} \right\} \quad (7)$$

where  $g(t) = \omega^2(\varepsilon - \varepsilon_0)[\rho^2(\psi) - a^2]$ . On calculating the representation (7) we take into account the approximation of the thin layer:  $H_\mu^{(1)}(k_0\rho(\psi)) \approx k_0\delta(\psi) \dot{H}_\mu^{(1)}(k_0a)$ , and also  $\mu - ka$ . It's obvious that

$$A_\mu(\psi) = \varphi_\mu(r_0) G_\mu^{WKB}(\psi, \psi_0)$$

is the initial approximation to the equation (6) and that the following terms of iterative procedure will have the values of the next orders with regard to the powers of  $\mu^{-1}$ . On restricting the consideration with the initial approximation we obtain the approximate non-periodical solution  $\tilde{u}(r, \psi)$  as

$$\tilde{u}(r, \psi) = \sum_\mu C_\mu^2 H_\mu^{(1)}(k_0r) H_\mu^{(1)}(k_0r_0) G_\mu^{WKB}(\psi, \psi_0),$$

and the approximate periodical solution of the problem (1) - (2) as

$$u(r, \psi) = \sum_\mu C_\mu^2 H_\mu^{(1)}(k_0r) H_\mu^{(1)}(k_0r_0) \sum_n G_\mu^{WKB}(\psi + 2\pi n, \psi_0) \quad (8)$$

On evaluating the second sum in (8) evidently we obtain

$$\sum_n G_\mu^{WKB}(\psi + 2\pi n, \psi_0) = \frac{\exp \frac{g(\psi) - g(\psi_0)}{4\mu^2} \cos \left\{ p_\mu(\psi - \psi_0) - \left( \left\lfloor \frac{|\psi - \psi_0|}{2\pi} \right\rfloor + \frac{1}{2} \right) W_\mu \right\}}{2\mu - \frac{g(\psi_0)}{\mu} \sin \frac{W_\mu}{2}};$$

$$\text{where } p_\mu(\psi - \psi_0) = \mu|\psi - \psi_0| - \frac{\text{sgn}(\psi - \psi_0)}{2\mu} \int_{\psi_0}^\psi g(t) dt; \quad W_\mu = 2\pi\mu - \frac{S}{2\mu}$$

and  $S = \int_0^{2\pi} g(t) dt$ . The most simple expression we have for the back scattering  $\psi = \psi_0$ :

$$u(r, \psi) = \sum_{\mu} \frac{1}{2\mu - \frac{g(\psi_0)}{\mu}} C_{\mu}^2 H_{\mu}^{(1)}(k_0 r) H_{\mu}^{(1)}(k_0 r_0) \operatorname{ctg} \frac{w_{\mu}}{2}.$$

#### REFERENCE

1. Sommerfeld A., Partielle Differentialgleichungen der Physik.- Leipzig, 1948.
2. Honl H., Maue A.W., Westpfahl K. Theorie der Beugung.- Springer-Verlag, 1961.
3. Babich V.M., Buldiren V.S. Asymptotical methods in the short wave diffraction problems.- Moscow, "Nauka", 1972.
4. Kamke E. Differentialgleichungen.- Leipzig, 1959.



# ON MODELING OF THE MICROWAVE SCATTERING AND ABSORPTION BY PLANT ELEMENTS

Ali Nadir ARSLAN

Department of Electrical and Electronics Engineering  
Çukurova University, 01330 Balcalı-Adana, TURKEY

## ABSTRACT

The simple case of scattering by a thin dielectric strip was examined. This problem was considered on the basis of the expansion of scattering operator into multiple scattering series. The calculations of inner field and the extinction cross section were conducted for certain dielectric constants and dimensions of strip corresponding to the parameters of vegetation elements. It has been shown that for values of  $kD|\epsilon - 1| \leq 0.5$ , where  $k$  is the wave number,  $D$  is the strip thickness, and  $\epsilon$  is the strip dielectric constant, the generalized Rayleigh-Gans approach can be successfully applied to calculate the extinction cross section of a dielectric strip. Radiation patterns of scattering by perfectly conducting strip and a thin dielectric strip was compared.

## INTRODUCTION

Development of reliable models for microwave emission and scattering from terrain, i.e., soil, vegetation, snow, forest, etc., is one of the important problems of microwave remote sensing. From theoretical point of view, this problem is of independent interest, because it concerns the studies about scattering by dielectric bodies of different shape and dimension, microwave propagation in random media, polarization properties of scattered waves, etc. On the other hand, the presence of reliable radiative models enables one to formulate the inverse problem of microwave remote sensing which is important for practical applications. Current investigations in microwave remote sensing field are mainly in the following directions: modeling of microwave emission and scattering from plant elements and vegetation as the whole, modeling of effective dielectric permittivity of natural media, modeling of microwave attenuation of forests. In this contribution, the grounds for the choice of the above mentioned models will be discussed and some results of modeling of microwave scattering and attenuation by plant elements are presented.

## MICROWAVE SCATTERING AND ABSORPTION BY PLANT ELEMENTS

The sizes of leaves and stalks in the microwave band are comparable with the wavelength, and, therefore, the scattering and absorption cross sections of plant elements must be calculated from diffraction models. Since the elements of plants are similar in shape to flat discs, strips (for example, leaves), and cylinders (for example, stalks), it is necessary to discuss the diffraction problem for bodies with the above shapes. The rigorous analytical solution of the diffraction problem for dielectric disc and strip is not yet known. In this case the cross sections can be found under some restrictive assumptions between the size of the element and the wavelength. The following models are most oftenly used: a. Small particles; b. Very large plane particles; c. Plane thin particles (the generalized Rayleigh-Gans approach). To establish the limits of applicability of these models a critical assesment of known solutions and further, development of theoretical approaches are required. We shall demonstrate this for a simple case and consider scattering by a thin dielectric strip.

## FORMULATION OF THE PROBLEM

In the case of E-polarization, the field at each point in space is given by the scattering operator

$$\mathbf{E}(x, y) = \mathbf{E}_i(x, y) + T\mathbf{E}(x', y') \quad (1)$$

$$TE(x', y') = \frac{ik^2(\epsilon - 1)}{4} \int_S E(x', y') H_0^{(1)}(k\sqrt{(x-x')^2 + (y-y')^2}) dx' dy' \quad (2)$$

$$E(x', y') = e^{-ik(x'\cos\vartheta + y'\sin\vartheta)} \quad (3)$$

where  $E_i(x, y)$  is the incident field,  $S$  is the cross section of the strip, and  $T$  is the integral scattering operator. Considering the point  $(x, y)$  as a point inside the strip the multiple scattering Born series (in mathematics this series is known as Neuman series) is obtained from (1)

$$E(x, y) = E_i(x, y) + TE_i(x', y') + TTE_i(x'', y'') + \dots \quad (4)$$

When there is a small parameter in the problem (for example, the strip thickness) it may be shown that series converges rapidly. In this case the accuracy of inner field estimation by some first terms of the series can be evaluated by considering the contribution of the next terms of the series. In the simple case of very thin strip, the inner field is considered to be equal to the incident field. This approximation is widely used in modeling of scattering by plant elements (the generalized Rayleigh-Gans approach [1,2]).

If we use well known integral representation of the Hankel function and substitute (3) in (1) and take integration over  $y'$  and  $x'$  respectively

$$E(x, y) = E_i(x, y) + \frac{ik^2(\epsilon - 1)}{2\pi} \int_{-\infty}^{\infty} \frac{\sin(ka(\cos\vartheta + \alpha))}{ka(\cos\vartheta + \alpha)} e^{-iky\cos\vartheta} f(\alpha, y) e^{ikx\alpha} \frac{d\alpha}{\sqrt{1-\alpha^2}} \quad (5)$$

where,

$$f(\alpha, y) = \frac{e^{-iky\sin\vartheta}}{ik(\alpha^2 - \cos^2\vartheta)} \{ 2\sqrt{1-\alpha^2} + (\sin\vartheta - \sqrt{1-\alpha^2})e^{ik(\sin\vartheta + \sqrt{1-\alpha^2})(d+y)} - (\sin\vartheta + \sqrt{1-\alpha^2})e^{-ik(\sin\vartheta - \sqrt{1-\alpha^2})(d-y)} \} \quad (6)$$

If we take into account,

$$\lim_{ka \rightarrow \infty} \frac{\sin(ka(\cos\vartheta + \alpha))}{(ka(\cos\vartheta + \alpha))} = \pi\delta(\cos\vartheta + \alpha) \quad (7)$$

When  $ka$  is changed from 5 to 30 that the accuracy of this approximation can be established in %10 and assume that  $kD \ll 1$ .

$$E(x, y) = E_i(x, y) + \frac{ik2d(\epsilon - 1)}{2} \frac{1}{\sin\vartheta} E_i(x, y), \quad \vartheta \neq n\pi, n = 0, 1, 2, \dots \quad (8)$$

### SOME NUMERICAL RESULTS

The absorption cross section of the dielectric strip is given by the expression [1,3]

$$\sigma_a = \frac{k \int_S |E|^2 \epsilon'' dx' dy'}{|E_i|^2} \quad (9)$$

When  $E(x', y') = E_i(x', y')$  is assumed

$$\sigma_a = k\epsilon'' S \quad (10)$$

is obtained which corresponds to the absorption length of a "Rayleigh" particle. Scattering cross section may be calculated with this approximation by the summation of scattering intensity.

$$\sigma_s = (kD)^2 |\epsilon - 1|^2 \frac{a}{2\pi ka} \int_0^{2\pi} \frac{\sin^2[ka(\cos\phi_0 - \cos\phi)]}{(\cos\phi_0 - \cos\phi)^2} d\phi \quad (11)$$

RELATIVE EXTINCTION CROSS SECTION,  $\sigma_e/\sigma_0$

EPS=20+J3, NORMAL INCIDENCE

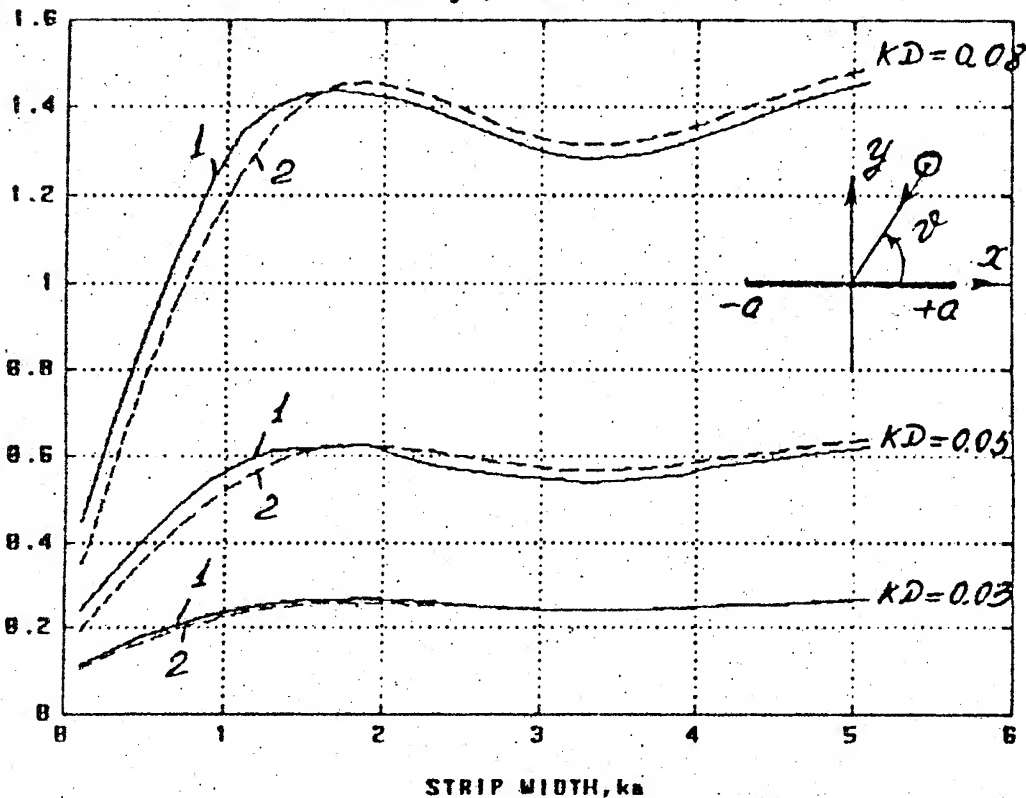


Fig. 1

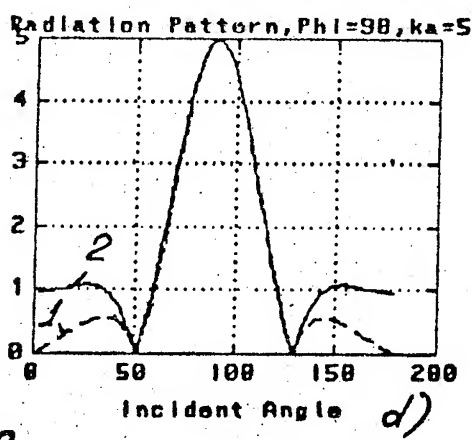
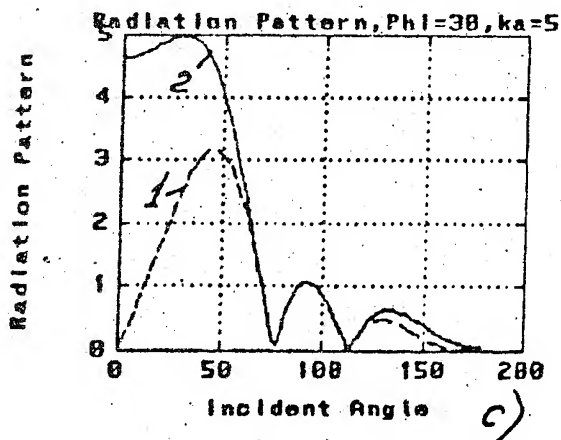
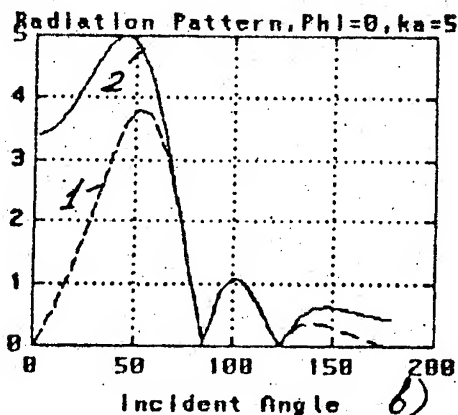
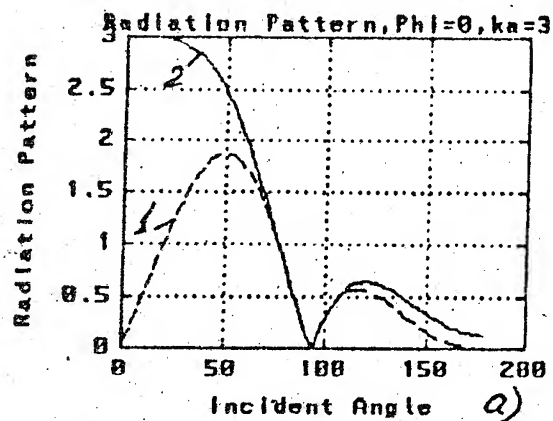


Fig. 2

where  $D$  is the thickness of the strip,  $2a$  is the width,  $k$  is the wave number,  $\epsilon$  is the dielectric permittivity, and  $\phi_0$  is the angle of incidence.

The extinction cross section is given by the expression[3],

$$\sigma_e = \sigma_a + \sigma_s \quad (12)$$

It is necessary to recall that in the above mentioned approach, the optical theorem (the law of energy conservation) is violated that may result in an error in the calculation of radiative parameters of a vegetation canopy modeled by the collection of strips. The accuracy of this approximation may be established by taking into account three terms of the series. Some results of the calculation of the relative extinction cross section ( $\frac{\sigma_e}{2a}$ ) are presented in Fig.1. It is seen that the zero order approximation may be used for values of  $kD |\epsilon - 1| \leq 0.5$ . Some results of the comparing radiation patterns of scattering by perfectly conducting strip and a thin dielectric strip for different values of  $ka$  are presented in Fig.2. It is seen that radiation patterns are same at a range of incident angle, but there is a certain difference out of the range.

### CONCLUSIONS

The results obtained are in a good agreement with the results provided by known methods; moreover, the accuracy of the solution obtained here can be estimated. Particularly, the limits of the applicability of the so-called generalized Rayleigh-Gans approach are established. The results obtained are also in a good agreement with the experimental data[1].

### REFERENCES

- 1.A.A.Chuklantsev, "Scattering and absorption of microwave radiation by elements of plants," Radiotekh.Elekt., vol.31, pp.1095-1104, 1986.
- 2.H.J.Eom, and A.K.Fung, "A scatter model for vegetation up to Ku-band," Remote Sensing Environ., vol.14, pp.185-200, 1984.
- 3.F.T.Ulaby, R.K.Moore, A.K.Fung, "Microwave remote sensing, active and passive" Volume I, Microwave Remote Sensing Fundamentals and Radiometry, 1981.

### ACKNOWLEDGMENT

The author is indebted to the Dr.A.A.Chuklantsev for his friendly help and useful discussions.

### FIGURE CAPTIONS

Fig.1.Spectral dependence of relative extinction cross section for strip-like plant element. 1-the Rayleigh-Gans approximation, 2-the current method with the second terms of the series taken into account.

Fig.2.Radiation patterns of scattering by perfectly conducting strip and a thin dielectric strip. (a)- $ka=3$  and observation angle  $\phi = 0$ , (b)- $ka=5$  and observation angle  $\phi = 0$ , (c)- $ka=5$  and observation angle  $\phi = 30$ , (d)- $ka=5$  and observation angle  $\phi = 90$ . 1-the perfectly conducting, 2-the thin dielectric strip.

# THE METHOD OF THE PROPER FUNCTIONS OF THE SINGULAR OPERATORS IN THE THEORY OF ANTENNAS.

Artemiev V.V., Eminov S.I.

The Novgorod state university, Novgorod.

In this work the method of the proper functions of the singular operators is developed with reference to the problems of the theory of the antennas.

The method of the proper functions was broadly conformed to the problems of the diffraction of E-polarization on the curved-linear screen. It appears that this method can successfully conform to the equations of diffraction of H-polarization and the equations of dipole antennas [1,2]. The structure of these equations has the view:

$$\begin{aligned} (Au)(\tau) + \lambda (Ku)(\tau) + (Bu)(\tau) = \\ = \frac{1}{\pi} \frac{\partial}{\partial \tau} \int_{-1}^1 u(t) \frac{\partial}{\partial t} \ln \frac{1}{|\tau-t|} dt + \lambda \frac{1}{\pi} \int_{-1}^1 u(t) \ln \frac{1}{|\tau-t|} dt + \\ + \int_{-1}^1 u(t) B(\tau, t) dt = e(\tau), \end{aligned} \quad (1)$$

The operator  $A$  is unlimited, symmetrical, positive definite. The orthonormalized basis of the power space  $H_A$  of this operator has the view:

$$\varphi_n(\tau) = \sqrt{\frac{2}{\pi n}} \sin[n \arccos(\tau)], \quad n=1,2,\dots, \quad (2)$$

The equation (1) we'll solve in  $H_A$ . With basis (2) the equation (1) comes equivalently to the infinite system of Fredholm of second kind. The subsequent development of the method of the proper functions is in the analytical definition of matrix of operator  $K$  in the basis (2). With series of the tabular integrals we'll find

$$(K\varphi_m, \varphi_n) = \begin{cases} \frac{(-1)^{i+j} \sqrt{(2i-1)(2j-1)} \Gamma(i+j-2)}{2\Gamma(i-j+2)\Gamma(j-i+2)\Gamma(i+j+1)}, & m=2i-1, n=2j-1, i+j>1, \\ \frac{(-1)^{i+j} 2\sqrt{ij} \Gamma(i+j-1)}{\Gamma(i-j+2)\Gamma(j-i+2)\Gamma(i+j+2)}, & m=2i, n=2j. \end{cases} \quad (3)$$

The correlation (3) permits to know asymptotical behaviour of the coefficients of the expansion of the solution (1) on the basis

$$u(\tau) = \sum_{n=1}^{+\infty} C_n \varphi_n(\tau) \quad (4)$$

Theorem. If  $e(\tau)$  is the infinite differentiating function then for  $C_n$  it's true:

$$|C_n| \leq \frac{\text{const}}{n^k}, \quad n = 1, 2, 3, \dots,$$

where  $k$  is arbitrary whole number.

For solution of the equation (1) should in (4) keep  $N$  of terms and solve the algebraical system of order  $N \times N$ . The rate of the tallieing of the approximate solution to the precision

solution is the following:

$$|\tilde{C} - C| = \sqrt{\sum_i (\tilde{C}_i - C_i)^2} \leq \frac{\text{const}}{N^k}.$$

If antenna stimulates oneself with the concentrated sources then the  $e(r)$  is special, i.e. it's slowly tallieing series. In this case it needs the additional regularization. One of the methods of the regularizations is in the following: the quite continuons kernel is substituted on the appoximate, infinite matrix is substituted on the finite. And right part is given precisely.

#### Literature:

1. Fainov S.I.: Radio-engineering and electronic, 1993, vol. 38, N 12, p. 2160.
2. Fainov S.I./Letter in JTF, 1993, vol. 19, N. 10, p. 41.



THE MODAL BASIS METHOD AND ELECTROMAGNETIC WAVES IN  
RANDOM MEDIA

Babiy V.I., Nazirov Z.F., Yantsevich A.A.

We study the problem of finding the middle field in the randomly nonstationary mediums. Here we follow the method using the representation of the field as the series of expansion on selfadjoint part of the Maxwell's operator ([1]). These expansions have scalar time-varying coefficients which satisfy the systems of ordinary stochastic differential equations. In first approach the presence of small medium's fluctuations leads to recounting of mediums contents. It is convenient to receive the equations for modal coefficients from rotor's Maxwell's equations for  $D_z$  and  $H_z$  when dielectrical permittivity has the form  $\epsilon = \epsilon(z - \xi(t))$  where  $\xi(t)$  - Markov's process. We have found the general form of equations for middle values of the corresponding coefficients of the expansions and analysed the case with  $\xi(t)$  is simplistic diffusion of Markov's process.

[1] . Tretyakov O.A. The modal Basis Method. Radiotekhnika i elektronika, N 6, 1986, pp. 1071-1082 (in Russian).

# SCATTERING OF ELECTROMAGNETIC WAVES FROM AN ANISOTROPIC INCLUSION EMBEDDED IN THE GYROTROPIC HALFSPACE.

O.V. Bagatskaya, D.O. Batrakov, S.N. Shulga, N.P. Zhuck.

310077 UKRAINE, Kharkov 77, pl. Svobody 4.

Kharkov State University, Department of Radiophysics.

## ABSTRACT

A 2-D problem of a TM polarized wave scattering from an infinitely long anisotropic inhomogeneous cylinder of arbitrary cross-section buried in the anisotropic homogeneous layer is considered. The scattering problem is formulated as a pair of integro-differential equations with respect to the electric field components over the cross-section of a scatterer. These equations are solved via the moment method using pulse basis functions and delta functions as the testing ones. Sample numerical results related to electrically gyrotropic media are presented.

## INTRODUCTION AND PROBLEM STATEMENT.

The problem of electromagnetic wave scattering from anisotropic objects has been studied extensively in the past decades mainly in connection with the radar determination of rocket launching using radar returns from rocket fumes. This problem has now emerged as one of major importance due to the development of new materials to be used in microwave and optical applications. Efficient approaches to treat scattering from anisotropic bodies has been developed e. g. in the recent papers [1,2].

We are interested in the following situation (see Fig.1). The isotropic volume is (I) characterized by the scalars  $\epsilon=\mu=1$ .

The half-space (II) is filled with a non-magnetic material whose permittivity tensor  $\hat{\epsilon}$  is represented in the rectangular coordinate system  $x, y, z$  as a matrix

$$\hat{\epsilon} = \begin{bmatrix} \epsilon_{xx} & 0 & 0 \\ 0 & \epsilon_{yy} & \epsilon_{yz} \\ 0 & \epsilon_{zy} & \epsilon_{zz} \end{bmatrix} \quad (1)$$

Here  $\epsilon_{xx}, \dots, \epsilon_{zz}$  are some constants, maybe complex-valued. Let insert in such a medium an infinitely long dielectric cylinder of arbitrary cross-section which is oriented along the  $x$  axis. The permittivity tensor  $\hat{\epsilon}_c$  of a cylinder has the form of (1), with the non-zero components  $\epsilon_{c_{xx}}, \dots, \epsilon_{c_{zz}}$  being some piecewise-continuous functions of the variable  $\vec{r} = (0, y, z)$ . It is assumed that the initial electromagnetic field  $\vec{E}_0, \vec{H}_0$  maintained by the time-harmonic ( $e^{-i\omega t}$ ) sources when the scatterer is absent depends on the variable  $\vec{r}$  only and is independent of  $x$ . In this situation the electromagnetic field does not depend on  $x$  as well.

The invariance of the problem when the translations are performed along  $x$  and the specific structure of permittivity tensors in the adopted coordinate system  $x, y, z$  ensures that the field  $\vec{E}, \vec{H}$  splits to the two independent constituents comprising the components  $E_x, H_y, H_z$  and  $H_x, E_y, E_z$  respectively. It is more complicated problem for the TM-polarized constituent that we intend to consider below.

In the case where external sources are located outside the body a 2D scattering of a TM-polarized wave by an anisotropic inhomogeneous cylinder can be formulated as an integral relation

[3]:

$$\vec{E}(\vec{r}) = \vec{E}_0(\vec{r}) - \frac{1}{4\pi} \frac{\omega}{\pi} \int_S d\vec{r}' \hat{G}_{ee}(\vec{r}, \vec{r}') \hat{\eta}(\vec{r}') \vec{E}(\vec{r}'). \quad (2)$$

Here  $\hat{G}_{..}$  is the electric dyadic Green's function of Maxwell's equations in the y-z plane with the scatterer being removed, S is the cross-section of a cylinder in the aforementioned plane,  $\hat{\eta} = \hat{\epsilon}_c - \hat{\epsilon}$ . On projecting relation (2) onto the y, z axes one obtains the following integro-differential equations within S with respect to  $E_y, E_z$ :

$$E_y(\vec{r}) = -\frac{1}{i a_c(\vec{r}) k} [\epsilon_{cyz}(\vec{r}) \frac{\partial}{\partial y} + \epsilon_{czz}(\vec{r}) \frac{\partial}{\partial z}] [H_{ox} + ikF(\vec{r})], \quad (3)$$

$$E_z(\vec{r}) = \frac{1}{i a_c(\vec{r}) k} [\epsilon_{cyy}(\vec{r}) \frac{\partial}{\partial y} + \epsilon_{czy}(\vec{r}) \frac{\partial}{\partial z}] [H_{ox} + ikF(\vec{r})].$$

In these equations  $k = \omega/c$ , c is the speed of light in vacuum,

$$F(\vec{r}) = \int_S d\vec{r}' [E_y(\vec{r}') L_y(\vec{r}, \vec{r}') + E_z(\vec{r}') L_z(\vec{r}, \vec{r}')]; \quad (4)$$

$$aL_q(\vec{r}, \vec{r}') = [\epsilon_{zy} \epsilon_{cyq}(\vec{r}') - \epsilon_{yy} \epsilon_{czq}(\vec{r}')] \frac{\partial G(\vec{r}, \vec{r}')}{\partial y'} + \\ + [\epsilon_{zz} \eta_{yq}(\vec{r}') - \epsilon_{yz} \eta_{zq}(\vec{r}')] \frac{\partial G(\vec{r}, \vec{r}')}{\partial z'}, \quad (q=y, z); \quad (5)$$

$$a = \epsilon_{zz} \epsilon_{yy} - \epsilon_{zy} \epsilon_{yz}, \quad a_c(\vec{r}) = \epsilon_{czz}(\vec{r}) \epsilon_{cyy}(\vec{r}) - \epsilon_{czy}(\vec{r}) \epsilon_{cyz}(\vec{r}). \quad (6)$$

The quantities  $\eta_{p,q}$ , (p, q=y, z), are the components of tensor  $\hat{\eta}$  in the coordinate system x, y, z, G is the scalar Green's function for the ambient medium. It is defined as a solution to the wave equation with a point-like source:

$$[\epsilon_{zz} \frac{\partial^2}{\partial z^2} + \epsilon_{yy} \frac{\partial^2}{\partial y^2} + (\epsilon_{yz} + \epsilon_{zy}) \frac{\partial^2}{\partial z \partial y} - k^2 a] G(\vec{r}, \vec{r}') = a \delta(\vec{r} - \vec{r}'), \quad (7)$$

which satisfies remaining boundary condition and demonstrates an outgoing wave behaviour at infinity.

Once the electric field within the scatterer is known, the quantities  $E_y, E_z$  in the outer region can be determined according to (2) via explicit formulae:

$$E_y(\vec{r}) = E_{oy}(\vec{r}) - \frac{1}{\alpha} [\epsilon_{yz} \frac{\partial}{\partial y} + \epsilon_{zz} \frac{\partial}{\partial z}] F(\vec{r}), \quad (8)$$

$$E_z(\vec{r}) = E_{oz}(\vec{r}) + \frac{1}{\alpha} [\epsilon_{yy} \frac{\partial}{\partial y} + \epsilon_{zy} \frac{\partial}{\partial z}] F(\vec{r}).$$

In order to calculate  $H_x$  one can employ the following expression:

$$H_x(\vec{r}) = H_{ox}(\vec{r}) + ikF(\vec{r}). \quad (9)$$

As a next step, we present a useful expression for the scattered field  $\vec{E}_s = \vec{E} - \vec{E}_0$ ,  $\vec{H}_s = \vec{H} - \vec{H}_0$  in the far-field zone. With this purpose, we introduce in the y-z plane a polar coordinate system  $L, \theta$  (see Fig.1).

One of the parameters of major interest in the scattering problems is the scattering cross-section  $\sigma(\theta)$  which is introduced as follows:

$$\sigma(\theta) = L P_s / P_o, \quad (kL \gg 1). \quad (10)$$

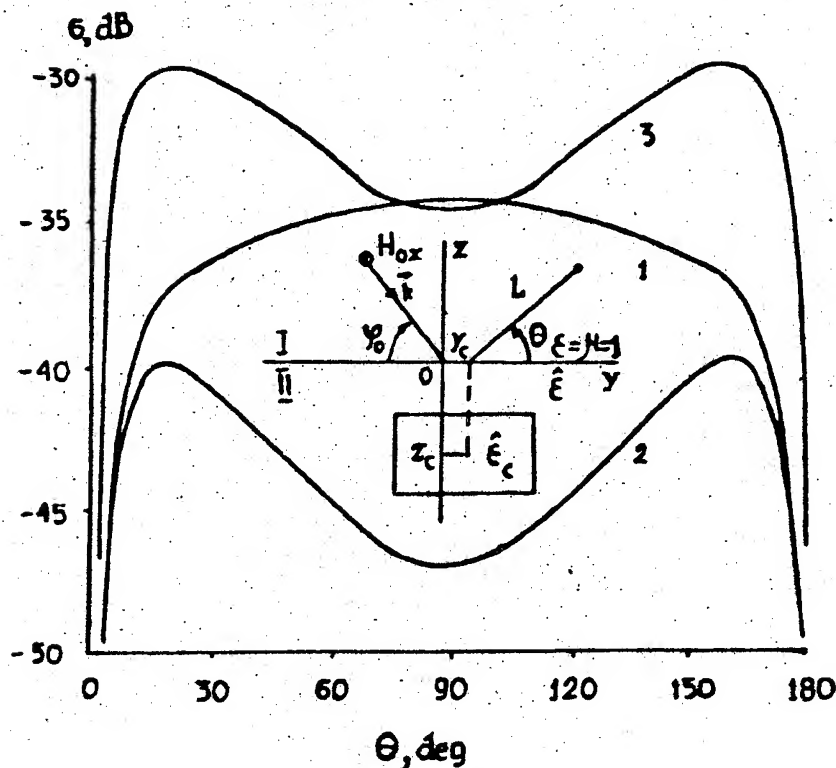
In this definition  $P_s$  and  $P_o$  are the values of the Poynting's vectors for the scattering field at an observation point  $(L, \theta)$  and for the initial field at the point  $\vec{r} = (0, y_o, 0)$ . Assume that the initial field is a TM-polarized plane wave which incidents from region (1) and propagates in the direction of the unit vector  $\vec{k}$ .

#### NUMERICAL SOLUTION AND ILLUSTRATIVE RESULTS.

The integro-differential equations (3) are solved numerically by the moments method [4]. Numerical computation have been performed to obtain  $\sigma(\theta)$  for the situation concerned with TM wave scattering from half-space region (II), which represents cold electron plasma. In this case  $\hat{\epsilon}$  and  $\hat{\epsilon}_c$  appear to be skew-symmetric. The ambient electrically gyrotropic medium is characterized by the parameters  $\epsilon_{yy} = \epsilon_{zz} = 1.1$ ,  $\epsilon_{yz} = -\epsilon_{zy} = i0.3$ . The

homogeneous scatterer has the rectangular cross-section with sides  $l$  and  $h$  and was centered at the point  $\vec{r}_c = (0, 0, z_c)$ ,  $k|z_c| = \pi$  (see Fig. 1.) The permittivity  $\hat{\epsilon}_c$  remains fixed throughout the computation and characterized by the components  $\epsilon_{czz} = \epsilon_{cyy} = 1$ ,  $\epsilon_{cyz} = -\epsilon_{czy} = i0.2$ . The initial field has the form of TM-polarized plane wave propagating in the negative  $z$ -direction. Three curves in Fig. 1 received for different scatterer cross-sections: 1- the rectangle is pulled along the  $y$ -direction ( $kl = 0.8\pi$ ,  $kh = 0.2\pi$ ); 2- the rectangle is pulled along the  $z$ -axis ( $kl = 0.2\pi$ ,  $kh = 0.8\pi$ ); 3- the scatterer has the quadratic cross-section ( $kl = kh = 0.8\pi$ ). This curves clearly show the influence of the shape of the scatterer to the scattering pattern.

Fig. 1. Geometry of the problem and angular distribution of the scattered field power.



#### REFERENCES.

1. R.D. Graglia and P.L.E. Uslenghi, "Electromagnetic scattering from anisotropic materials, Part 1: General Theory", IEEE Trans. Ant. & Propagat., vol. 32, pp.867-869, August 1984.
2. J.C. Monzon, "On a surface integral representation for homogeneous anisotropic regions: Two-dimensional case", IEEE Trans. Ant. & Propagat., vol.36, pp.1401-1406, Oct.1986.
3. A.J. Poggio and E.K. Miller, "Integral equation solution of three-dimensional scattering problems", in Computer Techniques for Electromagnetics, ed. R. Mittra. New York: Pergamon Press, 1973.
4. R.F. Harrington, Field Computation by Moment Methods. New York: MacMillan, 1986.



# TRANSFORMATION AND RADIATION OF SURFACE WAVE ON A BOUNDARY OF TIME-VARYING PLASMA

Michael Bakunov and Sergey Zhukov

University of Nizhny Novgorod  
Gagarin Ave. 23, Nizhny Novgorod, 603600, Russia

## ABSTRACT

Transformation of surface electromagnetic wave, supported by a boundary of plasma half-space, under instantaneous growth of plasma density in time is considered. It is shown that initial wave splits into two new surface waves propagating in the opposite directions and into transient bulk radiation. The frequencies of created surface and bulk modes as well as angular distribution of bulk radiation is investigated.

## INTRODUCTION

The theory of electromagnetic waves propagation in a time-varying, via ionizing processes, plasma was developed by many authors mainly with respect to the technical problem of tunable frequency up-shifting. The results were obtained both for the simultaneous ionization ("flash ionization") of the whole space [1], halfspace [2], slab [3] and for the moving ionization fronts [4]. However, the previous works in this area were concentrated exclusively on the transformation of the bulk (plane homogeneous) waves.

We extend here the theory to the transformation of surface waves in a non-stationary plasma structures. In theoretical aspects the problem is more rich comparing to the case of bulk waves transformation because the initial surface wave is converted not only into new waves of the same (surface) type but also into transient bulk radiation. As for practical application we believe that surface waves are very attractive to be used in devices with time-varying (solid-state or gaseous) plasmas due to their localization near the boundary and to their slowness.

Here we restrict our consideration of surface waves transformation to the important case of the instantaneous growth of plasma density of a half-space in a time. It plays the role of the basis (the "reference" case) for considering more complicated problems in this area.

## FORMULATION OF THE PROBLEM

Let cold collisionless plasma of plasma frequency  $\omega_{p1}$  occupies the half-space  $y < 0$  and bounds at  $y = 0$  with vacuum  $y > 0$ . A surface wave with magnetic field given by [5,6]

$$\vec{B}(x,y,t) = \vec{z}_0 B_0 \exp \left[ i\omega_0 t - ih_0 x - |y| \sqrt{h_0^2 - \frac{\omega_0^2}{c^2} \epsilon_1(y)} \right], \quad (1)$$

where

$$\epsilon_1(y) = \begin{cases} 1 & , y > 0 \\ \epsilon_1 = \epsilon_l \left( 1 - \frac{\omega_{p1}^2}{\omega^2} \right) & , y < 0 \end{cases} \quad (2)$$

$\epsilon_l$  - dielectric permittivity of the crystal lattice in the case of the solid-state plasma ( $\epsilon_l=1$  for the gaseous plasmas) and

$$h_0 = \frac{\omega_0}{c} \sqrt{\frac{\epsilon_1}{1 + \epsilon_1}}, \quad (3)$$

is travelling along the boundary  $y=0$  in the  $x$  direction when, at time  $t=0$ , the plasma density suddenly increases so that the plasma frequency changes from  $\omega_{p1}$  to  $\omega_{p2}$ . It causes transformation of initial wave (1) into new surface waves and into transient bulk radiation.

#### NEW SURFACE WAVES

The frequencies of created surface waves of the form  $\sim \exp(i\omega t - ihx)$  may be derived from treating dispersive equation for surface waves on a plasma-vacuum boundary [5,6]

$$\pm h = \frac{\omega}{c} \sqrt{\frac{\epsilon_2}{1 + \epsilon_2}}, \quad \epsilon_2 = \epsilon_l \left( 1 - \frac{\omega_{p2}^2}{\omega^2} \right) \quad (4)$$

together with the kinematic condition  $h=h_0$ , and are given by

$$\omega_{\pm} = \pm \frac{\omega_{p2}}{\sqrt{2}} \sqrt{1 + \frac{c^2 h_0^2}{\omega_s^2} - \sqrt{\left( 1 + \frac{c^2 h_0^2}{\omega_s^2} \right)^2 - 4 \frac{c^2 h_0^2}{\omega_{p2}^2}}} \quad (5)$$

where

$$\omega_s^2 = \omega_{p2}^2 \frac{\epsilon_l}{\epsilon_l + 1} \quad (6)$$

(see Fig.1).

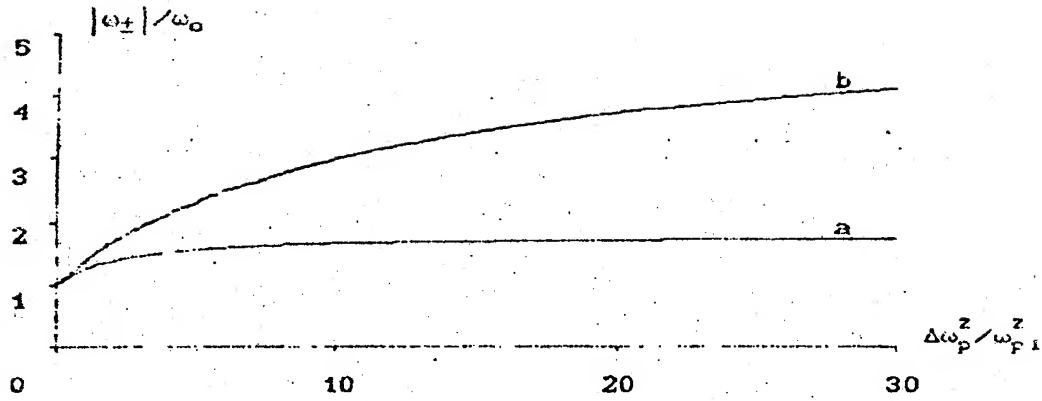


Fig.1. Frequencies absolute value of new surface waves as a function of plasma density jump ( $\Delta\omega_p^2 = \omega_{p2}^2 - \omega_{p1}^2$ ) for  $\epsilon_1=1$  and (a)  $\sqrt{2}\omega_0/\omega_{p1}=0,9$ , (b)  $\sqrt{2}\omega_0/\omega_{p1}=0,99$ .

Thus, the steady-state solution consists of two up-shifted ( $|\omega_{\pm}| > \omega_0$ ) surface waves. One of them, with frequency  $\omega_+ > 0$ , propagates in the same direction as the initial one and the other, with frequency  $\omega_- < 0$ , in the opposite direction.

Surface waves amplitudes obtained through the use of Laplace transforms are given by

$$B_{\pm} = E_0 \frac{\Delta\omega_p^2 \epsilon_2^2 \epsilon_1 (\omega_0 \sqrt{-(1+\epsilon_1)} - |\omega_{\pm}| \sqrt{-(1+\epsilon_2)})}{(\omega_0 - \omega_{\pm}) (\omega_0^2 \epsilon_1 - \omega_{\pm}^2 \epsilon_2) (1 - \epsilon_2) \sqrt{-(1+\epsilon_1)} (\epsilon_2^2 + \epsilon_1)} \quad (7)$$

The corresponding dependence of energy transformation coefficients  $W_{\pm}/W_0$  on the parameter  $\Delta\omega_p^2/\omega_{p1}^2$  is presented in Fig.2.

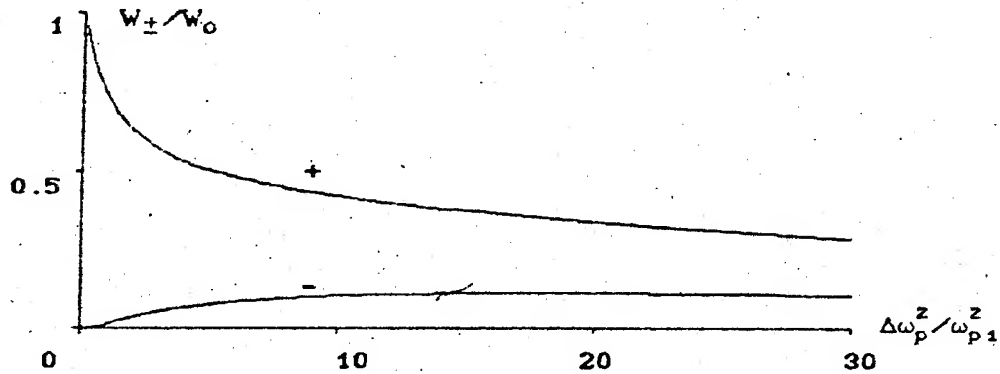


Fig.2. Energies of new surface waves vs plasma density jump for  $\sqrt{2}\omega_0/\omega_{p1}=0,99$ .

## TRANSIENT BULK RADIATION

Frequencies of bulk waves radiated into vacuum depend on the angle  $\theta$  between direction of wave propagation and the normal to a plasma surface according to the formula

$$\omega = \frac{c\omega_0}{\sin\theta} \quad (8)$$

where  $-\pi/2 < \theta < \pi/2$ .

The dependence of the portion of the whole energy  $W_r/W_0$  radiated both into vacuum and into plasma on the parameter  $\Delta\omega_p^2/\omega_{p1}^2$  is shown in Fig.3.

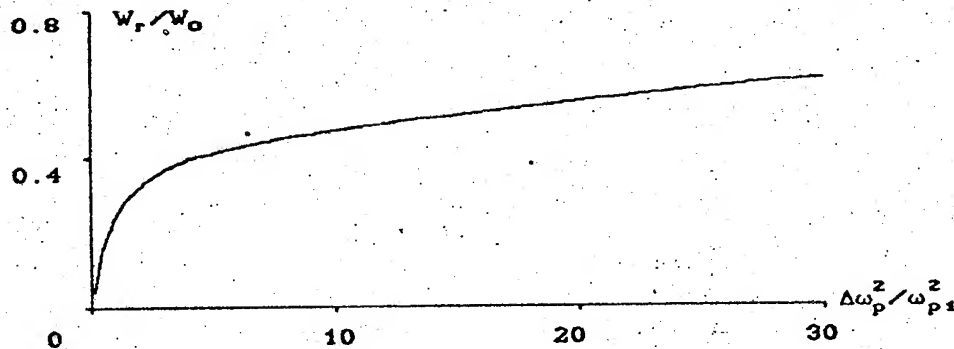


Fig. 3. Radiated energy as a function of plasma density jump for  $\sqrt{2}\omega_0/\omega_{p1}=0.99$ .

## REFERENCES

- (1) C.L.Jiang: "Wave propagation and dipole radiation in a suddenly created plasma", IEEE Trans. (1975), AP-23, 1, pp.83-90.
- (2) Kalluri D.K.: "On reflection from a suddenly created plasma half-space: transient solution", IEEE Trans. (1988), PS-16, 1, pp.11-16.
- (3) Kalluri D.K., Goteti V.R.: "Frequency shifting of electromagnetic radiation by sudden creation of a plasma slab", J.Appl.Phys. (1992), 72, 10, pp.4575-4580.
- (4) Wilks S.C. et al: "Frequency up-conversion of electromagnetic radiation with use of an overdense plasma", Phys.Rev.Lett. (1988), 61, 3, pp.337-340.
- (5) "Electromagnetic surface modes", edited by A.D.Boardman (Wiley, 1982).
- (6) "Surface polaritons", edited by D.I.Mills and V.M.Agranovich (North Holland, 1982).

Three-dimensional Inverse Problems of Geometric Optics  
in the Subsurface Radio Sounding.

V.A. Baranov, O. En Den, A.L. Karpenko, A.V. Popov  
Institute of Terrestrial Magnetism, Ionosphere and  
Radio Wave Propagation, Russian Academy of Sciences.  
IZMIRAN, 142092 Troitsk, Moscow region, Russia  
Fax: (095)3340908; Phone: (095)3340294

One of fast developing branches of radio location is sounding of objects and structures hidden under the earth surface, inside buildings or sometimes in living organisms [1,2]. Along with pure technical problems of constructing new transmitters, receivers and measuring equipment, a wide class of mathematical problems arises. They are concerned with interpretation of sounding data, determination of position, shape and material properties of the objects of interest. Despite of abundance of the developed methods, they often are inadequately complicated or, on the contrary, are based upon too simplified models of the horizontally stratified environment.

We discuss a wide class of essentially 3D inverse problems which can be solved exactly in the framework of geometric optics. The simplest problem is reconstruction of the shape of an ideally reflecting body embedded in a homogeneous or stratified medium from the measured travel times of the sounding pulse. The corresponding direct problem of ray tracing has a simple exact solution. Less trivial is the fact that the inverse problem also has a unified analytic solution provided the 2D travel time distribution over the earth surface is known. Here, we demonstrate an efficient numerical algorithm for the monostatic sounding problem.

Let a perfectly reflecting smooth surface  $z = h(\xi, \eta)$  be embedded into a stratified non-dispersive medium with dielectric permittivity  $\epsilon(z)$ . It is to be reconstructed using the data of monostatic radio sounding from the plane earth surface  $z = 0$ . We assume that the return signal at the transmitter/receiver point  $r_0 = (x_0, y_0)$  is formed by a monopulse specularly reflected from

a single point  $(\xi, \eta, h(\xi, \eta))$  of the reflecting surface. The measured travel time  $T = 2P/c$  is proportional to the group path  $P(x_0, y_0)$  being the function of the observation point  $(x_0, y_0)$ . As frequency dispersion is neglected ( $\partial \epsilon / \partial \omega \equiv 0$ ), it coincides with the optical path  $\psi = \int \sqrt{\epsilon} ds$  what greatly simplifies the following analysis.

It is obvious that, having performed observations at different points  $r_0$ , one gets a dual mapping of the reflecting boundary  $h(\xi, \eta)$  onto some surface  $P = \psi(x_0, y_0) > 0$  in the half-space  $(x, y, \psi)$ . Therefore, an inverse problem can be considered: to reconstruct the initial surface  $z = h(\xi, \eta)$  from measured values  $P = \psi(x_0, y_0)$ .

Within the framework of geometric optics, an exact solution of the corresponding direct problem has the following form:

$$x_0 = \xi + \sqrt{\epsilon(h)} n_x \tau, \quad y_0 = \eta + \sqrt{\epsilon(h)} n_y \tau$$

$$\tau = \int_0^{h(\xi, \eta)} \frac{dz}{\sqrt{\epsilon(z) - \epsilon(h)(n_x^2 + n_y^2)}} \quad (1)$$

$$\psi = \int_0^{h(\xi, \eta)} \frac{\epsilon(z) dz}{\sqrt{\epsilon(z) - \epsilon(h)(n_x^2 + n_y^2)}}$$

where  $n = (n_x, n_y, -\sqrt{1 - n_x^2 - n_y^2})$  is the unit normal vector to  $h(\xi, \eta)$  at the reflection point. The first three equations represent parametrically a ray in the stratified medium  $\epsilon(z)$  while the last equation gives its optical length [3].

The inverse problem can be solved via the same formulae (1) if one relates the normal components  $n_x, n_y$  with the measured values of  $\psi(x_0, y_0)$ . This relationship can be established by differentiating the last equation (1) with respect to  $\xi$  and  $\eta$ . It results in the following expressions

$$n_x = \frac{1}{\sqrt{\epsilon(h)}} \frac{\partial \psi}{\partial x}(x_0, y_0), \quad n_y = \frac{1}{\sqrt{\epsilon(h)}} \frac{\partial \psi}{\partial y}(x_0, y_0) \quad (2)$$

After substituting them into (1) the latter can be rearranged to the following form:

$$\xi = x_0 - \frac{\partial \psi}{\partial x}(x_0, y_0) \tau, \quad \eta = y_0 - \frac{\partial \psi}{\partial y}(x_0, y_0) \tau$$

$$\tau = \int_0^h \frac{dz}{\sqrt{\epsilon(z) - (\partial \psi / \partial x)^2 - (\partial \psi / \partial y)^2}} \quad (3)$$

$$\psi(x_0, y_0) = \int_0^h \frac{\epsilon(z) dz}{\sqrt{\epsilon(z) - (\partial \psi / \partial x)^2 - (\partial \psi / \partial y)^2}}$$

It can be easily seen that, for an arbitrary  $\epsilon(z)$ , these formulae give a parametric solution to the problem of reconstructing  $h(\xi, \eta)$ . In fact, given measured functions  $\psi$ ,  $\partial \psi / \partial x$ ,  $\partial \psi / \partial y$ , inversion of the last integral yields the reflection depth  $h$  as a function of the observation point  $(x_0, y_0)$ . Consequently, the ray parameter  $\tau$  and the coordinates  $(\xi, \eta)$  also can be calculated explicitly as functions of  $(x_0, y_0)$ .

In the particular case of a uniform medium  $\epsilon(z) = \epsilon_0 = \text{Const}$ , the solution (3) takes the simplest form:

$$\xi = x_0 - \frac{\psi}{\epsilon_0} \frac{\partial \psi}{\partial x}(x_0, y_0)$$

$$\eta = y_0 - \frac{\psi}{\epsilon_0} \frac{\partial \psi}{\partial y}(x_0, y_0) \quad (4)$$

$$h = \frac{\psi}{\epsilon_0} \sqrt{\epsilon_0 - (\partial \psi / \partial x)^2 - (\partial \psi / \partial y)^2}$$

Formulae (4) give an obvious generalization of the well-known results [4] concerning the 2D inverse problem (reconstruction of a cylindric surface  $h(\xi)$  from the measured group path  $P(x_0)$ ).

We demonstrate examples of numerical implementation of the above algorithm. We have simulated radio sounding of a given reflecting surface  $h(\xi, \eta)$  by calculating the group path  $\psi(x_0, y_0)$  and coordinates  $x_0(\xi, \eta)$ ,  $y_0(\xi, \eta)$  using formulae (1) over a rectangular grid in the  $(\xi, \eta)$  plane. As a result, we obtained travel time  $T = 2\psi/c$  as a function of the observation point  $(x_0, y_0)$ . The inverse problem was solved via the formulae (4). The derivatives  $\partial \psi / \partial x$ ,  $\partial \psi / \partial y$  have been calculated using finite



differences.

If the reflector is buried at a relatively small depth, the mapping  $h(\xi, \eta) \rightarrow \psi(x_0, y_0)$  is mutually unfold and the numerical solution reconstructs the given reflecting surface  $h(\xi, \eta)$  with small discrepancy due to a finite step between the observation points. For larger depths, caustics may occur and some modification of the algorithm is required [5].

More realistic models including rough boundaries characterized by certain scattering radiation patterns also can be considered. The radiation pattern, as well as the unknown dielectric permittivity profile of the host environment, can be determined from the data of the bistatic sounding.

#### REFERENCES

1. M.N.Finkelstein, V.A.Kutsev, V.P.Zolotarev. Application of Subsurface Radio Sounding to Engineering Geology (in Russian). Nedra, Moscow, 1986.
2. R.W.P.King, G.S.Smith. Antennas in Matter. The MIT Press, Cambridge, Massachusetts - London, 1981.
3. Yu.A.Kravtsov, Yu.I.Orlov. Geometric Optics of Inhomogeneous Media. Springer, Berlin - Heidelberg - New York, 1990.
4. C.H.Harrison. Reconstruction of Subglacial Relief from Radio Sounding Records. Geophysics, V.35, N 6, 1970, pp.1099-1115.
5. O.Weizman, V.Koltsov, A.Popov, S.Hoziosky. Reconstruction of Moving Reflecting Surface from Signal Lag Dynamics. Proc. of the Internat. Commsphere Symposium, 1991, Herzliya, Israel.

# THE INVERSE PROBLEM FOR A MULTILAYERED SLAB WITH CORRUGATED BOUND.

D. O. Batrakov, N. P. Zhuck.

310077 UKRAINE, Kharkov77, pl. Svobody 4,  
Kharkov State University, Dept. of Radiophysics.

## ABSTRACT

This report deals with the following electromagnetic inverse problem arising, for example, in geophysical exploration. We assume that the probed plane-layered slab of given thickness lies upon a uniform substrate. The upper halfspace from which sensing time harmonic plane wave is falling remain free. Permittivities of the substrate and the upper layer assumed to be known. The scattered field is then measured at a different frequencies or scattering angles. The problem is to find the unknown permittivity profile from these measurements. The proposed approach represents an extension and modification of the earlier proposed by the present authors iterative technique. The advantage of the present solution is that it permits due to the existence of the backscattered component to measure scattered field at only one observation point. So it allows to operate only with one antenna, situated, for example, at the airplane. The another novel idea is to formulate the problem via the intensity data registration. Then the nonlinear equation linking the informative parameter and the reconstructed quantity is inverted via the previously described Newton-Kantorovich iteration method and Tikhonov's regularization technique. Numerical results will be presented in graphical form to illustrate possibilities and prospects of the present method.

## INTRODUCTION AND PROBLEM STATEMENT

The previous research in the remote sensing has been focused on the direct scattering problems i.e. on finding the parameters of the scattered electromagnetic field under the assumption that the parameters of a medium as well as the statistical characteristics of the latter are known [1,2]. In some research areas such as radioceanography [1] and optics of light scattering [3] the efforts have been made to determine the parameters of a rough surface provided the properties of the underlying medium are given.

As it is well known, the internal structure of a medium bounded with a rough surface essentially affects the process of EM wave scattering [2]. This fact provides the physical basis for the inversion of physical characteristics of a  
n underlying medium by

using information concerning this medium which is contained in the non-coherent scattering data due to surface roughness. This is a completely new approach in the inverse scattering theory as compared with the existing inversion methods (see e.g. [4]) which have been developed for plane-layered media with a plane boundary and which utilize the (specular) coherent-wave reflection data.

We consider a plane-layered dielectric medium which consists of an inhomogeneous layer  $-b < z < 0$  and a uniform substrate  $-\infty < z < -b$  (see Fig.1). The outer boundary of a slab is covered with a statistical roughness determined by the equation  $z = z_{\Sigma}(r)$  where  $r = (x, y, 0)$ ,  $z_{\Sigma}$  is a random function with the zero mean value and the second statistical moment  $B(r-r') = \langle z_{\Sigma}(r) z_{\Sigma}(r') \rangle$ . The roughness is assumed to be slight [1]. A time-harmonic plane

wave polarized horizontally (p) or vertically (s) is obliquely incident from free space  $0 < z < +\infty$  upon the medium. Let  $\sigma_{p,s}$  designate the backscattering cross sections for the co-polarized constituents of non-coherent field at p,s polarizations respectively. It is assumed that the function  $B$  as well as the thickness  $b$  of a slab, the value  $\varepsilon(-0)$  of slab's permittivity at the unperturbed outer boundary and the permittivity of the substrate are known a priori. Suppose that a series of  $J = J_p + J_s$  experiments has been carried out, the  $j$ -th experiment being performed at a specific frequency and yielding the value  $u_j = \sigma_p$  for  $1 \leq j \leq J_p$  and  $u_j = \sigma_s$  for  $J_p < j \leq J_p + J_s$ , ( $j = 1, 2, \dots, J$ ). The task is to reconstruct the unknown permittivity distribution  $\varepsilon(z)$  within the slab from the non-coherent scattering data set  $u_j$ ,  $j = 1, \dots, J$ .

#### NUMERICAL SOLUTION AND SAMPLE RESULTS

For simplicity we limit ourselves to the case where the frequency dispersion of the constitutive parameters of all media involved can be ignored- at least in the frequency range employed. However we account for losses by allowing complex values for these constitutive parameters. Let us suppose that the medium within the slab whose permittivity distribution is unknown is replaced by an auxiliary medium with given permittivity distribution  $\varepsilon_a(z)$ , ( $-b < z < 0$ ), such that  $\varepsilon_a(-0) = \varepsilon(-0)$ . The outer boundary of the auxiliary medium is covered by the statistical roughness determined by the same random function  $z_\Sigma$  as for the probed medium. We calculated the BCS  $u, u_a$  for the probed and the auxiliary media within the framework of Born approximation [1,2]. Assume that  $\varepsilon_a$  differs

little from  $\epsilon$  so that the quantity  $\eta = \epsilon - \epsilon_a$  is small enough. On expanding  $u = \sigma_{p,s}$  in power of  $\eta$  and retaining two first terms one obtains the relation which links the difference  $u - u_a$  with  $\eta$ :

$$u - u_a = -ReL\eta \quad (1)$$

where  $L$  is some linear functional acting on  $z$  withing the interval  $-b < z < 0$  wich is determined by  $\epsilon_a$  and is independent of  $\epsilon$ . Then one can reconstruct  $\eta$  from the scattering data set  $u_j$  by employing an optimization approach where one minimizes the following cost functional:

$$F = \sum_{j=1}^J w_j |u_j - u_{j,a} + ReL_j \eta|^2 + \alpha \Omega(\eta). \quad (2)$$

Here  $w_j$  are the positive weighting coefficients,  $\alpha > 0$  is the regularization parameter,  $u_{j,a}$  and  $L_j$  are the quantities  $u$ ,  $L$  specified to the conditions of a  $j$ -th experiment,  $\Omega(\eta)$  is the quadratic smoothing functional. The minimization of  $F$  is performed analytically to yield an integral equation which easily lends itself to analytical solution. With  $\eta$  at hand, one arrives at the estimate  $\epsilon_{est} = \epsilon_a + \eta$  for the unknown function  $\epsilon$ . This estimate is employed in place of  $\epsilon_a$  and the preceding scheme is succescively repeated. This constitutes the Newton-Kantorovich iterative solution to the proposed inverse problem.

Sample results of profile reconstruction for measurements at  $p$  polarization are shown in Fig.2. Here the solid line depicts an actual permittivity profile, dashed with dots line - the initial guess, and the dotted line - reconstructed profile distribution respectively. It is assumed that the angle of incidence  $\psi$  takes  $J=40$  values disturbed equidistantly over the interval  $20^\circ \leq \psi \leq 80^\circ$ . The function  $B(r) = \sigma^2 \exp(-r^2/l^2)$  depicts the gaussian-correlated roughness with the rms height  $\sigma$  and correlation length  $l$ .

It is taken  $k_0 b = k_0 l = 0.92$ . From these results it is seen that the proposed inversion approach based on inverting the non-coherent scattering data provides quite feasible reconstruction of inhomogeneous permittivity profiles.

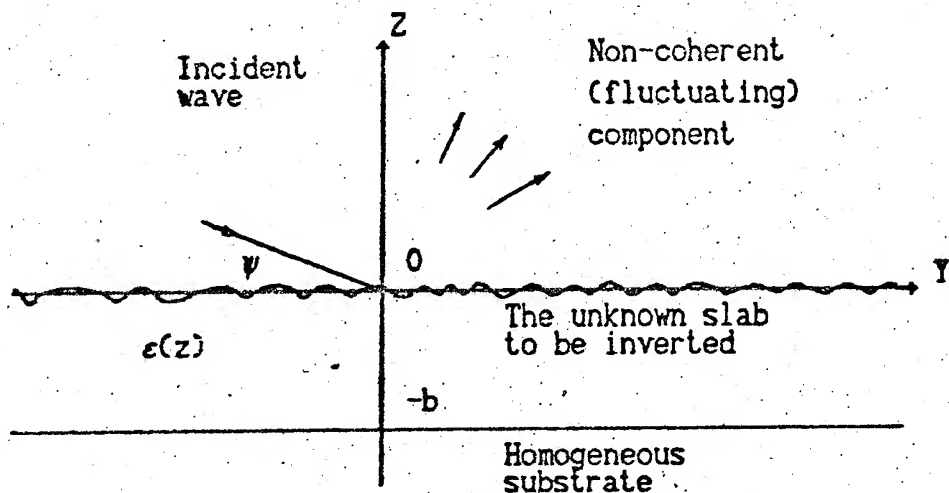


Fig.1 Two-dimensional sketch of the problem.

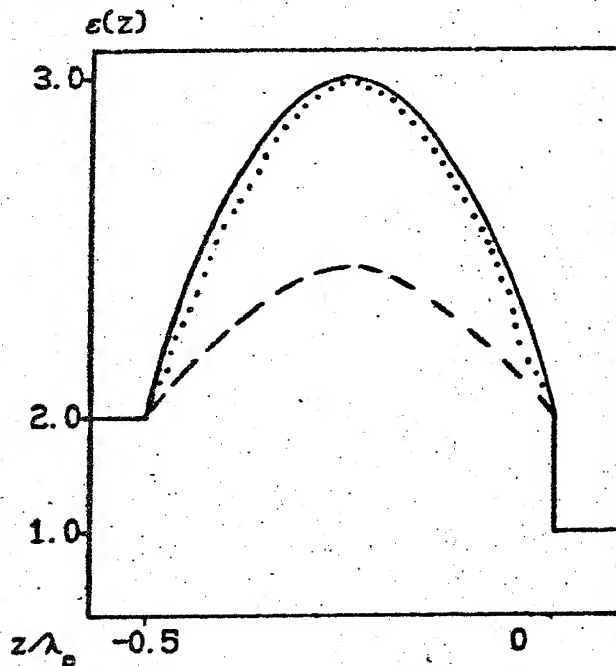


Fig.2 Example of profile reconstruction

#### REFERENCES

1. F.G.Bass and I.M.Fuks, Wave Scattering from Statistically Rough Surfaces, New York: Pergamon, 1979.
2. N.P.Zhuck, Theory of Waves in Statistically Inhomogeneous Media (in Russian), Dr Phys & Math Sci degree dissertation, Kharkov State University, Kharkov, 1990.
3. C.J.R.Sheppard, T.J.Connolly and M.Gu, "Imaging and reconstruction for rough surface scattering in the Kirchhoff approximation by confocal microscopy", J.Modern Optics, vol.40, No 12, pp.2407-2421, 1993.
4. T.Uno and S.Adachi, "Inverse scattering method for one-dimensional inhomogeneous layered media", IEEE Trans. Antennas Propagat., vol.35, No 12, pp.1455-1466, Dec.1987.

# DIELECTRIC SLAB EIGENMODE SCATTERING FROM A LOCAL CYLINDRICAL BOUNDARY DEFORMATION

Svetlana V. Boriskina and Alexander G. Yarovoy

Department of Radiophysics, Kharkov State University,  
Svobody Sq., 4, Kharkov, 310077, Ukraine

## ABSTRACT

The two-dimensional problem of dielectric slab eigenmode scattering from a penetrable body immersed into a stratified medium is solved by the numerical method based on the surface potentials approach. The original scattering problem is formulated in terms of a set of boundary integral equations. The layered geometry of the surrounding space is taken into account by using the Green's functions of the corresponding boundary problem. The Euler method is used to improve the convergence of Sommerfeld-type integrals which are contained in expressions for the Green's functions. Some illustrative numerical results are presented.

## INTRODUCTION

Discontinuity problems in open dielectric waveguides are essential to the design of various optical and millimeter-wave components, such as filters and grating couplers. They also play an important role in the simulation of splicing of two optical waveguides. The simplest model for these complicated discontinuities can be a dielectric cylinder immersed in a dielectric slab waveguide.

The scattering and mode conversion of the slab eigenmode from a circular cylinder outside the slab have been considered by an approximate method in [1] and rigorous method in [2]. Another rigorous method based on integral equations has been proposed in [3] for a symmetrical deformation of both boundaries of a slab. Modeling a splice of two dielectric waveguides has been performed in [4] by using the partial variational principle.

For consideration of an arbitrary local boundary deformation of an open waveguide we have proposed an approach based on the surface potentials method. By means of the single layer surface potential the original scattering problem is formulated in terms of a set of boundary integral equations. The stratified geometry of the host medium is taken into account in the kernels of the integral equations by using of the Green's functions of the corresponding boundary problem. The Euler transform is used to improve the convergence of Sommerfeld-type integrals which come into expressions for the Green's functions. Several numerical results, including scattering patterns, total scattered power and mode conversion coefficients have been calculated.

## PROBLEM FORMULATION AND SOLUTION

Consider a medium occupying the whole two-dimensional space which parameters can be described by

$$\epsilon(z) = \begin{cases} \epsilon_1, z > 0 \\ \epsilon_s, -d < z < 0, k(z) = k_0 \sqrt{\epsilon(z)} \\ \epsilon_3, z < -d \end{cases} \quad (1)$$



where  $\epsilon(z)$  and  $k(z)$  are the permittivity and the local wavenumber respectively,  $k_0$  is the free-space wavenumber and  $d$  is the thickness of the slab guiding region.

Consider a dielectric slab eigenmode scattering from a dielectric cylinder placed on the boundary between the slab and the upper halfspace. Cylinder cross-section  $S$  is bounded by an arbitrary smooth curve  $\Sigma$  and the permittivity of the cylinder is denoted as  $\epsilon_c$ .

The electric field component  $E_x$  of guided TE modes can be expressed as follows:

$$E_x = \Psi(z) e^{iky},$$

$$\Psi(z) = \begin{cases} A(1+Q)e^{-\rho_1 z}, & z > 0 \\ A(e^{-\gamma_1 z} + Qe^{\gamma_1 z}), & -d < z < 0 \\ A(e^{\gamma_1 d} + Qe^{-\gamma_1 d})e^{\rho_3(z+d)}, & z < -d \end{cases}, \quad Q = \frac{i\gamma_1 - \rho_1}{i\gamma_1 + \rho_1} \quad (2)$$

Here, we assume the  $e^{-i\omega t}$  time dependence, where

$$\gamma_1 = \sqrt{k_1^2 - h^2}, \quad \rho_3 = \sqrt{h^2 - k_3^2}, \quad \rho_1 = \sqrt{h^2 - k_1^2} \quad (3)$$

$\rho_1, \rho_3$  and  $\gamma_1$  satisfy the dispersion equation:

$$(\rho_1 + \rho_3) \cos \gamma_1 d + \left( \frac{\rho_1 \rho_3}{\gamma_1} - \gamma_1 \right) \sin \gamma_1 d = 0 \quad (4)$$

and mode amplitude  $A$  is looked for as meeting the condition:  $\int_{-\infty}^{\infty} \Psi^2(z) dz = 1$  (5)

Nonzero components of the scattered magnetic field are derived from the following

$$\text{relations: } H_y = \frac{1}{ik_0} \partial_z E_x, \quad H_z = \frac{i}{k_0} \partial_y E_x \quad (6)$$

The set of integral equations for the unknown potential densities  $\phi$  and  $\psi$  is obtained using the representing of the fields  $E$  and  $E^s$  by means of surface potentials.

$$\begin{cases} \int_{\Sigma} \{ \phi(\vec{\rho}) G_b(\vec{r}, \vec{\rho}) - \psi(\vec{\rho}) G(\vec{r}, \vec{\rho}) \} d\vec{\rho} = E^i(\vec{r}) \\ \frac{\Psi(\vec{r}) + \Phi(\vec{r})}{2} - \int_{\Sigma} \{ \phi(\vec{\rho}) \partial_n G_b(\vec{r}, \vec{\rho}) - \psi(\vec{\rho}) \partial_n G(\vec{r}, \vec{\rho}) \} d\vec{\rho} = -\partial_n E^i(\vec{r}) \end{cases} \quad (7)$$

The Green's functions  $G_b$  and  $G$  satisfy the Helmholtz equation with the Dirac-delta function in the right-hand part.

Consider singularities in the kernels of the integral equations (7).

When  $|\vec{r} - \vec{\rho}| \rightarrow 0$  the following estimations are valid:

$$G_b = G = O(\ln|\vec{r} - \vec{\rho}|), \quad \partial_n G_b = \partial_n G = O(1) \quad (8)$$

Assuming that the parametric expression for curve  $\Sigma$  is known, (7) can be expanded like follows:

$$\begin{cases} \int_0^{2\pi} \{\varphi(\tau)G_b(\tau, \xi) - \psi(\tau)G(\tau, \xi)\} d\tau = E^I(\xi) \\ \frac{\varphi(\xi) + \psi(\xi)}{2} - \int_0^{2\pi} \{\varphi(\tau)\partial_n G_b(\tau, \xi) - \psi(\tau)\partial_n G(\tau, \xi)\} d\tau = -\partial_n E^I(\xi) \end{cases} \quad (9)$$

The matrix equation is obtained using the quadrature formulas for both integrals with logarithmic singularities and regular integrals.

$$\begin{pmatrix} [G_b]N & -[G] \\ \frac{1}{2} - [\partial_n G_b] & \frac{1}{2} + [\partial_n G] \end{pmatrix} \times \begin{pmatrix} \varphi(\tau_0) \\ \varphi(\tau_{N-1}) \\ \psi(\tau_0) \\ \psi(\tau_{N-1}) \end{pmatrix} = \begin{pmatrix} E^I(\tau_0) \\ E^I(\tau_{N-1}) \\ -\partial_n E^I(\tau_0) \\ -\partial_n E^I(\tau_{N-1}) \end{pmatrix}, \quad (10)$$

$$\tau_k = \frac{2\pi k}{N}, \quad k = 0, N-1$$

The peculiarity of the problem is that a cylinder can be placed on the boundary between the slab and surrounding medium. When both the source and the observation points approach the boundary, integrals which are contained in expressions for the Green's functions become slowly convergent and the computation of matrix elements is time-consuming. The Euler method for slowly convergent series is used to improve convergence of these integrals because the integrand is the oscillating and slowly decreasing function and the integral over the half-period can be considered as a term of the series. The validity and usefulness of the proposed method is showed by the following numerical data:

Table 1. The comparing of two methods of Sommerfeld-type integrals evaluating.

( $d = 4, \epsilon_1 = \epsilon_3 = 1, \epsilon_2 = 3, k_0 = 1$ )

Z	Z'	The direct integration		The Euler transform application			
				eps=1.0E-07		eps=1.0E-06	
		Re{G}	t,c	Re{G}	t,c	Re{G}	t,c
2.0	2.0	-0.08951197	7	-0.08951197	7	-0.08951197	7
1.0	1.0	-0.06537017	7	-0.06537015	10	-0.06537025	8
0.5	0.5	-0.07469742	7	-0.07469741	13	-0.07469753	10
0.1	0.1	-0.08342145	10	-0.08342138	17	-0.08342189	14
0.05	0.05	-0.08411704	13	-0.08411694	18	-0.08411771	14
0.01	0.01	-0.08458928	20	-0.08458907	23	-0.08459031	16
0.005	0.005	-0.08464293	30	-0.08464270	24	-0.08464405	16
0.001	0.001	-0.08468500	32	-0.08468473	25	-0.08468632	17
0.0005	0.0005	-0.08469021	32	-0.08468994	25	-0.08469141	17

Matrix equation (10) can be solved numerically. The solutions of (10) enable the determination of the unknown scattered  $E^s$  and the total  $E$  electric fields.

Consider the expansion of the Green's function in terms of eigen functions of the slab:

$$G(\bar{r}, \bar{\rho}) = \sum_{\lambda} \frac{\bar{\Psi}(z, \lambda) \bar{\Psi}(z', \lambda) \exp(i\lambda|y - y'|)}{N^2(\lambda) 2i\lambda} \quad (11)$$

where  $\sum_{\lambda}$  includes the sum taken over the eigenvalues of the discrete spectrum and the integral with respect to the continuous spectrum of the problem:

$$\left\{ \frac{\partial^2}{\partial z^2} + k^2(z) + \lambda^2 \right\} \bar{\Psi}(z, \lambda) = 0, \quad -\infty < z < \infty \quad (12)$$

$|\bar{\Psi}(z, \lambda)| < \infty$  when  $z \rightarrow \pm\infty$

Coefficient  $N^2(\lambda)$  is obtained from the following condition:

$$\int_{-\infty}^{\infty} \bar{\Psi}(z, \lambda) \bar{\Psi}(z, \lambda') dz = N^2(\lambda) \delta_{\lambda\lambda'} \quad (13)$$

where  $\delta_{\lambda\lambda'}$  is the Dirac-delta function or the Kronecker coefficient.

Using (11) we obtain the scattered field expansion in the terms of eigen functions of the slab:

$$E^s(\bar{r}) = \begin{cases} \sum_{\lambda} C^+(\lambda) \bar{\Psi}(z, \lambda) \exp\{i\lambda y\} & , y > y_2 \\ \sum_{\lambda} C^-(\lambda) \bar{\Psi}(z, \lambda) \exp\{-i\lambda y\} & , y < y_1 \end{cases} \quad (14)$$

where  $y_1(y_2) = \min(\max)\{y \in S\}$  and  $C^{\pm}(\lambda)$  are mode conversion coefficients.

Integral with respect to the continuous spectrum of the problem in (11) can be evaluated by the steepest-descent method in the far zone of the cylinder outside the slab ( $z > 0$ ). Thus we obtain the expressions for the scattered power:

$$P_s = c \operatorname{Im}\{E^{s*} \nabla E^s\} / 8\pi k_0 \sqrt{\epsilon_1} \quad \text{-to the radiation modes,} \quad (15)$$

$$P_k^{\pm} = \frac{c}{8\pi k_0} \lambda_k N^2(\lambda_k) |C^{\pm}(\lambda_k)|^2 \quad \text{-to the k-th guided mode} \quad (16)$$

The scattering pattern: 
$$\sigma_s(\theta) = \lim_{L \rightarrow \infty} \frac{LP(L, \theta)}{P_0} \quad (17)$$

where  $P_0$  is the incident eigenmode total energy flow along the waveguide.

Fig. 1 shows the scattering pattern of the slab eigenmode scattering from a curvilinear cylinder embedded into the slab.

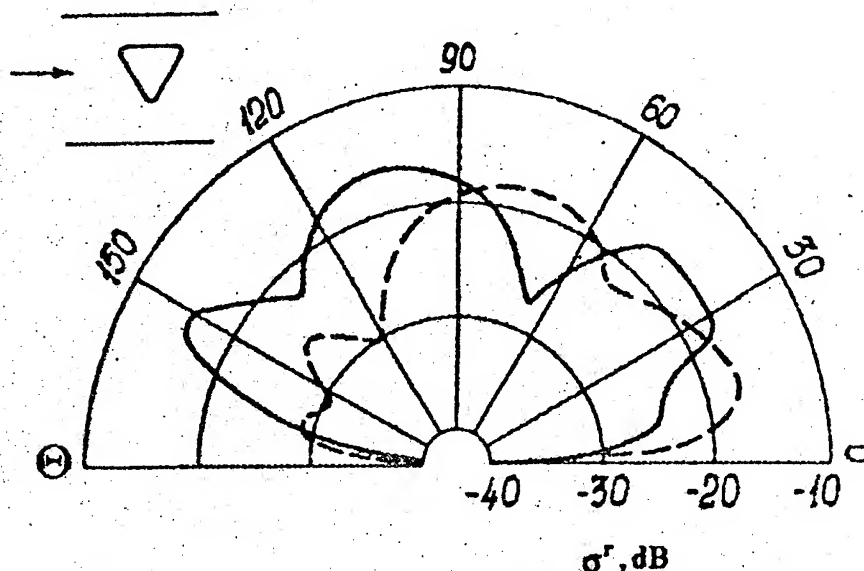


Fig. 1 Pattern of the scattering from a curvilinear cylinder immersed into the slab.

### CONCLUSIONS

The scattering and mode conversion of a dielectric slab eigenmode from a dielectric cylinder have been analyzed numerically by the method of a single-layer potential. The proposed method can treat cylindrical discontinuities with cross-section bounded by an arbitrary smooth curve. These cylinders can be placed inside the slab, outside it and on the slab boundary. This method can also solve the discontinuity problems with a TM mode incidence. Some illustrative numerical results for the scattering patterns, total scattered power and mode conversion coefficients have been presented.

### ACKNOWLEDGMENT

The authors are deeply indebted to Prof. A. Nosich for helpful advices.

### REFERENCES

- [1] N. Morita "Scattering and Mode Conversion of Guided modes of a Slab Waveguide by a Circular Cylinder", IEE Proc., 1980, v.27, Pt.H. N5, pp 263-269.
- [2] V.P. Kalinichev and P.N. Vadov "Numerical Investigation of Dielectric Resonator Excitation by a Dielectric Slab Waveguide", Radiotekhnika i Elektronika, vol.33, Mar. 1988, p. 464 (in Russian).
- [3] N. Morita "An Integral Equation Method for Electromagnetic Scattering of Guided Modes by Boundary Deformations of Dielectric Slab Waveguides", Radio Sci., vol.18, no.1, pp.39-47, 1983.
- [4] S.-J. Chung and C.H. Chen "Analysis of Irregularities in a Planar Dielectric Waveguide", IEEE Trans.MTT, vol. MTT-36, no.9, pp.1352-1358, sept. 1988.

THE METHOD OF THE LOCAL CHANGE OF VARIABLE  
DURING THE CALCULATIONS OF THE THERMAL RADIOEMISSION  
STATISTICAL CHARACTERISTICS OF THE ROUGH SEA SURFACE  
IN KIRHGOFF APPROXIMATION.

Igor Bubukin

Radiophysical Research Institute  
B. Pecherckay st. 25/14, Nizhny Novgorod, 603600, Russia

ABSTRACT

The method of development of the analytical expression for the brightness temperature statistic characteristics of the surface with the large-scale roughness was proposed. The method is based on the local coordinate introduction during the integral calculations by the pass method, using the infinitesimal of the surface inclination angle tangent variance. The theory of the sea surface thermal radioemission fluctuations for any polarization angle and large-scale waves was developed by means of this method.

The sea surface brightness temperature fluctuation investigations give a new opportunity to obtain the sea surface dynamic structure data. The brightness temperature fluctuation spectrum contains the information about the sea surface inclination spectrum and can be used both for sea waves and near surface wind velocity determination, and to calculate the average brightness temperature corrections. The progress in this field depends on the advance of the theory, which allows to produce the brightness temperature statistic characteristics of the surface with the large-scale roughness.

This method of development of the analytical expression for the brightness temperature statistic characteristics of the surface with the large-scale roughness is based on the local coordinate introduction during the integral calculations by the pass method [1]. For the large-scale roughness, when electromagnetic wavelength  $\lambda$  is much smaller than roughness dimension  $\Lambda$ :

$$\lambda \ll \Lambda$$

the wave surface brightness temperature  $T$  is defined by the surface characteristics at the point of intersection of sighting line with the surface. For this case the main statistic characteristic of the brightness temperature field—the correlation function is:

$$K(\vec{r}_1, t_1, \vec{r}_2, t_2, \psi, \alpha, \theta) = \Delta T(\zeta_1, \eta_2, \psi, \alpha, \theta) \cdot \Delta T(\zeta_2, \eta_2, \psi, \alpha, \theta) \quad (1)$$

where the surface conditions at the points  $\vec{r}_1, \vec{r}_2$  for moments  $t_1, t_2$  are defined by the surface inclination angle tangents  $\zeta_1, \eta_1$  and  $\zeta_2, \eta_2$  for X, Y axes, lying in the undisturbed sea surface plane (Y-axis is oriented in the opposite direction to the wind). The

horizontal line above  $T$  means the ensemble average.  $\alpha, \theta$  angles denote the observer direction at the polar coordinate system, where  $\alpha$  is measured from  $Y$ , and  $\theta$  from the normal to the undisturbed surface.  $\psi$  is a polarization angle, which is equal to zero for horizontal polarization of the receiver. The brightness temperature change is measured from the average value:

$$\Delta T(\zeta, \eta, \psi, \alpha, \theta) = T(\zeta, \eta, \psi, \alpha, \theta) - \bar{T}(\psi, \alpha, \theta) \quad (2)$$

The relationship (2) is expanded into the Taylor series, using the infinitesimal of the sea surface inclination angle tangent deviation:

$$\begin{aligned} \Delta T(\zeta, \eta, \psi, \alpha, \theta) = & \frac{\partial T}{\partial \zeta} \Big|_{\zeta, \eta=0} [\zeta - \bar{\zeta}] + \frac{\partial T}{\partial \eta} \Big|_{\zeta, \eta=0} [\eta - \bar{\eta}] + \\ & + \frac{1}{2} \frac{\partial^2 T}{\partial \zeta^2} \Big|_{\zeta, \eta=0} [\zeta^2 - \bar{\zeta}^2] + \frac{1}{2} \frac{\partial^2 T}{\partial \eta^2} \Big|_{\zeta, \eta=0} [\eta^2 - \bar{\eta}^2] + \\ & + \frac{\partial^2 T}{\partial \zeta \partial \eta} \Big|_{\zeta, \eta=0} [\zeta \eta - \bar{\zeta} \bar{\eta}] + \dots \end{aligned} \quad (3)$$

The brightness temperature momentary value  $T$  is expressed in terms of the local emission coefficient for vertical- $J_v$  and horizontal- $J_H$  polarization:

$$T(\psi, \zeta, \eta, \alpha, \theta) = T_0 \cdot [J_v - [J_v - J_H] \cdot \cos^2(\alpha - \psi)] \quad (4)$$

here  $T_0$  is the water kinetic temperature,  $\alpha(\zeta, \eta, \alpha, \theta)$  is the double-side angle between two observation planes, measuring from the undisturbed sea surface and from the tangential to the wave plane in the point where the observation line intersects the sea surface. The relationship (4) and the problem geometry allow to change differentiation variables in (3), that is modified to the expression:

$$\begin{aligned} \Delta T(\zeta, \eta, \psi, \alpha, \theta) = & T_0 \left\{ \left[ \frac{\partial J_B}{\partial \theta} - \left[ \frac{\partial J_B}{\partial \theta} - \frac{\partial J_B}{\partial \theta} \right] \cdot \cos^2 \psi \right] \cdot [\zeta_{\parallel} - \bar{\zeta}_{\parallel}] - \right. \\ & - \frac{[J_B - J_R]}{\sin \theta} \sin 2\psi [\zeta_{\perp} - \bar{\zeta}_{\perp}] + \frac{1}{2} \left[ \frac{\partial^2 J_B}{\partial \theta^2} - \left[ \frac{\partial^2 J_B}{\partial \theta^2} - \frac{\partial^2 J_R}{\partial \theta^2} \right] \cos^2 \psi \right] \cdot \\ & \cdot [\zeta_{\parallel}^2 - \bar{\zeta}_{\parallel}^2] + \frac{1}{2} \left[ \frac{1}{\tan \theta} \left[ \frac{\partial J_B}{\partial \theta} - \left[ \frac{\partial J_B}{\partial \theta} - \frac{\partial J_B}{\partial \theta} \right] \cos^2 \psi \right] + \right. \\ & + 2 \frac{[J_B - J_R]}{\sin^2 \theta} \cos 2\psi \cdot [\zeta_{\perp}^2 - \bar{\zeta}_{\perp}^2] + \\ & + \left. \left[ \frac{[J_B - J_R]}{\tan \theta} - \left[ \frac{\partial J_B}{\partial \theta} - \frac{\partial J_B}{\partial \theta} \right] \right] \frac{\sin 2\psi}{\sin \theta} [\zeta_{\parallel} \zeta_{\perp} - \bar{\zeta}_{\parallel} \bar{\zeta}_{\perp}] \right\} + \dots \end{aligned} \quad (5)$$

$\zeta_{\parallel}$  and  $\zeta_{\perp}$  denote the inclination angle tangents in the observation and perpendicular planes and they are related with  $\zeta$  and  $\eta$  by means of the expressions:

$$\zeta_{\parallel} = \zeta \cdot \sin \alpha + \eta \cdot \cos \alpha$$

$$\zeta_{\perp} = \eta \cdot \sin \alpha + \zeta \cdot \cos \alpha$$

For statistic homogeneous brightness temperature field the correlation function (1) depends on the difference of coordinates  $\vec{r} = \vec{r}_2 - \vec{r}_1$ ,  $\tau = t_1 - t_2$  and the brightness temperature fluctuation spectrum is related with the correlation function:

$$\Phi(\omega, \vec{r}, \psi, \alpha, \theta) = \frac{1}{(2\pi)^3} \int_{-\infty}^{+\infty} \int \int K(\vec{r}, \tau, \psi, \alpha, \theta) \cdot \exp[-i(\vec{r} \cdot \vec{r} - \omega \cdot \tau)] d^2 r d\tau \quad (6)$$

(1), (2), (4)-(6) relationships together with the model for two-points distribution function make statistic average possible and allow us to derive the brightness temperature spectrum and an inclination angle spectrum relation. Using this method for the brightness temperature average magnitude and its fluctuation spectrum is discussed in [2] more detailed. Relationships for the average brightness temperature change  $\Delta T = T - T_{fs}$  relative to the flat surface brightness temperature  $T_{fs}$  and for the fluctuation spectrum  $\Phi(\omega, \vec{r}, \psi, \alpha, \theta)$  were obtained accurate up to the second-order infinitesimal terms for the fluctuations:

$$\begin{aligned} \overline{\Delta T(\psi, \alpha, \theta)} = & \frac{T_0}{2} \left\{ \left[ \frac{\partial^2 J_B}{\partial \theta^2} - \left( \frac{\partial^2 J_B}{\partial \theta^2} - \frac{\partial^2 J_R}{\partial \theta^2} \right) \cdot \cos^2 \psi - \right. \right. \\ & \left. \left. - 2 \cdot \operatorname{tg} \theta \left[ \frac{\partial J_B}{\partial \theta} - \left( \frac{\partial J_B}{\partial \theta} - \frac{\partial J_R}{\partial \theta} \right) \cdot \cos^2 \psi \right] \right\} \cdot \sigma_{\parallel}^2 + \right. \\ & + \left\{ \frac{1}{\operatorname{tg} \theta} \left[ \frac{\partial J_B}{\partial \theta} - \left( \frac{\partial J_B}{\partial \theta} - \frac{\partial J_R}{\partial \theta} \right) \cdot \cos^2 \psi \right] + \frac{2}{\sin^2 \theta} (J_B - J_R) \cdot \cos 2\psi \right\} \cdot \sigma_{\perp}^2 + \\ & + \left[ \left( \frac{1}{\cos \theta} + \frac{1}{\sin \theta \cdot \operatorname{tg} \theta} \right) \cdot (J_B - J_R) - \frac{1}{\sin \theta} \left( \frac{\partial J_B}{\partial \theta} - \frac{\partial J_R}{\partial \theta} \right) \right] \cdot \sin 2\psi \cdot \quad (7) \\ & \cdot \left( \sigma_u^2 - \sigma_c^2 \right) \cdot \sin 2\alpha \end{aligned}$$

$$\sigma_{\parallel}^2 = \sigma_u^2 + \sigma_c^2$$

$$\sigma_{\perp}^2 = \sigma_u^2 + \sigma_c^2$$

$$\begin{aligned} \Phi(\omega, \vec{R}, \psi, \alpha, \theta) = T_0^2 & \left\{ \left[ \frac{\partial J_B}{\partial \theta} - \left( \frac{\partial J_B}{\partial \theta} - \frac{\partial J_R}{\partial \theta} \right) \cos^2 \psi \right]^2 \cdot \Phi_{\parallel}(\omega, \vec{R}, \alpha) + \right. \\ & + \frac{(J_B - J_R)}{\sin^2 \theta} \sin^2 2\psi \cdot \Phi_{\perp}(\omega, \vec{R}, \alpha) - \\ & \left. - \frac{(J_B - J_R)}{\sin \theta} \left[ \frac{\partial J_B}{\partial \theta} - \left( \frac{\partial J_B}{\partial \theta} - \frac{\partial J_R}{\partial \theta} \right) \cos^2 \psi \right] \cdot (\Phi_{\eta} - \Phi_{\zeta}) \sin 2\alpha \cdot \sin 2\psi \right\} \end{aligned} \quad (8)$$

$$\Phi_{\parallel} = \Phi_{\eta}(\omega, \vec{R}) \cos^2 \alpha + \Phi_{\zeta}(\omega, \vec{R}) \sin^2 \alpha$$

$$\Phi_{\perp} = \Phi_{\eta}(\omega, \vec{R}) \sin^2 \alpha + \Phi_{\zeta}(\omega, \vec{R}) \cos^2 \alpha$$

$\sigma_v, \Phi_{\eta}$  and  $\sigma_c, \Phi_{\zeta}$  are the surface inclination angle tangent deviations and fluctuation spectra along and across the wind and  $\sigma_{\parallel}, \Phi_{\parallel}$  and  $\sigma_{\perp}, \Phi_{\perp}$  are dispersions and spectra in the sighting and perpendicular plane respectively.

The analysis of the relationship (7) shows that the flat surface brightness temperature relationship at the polarization angle  $\psi$  differs from the relationship for the average temperatures:

$$\bar{T}(\psi) \neq \bar{T}_B \sin^2 \psi + \bar{T}_R \cos^2 \psi$$

It is related with the thermal electromagnetic field correlation for vertical and horizontal polarizations in the case of the rough surface, unlike the flat surface where they are statistically independent. In (8) the second and the third spectrum components are caused by the fluctuation correlation for vertical and horizontal polarization. They don't influence on the fluctuations for vertical and horizontal polarizations but they are substantial at an intermediate polarization angle. The brightness temperature fluctuation spectra for vertical and horizontal polarization depend on the inclination angle spectrum at the sighting plane, but for  $\psi \approx 45^\circ$  they depend on the inclination angle spectrum at the perpendicular plane. The experimental investigations of the rough sea surface brightness temperature fluctuations at various polarization angles verify this conclusion [2].

It is necessary to note that in (7), (8) and in other relationships produced by this method we haven't specified the local emission coefficient. It means, that  $J_v$  and  $J_h$  can describe both the local flat surface and the surface with the local structure: small-scale waves, pollutions and so on.

#### REFERENCE

- (1) I.T. Bubukin et al.: "Investigation of rough surface brightness temperature in Kirchhoff approximation", *Izvestiya vysshikh uchebnykh zavedenii, seriya radiofizika*, (1982) 25, 6, pp. 652-656.
- (2) I.T. Bubukin et al.: "The polarization investigation of the sea surface microwave radioemission fluctuations", *Radiotekhnika i elektronika*, in published.



# MATHEMATICAL METHODS OF THE ELECTROMAGNETIC WAVE THEORY IN URBAN MEDIA

Mihail Bulahov

The Tomsk State University  
Lenin st., 36, Tomsk, 634050 Russia

**Abstract:** Problems of electromagnetic field investigations in an urban media are considered. The Formulae and calculation algorithm for average attenuation of the field over a smoothly irregular terrain are offered. By the results of numerical simulation the radiomap of an urban area are constructed.

The exploration of electromagnetic fields in an artificial media and structures represents one of the vital directions of modern electromagnetic theory. Among the latters, there is an urban media, which differ from others by presence of the highest amount of inhomogeneity. At present, there are many different mathematical models for it, for example - one by Okumura /1/. But, to the author's mind, the most fundamental model is the analytical one /2/, which simulates the urban media by the set of plane opaque screens, placed casually and independently on the earth's surface. Basing on this insight, the authors of the model compute spatial - temporal urban field structure by calculating the multifold and multipath statistic, in the approach of geometric optics. Then, one of the important and the most informational at practice values is average intensity, for which the two asymptotical formulae faithfully representing its variability in the two limited cases were obtained /2/:

1. When the fixed station antenna is above the average level of the surrounding buildings roofs:

$$\langle I \rangle = \frac{1}{8\pi} \times R_1 \times \frac{z_2 - h}{d^3} . \quad (1)$$

2. In the case of its disposing below the level specified:

$$\langle I \rangle = \frac{1}{24\pi^2} \times R_1 \times R_2 \times \frac{\lambda}{d^3} . \quad (2)$$

Here:

$$R_{1,2} = \frac{\Gamma \lambda l_B}{\lambda^2 + [2\pi l_B \gamma (h - z_{1,2})]^2}$$

$\Gamma$  - the average magnitude of the luminous reflectance correlation function;  $\lambda$  - the wavelength;  $z_{1,2}$  the heights of the mobile and fixed station antennas respectively;  $d$  - the distance between them;  $\gamma$  - the average density of the building;  $h$  - the average height of the building;  $l_B$  - the vertical correlation scale of the luminous reflectance.

It is considered, that the mobile station antenna is disposed below the average height of the building both in the first and the second cases.

It is easy to detect, that at  $z_2 = h$  the equation (1) is equal to zero, because it is derived by using the onefold scattering theory approach. It makes the largest contribution for the forming of the field in the reception point during the high arrangement of the fixed station antenna, but tends to zero when it lowers to the roof level. Vice versa, the equation (2) is obtained in the multifold scattering theory approach, which begins to play the determinant role as soon as the fixed station antenna lowers below the roof level. Taking account of this singularity, as a matter of following convenience it would be advantageous to unite equations presented, that forms the part of this work.

As a result, the following united formula is offered:

$$\langle I \rangle = R_1 \times \left[ \eta + R_2' \frac{\lambda}{\pi^3 (1 + e^\xi)} \right] \frac{1}{d^3}, \quad (3)$$

which was obtained by the asymptotic joining of the equations (1) and (2) at  $z_2 = 0$ . Here:

$$R_2' = \frac{2\pi \Gamma \lambda l_B}{\lambda^2 + (2\pi l_B \gamma \zeta)^2}, \quad \eta = \begin{cases} z_2 - h, & z_2 > h \\ 0, & z_2 \leq h \end{cases}, \quad \zeta = \begin{cases} h - z_2, & h > z_2 \\ 0, & h \leq z_2 \end{cases}$$

The joint factor  $\xi = \frac{\eta}{\sqrt{2\lambda d}}$

is chosen on the base, that according to [2] the multifold scattering effects begins to play an appreciable role for the forming of field in the reseption point when  $z_2 - h \leq \sqrt{2\lambda d}$ .

Further, to correct the results obtained, the account of

influence of terrain relief is carried out. For these means, the fair irregularities of the earth's surface are approximated by spherical obstacles /3/ and the factor of added diffraction attenuation is introduced:

$$P = P_0 (de^{-2\alpha(d-d_0)} + oe^{-2\alpha\beta(d-d_0)}) \quad (4)$$

The latter is being constructed by joining Fok's diffraction asymptotic  $\frac{1}{r^2} e^{-2\alpha r}$  for field intensity over the horizon above the smooth earth's surface, where  $\alpha$  - attenuation factor, and the function  $\frac{1}{r^3}$ , which takes place for the field above the quasiplane urban area (i.e. ahead to the horizon). Basing on the described above mathematical model, the calculation algorithm for the average intensity was worked out and realized as a computer program. The results of the numerical simulation were compared with the set of experimental data obtained for the central part of Tomsk at the frequency 410 Mhz.

Utilization of the algorithm pointed out made it possible to construct the radiomap of the urban area, showed on fig.1. Here the results of numerical calculation are demonstrated by solid lines: The experimental data are marked by numbers in the circles. Value of zero db conforms to attenuation of the outer space field at the distance of 1 km from the radiation source. Besides, for example there are showed data for the two different radiopathes on fig.2,3. They correspond to the A and B sections on fig.1., and demonstrate the curves of the terrain relief profile and the attenuation values calculated. The experimental data are denoted by points with the indication of significant intervals.

As a whole, the results of numerical simulation is in accord with the experiment well, in such a way the average deviation of the values computed is 2.7 db. It provides the higher precision in comparison with the known empirical and graphical methods, including ones recommended by IRCC.

At the same time, the taking place deviations say about necessity of the search of ways for more detailed account of specific conditions. It seems, that the account of field polarization structure in urban areas is one of the possible ways of refinement the results obtained. This statement is based on the

fact that by nowadays the effects of radiation depolarization never has been taken into account during the computing of average intensity. However, these effects are present to a considerable extent /2/, and can influence on the prediction precision rather highly. It seems feasible to take account of the effects by introduction of the added attenuation factor, whose computation represents the separate problem.

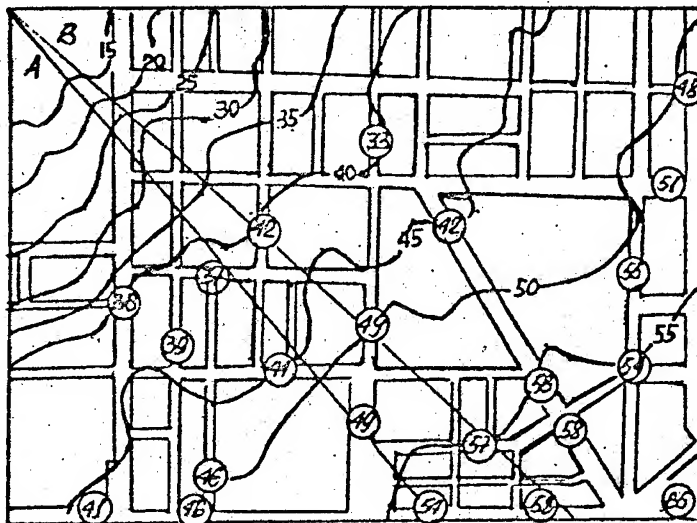


Fig. 1 Radiomap of an urban area.

$4x \langle I \rangle, \text{ dB}$

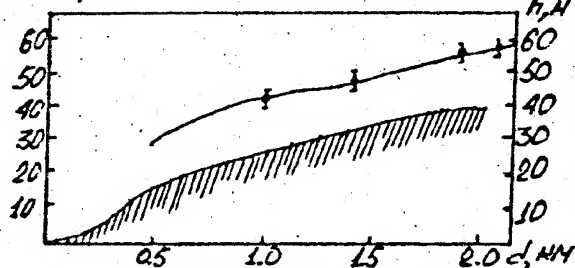


Fig. 2 Attenuation on path A.

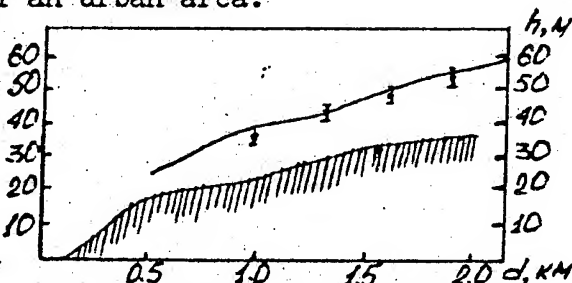


Fig. 3 Attenuation on path B.

#### References

- (1) Field strength and its variability in VHF and UHF land mobile radio service /J.Okumura, E.Ohmori, T.Kawano et al.// Rev. Elec. Com. Lab. 1968. Vol.16. N 9-10. P.825-873.
- (2) Пономарев Г.А., Куликов А.Н., Тельпуховский Е.Д. Распространение УКВ в городе.- Томск: МП "РАСКО", 1991.-223 с.
- (3) Калинин А.И. Распространение радиоволн на трассах наземных и космических радиолоний.- М.: Связь, 1979.- 296 с.
- (4) Фок В.А. Проблемы дифракции и распространения электромагнитных волн.- М.: Сов.радио, 1970.- 520 с.

# UNIFORM DESCRIPTION OF DOUBLE DIFFRACTION TRANSITION REGIONS AT A PLANE ANGULAR SECTOR

Filippo Capolino<sup>1</sup>, Stefano Maci<sup>1</sup>, Roberto Tiberio<sup>2</sup>, Alberto Toccafond<sup>2</sup>

<sup>1</sup>Dip. di Ing. Elett., Univ. di Firenze, via S. Marta 3, Firenze

<sup>2</sup>Facoltà di Ingegneria, Univ. di Siena, via Banchi di Sotto 55, Siena

## Abstract

A formulation is introduced, that provides a uniform description of the field scattered from a plane angular sector in the near zone, when it is illuminated by a plane wave. This formulation is based on the plane-wave far field response, that was derived in a previous work. The extension to observation point localized at finite distance has been obtained from spectral synthesis.

## 1. Introduction

A high-frequency description of the scattering from complex structures that exhibits surface discontinuities such as edges and vertices, is of importance in a wide variety of practical applications. To this end, the Geometrical Theory of Diffraction (GTD) and its uniform extension (UTD) provided very effective tools for most engineering purposes. Within this framework, an important canonical problem is that of a corner at the interconnection of two straight edges, joined by a plane angular sector.

It should be noted that for most practical purposes, the need for a corner diffraction coefficient in a UTD scheme mainly arises when the leading, edge diffracted field experiences a discontinuity, as it occurs when the diffraction point disappears from an edge or changes abruptly its location from one edge to the other.

The exact solution for this canonical problem was obtained in [1], but unfortunately is not well suited for practical calculations. A heuristic corner diffraction coefficient was conjectured in [2]. An improvement was introduced in [3], where the radiation integral of the currents induced by a single diffraction mechanism from one edge, is extended only to the plane angular domain delimited by the other adjacent edge. Although their solution is cast in a nicely uniform form, no estimate has been introduced therein of the distortion of the currents due to the presence of the second edge. A spectral PTD approach has been developed by Ivriissimtzis and Marehfska [4]. There, a significant improvement has been obtained by introducing secondary non-uniform currents; also, their solution includes a uniform formulation. Recently, corner diffraction coefficients have been derived in the plane wave-far field regime by using the induction theorem [5]. These non-uniform coefficients, that account for second order interactions between the two edges, exhibit the expected singularities at the caustics of single and doubly diffracted rays.

In this paper, the above solution is used to weight the plane wave spectrum representation of a source, located at a finite distance from the vertex. Next, via a suitable, asymptotic evaluation of the spectral integrals, a high-frequency uniform solution is obtained. For the sake of simplicity, the scalar case is treated in this paper and the formulation for hard boundary conditions is given explicitly hereinafter. The same basic procedure can be extended without any significant difficulty, to treat the more general electromagnetic vector problem.

## 2. Plane wave - far field diffraction coefficient

The geometry at a plane angular sector interconnecting two edges is shown in Fig. 1. Let us denote by  $\Omega$  the angle between the two edges. For the sake of simplicity in the discussion, let us suppose that hard boundary condition are imposed on the plane sector. At each edge ( $n=1,2$ ) it is useful to define a local coordinate system  $(x_n, y_n, z_n)$  with its origin at the vertex; the  $z_n$ -axis is chosen along the edge, and the  $y_n$ -axis is perpendicular to surface; accordingly, a spherical coordinate system  $(r, \beta_n, \phi_n)$  is also defined.

The far field that is scattered by the hard, plane angular sector, when it is illuminated by a plane wave propagating in a direction  $(\beta_n', \phi_n')$ , may be represented as [5]

$$D = D_{21}(\cos\beta_1, \cos\beta_2) + D_{12}(\cos\beta_2, \cos\beta_1) \quad (1)$$

In (1), the scattered far field has been normalized for  $\exp(-jkr)/(4\pi r)$ . Furthermore, the two term  $D_{21}$  and  $D_{12}$  are obtained from analogous diffraction mechanisms. In particular,  $D_{21}$  take into account for the field diffracted first at the edge 1 and next at the edge 2. For the sake of simplicity only the term  $D_{21}$  will be analyzed in the following. This term may be expressed as the sum of two contributions;

$$D_{21} = D_{21}' + D_{21}'' \quad (2)$$

$$D_{21}' = \frac{\bar{c}_{21}(c_{21}' - \frac{1}{2}\bar{s}_{21}) + \bar{c}_{21}(c_{21} - \frac{1}{2}\bar{s}_{21})}{jk(\cos\beta_1' - \cos\beta_1)(\cos\beta_2' - \cos\beta_2)}; \quad D_{21}'' = \frac{\bar{d}_{21}}{jk(c_{21}' + \bar{s}_{21})(c_{21} + \bar{s}_{21})\bar{d}_{21}} \quad (4)$$

which account for first order and second order diffraction mechanisms, respectively. In (8) and (9)

$$\bar{c}_{21} = \sqrt{\cos\beta_2 - \cos(\beta_1' + \Omega)}; \quad \bar{c}_{21} = \sqrt{\cos(\beta_2 - \Omega) - \cos\beta_1'} \quad (5a)$$

$$\bar{s}_{21} = \sqrt{\cos(\beta_1' - \Omega) - \cos\beta_2}; \quad \bar{s}_{21} = \sqrt{\cos\beta_1' - \cos(\beta_2 + \Omega)} \quad (5b)$$

$$c_{21}' = \pm \sqrt{\cos(\beta_1' - \Omega) - \cos\beta_2}; \quad c_{21} = \pm \sqrt{\cos\beta_1 - \cos(\beta_2 + \Omega)} \quad (5c)$$

$$\bar{d}_{21} = \sqrt{\sin\left(\frac{1}{2}(-\beta_2 + \beta_1' + \Omega)\right)}; \quad \bar{d}_{21} = \sqrt{\sin\left(\frac{1}{2}(-\beta_1' + \beta_2 + \Omega)\right)} \quad (5d)$$

where the upper (lower) sign apply for  $\phi_1 < \pi$  ( $> \pi$ ). It is worth noting that  $D_{21}'$  exhibit the expected singularities at the first order diffraction caustics. Furthermore, a square-root type singularity occurs in  $D_{21}''$  at the second order diffraction caustics ( $\bar{d}_{21}=0$ ).

### 3. Observation point at finite distance.

Let us consider an observation point P ( $x_2, y_2, z_2$ ) at finite distance from the tip. A spectral representation of the field in P may be cast in the form of superposition of spectral plane wave. For representing each plane wave it is convenient to use the two spectral cosines directors  $u_1$  and  $u_2$  of the two axis  $z_1$  and  $z_2$ . After some manipulations, the spectral representation of the scattered field in the near leads to

$$\mathcal{D}_{21} = \frac{-1}{8\pi^2 j} \int_{-\infty}^{\infty} \int_{-\infty}^{\infty} \frac{D_{21}(u_1, u_2)}{\sqrt{q(u_1, u_2)}} e^{-jkrp(u_1, u_2)} du_1 du_2 \quad (6)$$

$$q(u_1, u_2) = \sin^2\Omega - u_1^2 - u_2^2 + 2u_1 u_2; \quad p(u_1, u_2) = \frac{1}{\sin\Omega} [u_1 v_2 + u_2 v_1 + v\sqrt{q(u_1, u_2)}] \quad (8)$$

where  $v_1$  and  $v$  are the cosine directors with respect to the axes  $x_1$  and  $y$ , respectively,  $r$  is the finite distance of the observation point P from the tip,  $krp(u_1, u_2)$  is the phase shift between the observation point and the tip of each spectral plane wave.

It is easily seen that the integrand in (6) contains two separated poles in both the two variables of integration due to the term  $D_{21}'$ . These poles arise from the first order caustics of the corresponding plane-wave/far field representation. Furthermore, it contains the branch singularity of the term  $D_{21}''$  in the variable  $u_2$ , which arises from the double diffraction caustic.

The spectral integral representation (6) has been asymptotically evaluated. The two contributions that are associated to  $D_{21}'$  and  $D_{21}''$  have been approximated by two different asymptotic expressions. The first contribution (containing poles) is evaluated as in [3]. The second one is evaluated by means of cylindric parabolic functions.

$$\mathcal{D}_{21} = \mathcal{D}_{21}^{tip} + \mathcal{D}_2^{dd} U_2^{dd} + \frac{1}{2} \sum_{i=1}^2 U_i^d \mathcal{D}_i^d + \frac{1}{2} \mathcal{D}^{po} U^{po} \quad (9)$$

where

- $\mathfrak{D}^{go}$  is the geometrical optics contribution,  
 $\mathfrak{D}_i^d$  is the first order UTD diffraction coefficient at the  $i^{th}$  edge;  
 $\mathfrak{D}_2^{dd}$  is a double diffraction contribution from the second edge;  
 $\mathfrak{D}_{21}^{tip}$  is the diffraction tip contribution;  
 $U_i^d = U(\beta_i' - \beta_i)$ , accounts for the presence of first order diffraction point on the semi-infinite  $i^{th}$  edge;  
 $U^{so} = U(\pi - \phi_2 - \phi_2') U(\pi - \phi_1 - \phi_1')$ , accounts for the presence of a specular point within the plane angular sector;  
 $U_2^{dd} = U(\beta_1' - \Omega - \beta_2)$ ; accounts for the presence of second order diffraction point on the second edge.

It is worth pointing out that only a half of the total first order, diffracted field contribution comes from  $\mathfrak{D}_{21}$ ; the remaining part is obtained from  $\mathfrak{D}_{12}$ .

Herein after, explicit expression is presented for only the tip contribution since the other terms are rather standard:

$$\mathfrak{D}_{21}^{tip} = -\frac{e^{-jkr}}{4\pi r} \left[ D_{21}' + T''(2e^{-j\frac{\pi}{4}} \sqrt{kr} \bar{d}_{21}^2) D_{21}'' \right] T(\delta_1, \delta_1, \delta_2, \delta_2, kr) \quad (10)$$

where

$$\delta_i = \sqrt{2} \sin\left(\frac{\beta_i' - \beta_i}{2}\right) \quad ; \quad \bar{\delta}_i = \pm \sqrt{2 \sin\beta_i \sin\beta_i'} \cos\left(\frac{\phi_i' \pm \phi_i}{2}\right) \quad (11)$$

in which  $+$ ,  $-$  signs apply to  $\phi_i <, > \pi$ , respectively,

$$T''(x) = e^{-x^2/4} \sqrt{x} e^{-j\frac{\pi}{4}} D_{-\frac{1}{2}}(e^{-j\frac{\pi}{4}} |x|) \quad (12)$$

and

$$T(\bar{x}, x, \bar{y}, y, K) = jK \frac{(\bar{x}^2 + x^2)xy}{(x\bar{y} + y\bar{x})} (\epsilon_{\bar{x}} \epsilon_x G(K\bar{x}^2, Kx^2) + \epsilon_{\bar{y}} \epsilon_y G(K\bar{y}^2, Ky^2)) \quad (13)$$

in which  $\epsilon_z = \text{sgn}(z)$  and  $\epsilon = \text{sgn}(\beta_1' - \Omega - \beta_2)$ . The transition function  $T$  in (15) is the same as that defined in [3] and involves the generalized Fresnel integral  $G(a, b)$ . In (9) and (14) the transition function  $T''(x)$  involves a parabolic cylindric function  $D_{-\frac{1}{2}}$  of order  $-\frac{1}{2}$ .

## 5. Numerical results.

The first and second order diffraction contributions do exist whenever the observation point lies within the cones  $\beta_i = \beta_i'$  and  $\beta_i = \Omega - \beta_i'$ , respectively. These cones can be called first and second order shadow boundary cones (SBCs). When the observation point passes through these cones, a discontinuity occurs in the dominant contributions. This discontinuity is well compensated by the tip contribution by means of the transition functions  $T$  and  $T''$  involved therein. In the following numerical examples, the scattered field is observed on a scan plane, which is chosen to intersect SBCs. In all the curves, the dashed, dotted and continuous lines represent the first order UTD field, the tip contribution and the total scattered field, respectively. In Fig. 1 the amplitude of a field is plotted at distance  $r=2\lambda$  from the tip of a  $\Omega=90^\circ$  plane angular sector. The scan plane and the direction of the incident plane wave are specified in the inset of the same figure. When the point of observation  $P$  passes through this cone, the UTD diffracted field abruptly disappears and the tip contribution provides the required continuity of the total scattered field. This demonstrates the effectiveness of the transition functions  $T$ .

Fig. 2 shows the scattered field at a distance  $2\lambda$  ( $0 < \beta_1 < 180^\circ$ ,  $\phi_1 = 125^\circ$ ) for a plane wave incident from  $\phi_1' = 60^\circ$ ,  $\beta_1' = 80^\circ$  for the same plane angular sector ( $\Omega = 90^\circ$ ). The observation point passes through both first and second order SBCs. In this case both the two transition functions  $T$  and  $T''$  intervene when  $P$  approaches first and second order SBCs, respectively. Also in this case, tip contribution gives the expected continuity of the total field.



# References

- [1] Satterwhite, R. S., "Diffraction by a quarter plane, the exact solution and some numerical results", IEEE Trans. Antennas Propagat., AP-22 (5), 500-503, 1974.
- [2] Sikta, F. A., W. Burnside, T. T. Chu, L. Peters Jr., "First-order equivalent current and corner diffraction scattering from flat plate structures," IEEE Trans. Antennas Propagat., AP-31 (6), pp. 584-589, 1983.
- [3] K. C. Hill, "A UTD solution to the EM scattering by the vertex of a perfectly conducting plane angular sector" Ph. D. diss., Ohio State University, Dept. of Electrical Eng., 1990.
- [4] Ivrisimtzis, L. P., and R. J. Marhefka, "A uniform ray approximation of the scattering by polyhedral structures including higher terms," IEEE Trans. on Antennas Propagat., AP-40 (11), 1302-1312, 1992.
- [5] S. Maci, R. Tiberio, A. Toccafondi "Diffraction at a plane angular sector", to be published on Jour. on e.m. Wave and Applic. (Special issue on recent advances in Electromagnetics.), 1994

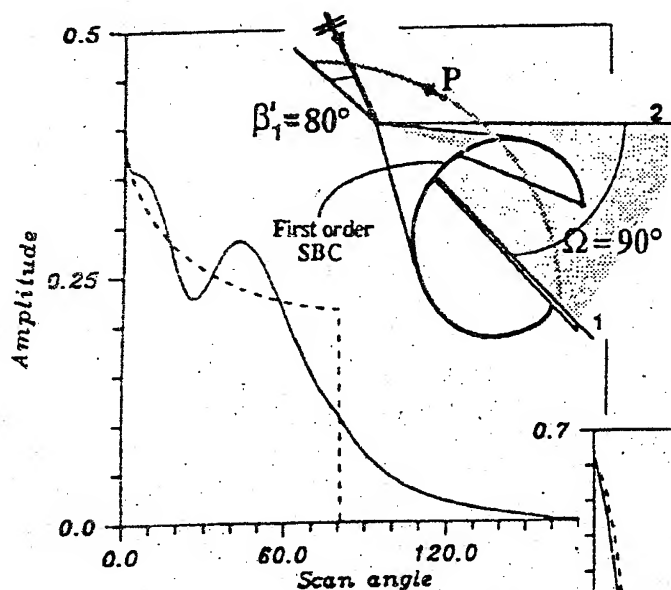


Fig.1

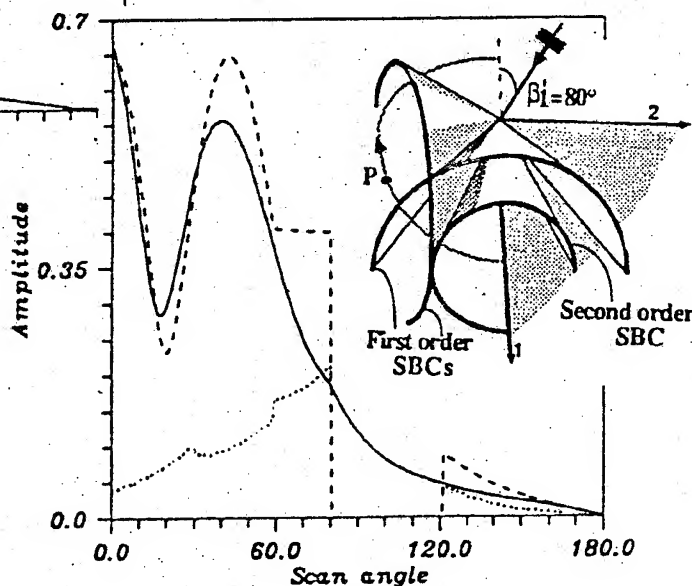
Amplitude of the field scattered from a plane angular sector. The distance of P from the tip is  $2\lambda$ . The scan-plane cuts only a first order shadow boundary cone (SBC).

----- First order UTD  
 ..... Tip contribution  
 ——— Total field

Fig. 2

Amplitude of the field scattered by a plane angular sector. The distance of P from the tip is  $2\lambda$ . The scan-plane cuts two first order SBCs and a second order SBC.

----- First order UTD  
 ..... Tip contribution  
 ——— Total field





# MATHEMATICAL QUESTIONS OF THE BOUNDARY EQUATION METHOD IN THE ELECTRODYNAMICS

Igor Chudinovich

Kharkov State University  
4, Svobody sq., Kharkov, 310077, Ukraine

The representation of solutions of mixed problems for Maxwell's system in a form of various combinations of the surface retarded potentials leads to the systems of nonstationary boundary equations. The results concerning to the unique solvability of these systems are presented. The properties of their solving operators in some functional spaces of Sobolev type are given too.

## INTRODUCTION

For some last years the interest to the mathematical questions of the boundary equation theory in hyperbolic mixed problems has been on increase. These equations arise after the limit transitions of a point to the boundary in the surface potentials representing solutions of original problems. It is well known that the question of the solvability of boundary equations both in the elliptic and in the parabolic cases was researched long ago, but in the hyperbolic case until very recently there were no results concerning to the solvability of corresponding boundary equations. Only in 1986 in the works by A. Bamberger and T. Ha Duong [1,2] the unique solvability of two boundary equations in two main mixed problems of the diffraction of acoustic waves was proved. In the early 90-es these investigations were continued in the cycle of author's works [3 - 6] devoted to boundary equations in the problems of the dynamic elasticity theory. This note is the first one in the cycle of papers devoted to the analogous questions in the electrodynamic problems for the nonstationary Maxwell's system.

## THE NOTATIONS AND THE FORMULATION OF THE PROBLEM

Let  $S$  be a smooth surface dividing  $\mathbb{R}^3$  into domains  $\Omega^+$  and  $\Omega^-$ . The electric and magnetic field vectors in a point  $x \in \mathbb{R}^3$  at the moment  $t \in \mathbb{R}_+ = (0, \infty)$  are denoted by  $E(X)$  and  $H(X)$  respectively where  $X = (x, t)$ . In the absence of the conduction current and free charges these vector fields either in  $G^+ = \Omega^+ \times \mathbb{R}_+$  or  $G^- = \Omega^- \times \mathbb{R}_+$  satisfy the Maxwell's system

$$\varepsilon \partial_t E(X) - \operatorname{rot} H(X) = 0$$

$$\operatorname{div} E(X) = 0$$

$$\mu \partial_t H(X) + \operatorname{rot} E(X) = 0$$

$$\operatorname{div} H(X) = 0$$

The initial conditions are supposed to be homogeneous

$$E(x, +0) = H(x, +0) = 0, \quad x \in \Omega^+$$

The boundary conditions have a form

$$E^\pm(X) \wedge \nu(x) = F(X), \quad (H^\pm(X), \nu(x)) = g(X), \quad X \in \Sigma^+ = S \times \mathbb{R}_+$$

where  $\nu(x)$  is an outward unit normal vector to  $S$  at a point  $x \in S$ , the symbols  $\wedge$  and  $(\dots)$  denote the vector and the scalar products in  $\mathbb{R}^3$  respectively, the superscripts " $\pm$ " denote the limit values of corresponding functions when their argument  $X$  tends to  $\Sigma^+$  from within  $G^\pm$  respectively. Excluding magnetic field we reduce this problem to the problem

$$\begin{aligned} \partial_t^2 E(X) - a^2 \Delta E(X) &= 0, & X \in G^\pm, \\ E(x, +0) = (\partial_t E)(x, +0) &= 0, & x \in \Omega^\pm, \\ E^\pm(X) \wedge \nu(x) = F(X), & \quad (\operatorname{div} E)^\pm(X) = 0, & X \in \Sigma^+, \end{aligned}$$

where  $a^2 = (\epsilon\mu)^{-1}$ . We consider even more general problem with the non-homogeneous boundary condition

$$(\operatorname{div} E)^\pm(X) = f(X), \quad X \in \Sigma^+.$$

Let us call this problem the dynamic electric problem.

### THE RETARDED POTENTIALS

Let  $\Phi(X)$  be the fundamental solution of the three-dimensional wave equation

$$\Phi(X) = (2\pi a)^{-1} \theta(t) \delta(a^2 t^2 - |x|^2)$$

where  $\theta$  is the characteristic function of  $\mathbb{R}_+$ ,  $\delta$  is the Dirac's function. The retarded single- and double-layer potentials with three-component densities  $\alpha$  and  $\beta = (\beta_\tau, \beta_\nu)$  defined on  $\Sigma^+$  are introduced by formulas

$$(V\alpha)(X) = \int_{\Sigma^+} \Phi(X - Y) \alpha(Y) ds_Y,$$

$$\begin{aligned} (W\beta)(X) = \int_{\Sigma^+} \sum_{j=1}^3 e_j \{ & (\operatorname{rot}_Y \Phi_j(X - Y) \wedge \nu(y), \beta_\tau(Y)) + \\ & + \operatorname{div}_Y \Phi_j(X - Y) \beta_\nu(Y) \} ds_Y \end{aligned}$$

where  $e_j$  is the  $j$ -th unit coordinate vector,  $\Phi_j(X) = \Phi(X)e_j$ ,  $\beta_\tau$  and  $\beta_\nu$  are the tangential and the normal to  $S$  components of  $\beta$ .  
Representing solution of the dynamic electric problem in a form

$$E(X) = (V\alpha)(X), \quad X \in G^\pm$$

and taking into account the boundary conditions one gets the system of boundary equations which is denoted by

$$Q_{V,\alpha}^\pm = \{F, f\}.$$

The representation

$$E(X) = (V\alpha_\tau)(X) + (W\beta_\nu)(X), \quad X \in G^\pm$$

in which  $\alpha_\tau$  and  $\beta_\nu$  are the tangential and the normal to  $S$  vector fields respectively leads to the system

$$Q_{V,W}^\pm(\alpha_\tau, \beta_\nu) = \{F, f\}.$$

The representation

$$E(X) = (W\beta_\tau)(X) + (V\alpha_\nu)(X), \quad X \in G^\pm$$

with the tangential density  $\beta_\tau$  and the normal density  $\alpha_\nu$  leads to the system

$$Q_{W,V}^\pm(\beta_\tau, \alpha_\nu) = \{F, f\}.$$

Lastly, representing solution in a form

$$E(X) = (W\beta)(X), \quad X \in G^\pm$$

one gets the system denoting by

$$Q_W^\pm \beta = \{F, f\}.$$

Our aim is to research the solvability of these systems.

### THE FUNCTIONAL SPACES

For any  $m \in \mathbb{R}$ ,  $z > 0$  let us introduce the standard Sobolev space  $H_{r,m,z}(\Sigma^+)$  consisting of three-component vector functions defined on  $\Sigma = S \times \mathbb{R}$  which vanish when  $t < 0$ , whose  $m$ -th (fractional) derivatives are square summable on  $\Sigma^+$  with the weight  $\exp(-2zt)$ . For any  $m, k \in \mathbb{R}$   $H_{r,m,k,z}(\Sigma^+)$  are the spaces consisting of vector functions  $U(X)$  vanishing when  $t < 0$  and such that  $(\partial_t^k U)(X) \in H_{r,m,z}(\Sigma^+)$ . Lastly,  $H_{r,m,k,z}^\tau(\Sigma^+)$  and  $H_{r,m,k,z}^\nu(\Sigma^+)$  are the subspaces in  $H_{r,m,k,z}(\Sigma^+)$  which consist of tangential and normal to  $S$  vector fields respectively.

## THE FORMULATION OF THE MAIN RESULT

The following statement answers the question of the unique solvability of the presented above systems of boundary equations.

**THEOREM.** The solving operators  $R_V^\pm = (Q_V^\pm)^{-1}$ ,  $R_{V,W}^\pm = (Q_{V,W}^\pm)^{-1}$ ,  $R_{W,V}^\pm = (Q_{W,V}^\pm)^{-1}$ ,  $R_W^\pm = (Q_W^\pm)^{-1}$  of four systems of boundary equations perform the maps

$$R_V^\pm: H_{r;1/2,k,z}^\tau(\Sigma^+) \times H_{r;-1/2,k,z}^\nu(\Sigma^+) \Rightarrow H_{r;-1/2,k-1,z}^\tau(\Sigma^+),$$

$$R_{V,W}^\pm: H_{r;1/2,k,z}^\tau(\Sigma^+) \times H_{r;-1/2,k,z}^\nu(\Sigma^+) \Rightarrow H_{r;-1/2,k-2,z}^\tau(\Sigma^+) \times H_{r;1/2,k-2,z}^\nu(\Sigma^+),$$

$$R_{W,V}^\pm: H_{r;1/2,k,z}^\tau(\Sigma^+) \times H_{r;-1/2,k,z}^\nu(\Sigma^+) \Rightarrow H_{r;1/2,k-2,z}^\tau(\Sigma^+) \times H_{r;-1/2,k-2,z}^\nu(\Sigma^+),$$

$$R_W^\pm: H_{r;1/2,k,z}^\tau(\Sigma^+) \times H_{r;3/2,k-2,z}^\nu(\Sigma^+) \Rightarrow H_{r;1/2,k-1,z}^\tau(\Sigma^+) \times H_{r;1/2,k,z}^\nu(\Sigma^+)$$

which are continuous for any  $k \in \mathbb{R}$ ,  $z > 0$ .

## REFERENCE

- (1) A. Bamberger and T. Ha Duong: "Formulation Variationnelle Espace-Temps pour le Calcul par Potentiel Retarde de la Diffraction d'une Onde Acoustique", Math. Meth. in the Appl. Sci., (1986), 8, pp. 405 - 435.
- (2) A. Bamberger and T. Ha Duong: "Formulation Variationnelle pour le Calcul de la Diffraction d'une Onde Acoustique par une Surface Rigide", Math. Meth. in the Appl. Sci., (1986), 8, pp. 598 - 608.
- (3) I. Chudinovich: "Boundary Equations in Dynamic Problems for Elastic Media", Dokl. Akad. Nauk of Ukraine, ser. A, (1990), 11, pp. 18 - 21.
- (4) I. Chudinovich: "Boundary equations in Nonstationary Diffraction Problems for Elastic Waves on Space Cracks", Matematicheskie zametki, (1991), 51, no. 4, pp. 119 - 123.
- (5) I. Chudinovich: "The Boundary Equation Method in the Third Initial Boundary Value Problem of the Theory of Elasticity Part 1. Existence Theorems", Math. Meth. in the Appl. Sci., (1993), 16, pp. 203 - 215.
- (6) I. Chudinovich: "The Boundary Equation Method in the Third Initial Boundary Value Problem of the Theory of Elasticity. Part 2. Methods for Approximate Solutions", Math. Meth. in the Appl. Sci., (1993), 16, pp. 217 - 227.

# THEORY OF THE INTEGRAL EQUATION OF THE IMPEDANCE DIPOLE

Danilchuk V.L., Plotnikov V.N., Radtsig J.J., Eminov S.I.

The Novgorod state university, Novgorod.

The impedance dipole was studied in numerous works of native and foreign investigations. But it is a problem of today of making of the effective methods of the calculation. The qualitative analysis of the integral equation is cited in this work. The effective program of the solution of the integral equation is built on its basis.

The initial equation of the impedance dipole has the view:

$$E_z(j_z) + E_z^0 = Z j_z, \quad (1)$$

where  $Z$  is the surface impedance;  $j_z$  is the density of current. Current is directed on the surfaces of the dipole by the primary field  $E_z^0$ . By the results of the works [1,2,3] the equation (1) may be written in the view:

$$\begin{aligned} & \lambda (AI)(\tau) + \frac{1}{2\pi a} (ZI)(\tau) + (KI)(\tau) = \\ & = \lambda \frac{1}{\pi} \frac{\partial}{\partial \tau} \int_{-1}^1 I(t) \frac{\partial}{\partial t} \ln \frac{1}{|\tau-t|} dt + \frac{1}{2\pi a} Z I(\tau) + \\ & + \int_{-1}^1 K(\tau, t) I(t) dt = e(\tau) \end{aligned} \quad (2)$$

where  $2l$ ,  $a$  - is length and radius of dipole. We'll consider the equation (2) in the power space  $H_A$  of the symmetrical, positive definite operator:

$$(AI)(\tau) = \frac{1}{\pi} \frac{\partial}{\partial \tau} \int_{-1}^1 I(t) \frac{\partial}{\partial t} \ln \frac{1}{|\tau-t|} dt \quad (3)$$

Theorem 1. The operator of multiplication on the function  $Z$  and integral operator  $K$  are operators of Hilbert-Schmidt in the space  $H_A$ .

The idea of the proof. The orthonormalize basis in  $H_A$  has view:

$$\varphi_n(\tau) = \sqrt{\frac{2}{\pi n}} \sin[n \arccos(\tau)], \quad n=1,2,\dots \quad (4)$$

the integral operator  $K$  has logarithmic peculiarity in the kernel. Asymptotic of the matrix elements of the operator  $K$  in basis  $\left\{ \varphi_n \right\}_{n=1}^{+\infty}$  is found on this basis. The asymptotic of the matrix elements of the operator of the multiplication on  $Z$ , if  $Z$  is piece-smooth is found also. It follows from this theorem that equation (2) is the equation of Fredholm of the second kind in the space  $H_A$ . The alternative of Fredholm is applied to this equation. Alternative: The equation has only one solution or the uniform equation has nonzero solution.

Theorem 2. If  $\operatorname{Re}(Z) \geq 0$  the uniform equation corresponding (2) has only zero solution.

The idea of the proof. If we'll submit the integral operator (2) in view of the Furje's integrals then the spectrum density has the positive real part. On this basis the assertion of the theorem 2 is proved easy. Then we'll expand the unknown current on the basis

$$I(\tau) = \sum_{i=1}^{+\infty} C_i \varphi_i(\tau) \quad (5)$$

and going to the infinite system of Fredholm of second kind

$$C_i + \sum_{j=1}^{+\infty} M_{ij} C_j = I_i, \quad 1 \leq i < +\infty, \quad (6)$$

For the constant impedance the asymptotic of the matrix elements  $M_{ij}$  is found and the theorem 3 is proved.

Theorem 3. If the right part of the integral equation is the smooth and differentiating by several times then the following estimation is correct for the coefficient of the system (6):

$$|C_i| \leq \frac{\text{const}}{i^3}, \quad (7)$$

There are two important conclusions from the theorem 3. At first, we can submit the function of current in view

$$I(\tau) = \rho(\tau) f(\tau),$$

where  $f(\tau)$  is smooth. At second, the solution of the integral of the integral equation is classic, it has to region of the definition of the unlimited operator  $A$ . Moreover, we can define the rate of the tallieing of the approximate solution  $C_N$ , founding from the solution of the truncated system of order  $N \times N$ , to precision. And the estimation is correct:

$$\|C_N - C\| \leq \frac{\text{const}}{N^{5/2}}, \quad (8)$$

where  $C = \left\{ C_i \right\}_{i=1}^{+\infty}$  is the solution of the infinite system (6). The constants in (7) and (8) is big values and the method of Galerkin is uneffective when exciting of dipole by the concentrated sources. The numeral-analytical method of the solution of the infinite system (6) is offered for this case. This method consists in the following: the first  $N$  of the

unknown values are found from the solution of the truncated system:

$$C_i + \sum_{j=1}^{+\infty} M_{ij} C_j = I_i, \quad 1 \leq i < N, \quad (9)$$

and other unknown values are found by analytical method:

$$C_i = I_i, \quad N \leq i < +\infty, \quad (10)$$

In this method the kernel of the integral equation is changed on the approximate but right part is set precisely.

It follows from the calculations that the numerical - analytical method has high effectiveness. The series of the calculations of the impedance dipole were carried out on the basis of this method for the constant impedance (distributed impedance) and for the piece-constant impedance. In the last case the space impedance models the loads. By the calculations the available of the capacitive and inductive loads permits to synthesize antenna with better characteristics as by the criterion of the co-ordination as by the coefficient of the directive action, with better weight-gabarit parameters.

#### Reference:

1. Eminov S.I.: Radio-engineering and electronic, 1993, vol. 38, N 12, p. 2160.
2. Eminov S.I./Letter in JTF, 1993, vol. 19, N. 10, p. 41.
3. Danilchuk V.L., Radtsig J.J., Eminov S.I.: Materials of the lectures of the All-Russian SPC - FAR-94, Kazan, 1994.



# THE NUMERICAL ANALYTICAL METHOD OF SOLVING THREE-DIMENSIONAL DIFFRACTION PROBLEMS IN THE COMPLEX GEOMETRY DOMAIN

Sergey G. Dmitryuk and Igor V. Petrusenko

Dniepropetrovsk State University  
Str. Gagarin 72, Dniepropetrovsk-10, 320625, Ukraine

## ABSTRACT

The technique of the partial inversion of the principal part of the mode-matching method's integral operator was developed and substantiated. An application of this method, named the method of partial overlapping regions, to solving a number of the waveguide discontinuity problems is discussed. Its basic advantages over other methods are illustrated.

## INTRODUCTION

Recent advances in microwave technology, such as the use of the millimetre-wave spectrum, lead to the increasing complexity of the electromagnetic structures employed. An accurate numerical tools are necessary for the design of electrodynamics systems. For the above reasons, highly sophisticated numerical techniques are required for computer-aided design.

The practically important problems requires construction of mathematical models for multiparametric analysis and computer optimization. Consequently they must be as efficient as possible from the point of accuracy and stability of numerical calculations. These models may be obtained by different methods of regularizing initial integral equations.

It is well known, that mode-matching technique usually leads to the convolution-type matrix operator. However, the condition of field continuity on a part of region's boundary allows to obtain sufficiently universal integral equations (IE) taking into account further transformations. In general case the kernel of IE contains one "moving" and two "moveless" singularities. When there is a "moveless" singularity with a certain weight in connection with a "moving" singularity, it is rarely possible to invert the principal part of the integral operator completely.

For the last instance the technique of the partial inversion of the principal part of the mode-matching method's integral operator was developed and substantiated. The operator of this method contains the "moveless" singularities on the edges of a boundary surface only. Thus, a resulting matrix operator consists of an idem-factor and a  $\omega$ -complete continuous operator in a suitable pair of spaces. On the basis of analytical Fredholm alternative theorem existence of bounded inverse operator and application of the reduction method for solving the matrix equation are proved.

According to this method, named the method of partial overlapping regions [1], a whole complex domain of field determination is divided into a number of overlapping regions. An integral equation to solve for one of the electromagnetic field vectors is formulated for each of overlapping regions using the integral theorems of the diffraction theory [2]. The field continuity on a common part of the overlapping regions leads to the system of interconnected integral equations. The last one is converted into an infinite matrix equation of the second kind, which permits efficient solving by a computer.

## THEORY

To compare the methods let us consider the problem of diffraction of LE-modes on the step discontinuity in the parallel-plane waveguide. Matching the electromagnetic fields at the aperture yields the integral equation of first kind

$$\int_0^a [G_1(x,0|x',0) + G_2(x,0|x',0)] U(x') dx' = U_{inc}(x), \quad (1)$$

where  $U_{inc}(x)$  represents an incident wave,  $a$  - is a relative aperture size and  $G_i(x,y|x',y')$  - is the Green's function for the  $i$ -th waveguide. For the moment method the unknown function  $U(x)$  can be given as the series of a complete orthonormal system of the transverse eigenfunctions that permits to invert the  $G_1(x,0|x',0)$ . Thus we obtain a matrix equation

$$(I + D_1) A = f_1, \quad (2)$$

where the elements of matrix operator  $D_1$  have the following asymptotic behaviour for  $p, q \gg 1$

$$d_{pq}^{(1)} \sim \frac{\sin \frac{\pi}{a}(p-q)}{p-q} h_{pq} + O\left(\frac{1}{p+q}\right), \quad (3)$$

( $h_{pq}$  - is the some combination of trigonometrical functions).

The (2) is the convolution-type equation and this fact is the consequence of the scalar product of two waveguides eigenfunctions properties. Presence of idem-factor in (2) does not mean from point of functional analysis because the unboundness of inverse operator in a pair of spaces  $\tilde{L}_2 \rightarrow \tilde{L}_2$  is fully determined by the singularite of matrix  $D_1$ . However it is principal according to the numerical calculation. By the reducing of matrix  $D_1$  we obtain invertible operator as the sum of idem-factor and compact operator. Therefor, the reducing of matrix leads to the self-regularization of the operator, and initial singular convolution-type operator is approached by the set of Hilbert-Schmidt-type operators. It is well-known from a number of applications of the mode-matching method that the obtained numerical results place near to the accurate values. But there is no rigorous mathematical proof of these numerical results convergence to correct values. Therefore, this method attributes to heuristics.

Method of partial overlapping regions possessing the calculation simplicity permits to create a correct mathematical model. Using of this method is equivalent to rearrange of the equation (1) to the form

$$\int_0^a [G_1(x,0|x',0) + M(x,x')] U(x') dx' = \frac{1}{2} U_{inc}(x), \quad (4)$$

where the kernel

$$M(x,x') = \frac{1}{2} [G_2(x,0|x',0) - G_1(x,0|x',0)]$$

obtains a single logarithm singularity in the point  $x=x'=a$ . Inverting of the kernel  $G_1(x,0|x',0)$  leads to the matrix equation of the form

$$(I + D_2) A = \frac{1}{2} f_1,$$

where the elements of matrix operator  $D_2$  have the following estimate

$$d_{pq}^{(2)} \sim \sum_m \frac{1}{mt+p} \cdot \frac{mt}{(mt)^2 - q^2}, \quad t = a^{-1}. \quad (5)$$

On the basis of results [3] it is proved that  $Dz$  is a  $\sigma$ -complete continuous operator in a pair of spaces  $l_1 \rightarrow l_2$ .

### ELECTRODYNAMIC MODELS AND NUMERICAL RESULTS

An application of the method of partial overlapping regions to the waveguide discontinuity problems is discussed to illustrate its basic advantages over other methods.

The problem of electromagnetic field diffraction in the H-plane modified power divider is solved. The used method permits to take into account a finite wall thickness between waveguides. The results of computer calculation of the junction parameters as a function of the coupling region length -  $l$ , thickness of the common wall -  $d$  and the wavelength in a waveguide -  $\lambda$  are shown in Fig. 1.

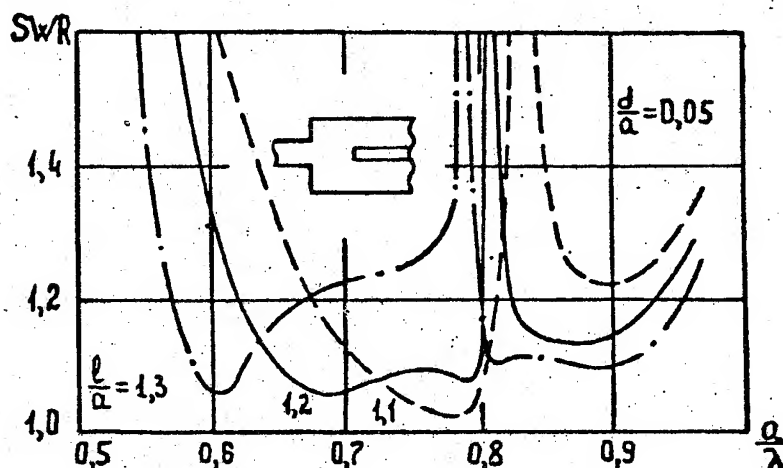


Fig. 1. Standing-wave ratio of the modified power divider with  $l$  and  $d$  as parameters.

It is seen from Fig. 1 that the operation frequency band of the power divider is extended when the coupling region length turns out near  $l=1.2$  of waveguide width. In this case a propagating  $H_{30}$  wave exists in the coupling region of junction. Hence,  $H_{30}$  wave may be used for extending the operation frequency band of the power divider. Physical processes of wave interaction in the coupling region of junction are studied.

The calculation of double-plane steps in the rectangular waveguide is performed. To solve the problem the numerical-analytical algorithm is developed based on the rigorous formulation of Huygens principle in form of integral theorems of three-dimensional diffraction. According to this theorem the electrical field vectors for each of overlapping regions may be written as follows [2]

$$\vec{E}(\vec{r}) = \vec{E}_{inc}(\vec{r}) - \nabla \times \int_S \vec{G}(\vec{r}, \vec{r}') \cdot [\vec{n} \times \vec{E}(\vec{r}')] ds', \quad (6)$$

where  $\vec{E}_{inc}(\vec{r})$  - is an incident field of  $TE_{10}$  -mode and  $\vec{G}(\vec{r}, \vec{r}')$  - is a dyadic Green's function of the electrical type of second kind for the rectangular waveguide, that satisfy the tensor equation

$$\nabla \times \nabla \times \vec{G}(\vec{r}, \vec{r}') - k^2 \vec{G}(\vec{r}, \vec{r}') = \vec{I} \delta(\vec{r} - \vec{r}') \quad (7)$$

and boundary conditions

$$\begin{cases} \vec{n} \times [\nabla \times \vec{G}(\vec{r}, \vec{r}')] = 0, \\ \vec{n} \cdot \vec{G}(\vec{r}, \vec{r}') = 0, \end{cases} \quad \vec{r}, \vec{r}' \in S. \quad (8)$$

The field continuity on a common part of the overlapping regions leads to the system of interconnected integral equations. The last one is converted into the matrix equation of the second kind.

Numerical convergence is confirmed by comparison with experimental data. Transmission and reflection coefficients behaviour over the frequency range is presented for various electrical dimensions of the waveguides.

The modified waveguide double bridge is investigated with the above method. The scattering matrix elements of junction are obtained. It's behaviour over the

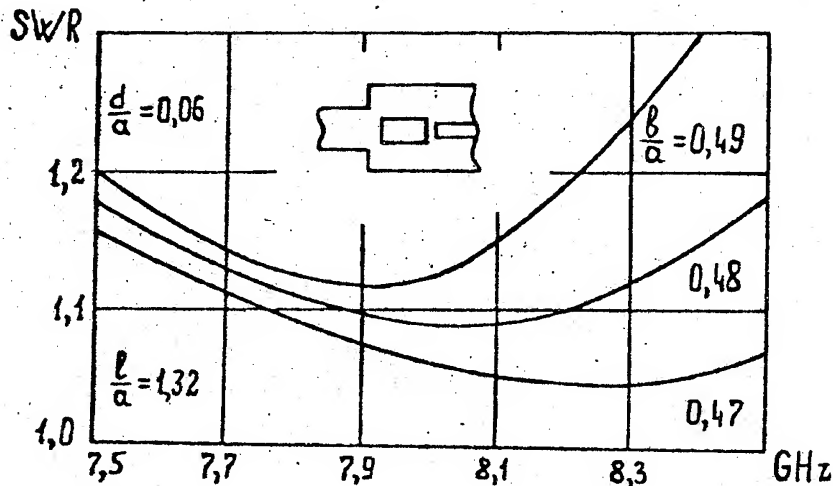


Fig. 2 Standing-wave ratio of the double bridge as a function of frequency and its geometrical dimensions.

frequency range is studied in order to extend the operation frequency band. Fig.2 demonstrates a number of obtained numerical results. It is shown that SWR in the H-port of junction is a function of frequency and geometrical dimensions. Comparison of the numerical results obtained from the analysis and published data shows good agreement.

### CONCLUSIONS

Thus, the method of partial overlapping regions possesses a number of advantages over other methods namely: the universality, the simplicity of realization, the mathematical correctness. It permits to solve a wide class of the internal and external electrodynamics problems.

### REFERENCES

- (1) I. Prokhoda, V. Chumachenko: "The method of partial overlapping regions to investigation of the complicated form waveguide-resonator systems", *Izv. Vuzov. Radiophysics*, (1973) v. 16, 10, pp. 1578-1581 (in Russian).
- (2) I. Prokhoda, S. Dmitryuk, V. Morozov: "Tensor Green's functions and their applications in the electrodynamics", (DSU, Dnepropetrovsk, 1985, in Russian).
- (3) I. Petrusenko, A. Yakovlev: "About complete continuity of some operators of the method of partial overlapping regions", in "Differential equations and its applications in physics", DSU, 1991, pp. 55-60 (in Russian).

THE SCATTERING OF THE PULSED ELECTRIC DIPOLE FIELD  
BY PERFECTLY CONDUCTING BODIES OF REVOLUTION

M. Doroshenko, R. Djobava, R. Zaridze

Department of Physics, Tbilisi University,  
Chavchavadze ave., 3, 380028, Tbilisi, Republic of Georgia

Abstract

Some results of the investigation of the pulsed electric dipole (PED) field scattered by the perfectly conducting prolate spheroid are presented. The excitation by sources with various time dependence of dipole moment is considered. The bistatic responses of spheroid in far zone and space-time distribution of the induced surface currents are investigated. The analysis of the physics of the transition processes is carried out.

1. Problem statement and solution method

Let us consider the PED field scattering from perfectly conducting prolate spheroid with semimajor axis  $C = 0.50$  and semiminor axis  $A = 0.25$  in a case when exciting dipole is located on the axis of revolution on the distance  $d = 0.20$  from the surface of the object. The dipole moment is polarized along the axis of revolution. The geometry of the problem is shown in Fig.1.

The problem is solved by using Fourier synthesis technique [1]. The frequency domain solutions are calculated by the auxiliary sources method (ASM) [2] and there is close relationship with the Yasuura method (mode-matching method) [3]. The basic idea of the ASM is the scattered field approximation as a superposition of the fields radiated by finite number of the auxiliary sources (AS) located inside the scatterer and constructed on a base of fundamental solutions of Helmholtz equation. For the purpose of increasing of the accuracy of the boundary problem solution and CPU time minimization the AS are located in the singularities regions of the fields extended inside the scatterer [3]. For solving of this concrete problem the effective modification of ASM based on the axial symmetry [4] is used. Followed from the symmetry of the problem and from excitation mode we use vertical electric dipoles as an auxiliary sources and locate them on the axis of revolution. There are two singularities region in this case: point of electrostatic image of exciting dipole and segment between focal points and the AS was located exactly in these two regions. Unknown coefficients of scattered field was determined from boundary conditions by collocations method as the solution of linear algebraic equations system with  $N \times M$  matrix [4] where  $M = N/2$ . " $M$ " is number of AS and " $N$ " is number of collocation points.

The frequency characteristic of spheroid was calculated over the interval  $0.1 \leq kL \leq 40.0$  with increment  $kL = 0.1$  ( $L = 2C$  and " $k$ " is the wave number in free space). Normalized residual of boundary condition over considered frequency interval is less than 0.001. In all figures real parts of currents and scattered fields are plotted.

2. Excitation by PED with non-modulated Gaussian moment

Let us consider that the exciting dipole moment  $p(t)$  has non-modulated Gaussian envelope with  $ct_0 = 1.0$  duration (we use  $ct$  units, " $c$ " is light velocity):

$$p(t) = \alpha \frac{1}{\sqrt{\pi}} \exp[-\alpha^2 (ct)^2], \quad (1)$$

" $\alpha$ " is parameter of Gaussian pulse.

Here we analyse induced surface currents. From geometry of the problem follows that for any AS with radius-vector  $\vec{r}'$  and any surface point with  $\vec{r}$  expression  $|\vec{r} - \vec{r}'| < cT_0$  is correct. At the same time for large part of the spheroid with the mean dimension  $L' = L - d$  (from top pole)  $L' < cT_0$  is correct. From this expressions and in correspondence with the mechanism of PED radiation [5] follows that surface large part located in "induction zone" in relation to both of AS and exciting dipole. Therefore induced surface current  $j$  consists of two terms: first term is proportional to dipole moment first time derivative (dominating term) and the second one - to second time derivative. Currents against time  $j = j(t)$  in surface different points are shown in Fig.2. Currents on poles are equal to zero. In the vicinity of top pole ( $\theta = 0.38^\circ$ ) one can observe two different components of current: pulse directly induced by the incident field - fundamental pulse (FP) and pulse reflected by bottom pole of spheroid - reflected pulse (RP). Duration of FP component is equal to  $cT_0$  and duration of RP is slightly large as  $cT_0$  since travelling pulse interferes with incident field. Time delay between FP and RP  $ct = 2.49$  is in good agreement with corresponding quantity in geometrical optics (GO) approximation  $ct = 2.50$ . In the vicinity of bottom pole ( $\theta = 177.37^\circ$ ) one can observe FP component and component reflected by top pole. During increasing the angle  $\theta$  one can observe following effects:

- 1) time delay between FP and RP is decreasing,
- 2) "retarding" of FP component in the point of observation,
- 3) increasing of RP amplitude; it can be explained by decreasing of part of spheroid generant traveled by RP.

Let us analyse currents distribution on the surface of the scatterer. Currents pattern  $j = j(\theta)$  at time fixed moments is shown in Fig.3. At time moment  $t = 0.38$  a peak of  $j(\theta)$  arises in point with  $\theta = 5.5^\circ$ . After this current pulse follows incident field. Later one can observe positive overshoot moving after dominate negative peak. This overshoot can be explained by "removing" electrons in the incident field propagation direction that causes positive charge region advection. Current reaches maximum at  $t = 0.6$  that is slightly later then peak of incident pulse reaches this point. Peak of current reaches bottom pole at  $t = 1.9$  and incident field peak - at  $t = 1.5$ . This time delay can be explained by fact that incident pulse moves along axis of revolution and current pulse moves along the generant which is longer then  $L$ . After this one can observe reflection of negative peak from bottom pole and current begin propagate to the opposite direction (i.e. to the top pole).

Here we investigate bistatic responses of the spheroid in far zone. The scattered field patterns against time at different angles of observation  $\theta = 30^\circ$ ,  $90^\circ$  and  $150^\circ$  are shown in Fig.4. Let us consider response at  $\theta = 30^\circ$ . This response consists of two terms: specularly reflected (SR) pulse which is proportional to  $dp(t)/dt$  and creeping wave (CW), proportional to  $d^2p(t)/dt^2$ . The SR duration is equal to  $cT_0$  and CW duration is slightly longer then  $cT_0$ . Time delay between SR and CW  $t = 2.1$  and this is in good agreement with corresponding quantity in GO approximation when angle of observation is taking into account. Note that calculations was carried out with creeping wave precise velocity which is differs from light velocity [6]. Small spike of scattered field at later time (specifically at large  $\theta$ ) can be explained by field radiation of current reflected from top pole.

During increasing the angle of observation  $\theta$  one can observe following effects:

- 1) smooth transition from the sum of two above mentioned terms to the pulse proportional to  $d^2p(t)/dt^2$ ,
- 2) time delay decreasing,
- 3) scattered field "retarding" in the point of observation,
- 4) increasing of the response amplitude.

### 3. Excitation by PED with modulated Gaussian moment

Let us consider that the exciting dipole moment has modulated Gaussian envelope with  $ct_0 = 1.0$  duration and modulation frequency  $\omega_m$  corresponding to  $k_0 L = 20.0$ :

$$p(t) = \alpha / \sqrt{\pi} \exp[-\alpha^2 (ct)^2] \exp(-i\omega_m t) \quad (2)$$

Here we describe briefly some results of this case.

Surface current patterns against time  $j = j(t)$  in the polar regions of spheroid are shown in Fig.5. In top pole region current consists of two terms: fundamental pulse (FP) and pulse reflected by bottom pole of spheroid - reflected pulse (RP). Duration of FP component is equal to  $ct_0$ . Time delay between FP and RP is  $t = 2.46$  that is in good agreement with GO approximation. Delay between time of current pulses arising in points with  $\theta = 0.38^\circ$  and  $\theta = 177.37^\circ$  is equal to 1.1 that is practically coincides in time with incident pulse leading edge propagates from top pole to the bottom one along the axis of revolution. In a point with  $\theta = 177.37^\circ$  both of this terms completely superimposed and RP is inverted in relation to FP. The rest of effects arising during increasing of angle of observation are similar to above mentioned effects in a case of PED moment given by (1).

Far field response at  $\theta = 30^\circ$  is shown in Fig.6. This response consists of SR and CW terms. Duration of SR is equal to  $ct_0$ . Time delay between SR and CW is equal to 2.07 (again we have good agreement with GO approximation). Small spike of scattered field at later time can be explained by radiation of current reflected from top pole. The effects arising during increasing of  $\theta$  are similar to above mentioned effects in a case of PED moment given by (1).

### Conclusion

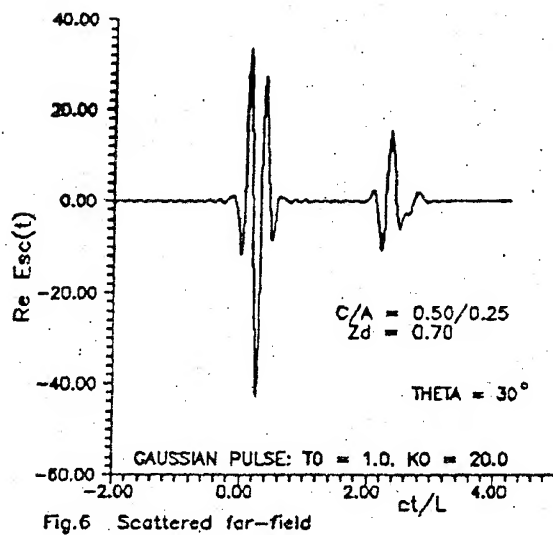
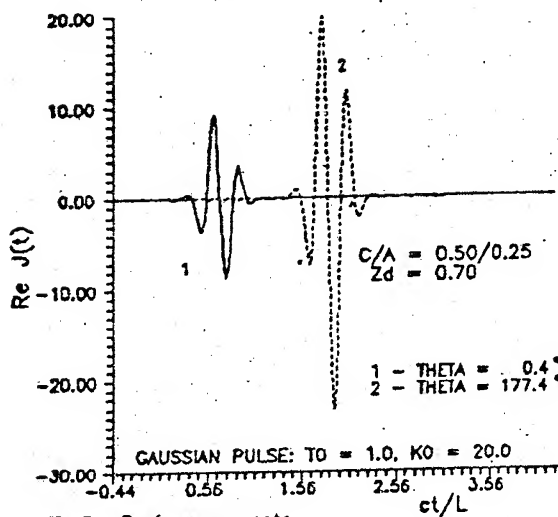
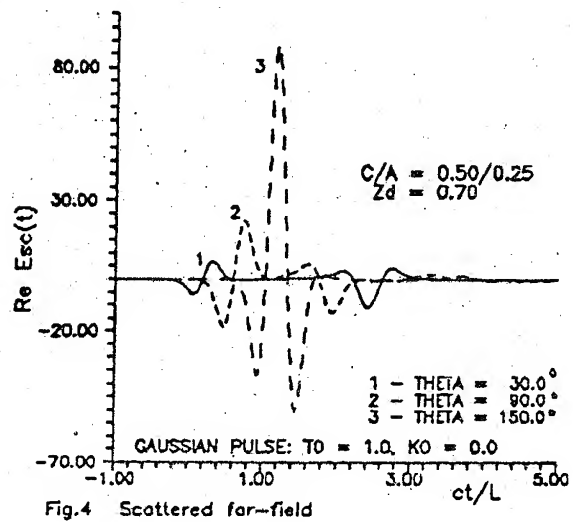
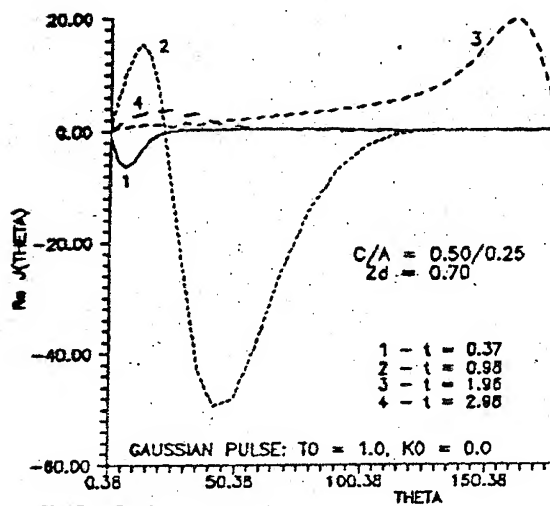
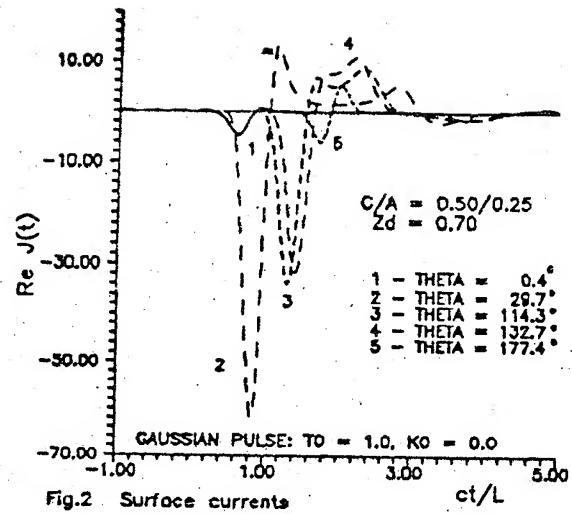
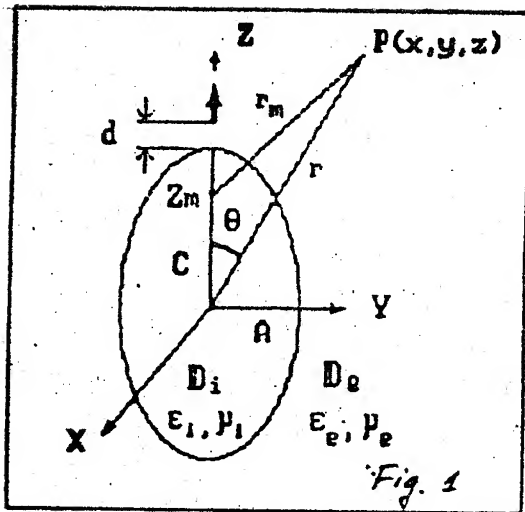
Let us briefly summarize presented results. Relation between scatterers geometry and dimensions from one side and time delay between SR and CW from another side is shown. Mechanism of arising and distribution of induced currents and charges is analysed. The exciting dipole moment envelope effect on surface current and scattered field is also investigated. All above mentioned effects are in good agreement with corresponding results of GO approximation, when angle of observation and CW precise velocity are taken into account.

Presented results demonstrated efficiency of the auxiliary sources method application in combination with Fourier synthesis technique for bodies of revolution.

### References

1. E.M. Kennaugh, D.L. Moffat, "Transient and Impulse Response Approximations" Proc. IEEE, vol.53, pp.893-901, 1965.
2. R.S. Zaridze et al., "A Method of Auxiliary Sources in Applied Electrodynamics", Proc. of URSI Int.Symp. on EM Theory, part A, p.104, Budapest, 1986.
3. H. Ikuno, M. Nishimoto, "Numerical analysis of three-dimensional scattering problems by the Yasuura method", Trans.IECC, vol.J72-C-1, pp.689-695, 1989.
4. Sveshnikov A.G., Eremin Yu.A, Orlov N.V., "Investigation of some mathematical models in the diffraction theory by the method of nonorthogonal series", Radiotekhnika i Elektronika, vol.30, No.4, pp.697-704, 1985 (in Russian).
5. G. Franceschetti, C.H. Papas, "Pulsed antennas", IEEE Trans., vol.AP-22, No.5, pp.651-661, 1974.
6. H.C. van de Hulst. Light Scattering by Small Particles, John Wiley & Sons, Inc., New York, 1957.







# THE INVESTIGATION OF TIME RESPONSES OF DIELECTRIC BODIES OF REVOLUTION

M. Doroshenko, R. Zaridze

Department of Physics, Tbilisi University,  
Chavchavadze ave., 3, 380028, Tbilisi, Georgia

## ABSTRACT

Some results of the investigation of both lossless and lossy prolate dielectric spheroids transient responses for different angles of observation in a case of excitation by pointwise vertical pulsed electric dipole are presented. Above mentioned scatterers bistatic transient responses are calculated by using Fourier synthesis technique. Scatterer's oscillations eigenfrequencies are determined numerically and relation between transient response structure and eigenfields radiation is shown.

## 1. INTRODUCTION

One of the most actual problems arising in various applications of transient electromagnetic fields [1] is a three-dimensional perfectly conducting and dielectric scatterers geometry and material determination. Accurate results for these problems are significant in microwave remote sensing and high resolution radar [2]. Most successfully this problem can be solved by the investigation of scatterers bistatic transient responses (TR). Specific resonance effects arising in the case of dielectric scatterers requires detail investigations of their frequency responses (FR).

For solving the above mentioned problems for dielectric objects the frequency approach is more preferable because it allows one to investigate both TR, FR and scattered fields in a case of monochromatic excitation simultaneously.

One of the most serious problems arising in frequency approach is frequency domain solution method choosing. This method must be flexible and it must allows one to minimize required CPU time. The frequency domain solutions are obtained by the Auxiliary Sources Method (ASM) [3, 4]. The ASM is one of the multiple expansion methods [5] and it is powerful and reliable numerical method for solving acoustic and electromagnetic boundary value problems.

Data transforming from the frequency domain into the time domain was carried out by Fourier synthesis technique [6].

## 2. PROBLEM STATEMENT AND SOLUTION METHOD

Let us consider the pulsed electric dipole (PED) field scattering by the dielectric prolate spheroid in a case when exciting dipole is located on the axis of revolution. The dipole moment is polarized along the axis of revolution. Problem's geometry is shown in Fig.1.

It was already mentioned that the frequency domain solutions was obtained by the ASM. The basic idea of this method is the scattered field representation as a superposition of fields radiated by finite number of the Auxiliary Sources (AS) located inside the scatterer and constructed on a base of Helmholtz equation fundamental solutions.

For solving of considered axial symmetric problems the effective modification of ASM based on the axial symmetry is used [7]. Following from the problem symmetry and from incident field polarization one can locate AS on the axis of revolution and polarize them along exciting dipole. From symmetry also follows that it is possible to satisfy boundary conditions only on the surface generant.

The criterion of the problem solution accuracy is the boundary condition residual in the norm of functional space  $L_2$ .

### 3. PED FIELD SCATTERING BY THE DIELECTRIC SPHEROID

Let us consider the pointwise vertical electric dipole field scattering by located in free space lossless prolate spheroid with semi-axis ratio  $C/A = 2.00$  and permittivity  $\epsilon_1 = 8.0 + i \cdot 0.0$ . It was assumed that permeability  $\mu_1 = 1$  and frequency dispersion is neglected. Exciting dipole is located on the axis of revolution at the distance  $d = 0.20 \cdot L$  from the top tip of the object ( $L = 2 \cdot C$  - length of spheroid).

The frequency response of spheroid was calculated over the interval  $0.05 \leq k_0 L \leq 20.00$  with increment  $\Delta(k_0 L) = 0.05$ . The boundary conditions normalized residual over considered frequency interval was less than 0.001.

Let us consider transient responses of lossless and lossy spheroids in a case of excitation by PED with non-modulated Gaussian dipole moment with relative duration  $ct_0/L = 1$  (we use relative  $ct/L$  units, "c" is light velocity).

Lossless spheroid TR at  $\theta = 30^\circ$  is presented in Fig. 2. This TR consists of three different components: specularly reflected (SR) pulse, creeping wave (CW), and oscillations corresponding to field radiation at resonance frequencies (RC). The SR relative duration is equal to  $ct_0/L$  and CW duration is slightly longer than  $ct_0/L$ . Time delay between SR and CW is equal to the same time delay in a case of perfectly conducting spheroid and it is in a good agreement with corresponding quantity in GO approximation.

When increasing angle  $\theta$  one can observe following effects:

- 1) amplitudes of SR, CW and RC are increasing;
- 2) time delay between SR and CW decreasing;
- 3) CW and RC superimposed.

These effects can be explained by all above mentioned components length of optical ways changing with observation angle increasing.

When increasing incident pulse duration all TR components are superimposed with each other.

Let us discuss the resonance component in more detail. There are some well known methods for resonances (eigenfrequencies) extraction from transient fields [8, 9]. For resonance frequencies extraction we use simple method which takes into account the fact that scattered field radiation pattern at the resonance frequencies significantly differs from radiation patterns at nonresonance frequencies.

For determination of frequencies at which occurs most intensive scattered field radiation along five arbitrarily taken directions  $\theta = 30^\circ, 60^\circ, 90^\circ, 120^\circ$  and  $150^\circ$  was analyzed following quantity:

$$\langle E^e(k_0 L) \rangle = \text{Pr} \{ E^e(k_0 L, \theta) \}$$

where "Pr" denotes production and  $E^e(k_0 L, \theta)$  denotes scattered E field y-component (in spherical coordinat system) spectrum along observation angle  $\theta$ . In Fig. 3 is shown  $\langle E^e(k_0 L) \rangle$  over considered frequency range. If compare it with scattered field spectra at various angles of observation, one can see that along all mentioned directions scattered field's most intensive radiation take place exactly at the resonance frequencies.

Let us investigate now the quantity

$$\langle E_T^e(k_0 L) \rangle = \text{Pr} \{ E_T^e(k_0 L, \theta) \}$$

$E_T^e(k_0 L, \theta)$  - spectrum of extracted from complete TR resonance component at angle  $\theta$ . Quantity  $\langle E_T^e(k_0 L) \rangle$  for  $ct_0/L = 1.0$  pulse is shown in Fig. 4. From comparison of this spectrum with corresponding  $\langle E^e(k_0 L) \rangle$  for scattered far field (spheroid's FR) (Fig. 3) follows that RC arises from eigenfields oscillations at the resonance frequencies.  $\langle E_T^e(k_0 L) \rangle$  in a case of Gaussian pulse with  $ct_0/L = 2.0$  is shown in

Fig. 5. Only two resonance frequencies occurs in this case and one can explain this fact by decreasing of the incident pulse spectrum width. In a case when exciting dipole moment has modulated Gaussian envelope with modulation frequency  $k_{mod}L = 10.0$  and  $ct_0/L = 1.0$  quantity  $\langle E_T^2(k_0, L) \rangle$  corresponding to this pulse is, practically, the same with plotted in Fig. 4. It corroborates the fact that RC is related with field radiation at the resonance frequencies. Resonance oscillations amplitudes are decreasing with increasing  $ct/L$  because of energy losses by radiation.

Responses of lossy spheroid consists only of SR and CW components (see Fig. 2, this response for convenience is shifted by  $-10.0$ ). SR practically completely correlate with lossless spheroid SR. Time delay between SR and CW is the same as for lossless spheroid and as for perfectly conducting one. From these follows that for imaging of strongly absorbing objects one can use methods which was developed for perfectly conducting targets [10]. RC is absent because of strong absorption.

The effects arising when increasing of  $\theta$  are similar to above mentioned effects in a case of lossless spheroid.

#### 4. CONCLUSION

Let us briefly summarize presented results.

Both lossless and lossy scatterers bistatic transient responses are calculated for excitation by pointwise PED with dipole moment various time dependence, modulation frequency and duration. Relation between scatterers geometry, dimensions and permittivity from one side and time delay between specular response and creeping wave from another side was investigated. All above mentioned effects are in a good agreement with corresponding results in GO approximation when angle of observation and CW precise velocity are taken into account.

The TR resonance component and scatterer's eigenfields radiation was also investigated and the possibility of scatterer's permittivity determination was shown.

Presented results demonstrated efficiency of using of Fourier synthesis technique and the ASM combination for transient scattering problems investigations.

Obtained results can be used in radar technology, inverse and target identification problems, microwave remote sensing.

#### REFERENCES

1. C.L. Bennet, G.F. Ross, "Time Domain Electromagnetics and Its Applications", Proc. IEEE, March 1978, pp. 299-318.
2. A.P. Agraval, W.M. Boerner, "Redevelopment of Kennaugh's target characteristic polarization state theory using the polarization transformation ratio formalism for the coherent case", IEEE Trans. Antennas Propagat., vol. AP-27, pp. 2-14, 1989.
3. R.S. Zaridze et al., "A Method of Auxiliary Sources in Applied Electrodynamics", Proc. of URSI Int. Symp. on EM Theory, part A, p.104, Budapest, 1986.
4. Apelcin V.F., Zaridze R.S., Karkashadze D.D. and oth. "Method of Auxiliary Sources. Fields Calculation Out of Boundary Surfaces", Thesis of 9 All Union School on Diffraction and Wave Propagation. Kazan 1988. Edt. KAI, p.59 (In Russian).
5. H. Ikuno, M. Nishimoto, "Numerical analysis of three-dimensional scattering problems by the Yasuura method", Trans. IEICE, J72-C-I, pp. 689-696, 1989.
6. E.M. Kennaugh, D.L. Moffat, "Transient and Impulse Response Approximations" Proc. IEEE, vol. 53, pp. 893-901, 1965.
7. Sveshnikov A.G., Eremin Yu.A., Orlov N.V., "Investigation of Some Mathematical Models in the Diffraction Theory by the Method of Nonorthogonal Series", Radiotekhnika i Elektronika, vol. 30, No. 4, pp. 697-704, 1985 (in Russian).
8. J. Auton, M. van Blaricum, "Investigation of Procedure for Automatic Resonance Extraction from Noisy Transient Electromagnetic Data", Math. Notes, 79, vol. 1-3, 1981.
9. A.G. Ramm, "Extraction of Resonances from Transient Fields", IEEE Trans., vol. AP-33, No. 2, 1985, pp. 223-226.
10. T. Uno, Y. Miki, S. Adachi, "One-Dimensional Radar Target Imaging of Lossy Dielectric Bodies of Revolution", IEICE Trans., vol. E74, No. 9, 1991, pp. 2915-2921.

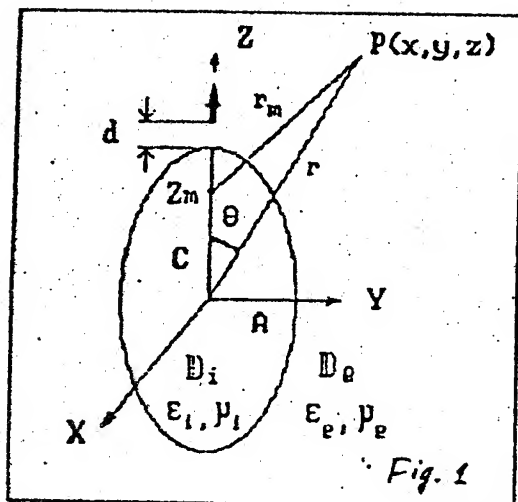


Fig. 1

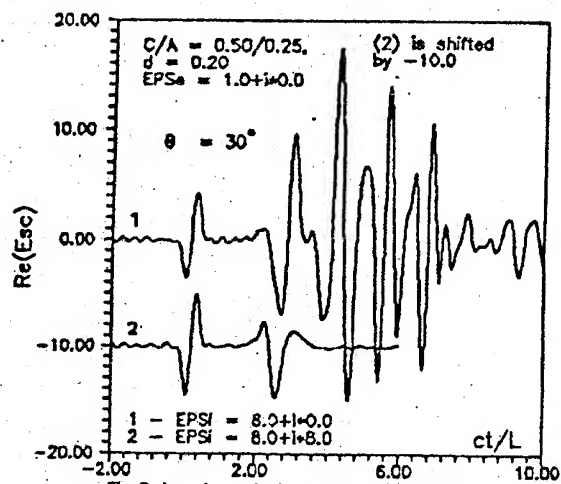


Fig. 2 Lossless & lossy spheroids TRs

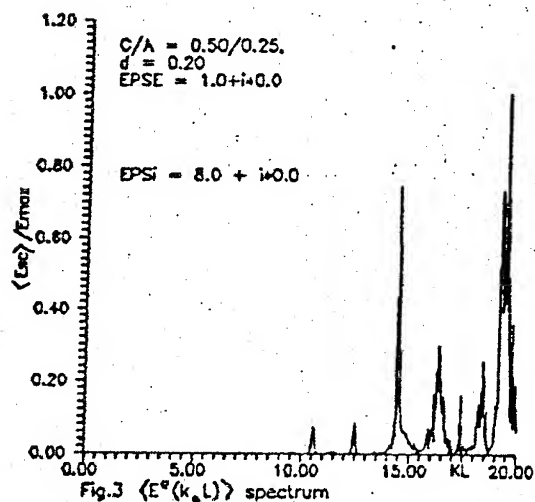


Fig. 3  $\langle E^*(k, L) \rangle$  spectrum

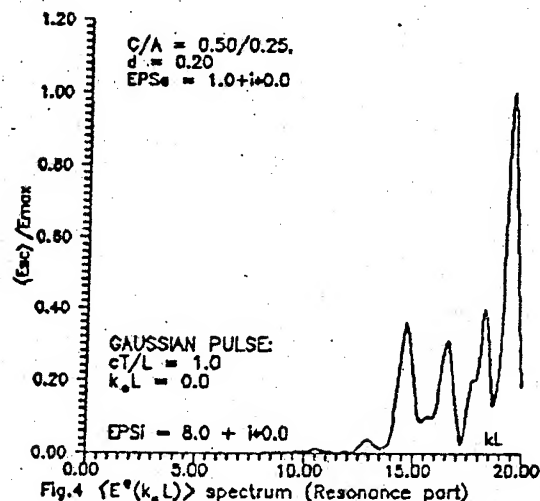


Fig. 4  $\langle E^*(k, L) \rangle$  spectrum (Resonance part)

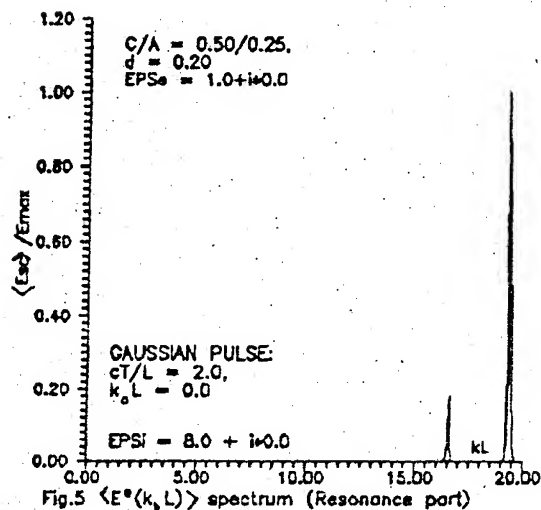


Fig. 5  $\langle E^*(k, L) \rangle$  spectrum (Resonance part)

# ANALYSIS OF IRREGULAR RECTANGULAR WAVEGUIDE STRUCTURE WITH ARBITRARY SHAPED CENTRAL SEPTUM

F.F.Dubrovka, Yu.V.Petrushevsky

Kijiv Polytechnical Institute, Theoretical Radioengineering Department  
KPI-2110, Peremohy prospect, 37, Kijiv, 252056, Ukraine  
(Phone: +7-044-441-9588, Fax: +7-044-274-0954)

## Abstract

The complete analysis of irregular rectangular waveguide structure with arbitrary shaped metal thin central septum is presented. The solution of ridged waveguide eigenvalue problem is obtained by the original formulation of an integral equation for infinitesimally thin ridges. The solution of discontinuity problem is obtained by formulation of an integral equation for each discontinuity type. The scattering matrices of discontinuities and regular transmission lines are progressively cascaded to determine the overall generalized scattering matrix of the structure:

## 1. Introduction

In-line configuration septum devices like [1,2] are exceptionally suitable for application in modern polarisation control systems due to their compactness and compatibility with typical requirements imposed on antenna array geometry. Such a device consists of a square or rectangular waveguide body divided by a thin central metal septum. The upper and lower septum parts together produce required differential phase shift between orthogonally polarized field components.

## 2. Formulations and Solutions

In order to determine the propagation characteristics of the septum devices, a generalised scattering matrix of the longitudinally irregular structure has to be obtained. The analysis is carried out in three steps. First, the structure is approximated by a number of regular section steps, being considered separately. Each septum region is equivalent to unsymmetrical double ridged waveguide. The solution of the ridged waveguide eigenvalue problem is well known [3,4]. But, as it is pointed out in [4], accuracy of the solutions degrades with decrease of the ridge thickness. We believe that the phenomenon occurs for errors of expanding fields components in terms of rectangular waveguide eigenfunctions in the gap region and errors, associated with the different edge singularity for thin and thick ridges.

In this report we describe a solution for ridged waveguide eigenvalue problem for infinitesimally thin ridges which excludes above-mentioned errors. The analysis is more accurate for thin ridges, than the finite ridges technique [3,4].

Geometries of the ridged and unsymmetrical ridged waveguides are illustrated in Fig.1 and Fig.2 accordingly. We have proposed two different solutions of the eigenvalue

problem: 1) with formulation in terms of electric field in the gap; 2) in terms of magnetic field on the ridges. As an example in this report we consider boundary condition for TE fields with the magnetic wall at YZ-plane. The TE modal fields are expressed in terms of a complete set of rectangular waveguide modes with unknown coefficients:

$$H_z = \sum_{n=0}^{\infty} A_n \sqrt{\frac{2 - \delta_{0n}}{b}} \cos \frac{n\pi y}{b} \cos \left( \left( \frac{a}{2} - x \right) \sqrt{k_c^2 - \left( \frac{n\pi}{a} \right)^2} \right), \quad (1)$$

where  $k_c$  - eigenvalues,  $A_n$  - unknown coefficients. By applying the boundary conditions we obtain the following integral eigenvalue equations: in term of electric field in the gap

$$\sum_{n=0}^{\infty} (2 - \delta_{0n}) \frac{\text{ctg} \frac{\sqrt{\varphi}}{2}}{\sqrt{\varphi}} \cos \frac{n\pi y}{b} \int_{-d}^{1+d} E_y(y) \cos \frac{n\pi y}{b} dy = 0, \quad (2)$$

and in term of magnetic field on the ridges

$$\sum_{n=0}^{\infty} (2 - \delta_{0n}) \text{tg} \frac{\sqrt{\varphi}}{2} \sqrt{\varphi} \cos \frac{n\pi y}{b} \left[ \int_0^{1-d} H_z(y) \cos \frac{n\pi y}{b} dy + \int_{1+d}^b H_z(y) \cos \left( \frac{n\pi y}{b} \right) dy \right] = 0, \quad (3)$$

where  $\varphi = (k_c a)^2 - \left( \frac{n\pi a}{b} \right)^2$ .

By expanding the aperture field in terms of special weighted Chebyshev polynomials with unknown coefficients [4] and then applying Galerkin's method, the eigenvalue equation is transformed into a matrix equation. The solution of the eigenvalue equation gives the associated eigenmode.

The second step in the analysis is obtaining generalized scattering matrices of changes (discontinuities) in waveguide cross-section. There are three types of waveguide discontinuities in this problem: a junction between empty and unsymmetrical double ridged waveguides; a junction between the two double ridged waveguides; a junction between the double ridged waveguide and waveguide entirely divided by thin metal septum into two independent equal rectangular sections. For all these discontinuities fields in the plane of the junction are expanded in terms of the unsymmetrical double ridged waveguide eigenmodes. By solving an integral equation the scattering matrix for the isolated discontinuity is obtained.

And finally, to determine the overall generalized scattering matrix, the scattering matrices of discontinuities and regular transmission lines are progressively cascaded.

### 3. Numerical Results and Practical Realizations

The most significant improvement of existing technique for analysis of irregular rectangular waveguide septum structure we have achieved by the new formulation of eigenvalue problem. The two different solutions of integral eigenvalue problem with formulation in term of electric field in the gap and in term of magnetic field on the ridges give upper and lower approximations to cut-off frequencies. Besides, the general order  $N$  of the eigenvalue matrix equation can be made lower than third (with 0.1% accuracy for cut-off frequency) due to appropriate expanding the aperture field in terms of special weighted Chebyshev polynomials with taking properly into account the edge singularity for thin ridges. These points effect a saving in computation time. The convergence of this approach for  $k_c a$  of the square ridged waveguide dominant mode is illustrated in tables 1 and 2 for integral eigenvalue formulation in term of electric field in the gap (2) and in term of magnetic field on the ridges (3) accordingly.

By means of the given technique we have designed extremely compact orthomode transducer with original upper and lower septum form (Fig.3), which provides the differential phase shift 90 degrees between orthogonally polarized field components. The measured performances in 15% frequency range are: VSWR - better than 1.15; isolation - better than 36 dB; ellipticity - better than 0.3 dB. Cross section dimensions are  $0.6\lambda \times 0.6\lambda$ , where  $\lambda$  is average wavelength.

With the results obtained we have also designed square waveguide rotator with VSWR less than 1.15 and differential phase shift 180 degrees over 25% frequency range.

### 4. Conclusion

We have described a new rigorous analysis of irregular rectangular waveguide structure with arbitrary shaped central septum. The technique can be used for design of extremely compact septum devices, such as differential phase shifters, ridged waveguide filters, orthomode transducers, polarization rotators, etc.

### References

- (1) N.D.Dang, S.Kapartis, and D.J.Brain: "A wide-band compact end-entry septum polariser OMT," Proc. ICAP-87, pp.419-424.
- (2) A.Witte, H.Wong, G.Kroupa: "Dual septum polarization rotator," EP 0482456, (1992).
- (3) J.P.Montgomery: "On the complete eigenvalue solution of ridged waveguide," Trans.IEEE,(1971) MTT-19, 6, pp.547-555
- (4) G.F.Zargano et al.: "Waveguides of complex cross section," Moscow, Radio and Communications, (1986), 124p.

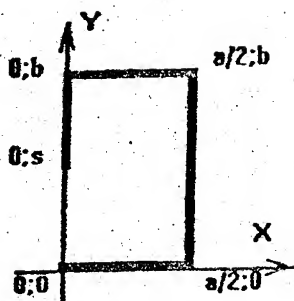


Fig. 1

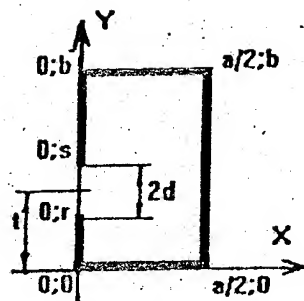


Fig. 2

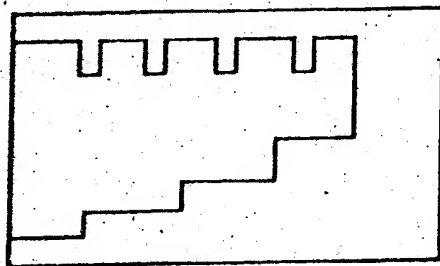


Fig. 3

Table 1

s/b	N=0	N=1	N=2
0,05	1,0250	1,0249	1,0249
0,1	1,1630	1,1630	1,1630
0,2	1,3768	1,3770	1,3770
0,3	1,5763	1,5769	1,5769
0,4	1,7888	1,7909	1,7909
0,5	2,0298	2,0341	2,0341
0,6	2,3094	2,3140	2,3142
0,7	2,6266	2,6245	2,6248
0,8	2,8129	2,9093	2,9103
0,9	2,6677	3,0863	3,0884
0,95	2,5595	3,1249	3,1289

Table 2

s/b	N=0	N=1	N=2
0,05	1,0273	1,0243	1,0231
0,1	1,1621	1,1621	1,1618
0,2	1,3771	1,3755	1,3754
0,3	1,5782	1,5754	1,5754
0,4	1,7924	1,7895	1,7895
0,5	2,0345	2,0325	2,0325
0,6	2,3146	2,3136	2,3135
0,7	2,6251	2,6248	2,6248
0,8	2,9101	2,9100	2,9100
0,9	3,0870	3,0868	3,0862
0,95	3,1287	3,1287	3,1287



# H-WAVEGUIDE WITH ROUNDED SHARP EDGES AND ANGLES

Anna G. Dudko, Victor I. Naidenko

Kiev Polytechnical Institute, KPI-2110, 37, prosp. Pobiedy,  
Kiev, 252056, Ukraine, Tel. +7-44-441-95-88, Fax: +7-44-274-59-32

## ABSTRACT

The eigenproblem for H-waveguide with rounded sharp edges and angles has been solved. It has been shown that proposed method has good convergency. Eigenvalues, fields have been calculated. Dependencies of eigenvalues on roundness radii are presented.

## INTRODUCTION

A conventional H-waveguide is not the best from the point of view of electrical parameters. To increase the transmitted power (breakdown power) it is expedient to do H-waveguide with rounded sharp edges (see fig.1) [1]. By rounding inner angle it is possible to decrease damping coefficient. Roundnesses are also expedient from the point of view of adaptability to production.

Such H-waveguide belongs to the class of electrodynamic objects with rounded sharp edges and angles, called below as objects with roundnesses. The objects with roundnesses have been investigated insufficiently. Complications to solve the boundary problem and absence of sufficiently effective and reliable calculation methods, satisfaction with characteristics of available devices were the main reasons of such state of affairs. However, due to the present more stringent requirements to the components and units, development of calculation methods,

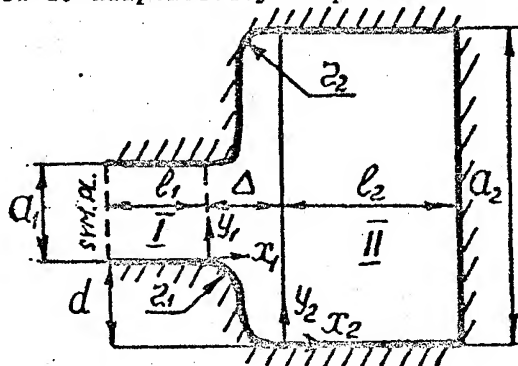


Fig.1

computer technology it is necessary and actual and possible in practice to solve problems for structures with rounded sharp edges and angles. The main difficulty is caused by the presence of straightforward and curve boundary sections. And, though from the point of view of convergency these problems are seemed to be simpler than the ones with sharp edges and angles, it is not trivial to obtain the constructive solution, and this problem is very actual.

## DESCRIPTION OF THE METHOD

To calculate eigenvalues, eigenfunctions and electrical parameters (characteristic impedance, maximum power, damping coefficient) of such H-waveguide various methods can be applied. But, investigation of this problem done by authors [2,3] has shown that the most effective method to solve it is one obtained as a result of synthesis of Ryaleigh hypothesis about analytical extension of solution of wave equation and mode matching method.

For H-waveguide with roundnesses problem is divided into two independent scalar ones, electric and magnetic. In its turn, due to the structure symmetry each of the latter is divided into two more with electric or magnetic wall in the symmetry plane (case of asymmetric location of contraction is considered).

Ryaleigh hypothesis applied to obtained problems consists in assumption that it is possible to present fields in region situated between planes  $x_2=0$  and  $x_2=-(r_1+r_2)$  (see fig.1) through expansion in eigenfunctions of rectangular region of larger cross section. The idea to use Ryaleigh hypothesis has appe-

ared in connection with advantages to solve boundary problem with minimum quantity of partial regions. In this case it is sufficient to consider only two partial regions (regions I and II in fig.1).

Fields in regions I and II are presented as for H-waves

$$H_z^I = \sum_{n=0}^{\infty} A_n^H \cos \frac{n\pi y_1}{a_1} \sin \left\{ \gamma_n (x_1 + l_1) \right\}, \quad H_z^{II} = \sum_{n=0}^{\infty} B_n^H \cos \frac{n\pi y_2}{a_2} \cos(\beta_n (x_2 - l_2)),$$

for E-waves

$$E_z^I = \sum_{n=1}^{\infty} A_n^E \sin \frac{n\pi y_1}{a_1} \cos \left\{ \gamma_n (x_1 + l_1) \right\}, \quad E_z^{II} = \sum_{n=1}^{\infty} B_n^E \sin \frac{n\pi y_2}{a_2} \sin(\beta_n (x_2 - l_2)).$$

Dependence on time and longitudinal coordinate  $\exp(i(\omega t - \alpha z))$  is omitted.

In the case of symmetrical H-waveguide summation in abovementioned expressions is done with respect to either odd or even  $m, n$ .

Expressing transverse components of the fields through longitudinal ones, matching tangential components on the boundary of regions I and II, using Galerkin method [2] homogeneous linear algebraic equation system (LAES) has been obtained

$$\sum_n B_n^{H(E)} \left[ \cos(\beta_n (l_2 + \Delta)) \sum_n d_{nm}^{H(E)} \frac{\operatorname{ctg} \left\{ \gamma_n l_1 \right\}}{\operatorname{tg} \left\{ \gamma_n l_1 \right\}} f_{nm}^{H(E)} f_{np}^{H(E)} \pm I_{np}^{H(E)} \right] = 0,$$

$p = (0) 1 \dots \infty$

where

$$I_{np}^{H(E)} = \int_0^{a_2} \phi_n^{H(E)} \frac{\cos \left( \frac{p\pi y_2}{a_2} \right)}{\sin \left( \frac{p\pi y_2}{a_2} \right)} dy_2,$$

$$\phi_n^H(y_2) = \beta_n \cos \frac{p\pi y_2(\alpha)}{a_2} \sin [\beta_n (f(y_2(\alpha)) - l_2)] \sin \alpha +$$

$$\frac{n\pi}{a_2} \sin \frac{p\pi y_2(\alpha)}{a_2} \cos [\beta_n (f(y_2(\alpha)) - l_2)] \cos \alpha,$$

$$\phi_n^E(y_2) = \sin \frac{p\pi y_2}{a_2} \sin [\beta_n (f(y_2) - l_2)],$$

$$f_{nm}^{H(E)} = \frac{2}{a_1} \int_0^{a_1} \cos \frac{n\pi(y_1 + d)}{a_2} \cos \frac{n\pi y_1}{a_1} dy_1,$$

$$d_{nm}^H = \frac{a_1}{4} \frac{1}{\delta_n} \gamma_n, \quad d_{nm}^E = \frac{a_1}{2} \frac{1}{\gamma_n} \beta_n, \quad \delta_n = \begin{cases} 1, & n=0, \\ 1/2, & n \neq 0, \end{cases}$$

$f(y_2(\alpha)), y_2(\alpha)$  - functions that describe surface formed by roundnesses, straightforward sections of lug and boundary of partial regions,  $\alpha$  - angle between axis  $y$  and tangent to the boundary.

Nontrivial solutions of LAES are only possible when  $\det(B)=0$ , where  $B$  - LAES coefficient matrix.

From the latter equation we find cutoff wave number, and from LAES - coefficients  $B_n^{H(E)}$ .

Thus, the eigenproblem for H-waveguide with rounded sharp edges and angles has been solved.

## RESULTS

Algorithm that makes it possible to find effectively roots of equation for cutoff wave numbers has been developed. Correctness of application of Rayleigh hypothesis to solve problems of such kind has been shown.

Eigenvalues and fields of the main and the higher modes of H-waveguide with roundnesses have been calculated for various roundness radii. Dimensions of tested waveguide were:  $a_1=6$ ,  $a_2=20$ ,  $l_1=11$ ,  $l_2=9$ ,  $d=7$  (all dimensions are given for the case when there are no roundnesses). Fig.2 shows the dependence of normalized wavenumber  $kl$  ( $l=l_1+l_2+r_1+r_2$ ) of the main mode of the symmetrical H-waveguide with rounded sharp edges ( $r_1 \neq 0$ ,  $r_2=0$ ) on roundness radius  $r_1$ . Under the calculations in region I 10 waves were taken into account, in region II - 30 waves. The ratio of numbers of waves being taken into account was determining by Mittra's rule. The order of LAES was equal to 30. The analogous dependencies for the first two E-waves (magnetic wall in symmetry plane  $x_1=-l_1$  and electric wall in symmetry plane  $y_1=a_1/2$ ) are presented in fig.3. In this case it was enough to take into account in region I - 5 waves and in region II - 15 waves. The order of LAES was equal to 15. It is seen that rounding of sharp edges diminishes the normalized wavenumbers, moreover, roundnesses influence on wavenumbers of H-waves more than on wavenumbers of E-waves that is in keeping with physical considerations. Fig.4 shows the dependencies of  $kl$  on radius  $r_2$  ( $r_1=1$ ) for E-wave. Small radii practically do not influence on  $kl$ , but with further increase there is increase in wavenumbers.

Results have been compared with ones obtained by finite element method [4], and in the case of absence of roundness and symmetrical location of contraction - with ones obtained by mode matching method with subject to singularity on the edge [5].

It has been shown that proposed method has good convergency both for the first and the higher modes of H-waveguide with rounded sharp edges and angles. As an example, table 1 shows the results of covergency investigation for the case of E-waves ( $r_1=0.75$ ,  $r_2=0$ ). In it  $N_{max}$  and  $M_{max}$  - numbers of waves taken into account in region I and II, correspondingly.

Table 1

$r_1$	$N_{max}$	$M_{max}$	$kl_1$	$kl_2$
0.75	3	9	9.33506	14.24780
	4	12	9.33623	14.25090
	5	15	9.33651	14.25220
	6	18	9.33628	14.25209

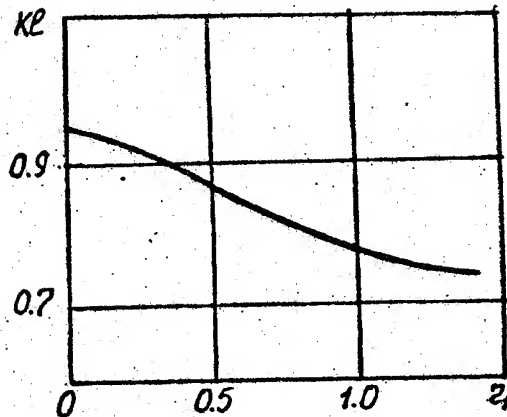


Fig.2

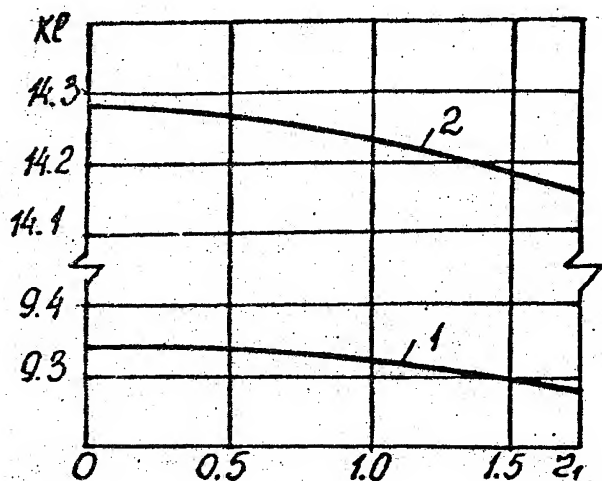


Fig. 3

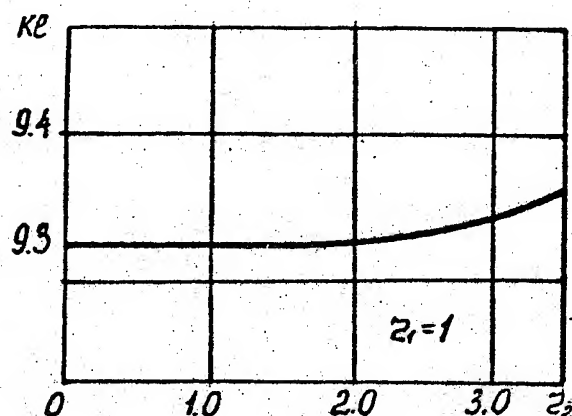


Fig. 4

#### REFERENCES

- [1] Koukharkin Eu.S., Sestroretski B.V. Electric strength of waveguide devices. - Moscow. - 1963. - 452 p.
- [2] Naidenko V.I. A Method to Calculate the Electrodynamical Systems with Rounded Sharp Edges //Dokl. AN Ukr.SSR, ser.A, 1990, N9.
- [3] Dudko A.G., Naidenko V.I. Calculation of H-plane Waveguide Tee with Rounded Sharp Edges and Conductive Lug by Method of Substitution of Wave Problem for Field Ones // 24th URSI GA, Japan, 1993.
- [4] Chepournykh I.P., Samoukhin G.S. Program to calculate the main electrodynamic characteristics of waveguides of arbitrary cross-section // Elektronika SVCh. - Ser.1, Elektronika SVCh. - 1976. - Is.2. - P.119-121.
- [5] Zargano G.F., Liapin V.P., Mikhalevski V.S. et al. Waveguides of complex cross-sections. - Moscow. - 1986. - 123 p.

# NUMERICAL REALISATION FOR THE DIFFRACTION PROBLEMS ON

## MULTIELEMENT GRATINGS

VLADIMIR DUSHKIN, YURJ GANDEL, NATALYA MOROZOVA

Department of Mechanics and Mathematics, Karkov State University  
4, Svobody Sq., Kharkov, 310077, Ukraine

Here is a suggestion to consider a new numerical and analytical method of solving the problem of electromagnetic wave diffraction by an infinite periodical grating constructed of perfectly conductive rectangular cross-section rods by the reduction it to a system of singular integral equations on an interval. The solution for which is made by the modified discrete singularities method.

Let a 2D-periodical structure constructed of the beams

$$B = \{ (x', y', z') : -\infty < x' < +\infty, |z'| < h, y' \in \bigcup_{n=-\infty}^{+\infty} CL_n \}$$

$$L_n = \bigcup_{i=1}^M (\alpha_i' + 2ln, \beta_i' + 2ln), \quad CL_n = [-1 + 2ln, 1 + 2ln] \setminus L_n,$$

be illuminated by a plane monochromatic wave. The dependance on time is supposed to be  $\exp(-i\omega t)$ . Due to the regularity of the structure along the OX axis the original problem can be reduced to the two scalar external boundary value problems for the Helmholtz equation with Dirichlet or Neumann boundary conditions. The solution will be sought with the following natural assumptions.

The field satisfies the Sommerfeld radiation condition, the conjugation conditions, the Meixner condition on the edge of a right dihedral angle:  $Ez \sim \rho^{-1/3}$ , where  $\rho$  is a space coordinate of a local in the edge vicinity polar coordinate system.

Let the grating be illuminated by an E-polarized wave  $u = e^{-ik(z'-h)}$  where  $k = \omega/c$  is the wave number.

The scattered field can be represented in the

$$e^{-k(z'-h)} + \sum_{n=-\infty}^{+\infty} a_n e^{-\bar{\gamma}_n(z'-h)} e^{i\frac{\pi}{l}ny'} \quad z' > h$$

$$\sum_{m=1}^{+\infty} (b_{1,m}^{(1)} \operatorname{ch}(\bar{\gamma}_{1,m} z') + b_{1,m}^{(2)} \operatorname{sh}(\bar{\gamma}_{1,m} z')) \sin\left(\frac{\pi m}{\beta_1' - \alpha_1'} (y' - \alpha_1')\right), \\ |z'| < h \quad y' \in (\alpha_i', \beta_i'), \quad i = 1..M$$

$$\sum_{n=-\infty}^{+\infty} a_n e^{-\bar{\gamma}_n(z'+h)} e^{i\frac{\pi}{l}ny'} \quad z' < h$$

where

$$\bar{\gamma}_n = \frac{\pi}{l} |n| \sqrt{1 - (kl)^2 / (n\pi)^2} \quad n \neq 0; \quad \bar{\gamma}_0 = -ik, \quad \bar{\gamma}_{1,m} = m \sqrt{\frac{\pi^2}{(\alpha_1' - \beta_1')^2} - \frac{k^2}{m^2}} \quad i = 1..m.$$

and  $\operatorname{Im}(\bar{\gamma}_n) \leq 0, \operatorname{Re}(\bar{\gamma}_n) \geq 0$

From the boundary conditions on the rods and the conjugation conditions two systems of the summator equations can be obtained:

for  $z=h$

$$1 + \sum_{n=-\infty}^{+\infty} A_n^+ e^{i \frac{\pi}{l} n y'} = 0, \quad y' \in \text{CLO}$$

$$1 + \sum_{n=-\infty}^{+\infty} A_n^+ e^{i \frac{\pi}{l} n y'} = \sum_{m=1}^{+\infty} (b_{1,m}^1 \text{ch}(\bar{r}_{1,m} h) + b_{1,m}^2 \text{sh}(\bar{r}_{1,m} h)) \sin\left(\frac{\pi m}{\beta_1' - \alpha_1'} (y' - \alpha_1')\right)$$

$$i k \sum_{n=-\infty}^{+\infty} A_n^+ \bar{r}_n e^{i \frac{\pi}{l} n y'} =$$

$$= - \sum_{m=1}^{+\infty} \bar{r}_{1,m} (b_{1,m}^1 \text{sh}(\bar{r}_{1,m} h) + b_{1,m}^2 \text{ch}(\bar{r}_{1,m} h)) \sin\left(\frac{\pi m}{\beta_1' - \alpha_1'} (y' - \alpha_1')\right),$$

$$y' \in (\alpha_1', \beta_1'), \quad 1=1..M,$$

and for  $z=-h$

$$\sum_{n=-\infty}^{+\infty} A_n^- e^{i \frac{\pi}{l} n y'} = 0, \quad y' \in \text{CLO}$$

$$\sum_{n=-\infty}^{+\infty} A_n^- e^{i \frac{\pi}{l} n y'} = \sum_{m=1}^{+\infty} (b_{1,m}^1 \text{ch}(\bar{r}_{1,m} h) - b_{1,m}^2 \text{sh}(\bar{r}_{1,m} h)) \sin\left(\frac{\pi m}{\beta_1' - \alpha_1'} (y' - \alpha_1')\right)$$

$$\sum_{n=-\infty}^{+\infty} A_n^- \bar{r}_n e^{i \frac{\pi}{l} n y'} =$$

$$= \sum_{m=1}^{+\infty} \bar{r}_{1,m} (-b_{1,m}^1 \text{sh}(\bar{r}_{1,m} h) + b_{1,m}^2 \text{ch}(\bar{r}_{1,m} h)) \sin\left(\frac{\pi m}{\beta_1' - \alpha_1'} (y' - \alpha_1')\right),$$

$$y' \in (\alpha_1', \beta_1'), \quad 1=1..M$$

Introducing the dimensionless variables ..

$$y = \frac{\pi}{l} y', \alpha_1 = \frac{\pi}{l} \alpha_1', \beta_1 = \frac{\pi}{l} \beta_1', x = \frac{l k}{\pi} = \frac{2l}{\lambda}, \quad 1=1..M$$

and denoting

$$r_n = |n| \sqrt{1 - (x/n)^2} \quad n \neq 0; \quad r_0 = -ix, \quad r_{1,m} = m \sqrt{1 - \frac{x^2 (\alpha_1' - \beta_1')^2}{m^2 \pi^2}}, \quad 1=1..M$$

after a simple transformations we can obtain a two systems of the summator equations:

$$\sum_{n=-\infty}^{+\infty} A_n e^{i n y} = 0, \quad y \in \text{CL} \quad (L = \bigcup_{l=1}^M (\alpha_l, \beta_l))$$

$$\sum_{n=-\infty}^{+\infty} A_n e^{i n y} = \sum_{m=1}^{+\infty} b_{1,m} \sin\left(\frac{\pi m}{\beta_1 - \alpha_1} (y - \alpha_1)\right) \quad y \in (\alpha_1, \beta_1) \quad 1=1..M$$

$$\sum_{n=-\infty}^{+\infty} A_n e^{i n y} = - \frac{\pi}{\beta_1 - \alpha_1} \sum_{m=1}^{+\infty} r_{1,m} W_{1,m} b_{1,m} \sin\left(\frac{\pi m}{\beta_1 - \alpha_1} (y - \alpha_1)\right) \quad y \in (\alpha_1, \beta_1) \quad 1=1..M$$

where  $A_n = A_n^+ + A_n^- + \delta_{n0}$ ,  $B_{1,m} = b_{1,m}^1 \text{ch}(\bar{r}_{1,m} h)$ ,  $W_{1,m} = \text{th}(\bar{r}_{1,m} h)$  in the first case and  $A_n = A_n^+ - A_n^- + \delta_{n0}$ ,  $B_{1,m} = b_{1,m}^2 \text{sh}(\bar{r}_{1,m} h)$ ,  $W_{1,m} = \text{cth}(\bar{r}_{1,m} h)$  in the second case.

Then, following the ideas of the works [1,2], we introduce the functions

$$F_0 = \sum_{n=-\infty}^{+\infty} A_n \ln e^{iny} \quad y \in [-\pi, \pi]$$

$$F_1 = \sum_{m=1}^{+\infty} \frac{\pi m}{\beta_1 - \alpha_1} b_{1,m} \sin\left(\frac{\pi m}{\beta_1 - \alpha_1} (y - \alpha_1)\right), \quad y \in (\alpha_1, \beta_1) \quad 1=1..M$$

with the properties  $F_0 = F_1$   $y \in (\alpha_1, \beta_1) \quad 1=1..M$

$$\int_{\alpha_1}^{\beta_1} F_1(t) dt = 0, \quad 1=1..M \quad (1.1)$$

The representation

$$A_n = \frac{1}{2\pi i n} \int_L F_0(t) e^{-int} dt \quad A_0 = \frac{1}{2\pi} \int_L F_0(t) dt$$

$$B_{1,m} = \frac{2}{\pi m} \int_{\alpha_1}^{\beta_1} F_1(t) \cos\left(\frac{\pi m}{\beta_1 - \alpha_1} (y - \alpha_1)\right) dt \quad 1=1..M$$

for the Fourier coefficients is based upon these properties. Using the Hilbert transformation, we come to a system of singular integral equations

$$\begin{aligned} & -\frac{1}{2\pi} \int_L \operatorname{ctg}\left(\frac{t-y}{2}\right) F_0(t) dt + \\ & + \frac{\pi}{\beta_1 - \alpha_1} \frac{1}{\pi} \int_{\alpha_1}^{\beta_1} \operatorname{ctg}\left(\frac{\pi}{\beta_1 - \alpha_1} \left(\frac{t-y}{2}\right)\right) + \operatorname{ctg}\left(\frac{\pi}{\beta_1 - \alpha_1} \left(\alpha_1 - \frac{t+y}{2}\right)\right) F_1(t) dt + \\ & + \frac{1}{\pi} \sum_{p=1}^M \int_{\alpha_p}^{\beta_p} K_p(y, t) F_p(t) dt = -ix \end{aligned} \quad (1.2)$$

with the additional conditions (1.1)

The solution for the system of the singular integral equations (1.2) with the additional conditions (1.1) is sought in the class of functions which may be represented in the form of:

$$F_1(y) = \frac{\tilde{V}_1(y)}{\sqrt{(\beta_1 - y)(y - \alpha_1)}}, \quad y \in (\alpha_1, \beta_1), \quad 1=1..M,$$

where  $\tilde{V}_1(y)$  is a function bounded on  $[\alpha_1, \beta_1]$ .

Introducing a linear map  $g_1(t): [-1, 1] \rightarrow [\alpha_1, \beta_1]$  and changing the variables in the system of the singular integral equations, we can obtain:

$$\frac{1}{\pi} \int_{-1}^1 K_{11}(\tau, t) \frac{V^1(t) dt}{\sqrt{(1-t^2)}} + \frac{1}{\pi} \sum_{p=1}^M \int_{-1}^1 K_{1p}(\tau, t) \frac{V^p(t) dt}{\sqrt{(1-t^2)}} = ix \quad 1=1..M, \quad (1.4)$$

where  $K_{1p}(\tau, t) = K_p(g_1(\tau), g_p(t))$  ( $p=1$ ) and  $V^p(t) = \tilde{V}_p(g_p(t))$   $p=1..M$ ,

$$\begin{aligned} K_{11}(\tau, t) = & K_1(g_1(\tau), g_1(t)) + \operatorname{ctg}\left(\frac{g_1(t-\tau)}{2}\right) + \\ & + \operatorname{ctg}\left(\frac{\pi}{\beta_1 - \alpha_1} \left(\frac{g_1(t-\tau)}{2}\right)\right) + \operatorname{ctg}\left(\frac{\pi}{\beta_1 - \alpha_1} \left(\alpha_1 - \frac{g_1(t+\tau)}{2}\right)\right) \end{aligned}$$



with the additional conditions

$$\int_{-1}^1 \frac{V^p(t)dt}{\sqrt{1-t^2}} = 0 \quad p=1..M, \quad (1.4)$$

For an approximate solution of the problem the discretization of the system of the singular integral equations (1.3) and the additional conditions (1.4) can be made by the discrete singularities method.

The interpolation points of the function  $V^p$  to be sought are chosen as the zeroes of the first kind Chebyshev polynomials of the power  $N_p$ . The integral equations are considered in the zeroes of the second kind Chebyshev polynomials of the power  $N_i-1$  ( $i=1..m$ ). This procedure leads to a system of linear algebraic equation with respect to the values of function  $V_h^p$  in the interpolation points.

$$\sum_{p=1}^M \sum_{r_p=1}^{N_p} \frac{1}{N_p} K_{ip}(\tau k_1^2, \tau r_p) V_h^p = I \alpha \quad i=1..M,$$

$$\sum_{r_p=1}^{N_p} \frac{1}{N_p} V_h^p = 0 \quad \begin{aligned} k_1 &= 1..N_1-1, \\ r_p &= 1..N_p, \\ p &= 1..M. \end{aligned}$$

The numerical results for the E- and H-polarized waves for one- or multielemental gratings for various values of grating parameters have been obtained.

- (1) Yu.Gandel: "On the paired Fourier series in some of the mixed boundary problems of mathematical physics," T.F.F.A. Kharkov, (1982) n.38, pp.15-18.
- (2) Yu.Gandel: "The Discrete Singularities Method for electrodynamics problems," Cybernetics problems, Moskov, (1986), pp.168-183.
- (3) S.Belotserskiy, I.Lifanov: "Numerical methods in singular integral equations", Moskov, (1985) pp 253-271.



ON THE PROBLEM OF WAVES DIFFRACTION  
BY SCREENS WITH NARROW SLOTS

Egorov M. B.

1. Introduction. The screens, perforated by narrow waveguide channels (their diameter  $d$  is essentially smaller than the wave length  $\lambda$ ) are used as the elements of different devices of electronic and antenna waveguide technique. When the number of such channels is sufficiently large, the considered domains have complicated structure of boundary. Even with the help of numerical methods often it is difficult to determine the solution. Hence, the natural question arises how to reduce the problem of such type to less difficult ones for the homogeneous medium and to determine the equations describing this equivalent medium.

The method of the present paper consists in obtaining of integral equations for certain limit function on the surface of screen in the case when the diameter of the waveguide channels vanishes. It is supposed that the number of channels  $N$  either finite or large, but their common measure is finite. In these narrow channels the one wave approximation is used with the error  $O(d/\lambda)$ . It is proved that the system of obtained integral equations is solvable and has the unique solution.

2. Formulation of the Integral Equation. The geometry of scattering problem is shown on Fig. 1, where the scatterer represents a plane metallic screen. Symmetric pairs of slots on the screen are connected with the waveguide channels being the space between two coaxial cylinders with the elements parallel to  $x$ -axis.

The incident wave is described by the formula

$$\vec{H}(y, z) = (\exp[ik(\beta y - \gamma z) - i\omega t], 0, 0) \quad (1)$$

The field in external space is represented as

$$H_x(y, z) = e^{ik(\beta y - \gamma z)} + e^{ik(\beta y + \gamma z)} - 2 \int_G H_0^{(1)}(k \sqrt{z^2 + (y - \eta)^2}) E(\eta) d\eta \quad (2)$$

where  $H_0^{(1)}(x)$  is the Bessel function,  $G = \bigcup G_n$ ,  $G_n$  is aperture of the  $n$ -th channel,  $E(\eta)$  - the tangential component of electric field on  $G$ .

The field in the  $n$ -th channel can be represented as

$$H_{xn}(r, \theta) = A_n \exp(ikr_n \sqrt{\epsilon_n} \theta) + B_n \exp(-ikr_n \sqrt{\epsilon_n} \theta) \quad (3)$$

where  $r_n$  is the middle radius of channel  $n$ ,  $\epsilon_n$  is the permittivity of medium inside the channel.

Let us determine the solution of this diffraction problem in the case  $d/\lambda \ll 1$ .

If the boundary conditions are fulfilled on  $G$  one have obtained two independent Fredholm equations of the second kind:

$$C_1(r) \Psi_1(r) = e^{-ik\beta r} + e^{ik\beta r} + \int [H_0^{(1)}(k|r-\eta|) - H_0^{(1)}(k|r+\eta|)] \Psi_1(\eta) d\eta \quad (4)$$

$$C_2(r) \Psi_2(r) = e^{-ik\beta r} + e^{ik\beta r} + \int [H_0^{(1)}(k|r+\eta|) + H_0^{(1)}(k|r-\eta|)] \Psi_2(\eta) d\eta$$

where

$$C_1(r) = -\operatorname{tg}(k\pi\sqrt{\epsilon}r/2) / (k\sqrt{1/\epsilon}), \quad C_2(r) = \operatorname{ctg}(k\pi\sqrt{\epsilon}r/2) / (k\sqrt{1/\epsilon})$$

$$\text{and } E(\eta) = (\Psi_1(\eta) + \Psi_2(\eta)) / 2.$$

3. Results. To obtain the equivalent boundary conditions for the dense grating it is necessary to do the passage to the limit  $\tau \rightarrow 0$  in the equation (4) and to take into account the representation (2). In the case of finite number of narrow slots one can solve the abovementioned integral equations by the method of progressive approximations. Substituting zero-order approximation in formula (2) and replacing the integral by the sum over all slots we obtain the description of the field over the screen.

$$H_x(y, z) = e^{ik(\beta y - \gamma z)} + e^{ik(\beta y + \gamma z)} + V_0(y, z).$$

$$V_0(R, \xi) = -4d\tau \sqrt{2k/\pi R} \frac{\exp[i(kR - \pi/4)]}{L} * \quad (5)$$

$$* \sum_{n=-N}^N n \{ e^{iknt(\beta - \cos \xi)} \operatorname{ctg}(knL) - e^{iknt(\beta + \cos \xi)} \operatorname{csc}(knL) \}$$

where  $R$  and  $\xi$  are the polar coordinates of observation point.

Function  $V_0$  is zero-order approximation of the field reradiated by slots. To obtain it we used simplifications permissible for antennas in far region. It is considered the most interesting from the practical point of view the case of equidistant grating, i.e.  $r_n = n\tau$ , with  $\sqrt{\epsilon_n} r_n = \text{const} = L$ . Such structure corresponds to the van-Att grating model.

The error of solution (5) is the value of order  $\alpha d/\lambda$ .

The representation (5) corresponds to the radiation field of two array antennas with linear phase and amplitude distributions. This phase distribution leads to the beam shift. The shift angle is determined by the angle of incidence of the wave. Hence, the maximal values of the reradiated field are observed at the

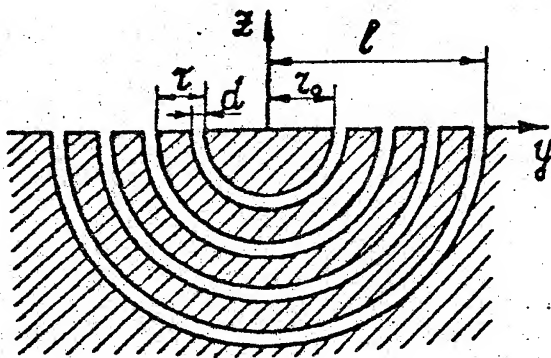


Fig. 1.

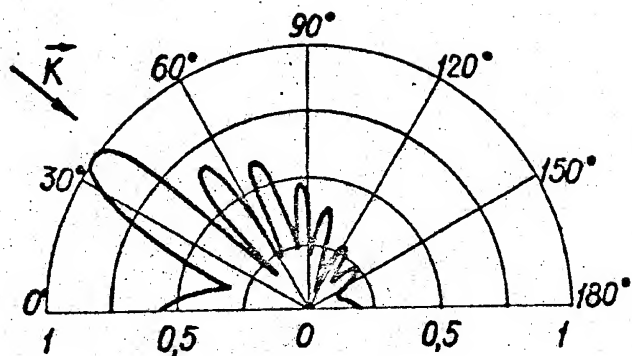


Fig. 2.

angles corresponding to the angle of arrival angle of specular reflection. From the formula (5) it follows that the quotient of the amplitude of specularly reradiated field to the amplitude of backscattered one is determined by the function

$$S = \frac{V_0(R, \pi/2 - \varphi)}{V_0(R, \pi/2 + \varphi)} \quad (6)$$

It is evident that the considered model provides the primary reflection of electromagnetic field in the direction to the source. For the given quotient of amplitudes  $S$  the parameters of wave-guide channels  $\epsilon_n$  and  $r_n$  must be chosen from the condition

$$L = \sqrt{\epsilon_n} r_n = \frac{\arccos S + 2\pi m}{k\pi}, \quad m = 0, 1, 2, \dots \quad (7)$$

On the Fig. 2 it is shown the scattering pattern of the van-Att grating model, which is calculated according to formula (5). The parameters of model are following:  $d = 0.09$ ,  $\tau = 0.1$ ,  $L = 6.2$ ,  $N = 20$ ,  $r_0 = 0.2$ .

# PROPOGATION OF PULSE WAVE BEAM IN THE VICINITY OF UNDERLYING SURRFACE

Nataliy Egorova, Nikolay Kolchigin

Kharkov State University

## ABSTRACT

A problem of scattering of wave pulse beam by flat boder between two dielectrics has been solved using the Green's function. Analytical solution has been obtained for distribution of density of field sources for Gaussian function and known time dependence.

## INTRODUCTION

Phisical phenomena of pulse wave beams observed both at propagation nearby a surface and scattering by various media differ substantially from those which occure in monochromatic wave beam cases. Distortion of pulse wave beam strusture is possible at its reflecting and transmitting through a dispersion medium. When a border is available between two media, one can observe a shift of maximum of wave beam spacial distribution relative to the position determined by geometrical optics. Focusing and defocusing of the beam, displacement of focus, change of the beam's polarization and etc. may to take place.

To investigate the above noted phenomena it's necessary to have solved proper boundary problems of wave beams propagation and diffraction allowing for an underlying surface.

## RESULTS AND DISSCUSIONS

Approach to solving these problems is based on Maxwell's equations with given external sources and uses the Green's function of the boundary problem. The latter fact justi-fies its generality. In this case solution of diffraction problem of thewave beam reduces to integration upon assigned cross-section for product of Green's function of a point source boundary problem and distribution density of point sources upon this cross-sec-

tion. This method permits to exclude the solution of boundary problem. Besides, the Green's function of this problem is in itself an explicit solution of the problem of finding a continual superposition of plane waves of the point source and includes all substantial physical effects of its field scattering on the border. Hence, the study of diffraction problem of wave beam reduces to analysis of scattering properties due to point sources distribution with given intensity at the surface.

For simplicity let us consider a scattering of pulse wave beam on the border between two dielectrics with refraction index  $n = \sqrt{\epsilon_1}/\sqrt{\epsilon_2}$  ( $\epsilon_1$  and  $\epsilon_2$  - dielectrical permittivity of upper and lower medium, respectively) (fig.1).

Let a distribution of sources, forming the original wave beam assigned by function  $f(y_i, t)$  at  $z_i = 0$ , to be known.

Electric (magnetic) dipoles, taken as sources, have the moments dependent on time in pulse regime as  $p(t - R/c)$

Function  $p(t)$  is represented as expansion into Fourier's integral:

$$p(t) = \frac{1}{2} \int_{-\infty}^{+\infty} e^{-i\omega t} \cdot g(\omega) d\omega \quad (1)$$

where  $g(\omega) = \frac{1}{\pi} \int_{-\infty}^{+\infty} p(t) e^{i\omega t} dt \quad (2)$

As  $p(t)$  is real function, the following equality is relevant

$$g(-\omega) = g^*(\omega)$$

Such dipoles excite the field, defined by one component electrical (respectively, magnetic) Hertz vector with unique component not equal zero, which is co-directional with orientation of the source's dipole moments.

Then the potential of electromagnetic field of radiated wave for two-dimension case may be written as:

$$G_i^U(y_i, z_i, t; y_j) = \frac{1}{2} \int_0^{\infty} \exp[-i(\omega t - kr_0 + \frac{\pi}{4})] g(\omega) \Psi(\omega, r_0) d\omega + c \quad (3)$$

$$\Psi_i(\omega, r_0) = \frac{1}{4} \exp(i\frac{\pi}{2}) \sqrt{\frac{2}{\pi k r_0}} \left( 1 - \frac{\theta_1 \exp(i\frac{\pi}{2}) \Gamma(\frac{3}{2})}{2 k r_0 \Gamma(-\frac{1}{2})} \right)$$

where

$$\theta_1 \text{ - small parameter, } |\theta_1| < 1; \quad r_0 = \sqrt{(x - h + y_i' \sin \theta_i)^2 + (y - y_i' \cos \theta_i)^2} \quad (4)$$

The field of original wave beam is defined by Green's theorem:

$$U_i(y_i, z_i, t) = \int_{-\infty}^{+\infty} \int_{-\infty}^{+\infty} f(y_i', t) G_i^v(y_i, z_i, t; y_i') dy_i' dt \quad (5)$$

where  $G_i^v(y_i, z_i, t; y_i')$  - Green function,  $f(y_i', t)$  - distribution function of dipoles density, defined by physical conditions of the problem and is given at plane  $z=0$ .

Generally, each one-component Hertz vector characterizes a five-component electromagnetic field.

To find out scattered fields in (5), corresponding Green's function of boundary problem ought to be available.

Further on we will use coordinates  $(y_i, z_i)$  with index  $i$  (incident) for original beam, and coordinates  $(y_r, z_r)$  with index  $r$  (reflected) for reflected field.

Using Green's function of boundary problem means practically that the spectral properties of the Maxwell's operator are not dealt with - discret and continual spectrums have been, as yet, taken into account and written in the explicit form by the Green's function of boundary problem.

Now, as seen from (3), in order to find the field of pulse radiator the scattered field Green's function is to be multiplied by  $1/2g(\omega)$  and then integrated from  $-\infty$  to  $+\infty$ . In view of properties of function  $g(\omega)$  we get:

$$G_r^v(y_r, z_r, t; y_i') = \frac{1}{2} \int_{-\infty}^{+\infty} \exp[-i(\omega t - kr_1 + \frac{\pi}{4})] g(\omega) \Psi(\omega, r_1) d\omega + c \quad (6)$$

where

$$\Psi_r(\omega, r_1) = \sqrt{\frac{2}{\pi k r_1}} (V(\theta_0) - iN/k r_1) \quad (7)$$

$$V(\theta_0) = \frac{m \cos \theta_0 - \sqrt{n^2 - \sin^2 \theta_0}}{m \cos \theta_0 + \sqrt{n^2 - \sin^2 \theta_0}}$$

Fresnel's coefficient for partial plane wave with incidence angle in the integral representation of the field of point source for solution of boundary problem is

$$\theta_0 = \arcsin \frac{(y_r + y_i') \cos \theta_i + z_r \sin \theta_i}{\sqrt{(y_r + y_i')^2 + z_r^2}}$$



$m = n^2$  for vertical electric dipole (polarization in incidence plane);  $m = 1$  for vertical magnetic dipole (polarization in plane perpendicular to incidence plane).

Correction coefficient  $N$  in formula (7) is defined by expression :

$$N = \frac{1}{2} [V''(\theta_0) + V'(\theta_0) \cot \theta_0]$$

Reflected field of wave pulse beam can be determined by formula (5) substituting the corresponding Green's function.

It remains only to integrate over the location region of sources with known function of their spacial distribution.

The advantage of this procedure is evident as the solution of diffraction problem for wave beams of higher order does not differ from the case of Gaussian beam.

Fig. 1 shows the amplitude distribution of the field for various moments in time, i.e., instant values. Calculations have been made according to formula 5 where  $G^V$  has been substituted instead  $G^H$ . Vertical magnetic dipoles are the sources ( $m = 1$  for reflection coefficient in (5)). Incidence angle is equal to  $\theta_i = 0.9$  rad.

Incidence is from medium with lesser density on to denser medium ( $\epsilon_1 = 1, \epsilon_2 = 2.53$ ). Distribution of sources density is described by Gaussian function  $f(y_i, 0) = e^{-y_i^2/W_0^2}$  where  $W_0$  - problem's parameter, characterizing the width in the sources plane upon which the radiation intensity decreases in  $e$  - times. Sources are excited synchronially.

Time-dependence form for dipole radiated impulse is like

$$p(t) = \xi / (\xi + t^2)$$

where  $\xi$  - impulse's width parameter.

Expansion into integral (2) is according to [1].

#### REFERENCE

1. B. R. Horowitz and T. Tamir " Lateral displacement of a light beam at a dielectric interface ," JOSA, 1971, v. 61, 5, p. p. 586-594.



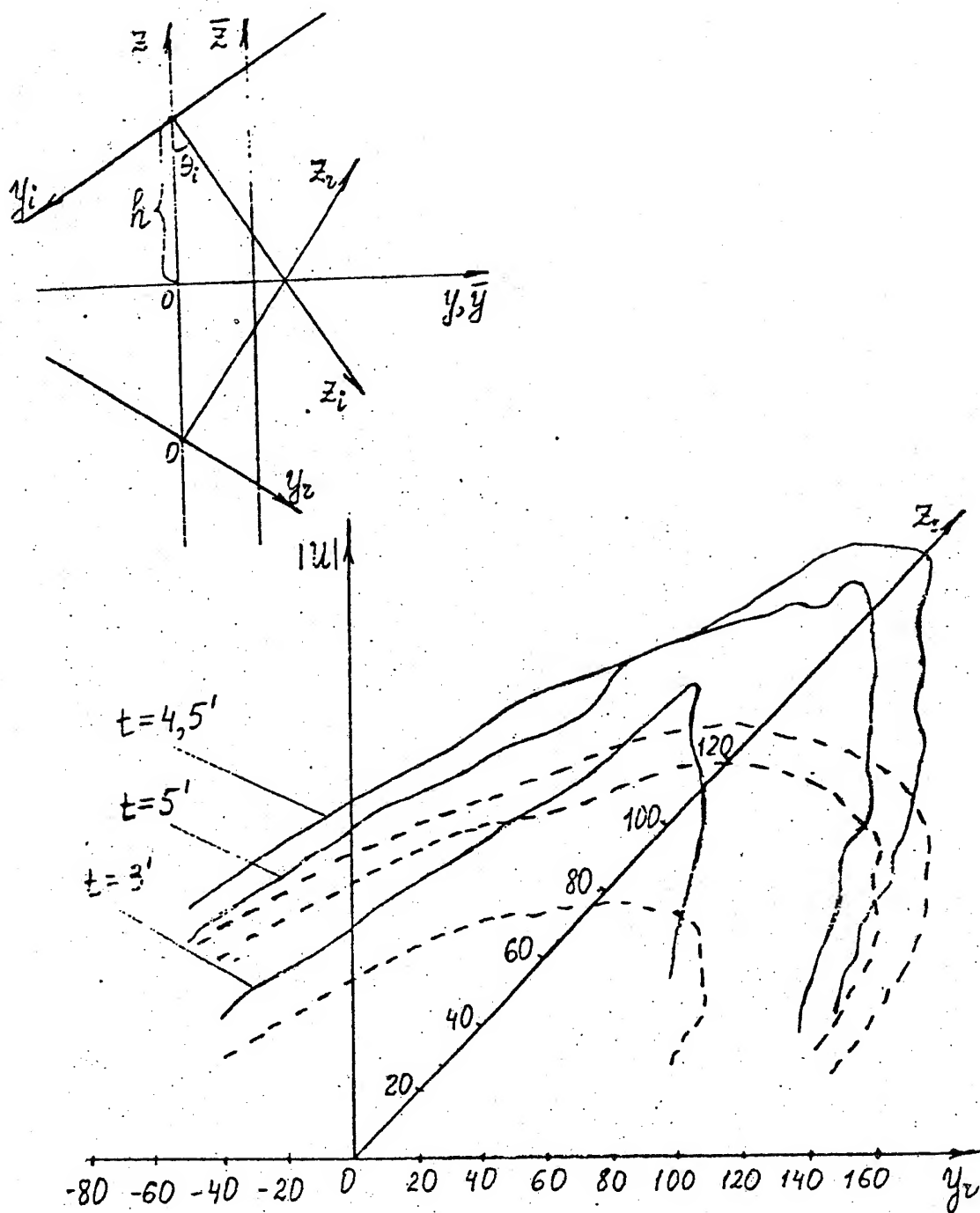


Fig 1. The space-time distribution of the field.

# MODE CONVERSION IN INHOMOGENEOUS CHIRAL MEDIUM

Nikolai Erokhin

Space Research Institute, Russian Academy of Sciences,  
Profsovnaya Str. 84/32, 117810 Moscow, Russia

## ABSTRACT

The electromagnetic waves propagation in an inhomogeneous, chiral, isotropic, plasma-type medium is considered. It has been found that in an isotropic, inhomogeneous medium the linear coupling of transverse electromagnetic waves, caused by chirality, results to new type of mode conversion. The mode conversion between the fast and slow electromagnetic waves is described by the set of two coupled equations with singularity at the plasma resonance layer which leads to a finite wave energy absorption independently on dissipation smallness. In the case of normal wave incidence on weakly inhomogeneous plasma with mode crossing layer, the plasma resonance region is the reflectionless layer and 100 % mode conversion takes place. The singular structure of wave fields at the plasma resonance region is studied.

## INTRODUCTION

Chiral media have been long known in optics as the optically active ones in which the electromagnetic waves of different polarization are propagating at different phase velocity. The chirality can significantly influences on a medium electrodynamics, for instance, the TE and TM modes linear coupling arises, the polarization plane rotation under the electromagnetic wave propagation in chiral medium occurs, the electromagnetic wave excitation and scattering are also changed and so on.

During the last years a number of papers on the fundamental problems of electromagnetic waves propagation in chiral medium have been published. The present paper is proposed to explore the chirality influence on the electromagnetic wave propagation in an weakly inhomogeneous, isotropic, plasma-type medium. Such medium can be considered, for example, as a specific type of dusty plasma with dusty particles to be a chiral objects.

The constitutive relations for lossless, re-

ciprocal, isotropic, chiral medium, under  $\exp(-i\omega t)$  time-dependence is assumed for the fields, are given by

$$D = \epsilon E + i \gamma B, \quad H = i \gamma E + B / \mu,$$

where  $\epsilon$  is the dielectric permittivity and  $\mu$  is the magnetic permeability of medium;  $\gamma$  is the chirality.

The principle feature of inhomogeneous plasma is possibility of the  $\epsilon$ -sign changing along a ray trace. In the case of such possibility, there is plasma layer where the dielectric permittivity  $\epsilon$  is small enough and, consequently, the chirality influence on electromagnetic wave propagation is of principle. We consider the electromagnetic waves propagation in the chiral plasma which is inhomogeneous in the one direction, say along  $z$ -axis. So  $\epsilon$ ,  $\mu$  and  $\gamma$  are a some functions of  $z$  only. We use the constitutive relations together with Maxwell's equations

$$\text{curl } E = i \omega B / c, \quad \text{curl } H = -i \omega D / c,$$

suppose that the fields depend on time and space variables as  $f(z)\exp(ikx - i\omega t)$ , where  $k = (\omega/c) \sin\theta$  and  $\theta$  is the electromagnetic wave incidence angle. Under this assumption, we have obtained the set of two coupled, ordinary differential equations of the second order each. This set of equations has been studied at the plasma resonance region and far from it.

## BASIC RESULTS

The theory of an electromagnetic waves propagation and mode conversion in the weakly inhomogeneous chiral plasma with the mode crossing layer is developed. In the case of chiral plasma the normal waves are the hybrid modes represented by superposition of the TE and TM modes. Consequently, the electromagnetic waves interaction with inhomogeneous chiral plasma will be described by the set of two coupled, differential equations of the second order each with variable coefficients which have singularity at the plasma resonance point. It is shown that plasma chirality affects significantly on the relative positions of the plasma resonance layer, the layers of wave reflection and the mode crossing layer. In particular, at the small incidence angle, the slow mode may, in contrast with the case of vanishing chirality, propagate into the overdense plasma region and, therefore, the plasma resonance layer becomes open. It is shown that chirality

leads to an appearance of the mode crossing layer but it always placed into the overdense plasma region. It is studied the singular structure of wave fields at the plasma resonance layer. Under a common boundary conditions, the electric field components parallel to the plane of wave incidence are singular at the plasma resonance point. Simultaneously, in contrast to the case of vanishing chirality, the magnetic field components, parallel to the plane of wave incidence, have singularity also. The wave field asymptotics valid at the vicinity of plasma resonance region have been obtained by the contour integration method. It is shown also that owing to chirality, the wave reflection from the weakly inhomogeneous plasma with the mode crossing layer and the wave resonant absorption may undergo the oscillatory behaviour in dependence on the incidence angle.

In the case of normal waves incidence on the inhomogeneous chiral plasma with linear spatial dependence of the plasma dielectric permittivity the exact analytical solution in terms of the Airy function has been obtained. This solution describes the mutual, 100 % mode conversion between the fast and slow electromagnetic waves. It is generalized to the case of an arbitrary, monotonic spatial profile of  $\epsilon(z)$  allowing the existence of the mode crossing layer. This solution is used to consider the polarization plane rotation and the magnetic helicity transport under waves propagation in the weakly inhomogeneous chiral plasma. It was shown that owing to chirality, the magnetic helicity of normal modes is nonzero and the magnetic helicity flux depends significantly on the wave polarization. At the mode crossing layer, the magnetic helicity density has maximum value which is proportional to the chirality parameter.

In the case of the fast mode oblique incidence on inhomogeneous plasma, the plasma resonance point is always placed in an evanescent layer and its thickness increases under the chirality growth.

# THEORY OF MULTIPLE SCATTERING FROM SYSTEMS WITH BOUND STATES

V. Freilikher, M. Kaveh, M. Pustilnik, I. Yurkevich

*The Jack and Pearl Resnick Institute of Advanced Technology,  
Department of Physics, Bar-Ilan University, Ramat-Gan 52900, Israel*

A. Maradudin,

*Department of Physics, University of California, Irvine, California 92717*

The interference of the multiply scattered random fields gives rise to a wide variety of physical phenomena such as strong and weak localization, backscattering enhancement, memory effect etc. Once these phenomena have been discovered in media with volume fluctuations, it was found during the recent few years that they may come into existence due to surface scattering also. Although the processes of reflection from the surface irregularities have much in common with volume scattering, there are many distinctive features which sometimes produce new and rather surprising and unexpected effects.

If the roughness sizes are large compared with the wavelength, multiple scattering are provided by reflections of beams from different randomly oriented parts of the surface. In the opposite case of slightly perturbed interface multiple scatterings are usually disregarded. This largely stems from the fact that a wave, after having been once scattered from a slightly rough surface to the upper half-space, propagates in a homogeneous medium without further interaction with the scattering boundary. In order to understand where the effects of multiple scattering comes from in this case, one has to take into account that the diffraction from surface irregularities makes also possible the resonant excitation of eigenmodes localized near the scattering boundary. These may be, for example, polariton-like surface waves (SW) or modes existing due to the size quantization in a slab bounded by scattering interface. These waves propagate along the boundary, interact repeatedly with the roughness, and being transformed into volume waves, give rise to enhanced diffuse scattering in the antispecular direction. The localization of surface waves, and effective absorption caused by their transformation into volume waves (VW) are the main factors which form the field in the antispecular direction and lead to a new scattering peaks to be observable. It is significant that in the presence of fluctuations surface wave (SW) is not a pure two-dimensional object since it is connected with upper volume through scattering.

Under some assumptions this connection may be taken into account by means of effective absorption in the Shrodinger equation with effective complex-valued potential which describes SW propagation along the surface. The real part of the random potential provides resonant scattering of SW, imaginary one represents nondissipative attenuation caused by the transformation of SW into volume waves (leakage). This leakage is indispensable in the SW propagation on real surface. It is very important distinctive feature which differentiates SW on random surface from volume wave in random medium, and gives rise to some characteristic properties of backscattered enhancement, its shape and magnitude being now dictated by characteristic relation between the leakage length  $l_{\text{leak}}$  and SW scattering mean free path

$l_{sc}$ . In the case of rough dielectric surface with large refractive index  $n$  the inequality  $l_{leak} \ll l_{sc}$  holds even for absolutely nonabsorbing media, which means that multiple scatterings of SW are not very much essential, and enhanced backscattered peak is completely described by second order approximation. In opposite case  $l_{leak} \gg l_{sc}$  the interference of multiply scattered SW has to be taken into account carefully.

From the mathematical point of view the description of the interaction of eigenmodes with rough boundary allows for approach which is general for all systems with discret spectrum, independent on the physical origin of eigenmodes. This approach is based on the fact that in the case of weak disorder the averaged Green function of such a system has a well emphasized pole structure. The unperturbed Green function  $G_0(p)$  has the pole at  $p=p_s$  (if interface is a boundary between vacuum and dielectric medium with  $\epsilon < -1$ ) or a set of poles  $\{p_n\}$ , corresponding to size quantization (due to the finiteness of a slab with  $\epsilon > 1$  in the  $z$ -direction). In the case of weak scattering  $l \gg (\Delta p_n)^{-1}$  ( $l$  is the mean free path;  $\Delta p_n$  is a characteristic distance between poles  $p_n$ ), the averaged Green function  $G(p)$  also has a well emphasized pole structure and can be represented in the form

$$G(p) = G_{reg}(p) + G_{sing}(p), \quad (1)$$

where  $G_{reg}(p)$  is a smooth function related to the continuous part of the spectrum and  $G_{sing}(p)$  describes the behavior of  $G(p)$  in vicinities of poles

$$G_{sing}(p) = \sum_{n=1}^N \frac{1}{\frac{p^2 - p_n^2}{C_n} - \Sigma(p)}, \quad C_n = \left( \frac{\partial}{\partial(p^2)} G_0^{-1}(p) \right)_{p=p_n} \quad (2)$$

where  $\Sigma(p)$  is the mass operator.

#### Single Interface with Polariton Eigenmode

In this case  $G_0(p)$  has the single pole at real  $p = p_s$  (discrete spectrum) which corresponds to surface waves (SW) with wave number  $p_s$ , propagating without attenuation in different directions along the surface. Continuous spectrum describes volume waves (VW), which, being reflected from the surface, propagate in the halfspace  $z > 0$  at angles  $\phi = \arccos p/k_0$ . Thus there are two well defined regions in momentum space. The first one is circle  $|p| < k_0$  which corresponds to phase volume of waves propagating above interface in free space. Another one is circumference  $|p| = p_s > k_0$ , that corresponds to isolated point of spectrum - surface waves propagating along the interface with wave numbers  $p_s$  and decaying exponentially in transverse to interface direction. Inhomogeneity of interface causes scatterings between different volume modes inside region  $|p| < k_0$  ( $VW \leftrightarrow VW$ ) as well as between surface ones ( $SW \leftrightarrow SW$ ). Scattering mixes waves of different nature, causing excitation of SW by incident wave ( $VW \leftrightarrow SW$ ) and leakage of surface wave into free space ( $SW \leftrightarrow VW$ ). This interaction leads to broadening of discrete spectrum and smears boundary of volume waves region in phase space. If scattering is weak enough, so that  $l^{-1}$  ( $l$  - mean free path) is much less than distance  $p_s - k_0$  between two different regions in momentum space, it is plausible to consider them as well distinguished and weakly affected by each other.

In this case coordinate representation of the SW part of the Green function, may be written in the Schrodinger equation form:

$$\frac{1}{C_0} (\Delta + p_s^2) G_{ss}(r, r') + (v_{ss}(r) + i\nu_v) G_{ss}(r, r') = \delta(r - r') \quad (3)$$

where  $v_{ss}$  is proportional to a sum of the Fourier harmonics of surface deviation with wavenumbers close to 0 and  $\pm 2p_s$  ( $SW \leftrightarrow SW$  scattering) and  $\nu_v$  is proportional to the part of the mass operator corresponding to the integration over wavenumbers less  $k_0$  ( $SW \leftrightarrow VW$  scattering).

Thus the problem of derivation of SW Green function is reduced to the problem with scattering potential  $v_{ss}$  and effective attenuation  $\nu_v$  which is of nondissipative nature, but is connected with transitions from surface waves to outgoing volume ones. The entire scattering rate  $\nu$  is made up of two parts  $\nu = \nu_s + \nu_v$  which effect the two-particle Green's function (scattered intensity) in different ways. Frequency  $\nu_s$  is connected with  $SW \leftrightarrow SW$  elastic scattering on random potential  $v_{ss}$  and may result in SW localization, whereas  $\nu_v$  comes from the imaginary part of potential  $\nu_v$  and therefore leads to the effective attenuation of SW. In the leading approximation in  $(p_s l)^{-1}$  we find

$$I_{diff}(p_{sc}, q_0) = 4\alpha(p_{sc})\alpha(p_{in}) |G(p_{sc})|^2 \left\{ \gamma(p_{sc}, p_{in}) + W \frac{\nu_s}{\nu_v} \right\} |G(p_{in})|^2 \quad (4)$$

In the case of slightly rough dielectric surface with large refractive index  $n$  ( $1/n \ll 1$ ) SW leakage to the volume is strong comparative to  $SW \leftrightarrow SW$  scattering and inequality holds  $\nu_v \gg \nu_s$ . It is clear that under this condition multiple scatterings are suppressed by effective attenuation, and  $\gamma(p_{sc}, p_{in})$  may be expand in powers of  $\nu_s / \nu_v \ll 1$  up to the second order only, which leads to the following form of enhanced backscattered peak

$$\gamma(p_{sc}, p_{in}) = W + W \frac{\nu_s}{\nu_v} \left( 1 + (p_{sc} + p_{in})^2 l_{leak}^2 \right)^{-1/d} \quad (5)$$

where  $l_{leak} = \nu_s / \nu_v$  is leakage mean free path,  $d$  is the dimensionality of the surface roughness.

If leakage of SW to the upper halfspace is weak  $\nu_v \ll \nu_s$ , which is the case, for example, if  $n \geq 1$ , SW multiple scatterings effect drastically the antispecular reflection, and infinite series of diagrams in  $\gamma(p_{sc}, p_{in})$  must be summarized. To do this the self-consistent theory of localization can be used, providing

$$I_{diff}(p_{sc}, p_{in}) = 4\alpha(p_{sc})\alpha(p_{in}) |G(p_{sc})|^2 W \left\{ \frac{\nu_s}{\nu_v + D(p_{sc} + p_{in})^2} + \frac{\nu_v}{\nu_v} \right\} |G(p_{in})|^2 \quad (6)$$

where diffusion coefficient  $D$  is the solution of self-consistent equation

$$\frac{D_0}{D} = 1 + \frac{p_s^{2-d}}{md} \int_0^{Q_0} \frac{Q^{d-1} dQ}{n_v + DQ^2}, \quad D_0 = \frac{\nu_s l_s}{d}, \quad Q_0 l_s \approx 1 \quad (7)$$

Solving this equation one can find  $D = \nu_v \alpha^2 l_s^2$ , where  $\alpha \sim 1$  for 1D and  $\alpha \sim e^{-2p_s l_s}$  for 2D case. The first term in brackets in Eq. (6) with  $D$  gives then the enhanced backscattered peak of the same magnitude as background and of width  $(\Delta \theta)^2 = \nu_v / D q_0^2$

**Slab with Size-Quantized Eigemodes**



Using multi-poles structure (2) one can calculate  $I_{\text{dif}}$  upon summarizing ladder and maximally crossed diagrams, which results in

$$I_{\text{dif}}(p_{\text{sc}}, p_{\text{in}}) = 4\alpha_0(p_{\text{sc}})\alpha_0(p_{\text{in}})|G^2(p_{\text{sc}})G^2(p_{\text{in}})|W \left\{ \frac{v}{v_v} + \frac{M(Q)}{1-M(Q)} \right\}, \quad (8)$$

where

$$Q = p_{\text{in}} + p_{\text{sc}},$$

$$M(Q) = W \int dp G(p + \frac{Q}{2}) G^*(p - \frac{Q}{2}) = \pi \frac{W}{v} + \sum \frac{a_{nm}}{1 + (\frac{Q - p_{nm}}{v_{nm}})^2}; \quad (9)$$

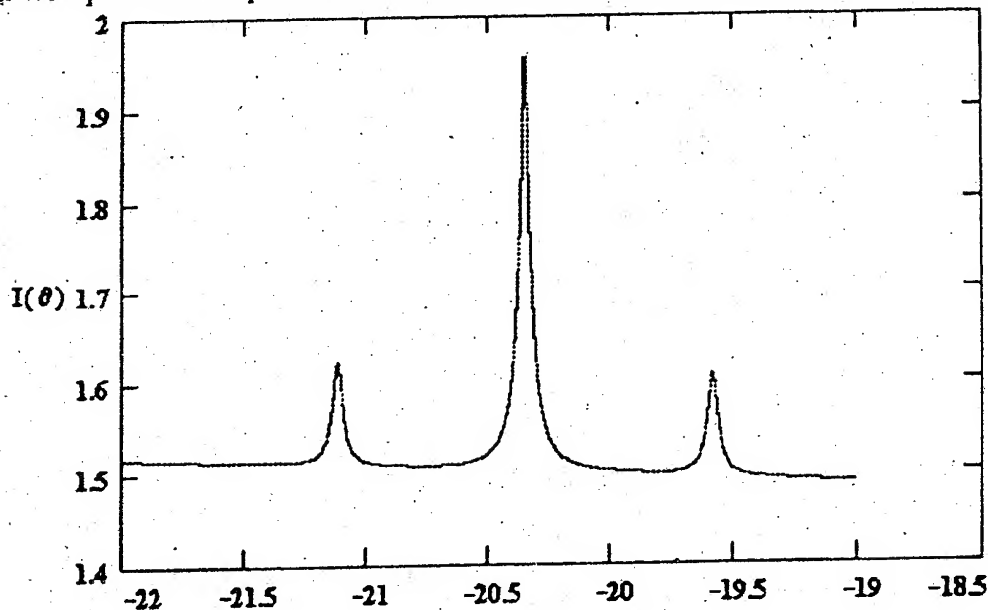
$$v_{nm} = \frac{v}{2} (a_n + a_m), \quad a_n = \frac{C_n}{p_n}, \quad a_{nm} = \frac{2a_n a_m}{a_n + a_m}, \quad p_{nm} = p_n - p_m.$$

The angular distribution of scattered intensity  $I_{\text{dif}}(p_{\text{sc}}, p_{\text{in}})$  exhibits peaks when the function  $M(Q)$  takes its maxima. When  $|Q| \gg v_n$ ,  $|Q + p_{nm}| \gg v_{nm}$  function  $M(Q) \ll 1$  and  $I_{\text{dif}}$  is a smooth function of scattering angles, determined by the first term in curly brackets of Eq.(8) (ladder approximation). In the vicinity of the retroreflection direction

( $|Q| \lesssim v_n$ ,  $|Q - p_{nm}| \gg v_{nm}$ ) the main contribution to  $M$  comes from the term with  $n = m$  and describes the well-known backscattered peak.

When the direction of scattering occurs in the vicinity of one of the angles, determined by the equation  $|Q| = |p_{nm}|$  ( $n \neq m$ ), the  $n=m$  term in  $M(Q)$  can be neglected, whereas the one non-diagonal ones contributes essentially and provides well-pronounced additional peaks of scattered intensity.

For example, in the case of S-polarized wave scattered from a slab with a slightly rough interface  $z = d + \xi(x)$ , potential  $v(p, q)$  can be represented in the form:  $v(p, q) = k_0^2 (\epsilon - 1) \xi(p - q)$ . For this case numerical calculations were carried out to illustrate predictions made above. The results are shown in Fig. and demonstrate two additional well-pronounced peaks for intensity of a wave scattered from a two-mode slab.





# RADIATION CHARACTERISTICS OF AN ELECTRIC CURRENT ELEMENT OVER A HIGH-INTRINSIC-IMPEDANCE SURFACE

Rabindra Nath Ghose  
Technology Research International, Inc.  
26672 Agoura Road, Calabasas, California, USA

## ABSTRACT

Electromagnetic fields due to an arbitrary electric current element over a high-intrinsic-impedance surface have been examined herein. The formulation of the problem is similar to that of Sommerfeld's problem involving radiation in the media comprising of two semi-infinite half-spaces such as the air and earth, although the radiation characteristics in air appear to change dramatically as the partially conducting earth's surface is replaced by a high-impedance surface.

## INTRODUCTION

As a conformal antenna on aircraft, a cavity-backed antenna is often used to enhance the antenna directivity and effectiveness, particularly when the radiating or receiving antenna element is parallel and close to the highly conducting or a very-low-intrinsic impedance surface such as the aircraft skin. The cavity in such a case deters the radiation toward, or reception from the backward direction of the antenna, and its effect may be viewed as a high-impedance connected in parallel with the antenna terminals. Similar effects may be expected when the radiating or receiving element of the antenna is placed over a very high intrinsic impedance surface. Such a possibility may eliminate the need of a cavity without affecting antenna directivity or effectiveness adversely.

One way to gain an insight into the problem is to examine the effect of such a high-impedance surface on an antenna without a cavity by evaluating the radiation characteristics of an arbitrary current element at the interference of two semi-infinite half-spaces, one corresponding to the air or free-space, and the other having an intrinsic impedance many times larger than that of free-space.

The classical problem of the electromagnetic radiation from an antenna situated near the ground or earth's surface and carrying a current periodic in time was formulated by A. Sommerfeld<sup>1</sup>, who derived the field solutions in the form of a single definite integrals. In principle, one may obtain from this time-periodic solution, the solution corresponding to an arbitrary variation with time of the current in the antenna. The problem of radiation due to an electric current element in two adjoining semi-infinite half-spaces has been addressed by many researchers<sup>2,3</sup> since Sommerfeld, although in all cases one of the two media is assumed to be highly conducting with its permeability same as that of the other medium or free-space. In general, the image of a horizontal current element at the highly conducting medium substantially cancels the field due to the current element due to an effective, near unity negative reflection coefficient at such a surface. If this reflection coefficient could be made positive by replacing the low-intrinsic impedance of the conducting medium with respect to the free-space by a high-intrinsic impedance surface, one should expect a substantial change in radiation characteristics. This turns out to be the case as evidenced in the discussions outlined in the following sections:

## FORMULATION OF THE PROBLEM

Let the radiation from the horizontal electric current element, carrying a periodic current and situated at the interface of a high-intrinsic-impedance Medium 1 and a free-space, Media 2, be considered first. The electromagnetic field in this case may be derived from the Hertzian Vector  $\vec{\Pi}$  that obeys the non-homogeneous wave equation

$$\nabla^2 \vec{\Pi} + \beta^2 \vec{\Pi} = j \frac{J_0}{\omega \epsilon}, \quad \vec{H} = j\omega \epsilon \nabla \times \vec{\Pi}, \quad \text{and} \quad \vec{E} = \beta^2 \vec{\Pi} + \nabla(\nabla \cdot \vec{\Pi}) \quad (1)$$

where a time factor,  $e^{j\omega t}$ ,  $\omega$  being the angular frequency is assumed, and  $\beta^2 = \omega^2 \mu \epsilon$ ,  $\mu$  and  $\epsilon$  are respectively the permeability and dielectric constant of the medium,  $J_0$  is the electric current density at

the source and  $\vec{E}$  and  $\vec{H}$  are the electric and magnetic field intensities.

Let  $\vec{J}_0 = \vec{u}_x p \delta(x) \delta(y) \delta(z-h)$  where  $p$  is the dipole moment for the current element of length  $L$ , such that  $p = \lim_{L \rightarrow 0} (IL)$ ,  $\vec{u}_x$  is a unit vector along  $x$  in the cartesian coordinate system,  $\delta$  is the delta function and  $h$  is the height of the current element above the interface of the two media in Medium 2,  $h$  approaching zero being the case of interest.

It is well known that unlike a vertical electric current element for the same two adjoining half-spaces under consideration that requires only the vertical component of  $\vec{\Pi}$ , the horizontal current element requires both  $x$  and  $z$  components to satisfy the boundary conditions at the interface. Let

$$\vec{\Pi} = \vec{u}_x \Pi_{x1} + \vec{u}_z \Pi_{z1} \quad , \quad z < 0 \quad , \quad \vec{\Pi} = \vec{u}_x \Pi_{x2} + \vec{u}_z \Pi_{z2} \quad , \quad z > 0 \quad (2)$$

$z=0$ , being the interface between the two media.

From (1) and (2) one obtains 4 scalar equations given by:

$$\begin{aligned} (\nabla^2 + \beta_1^2) \Pi_{x1} &= (\nabla^2 + \beta_1^2) \Pi_{z1} = (\nabla^2 + \beta_2^2) \Pi_{x2} = 0 \\ (\nabla^2 + \beta_2^2) \Pi_{z2} &= \frac{j p}{\omega \epsilon_2} \delta(x) \delta(y) \delta(z-h) \end{aligned} \quad (3)$$

where suffices 1 and 2 denote respectively the parameters relating to Media 1 and 2, the interest here being confined to the Medium 2.

From the two dimensional Fourier transforms and the boundary conditions that the tangential electric and magnetic field intensities must be continuous at  $z = 0$ , one may write the solution for  $\Pi_{x2}$  and  $\Pi_{z2}$  as

$$\begin{aligned} \Pi_{x2} &= \frac{-j p}{8 \pi^2 \omega \epsilon_2} \int_{-\infty}^{\infty} \int_{-\infty}^{\infty} \left[ \frac{e^{-\gamma_2 |z-h|}}{\gamma_2} + \frac{e^{-\gamma_2 (z+h)}}{\gamma_2} \frac{\mu_1 \gamma_2 - \mu_2 \gamma_1}{\mu_1 \gamma_2 + \mu_2 \gamma_1} \right] e^{j(\xi x + \eta y)} d\xi d\eta \\ \Pi_{z2} &= \frac{-j p}{4 \pi^2 \omega \epsilon_2} \frac{\partial}{\partial x} \int_{-\infty}^{\infty} \int_{-\infty}^{\infty} \left[ \frac{\mu_1 \epsilon_1 - \mu_2 \epsilon_2}{(\epsilon_2 \gamma_1 + \epsilon_1 \gamma_2)(\mu_1 \gamma_2 + \mu_2 \gamma_1)} \right] e^{j(\xi x + \eta y)} d\xi d\eta \end{aligned} \quad (4)$$

$$\text{where } \gamma_1^2 = \xi^2 + \eta^2 - \beta_1^2 \quad , \quad \gamma_2^2 = \xi^2 + \eta^2 - \beta_2^2$$

Subject to the approximation

$$\mu_1/\epsilon_1 \gg \mu_2/\epsilon_2 \quad , \quad \mu_1^2 \gg \mu_2^2 \quad \text{and in reality } \epsilon_1 > \epsilon_2 \quad (5)$$

$$\Pi_{x2} = \frac{-j p}{4 \pi \omega \epsilon_2} \left[ \frac{e^{-\gamma_2 R_1}}{R_1} + \frac{e^{-\gamma_2 R_2}}{R_2} - \frac{R \mu_2}{\mu_1} J_1 \right] \quad (6)$$

where

$$\begin{aligned} R_1^2 &= x^2 + y^2 + (z-h)^2 = \rho^2 + (z-h)^2 = R_2^2 - 4zh \\ \text{and } J_1 &= \int_0^{\infty} \frac{\gamma_1}{\gamma_2} J_0(\lambda \rho) e^{-\gamma_2 (z+h)} \lambda d\lambda \end{aligned} \quad (7)$$

$J_0(x)$  being the Bessel function of the first kind of  $x$ .

The striking difference between the principal component of the Hertz Vector, that is  $\Pi_z$ , due to the same current element along the  $x$ -direction for the cases of the conducting earth and the high-impedance surface may be noticed in (6). More specifically for the earth-free space case,

$$\Pi'_z = \frac{-jp}{4\pi\omega\epsilon_2} \left[ \frac{e^{-\beta_2 R_1}}{R_1} - \frac{e^{-\beta_2 R_2}}{R_2} + H \right] \quad (8)$$

where

$$H = 2 \int_0^\infty J_0(\lambda \rho) / (\gamma_1 + \gamma_2) e^{-\gamma_2(x+h)} \lambda d\lambda \quad (9)$$

As noted by Sommerfeld and others,  $H \rightarrow 0$  for an infinitely conducting earth. Similarly  $I_1 \rightarrow 0$  as the intrinsic impedance of the Medium 1 approaches infinity. For such cases,  $\Pi_z$  is reinforced by the image for the high-impedance surface while it is cancelled for the highly conducting earth, particularly when  $h \rightarrow 0$ . For the completeness of the field analysis, one needs to examine all the electric and magnetic field intensities due to the current element situated at the interface of the high-impedance surface and free-space in Medium 2. From (1)

$$\begin{aligned} E_z &= \left( \beta_2^2 + \frac{\partial^2}{\partial x^2} \right) \Pi_z + \frac{\partial^2 \Pi_z}{\partial x \partial z}, & H_z &= j\omega\epsilon_2 \frac{\Pi_z}{\partial y} \\ E_y &= \frac{\partial^2 \Pi_z}{\partial x \partial y} + \frac{\partial^2 \Pi_z}{\partial y \partial z}, & H_y &= -j\omega\epsilon_2 \left[ \frac{\partial \Pi_z}{\partial x} - \frac{\partial \Pi_z}{\partial z} \right] \\ E_x &= \left( \beta_2^2 + \frac{\partial^2}{\partial z^2} \right) \Pi_z + \frac{\partial^2 \Pi_z}{\partial x \partial z}, & H_x &= -j\omega\epsilon_2 \frac{\partial \Pi_z}{\partial y} \end{aligned} \quad (10)$$

The conventional means for evaluating the integral  $I_1$  in (6) is first to replace  $J_0(\lambda \rho)$  by  $H_0^{(2)}(\lambda \rho)$  and extend the limits of the integral from  $-\infty$  to  $\infty$ , since  $J_0(x) = 1/2 [H_0^{(2)}(x) + H_0^{(2)}(xe^{i\pi})]$ . The next step is to express the integral over a contour closed by a semi-circle in the lower half of the  $\lambda$ -plane with an indentation along the branch point  $\lambda = \beta_2$ , the branch cut being from  $\lambda = \beta_2 - i0$  to  $\beta_2 - j\infty$  in the lower half plane, the other branch points being avoidable. The major contributions toward the integral in most cases of interest above is from the residues at the poles, the value of each integral being  $-2\pi j$  times the residue at the pole. One thus obtains, subject to approximation in (5).

$$\begin{aligned} \frac{\partial \Pi_z}{\partial z} &= \frac{-jp}{2\pi\omega\epsilon_2} \frac{\partial}{\partial x} \left\{ \frac{\mu_2 \epsilon_1}{\mu_1 \epsilon_2} I - \frac{\mu_2^2 \epsilon_1}{\mu_1^2 \epsilon_2} I_1 \right\} \\ \text{and} \quad \left( \beta_2^2 + \frac{\partial^2}{\partial z^2} \right) \Pi_z &= \frac{-jp}{2\pi\omega\epsilon_2} \left\{ \frac{\mu_2 \epsilon_1}{\mu_1 \epsilon_2} \frac{\partial}{\partial z} I + \frac{\mu_2}{\mu_1} \beta_1^2 M \right\} \end{aligned} \quad (11)$$

$\eta_1$  and  $\eta_2$  being the intrinsic impedances of the Medium 1 and Medium 2 respectively,

$$\begin{aligned} I &= e^{-\beta_2 R} / R, & R &= R_1 = R_2 \quad \text{as } h \rightarrow 0 \\ I_1 &= (\pi/2) c H_0^{(2)}(\beta_2 \rho) \quad \text{and} \quad M = (\pi/2) \sqrt{\frac{2}{\pi c \rho}} e^{-\pi} e^{-\pi} \quad , \quad c = \beta_2 \eta_1 / \eta_2 \end{aligned}$$

The contributions toward the field components  $E_{x2}$  and  $E_{y2}$  due to  $\kappa_2$  become negligible in comparison with those due to  $\Pi_{x2}$ . Even for the field component  $E_{z2}$ , the contribution due to  $\kappa_2$  becomes vanishingly small as  $\eta_1/\eta_2$  and  $\mu_1/\mu_2$  approach large values. Thus the electric field components in Medium 2, for  $\phi = \tan^{-1}(y/x)$ , may be written as

$$[E_{x2}, E_{y2}, E_{z2}] = \frac{-jP}{2\pi\omega\epsilon_2} \left[ (\beta_2^2 I + \cos^2\phi \frac{\partial^2}{\partial \rho^2} I), \sin\phi \cos\phi \frac{\partial^2}{\partial \rho^2} I, \cos\phi \frac{\partial^2}{\partial \rho \partial z} I \right] \quad (12)$$

Since  $\frac{\partial^2}{\partial \rho^2} I$  and  $\frac{\partial^2 I}{\partial \rho \partial z}$  contains only terms which are proportional to  $1/R_1^2$ ,  $1/R_2^2$ , etc, their contributions in the radiation zone becomes negligible. Thus  $E_{z2}$  becomes the dominant, if not the only electric field at the radiation zone. In contrast when Medium 1 is a highly conducting medium with a very low intrinsic impedance,  $E_{z2}$ , although still proportional to  $\cos\phi$ , becomes the strongest field component. Equation (12) then shows that a conformal antenna situated at and parallel to the ground plane could be effective without a cavity at the base provided the ground-plane-impedance could be made high by employing a very-low-conductivity, and high permeability material such as a ferrite. Also, the high-impedance ground plane in such cases need not extend to infinity and in many cases a ground plane slightly larger than what is needed to accommodate the current element may be adequate. Additionally, one may note that the radiated electric field intensity in the presence of the high-impedance surface is twice as large as is obtained when the radiation is totally in free-space.

To examine the scattering from such an antenna element, one may first determine the current distribution at the antenna by the moment method while using the expression for  $E_{z2}$ , given in (6) as the Green's function. By equating the sum of  $E_z$  field at the antenna due to the impinging field and due to the current induced at the antenna by such a field to zero, one obtains the current distribution. Conventional methods can then be used to determine the scattering characteristics. Such techniques, being well known, are not discussed further in this paper.

#### ACKNOWLEDGEMENT

The assistance of Mrs. Patricia Van Ballegooijen toward the preparation of the manuscript is gratefully acknowledged.

#### REFERENCES

1. A. Sommerfeld, "Über die Ausbreitung der Wellen in der drachtlosen telegraphie", Ann. Physik, 28,655, 1909.
2. K. Norton, "The Propagation of Radio Waves over the Surface of the Earth and Upper Atmosphere", Proc. IRE, 25, 1203, Sept. 1937.
3. J. Wait, Electromagnetic Waves in Stratified Media, The MacMillian Co., New York, 1962.

# GTD ANALYSIS OF MICROSTRIP ANTENNAS AND VIBRATOR WITH PLANE SCREEN

N.N.Gorobetz, N.P.Ellseyeva

Electrodynamics department, Kharkov State University  
4 Svoboda Sq., Kharkov, p.o.310077, Ukraine

## ABSTRACT

Using the uniform geometrical theory of diffraction there has been obtained an asymptotic solution of the three-dimensional problem of the diffraction of electromagnetic radiation of the arbitrarily oriented and situated vibrator on an ideally conducting infinitely-thin screen of a rectangular form. There have been worked out fast-acting algorithms and programs for calculating and analyzing normalized amplitude directive patterns of microstrip antennas and vibrator with a screen in different observation planes. Comparing the known calculations with the strict method, it is shown that the worked-out algorithm provides sufficient accuracy beginning with the screen sizes of the order of the wave length for a small vibrator distance from the screen.

## INTRODUCTION

In the modern diffraction theory one of the most interesting aspects is diffraction of electromagnetic waves on metallic screens. To solve this problem there are used both the Integral Equation Formulation (IEF) and the approximated techniques based on assumptions of Physical Optics (PO) [ 1 ]. Calculation realization of the strict method is complicated and requires plenty of computation time, PO method leads to great errors when calculating antenna side radiation. Using the uniform geometrical theory of diffraction in our report there have been obtained the asymptotic solution of the three-dimensional problem of the diffraction of electromagnetic radiation of an vibrator on ideally conducting infinitely-thin screen of a rectangular form in cases, when vibrator is perpendicular to a screen and parallel to a larger or a smaller side of the screen. In a short wave approximation, superposition of these radiation fields allow to determine a field of an arbitrarily-oriented vibrator to a screen. There have been worked out fast-acting algorithms and programs for calculating and analyzing directional properties of the vibrator antennas with a screen over the whole observation space. At the same time, in [ 2 ] there have been compared our calculated directive patterns ( DP ) with the known ones calculated for the same geometrical parameters by means of the IEF and PO methods. It is shown that the worked-out algorithm provides reliable results, beginning with the screen sizes of the order of the wave length for the vibrator being distant from the screen in this case not more than  $0.3\lambda$ . With increasing the screen size, an accuracy appropriate for practice is provided when having the vibrator at a larger distance from the screen.

## FORMULATION OF THE RADIATION FIELDS

Let us introduce a Cartesian coordinate system  $X, Y, Z$  ( Fig. 1 ). The screen sides are  $W$  and  $L$ , respectively. A symmetrical electric vibrator used as a radiator is at the height  $h$  above the screen, being inclined with respect to the  $Z$ -axis at the angle  $\beta$ . The calculation algorithm of a geometrical-optical (GO) field of the vibrator with plane screen is based on the method of images



supposing for infinite sizes of the ideally conducting screen its replacement with image-radiator of a reflected wave. For a vibrator situated in the plane ZY, we resolve the current  $I$  flowing in the tilted vibrator into a horizontal ( $I_h = I \sin \beta$ ) and a vertical component ( $I_v = I \cos \beta$ ). For the screen being excited by the current component  $I_v$  the GO fields of the incident and reflected waves ( $i=1,2$ ) in the far zone are

$$E\theta_i(\theta, \varphi) = (-1)^{i+1} E_0 \exp(jkDi) [\cos(kl \cos \theta) - \cos kl] / \sin \theta, \quad (1)$$

where  $Di = h \cos(\alpha_i - \varphi) \sin \theta$  is the trajectory difference between the rays from the centre of the  $i$ -radiator and those from the coordinate system origin to the observation point;  $\alpha_i = 0, \pi$  is respectively for  $i=1,2$ ,  $E_0 = 0.5jW_0 (Idl/\lambda) \exp(-jkR)/R$  ( $Idl/\lambda$  is the Herzian dipole current,  $W_0 = 120\pi$  Ohm,  $k=2\pi/\lambda$ ).

For the screen being excited by the vibrator situated in a XY-plane and oriented at the angle  $\zeta$  to the X-axis, there have been derived the expressions for the GO field as

$$E\theta_{Li}(\theta, \varphi) = F_{Li}(\theta, \varphi) \cos(\varphi - \zeta_i) \cos \theta, \quad E\varphi_{Li}(\theta, \varphi) = F_{Li}(\theta, \varphi) \sin(\varphi - \zeta_i), \quad (2)$$

$$F_{Li}(\theta, \varphi) = E_0 \exp(jkDi) [\cos(kl \sin \theta \cos(\varphi - \zeta_i)) - \cos kl] / [1 - \sin^2 \theta \cos^2(\varphi - \zeta_i)]. \quad (3)$$

The DP of the edge wave with a phase centre in the origin of its own coordinate system on the  $n$ -edge ( $R_n, \theta_n, \varphi_n$ ) of the screen is defined as the DP of the wave diffracted by an ideally conducting half-plane under exciting by a dipole or its image. If the  $i$ -radiator is parallel to a screen edge, then an electric far-zone field of the primary diffraction wave is given by

$$E\theta_{in}(\theta, \varphi) = E\theta_i(\theta, \varphi) T(\xi_{in}), \quad T(\xi_{in}) = \pm [\Phi(|\xi_{in}| j^{1/2}) - 1] / 2. \quad (4)$$

The sign "+" stands for a light region of GO wave, and that of "-" is for a shadow one.  $\xi_{in} = (2kr_{in} \sin \theta_n)^{1/2} \cos[(\varphi_n - \varphi)/2]$ ,  $r_{in}$  and  $\varphi_{in}$  are the polar coordinates of the  $i$ -radiator in its own system on the  $n$ -edge.

In case when the radiator is perpendicular to a screen edge, the electric field intensity is expressed by

$$E\theta_{Lin}(\theta, \varphi) = E\theta_{Li}(\theta, \varphi) T(\xi_{in}) - p \cos \theta_n \sin(\varphi_n/2), \quad (5)$$

$$E\varphi_{Lin}(\theta, \varphi) = E\varphi_{Li}(\theta, \varphi) T(\xi_{in}) - p \cos(\varphi_n/2), \quad (6)$$

$$p = \sin(\xi_{in} - \varphi_{in}/2) [2 / (\pi k r_{in} \sin \theta_n)]^{1/2} \exp[-j(kr_{in} \sin \theta_n + \pi/4 - kDi)].$$

The fields of the twice diffracted waves between the parallel screen-edges are described by the uniform-observation-angle asymptotic expression

$$E_{mn} = \pm E_m [\pm \Phi(|\xi_{mn}| j^{1/2}) - 1], \quad \Phi(\xi j^{1/2}) = 2\pi - \frac{1}{2} \exp(j\pi/4) \int_0^\xi \exp(-jt^2) dt, \quad (7)$$

$$\xi_{21} = \sqrt{2kL \sin \theta} \sin(45 - \varphi/2), \quad \xi_{12} = \sqrt{2kL \sin \theta} \cos(45 - \varphi/2), \quad (8)$$

$$\xi_{34} = \sqrt{2kW \cos \varphi} \cos \theta/2, \quad \xi_{43} = \sqrt{2kW \cos \varphi} \sin \theta/2. \quad (9)$$

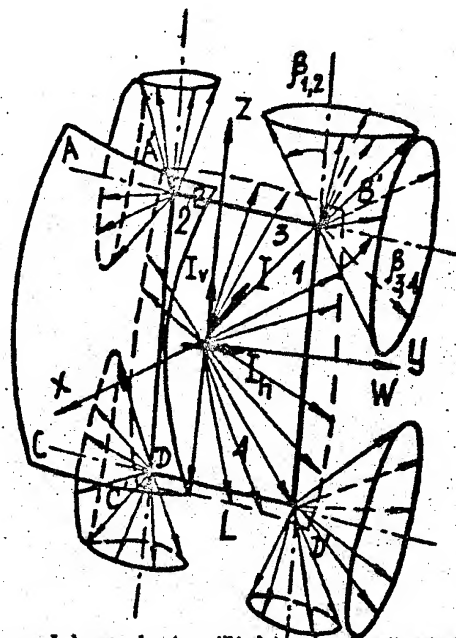


**Fig.1 Problem geometry and boundaries "light-shadow" of GO and edge waves**

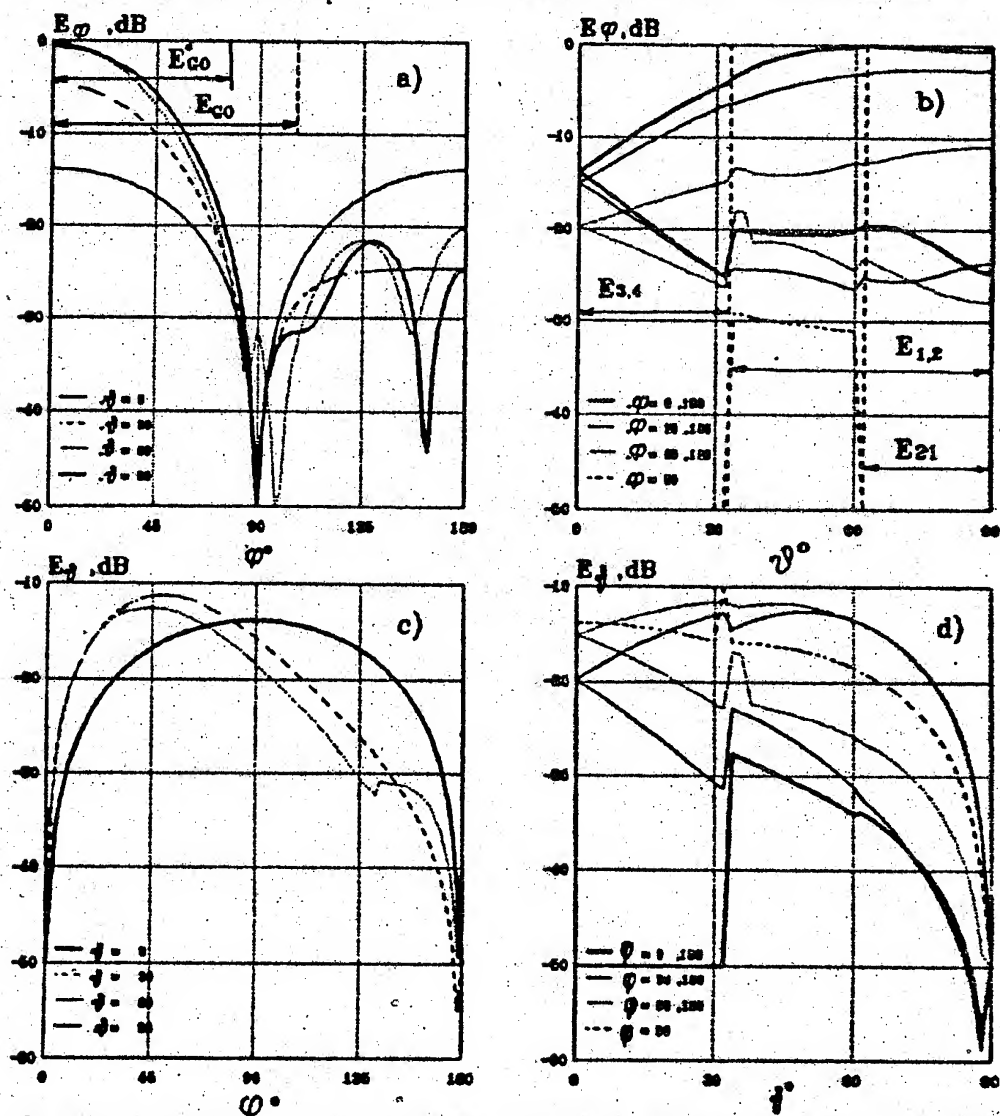


**Fig.2. Normalized amplitude directive patterns in different observation planes**

The first sign "+" in (7) stands for a light region of GO waves, the second sign "+" for a light region of singly diffracted waves, and that of "-" is for a shadow of these waves.  $E_m$  is defined by (4)...(6) as the uniform asymptotic of singly diffracted wave field on the edge  $m$ .

Because of finite sizes of the screen, each of the waves has a limited radiation region. The boundaries "light-shadow" of an incident spherical wave form a curved square ABCD (Fig. 1) and those of a spherical wave reflected from the screen form a curved square A'B'C'D'. The boundaries "light-shadow" are defined by the side equations of these squares. The edge rays breaking at angle points of the screen form cones of shadow. In case when a vibrator is above a centre of the screen, semivertex angles of the cones for edges 1 and 2, 3 and 4 are equal

$$\beta_{1,2} = \arctg \left[ \sqrt{k^2 + (L/2)^2} / (W/2) \right], \quad \beta_{3,4} = \arctg \left[ \sqrt{k^2 + (W/2)^2} / (L/2) \right]. \quad (10)$$

Fig. 2 shows the normalized DPs ( $F = 20 \lg (|E| / |E|_{\max})$ ) in the different observation planes for the screen with the sides  $W = 2.475\lambda$  and  $L = 1.5\lambda$  and  $h = 0.25\lambda$ , excited by the electric dipole oriented parallel to side  $L$ . The curves in Fig. 2(a,b) presents DPs for the  $E_{\varphi}$ -component, in Fig. 2(c,d) for  $E_{\theta}$ -component. Because of the DPs are defined by discontinuity functions, there are presented the angular light-regions for the GO and the edge waves.

The expressions for radiation field components in the main observation planes  $XZ$  ( $\varphi = 0^\circ$ , the upper half-plane) and  $XY$  ( $\theta = 90^\circ$ , the right half-plane) in case when the vibrator is parallel to  $Y$  axis are

$$E_{\varphi L}(\theta, \varphi) = E_{\varphi L q_0} + E_{\varphi L 1,2} + E_{\theta 1,3,4} + E_{\varphi L 2,1} + E_{\theta 1,1}, \quad (11)$$

$$E_{\theta L}(\theta = 90^\circ) = 0, \quad E_{\theta L}(\varphi = 0^\circ) = E_{\theta L 1,2} + E_{\theta L 2,1}. \quad (12)$$

In case of a grazing observation along a screen in directions when  $\varphi = 90^\circ$  or  $\theta = 0^\circ$ , the radiation fields are

$$E(\varphi = 90^\circ) = (E_2 + E_{21}) + E_1, \quad E(\theta = 0^\circ) = E_{q_0} + (E_4 + E_3) + E_3. \quad (13)$$

Taking into consideration that in (8), (9)  $\xi_{21} = 0$  under  $\varphi = 90^\circ$ ,  $\xi_3 = 0$  under  $\theta = 0^\circ$  and so  $E_2 + E_{21} = 0$ ,  $E_4 + E_3 = 0$ , we may say that in case of Neyman boundary conditions, diffracted field under  $\varphi = 90^\circ$  (Fig. 2b) in the light region of twice diffracted wave ( $E_{21}$ ) is equal to 0 because the edge waves of the incident and reflected ones are opposite in phase. In case of Dirichle boundary conditions the diffracted field is formed on the nearest edge (Fig. 2d). The radiation field components under  $\theta = 0^\circ$  (Fig. 2a,c) are the sums of GO field and the diffracted field on the nearest screen edge.

## REFERENCES

- (1) Yu. Pimenov, D. Khod'kov: "Radiation of an elementary electric vibrator situated parallel to a plane rectangular screen", Radiotekhnika, (1991), 7, pp. 61-63.
- (2) N. Gorobetz, N. Elisseyeva: "Algorithms and programs of calculation of directional response patterns of the vibrator antennas with plane screen" (in Russian), Proceedings of 2nd Crimean conference on Microwaves technology and Satellites reseption, Sevastopol, Ukraine, October 8-10, 1992, pp. 549-554.



# RADIATION OF VIDEO PULSE BY FINITE LENGTH DIPOLE ANTENNA.

N.N. Gorobetz, J. Yu. Shavorykina, A.V. Nechosa (Usina)

Electrodynamics department, Kharkov State University  
4 Svoboda Sq., Kharkov, p.o.310077, Ukraine  
( Phone: 0572+45-71-75; Fax: 0572+47-12-72 )

## ABSTRACT

Pulse radiation of linear vibrator is investigated. The exact formulas for E and H components of electromagnetic field were obtained for the cases of an arbitrary vector source; a linear source with an arbitrary time-dependence of the inducing current density and the case of pulse inducing current as a re-entering discharge. Last case was detally investigated by means of computer analysis of the exact formulas. Dependences of the radiated pulse shape, duration and amplitude on distance from the antenna, on time and on observation directions were studied. The exact formulas allowed to carry out this investigation for near field zone, far field zone and between them. The question of determination of these zones for pulse radiation is discussed.

## INTRODUCTION

Growing up for the last years interest to transient ( unharmonic ) signals is connected with an extension of possibilities of their application and generation. One well knows the areas of nonsinusoidal signal application from pulse weather-independent high-resolution radars up to radiocommunication with deeply dipped submarines.

In the present work the radiation of superbroadband pulse signal by weakly-directed exciters ( Gertz dipole and wire antenna of finite size ) is investigated.

## RADIATION OF LINEAR DIPOLE WITH ARBITRARY CURRENT TIME-DEPENDENCE.

Let us consider a radiation of Hertz dipole as a linear vibrator with a length equal 1 with an arbitrary time-dependence of inducing current described by the function  $j(t, r)$ ,  $r=(x, y, z)$ . For electrical component of electromagnetic field induced by a source with current density  $j$  but of presence of other sources the follows wave equation take place

$$\text{rot rot } \mathbf{E} + \frac{1}{v^2} \frac{\partial^2}{\partial t^2} \mathbf{E} = - \frac{4\pi}{c^2} \frac{\partial}{\partial t} \mathbf{j} \quad (1)$$

where  $v = c/\sqrt{\epsilon}$ ,  $\epsilon$  is a medium dielectric permittivity. The solution of this equation can be founded as a convolution of Green's function of the left part of the equation with the free term.

$$\mathbf{E} = \int_{-\infty}^{\infty} d\mathbf{x}' \hat{\mathbf{G}}(\mathbf{x} - \mathbf{x}') \frac{\partial \mathbf{j}(\mathbf{x}')}{\partial t'} \quad (2)$$

where Green's function is determined by the follows expressions found in the paper [1]:

$$\hat{G} = \frac{1}{s} (\text{grad div} - \frac{1}{v^2} \frac{\partial^2}{\partial t^2}), \quad (3)$$

$$f(x-x') = \frac{t-t'-\frac{|r-r'|}{v}}{|r-r'|} \theta(t-t'-\frac{|r-r'|}{v}),$$

where  $x$  and  $x'$  are four-dimensional vectors of spatial coordinates and time  $x=(t,r)$ ,  $\theta$  is Heviside unit function. Taking into account that

$$(\Delta - \frac{1}{v^2} \frac{\partial^2}{\partial t^2}) f(x-x') = -4\pi(t-t'-\frac{|r-r'|}{v}) \delta(|r-r'|),$$

the following expression for the field  $E$  out of the source can be found:

$$E = \frac{1}{s} \int_{-\infty}^{\infty} dx' \theta(t-t'-\frac{|r-r'|}{v}) \frac{t-t'-\frac{|r-r'|}{v}}{|r-r'|} \frac{\partial(t',r')}{\partial x'} \quad (4)$$

This formula determines the radiation of an arbitrary vector source with an arbitrary dependence of inducing current both on time and on spatial coordinates. For the linear vibrator of finite length  $l$  the inducing current density will be

$$J(t,r) = \delta(x)\delta(y)\theta(l/2-z)\theta(z+l/2)I(t), \quad (5)$$

where  $\delta$  is Dyra's delta-function.

Here an arbitrary time-dependence of  $I(t)$  is considered that one can consider a stationar source as well as a transient one. The vibrator is located in the choosen coordinate system as the figures 1 and 2 show. In the spherical coordinate system with a center in the point  $O'$  with coordinates  $(r \sin \theta, 0, r \cos \theta)$  and  $\rho = |r-r'|$  as it is on the figures 1 and 2 the expression (5) for the inducing current density becomes the follows

$$J(t',r') = \delta(r \sin \theta - \rho \sin \theta \cos \phi) \delta(\rho \sin \theta \sin \phi) \quad (6)$$

$$\theta(l/2 - r \cos \theta + \rho \cos \theta) \theta(r \cos \theta - \rho \cos \theta + l/2) I(t')$$

After integration of (4) for spatial coordinates accounting (6) one can consider the expression for the field  $E$  inside the layer  $|z| < l/2$  as

$$E = \frac{1}{s} \text{retrot} \left\{ \int_{-\infty}^{t-Q/v} dt' \frac{dI(t')}{dt'} (v(t-t') \ln \frac{Q}{r \sin \theta_0} - Q + r \sin \theta_0) + \right.$$

$$\left. + \int_{t-Q/v}^{t-r \sin \theta_0} dt' \frac{dI(t')}{dt'} (v(t-t') \ln \frac{v(t-t')}{r \sin \theta_0} - \frac{1}{v} (v(t-t') - r \sin \theta_0)) \right\}, \quad (7)$$

where  $Q = \sqrt{r^2 \sin^2 \theta + (r \cos \theta + 1/2)^2}$ .

This formula is available for the case of radiation of a vibrator with an arbitrary time-dependence of the inducing current density both for stationary and transient sources expressions for the case of pulse radiation. The formula (7) can be integrated for  $t$  for the concrete type of the time-dependence  $I(t)$ . One considered the case of radiation of the current as re-entering discharge [2].

$$I(t) = I_0 (e^{-t/\tau_1} - e^{-t/\tau_2}) \theta(t), \quad (8)$$

After integrating (7) for  $t$  for the current (8) and rotot calculation the following expression for the field E tangencial component take place:

$$E_\theta = \frac{I_0 v}{r^2} \sum_{l=1}^2 \frac{(-1)^l}{\lambda_l} \{ \theta(vt - r \sin \theta_0) \left[ \frac{2 \sin \theta_0}{r} e^{i \cos(t - r \sin \theta_0 / v)} (-\cos 2\theta_0 \lambda_l + \frac{2 \sin \theta_0}{r}) \right] + \theta(vt - Q) \left[ e^{i \cos(t - Q/v)} \left( \frac{\lambda_l r (Q_r')^2}{vQ} \sin \theta - \frac{\lambda_l Q_r' Q_\theta'}{vQ} \cos \theta + A(\theta, r) \right) \right] \},$$

$$A(\theta, r) = \left( \frac{3Q_r'}{Q} + \frac{rQ_{rr}''}{Q} - \frac{(Q_r')^2 r}{Q^2} \right) \sin \theta - \left( \frac{Q_{\theta r}''}{Q} - \frac{Q_\theta' Q_r'}{Q} \right) \cos \theta$$

(9)

where  $\lambda_l = 1/\tau_l$ ,  $Q'$ ,  $Q''$ , and  $Q'''$  are the derivations of  $Q$ .

Analogical expression for E radial component and for the field E for  $|z| > 1/2$  was obtained. These formulas allowed to obtained also expressions for magnetic component of the field using Maxwell's equations. All these obtained expressions are exact ones which allowed to study the radiated pulse behaviour in near field zone, far field zone and between them. Dependences of the pulse shape, duration and amplitude on distance from the antenna, on time and on observation directions (determined by the angle  $\theta$ ) were investigated by means of computer analysis of the obtained formulas. The question of determination of these zones for pulse radiation is discussed in connection with the obtained results.

## REFERENCE

- (1) Nerukh A.G., Khizhnyak N.A. Journal of Technic Physics, Leningrad, V.43., 1973, p.p. 1113-1120.
- (2) P.V.Bliokh, A.P.Nikolaenko, Yu.F.Filippov. Global electromagnetic resonances in the cavity Earth-ionosphere. Kiev, Naukova dumka publ., 1977, p.200.

# THE QUASITHREE-DIMENSIONAL PROBLEM ON EXCITATION OF THE WIRE SYSTEM LOCATED ON A CHIRAL HALF-SPACE

GENNADY GOSHIN, NATALIA LUGINA

Siberian Physico-Technical Institute  
Revolution Sq., 1, Tomsk, 634050, Russia

**ABSTRACT.** The quasithree-dimensional problem deal with the investigation of the straight line wire system located on a chiral-achiral interface. The rigorous solution of the problem is represented by the Fourier integrals. The spectra of the excited waves are explored and for the surface waves one-directional energy transmission are founded. The problem is devoted to the designing of wideband antennas with the needed polarised characteristics and nonreciprocal devices at microwave.

1. In the electromagnetic theory of the chiral media are absent papers devoted to the investigation of the wire system located on a chiral-achiral interface. Depending on concrete applications wire system may be considered as reflector array or delay system which able to support surface waves. Similar problems offer particular interest in the connection with the designing of new types of wideband low-profile antennas with the needed polarized characteristics and the corresponding transmission lines at microwave.
2. Let us consider in a Cartesian coordinate system  $x, y, z$  a plane  $z = 0$  perfectly conducting in the directions making up angle  $\psi$  with the positive axis  $z$  direction and non-conducting in other directions. A plane is situated on the interface of the two media. Region 1 ( $z > 0$ ) is magnetodielectric with the parameters  $\epsilon_1, \mu_1$ . Medium 2 ( $z < 0$ ) represents chiral half-space with the real parameters  $\epsilon_2, \mu_2, \xi$ . The parameter of the chirality  $\xi$  enters through the constitutive equations [1/

$$\begin{cases} \vec{D}_2 = \epsilon_2 \vec{E}_2 + i\xi \mu_2 \vec{H}_2 \\ \vec{B}_2 = \mu_2 \vec{H}_2 - i\xi \epsilon_2 \vec{E}_2 \end{cases} \quad (1)$$

where  $\epsilon_0 = \epsilon_2 + \mu_2 \xi^2$ . When  $\xi = 0$  we have magnetodielectric medium with the absolute parameters  $\epsilon_2, \mu_2$ . The primary field is produced by an electric line source with running wave current distribution  $I_y^*(y) = I_y^* e^{i\gamma y}$  located in the upper half-space parallel to the  $y$  axis and having coordinates  $x_0, z_0$ . The time dependens is assumed to be  $e^{-i\omega t}$ .

3. The method of the solution includes the introduction two vectors  $\overline{M}^{\pm}$  describing the fields of left and right circularly polarized waves /2/ and appropriate them scalar potentials  $U^{\pm}$ , which are superposition of the normal to the interface electrical and magnetic vector potentials  $A_{\pm}^{e,m}$ . In free-source region potentials  $U^{\pm}$  are the solutions of the homogeneous Helmholtz equations and are represented by the Fourier integrals. Unknown potential's spectral densities of the secondary field are defined from the boundary conditions for the components of field intensities on the plane  $z = 0$

$$\begin{cases} \alpha(E_{s1} + E_{s1}^0) + E_{v1} + E_{v1}^0 = 0, \\ \alpha(H_{s1} + H_{s1}^0) + H_{v1} = \alpha H_{s2} + H_{v2}, \\ E_{s1} + E_{s1}^0 = E_{s2}, E_{v1} + E_{v1}^0 = E_{v2}, \end{cases} \quad (2)$$

where  $\alpha = \text{ctg} \psi$  and primary field components are supplied by the symbol "0". The obtained solution for the potentials of the secondary field in the regions 1 and 2 has the form

$$\begin{cases} U_1^{\pm}(x, y, z) = \frac{w_1 I_y^0 e^{i\eta y}}{4\pi} \int_{-\infty}^{\infty} \left\{ \frac{(x \mp \eta \frac{\gamma_1}{\kappa_1})}{\frac{\gamma_1}{\kappa_1}(x^2 + \eta^2)} + \frac{2\alpha w_c}{D(x, \eta)} \left( \frac{\gamma_+}{\kappa_+} + \frac{\gamma_-}{\kappa_-} \right) \left[ \frac{\gamma_1(\alpha x + \eta) \pm (\alpha \eta - x)}{\kappa_1} \right] \right\} \\ \cdot e^{i\kappa(x - x_0) - \gamma_1(z + z_0)} dx, \\ U_2^{\pm}(x, y, z) = \frac{\alpha w_1 w_c I_y^0 e^{i\eta y}}{\pi} \int_{-\infty}^{\infty} \frac{\gamma_1}{\kappa_1} \left[ \frac{\frac{\gamma_{\mp}}{\kappa_{\mp}}(\alpha x + \eta) \mp (\alpha \eta - x)}{D(x, \eta)} \right] \\ \cdot e^{i\kappa(x - x_0) + \gamma_{\pm}z - \gamma_1 z_0} dx, \end{cases} \quad (3)$$

where

$$\begin{aligned} D(x, \eta) = & \left\{ 2 \frac{\gamma_1}{\kappa_1} w_1 \left[ (\alpha \eta - x) - \frac{\gamma_-}{\kappa_-} (\alpha x + \eta) \right] \left[ (\alpha \eta - x) + \frac{\gamma_+}{\kappa_+} (\alpha x + \eta) \right] \right. \\ & \left. + w_c \left[ \frac{\gamma_-}{\kappa_-} + \frac{\gamma_+}{\kappa_+} \right] \left[ (\alpha \eta - x)^2 - \left( \frac{\gamma_1}{\kappa_1} \right)^2 (\alpha x + \eta)^2 \right] \right\}, \end{aligned} \quad (4)$$

$\kappa_1 = \omega \sqrt{\epsilon_1 \mu_1}$ ,  $\kappa_{\pm} = \kappa_c (1 \pm \xi w_c)$ ,  $\kappa_c = \omega \sqrt{\epsilon_0 \mu_2}$ ,  $\gamma_1 = \sqrt{x^2 + \eta^2 - \kappa_1^2}$ ,  $\gamma_{\pm} = \sqrt{x^2 + \eta^2 - \kappa_{\pm}^2}$ ,  $w_1 = \sqrt{\mu_1 / \epsilon_1}$ ,  $w_c = \sqrt{\mu_2 / \epsilon_0}$ , the double signs correspond to the double potential signs. When  $\xi = 0$ ,  $\eta = 0$ ,  $\alpha = \infty$ , solution (3)—(4) completely coincides with the solution of the problem on excitation planar interface of the two magnetodielectric media by line source /3/.

4. From obtained solution follows, that there are excited both continuous and eigenvalue wave spectra in considered system. Wave propagation constants

of the continuous spectrum connect with the branch points  $\gamma_{\pm} = 0$ ,  $\gamma_1 = 0$  and are proportional to the plane wave propagational constants in infinite chiral and achiral media, i.e.  $\kappa_{\pm}$  and  $\kappa_1 = 0$ . Evaluation of the branch-cut integration for the branch point  $x_1 = \pm\sqrt{\kappa_1^2 - \eta^2}$  yields radiation field of the source in the upper half-space. Evaluation of the branch-cut integration for the points  $x_2 = \pm\sqrt{\kappa_+^2 - \eta^2}$  and  $x_3 = \pm\sqrt{\kappa_-^2 - \eta^2}$  describes the lateral waves /4/.

Eigenvalue wave spectrum is determined by roots of the equations  $D(x, \eta) = 0$ , which in general case will be complex. When  $|x| > \sqrt{\kappa_{\pm}^2 - \eta^2}$  roots are real and determine propagation constants of the surface waves which connect with the line wires system located on the two media interface. These solutions for the number of parameters are given on fig.1. The existence region of the surface waves is limited by dotted line. When the interface is absent, the expression for the propagation constants of the surface waves have the form

$$x_0 = \pm \kappa_1 \sqrt{1 + 1/\alpha^2} - \eta/\alpha, \quad (5)$$

where double signs correspond to the signs of the inequalities  $(x - x_0) \geq 0$ . These quantities correspond quantities of the cross wavenumbers

$$\gamma_0 = \frac{\kappa}{\alpha} \mp \eta \sqrt{1 + 1/\alpha^2}. \quad (6)$$

The condition for the existence of the surface waves are  $\gamma_0 > 0$  or  $\kappa > \eta \sqrt{1 + \alpha^2}$ .

It follows from curves on the fig.1 and formulae (5), (6) that in this system surface waves have different phase velocities in opposite directions and one-directional energy transmission will take place when exist certain relations between parameters. Similar effect may serve as basis for the designing of some microstrip nonreciprocal devices at microwave.

The research reported in this paper was supported by the Russian Fund of Fundamental Investigations (Project 93 - 02 - 3548).

#### REFERENCES

- (1) L.V. Lindell: "Simple variation of various Green dyadics for chiral media", AEU, (1990) 44, 5, s.427-429
- (2) H. Bateman: "The mathematical analysis of electrical and optical wave-motion on the basis Maxwell's equation", Dover Publications INC, (1958), 180p.
- (3) G.T. Marcov, A.F. Chaplin: "Excitation of the electromagnetic waves", Radio and svyas, (1983) 296p.
- (4) L.M. Brekovskikh: "Waves in layered media", Nauka, (1973), 314p.

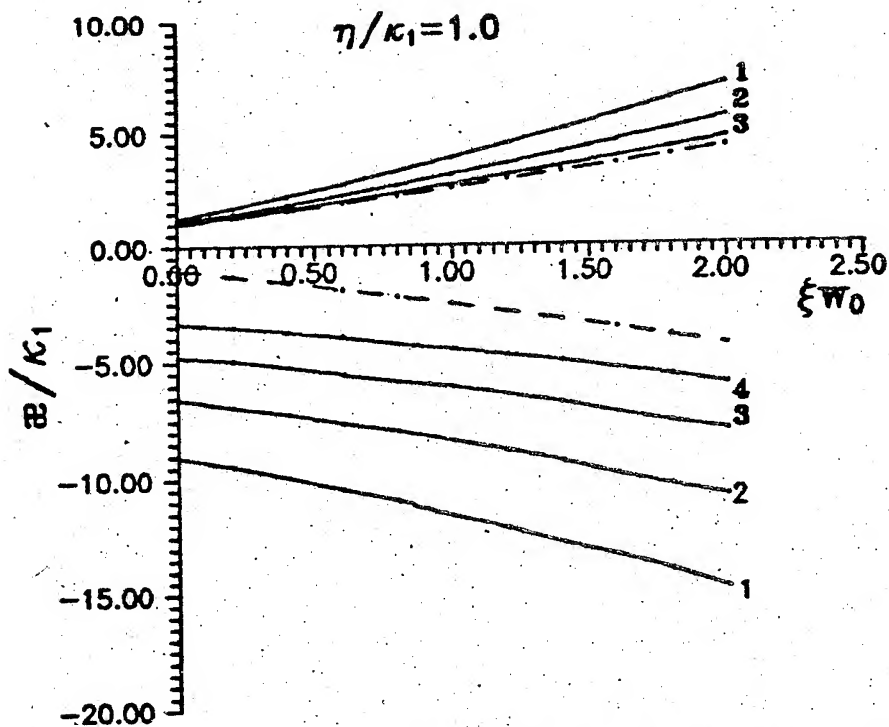
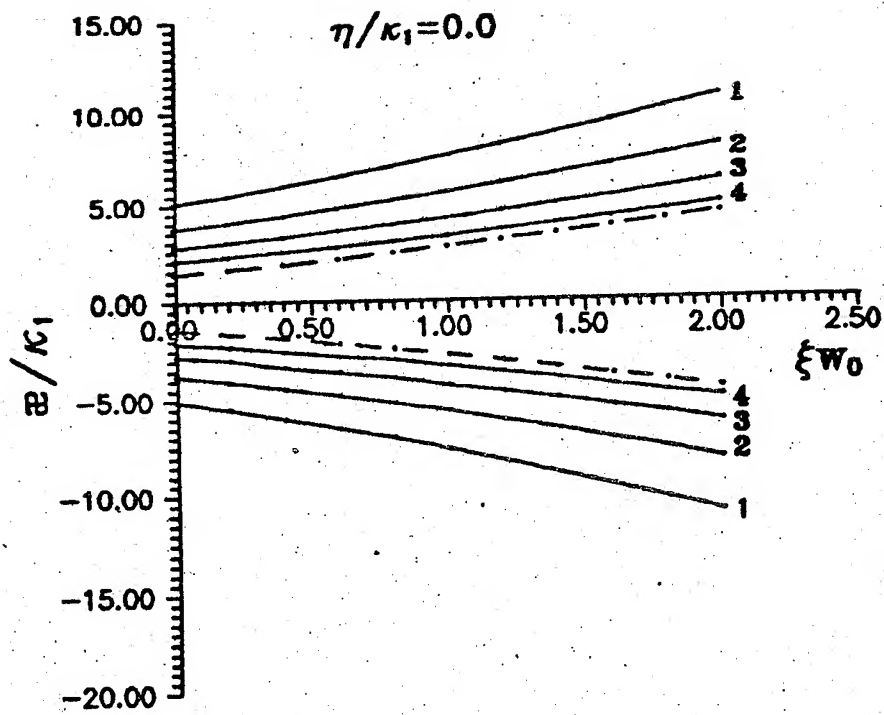


Fig. 1 Propagation constants of the surface waves ( $\epsilon_1=1.0, \epsilon_2=2.0$ ,  $w_0=120\pi$  cm; 1- $\alpha=0.25$ ; 2- $\alpha=0.35$ ; 3- $\alpha=0.50$ ; 4- $\alpha=0.75$ )



# CALCULATION OF DISPERSIONAL CHARACTERISTICS OF MULTIBEAM MULTISTAGE STRUCTURES WITH HIGHER SYMMETRIES

Elena V. Guseva, Victor I. Naidenko  
Radiotechnical Department of Kiev Politechnical Institute,  
pr. Peremogi, 37, KPI-2110, Kiev, Ukraine

## ABSTRACT

The real symmetrical linear algebraic equation system of comparatively low order accounting the higher symmetry of multistage periodic structure, unlimited number of coupling slots and interaction channels in each diaphragm has been obtained.

Results that show the possibility to calculate multibeam multislot multistage structures with high accuracy by personal computers have been presented.

## INTRODUCTION

At present time in microwave electron devices and accelerators of charged particles, as a rule, periodic structures with higher symmetries (with screw symmetry axis or glide symmetry plane) are used. Such structures are multibeam ones. They have more linear dispersive characteristic, wider bandwidth, better frequency dependence of energetic characteristics than the structures with lower symmetries. Structures being used in multibeam devices have, as a rule, great number of coupling slots. This makes it possible to achieve better field homogeneity in interaction channels and heat-dissipative capacity. Under calculation of properties of such systems a lot of serious difficulties are caused due to the great number of interaction channels and couplers, multistage character of the structure.

Integral equation system (IES) [1], that describes properties of waves in multistage periodic structures, does not take into account a higher symmetry of the structures, great number of coupling slots and transition holes, has high order and is complex. Due to this it is necessary to solve complex linear algebraic equation system (LAES) of high order that makes difficult, and sometimes, impossible to solve boundary-value problem for periodic structures being used in practice.

IES obtained in [2] is very promising. It takes into account a higher symmetry of the structure, unlimited number of coupling slots and interaction channels in each diaphragm, and is real and symmetrical. Reduction of IES order has been achieved by use of effective period of the structure with higher symmetry and generalized Floquet's theorem [3]. Pass from complex IES to real one has become possible due to the introduction of even and odd parts of tangential electric field.

The goal of the present work is to develop calculation method formulated in [2], investigation of characteristics of various structures, which are of practice interest and demonstrate a high effectivity of developed method under calculation of extremely complex sufficiently three dimensional electrodynamic systems.

## INTEGRAL EQUATION SYSTEM

Period of the structure with higher symmetries can be presented as a union of several effective periods. Effective period can be defined as a segment of periodic structure contained between chosen section and the same one but displaced on a minimal length and angle as a result of application operators of translation and rotation that lead to coincidence of the structure with its own.

Geometry of the effective period and notations are presented in fig 1 (regions 1,  $Q+1$  - cavities, regions 2, ...,  $Q$  - slots and channels for beams).

Fields in region  $q$  ( $q = 1, \dots, Q+1$ ) are presented as a sum of eigenwaves [4].

Let's denote the tangential electric field on the left boundary of regions with numbers 2, ...,  $Q$  as  $\vec{E}_q^-$ , on the right boundary of the same regions - as  $\vec{E}_q^+$ , introduce even and odd with respect to plane  $z_q = 0$  parts of electric field

$$(1) \quad \vec{E}_{qe} = (\vec{E}_q^+ + \vec{E}_q^-) / 2, \quad \vec{E}_{qo} = i(\vec{E}_q^+ - \vec{E}_q^-) / 2.$$

IES is presented as:

$$(2) \quad \sum_{P=1}^2 \sum_{m=1}^{\infty} \frac{\gamma_{ms1}^{(P)} \vec{\Phi}_{ms1}^{(P)}}{\sin(2\gamma_{ms1}^{(P)} l_1)} \sum_{s=2}^Q \int_{S_s} \left\{ \sin(\varphi + m_1 \psi_0) \vec{E}_{s0}^- - \left[ \cos(2\gamma_{ms1}^{(P)} l_1) \mp \cos(\varphi + m_1 \psi_0) \right] \vec{E}_{s0}^+ \right\} \vec{\Phi}_{ms1}^{(P)*} ds \pm$$

$$\pm \sum_{P=1}^2 \sum_{m=1}^{\infty} \gamma_{msq}^{(P)} \left\{ \frac{ig}{cig} (\gamma_{msq}^{(P)} l_q) \right\} \vec{\Phi}_{msq}^{(P)} \int_{S_q} \vec{E}_{q0}^- \vec{\Phi}_{msq}^{(P)*} ds = 0, \quad q = 2, \dots, Q.$$



The summation in (2) is done with respect to wave types ( $E$  and  $H$ , index  $P$ ) and transversal indices ( $m_q, s_q$ ) of eigenwaves of region  $q$ .  $\bar{\Phi}_{msq}^{(P)}$ ,  $\gamma_{msq}^{(P)}$  and  $\gamma_{msq}^{(P)}$  are orthonormalized vectorial eigenfunctions, wave admittance and longitudinal wave numbers of eigenwaves with transversal indices  $m_q, s_q$  of region with number  $q$ .

Upper (lower) indices of amplitudes of even and odd parts of transversal vector of electric field correspond to upper (lower) signs.

The IES order is determined by number of coupling channels and equal to  $2(Q-1)$ .

When there are no higher symmetries and phase shift  $\varphi = 0$  or  $\varphi = \pi$  IES (2) divides into two subsystems: solution of one of them gives odd or even parts of transversal electric field on the boundaries of partial regions (in dependence on  $\varphi$  and frequency), solution of other - zero. Thus, to determine boundaries of passbands of waves in structures with symmetries of translation or reflection types IES of order that is two times lesser than (2) can be used.

### LINEAR ALGEBRAIC EQUATION SYSTEM

Let's approximate  $\bar{\mathcal{E}}_{q0}^e$  with finite series of eigenfunctions of E- and H-waves

$$(3) \quad \bar{\mathcal{E}}_{qe} = \sum_{R=1}^2 \sum_{m_q}^M \sum_{s_q}^S B_{emsq}^{(R)} \bar{\Phi}_{msq}^{(R)}, \quad \bar{\mathcal{E}}_{qo} = \sum_{R=1}^2 \sum_{m_q}^M \sum_{s_q}^S B_{omsq}^{(R)} \bar{\Phi}_{msq}^{(R)}.$$

Substituting (3) into (2) and determining moments of obtained equations with functions  $\bar{\Phi}_{msq}^{(R)}$ , we come to real symmetrical LAES of the second kind for  $B_{emsq}^{(P)}$ ,  $B_{omsq}^{(P)}$ :

$$(4) \quad \begin{aligned} & \gamma_{ms_1}^{(P)} \frac{iq}{ctq} (\gamma_{ms_1}^{(P)} l_1) B_{oms_1}^{(P)} + \\ & + \sum_{s=2}^Q \sum_{R=1}^2 \sum_{m_q}^M \sum_{s_q}^S B_{emsq}^{(R)} \sum_{p=1}^2 \sum_{m_1}^M \sum_{s_1}^S \gamma_{ms_1}^{(P)} \frac{\cos(\varphi + m_1 \psi_1) \mp \cos(2\gamma_{ms_1}^{(P)} l_1)}{\sin(2\gamma_{ms_1}^{(P)} l_1)} \eta_{ms_1, ms_q}^{rp} \eta_{ms_1, ms_q}^{rp} \pm \\ & \pm \sum_{s=2}^Q \sum_{R=1}^2 \sum_{m_q}^M \sum_{s_q}^S B_{omsq}^{(R)} \sum_{p=1}^2 \sum_{m_1}^M \sum_{s_1}^S \gamma_{ms_1}^{(P)} \frac{\sin(\varphi + m_1 \psi_1)}{\sin(2\gamma_{ms_1}^{(P)} l_1)} \eta_{ms_1, ms_q}^{rp} \eta_{ms_1, ms_q}^{rp} = 0, \quad q = 2, \dots, Q, \quad p = 1, 2. \end{aligned}$$

Coupling coefficients

$$(5) \quad \eta_{ms_1, ms_q}^{PR} = \int_{S_q} \bar{\Phi}_{ms_1}^{(P)*} \bar{\Phi}_{ms_q}^{(R)} ds$$

reflect a couple on a hole of wave of  $P$  type with indices  $m_1, s_1$  of region 1 with wave of  $R$  type with indices  $m_q, s_q$  of region  $q$

LAES order is equal to  $\sum_{q=2}^Q K_{Pq} K_{mq} K_{sq}$ , where  $K_{Pq} = 2$ , if it is necessary to take into account  $E$ - and  $H$ -waves, or  $K_{Pq} = 1$ , if it is enough to consider waves of only one type,  $K_{mq}, K_{sq}$  - number of variations on azimuth and radius being taken into account.

Below we shall consider systems of circular cross-section of region 1 (or  $Q+1$ ) with circular transit and coupling holes. The circular shape of coupling holes has its own advantages: simplicity and accuracy of making, minimal losses in coupling holes, the highest cutoff frequency, and so, the most remote parasite passbands.

For such systems eigenfunctions are known [4]. To present eigenfunctions in region 1 in coordinate system of region  $q$  theorems of summation for Bessel functions are used. It has permitted to take all integrals (11) analytically in closed form.

Program to calculate the properties of multibeam multistage structures with higher symmetries with circular shield and coupling channels has been developed.

### CALCULATION OF CHARACTERISTICS OF SOME STRUCTURES

Fig 2 shows the calculated dispersional characteristic and dependencies of amplitudes  $B_{emsq}, B_{omsq}$  of expansions of even and odd parts of tangential electric field for single-beam structure with dimensions  $b=33, l=12, L=15, a=12$ , whose transit hole is situated on its

situated on its axis. Calculation was done for E-waves with azimuthal index  $m_1 = m_2 = 0$ . In cavity waves with radial indices  $s_1 = 1, \dots, 11$  have been taken into account, in hole - waves with radial indices  $s_2 = 1, \dots, 4$ .

Dispersional characteristics of single beam structure with the same dimensions as in fig. 2, whose transit hole was displacing from axis to shield (ratio  $R_2 / b$  was varying from 0 to 0.633) are shown in fig. 3. Character of dispersion, passband width, value and sign of group velocity changed with hole place being varied.

Tables 1-3 show the comparison of measured and calculated values  $\lambda / 2b$  for several  $\varphi$  for such structure with  $R_2 = 20$  whose holes in each next diaphragm are not displaced ( $\psi_0 = 0$ , table 1), are displaced on  $180^\circ$  ( $\psi_0 = 180^\circ$ , table 2), are displaced on  $90^\circ$  ( $\psi_0 = 90^\circ$ , table 3). Data "calc-1" have been obtained for  $m_2 = 0, 1$ ,  $s_2 = 1, 2$ ,  $m_1 = 0, \dots, 10$ ,  $s_1 = 1, 2, 3$ . Data "calc-2" have been obtained for  $m_2 = 0, 1, 2$ ,  $s_2 = 1, 2, 3$ ,  $m_1 = 0, \dots, 15$ ,  $s_1 = 1, \dots, 4$ .

Table 1.

$\frac{\varphi}{\pi}$	$\lambda / 2b$ exp.	$\lambda / 2b$ calc - 1	$\Delta, \%$	$\lambda / 2b$ calc - 2	$\Delta, \%$
0	1.3082	1.3079	0.046	1.3079	0.045
1/4	1.3157	1.3154	0.042	1.3153	0.040
2/4	1.3262	1.3253	0.002	1.3257	0.025
3/4	1.3315	1.3297	0.065	1.3306	0.003

Table 2.

$\frac{\varphi}{\pi}$	$\lambda / 2b$ exp.	$\lambda / 2b$ calc - 1	$\Delta, \%$	$\lambda / 2b$ calc - 2	$\Delta, \%$
0	1.3085	1.3082	0.045	1.3081	0.043
1/4	1.3145	1.3138	0.014	1.3139	0.023
2/4	1.3289	1.3279	0.008	1.3284	0.029
3/4	1.3443	1.3428	0.041	1.3438	0.030

Table 3.

$\frac{\varphi}{\pi}$	$\lambda / 2b$ exp.	$\lambda / 2b$ calc - 1	$\Delta, \%$	$\lambda / 2b$ calc - 2	$\Delta, \%$
0	1.3084	1.3082	0.053	1.3082	0.051
1/4	1.3144	1.3131	0.028	1.3132	0.023
2/4	1.3290	1.3260	0.16	1.3263	0.134
3/4	1.3450	1.3410	0.222	1.3418	0.167

Fig 4 shows a two row structure, that has the same main dimensions as in fig. 2, in which one hole of radius  $a_2 = 12$  is placed on system axis and four holes of radius  $a_3 = 6$  are placed on  $R_3 = 20$  ( $\psi_0 = 0$ ). This structure answers all the demands being make on structures of multibeam devices: distance between beams is comparative with a wavelength, heat-dissipative capacity is considerably high than in a usual coupled cavity chain, coupling elements and channels for beams are separated in space - central hole is used for coupling (or interaction with a hollow beam), holes of the second row - for interaction with four beams or inductive coupling with cavities. We want to call accelerators technology specialists attention as well to fact that such structure keeping all good properties of a corrugated waveguide distinguishes by higher vacuum conductance.

Measured and calculated values  $\lambda / 2b$  is given in table 4. Data "calc-1" have been obtained for  $m_2 = 0, 4, 8$ ,  $s_2 = 1, 2$ ,  $m_1 = 0, 1$ ,  $s_1 = 1, 2$ ,  $m_1 = 0, 4, \dots, 20$ ,  $s_1 = 1, \dots, 6$ , data "calc-2" - for  $m_2 = 0, 4, 8$ ,  $s_2 = 1, 2, 3$ ,  $m_1 = 0, 1, 2$ ,  $s_1 = 1, 2, 3$ ,  $m_1 = 0, 4, \dots, 32$ ,  $s_1 = 1, \dots, 9$ .

Table 4.

$\frac{\varphi}{\pi}$	$\lambda / 2b$ exp.	$\lambda / 2b$ calc - 1	$\Delta, \%$	$\lambda / 2b$ calc - 2	$\Delta, \%$
0	1.2735	1.2730	0.033	1.2716	0.075
1/5	1.2654	1.2633	0.096	1.2620	0.203
2/5	1.2428	1.2410	0.080	1.2397	0.186
3/5	1.2183	1.2181	0.056	1.2168	0.054
4/5	1.2014	1.2026	0.175	1.2012	0.020

Table 5.

$\frac{\varphi}{\pi}$	$\lambda / 2b$ exp.	$\lambda / 2b$ calc	$\Delta, \%$
0	1.27439	1.27481	0.0329
1/6	1.26968	1.27075	0.0844
2/6	1.26146	1.26075	0.0558
3/6	1.25028	1.24915	0.0910
4/6	1.24050	1.23931	0.0961

Structure with three rows of holes with dimensions  $b=45$ ,  $t=8$ ,  $L=10.5$ ,  $a_2=10$ ,  $a_3=6.4$ ,  $R_3=19.6$ ,  $a_4=3$ ,  $R_4=31.24$  ( $\psi_0 = 0$ ) is shown in fig. 5. Comparison of measured and calculated values  $\lambda / 2b$  is given in table 5. Numerical results have been obtained for  $m_2 = 0, 6$ ,  $s_2 = 1, 2, 3$ ,  $m_1 = 0, \dots, 3$ ,  $s_1 = 1, \dots, 4$ ,  $m_1 = 0, 1$ ,  $s_1 = 1$ ,  $m_1 = 0, 6, \dots, 36$ ,  $s_1 = 1, \dots, 14$ .

The results show that developed technique of mathematics permits extremely complex three-dimensional structures with several rows of coupling slots to be calculated with high accuracy by personal computers. Even for three row 13-beam structure with 6 coupling holes that is almost a "summit of the desires" calculation error does not exceed hundredth-tenth parts of per cent.

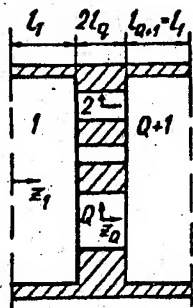


Fig. 1.

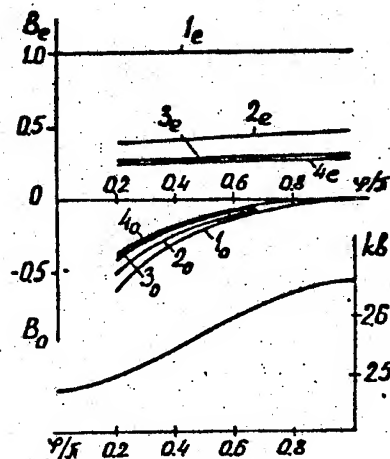


Fig. 2.

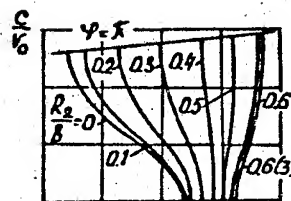


Fig. 3.

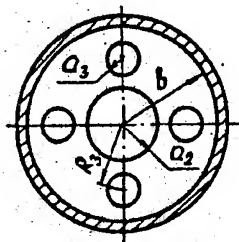


Fig. 4.

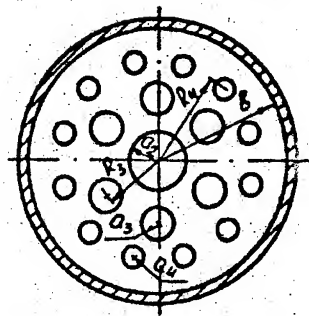


Fig. 5.

#### REFERENCE

1. Feld Ya.N., Benenson L.S. "Calculation of phase velocity of waves in coupled cavity chains", Radiotekhnika i elektronika, 1966, No. 10, pp. 1759-1770.
2. Naidenko V.I. "Integral equation system for multistage multibeam structures with higher symmetries", Voprosy atomnoy nauki i tekhniki. Ser. yadernaya fizika i tekhnika. Teoriya i eksperiment. 1992. Is. 4(25), pp. 61-64.
3. Hessel A., Chen M.H., Li R.C.M., Oliner A. "Propagation in Periodically Loaded Waveguide with Higher Symmetries", Proc. IEEE, 1973, v. 62, No. 2, pp. 183-195.
4. Marcuvitz N. Waveguide Handbook, New York: McGraw-Hill, 1951.

# DETERMINATION OF THE WAVE FRONTS BY PRESPECIFIED FOCAL LINE

Elman E.Hasanov, Agile S. Huseynova

Istanbul University, Faculty of Engineering

Istanbul, Avclar, 34850, Turkey

## ABSTRACT

Determination of the configuration of wave fronts by prespecified focal line has been considered. The problem in a sense may be thought as an inverse problem to the problems of catastrophe theory, where that configuration of wave fronts is specified to determine the singularity of fronts. Particularly, when focal line considered as a plane curve, the problem has been investigated earlier. On the other hand, if the focal line considered as a space curve this problem has not investigated up to now. This paper proposes a method for solving this problem under paraxial approximation.

## STATEMENT OF THE PROBLEM

Papers [1-3] have studied and developed the mathematical method for solving the laser focusing problem on line. In the case, when focal line considered as a plane curve, there its solution write down in explicit form under paraxial and non paraxial approximation. The goal of this paper is to investigate this problem, when the focal line prespecified as a space curve.

We shall consider this problem under paraxial approximation. Let the parametric equation of the focal line on the Cartesian coordinate system  $(u, v, z)$  be

$$C = (x(t), y(t), f(t))$$

and unknown wave front be  $S = S(u, v, z)$ , where  $S(u, v, z)$  satisfied the eikonal equation

$$\left(\frac{\partial S}{\partial u}\right)^2 + \left(\frac{\partial S}{\partial v}\right)^2 + \left(\frac{\partial S}{\partial z}\right)^2 = 1$$

The values of  $S(u, v, z)$  on domain  $G$  in the plane  $z = 0$  denote by  $\phi(u, v)$ :

$$S(u, v, 0) = \phi(u, v)$$

It will be shown that after finding  $\phi(u, v)$ , the function  $S(u, v, z)$  can be determined for any  $(u, v, z)$ . From Fig.1 we see that  $\vec{OA} + \vec{AB} = \vec{OB}$ , where  $\vec{OA} = (u, v, 0)$ ,  $\vec{AB} =$

$s(u, v) (\phi_u, \phi_v, \sqrt{1 - \phi_u^2 - \phi_v^2})$ ,  $OB = (x, y, f)$  and  $s(u, v)$  is the lengths of the optical path along the ray  $AB$ . Writing in coordinates, we obtain

$$\begin{aligned}x &= u + s\phi_u \\y &= v + s\phi_v \\f &= s\sqrt{1 - \phi_u^2 - \phi_v^2}\end{aligned}$$

Eliminating  $s = s(u, v)$  from this equation yields a mapping of the  $G$  onto curve  $(x(t), y(t), f(t))$ :

$$\begin{aligned}x &= u + f \frac{\phi_u}{\sqrt{1 - \phi_u^2 - \phi_v^2}} \\y &= v + f \frac{\phi_v}{\sqrt{1 - \phi_u^2 - \phi_v^2}}\end{aligned}$$

In paraxial approximation,  $|\phi_u| \ll 1, |\phi_v| \ll 1$ , this mapping becomes to the mapping:

$$\begin{aligned}x &= u + f\phi_u \\y &= v + f\phi_v\end{aligned} \quad (1)$$

Thus we have to choose the  $\phi(u, v)$  that the mapping (1) maps domain  $G$  onto the curve  $(x(t), y(t), f(t))$ . Let  $(u, v)$  be preimage of  $t$  under mapping (1). By this relation it is determined the function  $t = \tau(u, v)$  on  $G$ . It is clear, that if  $t = t_0$  then  $\tau(u, v) = t_0$  is some curve on plane  $(u, v)$ . On the other hand, it will be shown, that after finding the function  $\tau(u, v)$  phase function  $\phi(u, v)$  can be calculated in explicit form.

#### DETERMINATION OF PHASE FUNCTION

To determine  $\tau(u, v)$  to solve (1) for  $\phi_u, \phi_v$ :

$$\phi_u = \frac{x - u}{f} \quad \phi_v = \frac{y - v}{f} \quad (2)$$

Since,  $\phi_{uv} = \phi_{vu}$ , substituting  $t = \tau(u, v)$  into (2) and after differentiation, we obtain:

$$\begin{aligned}\phi_{uv} &= \frac{\dot{x} \frac{\partial \tau}{\partial v} f - f \frac{\partial \tau}{\partial v} (x - u)}{f^2} \\ \phi_{vu} &= \frac{\dot{x} \frac{\partial \tau}{\partial u} f - f \frac{\partial \tau}{\partial u} (y - v)}{f^2}\end{aligned}$$

or

$$\frac{\partial \tau}{\partial v} [\dot{x}f - \dot{f}(x - u)] - \frac{\partial \tau}{\partial u} [\dot{y}f - \dot{f}(y - v)] = 0 \quad (3)$$

(3) is a quasilinear partial equation in first order for  $\tau(u, v)$ . It can be solved by employing the characteristic method. In this case the equations of the characteristics are the following system of order differential equations :

$$\begin{aligned}\frac{du}{ds} &= -\dot{f}v - \dot{y}f + \dot{f}y \\ \frac{dv}{ds} &= \dot{f}u + \dot{x}f - \dot{f}x \\ \frac{d\tau}{ds} &= 0\end{aligned}\quad (4)$$

Let the solution of this system be  $u = u(s, r)$ ,  $v = v(s, r)$ ,  $\tau = \tau(s, r)$ , where  $r$  is the parameter along the unit curve  $u^0(r) = u(0, r)$ ,  $v^0(r) = v(0, r)$ ,  $\tau^0(r) = \tau(0, r)$ . Eliminating  $s, r$  we obtain the function  $\tau = \tau(u, v)$ . Substituting  $\tau(u, v)$  into (2) and after integrating, we obtain  $\phi(u, v)$  in explicit form :

$$\phi(u, v) = \int_L \frac{x(\tau(u, v)) - u}{f(\tau(u, v))} du + \frac{y(\tau(u, v)) - v}{f(\tau(u, v))} dv$$

where  $L$  is any curve in  $G$ .

It is very important in laser focusing theory is very important to know the preimage of point  $t$  under mapping (1). It can be shown, that the curves  $\phi(u, v) = C$  have a equation:

$$\begin{aligned}[(c_2 + b_2)^2 + c_2^2](u + b_2)^2 - 4c_2(c_1 + b_2)(u + b_2)\left(v - \frac{b_1}{f}\right) + \\ + [(c_1 + b_2)^2 + c_2^2]\left(v - \frac{b_1}{f}\right)^2 = [(c_1 + b_2)^2 - c_2^2]^2\end{aligned}\quad (5)$$

where  $b_1 = fy - yf$ ,  $b_2 = xf - fx$  and  $c_1, c_2$  are arbitrary constants, in other words, the preimage of  $t$  on the plane  $(u, v)$  is a conic section.

Since

$$\delta = \begin{vmatrix} (c_1 + b_2)^2 & -2c_2(c_1 + b_2) \\ -2c_2(c_1 + b_2) & (c_1 + b_2)^2 + c_2^2 \end{vmatrix} = [(c_1 + b_2)^2 - c_2^2]^2 > 0$$

then (5) is an ellipse. After transformation to main axis it becomes to form

$$\frac{2u_2^2}{(a+b)^2} + \frac{2v_2^2}{(a-b)^2} = 1$$

where  $a = c_1 + b_2$ ,  $b = c_2$ ,  $u_2 = \frac{u_1 + v_1}{2}$ ,  $v_2 = \frac{u_1 - v_1}{2}$ ,  $u_1 = u + b_2$ ,  $v_1 = v - \frac{b_1}{f}$ .

$s(u, v) (\phi_u, \phi_v, \sqrt{1 - \phi_u^2 - \phi_v^2})$ ,  $OB = (x, y, f)$  and  $s(u, v)$  is the lengths of the optical path along the ray  $AB$ . Writing in coordinates, we obtain

$$\begin{aligned}x &= u + s\phi_u \\y &= v + s\phi_v \\f &= s\sqrt{1 - \phi_u^2 - \phi_v^2}\end{aligned}$$

Eliminating  $s = s(u, v)$  from this equation yields a mapping of the  $G$  onto curve  $(x(t), y(t), f(t))$ :

$$\begin{aligned}x &= u + f \frac{\phi_u}{\sqrt{1 - \phi_u^2 - \phi_v^2}} \\y &= v + f \frac{\phi_v}{\sqrt{1 - \phi_u^2 - \phi_v^2}}\end{aligned}$$

In paraxial approximation,  $|\phi_u| \ll 1, |\phi_v| \ll 1$ , this mapping becomes to the mapping:

$$\begin{aligned}x &= u + f\phi_u \\y &= v + f\phi_v\end{aligned} \quad (1)$$

Thus we have to choose the  $\phi(u, v)$  that the mapping (1) maps domain  $G$  onto the curve  $(x(t), y(t), f(t))$ . Let  $(u, v)$  be preimage of  $t$  under mapping (1). By this relation it is determined the function  $t = \tau(u, v)$  on  $G$ . It is clear, that if  $t = t_0$  then  $\tau(u, v) = t_0$  is some curve on plane  $(u, v)$ . On the other hand, it will be shown, that after finding the function  $\tau(u, v)$  phase function  $\phi(u, v)$  can be calculated in explicit form.

#### DETERMINATION OF PHASE FUNCTION

To determine  $\tau(u, v)$  to solve (1) for  $\phi_u, \phi_v$ :

$$\phi_u = \frac{x - u}{f} \quad \phi_v = \frac{y - v}{f} \quad (2)$$

Since,  $\phi_{uv} = \phi_{vu}$ , substituting  $t = \tau(u, v)$  into (2) and after differentiation, we obtain :

$$\begin{aligned}\phi_{uv} &= \frac{\dot{x} \frac{\partial \tau}{\partial v} f - f \frac{\partial \tau}{\partial v} (x - u)}{f^2} \\ \phi_{vu} &= \frac{\dot{x} \frac{\partial \tau}{\partial u} f - f \frac{\partial \tau}{\partial u} (y - v)}{f^2}\end{aligned}$$

or

$$\frac{\partial \tau}{\partial v} [\dot{x}f - \dot{f}(x - u)] - \frac{\partial \tau}{\partial u} [\dot{y}f - \dot{f}(y - v)] = 0 \quad (3)$$

(3) is a quasilinear partial equation in first order for  $\tau(u, v)$ . It can be solved by employing the characteristic method. In this case the equations of the characteristics are the following system of order differential equations :

$$\begin{aligned}\frac{du}{ds} &= -\dot{f}v - \dot{y}f + \dot{f}y \\ \frac{dv}{ds} &= \dot{f}u + \dot{x}f - \dot{f}x \\ \frac{d\tau}{ds} &= 0\end{aligned}\quad (4)$$

Let the solution of this system be  $u = u(s, r)$ ,  $v = v(s, r)$ ,  $\tau = \tau(s, r)$ , where  $r$  is the parameter along the unit curve  $u^0(r) = u(0, r)$ ,  $v^0(r) = v(0, r)$ ,  $\tau^0(r) = \tau(0, r)$ . Eliminating  $s, r$  we obtain the function  $\tau = \tau(u, v)$ . Substituting  $\tau(u, v)$  into (2) and after integrating, we obtain  $\phi(u, v)$  in explicit form :

$$\phi(u, v) = \int_L \frac{x(\tau(u, v)) - u}{f(\tau(u, v))} du + \frac{y(\tau(u, v)) - v}{f(\tau(u, v))} dv$$

where  $L$  is any curve in  $G$ .

It is very important in laser focusing theory is very important to know the preimage of point  $t$  under mapping (1). It can be shown, that the curves  $\phi(u, v) = C$  have a equation:

$$\begin{aligned}[(c_2 + b_2)^2 + c_2^2](u + b_2)^2 - 4c_2(c_1 + b_2)(u + b_2)\left(v - \frac{b_1}{f}\right) + \\ + [(c_1 + b_2)^2 + c_2^2]\left(v - \frac{b_1}{f}\right)^2 = [(c_1 + b_2)^2 - c_2^2]^2\end{aligned}\quad (5)$$

where  $b_1 = fy - yf$ ,  $b_2 = xf - fx$  and  $c_1, c_2$  are arbitrary constants, in other words, the preimage of  $t$  on the plane  $(u, v)$  is a conic section.

Since

$$\delta = \begin{vmatrix} (c_1 + b_2)^2 & -2c_2(c_1 + b_2) \\ -2c_2(c_1 + b_2) & (c_1 + b_2)^2 + c_2^2 \end{vmatrix} = [(c_1 + b_2)^2 - c_2^2]^2 > 0$$

then (5) is an ellipse. After transformation to main axis it becomes to form

$$\frac{2u_2^2}{(a+b)^2} + \frac{2v_2^2}{(a-b)^2} = 1$$

where  $a = c_1 + b_2$ ,  $b = c_2$ ,  $u_2 = \frac{u_1 + v_1}{2}$ ,  $v_2 = \frac{u_1 - v_1}{2}$ ,  $u_1 = u + b_2$ ,  $v_1 = v - \frac{b_1}{f}$ .



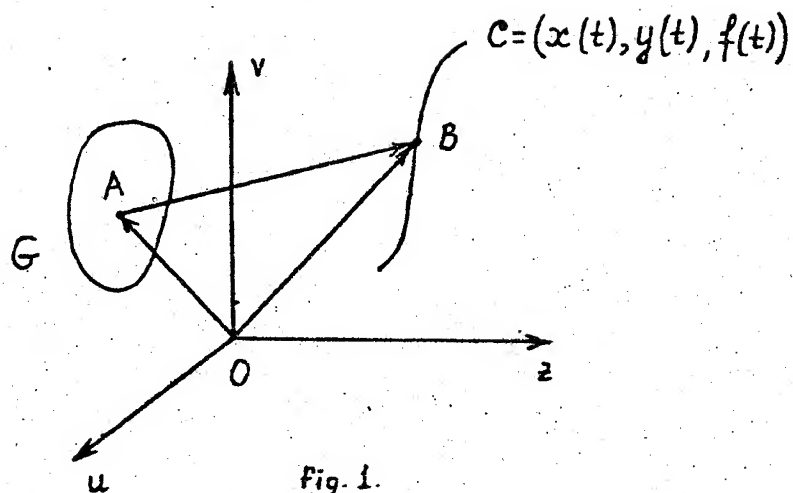


Fig. 1.

#### REFERENCES

- (1) A.V.Goncharskiy et.al. Dokl.Akad.Nauk SSSR, **273**, No.3, p.605.1983.
- (2) E.E.Gasanov "The Paraxial Approximation in the theory of Laser Beam Focusing".  
Sov.J. of Commun. Technol. and Electronics. **37**, No.5, pp.9-15.1992.
- (3) E.E.Gasanov "Theory of the Focusing of Laser Radiation into a Transmission Line".  
Sov.J. of Commun. Technol. and Electronics. **37**, No.6, pp.1-8.1992.

# Ray Technique for Stationary Waves in Guided Wave Structures

Masahiro Hashimoto

Department of Applied Electronic Engineering,  
Osaka Electro-Communication University, Neyagawa, Osaka 572, Japan.

## ABSTRACT

Ray optics deduced from Maupertuis' variational principle is presented. The ray deduced is shown to represent the path of propagation of a stationary wave strictly, and thus it does not coincide with the well-known ray of light which is the the path of energy transport of a dynamical wave. This novel optics provides an alternative description for high frequency fields excited by a monochromatic wave source, which may be useful for waves in open structures such as dielectric tapered waveguides. The basic physical features of this ray are discussed by applying it to Brekhovskikh's problem of reflection and transmission of a wave at a plane interface.

## INTRODUCTION

The ray techniques developed for simple structures in wave systems were successfully applied to layered and inhomogeneous waveguides [1]. The method involves including leakage of waves from a guide as a complex ray obtained by means of analytic continuation. The effect of ray shift can also be incorporated into the technique, which becomes nonnegligible for long waveguides used in real optical communication systems where the number of times of multiple reflection between two interfaces exceeds more than twenty. The incorporation of this high-order effect leads to the high-order optics [2]. However certain additional corrections are needed to improve the ray solution [3]. The author has shown that direct application and modification of the classical variational principle gives us a new formulation for high-order fields in geometrical optics which contains the effect of ray shift, and additional corrections as well [4].

The ray deduced in this way indicates the normal congruence representing the direction of wave-normal to the wave-surfaces, thus describing the path of motion of a stationary wave. In this paper, we present the geometrical theory of stationary waves based on the ray

congruence. Such a ray is referred to as the wave-normal ray. To illustrate the basic idea, the theory is outlined by treating the classical problem [3] of reflection and transmission of a cylindrical wave at a plane interface. The law of the inequality of the angles of incidence and reflection of a wave is derived from the principle. Snell's law for refraction is also renewed.

## VARIATIONAL PRINCIPLES

The theory of geometrical optics usually starts from Fermat's principle reported in a letter to Chambre in 1657 [5]. The principle was later modified as a general law of nature to describe the motion of a particle as well as light. This work was published in 1746 by Maupertuis [6] and is well known as the law of least action. His theory however had certain drawback from a dynamical point of view [7]. Hamilton gave the more complete theory of dynamical motion of light and particles [7].

The geometrical optics based on Hamilton's theory is called Hamiltonian optics. Hence, the ray is the path of dynamical motion of light. Since the ray direction differs from the wave-normal direction in generic media, the wave-surface or the normal congruence perpendicular to it is constructed via the ray configuration. In 1821, Fresnel discovered the wave-surface of a stationary wave, applying his famous construction technique [8], deduced from Huygens' theory, to the dynamical properties of light in crystalline bodies. Fresnel's wave-surface is constructed as the envelope of plane waves emitted from the origin and evidently it shows the equiphase surface of the stationary wave diverging from a point source. The direction of the normal congruence of a plane wavelet thus indicates the local direction of propagation of the stationary wave, whereas the sum of such plane wavelets forms a beam wave that represents a dynamical ray. This dynamical ray is referred here as an energy ray in order to distinguish from a stationary ray of wave-normal.

Expression of Hamilton's dynamical principle contains two parameters  $p$  and  $r$  which will be shifted independently when the variational calculation is implemented where  $p$  is a normalized momentum vector ( $=i, n$ ,  $i$  = the unit direction of the wave-normal ray,  $n$  is the refractive index) and  $r$  is a position vector. As a result of taking two independent variations in the dispersion relation  $F(p, r, \omega) = 0$ , the angular frequency  $\omega$  varies slightly from the center frequency  $\omega_0$ . The variation of  $\omega$  makes it possible to construct a dynamical ray in space [7]. On the other hand, in Maupertuis' principle  $\delta \int p \cdot r = 0$ , we can

choose a single parameter  $p$  or  $r$  in the variational process in which the value of  $\omega$  is kept constant, which means that making the first variation zero, we obtain the ray equations for the wave-normal rays of stationary waves. These ray equations were demonstrated by illustrating the wave surfaces of an extraordinary (cylindrical) wave propagating in an inhomogeneous anisotropic calcite [4].

For media containing certain classes of discontinuity, we may use the modified principle

$$\delta S = 0, \quad S = \int_p^q \mathbf{p} \cdot d\mathbf{r} - \frac{\phi \text{ or } \psi}{k} \quad (1)$$

which is applicable to the problem of reflection and transmission of a cylindrical wave at an interface, where  $k$  is the wavenumber ( $=\omega/c$ ;  $c$ =the

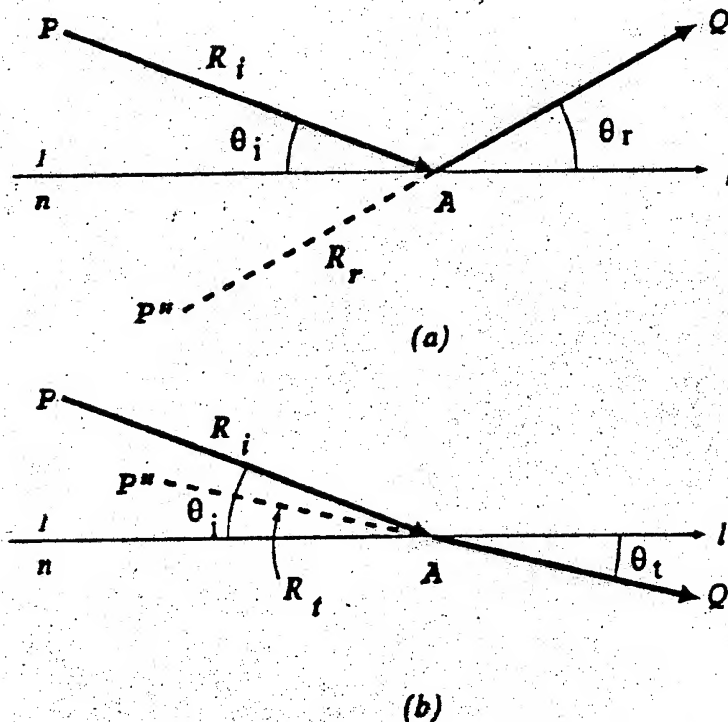


Fig.1 Reflection and transmission of wave-normal rays at a plane interface. The refractive indices of the upper and lower media are unity and  $n$ , respectively;  $R_i \equiv \overline{PA}$ ,  $R_r$  or  $R_t \equiv \overline{P''A}$ .  
(a) Reflection. (b) Transmission.

velocity of light in vacuum) and  $\Phi$  or  $\Psi$  denotes the phase increment due to reflection or transmission at the point of incidence located on the discontinuous interface, respectively. In what follows, the principle mentioned above is applied to Brekhovskikh's problem [3] as an example.

## REFLECTION AND TRANSMISSION OF A CYLINDRICAL WAVE

The action  $S$  in (1) denotes an optical distance from the source point  $P$  to the observation point  $Q$ :  $S = \overline{PA} + \overline{QA} - \Phi/k$  when Point  $Q$  is in the upper medium (air) or  $S = \overline{PA} + n\overline{QA} - \Psi/k$  when Point  $Q$  is in the lower medium with refractive index  $n$  (see Fig.1). Location of Point  $A$  is indicated by the coordinate  $l$  measured along the interface. Then  $S$  is given by a function of  $l$ . To minimize the value of  $S$ , we differentiate  $S$  with respect to  $l$  and put  $\partial S/\partial l = 0$ . From this stationary condition, the laws of reflection and refraction follow immediately. The resulting formulas for the angles of incidence, reflection and transmission,  $\theta_i, \theta_r, \theta_t$ , and the radii of curvature of the wavefronts of incident, reflected and transmitted waves at Point  $A$ ,  $R_i, R_r, R_t$ , are listed below.

$$\cos \theta_r = \cos \theta_i + \frac{\sin \theta_i}{kR_i} \Phi'(\theta_i) \quad (2)$$

$$n \cos \theta_t = \cos \theta_i + \frac{\sin \theta_i}{kR_i} \Psi'(\theta_i) \quad (3)$$

$$\frac{\sin^2 \theta_r}{R_r} = \frac{\sin^2 \theta_i}{R_i} - \frac{\sin^2 \theta_i}{kR_i^2} \left\{ \Phi''(\theta_i) + 2 \cot \theta_i \Phi'(\theta_i) \right\} \quad (4)$$

$$\frac{n \sin^2 \theta_t}{R_t} = \frac{\sin^2 \theta_i}{R_i} - \frac{\sin^2 \theta_i}{kR_i^2} \left\{ \Psi''(\theta_i) + 2 \cot \theta_i \Psi'(\theta_i) \right\} \quad (5)$$

where primes denote differentiation with respect to  $\theta_i$ . The first and second equations represent  $\partial S/\partial l = 0$ , and the last terms on their right hand sides arise from the derivatives of  $\Phi$  and  $\Psi$  with respect to  $l$ . The (4) and (5), respectively, are obtained by differentiating (2) and (3) again with respect to  $l$  and applying  $\partial/\partial l = -(\sin \theta_i/R_i) \partial/\partial \theta_i = -(\sin \theta_r/R_r) \partial/\partial \theta_r = -(\sin \theta_t/R_t) \partial/\partial \theta_t$ .

Now suppose that an incident cylindrical wave emanates from Point  $P$  and is reflected or transmitted at Point  $A$ . The wave-normal rays of the reflected or transmitted waves are seen to issue directly from the image source  $P''$  as indicated in Fig.1 where the values of  $\theta_i$  and  $R_i$  are specified. The angle  $\theta_r$  or  $\theta_t$  and the radius  $R_r$  or  $R_t$  are determined by (2)-(5). This means that locations of Point  $P''$ , which we demand to know in constituting the ray solution, are determined exactly.

The geometrical optics fields corresponding to incidence, reflection and transmission are given by  $\psi^i = K_i \exp(-jkr)/\sqrt{r}$ ,  $\psi^r = K_r \exp(-jkr)/\sqrt{r}$ ,  $\psi^t = K_t \exp(-jknr)/\sqrt{r}$ , respectively, where  $r$  denotes the distance between Point P" and Point Q and  $K_s$  are coefficients. The continuity of fields at Point A,  $\psi^i + \psi^r = \psi^t$ , with reflection coefficient  $\Gamma (= \psi^r / \psi^i)$  and transmission coefficient  $T (= \psi^t / \psi^i)$ , requires

$$K_r = K_i \sqrt{\frac{R_1}{R_1}} \Gamma e^{-jk(R_1 - R_r)} \quad (6)$$

$$K_t = K_i \sqrt{\frac{R_1}{R_1}} T e^{-jk(R_1 - nR_t)} \quad (7)$$

In the case of total reflection when the lower medium is optically rarer and further the value of  $\theta_i$  is taken to be less than the critical angle  $\theta_c = \cos^{-1}n$ , the law of conservation of energy flux in the incident ray tube and the reflected ray tube holds. Although it is evident from  $\partial\theta_r/\partial\theta_i \neq 1$  that the cone angles of ray tubes for the wave-normal rays at Point P and Point P" are different, those for the energy rays are identical [9]. This implies that the amplitudes of the real source at Point P and the image source at Point P" are the same;  $|K_r| = |K_i|$ . Thus we have [9]

$$\Gamma = \sqrt{\frac{R_1}{R_r}} e^{j\Phi} \quad (8)$$

According to the rule of analytic continuation, this expression is expected to be valid for both partial and total reflections.

The fields  $\psi^r$  and  $\psi^t$  obtained above are described in terms of  $\Phi$  and  $\Psi$  which are unknown. The value of  $\Psi$  can however be determined as follows by substituting (8) into  $T (= 1 + \Gamma)$ ,

$$T = 2 \sqrt{\frac{R_1}{R_r}} \cos\left(\frac{\Phi}{2}\right) e^{j\Psi} + o\left(\frac{1}{k^2}\right) \quad (9)$$

$$\Psi = \frac{\Phi}{2} - \frac{\Phi''}{4kR_1} \tan\left(\frac{\Phi}{2}\right) + o\left(\frac{1}{k^2}\right) \quad (10)$$

but  $\Phi$  still remain unknown. The most acceptable approximation for  $\Phi$  may be to use the phase of Fresnel's reflection coefficient,  $\Phi_r(\theta_i)$ ,

$$\Phi_r(\theta) = 2 \tan^{-1} \left( \frac{\sqrt{\cos^2 \theta - n^2}}{\sin \theta} \right) \quad (11)$$

which holds valid for plane wave incidence. The results obtained by this approximation will be discussed later.

# COMPLEX RAY IN THE EVANESCENT REGION

When the value of  $\theta_i$  becomes smaller than the value of  $\theta_c = \cos^{-1}n$ , the principal ray that obeys (3) is transmitted in the complex direction and the resulting transmitted ray arrives at a point located in complex space. This complex transmitted ray can analytically be continued to all points located in real space. It will be shown that the analytically continued field represents an evanescent field in the lower medium. For Point Q (x,y) fixed in real space as shown in Fig. 2, Point P" ( $x_{P''}$ ,  $y_{P''}$ ) moves in complex space as  $\theta_i$  goes along the real axis on a complex  $\theta_i$ -plane from  $\pi/2$  to zero, passing through the critical point  $\theta_c$ . The complex distance r from Point P" to Point Q is given by [4]

$$r = \sqrt{(x - x_{P''})^2 + (y - y_{P''})^2} = \sqrt{z - z^*} \quad (12)$$

where

$$z^* = x + jy - x_{P''} + jy_{P''} \quad (13)$$

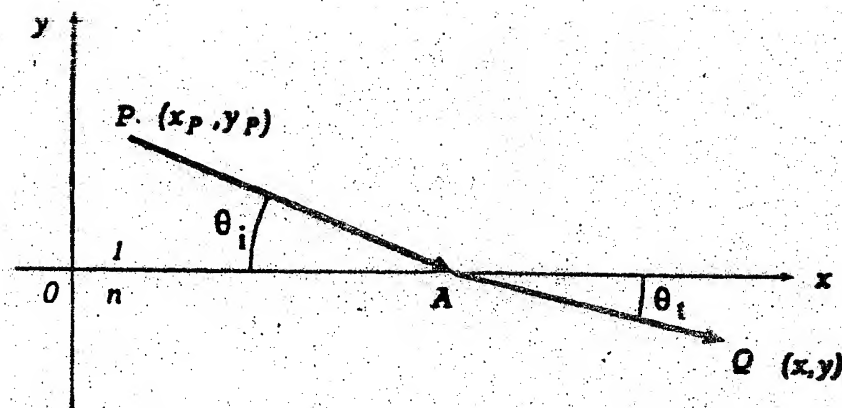


Fig.2 Principal wave-normal ray in the lower medium.



Figure 3 shows locations of the zeros of  $z^+$  and  $z^-$  on a complex  $\theta_i$ -plane (at which  $z^\pm = 0$ ). There is no distinction between the two zeros when  $\theta_i = \theta_c$  and  $y=0$ . These will however be separated upward and downward, respectively, if Point Q is apart from the boundary ( $y \neq 0$ ). The analytic continuation is carried out so that the variable  $\theta_i$  varies from  $\theta_c + 0$  to  $\theta_c - 0$  by going round the zero of  $z^-$  in a clockwise sense, as schematically shown in Fig.3. Note that the value of  $r$  tends to a large negative value as  $\theta_i$  approaches zero. The appearance of a small negative imaginary number in the expression of  $r$  gives rise to the evanescent wave; in fact, it decays in the vertical direction but propagates along the boundary.

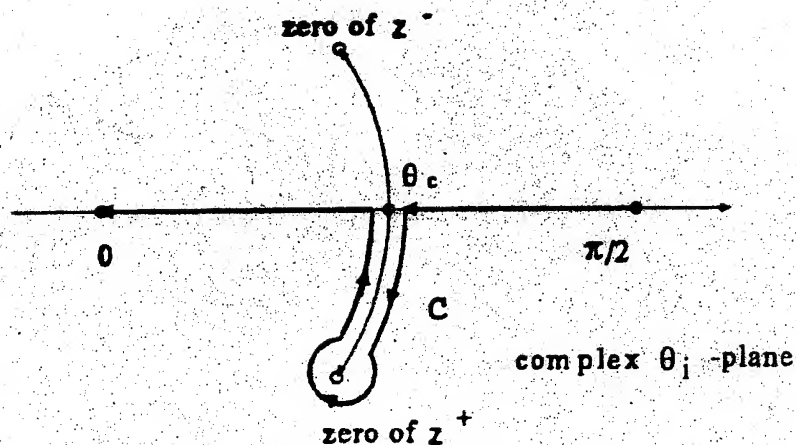
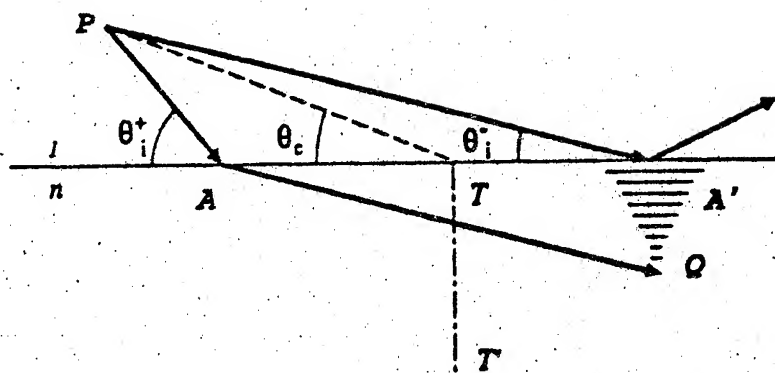


Fig.3 Zeros of the functions  $z^+$  and  $z^-$  on a complex  $\theta_i$ -plane.

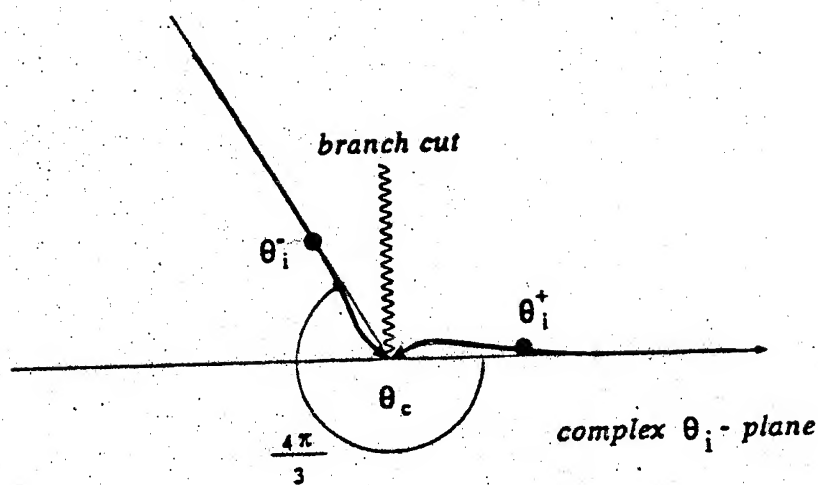
Consider two possible rays created in the right hand side of  $TT'$ , hitting the boundary from the upper side (see Fig.4a). One is a real ray incident with an angle  $\theta_i^+$  and the other is a complex ray incident with an angle  $\theta_i^-$ . These two rays are analytically continued, as stated above. The value of  $\theta_i^+$  or  $\theta_i^-$  is determined from

$$y_p \cot \theta_i^+ + (-y) \cot \theta_i^- = x - x_p \quad (14)$$





(a)



(b)

Fig.4 Real ray and complex ray in the lower medium.

(a) Solutions  $\theta_i^{\pm}$  for two rays.

(b) Locations of  $\theta_i^{\pm}$ .

together with (3). We see that the general solutions  $\theta_i$  are now complex quantities whose imaginary parts increase as  $\theta_i$  approach  $\theta_c$ . Figure 4b shows plot of  $\theta_i$  (·) approaching  $\theta_c$  when Point Q, lying on TT', moves toward the boundary from the lower side. All conclusions in this section however depends on the choice of the function  $\phi$  but are equally valid for real and complex rays, except for transit rays generated at the critical incidence.

#### DISCUSSION AND SUMMARY

For total reflection in the usual case, the values of  $\phi'$  or  $\psi'$  are negative, so that the values of  $\cos\theta_i$  are larger than those of  $\cos\theta_r$ , i.e.,  $\theta_i > \theta_r$ , and  $\cos\theta_i > n\cos\theta_r$ , although  $\theta_i$  takes a complex value. These formulas extend Snell's law to complex rays including the corrective terms of order  $1/k$ . This simple ray technique has been found to be very efficient for the analysis of dielectric tapered waveguides by checking the obtained solution with Feit-Fleck's propagating beam method solution (wave optics solution) [10].

Very similar but different formulas can also be derived [3, p.275] from wave optics calculations if the integration involved in the exact integral expression of  $\psi$  is carried out by the stationary phase method. Comparison has been made carefully. No discrepancy can be found between our result and the wave optics result within the range of order  $1/k$  unless  $\phi$  is misused; the best approximation is  $\phi(\theta_i) = \phi_r(\theta)$  where  $\theta = (\theta_i + \theta_r)/2$  [11]. However the wave optics solution is represented in terms of position-dependent parameters arising from the coordinates of the system introduced in the integral, for example,  $R_i$  and  $\theta_a$  in [3], which vary as Point Q moves in the ray direction. This is rather inconvenient for ray tracing in practical cases because unnecessary calculations are repeated to determine the ray paths along the reflected and refracted rays.

The advantage of using the present ray optics is that the local nature of waves in the neighborhood of the principal ray can exactly be described in terms of the radius of curvature of the wavefront. Such an idea, which dates from 1906 [12], can be applied to the tracing of wave-normal rays in inhomogeneous media containing some discontinuities [4]. The effect of diffraction is not considered here. We must take proper account of this in analyzing waves scattered at the critical angle. For this generalization, Keller's theory of diffraction [13], [14] may be helpful.

## REFERENCES

- [1] S.J.Maurer and L.B.Felsen. "Ray methods for trapped and slightly leaky modes in multilayered or multiwave regions," *IEEE Microwave Theory Tech.*, vol.MTT-18, no.9, pp.584-595, Sept. 1970.
- [2] L.B.Felsen and S.-Y. Shin. "Rays, beams, and modes pertaining to the excitation of dielectric waveguides," *IEEE Trans. Microwave Theory Tech.*, vol.MTT-23, no.1, pp.150-161, January 1975.
- [3] L.M.Brekhovskikh, *Waves in Layered Media*, 2nd ed., translated by R.T.Beyer. New York: Academic Press, 1973, Ch.IV.
- [4] M.Hashimoto, M.Idemen and O.A.Tretyakov (ed.). *Analytical and Numerical Methods in Electromagnetic Wave Theory*. Tokyo: Science House Co. Ltd., 1993, Ch.I.
- [5] P.Fermat, *Oeuvres de Fermat*, LXXXVI Fermat à de la Chambre, vol.2. Paris, 1894, pp.354-359.
- [6] P.L.M.Maupertuis, "Recherche des lois du mouvement" in *Oeuvres IV*, vol.4. Lyon, 1768
- [7] W.R.Hamilton, *The Mathematical Papers of Sir William Rowan Hamilton*, vol.I, Geometrical Optics, edited by A.W.Conway and J.L.Synge. Cambridge: Cambridge Univ. Press, 1931, vol.II, Dynamics, edited by A.W.Conway and A.J.McConnell, Cambridge: Cambridge Univ. Press, 1940.
- [8] E.Verdet, *Oeuvres complètes d'Augustin Fresnel*, vol.2. Paris, 1868, pp.257-623.
- [9] M.Hashimoto, "On the magnitude of the image source of a spherical and nonspherical wave reflected upon an interface," *Trans. IEICE*, vol.J75-C-I, no.8, pp.561-563, August 1992 (in Japanese).
- [10] M.Hashimoto and H.Hashimoto, "Ray-optical techniques in dielectric waveguides", *IEICE Trans. Electron.*, vol.E77-C, no.4, pp. 639-646, 1994.
- [11] M.Hashimoto, "Geometrical optics based on wave-normal rays: Application to dielectric waveguides," *Radio Sci.*, vol.28, no.6, pp.1245-1251, 1993.
- [12] A.Gullstrand, "Die reelle optische Abbildung," *Kungl. Svenska Vetenska. Handl.*, vol.41, no.3, pp.1-119, 1906.
- [13] J.B.Keller, "Geometrical theory of diffraction," *J. Opt. Soc. Am.*, vol.52, no.2, pp.116-130, Feb. 1962.
- [14] K.O.Friedrichs and J.B.Keller, "Geometrical acoustics II. Diffraction, reflection, and refraction of a weak spherical or cylindrical shock at a plane interface," *J. Appl. Phys.*, vol.26, no.8, pp.961-966, 1955.

# EFFECTS OF BISTABILITY IN THE NONLINEAR AND INHOMOGENEOUS TWO DIMENSIONAL SYSTEMS.

Michail V. Isakov

Moscow Power Engineering Institute.  
Krasnokazarmennaya 14, Moscow, 105835, Russia.

This work was supported by Russian Foundation  
of Fundamental Research (Grant No 93-02-16062).

## ABSTRACT

The propagation of intensive wave in the nonlinear waveguide and irradiation of slot antenna across nonlinear media were considered. A set of nonlinear laws of dependence of dielectric permittivity from intensity of electromagnetic waves were investigated. If permittivity was negative in absence of field and positive in presense of intensive fields the bistability of field structure had take places. The difference of bistability in two dimensional models from that in one dimensional models was showed. Also the influence of inhomogeneously of nonlinear parameters on field structure in nonlinear media was demonsrated.

## INTRODUCTION

The effects of bistability in radio and optics systems have a wide applications in phisios and technios [1]. This effects were founded in Fabri-Perrot resonators [1], in irradiation of antenna in nonlinear media [2] and in many others experiments. It is important that in these experiments the field structure was inhomogeneously and the media was inhomogeneous and nonlinear one. At present the bistability effects in problem of propagation of intensive waves was investigated theoretically on one dimensional models [3,4]. In these works the incidence of plane waves on plane nonlinear layers were considered. The model nonlinear dependences of permittivity from field intensity were investigated, including the positive ( $\partial\epsilon/\partial|E| > 0$ ) and negative ( $\partial\epsilon/\partial|E| < 0$ ) nonlinearity. But the limitation of one dimensional models do not allow to consider many special features of bistability effects in real phisical experiments and devices. For the culoulating the propagation of limiting beams in nonlinear media the method of parabolic equation is widely used. But the attempt to describe multystability in this approximation have not met with success. The main problem is that the method of parabolic equation can be used only for weak nonlinearity. The consideration of one dimensionally models showed that the bistability effects is followed by strong rearrange of field structure on small distance (near wave length). In this case the approximation of parabolic equation is not appropriate and for proper discription of propagation it is nessasary to solve Maxwell equation.

## STATEMENT OF THE PROBLEM

In this work we consider the problem of propagation of intensive electromagnetic wave in plane waveguide and irradiation of slot antenna across plane nonlinear plasma layer. If the waveguide (or slot) is exited by H-wave, then we can reduce our problem to solving nonlinear Helmholtz equation

$$\Delta E + k_0^2 \epsilon(|E|)E = 0. \quad (1)$$

A set of various local laws of dependence of dielectric permittivity from the field intensity was considered. In particular it was

$$\varepsilon = \varepsilon_0 + \varepsilon_2 \exp(\alpha |E|^2) \quad (2)$$

and

$$\varepsilon = \frac{\alpha + \beta |E|^2}{\gamma + \alpha |E|^2} \quad (3)$$

The dependences (2,3) can describe the positive or negative nonlinearity with saturation. In relatively weak field both these laws can be approximated by widely used so called "cubic" nonlinearity

$$\varepsilon = \varepsilon_0 + \varepsilon_2 |E|^2.$$

The equation (1) must be added by boundary conditions. For the metallic walls these conditions are

$$E(-d/2, z) = E(d/2, z) = 0. \quad (4)$$

where  $d$  - waveguides width. If the waveguide has an impedance walls the boundary conditions on walls may be written as

$$\left. \frac{\partial E}{\partial x} \right|_{x=\pm d/2} + \chi E = 0. \quad (5)$$

In (5)  $\chi = ik/Z_s$ ,  $Z_s$  - impedance of walls.

On the boundary of linear and nonlinear dielectric in waveguide the boundary conditions is written as

$$\left. \frac{\partial E}{\partial z} \right|_{z=0} - \frac{1}{d} \sum_{k=1}^{\infty} \gamma_k \phi_k(x) \int_{-d/2}^{d/2} E(x, 0) \phi_k(x) dx = -2 \sum_{k=1}^N \gamma_k \phi_k(x) E_k \quad (6)$$

$$\left. \frac{\partial E}{\partial z} \right|_{z=l} + \frac{1}{d} \sum_{k=1}^{\infty} \gamma_k \phi_k(x) \int_{-d/2}^{d/2} E(x, l) \phi_k(x) dx = 0. \quad (7)$$

where  $\phi_k$  - eigenfunctions of homogeneous plane waveguide.  $\gamma_k$  - propagation constant for mode  $k$ .

For solving the nonlinear Helmholtz equation the iteration method was used

$$\Delta E^{n+1} + k_0^2 \varepsilon(|E^n|) E^{n+1} = 0. \quad (8)$$

In (8)  $E^n$  is a field distribution in nonlinear media on  $n$ -s step of iterative procedure. To decide (8) the finite element method was used. The resulting system of linear algebraic equations was solved by biconjugate gradient method [5].

The irradiation of slot antenna across nonlinear layer can be described analogously as above problem. The main difficulties in this approach is the proper definition of boundary condition in open domains. But this problem may be approximated by the problem of irradiation of narrow waveguide in segment of wide waveguide with nonlinear media. This segment is closed by flange and radiate to the open space. The difference from waveguide propagations is only in boundary conditions on boundary of nonlinear dielectric with narrow waveguide and with open space. This conditions are

$$\left. \frac{\partial E}{\partial z} \right|_{z=0} - \frac{1}{d} \sum_{m=1}^{\infty} \phi_m(x) \sum_{p=1}^{\infty} W_1^{mp} \int_{-d/2}^{d/2} E(x, 0) \phi_p(x) dx = \sum_{m=1}^N W_2^{1m} E_m^n \phi_m(x), \quad (9)$$

where  $W_1$  and  $W_2$  - some matrices, linked with refraction matrix of waveguide width change on lighted boundary and

$$\left. \frac{\partial E}{\partial z} \right|_{z=l} + \frac{1}{2\pi} \int_{-\infty}^{\infty} \sqrt{k^2 - p^2} \left[ \int_{-\infty}^{\infty} E(x, l) e^{ipx} dx \right] e^{-ipx} dp = 0 \quad (10)$$

on opposite side.

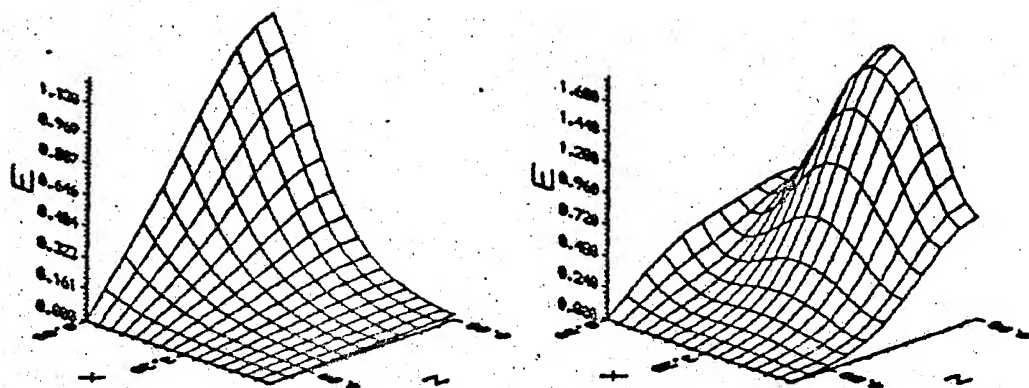


Fig. 1

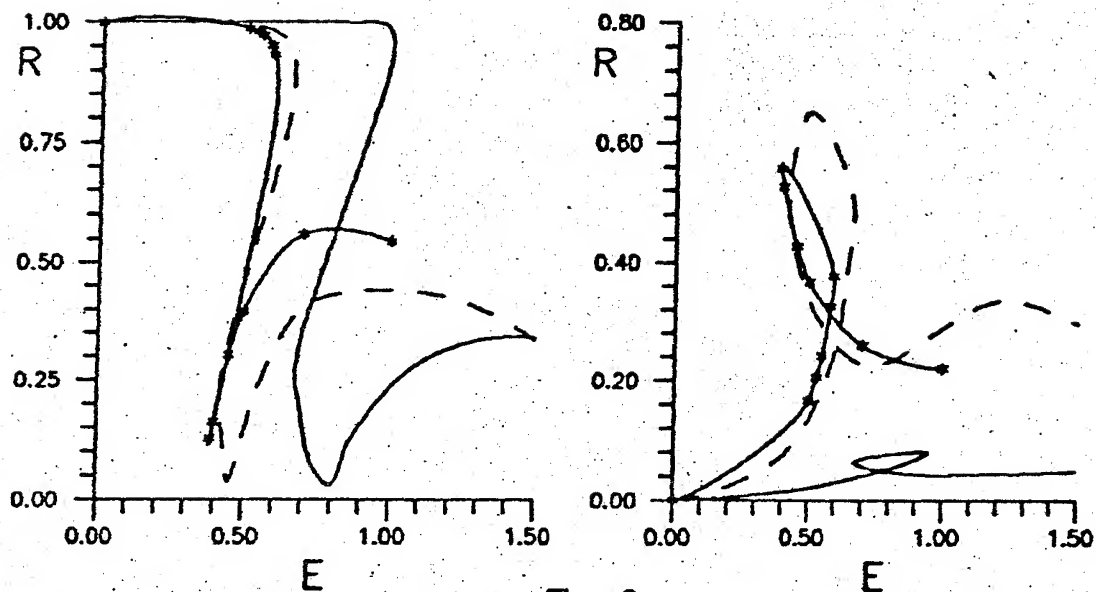


Fig. 2

a) First mode, b) third mode.  
 $kl = 6$ ; —  $kd = 6$ ; ---  $kd = 12$ ; —\*—  $kd = 18$

## PHYSICAL RESULTS

Most interesting results were obtained for positive nonlinearity when permittivity is negative in absence of field and becomes positive in sufficient intensive field. For thick layers (thickness near or more wavelength) the bistability of electromagnetic field structure in nonlinear media is obtained. Respectively we can look the hysteresis of reflection and transmission coefficient when we changed the intensity of incident wave. This effect was showed for waveguides various wide (from  $kd = 6$  to  $kd = 18$ ). Also analogous effect was showed for irradiation of slot antenna across nonlinear media. The distribution of electromagnetic field in nonlinear waveguide in some value of incident wave on both branches of hysteresis curve are showed on fig.1. Fig. 2 illustrated the dependence of reflection and transmission coefficients for first and third mode on intensity of incident wave. The common feature of field structure is that the field is compressed to lighted boundary when intensity of incident wave slowly increased from low value. When intensity increase some level, the field structure is rearranged and wave channel is formed. It is interesting that the width of this channel do not depended from transverse dependence of incident wave and approximately equal to one mode waveguide. Next if we decrease the intensity of incident wave the channel is saved to some level. It is important that this level is small that level when this channel was formed.

For negative nonlinearity we do not found a hysteresis solution. The main physical effect, that takes places is the limiting of the power value transmitting across nonlinear media. This effect was investigated previously on one dimensional models in [3]. The distinction between one-dimensional model and two-dimensional model lies in the fact that the level of limitation of transmitting power for two-dimensional model are greater that the level for one-dimensional model. This distinction may be explained by distinction between field structure for this two models. The possibility of bistability existence for two-dimensional nonlinear systems with negative nonlinearity is required further investigations.

Along with nonlinearity with homogeneous parameters (2,3) in this work also the influence of irregularity of nonlinearity parameters were investigated. In particular the dependence (2) was changed to

$$\epsilon = \epsilon_0(x,z) + \epsilon_2(x,z)\exp(\alpha|E|^2).$$

It was be founded that bistability is taken places for small irregularity and may disappear for strong irregularity.

## REFERENCE

1. Gibbs H.M. Optical bistability: Controlling light with light. 1985.
2. Taylor W.C., Sharfman W.E., Morita T. "Voltage breakdown of microwave antenna". Adv. Microwave v.7, No.1, p.59.
3. Bagdasaryan O.V., Permyakov V.A. "Bifurcation of modes and effect of limitation of energy flow of TE wave in media with ionized nonlinearity". Izv. VUZov. Radiophysika, 1978, v.21, No.9, p.1352 (in Russian).
4. Rozanov N.N. "Hysteresis phenomena in distributed optical system". Zurn. exp. i teor. phys. 1981. v.80, No.1, p.96 (in Russian).
5. Sarcoar T.K. "On the application of the generalized biconjugate gradient method". J. of Electromagnetic waves and applications. 1987. v.1, No.3, p.228.

# NUMERICAL COMPUTATION OF DIFFRACTION COEFFICIENTS FOR NEW CANONICAL PROBLEM

Vladimir Kalashnikov

Department of Radio Engineering, Moscow Power Engineering Institute  
Krasnokazarmennaya 14, Moscow 111250, Russia

## ABSTRACT

Direct numerical method is applied for the computation of diffraction coefficients for new canonical structure: joint of an infinite perfectly-conducting rectangular wedge with a semi-infinite dielectric slab.

## INTRODUCTION

The most important problem of the diffraction theory is scattering of electromagnetic wave from an object of complex form and structure. One was solved in resonance frequency domain, where scatterer's size is order of wavelength. In particular, the integral equation method can be used. It is very desirable to have such methods in a high frequency domain that are invariant for a form of scatter. The geometrical theory of diffraction (GTD) and the physical theory of diffraction (PTD) are developed for this domain. Both of these theories are not closed. They are historically based on the analytical solution of canonical problem: diffraction from a perfectly conducting wedge. It is difficult and often impossible to widen the range of problems amenable to analytical methods. An application of numerical solutions of new canonical problems is the most reasonable direction. There are set of canonical problems that were solved with help of the integral equation method [1-4].

Numerical solution for the new canonical problem is illustrated in the present research. With help that can to solve the wide range of scattering problems, which was being remained overboard of GTD and PTD.

The solution for this canonical problem is found for the first time.

## PROBLEM FORMULATION

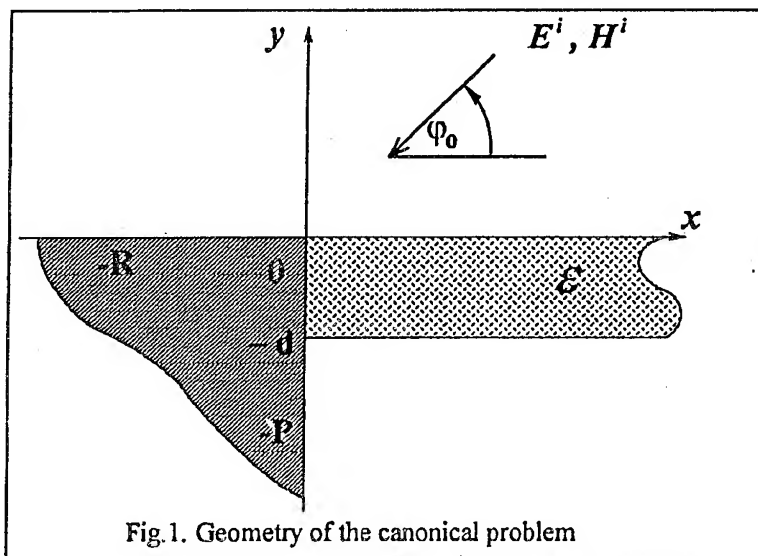


Fig. 1. Geometry of the canonical problem

We seek scattering from an infinite perfectly conducting rectangular wedge jointed to a semi-infinite dielectric slab, as shown in Fig. 1, upon illumination with a given incident electromagnetic plane wave  $E^i, H^i$ .

The slab has material with permittivity  $\epsilon_0$ . Let the wedge's edge is coincided with axis of  $z$ . Denoting the upper side of wedge by  $S_1: x \in ]-\infty; 0[, y = 0, z \in ]-\infty; +\infty[$ ; the area of lateral side of wedge, which contact with slab by  $S_2: x = 0, y \in ]0, -d[, z \in ]-\infty; +\infty[$ ; the rest area of lateral side- $S_3$ . Let's

denote the parts of cross section contour of wedge by  $L_1, L_2, L_3$  correspondingly.

Only monochromatic wave is considered, with time dependence  $\exp(i\omega t)$  suppressed throughout. The phase factor of incident wave is given by

$$\exp(ik_0 r_0) = \exp(ik_0 x \sin \theta_0 \cos \varphi_0 + ik_0 y \sin \theta_0 \cos \varphi_0 + ik_0 z \cos \theta_0), \quad \theta_0 \in ]0^\circ, 180^\circ[, \quad \varphi_0 \in ]-90^\circ, 180^\circ[.$$



## INTEGRAL EQUATION FORMULATION

The surface electric currents  $J^e$ , induced on an infinite wedge by an incident plane wave are the source of scattering field. We choose the distribution electric currents' density to determine. Let's use the following representation of the scattering field [5]:

$$E^{(s)} = \int_{\gamma} \mathcal{G}(x, y, z, u) J^e(u) du, \quad H^{(s)} = \int_{\gamma} \mathcal{H}(x, y, z, u) J^e(u) du,$$

where  $\mathcal{G}$  and  $\mathcal{H}$  are the tensor Green's functions,  $\gamma$ —contour of cross section wedge. We choose as a Green's function the field of an infinite current filament pointed inside and outside of infinite dielectric slab. The form of the Green's function is best viewed in [6]. This choice of a Green's function is taken into account the dielectric slab and the radiation condition. To take into account an infinite wedge we utilize the boundary conditions on the him external surface. Utilizing the boundary conditions results in the integral equations.

**Case 1. (total electric field).** We obtain a hyper singular integral equation of the first type, which are

known as electric field equation (EFIE) [7],  $[n, \int_{\gamma} \mathcal{G}(x, y, z, u) J^e(u) du] = -[n, E^p]$  utilizing

boundary conditions  $[n, E] = 0$ :  $n$ —external vector of normal to wedge;  $E = E^{(s)} + E^p$ —total electric field;  $E^p$ —primary electric field, which is found from a solution of problem about incidence of plane electromagnetic wave  $E^i, H^i$  on infinite dielectric slab.

**Case 2 (total magnetic field).** We obtain a Fredholm integral equation of the second type, which are

known as magnetic field integral equation (MFIE) [8],  $J^e - [n, \int_{\gamma} \mathcal{H}(x, y, z, u) J^e(u) du] = [n, H^p]$

satisfying boundary conditions  $[n, H] = J^e$ :  $H = H^{(s)} + H^p$ —total magnetic field;  $H^p$ —primary magnetic field (see above).

Obtained integral equations have been solved by the collocation method. We choose as basic functions to electric current density the following representation:

$$\begin{Bmatrix} J_x^e \\ J_y^e \\ J_z^e \end{Bmatrix} = \sum_{n=1}^N \chi(u, n, R) \begin{Bmatrix} A_n \\ B_n \end{Bmatrix} + \begin{Bmatrix} J_{\alpha}^e \\ J_{\beta}^e \end{Bmatrix} \exp(i\vartheta u) + \sigma(u - R) \frac{\exp(-i\beta u)}{\sqrt{u/R}} \left( \begin{Bmatrix} A_{N+1} \\ B_{N+1} \end{Bmatrix} + \begin{Bmatrix} A_{N+2} \\ B_{N+2} \end{Bmatrix} \frac{R}{u} \right), \quad u \in L_1;$$

$$\begin{Bmatrix} J_y^e \\ J_z^e \end{Bmatrix} = \sum_{k=1}^K \chi(u, k, d) \begin{Bmatrix} C_k \\ D_k \end{Bmatrix}, \quad u \in L_2;$$

$$\begin{Bmatrix} J_x^e \\ J_y^e \\ J_z^e \end{Bmatrix} = \sum_{m=1}^M \chi(u, m, P) \begin{Bmatrix} E_m \\ F_m \end{Bmatrix} + \sigma(u - d) \left[ \begin{Bmatrix} J_{\alpha}^e \\ J_{\beta}^e \end{Bmatrix} \exp(-\gamma_0(u - d)) + \begin{Bmatrix} J_{\alpha}^e \\ J_{\beta}^e \end{Bmatrix} \exp(\gamma_0(u - d)) \right] + \\ + \sigma(u - P) \frac{\exp(-i\beta u)}{\sqrt{u/P}} \left( \begin{Bmatrix} E_{M+1} \\ F_{M+1} \end{Bmatrix} + \begin{Bmatrix} E_{M+2} \\ F_{M+2} \end{Bmatrix} \frac{P}{u} \right), \quad u \in L_3;$$

where  $\chi(u, n, R) = \begin{cases} 1, & u \in [(n-1)\Delta_i, n\Delta_i] \\ 0, & u \notin [(n-1)\Delta_i, n\Delta_i] \end{cases}$ ,  $\Delta_i = \frac{R}{N}$ ;  $\sigma(u)$ —Heavyside's function;  $\vartheta = -k_0 \sin \theta_0 \cos \varphi_0$ ;

$\beta = k_0 \sin \theta_0$ ;  $\gamma_0 = ik_0 \sin \theta_0 |\sin \varphi_0|$ ;  $J_{\alpha}^e, J_{\beta}^e$ —amplitudes of physical optics currents, which depended from incident wave  $E^i, H^i$  and  $\varphi_0$ ; A, B, C, D, E, F—unknown values.

We are only interesting the scattering field in far region. The scattering field is writing in form:

$$\begin{Bmatrix} E_z \\ H_z \end{Bmatrix} = \frac{\exp[-i(k_0 r \sin \theta_0 - \pi/4)]}{\sqrt{k_0 r \sin \theta_0}} \exp(ik_0 z \cos \theta_0) \begin{Bmatrix} f(\varphi) \\ g(\varphi) \end{Bmatrix},$$

where  $f(\varphi)$  and  $g(\varphi)$ —diffraction coefficients.

### NUMERICAL RESULTS

It is stinted for the dielectric slab with parameters:  $d=0,44\lambda$  and  $\epsilon=2,7$ .

Let's seek diffraction coefficients for incident plane wave. The diffraction coefficients for different values of  $\varphi_0$  and for  $\theta_0=90^\circ$  are shown on the Fig.2. These diagrams were obtained with help the EFIE and the MFIE. The diffraction coefficients for  $\theta_0=70^\circ$  and  $\varphi_0=45^\circ$  are illustrated on the Fig.3.

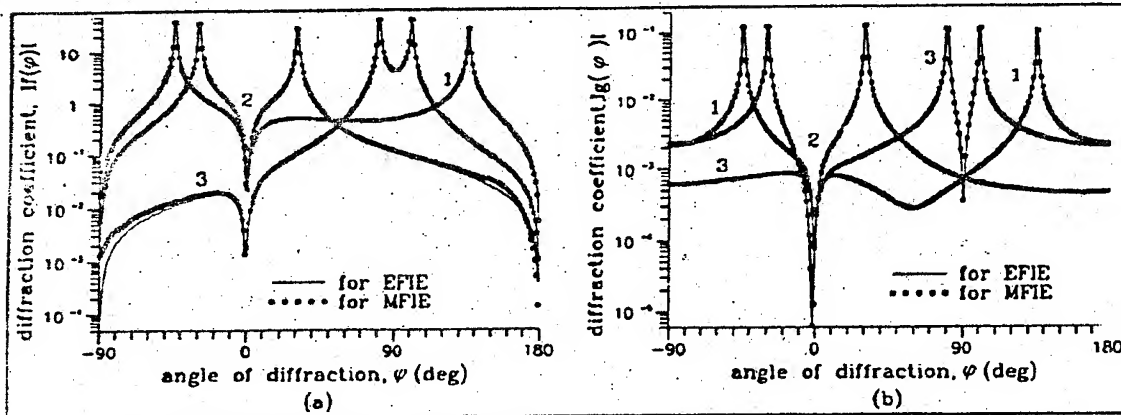


Fig.2. Diffraction coefficients:  $\theta_0=90^\circ$ ; 1—for  $\varphi_0=45^\circ$ , 2—for  $\varphi_0=150^\circ$ , 3—for  $\varphi_0=-80^\circ$ .  
(a) E-polarization. (b) H-polarization.

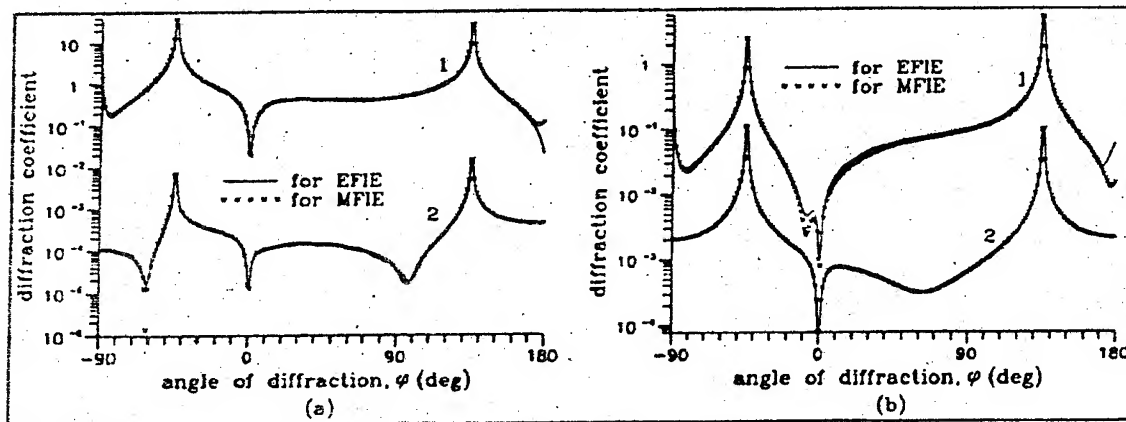


Fig.3. Diffraction coefficients:  $\theta_0=70^\circ$ ,  $\varphi_0=45^\circ$ ; 1—for  $|f(\varphi)|$ , 2—for  $|g(\varphi)|$ .  
(a) E-polarization. (b) H-polarization.

The diffraction of surface waves is also investigated. Illustrating some results. For primary field of surface wave inside the slab is given by

$$\begin{Bmatrix} E_z^s \\ E_x^s \end{Bmatrix} = \exp(i \begin{Bmatrix} \xi_i \\ \xi_j \end{Bmatrix} x) \begin{Bmatrix} \frac{sh(\gamma_s[y+d/2])}{sh(\gamma_s d/2)} \\ \frac{ch(\gamma_s[y+d/2])}{ch(\gamma_s d/2)} \end{Bmatrix}, \quad \begin{Bmatrix} H_z^s \\ H_x^s \end{Bmatrix} = \exp(i \begin{Bmatrix} \xi_i \\ \xi_j \end{Bmatrix} x) \begin{Bmatrix} \frac{ch(\gamma_s[y+d/2])}{sh(\gamma_s d/2)} \\ \frac{sh(\gamma_s d/2)}{sh(\gamma_s d/2)} \end{Bmatrix}$$

where  $\xi_m$ —traveling constant along axis  $x$  for  $m$  surface wave,  $\gamma_s = \sqrt{\xi_m^2 - \epsilon k_0^2}$ .

There are four traveling surface waves into slab with that parameters. The diffraction coefficients are shown on the Fig.4.

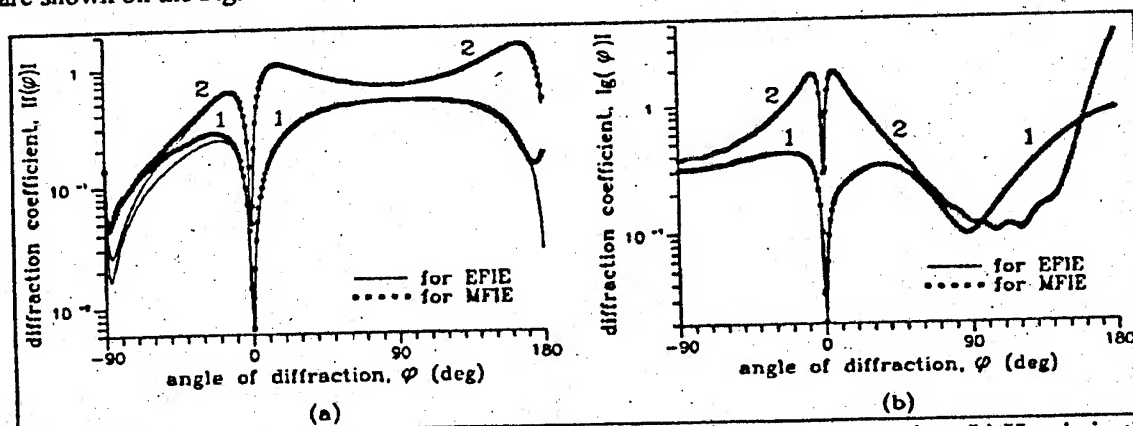


Fig.4. Diffraction coefficients: 1-for even wave; 2-for odd wave. (a) E-polarization. (b) H-polarization.

#### ACKNOWLEDGMENT

The author is totally indebted to E.N.Vasil'ev for many helpful discussions that have made this study possible. Discussions with A.I.Fedorenko were invaluable during the numerical solution stage of this work.

#### REFERENCE

- (1) E.N.Vasil'ev and V.V.Solodukhov: "Diffraction of electromagnetic waves by a dielectric wedge", *Izv.VUZ, Radiofizika*, (1974) 17, 10, pp.1518-1528.
- (2) E.N.Vasil'ev and V.V.Solodukhov: "Diffraction of electromagnetic wave by a wedge with a multi-layer absorbing covering", *Izv.VUZ, Radiofizika*, (1977) 20, 2, pp.280-289.
- (3) E.N.Vasil'ev and A.I.Fedorenko: "Diffraction from perfectly conducting wedge with dielectric covering on either side of wedge", *Izv.VUZ, Radiofizika*, (1983) 26, 3, pp.351-356.
- (4) E.N.Vasil'ev and A.I.Fedorenko: "Scattering of electromagnetic wave from the edge of semi-infinite dielectric slab, which placed into a perfectly conducting semi-infinite space", *Izv.VUZ, Radiofizika*, (1983) 26, 7, pp.860-866.
- (5) E.N.Vasil'ev. *Excitation of revolution bodies*.-M.: Radio i Svyaz, 1987.
- (6) V.I.Dmitriev and E.A.Fedorova: "Numerical investigation of electromagnetic fields into multi-layer mediums" in the book "Computation methods and programming" M.: MGU, 1980, vol.32, pp.150-183.
- (7) *Computation methods in electrodynamics*.-M.: Mir, 1977.
- (8) V.A.Fock: "Diffraction from convex body", *JETF*, (1945) 15, 12, pp.963-968.

# SURFACE MODE SCATTERING BY METAL STRIPS ON AN INTERFACE BETWEEN TWO DIELECTRIC LAYERS

Victor Kalinichev

Radio Engineering Department, Moscow Power Engineering Institute  
14 Krasnokazarmennaya, Moscow 111250, Russia

## ABSTRACT

The two-dimensional diffraction problem of surface mode scattering by a finite number of metal strips located inside a double-layer dielectric slab is analyzed. The influence of a higher leaky mode on the radiation behavior of the structure is clearly demonstrated.

## 1. INTRODUCTION

The goal of this work is to analyze radiation of surface mode caused by a metal-strip grating of finite extent located inside a double-layer dielectric slab. Such a structure may be used as a microwave or millimeter-wave planar antenna excited by a surface mode of the slab. In this work, radiation and scattering characteristics of the antenna are treated as a result of surface mode diffraction by a finite number of scatterers with mutual couplings. The analysis is based on the electromotive force technique and Kirchhoff-type equations in complex current amplitudes on the scatterers (1). It is shown that under certain conditions the higher leaky mode can affect the radiation properties of the structure. It should be noted that influence of leaky modes on radiation behavior of an electric dipole placed inside a substrate-superstrate dielectric structure was studied earlier by D. Jackson and A. Oliner (2).

## 2. METHOD OF ANALYSIS

The structure being analyzed is shown in Fig.1. A finite number  $N$  of zero-thickness and narrow metal strips of width  $2w$  separated by distance  $l$  are located on the interface between two dielectrics inside a grounded stratified dielectric slab. The top layer and the bottom one have thicknesses  $2a$ ,  $h$  and relative permittivities  $\epsilon_1$ ,  $\epsilon_2$  respectively. Assume that the surface  $TE_1$ -mode of the slab is incident normally on an input of the grating from the left. The real propagation constant  $\gamma = \gamma_{TE1}$  of this mode can be found from the dispersion equation:

$$p_{\epsilon_1} \text{th}(p_{\epsilon_2} h) [p_{\epsilon_1} \text{ch}(2p_{\epsilon_1} a) + p_{\epsilon_2} \text{sh}(2p_{\epsilon_1} a)] + p_{\epsilon_2} [p_{\epsilon_1} \text{sh}(2p_{\epsilon_1} a) + p_{\epsilon_2} \text{ch}(2p_{\epsilon_1} a)] = 0, \quad (1)$$

where  $p_{\epsilon_1} = (\gamma^2 - k^2 \epsilon_1)^{1/2}$ ,  $p_{\epsilon_2} = (\gamma^2 - k^2 \epsilon_2)^{1/2}$ ,  $p = (\gamma^2 - k^2)^{1/2}$ ,  $k = \omega/c$  and  $c$  is the velocity of light. It is assumed here that inequalities  $k(\epsilon_2)^{1/2} < \gamma_{TE1} < k(\epsilon_1)^{1/2}$  take place, so that the mode concentrates near the top layer.

Moreover, for the surface mode  $\text{Re } p > 0$  is used while the signs taken for the square roots of  $p_{\epsilon_1}$ ,  $p_{\epsilon_2}$  are arbitrary since these signs occur in even function fashion. It is implied here that the structure parameters are chosen to provide the single mode regime of the double-layer dielectric guide. As for the higher leaky modes of the slab, we must use  $\text{Re } p < 0$  and  $\text{Im } p > 0$  because of their improper character.

For finding a solution to the problem of diffraction of the  $TE_1$ -mode by the grating we employ the electromotive force technique. Let us suppose that the electric current density distribution on the  $n$ th strip is approximately

described by the formula:

$$i_n(z_n) \cong I_n / (w^2 - z_n^2)^{1/2}, \quad (2)$$

where the complex amplitudes  $I_n$ ,  $n=1, \dots, N$  will be determined below,  $z_n$  is measured from the center of the  $n$ th strip. By using the 2-D Green function of the stratified dielectric medium the secondary field generated by the current (2) at any observation point can be written via the Fourier-type integrals. For instance, the electric field in the upper free space region can be represented in the following way (suppressing  $e^{j\omega t}$ ):

$$E_{yn}(x \geq 2a, z_n) = \frac{-j\omega \mu_0 I_n}{2} \int_0^\infty \frac{p_{\epsilon_1} \text{th} p_{\epsilon_2} h}{D(x)} J_0(xw) \exp[-jxz_n - p(x-2a)] dx \quad (3)$$

with

$$D(x) = p_{\epsilon_1} \text{th}(p_{\epsilon_2} h) [p_{\epsilon_1} \text{ch}(2p_{\epsilon_1} a) + p_{\epsilon_2} \text{sh}(2p_{\epsilon_1} a)] + p_{\epsilon_2} [p_{\epsilon_1} \text{sh}(2p_{\epsilon_1} a) + p_{\epsilon_2} \text{ch}(2p_{\epsilon_1} a)], \quad (4)$$

where  $x$  is a spectral variable,  $J_0$  is a Bessel function of the zero kind,  $p_{\epsilon_1} = (x^2 - k^2 \epsilon_1)^{1/2}$ ,  $p_{\epsilon_2} = (x^2 - k^2 \epsilon_2)^{1/2}$ ,  $p = (x^2 - k^2)^{1/2}$  ( $\text{Re} p > 0$  if  $|x| > k$  and  $\text{Im} p > 0$  if  $|x| < k$  must be used to ensure the Sommerfeld radiation condition),  $\mu_0$  is free space permeability.

Next, the secondary fields generated by each of the strips must be superimposed. In addition, the primary field of the  $\text{TE}_1$ -mode must be included. Putting the observation point on the  $n$ th strip, equating the total tangential electric field in this point to zero and using the Galerkin technique, we obtain a set of the Kirchhoff-type equations of order  $N$  in the normalized complex current amplitudes  $\bar{I}_n = j\omega \mu_0 I_n$ :

$$\bar{I}_n Z_0 + \sum_{\substack{n=1 \\ (n \neq n)}}^N \bar{I}_n Z_{nn} = E_0 J_0(\gamma_{\text{TE}_1} w) \exp(-j\gamma_{\text{TE}_1} L_n), \quad n=1, \dots, N. \quad (5)$$

The value  $L_n$  denotes the distance from the origin of the coordinates to the center of the  $n$ th strip. For the equidistant array we have  $L_n = (n-1)l$ . The value  $E_0$  in the right-hand side of (5) depends on the amplitude of the primary  $\text{TE}_1$ -mode. The coefficient  $Z_{nn}$  viewed as a mutual impedance between the  $n$ th and  $n$ th strips is given by:

$$Z_{nn} = \int_0^\infty \frac{J_0^2(xw) \text{th}(p_{\epsilon_2} h) [p_{\epsilon_1} \text{sh}(2p_{\epsilon_1} a) + p_{\epsilon_2} \text{ch}(2p_{\epsilon_1} a)]}{D(x)} \exp(-jxL_{nn}) dx, \quad (6)$$

where  $L_{nn} = |L_n - L_n|$ . In a similar way, the coefficient  $Z_0$  may be treated as a self impedance of the  $n$ th strip, namely:  $Z_0 = Z_{nn}(n=n)$ .

The scattering and radiation characteristics (the reflection and transmission coefficients, the H-plane radiation pattern and the radiated power) can be straightforwardly determined from the solution of system (5) describing the complex current distribution in the grating.

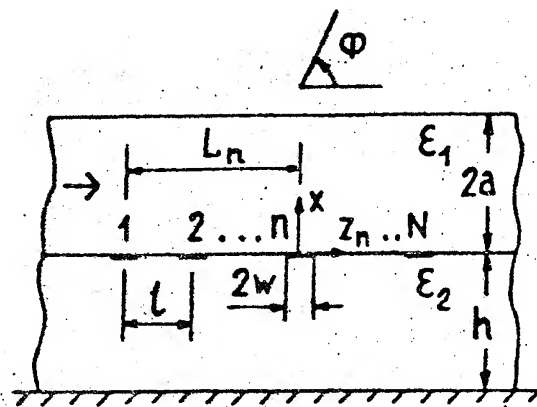


Fig.1 A planar antenna on a double-layer dielectric slab and a metal grating excited by the  $TE_1$ -surface mode.

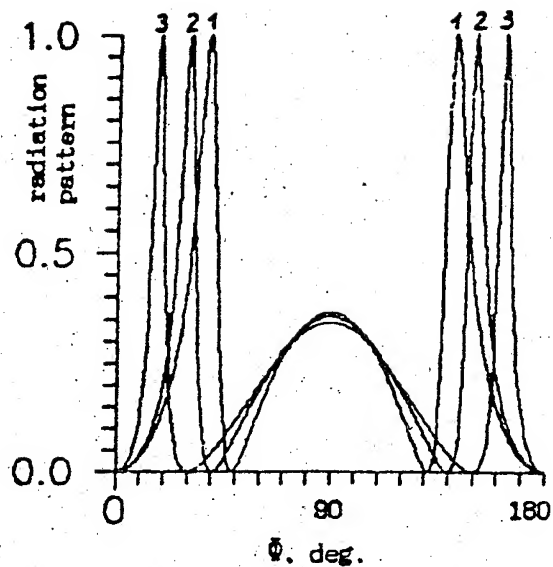


Fig.2 The H-plane radiation pattern for a single metal strip ( $N=1$ ):  
1 -  $f=60\text{GHz}$ , 2 -  $f=63\text{GHz}$ , 3 -  $f=67\text{GHz}$ .

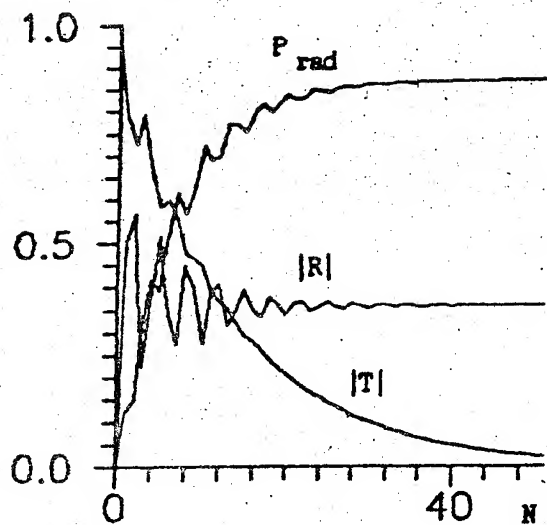


Fig.3 The radiation and scattering characteristics of the structure vs  $N$  ( $f=67\text{GHz}$ ).

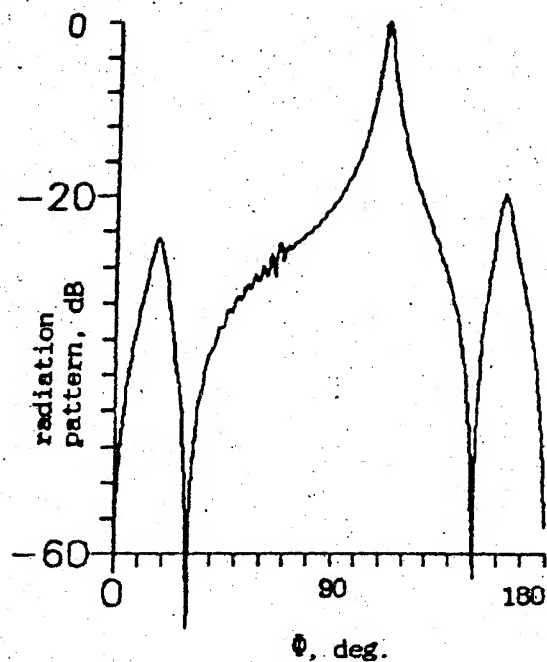


Fig.4 The H-plane radiation pattern for the grating consisting of  $N=51$  strips ( $f=67\text{GHz}$ ).

### 3. RESULTS

First, we considered the simplest structure with a single metal strip ( $N=1$ ). The parameters are chosen as follows:  $\epsilon_1=10.0$ ,  $\epsilon_2=2.0$ ,  $2a=0.5\text{mm}$ ,  $h=2.0\text{mm}$ ,  $2w=0.4\text{mm}$ . The calculated H-plane radiation patterns for some frequencies are shown in Fig.2. Physically, the two symmetrical beams near the grazing directions are attributable to the  $TE_2$  leaky mode, which is a part of the total diffracted field, propagating and weakly decaying on the double-layer slab. Indeed, as the frequency increases, the radiation peaks move symmetrically to the grazing directions taking the values  $\phi_0(60\text{GHz})=38^\circ$ ,  $\phi_0(63\text{GHz})=30^\circ$ ,  $\phi_0(67\text{GHz})=17^\circ$  and  $180^\circ-\phi_0$  correspondingly. On the other hand, the numerical solution of dispersion equation (1) in the leaky-mode region on these frequencies gives the following values:  $\gamma_{TE2}(60\text{GHz})=k(0.7655-j0.0529)$ ,  $\gamma_{TE2}(63\text{GHz})=k(0.8594-j0.0341)$ ,  $\gamma_{TE2}(67\text{GHz})=k(0.9546-j0.0163)$ . One can easily determine that  $\cos\phi_0 \approx \text{Re}(\gamma_{TE2})$  for every frequency. Consequently, the evolution of the peaks in Fig.2 completely conforms to the  $\gamma_{TE2}$ -vs- $f$  dependence in the complex  $\gamma$ -plane.

Thus, as follows from the afore-said discussion, the  $TE_2$  leaky mode can affect the radiation property of a single metal strip situated inside the double-layer dielectric structure. As was noted before, this conclusion closely agrees with a leaky-wave analysis of the narrow-beam "resonance gain" phenomena which may be produced in a substrate-superstrate geometry (2). Consequently, the  $TE_2$  leaky mode has to be taken into account in the further analysis of a finite number of scatterers with mutual couplings.

For instance, some radiation and scattering characteristics of a finite-periodic grating with period  $l=1.774\text{mm}$  were calculated on a frequency of  $f=67\text{GHz}$  (the other parameters remain as before). The reflection ( $|R|$ ) and transmission ( $|T|$ ) coefficients together with the relative radiated power ( $P_{\text{rad}}$ ) vs  $N$  are shown in Fig.3 ( $N$  varies up to 51). It should be noted that the reflection coefficient is high enough for this concrete situation. The H-plane radiation pattern for the case  $N=51$  is given in Fig.4. In accordance with the afore-discussed the  $TE_2$  leaky mode is responsible for the spikes occurring near the grazing directions. This clearly demonstrates the influence of the leaky mode on the radiation behavior of a planar beam antenna on a double-layer dielectric structure.

### 4. CONCLUSIONS

This paper discusses the approximate approach to the analysis of surface mode scattering by metal strips placed inside a double-layer dielectric slab. Impact of a higher-order leaky mode on the radiation behavior of the structure is analyzed for two situations. The first one concerns a single strip while the other situation deals with a grating of finite extent. The latter finite-periodic structure can be used as a planar beam antenna for microwave and millimeter-wave applications.

### REFERENCE

- (1) V. I. Kalinichev and Y. V. Kuranov, "Surface Wave Diffraction by a Finite Metal Grating and Numerical Model for Design of Leaky-Wave Antennas," IEEE Microwave and Guided Wave Letters, (1991) 1, 10, pp.282-284.
- (2) D. R. Jackson and A. A. Oliner: "A Leaky-Wave Analysis of the High-Gain Printed Antenna Configuration", IEEE Trans. Antennas Propagat., (1988) AP-36, 7, pp.905-910.

# ON THE PROBLEM OF SATELLITE MEASUREMENTS OF WIND SPEED

Karaev, V.Yu.

Institute of Applied Physics, Russian Academy of Science  
46, Uljanov Str., 603600, Nizhny Novgorod, Russia

## ABSTRACT

The dependence of the normalized radar cross section on the sea state at normal incidence is theoretically investigated. Slight dependence of the cross section on fetch for a developing sea waves is shown. A new algorithm of determining the wind speed using the independent altimetric measurements of the cross section and wave height is proposed.

## INTRODUCTION

At altimetric measurement over the ocean, the form of the backscattered pulse for determination of the wave height is used. The normalized radar cross section is applied to define the wind speed. However, the study performed in [1] has shown that the existing algorithms permit to determine the wind speed with the rms error equal to 1.7m/s. Fig.1 gives the comparison of the contact measurements of the wind speed with GEOSAT data (the wind speed was found by the empirical formula). The points are uniformly scattered near the correct value. Such behavior of the points and not very high accuracy of defining the wind speed is explained by the fact that the algorithms used now are regressive and are obtained by the set of experimental points. Using this approach it is impossible to achieve a better accuracy, because various wind speeds may correspond to identical values of measured cross section.

This paper considers the main factors affecting the cross section and studies the possibility of their taking into account.

## THE INITIAL ASSUMPTIONS AND RESULTS.

The cross section is defined by the state of the sea surface which unambiguously depends on the wind speed. When the incidence angles are small, the cross section measured along the direction of large-scale waves propagation (along the axis X) is defined by the well-known formula [2,3,4]:

$$\sigma_0 = \frac{|R(0)|^2}{2\sigma_x\sigma_y \cos^4 \theta_0} \cdot \exp[-\tan^2 \theta_0 / 2\sigma_x^2] \quad (1)$$

where  $\sigma_x^2$  and  $\sigma_y^2$  are the dispersions of the surface tilt along the axes X and Y;  $R(0)$  is the Fresnel coefficient of reflection at normal incidence;  $\theta_0$  is the incidence angle. To take into account the ripples effect on the reflected field the effective reflection coefficient  $R_{eff}$  is introduced [5,6]. In our calculations the JONSWAP spectrum was used [7]. In paper the following symbols are used:  $x$  is the length of the wind fetch in meters;  $\bar{x} = xg/U_{10}$  is the nondimensional fetch.

Let the wind speed at the height 10m  $U_{10}$  is equal 10m/s. The curve 1 in Fig.2 indicates the dependence of the cross section on the nondimensional fetch  $\bar{x}$ . It is seen from the Fig.2 that except the initial stage of the development of waves, the cross section is less in the process of the development in comparison with developed wind waves. This is explained by the fact that the dispersion of tilt is greater at the stage of wave development. The calculations are made at the fixed effective reflection coefficient corresponding to



increase of the fetch, the waves height will not change.

For  $U_{10} = 10 \text{ m/s}$ :  $x_k = 2.06 \cdot 10^5 \text{ m}$  or  $X_{kt} = 1.58 \cdot 10^5 \text{ m}$ . However, in the paper [10] occur also the fetches  $3 \cdot 10^5 \text{ m}$  and  $5 \cdot 10^5 \text{ m}$ . The simplest interpretation of this fact is that swell appears which increases the total waves height (at the fixed wind speed), and accordingly to the formula (3) it leads to the increase of  $X_g$ . Let  $U_{10} = 10 \text{ m/s}$ . We take from the Table given in [10] three intervals, whose left end refers to the stage of developing waves and the right one refers to the system of wind waves plus swell. We take also one point, which entirely refers to mixed waves. For definiteness we shall assume that the wavelength of swell is  $\Lambda = 150 \text{ m}$ . For swell the parameter  $\gamma$  in JONSWAP spectrum equals 10, and we find the value  $\alpha$  using the knowledge of the dispersion of swell deviation (in the system the wind waves plus swell).

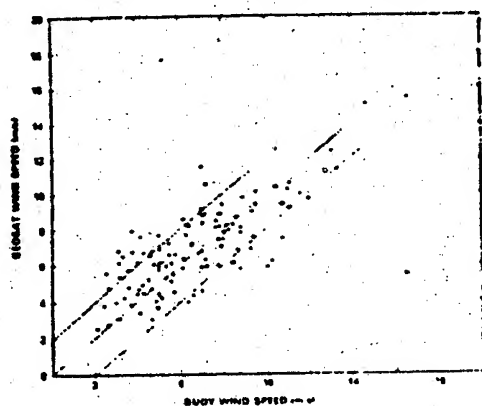


Fig. 1

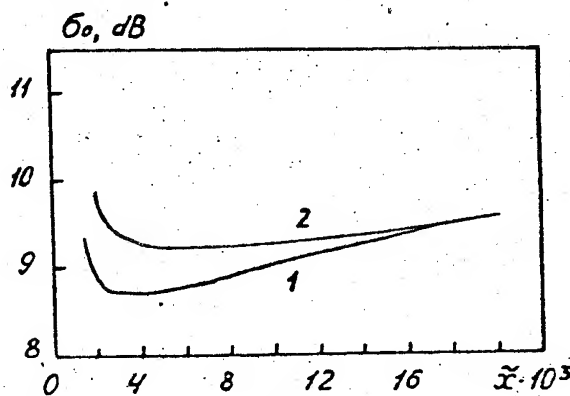


Fig. 2

The Fig. 3 shows two curves - the curve 1 is plotted on the basis of the experimental data and the curve 2 on the basis of our data. The theoretical curve 2 shows a good coincidence with the experimental data. For convenient comparison the cross section in the point  $X_g = 145 \text{ km}$  coincides and for the subsequent points the difference between the given point from the first one is used.

Let consider more carefully the case of mixed sea. The curve 1 in Fig. 4 shows the dependence of the cross section on the wind speed  $U_{10}$  for the developed wind waves. As the wind speed increases the wave height increases and the cross section decreases (the height of waves and the wind speed unambiguously relate to each other through spectrum). The wave height may increase also because of the swell arrival. The curve 2 corresponds the case, when there are developed waves on the surface corresponding to the wind speed  $U_{10} = 7 \text{ m/s}$  (the rms of the surface elevation  $\sigma_h = 0.29 \text{ m}$ ) and swell with  $\Lambda = 150 \text{ m}$ . The swell height is defined from the condition that the height of mixed waves is equal to the height of the wind waves. When plotting the curves on Fig. 4 we use the condition that wave heights are equal. It is seen from the Fig. 4 that the dependence of the cross section on wave heights differs essentially in both cases that permits to find the wind speed. Wind speed can be found as the solution of the following system:

$$\begin{cases} h_m = h_w(U_{10}) + h_s \\ \sigma_m = \sigma_0(U_{10}, h_s) \end{cases} \quad (4)$$

Here,  $h_m$  and  $\sigma_m$  are the measured wave height and cross section correspondingly;  $h_s$  is the height of swell;  $h_w$  is the height of wind waves. Thus for the case, when developed wind waves and swell present simultaneously on the surface, the solution of the system (4) gives the wind speed.

How can we present the algorithm of defining the wind speed? First we find the cross section by the known dependence  $\sigma_0$  on the waves height for the case of the developed wind waves. Three variants are possible - the coincidence of the measured cross section with the theoretical one - we assume that the wind speed is defined correctly. If the measured cross section is greater, then it will correspond to the case of mixed sea (the developed wind waves plus swell). In this case to define the wind speed it is necessary to solve the

the wind speed  $U_{10} = 10 \text{ m/s}$ . However, in the process of the wave development, the spectrum of ripple also develops. We have not found the experimental data concerning directly this problem, but there is indirect information.

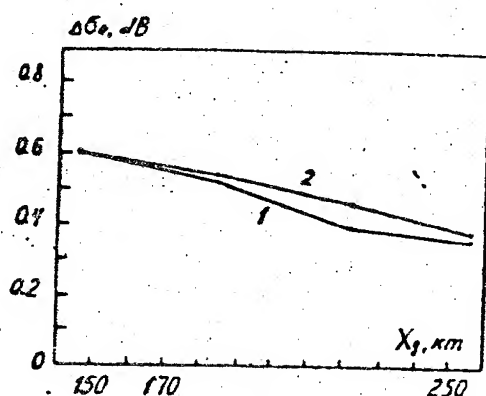


Fig. 3

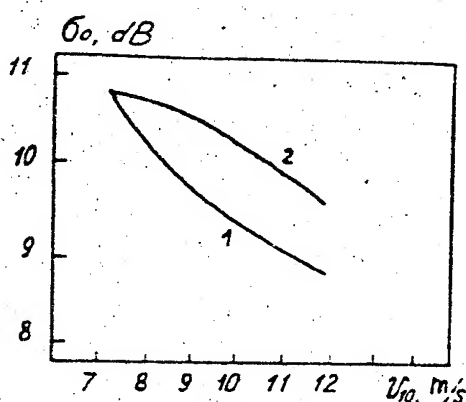


Fig. 4

In paper [8] on the basis of the analysis of extensive experimental material, the tendency of decreasing the wind speed, defined by the scatterometer was observed in comparison with the real data (measured by contact method) at the stage of the development of waves. In the first approximation we may account that this is associated with a less spectral ripple density on the process of waves development. The error caused by this fact may achieve 4.8 m/s [8] at the stage of waves development.

The analogous data are given in paper [9]. In particular, at  $\bar{x}_0 = 2 \cdot 10^3$  the error achieves 40 %. We shall assume that at the stage of the developed wind waves ( $\bar{x}_t \approx 2 \cdot 10^4$ ) the wind speed found by the cross section and the real wind speed coincide. To get the simplest estimate we assign the linear dependence of the effective wind speed on the fetch. Then for  $2000 \leq \bar{x} \leq 20000$ :

$$U_{eff} = 0.6U_{10} + 0.4U_{10}(\bar{x} - \bar{x}_0)/(\bar{x}_t - \bar{x}_0) \quad (2)$$

The two basic assumptions lay in the basis of the proposed method: 1) the measurements are made at middle angles show that the spectral density of ripple increases in the course of waves evolution. Thus we introduce the effective wind speed corresponding to the spectral density of the ripple at the given length of the fetch (formula (2)); 2) the formula for the scattering cross section (1) includes the coefficient  $R_{eff}$ , which depends on the wind speed (or the spectral density of ripple). Here the effective wind speed is used. The effective wind speed is found by the formula (2) and corresponds to the spectral density of ripple at the given stage of waves development.

Using the information on the dependence of the effective scattering coefficient on the wind speed [5], we have obtained the dependence of the cross section on the fetch. The curve 2 in Fig. 2 corresponds to this case. It is seen that cross section changes slightly at the stage of waves development. Let compare this theoretical result with the available experimental data.

In paper [10] the scattering cross section is analyzed on the basis of the experimental data for various lengths of fetch. Unfortunately, the space intervals in which the analysis was performed, are too large. In this reason, it is impossible to consider the interval corresponding only to the stage of waves development.

The authors [10] used the definition of the generalized fetch defined in the following way:

$$X_g = 4.2 \cdot 10^5 g H_s^2 / 1.29 U_{19}^2 \quad (3)$$

i.e.  $X_g \sim H_s^2 / U_{19}^2$ ,  $H_s$  is a significant height of waves;  $U_{19}$  is the wind speed at the height 19.5 m. When wind speed is constant, the ocean waves achieve the stage of the developed wind waves and at the further

system (4). In the opposite case we deal with developing wind waves and swell. This variant allows the analog consideration.

Consequently, having the independently obtained information on the cross section and the waves height (which permits to make the altimeter), using the proposed method one may try to define the wind speed for the case of mixed waves. To estimate the potentiality of this method one should process experimental data.

## CONCLUSION

In conclusion we mention that the paper theoretically shows that the cross section weakly depends on the fetch. The comparison with the experimental data shows that the following model of waves may be used: wind waves plus swell. The case of mixed sea is considered and this permits to propose a new method of defining the wind speed using the wave height and the cross section. In paper [11] the wave height is taken into account but in the regression algorithm. The comparison with the existing algorithms has shown that it has better accuracy; the rms error of defining the wind speed constitutes 1.4m/s.

A new method of determining the wind speed using the independent altimetric measurements of the cross section and the wave height is proposed for mixed sea. This method allow to remove the uncertainty when different wind speeds correspond to the same cross section. The further joint theoretical and experimental study of the cross section will permit to improve the estimation of the wind speed using the data of nadir probing.

Acknowledgments. The author is grateful to Dr.M.B.Kanevsky for help in writting the paper. This work was supported by the Russian Fund of Fundamental Investigation, grant 93-02-15892.

## REFERENCES

1. Dobson E. et al: Validation of Geosat altimeter derived wind speeds and significant wave heights using buoy data, Journ. of Geoph.Res., 1987, v.92, NC10, pp.10719-10732
2. Bass F.G., Fuks I.M.: Scattering of waves by the statistically rough surface, Moscow, Nauka publisher, 1972, p.424 (in Russian)
- 3.Barrick D.E.: Rough surface scattering based on the specular point theory, IEEE Trans. AP-16, 1968, v.16, pp. 499-454
4. Valenzuela G.R.: Theories for the interaction of electromagnetic and oceanic waves - A review, Boundary-Layer Meteorology, 1978, v.13, pp.61-86
- 5.Barrick D.E.: Wind dependence of quasi-specular microwave sea scatter, IEEE Trans. AP-22, 1974, v.22, N1, pp.135-136
- 6.Valenzuela G.R.: The effective reflection coefficients in forward scatter from a dielectric slightly rough surface, Proceedings of the IEEE, 1970, v.58, N8, p.1278
7. Karaev V.Yu.: On the normalized cross section problem by altimeter measurements of sea surface, Issled. Zemli iz Kosmosa, 1994, N1, pp.21-28, (in Russian)
- 8.R.E.Glazman, G.G.Pihos: Scatterometer wind speeds bias induced by the large-scale component of the wave, J.Geoph. Res., 1988, V.93, NC2, pp.1317-1328
9. Kavelin S.S, et al: Radar Sensing of Earth surface from space, 1990, Leningrad, Gidrometeoizdat, p.200 (in Russian)
10. R.E.Glazman, S.H.Pilors: Effects of sea maturity on satellite altimeter measurements, J.Geoph.Res., 1990,v.95, NC3, pp.2857-2870
11. R.E. Glazman, A.Greysukh: Satellite Altimeter Measurements of Surface Wind, J.Geoph. Res., 1993, v.98, NC2, pp.2475-2483

# Electromagnetics of Simplest H-Eigenwaves in Periodic Iris-Loaded Circular Waveguide

Serge K. Katenev  
Kharkov State University  
Svobody Sq., 4, 310077, Ukraine

**Abstract** - Using some routine rigorous computation procedure, general background of eigenwaves in periodic iris-loaded circular waveguide (PICW) is presented for theoretical treatment of EM-wave propagation in PICW to have started. A simplest H-wave event is treated in detail.

## 1. Introduction.

Widely practically used, PICW still has blank spots in its electromagnetics treatment both in general and in some specific aspects.

To save the argument, let's note that PICW, a periodic structure transmitting EM waves, is obeying of all the laws in effect, e.g.: a) pass/stop band nature of propagation [1]; b) linear dispersion origin of the waves behaviour [2]; c) coupled waves model in effect [3]. These general principles combining uniformly all the 3 types of waves, TE(H), TM(E), and hybrid ones, are to be kept to in order to succeed.

H-waves, the simplest ones in the trio, are the least in use and thus rare in papers, except some odd data concerning their dispersion curves mostly. But, this can't be made up for in view of, e.g., the theory. What is a number of eigenmodes in the guide or, at least, how to count them through? Which are eigenmodes' quantitative characteristics and what are they exactly? Which are major factors or, at least, major guide's dimensions in effect, and in what way do they work? No answer at the time to those questions should evidently provide solid proof for the absence-of-theory declaration as well as serve as best reasoning in why an attempt to develop such a one is worth trying.

## 2. Eigenwaves in Periodic Waveguide.

Generally, numerical info in the matter is of 2 kinds: Brillouin diagrams (BD) and energy characteristics (EC), e.g., Poynting vector  $S$  and power flow  $P$ . The both kinds of info are yielding in the study.

Infinitesimal iris in the regular guide transforms its BD as is in Fig.1, the perturbed regular modes are 1,2,3,6,11. Regular-periodic transition resides in: a) periodic, period 1, translation of regular dispersion curves tree; b) absence-of-propagation in the vicinity of

cross-points (called [4] Bragg wave numbers  $\kappa_B$ ) of neighbouring trees' branches. The both facts convey originally the 2 fundamental properties of periodic structure [4]: 1) availability of a set of space harmonics  $0, \pm 1, \pm 2, \dots$ ; 2) alteration of pass and stop bands. Of 1), 2) properties, 1) is equivalent to periodic structure itself, whereas 2) is a corollary of 1) and generally is a relative property, Fig. 1, 3.

Basic strip  $\kappa \in [0, 0.5]$ ,  $\kappa \in [0, \infty)$  suffices in the matter.

Exact fashion of modes' origination and transformation is determined foremost by the guide's period.

Admittedly [4], relationship  $\kappa_B = m/2$ ,  $m=1, 2, \dots$ , is relevant in periodic structures, and a model of added in phase successive reflections from perturbations is workable. But, since there are essentially other than that Bragg wave points in PICW, Fig. 1, and in view of both infiniteness of  $\kappa$  axis and general arbitrariness of  $\ell$ , the ratio  $\lambda_B/\ell$ ,  $\lambda_B$  being Bragg wavelength, seems to be as well arbitrary in the guide.

Points  $\kappa=0$  either correspond with the cut-off frequencies in regular guide, the eigenmodes concerned compose the 1-st group, or they are  $(0, \kappa_B)$  points which appear in PICW due to effect of periodicity, the modes concerned compose the 2-nd group.

In this way, periodic infinitesimal iris in regular waveguide results in identical mapping of its BD from the upper triangle  $\kappa > \kappa_B$  of I-st quadrant of  $(\kappa, \kappa)$  plane into the basic strip according to property 1) of periodic structure; the total number of eigenmodes is to be estimated as a unification of 2 countable sets of the 1-st and 2-nd type modes; all the eigenfrequencies are held constant at the mapping, except in Bragg-wave points where they generally vanish at all.

In the guide  $S_{nz} > 0$  ( $< 0$ ),  $P_n > 0$  ( $< 0$ ) at  $n > 0$  ( $n \leq 0$ ) provided  $d\kappa/d\kappa_B > 0$  and vv. This fact validates splitting of S, Fig. 2, and P as

$$Q = Q^- + Q^{*-} + Q^+ + Q^{*+}, \quad (Q = \vec{S}, P). \quad (1)$$

where superscripts "-", "+", "\*" denote  $\sum_{n=-\infty}^{-1}$ ,  $\sum_{n=0}^{\infty}$  summations and etc.

Vector fields (1) in Fig. 2,  $-\ell \leq z \leq \ell$ , present  $H_{01}$  mode and vector  $\vec{S}^- \equiv \vec{S}_R$  is contra-directional, vector  $\vec{S}^+ = \vec{S}_I \vec{S}^- + \vec{S}^+ + \vec{S}^{*+}$  is co-directional to vector  $\vec{S} \equiv \vec{S}_T$ , where T, R, I are for transmitted, reflected, initial.

$$\vec{S}_T(r, z) = \vec{S}_I(r, z) + \vec{S}_R(r, z). \quad (2)$$

None of the vectors (2) represents by itself the eigenwave, whereas any two of them do.

Similar relationship is relevant for P

$$P_T = P_I + P_R \Big|_{z=\ell, -\ell}. \quad (3)$$

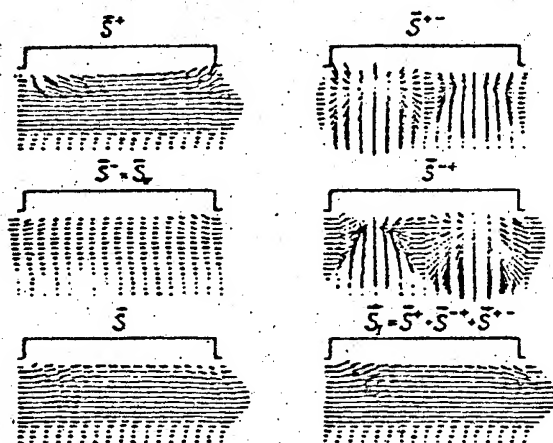


FIG. 2

Poynting vector  $\vec{S}$  field and all its ingredient portions over the unit cell (in the upper half) of the guide (3, 2.625, 24,  $H_w$ ,  $2\pi d = 0.32$ ).

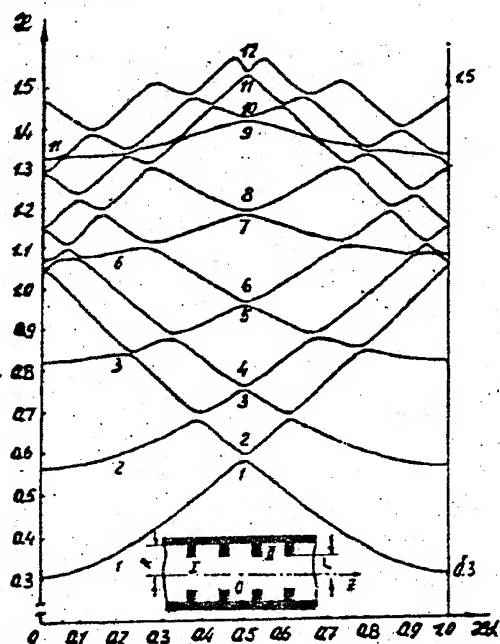


FIG. 1

Brillouin diagram of PTW at infinitesimal perturbations of regularity,  $R=3$ ,  $L=0.75$ ,  $d=0.65$ ,  $r=2.95$ .

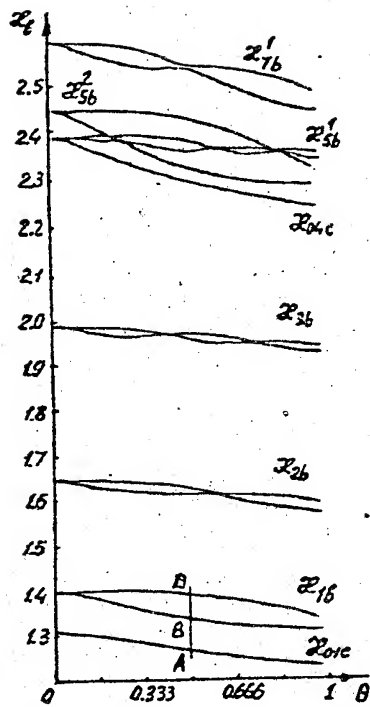


FIG. 4  
Boundary frequencies of modes of  
Fig. 3,  $r=2.8$ , vs  $\theta$ ; e.g.  $AB=\Delta\Omega$ ,  
 $BD=\Delta\omega$ , at  $\theta=0.5$ .

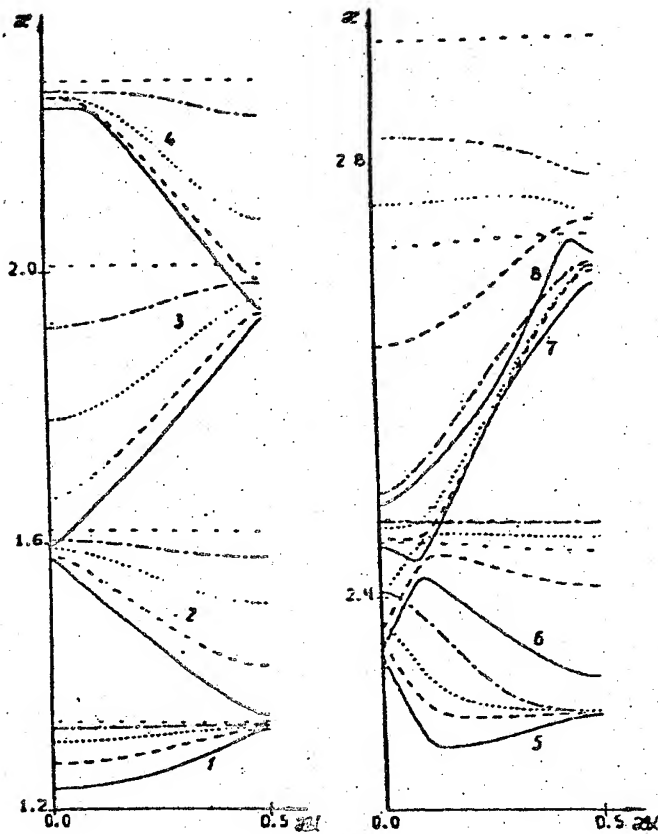


FIG. 3  
Brillouin diagram of PICW with large period  $l=3$ ,  $d=2.8$ ;  
 $r=2.8$  (solid line),  $r=2.4$  (dashed ---),  $r=2.0$  (dotted ...),  
 $r=1.6$  (dashed-dotted -.-.-),  $r=1.0$  (dashed - -).

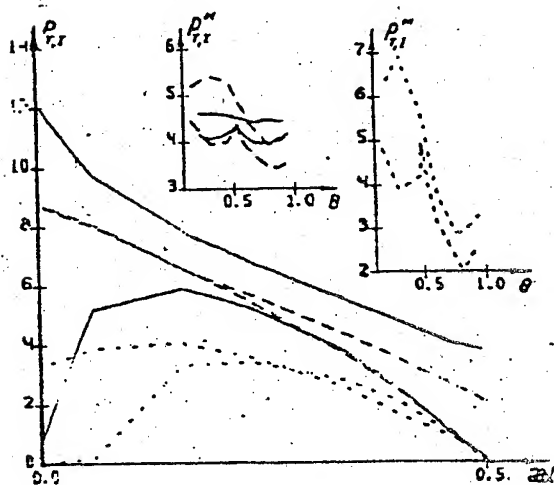


FIG. 6  
2-nd mode:  $P_r, P_i$  vs  $x$  at  $\Delta\omega$ , extremums,  $r=2.0$ ,  
and  $P_r^m, P_i^m$  vs  $\theta$ ,  $r=2.8, 2.4, 2.0$  (sol., dash., dot. lines).

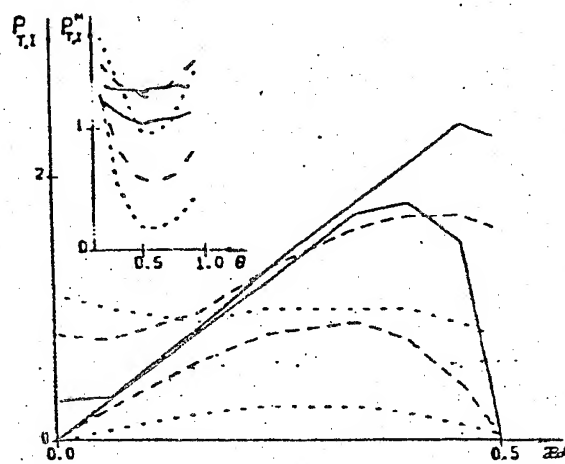


FIG. 5  
1-st mode:  $P_r, P_i$  vs  $x$  at  $\Delta\omega_{\max}$  and  $P_r^m, P_i^m$  vs  $\theta$   
for  $r=2.8$  (solid l.),  $2.4$  (dashed),  $2.0$  (dotted).

(3) quantitates mode's energy with respect to its distribution  $P(\alpha)$  upon basic interval and full mode's capacity  $P^M \approx \int_0^{\pi} P d\alpha$ .

### 3. Stop Bandwidth Extremums and Some Other Characteristics of H-Waves

BD of large period guide is presented in Fig. 3.  $H_{0i}$ ,  $i=1,2,\dots,8$  modes are available in the band. Frequencies  $(0,\pi), (0.5,\pi)$  vs  $\theta$  for some of the modes are plotted in Fig. 4. Stop bandwidths  $\Delta\omega_i$ ,  $i=1,2,3$ , have  $i$  maxima and  $i-1$  minima as well as similar  $\Delta\omega_5^2$ ,  $\Delta\omega_7^1$  bands have.

$H_{0i}$ 's  $P_{T,I}(\alpha)$  at  $d$  of  $\Delta\omega_{i,\max}$  (bigger plots) and  $P_{T,I}^M(\theta)$  dependencies are shown in Fig. 5. The highest level of  $P(\alpha;r)$  goes down and lowest level of  $P_R(\alpha;r)$  grows up at the growth of perturbation.  $P_I$  experiences a quite definite stability as  $r$  varies.

$H_{02}$ 's case is presented in Fig. 6.  $P_{T,I}(\alpha)$  are at  $d$ 's of  $\Delta\omega_2$  bandwidth extremums for  $r=2.0$ . 2 upper (minor) plots exhibit  $P_{T,I}^M(\theta)$  at  $r=2.8, 2.4, 2.0$ . There is strong reflection when  $\Delta\omega_2$  bandwidth is maximal and vv. The transparent  $\alpha$  interval of  $\Delta\omega_{2\min}$  is not bounded to  $\alpha=0$  vicinity. The 2-nd maximum's level of  $P$  is much lower than the 1-st one's, the greater perturbation, the greater is difference.

### 4. Conclusions

Both qualitative and quantitative principal background regarding eigenwave propagation in PICW has been formulated and put to effect.

It has been used in a specific simplest H-wave event. The left edge  $\alpha=0$  of  $H_{0i}$  mode is Bragg wave point,  $P_I \equiv P_R$ .  $H_{02}, H_{03}$  have the Bragg wave points on their both edges, except under some transparency conditions at certain  $d$ 's when there may be no Bragg points at all (e.g., in  $\Delta\omega_3$  bandwidth minima). These conditions are "lengthy" in  $\alpha$ .

H-wave eigenfrequencies monotonously grow up, varying in speed of the growth, at the growth ( $r$ ,  $\theta$  going down) of perturbations.

Each eigenwave has its reflected power flow portion  $P_R \neq 0$ , except at  $d$ -amount transparency conditions.

There is one-to-one correspondence among BD and EC kinds of info.

### 5. References

1. N. Brillouin. Wave propagation in periodic structures. -New York: Dover Publications, Inc., 1956.
2. G.B. Whitham. Linear and nonlinear waves. -Moscow: Mir, 1977. -622p.
3. G.R. Pierce. //Circuits for traveling wave tubes. //Proc. IRE. -1949. -v. 37. -p. 510.
4. C. Elachi. //Proc IEEE. -1976. -v. 64. -P. 1666.



# GUIDED WAVE REFLECTION FROM A JOINT BETWEEN THE REGULAR AND IRIS WAVEGUIDES

Vadim B. Kazanskiy, Dmitriy L. Litvinenko,  
Kharkov State University,

4 Svobody Sqr., 310077 Kharkov, Ukraine,

Leonid N. Litvinenko

Institute of Radio Astronomy of Ukrainian Academy of Science,

4 Krasnoznamennaya Str., 310002 Kharkov, Ukraine,

## ABSTRACT

Diffraction of waves is treated upon a joint of a regular and periodic loaded waveguides, both co-axial, half-infinite and of identical cross-sections. Repeated loading elements are a grating iris of conducting tapes with magnetodielectric spacer in between. The method employed is based upon equality of the input impedances of a loaded guide in the plane of a joint and in any cross-section a finite number of periods far from the joint.

The sought for coefficient of reflection from the half-infinite sequence of elements is determined using a single element's reflection characteristics obtainable as symmetric guided waves diffraction problem's solutions using the Vainstein-Sivov double-sided equivalent boundary conditions method.

The conditions of a absolute wave reflection on the joint have been revealed and the relation of those and the eigenwave conditions in infinite periodic loaded waveguide has been displayed.

## INVESTIGATED STRUCTURE

Object of investigation is a junction of the regular and periodically (period  $L$ ) loaded waveguides; both rectangular ( $a \times b$ ) and half-infinite. Amount  $L$  includes a magnetodielectric spacer's ( $\epsilon_1, \mu_1$ ) thickness  $D$ . Upon its surface there is a grating of a

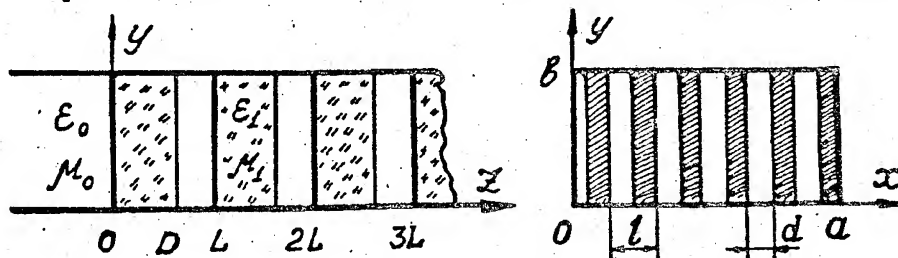


Fig. 1

period  $l$  and gap  $d$  composed of ideal conducting infinitissimally thin tapes parallel to the guide's narrow wall. The other part of the period ( $L - D$ ) is filled with the same ( $\epsilon_0, \mu_0$ ) medium as the regular guide (Fig.1). Assumingly, period  $l$  is much less than wavelength,  $\kappa = kl/2\pi \ll 1$ . Excitation shall be due to symmetric  $TE$ -waves. These assumptions do exclude a mode transformation and an elementary unit cell of the iris waveguide is representable as an equivalent four-pole.

## MODEL FOR THE HALF -INFINITE PERIODIC LOADING

Because of periodicity and half-infiniteness of the structure the waves propagating in the positive direction have equal input impedances in the cross-sections  $z = NL$  ( $N = 0, 1, 2, \dots$ ) [1]. For

this reason the sought for reflection coefficient ( $R$ ) just on the joint ( $z = 0$ ) and these same at the input of any two (neighbouring, e.g.) out of the whole lot of the equivalent four-poles are equal. This fact does determine the relation between  $R$  and the wave matrix  $S$  of the four-pole as

$$R = S_{11} + S_{12} S_{21} R / (1 - S_{22} R) \quad (1)$$

Suchlike approach is also valid in asymmetric wave and/or anisotropic filling events when the mode transformation is occurring. In that case the composing elements of the loading are representable by respecting multi-poles while the reflected field is described via a vector-column of the reflection and transformation coefficients.

For finding out the wave matrix  $S$  both the ordinary and the generalized double-sided equivalent boundary conditions upon a top grating ought to be used [2]. At arbitrary the structure's parameters and the exciting field  $|S_{11}/S_{22}| = 1$ . As the roots square (1) are related due to relationship  $|R_1| = |R_2|^{-1}$ , an obvious condition  $|R_k| \leq 1$  provides a uniqueness of solution.

### REFLECTION CHARACTERISTICS

The peculiarities about the structure in question are the availability of bands of full reflection (stop-band) and a polarization susceptibility. While the first is due no-propagation conditions in periodic loaded waveguide, the second is due to the anisotropic conductivity of the grating. The wave propagation conditions are the effects of the eigenwave conditions' cause in the infinite guide formed up by the sequence of the elementary cells considered. The output and input field amplitudes for each of them, according to Floquet theorem, are related through the factor  $\exp(-i\gamma L)$ . The "averaged" propagation constant  $\gamma$  - is obtainable from dispersion equation:

$$\cos \gamma L = (1 - S_{11} S_{22} + S_{12} S_{21}) / 2S_{22} \quad (2)$$

When  $|\cos \gamma L| \geq 1$  the waves in the infinite guide do not propagate. The parameters of the structure regarding the last inequality define the full reflection conditions in effect. While in  $TE_{m0}$ -event at arbitrary ratio  $d/l$  the upper boundary of the stop band appears to be fixed on the scale  $kL$ , in  $TE_{0n}$ -event it is the lower one that is fixed. In the both cases, growing narrower (at  $d/l \rightarrow 1$ ), the stop bands go somewhat shrinking towards their fixed border. In the absence of magnetodielectric spacers ( $Z_0 = Z_1 = Z = k\mu/\gamma$ ) for the "overlapping" of the bands of partial transition for the both types of waves ( $e, h$ ), it is necessary that in one time the two relationships be valid

$$2Z e^{\pi} |\ln \sin(\pi d/2l)| < 1 \quad \text{and} \quad 2Z^h / e^{\pi} |\ln \cos(\pi d/2l)| < 1.$$

In  $0.1 \leq d/l \leq 0.9$  interval, the first condition is ever valid and the bands of the partial transition of  $TE_{0n}$ -waves are wider than those of  $TE_{m0}$ -waves.

Dependence of the reflection coefficient's  $R$  module vs  $kL$  may be described as the "beatings" of oscillatory functions of diverse

periods. Their mutual period grows up at the growth of both the ratio  $D/L$  and optical density of the spacer. The grating causes weak perturbations in the dispersed  $TE_{0n}$ -wave field. In the  $TE_{m0}$ -event even at  $d/l \geq 0.9$  the grating not only causes an increase in the minimal level of the reflection, but makes principal changes in its character (Fig.2).

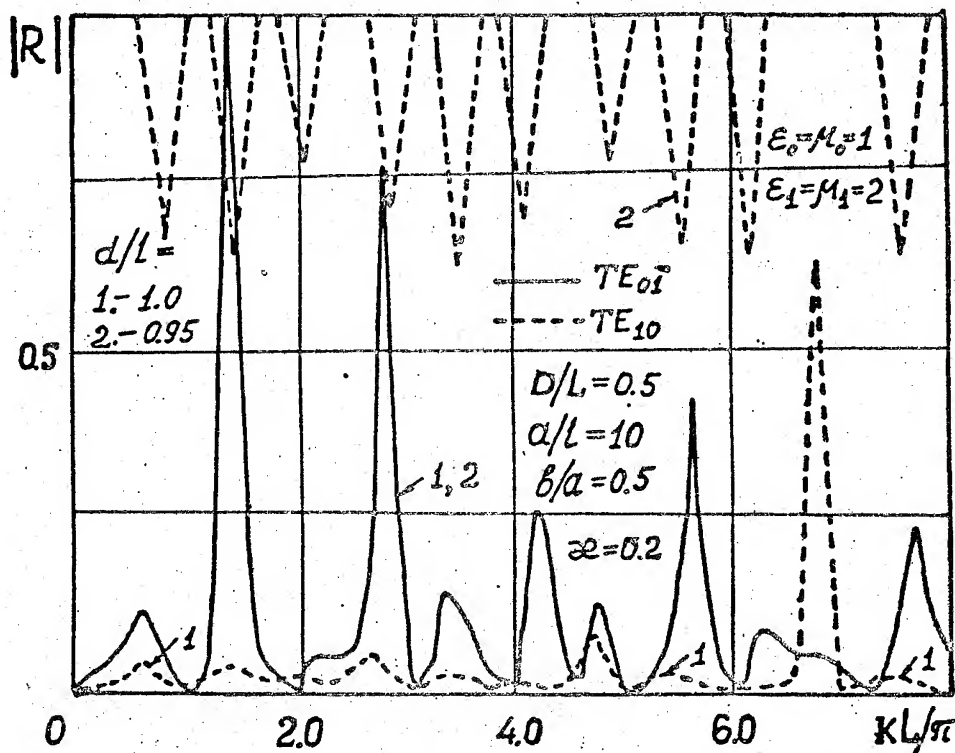


Fig.2

The decisive for  $R$  vs  $D/L$  is whether the interferential resonances exist ( $kL/Z > \pi/2$ ) or not ( $kL/Z < \pi/2$ ). In no-resonant case,  $R$  vs  $D/L$  dependency is monotoneous (without oscillations). It's level, when grating is used, depends upon the excitation field's type.

#### RESUME

The loading of a half-infinite periodic iris waveguide possesses of vast functional capabilities. It models important in practical applications the control systems, namely: a selector, a wave type transducer and stabilizer, band and resonant frequency filters, a standard reflector, etc.

#### REFERENCES

1. Litvinenko L.N., Reznick I.I., Litvinenko D.L. Diffraction of waves upon half-infinite periodical structures // Dokl. AN UK. SSR, 1991, N 6, pp. 62-67.
2. Kazanskiy V.B. Theory of multifunctional control system in the multimode transmission lines, Proc. International Conference "Physics in Ukraine", Kiev 22-27 June 1993. -Kiev. Bogolyubov Institute for Theoretical Physics. 1993- pp. 140-143.

# MATHEMATICAL MODEL OF QUASIOPTICAL COMMUNICATION CHANNELS WITH RESONANT CAVITIES

Vadim B. Kazansky, Valentina A. Gridina

Department of Radiophysics, Kharkov State University,  
4 Svobody Sqr., 310077 Kharkov, Ukraine.

## ABSTRACT

The matrix method of diffraction theory with discrete and integral scattering operator for a individual inhomogeneity is developed. Quasi-optical transmission lines, reentrant and one-entry resonators with resonant and wide-band coupling elements were investigated.

## INTRODUCTION

A resonant radiating module of phased array, transmission and load resonators and like [Fig.1-3] are modelled by the set of elementary heterogeneities. They consist of waveguide joint of differently dimensioned and a half-infinite flanged waveguide. From the rigorous solution of the diffraction problem for each individual heterogeneity a matrix or integral scattering operators have been found. Original scattering fields have been determined in the form of the Neuman operator series [1].

## THEORETICAL BASIS

To find the scattering operators of the half-- infinite

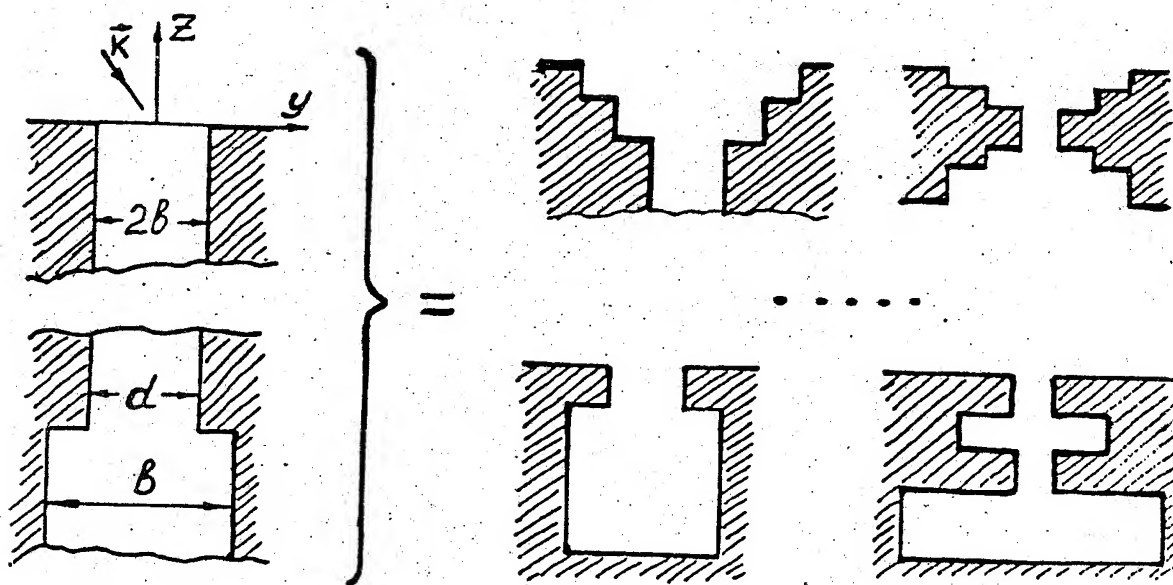


Fig.1

flat waveguide with infinite flanged waveguide [Fig.1] we must consider radiation and excitation problems. Since the structure is homogeneous in axis  $Ox$ , the scattering fields for H-polarized excited wave may be written in the form ( $H = \{\phi(y,z) \exp(-i\omega t), 0, 0\}$ ):

$$\phi = \begin{cases} e^{ik(\alpha y - \gamma z)} + e^{ik(\alpha y + \gamma z)} + \int_{-\infty}^{\infty} \alpha(\xi) e^{ik(\sqrt{1-\xi^2} z + \xi y)} d\xi, \\ \sum_{m=0}^{\infty} b_m e^{-iq_m z} \cos m\pi(y+b)/2b, \quad q_m = \sqrt{k^2 - (\pi m/b)^2} \end{cases}$$

Using the reexpansion technique and Neuman boundary conditions we can find the coupling between amplitudes of discrete spectrum of guided waves and Fourier components of scattering field:

$$\alpha(\xi) \sqrt{1-\xi^2} = \sum b_m D_m(\xi)$$

$$b_n = A_n + \int_{-\infty}^{\infty} L_n(\xi) \alpha(\xi) d\xi$$

If the structure is analyzed in the long wave range ( $\lambda \gg d$ ) then the last expressions are reduced to the integral equation for  $\alpha(\xi)$  which is more preferably solved by iteration technique. In resonance regime ( $\lambda \cong d$ ) the use of a system of linear algebraic equations of the second kind is more effective. The found scattering operator simultaneously with the scattering operators of differently dimensioned waveguides joint open a prospect for modelling and reseaching of complex shaped constructions.

## RESULTS AND DISCUSSION

Frequency characteristic ( $x = b/\lambda$ ) of the reflection coefficient of phased array's resonant radiating module is shown in Fig.2. For single wave regime ( $x < 1$ ) this characteristic has oscillate behaviour with a period which depends on flanged thickness ( $a_1$ ). When frequency increases the structure does not radiate practically for the basic harmonic of the electromagnetic field. In this range the character of scattering is determined by the fields of higher-order modes. The high -Q factor resonances with the phased inversion which is equal to  $\pi$  (cut off modes) have been found on the dependences of reflection coefficient as a function of resonator's length ( $ka$ ). It has been shown that under certain conditions 0-mode and the higher-order modes contribute equally to the total scattering field.

The approach developed in this work permits to study the scattering problems of electromagnetic waves by more complex constructions than ones which has been considered earlier. Here we present the frequency characteristics of transmission coefficient of the electromagnetic wave through the

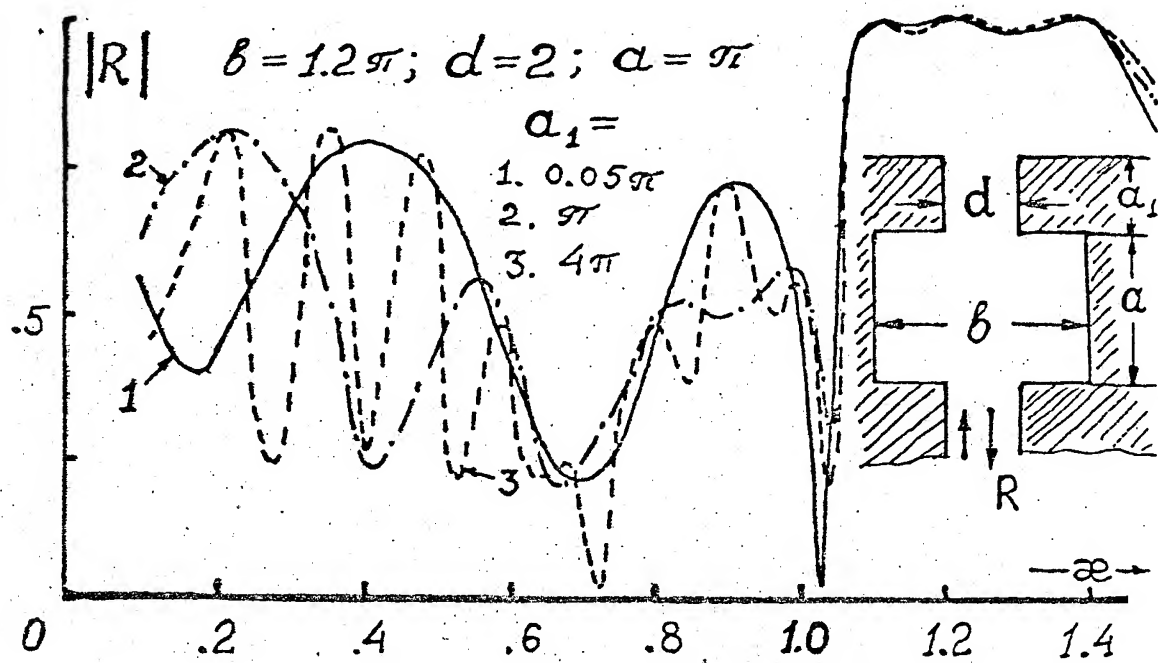


Fig. 2

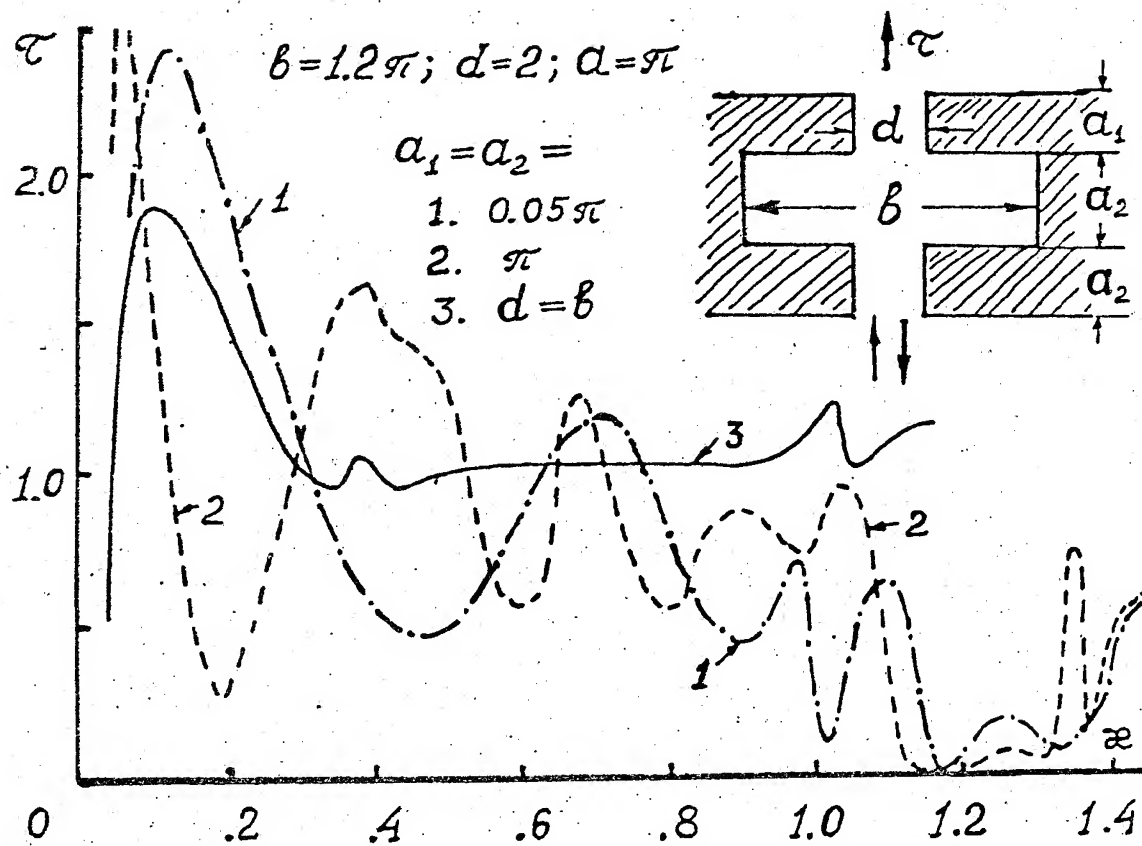


Fig. 3

profiled slit in a conducting thick screen. The transmission coefficient dependences as a function of frequency parameter  $x = b/\lambda$  are shown in Fig. 3.

Its comparison with the similar characteristic of the screen with the same thickness but with the regular slit ( $d=b$ ) proves the ability of substantial increase of maximal transmission level. Specially it should be noted the weak dependence of incident angle of electromagnetic wave. Such reradiating system may be used in constructions of electromagnetic screens. A number of resonances and their Q-factor are determined as by the length of resonant cavity ( $a$ ) and feed channels ( $a_1, a_2$ ) as by the level of their coupling ( $d/b$ ).

### CONCLUSIONS

Thus using the operator technique and knowing the scattering operators of basic elements permits to study electromagnetic characteristics of much more complex constructions modelling the well-known devices and new facilities of millimeter and quasioptic wave band.

### REFERENCES

1. R. Mittra and S. W. Lee. Analytical Techniques In The Theory Of Guided Waves. New-York - London, 1971.
2. Gridina V. A., Kazanskiy V. B. Electrodynamic characteristics of septate waveguide. // Izv. vuzov USSR. Radioelektronika -1981. -v. 24, N. 9, pp. 10-15.



# THE SIMPLIFIED REAL-FREQUENCY METHOD APPLIED TO THE LOW-NOISE AMPLIFIERS SYNTHESIS.

E.KERHERVE\*, P.JARRY\*, B.THERON\*\*, C.TRONCHE\*\*

\*Laboratoire de télécommunications-ENSERB-351, Cours de la libération 33405 Talence Cedex FRANCE.  
\*\*ALCATEL ESPACE-26, Avenue Champollion BP 1187, 31037 Toulouse Cedex FRANCE.

## INTRODUCTION

The microwave amplifiers are commonly used in the repeaters of telecommunication's satellites. Their creation remains yet empirical, particularly at the level of the interstage matching networks (equalizers). We present in this work the "simplified real-frequency method" which allow us the determination of the equalizers in a systematic and rigorous way. The published documents about this subject, have never taken a matter of interest by the industrialists as a major issue: taking into account the input and output polarization of the transistors; which corresponds to the effective realization of the amplifier. In this communication, we describe the modified method taking into consideration the polarization of transistors, and we present the circuit mask, result of a study which is the subject of an experimental realization in collaboration with ALCATEL ESPACE FRANCE.

## D DESCRIPTION OF THE METHOD

The efficacy of the "simplified real-frequency method" introduced by H.J. CARLIN and B.J. YARMAN [1] resides in its simplicity of use: no equivalent schema of transistors is necessary; it utilizes only, the measured of the scattering parameters [S] and the noise parameters of the FET devices, to work out in a recursive way the matching networks of a multistage amplifier for narrow bands as well as wide bands. Neither a priori knowledge of an equalizer topology is assumed. No approximation is made over the transistor, due their non-unilateral behaviour. The algorithm of J.J. MORE [2] based on a modified MARQUARDT routine for least-squares allows us to make the simultaneous optimization of the gain, the input and output VSWR, and the noise factor. The method based on the BELEVITCH's representation [3] of the equalizers assures it a systematic stability.

## II LOW-NOISE AMPLIFIER

This method allows in this case to synthetize the distributed elements of the matching quadripoles of the amplification chain made by up the transistors, their input and output polarization, and the equalizers (fig.1). In dynamic, the polarization (input, as well as output) permit us to carried out an open circuit at the level of the transistor's grid. The design with the [S] parameters of the transistor-polarizations block, give us the expression of the gain for the k stages of the amplifier:

$$G_{v_k} = G_{v_{k-1}} \frac{|e_{21_k}|^2 |S_{21_k}|^2}{|1 - e_{11_k}|^2 |1 - \hat{e}_{22_k} S_{11_k}|^2}$$

with  $G_{v_{k-1}}$  : available gain of the k-1 first stages,  
 $e_{ijk}$  : scattering parameters of the kth equalizer  $E_k$ ,  
 $\hat{e}_{22k}$  : reflection coefficient measured at the output of  $E_k$  to the left,  
 $S_{ijk}$  : scattering parameters of the kth whole transistor-polarisations.

The  $e_{ijk}$  paramaters represents themselves from the  $h(t)$  and  $g(t)$  polynomials relied by the relation of non-dissipativity of passive networks:

$$g(t) g(-t) = h(t) h(-t) + (1-t^2)^n$$

where n represents the number of distributed elements of the equalizer.  $h(t)$  then characterizes the equalizer thoroughly and is used as unknown at the time of the optimization.

<b>Specifications:</b>	Passband	5,925-6,425 GHz
	Gain	$\geq 29,5$ dB
	Noise Factor	$\leq 1,6$ dB
	Input VSWR	$\leq -10$ dB
	Output VSWR	$\leq -15$ dB

We give the performances (fig.2,3,4) of a low-noise 4-8 GHz amplifier. The parameters optimization is made between 5,925-6,425 GHz. Like these obtained results satisfy the specifications, we have decided to make the realization of this amplifier. The fig. 5 shows the one scale mask of this circuit. The fig. 6 represents an enlargement of this mask.



## REFERENCES

- [1] H.J. CARLIN-B.S. YARMAN. "A simplified real frequency technique applied to broadband multistage microwave amplifiers". IEEE Trans. on MTT, Vol MTT-30, n°12, dec 1982.
- [2] J.J. MORE. "The Levenberg-Marquardt algorithm: implementation and theory". Lecture notes in Mathematics 630, Springer Verlag, 1978.
- [3] V. BELEVITCH. "Elementary application of the scattering formalism to network design". IRE Trans. Circuit Theory, CT-Vol 3, June 1956.

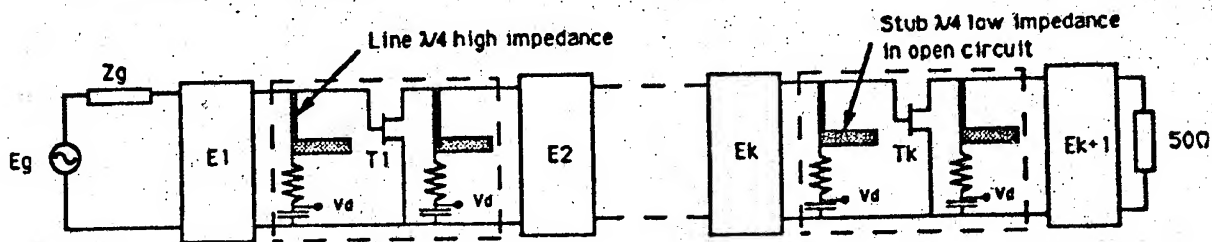


Fig. 1: Schema of the low-noise amplifier

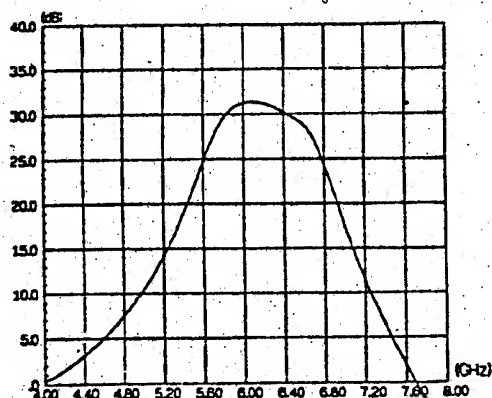


Fig. 2: Gain response

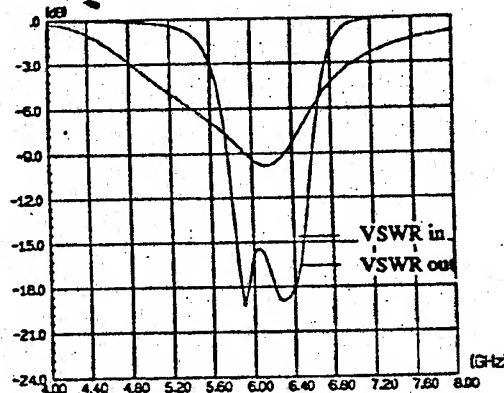


Fig. 3: VSWR responses

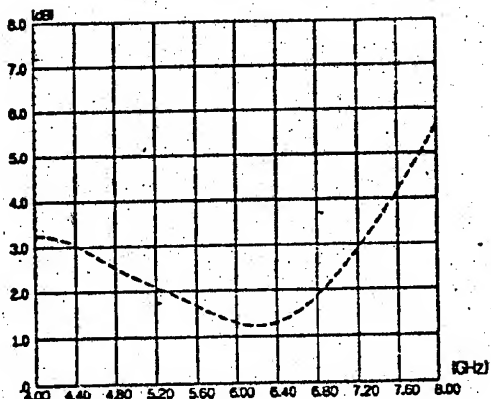


Fig. 4: Noise Factor response

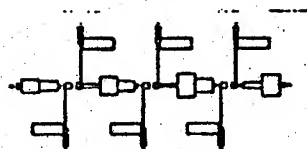


Fig. 5: One scale mask

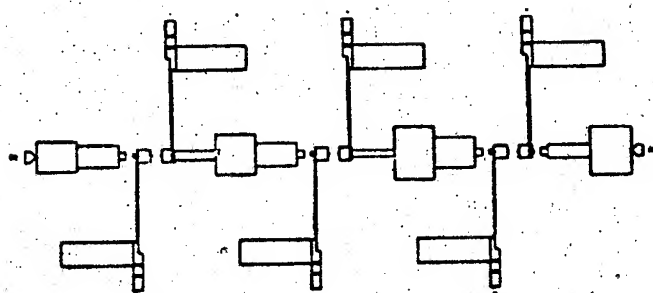


Fig. 6: Circuit mask with distributed elements

# METHOD OF VIRTUAL DECOMPOSITION FOR SOLUTION OF 3-D DIFFRACTION PROBLEMS

Kirilenko A.A., Vassilyeva T.I., Rud' L.A., Tkachenko V.I.

Institute of Radiophysics and Electronics  
of National Academy of Sciences of Ukraine  
12, Ac.Proskura st., Kharkov, 310085, Ukraine

## ABSTRACT

A method of virtual decomposition consisting in breaking a 3-D waveguide or grating component into a set of one-dimensional discontinuities by insertion of auxiliary virtual waveguides or gratings is proposed. This method is applied for scalarization of 3-D waveguide problems for structures with rectangular or round apertures, diaphragms, slots or coupling windows, to diffraction gratings with two-dimensional periodicity, to some noncoordinate problems. There exist problems which cannot be solved by other methods.

Many effective numerical-analytical techniques which have proved their advantages are available now, such as the modified residual technique [1] or the semi-inversion of the differential part of the matrix operator [2], but all of them almost without exception are used for solution of scalar two-dimensional diffraction problems. Whereas the solution of a vector waveguide problem mostly is obtained by direct numerical techniques. The technique discussed below permits to extend the field of numerical-analytical techniques application on a wide class of vector waveguide problems. The diffraction on any waveguide structure which can be virtually broke into appropriate separate elements representing a discontinuity only along one axis can be considered by this technique.

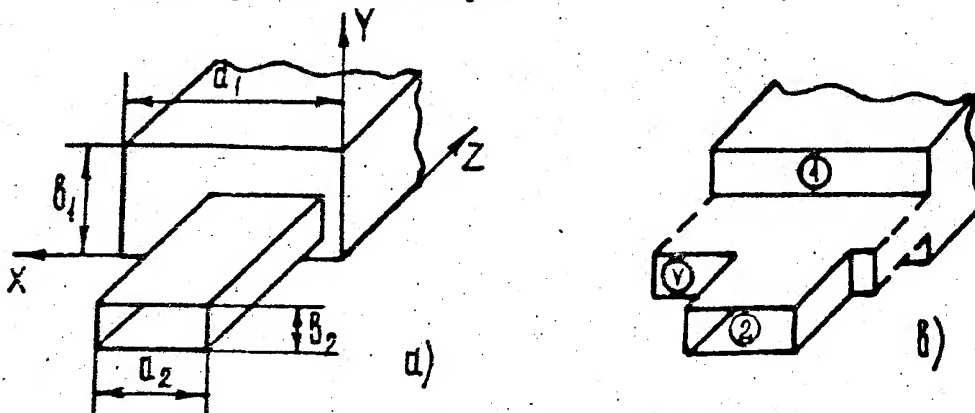


Fig.1. Vector waveguide junction.

The simplest example of the problem tractable by the proposed technique is the junction of two rectangular waveguides of different cross-sections which can be presented as a succession of two "scalar" E- and H-plane steps joined by a virtual waveguide of zero length ( Fig.1). A more complicated structure - rectangular slot in common wall of two waveguides ( Fig.2 ) - can be represented for instance as a junction of two tees each of

them in their turn is decomposed in "scalar" tee and step.

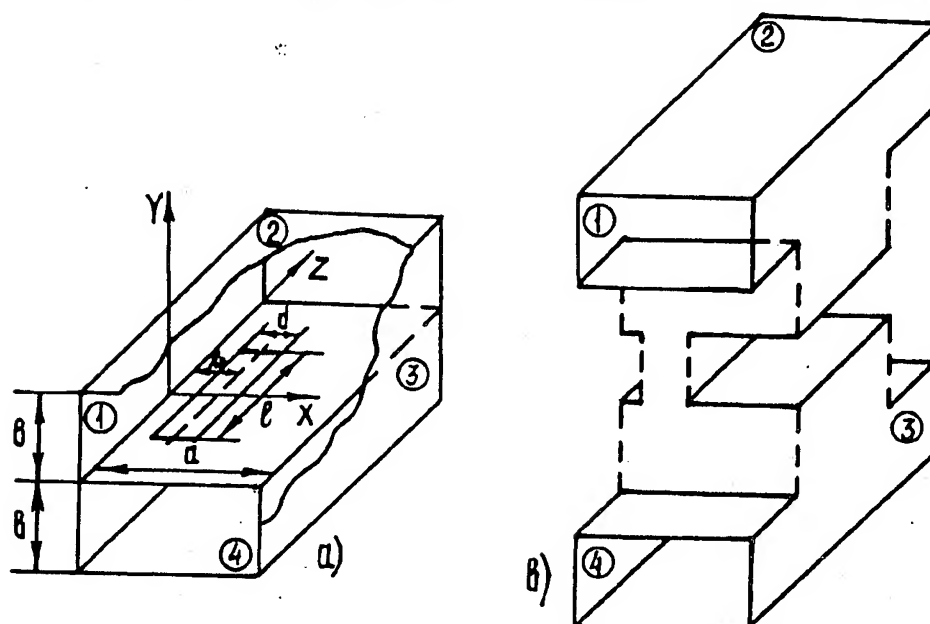


Fig.2. Rectangular slot in common wall of two waveguides

Let's consider the simplest case of the rectangular waveguides junction (Fig.1). We will present the fields in regular sections of the first, second and virtual waveguides as the superposition of lateral TE and TM-modes. Either using the step-by-step matching of the fields of the first and virtual waveguides and then of the virtual and second ones or applying immediately the generalized matrix method [1] to the component consisting of two "scalar" steps the scattering matrix of the two-step discontinuity S will be found.

$$S_{11} = S_{11}^{(1)} + S_{12}^{(1)} * S_{21}^{(1)} * S_{11}^{(2)} * (I - S_{22}^{(1)} * S_{11}^{(2)})^{-1},$$

$$S_{21} = S_{21}^{(1)} * S_{21}^{(2)} * (I - S_{22}^{(1)} * S_{11}^{(2)})^{-1},$$

where I is unit matrix,  $S_{11}$  and  $S_{21}$  are matrices of reflection and transition coefficients correspondingly of the two-step junction at the excitation from the first waveguide,  $S_{ij}^{(k)}$  ( $i, j, k=1, 2$ ) are the matrices of the reflection ( $i=j$ ) and transition ( $i \neq j$ ) coefficients of the k-th "scalar" junction at the excitation from the j-th arm.

Let's now consider the scattering matrices  $S^{(1)}$  and  $S^{(2)}$  in the basis of TE and TM-modes. It is very important that each of them is related with a component uniform along one of the axis. Then let's represent the incident lateral  $TE_{qp}$  or  $TM_{qp}$ -mode as the linear combination of longitudinal  $LE_{qp}$  and  $LM_{qp}$ -modes polarized along the x-axis which is the axis of uniformity for the first discontinuity and having the same indexes.

$$TE_{qp} = H_x^h * LE_{qp} + E_x^h * LM_{qp},$$

$$TM_{qp} = H_x^e * LE_{qp} + E_x^e * LM_{qp},$$

where  $H(E)_x^{h(e)}$  coefficient at x-component of the magnetic

(electric) field of the  $TE_{qp}$  ( $TM_{qp}$ )-mode.

Let's consider the diffraction of these partials.

Proceeding from the equivalence of the plate-plane and rectangular waveguides [3] the solution of the problem of the diffraction on the component uniform in the  $x$ -direction in a rectangular waveguide with width  $a$  for  $LE_{qp}$  - modes polarized along the  $x$ -axis can be obtained from the solution of this problem in the plate-plane region changing the wave number  $k$  on  $k'$

$$k'^2 = k^2 - (q\pi/a)^2$$

It is clear that this principle can be extended on the longitudinal magnetic modes as well as on the another polarization. It means that knowing the solution of the problem for plane step in E- and H-planes the scattering matrices of  $LE$ - and  $LM$ -modes polarized along  $x$ -axis on the junction of the first and virtual waveguides and polarized along  $y$  one on the junction of the virtual and second waveguides can be obtained.

So knowing how the longitudinal modes constituting incident lateral mode with indexes  $q$  and  $p$  were scattered and representing the diffract longitudinal modes with indexes  $m$  and  $n$  in their turn as a linear combination of lateral modes with the same indexes the element of the scattering matrix  $S_{mn,qp}^{(1)}$  will be

found. The scattering matrix for the second junction can be found from the decomposition of the lateral electromagnetic modes into longitudinal ones polarized along  $y$ -axis and vice versa.

As a result the substantially vector problem proved to be reduced to the determination of the scattering matrices of two "quasi vector" elements and to the system of linear algebraic equations whose operator is built of this scattering matrices. Each of those "quasi vector" problems of diffraction on the element uniform along one of the axis which are distinguished only by the number of field variation along the axis of uniformity in its turn can be broke into two "scalar" ones with boundary conditions of Neumann or Dirichlet type. And any suitable numerical-analytical techniques can be applied just to those "scalar" problems.

In this manner to obtain the scattering matrix of the considered vector structure accounting  $TE_{mn}$  and  $TM_{mn}$ -modes with  $0 < m < M$  and  $0 < n < N$  it is necessary for the first junction uniform along  $x$ -axis to solve the "scalar" diffraction problem with the Dirichlet boundary conditions  $N+1$  times to obtain matrix  $(M \times N)$  and to solve Neumann problem  $N$  times obtaining matrix with  $(M+1) \times (M+1)$  dimensions. And for the junction uniform along  $y$ -axis it is necessary  $M+1$  and  $M$  times to solve corresponding problems for obtaining "scalar" matrices of the dimensions  $N \times N$  and  $(N+1) \times (N+1)$  correspondingly.

The accuracy of the vector problem solution as well as the cpu time depend on the accuracy of the "scalar" problems solutions as well as on the number of the modes accounted in the virtual waveguide. Comparing the cpu time for the scattering matrix of the two-step junction by direct numerical technique and by the virtual decomposition one it can be stated that they are close if the "scalar" problems are as well solved by the direct moment technique as the solution procedure is reduced to the equivalent matrix manipulations and the numbers of division and multiplication operations are the same. The essential difference

take place when an effective technique of "scalar" problem solution requiring opu time a few tens times lesser is used. The total opu time turned to be 5-7 times lesser. It is necessary to note that the solutions based on the special basis taking into account edge condition permit to separate a frequency independent part and it reduce the opu time of frequency characteristics of the component by a factor of 2-3. It is especially important at the frequency-selective device synthesis.

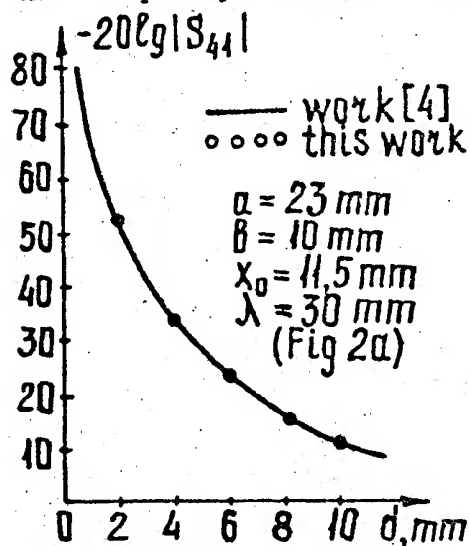


Fig.3. The  $S_{41}$  - dependence of  $d$  for rectangular window in common wall of two waveguides.

The advantage of the proposed approach consists in the extending of the field of application of the numerical-analytical techniques on the wide class of vector diffraction problems. Its merits are cyclicity, possibility to work with the low dimensional matrices. Thanks to effective numerical techniques the opu time decreases substantially as well as in the cases when only one dimension or only frequency is changed and only corresponding part of the algorithm must be repeated.

The comparison of the results of the work [4] and ones obtained by this technique for the calculations of the asymmetrical rectangular slot in the common wide wall of two waveguides is presented on the Fig.3. The good coincidence of the results proves the accuracy of the proposed technique.

#### REFERENCES

- [1] Mittra R. and Lee S.W., "Analytical technique in the theory of guided waves", New York: The Macmillan company, 1971.
- [2] Shestopalov V.P., Kirilenko A.A., Masalov S.A., "matrix equations with a difference type operator in diffraction theory", Kiev: Naukova dumka, 1984.
- [3] Levin L., "Theory of waveguides", London: Newnes-Butterworths, 1975.
- [4] Garb Kh.L., Meyerova R.S., Pochikayev G.V., Fridberg P.Sh., "Diffraction of the H<sub>10</sub>-mode on the rectangular aperture in the common wall of two rectangular waveguides", Radiotekhnika i elektronika", v.34, pp. 1150-1157, June 1989.

# INTERACTION OF THE MODES IN QUASI-OPTICAL RESONATORS

A. I. Kleev and A. B. Manenkov

P.Kapitza Institute for Physical Problems, Russian Academy of Sciences

Kosygina 2, Moscow, 117334, Russia

Fax: 7(095) 938 2030, E-mail: kleev@magnit.msk.ru

**Abstract** — The modes coupling in the quasi-optical resonators is studied. The analysis is made numerically by the Galerkin technique. The effects of different factors (for example, the screens and mirror aberrations) on the coupling are examined.

## Introduction

Using the quasi-optical resonators (QORs) one frequently is faced with the instabilities of the mode structure [1-3]. These effects result from different reasons, for example, because of the resonator surface deformations, which destroy the caustics or couple the modes. In many papers unstable geometries of the QORs (for example, the resonators with different curvature radii of the mirrors) have been examined by the theory of the geometrical optics. In practice, the instabilities, which destroy the caustics, are dominant, but in some cases they can be excluded. There are only partial studies of the problem of the modes coupling in the QORs. For example, the effects of the mirrors aberrations (or other deformations of the cavity) on the coupling are practically not examined for the QORs.

In the present paper the numerical analysis of the modes coupling in two dimensional QORs near degeneration points is made. The waveguide and open QORs are investigated (Fig. 1). We treat the systems, which are stable from the viewpoint of the geometrical optics.

### 1. The modes coupling in the waveguide QOR

Consider the modes of the closed (screen) QOR, shown schematically in Fig. 1,a. Assume, that the left and right mirrors are identical, and both perturbed and unperturbed resonators are symmetrical about the plane  $XZ$ . Later on we shall examine the even modes with the single magnetic field component  $H_z$  ( $H_y = H_x = 0$ ). We shall denote these modes as  $E_{jq}$ . All dimensions of the QOR are assumed to be greater than the light wavelength  $\lambda$ . Below we omit the time factor  $\exp(-i\omega\tau)$ , where  $\omega = kv_z$  is the frequency,  $k = 2\pi/\lambda$  is the wavenumber,  $v_z$  is the light velocity. In this section we suppose, that the mirrors are parabolic and their curvature radius for  $y=0$  is equal to  $R$ .

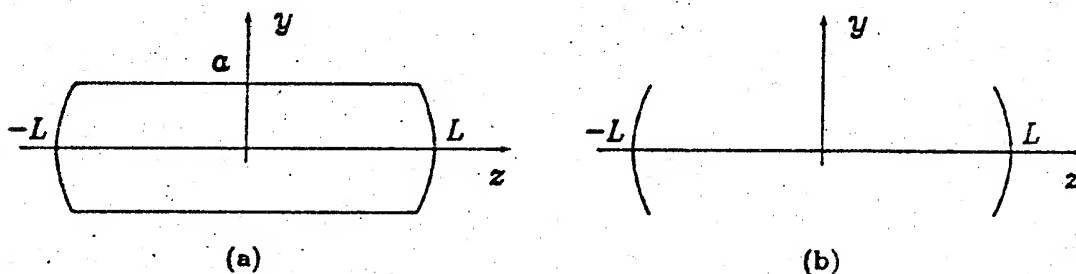


Fig. 1 The geometries of the QORs

All the fields components of the mode are expressed in terms of the transverse electric field component

$$E_y = \Phi(y, z) - (-1)^q \Phi(y, -z). \quad (1)$$

The impedance boundary conditions on the walls of the waveguide ( $z = \pm a$ ) and on the mirrors are satisfied. The function  $\Phi$  is expanded in the series of the waveguide modes [4]

$$\Phi(y, z) = i \sum_n A_n h_n \cos(v_n y) \exp(i h_n z), \quad h_n^2 = k^2 - v_n^2. \quad (2)$$

All the terms of the above series obey the wave equation. The transverse wavenumbers  $v_n$  are defined by the boundary conditions on the plates  $z = \pm a$ . Assuming  $a/L = \gamma \ll 1$  and using the standard quasi-optics approximations, we can derive the integral equation

$$\Gamma f(t) = \int_{-1}^1 K^{(w)}(t, t_1) f(t_1) dt_1, \quad f(t) = \sum_n A_n \cos(\beta_n t) \exp\left(i \frac{\beta_n^2}{4c} + i c \varphi(t)\right), \quad (3)$$

$$K^{(w)}(t, t_1) = \exp[-i c (\varphi(t) + \varphi(t_1))] G^{(w)}(t, t_1, 1, -1), \quad (4)$$

$$G^{(w)}(t, t_1, \theta, \theta_1) = \sum_{n=1}^{\infty} \frac{1}{p_n} \exp\left(-i \frac{\beta_n^2 (\theta - \theta_1)}{4c}\right) \cos(\beta_n t_1) \cos(\beta_n t), \quad p_n = \int_{-1}^1 \cos^2(\beta_n t) dt, \quad (5)$$

$$c = k a^2 / 2L, \quad \beta_n = v_n a, \quad t = y/a, \quad g = 1 - 2L/R, \quad \Gamma = (-1)^g \exp(-2ikL). \quad (6)$$

Here  $G^{(w)}$  is the Green function of the waveguide, obtained by the approximation of parabolic equation [3, 4],  $\varphi(t)$  is the function, defining the mirrors surfaces. Deriving this equation we omit all the terms of the order  $\gamma^2$ . Using the Galerkin technique transforms the above equation to the eigenvalue one

$$SC = \Gamma C, \quad (7)$$

where  $S$  is a matrix,  $C$  is the column matrix. The elements of the  $C$  are proportional to the expansion coefficients  $A_n$  of the function  $\Phi$ .

The guide Green function  $G^{(w)}$  may be divided into two terms:

$$G^{(w)}(t, t_1, \theta, \theta_1) = G^{(*)}(t, t_1, \theta, \theta_1) + G^{(p)}(t, t_1, \theta, \theta_1), \quad |t|, |t_1| \leq 1, \quad (8)$$

where

$$G^{(*)}(t, t_1, \theta, \theta_1) = \frac{1}{2} \sqrt{\frac{\tilde{c}}{\pi i}} \left\{ \exp[i\tilde{c}(t - t_1)^2] + \exp[i\tilde{c}(t + t_1)^2] \right\}, \quad \tilde{c} = \frac{c}{(\theta - \theta_1)}, \quad (9)$$

is the Green function of the free space,  $G^{(p)}$  is an additional term, which describes the influence of the guide walls on the mode fields. Under condition  $c \gg 1$  the last term is small, i.e. the walls slightly perturb the fields and in the QOR the waves transmit from one mirror to other practically as in the free space. Using the above separation of the function  $G^{(w)}$  leads to the following division of the kernel of the integral equation:  $K^{(w)} = K^{(*)} + K^{(p)}$ , where  $|K^{(p)}| \ll |K^{(*)}|$ ; therefore we can consider the plates as the small perturbation factor. The perturbations may appreciably change the features of the modes in the degeneration points of the frequencies. Later on we shall treat the case, when the modes  $E_{0q}$  and  $E_{2q}$  have close frequencies. Applying the perturbation technique we derive the approximation equation for the eigenvalues  $\Gamma$  of two coupling modes

$$\Theta^2 - \Omega^2 = \Upsilon^2, \quad \Theta = \left[ \ln \Gamma - \frac{i}{2} (\Theta_0 + \Theta_2) \right], \quad \Omega = \frac{i}{2} (\Theta_0 - \Theta_2), \quad (10)$$

where  $\tilde{\Gamma}_j = \exp(i\Theta_j)$  is the perturbed eigenvalues ( $j = 0, 2$ ), calculated without the coupling, and  $\Upsilon$  is the coupling coefficient:

$$\Gamma = (\tilde{\Gamma}_0 \tilde{\Gamma}_2)^{-1/2} \int_{-1}^1 \int_{-1}^1 f_0(t) f_2(t_1) K^{(p)}(t, t_1) dt_1 dt. \quad (11)$$

It describes the effects of the guide walls on the modes.

The features of the solutions of the coupling mode equation are defined by the relation between the parameters  $\Omega$  and  $\Gamma$ . The estimations demonstrate, that in practice the decrements of the coupling modes are far from each other, i.e.  $|\text{Im}(k_0 - k_2)|L \gg |\Gamma|$ . In this case the modes coupling is small and near degeneration points ( $\text{Re } k_{0q} = \text{Re } k_{0q'}$ ) the field distribution of the interaction modes is changed slightly. But in such points the decrement of the dominant mode  $E_{0q}$  can be appreciably decreased.

Considering the mode losses, we shall use the auxiliary parameter  $\Lambda = -20 \lg |\Gamma|$ . Fig. 2 presents the parameter  $\Lambda$  of the mode  $E_{0q}$  versus the  $g$  for different values of the parameter  $c$ . The impedance parameter  $ka\zeta'$  is assumed to be equal to 2 ( $\zeta = (1 - i)\zeta'$  is the wall impedance). For simplicity we suppose, that the mirrors are ideally conductive. It is known [3], that for the QOR, in which we can neglect the intermodal coupling, the losses parameter  $\Lambda$  is minimal near the point  $g = 0$ . The calculation shows, that near this point the losses can considerably increase. This effect is explained by the coupling of the

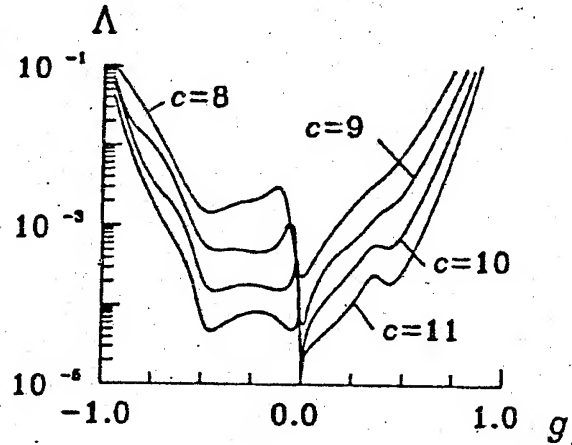


Fig. 2 The losses parameter  $\Lambda$  versus the  $g$

modes, which have close frequencies. In turn the coupling is the result of the influence of the waveguide on the modes. For the values  $c \sim 10 \div 20$  only the two lower order modes are coupled: the losses of higher order modes are large (i.e. their complex frequencies are very different) and these modes practically do not influence the mode  $E_{0q}$ .

In the QOR under study the losses of the dominant mode  $E_{0q}$  are the smallest since the mode has the caustic and its fields on the walls are small. The coupling between the modes  $E_{0q}$  and  $E_{2q'}$  results in the increase of the dominant mode losses (see Fig. 2). When the parameter  $c$  decreases, the intermodal coupling increases (see eqn. 11). In this case the interval of the parameter  $g$ , in which the losses are abruptly changed, becomes smaller.

## 2. Intermodal coupling in the open QOR

The modes of the open QOR (Fig. 1,b) are defined by the integral equation of the same type as eqn. 3 with the kernel  $K^{(o)}(t, t_1)$ . The kernel  $K^{(o)}(t, t_1)$  is expressed through the Green function  $G^{(s)}(t, t_1)$  and the function, which defines the mirrors form. The expression for the  $K^{(o)}(t, t_1)$  can be derived, if we expand the  $G^{(s)}(t, t_1)$  in terms of the Fourier series:

$$G^{(s)}(t, t_1) = \sum_{m,n} \tilde{G}_{m,n}^{(s)} \cos(\beta_n t) \cos(\beta_m t_1), \quad \tilde{G}_{m,n}^{(s)} = G_{m,n}^{(p)}, \quad m \neq n, \quad \tilde{G}_{n,n}^{(s)} = \frac{1}{p_n} \exp\left(-i \frac{\beta_n^2}{4\epsilon}\right) - G_{n,n}^{(p)}. \quad (12)$$



In the expansion (12) the values of  $\beta_n$  should be chosen so that the functions system  $\{\cos(\beta_n t)\}$  become complete and orthogonal on the interval  $(-1, 1)$ . Using the Galerkin technique (with the same basis and test functions) results in the algebraic eigenvalue problem (cf. eqn. 7), which can be numerically solved.

To illustrate the effects of the intermodal coupling in the open QOR, we consider the influence of mirrors deformations on the mode losses. We suppose, that the mirrors surface is determined by the function  $\psi(y) = y^2/2R + \xi y^4/4a^2L$ . Assuming  $|\xi| \ll 1$  we can approximately solve the integral

equation by the perturbation method, separating the small term  $K^{(1)}(t, t_1)$  from the kernel  $K^{(0)}(t, t_1)$ . It is associated with the second term of the function  $\psi(y)$  and is proportional to the small parameter  $\xi$ . The equation derived is similar to eqns. 10-11, where  $\Upsilon \propto \xi$ .

Fig. 3 shows the dominant mode losses versus the parameter  $g$ . The curves are constructed for different values of the  $c$ . Note, that near the point  $g = 0$  the two effects define the losses of the mode  $E_{0q}$ . First, the losses decrease, since the size of the caustic increases [3]. Second, the losses increase because of the coupling of the mode  $E_{0q}$  with the mode  $E_{2q}$  (and others). The calculations show, that the coupling is generally small, therefore the field structure of the mode  $E_{0q}$  is practically not changed, but the losses of the dominant mode can be considerably increased due to this effect.

### Conclusion

The results presented above demonstrate that the losses in the QORs play an important role for the intermodal coupling analysis. The losses can significantly separate the complex frequencies of the modes interacting. For the typical parameters of the QORs the coupling is usually small, since the difference between the decrements of the modes interacting is considerably larger, than the coupling coefficient. The calculations have shown, that in this case the coupling can appreciably change only the losses of the dominant mode. The fields structure of the mode is practically not changed.

### References

- (1) S. F. Dyubko, V. V. Kamyshan, V. P. Sheiko: "On the Instability of the Confocal Systems", Zh. Tekh. Fiz. (1965) 35, 10, pp. 1806-1816 (in Russian).
- (2) R. L. Sanderson, W. Streifer: "Unstable Laser Resonator Modes", Appl. Opt. (1969) 8, 10, pp. 2129-2136.
- (3) L. A. Weinstein: "Open Resonators and Open Waveguides". Boulder, Colorado: Golem Press, 1969.
- (4) A. I. Kleev: "Ohmic Losses in Shielded Quasioptical Resonator", Journal of Communications Technology & Electronics, (1993) 38, 3, pp. 119-124.

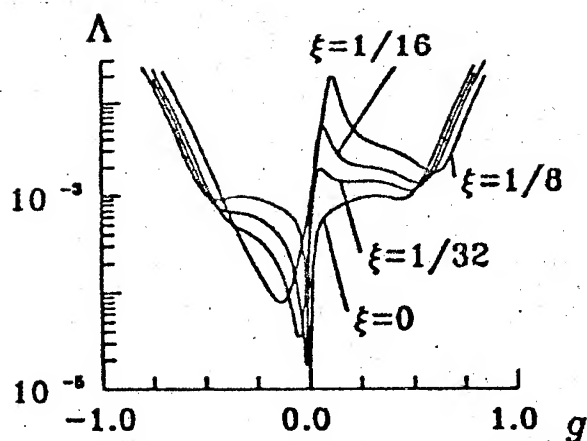


Fig. 2 The losses parameter  $\Lambda$  versus the  $g$

# Analysis of Electromagnetic Wave Scattering by Complex Screens with Edges in a Cases of Plane and Axial Symmetry

Valery N. Kochin, Sergey L. Prosvirnin and Tatyana D. Vasilieva

*Institute of Radio Astronomy,  
#4, Krasnosnamennaya str., Kharkov 310002 Ukraine,  
Tel.:(0572)44-8596, Fax:(0572)47-6506,  
E-mail: rai@ira.kharkov.ua@relay.usar.eu.net*

## Abstract

Analysis of electromagnetic wave scattering by polygonal cylindrical screens with closed and open cross-section contour and wave scattering by axially symmetrical screen consisting of joined cylinders and disks is carried out on the base of the spectral method with the partial operator inversion. There are mathematical ground of the spectral method using and the numerical results of investigation of electromagnetic wave radiation and scattering.

## INTRODUCTION

The purpose of this work consist in a rigorous theoretical investigation of important problems of electromagnetic wave scattering by composite closed or open perfectly conducting screens with edges in the cases of plane and axial symmetry carried out on the base of the analytical-numerical method. The main problems are wave scattering by polygonal cylindrical screens with closed and open cross-section contour and wave scattering by axially symmetrical screen consisting of joined cylinders and disks. A peculiarity of this problems of wave diffraction is in different degree of transverse field components increasing near the different edges of the screen and a strong interaction of a adjacent elements of a screen.

## SPECTRAL METHOD FOR THE SOLUTION OF THE BOUNDARY VALUE PROBLEM

Let us consider the 2-D problem of a TM wave  $U^i$  diffraction by a metal screen with a smooth piecewise cross-section countor  $L = \cup_{j=1}^N L_j$ ,  $N$  is the number of its faces. The total field may be represented in the form

$$U = U^i + U^s.$$

The scattered field  $U^s$  may be expressed in terms of potentials of the double layer

$$U^s = \sum_{j=1}^N \int_{L_j} \mu_j(s_j) \frac{\partial G}{\partial n_j} ds_j,$$

$G$  is the Green function,  $s_j$  is coordinate along  $L_j$  in the local system of coordinate which connected with the face number  $j$ . The transformation  $u = f_j(s_j)$  is used on an every face in such way that  $s_j \in L_j$  corresponds to  $u \in [-1, 1]$ . As a complete system of expansion functions in the space  $C[-1, 1]$  one may take the functions  $1, u, \sqrt{1-u^2}U_n(u), n = 0, 1, 2, \dots$ , where  $U_n(u)$  are the Chebyshev polynomials of the second kind. We represent the potential density in the form

$$\mu_j(u) = \nu_{j-1}(1-u) + \nu_j(1+u) + \sqrt{1-u^2} \sum_{n=0}^{\infty} C_n^j U_n(u), \quad \nu_0 = \nu_N, \quad j = 1, 2, \dots, N.$$

If any faces  $j$  and  $j+1$  are unconnected, it leads to  $\nu_j = 0$ . It is  $\nu_0 = \nu_N = 0$  if the faces 1 and  $N$  are unconnected. It follows from the condition which ensures the field energy to be finite in any bounded region including the vicinities of the edges that  $C^j \in l_2 = \{ \{C_n^j\}_0^\infty | \sum_{n=0}^{\infty} |C_n^j|^2 (n+1) < \infty \}$ .

As the normal derivative has no sense on a screen edges, one should require a boundary condition as following. Let  $q$  be an arbitrary function which is continuous in all space and on  $L$ . We take a curve  $\bar{L}$  with continuous curvature near a corner points of  $L$  and formulate the problem to find  $U^*$  for which

$$\int_L q \frac{\partial U^*}{\partial n} ds = - \sum_{j=1}^N \int_{L_j} q(s_j) \frac{\partial U^j}{\partial n_j} ds_j$$

is satisfied for any of functions  $q$  when  $\bar{L}$  tends to  $L$ . The requirement of the boundary condition to be satisfied (when functions  $q$  on  $L$  are chosen as the basis elements in the space of continuous functions) reduces the procedure to using of the projection method. Let us take the system described above as the system of testing functions in  $C[-1, 1]$ . As a result we obtain  $N$  infinite connected systems of linear algebraic equations in  $\nu_j$  and  $C_n^j$ .

The operator of the each infinite system of equations consists of two parts [1], [2]. The first describes the diffraction by one of the faces of the screen and the other parts describe the interaction with all rest faces. Dynamic parts of operators (being equal to zero when  $\omega = 0$ ) and static parts (being non-equal to zero when  $\omega = 0$ ) of interaction operators of non-connected faces is entirely continuous in  $l_2$ . A static part of the operator being relevant to the one face of the screen can be inverted easily. The analytical inversion of this part of the operator becomes possible by choosing Chebyshev polynomials as the elements of the basis. Rest static parts of operators are closed operators [1]. Therefore as it can be show the infinite system of linear equations is correctly solvable thus a numerical solution of it is stable for any real values of frequency if the screen is open. If the screen is closed the system of equations has a stable solution for any real frequency with the exception of own frequencies of the internal region of the screen.

The problems of radiation and scattering of electromagnetic waves by structures with axial symmetry consisting of jointed metal circle cylinders segments with one or two closed butt-ends, circle cylinders segments with co-axial disk of equal or greater diameter are reduced to the integral equation for a surface current density and analysed by the same method.

As an expansion functions for a surface current density on the cylinder segment the Chebyshev polynomials of the second kind and for a current density on the disk the Legendre associated functions  $P_n^{(1)}(\sqrt{1-p^2})$  are used.

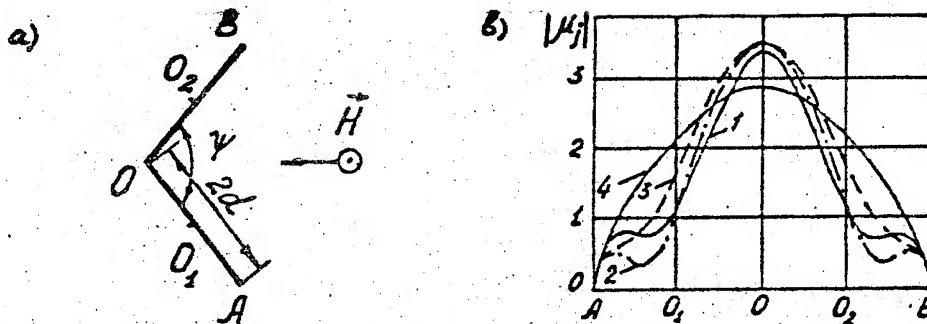


Figure 1: a) Corner screen geometry; b) Surface current density distribution:  $2d/\lambda = 0.5$ ; 1-  $\psi = 60^\circ$ , 2-  $\psi = 90^\circ$ , 3-  $\psi = 150^\circ$ , 4-  $\psi = 180^\circ$ .

### NUMERICAL RESULTS

The method was applied for 2-D problems analysis of the plane wave diffraction and the model of dipol radiation scattering by corner screen [2], rectangular and  $\Gamma$ -type projection on a metal plane. Algorithms are used for the investigation of the influence of metal screens of this type on the radiation of short dipol antennas. The mathematical model of a monopole with a disk on its top was investigated [3].

Fig. 1 shows the distribution of surface current density on the corner screen. The method allows one to find the solution of the problem at an arbitrary value of angle  $\psi$ , in particular, for  $\psi = \pi$ , when the corner screen transforms into a strip with a width of  $4d$ . The results of the computation of the surface current density for the strip obtained by the present method coincide with earlier results in [4] obtained independently and with an exact solution.

Fig. 2 presents the frequency dependence of the effective scattering cross-section of the corner screen which has a resonance behavior. Resonances occurs when odd number of half-waves are present along the screen cross-section. The dotted straight lines indicate the values of the scattering cross-section at  $\lambda \rightarrow 0$ . From geometrical optics, it follows that  $\sigma_{\lambda \rightarrow 0} = 8d \sin(\psi/2)$ . The computation results show that to get a value of  $\sigma/2d$  to an accuracy of two true decimal places, it is necessary to take the number of equations in the reduced system equal to integer part of  $kd$  plus three.

Frequency dependence of the scattering coefficient of the 2-D dipol radiation by  $\Gamma$ -type projection on a metal plane is shown in Fig. 3.

The mathematical model of a short monopole with a disk on its top was investigated. Fig. 4 shows the frequency dependence of the input impedance imaginary part of a short monopole with the load.

### REFERENCES

- [1] T.D.Vasilieva, L.N.Litvinenko, and S.L.Prosvirnin, "Wave diffraction by a two-dimensional corner screen", *Dokl. Akad. Nauk USSR, ser. A*, no. 6, pp. 58-62, 1990.
- [2] T.D.Vasilieva, L.N.Litvinenko, and S.L.Prosvirnin, "The diffraction of  $H$ -polarized electromagnetic waves by a two-dimensional corner screen", *IEEE Trans. Antennas Propagat.*, vol. 42, no. 4, April 1994.
- [3] A.A.Gridin, V.N.Kochin, Yu.B.Nechasov, and S.L.Prosvirnin, "Characteristics of a short monopole with a disk on its top", *Radiotekhnika i Elektronika*, vol. 38, no. 9, 1994.
- [4] L.N.Litvinenko and S.L.Prosvirnin, "Spectral scattering operators in problems of wave diffraction by plane screens", Kiev, Naukova Dumka, 240 p., 1984.

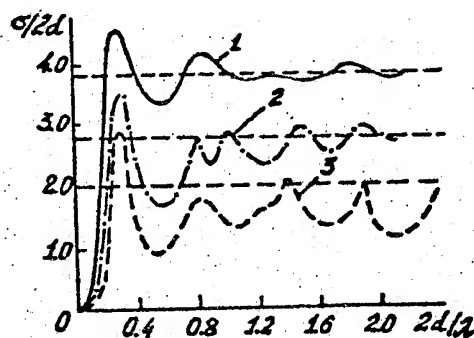


Figure 2: Normalized effective scattering cross-section versus frequency; 1-  $\psi = 150^\circ$ , 2-  $\psi = 90^\circ$ , 3-  $\psi = 60^\circ$ .

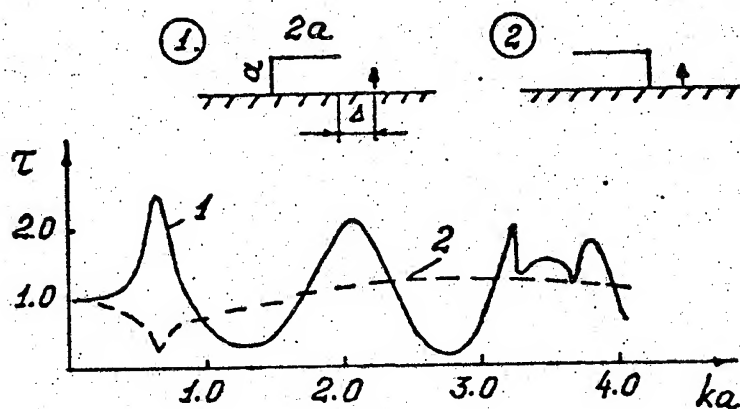


Figure 3: Frequency dependence of the scattering coefficient;  $k\Delta = 1.0$ .

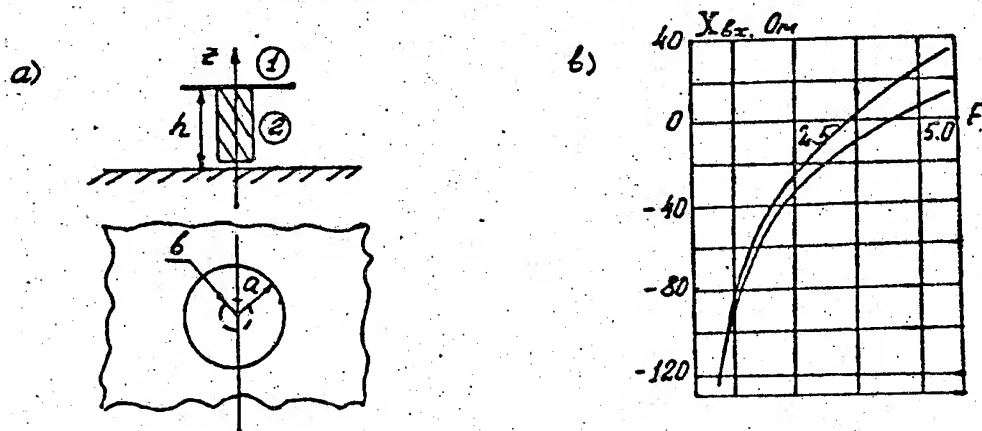


Figure 4: a) Short monopole with disk; b) Imaginary part of the input impedance versus  $F = 100h/\lambda$ :  $a/h = 3.0$ , 1-  $b/h = 0.2$ , 2-  $b/h = 0.52$ .

# MODES IN MULTICORE OPTICAL FIBRE STRUCTURES.

Yury V. Kolesnichenko

Institute of Radioengineering and Electronics  
Russian Academy of Sciences

Mokhovaya str.11, Moscow, 103907, Russia

A scalar shift-formula method is developed for optical fibres with several nonidentical circle homogeneous cores. Numerical calculations of dispersion curves were made for different cases. The our numerical results are obtained to be close to these of approximate method for identical core case. For a nonidentical core case at first synchronism conditions of noncoupled cores are found and after that dispersion dependencies are calculated for different distances between the cores.

## INTRODUCTION

We studied structural and dispersion properties of guided waves (modes) in optical fibre with several identical (first case) and nonidentical (second case) circle homogeneous cores. For the above structures we develop the shift-formula method [1] which was applied earlier in our works to noncircular optical waveguides [2,3] and in the beginning of the study to coupled optical fibres [4]. By using this method we obtained exact numerical solutions for the modal parameters and their dependencies on the frequency and waveguide parameters. For the first case our results compare with results of other works. For the second case we look for condition of synchronism, i.e. equality of separated core propagation constants. After that we calculate dispersion dependencies for different distances between the cores.

## 1. SYNCHRONISM

Multicore optical fibres are of interest now because of these new application possibilities in switchers and multichannel lines. Special interest is present region of synchronism, i.e. parameters region with equal propagation constants  $h$  of fundamental modes in separated cores. In this region it is able maximum power transfer between cores. This region occupy all frequency axis for most investigated identical core case. Synchronism for case of nonidentical cores takes place only on some fixed frequency points and if some proportions exist between dielectric permittivities and sizes of core. Fig.1 show ones for two circle homogeneous cores with  $R_1$  and  $R_2$  radii and dielectric permittivities  $\epsilon_1$  and  $\epsilon_2$ . Cores have common cladding with dielectric permittivity  $\epsilon_0$ . Here and below we use next values:  $\Delta_i = (\epsilon_i - \epsilon_0) / 2\epsilon_0$ ,  $i=1,2,\dots$ ,  $V = R_1(\epsilon_1 - \epsilon_0)^{1/2} \omega/c$ , where  $\omega$  - angular frequency,  $c$  - light velocity.

Fig.3 demonstrate possibility of three frequency point synchronism in three nonidentical core waveguide. There are phase parameter ( $B = \alpha^2 R_1^2 / V^2$ ) dependencies on normalized frequency  $V$ , where  $\alpha$  - transverse wave number. In principle here it is possible channel transfer between three channels on three different frequencies.

## 2. CALCULATION BY SHIFT-FORMULA METHOD

For above structure analysis it is convenient the shift-formula method [1-4]. Here one used for exact numerical calculations of dispersion curves in case of finite distance between cores. Identical core case results were used for comparison with results obtained by approximate method (see [5]). Dispersion curves for case of finite distance between nonidentical cores is shown on Fig.3. Here we used value  $p = (R_1 + R_2)/d$ , where  $d$  is distance between core centers.  $p=1$  means that the cores are touching. We mark that curves for  $p < 0.5$  practically merge with ones for  $p=0$  ( $p=0$  case correspond to dashed curves in Fig.3). The shift-formula method allowed to observe degeneration taking off as distance decreased.

The research described in this publication was made possible in part by Grant N MMB000 from the International Science Foundation.

## REFERENCES

- (1) V.V.Shevchenko : "Shift-formula methods in the theory of dielectric waveguides and fiber lightguides (review)". Radiotekhnika i Elektronika, (1986) 31, 5, pp.849-864 (Engl. transl. in: Sov.J. of Communications Technology and Electronics, (1986) 31, 9, pp.28-42).
- (2) Yu.V.Kolesnichenko, V.V.Shevchenko : "Fibre-optic dielectric waveguides with a noncircular core". Radiotekhnika i Elektronika, (1988) 33, 7, pp.1399-1409 (Engl. transl. in: Sov. Journal of Communication Technology and Electronics, (1988) 33, 11, pp.127-136).
- (3) Yu.V.Kolesnichenko, V.V.Shevchenko : "Dispersion and polarization characteristics of modes in fiber lightguides with noncircular cores". Radiotekhnika, (1988) 8, pp.78-84 (Engl. transl. in: Telecommunications and Radio Engineering, (1988) 43, 9, pp.116-124).
- (4) Yu.V.Kolesnichenko : "Optical fibres with two noncircular cores". Radiotekhnika, (1989) N8, pp.79-80 (Engl. transl. in Telecommunications and Radio Engineering, (1989) 44, 9, pp.109-111).
- (5) V.V.Shevchenko, A.D. Skaballanovich : "Modes of double core optical fibre with nonidentical cores", this issue (1994).



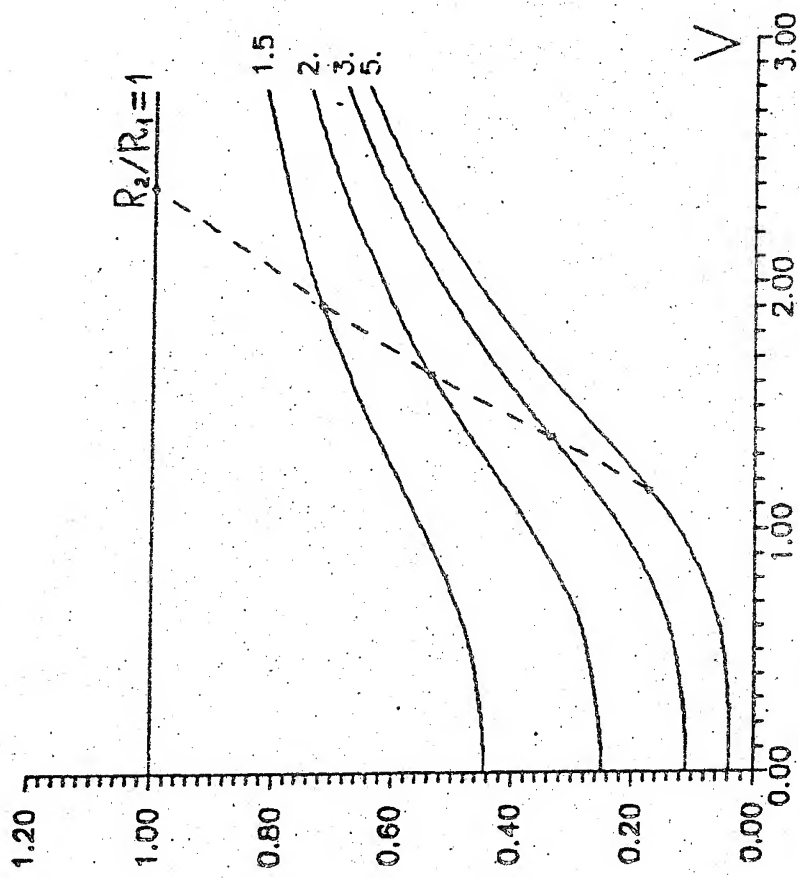


Fig.1. Dependencies ensuring synchronism of two nonidentical noncoupled cores. Dashed curve is two mode regime boundary.

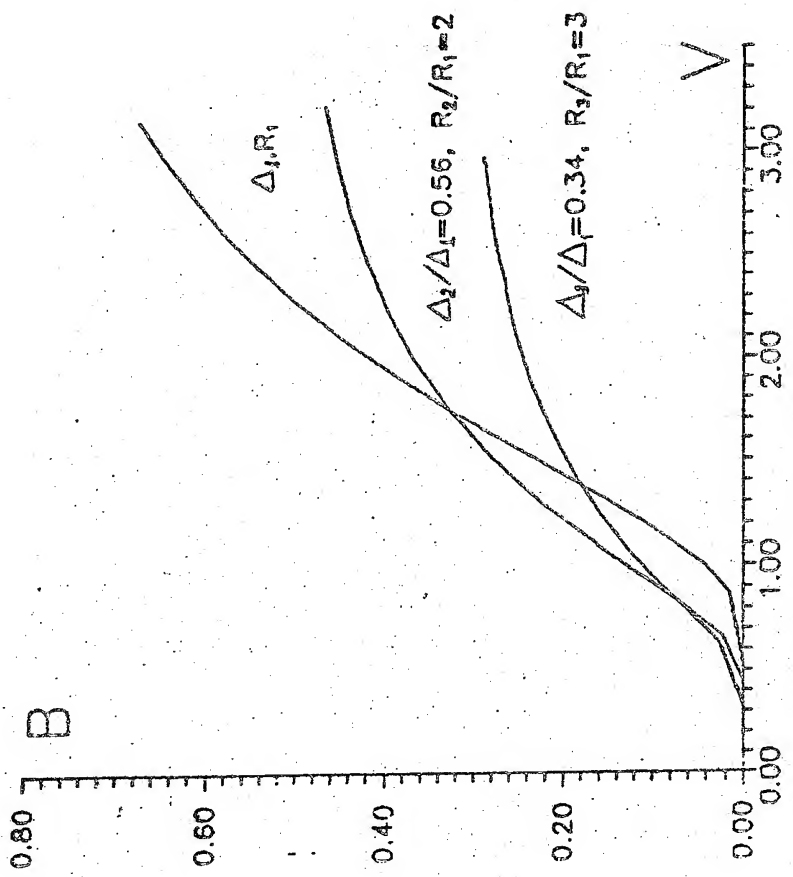


Fig.2. Dispersion dependencies of fibre with three nonidentical noncoupled cores.



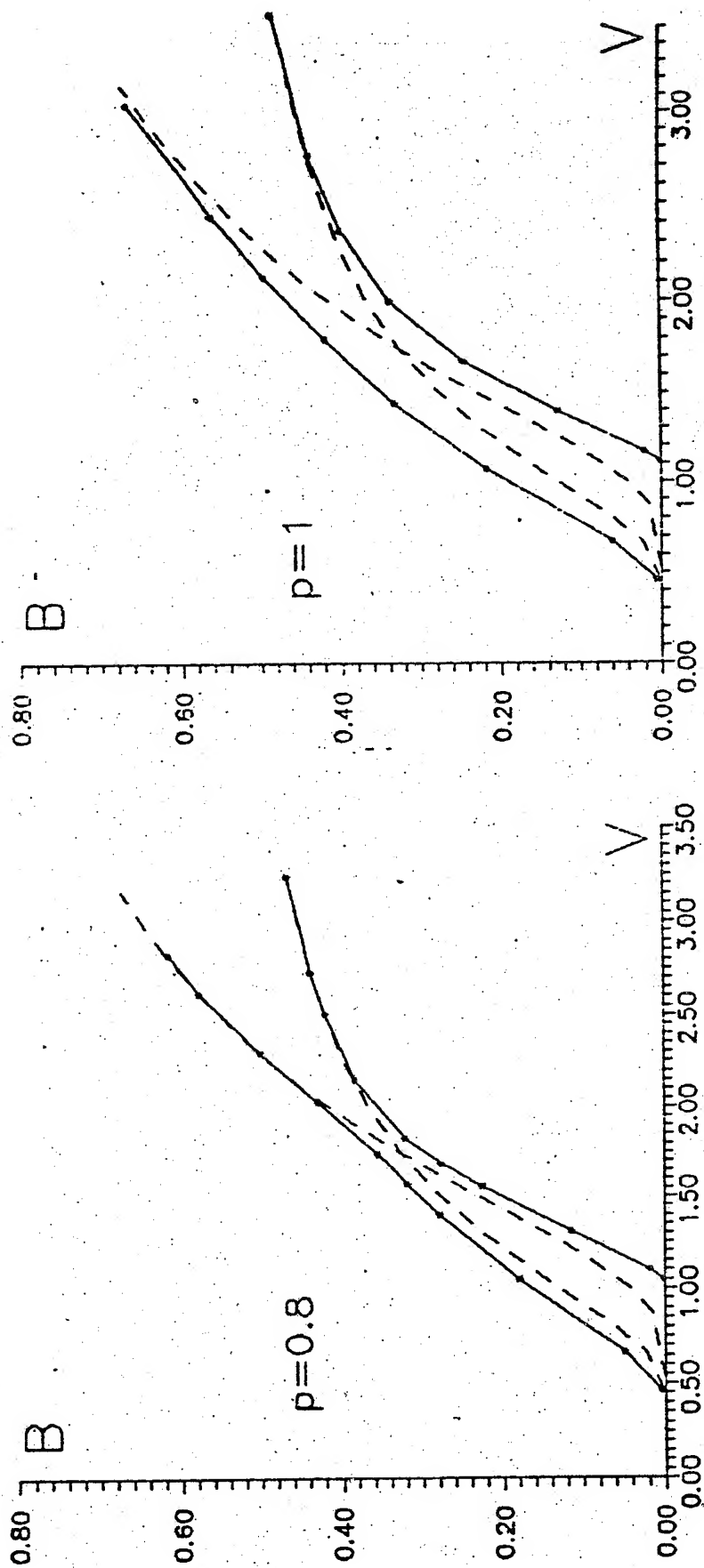


Fig.3. Dispersion dependencies of optical fibre with two nonidentical cores ( $R_2/R_1=2$ ,  $\Delta_2/\Delta_1=0.56$ ) and for two different distances between ones. Dashed curves are shown noncoupled case ( $p=0$ ).

# THREE-DIMENSIONAL TECHNIQUE USED FOR THE NUMERICAL COMPUTATION OF EF CREATED AROUND FRACTAL CLUSTERS IN THE INSULATION

Konotop V.V., Rezinkina M.M., Rezinkin O.L.

Kharkov polytechnic university

NIPKI "Molniya" Shevchenko 47 310013 Kharkov UKRAINE

## ABSTRACT

The calculation technique of 3-D EF intensity distribution in the inhomogeneous dielectric has been described. The numerical solution was obtained using the method of finite differences. The program for IBM PC has been developed and tested. The electric field intensity distribution near the broken-down dielectric aries of different configurations has been determined. These areas have fractal structure.

## INTRODUCTION

The simulations of the processes of the insulation breakdown under action of electric field requires the analyses of electrical field distribution around the conducting clusters with fractal structure. This requires information on the levels of EF intensity in the whole dielectric area being investigated taking into account the changes of the volumetric configuration of the distracted areas. The analytic solution of such problem is impossible. This stipulated the choice of the finite differences method for the estimation of the potentials distribution in the dielectric containing the conducting clusters. The 3-dimensional Laplace equation was solved using the iteration method of variable trends at each time step. The IBM PC program developed on the basis of this technique allowed for the calculation of the EF intensity in the dielectric containing fractal structures of different configuration.

Let us consider the system of flat linings. Between these linings the dielectric with conducting zones has been placed. The rectangular grid is applied on the dielectric in such a way that its nodes are located at the media boundaries. Assume that the media properties within each formed cell are the same. We shall write down the first Maxwell law for each node of calculation grid., define the divergence from both sides and integrate each term by S (where S is surface that embracing the node divides the distance between two adjacent nodes into two equal parts). Integrating the latter expression by time we shall obtain the following:

$$\oint_{\cdot S} \gamma E_n ds + \oint_S \epsilon E_n ds = 0, \quad (1)$$

where E is an electric field intensity;  $\gamma$  and  $\epsilon$  - conductivity and permeability of the media accordingly; index n

denotes the projection of vector to the normal of S surface.

The first term of expression (1) corresponds to the charge stored at the media boundary by the time  $t$ . After replacement the integration by summation using the trapezoid formulae we shall transfer the terms that correspond to the previous time step to the right side, i.e. to the known ones and after insertion of  $E = -\text{grad } \varphi$  we shall write the equation (1) in a differential form:

$$\Lambda_x \varphi_{i,j,k} + \Lambda_y \varphi_{i,j,k} + \Lambda_z \varphi_{i,j,k} = f_{i,j,k} \quad (2)$$

$$\text{where } \Lambda_z \varphi_{i,j,k} = \varphi_{i-1,j,k} \cdot AX_{i,j,k} - \varphi_{i,j,k} \cdot (AX_{i,j,k} + BX_{i,j,k}) -$$

$$+ \varphi_{i+1,j,k} \cdot BX_{i,j,k}$$

$$\Lambda_y \varphi_{i,j,k} = \varphi_{i,j-1,k} \cdot AY_{i,j,k} - \varphi_{i,j,k} \cdot (AY_{i,j,k} + BY_{i,j,k}) +$$

$$+ \varphi_{i,j+1,k} \cdot BY_{i,j,k}$$

$$\Lambda_z \varphi_{i,j,k} = \varphi_{i,j,k-1} \cdot AZ_{i,j,k} - \varphi_{i,j,k} \cdot (AZ_{i,j,k} + BZ_{i,j,k}) +$$

$$+ \varphi_{i,j,k+1} \cdot BZ_{i,j,k}$$

$AX_{i,j,k}, BX_{i,j,k}, AY_{i,j,k}, BY_{i,j,k}, AZ_{i,j,k}, BZ_{i,j,k}$  are run coefficients;  $f_{i,j,k}$  - is a differential analog of the expression for the charge stored at the media boundary without a term that corresponds to a current moment of time.

For the solution of this equation we used the iteration method of a variable directions. It is known from [1] that this method is used for the solution of two-dimensional elliptic problems. According to [2] it works perfectly well in many cases in spite of the absence of complete theoretical grounding. By analogy with the method of locally one-dimensional patterns [3] the transition from  $k$ -th to  $(k+1)$ -th iteration was performed through the sequential use of the run method in the X,Y,Z directions for three-point equations:

$$F_{IT} \cdot \varphi_{i,j,k}^{k+1/2} - \Lambda_z \varphi_{i,j,k}^{k+1/2} = F_{zy}^k \quad F_{zy}^k = \Lambda_y \varphi_{i,j,k}^k + \Lambda_z \varphi_{i,j,k}^k +$$

$$+ f_{i,j,k} + F_{IT} \cdot \varphi_{i,j,k}^k \quad (3)$$

$$F_{IT} \cdot \varphi_{i,j,k}^{k+2/2} - \Lambda_y \varphi_{i,j,k}^{k+2/2} = F_{zx}^{k+1/2}, \quad F_{zx}^{k+1/2} = \Lambda_x \varphi_{i,j,k}^{k+1/2} + \Lambda_z \varphi_{i,j,k}^{k+1/2} +$$

$$+ f_{i,j,k} + F_{IT} \cdot \phi_{i,j,k}^{k+2/3}; \quad (4)$$

$$F_{IT} \cdot \phi_{i,j,k}^{k+2/3} - \Lambda_z \phi_{i,j,k}^{k+2/3} = F_{yx}^{k+2/3}, \quad F_{yx}^{k+2/3} = \Lambda_x \phi_{i,j,k}^{k+2/3} + \Lambda_z \phi_{i,j,k}^{k+2/3} +$$

$$+ f_{i,j,k} + F_{IT} \cdot \phi_{i,j,k}^{k+2/3}. \quad (5)$$

where  $F_{IT}$  is iteration parameter.

The running over X (see (3)) was performed in the whole area of investigation at each Y sequentially at all layers of Z. In the same way the running over Y was performed (see equation (4)) and over Z (see equation (5)). During the calculations the following boundary conditions have been used: over Y - the prescribed potentials at the electrodes; over X and Z - the uniform Neuman equations [1].

The described scheme for the solution of 3-D equation (2) has been realized in the form of program for IBM PC, FORTRAN-77.

The testing of this program by the comparison with the precise analytical solutions [3] has shown that the relative difference between electric field intensity levels doesn't exceed 5%, i.e. it is within the value prescribed for the numerical calculation of relative error.

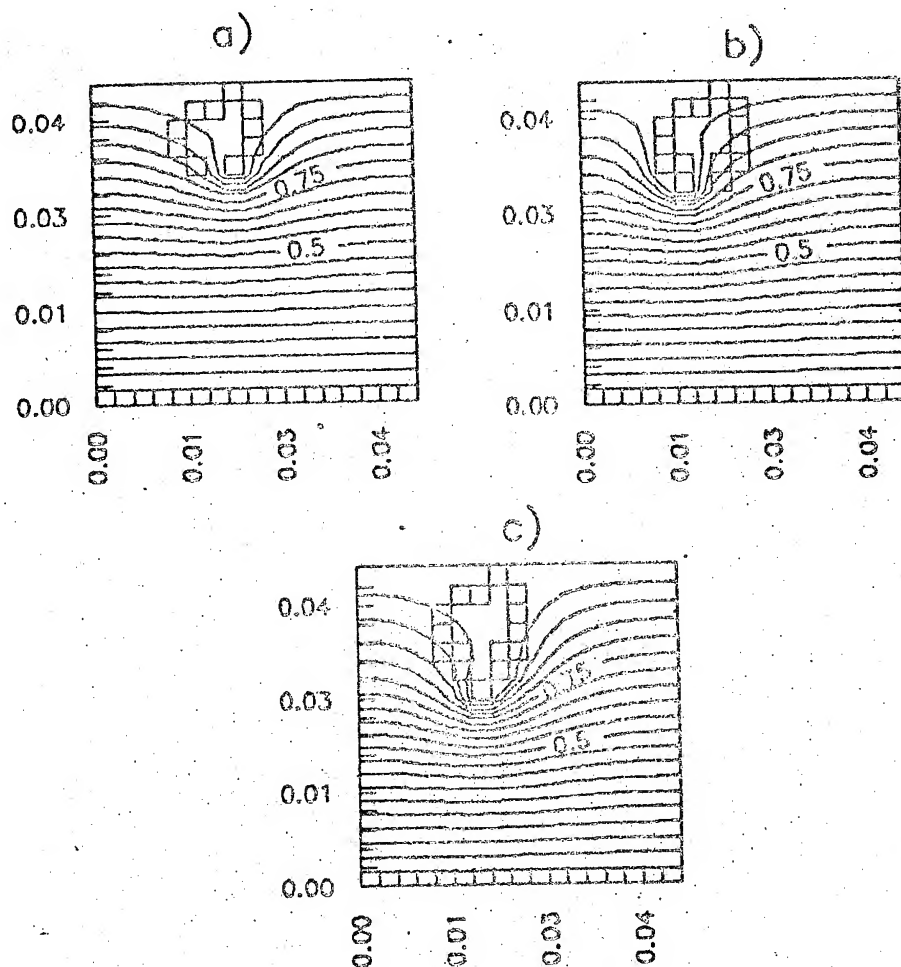
In the process of electric aging of some insulation materials, for example polyethylene the treeing of structure deep inside takes place. The so-called dendrites are formed. The experimental data obtained for the specific surface conductivity of dendrites channels show that this channels can be considered as conductive [4]. The developed technique has been used for the calculation of electric field distortion by dendrites observed in the experiments. The figure shows the patterns of equipotential lines around the dendrites in the process of electric aging of polyethylene insulation (see a), b), c). Equipotential lines are shown in the section  $Z=\text{const}$  that run through the middle of dendrite. The figure shows also the dendrites projection to the plane  $Z=\text{const}$ .

#### Conclusions.

1. The volume distribution of electric field intensity in the dielectric that contains the conductive inclusions of arbitrary shape has been calculated using PC program, which has developed and realized for this purpose. The program allows for the analysis of the effect produced by the form of conductive inclusions on distortion of electric field in the dielectric.

2. The method of variable directions that was developed for the solution of two-dimensional elliptic equations and was applied to the solution of 3-D problems allowed for the calculation of volumetric electric field distribution.

3. The developed IBM PC program allowed for the calculation of EF intensity distribution around the broken-down areas with fractal structure. These areas are formed in the process of electric aging of dielectric.



The patterns of equipotential lines distribution around the dendrites that are formed in the process of electric aging of polyethylene insulation (a), b), c) - phases of dendrites development).

#### References.

1. Самарский А.А., Теория разностных схем., М., "Наука", 1977, 656 с.
2. Хейгеман Л., Янг Д., Прикладные итерационные методы., М., "Мир", 1986, 446 с.
3. Кучинский Г.С., Кизеветтер В.Е., Пинталь Д.С. Изоляция установок высокого напряжения. -М., Энергоатомиздат, 1987, 368 с.
5. Кучинский Г.С., Частичные разряды в высоковольтных конструкциях., Л., "Энергия", 1979, 233 с.

# FULLY ANTI-MIRROR REFLECTION FROM CORRUGATED BOUNDARY OF DIELECTRICS DIELECTRICAL ECHELETTE. DIELECTRICAL ECHELETTE RESONATORS

E.V.Koposova, S.N.Vlasov

Institute of Applied Physics, Russian Academy of Science  
46 Uljanov St., 603600 Nizhny Novgorod, Russia

## ABSTRACT

We consider a new effect of diffraction of electromagnetic waves at the gratings, such as the full anti-mirror reflection from the corrugated boundary of dielectrics. Quasioptical dielectrical echelette resonator with high selective properties is designed.

The results obtained are applied for design of the resonators for high frequency electron devices.

## HISTORY

Diffraction gratings with different profiles are used in many fields of physics and technology, such as optics, acoustics, antennas and measurements, for a long time. The analysis of properties of electromagnetic fields, scattered by periodical structures, was restricted by approximation methods, such as long-wave quasi-static approximation or geometric optics. Recently there are the number of papers devoted to the rigorous analysis of gratings with elements of different profile scales, compared to wavelength. More accurate definition of the theory made it possible to observe the new interesting effects in the wave scattering by gratings.

As is well known, for wave diffraction at gratings there arise space harmonics, propagated in the directions determined by the main diffraction parameter  $\kappa = d/\lambda$  and the angle of incidence of the wave  $\theta_1$  (fig.1). The interested cases are of the given energy distribution on directions of scattering, for instance maximal selective, that is, the existence of the one beam only in the scattered field, usually anti-mirror reflected beam.

The simplest example of the grating with such properties is a step-wise echelette<sup>1</sup> (fig.2), one step side of whose is normal to the direction of incidence, the other step side contains an integer number of semi-wavelengths. For the incidence at such a structure of wave with E-vector, perpendicular to the touches of grating, the energy reflects fully in the anti-mirror directions. The nature of the effect of fully anti-mirror reflection is obvious in this case because a standing wave satisfies to the boundary condition at the echelette surface.

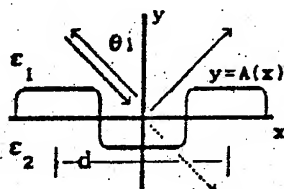


fig.1

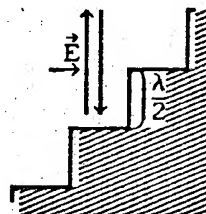


fig.2

For a surface of more complicated shape and for the other field polarization the existence of such effects still not so obvious. To study a possibility of these effects it is necessary to solve exactly the diffraction problem<sup>2,3</sup>.

The calculations show the regime of fully anti-mirror reflection of  $-1$  space harmonics becomes possible<sup>3-6</sup>, i.e. reflective coefficient and energy in anti-mirror direction can equal unity  $W_{-1}=1$ , if the sufficient depth of an arbitrary profile of the infinitely conducting grating.

The fully anti-mirror reflection can be provided not only for reflection at metallic grating, but at the corrugated boundary of dielectrics, when  $\epsilon_1 > \epsilon_2$  (fig.1) and the fully inner reflection condition is fulfilled at the smooth boundary. Under the needed conditions there are only two propagating waves: 0 and  $(-1)$  harmonics. Under the autocollimation condition  $2\kappa \sin \theta = 1$ , where  $\kappa = d\sqrt{\epsilon}/\lambda$ ,  $\epsilon = \epsilon_1/\epsilon_2$ , the  $(-1)$  harmonics propagates

in the direction opposite to the incidence one and its energy can arrive unity for the sufficient depth of groove.

### METHOD

The problem may be solved by method of integral equation<sup>2</sup>. Fig.1 shows the general periodic structure with arbitrary profile  $y=A(x)$ . For example we consider one which is given by function

$$y=A(x)=A_0 \sin \frac{2\pi}{d}x$$

with period  $d=2\pi$ , which is a dielectric boundary, separating two media having dielectric permittivities of  $\epsilon_1$  and  $\epsilon_2$ , uniform in one direction  $z$  in a rectangular coordinate system Oxyz. Let consider  $\epsilon_1=\epsilon_2=1$ .

An electromagnetic monochromatic plane wave whose amplitude is unity with electric or magnetic field being parallel to grooves strikes the grating at the angle  $\theta_1$  in a plane normal to uniform direction  $z$

$$E^{(1)} = e_z^0 \exp(ik\sqrt{\epsilon} \sin\theta x - ik\sqrt{\epsilon} \cos\theta y) = \exp(ik_{ox} x - ik_{oy} y).$$

We consider an electric field of the wave is polarized along the grating edges.

At scattering of the plane wave on the grating, there arise space harmonics with amplitudes  $R_n$  and  $T_n$ .

$$E_n^{(1)} = R_n \exp(ik_{nx} x + ik_{ny}^{(1)} y), \quad E_n^{(2)} = T_n \exp(ik_{nx} x - ik_{ny}^{(2)} y).$$

Their projection of wave vector in the first and second media to  $x$ -direction follow from known grating formula, so

$$E_n^{(1)} = R_n \exp(i(k\sqrt{\epsilon} \sin\theta + n \frac{2\pi}{d})x + i\sqrt{k^2 \epsilon - (k\sqrt{\epsilon} \sin\theta + n \frac{2\pi}{d})^2} y)$$

$$E_n^{(2)} = T_n \exp(i(k\sqrt{\epsilon} \sin\theta + n \frac{2\pi}{d})x - i\sqrt{k^2 - (k\sqrt{\epsilon} \sin\theta + n \frac{2\pi}{d})^2} y)$$

The integral equation, which described the field, scattered at the grating, can be obtained by the following manner. In accordance to Huygens principle, the field in the up and down medium can be expressed, using the field value and the derivative of field on the both sides of the boundary:

$$E^{(1)}(x,y) = E^{(1)}(x,y) + \int ds' \left\{ G^{(1)}(x-x', y-y') \frac{\partial}{\partial n'} E^{(1)}(x', y') - E^{(1)}(x', y') \frac{\partial}{\partial n'} G^{(1)}(x-x', y-y') \right\},$$

$$E^{(2)}(x,y) = - \int ds' \left\{ G^{(2)}(x-x', y-y') \frac{\partial}{\partial n'} E^{(2)}(x', y') - E^{(2)}(x', y') \frac{\partial}{\partial n'} G^{(2)}(x-x', y-y') \right\},$$

where  $y'=A(x')$ ,  $ds'=dx' \sqrt{1 + \left(\frac{dy'}{dx'}\right)^2}$ . Here the integral is taken over the period.

The two-dimensional Green functions

$$G^{(j)}(x-x', y-y') = \frac{1}{2id} \sum_{n=-\infty}^{\infty} \frac{1}{k_{ny}^{(j)}} \exp\left(ik_{xn} (x-x') + ik_{yn}^{(j)} (y-y')\right)$$

for the first and the second medium correspond to the field, which is radiated by the array of collinear in  $z$ -direction sources. These sources are placed periodically in  $x$ -direction and the phase shift between neighbour elements equals  $k^{(j)} d \sin\theta$ . The field and its derivative on the both sides of the boundary are coupled by the boundary conditions:

$$E^{(1)}(x,y) = E^{(2)}(x,y) \Big|_{y=A(x)}, \quad \frac{\partial}{\partial n} E^{(1)}(x,y) = \frac{\partial}{\partial n} E^{(2)}(x,y) \Big|_{y=A(x)}.$$

Let us introduce an unknown function in accordance to the combination:

$$\begin{aligned} \int ds' \left\{ G^{(1)}(x-x', y-y') \frac{\partial}{\partial n'} E^{(1)}(x', y') - E^{(1)}(x', y') \frac{\partial}{\partial n'} G^{(1)}(x-x', y-y') \right\} = \\ = \int ds' G^{(1)}(x-x', y-y') \phi(x', y') \end{aligned}$$

Using this function, we express the field in the up and down medium and put a point of view to the surface. We get the integral equation under the boundary conditions:



$$\int ds' \left\{ \frac{1}{2} \left( G^{(1)}(x-x', y-y') + G^{(2)}(x-x', y-y') \right) + \int ds'' \left[ G^{(2)}(x-x'', y-y'') \frac{\partial}{\partial n''} G^{(1)}(x''-x', y''-y') - \frac{\partial}{\partial n''} G^{(2)}(x-x'', y-y'') G^{(1)}(x''-x', y''-y') \right] \right\} \phi(x', y') + \frac{1}{2} E^{(1)}(x, y) + \int ds' \left[ G^{(2)}(x-x', y-y') \frac{\partial}{\partial n} E^{(1)}(x', y') - \frac{\partial}{\partial n} G^{(2)}(x-x', y-y') E^{(1)}(x', y') \right] = 0 \Big|_{y=A(x)}$$

The amplitudes of the space harmonics of diffraction field in the both media that are the reflection and transmission coefficients can be expressed by solution of the equation:

$$R_n = \int ds' \frac{1}{2i d k_{ny}^{(1)}} \exp(-i k_{ny}^{(1)} y' - i n \frac{2\pi}{d} x') \phi(x', y');$$

$$T_n = - \int ds' \left\{ \frac{1}{2i d k_{ny}^{(2)}} \exp(i k_{ny}^{(2)} y' - i n \frac{2\pi}{d} x') \left[ \frac{\partial}{\partial n} E^{(1)}(x', y') + \frac{1}{2} \phi(x', y') + \int ds'' \frac{\partial}{\partial n''} G^{(1)}(x'-x'', y'-y'') \phi(x'', y'') \right] + \frac{1}{2d \sqrt{1 + \left( \frac{dy'}{dx'} \right)^2}} \left( -1 - \frac{k_{nx}}{k_{(j)}} \frac{dy'}{dx'} \right) \exp(i k_{ny}^{(2)} y' - i n \frac{2\pi}{d} x') \left[ E^{(1)}(x', y') + \int ds'' G^{(1)}(x'-x'', y'-y'') \phi(x'', y'') \right] \right\}$$

The integral equation have the general symbolic representation<sup>2</sup>:

$$\int_0^d W(x, x') \phi(x') dx' + V(x) = 0$$

where  $V, U$  are periodic functions,  $W$  is a kernel, that may be singular, but integrable.

The simplest method to solve the equations is to represent an unknown function by  $N$  values at the period  $\phi_m = \phi(x_m)$ . Then the integral equation can be expressed by the system of linear algebraic equations:

$$\sum_{l=1}^M W_{ml} \phi_l + V_m = 0,$$

where  $V_m = V(x_m)$ ,  $W_m = W(x_m, x_n')$ , which is solved numerically.

The other method, which we used for solving equation is to use the Fourier series for an unknown function

$$\tilde{\phi}(x) = \sum_{n=-\infty}^{\infty} \phi_n \exp(i n \frac{2\pi}{d} x).$$

In this case the integral equation can be expressed by the analogical system of linear algebraic equations. Now this system is for the Fourier coefficients of an unknown function  $\phi_n$  where right-hand member and kernel are

$$V_n = \frac{1}{d} \int_0^d V(x) \exp\left(-i n \frac{2\pi}{d} x\right) dx,$$

$$W_{nm} = \frac{1}{d^2} \int_0^d \int_0^d W(x, x') \exp\left(-i n \frac{2\pi}{d} x + i m \frac{2\pi}{d} x'\right) dx dx',$$

the coefficient of the Fourier transform which can be easily calculated using the FFT<sup>7</sup>.

As the result, the coefficients of reflection in all diffraction mounts can be determined.

### FULLY ANTI-MIRROR REFLECTION REGIME

Figs.3ab show the efficiency curves of (-1)-order Littrow mount, in dependence on



the groove amplitude and the wave number for the field with  $E$  parallel to the grooves, sinusoidal profile with amplitude  $A_0$  and the absence of wave transmission. Fig.4 shows curves at the plane of parameters  $(A_0, \kappa)$ , which correspond to the fully anti-mirror reflection  $W=1$  and the fully mirror reflection  $W=0$ . Dashed curves correspond to the case of wave incident to the perfectly conductive surface whose corrugation is the same. Only for the quite large value of the ratio  $\epsilon_1/\epsilon_2$  the curves for dielectrics are close to the curves for metal. The dependence of curve on the ratio  $\epsilon_1/\epsilon_2$  is very weak. With changing of this ratio from 1.5 up to 10 curves are practically coincident for the intervals which correspond to the absence of transmission waves.

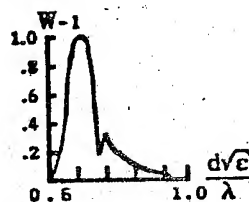


fig.3a

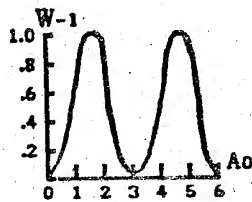


fig.3b

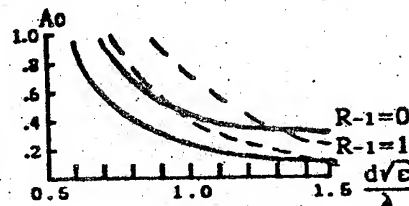


fig.4

### DIELECTRICAL ECHELETTE

Observation of the effect of fully anti-mirror reflection at a corrugated boundary of dielectrics gives possibility of building of dielectric echelettes and dielectric echelette resonators with a comparably rare spectrum.

Such a resonator was studied experimentally. We have designed the two-mirror resonator. One of the mirrors was made from dielectric  $\epsilon=2$  and had the echelette side for the reflecting of wave incident from dielectric. The second mirror was made as plane metallic (fig.5). Resonator mode was organized by the wave which propagated normal to the plane metal mirror and reflected at the dielectric echelette with the coefficient near equal to unity.

There were observed one high-Q-factor oscillation with  $Q \sim 900+1000$  and the low-Q-factor oscillation with Q-factor no exceeded  $Q \sim 250-350$ . The module of the reflection coefficient was defined by the Q-factor and was  $R=0.95+0.98$  at the frequency where the theoretical value is unity (fig.6).

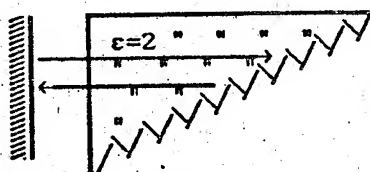


fig.5

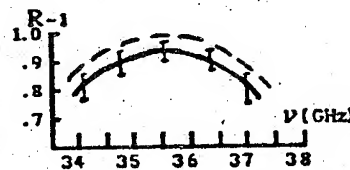


fig.6

The work is supported RFFI (grant 93-02-15423).

### REFERENCES

1. Kosarev E.L. Rarefaction of spectrum of the open resonator using the echelette. Pis'ma v ZETF, Vol.3, P.295, 1966.
2. Shestopalov V.P., Litvinenko L.N., Masalov S.A., Sologub V.G. Wave diffraction at Gratings. - Kharkov, 1973 (in Russian).
3. Electromagnetic Theory of Grating /Ed. Petit R. New-York: Springer-Verlag, 1980.
4. Shestopalov V.P., Kirilenko A.A., Masalov S.A., Sirenko Yu.K. Resonance wave scattering, Vol.1, Kiev, 1986 (in Russian).
5. Kirilenko A.A., Kusaikin A.P., Sirenko Yu.K. Non-mirror reflection by waveguide-tape gratings. Specific laws of scattering. Izv.VUZ, Radiofizika, 1986, Vol.29-10, p.1182.
6. Sheinina E.V. Fully auto-collimation reflection for different profiles of corrugated surfaces. Izv.VUZ, Radiofizika, 1988, Vol.31, p.885.
7. Vainshtein L.A., Sukov A.I. Diffraction at rough surface// Radiotekhnika i Elektronika. - 1984. - V. 29, N8. - P.1472.

# RECOGNITION OF ELECTROMAGNETIC FIELDS

Igor Koritzev

Cukurova University, 01330, Adana, Turkey.

## ABSTRACT

Classification of electromagnetic fields becomes very important in the problems of electromagnetic hazard and electromagnetic compatibility. This paper considers field presentation and its recognition in a real time scale. Field presentation is produced in the space of its time realizations. The optimal decision rule uses recognition signs built with the Karunen - Loev's decomposition technique.

## INTRODUCTION

Time investigations of electric or magnetic components of a field in any plane have a random character. Description of fields in purpose of their recognition may be produced with probability densities, covariation matrices, spectra or time realizations/1,2/. This paper deals with field presentation by discrete time functions and construction of recognition signs in the space of common Karunen - Loev's signs.

## FORMULATION OF THE PROBLEM

The  $i$ -th field type is assumed to be one of  $M$  possible types with probability  $P_i$ , such that

$\sum_{i=1}^M P_i = 1$ . A field is presented in the space of time realizations. Statistical characteristics of a field are unknown, but a teaching classified sample is given. Necessary to construct field recognition signs and an optimal decision rule.

## FIELD PRESENTATION WITH DISCRETE TIME FUNCTIONS

An electromagnetic field represents a random field  $\vec{F}(t, \vec{r})$  in a space point  $\vec{r}$  with coordinates  $(x, y, z)$ . The full statistical description of a three-dimensional field may be given by a set of three  $N$ -dimensional probability densities. We will be limited with the correlation theory level and assume that a field is stationary. The  $i$ -th field type will be described with a matrix function of the dimension  $3 \times 1$

$$\vec{F}^i = [F_x^i(t), F_y^i(t), F_z^i(t)]^T. \quad (1)$$

A function  $\vec{F}^i(t)$  is generally a complex function and may be described at the level of the correlation theory by a matrix correlation function

$$[R^i(\tau)] = [E(F_{i1}^i(t) - m_{i1}^i)(F_{i2}^i(t + \tau) - m_{i2}^i)^*] \quad (2)$$

where  $E$  is a sign of averaging;  $m_{ij}^i = E F_{ij}^i(t)$ ; the bar indicates the complex conjugate.

In practice a function  $\vec{F}^i(t)$  is observed a finite time and measured in a discrete form. Therefore assume, that we deal with a discrete matrix function, given within a finite interval

$$\vec{F}^i(k), \quad k = 0, 1, \dots, L-1. \quad (3)$$

Decompose a function  $\vec{F}^i(k)$  into the Fourier series in the basis set  $\left\{ \exp\left(\sqrt{-1} \frac{1}{L} 2\pi f k\right) \right\}$ :

$$\bar{F}^i(k) = \sum_{l=0}^{L-1} \bar{S}^i(f) \exp(\sqrt{-1} \frac{1}{L} 2\pi f k), \quad (4)$$

where  $\bar{S}^i(f)$  is a matrix function, which defines a field spectrum in the mentioned basis set

$$\bar{S}^i(f) = \frac{1}{L} \sum_{k=0}^{L-1} \bar{F}^i(k) \exp(\sqrt{-1} \frac{1}{L} 2\pi f k). \quad (5)$$

### CONSTRUCTING RECOGNITION SIGNS

The chosen basis set performs the role of field primary signs. Now we will define the informative recognition signs of fields as a common Karunen-Loev's signs.

Introduce the space of matrix functions  $\bar{F}(k)$  with the following inner product, length and distance

$$_k([\bar{F}^1], [\bar{F}^2]) = \sum_{l=1}^3 \sum_{k=0}^{L-1} F_l^1(k) \overline{F_l^2(k)}; \quad (6)$$

$$\|[\bar{F}]\| = \sqrt{\sum_{l=1}^3 \sum_{k=0}^{L-1} |F_l(k)|^2}; \quad (7)$$

$$\rho([\bar{F}^1], [\bar{F}^2]) = \sqrt{\sum_{l=1}^3 \sum_{k=0}^{L-1} |F_l^1(k) - F_l^2(k)|^2}. \quad (8)$$

Decompose the function  $\bar{F}^i(k)$  into the general Fourier series with the orthonormalised basis set

$$\{\bar{\psi}(s, k)\}$$

$$\bar{F}^i(k) = \sum_{s=0}^{L-1} \alpha^i(s) \bar{\psi}(s, k), \quad (9)$$

where

$$_k(\bar{\psi}(s_1, k), \bar{\psi}(s_2, k)) = \sum_{l=1}^3 \sum_{k=0}^{L-1} \psi_l(s_1, k) \psi_l(s_2, k); \quad (10)$$

$$\alpha^i(s) = \sum_{l=1}^3 \sum_{k=0}^{L-1} F_l^i(k) \psi_l(s, k). \quad (11)$$

We will be limited with a partial sum

$$\bar{F}_{N_s}^i(k) = \sum_{s=0}^{N_s-1} \alpha^i(s) \bar{\psi}(s, k). \quad (12)$$

Consider the expression

$$\hat{\rho}^2(\bar{F}, \bar{F}_{N_s}) = \hat{E} \sum_{i=1}^M P_i \rho^2([\bar{F}^i], [\bar{F}_{N_s}^i]), \quad (13)$$

where the value  $\rho([\bar{F}], [\bar{F}_{N_s}])$  is defined according to (8). It represents the squared distance between field realizations  $\bar{F}^i$  and  $\bar{F}_{N_s}^i$  averaged through the  $M$  field types and with additional averaging through a set of realizations. Transform (13) to the next expression

$$\begin{aligned} \hat{\rho}^2([\bar{F}], [\bar{F}_{N_s}]) &= \hat{E} \sum_{i=1}^M P_i (\bar{F}^i, \bar{F}^i) - \hat{E} \sum_{i=1}^M P_i \times \\ &\times \sum_{s=0}^{N_s-1} \sum_{l_1, l_2=1}^3 \sum_{k_1, k_2=0}^{L-1} F_{l_1}^i(k_1) \overline{F_{l_2}^i(k_2)} \psi_{l_1}(s, k_1) \overline{\psi_{l_2}(s, k_2)}; \end{aligned} \quad (14)$$

introducing  $\sum_{i=1}^M P_i \hat{E} F_{i1}(k_1) \overline{F_{i2}(k_2)} = \hat{R}_{11,12}(k_1, k_2)$ , the (14) may be written as

$$\hat{p}^* \left( [\bar{F}], [\bar{F}_N] \right) = \hat{E} \sum_{i=1}^M P_i (\bar{F}^i, \bar{F}^i) - \sum_{s=0}^{N_s-1} \sum_{n,12=1}^3 \sum_{k_1,k_2=0}^{L-1} \hat{R}_{11,12}(k_1, k_2) \psi_{11}(s, k_1) \overline{\psi_{12}(s, k_2)}. \quad (15)$$

Let us find the basis set  $\{\bar{\psi}(s, k)\}$  for which the expression (15) will be minimum. For this case the error mean square of a field presentation with a partial sum (12) will be also minimum. According to (15) the problem of such basis finding goes to the maximum of the expression

$$\sum_{s=0}^{N_s-1} \sum_{n,12=1}^3 \sum_{k_1,k_2=0}^{L-1} \hat{R}_{11,12}(k_1, k_2) \psi_{11}(s, k_1) \overline{\psi_{12}(s, k_2)} = \sum_{s=0}^{N_s-1} \sum_{n,12=1}^3 \left( \left[ \hat{R}_{11,12}(k_1, k_2) \right], \left[ \psi_{11}(s, k_1) \right], \left[ \overline{\psi_{12}(s, k_2)} \right] \right). \quad (16)$$

After introducing the operator  $\hat{R}$  according to the expression

$$\hat{R} \left[ \psi_{12}(s, k_2) \right] = \sum_{n,12=1}^3 \left( \left[ \hat{R}_{11,12}(k_1, k_2) \right], \left[ \psi_{11}(s, k_1) \right] \right). \quad (17)$$

the maximum of (16) will be reached, if characteristic vectors of this operator are chosen, as a matrix

$\left[ \psi_i(s, k) \right]$ . They are defined from the equation

$$\hat{R} \left[ \psi_i(s, k) \right] = \lambda_i \left[ \psi_i(s, k) \right]. \quad (18)$$

Taking into account (17) the last equation after expanding may be written as

$$\sum_{n=1}^3 \sum_{k_1=1}^{L-1} \hat{R}_{11,12}(k_1, k_2) \overline{\psi_{11}(s, k_1)} = \lambda_i \left[ \overline{\psi_{12}(s, k_2)} \right]. \quad (19)$$

Expression (19) represents a system of three equations for definition of the characteristic values and characteristic vectors. Characteristic vectors perform the role of common Karunen-Loev's signs. In the space of this signs the  $i$ -th field type is described by a vector

$$\bar{\alpha}^i = (\alpha^i(0), \dots, \alpha^i(s), \dots, \alpha^i(N-1))^T. \quad (20)$$

From a teaching Sample  $\{\alpha^i(s, r); r = 1, \dots, n_i; i = 1, \dots, M\}$  an estimation of the  $i$ -th field type probability density may be defined for constructing a decision rule as a partial sum of the series

$$p^*(\bar{\alpha}) = \sum_{k=1}^K d_k^i(k) e_k(\bar{\alpha}). \quad d_k^i(k) = \frac{1}{n_i} \sum_{r=1}^{n_i} e_k(\bar{\alpha}^i, r). \quad (21)$$

On finding decomposition coefficients, we receive the estimation  $p^*(\bar{\alpha})$  and construct in the space with the adaptive Byes' principle an asymptotic optimal decision rule as follows

$$P_i p^*(\bar{\alpha}) \geq P_l p^*(\bar{\alpha}), \quad l = 1, \dots, M; \quad l \neq i. \quad (22)$$

Such construction of a decision rule in the space with a small number of recognition signs provides realization of a specialized recognition system.

#### REFERENCES

- (1) V. Omelchenko: "Orthogonal decomposition of random signals and fields" Kiev, 1980
- (2) I. Koritzhev: "Estimation of the field spectral density" Coll. vol. "Probable models, processing of random signals and fields". Lvov, 1993, pp. 191-193

# DIFFRACTION BY A TERMINATED, SEMI-INFINITE PARALLEL-PLATE WAVEGUIDE WITH THREE DIFFERENT MATERIAL LOADING: PART I - THE CASE OF *E* POLARIZATION

Shoichi Koshikawa and Kazuya Kobayashi

Department of Electrical and Electronic Engineering, Chuo University

1-13-27 Kasuga, Bunkyo-ku, Tokyo 112, Japan

(Tel: +81-3-3817-1869, Fax: +81-3-3817-1847, E-mail: kazuya@kawa.elect.chuo-u.ac.jp)

**Abstract** - The plane wave diffraction by a terminated, semi-infinite parallel-plate waveguide with three different material loading is rigorously analyzed for the *E*-polarized case using the Wiener-Hopf technique. Representative numerical examples of the radar cross section (RCS) are presented and the far field back-scattering characteristics are discussed. It is shown that the three-layer lossy material loading on the endplate inside the waveguide results in significant RCS reduction over broad frequency range.

## 1. INTRODUCTION

Analysis of the scattering from open-ended metallic waveguide cavities is an important subject in target identification problems since these obstacles contribute significantly to the radar cross section (RCS) due to the interior irradiation. Cavity structures are encountered in many radar targets such as jet aircrafts and ships; therefore it is often required to reduce the RCS either by loading the interior of cavities with absorbing materials or by shaping cavities. Some of the cavity diffraction problems have been analyzed thus far using various analytical and numerical methods [1]. It appears, however, that the solutions deduced via these methods are not uniformly valid for arbitrary cavity dimensions.

In the previous papers [2, 3], we have considered a finite parallel-plate waveguide with a planar termination at the open end as an example of two-dimensional cavity structures, and analyzed rigorously the plane wave diffraction using the Wiener-Hopf technique, where the efficient approximate solution is obtained which is valid for cavity depth greater than about the wavelength. In this paper, as a related two-dimensional geometry, we shall consider a material-loaded cavity formed by a semi-infinite parallel-plate waveguide with an interior planar termination, and analyze the diffraction of an *E*-polarized plane wave using the Wiener-Hopf technique. Introducing the Fourier transform for the scattered field and applying boundary conditions in the transform domain, the problem is formulated in terms of the simultaneous Wiener-Hopf equations, which are solved rigorously via the factorization and decomposition procedure. It is to be noted that the solution is valid for arbitrary cavity dimensions. The scattered field is evaluated by taking the inverse Fourier transform together with the use of the saddle point method. Illustrative numerical examples on the RCS are presented for various physical parameters and the far field backscattering characteristics are discussed. It is shown that the interior irradiation is significantly reduced over broad frequency range by loading the interior of the cavity with three-layer lossy material.

The time factor is assumed to be  $e^{-i\omega t}$  and suppressed throughout this paper.

## 2. RIGOROUS WIENER-HOPF SOLUTION

We consider the diffraction of an *E*-polarized plane wave by a terminated, semi-infinite parallel-plate waveguide with material loading, as shown in Fig. 1, where the upper and lower plates of the waveguide and the endplate at  $z = -d_1$  are infinitely thin, perfectly conducting, and uniform in the *y*-direction. The material layers I ( $-d_1 < z < -d_2$ ), II ( $-d_2 < z < -d_3$ ), and

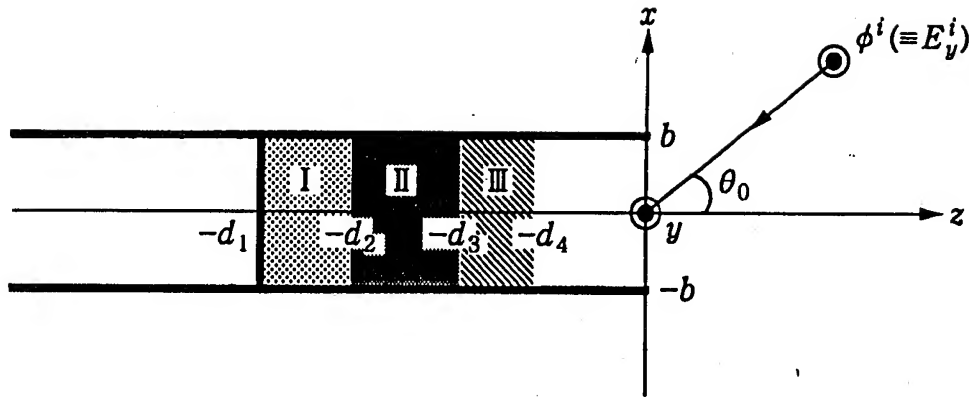


Fig. 1. Geometry of the problem.

III ( $-d_3 < z < -d_4$ ) are characterized by the relative permittivity/permeability  $(\epsilon_1, \mu_1)$ ,  $(\epsilon_2, \mu_2)$ , and  $(\epsilon_3, \mu_3)$ , respectively.

Let the total electric field  $\phi^i(x, z) [\equiv E_y^i(x, z)]$  be

$$\phi^i(x, z) = \phi^i(x, z) + \phi(x, z), \quad (1)$$

where  $\phi^i(x, z)$  is the incident field defined by

$$\phi^i(x, z) = e^{-ik(x \sin \theta_0 + z \cos \theta_0)}, \quad 0 < \theta_0 < \pi/2 \quad (2)$$

with  $k [= \omega(\mu_0 \epsilon_0)^{1/2}]$  being the free-space wavenumber. For analytical convenience, we shall assume that the vacuum is slightly lossy as in  $k = k_1 + ik_2$  with  $0 < k_2 \ll k_1$ . The solution for real  $k$  is obtained by letting  $k_2 \rightarrow +0$  at the end of analysis. Let us define the Fourier transform of the unknown scattered field  $\phi(x, z)$  as

$$\Phi(x, \alpha) = (2\pi)^{-1/2} \int_{-\infty}^{\infty} \phi(x, z) e^{iaz} dz, \quad \alpha = \text{Re } \alpha + i \text{Im } \alpha (\equiv \sigma + i\tau). \quad (3)$$

In view of the radiation condition, it follows that  $\Phi(x, \alpha)$  is regular in the strip  $-k_2 < \tau < k_2 \cos \theta_0$  of the  $\alpha$ -plane. Taking the Fourier transform of the two-dimensional Helmholtz equation and solving the resultant equations, we may derive the scattered field representation in the transform domain. In particular, the field for  $x \gtrless \pm b$  is given by

$$\Phi(x, \alpha) = (1/2)[U_{(+)}^e(\alpha) \pm V_{(+)}^e(\alpha)]e^{\mp \gamma(x \mp b)}, \quad (4)$$

where  $\gamma = (\alpha^2 - k^2)^{1/2}$  with  $\text{Re } \gamma > 0$ , and

$$U_{(+)}^e(\alpha) = \Psi_{(+)}(b, \alpha) + \Psi_{(+)}(-b, \alpha), \quad V_{(+)}^e(\alpha) = \Psi_{(+)}(b, \alpha) - \Psi_{(+)}(-b, \alpha), \quad (5)$$

$$\Psi_{(+)}(x, \alpha) = \Phi_{+}(x, \alpha) - \frac{e^{-ikx \sin \theta_0}}{(2\pi)^{1/2} i(\alpha - k \cos \theta_0)}, \quad (6)$$

$$\Phi_{+}(x, \alpha) = (2\pi)^{-1/2} \int_0^{\infty} \phi(x, z) e^{iaz} dz. \quad (7)$$

Applying the boundary conditions in the transform domain, the problem is formulated in terms of the simultaneous Wiener-Hopf equations satisfied by the unknown functions  $U_{(+)}^e(\alpha)$  and  $V_{(+)}^e(\alpha)$ . The Wiener-Hopf equations can be solved via the factorization and decomposition procedure leading to the following exact solution:

$$\frac{U_{(+)}^e(\alpha)}{b} = \frac{M_{+}^e(\alpha)}{b^{1/2}} \left[ -\frac{A_e}{b(\alpha - k \cos \theta_0)} + \sum_{n=1}^{\infty} \frac{e^{-2\gamma_{2n-1}d_4} \kappa_{2n-1}^e a_n^e p_n^e u_{en}^+}{b(\alpha + i\gamma_{2n-1})} \right], \quad (8)$$

$$\frac{V_{(+)}^e(\alpha)}{b} = \frac{N_{+}^e(\alpha)}{b^{1/2}} \left[ \frac{B_e}{b(\alpha - k \cos \theta_0)} + \sum_{n=1}^{\infty} \frac{e^{-2\gamma_{2n}d_4} \kappa_{2n}^e b_n^e q_n^e v_{en}^+}{b(\alpha + i\gamma_{2n})} \right], \quad (9)$$

where  $M_{+}^e(\alpha)$  and  $N_{+}^e(\alpha)$  are split functions of the Wiener-Hopf kernels [4], and

$$a_n^e = [(n-1/2)\pi]^2 / b i \gamma_{2n-1}, \quad b_n^e = (n\pi)^2 / b i \gamma_{2n}, \quad (10)$$

$$p_n^e = M_+^e(i\gamma_{2n-1})/b^{1/2}, \quad q_n^e = N_+^e(i\gamma_{2n})/b^{1/2}, \quad (11)$$

$$u_{en}^+ = U_{(+)}^e(i\gamma_{2n-1})/b, \quad v_{en}^+ = V_{(+)}^e(i\gamma_{2n})/b, \quad (12)$$

$$\kappa_n^e = \frac{\rho_{2n}^e e^{-2\Gamma_{2n}(d_2-d_1)} - \rho_{3n}^e}{1 - \rho_{2n}^e \rho_{3n}^e e^{-2\Gamma_{2n}(d_2-d_1)}}, \quad \rho_{3n}^e = \frac{\mu_3 \gamma_n - \Gamma_{3n}}{\mu_3 \gamma_n + \Gamma_{3n}}, \quad (13)$$

$$\rho_{1n}^e = \frac{(\mu_2/\mu_1)\Gamma_{1n} - \zeta_{1n}^e \Gamma_{2n}}{(\mu_2/\mu_1)\Gamma_{1n} + \zeta_{1n}^e \Gamma_{2n}}, \quad \zeta_{1n}^e = \frac{1 - e^{-2\Gamma_{1n}(d_1-d_2)}}{1 + e^{-2\Gamma_{1n}(d_1-d_2)}}, \quad (14)$$

$$\rho_{2n}^e = \frac{(\mu_3/\mu_2)\Gamma_{2n} - \zeta_{2n}^e \Gamma_{3n}}{(\mu_3/\mu_2)\Gamma_{2n} + \zeta_{2n}^e \Gamma_{3n}}, \quad \zeta_{2n}^e = \frac{1 - \rho_{1n}^e e^{-2\Gamma_{2n}(d_2-d_1)}}{1 + \rho_{1n}^e e^{-2\Gamma_{2n}(d_2-d_1)}}, \quad (15)$$

$$A_e = -\left(\frac{2b}{\pi}\right)^{1/2} \frac{\text{icos}(kb \sin \theta_0)}{M_+^e(k \cos \theta_0)}, \quad B_e = \left(\frac{2b}{\pi}\right)^{1/2} \frac{\sin(kb \sin \theta_0)}{N_+^e(k \cos \theta_0)}, \quad (16)$$

$$r_n = [(n\pi/2b)^2 - k^2]^{1/2}, \quad \Gamma_{mn} = [(n\pi/2b)^2 - \mu_m \varepsilon_m k^2]^{1/2} \text{ for } m = 1, 2, 3. \quad (17)$$

In (8) and (9), the unknowns  $u_{en}^+$  and  $v_{en}^+$  for  $n = 1, 2, 3, \dots$  are determined by solving appropriate matrix equations numerically. The above solution is valid for arbitrary cavity dimensions. The scattered field in real space for  $|x| > b$  can be derived by substituting (8) and (9) into (4) and evaluating the inverse Fourier transform asymptotically with the aid of the saddle point method. The analysis has thus far been carried out by assuming  $0 < \theta_0 < \pi/2$ , but the results are in fact true for arbitrary  $\theta_0$ .

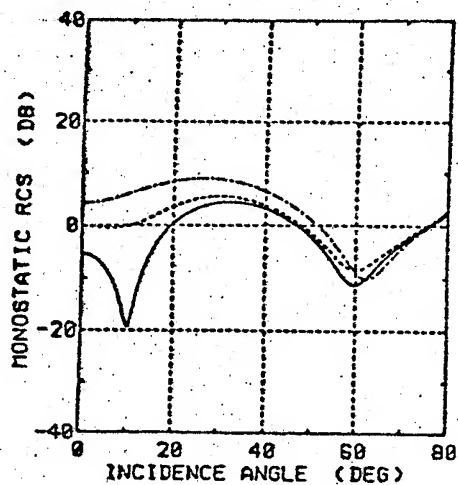
### 3. NUMERICAL RESULTS AND DISCUSSION

Figures 2 and 3 show numerical results of the monostatic RCS versus the incidence angle  $\theta_0$ . In numerical computations, cavity dimensions have been taken as  $kb = 3.14, 15.7, 31.4$  with  $d_1/2b = 1.0$  (Fig. 2) and  $2.0$  (Fig. 3). We have chosen Emerson & Cuming AN-73 as an example of existing three-layer materials, where the material constants are  $\varepsilon_1 = 3.4 + i10.0$ ,  $\varepsilon_2 = 1.6 + i0.9$ ,  $\varepsilon_3 = 1.4 + i0.35$ ,  $\mu_1 = \mu_2 = \mu_3 = 1.0$ , and the thickness of each layer is  $d_1 - d_2 = d_2 - d_3 = d_3 - d_4 (=t/3)$ . In order to investigate the effect of multilayer material loading, we have also computed the RCS for the single-layer case with  $\varepsilon_1 = \varepsilon_2 = \varepsilon_3 = 1.4 + i0.35$ ,  $\mu_1 = \mu_2 = \mu_3 = 1.0$ , and  $d_1 - d_4 = t$ . The thickness of the single- and three-layer materials is taken as  $kt = 2.08$ . In the figures, the results for no material loading have been added for comparison.

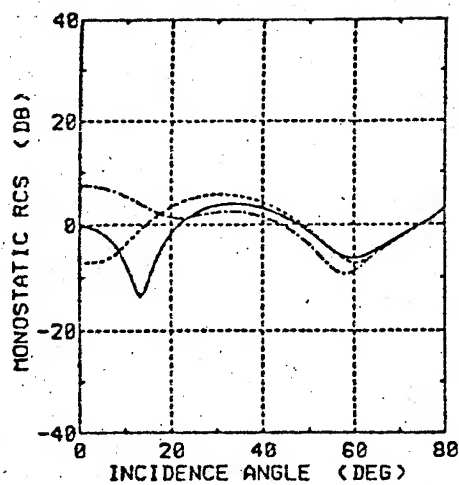
It is seen from the figures that, for empty cavities, the RCS exhibits large values due to the effect of interior irradiation, whereas the irradiation is reduced for the material-loaded case, particularly over  $0^\circ < \theta_0 < 60^\circ$ . Comparing the results for single- and three-layer loaded cavities, we observe that the RCS reduction is generally significant in the three-layer case. Therefore, it is inferred that multilayer lossy materials can be used as broadband absorbing structures. Similar analysis for the  $H$  polarization is carried out in the companion paper [4].

### REFERENCES

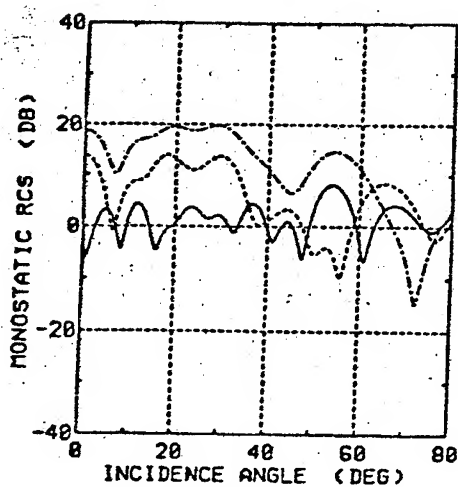
- [1] W. R. Stone, Ed., *Radar Cross Sections of Complex Objects*, IEEE Press, New York, 1990.
- [2] K. Kobayashi and A. Sawai, "Plane wave diffraction by an open-ended parallel plate waveguide cavity," *J. Electromagn. Waves Appl.*, **6**, 475, 1992.
- [3] S. Koshikawa and K. Kobayashi, "Wiener-Hopf analysis of the diffraction by a parallel-plate waveguide cavity with partial material loading," *IEICE Trans. Electron.*, **E77-C**, 1994, in press.
- [4] S. Koshikawa and K. Kobayashi, "Diffraction by a terminated, semi-infinite parallel-plate waveguide with three different material loading: part II - the case of  $H$  polarization," to be presented at *1994 International Conference on Mathematical Methods in Electromagnetic Theory (MMET-94)*, Kharkov, Ukraine, September 7-10, 1994.



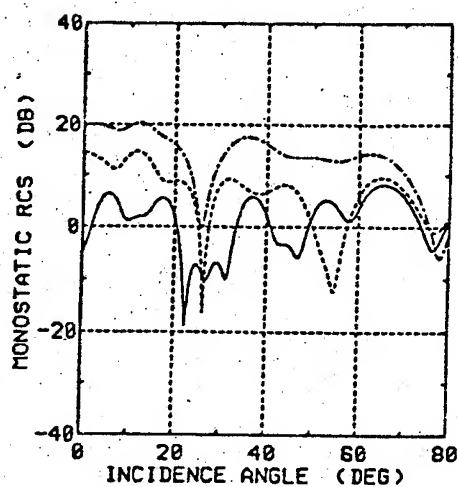
(a)  $kb = 3.14$ .



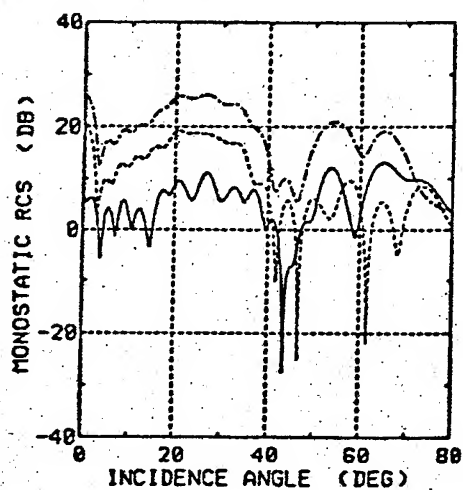
(a)  $kb = 3.14$ .



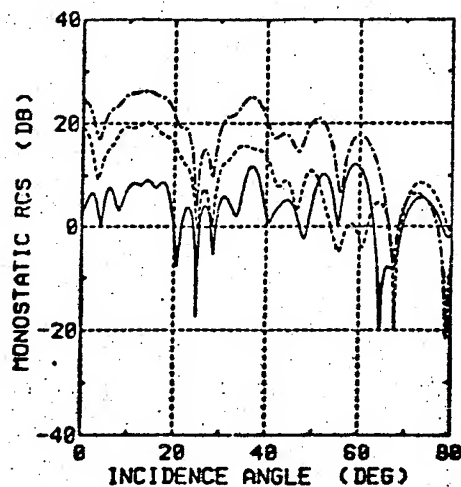
(b)  $kb = 15.7$ .



(b)  $kb = 15.7$ .



(c)  $kb = 31.4$ .



(c)  $kb = 31.4$ .

Fig. 2. Monostatic RCS [dB] versus incidence angle for  $d_1/2b = 1.0$ . — : empty.  
 ..... : single-layer.  
 — : three-layer.

Fig. 3. Monostatic RCS [dB] versus incidence angle for  $d_1/2b = 2.0$ . — : empty.  
 ..... : single-layer.  
 — : three-layer.



# DIFFRACTION BY A TERMINATED, SEMI-INFINITE PARALLEL-PLATE WAVEGUIDE WITH THREE DIFFERENT MATERIAL LOADING: PART II - THE CASE OF $H$ POLARIZATION

Shoichi Koshikawa and Kazuya Kobayashi

Department of Electrical and Electronic Engineering, Chuo University

1-13-27 Kasuga, Bunkyo-ku, Tokyo 112, Japan

(Tel: +81-3-3817-1869, Fax: +81-3-3817-1847, E-mail: kazuya@kawa.elect.chuo-u.ac.jp)

**Abstract** - In this second part of a two-part paper, the plane wave diffraction by a terminated, semi-infinite parallel-plate waveguide with three different material loading is rigorously analyzed for the  $H$ -polarized case using the Wiener-Hopf technique. The method of solution is similar to that developed in Part I for the case of  $E$  polarization. Illustrative numerical examples of the radar cross section (RCS) are given and the far field backscattering characteristics are discussed. It is confirmed that the effect of three-layer loading is more significant in the  $H$  polarization than in the  $E$  polarization.

## 1. INTRODUCTION

Analysis of the scattering by open-ended metallic waveguide cavities with material loading has received much attention recently in connection with the radar cross section (RCS) reduction of a target [1-4]. In Part I [5] of this two-part paper, we have considered a terminated, semi-infinite parallel-plate waveguide with three-layer material loading as an example of two-dimensional loaded cavities, and carried out a rigorous Wiener-Hopf analysis of the plane wave diffraction for the case of  $E$  polarization. It has been shown via numerical examples that, for large cavities, significant RCS reduction can be achieved by lossy material loading inside the cavity. Comparing the characteristics for single- and three-layer loaded cavities, we have also confirmed that the three-layer case generally gives better RCS reduction than the single-layer case.

In this second part, we shall treat the plane wave diffraction by the same cavity structure for the  $H$  polarization and derive the rigorous Wiener-Hopf solution following a method similar to that employed in Part I. Representative numerical examples on the RCS are presented for various physical parameters and the far field backscattering characteristics are investigated in detail. It is shown that the effect of three-layer loading is significant in the  $H$ -polarized case compared to the  $E$  polarization [5]. In the following, we shall use abbreviated citation of the equations and figures in Part I such as (I.1) and Fig. I.1 if necessary, where the prefix I and the second number denote Part I and the equation/figure number, respectively.

The time factor is assumed to be  $e^{-i\omega t}$  and suppressed throughout this paper.

## 2. RIGOROUS WIENER-HOPF SOLUTION

We consider a two-dimensional parallel-plate cavity with three-layer material loading, being illuminated by an  $H$ -polarized plane wave, as shown in Fig. 1, where the upper and lower plates of the waveguide and the endplate at  $z = -d_1$  are perfectly conducting and of zero thickness. The material layers I ( $-d_1 < z < -d_2$ ), II ( $-d_2 < z < -d_3$ ), and III ( $-d_3 < z < -d_4$ ) are, respectively, characterized by the relative permittivity/permeability  $(\epsilon_1, \mu_1)$ ,  $(\epsilon_2, \mu_2)$ , and  $(\epsilon_3, \mu_3)$ .

Let us define the total magnetic field  $\phi^i(x, z) [\equiv H_y^i(x, z)]$  as in (I.1), with the incident field  $\phi^i(x, z)$  being given by (I.2). As in the case of  $E$  polarization, we shall assume the vacuum to be slightly lossy so that the free-space wavenumber  $k$  has a small positive imaginary part.

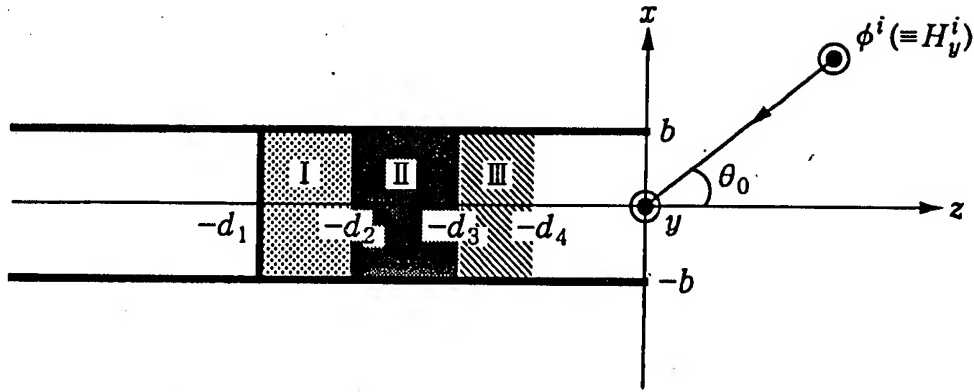


Fig. 1. Geometry of the problem.

If we define the Fourier transform of the scattered field  $\phi(x, z)$  as (I.3), it is seen that  $\Phi(x, \alpha)$  is regular in the strip  $-k_2 < \tau < k_2 \cos \theta_0$  of the  $\alpha$ -plane. Proceeding the same procedure as in the  $E$ -polarized case [5], the Fourier transform representation of the scattered field for  $x \geq \pm b$  is found to be

$$\Phi(x, \alpha) = \mp (1/2\gamma) [U_{(+)}^h(\alpha) \pm V_{(+)}^h(\alpha)] e^{\mp \gamma(x \mp b)} \quad (1)$$

with  $\gamma$  being defined in Part I, where

$$U_{(+)}^h(\alpha) = \Psi_{(+)}'(b, \alpha) + \Psi_{(+)}'(-b, \alpha), \quad V_{(+)}^h(\alpha) = \Psi_{(+)}'(b, \alpha) - \Psi_{(+)}'(-b, \alpha), \quad (2)$$

$$\Psi_{(+)}'(x, \alpha) = \Phi_+'(x, \alpha) + \frac{k \sin \theta_0 e^{-ikx \sin \theta_0}}{(2\pi)^{1/2}(\alpha - k \cos \theta_0)}, \quad (3)$$

$$\Phi_+'(x, \alpha) = (2\pi)^{-1/2} \int_0^\infty \frac{\partial \phi(x, z)}{\partial x} e^{iaz} dz. \quad (4)$$

In accordance with the Wiener-Hopf procedure as explained in Part I, the unknown functions  $U_{(+)}^h(\alpha)$  and  $V_{(+)}^h(\alpha)$  in (1) are determined as follows:

$$U_{(+)}^h(\alpha) = b^{1/2} M_+^h(\alpha) \left[ -\frac{A_h}{b(\alpha - k \cos \theta_0)} - \sum_{n=1}^{\infty} \frac{e^{-2\gamma_{2n-1} d_4} \kappa_{2n-1}^h a_n^h p_n^h u_{hn}^+}{b(\alpha + i\gamma_{2n-1})} \right], \quad (5)$$

$$V_{(+)}^h(\alpha) = b^{1/2} N_+^h(\alpha) \left[ \frac{B_h}{b(\alpha - k \cos \theta_0)} - \sum_{n=1}^{\infty} \frac{e^{-2\gamma_{2n-2} d_4} \delta_{2n-2}^h \kappa_{2n-2}^h b_n^h q_n^h v_{hn}^+}{b(\alpha + i\gamma_{2n-2})} \right], \quad (6)$$

where  $M_+^h(\alpha)$  and  $N_+^h(\alpha)$  are split functions of the Wiener-Hopf kernels (see Appendix), and

$$\delta_n = 1/2 \text{ for } n=0; \quad = 1 \text{ for } n \geq 1, \quad (7)$$

$$a_n^h = (bi\gamma_{2n-1})^{-1}, \quad b_n^h = (bi\gamma_{2n-2})^{-1}, \quad (8)$$

$$p_n^h = b^{1/2} M_+^h(i\gamma_{2n-1}), \quad q_n^h = b^{1/2} N_+^h(i\gamma_{2n-2}), \quad (9)$$

$$u_{hn}^+ = U_{(+)}^h(i\gamma_{2n-1}), \quad v_{hn}^+ = V_{(+)}^h(i\gamma_{2n-2}), \quad (10)$$

$$\kappa_n^h = \frac{\rho_{2n}^h e^{-2\Gamma_{3n}(d_3-d_4)} - \rho_{3n}^h}{1 - \rho_{2n}^h \rho_{3n}^h e^{-2\Gamma_{3n}(d_3-d_4)}}, \quad \rho_{3n}^h = \frac{\varepsilon_3 \gamma_n - \Gamma_{3n}}{\varepsilon_3 \gamma_n + \Gamma_{3n}}, \quad (11)$$

$$\rho_{1n}^h = \frac{(\varepsilon_2/\varepsilon_1) \zeta_{1n}^h \Gamma_{1n} - \Gamma_{2n}}{(\varepsilon_2/\varepsilon_1) \zeta_{1n}^h \Gamma_{1n} + \Gamma_{2n}}, \quad \zeta_{1n}^h = \frac{1 - e^{-2\Gamma_{1n}(d_1-d_2)}}{1 + e^{-2\Gamma_{1n}(d_1-d_2)}}, \quad (12)$$

$$\rho_{2n}^h = \frac{(\varepsilon_3/\varepsilon_2) \zeta_{2n}^h \Gamma_{2n} - \Gamma_{3n}}{(\varepsilon_3/\varepsilon_2) \zeta_{2n}^h \Gamma_{2n} + \Gamma_{3n}}, \quad \zeta_{2n}^h = \frac{1 + \rho_{1n}^h e^{-2\Gamma_{2n}(d_2-d_3)}}{1 - \rho_{1n}^h e^{-2\Gamma_{2n}(d_2-d_3)}}, \quad (13)$$

$$A_h = -\left(\frac{2b}{\pi}\right)^{1/2} \frac{k \sin \theta_0 \cos(kb \sin \theta_0)}{M_+^h(k \cos \theta_0)}, \quad B_h = -\left(\frac{2b}{\pi}\right)^{1/2} \frac{ik \sin \theta_0 \sin(kb \sin \theta_0)}{N_+^h(k \cos \theta_0)}. \quad (14)$$

In the above,  $\tau_0 = -ik$  and  $\Gamma_{m0} = -i(\mu_m \epsilon_m)^{1/2} k$  with  $m = 1, 2, 3$ , whereas  $\tau_n$  and  $\Gamma_{mn}$  with  $m = 1, 2, 3$  for  $n \geq 1$  have already been introduced in Part I. The unknowns  $u_{hn}^+$  and  $v_{hn}^+$  for  $n = 1, 2, 3, \dots$  in (5) and (6) are determined by solving appropriate matrix equations numerically. It is to be noted that the above solution is valid for arbitrary cavity dimensions. The scattered field in real space for  $|x| > b$  can be derived by substituting (5) and (6) into (1) and taking the Fourier inverse together with the use of the saddle point method.

### 3. NUMERICAL RESULTS AND DISCUSSION

Figures 2 and 3 show the monostatic RCS versus the incidence angle  $\theta_0$ , where all the parameters for numerical computation are the same as in Part I. It is noted from the figures that the RCS for empty cavities show large values due to the effect of interior irradiation, whereas the RCS is reduced for the case of material loading with all chosen values of  $kb$ . Comparing the results for empty cavities between the  $E$  and the  $H$  polarization, we notice that if the cavity dimension is small as in Figs. 1.2(a), 1.3(a), 2(a), and 3(a), there are great differences depending on the incident polarization. On the other hand, the RCS for both polarizations exhibits close features with an increase of the cavity dimension, as may be seen from Figs. 1.2(c), 1.3(c), 2(c), and 3(c). As regards loaded cavities, we find by comparing the results for the single- and three-layer cases between different polarizations that the effect of three-layer loading is more significant in the  $H$ -polarized case than in the  $E$  polarization.

### APPENDIX: SPLIT FUNCTIONS OF THE WIENER-HOPF KERNELS

The split functions appearing in this two-part paper are defined as

$$M_+^e(\alpha) = (\cos kb)^{1/2} e^{i\pi/4} (k + \alpha)^{-1/2} \exp[f(\alpha) - (iab/\pi) \ln 2] P_+(\alpha), \quad (A.1)$$

$$N_+^e(\alpha) = (\sin kb/k)^{1/2} \exp[f(\alpha) + (iab/\pi) \ln 2] Q_+(\alpha), \quad (A.2)$$

$$M_+^h(\alpha) = (\cos kb)^{1/2} e^{i3\pi/4} (k + \alpha)^{1/2} \exp[f(\alpha) - (iab/\pi) \ln 2] P_+(\alpha), \quad (A.3)$$

$$N_+^h(\alpha) = (k \sin kb)^{1/2} e^{i\pi/2} (1 + \alpha/i\tau_0) \exp[f(\alpha) + (iab/\pi) \ln 2] Q_+(\alpha), \quad (A.4)$$

where

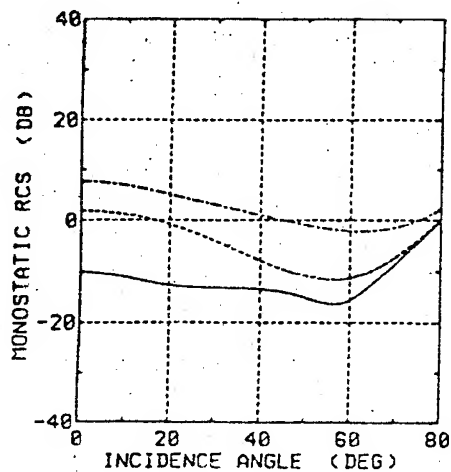
$$f(\alpha) = (i\tau b/\pi) \ln[(\alpha - \tau)/k] + (iab/\pi)[1 - C + \ln(\pi/kb) + i\pi/2], \quad (A.5)$$

$$P_+(\alpha) = \prod_{n=1, \text{odd}}^{\infty} (1 + \alpha/i\tau_n) e^{2iab/n\pi}, \quad Q_+(\alpha) = \prod_{n=2, \text{even}}^{\infty} (1 + \alpha/i\tau_n) e^{2iab/n\pi} \quad (A.6)$$

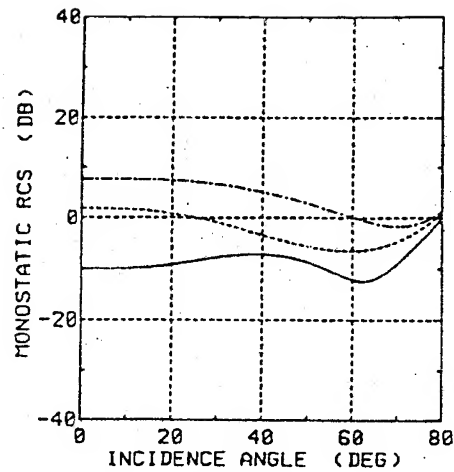
with  $C (= 0.57721566 \dots)$  being Euler's constant.

### REFERENCES

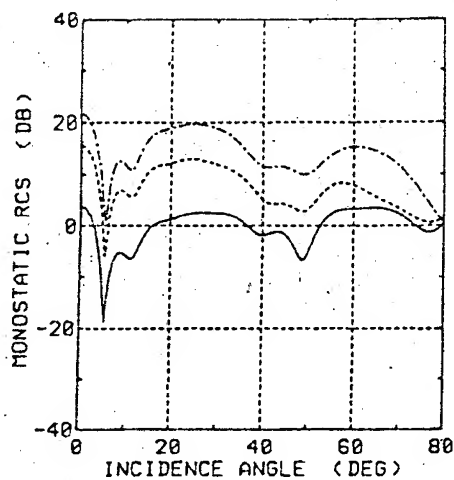
- [1] S.-W. Lee and H. Ling, "Data book for cavity RCS: Version 1," *Tech. Rep., Univ. Illinois*, No. SWL 89-1, 1989.
- [2] K. Kobayashi, S. Koshikawa, and A. Sawai, "Diffraction by a parallel-plate waveguide cavity with dielectric/ferrite loading: part I - the case of  $E$  polarization," in *Progress in Electromagnetics Research, PIER 8*, J. A. Kong, Ed., Elsevier, New York, 1994, in press.
- [3] S. Koshikawa and K. Kobayashi, "Diffraction by a parallel-plate waveguide cavity with dielectric/ferrite loading: part II - the case of  $H$  polarization," in *Progress in Electromagnetics Research, PIER 8*, J. A. Kong, Ed., Elsevier, New York, 1994, in press.
- [4] S. Koshikawa and K. Kobayashi, "Wiener-Hopf analysis of the diffraction by a parallel-plate waveguide cavity with partial material loading," *IEICE Trans. Electron.*, E77-C, 1994, in press.
- [5] S. Koshikawa and K. Kobayashi, "Diffraction by a terminated, semi-infinite parallel-plate waveguide with three different material loading: part I - the case of  $E$  polarization," to be presented at *1994 International Conference on Mathematical Methods in Electromagnetic Theory (MMET\* 94)*, Kharkov, Ukraine, September 7-10, 1994.



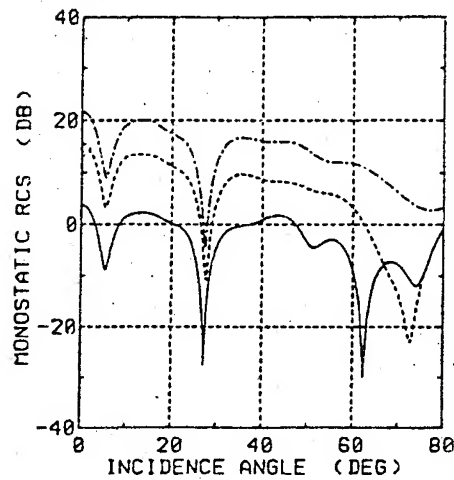
(a)  $kb = 3.14$ .



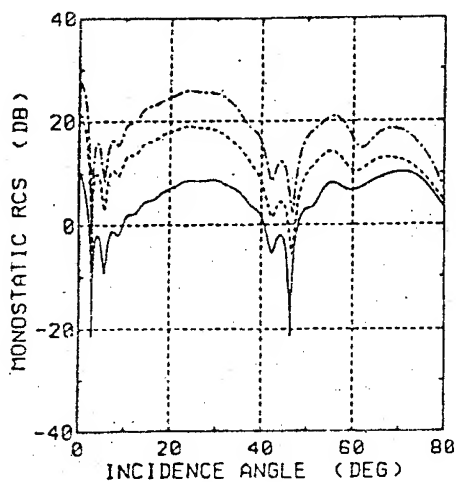
(a)  $kb = 3.14$ .



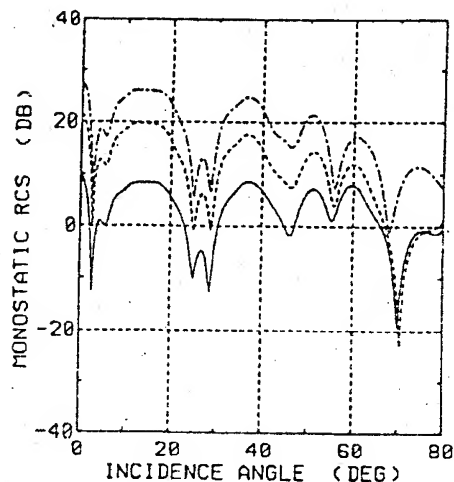
(b)  $kb = 15.7$ .



(b)  $kb = 15.7$ .



(c)  $kb = 31.4$ .



(c)  $kb = 31.4$ .

Fig. 2. Monostatic RCS [dB] versus incidence angle for  $d_1/2b = 1.0$ . — : empty.  
 ..... : single-layer.  
 — : three-layer.

Fig. 3. Monostatic RCS [dB] versus incidence angle for  $d_1/2b = 2.0$ . — : empty.  
 ..... : single-layer.  
 — : three-layer.

# THE IMPROVED POINT-MATCHING METHOD WITH MATHIEU FUNCTION EXPANSION FOR ELLIPTICAL FIBERS

Zygmunt Krasiński and Adam Majewski

Institute of Electronics Fundamentals, Warsaw University of Technology  
Nowowiejska 15/19, 00-665 Warsaw, Poland

Takashi Hinata

College of Science & Technology, Nihon University  
1-8 Surugadai, Chiyoda-ku, Tokyo 101, Japan

## ABSTRACT

We present the improved point-matching method with Mathieu function expansion for the accurate analysis of the W-type elliptical fiber with layers of any ellipticity. Limitations of previously reported method are discussed. Numerical results illustrating the application of our method to investigate the highly-birefringent elliptical fibers with a hollow layer are presented. From the convergence tests, it is confirmed that the relative error of the modal birefringence is less than 0.01%. The proposed method can be extended for analysis of the elliptical fibers with hollow pits and electromagnetic scattering problems by targets of the complex elliptical geometry.

## INTRODUCTION

The double-step confocal-elliptical fibers were analyzed by the exact analytical method with Mathieu function expansion [1], [2]. Among several structures of such fibers, the W-type fiber was suggested for low-dispersion and polarization-maintaining applications. In order to investigate the W-type elliptical fibers with layers of any ellipticity  $e_j$  [ $=1-b_j/a_j$ ,  $j=\{1,2\}$ , see Fig. 1], a few numerical methods were proposed, f.e. the point-matching method with Bessel function expansion [3] and the Yasuura's mode-matching method (Y-MMM) with Bessel function expansion [4]. In these methods, however, high accuracy may not be expected for larger ellipticities ( $e_j > 0.5$ ) [4].

In this paper we present the improved point-matching method (IPMM) with Mathieu function expansion for the accurate analysis of the polarization-maintaining W-type elliptical fiber with layers of any ellipticity. It is shown that the numerical results by IPMM are quite reliable. Our results are compared with those by Y-MMM. Numerical results illustrating the application of our IPMM to investigate the highly-birefringent elliptical fibers with a hollow layer are also included.

## FORMULATION

The cross section of the W-type elliptical fiber is shown in Fig. 1. Two elliptical coordinate systems  $(\xi_1, \eta_1, z)$  and  $(\xi_2, \eta_2, z)$  are introduced for the complete modal expansions and two of the elliptical cylinders with  $\xi_1 = \xi_{10}$  and  $\xi_2 = \xi_{20}$  are assumed to coincide with the boundaries of the layer 1 and 2, respectively. The refractive index in the layer of a number  $i$  is denoted by  $n_i$ , where

$i=\{1,2,3\}$  and it is assumed, that  $n_1 > n_3 > n_2$ . The propagation factor  $e^{j(\omega t - \beta z)}$ , where  $\beta$  is the propagation constant in the  $z$ -direction and  $\omega$  is the angular frequency, will be omitted in the expressions for the field components. Since the fiber structure is symmetrical about the  $x$  axis, the electromagnetic fields can be separated into the odd modes  ${}_o\text{HE}_{mp}$ ,  ${}_o\text{EH}_{mp}$  and the even modes  ${}_e\text{HE}_{mp}$ ,  ${}_e\text{EH}_{mp}$ . In our IPMM the  $z$ -components of electric and magnetic fields ( $E_z$  and  $H_z$ ) for the odd modes are approximated by the complete modal expansions with the Mathieu functions as follows:

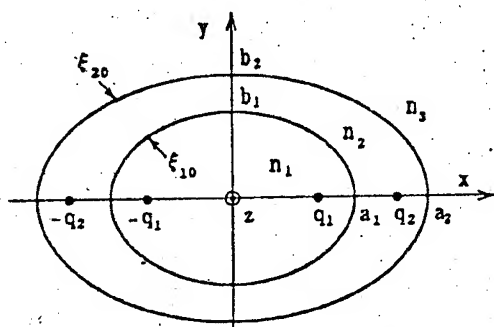


Fig. 1 Cross section of the W-type elliptical fiber:  $n_1 > n_3 > n_2$

In layer 1:

$$E_z^{(1)} = \sum_{n=0}^{N-1} A_n^{(1)} Ce_n(\xi_1, \gamma_1^2) ce_n(\eta_1, \gamma_1^2) \quad (1)$$

$$H_z^{(1)} = \sum_{n=1}^{N-1} B_n^{(1)} Se_n(\xi_1, \gamma_1^2) se_n(\eta_1, \gamma_1^2) \quad (2)$$

In layer 2:

$$E_z^{(2)} = \sum_{l=0}^{L-1} A_l^{(2)} Ce_l(\xi_2, -\gamma_{22}^2) ce_l(\eta_2, -\gamma_{22}^2) + \sum_{n=0}^{N-1} C_n^{(2)} Fek_n(\xi_1, -\gamma_{21}^2) ce_n(\eta_1, -\gamma_{21}^2) \quad (3)$$

$$H_z^{(2)} = \sum_{l=1}^{L-1} B_l^{(2)} Se_l(\xi_2, -\gamma_{22}^2) se_l(\eta_2, -\gamma_{22}^2) + \sum_{n=1}^{N-1} D_n^{(2)} Gek_n(\xi_1, -\gamma_{21}^2) se_n(\eta_1, -\gamma_{21}^2) \quad (4)$$

In layer 3 (the cladding):

$$E_z^{(3)} = \sum_{l=0}^{L-1} A_l^{(3)} Fek_l(\xi_2, -\gamma_3^2) ce_l(\eta_2, -\gamma_3^2) \quad (5)$$

$$H_z^{(3)} = \sum_{l=1}^{L-1} B_l^{(3)} Gek_l(\xi_2, -\gamma_3^2) se_l(\eta_2, -\gamma_3^2) \quad (6)$$

where  $\gamma_1^2 = q_1^2(k_1^2 - \beta^2)/4$ ,  $-\gamma_{2j}^2 = q_j^2(k_2^2 - \beta^2)/4$ ,  $-\gamma_3^2 = q_2^2(k_3^2 - \beta^2)/4$  and  $k_i = k n_i$ ,  $q_j$  is the semifocal length in elliptical coordinate system of a number  $j$ ,  $j = \{1, 2\}$ ,  $k$  is the wavenumber in free space;  $ce_n(\cdot)$ ,  $se_n(\cdot)$  are the even and odd Mathieu functions of the first kind;  $Ce_n(\cdot)$ ,  $Se_n(\cdot)$  are the even and odd modified Mathieu functions of the first kind;  $Fek_n(\cdot)$ ,  $Gek_n(\cdot)$  are the even and odd modified Mathieu functions of the second kind.  $N$  and  $L$  are the number of space harmonics taken in our IPMM. The coefficients  $A_n^{(1)} \sim B_l^{(3)}$  of Eqs. 1-6 are determined from the boundary conditions. Axial field components for the even modes are in the form of Eqs. 1-6, when the even Mathieu functions are replaced by the odd ones and vice versa. The total transverse components of the field in layer 2 can be expressed by combining the fractional  $\xi$ -component and  $\eta$ -component in two elliptical coordinate systems at any points at  $\xi_{10}$  and  $\xi_{20}$  as [5]:

$$\Psi_{\eta_1} = \phi_{\eta_1} + \phi_{\eta_2} \cos \gamma_1 - \rho_1 \phi_{\xi_2} \sin \gamma_1 \quad (7)$$

$$\Psi_{\eta_2} = \phi_{\eta_2} + \phi_{\eta_1} \cos \gamma_2 + \rho_2 \phi_{\xi_1} \sin \gamma_2 \quad (8)$$

where  $\Psi$  and  $\phi$  are the total and fractional field components ( $= \{E^{(2)}, H^{(2)}\}$ ), respectively,  $\gamma_j$  is the angle between  $\eta_1$ -component and  $\eta_2$ -component,  $\rho_j = 1$  or  $-1$ .

Because of the symmetry of the structure, only the first quadrant of the fiber cross-section is used in the analysis. The propagation constants of modes are computed for the even mode number expansions (EMNE) and the odd mode number expansions (OMNE) of the fields. By matching the tangential fields at the equiangularly spaced points around the boundaries between layers of the fiber, we obtain simultaneously homogeneous linear equations:  $4(N+L-1)$  for EMNE and  $4(N+L)$  for OMNE and finally the characteristic equation, from which we can get the propagation constants.

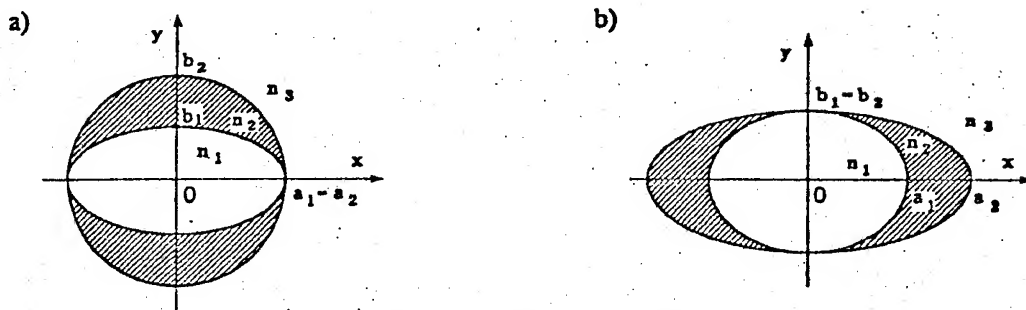


Fig. 2 Models of W-type elliptical fibers:  $n_1 > n_3 > n_2$

In the following analysis the parameters are defined as follows:  $P_{o,e} = [(\beta_{o,e}/k)^2 - n_3^2] / (n_1^2 - n_3^2)$  is the normalized propagation constant and  $V = ka_1(n_1^2 - n_3^2)^{1/2}$  is the normalized frequency, where  $\beta_o$  and  $\beta_e$  denote the propagation constants of the odd and even fundamental mode, respectively. The propagation constants  $\beta_o$  and  $\beta_e$  are the maximum values of  $\beta$  for the even and the odd mode number expansions of the modes. The results are presented for the case, when  $N=L$ .

### RESULTS AND DISCUSSION

The Fortran programs for the Mathieu functions which we use in our numerical computations have been developed by Yamashita [6], [7]. The accuracy of the Mathieu functions is confirmed to be of more than ten significant digits for the double precision computations. Such accuracy is necessary in view of the computational errors involved in large matrix operations.

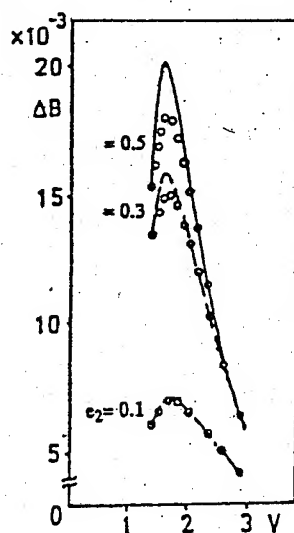


Fig. 3 Characteristics of  $\Delta B$  versus  $V$  for fibers as shown in Fig. 2(b) with different values of  $e_2$ ,  $e_1=0$ ,  $n_1=1.5$ ,  $n_2=1.3$  and  $n_3=1.4$

Curves correspond to Ref. [4] and  
circle-points correspond to our IPMM

Fig. 3 shows the dependence of the difference in normalized propagation constants  $\Delta B = |P_o - P_e|$  on the normalized frequency  $V$  for fibers as shown in Fig. 2(b), having different ellipticities  $e_2$ ,  $e_1=0$ ,  $n_1=1.5$ ,  $n_2=1.3$  and  $n_3=1.4$ . The difference  $\Delta B$  is proportional to the modal birefringence  $B = |(\beta_o - \beta_e)/k|$  and it was used by Miyamoto to express a degree of polarization-preservation in fibers. As can be seen from Fig. 3, the results reported in [4] (curves) are in substantial disagreement with our results (circle-points) in the region of interest, namely near the  $V$ -value corresponding to maximum birefringence. In the presented case, results of Y-MMM are accurate enough for fibers of very small  $e_1$ . The convergence tests for  $\Delta B$  as a parameter of  $e_2$ , for fibers as considered in Fig. 3 (with the additional case of  $e_2=0.7$ ), when  $V=1.6$ , are illustrated in Fig. 4. It is noted that the convergence of  $\Delta B$  depends significantly on ellipticity of the layer 2. Numerical computations were carried out by using the truncation number  $N$ , which

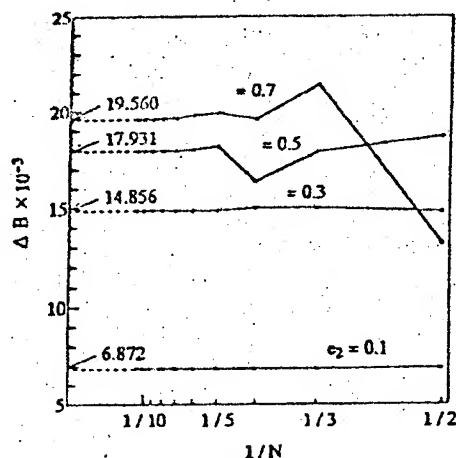


Fig. 4  $\Delta B$  versus  $1/N$  for fibers as analyzed in Fig. 3 with different values of  $e_2$ ,  $e_1=0$ ,  $n_1=1.5$ ,  $n_2=1.3$  and  $n_3=1.4$

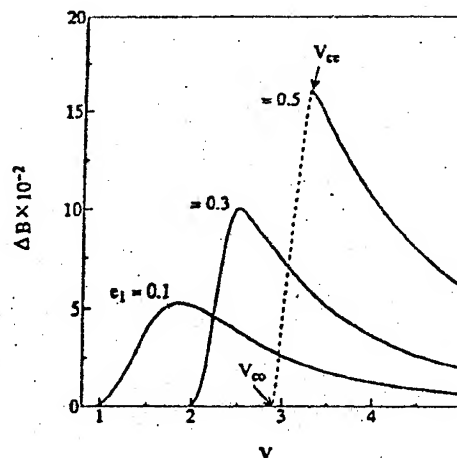


Fig. 5 Characteristics of  $\Delta B$  versus  $V$  for W-type fibers as shown in Fig. 2(a) with a hollow layer 2, different values of  $e_1$ ,  $e_2=0$ ,  $n_1=1.5$  and  $n_3=1.4$

makes the relative error of  $\Delta B$  less than 0.01%. Fig. 5 shows the dependence of  $\Delta B$  on  $V$  for the elliptical fibers with a hollow layer 2 and  $a_1=a_2$  (Fig. 2(a)), having different ellipticities  $e_1$ ,  $e_2=0$ ,  $n_1=1.5$  and  $n_3=1.4$ . It is noted that such fibers can realize the large value of modal birefringence. In the frequency range  $V_{co} < V < V_{cc}$  for  $e_1=0.5$  (broken-line curves) the single-polarization transmission is possible and we have that  $V_{cc} \cong 3.276$  and  $V_{co} \cong 2.889$  ( $V_{cc}$  and  $V_{co}$  denote the normalized cut-off frequencies of the even and odd fundamental mode, respectively).

### CONCLUSIONS

We have presented the improved point-matching method with Mathieu function expansion for the analysis of the W-type elliptical fibers. Results of our IPMM are quite reliable for the fibers with layers of any ellipticity, because: 1. The electromagnetic fields in each layer of the fiber are expanded by a sum of the complete set of wave functions; 2. The Mathieu functions are calculated to more than ten significant digits over the range of arguments and orders used; 3. From the convergence tests, it is confirmed that the relative error of the modal birefringence is less than 0.01%; 4. Our method never produces spurious numerical solutions. From the numerical analysis it was found that W-type fibers as shown in Fig. 2(a), with a hollow layer 2, can realize the large value of modal birefringence and they may be useful for the single-mode single-polarization transmission.

Owing to its flexibility and accuracy, the IPMM proposed in this paper can be a useful tool for analysis of a large class of fibers (f.e. elliptical fibers with hollow pits) and electromagnetic scattering problems by targets of the complex elliptical geometry.

### REFERENCES

- (1) S.R. RENGARAJAN and J.E. LEWIS: 'Single-mode propagation in multi-layer elliptical fiber waveguides', *Radio Science*, 1981, 16, (4), pp. 541-547.
- (2) Z. KRASIŃSKI and A. MAJEWSKI: 'Numerical analysis of single-mode confocal-elliptical fibers. II', *Bulletin of Polish Academy of Sciences*, 1991, 39, (4), pp. 695-709.
- (3) E. YAMASHITA, K. ATSUKI and Y. NISHINO: 'Composite dielectric waveguides with two elliptic-cylinder boundaries', *IEEE Trans.*, 1981, MTT-29, (9), pp. 987-990.
- (4) T. MIYAMOTO: 'Accurate numerical analysis of polarisation-preserving optical fibre with three-layer elliptical cross-section', *IEE Proc. J*, 1991, 138, (1), pp. 1-6.
- (5) Z. KRASIŃSKI, A. MAJEWSKI and T. HINATA: 'Accurate numerical analysis of polarization-maintaining W-type elliptical fibers', *Opto-Electronics Review*, 1993, 4, pp. 111-114.
- (6) S. YAMASHITA: 'On the calculation of eigenvalues of Mathieu function', *Trans. IPS Japan*, 1992, 33, (11), pp. 1290-1295 (in Japanese).
- (7) S. YAMASHITA: 'Note on the recurrence techniques for Bessel function and its application to Mathieu function', *Trans. IPS Japan*, 1993, 34, (2), pp. 191-195 (in Japanese).



# DIFFRACTION EFFECTS AT THE ELECTROMAGNETIC SCATTERING BY AN INHOMOGENEOUS PLASMA

Sergey V. Krestyaninov, Andrey M. Lebedev, Valeriy A. Permyakov  
Department of Radio Engineering, The Moscow Power Engineering  
Institute, Krasnokazarmennaya, 14, Moscow, 111250, USSR

## ABSTRACT

Two diffraction effects in the illuminated region of inhomogeneous plasma bodies are discussed.

## INTRODUCTION

We investigate two diffraction effects arising in the illuminated region of an inhomogeneous isotropic plasma with an overdense core. The first effect is conditioned by peculiarities of E-wave ( $\nabla \epsilon \neq 0$ ) propagation in a smoothly inhomogeneous plasma which is not taken into account by classical geometrical optics (GO). This effect is described with special modification of geometrical optics (MGO - see Ref. [1]). Another diffraction effect in the lit plasma region is observed when local curvature radius is small compared with the phase deviation scale for a local plane wave.

## METHODS OF ANALYSIS

For investigation of diffraction effects in the lit region of inhomogeneous plasma we apply two groups of methods: numerical and asymptotical.

Numerical methods. For radially inhomogeneous scatterers (cylinder, sphere) was used the well-known eigen-function method. For two-dimensionally inhomogeneous plasma cylinder was used the method of finite elements. The peculiarities of E-wave ( $\nabla \epsilon \neq 0$ ) propagation in an inhomogeneous plasma are taken into account on numerical realization of methods. For this purpose we apply the method of analytical extension in the region  $\epsilon \approx 0$ .

Asymptotical methods. For asymptotical solution we apply the geometrical optics and the method of interferential integrals (by H-polarisation of incident wave, when  $H \nabla \epsilon \neq 0$ ), and modifications of the geometrical optics and of the method of interferential integrals (by E-polarisation of incident wave, when  $E \nabla \epsilon \neq 0$ ). Also we apply the parabolic equation method.

## PHYSICAL RESULTS

Consider the first effect which is conditioned by peculiarities of E-wave ( $\nabla \epsilon \neq 0$ ) propagation in a smoothly inhomogeneous plasma and is not taken into account by classical GO (see ref. [1]).

Let the plane wave be diffracted on inhomogeneous plasma bodies of the finite dimensions. The divergence of the E- and H-rays reflected from a finite dimension, plasma bodies can be considerably distinguished in the far zone. The divergence of the E-rays is less than that of the H-rays because  $|\nabla \epsilon_{ef}| > |\nabla \epsilon|$  and  $r_{10} > r_0$ . (The effective overdense core radius  $r_{10}$  and the overdense core radius  $r_0$  are defined by equations  $\epsilon_{ef}(r_{10})=0$  and  $\epsilon(r_0)=0$ , respectively). In accordance with this conclusion the bistatic cross-section near backscattering direction (when the resonant attenuation in region  $\epsilon \approx 0$  is neglected) is greater for E-rays than for H-rays. For example consider the back-scattering cross-section for a radially inhomogeneous plasma sphere

$$\sigma = \pi \rho^2 \left| (2I_H)^{-1} \exp(-2i\Phi_H) - R_E(0) (2I_E)^{-1} \exp(-2i\Phi_E) - \varepsilon'(\rho)/8 \right|^2 \alpha, \quad (1)$$

where the  $\rho$  - external sphere radius (at  $\varepsilon=1$ ),  $r_0$  and  $r_{10}$  are defined above,

$$\Phi_H = k_0 \int_{r_0}^{\rho} \sqrt{\varepsilon} dr, \quad I_H = 1 + \rho \int_{r_0}^{\rho} dr/r^2 \sqrt{\varepsilon}, \quad (2)$$

$$\Phi_E = k_0 \int_{r_{10}}^{\rho} \sqrt{\varepsilon_{ef}} dr, \quad I_E = 1 + \rho \int_{r_{10}}^{\rho} dr/r^2 \sqrt{\varepsilon_{ef}},$$

and  $R_E(0) = R_E$  at  $h=0$ . We take into account also the jump of the permittivity derivative at the boundary of the sphere together with divergent E- and H-rays in Eqn. (2).

Analogous expressions for the radially inhomogeneous cylinder back-scattering cross-sections for a perpendicular plane wave incidence (the jump  $\varepsilon(\rho)$  is neglected) are given by

$$\sigma_E = \pi \rho I_E^{-1} \text{ at } (\nabla \varepsilon) \neq 0, \quad \sigma_H = \pi \rho I_H^{-1} \text{ at } (\nabla \varepsilon) = 0 \quad (3)$$

where  $I_E$  and  $I_H$  are defined in Eqn. (2), the  $\rho$  - external cylinder radius.

As opposed to back-scattering, the bistatic cross-section in the vicinity of resonant attenuation maximum defined by condition  $h|k_0/\nabla \varepsilon| \approx 0.7$  is less for E rays than for H rays.

The considerations mentioned above are confirmed by comparing of MGO approximation with the numerical solution for the diffraction of a plane wave from radially inhomogeneous scatterers.

Consider a few numerical examples. The back-scattering cross-section of the radially inhomogeneous sphere with linear law  $\varepsilon = a(r - r_0)$  as a function of the permittivity gradient "a" is shown in Fig. 1 for  $k_0 r_0 = 8$ . The solid line represents the results of computer calculations using the eigenfunction method. The dash-star line indicates MGO and the dashed line gives the standard GO (the same notations are also used in Figures below). Fig. 1 shows that the inhomogeneous sphere back-scattering cross-section is described well by MGO as opposed to GO which gives a lower value for backscatter. The scattering amplitude diagrams for a radially inhomogeneous cylinder with Gaussian law  $\varepsilon(r) = 1 - B \exp(-\alpha k_0^2 r^2)$  at  $B=5.75$ ,  $\alpha=0.51$  are plotted in Fig. 2 for two polarisations of an incident plane wave. From this figure one can see that in the lit region the bistatic cross-section of the radially inhomogeneous cylinder (at  $E \nabla \varepsilon \neq 0, H \nabla \varepsilon = 0$ ) is satisfactorily described by MGO.

Consider now the diffraction effect arising from the small overdense core of a plasma body. Physically, the existence of this effect seems obvious by the absence of an overdense core when the back-scattering field is equal to zero in GO approximation, but in fact, it is not equal to zero. We shall find the criterion of this effect with the parabolic equation approximation. The permittivity  $\varepsilon(x, y, z)$  near the surface  $\varepsilon = \text{const}$  is described by expansion

$$\begin{aligned} \varepsilon(x, y, z) = & \varepsilon(0, 0, t) + \varepsilon'_t(0, 0, t)(z - t) + 0.5\varepsilon''_{xx}(x, 0, t)|_{x=0}x^2 + \\ & + 0.5\varepsilon''_{yy}(0, y, t)|_{y=0}y^2 \dots \end{aligned} \quad (4)$$

when the z axis is parallel  $\nabla \varepsilon$ . Let the plane wave go to the surface  $\varepsilon = \text{const}$  in an inhomogeneous media in direction z.

The criterion of this diffraction effect can be obtained from parabolic equation and can be written in the form [2]

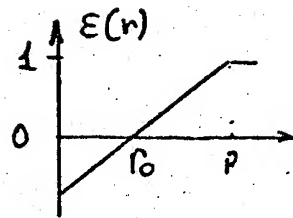
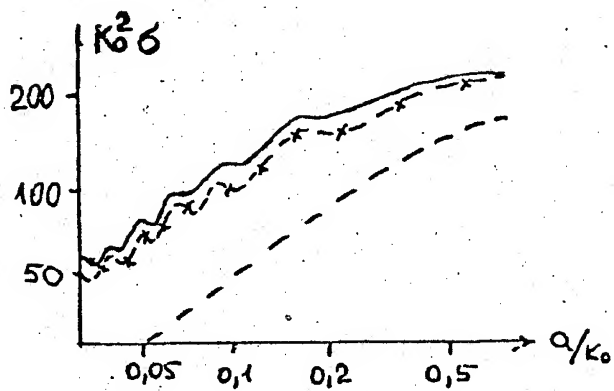


Fig. 1.

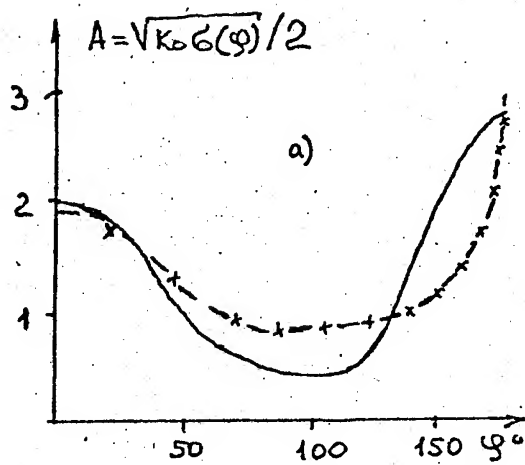
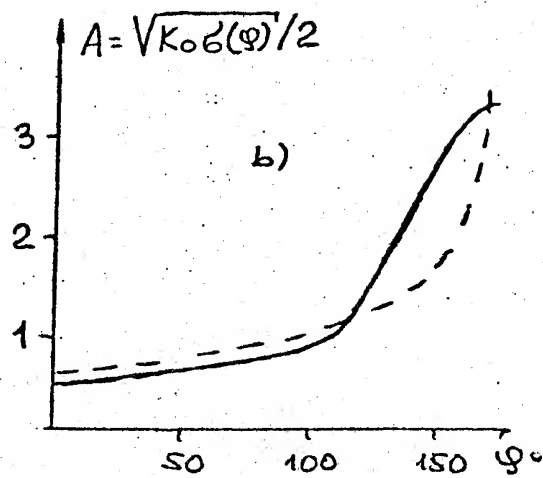


Fig 2 a)  $\bar{E} \nabla E \neq 0, \bar{H} \nabla E = 0$



b)  $\bar{E} \nabla E = 0, \bar{H} \nabla E \neq 0$

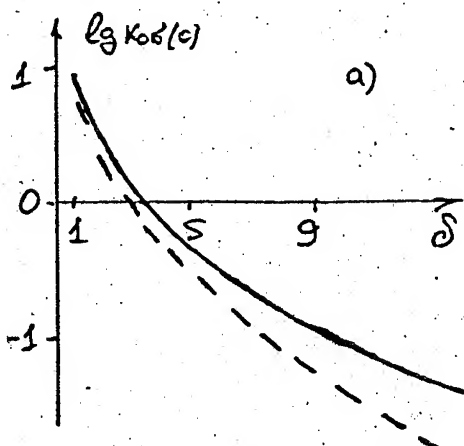
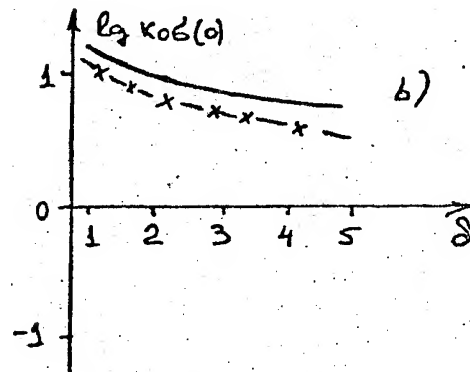


Fig 3. a)  $\bar{E} \nabla E = 0, \bar{H} \nabla E \neq 0$



b)  $\bar{E} \nabla E \neq 0, \bar{H} \nabla E = 0$

$$R_m = 2 \left[ \left| \frac{\partial \varepsilon / \partial z}{\partial^2 \varepsilon / \partial x^2} \right| + \left| \frac{\partial \varepsilon / \partial z}{\partial^2 \varepsilon / \partial y^2} \right| \right]^{-1} < L_\varphi = \begin{cases} (k_0 \varepsilon)^{-1}, & \varepsilon \neq 0 \\ k_0^{-1} (\partial \varepsilon / \partial k_0 z)^{-1/3}, & \varepsilon \approx 0 \end{cases} \quad (5)$$

The approximate expression for the mean curvature radius  $R$  in the point  $(0,0,t)$  of surface  $\varepsilon = \text{const}$  is in the left-hand side of this inequality. The phase deviation scale is in the right-hand side.

Thus, this diffraction effect arises when surface  $\varepsilon = 0$  local curvature radius becomes less than the phase deviation scale for a local plane wave. The criterion (5) is defined for scalar case.

The diffraction effect described above was analytically investigated for the plane wave diffraction from radially inhomogeneous sphere. The asymptotic investigation of the scattered field, with the help of E- and H-waves WKB asymptotics gives the following expression for the back-scattering cross-section of a plasma sphere with power profile  $\varepsilon = a r^m$ :

$$\sigma = \frac{\lambda^2}{4\pi} \left| \left( \frac{m+2}{2\pi} \right)^2 \exp \left[ -\frac{14k_0 \rho}{m+2} \right] + (i\pi - 1) \left( \frac{m+2}{2\pi} \right)^2 \exp \left[ -\frac{14k_0 \rho}{m+2} + i\pi \right] + \frac{i\varepsilon(\rho)k_0 \rho}{8} \right|^2, \quad (6)$$

where  $\mu = (2/(m+2)) \sqrt{m^2/4 + m/2}$ , and  $\rho = a \frac{1}{m}$ , the  $\lambda$ -wave length in a free space. If we can neglect  $\nabla \varepsilon$  jump at the boundary of the sphere, we see from Eqn. (6) that back-scattering cross-section has a value  $\approx \lambda^2$  for  $\varepsilon(0) = 0$ .

To determine this diffraction effect value for two-dimensional and three-dimensional scatterers, we must apply numerical methods. Consider the results of the back-scattering cross-section calculations for a two-dimensional inhomogeneous cylinder with law  $\varepsilon = 1 - B \exp(-\alpha k^2(x^2 + \delta y^2))$  where  $\delta \geq 1$ , and the direction of wave incidence is along axis  $x$ . The cross-sections of inhomogeneous plasma cylinder for two polarisations of incident plane wave are plotted in Fig. 3 for  $B=2.818$ ,  $\alpha=0.0625$ . They were calculated by the finite element method (solid line) and by the GO approximation (dashed line, Fig. 3a) or the MGO approximation (dashed and star line, Fig 3b, in this case we drop the term  $\Delta \varepsilon$  in  $\varepsilon$  ef). One can see good agreement between GO (or MGO for another polarisation) and numerical results when parameter  $\delta$  is near unit. We see also that diffraction effects arise with an increase in parameter  $\delta$ , in accordance with estimation (5).

### CONCLUSION

Interesting diffraction effects may be observed in experiments on electromagnetic wave scattering by natural and artificial plasma inhomogeneities. For example it has been shown that for the case of scattering by meteor trails with a big (i.e.  $> \lambda/2\pi$ ) overdenoe region radius, the MGO approximation can explain the increase in E-wave ( $E \nabla \varepsilon \neq 0$ ) scattering, as compared to H-wave ( $E \nabla \varepsilon = 0$ ) scattering.

### REFERENCES

1. Permyakov V.A., Kreстьяninov S.V. Modified geometrical optics for an inhomogeneous isotropic plasma. MMET-94.
2. Permyakov V.A. The criterions of diffraction effects in the lit region of an inhomogeneous plasma's bodies. Pisma v zhurnal tekhnicheskoi fiziki. 1993. V.I9. N.I6. P.70-73. (In Russian)

# DETERMINATION OF SPRAY DISTRIBUTION OVER THE SEA SURFACE BY RADAR

G.P.Kulemin, S.A.Velichko  
Institute of Radiophysics and Electronics,  
National Academy of Science,  
12, Ak.Proskury St., 310085, Kharkov, Ukraine

## ABSTRACT

It has been analysed the possibility to obtain the velocity and the size distributions of the drops appeared over the sea surface during the wave breaking. Bimodal current power spectra of the scattered signals were took into account; on this base the spectra parts connected with the spray removing by air flows were investigated; as a result it allowed to formulate the relation between the velocity and size drops distribution and the noted spectra parts. Moreover, the mean windspeed at the medium heights above the surface has been estimated, as well as the mean height of the layer included the drops transferring.

## 1. INTRODUCTION

It is need for the various applications to know the distribution features of the water drops, generated during the wave crests breaking and carried away from these crests by the wind flow. They are both the oceanology investigations, and the radar clutter level estimation for the sea monitoring by X- and Ku- radiowave bands. As a rule, in-situ methods are used successfully to study these distributions [1] for the heights more than ten of meters above the sea surface, while there is a problem to use these methods for the lower heights. The last resulted in the fact, that at present there are not practically the complete and reliable data about the size and velocity distributions of the drops at small height above the sea surface, where main part of drops is concentrated.

Meanwhile, as it was presented at [2], the current radar spectra of scattering by the sea surface have often the bimodal form in the instants of scattered signals "splashes", and the second peak at higher frequency is caused by the scattering by the drops formed after the wave breaking and moved by the wind flow. Drops mean velocity, determined as

$$\bar{V} = \frac{\int_0^{\infty} p(V) V dV}{\int_0^{\infty} p(V) dV} \quad (1)$$

where  $p(V)$  - drops velocity distribution and  $V$  - velocity, is not varied practically under the air turbulence effect and results in the frequency shift of the Dopler spectrum of the scattered signal, as

$$F_0 = \frac{2V}{\lambda} \cos \psi \cos \theta \quad (2)$$

where  $\psi$  - grazing angle,  $\theta$  - angle between the wind vector and the look radiowave propagation one.

The spectrum width of the signal scattered by drops correlates with the drops velocity distribution, and, as a result, with their size distribution. This fact allows the opportunity on the base on the scattered signal radar measurement to derive the particles velocity and size distribution on the low heights above the sea surface.

## 2. POWER SPECTRA.

During a great number of experiments, carried out with the short part of centimeter and millimeter radiowave bands, it has been shown, that the resulting spectrum of the backscattered signals could be presented as a sum of two spectra

$$G(F) = G_{SB}(F) + G_{SP}(F) \quad (3)$$

Here the first term in the right part is determined by the scattering by the sea surface, and the second - by the scattering on the drops appeared during the wave breaking and transferred by wind flow.

As for the first term, the features of the power spectra for the signals backscattered by the sea surface has been studied enough complete [3].

However, the current power spectra, measured in the instants of the scattered signals "splashes", have in some cases the second peak in their high frequency part. To study it, experiments were carried out, that had resulted in the following data: the current power spectra for the sea surface backscattering during the splashes were obtained for the 3 cm and 8 mm radiowave bands in the continuous wave regime. The integration times for these spectra realising were 1.024 sec for 3 cm waveband and 0.819 sec for 8 cm waveband. In the spectra the second peaks appear clearly in 220..380 Hz band for 3 cm wavelength and in 900..1300 Hz band for 8 mm wavelength. The wind velocity had been measured by the standard meteorological station situated on the 10 m level over the sea, and was about  $8..10 \text{ ms}^{-1}$  during experiments; mean wave height was about 1.5 m.

To explain the second peak appearing, it is need to suppose the scatterers speed to be existed is about  $5.2..5.4 \text{ ms}^{-1}$ , that is essential more than possible scatterers speed in the frames of the two-scale scattering model. The speed for the real scatterers here must be about 60% of the wind speed.

From the other hand, the horizontal spray relocation by wind flows could explain these high velocity of the scatterers. It is also proved by the depolarization coefficient increasing during the splashes, as well as by the fact, that the doppler frequency shift of the 1st peak was opposite to the 2nd one, while the wave propagated upwind in some experiments.

If the spectrum of the scattering by the sea is used in the form

$$G_{SB}(F) = G_{0SB} \left[ 1 + \left| \frac{F - F_{01}}{\Delta F_1} \right|^n \right]^{-1} \quad (4)$$

and it is proposed the spectrum of the scattering by the spray is symmetrical in respect to the frequency  $F_{02}$  and could be presented in the type like

$$G_{SP}(F) = G_{0SP} \left[ 1 + \left| \frac{F - F_{02}}{\Delta F_2} \right|^m \right]^{-1} \quad (5)$$

it is possible to obtain the dependence between the real spectrum of the scattering by spray and the estimation one:

$$\frac{\hat{G}_{SP}(F)}{G_{SP}(F)} \approx \begin{cases} \left[ 1 + \frac{G_{0SB}}{G_{0SP}} \left( \frac{\Delta F_1}{F} \right)^m \right] & \text{when } |F - F_{02}| < \Delta F_2 \\ \left[ 1 + \frac{G_{0SB}}{G_{0SP}} \frac{\Delta F_1^m}{\Delta F_2^m} \left( \frac{F - F_{02}}{F - F_{01}} \right)^m \right] & \text{when } |F - F_{02}| > \Delta F_2 \end{cases} \quad (6)$$

Taking into account the known wind velocity dependence via the height as

$$\frac{V}{V_0} = \left( \frac{h}{h_0} \right)^{0.26} \quad (7)$$

that allows to estimate the doppler shift is equal 375 Hz on 3 cm waveband and 1400 Hz on 8 mm waveband for the height 1 m above the surface, and while  $V_0 = 10 \text{ ms}^{-1}$  on the 1 m height. The values estimated are enough well agreed with the experimental ones. The last expression can be used too for the layer mean height deriving, where there is the spray transferring by the wind.

$$h_m = \left( \frac{F_{02} \lambda}{2V_0} \right)^4 h_0 \quad (8)$$

The correlation function of the scattered signal were searched in the terms of the "wandering inhomogeneties" theory [4,5]. It performed to present the power spectrum of the scattered signal as

$$\begin{aligned} G(F) &= \int_{-\infty}^{\infty} \overline{EE_S^*} \cos 2\pi f S \, dS = \\ &= \int_{-\infty}^{\infty} W(V) \, dV \int_{-\infty}^{\infty} N^2 a^2 \cos(2kV S \Delta S) \cos 2\pi f S \, dS \end{aligned} \quad (9)$$

where  $W(V)$  - scatterers velocity projections distribution. Besides, the amplitude of the signal is a function of the drop diameter, i.e. the velocity of the particle

$$\alpha_i^2 = c \varphi(V_{ir})$$

and if to present

$$p(V) = \frac{\varphi(V)}{\bar{\varphi}(V)} W(V) \quad (10)$$

it is possible to show, that



$$G(F) = \overline{A} p(V) \quad (11)$$

where  $\overline{A} = \overline{N c \varphi(V)}$ , i.e. the spectrum in the phase detector output is similar to the form of the distribution of the scatterers velocity projections on the observation direction.

#### REFERENCE

- (1) Monahan E.S. "Sea spray as a function of low elevation wind speed", J.Geophys.Res. (1968) v.73, N4. - P.1127-1137.
- (2) Kulemin G.P., Rasskasovsky V.B. "Millimeter radiowave scattering by Earth under the grazing angles", Kiev, Nauk. Dumka (1987), 230pp. (in Russian).
- (3) Blanchard D.C. "The electrification of the atmosphere by particles from bubbles in the sea", Prog.Oceanogr. - 1963. - N1. - P.71-202.
- (4) Gorelik G.S. "On the theory of the radiowave scattering by the wandering inhomogeneties", Radiotekhnika i Elektronika (1956), v.1, N6, pp.695-703.
- (5) Gorelik G.S. "Scatterers velocities correlation effect on the scattered signal statistical properties", Radiotekhnika i Elektronika (1957), v.2, N10, pp.1227-1233.



# THE SEMI-INVERSION METHOD FOR GENERALIZED CYLINDRICAL MICROWAVE STRUCTURES

Alexander LERER, Igor DONETS, Sergey Bryzgalo

ROSTOV STATE UNIVERSITY, Institute of Physics, 194 Stachky street,  
344104, Rostov on Don, Russia.

## ABSTRACT

A new effective numerical-analytical method of analysis of cylindrical structures with arbitrary cross-section is presented. The method is based on an inversion of the main singular part of operator equation. It is reached by using in Galerkin method the basis functions being the eigenfunctions of the boundary value problem for the electromagnetic wave diffraction by a circular cylinder. The method was used to investigate diffraction by inhomogeneous dielectric bodies, to treat discontinuities in a waveguide, to analyze waveguides and strip lines with a complex cross-sections.

## INTRODUCTION

The semi-inversion method (SIM) is one of the most effective numerical-analytical methods for solving boundary value problems of microwave electrodynamics (see [1],[2] and their references). The method is based on an inversion of the main singular part of operator equation. As a result operator equation of the first kind is transformed to equation of the second kind. The various ways to invert the singular part of the operator are known.

In most cases the inverted operator in the SIM describes key structure for which the solution of the boundary problem exists in the closed form (diffraction by semi-infinite screens, electrostatic field of a metallic strip or a slot in metallic screen, etc.). Therefore, the SIM application can be started with searching for a key structure.

To solve the boundary problem for cylindrical structures with an arbitrary cross-section it is suggested to use the solution of the boundary problem for circular cylinder of radius  $a$  as the key problem which is known to have a solution in the closed form both for static and electromagnetic fields.

In present paper the use is made of that the functions  $\cos(jt)$ ,  $\sin(jt)$  are the eigenfunctions of integral operators with kernels:

$$G_{\bullet}^0(t, t') = \frac{1}{2\pi} \ln \left| \sin \frac{t-t'}{2} \right| \quad (1)$$

$$G_{\bullet}^0(t, t') = -\frac{i}{4} H_0^{(2)}(2ka \left| \sin \frac{t-t'}{2} \right|) \quad (2)$$

$$\bar{G}_h^0(t, t') = \frac{i}{2} ka \left| \sin \frac{t-t'}{2} \right| H_1^{(2)}(2ka \left| \sin \frac{t-t'}{2} \right|) \quad (3)$$

$$G_0(r, t, r', t') = -\frac{i}{4} H_0^{(2)}(ka\sqrt{\epsilon_1} \sqrt{r'^2 + r^2 - 2rr' \cos(t-t')}) \quad (4)$$

$k$  - is wavenumber,  $H_{0,1}^{(2)}$  - are Hankel functions.

This is the consequence of well-known formulas:

$$\int_0^{2\pi} \begin{Bmatrix} \cos(mt) \\ \sin(mt) \end{Bmatrix} G_{\bullet}^0(t, t') dt = - \begin{Bmatrix} \cos(mt') \\ \sin(mt') \end{Bmatrix} \begin{Bmatrix} \ln(2) & m=0 \\ 1/\sqrt{2m} & m \neq 0 \end{Bmatrix} \quad (5)$$

$$\int_0^{2\pi} \begin{Bmatrix} \cos(mt) \\ \sin(mt) \end{Bmatrix} G_{\bullet}^0(t, t') dt = -\frac{\pi i}{2} J_m(ka) H_m^{(2)}(ka) \begin{Bmatrix} \cos(mt') \\ \sin(mt') \end{Bmatrix} \quad (6)$$

$$\int_0^{2\pi} \begin{Bmatrix} \cos(mt) \\ \sin(mt) \end{Bmatrix} \bar{G}_h^0(t, t') dt = -\frac{\pi i}{2} ka \frac{d}{d(ka)} \left[ J_m(ka) H_m^{(2)}(ka) \right] \begin{Bmatrix} \cos(mt') \\ \sin(mt') \end{Bmatrix} \quad (7)$$

$$\int_0^{2\pi} \begin{Bmatrix} \cos \\ \sin \end{Bmatrix} (mt) G_0(r, t, r', t') dt = 2\pi \begin{Bmatrix} \cos \\ \sin \end{Bmatrix} (mt') \begin{cases} J_m(ka\sqrt{\epsilon_1} r) H_m^{(2)}(ka\sqrt{\epsilon_1} r'), & r \leq r' \\ J_m(ka\sqrt{\epsilon_1} r') H_m^{(2)}(ka\sqrt{\epsilon_1} r), & r \geq r' \end{cases} \quad (8)$$

#### ANALYSIS COMPLEX STRUCTURES BY THE SEMI-INVERSION METHOD

For strip and microstrip (quasi-TEM solution) lines with conductors of complex cross-sections, and for electromagnetic wave diffraction by the metallic cylindrical structures in the case of E-polarization ( $E_z \neq 0$ ,  $H_z = 0$ , the axis  $Oz$  is parallel to the cylindrical generating line) the following equation was solved:

$$\oint_L f(x, y) G(x, x', y, y') dl = g(x', y'), \quad x', y' \in L, \quad (9)$$

where  $L$  is the contour of conductor's cross-section,  $g$  is known excitation function,  $f$  is unknown function,  $G$  is the Green's function. This function has logarithmic singularity as  $x, y \rightarrow x', y'$ :

$$G(x, x', y, y') \sim \frac{1}{4\pi} \ln[(x-x')^2 + (y-y')^2].$$

Let's assume that  $L$  is a simple connected closed curve. Then let's write the equation of  $L$  in parametric form:  $x=x(t)$ ,  $y=y(t)$   $0 \leq t \leq 2\pi$

The equation (9) is transforming into:

$$\int_0^{2\pi} \bar{f}(t) G(t, t') dt = g(t') \quad 0 \leq t' \leq 2\pi, \quad (10)$$

where  $\bar{f}(t) = f(x(t), y(t))$ ;  $s(t) = \sqrt{\left(\frac{dx}{dt}\right)^2 + \left(\frac{dy}{dt}\right)^2}$ .

Let's present the equation (10) in the form:

$$\int_0^{2\pi} \bar{f}(t) G(t, t') dt = \int_0^{2\pi} \bar{f}(t) G^0(t, t') dt + \int_0^{2\pi} \bar{f}(t) [G(t, t') - G^0(t, t')] dt = g(t') \quad (11)$$

The expression of  $G^0(t, t')$  is given by expressions (1) or (2) or (3). The function  $G - G^0$  will not have a singularity. We search for the solution of (11) in the form:

$$\bar{f}(t) = \sum_{j=0}^{\infty} X_j^c \cos(jt) + \sum_{j=0}^{\infty} X_j^s \sin(jt) \quad (12)$$

Let us substitute (12) into (11) using expressions either (5) or (6) and  $\cos(jt)$ ,  $\sin(jt)$  orthogonality. As a result the infinite set of linear algebraic equations (SLAE) of the second kind is obtained.

The matrix elements of SLAE are represented by double integrals of the smooth function  $G(t, t') - G^0(t, t')$ , and can be easily approximated by one-point rectangular rule numerical quadrature.

The formulas (1) and (5) were used for strip and microstrip lines. The formulas (2) and (6) were used for metallic cylindrical structures in rectangular waveguide.

For the problem of electromagnetic wave diffraction by the cylindrical structures in the case of H-polarization ( $H_z \neq 0$ ,  $E_z = 0$ ) the following equation was solved:

$$H_z^0(x', y') = -J_\varphi(x', y')/2 + \oint_L J_\varphi(x, y) \frac{\partial G_h(x, x', y, y')}{\partial n} dl, \quad x', y' \in L$$

where  $H_z^0$  is component of incident field,  $J_\varphi$  is transversal component of electric current density,  $\vec{n}$  - is a unit vector normal to cylinder surface. This equation was solved using the scheme of solving the equation (9) and formulas (3) and (7).

In order to solve the two-dimensional problem of E-polarized electromagnetic wave diffraction by dielectric body with arbitrary cross-section  $S$  and permittivity  $\epsilon_2(x, y)$  we use an integral equation

$$E(x', y') = E^0(x', y') + k^2 \int_S \tau(x, y) \cdot E(x, y) \cdot G(x, y, x', y') \cdot dS, \quad (13)$$

where  $E$  is unknown field inside the body;

$$\tau(x, y) = \frac{\epsilon_2(x, y) - \epsilon_1}{\epsilon_1};$$

$$G(x, y, x', y') = -\frac{1}{4} H_0^{(2)}(k\sqrt{\epsilon_1} \sqrt{(x-x')^2 + (y-y')^2}) - \text{Green function.}$$

The body is situated in free space with permittivity  $\epsilon_1$ .

After transformation of coordinates:

$$x = X(r, t), \quad y = Y(r, t); \quad 0 \leq t \leq 2\pi, \quad 0 \leq r \leq 1; \quad (14)$$

and extraction of the integral equation kernel singularity instead the equation (13) we have:

$$\frac{F(r', t')}{J(r', t')} = E^0(r', t') + \int_0^1 \int_0^{2\pi} F(r, t) \cdot G_0(r, t, r', t') \cdot dt \cdot dr + \int_0^1 \int_0^{2\pi} F(r, t) \cdot [G(r, t, r', t') - G_0(r, t, r', t')] \cdot dt \cdot dr, \quad (15)$$

where  $G_0(r, t, r', t')$  is given by (4);

$$F(r, t) = k^2 \cdot \tau(r, t) \cdot E(r, t) \cdot J(r, t);$$

$J(r, t)$  is Jacobian of coordinates transformation (14).

The equation (15) is solved as described above with using (8). But in this case  $X_j^0, X_j^1$  are functions of  $r$ . Using the numerical integrating procedure to calculate radius integrals we obtain the set of linear algebraic equations of  $(2M+1) \cdot N$  order, where  $M$  is number of basis functions,  $N$  is number of nodes over the radius in the numerical quadrature.

The method was used by us to analyze the variety of microwave structures. The following computational results were obtained:

- wave impedances and delay ratio values of fundamental mode in strip and microstrip (quasi-TEM solution) lines, the inner conductors of which have the circular, elliptical, rectangular with the rounded edges contour.
- cutoff wavelengths of elliptical metallic waveguide
- scattering matrix of perfectly conducting and impedance posts placed across the rectangular guide parallel to the narrow wall; the shape of posts' cross-section is elliptical and cross-shaped
- effective scattering width of inhomogeneous dielectric cylinder with elliptical cross-section.

The computational results shown the inner convergence of method are presented in Tables 1-4. In the Tables:  $M$  is the number of terms in series (12). The Table 1 shows the values of magnitude  $R$  and phase  $\varphi$  of reflection coefficient of the metallic elliptic post in a rectangular waveguide with parameters  $l/a' = 0.3$ ;  $l'/a' = 0.1$ ;  $\lambda/a' = 1.4$ ;  $a' = 20$  mm.; conductivity  $\sigma = 6.1 \cdot 10^7$  Sm/m, free space wavelength  $\lambda$ ,  $l$  and

$2a$  are axes of ellipse,  $l$  is perpendicular to the waveguide, width of the wide wall is  $a'$ , the post is placed in the middle of waveguide. Table 2 presents the values of wave impedance of a single strip line with rectangular conductor with rounded-off edges with dimensions  $d/b=0.3$ ;  $r/b=0.1$ ;  $c/b=0.4$ , where  $d$  and  $c$  are height and width of rectangular,  $r$  is the rounded-off radius,  $b$  is distance between grounded planes.

Table.1

	H						
	1	2	3	4	5	6	7
K	0.99939	0.99276	0.99356	0.99355	0.99355	0.99355	0.99355
$\rho$	3.10943	3.19656	3.20330	3.20347	3.20347	3.20347	3.20347

Table.2

H				
1	2	3	4	5
86.734	84.664	84.652	84.579	84.577

Tables 3, 4 show convergence of effective scattering width  $W$  for two cases: 1. the dielectric cylinder of elliptical cross-section with  $l'/l=0.5$ ,  $\alpha=30^\circ$ ,  $2\lambda/l=4$ ,  $\epsilon_2=4$ ; 2. the cylinder with  $l'/l=0.5$ ,  $\alpha=30^\circ$ ,  $2\lambda/l=12$ ,  $\epsilon_2(r, l) = (2(1-r^2)+4) \cdot \begin{cases} (\cos(l)+1), & -\pi/2 \leq l \leq \pi/2; \\ (-\cos(\pi-l)+1), & \pi/2 \leq l \leq 3\pi/2. \end{cases}$

The results of the convergence with increasing  $N$  are presented in the table 3 for  $M=5$ . The table 4 shows the data for the convergence with respect to  $H$  for  $N=10$ .

Table 3

N	W1	W2
4	6.25203	6.01382
6	6.25182	6.01089
8	6.25104	6.00831
10	6.25204	6.00788
12	6.25211	6.00747

Table 4

H	W1	W2
3	6.2504	6.00203
4	6.25201	6.0089
5	6.25204	6.00788
6	6.25203	6.01044
7	6.25203	6.01012

It is shown in this work that the method has many advantages, such as fast inner convergence, high accuracy, universality (it makes it possible to solve effectively the problems of electrostatics and electrodynamics, the vector boundary problems, moreover, there is possibility to generalize the method for solving the three-dimensional boundary problems).

Thus the above method elaborated and demonstrated by us is an effective means of analysis of a vast class of microwave structures with the arbitrary cross-section.

#### REFERENCES

1. V.P. Shestopalov, A.A. Kirilenko, S.A. Masalov, Matrix Equations With a Difference Type Operator in Diffraction Theory. Kiev: Naukova Dumka, 1984 (in Russian)
2. L.P. Litvinenko, S.L. Prosvirnin, Spectral Operators for Problem of Diffraction by Screens. Kiev: Naukova Dumka, 1984 (in Russian)

# EXPERT SYSTEM FOR RADAR IMAGE RECOGNITION / FILTERING

Lukin V.V., Melnik V.V., Miao Zhenjiang\*, Ponomarenko N.N.,  
Zelensky A.A.

Kharkov Aviation Institute, Chkalova Str., 17, 310070, Kharkov, Ukraine,  
tel. (0572) 442352, fax (0572) 441131

\*Institute of Information Science, Northern Jiaotong University,  
100044, Beijing, China, tel. (861) 3240616, fax (861) 8315891

**Abstract.** The approach to adaptive filtering based on image pixel type recognition is proposed. The expert system using local statistical parameter analysis in the scanning window for proper filtering algorithm selection and remote sensing data interpreting is described.

## INTRODUCTION

Usually image filtering and recognition are considered as separate operations of remote sensing radar data processing. At the same time many new algorithms of adaptive robust image filtering include the elements of scanning window central pixel neighborhood analysis having the aim to determine its probable belonging to several classes of fragments [1], i. e. realizing principles of image recognition. That is why here we propose a new approach which puts into the basis the use of expert system with fuzzy logic for estimation of correct recognition probability and making up the decision. The results of this operation can be used for both locally optimal filtering algorithm selection enhancing radar image segmentation and data interpreting.

In this paper we sequently discuss local parameters which are analyzed and classes of fragments, present the techniques of expert system operation, give the background of filter type selection depending upon recognition results, show the efficiency of proposed approach for test model and real data, estimate the probability of correct decision for simulated images having different characteristics.

## RECOGNITION PROCEDURE

For recognition executing the several local scanning window statistical parameters have to be calculated. The authors analyzed many local values and propose here ones which can be considered to be the most informative. So let us assume that the scanning window dimensions are chosen and equal to  $N=M \times L$  image pixels - it must contain at least 10-15 independent image elements taking into account the correlation between neighbor pixels. The local parameters are the following:

a) ratio  $\sigma_{ij}^2 / \sigma_0^2$ , where  $\sigma_{ij}^2$  is the relative (normalized by  $\bar{I}_{ij}^2$ ) local variance,



$\sigma_0^2$  - speckle (multiplicative noise) relative variance,  $\bar{I}_y$  local mean value;

b) quasirange  $Q_y = (I_y^p - I_y^q) / \bar{I}_y$  where  $I_y^p$  and  $I_y^q$  denote  $p$ -th and  $q$ -th scanning window sample order statistics;

c)  $r_{mn} = |\bar{I}_y - I_y^{med}| / \bar{I}_y \sigma_0$ , where  $I_y^{med}$  is the median value of the sampling;

d) the coefficient of neighborhood belonging  $l$ , which is equal to the ratio  $N_b/N$ , where  $N_b$  is the number of image values belonging to the area  $[I_y(1-2\sigma_0); I_y(1+2\sigma_0)]$ ;

e) the coefficient of pixel rank position  $z = |I_y - \frac{N+1}{2}| / N$ , where  $I_y$  is the rank number of the central scanning window value in the ordered sampling formed by pixels of its aperture;

f) the non-symmetry coefficient  $S_n = |I_y^N + I_y^1 - 2\bar{I}_y| / \bar{I}_y$ .

Evidently these parameters are sensitive to different situations (local distribution laws) but no one of them being used separately can not distinctly recognize different fragment types. For instance, large  $\sigma_y^2 / \sigma_0^2$  value may correspond to edges, small-dimension objects and impulse noise presense in the scanning window aperture. Only their common using and knowledge of their specific properties ensures the perfect solution of recognition problem.

The situations which are the most typical and important for image processing are the following: 1) the homogeneous lot (large-dimension "flat" object; 2) central pixel edge belonging; 3) spike noise presense in the scanning window but the central position pixel is not a spike; 4) central position value corresponds to impulse noise (spike); 5) small-dimension object presense in the window and central pixel belonging to it; 6) the neighbourhood of small-dimension objects when central pixel does not belong to it. Several situations can not be distinctly interpreted, for example, when aperture contains the small part (sharp edge) of large dimension object the solution variants 3 and 6 are reasonable. To the word, the difficulty of these situations recognition is not important because for both cases the same filtering algorithms occur to be efficient. Moreover from recognition procedure point of view only variants 1, 2, 4 and 5 are important, other situations must be taken into account mainly during filtering and for spikes removal.

Using test image models and easily recognizable fragments of real data characterized by the variety of object contrasts, dimensions and configurations and having different noise and spikes properties the dependences of controlled parameter distribution laws on possible situations were obtained. Taking into consideration expert knowledge they were extrapolated and corrected for image and noise properties not scoped by simulation data.

After this for every pixel the probability  $P_y^m$  of its relating to  $m$ -th situation mentioned above was calculated. The probability of the event that the correct solution  $P_y^m$ ,  $m=1,6$  is the largest varied from 0.8 to 1.0 depending upon image and

noise characteristics. For every pixel we controlled not only the largest  $P_{ij}^m$  value, but also the second large one. The probability that the correct recognition solution has one among two largest  $P_{ij}^m$  values is even greater and usually exceeds 0.9.

### ADAPTIVE FILTERING

For every pair of the most probable situations the filtering algorithm was proposed. It must be chosen according to the Table from the set of following scanning window image processing algorithms: 1) modified rank filter supposing censored non-weighted data averaging [2]; 2) median one realizing the calculation of  $\frac{N+1}{2}$ -th order statistic of the pixel value sampling; 3) modified sigma-filter [3] fulfilling the averaging of scanning window image value belonging to the  $2\sigma_0$  - neighborhood of  $I_{ij}$ -pixel value. These algorithms differ greatly by their main properties - the ability to suppress noise, to eliminate spikes, to preserve edges and small-dimension objects. Besides all these filters are characterized by high computation efficiency, i.e. they need minimal time expenses for their executing, are enough simple, there exist the special digital processors for fast realization of these algorithms. We carried out a thorough investigation of wide range of various filtering algorithms and concluded that the selection of these three ones is the most expedient, especially taking into account that during preliminary calculation of considered parameters the values  $I_{ij}^p, I_{ij}^q, I_{ij}^{med}$  and the neighborhood  $[I_{ij}(1-2\sigma_0), I_{ij}(1+2\sigma_0)]$  have to be derived. As the filtered value for modified rank algorithm the value  $(I_{ij}^p + I_{ij}^q)/2$  can be accepted.

Table

Situation having the largest $P_{ij}$	homogen. lot (flat obj.)	central pixel edge belonging	spike presence in the window	spike in the centr. pixel	central pixel belong to sm.-dim obj	the neighborhood of sm.-dim. obj.
Situation having the second magn. prob. $P_{ij}$						
homogen. lot	mod.rank	sigma	mod.rank	mod.rank	sigma	median
central pix. edge belonging	mod.rank	sigma	median	median	sigma	sigma
spike presence in the window	median	median	median	median	sigma	median
spike in the central pixel	median	median	median	median	sigma	median
cen. pix. bel. to sm.-dim. object	sigma	sigma	sigma	sigma	sigma	sigma
the neighborhood of sm.-dim. object	median	sigma	median	median	sigma	sigma

The diagonal elements of the Table correspond to pixels for which the largest  $P_{ij}$  is much greater than the second one.

The investigation has shown that the proposed filtering algorithms provided better results than any other one both according to quantitative image quality integral and/or local criteria and to visual impression, especially when the images contain the variety of objects. It was proved for test and real data. When usual computer means are used the main part of processing time is needed for local parameter calculation. The way for its reducing is the realization of parallel computations using specialized processors.

### CONCLUSION

The new approach to radar image filtering and the first stage data recognition based on expert system using is proposed. The problems of algorithm practical realization are discussed. The considered approach can be useful both for visual image quality enhancement and the reliability increasing of segmentation procedure. Besides it can serve as the basis for further recognition of flat object types, their parameter estimation, spike noise removal, small-dimension object detection and localization, multichannel radar image superimposing etc.

### REFERENCES

- (1) A.A.Zelensky, G.P.Kulemin, V.V.Lukin, V.P.Melnik: "Locally-adaptive robust algorithms for radar image processing", Preprint 93-143 issued by Institute of Radiophysics and Electronics of Ukrainian Academy of Science, 1993, 39 p.
- (2) Lukin V.V., Miao Zhenjiang, Yuan Baozong: "Multifrequency remote sensing radar images processing and analysis", Proceedings of IEEE TENCON-93, Beijing, China, pp. 1042-1045.
- (3) Jong-Sen Lee: "Digital Image Smoothing and the Sigma Filter", Comp. Vision, Graphics and Im. Processing, 1983. v. 24, pp. 255-269.



# POLARIMETRIC RADAR BACKSCATTER

Ernst A.F. Lüneburg

German Aerospace Research Establishment (DLR)  
Institute for Radio Frequency Technology  
D-82234 Oberpfaffenhofen, Germany

## Abstract

The concept of a linear radar backscatter operator entails internal mathematical inconsistencies. The present contribution tries to point out the prevailing shortcomings and misconceptions and to provide a satisfactory solution by introducing the concept of an antilinear backscatter operator.

## Introduction

Vector scattering theory that makes full use of the transverse nature of the electromagnetic radiation field becomes increasingly more important for a variety of scientific problems like inverse scattering theory, three-dimensional reconstruction, vector diffraction tomography or remote sensing with real or synthetic aperture radars.

In radar polarimetry, the merging of the technological concept of radar (radio detection and ranging) and the fundamental concept of polarimetry, the backscatter operator determines the far field backscatter characteristics of a deterministic or random target illuminated by an incident (plane) electromagnetic wave. For a deterministic target it is traditionally considered to be a linear operator represented by the complex symmetric  $2 \times 2$  Sinclair (radar scattering) matrix  $S$  in a common polarization basis. Symmetry is due to reciprocity for backscattering.

For a stationary and ergodic random target the Sinclair matrix  $S$  is a random variable. Assuming that the random target can be modelled as a Gaussian random field (with only slowly varying mean characteristics) the backscatter process can be described completely by the Mueller or Kennaugh matrix composed by averaging second order moments of the Sinclair matrices  $S$ . This requires the introduction of the Stokes vector concept.

Due to a medley of mathematical and heuristic reasonings the concept of a linear backscatter operator entails internal mathematical inconsistencies if proper care is not taken. The appearance of seemingly unrelated new concepts like Kennaugh's pseudo eigenvalue equation [13] (concigenvalue equation), the unitary T-congruence (consimilarity) change of basis ( $U^T S U$ ), the distinction

between voltage and operator transformations under basis changes [14], the difference between the conventionally defined Kennaugh and Mueller matrices [5], the proper formulation and transformation behavior of the bilinear voltage (power transfer) equation and the indiscriminated use of different coordinate systems (forward scattering alignment FSA versus backward scattering alignment BSA convention) are examples for the unsatisfactory and even confusing present state-of-art of the theoretical basis of radar backscattering theory.

The difficulties arise mainly due to the fact that the incoming and outgoing plane wave polarization spaces (spin spaces) are not properly identified and clearly distinguished. The utilization of different coordinate systems (FSA, BSA) does not eliminate these difficulties and inconsistencies but tends to increase the prevailing confusion. The classical backscatter operator  $S^1$  with the Sinclair radar backscatter matrix  $S$  as its matrix representation in a common 2-dimensional polarization basis maps the incoming plane wave polarization space  $\mathcal{P}_+$ , the domain of  $S$ , onto the outgoing plane wave polarization space  $\mathcal{P}_-$ , the range of  $S$ . Both spaces are different but anti-isomorphic. The bijective mapping of  $\mathcal{P}_+$  onto  $\mathcal{P}_-$  or vice versa is accomplished by the nonlinear conjugation operator  $\mathcal{K}$  which is realized in the 2-dimensional complex column vector space as the complex conjugation operation  $K$  ( $K$  takes the complex conjugate of all entries to its right).

An alternative mathematical description is provided by introducing a generalized backscatter operator  $\mathcal{S}_a$  that combines the linear mapping of the Sinclair operator  $S$  and the nonlinear operator  $\mathcal{K}$  and maps each one of the polarization spaces  $\mathcal{P}_+$  or  $\mathcal{P}_-$  onto itself. By construction this is a antilinear operator that is Hermitian if  $S$  is symmetric. The realization of this operator in an orthonormal polarization basis common to the range and the domain of  $\mathcal{S}_a$ , has the form of an antimatrix  $KS$  for  $\mathcal{P}_+$  or  $SK$  for  $\mathcal{P}_-$ . In this formulation (i) the change of basis is effected by a unitary similarity transformation for  $KS$  (or  $SK$ ), implying a consimilarity transformation (unitary T-congruence) for the matrix part  $S$  of  $\mathcal{S}_a$ ; (ii) Kennaugh's pseudoeigenvalue equation appears to be the eigenvalue equation of an antilinear operator; (iii) the difference between voltage and operator transformation disappears; and (iv) the definitions of the Kennaugh and the Mueller matrix can be reconciled if the corresponding Stokes vector propagation spaces and representations are properly introduced. Furthermore, (V) the basis transformation of the voltage equation in its bilinear form can be properly formulated and its representation as a Hermitian scalar product in  $\mathcal{P}_+$  (or  $\mathcal{P}_-$ ) be derived. The square of the antilinear scattering operator  $\mathcal{S}_a$ , the simplest linear operator that can be formed with  $\mathcal{S}_a$ , is represented by the Graves power density matrix  $G = S^1 S$  (or  $G = SS^1$ ).

Optimal polarizations in radar backscattering are by definition those states of polarization of an incident plane electromagnetic waves that maximize or min-

<sup>1</sup>Capital calligraphic letters are used for abstract operators whereas their realizations (representations) are denoted by the same capital latin letter

imize the received co- and cross-polar power. For a deterministic target with a complex-valued symmetric Sinclair matrix  $S$  co-pol maxima and cross-pol nulls coincide and are given by the so-called coneigenvectors of  $S$ . Together with the co-polar nulls they form the well-known Huynen fork on the Poincaré sphere. The deeper reasons behind these polarimetric manifestations are intriguing matrix analytical properties: diagonalization of a complex symmetric matrix by unitary consimilarity and off-diagonalization by T-congruence. These properties are direct consequences of the antilinear nature of the backscatter operator.

In the Stokes vector formulation the Mueller and Kennaugh matrices can be shown to agree if proper care is taken of the domain and range of these matrices. For a deterministic target the Mueller-Kennaugh matrix is (up to a constant) a proper Lorentz transformation. Optimal polarizations have important applications in target detection, identification and discrimination as well as in target/clutter separation problems.

### Phase Conjugation

The 3-dimensional real physical Euclidean space  $R^3$  is endowed with a right-handed orthonormal basis  $B = \{\hat{x}, \hat{y}, \hat{z}\}$  at the common transmitting and receiving antenna site, with the  $z$ -direction pointing towards the target. This is the so-called backscatter alignment convention BSA. The origin of the coordinate system is assumed to lie inside the target.

The transverse character of a plane wave propagating either along the positive direction of the  $z$ -axis, denoted in the following as  $|_+$ , or along the negative  $z$ -direction, denoted as  $|_-$ , implies that their electric field vectors lie in the subspace  $\mathcal{R}^2 = \text{span}\{\hat{x}, \hat{y}\}$ . The complexification of  $\mathcal{R}^2$  leads to the following expression for a general plane wave propagating in the positive  $z$ -direction

$$\vec{E}_+(z, t) = \vec{E}_+ \exp[j\{\omega t - kz\}] \exp\{j\omega t\} \quad (1)$$

and in the negative  $z$ -direction

$$\vec{E}_-(z, t) = \vec{E}_- \exp[j\{\omega t + kz\}]. \quad (2)$$

The assumed harmonic time variation  $\exp\{j\omega t\}$  for all field quantities will be suppressed whenever convenient.

The  $z$ - and  $t$ -independent complex amplitudes  $\vec{E}_+$  and  $\vec{E}_-$  belong to the incoming and outgoing polarization spaces  $\mathcal{P}_+$  and  $\mathcal{P}_-$ . These different spaces must be clearly identified and distinguished. The latter correspond to the undotted and dotted 2-spinor spaces used by Bebbington [2] in his recent innovative studies of polarimetry.

Following the IEEE convention [12] that there exists a bijective (one-to-one and onto) phase conjugation mapping between the vector spaces  $\mathcal{P}_+$  and  $\mathcal{P}_-$ :

$$\vec{E}_- := K \vec{E}_+ \quad \text{and} \quad \vec{E}_+ := K \vec{E}_- \quad (3)$$

(:= means defined by) where  $K$  is the complex conjugation operator such that the vectors  $\vec{E}_+$  and  $\vec{E}_-$  possess the same polarization:

$$\text{Polarization}(\vec{E}_-) = \text{Polarization}(\vec{E}_+) \left\{ \begin{array}{l} \text{if and} \\ \text{only if} \end{array} \right\} \vec{E}_- = K\vec{E}_+ \quad (4)$$

In this context see also [16] and [15].

The operator  $K$  is involutory, i.e.  $K^2 = I$  (identity). Since  $K$  is a nonlinear operator it cannot be represented by a matrix.

This behavior is related to the time reversal operation in spin spaces.

The total polarization space  $\mathcal{P}$  can be written as

$$\mathcal{P} = \sum_{\vec{k}} \cup \left\{ \mathcal{P}_+(\vec{k}) \cup \mathcal{P}_-(\vec{k}) \right\} \quad (5)$$

The usual convention is that

$$\text{Polarization} \left\{ \mathcal{P}_+(\vec{k}) \right\} \text{ independent of } \vec{k} \quad (6)$$

where  $\vec{k}$  is measured in a conventional spherical coordinate system  $\{\hat{r}, \hat{\theta}, \hat{\phi}\}$ . This implies, however, that  $\mathcal{P}_-(\vec{k}) \neq \mathcal{P}_+(-\vec{k})$ . This is the reason for putting  $\mathcal{P}_+(\vec{k})$  and  $\mathcal{P}_-(\vec{k})$  side by side in equation (5) since both are endowed with the same orthonormal basis (BSA convention) and satisfy the relation

$$\mathcal{P}_-(\vec{k}) = K\mathcal{P}_+(\vec{k}). \quad (7)$$

in the sense of equation (4).

## Radar & Voltage Equation

The (normalized) radar equation reads

$$\vec{E}'_- = S \vec{E}_+^i \quad (8)$$

where the superscripts 'i' and 's' denote 'incident' and 'scattered' wave, respectively. Here  $\vec{E}_+^i \in \mathcal{P}_+$  and  $\vec{E}'_- \in \mathcal{P}_-$  and  $\mathcal{P}_+$  is the domain and  $\mathcal{P}_-$  is the range of the linear backscatter operator  $S$ . For reciprocal targets the corresponding Sinclair backscatter matrix  $S$  is complex symmetric. In the literature the propagation indices  $|_+$  and  $|_-$  are almost always omitted. A notable exception is the fundamental paper by Graves [4]. This omission and the resulting ambiguity leads to considerable confusion when going over to other polarization bases.

The standard radar equation (8) has the disadvantage that the domain and the range of the matrix  $S$  belong to the different linear vector spaces  $\mathcal{P}_+$  and  $\mathcal{P}_-$ .

Referring not only to a common basis but more importantly also to a common linear vector space,  $\mathcal{P}_+$ , say, the radar equation can be written as

$$\vec{E}_+^* = \vec{E}_+^{**} = KS\vec{E}_+^i \quad (9)$$

The term  $KS$  on the right hand side is the realization of the antilinear backscatter operator [6]

$$\mathcal{S}_a = K\mathcal{S} \quad (10)$$

where  $S$  is the matrix representation of  $\mathcal{S}$  in the appropriate basis of  $\mathcal{C}^2$  and  $K$  denotes complex conjugation.

In abstract operator notation the radar equation (9) can now be written as

$$\mathcal{E}_+^* = \mathcal{S}_a \mathcal{E}_+^i \quad (11)$$

Here the incident as well as the scattered field belong to one and the same polarization space  $\mathcal{P}_+$ .

The matrix part  $S$  of the antilinear operator  $\mathcal{S}_a$  is called an antimatrix [7]. Hence, it is more precise to call  $S$  the Sinclair scatter antimatrix. Symmetry of the antimatrix  $S$  implies Hermiticity of  $\mathcal{S}_a$  and vice versa.

It should be stressed that the correct formulation of the radar equation is not in any fundamental way related to the choice of the backward or forward scattering alignment convention BSA or FSA. The passage from BSA to FSA or vice versa is simply affected by multiplying the corresponding vectors with the diagonal matrix  $\text{diag}[1, -1]$ . This transition matrix does not establish, however, a connection between polarization states in the physically different linear vector spaces  $\mathcal{P}_+$  and  $\mathcal{P}_-$ , but cf. [5].

The voltage (energy transfer) equation is conventionally written in the apparently bilinear form

$$V = \vec{h}_+ \cdot \vec{E}_- \equiv (\vec{h}_+, \vec{E}_-) \equiv \vec{h}_+^T \vec{E}_- \quad (12)$$

where  $\vec{h}_+$  is the receiving antenna polarization (height) and  $\vec{E}_-$  is the backscattered field. The common practice to delete the propagation indices again may lead to confusion. Use of eq. (3) yields the expression

$$V = (\vec{h}_+, \vec{E}_-) = (\vec{h}_+, \vec{E}_+^*) = \vec{E}_+^T \vec{h}_+ = \langle \vec{h}_+, \vec{E}_+ \rangle \quad (13)$$

involving directional Jones vectors from the same polarization space. Here the brackets  $\langle \rangle$  indicate the usual unitary Hermitian scalar product  $\langle x, y \rangle = y^T x$ .

A general change of polarization basis

$$\vec{E}_+ \rightarrow A\vec{E}_+^i \quad (A \text{ nonsingular}) \quad (14)$$

leads according to eq. (3) to

$$\vec{E}_- \rightarrow A^* \vec{E}_+^i \quad (15)$$

and similarly for all polarization vectors in  $\mathcal{P}_+$  and  $\mathcal{P}_-$ .

Hence, from any form of the radar equation or the voltage equation follows consistently

$$S \rightarrow S' = A^{-1*}SA \quad (16)$$

i.e. the Sinclair (anti)matrix  $S$  transforms by consimilarity (see [9]) and not by similarity. If  $A$  is unitary then

$$S \rightarrow S' = U^T S U \quad (17)$$

and unitary consimilarity and unitary  $T$  congruence coincide. In this case symmetry of  $S$  is conserved. Consimilarity has been investigated extensively by R. Horn and Yoo Pyo Hong [8] during the last ten years and significant differences with respect to ordinary similarity have been pointed out.

## Optimal Polarizations

Consimilarity and  $T$  congruence are equivalence relations (reflexive, symmetric, transitive). Thus the set of all scattering matrices is partitioned into disjoint equivalence classes which each describe one and the same abstract scattering operator with different representations for all possible coordinate systems characterized by the columns of the corresponding transition matrix.

The equivalence class of complex symmetric matrices under unitary consimilarity contains as canonical matrices diagonal matrices [1, 17, 8, 9]

$$U^T S U = \begin{pmatrix} \lambda_1 & 0 \\ 0 & \lambda_2 \end{pmatrix} \quad (18)$$

where the coneigenvalues  $\lambda_{1,2}$  can be taken as nonnegative with  $0 \leq \lambda_2 \leq \lambda_1$ . Writing  $U = [x_1, x_2]$  this equation leads to the coneigenvector equation

$$S x_i = \lambda_i x_i^* \quad (i = 1, 2). \quad (19)$$

In radar polarimetry this equation is known as Kennaugh's pseudo eigenvector equation [13]. It is not a usual eigenvalue equation due to the complex conjugation on the right hand side. It is, however, the appropriate eigenvalue/eigenvector equation for the nonlinear backscatter problem. The linear forward (transmission) problem on the other hand is dealt with by the familiar eigenvalue problem. Symmetry for the Sinclair backscatter antimatrix corresponds to normality of the Jones transmission matrix as far as the corresponding coneigenvectors and eigenvectors are orthogonal. The applicability and restriction of the coneigenvector equation to backscattering and of the common eigenvector equation to forward scattering (transmission) is unfortunately still not always recognized [10].

Any phase terms in eq. (18) resulting from the requirement that  $U \in SU(2)$ , i.e.  $\det(U) = 1$ , can be restored after calculating the co- and crosspolar optimal polarizations. The coneigenvectors  $x_i$  ( $i = 1, 2$ ) are eigenvectors of the Hermitian positive semi-definite linear Graves power matrix  $G = S^\dagger S$  and the squares of the coneigenvalues  $\lambda_{1,2}^2$  (the squared absolute values in the general case) are the eigenvalues of  $G$ .

On the other hand the equivalence class of the complex symmetric matrix  $S$  under  $T$  congruence contains all symmetric matrices with the same rank as  $S$  [9]. The  $2 \times 2$  symmetric Sinclair matrix, in particular, is  $T$  congruent to the backward identity matrix

$$A^T S A = \mu \begin{pmatrix} 0 & 1 \\ 1 & 0 \end{pmatrix}, \det(A) \neq 0. \quad (20)$$

Writing  $A = [y_1, y_2]$  with  $\det(A) = 1$  this equation reads

$$S y_i = \mu y_i^{\perp*} \quad (i = 1, 2) \quad (21)$$

where  $y^\perp$  is orthogonal to  $y$ . These are the Kennaugh-Huynen copolar null polarization equations [11]. In the coneigenvector basis these vectors assume the form

$$y_{1,2} = \frac{1}{\sqrt{\lambda_1 + \lambda_2}} \begin{bmatrix} \sqrt{\lambda_2} \\ \pm j \sqrt{\lambda_1} \end{bmatrix}. \quad (22)$$

They are orthogonal if and only if  $\lambda_1 = \lambda_2$ .

Unitary matrices that produce a zero in the 1-1 element of  $S$  under consimilarity can be found as  $U_{1,2} = [y_{1,2}, y_{1,2}^\perp]$ .

The most important optimal polarizations are the extrema of the copolar and crosspolar power defined by

$$P_{co}(p) = |V_{co}(p)|^2 = |(p, Sp)|^2 \quad (23)$$

and

$$P_{\perp}(p) = |V_{\perp}(p)|^2 = |(p^\perp, Sp)|^2 \quad (24)$$

with  $\|p\|^2 = (p, p) = 1$ . Using a general ansatz for  $p$  it follows immediately from the preceding matrix representations that

$$\left. \begin{array}{l} \max P_{co}(p) = \lambda_1^2 \\ \text{null } P_{\perp}(p) = 0 \end{array} \right\} \text{ for } p = x_1 \quad (25)$$

$$\left. \begin{array}{l} \text{submax } P_{co}(p) = \lambda_2^2 \\ \text{null } P_{\perp}(p) = 0 \end{array} \right\} \text{ for } p = x_2. \quad (26)$$

Furthermore

$$\text{null } P_{co}(p) \quad \text{for } p = y_{1,2} \quad (27)$$

and

$$\max P_e = \frac{1}{4} \{\lambda_1 + \lambda_2\}^2 \text{ for } p = \frac{1}{\sqrt{2}} \begin{bmatrix} 1 \\ \pm j \end{bmatrix} \quad (28)$$

in the concigenvector basis. These results are in agreement with the literature [3] and lead to the well-known Huynen fork representation on the Poincare sphere [11, 3].

The result about the copolar nulls expressed in eqs. (21,22,23) can also directly be derived in the following way: Denoting the square root of the diagonal matrix on the right hand side of eq. (18) by  $D^{1/2} = \text{diag}[\sqrt{\lambda_1}, \sqrt{\lambda_2}]$  the matrix  $S$  can be written as

$$S = B^T B \text{ with } B = D^{1/2} U^{-1} \quad (29)$$

Vanishing of the copolar voltage  $V_{co}$  of eq. (23) leads to

$$V_{co} = q^T q = 0 \text{ with } q = Bp \quad (30)$$

This expression can only vanish if  $q$  is a vector of the form ( $c$  is a normalization constant)

$$q = c \begin{bmatrix} 1 \\ \pm j \end{bmatrix} \text{ (isotropic vector)} \quad (31)$$

Hence,

$$p = B^{-1} q = U D^{-1/2} q = \frac{c}{\sqrt{\lambda_1 \lambda_2}} \begin{bmatrix} \sqrt{\lambda_2} \\ \pm j \sqrt{\lambda_1} \end{bmatrix} \quad (32)$$

This agrees with eq. (22) in the concigenvector basis if normalized to one.

The following 4-channel conservation of energy relation

$$P_{co}(p) + P_{co}(p^\perp) + 2P_e(p) = \lambda_1^2 + \lambda_2^2 \quad (33)$$

should be noted.

## Stokes Vectors & Mueller Matrix

For random target interrogation and partially polarized waves it is necessary and expedient to introduce directional Stokes vectors corresponding to propagation in the  $+$  and  $-$  direction:

$$\vec{g}_\pm = \begin{bmatrix} 1 \\ \langle |E_{1\pm}|^2 \rangle - \langle |E_{2\pm}|^2 \rangle \\ 2 \langle \text{Re}(E_{1\pm}^* E_{2\pm}) \rangle \\ \pm 2 \langle \text{Im}(E_{1\pm}^* E_{2\pm}) \rangle \end{bmatrix} \quad (34)$$

The directional Stokes vectors  $\vec{g}_+$  and  $\vec{g}_-$  are realizations of vectors in the polarization spaces  $\mathcal{P}_\pm$  analog to the directional Jones vectors.



Both Stokes vectors describe the same state of polarization if

$$\vec{g}_+ := K\vec{g}_- \quad \text{or} \quad \vec{g}_- := K\vec{g}_+ \quad (35)$$

where  $K = \text{diag}(1, 1, 1, -1)$  is involutory ( $K^2 = I$ ) in analogy to the involutory complex conjugation operation.

A Stokes vector  $\vec{g}$  belongs to the 4-dimensional real linear Minkowski space and satisfies the so-called Lorentz norm  $\|\vec{g}\|^2 = g_0^2 - g_1^2 - g_2^2 - g_3^2 \geq 0$ . For partially polarized waves  $\|\vec{g}\| > 0$  whereas for partially polarized waves  $\|\vec{g}\| = 0$  ('time-like'/'null-cone').

The norm can be written more conveniently as

$$\|\vec{g}\|^2 = \vec{g}^T \eta \vec{g} \quad (36)$$

where  $\eta = \text{diag}(1, -1, -1, -1)$  is the Minkowski metric tensor.

The Mueller matrix  $M$  connects the Stokes vectors of the incident and the scattered fields. For a coherent target

$$\vec{g}_-^s = KM\vec{g}_+^i, \quad \vec{g}_+^s = K\vec{g}_-^i = M\vec{g}_+^i \quad (37)$$

where

$$M = 2A^{T-1}(S \otimes S^*)A^{-1}. \quad (38)$$

Here  $\otimes$  denotes the Kronecker product and

$$A = \begin{pmatrix} 1 & 0 & 0 & 1 \\ 1 & 0 & 0 & -1 \\ 0 & 1 & 1 & 0 \\ 0 & j & -j & 0 \end{pmatrix} \quad (39)$$

The power received by an antenna with polarization vector  $\vec{h}_r$  (r received) is given by

$$P = |\vec{h}_r \cdot \vec{E}^s|^2 = |\vec{h}_r \cdot K\vec{E}^i|^2. \quad (40)$$

This can be written as

$$P = \frac{1}{2}\vec{g}_+^{iT} K \vec{g}_-^s = \frac{1}{2}\vec{g}_+^{iT} \vec{g}_+^s = \frac{1}{2}\vec{g}_+^{iT} M \vec{g}_+^i. \quad (41)$$

Traditionally the expression  $KM$  was called Mueller matrix and is non symmetric whereas the so-called Kennaugh matrix  $M$  is symmetric.  $MK$  and  $M$  differ by the sign of the fourth row. If proper care is taken to involve only quantities belonging to one and the same polarization space  $\mathcal{P}_+$  (or  $\mathcal{P}_-$ ) only the matrix  $M$  of eq. (38) appears and is called Mueller matrix here.

For a single deterministic target the symmetric Mueller matrix (38) is (up to a constant) a proper orthochronous Lorentz transformation

$$M^T \eta M = |\Delta|^2 \eta \quad (42)$$

where  $\Delta = \det(S)$ .

From eq. (37) follows

$$\|\vec{g}_+^*\| = \|\vec{g}_-^*\| = |\Delta| \|\vec{g}_+^*\| \quad (43)$$

For the coherent case the theory of optimal polarizations can directly be taken over from the previous considerations. For instance denoting the angle between the Stokes vectors on the Poincare sphere corresponding to the copolar nulls  $y_i$  ( $i = 1, 2$ ) of eq. (22) by  $4\gamma$  it follows from  $\cos 2\gamma = |(y_1, y_2^*)|$  that  $\tan^2 \gamma = \lambda_2/\lambda_1$  [11].

The theory of optimal polarizations can also be formulated in the Minkowski space setting itself with interesting particularities. The latter approach is important regarding the incoherent scatter case.

The received copolar and crosspolar power read

$$P_{co} = \frac{1}{2} \vec{g} M \vec{g}, \quad P_{\perp} = \frac{1}{2} \vec{g}_{\perp} M \vec{g} \quad (44)$$

where

$$\vec{g} = \begin{bmatrix} 1 \\ \vec{p} \end{bmatrix}, \quad \vec{g}_{\perp} = \begin{bmatrix} 1 \\ -\vec{p} \end{bmatrix} \quad (45)$$

The symmetric Mueller matrix is written as

$$M = M^T = \begin{bmatrix} m_{00} & \vec{a}^T \\ \vec{a} & M_3 \end{bmatrix} \quad (46)$$

Then

$$P_{\perp} = \frac{1}{2} \vec{p}^T \{m_{00} I - M_3\} \vec{p} \quad (47)$$

This is a real symmetric form. The eigenvectors/-values

$$\{M_{00} I - M_3\} \vec{p}_i = \mu_i \vec{p}_i, \quad i = 1, 2, 3 \quad (48)$$

( $0 \leq \mu_1 \leq \mu_2 \leq \mu_3$ ) determine minimal and maximal crosspolar power.

$$\min P_{\perp} = \frac{1}{2} \mu_1, \quad \max P_{\perp} = \frac{1}{2} \mu_3. \quad (49)$$

For a deterministic target  $\mu_1 = 0$  and  $\vec{p}_1 = \vec{a}$ .

The copolar power in the general incoherent scatter case can be expressed in terms of an inhomogeneous quadratic form and the search for optimal solutions requires the numerical solution of a 6.th order polynomial. For details see for instance [18] and the literature cited there.

## References

- [1] L. Autonne: "Sur les matrices hypohermitiennes et sur les matrices unitaires," *Annales De L'Universite de Lyon, Nouvelle Serie I, Fasc. 38* (1915) pp. 1-77
- [2] D.H.O. Bebbington: "Target vectors - spinorial concepts," *Second International Workshop on Radar Polarimetry, IRESTE, Sept. 9 - 10, 1992, Nantes, France*, pp. 26-36
- [3] W.-M. Boerner, L.-L. Liu, and X. Zhang: "Comparison of optimization procedures for  $2 \times 2$  Sinclair,  $2 \times$  Graves,  $3 \times$  covariance and  $4 \times 4$  Mueller (Kennaugh) matrices in coherent radar polarimetry and its application to target versus background clutter discrimination in microwave remote sensing and imaging," *EARSel, Advances in Remote Sensing, Vol. 2, No. 1*, (1993) pp. 55-82
- [4] C.D. Graves: "Radar polarization power scattering matrix," *Proc. IRE, Vol. 44* (1956) pp. 248-252
- [5] A. Guissard: "Mueller and Kennaugh matrices in radar polarimetry," *Trans. Geoscience and Remote Sensing Vol. 32,3* (1994)
- [6] F. Herbut F and M. Vujičić: "Basic algebra of antilinear operators and some applications. I," *J. Math. Phys. Vol. 8* (1967) pp. 1345-1354
- [7] F. Herbut, M. Vujičić, and Z. Papadopolos: "A new look at unitary-antiunitary representations of groups and their construction," *J. Phys. A: Math. Gen. 13* (1980) pp. 2577-2589
- [8] Yoo Pyo Hong and R.A. Horn: "A canonical form for matrices under consistency," *Linear Algebra and its Applications, Vol. 102* (1988) pp. 143-168
- [9] R.A. Horn and C.A. Johnson: "Matrix Analysis," *Cambridge University Press, New York*, 1985
- [10] J.C. Hubbert: "A comparison of radar, optic, and specular null polarization theories," *Trans. Geoscience and Remote Sensing Vol. 32,3* (1994)
- [11] J.R. Huynen: "Phenomenological Theory of Radar Targets," *Ph.D. Thesis, Technical University, Delft, The Netherlands*, 1970
- [12] IEEE Standard Definitions of Terms for Antennas, *IEEE Transactions on Antennas and Propagation, AP-31*, 1983
- [13] E.M. Kennaugh: "Effects of type of polarization on echo characteristics," *The Ohio State University, Antennas Laboratory, Columbus, OH, Reports 381-1 to 394-24, 1949-1954, in particular Report 389-12 (M.Sc. Thesis:*

March 1952); also see: Moffat D L, Grarbacz R J, "Research Studies on the Polarization Properties of Radar Targets" by Prof. Edward M. Kennaugh, The Ohio State University, Electro Science Laboratory, 1420 Kinnaer Rd., Columbus, OH 43212, July 1984, Vol. 1 & 2

- [14] A.B. Kostinski and W.-M. Boerner: "On foundations of radar polarimetry," IEEE Trans. Antennas Propagation, Vol. AP-34 (1986) pp. 1395-1404; H. Micras: Comments on "Foundations of radar polarimetry", ibid. pp. 1470-1471; Authors's reply to Comments by H. Micras, ibid. pp. 1471-1473
- [15] E. Krogager: "Aspects of polarimetric radar imaging," Ph.D. Thesis, Technical University of Denmark, 1993
- [16] E. Pottier and S. Saillard: "Fondements mathématique de la la polimétrie et son application au domain du radar," Ann. Télécommun., 47 (7-8) (1992) pp. 314-336
- [17] D.C. Youla: "A normal form for a matrix under the unitary congruence group," J. Math., Vol. 13 (1961) pp. 694-704
- [18] Lüneburg E, Ziegler V, Schroth A, Tragl K 1991, "Polarimetric covariance matrix analysis of random radar targets," ADARD-CP-501, Target and Clutter Scattering and their Effects on Military Radar Performance, May 6-9, 1991, Ottawa, Canada, pp. 27-1-27-12

# ASYMPTOTICS OF ELECTROMAGNETIC FIELD IN THE PROBLEM OF DIFFRACTION BY A WEDGE WITH ANISOTROPIC FACE IMPEDANCES

Mikhail A. Ljalinov

Department of Mathem. Physics, Institute of Physics, S. Petersburg University, Uljanovskaja 1-1, Petrodvorec, 198904, Russia.

## ABSTRACT

The asymptotic procedure developed for coupled Maliuzhinets' system of functional equations gives effective asymptotic formulae for the electromagnetic field scattered by a wedge with anisotropic impedance faces. The analytic technique for solving of recurrent system is based on modified Fourier transformation and theory of Maliuzhinets' functional equations. Investigation of the spectral function leads to extraction of their singularities which correspond to different waves: reflected, leaky or scattered. When  $kp \gg 1$  high frequency asymptotics can be deduced using closed integral representation of the wave field. Via matching of local series one can construct a uniform asymptotic representation.

## INTRODUCTION

The problem of diffraction by a wedge is the key problem in many practical situations. Particular interest to the problem of diffraction by a wedge with anisotropic coatings arises recently due to the development of new technologies and their applications in construction of scattering surfaces with prescribed properties [1-9].

Electromagnetic field in our case can be expressed via  $E_z$ ,  $H_z$  components which are directed along the edge of the wedge. The  $E_z, H_z$  components satisfy the wave equation (with  $\exp(-i\omega t)$  time dependence which is suppressed in this paper) and anisotropic boundary conditions. Using Sommerfeld integrals we reduce the problem under consideration to the system of coupled Maliuzhinets' functional equations for the pair of spectral functions. Spectral functions are to be chosen from a special class of meromorphic functions to represent physical solution. For weak anisotropy the system of functional equations can be solved by asymptotic method. It is shown that the leading terms and the first correction can be determined in closed form by means of modified Fourier transformation. In the case of  $E_z$  polarization interaction of the incident wave with an anisotropic wedge generates an  $H_z$  component of scattered field which is proportional to the magnitude of anisotropy. Analysis of the obtained formulae leads to extraction of waves of different physical nature: reflected, scattered or leaky waves. Standard uniform asymptotic analysis is applied to construct uniform asymptotics of the field outside the vicinity of the edge. Our approach uses Maliuzhinets' method which has to be modified appropriately and applied to asymptotic procedure [10].

# FORMULATION AND ANALYSIS

A plane wave

$$E_z^i = e^{-ik\rho\cos(\varphi - \varphi_0)} E_{0g}, \quad H_z^i = e^{-ik\rho\cos(\varphi - \varphi_0)} E_{0g} \quad (1)$$

is incident on a wedge, whose faces are  $\varphi = \pm \tilde{\varphi}$ , where  $\rho, \varphi, z$  are cylindrical polar coordinates with  $z$ -axes directed along the edge (Fig. 1). Local coordinates  $X^\pm, Y^\pm$  with  $(\pm)$  related to the faces  $\varphi = \pm \tilde{\varphi}$  are determined as

$$X^\pm = \mp \rho \cos(\tilde{\varphi} \mp \varphi), \quad Y^\pm = \rho \sin(\tilde{\varphi} \mp \varphi)$$

where  $Y$  is local normal coordinate. Electromagnetic field can be expressed via  $E_z, H_z$  [10]. In the leading approximation for a weak anisotropy ( $\varepsilon$  is small) one has

$$E_z(\rho, \varphi) = \frac{1}{2\pi i} \int_{\gamma} e^{-ik\rho\cos\alpha} \frac{\psi_g(\alpha + \varphi)(\pi/2\tilde{\varphi})\cos(\pi\varphi_0/2\tilde{\varphi})E_{0g}}{\left[\sin \frac{\pi(\alpha + \varphi)}{2\tilde{\varphi}} - \sin \frac{\pi\varphi_0}{2\tilde{\varphi}}\right]} d\alpha (1+O(\varepsilon^2))$$

$$H_z(\rho, \varphi) = \frac{\varepsilon}{2\pi i} \int_{\gamma} e^{-ik\rho\cos\alpha} \frac{\psi_g(\alpha + \varphi)(\pi/2\tilde{\varphi})\cos(\pi\varphi_0/2\tilde{\varphi})E_{0g}}{\left[\sin \frac{\pi(\alpha + \varphi)}{2\tilde{\varphi}} - \sin \frac{\pi\varphi_0}{2\tilde{\varphi}}\right]} d\alpha \quad (1)$$

$$* \int_{\gamma} (\alpha + \varphi) d\alpha (1+O(\varepsilon^2))$$

where all notations are defined in [10]. We consider the integrand of  $H_z$  (1) and construct uniform asymptotic formulae when  $k\rho \gg 1$ . The investigation of asymptotics of  $E_z$  component is standard [4].

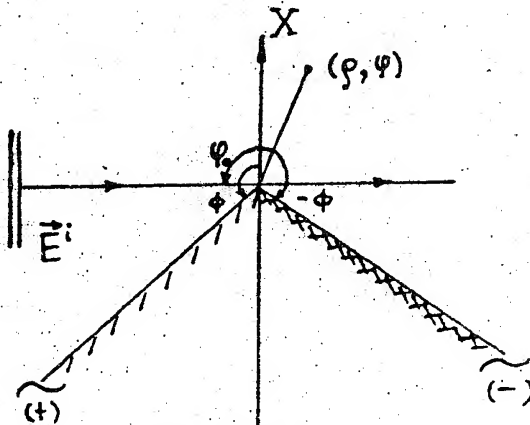


Figure 1.

Let  $\tilde{\varphi} > \pi/2$ , then in general case integrand in (1) for  $H_z$  may have poles  $\alpha_{\pm}^{\pm} = \pm 2\tilde{\varphi} - \varphi_0 - \varphi$ ,  $\alpha_{\pm}^{\theta} = -\varphi \pm (\pi + \tilde{\varphi} + \theta_{\pm}^{\pm})$  and  $\alpha_{\pm}^{\chi} = -\varphi \pm (\pi + \tilde{\varphi} + \chi_{\pm}^{\pm})$  [10]. We omit consideration of  $\alpha_{\pm}^{\chi}$ , since it

is the same as for  $\alpha_{\pm}^{\theta}$ . When deformation of integration contour  $\gamma$  into steepest descent path [4] is performed, these poles can be captured. The residues in the poles  $\alpha_{\pm}$  give leaky wave terms

$$r_{\pm}^{\theta} = \varepsilon C_{\pm} \exp[ik\rho \cos(\mp + \theta \mp \varphi)] U(\pm\rho - \rho_0^{\pm}),$$

and  $U(x)$  is Heaviside function:  $U(x) = 1$  ( $x > 0$ ),  $U(x) = 0$  ( $x < 0$ ). If  $\text{Im}\theta > 0$  we can neglect these waves in asymptotics when  $k\rho \gg 1$ . Analogously contribution given by residues at the poles  $\alpha_p^{\pm} = \pm 2\bar{\varphi} - \varphi_0$  can be interpreted as reflected secondary waves arising due to anisotropy of the wedge faces

$$r_n^{\pm} = \varepsilon e^{-ik\rho \cos(\pm 2\bar{\varphi} - \varphi - \varphi_0)} E_{og} U(\pi - |\pm 2\bar{\varphi} - \varphi - \varphi_0|) * \\ * (-\psi_g(\pm 2\bar{\varphi} - \varphi_0)) * \xi(\pm 2\bar{\varphi} - \varphi_0)$$

where  $\psi_g(\pm 2\bar{\varphi} - \varphi_0)$  and  $\xi(\pm 2\bar{\varphi} - \varphi_0)$  are easily computed

$$\xi(\pm 2\bar{\varphi} - \varphi_0) = \pm A_{11}^{\pm} / a_{21}^{\pm} 2\sin(\varphi_0 \mp \bar{\varphi}) / (\pm \sin(-\varphi_0 \mp \bar{\varphi}) + \sin\theta^{\pm}) / \\ / (\pm \sin(-\varphi_0 \mp \bar{\varphi}) - \sin\chi^{\pm})$$

$$\psi_g(\pm 2\bar{\varphi} - \varphi_0) = - \frac{\sin(-\varphi_0 \mp \bar{\varphi}) \pm (-\sin\chi^{\pm})}{\sin(-\varphi_0 \mp \bar{\varphi}) \pm \sin\chi^{\pm}}$$

Cylindrical wave arises due to saddle points and given by

$$H_{sp}(\rho, \varphi) \sim \frac{\varepsilon e^{ik\rho + i\pi/4}}{\sqrt{2\pi k\rho}} E_{og} \pi/2\bar{\varphi} \cos \frac{\pi\varphi_0}{2\bar{\varphi}} \left\{ \frac{\psi_g(\varphi - \pi)\xi(\varphi - \pi)}{\left[ \sin \frac{\pi(\varphi - \pi)}{2\bar{\varphi}} - \sin \frac{\pi\varphi_0}{2\bar{\varphi}} \right]} - \right. \\ \left. - \frac{\psi_g(\varphi + \pi)\xi(\varphi + \pi)}{\left[ \sin \frac{\pi(\varphi + \pi)}{2\bar{\varphi}} - \sin \frac{\pi\varphi_0}{2\bar{\varphi}} \right]} \right\}$$

Nonuniform asymptotic representation of the wavefield is used to construct a uniform one [10]. For simplicity we are restricted by angles of incidence  $\bar{\varphi} > \varphi_0 > \pi - \bar{\varphi}$  when only one face of wedge is illuminated by incident wave. We neglect the terms  $r_{\pm}^{\theta, \chi}$  for  $k\rho \gg 1$ .

1. Using the method of matching of local asymptotics [9] one has

$$H_z \sim \varepsilon E_{og} e^{-ik\rho \cos(2\bar{\varphi} - \varphi_0 - \varphi)} (-\psi_g(2\bar{\varphi} - \varphi_0)\xi(2\bar{\varphi} - \varphi_0)) * \\ * F\left[\sqrt{2k\rho} \cos\left[\frac{2\bar{\varphi} - \varphi - \varphi_0}{2}\right]\right] + \frac{e^{ik\rho + i\pi/4}}{\sqrt{2\pi k\rho}} \varepsilon E_{og} \left\{ \frac{-\psi_g(2\bar{\varphi} - \varphi_0)\xi(2\bar{\varphi} - \varphi_0)}{2\cos\left[\frac{2\bar{\varphi} - \varphi - \varphi_0}{2}\right]} - \right.$$

$$\begin{aligned}
& - \frac{(\pi/2\Phi) \cos \frac{\pi\varphi_0}{2\Phi} \psi_g(\pi+\varphi) \xi(\pi+\varphi)}{2\sin\left[\frac{\pi}{4\Phi}(\pi+\varphi-\varphi_0)\right] \cos\left[\frac{\pi}{4\Phi}(\pi+\varphi+\varphi_0)\right]} \Bigg\} + \frac{e^{ik\rho+i\pi/4}}{\sqrt{2\pi k\rho}} * \\
& * cE_{og} \Bigg\{ \frac{(\pi/2\Phi) \cos \frac{\pi\varphi_0}{2\Phi} \psi_g(\varphi-\pi) \xi(\varphi-\pi)}{2\sin\left[\frac{\pi}{4\Phi}(\varphi-\pi-\varphi_0)\right] \cos\left[\frac{\pi}{4\Phi}(\varphi-\pi+\varphi_0)\right]} \Bigg\} \quad (2)
\end{aligned}$$

where  $F(x)$  is Fresnel integral. For chosen angles of incidence, the wave field has one transition region in the vicinity of the ray  $\varphi = 2\Phi - \varphi_0 - \pi$ , when the argument of Fresnel integral is equal to zero. Denominators of the second term in (2) are also equal to zero, but singularities cancel each other. Formula (2) is generalized easily to the case when both wedge faces are illuminated. The effectiveness of formula (2) is determined by the effectiveness of numerical computation of  $\xi(\pm\pi+\varphi)$  [10]. Initially this function is derived in the strip  $|\operatorname{Re} \alpha| < \Phi$ . As shown in [10]  $\xi(\alpha)$  can be continued analytically to wider strip  $|\operatorname{Re} \alpha| < 3\Phi$ . Then the problem of tabulation for  $\xi(\alpha)$  consists in fast numerical calculation of exponentially converging integrals.

#### REFERENCES

- (1) Miller (M.A.) and (V.I.) Talanov, Usage of conception of surface impedance in the theory of surface waves. Sov. Radiophysics, (1961) 4(6), pp.795-830
- (2) Kurushin (E.P.) et.al., Diffraction of electromagnetic waves by anisotropic structures, (1975), Nauka, Moscow, 196 p.
- (3) Nefedov (E.I.) and (A.T.) Fialkovskij, Electromagnetic plane wave diffraction by anisotropic halfplane in free space and plane waveguide, Radiotechnics & Electronics, (1972), 17(6), pp.1141-1152
- (4) Maliuzhinets (G.D.), Excitation, reflection and emission of surface waves from a wedge with given face impedances, Sov. Phys. Dokl., (1958) 3, pp.752-755.
- (5) Maliuzhinets (G.D.), Inversion formula for the Sommerfeld integral, Sov. Phys. Dokl., (1958) 3, pp.52-56.
- (6) Tuzhilin (A.A). Theory of inhomogeneous functional Maliuzhinets equations. Differential equations. (1973), 9(11), pp.2058-2064.
- (7) Senior (T.B.A.), Diffraction by a generalized impedance halfplane. Radio Sci., (1991), 26(1), pp.163-167.
- (8) Bernard (J.-M.L.), Diffraction by a metallic wedge covered with a dielectric material, Wave Motion, (1987) 9, pp.543-561.
- (9) Borovikov (V.A.) and (B.E.) Kinber, Geometrical theory of diffraction, (1978), Svyas', Moscow, 248 p.
- (10) Ljalinov M.A. "On one approach to an electromagnetic diffraction problem in a wedge shaped region" J.Phys.A (1994) 27, L183-L189.



# UNIFORM DIFFRACTION COEFFICIENTS AT EDGES IN A GROUNDED DIELECTRIC SLAB

Stefano Maci, Leonardo Borselli, C. Salvador, Lorenzo Rossi  
Department of Electronic Engineering, University of Florence,  
via S. Marta 3, 50139, Florence, Italy,

## Abstract

Uniform diffraction coefficients has been derived for predicting far field pattern of an horizontal electric dipole placed on a truncated, grounded dielectric slab. The formulation is based on a Physical Optics (PO) approximation for both the volumetric currents in the slab and the surface currents on the ground plane. This approach leads to a spectral integral, which is uniformly evaluated by taking into account the presence of surface waves and leaky waves poles.

## 1. Introduction

The prediction of the diffraction mechanisms at edges in a grounded dielectric slab is of importance in patch antennas applications. The need for taking into account such effects mostly arises when the patches are printed on free standing structures, in which the front-to-back ratio has to be maximized for interferences reduction. Furthermore, these diffraction mechanisms may considerably affect the radiation pattern [1]-[2] and have an influence on the directivity, mostly when surface waves are strongly excited.

GTD diffraction coefficients for an electric dipole placed at the interface of a dielectric slab and in proximity of its interruption, would provide an efficient tool for predicting diffraction contributions. Diffraction coefficients may be derived from the exact solution of an half-plane with surface impedance boundary conditions (b.c.) on one face and perfectly conducting b.c. on the other face [3]. However, this kind of solution loses validity for increasing substrate thicknesses, when the impedance boundary condition approximation fails. Then, it cannot be easily applied to patch antennas problems.

A more general solution of the canonical half-plane problem was derived by the Wiener-Hopf technique in [4], in which generalized impedance boundary conditions were employed to model the slab. Unfortunately, due to the extreme complication of the problem, the diffraction coefficients that can be deduced from this solution are not simply to manipulate.

In this paper, a uniform diffraction coefficient has been derived for an horizontal electric dipole on an interrupted slab. To this end a Physical Optics (PO) estimate is adopted for both the volumetric currents in the slab and the surface currents on the ground plane. In particular, the analysis consists of four steps. a) First, by applying the equivalence theorem, the half-slab and the half-ground plane are replaced by polarization and surface currents, respectively, radiating in free space; b) next, according to PO, these currents are estimated from those existing in an infinite grounded slab, that are represented in terms of spectral plane-wave; c) then, the far field is obtained by the end-point evaluation of the radiation integral of such currents; d) finally, the spectral integral which is obtained at the previous step is asymptotically evaluated by the Van der Waerden method of the steepest descent, taking also into account for the presence of surface waves and leaky waves poles.

## 2. Formulation

Let us consider a semi-infinite dielectric slab and an infinitesimal, horizontal electric dipole (HED) located at the air-dielectric interface, at distance  $L_y$  from the edge. For the sake of simplicity, let us suppose the HED parallel to the edge. A coordinate system  $(x, y, z)$  of unit vectors  $(\hat{x}, \hat{y}, \hat{z})$  is introduced, with its origin at the HED. The  $z$  axis is perpendicular to the surface and the  $x$ -axis is parallel to the edge and along the HED. A spherical coordinate system  $(r, \theta, \phi)$  of unit vectors  $(\hat{r}, \hat{\theta}, \hat{\phi})$  is also introduced in order to describe the far field pattern.

By resorting to the equivalence theorem, the dielectric and the ground plane can be replaced by electric polarization currents and surface electric currents, respectively. These currents may be estimated in the hypothesis of infinite grounded dielectric slab, by resorting to the PO approximation. In such a way, all the currents components may be expressed by a spectral-Fourier representation; i.e.,

$$\vec{J}_p(x, y) = \frac{1}{2\pi} \int_{-\infty}^{\infty} \int_{-\infty}^{\infty} \vec{J}_p(k_x, k_y) e^{-j(k_x x + k_y y)} dk_x dk_y \quad (1)$$

where the apex  $p = x, y, z$  denotes the directions of the current components and the index  $q = g, d$  refers to the ground-plane currents and the dielectric currents, respectively. It is worth noting that  $\vec{J}_p^d$  and  $\vec{J}_p^g$  have also a dependence from the  $z$  variable. This dependence is not explicitly expressed in (1) for obtaining a more compact notation.

In order to obtain the magnetic potential components, the electric current  $\vec{J}_p^g$  is integrated all over the semi-infinite extent  $y \leq L_y$  after weighting with the free-space, far-field Green's function. By starting from this potential components it is a straightforward matter to obtain the far field contribution at any point  $P \equiv (r, \theta, \phi)$

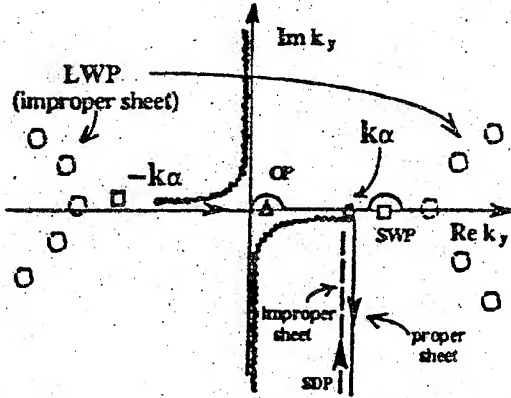


Fig. 1. Topology of the proper and improper  $k_y$  complex plane.

$$\vec{E}(r, \theta, \phi) = -jk \frac{\exp(-jk r)}{4\pi r} (a_\theta \hat{\theta} + a_\phi \hat{\phi}) \quad (2)$$

in which

$$a_\xi = \sum_{p,q} a_p^q \hat{p} \cdot \hat{\xi} + \hat{x} \cdot \hat{\xi}, \quad \xi = \theta, \phi \quad (3)$$

$$a_p^q = \int_{-\infty}^{\infty} \int_{-\infty}^{\infty} \int_0^h \vec{J}_p(x, y, z) e^{jk(xu + yv + wz)} dx dy dz \quad (4)$$

in which

$$u = \sin\theta \cos\phi; v = \sin\theta \sin\phi; w = \cos\theta. \quad (5)$$

and  $h$  is the thickness of the substrate. In (4), the integral in  $z$  applies only to the dielectric currents  $\vec{J}_p^d$ . It is worth noting that the term  $\hat{x} \cdot \hat{\xi}$  in (3) represents the direct far field contribution from the unit dipole.

The double spectral Fourier representation (1) is now introduced in (4). Changing the order of integration and performing in a closed form both the couple of integral in  $k_x$ - $x$  and the integral in  $y$ , leads to

$$a_p^q = \int_{-\infty}^{\infty} \frac{j \vec{J}_p^q(ku, k_y)}{(k_y - kv)} e^{-jL_y(k_y - kv)} dk_y \quad (6)$$

in which  $\vec{J}_p^g(k_x, k_y) = \vec{J}_p^g(k_x, k_y)$  for  $q=g$  and  $\vec{J}_p^d(k_x, k_y) = \int_0^h \vec{J}_p^d(k_x, k_y) e^{jk_z w} dz$  for  $q=d$ .

The integrand in (6) exhibits an optical pole (OP) at  $k_y = kv$  with a small, negative imaginary part due to small losses in the surrounding medium which can be assumed. Otherwise, one can suppose this imaginary part tends to zero, thus producing a clockwise indentation of the integration path, as shown in Fig. 1.

The numerical evaluation of the integral in (6) presents two main difficulties. First, the poles have to be extracted in order to obtain a smooth function suitable for numerical integration. Next, the behaviour of  $\vec{J}_p^g(ku, k_y)$  for  $k_y$  large is such that the integrand in (6) is rapidly oscillating and slowly decaying, thus resulting in a poor convergence of the integral for large value of  $kL_y$ . To overcome these limitations, asymptotic, closed-form expression of  $a_p^q$  will be developed in the next sections.

### 3. Pole structure and asymptotic evaluation.

In (6), the relevant topology of the proper Riemann sheet ( $\text{Im} \sqrt{k^2(1-u^2) - k_y^2} < 0$ ) of the complex  $k_y$  plane is depicted in Fig. 1. This sheet contains two branch points at

$$k_y = \pm k\alpha = \pm k(1-u^2)^{1/2} \quad (7)$$

that depend on the observation aspects. Apart from the optical pole OP at  $kv$ , there are surface wave poles (SWP) at  $k_y = \pm k_{y_{sw}}^{(n)}$  ( $n=1,2,\dots$ ). Other complex poles  $k_y = \pm k_{y_{lw}}^{(i)}$

( $i=1,2..$ ) are located on the improper Riemann sheet ( $\text{Im}((k\alpha)^2 - k_y^2)^{1/2} > 0$ ) of the  $k_y$  plane.

In the conventional Sommerfeld representation, these poles correspond to the leaky wave poles (LWP). When  $kh$  or  $\epsilon_r$  increase, the LWP migrate toward the branch point and emerge on the proper Riemann sheet when the prime condition of SW is met.

The topology of the  $k_y$  plane is not much convenient for the asymptotic evaluation in (6), since the steepest descent path (SDP) does not lie completely on the proper Riemann sheet. As shown in Fig. 1, in this plane the SDP starts from  $k\alpha - j\infty$  on the improper sheet, passes through the branch point  $k\alpha$  and goes to  $k\alpha + j\infty$  on the proper sheet.

By employing the substitution

$$k_y = k\alpha - jks^2; \sqrt{(k\alpha)^2 - k_y^2} = ks\sqrt{s^2 + 2j\alpha} \quad (8)$$

the integral in (6) is rewritten as

$$a_p^q = 2j e^{-j\Omega(\alpha-v)} \int_{-\infty \exp(j\pi/4)}^{\infty \exp(j\pi/4)} \frac{s b(s)}{s^2 - s_0^2} e^{-\Omega s^2} ds \quad (9)$$

where

$$s_0 = e^{-j\pi/4} \sqrt{\alpha - v}; \quad b(s) = J_p^N(ku, k_y); \quad \Omega = kL_y \quad (10)$$

The conditions (8) map the SDP onto the real axis of the top Riemann sheet of the complex  $s$ -plane, as shown in Fig. 2. Here, the saddle point lies at  $s=0$ . It is worth noting that the integrand in (9) has OP at  $\pm s_0$ , SWP at

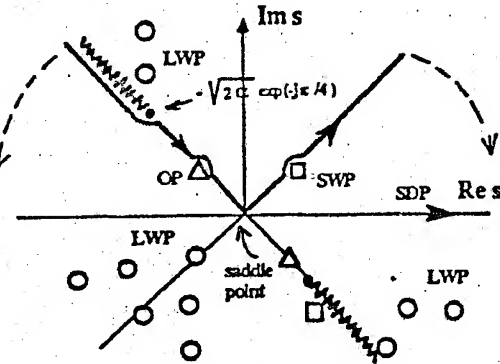


Fig. 2. Topology of the top sheet of the complex  $s$ -plane

$$s_{sw}^{(n)} = e^{j\pi/4} \sqrt{k_{y,sw}^{(n)}/k - \alpha} \quad (n=1,2..), \text{ and LWP at } s_w^{(i)} = -e^{j\pi/4} \sqrt{k_{y,w}^{(i)}/k - \alpha} \quad (i=1,2..) \quad (11)$$

The path of integration in (8) is now deformed onto the SDP through this saddle point (Fig. 2). In this deformation the SWPs and an OP are captured, thus leading to

$$a_p^q = 2\pi J_p^N(ku, kv) - 2\pi j \sum_n R_{sw}^{(n)} e^{-j\Omega(k_{y,w}^{(n)}/k - v)} + I_{sdp} \quad (12)$$

where  $I_{sdp}$  is the integral along the real axis of the complex  $s$ -plane, and  $R_{sw}^{(n)}$  are the residues of the SWP.

The integral on the SDP can be evaluated by means of the Van der Waerden method of SD [5]. In principle, in all the poles in (11), including the LWPs, affect the asymptotic value of this integral; in most practical cases, only the inclusion of the LWP closer to the origin results in a significant improvement of the asymptotic evaluation [6]. The inclusion of this pole ensures uniformity in the asymptotic solution also very close to the SW prime conditions. In order to evaluate asymptotically the integral, the significant singularities are extracted and the resulting regular function is approximated by the first two nonvanishing terms of its Taylor expansion around  $s=0$ , thus obtaining

$$I_{sdp} = \frac{\sqrt{\pi}}{2} e^{-j\Omega(\alpha-v)} + j\frac{\pi}{4} \left( \sum_n R_w^{(n)} f(j\Omega(s_w^{(n)})^2) + [b(s_0) - b(-s_0)] f(j\Omega s_0^2) - \frac{e^{-j\pi/4} b'(0)}{(s_0)^2} \Omega^{-3/2} \right) \quad (13)$$

where  $s_w^{(i)}$  represents either  $s_{sw}^{(i)}$  or  $s_w^{(i)}$ ,  $R_w^{(i)}$  is its residue, and

$$f(x) = \frac{1}{\sqrt{x}} \left[ 1 - F(x) - \frac{1}{2jx} \right] \quad (14)$$

in which  $F(x)$  is the UTD transition function.

The asymptotic expansion in (12) shows three contributions. 1) The first, due to the residue of the optical pole, is the geometrical optics (GO) contribution. 2) As can be easily inferred from the phase term  $\exp(-j\Omega(\alpha-v))$ , the SDP integral represents a field which

arises from a diffraction-point  $Q'$  that satisfies the conventional GTD condition in free-space (see Fig. 3). Then the last contribution in (12) represents a space-wave diffracted field. 3) The residues of SWP represents the field diffracted from surface waves in the PO approximation. The SW diffracted field arises from a diffraction-point  $Q_{sw}^{(n)}$  that satisfy the generalized Fermat principle; this point does not coincide with the space-wave diffraction point  $Q'$ ; in particular, as shown in Fig. 3,  $Q_{sw}^{(n)}$  precedes  $Q'$  due to the slow phase-velocity of the surface waves.

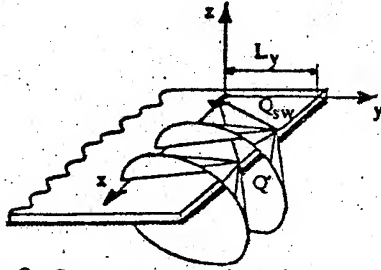


Fig. 3. Space waves and surface waves diffraction cones.

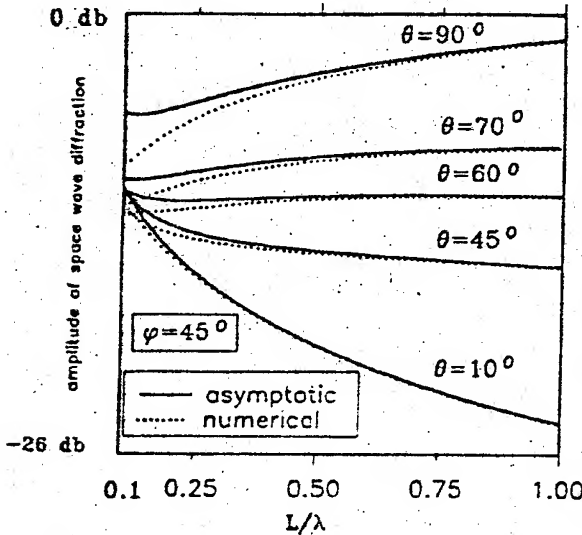


Fig. 4. Amplitude of the space-wave diffracted field; ( $\phi=45^\circ$ ,  $\epsilon_r=2.2$ ,  $\theta$ -components).

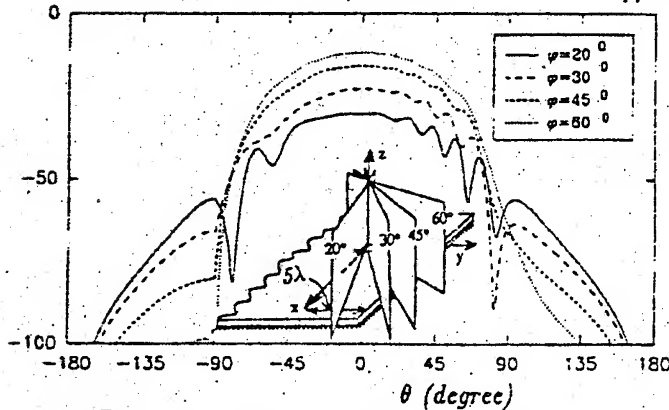


Fig. 5. Far field pattern ( $\phi$ -component) of a dipole placed at  $5\lambda$  from the edge, for different plane cuts.

#### 4. Numerical results

Preliminary results has been obtained by the formulation presented here. The examples refer to  $\epsilon_r=2.2$  and  $h=\lambda/20$ . Under these conditions, only the fundamental TM mode is primed in the slab.

Fig. 3 shows the amplitude of the space diffracted field ( $I_{sd\phi}$ ,  $\theta$ -component) as a function of  $L_y/\lambda$  for different values of  $\theta$  in the plane cut  $\phi=45^\circ$ . The plots compare the numerical integration (continuous line) with the asymptotic approximation in (13) (dashed line). Although the asymptotic approximation requires  $\Omega=kL_y$  large, a surprising agreement has been found also for  $L_y=\lambda/2$ .

Fig. 4 shows the total, normalized far-field ( $\phi$ -component) of a dipole which is placed at  $L_y=5\lambda$  from the edge, for different plane cuts  $\phi=C$  ( $C=60^\circ, 45^\circ, 30^\circ$ ). It is worth pointing out that, when  $C$  decreases, the field amplitude decreases due to the low contribution of GO to the  $E_\phi$ -component. Furthermore, side-lobes gradually appear, which arise from the interference between SW-diffraction and GO contributions.

#### References

- [1] E. Lier, and K.R. Jacobsen "Rectangular microstrip antennas with infinite and finite ground plane dimensions" *IEEE Trans. on Antennas and Propagat.*, Vol. AP-31, pp. 978-984, 1983.
- [2] S.A. Bokhari, J.R. Mosig, F.E. Gardiol, "Radiation pattern computation of microstrip antennas on finite size ground plane," *IEE Proceedings-H*, Vol. 139, N. 3, pp. 278-286, 1992
- [3] R.G. Rojas, "Electromagnetic diffraction of an obliquely incident plane wave field by a wedge with impedance faces," *IEEE Trans. Antennas Propagat.*, Vol. AP-36, No. 7, pp. 956-970, July 1988.
- [4] H.C. Ly, G. Rojas, P.H. Pathak "EM plane wave diffraction by a planar junction of two thin material half-plane: oblique incidence" *IEEE Trans. on Ant. and Propagat.*, Vol. AP-41, No. 4, pp 429-441 1993.
- [5] B. L. Van der Waerden, "On the method of saddle points" *Appl. Sci. Res.*, Vol. B2, pp. 33-45, 1951.
- [6] M. A. Marin, S. Barkeshli, P.H. Pathak, "On the location of proper and improper surface waves poles for the grounded dielectric slab," *IEEE Trans. Antennas Propagat.*, Vol. AP-38, No. 4, pp. 570-573, 1990.

# MILLIMETER WAVE DIELECTRIC STRIP WAVEGUIDES USING FERRITES AND SEMICONDUCTORS

V.V.Meriakri, B.A.Murmuzhev, M.P.Parkhomenko

Institute of Radio Engineering and Electronics  
of the Russian Academy of Sciences,  
1 Vvedenski sq., Fryazino Moscow reg., 141120, Russia.

## ABSTRACT

Devices based on dielectric strip waveguides made of low loss ferrites and semiconductors have been created. Circuit elements, such as attenuators, phase shifters, switches, dividers, couplers, in particular with optical and electrical control, nonreciprocal devices, were applied to some millimeter wave systems, including communication systems..

## INTRODUCTION

Dielectric strip waveguides (DSW) are well known in microwave and millimeter wave techniques.<sup>1,2,3</sup>

Here, we present some results of investigation of the DSW made of ferrites and semiconductors. These materials permit to realize all of the components necessary for measurement and antenna-feeder subsystems at frequencies from 30 to 200 GHz.

## MATERIALS FOR DSW

The parameters of low loss dielectrics, ferrites and semiconductors, used for DSW fabrication are shown in Table 1. The measurements of these parameters were carried out using beam waveguide spectroscopy methods.

DSW sections made of TGS crystal were used as polarization filters. TGS crystal parameters for the wave propagating along three crystallographic axes were measured to be  $n_1 = 2.74$ ,  $\tan\delta_1 = 0.62$ ;  $n_2 = 2.31$ ,  $\tan\delta_2 = 8.4 \cdot 10^{-3}$ ;  $n_3 = 2.91$ ,  $\tan\delta_3 = 1.5 \cdot 10^{-2}$ , respectively, at  $\lambda = 1.1$  mm.

Expression

$$\alpha \text{ [dB/cm]} = 27.3 \tan\delta \, n/\lambda \quad (1)$$

allows us to estimate losses in DSW, made of materials of Tab.1. Losses at frequencies about 150 GHz amount to some dozen dB/cm.

Table 1.

#	Material	$n \pm 0,3\%$	$\tan\delta \cdot 10^{-3} \pm 5\%$	$\lambda, \text{ mm}$
1	PTFE	1.437	0.63	0.63
2	Polyethylene	1.512	0.62	1.0
3	SiO <sub>2</sub> (ceramic)	1.820	1.70	0.75
4	SiO <sub>2</sub> (fused)	1.951	1.47	0.86
5	Al <sub>2</sub> O <sub>3</sub> (ceramic)	3.031	1.30	0.95
6	Ferrite (NiZn)	3.65	1.52	1.3
7	Ferrite (Li)	3.95	1.24	2.16
8	Ferrite (FeY)	3.88	0.75	2.16
9	Si ( $\rho > 10^4 \Omega \text{ cm}$ )	3.42	0.2	1.0
10	GaAs ( $\rho > 10^7 \Omega \text{ cm}$ )	3.61	0.2	2.2

$n$  - refractive index,  $\tan\delta$  - loss tangent

#### DEVICES BASED ON DSW

Main components for measurement equipment and subsystems for frequencies 26 - 48, 80 - 120 and 115 - 145 GHz have been elaborated. Components are based on PTFE, SiO<sub>2</sub>, Al<sub>2</sub>O<sub>3</sub>, Si, TGS and ferrites (Tab.1). For the above mentioned frequency ranges, DSW - rectangular waveguide transition sections, couplers, frequency and polarization filters, attenuators, phase shifters, nonreciprocal devices have been elaborated.

For example, complete set of devices for frequency range 26 - 37 GHz has been fabricated on the basis of NiZn ferrite on foamed PTFE substrate. For 3 and 4 port switches, two T-bridges were used, based on electrically controlled square cross-section DSW and metal gratings. Switching loss is less than 0.6 dB, channel isolation 20 dB. Rectangular cross-section ferrite DSW with the same coil is used as an electrically controlled phase shifter. Phase shift is about 80 deg/cm, insertion loss 0.4 dB. DSW made of Si is used as an optically controlled attenuator. In this case, three light emitting diodes enable to change attenuation from 0.5 to 25 dB at the 26 - 37 GHz range.

#### SOME SUBSYSTEMS BASED ON IMAGE DSW

Components based on image DSW have been created for the frequency ranges 80 - 120 and 115 - 145 GHz. For example, isolators

with insertion losses not exceeding 2.5 dB and return losses 15 dB have been elaborated.<sup>5</sup> Filter-resonator, using ferrite disc resonator had 20 dB stopband and insertion loss 0.5 dB.<sup>6</sup> Broadband directional coupler has coupling  $15.5 \pm 1.5$  dB at the frequency range 80 - 120 GHz.

Receiving and transmitting subsystems consisting of image DSW - metal waveguide transition section, ferrite isolator, directional coupler, optically controlled attenuator and modulator have been elaborated for the frequency range 80 - 120 GHz. Insertion losses  $\leq 14$  dB, VSWR  $< 1.4$ , isolation  $> 14$  dB, attenuation range 15 dB, dimensions  $20 \times 40 \times 120$  mm<sup>3</sup>, weight 200 grams.

#### REFERENCES

1. R.M.Knox, P.P.Toulios, "Integrated circuits for the millimeter through optical frequency range," Symposium on Submillimeter waves. Polytechnical Institute of Brooklyn, pp.497-515, 1970.
2. T.Itoh, "Inverted strip dielectric waveguide for millimeter wave integrated circuits," IEEE Trans. on MTT, vol.MTT-24, pp. 821-830, November 1976.
3. L.N.Vershina, V.V.Meriakri, "Dielectric strip waveguide for short millimeter range," Radiotekhnika i elektronika, vol.27, No.7, pp.1348-1351, 1980 (in Russian).
4. V.V.Meriakri et al, "Submillimeter beam waveguide spectroscopy and its applications" in book Problems of modern radio engineering and electronics, Nauka Publishers, Moscow, pp. 179-197, 1985.
5. S.S.Gigoyan, B.A.Murmuzev, "Millimeter wave dielectric image line ferrite isolator," Radiotekhnika, No.4, pp.84-85, 1986 (in Russian).
6. A.A.Akhumyan, S.S.Gigoyan, B.A.Murmuzev, R.M.Martirosyan, "Millimeter wave alumina image line ferrite isolators," Radiotekhnika, No.2, pp.41-43, 1990 (in Russian).



# MILLIMETER WAVE ELECTRICALLY AND OPTICALLY CONTROLLED SCREENS

V.V.Meriakri, I.P.Nikitin, M.P.Parkhomenko

Institute of Radio Engineering and Electronics  
of the Russian Academy of Sciences,  
1 Vvedensky sq., Fryazino, Moscow reg., 141120, Russia.

## ABSTRACT

The results of numerical and experimental analysis of frequency selective properties of periodic gratings, consisting of bare or metallized dielectric (semiconductor) rods of rectangular cross-section are presented. The emphasis is put on optical and electrical control of gratings' frequency selective properties.

## INTRODUCTION

Frequency Selective Screens or Surfaces (FSSs) find widespread applications in microwaves as filters, antenna subreflectors, wave polarizers, resonator walls etc.<sup>1,2</sup> The common types of FSS consist of periodical arrays of conductive patches or apertures on a conducting screen. An alternative way of FSS design is a dielectric layer with periodically varying dielectric constant or dielectric grating.<sup>3,4</sup>

Earlier,<sup>4</sup> electrically controlled grating composed of NiZn ferrite rods was demonstrated. Axial magnetization of the rods provided effective control of transmission and reflection coefficients of the E-polarized wave.

Optical and electrical (by means of electric rather than magnetic field) control of grating parameters seems to be faster, since it does not require rather inertial magnetic loops. For the purpose, two types of gratings, consisting of high-resistivity silicon rods have been considered. The first type of grating consists of silicon rods of rectangular cross-section. The second type is a metal dielectric grating, i.e. the grating of the first type, in which the inner faces of rods are coated with thin conducting strips. In<sup>5</sup>, some interesting frequency selective properties of such gratings have been demonstrated. There is an obvious advantage of this type of grating, concerned with the presence of conductive strips, which may serve as electrodes for electrical control of grating parameters.

The present paper reports the results of numerical and experimental



rimental study of silicon made electrically and optically controlled frequency selective periodical gratings.

### OPTICALLY CONTROLLED SILICON GRATING

Fig. 1 represents the cross section of the grating made of silicon rods. High-resistivity silicon ( $\rho > 2 \cdot 10^4 \Omega \text{ cm}$ ) demonstrates extremely low-losses in the millimeter wave range at room temperatures. The parameters of the material have been measured to be  $\epsilon = 11.7$  and  $\tan \delta < 10^{-4}$  in the 1 - 6 mm wavelengths.

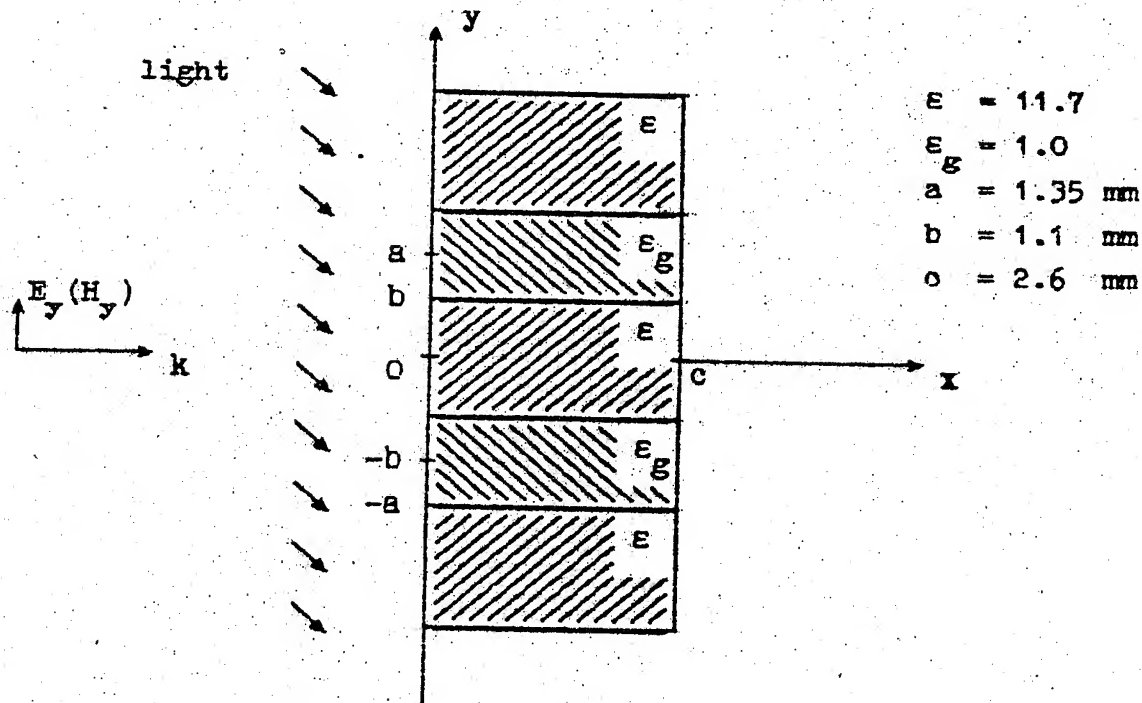


Fig.1. Cross-section of the grating.

For the normal incidence of plane linearly polarized wave, the transmission coefficients versus dimensionless parameter  $\alpha = 2a/\lambda$  are shown in Figs 2 and 3 for the E- and H-polarization cases, respectively. The solid curves correspond to the measured characteristics, while the dashed curves - to the computed ones. When the grating is illuminated by quartz halogen lamp, the transmission is levelled and suppressed to -15 dB throughout the frequency range (dotted lines). Similar measurements of the reflection coefficients resulted in suppression of reflection coefficients to -4 - 6 dB.

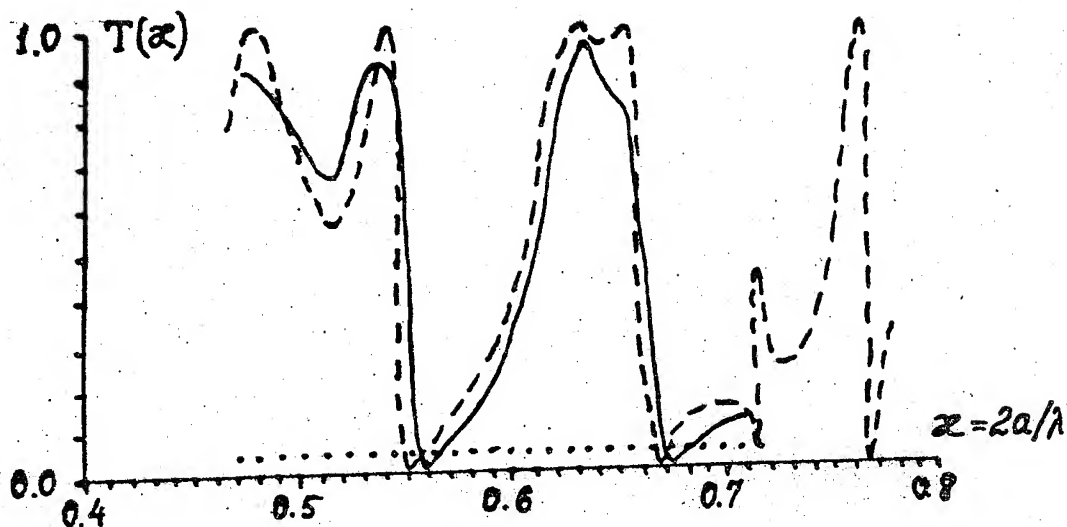


Fig.2. E-polarization case.

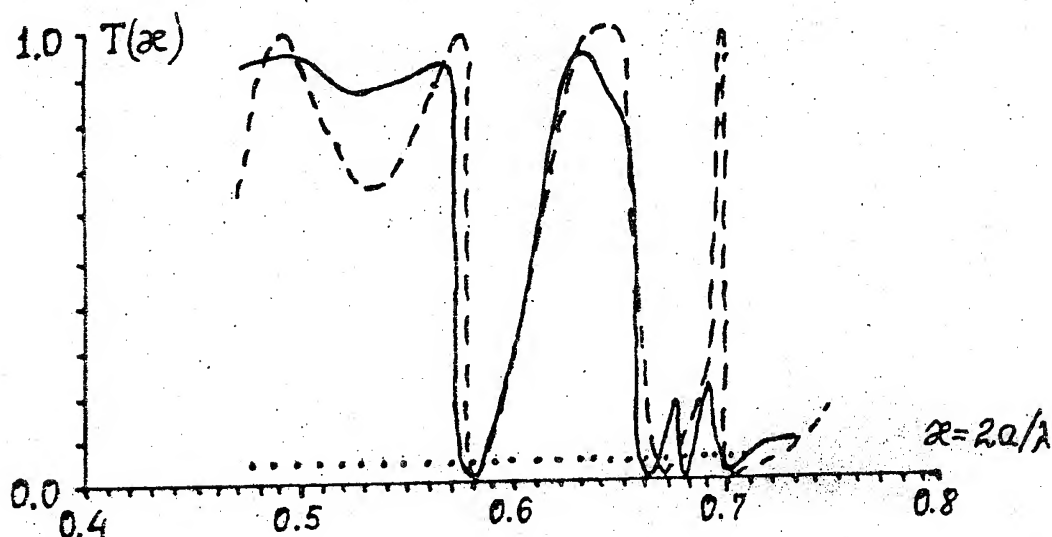


Fig.3. H-polarization case.

#### ELECTRICALLY CONTROLLED SILICON GRATING

Metal-dielectric grating, composed of thin metallized semiconductor slabs, can be effectively controlled by the electric field applied to the slabs' metallized faces. Results of numerical study of grating made of metallized silicon slabs are presented in Fig.4. Parameters of the grating are:  $a = 1.5$  mm,  $b = .15$  mm,  $c = 1.5$  mm,  $\epsilon_g = 1$ . The solid curve corresponds to the grating with  $\epsilon'' = 10^{-2}$  ( $\epsilon = \epsilon' - i\epsilon''$ ,  $\epsilon' = 11.8$ ), the dashed curve - to  $\epsilon'' = 1$  and the dotted curve - to  $\epsilon'' = 10$ .

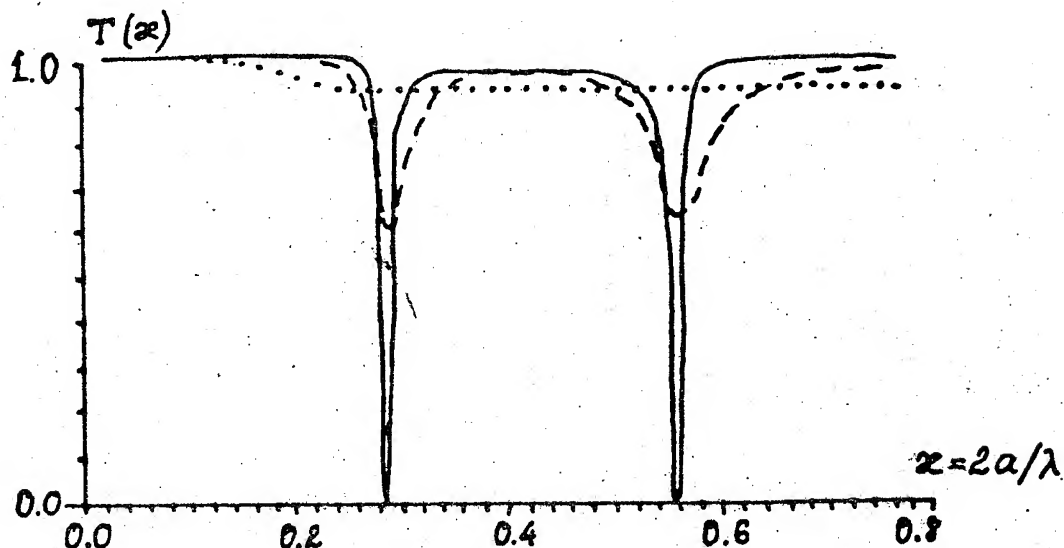


Fig.4. Metallized silicon grating. Transmission vs  $\alpha$ .

### CONCLUSIONS

Control of grating characteristics by generation of charge carriers in semiconductors by means of electric field or by light is demonstrated on two types of silicon gratings. Besides the change of transmission and reflection coefficients, the effect of light or electric field is also in the suppression of frequency selective properties of the gratings.

### REFERENCES

1. R.Mitra et al., "Techniques for analyzing frequency selective surfaces.- A review", *Proc. IEEE*, (1988), V.76, 12, pp. 1593-1615.
2. W.V.T.Rusch, "The current state of the reflector antenna art", *IEEE Trans.*, 1984, AP-32, 4, pp.313-329.
3. H.L.Bertoni et al., "Frequency-selective reflection and transmission by a periodic dielectric layer", *IEEE Trans.* 1988, AP-37, 1, pp.78-83.
4. V.V.Meriakri et al. "Ferrite rod gratings at millimetre waves", *20-th European Microwave Conf. Proc.*, Budapest, 1990, Vol.2, pp. 1383-1386.
5. V.V.Meriakri et al., "Frequency characteristics of Metal-Dielectric Gratings", *Radiotekhnika i elektronika*, 1992, V.37, 4, pp. 604-611.

# THE ELECTROMAGNETIC WAVE SCATTERING BY SCREEN SYSTEM IN STRATIFIED MEDIUM

Zinovy T. Nazarchuk and Oleg I. Ovsyannikov

Physico-Mechanical Institute of the  
National Academy of Sciences of Ukraine  
Naukova St. 5, Lviv 290601, Ukraine

## ABSTRACT

A general approach to rigorous solution of two-dimensional problem of electromagnetic wave diffraction on the system of infinitely thin and perfectly conductive screens inside a stratified medium is presented. There are three layers with different electromagnetic properties that are excited by a two-dimensional  $E$ - or  $H$ -polarized electromagnetic wave. The medium surfaces are formed by two parallel planes. In the middle layer we situate a system of cylindrical screens and assume that their cross-sections are arbitrary. The integral equations of the corresponding diffraction problem are suggested and a numerical method of solution is developed. The integral equation kernels contain the usual free-space Green function and the Sommerfeld-type integrals of two variables. An efficient method of the second kernel part evaluation is proposed using contour integration and construction Lagrange type interpolation polynomial. Some field calculation results are presented and discussed.

## INTRODUCTION

An analysis of electromagnetic wave scattering by different type inhomogeneities in stratified medium is one of the interesting problems in radiophysics [1-3], geophysics [4] and non-destructive testing. In the resonance region - the most difficult case for theoretical investigation - the integral equations technique is widely applied to solve the corresponding diffraction problems. Concerning conductive cylinders such equations are formulated regarding unknown surface current densities [5,6] or internal fields [7-10]. Numerical investigation of electromagnetic scattering by screens with resonance size within planar stratified medium have been carried out up to the present only for a strip [11], circular cylinder with a slot [12,13] or combination of them [14].

This paper presents a general technique of singular integral equations rigorous solution of the two-dimensional diffraction problem for a system of arbitrary cylindrical screens in open three-layer medium. The proposed algorithm is based on the potential method application in boundary integral equations [15]; the direct numerical treatment of the obtained singular integral equations using the mechanical quadrature method [16]; the manner of Green functions calculation by contour integration and polynomial approximation [17]. The algorithm serviceability and validity are shown by solution of scattering problem in the case of two resonant elliptical screens in a dielectric slab.

## STATEMENT OF THE PROBLEM AND GREEN FUNCTION CALCULATION

Let the planes  $y=0$  and  $y=-d$  (relating to Cartesian coordinates  $xyz$ ) form the medium interfaces with wave numbers  $\chi_1, \chi_2, \chi_3$ . The system of cylindrical infinitely thin perfectly conductive screens with cross-section of  $L_k, k=\overline{1,N}$  is arbitrary situated in the strip  $-d < y < 0$  parallel to  $Oz$ -axis. The arcs  $L_k$  are assumed as the Lyapunov type contours of arbitrary curvature. The external source of two-dimensional  $E$ - or  $H$ -polarized electromagnetic wave (the time dependence  $\exp(-i\omega t)$ ) with a  $W^*(x,y)$  longitudinal (along  $Oz$ -axis) component excites presented structure. Let  $W^* \equiv E^*(H^*)$  in the case of  $E(H)$ -polarization. Once the  $z$ -coordinate in the scattering problem is dropped, use symbol  $z$  to denote the  $(x,y)$  point, i.e. define  $z=x+iy, \bar{z}=x-iy, W^*(x,y) \equiv W^*(z)$ .

The diffraction problem is reduced to find two-dimensional Helmholtz equation solution which satisfies the conditions of continuity on the medium interfaces; of waves absence from infinity (except exciting one); of Dirichlet ( $E$ -polarization) or Neumann ( $H$ -polarization) on the arc  $L_k, k=\overline{1,N}$ ; of Meixner-type near the screen ribs ( $L_k$  arc end-points) [13,18].

Considering the radiation condition we obtain (look also [13,19])

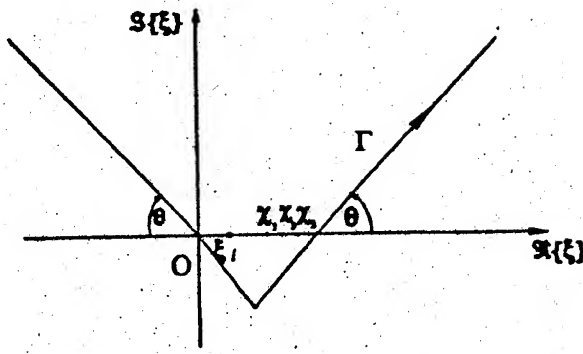


Fig. 1 The integration contour in  $\xi$ -plane.

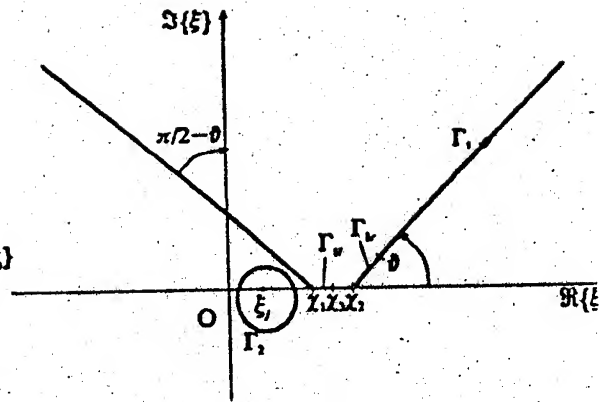


Fig. 2 Modified integration contour in the case of existing  $\xi_i$ -poles.

$$G_{E,H}(t,z) \equiv G_{E,H}^2(t,z), -d \leq \Im\{z\} \leq 0; G_{E,H}^2(t,z) = \frac{1}{4} H_0^{(0)}(\chi_2^2) + S_{E,H}^2(t,z); \quad (1)$$

$$S_{E,H}^2(t,z) = \sum_{p=1}^4 \frac{1}{4\pi} \int_{-\infty}^{+\infty} \frac{g_p \exp[\theta_p v_2 + i\xi \Re\{t-z\}]}{v_2 g} d\xi, -d \leq \Im\{z\} \leq 0,$$

$$g_1 = (v_2 p_{13} - v_1 p_{23})(v_2 p_{13} + v_3 p_{23}); \theta_1 = \Im\{t-z\};$$

$$g_2 = (v_2 p_{13} - v_1 p_{23})(v_2 p_{13} - v_3 p_{23}); \theta_2 = -2d + \Im\{t-z\};$$

$$g_3 = (v_2 p_{13} + v_1 p_{23})(v_2 p_{13} - v_3 p_{23}); \theta_3 = -2d - \Im\{t-z\};$$

$$g_4 = g_2; \theta_4 = -2d - \Im\{t-z\}; g = (v_2 p_{13} + v_1 p_{23})(v_2 p_{13} + v_3 p_{21}) - (v_2 p_{13} - v_1 p_{23})(v_2 p_{13} + v_3 p_{21}) \exp[-2d v_2]; r = |t-z|; v_i = \sqrt{\xi^2 - \chi_i^2}, \Re\{v_i\} \geq 0,$$

where  $p_{ji}=1$  in the case of  $E$ -polarization,  $p_{ij}=\chi_i^2 \chi_j^2$  in the  $H$ -case ( $i,j=1,2,3$ ),  $\Im\{\}$  and  $\Re\{\}$  marks the real and imaginary part of complex value.

To obtain the solution of problem the numerical evaluation of the Green functions (1) and their normal derivatives must be done carefully. It is hard especially in the cases when  $|\Re(t-t_0)|$  is large and integrands in (1) become highly oscillate. The necessity of such integration can be avoided by integral conversion according to scheme

$$I(\alpha, \beta) \equiv \int_{-\infty}^{+\infty} \frac{\varphi(\xi)}{v_2} \exp(-\alpha v_2 + i\xi \beta) d\xi = \int_{\Gamma} \frac{\varphi(\xi)}{v_2} \exp(-\alpha v_2 + i\xi \beta) d\xi, \quad (2)$$

where the contour  $\Gamma$  is shown in Fig. 1 and is chosen from the condition

$$\Im(-\alpha v_2 + i\xi \beta) \Big|_{\xi \rightarrow \infty} \sim \text{const}, \tan \theta = \beta/\alpha, \xi \in \Gamma. \quad (3)$$

Condition (3) quenches an oscillation of integrand in (2) and causes its rapid decrease at infinity. It should be stressed that the foregoing method of Green functions calculation is effective in the case of waveguide modes absence. However, the non-attenuated wave propagation may exist in dielectric layer. Mathematically it means the presence of the real poles  $\xi_i$  in complex  $\xi$ -plane. Such poles are the solutions of equation  $g(\xi_i)=0$ ,  $g'(\xi_i) \neq 0$ ,  $i=1, \bar{n}_p$  (see (1)) and always exist for condition  $\chi_2 > \chi_{1,3}$ . Allowing for this circumstance we change the contour  $\Gamma$  according to Fig. 2. Then we

obtain  $\int_{\Gamma} d\xi = \int_{\Gamma_1} d\xi + \int_{\Gamma_2} d\xi$ . The integral over  $\Gamma_1$  vanishes at  $r=|z| \rightarrow \infty$  as  $1/\sqrt{r}$ . The integral over

$\Gamma_2$  is equal to sum of residues and describes the waveguide modes.

Let us consider the integrand behavior over  $\Gamma_{1l}$  (left) and  $\Gamma_{1r}$  (right) parts of contour  $\Gamma$  at point  $\xi = \chi_2$ . When  $\xi = (\chi_2 - \xi'_{lr}) + \xi'_{lr} \tau$  (where parameter  $\tau = [0; 1]$ ,  $\xi'_{lr} = d\xi/d\tau$ ,  $\xi \in \Gamma_{1l,r}$ ) we obtain

$$\frac{1}{v_2} = \frac{1}{\sqrt{1-\tau^2}} \left[ \frac{\sqrt{1-\tau^2}}{\sqrt{\xi^2 - \chi_2^2}} \right] = \frac{1}{\sqrt{1-\tau^2}} \frac{\sqrt{1+\tau}}{\sqrt{\xi'_{lr} \{ (\xi'_{lr} - \chi_2 - \xi'_{lr} \tau) - \chi_2 \}}}$$

We chose the value of radicals for right-hand part contour  $\Gamma_1$  from  $\chi_2$  so that  $\Re \left\{ \sqrt{\xi'_{lr} \{ (\xi'_{lr} - \chi_2 - \xi'_{lr} \tau) - \chi_2 \}} \right\}, \Re \{v_2\} \geq 0$ , for left-hand part contour  $\Gamma_1$  from  $\chi_2$  so that  $\Im \left\{ \sqrt{\xi'_{lr} \{ (\xi'_{lr} - \chi_2 - \xi'_{lr} \tau) - \chi_2 \}} \right\}, \Im \{v_2\} \leq 0$ . Here for  $\Re \{\xi\} \geq \chi_{1,2}$ , the  $\Re \{v_{1,2}\} \geq 0$ ; for  $\Re \{\xi\} \leq \chi_{1,2}$ , the  $\Im \{v_{1,2}\} \leq 0$ .

To calculate an integral along contours  $\Gamma_{1r}$  and  $\Gamma_{1l}$  we can apply a special quadrature Gauss-Chebyshev formulae which account stationary singularities at  $\chi_2$  [15]. Another way of evaluation those integrals consists in transformations

$$\begin{aligned} I_{ca} &= \int_{\Gamma_{1r,l}} \frac{\varphi(\xi)}{v_2} e^{-v_2 \alpha + i \xi \beta} d\xi = \int_0^1 \frac{\varphi(\xi)}{v_2} e^{-v_2 \alpha + i \xi \beta} \xi'_{lr} d\tau = \\ &= \xi'_{lr} \left[ \int_0^1 \frac{1}{v_2} \left\{ \varphi(\xi) e^{-v_2 \alpha + i \xi \beta} - \frac{\xi}{\chi_2} \varphi(\chi_2) e^{i \chi_2 \beta} \right\} d\tau \right] - \frac{\varphi(\chi_2) e^{i \chi_2 \beta}}{\chi_2} v_2 \Big|_{\tau=0}. \end{aligned} \quad (4)$$

Thus the calculation of a singular integral is reduced to evaluation of a regular one. The numerical testing of two approaches shows that the second algorithm is preferable.

For additional computer time decrease during evaluation of oscillatory integrals at near field zone we build for them the Lagrange type interpolation polynomial of two variables

$$I(\alpha, \beta) = \omega(\alpha, \beta) \frac{T_{M_1}(\delta) T_{M_2}(\zeta)}{M_1 M_2} \sum_{k=1}^{M_1} \frac{1}{\delta_k - \delta} \sum_{l=1}^{M_2} \frac{1}{\zeta_l - \zeta} I_0^*(\alpha^* \delta_k \beta^* \zeta_l). \quad (5)$$

Here  $\delta_k = \cos[\pi(2k-1)/(2M_1)]$ ,  $\zeta_l = \cos[\pi(2l-1)/(2M_2)]$ ;  $T_M(\zeta) = \cos[\text{Marccos}(\zeta)]$ ;  $\delta = \alpha/\alpha^*$ ,  $\zeta = \beta/\beta^*$ ,  $-1 \leq \delta, \zeta \leq 1$ ;  $I_0^*(\alpha^* \delta_k \beta^* \zeta_l) = I(\alpha^* \delta_k \beta^* \zeta_l) T_{M_1-1}(\delta_k) T_{M_2-1}(\zeta_l) / \omega(\alpha, \beta)$ ;  $\alpha^*$  and  $\beta^*$  are the greatest values of the variables  $\alpha$  and  $\beta$ , which are necessary for solution of integral equation system; function  $\omega(\alpha, \beta)$  is proportional to Sommerfeld-type integral asymptotic behavior (in our case  $\omega(\alpha, \beta) = \exp[i\chi_2|\alpha + i\beta|]$ ).

One time numerically calculated values  $I_0^*(\alpha^* \delta_k \beta^* \zeta_l)$ ,  $k = \overline{1, M_1}$ ,  $l = \overline{1, M_2}$  give us according to (5) the analytical representation of integral  $I(\alpha, \beta)$  at arbitrary  $\alpha$  and  $\beta$ .

## SYSTEM OF INTEGRAL EQUATIONS AND ITS SOLUTION

Using the Green function  $G_E(t, z)$  the solution of diffraction problem in the case of  $E$ -polarization is sought as the simple layer potential

$$E(z) = E^*(z) + 2\pi \sum_{k=1}^N \int_{L_k} J_k(t_k) G_E(t_k, z) ds_k \quad (6)$$

and in the case of  $H$ -polarization - as a double-layer potential

$$H(z) = H^*(z) + 2\pi \sum_{k=1}^N \int_{L_k} m_k(t_k) \frac{\partial}{\partial n_k} G_H(t_k, z) ds_k \quad (7)$$

Here  $J_k(t_k)$  and  $m_k(t_k)$  are unknown functions proportional to surface current densities induced on screens by excited wave,  $\partial/\partial n_k$  marks a partial derivative by normal at the internal point  $t_k = x_k + iy_k$  with arc abscissa  $s_k$  of contour  $L_k$ .

Let the contours  $L_k$ ,  $k = \overline{1, N}$  are described parametrically  $t_k = t_k(\tau)$ ,  $\tau \in [-1; 1]$  by complex-valued functions of real parameter  $\tau$  and we can have  $ds_k = |t'_k(\tau)| d\tau$ . We satisfy the Dirichlet (*E*-case) or the Neumann (*H*-case) conditions on  $N$  contours  $L_k$  and obtain the system of integral equations with logarithmic singularities (*E*-case)

$$-\int_{-1}^1 j_k(\tau) \ln|\tau - \tau_0| d\tau + \int_{-1}^1 j_k(\tau) K(\tau, \tau_0) d\tau + 2\pi \sum_{k=1}^N \int_{-1}^1 j_k(\tau) G_E^2(t_k, t_l^0) d\tau = E^*(t_l^0), \quad l = \overline{1, N}, \quad (8)$$

or get the system of hypersingular integral equations (*H*-case)

$$\int_{-1}^1 \frac{m'_k(\tau)}{\tau - \tau_0} d\tau - \int_{-1}^1 m_k(\tau) K_1(\tau, \tau_0) \ln|\tau - \tau_0| d\tau + \int_{-1}^1 m_k(\tau) K_2(\tau, \tau_0) d\tau + 2\pi |(t_l^0)| \sum_{k=1}^N \int_{-1}^1 m_k(\tau) \frac{\partial}{\partial n_l^0 \partial n_k} G_H^2(t_k, t_l^0) |t'_k| d\tau = |(t_l^0)| \frac{\partial}{\partial n_l^0} H^*(t_l^0), \quad l = \overline{1, N}, \quad (9)$$

The designations  $j_k(\tau) = J_k(t_k(\tau))|t'_k|$ ,  $m_k(\tau) = m_k(t_k(\tau))$ ,  $t_k = t_k(\tau) \in L_k$ ,  $t'_k = t'_k(\tau)$ ,  $t_l^0 = t_l^0(\tau_0) \in L_l$  are made in systems (8), (9). Due to edge condition the expressions  $j_k(t) = j_k^*(t)/\sqrt{1-t^2}$ ,  $m_k(t) = m_k^*(t)/\sqrt{1-t^2}$  hold ( $j_k^*(\tau)$ ,  $m_k^*(\tau)$  are Hölder continuous functions, bounded and nonzero at  $\tau = \pm 1$ ). The kernels  $K(\tau, \tau_0)$ ,  $K_{1,2}(\tau, \tau_0)$  are regular functions in square  $-1 < \tau, \tau_0 < 1$ , primes designate the derivatives with respect to arguments.

To obtain the discrete analog of equations (8), (9) we apply the mechanical quadratures method [15, 16]. To achieve the algorithm effectiveness in the case of scattering by a screen system we use the procedure of successive approximations with allowance for wave rereflection. Thus the problem solution is performed in a step by step handling of  $N$  independent linear algebraic systems.

## RESULTS AND DISCUSSION

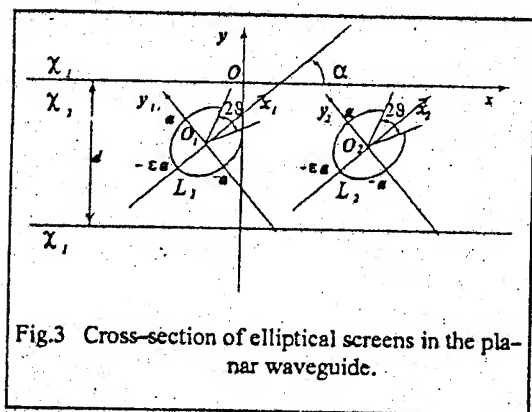


Fig.3 Cross-section of elliptical screens in the planar waveguide.

Let's consider a question of the obtained results validity. The validity of equation (5) is proved by comparison of the obtained values and the appropriate Sommerfeld type integrals calculated numerically by contour integration (see (2) and (5)). In all these cases the accuracy of the Green function was 0.01% when node numbers  $M_{1,2} = 15$  per wave length. The comparison of the Green function in general case  $\chi_1 \neq \chi_2 \neq \chi_3$  with the results of [19] was carried out at *E*-polarization excitation.

Mathematical ground and convergence properties of the proposed technique are shown in [20, 21]. Its practical examination was performed by comparison of the solutions at different nodes

number  $n$ . The increase of  $n$  stopped when error was 0.01%. The procedure of successive approximation was examined by the rigorous solution of integral system (8) and (9). We also checked the calculation results of *E*-polarized field scattered by strip in half-space [6] and of *H*-polarized wave diffracted by a circular cylinder in planar waveguide [13].

Let's apply the numerical method of diffraction problem solution to determine the field on the interface  $y=0$  at  $x \rightarrow \pm\infty$  (wave zone or far-field pattern). We consider the particular case when excitation is a normal incident plane wave

$$W^*(z) = \exp[-i\chi_1 \Im(z)] \quad (10)$$

or own waveguide mode



$$\vec{W}(x) = \begin{cases} \cos \\ \sin \end{cases} (p_k \chi_2 (y-d/2)) \exp[ih_k \chi_2 x], \quad -d/2 \leq x \leq d/2, \quad x_1 = x_3 \quad (11)$$

( $2\pi/(h_k \chi_2)$  is  $k$ -th waveguide mode wavelength;  $p_k = \sqrt{\epsilon_2^2 - h_k^2}$ ,  $\epsilon_i$ ,  $i=1,3$  are dielectric constants of the medium).

The numerical results given below correspond to configuration shown in Fig.3 at  $\chi_2/\chi_1=1.5$ ;  $\chi_2 d=3$ . Calculations were carried out during slab sounding both by  $E$ - and  $H$ -polarized non-attenuated planar waveguide mode. We consider the transmission  $T_{jk}(x \rightarrow +\infty)$  and reflection  $R_{jk}(x \rightarrow -\infty)$  coefficients of such waveguide modes which are specified by formula

$$W(z) - W^*(z) = \Psi_j(\varphi) \left( \frac{2}{i\pi \chi_2 r} \right)^{1/2} \exp(i\chi_2 r) + \sum_{n=1}^{n_p} \begin{cases} T_n - \delta_n, & x > 0 \\ R_n, & x < 0 \end{cases} \begin{cases} \cos \\ \sin \end{cases} (p_n \chi_2 y) \exp(ih_n \chi_2 |x|), \quad (12)$$

where  $\delta_{jk}$  is Kronecker delta symbol;  $\Psi_j$  is far-field pattern;  $n_p \geq 1$  is a number of non-attenuated waveguide modes;  $1 \leq n_p$  is an index of the exciting waveguide mode. In our case (see (11)) we have  $j=n_p=1$ ,  $T_{11}=T$ ,  $R_{11}=R$ . In the layer region and at the single-mode excitation the squares of these coefficients define respectively the transmitted ( $P^t=|T|^2 P^{inc}$ ), reflected ( $P^r=|R|^2 P^{inc}$ ) as well as dissipated ( $E/P^{inc}=1-|T|^2+|R|^2$ ) field energy normalized by the incident mode power  $P^{inc}$ .

Let the parametrical equations of contours  $L_k$ ,  $k=1,2$  are described by formula

$$L_k(\tau) = a \cos((\pi - \vartheta)\tau) + i \varepsilon \sin((\pi - \vartheta)\tau) \exp[i\alpha] - id/2 + (2a + i)(k-1), \quad -1 \leq \tau \leq 1, \quad (13)$$

where  $a$  and  $\varepsilon$  are the ellipses half-axis;  $l$  is a distance between screens;  $2\vartheta$  is an angular size of the screen slot;  $\alpha$  is an angle of screen orientation relatively to the  $y=0$  plane. Calculations were performed when  $\chi_2 a=0.35$ ,  $\alpha=\pi/2$ ,  $\vartheta=\pi$  in a case of  $E$ -polarization and  $\alpha=\pi/6$ ,  $\vartheta=\pi/6$ ,  $\varepsilon=0.6$  at  $H$ -polarized excitation.

The  $E$ -polarized wave transmission coefficient as functions of distance between screens  $\chi_2 l$  and their curvature  $\varepsilon$  are shown in Fig.4. The function maximums depend on the distance between screens and on parameter  $\varepsilon$  (according to (13) the change of curvature  $\varepsilon$  is equivalent to the change of size of screens). Note that location of the maximums of functions slightly depends on  $\varepsilon$ . For small

curvature  $\varepsilon$  we observe the transmission maximum at  $l \approx 0.4\lambda$  and minimum - at  $l \approx 0.27\lambda$  ( $\lambda$  - is wavelength). Increase of size of screens causes shift of the functions  $|T-1|$  extremes to high frequency range. The results of  $H$ -polarized scattered field calculations as function of distance  $\chi_2 l$  and size of screens  $\chi_2 a$  are illustrated in Fig.5. We see that value  $\chi_2 a=0.52$  which corresponds to the resonance size of each screen remains extreme in the case of their system. The resonance amplitude slightly depends on the distance between screens. The corresponding analysis of energy dissipation (Fig.5) shows that the single slotted screen resonance is the reason of powerful energy dissipation and the system of screens decreases these losses.

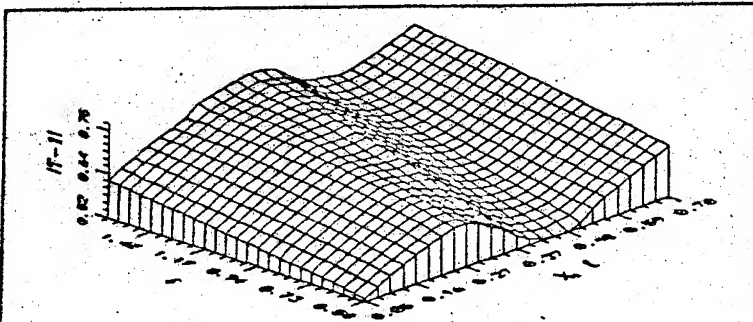


Fig.4 The  $E$ -polarized waveguide mode transmission as screen curvature  $\varepsilon$  and distance  $\chi_2 l$  functions.

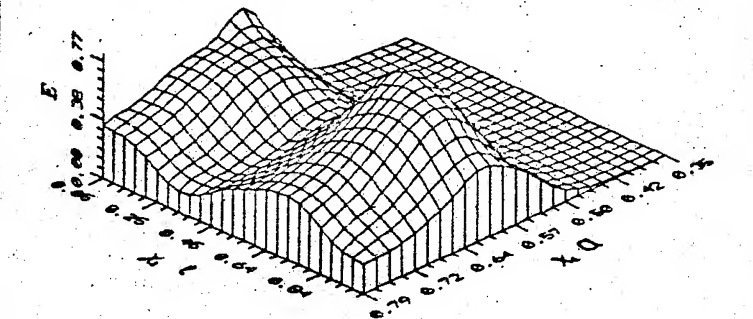


Fig.5 The  $H$ -polarized wave energy dissipation as the function of distance  $\chi_2 l$  and size  $\chi_2 a$ .



Thus the general approach to accurate calculation of two-dimensional electromagnetic field scattered by the system of cylindrical screens in slab is proposed. The geometrical and physical parameters in the problem are supposed to be arbitrary. The developed numerical schemes in fast acting and on-line request memory can analyze the scattering on screens up to few tens of  $\lambda$  by a modern personal computer. The accuracy of the obtained results above confirms high effectiveness of the approach and wide areas of its application.

## REFERENCES

1. Butler, Ch., "General analysis of a narrow slot in a conducting screen between half-spaces of different electromagnetic properties," *Radio Sci.*, Vol. 22, N7, 1149-1154, 1987.
2. Chammeloux, L., Pichot, Ch., and Bolomey, J.-Ch., "Electromagnetic modeling for microwave imaging of cylindrical buried inhomogeneities," *IEEE Trans. Microwave Theory Techn.*, Vol. 34, N10, 1064-1076, 1986.
3. Hongo Kohel, and Hamamura Akihiko, "Asymptotic solution for the scattered field of plane wave by a cylindrical obstacle buried in a dielectric half-space," *IEEE Trans. Antennas Propag.*, Vol. 34, N1, 1306-1312, 1986.
4. Uzunoglu, N.K., and Kannelopoulos, J.D., "Scattering from underground tunnels," *J. Phys. A: Math. and Gen.*, Vol. 15, N2, 459-471, 1982.
5. Xu, X.B., and Butler, Ch., "Current induced by TE excitation on a conducting cylinder located near planar interface between two semi-infinite half-spaces," *IEEE Trans. Antennas Propag.*, Vol. 34, N7, 880-890, 1986.
6. Xu, X.B., and Butler, Ch., "Scattering of TM excitation by coupled and partially buried cylinders at the interface between two medium," *Ibid.*, Vol. 35, N 5, 529-539, 1987.
7. Morita, N., "Scattering and mode conversion of guided modes of a slab waveguide by a circular cylinder," *IEE Proc.*, Vol. H127, N5, 263-269, 1980.
8. Uzunoglu, N.K., and Fikioris, J.G., "Scattering from an inhomogeneity inside a dielectric slab waveguide," *J. Opt. Soc. of America.*, Vol. 72, N5, 628-637, 1992.
9. Yarovoy, A.G., "Wave scattering from permeable inhomogeneities in open acoustic waveguides," *Akustichesky Zhurnal.*, Vol. 38, N4, 756-763, 1992 (in Russian).
10. Zhuk, N.P., and Shulga, S.B., "Two-dimensional problem of electromagnetic waves scattering by cylindrical inclusion in stratified medium," *Radiotekhnika (Kharkiv)*, Vol. 90, 93-101, 1989 (in Russian).
11. Michalski, K.A., and Butler, Ch., "Determination of a conducting strip embedded in a dielectric slab," *Radio Sci.*, Vol. 18, N6, 1195-1206, 1988.
12. Nosich, A.I., and Shestopalov, V.P., "Self-agreed solution of diffraction problem for inhomogeneity in open waveguide," *Dokl. Akad. Nauk SSSR*, Vol. 311, N5, 1110-1115, 1990 (in Russian).
13. Andrenko, A.S., and Nosich, A.I., "Diffraction of dielectric waveguide modes on the inhomogeneities," *Dokl. Akad. Nauk Ukr.SSR.*, Vol. A, N4, 61-66, 1989 (in Russian).
14. Nosich, A.I., (1993) "Green's function-dual series approach in wave scattering by combined resonant scatterers," 419-471, In: "Analytical and Numerical Methods in Electromagnetic Wave Theory," Edited by M.Hashimoto, M.Idemen, and O.Tretyakov, Science House Co.-Tokyo.
15. Panasyuk, V.V., Savruk, M.P., and Nazarchuk, Z.T., (1984) "Method of singular integral equations in two-dimensional diffraction problems", *Naukova Dumka Publ. House.-Kyiv* (in Russian).
16. Nazarchuk, Z.T., (1989) "Numerical investigation of waves diffraction by cylindrical structures", *Naukova Dumka Publ. House.-Kyiv* (in Russian).
17. Ovsyannikov, O.I., "On calculation of Green's function in diffraction two-dimensional problems," *Proc. First Intern. Conf. on Information Technologies for Image Analysis and Pattern Recognition.-Lviv, Ukraine*, Vol. 2, 336-340, 1990.
18. Nosich, A.I., and Shestopalov, V.P., "Radiation conditions and uniqueness theorems for open waveguides," *Radiotekhn. and Elektron.* Vol. 33, N12, 2493-2500, 1988 (in Russian).
19. Tsetsokho, V.A., "Green function calculation for medium with plane-parallel layer (the E-polarization case)," *Geologiya and Razvedka.*, Vol. 4, 77-88, 1972 (in Russian).
20. Gabdulkaev, B.G., "Optimization of the direct methods of the first kind logarithmic integral equations solution," *Integral Equations in Applied Modeling (Abstract if the 2nd Ukrainian Conference)-Kyiv*, Vol. 1, 22-23, 1986 (in Russian).
21. Akhmadiev, M.G., and Gabdulkaev, B.G., "Approximate Methods of Solving of the Singular Integrodifferential Equations at Non-closed Contours," *VINITI, Moscow.*, N1167-B88, 1988 (in Russian).

# WAVE EQUATION GREEN'S FUNCTION FOR THE CASE OF PIECEWISE HOMOGENEOUS AND TEMPORALLY CONSTANT MEDIUM

Alexander Nerukh

Kharkov State Technical University of Radioelectronics  
Lenin av., 14, Kharkov, 310726, The Ukraine

## ABSTRACT

A space-time tensor Green's function of Maxwell's equation for a three-dimensional case of two half-spaces is derived. A plane boundary separates these half-spaces and in one of them a permittivity changes abruptly in time beginning from zero moment. The obtained Green's function allows to formulate integral equations for an electromagnetic field when a nonstationary inhomogeneity is placed in any half-space. The symmetry of this equations is controlled by an inhomogeneity alignment with respect to an interface between media rather than a nonstationary alignment.

## INTRODUCTION

In a background that is described by a continuous vector-function of an electric

polarization  $\mathbf{P}_{ex} = \frac{1}{4\pi}(\epsilon - 1)\mathbf{E}$ , where  $\epsilon$  is a permittivity of this medium, there is a region  $V_1(t)$  involving a subregion  $V_2(t)$ . A medium in these complementary subregions  $V_1 \setminus V_2$  and  $V_2$  is described by functions, respectively  $\mathbf{P}_1$  and  $\mathbf{P}_2$ . A function described a medium throughout the space can be presented in the form

$$\mathbf{P} = \chi_2(\mathbf{P}_2 - \mathbf{P}_1) + \chi_1(\mathbf{P}_1 - \mathbf{P}_{ex}) + \mathbf{P}_{ex}, \quad (1)$$

Here,  $\chi_{1,2}$  are characteristic functions for regions  $V_{1,2}$ . Then, in view of Eq. (1), a generalized inhomogeneous wave equation for a vector of an electric field  $\mathbf{E}$  will take the form [1]

$$\text{rot rot } \mathbf{E} + \frac{1}{c^2} \frac{\partial^2}{\partial t^2} \epsilon \mu \mathbf{E} + \frac{4\pi}{c^2} \frac{\partial^2}{\partial t^2} \mu \chi_1 (\mathbf{P}_1 - \mathbf{P}_{ex}) = \mathbf{F}_2 - \frac{4\pi}{c^2} \frac{\partial}{\partial t} \mu \mathbf{j}_{extr} \quad (2)$$

Here,  $\mu$  is a background medium permeability,  $\mathbf{j}_{extr}$  is an external electric current density, and items with coefficients that have discontinuities at the boundary of the region  $V_2$  are referred to the right-hand side:

$$\mathbf{F}_2 = -\frac{4\pi}{c^2} \frac{\partial^2}{\partial t^2} \mu \chi_2 (\mathbf{P}_2 - \mathbf{P}_1) \quad (3)$$

The solution of Eq. (2) can be represented by a convolution of the right-hand part of this equation with its fundamental solution  $G_1$  (Green's function) [2]

$$\mathbf{E} = \mathbf{E}_0 + G_1 * \left( \mathbf{F}_2 - \frac{4\pi}{c^2} \frac{\partial}{\partial t} \mu \mathbf{j}_{extr} \right). \quad (4)$$

Here,  $\mathbf{E}_0$  is a solution of Eq. (2), whose right side is equal to zero, that is a field in a medium whose parameters have discontinuities only at the boundary of the region  $V_1$ . As Eq. (2) involves the boundary conditions at all discontinuity surfaces,  $\mathbf{E}_0$  meets these conditions at the boundary of the region  $V_1$ .

It is known, that in the general case a Green's function of the equation (2) is defined ambiguous because an arbitrary solution of the homogeneous equation can be added to it. This solution is presented in Eq. (4) by the item  $\mathbf{E}_0$ , so in the following

one will be needed only a singularity part of Green's function that satisfies to the equation

$$\text{rot rot } G_1 + \frac{1}{c^2} \frac{\partial^2}{\partial t^2} \epsilon \mu G_1 + \frac{4\pi}{c^2} \frac{\partial^2}{\partial t^2} \mu \chi_1 (\hat{P}_1 - \hat{P}_{ex}) G_1 = \hat{I} \delta(\mathbf{x} - \mathbf{x}') \quad (5)$$

Here,  $\hat{P}$  is an operator corresponding a function  $\mathbf{P}$ ,  $\hat{I}$  is an identical operator,  $\delta(\mathbf{x})$  - the delta-function and  $\mathbf{x}=(t, \mathbf{r})$ .

This equation takes into account the boundary conditions at the surface of the region  $V_1$ , consequently, its solution, that is the function  $G_1$ , also meets these conditions.

It is essentially for an approach used in this paper that a medium nonstationarity begins at a finite moment of time. This moment is assigned to  $t=0$  here. Let a medium nonstationarity be caused by the occurrence of the region  $V_1$  at this moment. It means that,  $\hat{P}_1 = \hat{P}_{ex}$  for  $t < 0$ . Then Eq. (5) can be converted to the integral equation

$$G_1 = G_0 + \hat{K} G_1, \quad (6)$$

Here,

$$\hat{K} = -\frac{4\pi\mu}{c^2} \int d\mathbf{x}' \frac{\partial^2 G_0(\mathbf{x} - \mathbf{x}')}{\partial t'^2} \chi_1(\mathbf{x}') (\hat{P}_1 - \hat{P}_{ex}) \quad (7)$$

the integral  $\int d\mathbf{x}'$  is over the four-dimensional half-space  $t \geq 0$ . The operator  $\hat{K}$  properties are controlled by the function  $G_0$  properties which is the Green's function of the wave equation in the background

$$G_0 = -\frac{v^2}{4\pi} \left( \nabla \nabla - \frac{1}{v^2} \frac{\partial^2}{\partial t^2} \right) \frac{t - t' - \frac{|\mathbf{r} - \mathbf{r}'|}{v}}{|\mathbf{r} - \mathbf{r}'|} \theta(t - t' - \frac{|\mathbf{r} - \mathbf{r}'|}{v}), \quad (8)$$

where  $v = \frac{c}{\sqrt{\epsilon\mu}}$  and  $\theta(t)$  is the Heviside unit function.

The carrier of the function  $G_0$  is the light cone for  $t < 0$  with the vertex at the observation point. As this function has an integrable singularity in a four-dimensional space, the operator  $\hat{K}$  is a Volterra integral operator.

As well as in a general theory of an integral equation method [3], a sense of the expression (6) essentially depends on the observation point  $\mathbf{r}$  locating. Inside the region  $V_1$ , ( $\chi_1=1$ ), Eq. (6) is the Volterra equation of the second kind and its solution can be made by the resolvent  $\hat{R}$  [4]. Outside this region, ( $1-\chi_1=1$ ), Eq. (6) is a quadrature. So, the expression for the desired Green's function can be defined by the form

$$G_1 = G_0 + \chi_1 \hat{R} \chi_1 G_0 + (1 - \chi_1) \hat{K}^{(ex)} (\hat{I} + \chi_1 \hat{R}) \chi_1 G_0. \quad (9)$$

where superscript  $(ex)$  on the operator  $\hat{K}$  denotes that the argument  $\mathbf{r}$  is checked outside the region  $V_1$ .

# GREEN'S FUNCTION

The specific construction of the Green's function is made for the case of a nonstationary dielectric half-space bounded with a plane. In this case,  $\chi_1 = \theta(x)$ ,

$\hat{R} = (\epsilon_1 - 1) / 4\pi$ ,  $\mu = 1$ . Then the calculation carried out by the formula (9) gives the expression of the desired Green's function for  $t \geq 0$ :

$$G_1 = \theta(x) \{ [G_{n1} \theta(x - x') + G_{n2} \theta(x' - x) - G_{n3}] \theta(x') + G_{n4} \theta(-x') \} + \theta(-x) \{ G_{s1} \theta(x') + G_{s2} \theta(-x') \} + \theta(-x) G_0 \theta(-x'). \quad (10)$$

For  $t < 0$   $G_1 = G_0$ .

In Eq. (10):

$$\begin{aligned} G_{n1}(x - x') &= \hat{L} \frac{v_1}{\phi_1 p^2} \left[ v_1^2 \begin{pmatrix} -\frac{\phi_1^2}{v_1^2} & i \frac{\phi_1}{v_1} k_{\perp} \\ i \frac{\phi_1}{v_1} k_{\perp}^* & k_{\perp}^* k_{\perp} \end{pmatrix} + p^2 I_{\perp} \right] e^{-\frac{\phi_1}{v_1}(x - x')}, \\ G_{n2}(x - x') &= \hat{L} \frac{v_1}{\phi_1 p^2} \left[ v_1^2 \begin{pmatrix} -\frac{\phi_1^2}{v_1^2} & -i \frac{\phi_1}{v_1} k_{\perp} \\ -i \frac{\phi_1}{v_1} k_{\perp}^* & k_{\perp}^* k_{\perp} \end{pmatrix} + p^2 I_{\perp} \right] e^{\frac{\phi_1}{v_1}(x - x')}, \\ G_{n3}(x + x') &= \hat{L} \frac{v_1}{\phi_1 p^2} X e^{-\frac{\phi_1}{v_1}(x + x')}, \\ G_{n4}(x, x') &= \hat{L} \frac{v}{\phi p^2} \left[ v v_1 T_m \begin{pmatrix} -k_{\perp}^2 & i \frac{\phi}{v} k_{\perp} \\ i \frac{\phi}{v_1} k_{\perp}^* & k_{\perp}^* k_{\perp} \end{pmatrix} + p^2 T_e I_{\perp} \right] e^{-\frac{\phi_1}{v_1}x + \frac{\phi}{v}x'}, \\ G_{s1}(x, x') &= \hat{L} \frac{v}{\phi p^2} \left[ v v_1 T_m \begin{pmatrix} -k_{\perp}^2 & -i \frac{\phi_1}{v_1} k_{\perp} \\ -i \frac{\phi}{v} k_{\perp}^* & k_{\perp}^* k_{\perp} \end{pmatrix} + p^2 T_e I_{\perp} \right] e^{\frac{\phi}{v}x - \frac{\phi_1}{v_1}x'}, \\ G_{s2}(x + x') &= \hat{L} \frac{v}{\phi p^2} X(e x) e^{\frac{\phi}{v}(x + x')}, \end{aligned}$$

(11)

where

$$\begin{aligned} \hat{L} &= \frac{1}{2} \int_{-\infty}^{\infty} \frac{dp}{2\pi i} \int_{\infty}^{\infty} \frac{dk_{\perp}}{(2\pi)^2} e^{p(t-t') + ik_{\perp}(r_{\perp} - r'_{\perp})}, \\ X &= -v_1^2 V_m \begin{pmatrix} k_{\perp}^2 & i \frac{\phi_1}{v_1} k_{\perp} \\ -i \frac{\phi_1}{v_1} k_{\perp}^* & k_{\perp}^* k_{\perp} \end{pmatrix} + 2v v_1 V_{em} \begin{pmatrix} 0 & 0 \\ 0 & k_{\perp}^* k_{\perp} \end{pmatrix} + p^2 V_e I_{\perp}, \end{aligned}$$

$$X(ex) = -v^2 V_m \begin{pmatrix} k_{\perp}^2 & -i \frac{\varphi}{v} k_{\perp} \\ i \frac{\varphi}{v} k_{\perp}^* & k_{\perp}^* k_{\perp} \end{pmatrix} + 2vv_1 V_{em} \begin{pmatrix} 0 & 0 \\ 0 & k_{\perp}^* k_{\perp} \end{pmatrix} + p^2 V_e I_{\perp}.$$

$$V_m = \frac{v\varphi - v_1\varphi_1}{v\varphi + v_1\varphi_1}, \quad V_{em} = \frac{v_1\varphi - v\varphi_1}{v\varphi + v_1\varphi_1}, \quad V_e = \frac{v_1\varphi - v\varphi_1}{v_1\varphi + v\varphi_1}, \quad I_{\perp} = \begin{pmatrix} 0 & 0 & 0 \\ 0 & 1 & 0 \\ 0 & 0 & 1 \end{pmatrix}.$$

$$T_m = \frac{2v_1\varphi}{v\varphi + v_1\varphi_1}, \quad T_e = \frac{2v_1\varphi}{v_1\varphi + v\varphi_1}, \quad \varphi_i = \sqrt{p^2 + v_i^2 k^2}, \quad \operatorname{Re} \varphi_i > 0, \quad \mathbf{r}_{\perp} = (y, z).$$

All  $G_{ai}$  functions equal to zero for  $t-t' < 0$  by virtue of its analytical features. For  $v_1 \rightarrow v$  the function  $G_1$  transfers to  $G_0$ .

From the properties of the obtained Green's function on the discontinuity lines it is follows: the action of the Green's function on any vector gives a vector that has discontinuity on the line  $x'=0$ , but this discontinuity is caused by an initial vector component that is normal to an interface between media. On the line  $x=0$  only a resulting vector component, that is normal to the boundary, has a discontinuity.

The obtained Green's function allows to write out the expression to whom an electric field satisfies in the case when the inhomogeneity  $V_2(t)$  is placed in the medium that presents two dielectric half-spaces devided by a plane boundary. In one of them a permittivity can change abruptly in time. If until  $t=0$  a permittivity in both half-spaces was the same and equal to  $\epsilon$ , and at  $t=0$  it changes by jump to  $\epsilon_1$  in the half-space  $x>0$ , than from Eq. (2) we have the integral equation for  $t>0$

$$\mathbf{E} = \mathbf{F} - \frac{4\pi}{c^2} \frac{\partial^2 G_1}{\partial t^2} * \theta(t) \chi_2 (\mathbf{P}_2 - \mathbf{P}_1). \quad (12)$$

Here,  $\mathbf{F} = \mathbf{E}'_0 - \frac{4\pi}{c^2} G_1 * \frac{\partial}{\partial t} \mathbf{j}_{extr} - \frac{4\pi}{c^2} \frac{\partial^2 G_1}{\partial t^2} * \theta(-t) \chi_2 (\mathbf{P}_2 - \mathbf{P}_{ex})$ , and  $\mathbf{E}'_0$  is a field in a piecewise homogeneous medium without  $V_2$ . Analysis of (12) shows that its specific form depends on in what half-space the region  $V_2$  is placed rather than where a permittivity jump has occurred.

- (1) Nerukh A.G. and Khizhnjak N.A.: Modern problems of transient macroscopic electrodynamics (in Russian), "Test-radio", Kharkov. (1991) 280 pp.
- (2) Vladimirov V.S.: Generalized functions in mathematical physics (in Russian), Moscow, "Nauka" (1979), 320 pp.
- (3) Khizhnjak N.A.: Integral equations of macroscopic electrodynamics (in Russian), "Naukova dumka", Kiev. (1986), 280 p.
- (4) Nerukh A.G.: "Refocussing of electromagnetic radiation by a plane boundary of non stationary dielectric" (in Russian), Pisma v "Zhurnal tekhnicheskoi fiziki", (1992), 18(12), pp. 47-51.

# **STEPPED FUNCTION APPROXIMATION OF NONSTATIONARITY OF BOUNDED ABSORBING DIELECTRIC**

Nerukh A.G., Scherbinin D.G.  
Kharkov State Technical University of Radio electronics,  
Lenin Avenue, 14, Kharkov, 310726, the Ukraine.

## **ABSTRACT**

An electromagnetic field interaction with a transient conductive medium bounded by a plane is investigated. This interaction is described by the four-dimensional integral Volterra equation of the second kind. The exact resolvent of this equation for the case of one time jump of medium parameters is obtained. It allows to consider a transformation of an arbitrary primary electromagnetic signal caused by time changing of medium features. It is shown that the obtained resolvent operator can be used to take into account a sequence of time jumps of medium parameters.

## **SCATTERING OPERATOR FOR THE CASE OF ONE JUMP**

Let the half-space  $x > 0$  be filled with the transient medium, that is characterised by the permittivity  $\epsilon_0 + \theta(t)[\epsilon(t) - \epsilon_0]$  and conductivity  $\sigma_0 + \theta(t)[\sigma(t) - \sigma_0]$ , where  $\theta(t)$  is Heaviside function. The background is described by the permittivity  $\epsilon' = \text{const}$ .

An electromagnetic field in this case satisfies to the integral equation

$$\vec{E}(\vec{x}) = \vec{E}^{(0)}(\vec{x}) + \int_0^\infty dt' \int_{x' \geq 0} \hat{K}(\vec{x}, \vec{x}') \vec{E}(\vec{x}') d\vec{r}', \quad \vec{x} = (t, \vec{r}) \quad (1)$$

Here,

$$\hat{K}(\vec{x}, \vec{x}') = \frac{1}{4\pi\epsilon'} \left( \nabla \nabla - \frac{1}{v^2} \frac{\partial^2}{\partial t^2} \right) \frac{(\epsilon(t) - \epsilon') \frac{\partial}{\partial t} + \sigma(t)}{|\vec{r} - \vec{r}'|} \theta \left( t - t' - \frac{|\vec{r} - \vec{r}'|}{v} \right) \quad (2)$$

is the kernel of this equation,  $v^2 = c^2/\epsilon'$  and

$$\vec{E}^{(0)}(\vec{x}) = \vec{E}_{pr} + \int_{-\infty}^0 dt' \int_{x' \geq 0} \hat{K}^{(0)}(\vec{x}, \vec{x}') \vec{E}^{(0)}(\vec{x}') d\vec{r}' \quad (3)$$

is the free term.  $\vec{E}_{pr}$  is a primary field that is an arbitrary source field in the background,  $\vec{E}^{(0)}$  is a field in the halfspace  $x > 0$  until  $t=0$ .  $\hat{K}^{(0)}$  in Eq. (3) is obtained from Eq. 2 by the substitution of  $\epsilon(t)$  for  $\epsilon_0$  and  $\sigma(t)$  for zero.

Inside the non-stationary medium Eq. 1 is an integral Volterra equation of the second kind and it's solution is given by the resolvent  $\hat{R}$ :

$$\vec{E}(\vec{x}) = \vec{E}^{(0)}(\vec{x}) + \int_0^\infty dt' \int_{x' \geq 0} \hat{R}(\vec{x}, \vec{x}') \vec{E}^{(0)}(\vec{x}') d\vec{r}' \quad (4)$$

The exact expression for the resolvent operator of the 3-dimensional problem is derived in the case of a jump change of conductivity and permittivity at zero moment of time in the region  $x > 0$ . In this case  $\epsilon(t) = \epsilon_1 = \text{const}$ ,  $\sigma(t) = \sigma_1 = \text{const}$  and the resolvent has the form:

$$\hat{R}(\vec{x}, \vec{x}') = \left\{ \hat{R}_1 + v_1^2 \begin{pmatrix} \nabla_1^2 & \frac{\partial}{\partial x} \nabla_1 \\ -\frac{\partial}{\partial x} \nabla_1 & \hat{Q}_1 \end{pmatrix} \hat{V}_m + 2vv_1 \begin{pmatrix} 0 & 0 \\ 0 & \hat{Q}_1 \end{pmatrix} \hat{V}_{em} - \frac{\partial^2}{\partial t^2} \begin{pmatrix} 0 & 0 \\ 0 & \hat{I} \end{pmatrix} \hat{V}_e \right\} \theta(x') \quad (5)$$

Here,

$\nabla_1 = \left( \frac{\partial}{\partial y}, \frac{\partial}{\partial z} \right)$ ;  $\nabla_1'$  is transposed to  $\nabla_1$ ,  $\hat{Q}_1 = \nabla_1' \times \nabla_1$ ,  $v_1 = c/\sqrt{\epsilon(t)}$ ,  $\hat{I}$  is the unit

matrix. The operators  $\hat{V}_a$  are equal:

$$\hat{V}_a = \int_{\alpha-i\infty}^{\alpha+i\infty} \frac{dp}{2\pi i} \int_0^\infty \frac{dk}{2\pi} k V_a(p, l, \sigma) J_0(k|\vec{\rho} - \vec{\rho}'|) e^{p(t-t') - l(x+x')/v_1}$$

where  $l = \sqrt{p^2 + 4\pi\sigma_1 p/\epsilon_1 + v_1^2 k^2}$ ,  $\text{Re } l \geq 0$ ,  $\vec{\rho} = (y, z)$ ,  $J_0$  - the Bessel function and  $V_a(p, l, \sigma)$  is determined by the analogous of the reflectance corresponding various polarization of a vector  $\vec{E}$ :

$$V_e = \frac{v\varphi(p+2\sigma) - v_2 l p}{v\varphi(p+2\sigma) + v_2 l p}; V_m = \frac{vl - v_2 \varphi}{v\varphi(p+2\sigma) + v_2 l p}; V_{em} = \frac{vl - v_2 \varphi}{vl + v_2 \varphi};$$

$$\varphi = \sqrt{p^2 + v^2 k^2}.$$

The first item  $\hat{R}_1$  in (5) corresponds to an unbounded problem and account for the medium features time changing only [3]. The other items account for the boundary influence.

Outside the non-stationary medium ( $x < 0$ ), if one takes into account Eq. (2) and (3), Eq. (1) has the form:

$$\vec{E}(\vec{x}) = \vec{F}(\vec{x}) + \int_0^\infty dt' \int_{x' \geq 0} \hat{N}(\vec{x}, \vec{x}') \vec{F}(\vec{x}') d\vec{r}' \quad (6)$$

Here,

$$\hat{N} = \int_{\alpha-i\infty}^{\alpha+i\infty} \frac{dp}{2\pi i} \int_0^\infty \frac{dk}{2\pi} k \left[ \frac{v^2(p+2\sigma) - pv_1^2}{v\varphi(p+2\sigma) - lpv_1} \begin{pmatrix} -\nabla_1^2 & \frac{l}{v_1} \nabla_1 \\ \frac{\varphi}{v} \nabla_1' & \hat{Q}_1 \end{pmatrix} - \right. \\ \left. - \frac{v^2(p+2\sigma) - pv_1^2}{vv_1(vl + v_1\varphi)} \begin{pmatrix} 0 & 0 \\ 0 & \hat{I} \end{pmatrix} \right] J_0(k|\vec{\rho} - \vec{\rho}'|) e^{p(t-t') - lx'/v_1 + \varphi x/v}, \quad (7)$$

The obtained resolvent allows to consider situation when in a homogeneous dielectric medium with the permittivity  $\epsilon'$  the region  $x > 0$  with permittivity  $\epsilon_1$  and conductivity  $\sigma_1$  is formed at zero moment of time. In this case the free term in the integral equation (1) is equal to a primary electromagnetic field. The field transformation is illustrated by the case of a primary plane electromagnetic wave  $\vec{E} = \vec{E}_0 \exp[i(\omega t - \vec{s}\vec{r})]$ . All transients begin in the neighbourhood of the plane  $x=0$  because this plane has become a boundary that separates the background medium from the nonstationary medium. As it follows from this the plane  $x=v_1 t$  breaks away from the boundary at  $t=0$  and then moves deep into the nonstationary half-space, dividing the latter into two regions with qualitatively different structure of a

field. In the region  $x > v_1 t$  there is a known splitting of a plane wave up two opposite directed damped waves:

$$\bar{E}_{1,2}(x) = \bar{E}_0 E^\pm e^{(-\sigma \pm \sqrt{\sigma^2 - \omega'^2})t - i\bar{s}x} \quad (8)$$

Here,  $E^\pm$  is the amplitudes depending on  $s$ ,  $\sigma$  and  $\varepsilon$ ,  $s = |\bar{s}|$  is the wave number,  $\omega' = v_1 s$ . In this region the field does not depend on the presence of the formed boundary and coincides to a field relevant to an unbounded medium case.

The region  $0 < x < v_1 t$  is characterized by the boundary influence. In the case of the perpendicular polarization of the primary field ( $\bar{E}_0 = (0, 0, E_0)$ ,  $\bar{s} = (s_1, s_2, 0)$ ) the exact expression for the transformed field in this region has the form:

$$\bar{E}(x) = \bar{E}_1 + \bar{E}_2 + \theta(v_1 t - x) \bar{E}_0 e^{i\bar{s}x} [\hat{\alpha}_1 A(t, x) + \hat{\alpha}_2 B(t, x)] \quad (9)$$

Here:  $\bar{E}_{1,2}$  is given by the expression (8); the operators

$$\hat{\alpha}_i = \left( \alpha_{i1} \frac{\partial^2}{\partial t^2} + \alpha_{i2} \frac{\partial}{\partial t} + \alpha_{i3} \right) \left( \alpha_{i4} \frac{\partial}{\partial x} + \alpha_{i5} \right), \quad (i = 1, 2, 3, 4), \text{ where}$$

coefficients  $\alpha_{ik}$ , that have rather cumbersome form, depend on parameters  $s$ ,  $\sigma$  and  $\varepsilon$ . The transients are described by the functions  $A(t, x)$  and  $B(t, x)$ . The function  $A$  is equal to:

$$A(t, x) = \sum_{k=0}^2 a_k A_k(t, x), \text{ where } a_k = a_k(s, \sigma, \varepsilon) \text{ are known coefficients}$$

$$\text{and } A_k(t, x) = e^{w_k t} \int_{x/v_1}^t e^{-(w_k + \sigma)\tau} I_0 \left( \sqrt{(\sigma^2 - v_1^2 s_2^2)(\tau^2 - x^2/v_1^2)} \right) d\tau$$

Here,  $I_0$  is the modified Bessel function,  $w_0 = i\omega$ ,  $w_{1,2} = -\sigma \pm (\sigma^2 - \omega'^2)^{1/2}$ . The functions  $A_k(t, x)$  has the continuous Fourier-spectrum. Monochromatic waves are separated out from this spectrum when  $t \rightarrow \infty$ :  $a_0 A_0$  forms partially an ordinary stationary wave, refracting on the plane boundary;  $a_1 A_1$  quenches the wave  $\bar{E}_1$ ;  $a_2 A_2$  turns into zero.

The function  $B$  is equal to:

$$B(t, x) = \hat{\alpha}_3 \sum_{k=0}^4 b_k A_k(t, x) + \hat{\alpha}_4 \int_{x/v_1}^t A(\tau, x) [C(t - \tau) * D(t - \tau)] d\tau$$

Here,  $w_3 = -2\sigma\varepsilon_1/(s_1 - \varepsilon)$ ,  $w_4 = 0$ ,  $b_k = b_k(s, \sigma, \varepsilon)$ ,  $C * D$  is a convolution, in which

$$C(t) = (\pi t)^{-1/2} e^{-\gamma t} + \sqrt{\gamma} \operatorname{Erf}(\sqrt{\gamma t}), \quad \gamma = -iv s_2;$$

$$D(t) = (\pi t)^{-1/2} e^{\eta t} + \sqrt{\eta} \operatorname{Erf}(\sqrt{\eta t}) e^{(\gamma + \eta)t}, \quad \eta = iv s_2 - 2\sigma\varepsilon_1(\varepsilon_1 - \varepsilon)^{-1};$$

$\operatorname{Erf}(x)$  is the error function.

When  $t \rightarrow \infty$  the function  $B(t, x)$  describes two wave processes, namely: 1) the process that along with the one described by the part of the function  $A(t, x)$  forms the ordinary stationary refracting wave, whose amplitude corresponds to the Fresnel law; 2) the wave caused by the reflection of the wave  $\bar{E}_2$  from the formed boundary of the nonstationary half-space.



## A SEQUENCE OF TIME JUMPS OF MEDIUM PARAMETERS

Let functions  $\epsilon(t)$  and  $\sigma(t)$  after  $t=0$  be given by the stepped functions:

$$\epsilon = \sum_{k=1}^N \epsilon_k \theta(t - t_k), \quad \sigma = \sum_{k=1}^N \sigma_k \theta(t - t_k). \quad (10)$$

Here,  $\epsilon_k, \sigma_k$  are constants,  $t_1 = 0$  and  $t_k$  corresponds to the  $k$ -th jump of medium parameters.

In the interval  $[t_1, t_2]$  the field is derived by the formulae (2)-(4) inside the nonstationary medium and by the formulae (6) and (7) outside it.

The derivation of the field in the interval  $[t_2, t_3]$  needs to transfer the non-stationarity initial moment at point  $t_2$  by the substitution of  $t$  for  $t-t_2$ . After appropriate changing of variables in Eq. 2-4 the field inside the non-stationary will take the form

$$\vec{E}^{(2)}(\vec{x}) = \vec{F}^{(2)}(\vec{x}) + \int_{t_2}^{\infty} dt' \int_{x' \geq 0} \hat{R}_2(\vec{x}, \vec{x}') \vec{F}^{(2)}(\vec{x}') d\vec{r}'$$

Here,  $\hat{R}_N$  follows from  $\hat{R}_1$  by changing  $\epsilon_1$  for  $\epsilon_N$ ;  $\sigma_1$  for  $\sigma_N$ :

$$\vec{F}^{(2)}(\vec{x}) = \vec{F}^{(1)}(\vec{x}) + \int_{t_1}^{t_2} dt' \int_{x' \geq 0} \hat{K}^{(1)}(\vec{x}, \vec{x}') \vec{E}^{(1)}(\vec{x}') d\vec{r}'$$

One takes into account that  $\vec{F}^{(1)}(\vec{x}) = \vec{F}^{(0)}(\vec{x})$  and  $\hat{K}^{(k)}$  is obtained from (2) by the substitution  $\epsilon, \sigma$  for  $\epsilon_k, \sigma_k$ .

Successive account of  $N$  jumps leads to a sequence of equations, that allows to derive electromagnetic field after the  $N$ -th jump of the medium parameters

$$\vec{E}^{(N)}(\vec{x}) = \vec{F}^{(N)}(\vec{x}) + \int_{t_N}^{\infty} dt' \int_{x' \geq 0} \hat{R}_N(\vec{x}, \vec{x}') \vec{F}^{(N)}(\vec{x}') d\vec{r}' \quad (11)$$

Here,

$$\vec{F}^{(N)}(\vec{x}) = \vec{F}^{(N)}(\vec{x}) + \sum_{k=1}^{N-1} \int_{t_k}^{t_{k+1}} dt' \int_{x' \geq 0} \hat{K}^{(k)}(\vec{x}, \vec{x}') \vec{E}^{(k)}(\vec{x}') d\vec{r}' \quad (12)$$

The transients in the region  $x < 0$  is determined by integrating in (6).

The expressions (11) and (12) allow to investigate a transformation of an arbitrary primary electromagnetic signal caused by an any number of the time jumps of medium features.

### REFERENCES

- (1) Borisov V.V., "Electromagnetic field transformation under time changing of conductivity" (in Russian), *Geomagnetism i aeronomia*, (1989) v. 29, No 5, p. 730.
- (2) Nerukh A.G., Shavorykina I.Yu., "Electromagnetic impulse return from a conductive medium which has come into being". *Proc. Int. Symp. Anten. Prop.*, (1992) v. 2, p. 585-588, Sapporo, Japan.
- (3) Nerukh A.G. and Khizhnjak N.A.: Modern problems of transient macroscopic electrodynamics (in Russian), "Test-radio", Kharkov. (1991) 280 pp.

# CHAOTIC BEHAVIOR in VARACTOR CIRCUITS

A. Oksasoglu

Department of Electrical & Electronics Engineering

Çukurova University

Balçalı, Adana TURKEY

**Abstract** Chaotic behavior of a varactor circuit with quasiperiodic excitation is studied. It is shown that, compared to a single frequency forcing, a quasiperiodic input, such as an amplitude modulated signal, can cause a considerable drop in the threshold for chaotic onset. Analytical conditions for chaos to arise are also obtained.

**Introduction** It has been repeatedly demonstrated that chaotic oscillations can arise in varactor diode tuning circuits similar to the one given in Fig. 1 with a harmonic external force  $i(t) = I_0 \cos \omega t$  (e.g. [1]). The chaotic oscillations appear here via the period-doubling bifurcations of the period  $T = 2\pi/\omega$ . Such chaotic oscillations can arise only in substantially nonlinear systems when the amplitude of the external signal is usually considerably larger than the value of biasing voltage, in which case, the circuit loses its resonance property. However, such high values of amplitude are not typical for most practical systems, and therefore chaotic behavior is usually ignored when analyzing the stability and noise performance of such systems. The situation is quite different when real signals containing several independent frequencies are considered. In this paper, we show that chaotic instability can manifest itself in the weakly nonlinear limit for practically low amplitudes of the forcing function.

**Analysis** To illustrate the above-mentioned case, we consider an amplitude modulated input  $i(t) = I_0(1 + m \cos \Omega t) \cos \omega t$ . The varactor diode in Fig. 1 is modeled as a parallel combination of a p-n junction transition capacitance  $C_T(V_j) = C_{T0}(1 + V_j/V_\phi)^{-\gamma}$  and a nonlinear resistance whose  $i-v$  characteristic is  $i_R \equiv f(V_j) = I_s[\exp(\Lambda V_j) - 1]$  (see [2] for details). The junction voltage  $V_j$  is the sum of the biasing voltage  $V_B$  (not shown in Fig. 1) and the ac component  $v$ . The equation describing the circuit's behavior can be given as

$$C_T(V_j) \frac{dv}{dt} + \frac{1}{L} \int v dt + f(V_j) + \frac{v}{R} = i(t) = I_0(1 + m \cos \Omega t) \cos \omega t \quad (1)$$

Since we consider a weakly nonlinear system, it is possible to look for solutions of the form  $v(t) = A \cos(\omega t + \phi)$ , where  $A$  and  $\phi$  are slow-varying functions of time. By using the method of averaging

[3] and the cubic approximation for the diode characteristics, we find

$$\begin{aligned}\frac{dA}{d\tau} &= -A - \beta A^3 - P(1 + m \cos \bar{\Omega}) \sin \phi \\ A \frac{d\phi}{d\tau} &= \Delta A - \delta_1 A^3 - P(1 + m \cos \bar{\Omega}) \cos \phi\end{aligned}\quad (2)$$

Here,  $\tau = \omega t / 2Q$ ,  $P = QI_0 / \omega C_0$ ,  $\bar{\Omega} = 2Q\Omega / \omega$ ,  $\Delta = 2Q(\omega - \omega_0) / \omega$ , where  $C_0 = C_{T0}(1 - V_B/V_\phi)^{-\gamma}$ ,  $\omega_0$  and  $Q$  are respectively the natural frequency and the quality factor of the circuit, and  $\beta = QI_0 A^3 (8C_0 \omega)^{-1} \exp(\Lambda V_B)$ ,  $\delta_1 = (1/8)Q\gamma(\gamma + 1)(V_\phi - V_B)^{-2}$  are the parameters of the dissipative and reactive nonlinearity, respectively.

As can be seen, the system (2) can exhibit no chaotic behavior in the case of harmonic forcing ( $m = 0$ ), since it is reduced to a two-dimensional autonomous system. This means that chaotic oscillations cannot occur in the weakly nonlinear limit with harmonic excitation. However, when  $m \neq 0$ , this system can demonstrate chaotic behavior in a finite region of system parameters. The fact that chaotic states arise in the averaged equation means that chaos can arise in the original system (1) regardless of the degree of nonlinearity. In order to find the condition for chaos, we use the method of current Lyapunov exponents and Melnikov technique [4,5]. As a result, for chaos to arise, the maximum value of the voltage across the diode  $\max\{v(t)\} \equiv v_{max}$  must exceed the threshold

$$v_{max} \geq [(\beta^2 + \delta_1^2)^{1/2} - 2\beta]^{-1/2} \quad (3)$$

We see from (3) that the threshold for chaos increases as  $\beta$  increases, and when  $\beta > \delta_1/\sqrt{3}$ , then no chaotic oscillations can arise for any values of the external force. Hence, we can say that reactive and dissipative nonlinearities play quite different roles in terms of the circuit's stability performance. Since, for most practical diodes,  $\beta$  is much less than  $\delta_1$  due to the reversed-biased operation mode, the condition for chaos to arise is not stringent. Neglecting  $\beta$ , we can rewrite (3) in terms of the actual diode parameters as

$$v_{max} \approx I_0 R \geq 2\sqrt{2}|V_B - V_\phi|/\sqrt{\gamma(\gamma + 1)Q} \quad (4)$$

As an example, let us choose  $\gamma = 0.5$ ,  $V_\phi = 0.3V$ , which are typical for some diodes, then for the biasing voltage  $V_B = -2V$ , and  $Q = 100$ , we find that chaos can arise when  $v_{max} \geq 0.75V$  (or  $I_0 \geq 0.75/R$  A), which is less than  $V_B$  in magnitude. It should be noted that increasing  $Q$  sharply decreases the threshold value for chaotic onset. By analyzing the original system (1), it can be shown that this threshold value is lower than that of the harmonic excitation case by a factor of  $Q$ .

When (4) is met, chaotic oscillations can arise in some region of  $\bar{\Omega}$  and  $m$  variations. A typical two-dimensional bifurcation diagram in parameter plane  $m - \bar{\Omega}$  is shown in Fig. 2. The most

dangerous case in terms of chaotic instability occurs when  $\Omega \cong \omega_0/Q$ . The typical road to chaos is the period-doubling bifurcations of the period of modulation  $T_\Omega = 2\pi/\Omega$  which corresponds to the destruction of two-dimensional torus in the original physical system. Since the bandwidth of the chaotic oscillations has the same order as that of the original system ( $\omega_0/Q$ ), the resonance property is preserved.

**Conclusion** The results obtained show that the stable operation of the resonant varactor circuits under harmonic excitation will not necessarily hold under multi-frequency excitation. In the multi-frequency case, chaotic instability arises under weakly nonlinear excitation conditions, and thus can exert strong influence on the stability and noise performance of practical systems. Qualitatively, these results do not depend on the type of the external forcing, i.e., being amplitude, frequency or phase modulated. One other aspect worth mentioning here is that increasing the dissipative nonlinearity is a promising way of preventing the chaotic behavior of such systems.

#### REFERENCES

- [1] P. S. Linsay, "Period Doubling and Chaotic Behavior in a Driven Unharmonic Oscillator," *Phys. Rev. Lett.*, vol. 47, no. 19, pp. 1349-1352, 1981.
- [2] R. W. Landee, D. C. Davis, and A. P. Albrecht, *Electronics Designers' Handbook*. Second Edition, Mc Graw-Hill: New York, 1977.
- [3] N. N. Bogoliubov, and Y. A. Mitropolski, *Asymptotic Methods in the Theory of Nonlinear Oscillations*. Gordon & Breach: New York, 1961.
- [4] D. M. Vavriv, and V. B. Ryabov, "Current Lyapunov Exponents and the Conditions of Chaos Arising," *Zh. Vysishlit. Mat. i Mat. Fiz.*, vol.32, pp. 1409-1421, 1992.
- [5] V. B. Ryabov, and D. M. Vavriv, "Conditions of Quasiperiodic Oscillation Destruction in the Weakly Nonlinear Duffing Oscillator," *Phys. Lett.*, vol. A153, pp. 431-436, 1991.

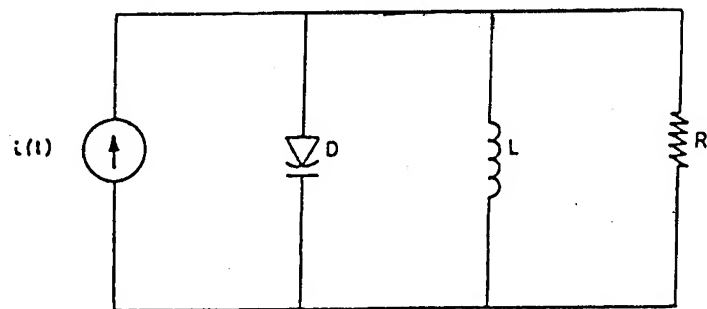


Fig. 1. A Varactor diode tuning circuit.

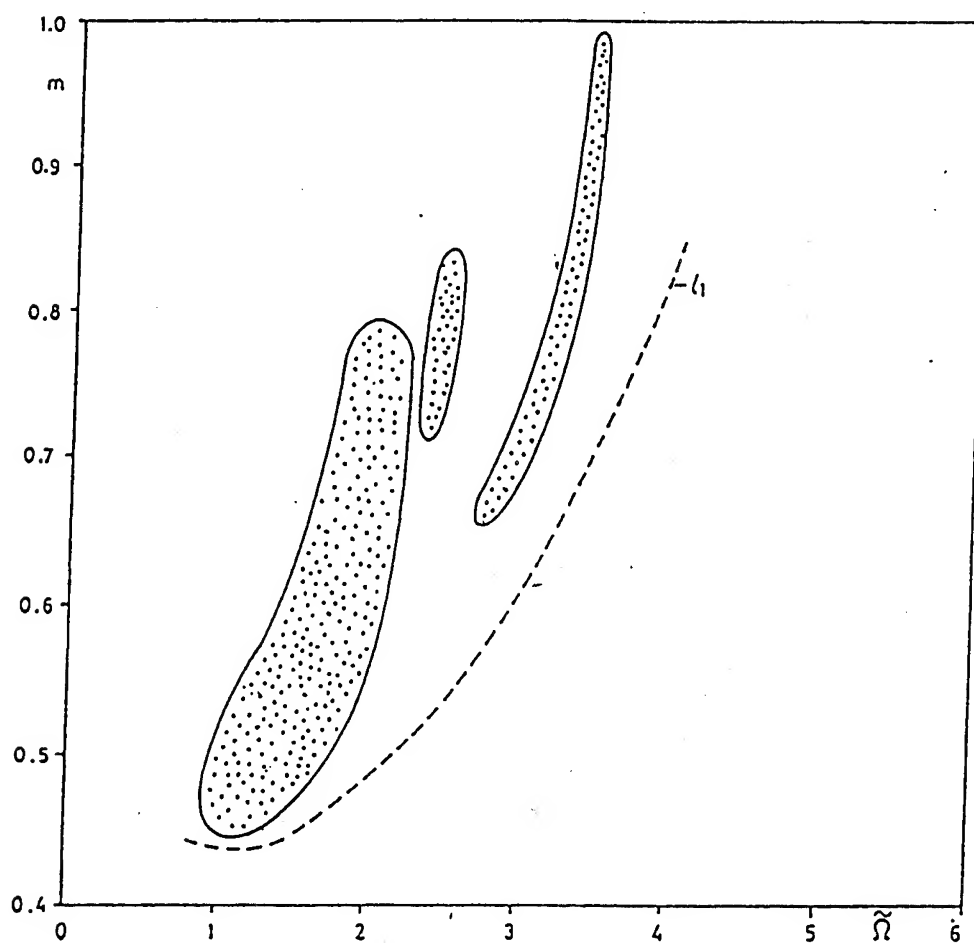


Fig. 2. Bifurcation diagram of regimes of the nonlinear circuit in the plane of parameters  $m$ ,  $\tilde{Q}$ . The chaotic region is dotted. Line of the first period doubling bifurcation is indicated by  $l_1$ .  $\Delta = 4$ ,  $P = 1.85V$ ,  $\gamma = 0.5$ ,  $V_\phi = 0.3V$ ,  $V_B = -2V$ ,  $Q = 100$ .

# A Duality Relationship between Scattered Field and Current Density Calculation in the Yasuura Method

Yoichi Okuno

## Abstract

After an introduction to the Yasuura's mode-matching methods for solving boundary value problems to the Helmholtz equation in homogeneous media, a duality relationship will be established, the relationship which holds between scattered field and current density calculation. Although the methods of calculation have been explained separately as a least-squares boundary residual method (scattered field) and as a least-squares approximation for an unknown target function (current density), they may be understood as a technique to find a stationary point of Rumsey's reaction between the incident wave to and the scattered wave from a perfectly conducting obstacle. This will make clear the hidden structure of the methods and will facilitate the understanding.

## 1. Introduction to the Yasuura's Methods

Here, we briefly see what are the Yasuura's methods taking a 2-D E-wave scattering as an example.<sup>1</sup>

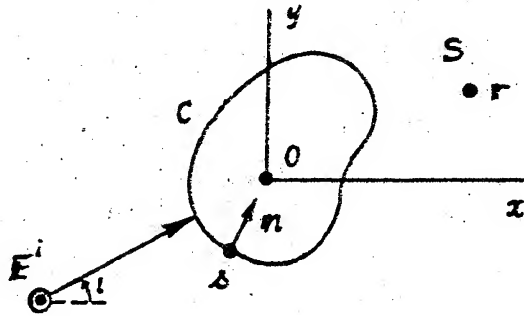


Figure 1: A 2-D obstacle with an incident wave. The total length of  $C$  is assumed to be 1.

**Formulation of the problem.** Consider a 2-D obstacle made of a perfect conductor shown in Fig. 1. When a plane E-wave,  $E^i(r) = u, F(r)$  ( $F(r) = \exp[-ikr \cos(\theta - \iota)]$ ), is incident, a surface current  $K(s) = u, K(s)$  flows to induce the scattered wave  $E^s(r) = u, \Psi(r)$ . The  $\Psi(r)$  function satisfies the Helmholtz equation

$$\nabla^2 \Psi(r) + k^2 \Psi(r) = 0 \quad (r \in S), \quad (1)$$

the radiation condition, and the boundary condition

$$\Psi(s) = f(s) = -F(s) \quad (0 \leq s \leq 1). \quad (2)$$

Here,  $k = 2\pi/\lambda$  is a positive wavenumber and  $\iota$  is the angle of incidence shown in Fig. 1. The current density  $K(s)$  is in proportion to the total magnetic field on  $C$  and is given by

$$K(s) = -(i\omega\mu)^{-1} \partial \Phi(s) / \partial n = -(i\omega\mu)^{-1} \partial (F + \Psi)(s) / \partial n.$$

For simplicity, we omit the coefficient and term the function

$$j(s) = -i\omega\mu K(s) = \partial \Phi(s) / \partial n \quad (3)$$

the current density.

Y. Okuno is with the Department of Electrical Engineering and Computer Science, Kumamoto University, Kumamoto 860, Japan. Fax.: +81-96-345-1553. E-mail: okuno@qpo.kumamoto-u.ac.jp

<sup>1</sup>The details may be found in references from (1) through (3). Although we do not include in this small article the relationship between the methods with the smoothing procedure, we can easily modify the discussion below in order to find it.

A method for finding  $\Psi(r)$ . Let

$$\varphi_m(r) = H_m^{(2)}(kr) \exp(im\theta) \quad (m = 0, \pm 1, \dots) \quad (4)$$

be the modal functions.<sup>2</sup> The set of  $\varphi_m$  functions meets the following conditions: 1) Each  $\varphi_m$  function is an outgoing solution to the Helmholtz equation in S; 2) The set of boundary values  $\{\varphi_m(s)\}$  is complete in  $H = L^2(C)$ . An approximation to the scattered field is defined as a finite linear combination of the  $\varphi_m$  functions:

$$\Psi_N(r) = \sum_{m=-N}^N A_m(N) \varphi_m(r). \quad (5)$$

The unknown coefficients  $A_m(N)$  are determined so that the mean-square error on the boundary condition

$$E_N = \|\Psi_N - f\|^2 \quad (6)$$

becomes minimal. Such coefficients, theoretically, may be obtained by

$$HA = f. \quad (7)$$

Here,  $H$  is a  $(2N+1) \times (2N+1)$  positive definite Hermitean matrix whose elements  $(\varphi_m, \varphi_n)$  are inner products between  $\varphi_m$  and  $\varphi_n$ ;  $A$  is a  $(2N+1)$ -dimensional column vector with the elements  $A_m(N)$ ; and  $f$  is a  $(2N+1)$ -dimensional right-hand-side vector consists of  $(\varphi_m, f)$ 's.<sup>3</sup> We can prove that the sequence of approximate solutions obtained by the method above converges to the true solution uniformly in wider sense in S.

A method for finding  $j(s)$ . Define an approximation of  $j(s)$  by

$$j_N(s) = \sum_{m=-N}^N C_m(N) \overline{\varphi_m(s)}. \quad (8)$$

The  $C_m$  coefficients are determined so that  $j_N(s)$  be the best approximation of  $j(s)$  in the mean-squares sense. Minimize the distance  $\|j_N - j\|$ . This leads us to

$$CH = -g. \quad (9)$$

Here,  $C$  is a  $(2N+1)$ -dimensional row vector whose elements are  $C_n(N)$  and  $g$  denotes a  $(2N+1)$ -dimensional vector whose  $n$ th element is

$$\langle F, \varphi_n \rangle = \int_0^1 [F(s) \partial \varphi_n(s) / \partial n - \varphi_n(s) \partial F(s) / \partial n] ds. \quad (10)$$

The quantity  $\langle F, \varphi_n \rangle$  is a particular form of the reaction introduced by Rumsey.<sup>(4)</sup> Because  $F(r)$  is a plane wave and  $\varphi_n(r)$  is given by (4), we have  $\langle F, \varphi_n \rangle = -4i \exp[in(i + \pi/2)]$ .

## 2. A Stationary Representation of the Reaction

In the figure below we show two incident waves  $F^{(1)}(r)$  and  $F^{(2)}(r)$ , and corresponding scattered waves  $\Psi^{(1)}(r)$  and  $\Psi^{(2)}(r)$ . The scattered waves satisfy the Helmholtz equation in S, the radiation condition at infinity, and the boundary condition

$$\Psi^{(i)}(s) = -F^{(i)}(s) \quad (i = 1, 2) \quad (11)$$

on C.

**Definition of the reaction and a quadratic form.** Let us define the reaction between two wave functions  $\varphi(r)$  and  $\psi(r)$  by

$$\langle \varphi, \psi \rangle = \int_0^1 [\varphi(s) \partial \psi(s) / \partial n - \psi(s) \partial \varphi(s) / \partial n] ds. \quad (12)$$

The reaction between  $F^{(2)}$  and  $\Psi^{(1)}$  is equal to one between  $F^{(1)}$  and  $\Psi^{(2)}$ :

$$J = \langle F^{(2)}, \Psi^{(1)} \rangle = \langle F^{(1)}, \Psi^{(2)} \rangle. \quad (13)$$

<sup>2</sup>This is an example of the set of exterior modal functions, which is an ensemble of functions satisfying the requirements below. It is often recommendable to employ another set of modal functions such as monopole fields whose sources are located inside C.

<sup>3</sup>The implementation of numerical computation requires a discretizing procedure, which is not less important than the analytical treatment. See (3) for example.

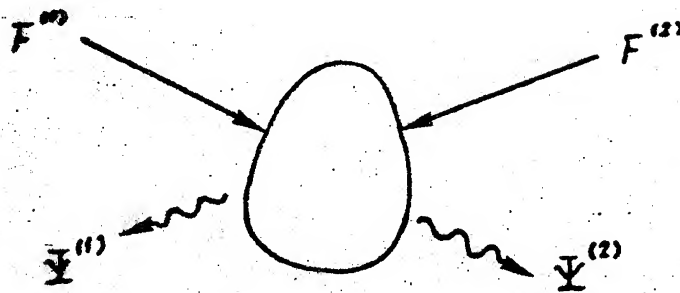


Figure 2 Incident waves  $F^{(1)}$  and  $F^{(2)}$  and corresponding scattered waves  $\Psi^{(1)}$  and  $\Psi^{(2)}$ .

Use of the fact that the reaction between outgoing waves and one between incoming waves are zero yields alternative representations of  $J$  such as

$$J = \langle F^{(2)}, \Phi^{(1)} \rangle = \langle F^{(1)}, \Phi^{(2)} \rangle = \langle \Phi^{(2)}, \Psi^{(1)} \rangle = \langle \Phi^{(1)}, \Psi^{(2)} \rangle. \quad (14)$$

Here,  $\Phi^{(1)}(r)$  and  $\Phi^{(2)}(r)$  denote the total field defined by  $\Phi^{(i)}(r) = F^{(i)}(r) + \Psi^{(i)}(r)$  ( $i = 1, 2$ ).

From (13) and (14) we have a quadratic form of  $J$ :

$$J = -\langle F^{(2)}, \Psi^{(1)} \rangle = \langle \Phi^{(2)}, F^{(1)} \rangle = \langle \Phi^{(2)}, \Psi^{(1)} \rangle. \quad (15)$$

Here, the relationship  $\langle \varphi, \psi \rangle = -\langle \psi, \varphi \rangle$  is used. Making use of the boundary conditions  $\Phi^{(i)}(s) = 0$  ( $i = 1, 2$ ), we can modify the right-hand side of (15) to

$$J = -\langle F^{(2)}, \Psi^{(1)} \rangle = \int_0^1 \frac{\partial \Phi^{(2)}(s)}{\partial n} F^{(1)}(s) ds / \int_0^1 \frac{\partial \Phi^{(2)}(s)}{\partial n} \Psi^{(1)}(s) ds. \quad (16)$$

**Proof of stationarity.** Let us now show that (16) is a stationary representation of  $J$  for any permissible variation of  $\Psi^{(2)}(s)$  or  $\partial \Phi^{(2)}(s)/\partial n$ . First, we assume a small variation in  $\partial \Phi^{(2)}(s)/\partial n$  and denote it by  $\delta[\partial \Phi^{(2)}(s)/\partial n]$ . Then, taking the first variation of (16), we have

$$\delta J \int_0^1 \frac{\partial \Phi^{(2)}(s)}{\partial n} \Psi^{(1)}(s) ds + J \int_0^1 \delta \left[ \frac{\partial \Phi^{(2)}(s)}{\partial n} \right] \Psi^{(1)}(s) ds = -\langle F^{(2)}, \Psi^{(1)} \rangle \int_0^1 F^{(1)}(s) \delta \left[ \frac{\partial \Phi^{(2)}(s)}{\partial n} \right] ds.$$

Because

$$\int_0^1 \Psi^{(1)}(s) \delta \left[ \frac{\partial \Phi^{(2)}(s)}{\partial n} \right] ds = - \int_0^1 F^{(1)}(s) \delta \left[ \frac{\partial \Phi^{(2)}(s)}{\partial n} \right] ds, \quad (17)$$

the second term on the left-hand side of the variational relationship above is equal to the right-hand member. Consequently, we find that  $\delta J = 0$ .

Second, we assume a small variation in  $\Psi^{(2)}(s)$ . Taking the first variation of (16) and making some manipulation, we have

$$\delta J \int_0^1 \frac{\partial \Phi^{(1)}(s)}{\partial n} \Psi^{(2)}(s) ds + J \int_0^1 \frac{\partial \Phi^{(1)}(s)}{\partial n} \delta \Psi^{(2)}(s) ds = -\langle F^{(1)}, \delta \Psi^{(2)} \rangle \int_0^1 \frac{\partial \Phi^{(1)}(s)}{\partial n} F^{(2)}(s) ds.$$

Because  $\delta \Psi^{(2)}(s)$  must be the boundary value of an outgoing wave function, the reaction between  $\Psi^{(1)}(r)$  and  $\delta \Psi^{(2)}(r)$  is zero:  $\langle \Psi^{(1)}, \delta \Psi^{(2)} \rangle = 0$ . Hence,

$$\langle F^{(1)}, \delta \Psi^{(2)} \rangle = \langle \Phi^{(1)}, \delta \Psi^{(2)} \rangle = - \int_0^1 \frac{\partial \Phi^{(1)}(s)}{\partial n} \delta \Psi^{(2)}(s) ds. \quad (18)$$

Combining this equation with the variational relationship above, we have  $\delta J = 0$ .

It is noted here that (17) and (18) are fundamental relationships for finding the scattered field and the current density, respectively. That is, if a radiative solution of the Helmholtz equation, say  $\Psi^{(1)}(r)$ , satisfies (17) for any possible variation  $\delta[\partial \Phi^{(2)}(s)/\partial n]$ , then the  $\Psi^{(1)}(r)$  is the true solution of the problem. Conversely, if a current density  $\partial \Phi^{(1)}(s)/\partial n$  satisfies (18) for any permissible variation  $\delta \Psi^{(2)}(s)$ , then the  $\partial \Phi^{(1)}(s)/\partial n$  is the true density.



### 3. A Duality between Scattered Field and Current Density Calculation

The permissible variation,  $\delta[\partial\Phi^{(2)}(s)/\partial n]$  or  $\delta\Psi^{(2)}(s)$ , in principle, should cover the function space  $H$ . In the context of the Yasuura's methods stated in 1, we have made use of the completeness of the set of boundary values of modal functions.

The method for the scattered field. In 1 we have defined an approximate solution by (5). Thus the boundary value of our approximate solution,  $\Psi_N^{(1)}(s)$  belongs to a subspace of  $H$  spanned by  $\{\varphi_m(s): m = 0, \pm 1, \dots, \pm N\}$ . Substituting  $\Psi_N^{(1)}(s)$  for  $\Psi^{(1)}(s)$  in (17), we have

$$\int_0^1 \Psi_N^{(1)}(s) \delta \left[ \frac{\partial \Phi^{(2)}(s)}{\partial n} \right] ds = - \int_0^1 F^{(1)}(s) \delta \left[ \frac{\partial \Phi^{(2)}(s)}{\partial n} \right] ds.$$

Of course this equality no longer holds for any possible variation, and we should give the meaning of the sign of equality. It is natural that if the  $\Psi_N^{(1)}(s)$  is so restricted as stated above, then the variation in the current density covers a subspace of  $H$  spanned by  $\{\varphi_m(s): m = 0, \pm 1, \dots, \pm N\}$ . Hence, setting

$$\delta \left[ \frac{\partial \Phi^{(2)}(s)}{\partial n} \right] = \overline{\varphi_m(s)} \quad (m = 0, \pm 1, \dots, \pm N),$$

we have a set of linear equations (7) for finding the  $A_m(N)$  coefficients.

The method for the current density. Because the  $\delta\Psi^{(2)}(s)$  in (18) must be the boundary value of an outgoing wave function, let us set  $\delta\Psi^{(2)}(s) = \varphi_m(s)$  ( $m = 0, \pm 1, \dots, \pm N$ ). Then, an approximation of the current density should be inside a subspace of  $H$  spanned by  $\{\varphi_m(s): m = 0, \pm 1, \dots, \pm N\}$ . Hence, if we define an approximate density by (8), we have (9) from (18).

The duality. Let us now set  $F^{(1)}(r) = F^{(2)}(r) = F(r)$  and, hence,  $\Psi^{(1)}(r) = \Psi^{(2)}(r) = \Psi(r)$  and  $\Phi^{(1)}(r) = \Phi^{(2)}(r) = \Phi(r)$  in the discussion above. In the circumstances the quadratic form (15) takes the form

$$J = -\langle F, \Psi \rangle \langle \Phi, F \rangle / \langle \Phi, \Psi \rangle.$$

Reference to (16) gives an approximation to  $J$ , which, in vector-matrix notation, may be represented as

$$J_N = -(gA)(Cf)/CHA. \quad (19)$$

It is easy to show that  $A$  and  $C$ , which respectively are the solutions to (7) and (9), make the representation (19) stationary. We can conclude that if we examine the methods in 1 from the viewpoint of reaction relations, they are nothing other than procedures to find stationary points of the  $J_N$  given in (19). Similar duality holds between the methods with the smoothing procedure.

### References

- (1) Y. Okuno, Mathematical foundations of the Yasuura method, *Proc. MMET\*90*, 89-99, Test-Radio, Kharkov, 1991.
- (2) Y. Okuno, Yasuura's methods for calculating the surface current density on a cylindrical obstacle, *Proc. MMET\*91*, 106-117, Test-Radio, Kharkov, 1991.
- (3) Y. Okuno and H. Ikuno, The Yasuura method for solving the boundary value problems to the Helmholtz equation in homogeneous media, *Radiotekhnika i Elektronika*, **33**, 10, 1744-1763, 1992.
- (4) V. H. Rumsey, Reaction concept in electromagnetic theory, *Phys. Rev.*, **94**, 1483-1491, 1954.

# ELECTROMAGNETIC DIFFRACTION BY A SYSTEM OF COUPLED RECTANGULAR WEDGES: EFFICIENT SOLUTION VIA THE SEMI-INVERSION METHOD

Andrey Osipov

Radiophysics Dept., Inst. of Physics, St. Petersburg State University  
Ulianovskaya 1 - 1, Petrodvorets, 198904 St. Petersburg, Russia

## ABSTRACT

Using a closed solution of a matrix Riemann-Hilbert problem, a two-dimensional diffraction problem for a wave field excited by a line source in a system consisted of a pair of quarter-spaces and a half-space filled with isotropic homogeneous media is accurately reduced to a scalar one-dimensional integral equation of the Fredholm's type convenient for both numerical and analytical approaches.

## INTRODUCTION

This paper investigates electromagnetic diffraction by a system of coupled rectangular wedges which is of importance to predict the influence of a step-like material discontinuity on radiowave propagation over a flat surface [1] as well as on microwave/light scattering from junctions in open dielectric waveguides and resonators [2,3]. With few exceptions, there are no exact solutions in any closed form for this class of diffraction problems (see, for example, [4,5]). In classical works of V.A.Fock and G.A.Greenberg on coastal refraction of radiowaves [1] an approximate solution has been constructed by applying impedance boundary conditions on outer faces of the wedges. Other approaches based on certain physically reasonable simplifications are also possible [6,7].

Mathematically rigorous examinations have been carried out in [4,8] by transformation of the problem to systems of two-dimensional integral equations (in both coordinate and spectral spaces) that prove to be fruitful for general theoretical analysis but cumbersome in obtaining physical results. For anisotropic media with a special structure of their permittivity tensors, one-dimensional singular integral equations have been deduced by V.I.Kurillo and co-authors [9] using Fourier representations of the wave fields. G.I.Makarov and A.P.Sazonov have given an exhaustive consideration of the particular case in which one of the rectangular wedges is perfectly conducting [10-12]. A rigorous theory, applicable to the general case, which reduces the diffraction problem to a system of integral-functional equations has been proposed recently [13,14]. Their asymptotic solutions and applications to various physical problems have been discussed in a number of publications [15-18].

In this paper, the ideas of the semi-inversion method [19] are developed in application to open structures with continuous spectrum, which results in obtaining one-dimensional integral equation of the Fredholm's type, accessible for analytical and numerical treatments [16]. To illustrate the possibilities being offered by the technique, the paper describes the wave fields propagating over an electrically nonuniform surface as well as radiated from certain dielectric structures (both loss-free and absorbing).

## STATEMENT OF THE PROBLEM AND MAIN RESULTS

Let us suppose that in the Cartesian coordinate system  $(x, y, z)$  a homogeneous isotropic medium occupies the upper half-space ( $y > 0$ ) whereas the lower half-space is divided into a pair of quarter-spaces, left ( $x < 0$ ) and right ( $x > 0$ ), filled with different isotropic materials. Then the two-dimensional harmonical ( $\exp(-i\omega t)$ ) wave field excited by a line source, infinitely long and uniform in  $z$ -direction, located at a point  $x = x_0, y = y_0$ ,

can be expressed through the Green's function  $G(x, x_0, y, y_0)$  of the Helmholtz' equation

$$\left( \frac{\partial^2}{\partial x^2} + \frac{\partial^2}{\partial y^2} + k^2 \right) G(x, x_0, y, y_0) = \delta(x - x_0) \delta(y - y_0) \quad (1)$$

which meets transition conditions  $[G] = 0$ ,  $[\rho^{-1} \frac{\partial}{\partial n} G] = 0$  at every material boundary (square brackets denote the jump of the quantity across the boundary,  $\frac{\partial}{\partial n}$  is the normal derivative with respect the boundary) together with proper conditions at the edge [20] and infinity. In each portion of the structure the parameters  $k, \rho$  take different values  $k_j, \rho_j, j = 1, 2, 3$ , with  $k_j = \omega(\epsilon_j \mu_j)^{1/2}$ ,  $\rho_j = \epsilon_j$  in  $H$ -polarisation case ( $G \sim H_z$ ) or  $\rho_j = \mu_j$  in  $E$ -polarisation case where  $\epsilon_j, \mu_j$  being complex permittivities and permeabilities of the media ( $j = 1$  for the upper half-space and  $j = 2, 3$  for the left and right quarter-spaces, respectively). Nonzero conductivities of the media are assumed hereinafter to make clearer the mathematical procedure to be used.

Represent the wave fields scattered from the boundary  $y = 0$  into the upper half-space through the Fourier integral

$$G_+ = \int_{-\infty}^{+\infty} e^{itx + i\gamma_1(t)y} A_+(t) dt \quad (2)$$

and the wave fields scattered into the lower half-space through the following expansion

$$G_- = \int_0^{+\infty} \left( B(t) w_1(x, t) e^{-i\gamma_2(t)y} + C(t) w_2(x, t) e^{-i\gamma_3(t)y} \right) dt \quad (3)$$

with  $\gamma_j(t) = \sqrt{k_j^2 - t^2}$ ,  $\text{Im}(\gamma_j(t)) > 0$ ,  $j = 1, 2, 3$  [13,14]. The spectral functions

$$w_1(x, t) = \begin{cases} T_1(t) e^{ix\sqrt{t^2 - q^2}}, & \text{if } x \geq 0, \\ e^{itx} + R_1(t) e^{-itx}, & \text{if } x \leq 0, \end{cases} \quad \begin{aligned} T_1(t) &= \frac{2t}{t + \epsilon_{22}\sqrt{t^2 - q^2}}, \\ R_1(t) &= T_1(t) - 1, \end{aligned}$$

$$w_2(x, t) = \begin{cases} T_2(t) e^{-ix\sqrt{t^2 + q^2}}, & \text{if } x \leq 0, \\ e^{-itx} + R_2(t) e^{itx}, & \text{if } x \geq 0, \end{cases} \quad \begin{aligned} T_2(t) &= \frac{2t}{t + \epsilon_{32}\sqrt{t^2 + q^2}}, \\ R_2(t) &= T_2(t) - 1, \end{aligned}$$

$q^2 = k_2^2 - k_3^2$ ,  $\epsilon_{jm} = \epsilon_j / \epsilon_m$ ,  $j, m = 2, 3$ ,  $\text{Im}(\sqrt{t^2 \pm q^2}) \geq 0$ , compose a complete system of basis functions [13].

Represented by Eq.(2),(3), for arbitrary coefficients  $A_+(t)$ ,  $B(t)$ ,  $C(t)$ , functions  $G_{\pm}$  satisfy Helmholtz' equations (1), conditions at infinity, and transition conditions along the common face of the wedges. To meet conditions at the edge, these coefficients are required to be of order  $o(t^{-1})$  when  $t \rightarrow \infty$ . Then substituting (2),(3) into the rest of transition conditions followed by elimination of  $B(t)$ ,  $C(t)$  leads to the system of integral-functional equations [13,14]

$$\varphi^+(t) + R_1(-t)\varphi^+(-t) - T_1(-t)\Phi^-(-\sqrt{t^2 - q^2}) = f_1(t) + \kappa_1 A_+ \quad (4)$$

$$\Phi^-(-t) + R_2(-t)\Phi^-(t) - T_2(-t)\varphi^+(\sqrt{t^2 + q^2}) = f_2(t) + \kappa_2 A_+$$

$t \in (-\infty, +\infty)$ , where  $\hat{K}_p$  are integral operators with smooth kernels and  $f_p(t)$  represent given functions of the incident field,  $p = 1, 2$ . Functions  $\varphi^+(t)$ ,  $\Phi^-(t)$ , analytical in the upper and lower half-planes of the complex  $t$ -plane respectively, are connected with the Fourier transformation of the scattering field through the relation

$$A_+(t) = \frac{\Lambda(t)}{2\pi i} \int_{-\infty}^{+\infty} \left( \frac{\varphi^+(\tau)}{X^-(\tau)(\tau - t - i0)} + \frac{\Phi^-(\tau)}{X^+(\tau)(\tau - t + i0)} \right) d\tau \quad (5)$$

where symbols  $\pm i0$  show the displacements of the pole  $\tau = t$  with respect to the contour of integration. Function  $\Lambda(t)$  can be written in either of the two forms

$$\Lambda(t) = \frac{X^+(t)}{\gamma_1(t) + \varepsilon_{12}\gamma_2(t)} = \frac{X^-(t)}{\gamma_1(t) + \varepsilon_{12}\gamma_2(t)}$$

because  $X^\pm(t)$  are introduced as certain solutions to the corresponding factorization problem when  $t \in (-\infty, +\infty)$ .

The method for handling Eq. (4) is the following semi-inversion procedure [18]. Consider an auxiliary matrix Riemann-Hilbert problem resulting from (4) if its right parts are regarded as certain known functions  $g_{1,2}(t)$  meeting the relations  $g_{1,2}(-t) = R_{1,2}(t)g_{1,2}(t)$ . Applying Cauchy operators to each of the equations of the auxiliary system produces, on rearrangement of the contour integrals, its exact solutions in the form

$$\varphi^+(z) = \frac{1}{4\pi i} \int_{-\infty}^{+\infty} \left( \frac{2g_1(\tau)}{\tau - z} + \varepsilon_{12} \frac{T_2(\tau)g_2(\tau)}{\sqrt{\tau^2 + q^2 + z}} \right) d\tau, \quad (\text{Im}(z) > 0) \quad (6)$$

$$\Phi^-(z) = \frac{1}{4\pi i} \int_{-\infty}^{+\infty} \left( \frac{2g_2(\tau)}{\tau + z} + \varepsilon_{23} \frac{T_1(\tau)g_1(\tau)}{\sqrt{\tau^2 - q^2 - z}} \right) d\tau, \quad (\text{Im}(z) < 0).$$

When combined according to (5), Eq. (6) lead, on substitutions  $g_p(t) = f_p(t) + \hat{K}_p A_+$ ,  $p = 1, 2$ , to an integral equation for function  $A_+(t)$ , which, for more convenience, can be written with respect the Fourier transformation of the total field in the upper half-space

$$A(t) = \begin{cases} A_+(t) + A_0(t), & \text{if } y_0 > 0 \\ A_+(t), & \text{if } y_0 < 0 \end{cases}$$

where  $A_0(t) = \exp(-itx_0 + i\gamma_1(t)y_0)/(4\pi i\gamma_1(t))$ . This equation has a form of an integral equation of the second kind

$$A(t) = f(t) + \int_{-\infty}^{+\infty} H(t, \tau) A(\tau) d\tau, \quad t \in (-\infty, +\infty), \quad (7)$$

with a smooth kernel being expressed as the sum  $H(t, \tau) = \frac{\Lambda(t)}{2\pi i} (I_2(t, \tau) + I_3(t, \tau))$  of the contour integrals

$$I_2(t, \tau) = \frac{\varepsilon_{12}}{2\pi i} \int_{\Gamma_2} \frac{\gamma_2(\tau_1)}{X^-(\tau_1)(\tau_1 - \tau)} \left( \frac{1}{\tau_1 - \tau} - \frac{R_1(-\tau_1)}{\tau_1 + \tau} + \frac{\varepsilon_{23}T_1(-\tau_1)}{\sqrt{\tau_1^2 - q^2 + \tau}} \right) d\tau_1,$$

$$I_2(t, \tau) = \frac{\varepsilon_{12}}{2\pi i} \int_{\Gamma_2} \frac{\gamma_2(\tau_1)}{X^+(\tau_1)(\tau_1 - t)} \left( \frac{1}{\tau_1 - t} - \frac{R_2(\tau_1)}{\tau_1 + \tau} - \frac{\varepsilon_{22} T_2(\tau_1)}{\sqrt{\tau_1^2 + q^2} - \tau} \right) d\tau_1$$

where contours  $\Gamma_{2,3}$  envelop the branch lines  $Im(\gamma_{2,3}(t)) = 0$  issued out of the points  $\tau_1 = -k_2, k_3$ , respectively. Depending on source location,  $f(t)$  is given by the formulas

$$f(t) = A_0(t) + \frac{\Lambda(t)}{2\pi i} \int_{-\infty}^{+\infty} \frac{A_0(\tau)}{\Lambda(\tau)} \left( \frac{R_{12}(\tau)}{\tau - t - i0} - \frac{R_{13}(\tau)}{\tau - t + i0} \right) d\tau,$$

$$R_{mj}(t) = \frac{\gamma_m(t) - \varepsilon_{mj} \gamma_j(t)}{\gamma_m(t) + \varepsilon_{mj} \gamma_j(t)}, \text{ if } y_0 > 0;$$

$$f(t) = \frac{\Lambda(t)}{4\pi i} \int_{-\infty}^{+\infty} \left( \frac{2f_1(\tau)}{X^-(\tau)(\tau - t - i0)} + \frac{\varepsilon_{22} T_1(\tau) f_1(\tau)}{X^+(\sqrt{\tau^2 - q^2})(t - \sqrt{\tau^2 - q^2})} \right) d\tau + \frac{\Lambda(t)}{4\pi i} \int_{-\infty}^{+\infty} \left( \frac{\varepsilon_{22} T_2(\tau) f_2(\tau)}{X^-(-\sqrt{\tau^2 + q^2})(t + \sqrt{\tau^2 + q^2})} + \frac{2f_2(-\tau)}{X^+(\tau)(\tau - t + i0)} \right) d\tau,$$

if  $y_0 < 0$ .

Integral equation (8) provides known solutions in the limit case of quasistatics ( $k_j \rightarrow 0$ ,  $j = 1, 2, 3$ ) [21] as well as in the case of homogeneous lower half-space ( $\varepsilon_3 \rightarrow \varepsilon_2$ ,  $k_3 \rightarrow k_2$ ). For perfectly conducting quater-space ( $Im(k_3) = \infty$ ), it proves to be consistent with convolution-type integral equations obtained by Makarov and Sozonov [10]. In general, Eq.(8) is of Fredholm's type and, consequently, has one and only one solution, trivial if  $f(t) = 0$ . When  $t \rightarrow \infty$ , its solution is of order  $O(t^{-1-\alpha_1})$  where  $\alpha_1$  is a non-negative root of a Moirner's type equation from strip  $0 < Re(\alpha_1) < 1$  [20-22]. If parameters either  $|\varepsilon_{12}|$ ,  $|\varepsilon_{13}|$  or  $|\varepsilon_3 - \varepsilon_2|/(\varepsilon_3 + \varepsilon_2)$ ,  $|(k_3 - k_2)/(k_3 + k_2)|$  are small enough, then Neumann's procedure can be used to get approximate solutions of Eq.(8) in the form

$$A(t) = f(t) + \hat{H}f + \hat{H}^2 f + \dots$$

giving convenient and justified representations of the Green's function applicable to analyze a broad spectrum of electromagnetic problems [13,15-17].

## REFERENCES

- [1] Fock V.A. Electromagnetic Diffraction and Propagation Problems. 1965 (Pergamon: London);
- [2] Weinstein L.A. The Theory of Diffraction and the Factorisation Method. 1969 (Golem: Boulder Colo.);
- [3] Marcuse D. Theory of Dielectric Optical Waveguides. 1974 (Academic: New York);
- [4] Lats N. *J.Math.Analysis and Appl.* (1973) Vol.43, 2, p.373; [5] Osipov A.V. *Vestn.St.Petersburg Univ. Ser.4* (1993) No 2, p.10; [6] Kurilko V.I. *Izv.Vuzov. Radiofizika* (1983) Vol.11, 8, p.1221; [7] Ryan J., Walsh J. *Radio Sci.* (1985) Vol.20, 6, p.1518; [8] Melster E., Lats N. *ZAMM* (1984) Vol.44, 8-H., p.47; [9] Boots V.A., Kalmykova S.S., Kurilko V.I. *Izv.Vuzov. Radiofizika* (1983) Vol.11, 1, p.62; [10] Makarov G.I., Sozonov A.P. *Izv.Vuzov. Radiofizika* (1984) Vol.27, 4, p.481; [11] Makarov G.I., Sozonov A.P. *Vestn.Leningr.Univ. Ser.4* (1985) No 1, p.98; [12] Makarov G.I., Sozonov A.P. *Vestn.Leningr.Univ. Ser.4* (1985) No 4, p.85; [13] Osipov A.V. *Ph.D.Thesis* 1985, Leningrad State University; [14] Osipov A.V. *Vestn.Leningr.Univ. Ser.4* (1983) No 3, p.44; [15] Osipov A.V. *Vestn.Leningr.Univ. Ser.4* (1986) No 4, p.86; [16] Makarov G.I., Osipov A.V. *Vestn.Leningr.Univ. Ser.4* (1989) No 1, p.31; [17] Osipov A.V. In: *Problems of Diffraction and Wave Propagation (St.Petersburg State Univ.)* (1992) No 24, p.61; [18] Osipov A.V. *Vestn.St.Petersburg Univ. Ser.4* (1993) No 3, p.15; [19] Shestopalov V.P., Kirilenko A.A., Masalov S.A. Convolution-type Matrix Equations in the Theory of Diffraction. 1984 (Naukova Dumka: Kiev); [20] Moirner J. *IEEE Trans.AP* (1972) Vol.20, p.442; [21] Greenberg G.A. Selected Problems of the Mathematical Theory of Electrical and Magnetic Phenomena. 1948 (Academy Sci.: Leningrad - Moscow); [22] Makarov G.I., Osipov A.V. *Izv.Vuzov. Radiofizika* (1986) Vol.29, p.714.

# APPLICATION OF THE HOMOGENIZATION THEORY IN SUPERCONDUCTIVITY PROBLEMS

L.S. Pankratov

B. Verkin Institute for Low Temperature Physics & Engineering  
National Academy of Sciences of Ukraine  
47, Lenin Ave., 310164 Kharkov, Ukraine

## ABSTRACT

The asymptotic behavior of the solutions of the boundary value problem for Ginzburg-Landau equation in domains with complicated boundary is considered. It is shown that the limit function is the solution of some modified boundary value problem considered in the simple domain.

## INTRODUCTION

Since early 60s a considerable number of papers devoted to homogenization of partial differential equations describing various physical processes in strongly inhomogeneous media were presented (see for example [1-5]). Such media possess of local physical characteristics enduring rapid oscillations in space and therefore corresponding differential equations either have rapidly oscillating coefficients or are considered in strongly perforated domains. The complicated structure of strongly perforated domain does not contribute any additional difficulties to the question of solvability of boundary value problems in such domains but the determination of the solution is practically impossible either by analytical or by numerical approaches. However, if the characteristic scale of the microstructure of the medium is much smaller than the scale of the domain in which the process is studied then the homogenized description of the process may be proposed.

The present paper is related with homogenization theory in strongly perforated domains and devoted to its application to the boundary value problem in so called weakly connected domains for Ginzburg-Landau equation which is a fundamental macroscopic model of the weak superconductivity theory in the absence of a magnetic field [6].

Note that the asymptotic behavior of nonlinear variational problems in weakly connected domains was studied by the writer in paper [7].

## FORMULATION OF THE PROBLEM AND THE MAIN RESULT

Let  $\Omega$  is a composite superconductor consisting of a melange of a superconducting material  $\Omega \setminus F^{(s)}$  and of dielectric  $F^{(s)}$ , where the parameter  $s$  ( $s = 1, 2, \dots$ ) is the characteristic of the scale of microstructure. Since the current does not penetrate the dielectric the Neumann boundary condition is fulfilled on the boundary  $\partial F^{(s)}$ .

We shall assume that  $\Omega$  is a unit cube  $\Omega = \{(x_1, x_2, x_3) : -1/2 \leq x_k \leq 1/2\}$  in three-dimensional Euclidean space and the set  $F^{(s)}$  is located in an arbitrary small neighbourhood of the plane  $x_3 = 0$ .

Consider the following boundary value problem for determination of the complex-valued wave function  $\psi^{(s)}(x)$  in the domains  $\Omega^{(s)} = \Omega \setminus F^{(s)}$ :

$$\Delta \psi^{(s)} + \psi^{(s)} - \psi^{(s)} |\psi^{(s)}|^2 = 0, \quad x \in \Omega^{(s)}, \quad (1)$$



$$\frac{\partial \psi^{(s)}}{\partial \nu} = 0, \quad x \in \partial F^{(s)} \cup \partial \Omega \setminus (\Gamma_1 \cup \Gamma_2), \quad (2)$$

$$\psi^{(s)}|_{\Gamma_1} = \Psi_1(x), \quad \psi^{(s)}|_{\Gamma_2} = \Psi_2(x), \quad (3)$$

$$\psi^{(s)}(x) \in W_2^1(\Omega^{(s)}) \cap W_2^2(\Omega^{(s)}, loc), \quad (4)$$

where  $\Gamma_1$  and  $\Gamma_2$  are top and bottom faces of the cube  $\Omega$ , respectively;  $\partial/\partial \nu$  is the normal derivative on the domain's boundary;  $\Psi_{1,2}(x)$  are complex-valued functions defined in the domain  $\Omega$ , belonging to the class  $W_2^2(\Omega) \cap C^\infty(\bar{\Omega})$ , and satisfying the condition  $\partial \Psi_s / \partial \nu = 0$  on  $\partial \Omega \setminus (\Gamma_1 \cup \Gamma_2)$ . Boundary condition is understood in the sense of distributions [8].

It is known that there exists at least one generalized solution  $\psi^{(s)}(x)$  of the boundary value problem (1)-(4).

We shall study the asymptotic behavior of the solutions  $\psi^{(s)}(x)$  as  $s \rightarrow \infty$  in the domains  $\Omega^{(s)} = \Omega \setminus F^{(s)}$ , when the sets  $F^{(s)}$  unrestrictedly approach the surface  $x_3 = 0$ .

To formulate the main result of the paper, we shall first introduce a quantitative characteristic of the sets  $F^{(s)}$  ("permeability"). Let  $\Gamma = \{x_3 = 0\} \cap \Omega$  and  $\gamma$  is an arbitrary portion of  $\Gamma$ , i.e., an open connected set on  $\Gamma$ ,  $T(\gamma, \delta)$  is a layer of thickness  $2\delta$  with mid surface  $\gamma$ , so that  $\gamma_\delta^\pm$  are the bases of the layer  $T(\gamma, \delta)$ , i.e., the plane surfaces located on the different sides of  $\gamma$  at the distance  $\delta$  and  $T^{(s)}(\gamma, \delta) = T(\gamma, \delta) \setminus F^{(s)}$ . Now we shall define the function of sets  $\gamma \subset \Gamma$ :

$$P(\gamma, s, \delta) = \inf_{\psi^{(s)}} \int_{T^{(s)}(\gamma, \delta)} |\nabla \psi^{(s)}|^2 dx, \quad (5)$$

where the infimum is taken over the class of functions  $\psi^{(s)}(x) \in W_2^1(T^{(s)}(\gamma, \delta))$  which are equal to one and zero on  $\gamma_\delta^+$  and  $\gamma_\delta^-$ , respectively.

Now we shall formulate the main result of the present paper. The theorem is valid.

**Theorem 1.** Let the following conditions are fulfilled as  $s \rightarrow \infty$ :

- (i) the sets  $F^{(s)}$  are contained in a layer of arbitrarily small width with mid surface  $\Gamma \subset \Omega$ ;
- (ii) for any portion  $\gamma \subset \Gamma$  the equality holds

$$\lim_{\delta \rightarrow 0} \lim_{s \rightarrow \infty} P(\gamma, s, \delta) = \lim_{\delta \rightarrow 0} \lim_{s \rightarrow \infty} \overline{\lim}_{\gamma} P(\gamma, s, \delta) = \int_{\gamma} p(x) d\Gamma, \quad (6)$$

where  $p(x)$  is a measurable function on  $\Gamma$  and  $p(x) \geq 0$ . Then every sequence of solutions  $\{\psi^{(s)}(x)\}_{s=1}^\infty$  of the boundary value problem (1)-(4) converges in  $L_2(\Omega^{(s)})$  to the solution  $\psi(x)$  of the boundary value problem

$$\Delta \psi + \psi - \psi |\psi|^2 = 0, \quad x \in \Omega \setminus \Gamma, \quad (7)$$

$$\left(\frac{\partial \psi}{\partial \nu}\right)_+ = \left(\frac{\partial \psi}{\partial \nu}\right)_- = p(x)[\psi_+ - \psi_-], \quad x \in \Gamma, \quad (8)$$

$$\psi|_{\Gamma_1} = \Psi_1(x), \quad \psi|_{\Gamma_2} = \Psi_2(x), \quad (9)$$

$$\frac{\partial \psi}{\partial \nu} = 0, \quad x \in \partial \Omega \setminus (\Gamma_1 \cup \Gamma_2), \quad (10)$$

where the signs "+" and "-" indicate the boundary values of functions on the different sides of  $\Gamma$ , and  $\partial/\partial \nu$  is the normal derivative to  $\Gamma$  in the direction corresponding to "+".

There exists one and only one solution of the boundary value problem (7)-(10).

The proof of the Theorem 1 is based on application of the results of the monograph [1] to the boundary value problem (1)-(4) and will appear among some other results concerning with this boundary value problem in paper [9].

### STATIONARY JOSEFSON EFFECT

Let us obtain the expression for the normal component of superconducting current flowing through a weak connection. The homogenized density is calculated by the formula

$$j = -\frac{i}{2} \left[ \bar{\psi}_\pm \left(\frac{\partial \psi}{\partial \nu}\right)_\pm - \psi_\pm \left(\frac{\partial \bar{\psi}}{\partial \nu}\right)_\pm \right]. \quad (11)$$

By virtue of the boundary condition (8) it is easy to obtain that

$$j = \frac{ip(x)}{2} [\bar{\psi}_+ \psi_- - \psi_+ \bar{\psi}_-]. \quad (12)$$

Let  $|\psi_\pm|$  and  $\varphi_\pm$  are the modulus and the phase of the complex-valued function  $\psi_\pm$ , respectively, then

$$j = p(x) |\psi_+| |\psi_-| \sin(\varphi_+ - \varphi_-), \quad (13)$$

which is mathematical expression of the stationary Josephson effect [6].

### CONCLUSIONS

The results of the paper may be interpreted as follows. Let  $\Omega$  is a composite superconductor which for the sake of simplicity is considered as unit cube and the wave function  $\psi^{(s)}(x)$  is given



on the top  $\Gamma_1$  and bottom  $\Gamma_2$  faces of the cube, i.e.,  $\psi^{(s)}(x)$  satisfies the Dirichlet boundary condition on  $\Gamma_{1,2}$  and satisfies the Neumann condition on the remaining part of the boundary. Let us also assume that the sets  $F^{(s)}$  (dielectric) approach the plane  $x_3 = 0$ . Then the wave function  $\psi^{(s)}(x)$  and the current density

$$j^{(s)} = \text{Im}(\nabla \psi^{(s)}(x) \bar{\psi}^{(s)}(x))$$

converge to the limit function  $\psi$  and current density  $j$ , respectively. The function  $\psi$  is the solution of the boundary value problem (7)–(10) and at every point of the plane  $x_3 = 0$  the relation (13) is valid. This relation is a mathematical expression for well-known Josefsen effect.

## REFERENCES

- (1) V.A. Marchenko and E.Ya. Khruslov "Boundary Value Problems in the Domains with Fine-Grained boundary", Naukova Dumka, Kiev (1974), 279 p. (Russian)
- (2) A. Bensoussan, J.-L. Lions and G. Papanicolau "Asymptotic Analysis for Periodic Structures", Studies in Mathematics and its Applications, vol.5, North-Holland, Amsterdam (1978).
- (3) E. Sanchez-Palencia "Non-Homogeneous Media and Vibration Theory. Lectures Notes in Physics, Springer-Verlag, New York (1980), 469 p.
- (4) N.S. Bakhvalov and G.P. Panasenko "Homogenization of Processes in Periodic Media", Nauka, Moscow (1984). (Russian)
- (5) V.V. Zhikov, S.M. Kozlov and O.A. Oleinik "Homogenization of Differential Operators", Fiz.-Mat. Lit., Moscow (1993), 461 p. (Russian)
- (6) V.V. Schmidt "Introduction to the Superconductor Physics", Nauka, Moscow (1982), 240 p. (Russian)
- (7) L.S. Pankratov "On convergence of variational problems solutions in weakly connected domains" Kharkov, Preprint FTINT AN UkrSSR (1988), 53–88, 25 p. (Russian).
- (8) S.L. Sobolev "Some Applications of Functional Analysis in Mathematical Physics", Siberia Department of AN SSSR, Novosibirsk (1962), 255 p. (Russian)
- (9) E.Ya. Khruslov and L.S. Pankratov "Homogenization of Boundary Problems for the Ginzburg-Landau Equation in Weakly Connected Domains", In : Advances in Soviet Mathematics, AMS Providence, 1994 (to appear).

# On wave propagation over a plane surface of variable conductivity

L.A. Pazynin

Institute of Radiophysics and Electronics  
Kharkov, Ukraine

**Abstract:** The problem of propagating an electromagnetic wave over a surface of variable impedance is studied. The new class of surface impedance distributions for which the solution can be found in an explicit form is defined. For this the problem must be reduced to the Carleman boundary problem for a strip in the complex variable plane. In the case of small impedance values the estimation of the back scattering by an impedance inhomogeneity, depending on its width referred to wavelength, is given.

The characteristics of electromagnetic wave propagation over a surface of variable conductivity are analyzed theoretically in a great number of works, beginning from [1]. As a rule, studying the problem is based on the solution of Volterra's integral equation for the power attenuation factor over an impedance surface as a function of distance from a source [2-5]. This equation is approximate in virtue of the assumption on smoothness of surface impedance variations, therefore, in particular, its solution does not include the back scattered waves. The exceptions from this approach are investigations begun in works by Grinberg, Fok [1,6] for the case of the plane surface impedance being a *discontinuous* function with a jump on the wave path from one constant value  $\eta_2$  to another  $\eta_1$ . The exact solution of the problem on plane wave propagation over such a surface has been found in a closed form [1,6,7]. Bass [8] has generalized the results of the works [1,6] to the case of a curvilinear coast.

In the present work a new model is suggested to describe electromagnetic wave propagation over the plane surface whose impedance  $\eta(x)$ , as distinct from [1,6,7,8] is a *continuous* function of a special form varying monotonically from  $\eta_2$  to  $\eta_1$ .

In addition to these two parameters, the description of the function  $\eta(x)$  includes the parameter  $\delta$  defining the "transient" region width and varying from zero to infinity. The Grinberg-Fok model is its limiting case at  $\delta = 0$ . For the model suggested the exact solution of the corresponding boundary value problem is found.

A sought-for value is an electromagnetic field in the upper half-space  $z > 0$  limited by the plane  $z = 0$  with the impedance  $\eta(x, y)$ . The source geometry and dependence  $\eta(x, y)$  are described further. Starting from Green's integral formula and following [6] we obtain the integral representation for  $z$ -component of a full field in the half-space  $z > 0$

$$E_z(x, y, z) = E_z^0(x, y, z) - \iint_{-\infty}^{\infty} \left\{ \frac{\partial E_z(x', y', 0)}{\partial z'} v(r) - E_z(x', y', 0) \frac{\partial v(r)}{\partial z'} \right\} dx' dy' \quad (1)$$

where

$$v(r) = \exp(ikr) / (4\pi r), \quad r = \sqrt{(x-x')^2 + (y-y')^2 + z^2},$$

$$k = k_1 = k_0 \sqrt{\epsilon_1 \mu_1}, \quad \text{Im } k > 0.$$

The modified Leontovich's boundary condition for the normal component of the electric field  $E$  has the following form [6,9,10]

$$\frac{\partial E_z(x,y,0)}{\partial z} = -ik \eta(x,y) E_z(x,y,0). \quad (2)$$

where  $\eta(x,y) = \sqrt{\epsilon_1 \mu_2 / \epsilon_2' \mu_1}$  is the relative surface impedance plane  $z=0$ ,  $\epsilon_2' = \epsilon_2'(x,y)$  is the complex dielectric constant of the half-space  $z < 0$ . After substitution of (2) in the integral equation we have

$$E_z(x,y,0) = 2E_z^0(x,y,0) + 2ik \iint_{-\infty}^{\infty} \eta(x',y') E_z(x',y',0) v(r_0) dx' dy'. \quad (3)$$

Our consideration will be restricted to the two-dimensional case. Let  $\eta(x,y) = \eta(x)$ , and the source is a linear magnetic current [12]

$$J^{(m)} = J_y I^{(m)} \delta(\bar{\rho} - \bar{\rho}_0), \quad E^0 = i\omega \mu_0 \mu_1 \nabla \times \Pi^{(m)}, \quad \bar{\rho} = \{x, 0, z\},$$

$$\Pi_x^{(m)} = \Pi_z^{(m)} = 0, \quad \Pi_y^{(m)} = -\frac{I^{(m)}}{4\omega \mu_0 \mu_1} H_0^{(1)}(k|\bar{\rho} - \bar{\rho}_0|).$$

We obtain

$$\bar{I}(x) = \bar{g}(x) - \frac{k}{2} \eta(x) \int_{-\infty}^{\infty} \bar{I}(x') H_0^{(1)}(k|x-x'|) dx', \quad (4)$$

where

$$\bar{I}(x) = \eta(x) E_z(x,0), \quad \bar{g}(x) = 2\eta(x) E_z^0(x,0).$$

Consider the following three-parameter class of surface impedance distributions, each of them describing the impedance continuous transition from one fixed complex value  $\eta_2 = \eta(-\infty)$  to another  $\eta_1 = \eta(+\infty)$

$$\eta(x) = \frac{\eta_1 + \eta_2 e^{-ix}}{1 + e^{-ix}} = \frac{\eta_1 + \eta_2}{2} + \frac{\eta_1 - \eta_2}{2} \operatorname{th} \frac{x}{2\delta},$$

where  $\delta = 1/\tau$ ,  $\tau > 0$ . The equation (4) for such  $\eta(x)$  after substitution  $ix = s$ ,  $f(s) = \bar{I}(\delta s)$ ,  $g(s) = \bar{g}(\delta s)$  belongs to the type of smooth-transition equations introduced by Cherskii [11]

$$f(s) + \frac{1}{\sqrt{2\pi}} \int_{-\infty}^{\infty} n_1(s-t) f(t) dt + \frac{1}{\sqrt{2\pi}} \operatorname{th} \frac{s}{2} \int_{-\infty}^{\infty} n_2(s-t) f(t) dt = g(s), \quad (5)$$

( $-\infty < s < \infty$ )

$$n_{1,2}(s-t) = \sqrt{\pi/2} k\delta \frac{\eta_1 \pm \eta_2}{2} H_0^{(1)}(k\delta|s-t|).$$

The solvability of eq.(5) by quadrature in the space  $L_2$  under the condition  $g(s) \in L_2$  has been proved in [11]. With use of the Fourier transform Eq.(5) is reduced to the Carleman boundary problem for a strip which is reduced by some conformal transform to the Riemann problem on the real axis. The solution of eq.(4) can be written as

$$\bar{f}(x) = -\frac{1}{4} I^{(2)} \frac{1}{\sqrt{2k}} \int_{-\infty}^{\infty} [\tau G(\tau t) + e^{x\tau} \omega^*(e^{2x\tau})] e^{-i\bar{x}\tau} \frac{\sqrt{k^2 - t^2}}{\sqrt{k^2 - t^2} + k\eta_2} dt, \quad (6)$$

$$G(\tau t) = \sqrt{2/k} \frac{\partial}{\partial \bar{x}_0} \int_{-\infty}^{\infty} \frac{\eta_1 + \eta_2 e^{-y}}{1 + e^{-y}} H_0^{(1)}(k\sqrt{(y - \bar{x}_0)^2 + \bar{z}_0^2}) e^{i\tau y} dy.$$

$$X^{\pm}(e^{2x\tau}) = \exp \left\{ \frac{e^{2x\tau} + 1}{1} \int_{-\infty}^{\infty} \ln \frac{\sqrt{k^2 - s^2 + k\eta_2}}{\sqrt{k^2 - s^2 + k\eta_1}} \frac{e^{2xs} ds}{(e^{2xs} + 1)(e^{2xs} - e^{2x\tau})} \right\}.$$

$$\omega^*(e^{2x\tau}) = -i\tau X^+(e^{2x\tau}) k(\eta_2 - \eta_1) \int_{-\infty}^{\infty} \frac{G(\tau\lambda) e^{x\lambda} d\lambda}{(\sqrt{k^2 - \lambda^2 + k\eta_1}) X^+(e^{2x\lambda}) (e^{2x\lambda} - e^{2x\tau})},$$

where  $\bar{k} = k\delta$ ,  $\bar{x} = x\tau$ ,  $\bar{z} = z\tau$  and the integration contour bypasses the pole in the point  $t$  from above and below for the functions designated by "+" and "-", respectively. These relations give the explicit expression for Green's function of the two-dimensional boundary problem considered without any restrictions on parameter values.

In the case of a plane wave the relations (6) can be simplified. For the sake of simplicity we restrict our consideration to the sliding incidence ( $x_0 \rightarrow \infty$ ) and  $\eta_2 = 0$ .

We obtain the resulting expression for the vertical component of the full electric field on an impedance surface

$$E_z(x, 0) = 2e^{ikx} - \frac{i k \eta_1}{X^-(e^{2x(-\bar{k}+1)})} \int_{-\infty}^{\infty} \frac{X^+(e^{2x\tau})}{\sqrt{k^2 - t^2} \operatorname{sh}(\pi(\bar{k} + t))} e^{-i\bar{x}\tau} d\tau, \quad (7)$$

here the pole  $t = -\bar{k}$  is bypassed from above. The relation (7) is convenient for studying the field in the region  $x < 0$ , with first term of (7) representing the full field of a plane wave on a perfectly conducting plane and the integral term describing the scattering by an impedance inhomogeneity. The representation convenient in the region  $x > 0$  can be obtained from here

$$E_z(x, 0) = \frac{-i k \eta_1}{X^-(e^{2x(-\bar{k}+1)})} \int_{-\infty}^{\infty} \frac{X^-(e^{2x(t+1)})}{(\sqrt{k^2 - t^2} + k\eta_1) \operatorname{sh}(\pi(\bar{k} + t))} e^{-i\bar{x}\tau} d\tau, \quad (8)$$

with the path-tracing of the pole  $t = -\bar{k}$  from below. The field in the half-space  $z > 0$  can be restored by the field found on the plane  $z = 0$  (7) or (8) with use of Eq. (1).

The expression (8) for  $E_z(x, 0)$  at  $\delta \rightarrow 0$  is easily shown to go over into the known representation [10] for the field  $E_z(x, 0)$  on the plane with the impedance equal to zero at  $x < 0$  and  $\eta_1$  at  $x > 0$ . Note that this solution obtained by Grinberg and Fok [6] can be considered as the leading term of the long-wavelength asymptotic expression of our solution, i.e. as one corresponding to the case of the "transient" region width being much less than the source wavelength, i.e.  $2k\delta \ll 1$ .

In the theory of radio wave propagation the inequality  $|\eta| \ll 1$  is usually satisfied. Then the functions  $X^{\pm}(e^{2x\tau})$  can be shown

to be unit with the accuracy of the order of  $O(|\eta_1|)$ .

From (7) at  $|\eta_1| \ll 1$  we find the field  $E_z^*(x, 0)$  scattered by the impedance inhomogeneity far from it ( $k|x| \gg 1, \tau|x| \gg 1$ ) for  $x < 0$

$$E_z^*(x, 0) \approx \frac{1}{\sqrt{2\pi}} e^{ikx/4} \eta_1 A^* \frac{e^{-ikx}}{\sqrt{k|x|}} \quad (x < 0) \quad (9)$$

whose amplitude is proportionate to the factor

$$A^* = \frac{2\pi k \delta}{\text{sh}(2\pi k \delta)} \quad (10)$$

defining the effect of size of the "transient" region width  $2\delta$  referred to wavelength on the field scattered. As seen from (10), the back scattering is exponentially decreases with increasing  $\delta/\lambda$  and at  $2\pi k \delta \gg 3$  can be neglected, then the approximations [3,4] can be used. For the surface impedance distributions with less "transient" region widths the back scattering amplitude is not small and estimating the field over such a surface can be reliable only when relations (7) or (8) of the present work is used.

### References

1. Grinberg, G.A.: 'Theory of the coastal refraction of electromagnetic waves', J. Phys. USSR, 1942, vol. 6, pp. 185-209
2. Feinberg, E.L.: 'On the propagation of radio waves along an imperfect surface', J. Phys. USSR, 1944, vol. 8, pp. 317-330
3. Feinberg, E.L.: 'The propagation of radio waves along the surface of the earth', by Ye. L. Feynberg, tr. from Russian. Wright-Patterson Air Force Base, Ohio: Foreign Techn. Div., AF Systems Command, 1967
4. Wait, J.R.: 'Electromagnetic Wave Theory', Harper and Row, New York, 1985
5. Forget, P., and Broche, P.: 'A study of VHF radio waves propagation over a water surface of variable conductivity', Radio Science, 1991, 26, No 5, pp. 1229-1237
6. Fok, V.A.: 'Electromagnetic diffraction and propagation problems', in International Series of Monographs on Electromagnetic Waves, Pergamon, New York, 1965
7. Rojas, R.G.: 'Wiener-Hopf Analysis of the EM Diffraction by an Impedance Discontinuity in a Planar Surface and by an Impedance Half-Plane', IEEE Trans. Antennas Propagat., 1988, vol. 36, No 1, pp. 71-83
8. Bass, F.G., Slepian, G.Ya., Slepian, A.Ya.: 'On the theory of coastal refraction of electromagnetic waves', Dokl. Akad. Nauk SSSR, 1991, 317, No 1, pp. 82-85 ( in Russian )
9. Senior, T.B.A., and Volakis, J.L.: 'Generalized Impedance Boundary Conditions in Scattering', Proceedings of the IEEE, 1991, vol. 79, No 10, pp. 1413-1420
10. Weinstein, L.A.: 'The Theory of Diffraction and the Factorization Method', Boulder, CO: Golem, 1969
11. Cherskii, Yu. I.: 'Normally solvable smooth-transition equation', Dokl. Akad. Nauk SSSR, 1970, 190, No 1, pp. 57-60 ( in Russian )
12. Tyras, G.: 'Radiation and propagation of electromagnetic waves', in a Series of Monographs and Texts, Academic Press, New York and London, 1969

# MODIFIED GEOMETRICAL OPTICS FOR AN INHOMOGENEOUS ISOTROPIC PLASMA

Valeriy A. Permyakov and Sergey V. Krestyaninov

Department of Radio Engineering, The Moscow Power Engineering Institute, Krasnokazarmennaya, 14, Moscow, 111250, Russia

## ABSTRACT

A modified geometrical optics procedure (MGO) was formulated for an arbitrary, smoothly inhomogeneous plasma. MGO is taken into account the peculiarities of E-wave ( $\nabla E_z \neq 0$ ) propagation in an inhomogeneous plasma with overdense core.

## INTRODUCTION

It is well known that the peculiarities of E-wave ( $\nabla E_z \neq 0$ ) propagation in a smoothly inhomogeneous plasma are not taken into account by classical geometrical optics (GO). The problem lies in the correct description of E-field amplitude and phase near the backscattering direction and E-wave resonant attenuation in the vicinity of plasma permittivity simple zero [1]. The analytic solutions for standard problems of a plane E-wave diffraction and magnetic current filament radiation in a plane-stratified plasma permit interpretation of the E-field, in terms of MGO, as the field in a medium with effective permittivity  $\epsilon_{ef} = \epsilon + k_0^{-2} [\epsilon'(z)/2\epsilon - (\epsilon'(z)/\epsilon)^2]$ , and allows as to find the magnetic field reflection coefficient in a turning point, taking into account the effect of resonant attenuation. A MGO procedure is formulated on the basis of solutions for standard problems of an arbitrary, smoothly inhomogeneous plasma and include special diffraction effects for an E-field connected with the corrections  $O(k_0^{-2})$  in  $\epsilon_{ef}$ .

## PROPAGATION OF A PLANE E-WAVE IN A PLANE-STRATIFIED PLASMA.

MGO given below is based on the local plane-stratified approximation of the medium in the ray vicinity. The first step in MGO construction is the WKB solution for the problem of plane E-wave propagation in the media with local (i.e., in the vicinity of the zero of  $\epsilon$ ) linear approximation for the permittivity. The solution of this problem see in Ref. [2]. Here we discuss the conclusions in [2]. The harmonic time-dependence  $\exp(i\omega t)$  is used in this paper.

The dependence of the E-wave magnetic field component

$$H_x = U(z) \exp(-ik_0 h(\theta)y) \quad (1)$$

is defined by the equation

$$U''_{zz} - \frac{\epsilon'(z)}{\epsilon(z)} U'_z + k_0^2 (\epsilon(z) - h^2) U = 0, \quad h = \sin\theta. \quad (2)$$

By means of the substitution  $U = \sqrt{\epsilon} F$ , Eqn. (2) is reduced to equation

$$F''_{zz} + (k_0^2 q(z) + r(z)) F = 0, \quad (3)$$

where

$$q(z) = \epsilon_{ef}(z) - h^2, \quad \epsilon_{ef} = \epsilon + k_0^{-2} [\epsilon''(z)/2\epsilon - (\epsilon'(z)/\epsilon)^2], \quad r(z) = (\epsilon'(z)/2\epsilon)^2 \quad (4)$$

The WKB solution (3), satisfying the condition  $F \rightarrow 0$  at  $z \rightarrow +\infty$

( $\varepsilon \rightarrow -\infty$ ) was found in [2] by going around the zeros of  $q(z)$  in the upper half-plane  $z$ . It was assumed that the zeros of  $q(z)$  are isolated and that the Stokes constant  $T = 1$  was used (for discussion on this question see Ref. [2]). It should be mentioned that the free term coefficient presentation of Eqn. (3) in the form of Eqn. (4) ensures the application of the WKB solution in the vicinity of the  $\varepsilon$ -zero.

The final result is

$$U(z) = \sqrt{\varepsilon} F_2(z) + iR_E \sqrt{\varepsilon} F_1(z), \quad (5)$$

where

$$F_k^m = q^{-1/4} \exp((-1)^{k-1} i k_0 \int_{z_m}^z \sqrt{q} dz), \quad (6)$$

$z_m$  - zeros of function  $q(z)$ ,

$$R_E = 1 + \exp(-2ik_0 \int_{z_1}^{z_2} \sqrt{q} dz). \quad (7)$$

In nondissipative plasma point  $z_1$  lies in real axis  $z$ , point  $z_2$  - in upper half-plane  $z$  (disposition of the zeros of the function  $q(z)$ , and the Stokes and anti-Stokes lines for the Eqn. (3) see in Ref. [2]). The WKB solution (5) defines the magnetic field structure of the E-wave in the transparent region and can be interpreted in terms of the MGO as the magnetic field of E-wave (E-ray) in a medium with effective permittivity  $\varepsilon_{ef}$  (see Eqn. (4)).  $R_0 = iR_E$  can be interpreted as the reflection coefficient of the wave running to the turning point  $z_1$ . For a plane wave, the turning point position coincides with the caustic.

It is shown for the linear dependence of  $\varepsilon$  that  $|R_E| = 1$  for  $\theta = 0$  and  $|R_E| < 1$  for  $\theta \neq 0$ . Thus, solution (5) takes into account the effect of resonant attenuation in the vicinity of the  $\varepsilon$ -zero [2]. The WKB solution (5) for the E-wave magnetic field gives a physical interpretation and a fairly good accuracy of the E-wave field; it yields WKB reflection coefficient calculations which are better than the accuracy of approximations suggested in another papers (see reference in [1,2]). Standard GO gives a big error in this region, on condition  $(k_0/\nabla\varepsilon)^{2/3} h^2 < 2$ .

#### RADIATION OF THE MAGNETIC CURRENT FILAMENT IN PLANE-STRATIFIED PLASMA

The next step in the MGO construction is the analysis of magnetic current filament radiation in a plane-stratified plasma with  $\varepsilon(z)$  varying monotonically in  $z$ .

Let the magnetic current filament  $J_x^M = I_x \delta(z-z_0) \delta(y=0), z_0 < 0$  be placed in a free space near the plasma half-space ( $z > 0$ ). The magnetic field structure inside the plasma is determined by integral

$$H_x = \int_{-\infty}^{\infty} \frac{U(x, z)}{\sqrt{k_0^2 - x^2}} \exp(-ixy + i \sqrt{k_0^2 - x^2} z_0) dx, \quad (8)$$

For evaluation (8), we employ the solution (5), assuming the slow dependence  $R_E(x)$ . Then the asymptotic evaluation (8) gives, by the stationary phase method, the following expression for the field in



the medium

$$H_x \approx A \sqrt{\frac{2\pi\epsilon}{|\Psi''_{1z\alpha}|}} \left[ (1-h^2)(\epsilon_{ef}-h^2) \right]^{-1/4} \exp(-i\Psi_1(z,y,\alpha) + i\pi/4) + A \sqrt{\frac{2\pi\epsilon}{|\Psi''_{2z\alpha}|}} R_r \left[ (1-h^2)(\epsilon_{ef}-h^2) \right]^{1/4} \exp(-i\Psi_2(z,y,\alpha) + i\pi/2 - i\pi/4 \text{sign}(\Psi''_{2z\alpha})) \quad (9)$$

where  $A = -I_x / 4\pi\sqrt{\mu_0/\epsilon_0}$ ,

$$\Psi_{1,2} = k_0 \phi = -k_0 \int_0^{z_1} \sqrt{1-h^2} dz + k_0 \int_0^{z_1} \sqrt{\epsilon_{ef}-h^2} dz \pm k_0 \int_z^{z_1} \sqrt{\epsilon_{ef}-h^2} dz + \alpha y,$$

$h = \alpha/k_0$ ,  $R_r$  is defined in Eqn. (7),  $\alpha$  and  $h$  in (9) relate to real (in absence of collisions) points of stationary phase.

Magnetic current filament radiation analysis shows that the reflected (inside media) ray amplitude and phase change at the turning point  $z_1$ , as opposed to the standard GO where they are continuous at the turning point. Moreover, the reflected field phase change by  $\pi/2$ , when the ray touches the caustic, as in standard GO.

MGO permits finding new physical peculiarities of the magnetic field radiated by magnetic current filament, as compared with the electric field radiated by an electric current filament. Inside the media, the reflected E-ray amplitude depends on two factors. The first one is the E-rays diverge. This effect is less pronounced for media with monotonic decrease in  $\epsilon$ , as compared to H-rays described by standard GO. The second factor is the effect of the E-wave resonant attenuation in the region  $\epsilon \approx 0$ . In the far zone the divergence of E- and H-rays reflected from plane-stratified plasma is not diminished. Thus the difference between the amplitudes of E- and H-rays is defined only by  $|R_r|$ .

#### MODIFICATION OF GEOMETRICAL OPTICS FOR THREE-DIMENSIONALLY INHOMOGENEOUS PLASMA WITH AN OVERDENSE CORE.

Here we construct MGO on the basis of solutions to two problems (i.e., that of plane E-wave propagation, and that of magnetic current filament radiation in a plane-stratified plasma).

Let the electric and magnetic fields in the inhomogeneous plasma be written in the following form

$$\vec{E} = \vec{A} \exp(-ik_0 \phi_H) + (ik_0 \epsilon)^{-1} \text{rot}(\sqrt{\epsilon} \vec{B} \exp(-ik_0 \phi_E))$$

$$\vec{H} = \frac{i}{k_0} \text{rot}(\vec{A} \exp(-ik_0 \phi_H) + \sqrt{\epsilon} \vec{B} \exp(-ik_0 \phi_E)), \quad (10)$$

where vector amplitudes  $\vec{A}$  and  $\vec{B}$  are expressed by the series

$$\vec{A} = \sum_{m=0}^{\infty} \frac{\vec{A}_m}{(ik_0)^m}, \quad \vec{B} = \sum_{m=0}^{\infty} \frac{\vec{B}_m}{(ik_0)^m}.$$

The first terms in Eqn. (10) are related to H-ray fields defined in the zero approximation by the condition  $(\vec{A}_0 \nabla \epsilon \neq 0)$ . The second terms are related to E-ray fields defined by condition  $(\vec{B}_0 \nabla \epsilon \neq 0)$ . The



supposition of independence of E and H fields in the zero approximation ( $m=0$ ) is justified locally, in vicinity of the point  $\vec{r}_0$ , on distance  $L_N \sim |\epsilon/\nabla\epsilon|$  under condition  $L_N \ll L_r$  where  $L_r$  is radius of torsion of ray. After substitution Eqn. (10) into Maxwell's equations, we use the expansions  $\vec{A}$  and  $\vec{B}$  in a power series in  $k_0^{-1}$  and obtain the standard eiconal and transport equations for H-ray fields. For E-ray fields the eiconal equation is postulated in the form

$$(\nabla\phi_r)^2 = \epsilon_{ef}(\vec{r}) = \epsilon(\vec{r}) + \frac{\Delta\epsilon}{2k_0^2\epsilon} - \left[ \frac{\nabla\epsilon}{k_0\epsilon} \right]^2, \quad (11)$$

where the dependence  $\epsilon_{ef}$  is introduced by analogy with the plane-stratified medium [2]. The transport equations for  $\vec{A}_0$  and  $\vec{B}_0$  have a standard form.

The effect of the E-field's resonant attenuation in the region  $\epsilon \approx 0$  is taken into account by introduction of reflection coefficient for the E-ray which has gone through the turning point. The condition for this ray is  $\vec{B}_{02} = R_E \vec{B}_{01}$ , where  $\vec{B}_{01}$  is the amplitude of the ray branch going to the turning point  $z_1$ , and  $\vec{B}_{02}$  is the amplitude on the ray branch leaving  $z_1$ .  $R_E$  is defined in Eqn. (7), where  $z_1$  and  $z_2$  are the coordinates of the turning points in the local Cartesian coordinates for the linear approximation  $\epsilon(\vec{r}) = \epsilon'(0)z$  in the vicinity of the turning point  $z_1$  (see Fig.1), and  $h$  is the value  $(\nabla\phi_r)^2$  of the turning point  $z_1$ . Coordinates  $z_1$  and  $z_2$  are defined in absence of collisions by conditions  $\text{Im } z_1 = 0$ ,  $\text{Im } z_2 > 0$ , the axis  $z$  is directed into the region  $\epsilon < 0$ . If the linear approximation  $\epsilon$  is unacceptable, then  $R_E$  is calculated by numerical methods.

Consider some aspects of the plane wave diffraction on inhomogeneous plasma bodies of the finite dimensions. In contrast to plane-stratified medium divergence of the E- and H-rays reflected from a finite dimension, plasma bodies can be considerably distinguished in the far zone. The divergence of the E-rays is less than that of the H-rays because  $|\nabla\epsilon_{ef}| > |\nabla\epsilon|$  and  $r_{10} > r_0$ . (The effective overdenance core radius  $r_{10}$  and the overdenance core radius  $r_0$  are defined by equations  $\epsilon_{ef}(r_{10})=0$  and  $\epsilon(r_0)=0$ , respectively). In accordance with this conclusion the bistatic cross-section near backscattering direction (when the resonant attenuation in region  $\epsilon \approx 0$  is neglected) is greater for E-rays than for H-rays. Some example see in Ref.[1].

#### REFERENCE

1. Krestyaninov S.V., Lebedev A.M., Permyakov V.A., Yakushkin I.G. Modified geometrical optics and diffraction effects at the electromagnetic scattering by an inhomogeneous plasma. Electromagnetics, 1992. V.12. N 1, P. 93.
2. Permyakov V.A., Yakushkin I.G. On analytic description of the E wave reflection in bounded smoothly inhomogeneous cold plasma, Fisika plazmy, 1988, V.14, N.8, P.943. (in Russian).

# EFFECTIVE NUMERICAL PROCEDURES FOR EVALUATION OF H AND E-WAVE DIFFRACTION ON THE TWO-DIMENSIONALLY INHOMOGENEOUS PLASMA CYLINDER.

Valeriy A. Permyakov, Andrey M. Lebedev

Department of Radio Engineering, Moscow Power Engineering Institute, Krasnokazarmennaya, 14, Moscow, 111250, Russia

## ABSTRACT

Numerical procedures based on finite element method, decomposition of scatterer and round of field peculiarity in complex space are discussed. Physical results obtained are reported.

## INTRODUCTION

Plasma objects, both artificial and natural, are often stretched in a direction, in which their parameters are changing slowly, but a media is substantially two-dimensionally inhomogeneous in the cross-section plane. We would mention here streams of jet engine and meteors trails at the height about 100 km, anisotropically extending in the Earth magnetic field. Scattering properties research for such objects represents the foundation for many applications such as a discovery and diagnostics, radio communication using plasma objects.

Consideration of two - dimensional model is a reasonable choice. In fact when finite element method is used the time of problem's decision rises as  $10(R/h)$  in one-dimensional case, and much more faster in multi-dimensional cases: proportionally to  $(R/h)^4$  in two- or  $(R/h)^7$  in three-dimensional case, there  $R$  is the radius of containing surface,  $h$  is the discretization step. It's possible using 386 processor based computer to solve in the same time about four hours one-dimensional problem with  $R/h \sim 10^7$  (up to one million wavelengths over diameter in dielectric supposing 30 steps per wavelength) or two-dimensional problem with  $R/h \sim 100$  (7 wavelengths) or three-dimensional problem with  $R/h \sim 10$  (less than one wavelength). Two-dimensional model permits, firstly, to investigate scattering regularities in more realistic situations as regards to one-dimensional inhomogeneous cylinder, and, secondly, to compare the calculation results for strict numerical and approximate optics methods.

Let plasma cylinder has permittivity  $\epsilon(r, \varphi) = \epsilon' - i\epsilon''$ . The fall along  $X$  axis of  $H$ -wave ( $\nabla \epsilon \cdot \vec{E} = 0$ ) and  $E$ -wave ( $\nabla \epsilon \cdot \vec{H} = 0$ ) is considered. Plasma may has negative kernel, i.e. the region with  $\epsilon' < 0$ . It's supposed that  $\epsilon'' \geq 0$ , the loses may be of any level including evanescently little.

It's known that for  $E$ -wave in plasma with low loses field components are changing in complex manner in the vicinity of  $\epsilon'$  transition through zero [1]. It's physically caused by plasma oscillations excitation and mathematically connected with presence of  $E$ -field peculiarity on  $\epsilon = 0$  curve, which is situated in the complex coordinates space. For low loses the peculiarity curve is passing closely to the plane of cross-section real coordinates - for peculiarity curve  $\xi \approx 1 - \frac{S}{\nabla \epsilon'} = iL_{\epsilon}$ , where  $\xi$  axis is oriented in  $\nabla \epsilon'$ .

direction,  $\xi=0$  when  $\varepsilon'=0$ ,  $S=\frac{\nu_e}{\omega}$  is the losses level,  $\nu_e$  is the frequency of electron collisions with heavy particles. In the vicinity of peculiarity the mesh step has to be less or order than  $L_E$ .

So far as the time of region counting up is proportional to  $\frac{1}{h^4}$ , thus the losses in common with scatterer size determines the possibility to get numerical decision under the  $\varepsilon'(r, \varphi)$  function has been settled.

## NUMERICAL PROCEDURES

Method of finite elements (MFE) used in current work has some preferences. Firstly it's characterized with sparse matrix of coefficients. Secondly it has been developed for nonregular mesh. thirdly it fits to take into account inhomogeneous parameters of media and, if necessary, complex borders of objects.

Special methods have been used to improve effectiveness of numerical procedures. Firstly the scatterer decomposition into a series of cylindrical lays is carrying out because computer reserves consumption is reduced since the dimension of sequently solved problems is diminished [2]. The time of decision rises as  $(R/h)^{7/2}$ , and for 100 knots per radius it takes a quarter of time compared to decision without decomposition. Required storage capacity rises as  $(R/h)^2$  as regards to  $(R/h)^3$  without decomposition. For  $(R/h) \sim 100$  the economy of memory is about 2 orders, the consumption is less than 1Mb. Secondly the task of getting numerical decision without reducing mesh step in E-wave case while losses are low is solved here using peculiarity round in complex space. This means the cylinder cross - section bend in complex plane with the aim to go away from peculiarity curve.

Analogous to [3], field in cylindrical lay is decayed over the previously found series of wave equation decisions for linearly independent border conditions of Dirichle or Neyman. This equation taken for "z" field components, is solved using MFE. Note that the second tangential to border component  $H_\tau$  or  $E_\tau$  is proportional to partial derivation of "z" field component with respect to border normal. This permits to characterize separate regions through impedance or admittance matrices. Recomposing is executed in ordinary way.

Pyramidal basis-weighting functions were used in projection scheme. Functions are connected to the knot of triangular mesh and differ from zero only at finite elements having knot as a vertex.

Let previously mentioned  $\xi = \xi' + i\xi''$  axis is described by equation  $Y = kX + q$ ,  $k = \tan \psi$  and  $q$  are real. So  $\xi$  reflects on imagine coordinates plane as an axis  $\xi''$  going through the source of coordinates under the angle  $\psi$ .

We gave imaginary additions to coordinates of cross - section points according to  $\Delta r''(\Delta r')$  with respect to certain point, say C, inside negative kernel, not coincident with the source of coordinates. It's enough for vertex kernels. For kernels having parts with difference between inclination  $\psi$  angle and angle of observation from point C more than  $\pi/2$  on the real coordinates plane, such a simple way of giving additions to coordinates is unacceptable, because it leads not to removal, but to approaching of cross - section and  $\varepsilon=0$  curve. Then it's necessary to give additions to coordinates of points near kernel border in more

accurate way: to add imaginary coordinates in a direction of  $(-\xi)$  growing.

Dependencies of  $X$  and  $Y$  from  $X'$  and  $Y'$  were approached with the help of the same pyramidal functions. For integration over cross - section

$$\int_{\Omega} F(X,Y) dX dY = \int_{\Omega'} F(X',Y') \det J dX' dY' ,$$

was used, where  $J$  is Jacobian of coordinates transformation.

According to numerical experiments, for obtaining satisfactory accuracy it's necessary to remove cross - section from peculiarity curve on a relatively little distance about or more than a half of used mesh step.

## PHYSICAL RESULTS

Diffraction on radially inhomogeneous plasma cylinders with Gaussian electrons distribution  $\varepsilon = 1 - B \cdot (1 + iS) \cdot \exp(-r^2/r_t^2)$  was investigated in connection with meteors trails scattering research. Here  $r_t$  is a characteristic size of plasma cylinder,

$$4 \cdot r_e \cdot \alpha$$

$B = \frac{r_e^2}{r_t^2}$ ,  $r_e$  is classical electron radius,  $\alpha$  is linear electrons density [1]. In [4] for wide range of parameters  $r_t = (0.4 + 4)$  and

$\alpha = (10^{11} + 10^{13}) \text{ cm}^{-1}$ ,  $S = 0.1$  and  $0.01$  back - scattering coefficients

$\hat{\sigma} = \frac{\sqrt{\sigma(0)}}{2}$  have been given for  $H$  and  $E$ -waves, here  $\sigma(\varphi)$  is the

scattering cross section of cylinder. Widely known dipole resonance of internal field in homogeneous elliptical cylinder placed in a field of relatively low frequency perpendicular to  $E$  vector plane, is connected with plasma waves excitation. The resonance displays itself in rising of polarization relation  $\hat{\sigma}_E / \hat{\sigma}_H$ . For radially one- and two-dimensionally inhomogeneous cylinder the resonance is weakened because the field absorption in the  $\varepsilon \approx 0$  region. The rising of polarization relation was reported in [4], but no more than to 2.

Calculations for plasma cylinders with elliptical level's lines flattened or stretched along  $Y$  axis were conducted. For  $\varepsilon = 1 - B \cdot (1 + iS) \cdot \exp[-(x^2 + \delta \cdot y^2)/r_t^2]$   $r_t = 0.6$  was chosen, which means that negative kernel size in wave fall direction is much less than wavelength. Also  $\alpha = (10^{11} + 10^{13}) \text{ cm}^{-1}$ , hence  $B = (0.3 + 30)$ ,  $S = 0.01$  and  $\delta = 9$ ,  $\delta = 1$ , or  $\delta = 1/9$  were taken. The calculated back - scattering coefficients for two polarizations vs  $\alpha$  are represented on Fig. 1a. The polarization relation vs  $\alpha$  is shown on Fig. 1b. The back - scattering coefficients decrease for flattened ( $\delta = 9$ ) and increase for stretched ( $\delta = 1/9$ ) cylinders as compared to radially inhomogeneous cylinder, it's connected with cross size changing. The increase of back scattered field with growth of  $\alpha$  is observed. For flattened cylinder polarization relation maximum is taking place for lesser  $\alpha$  - quicker after negative kernel appearance, and oppositely for stretched cylinder maximum is shifted to greater  $\alpha$ . This is in qualitative accordance with homogeneous cylinder static

resonance consideration. Since negative kernel is closer to plane lay for  $\delta=9$  thus the resonance is more pronounced and maximum becomes greater than 2. For  $\delta=1/9$  maximum is so close to 1, that there is no sense in talking about resonance manifestation.

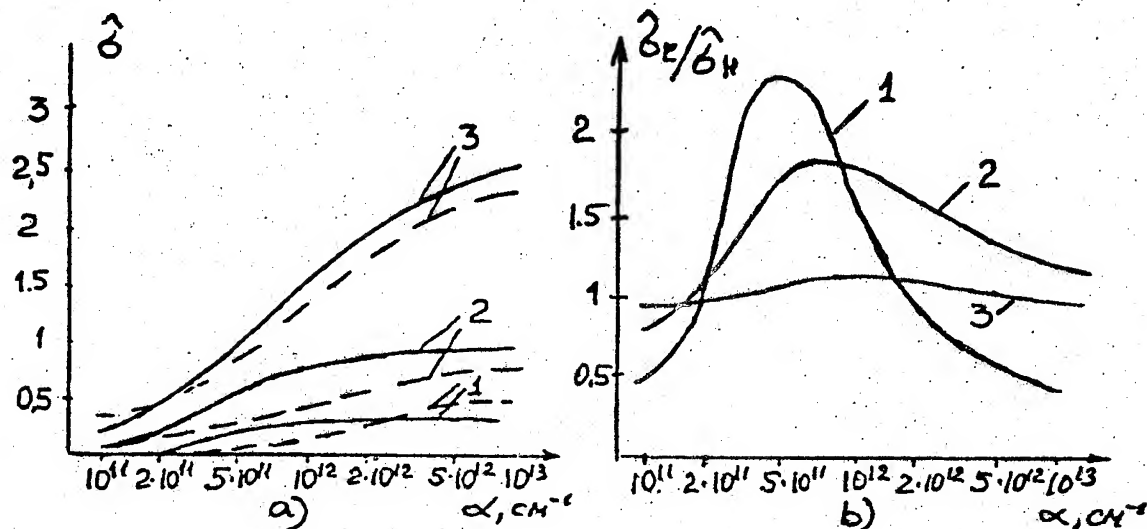


Fig.1. Back-scattering coefficients (a) and polarization relation (b) vs linear electrons density for H and E-waves (stroked and solid lines). Curves 1 - 3 are for  $\delta=9$ ; 1;  $1/9$ .

Developed procedures permits to estimate the limits of applicability for geometrical optics (H-wave case) and modified geometrical optics (E-wave case) [5] so as it's discussed in [6].

## REFERENCES

- [1] V.L. Ginsburg: "Propagation of electromagnetic waves in plasma", New York: Gordon and Breach, 1961.
- [2] A.M. Lebedev, V.A. Permyakov: "Usage of optimal decomposition into lays and finite element method for solving the problems of diffraction on the extended two-dimensionally inhomogeneous objects", Taganrog: Electromagnetic waves scattering (1991), vol. 8, pp. 24-28.
- [3] S.-K.Chang, K.Mei: "Application of the unimoment method to electromagnetic scattering of dielectric cylinders", Trans.IEEE (1976), AP-24, pp.35-42.
- [4] U.V.Chumak, R.I.Moysia. "Scattering of radiowaves by plasma cylinder", Izv. vuzov. Radio physics (1977), vol.20, pp.51-...
- [5] V.A. Permyakov, S.V. Krestyaninov: "Modified geometrical optics for an inhomogeneous isotropic plasma", MMET-94.
- [6] S.V. Krestyaninov, A.M. Lebedev, V.A. Permyakov: "Diffraction effects at the electromagnetic scattering by an inhomogeneous plasma", MMET-94.

# FROM FUNCTIONAL ANALYSIS TO THE METHOD OF FICTITIOUS SOURCES IN E. M. DIFFRACTION

by R. PETIT

Laboratoire d'Optique Electromagnétique, U.R.A. CNRS n° 843  
Faculté des Sciences de St-Jérôme, Case 262, 13397 Marseille Cedex 20, France

## ABSTRACT

We first recall that the Method of Fictitious Sources is not only an efficient numerical recipe but, on the contrary, an algorithm whose convergence can be established on a sound theoretical basis. We also report on some recent practical applications.

## 1. INTRODUCTION

I have been very honoured with your invitation to this meeting devoted to Mathematical Methods in Electromagnetic Theory. I thought it was probably for me a good opportunity to get in touch with numerous colleagues that we have not been able to meet during a very long time. One of the problems I had to solve was to find a subject for this invited paper. The Chairman (E.I. Veliev) suggested to present a paper based on my recent research ... or on other appropriate topics. Most of this audience is probably waiting for a review paper on relatively recent and broad topics. Such a paper requires from the author to quote an important list of recent publications. Unfortunately, I have to confess that I have no gift for an exhaustive bibliographical research... Consequently I decided to summarize the work carried out in our Laboratory concerning what we call the Method of Fictitious Sources (M.F.S.), an approach to diffraction problems which has become as important as integral, differential, modal and finite element methods. As a consequence, most of what follows has already been published. But the papers devoted to pioneering works are not always very clear ; they are often written to have a prior claim and consequently the didactic aspect is sometimes somewhat neglected. Moreover, very often it appears that, on further consideration, the contents of several papers can be presented in a more concise and unified manner through the help of some leading idea. I will be satisfied if this paper allows my colleagues (and mainly those of the former Soviet Union) to have an idea of what has been done in the "Laboratoire d'Optique Electromagnétique de Marseille", concerning the theoretical aspects of the M.F.S.

We will only deal with time harmonic field and cylindrical diffracting obstacles (rods and gratings). The electrical and magnetic fields will be represented by the complex vectors  $\vec{E}$  and  $\vec{H}$  taking into account a time dependance in  $\exp(-i\omega t)$ . An homogeneous medium will be characterized by its permittivity  $\epsilon$ , its permeability  $\mu$ , and  $k^2 \stackrel{\text{def}}{=} \epsilon \mu \omega^2$ . As we did in all our previous papers, I will assume that all the media have the permittivity  $\mu_0$  of a vacuum. For a metal, it will be always understood that the conductivity has been included in the permittivity and, consequently, the complex optical index  $v$  will be defined as the square root of the ratio of the permittivity  $\epsilon$  to the permittivity  $\epsilon_0$  of a vacuum. Starting with a simple scalar problem, we will arrive, step by step, to rather complicated problems. For example, we will say a few words about the diffraction by a dielectric (or metallic) grating illuminated by a plane wave whose the incident vector is not perpendicular to the grooves (conical diffraction).



Before diving into mathematics, maybe it is useful to remind briefly the physicists<sup>1</sup> of the basic idea of the M.F.S. Let us therefore consider an obstacle whose boundary is a closed surface  $S$ . We call respectively  $\Omega_1$  and  $\Omega_2$  the exterior and the interior of  $S$ . These two regions are respectively filled with homogeneous and isotropic materials 1 ( $\epsilon_1, \mu_0$ ) and 2 ( $\epsilon_2, \mu_0$ ). The obstacle is illuminated by a known incident field  $\vec{E}^{inc}, \vec{H}^{inc}$  and we look for the total field  $\vec{E}, \vec{H}$ . In  $\Omega_2$  the total field must satisfy the Maxwell equations in medium 2 ( $\epsilon_2, \mu_0$ ); therefore, we can hope it can be considered as radiated by adequate fictitious sources (charges and currents) located in region  $\Omega_1$  but radiating in the whole space filled with material 2 ( $\epsilon_2, \mu_0$ ). In the same way, we can hope that in  $\Omega_1$  the diffracted field (which must satisfy a radiation condition) can be generated by some fictitious sources located in  $\Omega_2$  and radiating in the whole space filled with material 1 ( $\epsilon_1, \mu_0$ ). The problem is now how to determine the nature and the location of the adequate fictitious sources. Of course, this must be done in such a way that the so-called boundary conditions be satisfied: i.e., for  $\vec{E}$ , and  $\vec{H}$  as well, the tangential components must have no jump on  $S$ . The idea, which in some sense appears as a generalization of Huygens' Principle, is certainly seductive but a question immediately comes to our mind. If, for numerical purposes, we take only a finite number of fictitious sources, will it be possible to satisfy rigorously the boundary conditions? Intuitively we are led to give a negative answer; we guess that we will have to be content with imposing only approximate boundary conditions, obtaining thus an approximate solution. Depending on the precise meaning of approximate (when speaking of approximate boundary conditions), we have to discuss (from a mathematical point of view) the quality of the associated approximate solution, and to prove that it tends to the exact solution of the physical problem. This is indeed an ambitious research programme ... we cannot manage it without the help of functional analysis.

## 2 - DIFFRACTION BY A ROD : THE SCALAR PROBLEM

### 2.1. Notations.

Let us now consider (fig. 1) a cylindrical rod whose generatrices are parallel to the  $z$  axis and whose cross section is the interior  $\Omega_2$  of the closed curve  $\Gamma$ . We denote by  $\Omega_1$  the exterior of  $\Gamma$ . The regions  $\Omega_1$  and  $\Omega_2$  are respectively filled with a material characterized by  $k_1$  and  $k_2$ . The constant  $k_1$  is real but, to skip over some theoretical complications,  $k_2$  is assumed to be a complex number whose imaginary part is strictly positive.<sup>2</sup> We assume that the electric field is linearly polarized in a parallel direction to the  $z$  axis and depends only on  $x$  and  $y$ . Consequently the total (electric) field, and the known incident field as well, can be described by only one scalar function (namely their  $z$ -component) that we call respectively  $U(x,y)$  and  $U^{inc}(x,y)$ .

### 2.2. The field representation.

The total field  $U$  we are looking for, will be represented by an ordered pair of functions  $u$  and  $v$ , defined on  $\Gamma$  as follows:  $u$  is the restriction of  $U$  to  $\Gamma$ , and  $v$  is the normal derivative  $\partial_n U$  of  $U$  on  $\Gamma$ . The pair will be denoted by  $F$  (the first letter of field). With usual notation we have therefore:

<sup>1</sup> Using their own language and without more or less esoteric mathematical words.

<sup>2</sup> From the practical point of view, this restriction is not essential; see section 2.7

$$(1) \quad u = U|_{\Gamma}, \quad v = \partial_n U \text{ or } D_{\Gamma} U, \quad F = (u, v).$$

It must be noticed that  $U(x, y)$  is a function defined on  $\mathbb{R}^2$  whereas  $u, v$  and  $F$  are functions of one variable (the curvilinear abscissa  $\ell$  or some other parameter) defined on the curve  $\Gamma$ . Functions  $u$  and  $v$  are **unambiguously defined** because, due to the boundary conditions,  $U$  is continuous and its normal derivative has not jump on  $\Gamma$ .

Similarly, a known and unambiguously defined pair  $F^{\text{inc}}$  can be associated to the incident field  $U^{\text{inc}}$ :

$$(2) \quad F^{\text{inc}} = (u^{\text{inc}}, v^{\text{inc}}), \quad u^{\text{inc}} = U^{\text{inc}}|_{\Gamma}, \quad v^{\text{inc}} = D_{\Gamma} U^{\text{inc}}.$$

It must be emphasized that  $F$  is a good representation of  $U(x, y)$  in the following sense: if  $F$  is known, we know  $U|_{\Gamma}$  and  $D_{\Gamma} U$ , which allows us to compute  $U$  everywhere in  $\Omega_2$  using the Kirchhoff-Helmholtz formula. But, because  $F^{\text{inc}}$  is given, we also know the value of the diffracted field<sup>3</sup> and its normal derivative on  $\Gamma$ , which allows us to compute this out-going field<sup>4</sup> in  $\Omega_1$ , using again the Kirchhoff-Helmholtz formula (K.H. formula). In other words, as soon as  $F$  is known, the diffraction problem is reduced to standard computations requiring only a good computer code for Hankel functions.

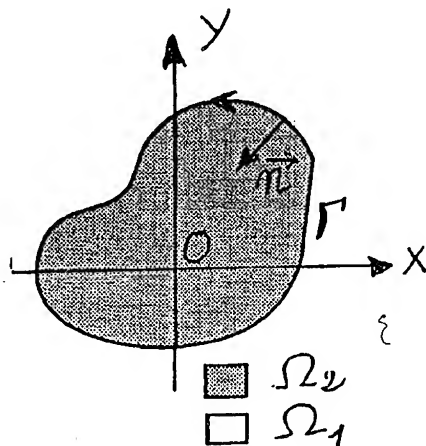


**Fig. 1.**  $\Omega_2$  is bounded but  $\Omega_1$  is not. The arrow gives the conventional direction of the tangent unit vector  $\vec{t}$ . The normal unit vector  $\vec{n} = \vec{e}_z \wedge \vec{t}$  points towards  $\Omega_2$ .

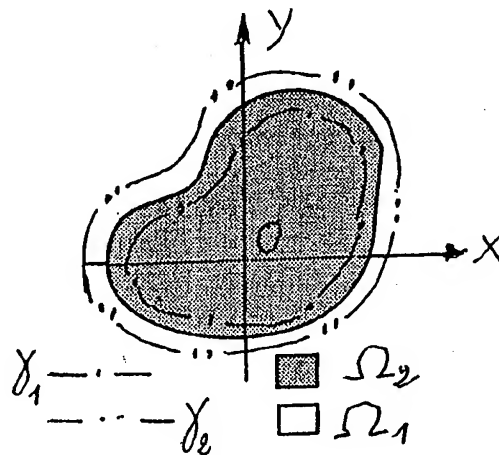


**Fig. 2.** Example of curves  $\gamma_1$  and  $\gamma_2$  on which we can put the fictitious sources.

Let us now make some further comments about functions  $u$  and  $v$ . A physicist will certainly agree that the diffraction problem we are dealing with has one and only one solution. On the contrary, a mathematician cannot discuss existence and uniqueness without knowing in what function space he has to find a solution. It seems judicious to require that the solution belong to  $H_{\text{loc}}^1(\mathbb{R}^2, \Delta)$  in order to be able to define an electromagnetic energy.<sup>5</sup> Under this requirement, existence and uniqueness are established and it can be shown that  $u$  and  $v$  necessarily belong respectively to the Sobolev spaces  $H^{1/2}(\Gamma)$  and  $H^{-1/2}(\Gamma)$ . Unfortunately, and from the numerical point of view, the scalar products associated to these spaces are not easy to handle ... But the mathematicians [1] also say that provided  $\Gamma$  is sufficiently regular (class  $C^2$  for example),

<sup>3</sup> defined in  $\Omega_1$  as  $U - U^{\text{inc}}$ .

<sup>4</sup> a field satisfying the Sommerfeld radiation condition.

<sup>5</sup>  $H_{\text{loc}}^1(\mathbb{R}^2, \Delta)$  is the space of functions  $f$  such that  $f$  and  $\Delta f$  belongs to  $H_{\text{loc}}^1(\mathbb{R}^2)$ .



and if the solution is required to belong to  $H_{loc}^{3/2}(R^2)$ , then  $u$  and  $v$  necessarily belong respectively to  $H^1(\Gamma)$  and  $H^0(\Gamma)$ . Notice that  $H^0(\Gamma)$  is nothing but the familiar space  $L^2(\Gamma)$ . In other words, and from now on, we will assume, in all our theoretical considerations, that  $\Gamma$  is a  $C^2$  curve and that the total field  $U(x,y)$  is somewhat more regular than it should be to only ensure the existence of the electromagnetic energy. Correlatively we will claim that  $u$  and  $v$  respectively belongs to  $H^1(\Gamma)$  and  $L^2(\Gamma)$ .<sup>6</sup> Clearly this proposition also holds for  $u^{inc}$  and  $v^{inc}$ , since the incident field  $U^{inc}(x,y)$  is indefinitely differentiable.

### 2.3. Some function spaces and their fundamental properties.

We call  $\mathcal{V}$  the vector space whose elements  $\phi$  are pairs of functions  $u$  and  $v$  defined on  $\Gamma$  and such that  $u \in H^1(\Gamma)$  and  $v \in L^2(\Gamma)$ . In other words  $\mathcal{V} = H^1(\Gamma) \times L^2(\Gamma)$ . Space  $\mathcal{V}$  is endowed with a scalar product  $(\cdot, \cdot)_{\mathcal{V}}$  inducing a norm  $\|\cdot\|_{\mathcal{V}}$ . If  $\partial_t$  and  $\partial_n$  denote respectively the tangential and normal derivatives on  $\Gamma$ :

$$(3) \quad (\phi_1 | \phi_2)_{\mathcal{V}} \stackrel{\text{def}}{=} a_1 \int_{\Gamma} u_1 \overline{u_2} d\ell + a_2 \int_{\Gamma} \partial_t u_1 \partial_t \overline{u_2} d\ell + a_3 \int_{\Gamma} \partial_n v_1 \partial_n \overline{v_2} d\ell, \quad \|\phi\|_{\mathcal{V}} \stackrel{\text{def}}{=} (\phi | \phi)_{\mathcal{V}}$$

It is of course recommended to choose the positive numbers  $a_1, a_2, a_3$  in such a way that the three terms appearing in the right side of (3) have the same dimension; as for their numerical values, it is a matter of numerical optimization.

For what follows it is convenient to introduce two subspaces of  $\mathcal{V}$ , denoted by  $\mathcal{V}_1$  and  $\mathcal{V}_2$ . A pair  $\phi = (u, v)$  is said to be element of  $\mathcal{V}_2$  if there exists a function, defined and continuous in  $\Omega_2 \cup \Gamma$ , and such that:

$$a) \quad \Delta f + k_2^2 f = 0 \text{ in } \Omega_2, \quad b) \quad u = f|_{\Gamma}, \quad v = D_{\Gamma} f.$$

Briefly we can say that  $u$  and  $v$  must be "the boundary values on  $\Gamma$ " of a two variable function satisfying the Helmholtz equation in  $\Omega_2$ .

Subspace  $\mathcal{V}_1$  is defined in a similar way replacing  $\Omega_2$  by  $\Omega_1$  and  $k_2$  by  $k_1$ ; but, because  $\Omega_1$  is unbounded, we moreover require  $f$  to satisfy the Sommerfeld radiation condition.

Clearly, if  $f(x,y)$  is looked on as the  $z$  component of an electric field, then  $v$  can be interpreted (within a multiplicative constant) as the tangential component of the associated magnetic field. Anyway, and as pointed out in [3], we can attach<sup>7</sup> to each of the  $\mathcal{V}_j$  ( $j=1,2$ ) an impedance operator  $Z_j$  and an admittance operator  $Y_j$  defined by:

$$(4) \quad v = Y_j u, \quad u = Z_j v.$$

Referring to Cessenat's work [4,2], these operators, also often called capacity operators, have an extremely important property. They are inverse of each other and they are both linear and continuous. It must be emphasized that the continuity (that will play an essential role subsequently) could not be established assuming that  $u$  belongs to  $L^2(\Gamma)$  rather than to  $H^1(\Gamma)$ . Of course, since we speak of continuity,  $\mathcal{V}_1$  and  $\mathcal{V}_2$  must be topological spaces. For each of them, we have to define what we mean when we say that a

<sup>6</sup>  $H^1(\Gamma)$  is the Sobolev space of functions which are square integrable on  $\Gamma$ , as well as their generalized first derivative.

<sup>7</sup> This is to ensure the existence of these operators that we required  $k_2$  not to be real

sequence of functions tends to zero. We will say that  $\phi_n \rightarrow 0$  in  $\mathcal{Y}_j$  if  $\|\phi_n\|_{\mathcal{Y}} \rightarrow 0$ . In other words, we will use on  $\mathcal{Y}_j$  the topology induced by the  $\mathcal{Y}$  topology.

As a first consequence of the continuity of the impedance and admittance operators, it is worth noting that  $\mathcal{Y}_1$  and  $\mathcal{Y}_2$  are both closed subset. As a matter of fact, let us consider a sequence of pairs  $\phi_n = (u_n, v_n)$  belonging to  $\mathcal{Y}_j$  and such that  $\lim \phi_n = \phi = (u, v)$ . Due to the continuity of  $Y_j$ ,  $\lim v_n = \lim(Y_j u_n) = Y_j u$ . Therefore  $v = Y_j u$ , which means that  $\phi \in \mathcal{Y}_j$  (QED).

Last but not the least, it can be proved that any pair  $\phi \in \mathcal{Y}$  can be decomposed into the sum of two pairs  $\phi_1$  and  $\phi_2$ , with  $\phi_1 \in \mathcal{Y}_1$  and  $\phi_2 \in \mathcal{Y}_2$ . Moreover this decomposition is unique. In other terms  $\mathcal{Y}$  is the direct sum of  $\mathcal{Y}_1$  and  $\mathcal{Y}_2$  :

$$(5) \quad \mathcal{Y} = \mathcal{Y}_1 \oplus \mathcal{Y}_2 .$$

The proof of this fundamental theorem, called hereafter theorem of the direct sum, is given in Appendix A. Referring to the specialized literature, the reader will be able to convince himself that, because  $\mathcal{Y}_1$  and  $\mathcal{Y}_2$  are closed subsets,  $\mathcal{Y}$ , as given by (5), is not only an algebraic direct sum but also a topological one. As for us, we reached this conclusion by reading the famous book by T. Kato [5].

#### 2.4. The solution of the diffraction problem.

As noted at the end of section 2.2, the known pair  $F^{inc}$  (associated to the incident field) belongs to  $\mathcal{Y}$ . This known pair  $F^{inc}$  can therefore be decomposed in a unique way as :

$$(6) \quad F^{inc} = \phi_1 + \phi_2, \quad \phi_1 \in \mathcal{Y}_1, \quad \phi_2 \in \mathcal{Y}_2 .$$

Now, it must be understood that, if this decomposition has been successfully completed, the diffraction problem can be considered as virtually solved because the pair  $\phi_2$  is nothing other than the pair  $F$  we are looking for. As a matter of fact, we can write :

$$(7) \quad F^{inc} = F^{inc} - F + F .$$

Obviously  $F^{inc} - F$  and  $F$  respectively belong to  $\mathcal{Y}_1$  and  $\mathcal{Y}_2$  and, since the decomposition of  $F^{inc}$  is unique, we get, comparing (7) with (6) :

$$(8) \quad F^{inc} - F = \phi_1 \quad \text{and} \quad F = \phi_2 \quad (\text{Q.E.D.}) .$$

The question is now how to achieve decomposition (6). There exists for that a general procedure. Let us suppose that we know a total family  $\phi_{1,n}$  in  $\mathcal{Y}_1$  and a total family  $\phi_{2,n}$  in  $\mathcal{Y}_2$ . For a fixed integer  $N$ , we consider the positif number  $\Delta_N$  defined as :

$$(9) \quad \Delta_N = \left\| F^{inc} - \sum_{n=1}^N c_{1,n} \phi_{1,n} - \sum_{n=1}^N c_{2,n} \phi_{2,n} \right\|_{\mathcal{Y}}^2$$

where the  $c_{1,n}$  and the  $c_{2,n}$  are complex coefficients. Then, using a least squares algorithm (L.S.A.), we determine those coefficients  $\bar{c}_{1,n}(N)$  and  $\bar{c}_{2,n}(N)$  that give to  $\Delta_N$  its minimal value  $\bar{\Delta}_N$ . We thus obtain approximants  $\bar{\phi}_1^N$  and  $\bar{\phi}_2^N$  for  $\phi_1$  and  $\phi_2$ , that is to say, from (8), for  $F^{inc} - F$  and  $F$  :

$$(10) \quad \bar{\phi}_1^N = \sum_{n=1}^N \bar{c}_{1,n} \phi_{1,n}, \quad \bar{\phi}_2^N = \sum_{n=1}^N \bar{c}_{2,n} \phi_{2,n} .$$

Of course, intuitively, the larger  $N$ , the better the approximation .. Mathematically speaking the procedure is convergent in the following sense :

$$(a) \quad \lim_{N \rightarrow \infty} \bar{\Delta}_N = 0, \quad (b) \quad \lim_{N \rightarrow \infty} \|\phi_j - \bar{\phi}_j^N\|_{\mathcal{V}}^2 = 0, \quad j = 1, 2$$

The last point is a consequence of the continuity of the applications  $\phi \mapsto \phi_1$  and  $\phi \mapsto \phi_2$  (namely the projection of  $\mathcal{V}$  on  $\mathcal{V}_1$  along  $\mathcal{V}_2$ , and the projection of  $\mathcal{V}$  on  $\mathcal{V}_2$  along  $\mathcal{V}_1$ ). In the book by Kato [5], this continuity is established as a consequence of the closed graph theorem. (see p. 156 and 166). Again we are rather far from elementary mathematics ...

## 2.5. Examples of total families in $\mathcal{V}_1$ and $\mathcal{V}_2$ .

In a previous paper [3], we establish the two following theorems:

**Theorem 1.** (This theorem applies if  $\Gamma$  is a  $C^2$  curve).

Let  $\gamma_1$  (resp.  $\gamma_2$ ) be a simple closed  $C^2$  curve located in  $\Omega_2$  (resp.  $\Omega_1$ ) and following the curve  $\Gamma$  at some distance (Fig. 2). Let us introduce a set of function  $s_{1,n}$  (resp.  $s_{2,n}$ ) which form a total family in  $L^2(\gamma_1)$  (resp.  $L^2(\gamma_2)$ ). For  $j = 1, 2$ , let  $e_{j,n}$  be the solution of  $\Delta e_{j,n} + k_j^2 e_{j,n} = s_{j,n} \delta_{\gamma_j}$  satisfying the radiation condition. Then the pairs  $\phi_{j,n}$  defined on  $\Gamma$  by:

$$\phi_{j,n} = \left( e_{j,n}|_{\Gamma}, D_{\Gamma} e_{j,n} \right)$$

form, for a fixed  $j$  ( $j = 1$  or  $2$ ) a total family in  $\mathcal{V}_j$ . It must be noticed that, because  $e_{j,n}$  is the field radiated by a source  $s_{j,n} \delta_{\gamma_j}$  (whose support belongs to  $\gamma_j$ ),  $e_{j,n}$  is analytic in the neighbourhood of  $\Gamma$ , which of course allows us to claim that the components of  $\phi_{j,n}$  indeed belong to  $H^1(\Gamma)$  and  $L^2(\Gamma)$ . The proof of the theorem can be found in [3]; but, because of its importance, it is given again in appendix B with only slight modifications, which I think are changes for the better.

**Theorem 2.** (This theorem applies if  $\Gamma$  is a  $C^\infty$  curve).

Curves  $\gamma_1$  and  $\gamma_2$  being defined as in theorem 1, consider a countable and dense set of points  $P_{j,n}$  on  $\gamma_j$  ( $n \in \mathbb{N}$ ). Let  $e_{j,n}(M)$  be now the solution of  $\Delta e_{j,n} + k_j^2 e_{j,n} = \delta(M - P_{j,n})$  and satisfying the radiation condition. Then the pairs  $\phi_{j,n}$  defined on  $\Gamma$  by:

$$\phi_{j,n} = \left( e_{j,n}|_{\Gamma}, D_{\Gamma} e_{j,n} \right)$$

form, for a fixed  $j$  ( $j = 1$  or  $2$ ) a total family in  $\mathcal{V}_j$ .

It must be noticed that  $e_{j,n}(M)$  is now the field radiated by a point source. Therefore,  $e_{j,n}(M)$  is nothing other than  $H_0^+(k_j R_{j,n})$ , where  $R_{j,n}$  is the distance between points  $M$  and  $P_{j,n}$ . Again one can refer to [3] for the proof which, once more, requires a good background in Mathematics. We had to make use of the famous Hahn-Banach theorem and also of the notion of total family of distributions: see appendices C, D, E in [3]. As a by-product, we got a form of the reciprocity relations that I never saw in the literature.<sup>8</sup> I cannot keep myself from giving it, although reciprocity theorems are not the subject of this paper.

**Theorem 3.** Let  $\gamma$  and  $\bar{\gamma}$  be two closed  $C^\infty$  curves which do not intersect. As usual, we denote by  $\mathcal{D}(\gamma)$  and  $\mathcal{D}(\bar{\gamma})$  the spaces of indefinitely differentiable complex functions

<sup>8</sup> which, of course, is not a proof of its originality.

respectively defined on  $\gamma$  and  $\bar{\gamma}$ . Of course  $\mathcal{D}'(\gamma)$  and  $\mathcal{D}'(\bar{\gamma})$  are the corresponding spaces of distributions. To any  $s \in \mathcal{D}'(\gamma)$  we associate  $s\delta_\gamma \in \mathcal{D}'(\mathbb{R}^2)$  :

$$\forall \psi \in \mathcal{D}(\mathbb{R}^2), \quad \langle s\delta_\gamma, \psi \rangle \stackrel{\text{def}}{=} \langle s, \psi|_\gamma \rangle, \text{ where } \psi|_\gamma \text{ denotes the restriction of } \psi \text{ to } \gamma.$$

Consider  $s \in \mathcal{D}'(\gamma)$ ,  $\bar{s} \in \mathcal{D}'(\bar{\gamma})$ ,  $u$  defined as the unique solution of  $\Delta u + k^2 u = s\delta_\gamma$  with radiation condition,  $\bar{u}$  defined as the unique solution of  $\Delta \bar{u} + k^2 \bar{u} = \bar{s}\delta_{\bar{\gamma}}$  with radiation condition. We call  $\phi$  the restriction of  $\bar{u}$  to  $\gamma$  ( $\phi = \bar{u}|_\gamma$ ) and  $\bar{\phi}$  the restriction of  $u$  to  $\bar{\gamma}$  ( $\bar{\phi} = u|_{\bar{\gamma}}$ ). We claim that  $\langle s, \phi \rangle = \langle \bar{s}, \bar{\phi} \rangle$ , where a bracket such as  $\langle s, \phi \rangle$  represents, as usual, the number associated to  $\phi \in \mathcal{D}(\gamma)$  by a distribution  $s$ ; if  $s$  is a function, this number is given by the integral  $\int_\gamma s \phi d\ell$  (See [3] for the proof).

## 2.6. The fictitious sources and the numerical recipe.

In the statement of theorem 1 (and of theorem 2 as well), the components of a pair  $\phi_{1,n}$  are the "boundary values on  $\Gamma$ " of the field  $e_{j,n}$  radiated in  $\Omega_j$  by a source<sup>9</sup>  $S_{j,n}$  located on  $\gamma_j$ . As previously explained, and using K.H. formulas, the knowledge of  $\phi_{2,n}$  (resp.  $\phi_{1,n}$ ) allows us to find the total field (resp. diffracted field) in  $\Omega_2$  (resp.  $\Omega_1$ ). But, in fact, the use of K.H. formulas is not necessary: the field associated in  $\Omega_j$  with the pair  $\phi_{j,n}$  is nothing other than the field  $e_{j,n}$  itself (since the difference of these two fields would be a field described by the null pair). As a consequence, all the theoretical and rather subtle considerations developed up to now, indeed lead to a numerical recipe very easy to understand and to implement on a computer:

Consider  $N$  sources  $S_{1,n}$  located on  $\gamma_1$  and  $N$  sources  $S_{2,n}$  located on  $\gamma_2$ . Let us call  $e_{1,n}$  (resp.  $e_{2,n}$ ) the field radiated in the whole space filled with an homogeneous material described by  $k_1$  (resp.  $k_2$ ). Then we retain as a approximant of the total field the field  $\bar{U}_N$  defined as follows :

$$(11) \quad \bar{U}_N = \begin{cases} \bar{U}_{1,N} = \sum_{n=1}^N \bar{c}_{1,n}(N) e_{1,n} + U^{\text{inc}} & \text{in } \Omega_1 \\ \bar{U}_{2,N} = \sum_{n=1}^N \bar{c}_{2,n}(N) e_{2,n} & \text{in } \Omega_2 \end{cases}$$

where  $\bar{c}_{1,n}$  and  $\bar{c}_{2,n}$  are those coefficients  $c_{1,n}$  and  $c_{2,n}$  that minimize :

$$\Delta_N = \left| F^{\text{inc}} + \sum_{n=1}^N c_{1,n} \phi_{1,n} - \sum_{n=1}^N c_{2,n} \phi_{2,n} \right|_\gamma^2.$$

Calling  $\bar{\Delta}_N$  the minimal value of  $\Delta_N$ , we can use the value of  $\bar{\Delta}_N$  as a measurement of the quality of our approximate solution (remember that  $\bar{\Delta}_N$  must decrease and tend to zero if  $N$  is going to infinity). It is worth noting that, from the classical boundary conditions,<sup>10</sup>

$\Delta_N$  would be zero if  $\sum_{n=1}^N c_{1,n} \phi_{1,n}$  and  $\sum_{n=1}^N c_{2,n} \phi_{2,n}$  were respectively replaced by the

<sup>9</sup> This source is a surface current with current density  $S_{j,n}$  in theorem 1, and a 1D wire current in theorem 2.

Up to now, in our computations,  $s_{j,n}(\ell) = \exp(i n (2\pi/L_j) \ell)$  where  $L_j$  is the length of  $\gamma_j$ .

<sup>10</sup> On  $\Gamma$ , both the field and its normal derivative have no jump.

(unknown) pair associated to the diffracted field in  $\Omega_1$  and the (unknown) pair associated with the total field in  $\Omega_2$ . We can say that minimizing  $\Delta_N$  is the means used in the M.S.F. to enforce the boundary conditions on  $\Gamma$ . The idea of expressing the boundary conditions through the minimization of a convenient norm is not new. For example, it has been intensively used in Japan (using a classical  $L^2$  norm) by K. Yasuura and his collaborators [6]. As mentioned in [7,8,9], the Yasuura method can be considered as a particular case of the M.F.S.

At this stage of the analysis, it must be emphasized that the M.F.S. reduces the diffraction problem to two canonical problems namely : (a) - the computation of the field radiated in an infinite homogeneous medium by a known distribution of current, (b) the least square problem. The former is a matter of integral calculus ; since the Green's function is known (i.e. a Hankel function), at most we have to perform a convolution product. The latter is a traditional chapter of any text book concerned with applied mathematics. Nevertheless we encountered some numerical problems when dealing with the famous Gauss normal equations ... but fortunately we benefitted from the advice given in "Solving Least Squares Problems" by C.L. Lawson and R.J. Hanson, Prentice-Hall, 1974 (Use of Householder transformation, singular value decomposition ... etc).

**Remark :** In our theoretical work, we have been especially concerned with two types of fictitious sources (see theorem 1 and 2) but, from the practical point of view, other sources can, of course, be used. Let us refer to fig. 3 and suppose we have got a satisfactory solution assuming for the diffracted field to be generated by  $N$  wires represented by  $N$  points on  $\gamma_1$ . Moreover suppose that, as shown in the figure, a certain number of points  $P_n$  (say those corresponding to  $n=1,2,\dots,N_1$ ) are in a disk  $D_1$  centered at  $C$  and contained in  $\Omega_2$ . Then, taking the origine  $O$  of the coordinate system at  $C$ , and putting  $R_n = P_n M$ ,  $CP_n = OP_n = r_n$  and  $CM = OM = r$ , we have<sup>11</sup> for  $n=1,2,\dots,N_1$ , and for any  $M \in \Omega_1$ :

$$H_0^+(k_1 R_n) = \sum_{m \in \mathbb{Z}} H_m^+(k_1 r) J_m(k_1 r_n) e^{im\theta} e^{-im\theta_n}$$

The contribution of all the points  $P_n$  located in  $D_1$  is therefore :

$$\sum_{m \in \mathbb{Z}} \left( \sum_{n=1}^{N_1} \tilde{c}_n J_m(k_1 r_n) e^{-im\theta_n} \right) H_m^+(k_1 r) e^{im\theta}$$

which can be interpreted as the field of a multipole. In other words, we can replace the  $N_1$  point-sources (monopoles) lying in  $D_1$ , by a multipole source. This remark shows there is a link between our work and the work done by C. Hafner and his collaborators at the Institute für Feldtheorie in Zurich. They used extensively the multipoles as recalled by the title of their book [10].

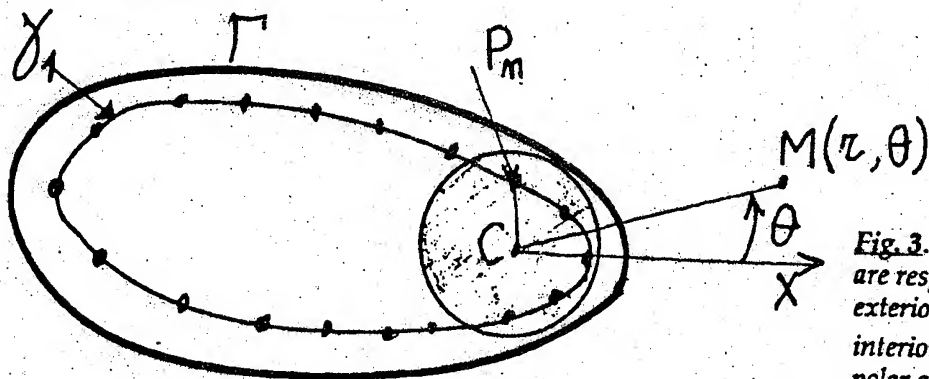


Fig. 3.  $\Omega_1$  and  $\Omega_2$  are respectively the exterior and the interior of  $\Gamma$ .  $\theta_n$  is the polar angle of  $CP_n$ .  $N=18$ ,  $N_1=5$ .

<sup>11</sup> From the "addition theorem" for Hankel functions, since  $r_n < r$ .

### 2.7. Straightforward generalizations.

If it is the magnetic field (rather than the electric field) which is parallel to the  $z$  axis, our unknown function  $U(x,y)$  must be defined as the  $z$  component of  $\vec{\mathcal{H}}$ . Then we have only to change the definition of the pairs and to make some suitable modifications in the theoretical considerations. The first component of the pair  $F$  is still  $u = U|_{\Gamma}$  but the second is now  $(\epsilon_0 / \epsilon) \partial_n U$  on  $\Gamma$ . As a rule, the components of a pair must be unambiguously defined functions ; here, and due to the boundary conditions,  $v$  has indeed the same value on both side of  $\Gamma$ .

Up to now, we assumed  $\text{Im}(k_2)$  to be strictly positive, but our conclusions still hold if  $\text{Im}(k_2)=0$ , except for some isolated values of  $k_2$  (linked with the eigenvalues of the Laplacian operator in  $\Omega_2$ ). From the practical point of view, it can be said that the M.F.S. also works for dielectric rods. Maybe we are lucky but, up to now, we never encountered difficulties in our computations.

The M.F.S. also works for an infinitely conducting obstacle. In this case, we have only to suppress the fictitious sources associated to  $\gamma_2$ . The rule is indeed very simple : the total field  $U$  being now null in  $\Omega_2$ , we can suppress the sources introduced to produce  $U$  in  $\Omega_2$  when this region was filled with a metal of finite conductivity.

## 3 - DIFFRACTION BY SEVERAL RODS

In this section we suppose that the diffraction obstacle consists of two rods which are parallel to the  $z$  axis and whose cross sections are, to a large extent, arbitrary. We will be brief because a detailed paper has been published in the J.O.S.A. [11]. Dealing with the case of polarization already used in sect. 2, we only want to draw the reader's attention to the main problems we had to face with.

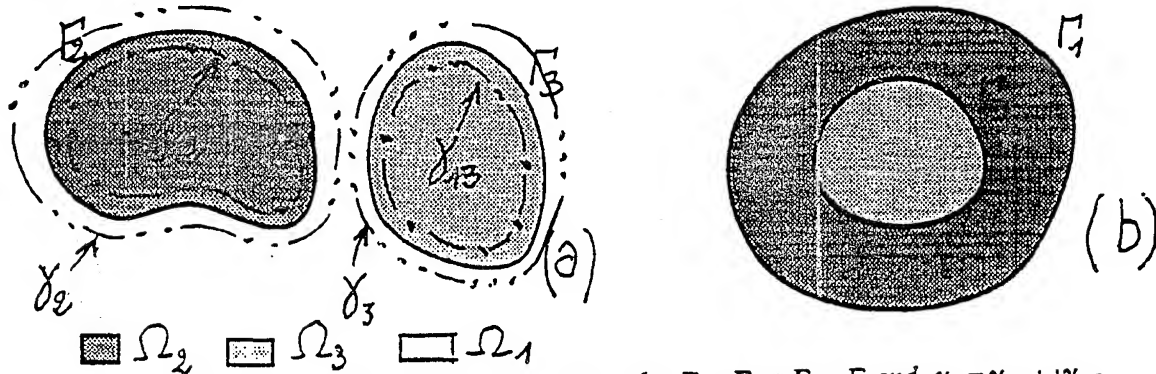


Fig. 4. Diffraction by several rods : (a) - two rods :  $\Gamma_1 = \Gamma_2 \cup \Gamma_3 = \Gamma$  and  $\gamma_1 = \gamma_{1,2} \cup \gamma_{1,3}$

(b) - a coated rod :  $\Gamma_2 = \Gamma_1 \cup \Gamma_3 = \Gamma$

### 3.1. Notations.

It is convenient to introduce three regions  $\Omega_1, \Omega_2, \Omega_3$ . We denote by  $\Gamma_j$  the boundary of  $\Omega_j$  and we characterize the homogeneous material which filled  $\Omega_j$  by  $k_j^2 = \omega^2 \epsilon_j \mu_0$ . What we call now  $\Gamma$  is the union of the  $\Gamma_j$  ( $\Gamma = \cup_j \Gamma_j$ ). At any point of  $\Gamma$ , we define the tangent unit vector  $\vec{t}$  (with a conventional direction) and the normal unit vector  $\vec{n} = \vec{e}_z \wedge \vec{t}$ . One can see in Fig. 4 two different possible situations, namely two separated rods (Fig. 4a) and a coated rod (Fig. 4b). It is worth noting that region  $\Omega_1$ , in which the incident field is propagating, is not bounded contrarily to  $\Omega_2$  and  $\Omega_3$ . As we did in Sec. 1, the fields  $U$  is still represented by a pair  $F = (u,v)$  and the definition of the



pair components remains unchanged. On the other hand, the incident field  $U^{inc}$  is represented by a pair in a slightly different way :

$$(12) \quad F^{inc} = (E^{inc}|_{\Gamma_1}, D_{\Gamma_1} E^{inc}) \text{ on } \Gamma_1 \text{ and } (0,0) \text{ elsewhere.}$$

Space  $\mathcal{V}$  is still  $H^1(\Gamma) \times L^2(\Gamma)$  and subspace  $\mathcal{V}_j$  ( $j=1,2,3$ ) are defined as in section 2 : briefly, a pair  $(u,v)$  belongs to  $\mathcal{V}_j$  if  $u$  and  $v$  are "the boundary values on  $\Gamma_j$ " of a function  $f_j$  satisfying the Helmholtz equation  $\Delta f_j + k_j^2 f_j = 0$  in  $\Omega_j$  (and the radiation condition if  $j=1$ ).

### 3.2. The theorem of the direct sum.

This theorem still holds. We have now :  $\mathcal{V} = \mathcal{V}_1 \oplus \mathcal{V}_2 \oplus \mathcal{V}_3$  and the generalization to  $N$  regions would be straightforward. The proof, given in [11], is unfortunately more intricate ; let say only that we have not been able to avoid the introduction of new functions  $\sigma_j$  ( $j=1,2,3$ ) defined on  $\Gamma$ , which maybe makes the reasoning somewhat difficult to follow in details.

### 3.3. The numerical recipe.

On the contrary, the numerical implementation do not present new difficulties. Let us explain what we have to do, referring to fig.4a. For each  $j$ , we introduce a curved (or a union of disjoint closed curves)  $\gamma_j$  lying in the complement of  $\Omega_j \cup \Gamma_j$  and following the curve  $\Gamma_j$  at some distance. Possible curves are shown in the figure using the following convention : curve  $\gamma_j$  ( $j=1,2,3$ ) is composed of dashes separated by groups of  $j$  dots. Since  $\Gamma_1$  is the union of  $\Gamma_2$  and  $\Gamma_3$ , it must be noticed that  $\gamma_1$  is the union of  $\gamma_{1,2}$  (a curve lying in  $\Omega_2$ ) and  $\gamma_{1,3}$  (a curve lying in  $\Omega_3$ ). To each curve  $\gamma_j$  we attach  $N$  fictitious sources  $S_{j,n}$  ( $n=1,N$ ) which radiate a field  $e_{j,n}$  in the whole space supposed to be filled with the material described by  $k_j$ . We look for an approximate solution  $\bar{U}_N$ . In  $\Omega_2$  or in  $\Omega_3$ ,  $\bar{U}_N$  is defined as a linear combination of the  $e_{j,n}$  :

$$(13) \quad \bar{U}_{j,n} = \sum_{n=1}^N c_{j,n} e_{j,n} \quad j=2,3$$

and in  $\Omega_1$ , where we have to take account of the incident field :

$$(13') \quad \bar{U}_{1,N} = \sum_{n=1}^N c_{1,n} e_{1,n} + U^i.$$

Now, as we did in Sect. 1, we have to express the boundary conditions on  $\Gamma$  through the minimization of a certain positive expression. Since  $\Gamma$  is the union of  $\Gamma_1$  and  $\Gamma_2$  (Fig. 4a), the squared norm of a pair defined on  $\Gamma$  is now the sum of two integrals (one on  $\Gamma_1$  and one on  $\Gamma_2$ ) ; with obvious notations :

$$(14) \quad \| \cdot \|_{\Gamma}^2 = \| \cdot \|_{\Gamma_1}^2 + \| \cdot \|_{\Gamma_2}^2.$$

It is convenient to denote by  $F_{1,2}^N$  and  $F_{1,3}^N$  the pairs representing the field radiated by the fictitious sources placed on  $\gamma_{1,2}$  and  $\gamma_{1,3}$  respectively. In a similar way, for  $j=2$  or  $3$ , we denote by  $F_j^N$  the pair representing the field radiated by the fictitious sources placed on  $\gamma_j$ . The determination of coefficient  $c_{j,n}$  is carried out by minimalization of :

$$(15) \quad \Delta_N = \| F^{inc} + F_{1,2}^N + F_{1,3}^N - F_2^N \|_{\Gamma_2}^2 + \| F^{inc} + F_{1,2}^N + F_{1,3}^N - F_3^N \|_{\Gamma_3}^2.$$

For the study of the coated rod (Fig. 4b), the reader can refer to [11].

### 3.3. An important comment.

Fig. 5 shows another diffraction problem in which the diffracting obstacle is a heterogeneous rod made of two jointed homogeneous rods. We have indeed solved the associated problem with the M.F.S. putting the fictitious sources on curves  $\gamma_j$  looking like the ones shown on fig. 5b. But, as explained in [11], we are, in such a case, confronted with new theoretical difficulties. The M.F.S. indeed seems to work (as shown by our numerical experiments), but we have not been able to give a theoretical proof of its convergence.

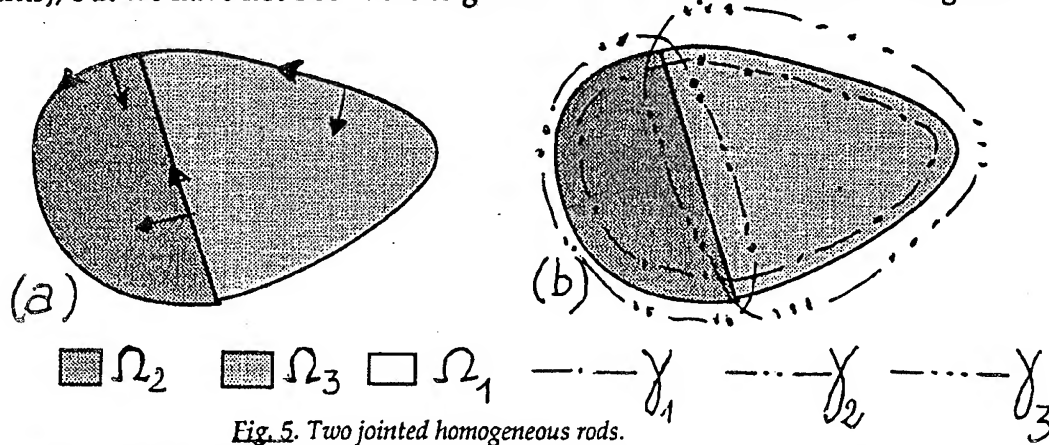


Fig. 5. Two jointed homogeneous rods.

## 4. DIFFRACTION BY ONE ROD ILLUMINATED BY A PLANE WAVE WHOSE WAVE VECTOR $\vec{k}^{\text{inc}}$ IS NOT PERPENDICULAR TO THE ROD

This question that cannot be reduced to a scalar problem has been also solved using the M.F.S., as recently described in the J.E.W.A. [12]. Putting  $\gamma = \vec{k}^{\text{inc}} \cdot \vec{e}_z$ , it can be shown that  $\vec{\mathcal{E}}(x, y, z) = \vec{E}(x, y) \exp(i\gamma z)$  and  $\vec{\mathcal{H}}(x, y, z) = \vec{H}(x, y) \exp(i\gamma z)$ .

As well known, it is possible to express the tangential components (on  $\Gamma$ ) of  $\vec{E}$  and  $\vec{H}$  in terms of  $E_z$  and  $H_z$ . These components are unambiguously defined (they take the same values on both sides of  $\Gamma$ ); they form a ordered set of functions (a quadruplet  $F$ ) that we use to represent the total field. More generally, any field sufficiently regular can be represented by such a quadruplet (rather than by a pair as we do for  $(\gamma = \vec{k}^{\text{inc}} \cdot \vec{e}_z = 0)$ ). For space limitation reasons, it is impossible to go into all the details. Let us only say that, again the problem can be reduced to the minimization of a norm which, by the way, is for  $\gamma \neq 0$  a traditional  $L^2$  norm. However, for  $\gamma \neq 0$ , we have now to determine four sequences of coefficients instead of two (for  $\gamma = 0$ ). In conclusion, the algorithm proposed and justified in [12], which seems at first glance rather intricate is, after due consideration, a straightforward generalization of the algorithm described in section 2. The associated numerical recipe is again simple to understand ... but of course the programming becomes cumbersome and the computation time increases. Anyway the numerical results given in [12] show that it works!

## 5. DIFFRACTION OF A PLANE WAVE BY A GRATING

From the mathematical point of view, there exists indeed a strong correlation between the diffraction by a rod (Problem 1) and the diffraction by a grating (Problem 2). In the first problem, the fields are functions of the polar coordinates  $r, \theta$ ; these functions are, for fixed  $r$ , periodic in  $\theta$ , with period  $2\pi$ ; very often, the cross section of the rod can be



described by a function  $f(\theta)$  which has itself the period  $2\pi$ . In the second problem, the fields are functions of the cartesian coordinate  $x, y$ ; in normal incidence,<sup>12</sup> these functions are, for fixed  $y$ , periodic in  $x$  with period  $d = 2\pi$  (provided we choose conveniently the unit of length); very often, the grating profile can be described by a periodic function  $f(x)$  with period  $2\pi$ . Thanks to this preliminary remark, it is possible to make M.F.S. algorithms suitable for the Electromagnetic Theory of Gratings [13, 7]. Even the case of conical diffraction ( $\gamma = \bar{k}^{\text{inc}} \cdot \bar{e}_z \neq 0$ ) has been recently solved, in collaboration with F. Zolla, as an adaptation of our paper in the J.E.W.A. [12]. This last work, carried out in the framework of a contract, has not yet been published ... we are now preparing a paper.

When passing from rods to gratings, there is however something which is worth noting. In both cases, an important step is the computation of the fields radiated by the fictitious sources. We need therefore to make the convolution product of a given distribution with a Green's function. For a rod, this Green's function is nothing other than a Hankel function for which efficient programmes do exist in any computer library. On the contrary, in grating Theory [13], and taking  $d = 2\pi$ , the Green function is

$$g(x-x_0, y-y_0) \text{ with } g(x, y) = \frac{1}{4i\pi} \sum_{n=-\infty}^{+\infty} \frac{1}{\chi_n} e^{i\alpha_n x + i\chi_n |y|}, \quad \chi_n = \sqrt{k^2 - \alpha_n^2}, \quad \alpha_n = n + k \sin(\theta^{\text{inc}})$$

This series converges slowly for small values of  $|y|$  and is not absolutely convergent for  $y = 0$ . However, when dealing with the M.F.S., we must be able to compute  $g(x_0, y_0)$  with a great accuracy<sup>13</sup> ( $10^{-10}$  for example) and in a reasonable time, whatever  $x_0$  and  $y_0$  (except for  $x_0 = 0$  and  $y_0 = 0$ ). We have been working a lot on this affair during the last months. As explained in [14], it turns out that, after a Kummer's transformation, we are led to series whose sum can be expressed in terms of polylogarithms [15]. The values of these rather exotic special function are available in MATHEMATICA but they seem difficult to get from a FORTRAN library. We first computed them with a "home-made programme", but we use now a much more efficient one provided by Dr. G.A. Erskine (C.E.R.N. - Genève). It is worth noting that very recently my colleague Cadilhac suggested to express the grating Green's function by an integral rather than by a series. He allows me to show you the result of his unpublished work; assuming again  $d=2\pi$ :

$$(16) \quad g(x, y) = \frac{1}{4i} H_0^{(1)}(kr) - \frac{1}{2i\pi} \int_{\Delta} \left( \frac{e^{iax}}{1 - e^{-2i\pi(a-a_0)}} + \frac{e^{-iax}}{1 - e^{-2i\pi(a+a_0)}} \right) \frac{\cos by}{a} db$$

with  $r = \sqrt{x^2 + y^2}$ ,  $a = \sqrt{k^2 - b^2}$ ,  $a_0 = k \sin(\theta^{\text{inc}})$ , the integration path being in the complex plane, the curve  $b = (1-i)t$ ,  $t > 0$ . We checked that the results obtained with the polylogarithm method are in perfect agreement (within  $10^{-8}$ ) with those obtained from (16) after numerical integration. Moreover for certain points  $(x, y)$ , Cadilhac's method is the most rapid (often by a factor 5). This is why it will be likely introduced in our programmes (at least as a conditional branch) in the near future.

## 6 - CONCLUSION AND ACKNOWLEDGMENTS

Since officially such a paper must not exceed twelve pages ... it is about time that I conclude very briefly. In this paper, we have been mainly interested with the theoretical aspects of the M.F.S. but, during the last years, we performed a lot of numerical

<sup>12</sup> For an arbitrary incidence  $\theta^{\text{inc}}$ , the fields are only pseudo-periodic but, as explained in [13], this is not a serious complication.

<sup>13</sup> Indeed we need not only the Green's function but its first derivatives as well.

experiments [3, 11, 12] to get some ideas on the efficiency and on the limits of the method. Indeed it must be emphasized that the "speed of convergence" strongly depends on the choice and on the location of fictitious sources. This is clearly shown in our previous papers, in Hafner's book [10], or in the numerous papers written in Israël by Leviatan and his collaborators [16]. From the theoretical point of view, the choice of curves  $\gamma_1$  and  $\gamma_2$  is, to a large extent arbitrary ; but, for a given problem, there is in fact an optimal choice which is a matter of habit. The M.F.S. is a powerful and a very flexible method but its use can be a tricky job. An inexperienced user will not choose the "good sources" at the first attempt ...

Because this paper is essentially concerned with already published results, I am very grateful to my colleagues M. Cadilhac, G. Tayeb and F. Zolla who have been my co-workers and co-authors, and without whom this invited paper would never have been possible.

## REFERENCES

- [1] We had numerous discussions with the mathematicians, especially with M. Cessenat, who is with the Commissariat à l'Energie Atomique (C.E.A.), CEL-V, B.P. 27, 91190 Villeneuve St-Georges, France. M. Cessenat plays more than a minor role in the preparation of the book quoted in ref. [2], especially chap. XI. He is now preparing a book on mathematical methods in electromagnetism.
- [2] R. Dautray and J.L. Lions, *Analyse mathématique et Calcul numérique pour les Sciences et les Techniques*, Masson, 1985 (now translated in english).
- [3] M. Cadilhac and R. Petit, "On the diffraction problem in electromagnetic theory : a discussion based on concepts of functional analysis including an example of practical application", in Huyghens' Principle 1690-1990, Theory and Applications, H. Block, H.A. Ferwerda and H.K. Kuiken, ed., Vol. 3 of Studies in Mathematical Physics (North-Holland Elsevier Science Publishers B.V, 1990), pp.249-272.
- [4] M. Cessenat, "Résolution de problèmes de Maxwell en régime harmonique par des méthodes intégrales", Rapport C.E.A., CEL-V/DS-EM, n° 587, 1978.
- [5] T. Kato, "Perturbation Theory for Linear Operators" - Second corrected printing of the second edition, Springer Verlag, 1984.
- [6] K. Yasuura and Y. Okuno, J. Opt. Soc. Am., 72, 847-852, 1982.
- [7] G. Tayeb, Thèse de Doctorat en Sciences (Faculté des Sciences de St-Jérôme, Marseille, France, 1990).
- [8] R. Petit and M. Cadilhac, "Electromagnetic theory of gratings : some advances and some comments on the use of the operator formalism", J. Opt. Soc. Am. A, 7, 1666-1674 (1990).
- [9] F. Zolla, Thèse de Doctorat en Sciences (Faculté des Sciences de St-Jérôme, Marseille, France, 1993).
- [10] G. C. Hafner, "Generalized multipole technique for computational electromagnetics", (Boston, Artech, 1990).
- [11] F. Zolla, R. Petit, M. Cadilhac, "Electromagnetic theory of diffraction by a system of parallel rods : the method of fictitious sources", J. Opt. Soc. Am. A, Vol. 11, n° 3, 1087-1096, 1994.
- [12] R. Petit, F. Zolla, "The method of fictitious sources as applied to the conical diffraction by a homogeneous rod", J. of Electromagnetic Waves and Applications, Vol. 8, n° 1, 1-18, 1994.
- [13] R. Petit, (Ed.), *Electromagnetic Theory of Gratings*, Vol. 22 of Topics in Current Physics (Springer, 1980).
- [14] N.A. Nicorovici, R.C. McPhedran and R. Petit, "Efficient calculation of the Green's function for electromagnetic scattering by gratings", Phys. Review E, Vol. 49, Issue 5, May 1994.
- [15] L. Lewin, "Dilogarithms and associated functions", Mac Donald London, 1958.
- [16] Yehuda Leviatan is with the Department of Electrical Engineering, Technion Israël, Institute of Technology, Haïfa 32000, Israël. With his collaborators, he published a lot of papers (our previous papers can be used as a key for references).

## Appendix A : Proof of the fundamental theorem $\mathcal{V} = \mathcal{V}_1 \oplus \mathcal{V}_2$ .

Given a pair  $\phi = (u, v)$ , let us consider the unique function  $g$  that satisfy the Sommerfeld radiation solution and is the solution of :<sup>14</sup>

$$\Delta g + k^2 g = v \delta_\Gamma + \text{div}(u \bar{n} \delta_\Gamma)$$

<sup>14</sup> Given a curve  $\Gamma$  and a function  $\alpha$  defined on  $\Gamma$ ,  $\alpha \delta_\Gamma$  is the distribution defined as :

$$\forall \phi \in \mathcal{D}, (\alpha \delta_\Gamma) = \int_\Gamma \alpha \phi d\ell.$$

As usual,  $\mathcal{D}$  is the space of all complex-valued functions of two variables having derivatives of all orders, all of which with compact support. The operator  $\text{div}$  must be understood in the sense of distribution theory.

where  $k^2$  is the piecewise-constant function almost everywhere defined on  $R^2$  as :

$$k^2(M) = k_1^2 \text{ si } M \in \Omega_1, \text{ or } k_2^2 \text{ si } M \in \Omega_2$$

As well known in distribution theory, functions  $u$  and  $v$  are the jumps (on  $\Gamma$ ) of  $g$  and its normal derivative  $Dg$ . We have therefore, at any point :

$$(u(P), v(P)) = (g_2(P) - g_1(P), Dg_2(P) - Dg_1(P)) ,$$

the subscripts 1 and 2 denoting the region in which the boundary values and the normal derivatives have to be evaluated. In other terms, if we introduce the pairs  $\phi_1 = (-g_1, -Dg_1)$  and  $\phi_2 = (g_2, Dg_2)$  which belong to  $\mathcal{X}_1$  and  $\mathcal{X}_2$  respectively, we can write :  $\forall \phi \in \mathcal{X}, \phi = \phi_1 + \phi_2$ .

The uniqueness of this decomposition can be established using a *reductio ad absurdum method of reasoning*. If this decomposition were not unique, it would be possible to find two pairs (say  $\psi_1$  and  $\psi_2$ ) such that  $0 = \psi_1 + \psi_2$  with  $\psi_1 \in \mathcal{X}_1$ , one of these pair at least being different from zero. In this case, we would be able to build a function  $g_1$ , defined in  $\Omega_1$ , having as "boundary values on  $\Gamma$ " the opposites of the components of the pair  $\psi_1$ , satisfying the radiation condition and the Helmholtz equation  $\Delta g_1 + k_1^2 g_1 = 0$ . We would be also able to build a function  $g_2$ , defined in  $\Omega_2$ , having as "boundary values on  $\Gamma$ " the components of the pair  $\psi_2$  and satisfying  $\Delta g_2 + k_2^2 g_2 = 0$ . Then the function  $g$  defined as :

$$g(M) = g_1(M) \text{ si } M \in \Omega_1, \text{ or } g_2(M) \text{ si } M \in \Omega_2$$

would be in the sense of distribution a nonvanishing solution of the equation  $\Delta g + k^2 g = 0$ , where  $k^2$  is again the piecewise-constant function defined above ; but it is known that such a solution cannot exist.

#### Appendix B : proof of theorem 1.

We suppose that function  $s_{1,n}$  form a total family in  $L^2(\gamma_1)$ . Considering functions  $e_{1,n}$  which satisfy the radiation condition and are solutions of :  $\Delta e_{1,n} + k_1^2 e_{1,n} = s_{1,n} \delta_{\gamma_1}$ , we first establish that their normal derivatives  $v_n$  on  $\Gamma$  form a total family in  $L^2(\Gamma)$ .

Let  $\alpha \in L^2(\Gamma)$  be a function such that, for any  $v_n$ , we have  $(v_n | \bar{\alpha})_\Gamma = 0$ . As is well known, what we have to show is that necessarily  $\alpha$  is null almost everywhere on  $\Gamma$ . Let  $w$  be the unique and almost everywhere defined function satisfying the radiation condition and such that :  $\Delta w + k_1^2 w = \text{div}(\bar{n} \alpha \delta_\Gamma)$ .

After classical manipulations, we get :  $e_{1,n} \Delta w - w \Delta e_{1,n} = e_{1,n} \text{div}(\bar{n} \alpha \delta_\Gamma) - w s_{1,n} \delta_{\gamma_1}$ , an equation which must be interpreted in the sense of distributions. Letting each member operate on a two variables constant function,<sup>15</sup> we are led to :  $0 = \int_\Gamma \alpha \partial_n(e_{1,n}) d\ell + \int_{\gamma_1} w s_{1,n} d\ell$ .

The first integral which is nothing other than  $(v_n | \bar{\alpha})_\Gamma$  is zero (from our hypothesis) and consequently, for any  $n$  :  $\int_{\gamma_1} w s_{1,n} d\ell = 0$ .

This means that  $\bar{w}$  (and  $w$  as well) is null (almost everywhere) on  $\gamma_1$ , since the functions  $s_{1,n}$  form a total family on  $\gamma_1$ . But  $w$  being continuous in the complementary of  $\Gamma$ , we conclude that  $w$  is null on  $\gamma_1$ . Thus  $w$ , which vanishes on  $\gamma_1$  and satisfies the Helmholtz equation  $\Delta w + k_1^2 w = 0$  in the interior of  $\gamma_1$ , vanishes<sup>16</sup> in the interior of  $\gamma_1$  and, therefore, in  $\Omega_2$  (a property of the Helmholtz equation). Consequently  $\partial_n w$  is zero on both sides of  $\gamma$  since, as a consequence of the definition of  $w$ , the jump on  $\Gamma$  of  $\partial_n w$  is zero. Then, we can claim that  $w$ , which satisfies the radiation condition, also vanishes in  $\Omega_1$  (uniqueness for the Neumann problem). In other words,  $w$  is the null function and consequently  $\text{div}(\bar{n} \alpha \delta_\Gamma)$  is the null distribution which implies<sup>17</sup> that  $\alpha = 0$ , almost everywhere on  $\Gamma$  (Q.E.D.).

Let us consider now the mapping which to any function  $v \in L^2(\Gamma)$ , associates the pair  $(Z_1 v, v)$ . This mapping is a continuous bijection from  $L^2(\Gamma)$  to  $\mathcal{X}_1$ , which implies that the pairs  $\phi_{1,n}$ , whose components are  $Z_1 v_n$  and  $v_n$ , form a total family in  $\mathcal{X}_1$ .

Of course, similar considerations allow us to show that the pair  $\phi_{2,n}$  form a total family in  $\mathcal{X}_2$ .

<sup>15</sup> This is possible since each member is a distribution whose support belongs to  $\Gamma \cup \gamma_1$  and is therefore bounded

<sup>16</sup> except if  $k_1^2$  is an eigenvalue of the Laplacien with a Dirichlet condition on  $\gamma_1$ .

<sup>17</sup> See Appendix F in [3]

# COUPLED POWER EQUATION USE FOR ANALYSIS OF OPTICAL FIBERS WITH UNSTEADY STATE POWER DISTRIBUTION

Sergey Petrov and Igor Sukhoivanov

The Technical University of Radio Electronics  
14, Lenin av., Kharkov, 310726, The Ukraine

## ABSTRACT

The authors have developed the methods consisting in introduction the static mode cut-off criterion, extended boundary condition in power diffusion equation solution and a special condition for solving the diffusion in time-dependent case. The developed methods have allowed to apply the coupled power equation to analysis of the irregular optical fibers of any length irrespective of the mode power distribution nature.

## THEORY

At present optical fibers are perspective means to create the most qualitative local systems. The peculiarity of these systems functioning is their characteristics dependence on the real mode distribution in the optical fiber that in its turn is the function of the many characteristics and conditions. Real value of different parameters in such systems may differ significantly (sometimes to 60 percent) from the individual measuring results. To analyse the multimode irregular optical fibers we used the coupled power equations:

$$\frac{d\bar{P}_m}{dz} + \tau_m \frac{d\bar{P}_m}{dz} = -2\gamma_m \bar{P}_m + \sum_{k=1}^N h_{mk} (\bar{P}_k - \bar{P}_m), \quad (1)$$

where  $\tau_m$  is the delay time for the length unit for the  $m$ -th mode. The boundary conditions:

$$\bar{P}(m, z, t)|_{m=0} = 0, \text{ and } \bar{P}(m, z, t)|_{m=M_0} = 0, \quad (2)$$

The unsteady state power distribution is also determined by the cladding modes excited by the source. With the influence of irregularity in the core and in the cover and also on border between them the couple arise. This couple is mutual and there's the reverse energy flow. That's why we introduce the wide boundary condition, taking into account the guiding qualities of the border between the cover and casing [1]

$$\bar{P}(m, z, t)|_{m=M_c} = 0, \quad (3)$$

where  $M_c$  is the largest mode number of the cladding modes.

The general solution of the power flow equation (2), describing the diffusion of the power distribution along the optical fiber, is expressed by the equation solution superposition :

$$F(z, x, t) = \sum_{i=1}^2 \sum_{k=1}^{\infty} W_k U_k(x) \exp(-(2\gamma(x) + \Gamma_{1,k})z) F_1(x, t), \quad (4)$$

To analyse the unsteady state power distribution optical fibers using the diffusing equation the criterion, described in [2] is used, this criterion allows to find the necessary and sufficient number  $K_{\max}$  determining the highest summing up limit in the equation (4)

$$(\Gamma_{1,k} - \Gamma_{1,1})z < 10 \text{ db}, \quad (5)$$

The expression for  $W_k, U_k(x), \Gamma_{1,k}$  is presented in details in [5].

The full power on the output of the optical fiber with the length of consists of the optical power that propagation in the core and in the cover.

To analyse the dispersion of the impuls signal, spreading along the multimode optical fiber with the unsteady state power distribution the power diffusion equation is used. Taking into account the function  $F_1(x, t)$  determining the character of the power diffusion in time [3], the solution of the equation may be presented as

$$F(z, x, t) = \frac{2}{\pi} \sum_{i=1}^2 \sum_{k=1}^{K_{\max}} \frac{W_k}{\Gamma_{1,k}} U_k(x) \exp(-(2\gamma(x) + \Gamma_{1,k})z) * \exp\left(-\frac{4(t - \tau_{1,k}^2 z)}{t_{1,k}^2 z}\right), \quad (6)$$

where  $\tau_{1,k}$  is the delay of the  $k$ -th statistical mode, and  $t_{1,k}$  is the width of this mode impuls response.

The delay of the statistical mode and the width may be presented as [2]:

$$\tau_{1,k} = 2 \int_0^1 x \tau_1(x) U_k(x) dx, \quad (7)$$

$$t_{1,k} = 4 \left( \sum_{k,j > k}^{K_{\max}} \frac{\left( \int_0^1 x \tau_1(x) U_k(x) U_j(x) dx \right)^2}{\Gamma_{1,j} - \Gamma_{1,k}} \right)^{1/2} z. \quad (8)$$

## RESULTS AND DISCUSSION

Using the developed method we analysed the power  $F(x, z, t)$  redistribution processes when the optical signal with the initial dis-

tribution  $P(x,0,t)$  goes along the 1...100 m long optical fiber and also the optical and geometric parameters influence on the power redistribution. On the Figure 1 and 2 the characteristics of the mode power distribution for  $z=5$  m long (Fig. 1) and  $z=50$  m long (Fig.2) optical fibers. Two regimes may be realized here: 1) the regime of the "weak radiations" of the cladding modes, when as a result of a gradual power redistribution between the guided and cladding modes, part of the mode power presents in the cover and takes part in the optical signal transmission. 2) the regime of the "strong radiation" of the cladding modes, when with the increase of the optical fiber length, the power diffusing to the cover doesn't accumulate there but radiate to the casing. From the point of view of the energy characteristics for the most qualitative local communication systems the first regime is expedient the "weak radiation" of the cladding modes.

On the Figure 3 the losses dependence on the length of the optical fiber when it is excited by different types of sources. It's necessary to mention that when changing the value of  $\alpha$  and  $E_3$  it's possible to change the conditions of the cladding modes spreading, without influence on the guided modes.

On the Figure 4 the signal dispersion dependence on the length of the optical fiber is shown when the optical fiber is excited by the laser diode. Positive results may be obtained with values  $\alpha = 0.2 \dots 0.5 \text{ m}^{-1}$ , with casing thickness  $c \geq 500 \text{ mkm}$ , elasticity module of the cover material not more than 1 GPa or depending on the values  $E_2$ ,  $E_3$ , under condition  $p > 1$ .

In conclusion we'd like to underline again that the spreading conditions of signals in the optical fibers with the unsteady-state power distribution have some peculiarities connected with the significant role of the cladding modes and their influence on the effects of intermode interaction and as a result on the quality of the transmitted signal. That's why such optical fibers cannot be simply considered as short optical fibers but must be separated into a special class.

#### REFERENCES

1. J.Kanka: "Modelling of attenuation properties of PCS fiber", Opt. and Quant. Electron., (1987), 19, pp.191-198.
2. S.Petrov, I.Suchoivanov: "Influence of cladding modes on the power diffusion into short fibers", Radiotechnics (1990), 93, pp.126-130.
3. I.Suchoivanov, S.Petrov: "Influence of the microbendings on the power diffusion in the short fibers" Radiotechnics (1990), 79, pp.87-90.

# STATISTICAL PROPERTIES OF DECAMETRIC RADAR SIGNALS REFLECTED BY EARTH SURFACE

S.F.Pimenov

Institute of Physics, Stachky, 194,  
344104, Rostov on Don, Russia

## ABSTRACT

The report summarizes the theoretical and experimental results achieved in the active decametric remote sensing of soil moisture, subsoil water levels and mineralization of freshwater reservoirs. As shown, the decametric wave range allows direct estimations of dielectric constant and moisture of soil in the near-surface layer of thickness about 1 m. A correlation is found between subsoil water levels (up to depth about 10 m) and the amplitude fluctuations of the reflected radiation. A high sensitivity of the mean amplitude of the reflected radiation to the level of mineralization of freshwater reservoirs is proved.

Keywords: decametric radar, soil moisture, water mineralization, subsoil water levels

## 1. INTRODUCTION

Recent years a number of works were devoted to remote determination of soil moisture content with use of the microwave range /1-4/. A series of experiments were carried out also in the meter range /5/. As a result, different factors are found to effect on the accuracy of measurements, such as shielding of soils by vegetation, roughnesses of the surface. The influence of a soil type on the dielectric permittivity dependence on moisture  $\epsilon(W)$  and the depth of the sensed layer were estimated /4/. It was shown that the layer thickness  $L$  in which one can successfully estimate the moisture content using microwave measurements was  $\sim 5$  cm /4/. However, many agricultural applications usually need the soil moisture known in an upper soil layer of about 1 m thickness. Such problem can be solved by using lower frequencies including decametric range /6/. A large penetration depth ( $\sim 10$  m) and strong dependence of complex dielectric constant on conductivity are those advantages which make this range unique for subsoil remote sensing and for water mineralization measurements /7/.

## 2. EXPERIMENTS AND CONCLUSIONS

A series of experiments were carried out in 1987-1993 to clarify the possibilities of using the decametric band for monitoring soil moisture, freshwater reservoir mineralization and SWL. Radar measurements were carried out on the board of AN-2



plane from the heights of 300-1000 m at the flight speed of 180-190 km/h. The carrier frequencies of the transmitter was 30 and 15 MHz, the length of the emitted pulse was 1  $\mu$ s, and the frequency of repetition was 1 kHz. There was also a possibility to sweep the frequency from 30 to 42 MHz. The quarter wave vibrator was used as a radiator. The influence of side reflections was removed by using the peak detector and strobing of the receiver. The spatial resolution is estimated as first Fresnel zone size. The average amplitude of 10 pulses  $a(t)$  was written to the computer memory every 10ms.

The instrument was calibrated by measuring  $a'$  on a quiet water surface for which reflection coefficient  $R'$  was considered known. The reflection coefficient from the Earth surface (for a constant flight height) was calculated with the equation  $R=R' \cdot a/a'$ . The mean  $a(t)$  amplitude  $\langle a \rangle$  was also used (averaging time was from 1s to 10s). Assuming  $\text{Im} \epsilon \ll \text{Re} \epsilon$  we estimated the soil dielectric constant  $\epsilon_R$  with the Fresnel equation.

The correlation between  $\epsilon_R$  and soil moisture  $W$  (by weight) in five upper layers (0-20cm, 20-40cm, 40-60cm, 60-80cm, 80-100cm) was studied. About thirty experiments were carried out (length of each route about 10km) on the territories of Rostov and Dnepropetrovsk Regions. The main result is that at 30MHz maximum correlation is observed between  $\epsilon_R$  and soil moisture in two upper layers 0-20cm and 20-40cm. At 15MHz the best correlation takes place in the layers 20-40 and 40-60cm. The result agrees with formula for depth of sensing  $d/6$ :

$$d \sim \lambda / (16 |\bar{\epsilon}|^{1/2}). \quad (1)$$

Here  $\bar{\epsilon} = d^{-1} \int_0^d \epsilon(x) dx$ ,  $\epsilon(x)$  is the distribution of the dielectric constant. Corresponding correlation coefficients  $\rho$  both range from 0.7 to 0.9. Minimum correlation was obtained between  $\epsilon_R$  and  $W$  in layer 80-100cm ( $\rho \sim 0.6$ ). The dependence of regression coefficients on soil type was also observed. The results of one of the experiments are shown in Fig.1.

In 1989-1991 the research program was performed of airborne measuring of reflection coefficients from freshwater reservoirs at the frequency of 30MHz. The studied objects were: 1. Tsymlyansk reservoir (mineralization  $S = 0.3-0.6\text{g/kg}$ ), 2. Vesely reservoir ( $S = 1-3\text{g/kg}$ ), 3. Proletarsk reservoir ( $S = 3-10\text{g/kg}$ ), 4. Manych - Gudilo Lake ( $S = 10-30\text{g/kg}$ ), 5. Taganrog Gulf ( $S = 10-20\text{g/kg}$ ). The considerable sensitivity was found of the radar signal to the mineralization changes with the best sensitivity fits into 0.5- 5g/kg mineralization range. The data of one of the route (Manych - Gudilo Lake - Proletarsk - Vesely) are presented in Fig.2. The correlation coefficients between average radar signal  $\langle a \rangle$  and water mineralization  $S$  usually range from 0.7 to 0.8. The mean radar contrast between Tsymlyansk reservoir and Vesely, Proletarsk and Manych - Gudilo ones equals to 0.35dB, 1.05dB and 1.55dB correspondingly.

The considerable part of the decametric radar research program was directed to investigations of fluctuations of the signals reflected by the Earth surface. At first, a lot of experiments was



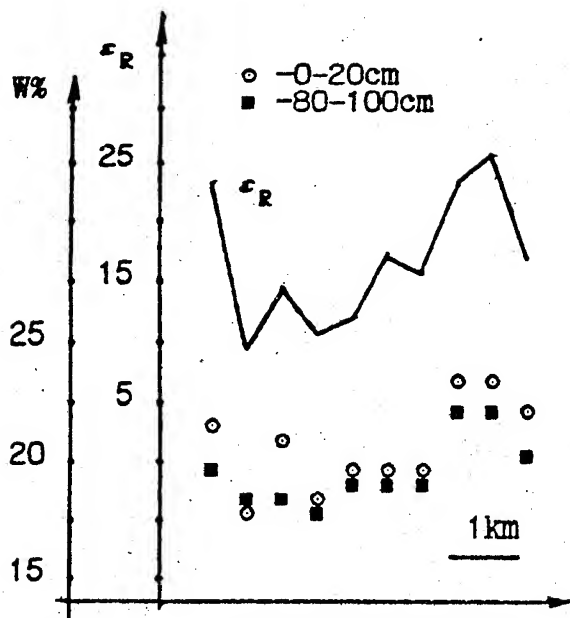


Fig.1. The results of soil moisture measurements, Rostov Region, October, 1989.

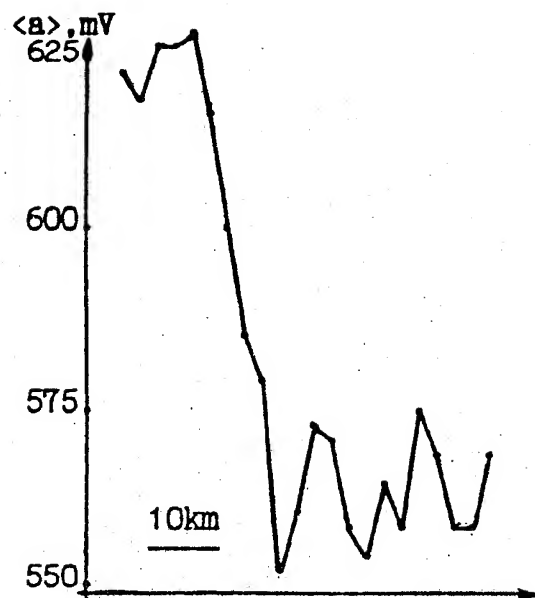


Fig.2. The results of Manych-Gudilo-Vesely route measurements, November, 1989.

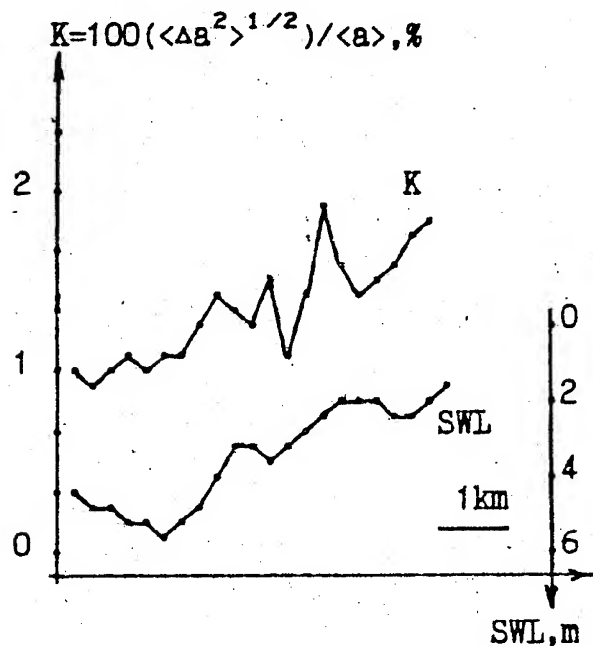


Fig.3. The results of SWL measurements, Dnepropetrovsk Region, July, 1988.

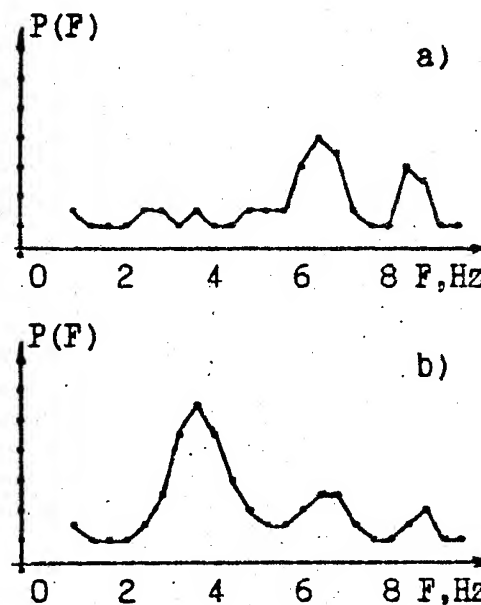


Fig.4. The spectrum of radar signal. Taganrog Gulf, June, 1991.

carried out to study the possibility of underground sounding with use the scattered power /6/. The correlation was studied between the fluctuation coefficient  $K$  (see Fig.3 ) and SWL. The correlation coefficients between  $K$  and SWL are found to be in 0.6 - 0.7 range. The good correlation ( $\rho \sim 0.7$ ) is also observed between SWL and the values estimated from  $K$  oscillations when sweeping the carrier frequency. The regression coefficient shows the strong dependence on a soil type. At second, such an important property of the fluctuation spectrum  $P(F)$  is found: it has rather a power-law dependence on the fluctuation frequency  $F$ :  $P(F) \sim F^{-\alpha}$  ( $\alpha \sim 1.5 - 2.5$ ) /8/ ( i.e. about 80% of spectra with only 20% being Gaussian ).  $F$  is defined by the inhomogeneity scale  $l$  and the aircraft speed  $v$  as:  $F \sim l/v$ .

The program also started with the freshwater reservoir and sea gravity wave spectrum investigation. Some experiments have been carried out accordingly to the program. Preliminary results are that in the freshwater reservoirs the spectra usually showed the series of lines with the width  $\Delta F/F \sim 0.02 - 0.07$  /8/. Sea wave spectra usually showed more wide lines and group of lines. The example of the spectrum of weak sea gravity waves is shown in Fig.4. The two spectra illustrate the spatial development of waves. The spectrum in fig.4a obtained 3km north of the south coast of the Gulf ( Port Caton ) shows only two lines at 6.5 and 8.5 Hz. The spectrum in fig.4b obtained 10km north of Port Caton shows the growth of new area of waves having another wavelength (corresponding to 3.9Hz fluctuation frequency ).

#### REFERENCES

- (1) N.A.Armand and A.E.Basharinov: "Study of the Earth with airborne instruments. Results using radiophysics methods", Vestn. AN SSSR, (1977) 8, pp.27-38.
- (2) K.Ya.Kondrat'ev, V.V.Melent'ev, Yu.I.Rabinovich, et al.: "Some physical characteristics of the soil surface layer with thermal radio emission", DAN SSSR, (1973) 200, 2, pp.342-345.
- (3) A.M.Shutko: "Microwave radiometry of lands under natural and artificial moistening", IEEE Trans. Geosci. and Remote Sens., (1982) GE-20, 1, pp.18-26.
- (4) T.J.Schmugge: "Remote Sensing of Soil Moisture", in: Hydrological Forecasting/Ed.by M.G.Anderson, T.P.Burt, New York, Wiley and Sons, 1985.
- (5) V.V.Popov, et.al.: "Construction of calibration curves of soil moisture radar measurements", in Proc.of All-Union Conf. on Statistical Data Procession in Remote Sens. of Environ., Riga, 1986, p.81.
- (6) A.S.Afanas'ev et al.: "Remote Sensing of Soils in Decametric Range", Sov.J. Remote Sens., (1990) 8(1), pp.86-98.
- (7) M.V.Kachan, S.F.Pimenov: "Decametric Radar Measuring of reservoirs mineralization", in Proc. of Conf. on Radiophysical Informatics, Moscow, 1990, p.47.
- (8) S.I.Gavronsky, M.V.Kachan, S.F.Pimenov, V.N.Stepchenko: "Statistical properties of radar signals reflected by Earth surface in meter and decameter range", in Proc. of Conf. on Statistical Methods of signal and image processing, Novorossiysk, 1991, p.80.

# SECOND ORDER SCATTERING OF RADIO WAVES BY TWO-LAYER MEDIUM WITH ROUGH BOUNDARIES

S.F.Pimenov and N.A.Stepanova

Institute of Physics, Stachky, 194,  
344104, Rostov on Don, Russia

Institute of Radio Astronomy, Krasnoznamennaya 4,  
310002, Kharkov, Ukraine

## ABSTRACT

When considering incidence of a plane wave arbitrarily polarized on a two-layer medium with rough surfaces, the average and scattered field is studied with use of the perturbation theory by small roughness. The important fact revealed is that the account of the second - order terms by roughnesses in the boundary conditions is essential for correct obtaining the average field in the lower half-space (medium), with they being not needed for defining its value in the upper half-space (from which the wave comes). The second momentum of the scattered field is also presented for the orthogonal polarization. It is shown also that such an effect as fading of scattering appears when correlation between roughnesses of upper and lower boundaries occurs.

Keywords: scattering of radio waves by rough surfaces, second order perturbation theory, layered medium.

Scattering of electromagnetic waves (SEW) by statistically rough boundaries in a layered medium was studied in a number of works. ( see /1-5/ ). The problem was solved by the method of equivalent boundary conditions in /1,2/, in the frameworks of the first approximation of the perturbation theory in /3/ and by the Kirchhoff method in /4,5/. In the present work SEW by a two-layer medium with rough boundaries is considered using the perturbation approach to the second-order accuracy.

Consider in the lower half-space a medium divided in average by plane boundaries onto such two layers: an upper one (second medium) of  $H$  thickness with dielectric constant  $\epsilon$  and lower half-infinite one (third medium) with  $\epsilon$ . The dielectric constant of the upper half-space (first medium) is equal to 1. The indices  $a$  and  $b$  denote values related to upper and lower boundaries, respectively. A monochromatic plane electromagnetic wave with wave vector  $\mathbf{k}$  is incident from the upper half-space on the medium. In particular, in the case of an incident horizontal polarization, the perturbation theory gives for the tangent Fourier component of the perturbation of the mean electric field in the lower (third) medium ( the boundary roughnesses are considered noncorrelated ) the following expression:

$$\begin{aligned}
\langle E_{32\tau} \rangle = & E_{10\tau} \cdot \tilde{D}(\vec{q}-\vec{q}_0) \cdot \tilde{D}(\vec{q}_0) \cdot (k^2/2) \cdot \left[ \{(\epsilon)_a \sigma_a^2 + (\epsilon)_b \sigma_b^2\} - (\epsilon)_a (1 + \right. \\
& + \tilde{V}_a(\vec{q}_0)) \cdot (\sigma_a^2 + \{(\epsilon)_a/2\} \tilde{Z}_1(\vec{q}_0) \int d\vec{q}_1 \Phi_a(\vec{q}_0 - \vec{q}_1) [\tilde{Z}_1(\vec{q}_1) (1 + \tilde{V}_a(\vec{q}_1)) \times \\
& \times \cos^2 \varphi + Z_1(\vec{q}_1) (1 + V_a(\vec{q}_1)) \sin^2 \varphi]) - (\epsilon)_b \cdot ((1 - \tilde{V}_b(\vec{q}_0)) \sigma_b^2 + \\
& + \{(\epsilon)_b/2\} \tilde{Z}_3(\vec{q}_0) (1 + \tilde{V}_b(\vec{q}_0) \int d\vec{q}_1 \Phi_b(\vec{q}_0 - \vec{q}_1) [\tilde{Z}_3(\vec{q}_1) (1 + \tilde{V}_b(\vec{q}_1)) \times \\
& \times \cos^2 \varphi + Z_3(\vec{q}_1) (1 + V_b(\vec{q}_1)) \sin^2 \varphi]) \left. \right] \quad (1)
\end{aligned}$$

Here and after:

$E_{10\tau}$  is the incident wave amplitude ( with first, second and third indices denoting a number of medium, an approximation order and a kind of polarization , respectively),

$\vec{q}_0$  and  $\vec{q}$  are the transverse components of the wave vector of the incident and scattered waves, respectively,

$\tilde{D}$  is the transmission coefficient of the layer for waves of horizontal polarization,

$\{\epsilon\}_a = \epsilon - 1$ ,  $\{\epsilon\}_b = \tilde{\epsilon} - \epsilon$  are the jumps of the dielectric constants,

$\sigma_{a,b}^2$  and  $\Phi_{a,b}$  are the dispersions and spectra of boundary roughnesses,

$\varphi$  is the angle between  $\vec{q}_0$  and  $\vec{q}_1$ ,

$\tilde{V}_{a,b}$ ,  $V_{a,b}$  и  $\tilde{Z}_{1,3}$ ,  $Z_{1,3}$  are the reflection coefficients from boundaries and impedances of the media 1 and 3 for waves of horizontal ( with  $\sim$  ) and vertical polarization ( see e.g. /6/ ).

The following case should be pointed out specially. In the second order of the perturbation theory the expressions for the mean fields of main polarization in the upper half-space prove to coincide with those, for example, obtained in /2/ with use of the equivalent boundary condition technique /1/. However, in the lower half-space and in the layer the mean fields of main polarization ( including the expression (1), in particular ) resulted from the perturbation theory differ from expressions obtained in /2/. This is due to neglecting in /1/ the second-order terms by boundary roughnesses. For example, the additional terms  $\langle \Delta \vec{E} \rangle$ ,  $\langle \Delta \vec{H} \rangle$  obtained for the electric and magnetic fields in the lower medium from the perturbation theory as compared to those from /2/. When roughnesses of lower boundary are absent we obtain:

$$\langle \Delta \vec{H} \rangle = \sigma_a^2 k^2 \{\epsilon\}_a \vec{H}_{30} / 2, \quad \langle \Delta \vec{E} \rangle = \sigma_a^2 k^2 \{\epsilon\}_a \vec{E}_{30} / 2. \quad (2)$$

where  $\vec{H}_{30}$ ,  $\vec{E}_{30}$  are the fields of zero approximation. For the many-layered medium the corresponding corrections to the mean field have the same structure, i.e. the amplitudes of the reflected fields in the upper half-space are not changed, but in the lower half-space and in the layer they have additional terms equal to the zero-order fields with the factor:

$$\mu_a = \sigma_a^2 k^2 (\epsilon)_a / 2. \quad (3)$$

At last, similar corrections due to roughnesses of an inner boundary  $c$ , also turn to zero in the upper region (above this boundary), and in the lower region are equal to zero-order field with the coefficient:

$$\mu_c = \sigma_c^2 k^2 (\epsilon)_c / 2. \quad (4)$$

In particular, these corrections correspond to the first term in rectangular brackets in (1).

The expressions for the second momenta of the scattered in the incidence plane fields of main and orthogonal polarizations are given below. For example, in the first order the second momentum of the back scattered field of horizontal polarization with inner boundary roughnesses being absent takes the following form (in agreement with [3]):

$$G_1 = \langle E_{11\tau}^* \cdot E_{11\tau} \rangle = E_{10\tau}^* \cdot E_{10\tau} \cdot (k/2) \tilde{Z}(\tilde{q}_0) (\epsilon)_a (1 + \tilde{V}(\tilde{q}_0))^2 |^2 \times \\ \times \delta(\tilde{q} + \tilde{q}_0) \cdot \Phi_a(-2\tilde{q}_0). \quad (5)$$

For the field of orthogonal polarization under the same conditions we have ( $G_2$  is not zero only beginning from the second order approximation):

$$G_2 = \langle E_{12q}^* \cdot E_{12q} \rangle = E_{10\tau}^* \cdot E_{10\tau} \cdot (k/2) Z(\tilde{q}_0) (\epsilon)_a (1 + \tilde{V}(\tilde{q}_0)) (1 + V(\tilde{q}_0)) |^2 \times \\ \times \delta(\tilde{q} + \tilde{q}_0) \cdot I(-2\tilde{q}_0). \quad (6)$$

Here the value  $I$  implies an effective spectrum of roughnesses and can be described by the expression:

$$I = ((\epsilon)_a k/4)^2 \cdot \int d\tilde{q}_1 \Phi_a(\tilde{q}_1 + \tilde{q}_0) \Phi_a(\tilde{q}_1 - \tilde{q}_0) (1 - \cos 4\varphi) |Z(\tilde{q}_1) (1 + V(\tilde{q}_1)) - \\ - \tilde{Z}(\tilde{q}_1) (1 + \tilde{V}(\tilde{q}_1))|^2. \quad (7)$$

As follows from the properties of the reflection coefficients  $\tilde{V}$ ,  $V$ , the second momenta of the scattered fields (5) and (6) are the oscillating functions of the layer thickness  $H$  and wave number due to the factors  $|1 + \tilde{V}|$  and  $|1 + V|$  with the period of  $\tilde{V}$  and  $V$  oscillations by the parameter  $S = 2kH$  being defined by the incidence angle:

$$T = 2\pi(\epsilon - q_0^2/k^2)^{-1/2}.$$

The expression (6) differs from (5) essentially by the dependence of  $I$  on the parameter  $S$ . In a number of cases this dependence is also oscillating with the period defined not only by the incidence angle but the roughness spectra as well. For the Gaussian spectrum:

$$\Phi_a(\tilde{p}) = \sigma_a^2 \exp(-q^2/p^2) / (\pi p^2)$$

the dependence  $I(S)$  takes the form:

$$I = ((\epsilon)_a k \sigma_a^2)^2 / (8\pi p^4) \cdot \exp(-2q_0^2/p^2) \int dq_1 q_1 \exp(-2q_1^2/p^2) \times \\ \times |Z(\tilde{q}_1) (1 + V(\tilde{q}_1)) - \tilde{Z}(\tilde{q}_1) (1 + \tilde{V}(\tilde{q}_1))|^2. \quad (8)$$

The value (8) has been calculated for  $2 \leq \epsilon < \tilde{\epsilon} \leq 9$ ,  $p \leq 4k$ . In all the cases studied numerically quasi periodic oscillations of  $I(S)$

are obtained. At  $p > k$  the period is almost independent of  $p$ . For example, at  $p=2k$  and  $p=4k$  for  $\varepsilon=4$ ,  $\varepsilon=9$  the period  $I(S)$  is equal to:

$$T_s \approx 3.6 \approx 2\pi(\varepsilon-1)^{-1/2},$$

at the same values  $p$ , but for  $\varepsilon=2$ ,  $\varepsilon=9$  it is:

$$T_s \approx 6.3 \approx 2\pi(\varepsilon-1)^{-1/2}.$$

When  $p < k$  the period of  $I(S)$  oscillations is determined by the boundary of a roughness spectrum and at  $p \ll k$  reduces to the value:

$$T_s \approx 2\pi\varepsilon^{-1/2}.$$

In the cases above the relative amplitudes of  $I(S)$  oscillations vary from tens of percents at  $S$  of the order of unity to few percents at  $S$  of the order of tens. They tend to decrease with increasing  $p$ .

In the case of full correlation between upper and lower boundary roughnesses similar to the case of large scale roughnesses (see /5/) fading effect for scattering occurs. For example, to the first order accuracy its condition for horizontally polarized wave reduces to the following:

$$\xi_b(\vec{q}-\vec{q}_0)/\xi_a(\vec{q}-\vec{q}_0) = -\{\varepsilon\}_a(1+\tilde{v}_1(\vec{q}_0))(1+\tilde{v}_1(\vec{q})) / (\{\varepsilon\}_b\tilde{D}(\vec{q}_0)\tilde{D}(\vec{q})). \quad (9)$$

This requirement and the same conditions for other processes correspond to infinitely narrow directivity patterns of source and receiver antennae. Allowance for a finite pattern width leads to another expressions. Particularly, for wide patterns at normal incidence the following condition takes place:

$$\xi_b(\vec{\rho})/\xi_a(\vec{\rho}) = -\{\varepsilon\}_a(1+\tilde{v}_1(0))(1+\tilde{v}_1(0)) / (\{\varepsilon\}_b\tilde{D}(0)\tilde{D}(0)), \quad (10)$$

Here  $\vec{\rho} = ix + jy$ ,  $x$ ,  $y$  are horizontal coordinates. Note that the condition (10) coincides with the corresponding one in /5/ obtained earlier by Kirchhoff method.

#### REFERENCES

- (1) N.P.Zhuk and O.A.Tret'yakov: "Two-side boundary conditions for mean electromagnetic field on a rough surface", *Izvestiya vysshikh uchebnykh zavedenii, seriya radiofizika*, (1981) 24, 12, pp.1476-1483.
- (2) N.P.Zhuk: "Coherent scattering of electromagnetic waves by a rough boundary of one-axis layered half-space" *Zhurnal tech. fiziki*, (1989) 59, 6, pp.12-17.
- (3) A.S.Bryukhovetski: "Incoherent scattering of radio waves by a rough layered soil. Born's approximation", in *Proc. of Conf. on Statistical Methods and Remote Sensing Systems*, November 1989, Minsk, p.81-82.
- (4) S.G.Zubkovich, *Statistical Properties of Radio Waves, Reflected by Earth Surface*, M.: Radio i svyaz', 1968.
- (5) S.F.Pimenov and M.A.Rudenko: "Reflection of Radio waves by Two-layer medium", *Izvestiya vysshikh uchebnykh zavedenii, seriya radiofizika*, (1992) 35, 3-4, pp.275-284.
- (6) L.M.Brekhovskich, *Waves in layered medium* M.: Ed. of the Acad. of Sci. of the USSR, 1957.

# STRONG SCATTERING OF RADIO WAVES BY LAYERED MEDIA WITH ROUGH SURFACE

S.F.Pimenov and N.A.Stepanova

Institute of Physics, Stachky, 194,  
344104, Rostov on Don, Russia

Institute of Radio Astronomy, Krasnoznamennaya 4,  
310002, Kharkov, Ukraine

## ABSTRACT

Theoretical consideration of wave scattering by rough surfaces within the frameworks of the perturbation theory is usually based on expanding the boundary conditions by powers of the surface roughness height  $\xi$ . When using such an approach, it would not be managed to account for effects of strong scattering described by high order terms of the expansion. In the method developed here the boundary jump  $\{\epsilon\}$  of the dielectric constant is used as a small parameter for obtaining the perturbation series. This allows to consider the effects appearing at roughness height large compared to the wavelength  $\xi \gg \lambda$ .

Keywords: strong scattering theory by rough surfaces, layered media.

Consider scattering of a plane monochromatic wave by a two-layer medium with an upper rough boundary. Let the dielectric constants be equal to  $\epsilon$  and 1 in the layer and upper half-space, respectively. Start with the electric field strength taken in the integral form /1/:

$$\vec{E}(\vec{r}, t) = \vec{E}_0(\vec{r}, t) - (4\pi/c) \int d\vec{r}' dt' \hat{G}(\vec{r}, t, \vec{r}', t') \vec{j}(\vec{r}', t'). \quad (1)$$

Here  $\hat{G}$  and  $\vec{j}$  are the tensor electrical Green function and density of current, respectively.  $\vec{E}$  is the electric field in unperturbed media. For the problem of interest the current density  $\vec{j}$  is considered as induced by the field in perturbations  $\delta\epsilon$  of the dielectric constant:

$$\vec{j}(\vec{r}', t') = (c/4\pi) \delta\epsilon \partial / \partial t \vec{E}(\vec{r}', t'). \quad (2)$$

The  $\delta\epsilon$  value can be written as:

$$\delta\epsilon = \begin{cases} \{\epsilon\} \text{sign} \xi, & \text{for } z(z-\xi) < 0, \\ 0, & \text{in another case.} \end{cases} \quad (3)$$

Here,  $\{\epsilon\} = \epsilon - 1$  is the dielectric constant jump at the upper boundary, the axis  $z$  is the normal to the layer plane. The solution of the system of equations (1)-(3) can be expressed as the Neumann series. Particularly, to the first-order by  $\{\epsilon\}$  accuracy with an incident wave of horizontal polarization taken in the form:

$$\vec{E} = \vec{E}_\tau \cdot \vec{E}_0 \cdot \exp(i(\vec{k}_0 \vec{r} - \omega_0 t)),$$



we obtain the following expression where Fourier transformation by horizontal coordinates  $\vec{\rho}$  and time  $t$  was performed:

$$\vec{E}(\omega, \vec{q}, z) = \vec{E}_0 + \Delta \vec{E} \approx \delta(\omega - \omega_0) \left[ \delta(\vec{q} - \vec{q}_0) \vec{E}_0(\omega, \vec{q}, z) + \right. \\ \left. + 2\pi i \omega_0 \{\epsilon\} \int d\vec{\rho}' \exp\{i((\vec{q}_0 - \vec{q})\vec{\rho}')\} \int dz' \hat{G}(\omega, \vec{q}, z, z') \vec{E}_0(\omega, \vec{q}, z') \right]. \quad (4)$$

Here the integral over  $dz'$  is taken in the limits from 0 to  $\xi(\vec{\rho}')$  with  $\vec{q}_0$  and  $\vec{q}$  being the transverse components of the incident and scattered wave vectors. Such values in (4) as the Fourier component of the unperturbed field:

$$\vec{E}_0(\omega, \vec{q}, z) \delta(\omega - \omega_0) \delta(\vec{q} - \vec{q}_0)$$

and the tensor electric Green's function  $\hat{G}(\omega, \vec{q}, z, z')$  can be found with use of the relations given in /2,3/. When the inequality:

$$1 \ll \{k_0 \epsilon \ll \epsilon / \{\epsilon\}, \quad (5)$$

is valid, the expressions mentioned take the most simple form. In this case, for example, the tangent component of the perturbation of the mean electric field strength  $\langle \Delta E_T \rangle$  has the following form:

$$\langle \Delta E_T(\vec{q}) \rangle = E_0(\vec{e}_T \vec{e}_{T_0}) \delta(\omega - \omega_0) \delta(\vec{q} - \vec{q}_0) \tilde{v}(q_0) \exp\{-2\sigma^2 k_{2z}^2(q_0)\} \times \\ \times (1 - \tilde{v}_b^2(q_0)) \exp(4ik_{2z}(q_0)H). \quad (6)$$

Here,

$H$  is the layer thickness,

$\sigma^2$  is the dispersion of the upper boundary roughness,

$k_{2z}(q_0)$  is the longitudinal component of the wave vector in the layer,

$\tilde{v}$ ,  $\tilde{v}_b$  are the reflection coefficients for waves of horizontal polarization from the upper and lower boundaries of the layer, respectively.

Note that the value  $\langle \Delta E_T \rangle$  at large  $\sigma^2$  proves to be exponentially small due to the term  $\exp\{-2\sigma^2 k_{2z}^2\}$ .

On calculating the second momentum of the electric field perturbation  $\langle \Delta E_{T1} \Delta E_{T2} \rangle$  we obtain the following sum:

$$\langle \Delta E_{T1} \Delta E_{T2} \rangle = \sum_j A_j I_j. \quad (7)$$

Here,

$$I_j = (2\pi)^{-4} \int d\vec{\rho}_1 d\vec{\rho}_2 \exp\{-1((\vec{q}_{01} - \vec{q}_1)\vec{\rho}_1 + (\vec{q}_{02} - \vec{q}_2)\vec{\rho}_2)\} P_j(\vec{\rho}_1, \vec{\rho}_2). \quad (8)$$

$$P_j(\vec{\rho}_1, \vec{\rho}_2) = \langle \exp\{-1(\beta_1 \xi(\vec{\rho}_1) + \beta_2 \xi(\vec{\rho}_2))\} \rangle =$$

$$= \exp\{-\sigma^2(\beta_1^2 + \beta_2^2 + 2\beta_1 \beta_2 r(\Delta \vec{\rho})) / 2\}, \quad (9)$$

$$\beta_+ = k_{2z}(q) + k_{2z}(q_0), \quad \beta_- = k_{2z}(q) - k_{2z}(q_0). \quad (10)$$

$\beta_n = \nu \beta_{\pm}$ ,  $\nu = \pm 1$ ,  $n=1,2$ , the values  $j$  correspond to various combinations of  $\nu$  and signs  $\pm$ ,  $r(\Delta \vec{\rho})$  is the correlation radius of the



upper boundary roughnesses.

In the case of isotropic roughnesses at  $\beta_1\beta_2 < 0$  the following asymptotic ( $\sigma \rightarrow \infty$ ) expression can be found:

$$I_j = \delta(\tilde{q}_{01} - \tilde{q}_1 + \tilde{q}_{02} - \tilde{q}_2) \exp(-\sigma^2(\beta_1^2 + \beta_2^2)/2) (2\pi)^{-2} \int d\Delta \tilde{\rho} \exp(-\sigma^2 \beta_1 \beta_2 r(\Delta \tilde{\rho}) - \\ - \Delta \tilde{\rho}(\tilde{q}_{01} - \tilde{q}_1)) = \delta(\tilde{q}_{01} - \tilde{q}_1 + \tilde{q}_{02} - \tilde{q}_2) \exp(-(\tilde{q}_{01} - \tilde{q}_1)^2 / (2\sigma^2 \beta_1 \beta_2 r''(0))) \times \\ \times \exp(-\sigma^2(\beta_1 + \beta_2)^2 / 2) / (2\pi \sigma^2 \beta_1 \beta_2 r''(0)). \quad (11)$$

Generally, the values (11) and, at the same time, the value (7) are exponentially small by the parameter  $\sigma$ . However, in the case:

$$\beta_1 + \beta_2 = 0 \quad (12)$$

the exponential decreasing of the value (7) is replaced by the power law one. It reveals some resonant frequencies and directions of incidence and scattering which prove to be most sensitive to existence of a layer. When defining a layer thickness from the scattered field the most reasonable approach is to use these frequencies and directions as most informative.

#### REFERENCES

- (1) L.B.Felsen and N.Marcuvitz, Radiation and Scattering of Waves, Prentice-Hall Inc., Englewood Cliffs, New Jersey, 1973.
- (2) F.G.Bass and I.M.Fuks, Wave scattering from statistically rough surface, M.: Nauka, 1972.
- (3) L.M.Brekhovskich, Waves in layered medium, M.: Ed. of the Acad. of Sci. of the USSR, 1957.

Institute of Radiophysics and Electronics Ukrainian Academy of Sciences, 12, ac. Proskura st., Kharkov, 310085, Ukraine  
(Tel. (7-0572)-44-85-43; FAX: (7-0572)-79-11-11)

The heart of interest in different microwave devices designing is investigation of resonant phenomena in their various displaying. Understanding the nature of these processes may provide designer with possibilities to utilize and explore their advantages and avoid their drawbacks.

The reliable and trustworthy description of electromagnetic processes in resonant parameter region can be obtained only by means of correct mathematical models and their correct computer realization. Different numerical approaches, based on such direct ones as moment method, finite element method fail in investigation of fast oscillating scattering characteristics near resonant frequencies. All these make clear the advantages of correct mathematical approaches for investigating of resonant phenomena. Moreover, only this kind of approaches and developed on it's base spectral theory with utilizing of catastrophe theory, provide trustworthy description and explanation of several complicated phenomena, arising in resonant region. Spectral theory of open waveguide resonators deals with eigen modes of structures (possible natural modes of electromagnetic field), their "coupling" and role in forming of resonant respond of cavity to any of (stationary and nonstationary) excitation. Canonic problems of the theory consist in determination of nontrivial time harmonic solutions of homogeneous Maxwell equations. This solutions have to satisfy usual in electromagnetics boundary conditions and Reichardt radiation conditions in regular semiinfinite waveguides that are connected (via junction windows) with bounded resonant volume. The number and configuration of every of this (maybe of different type) radiating channels define the spectral parameter variation region, i.e. the region where eigen frequencies are searching for. The complete set of eigen frequencies and relevant eigen modes is the minimal basis, that defines all electromagnetic properties of subject. Analytical description of correspondent connections is given by various (local and global) expansion theorems and act as the base on which the modern physics of resonant wave scattering is created. The physics that not only certify anomalous effects and phenomena, but uniquely determines their nature and regularities in realizations, provides the reliable qualitative predictions.

This report is devoted to the discussion of physical results, obtained in the frames of the approach described above, based on one of semiinversion method [1]. The key point of approach is the construction of correct solution of initial boundary value problem. In the case when resonant phenomena and their particularities are of special interest, it is necessary to solve the spectral problem and receive boundary value problem function that adequately describe the physical problem.

The resonators, considered herein, are constructed by coaxial junctions of cylindric and coaxial waveguides (see Fig.1,2). The initial boundary value spectral problem for them may be reduced to

$$(\Delta - \kappa^2)U(r, \kappa) = 0, \quad r \in Q, \quad \kappa \in K \quad (1)$$

$$U(r, \kappa) \left\{ \frac{\partial}{\partial n_i} U(r, \kappa) \right\} = 0, \quad r \in S \quad (2)$$

$$U(r, \kappa) = \sum_{n=1}^{\infty} a_{nj} U_{nj}(p) \exp\{i\omega_{nj} Z_j\}, \quad r \in Q, \quad j = 1, 2, \dots, M, \quad (3)$$

where:  $M$  - the number of regular waveguide regions,  $K$  - infinitely foliated Riemann surface with second order branching points  $\kappa_{nj}$ :  $\omega_{nj} = \sqrt{\kappa^2 - (\nu_n/\theta_j)^2} = 0, \kappa = \kappa' + i\kappa'', \nu_n$  - roots of  $J_0(\kappa) = 0, n = 1, 2, \dots, j = 1, 2, \dots, M, \theta_j$  - relative radii of waveguides. The configuration of cuts is arbitrary (the possible nonuniqueness of solution may be eliminated by complete posing of the problem in Riemann surface), but quarters of their disposition in plane  $\kappa$  are strictly determined by the necessity of being valid at axis  $R^1$  in the first foliate physically proved condition that all waveguide modes in (3) may be not arriving from the infinity  $\text{Im } \omega_{nj} \geq 0, n = 1, 2, \dots, j = 1, 2, \dots, M$ . In the Dirichlet problem case spectrum points  $\kappa$  and relevant

nontrivial solutions  $U(r, \bar{\kappa}), \bar{\kappa} \in \Omega$ , describe  $H_{0n}$  eigen modes, and in the case of Neimaun boundary problem -  $E_{0n}$  eigen modes.

It is necessary to point out that in difference from classic (selfadjoint or  $Z_2(Q)$ ) theory of open resonators, theory, based on the solution of nonselfadjoint problem (1)-(3), enables us to analyze eigen modes of any type (including leaky modes i.e. the kind of modes with exponentially increasing amplitudes when  $|z_j| \rightarrow \infty$ ). This theory does not operate with such notions as "continuous" spectrum, not filled by clear physical contents and eliminate subjective elements, that appear inevitably in attempts to consider the spectral problem in simple "physical" spectral parameter region of variation.

It is proved, [1] that spectrum  $\Omega$  (the set of points  $\bar{\kappa} \in K$ , where the problem (1)-(3) has nontrivial solution) is of finite multiplicity and discrete and is not empty in any finite region from  $K$ , and fundamental solution of (1)-(3) (Green function  $G(r, r_0, \kappa)$ ) is meromorphic (in respect to local on  $K$  variables) function with poles of finite order in points  $\bar{\kappa} \in \Omega$ . The rough localization of spectrum  $\Omega$  on  $K$  is carried out (the regions of surface free of spectrum point  $\Omega$  are determined). The representation of open waveguide cavities electromagnetic characteristics via their spectral characteristics are proceeded: local ones (in frequency domain) and global ones (in time domain when  $t \rightarrow \infty$ ).

In the way [1] the spectral problems is reduced to the problem of finding out the characteristic numbers of analitical operator-function,  $I - A(\kappa)$  in  $K$  where  $A(\kappa)$  is compact and even kernel operator for any complex  $\kappa \in K$ . That is why the function

$$F(\kappa, L) = \det\{I - A(\kappa, L)\} \quad (4)$$

exists and spectral problem is reduced to the solving of the equation

$$F(\kappa, L) = 0 \quad (5)$$

giving us the spectrum of resonant cavity and eigen functions i.e. natural modes of resonant cavity

Using this results as a background and utilizing results of parallel numerical examples of the solution of diffraction and spectral problems the following problems are investigated:

- anomalous phenomena connected with changing of numbers of open radiation channels (the number of waves in fields (3));
- the complete energy reflection and transmission via open waveguide resonator, and their connection with excitation in resonator's volume oscillations close to natural ones;
- phenomenon, coursed by "interaction" of possible natural oscillations when their own frequencies are approaching in complex space metric, including effect of existence of super high  $Q$  oscillation ( $\bar{\kappa} \in R^1$ ) in open resonators (there exist  $n$  and  $j$  such, that when  $\bar{\kappa} \in R^1, \bar{\kappa} \in \Omega, \text{Re} \omega_{nj} > 0, \text{Im} \omega_{nj} = 0$ );
- trap effect and effect of energy accumulation: nonstationary wave scatters. In this case the energy of secondary near field of resonant cavity after source instantly have been operated do not decrease or when source operates constantly is accumulated;
- effects of complete transformation of propagating packet of waveguide modes, and many other resonant effects and phenomena, defining interesting, from point of view of applications, properties of open waveguide cavities, as device, enabling to realize required frequency, space and type selection of signals.

The regularities of these effects displaying and conditions, necessary for their realizations are to be discussed in the report.

Herein we shall dwell only on one example, illustrating the connection between the effects of complete wave packet transformation and eigen regimes of open waveguide resonators existing on real eigen frequencies ( $\text{Im} \bar{\kappa} = 0$ ) on "nonphysical" (higher) sheets of surface  $K$ . So as these sheets are defined completely by values of couples  $\{\kappa; \omega_{nj}(\kappa), n = 1, 2, \dots, j = 1, 2, \dots, M\}$ , they differ from each other only by the fact that signs of finite number of values  $\omega_{nj}(\kappa)$  are changed to opposite, then radiating field of real frequency  $\bar{\kappa}$  in higher sheets  $K$  (see (3)) contains finite number of "arriving" waveguide modes. Hence the total identification of the eigen mode field on real eigen frequency  $\kappa$ , with complete diffraction field of frequency  $\kappa \in R^1$ , that is projection  $\bar{\kappa}$  into the first sheet of  $K$  is possible. And in that total diffraction field part of modes in (3) will propagate towards the cavity (waves of excitation), and other part with not coinciding with previous ones indexes  $n$  and  $j$  - will propagate from cavity (secondary diffraction field). Thus, the total field will be divided into two noncoinciding packets, that is the complete transformation of one wave packet into another is realized. All characteristics of the regime (amplitude of arriving and outgoing wave  $a_{nj}$ , the excitation

frequency  $\kappa$ ) are determined from the solution of spectral problem on the line segment of axis  $\kappa'$  of higher sheet of surface. Both the line segment and the sheet are uniquely defined by main parameter of regime - by set of indexes  $n$  and  $j$ , corresponding to outgoing and arriving waves.

The results shown in Fig.1,2 illustrate these statements. The parameters of the simplest model - coaxial cavity in circular waveguide as waveguide tuner and reflection mode transformer are defined. In Fig.1 the point  $\kappa' = 1.2214, L = 0.658$ , where curve  $\kappa''(L)$  crosses axes of real  $\kappa'$  after passing through cut line  $\omega_{12}(\kappa) = 0$  into second sheet of  $K$ , corresponds to the complete tuning of two circular waveguides or different radii. The point  $\kappa' = 1.3967, L = 0.387$  in Fig.2 provides the regime of complete transformation of  $H_{02}$  arriving wave into  $H_{01}$  reflected. The lines of equal values of  $H_{02}$  transmitted wave energy (Fig.1) and  $H_{01}$  reflected (Fig.2) in coordinates  $\kappa, L$  obtained by labor-consuming numerical solving of diffraction problem in considerable parameter region demonstrate the advantages of spectral approach in defining particular regimes of electromagnetic devices. (The points of complete mode transformation are marked by asterisks).

Consideration of  $F(\kappa, L)$  in the region of complex  $L$  (or any other parameters) provide the investigation of more "intimate" processes existing only in resonant regions among natural modes such as mode degeneracy and coupling. In order to determine the coordinates of degeneracy points  $\{\kappa_d, L_d\}$ , which are causing the degeneracy phenomenon, we have to solve the system:

$$\begin{cases} F'_\kappa(\kappa, L), & \kappa = \kappa' + i\kappa'' \\ F(\kappa, L), & L = L' + iL'' \end{cases} \quad (6)$$

In the local vicinity of the degeneracy point  $(\kappa_d, L_d)$  can be written in the form

$$F(\kappa, L) = F'_L(L - L_d) + \frac{1}{2}\{F''_{\kappa\kappa}(\kappa - \kappa_d)^2 + 2F''_{\kappa L}(\kappa - \kappa_d)(L - L_d) + F''_{LL}(L - L_d)^2\} + \dots$$

Their investigation can give the picture of degeneracy's transformation and even disappearance, that are displaying in resonator when its parameters are changing (the diffraction losses increasing, volume is varying and etc). To determine the Morce critical points coordinates  $\kappa_M, L_M$ , causing the mode coupling, we have to solve the following system:

$$\begin{cases} F'_\kappa(\kappa, L) = 0 \\ F'_L(\kappa, L) = 0 \end{cases} \quad (7)$$

with condition

$$F''_{\kappa\kappa}F''_{LL} - (F''_{\kappa L})^2 \neq 0 \quad (8)$$

In local vicinity of Morce critical point spectral curves may be computed by means of rather simple form:

$$\frac{1}{2}\{F''_{\kappa\kappa}(\kappa - \kappa_M)^2 + 2F''_{\kappa L}(\kappa - \kappa_M)(L - L_M) + F''_{LL}(L - L_M)^2\} + \delta = 0 \quad (9)$$

where  $\delta = F(\kappa_M, L_M), F''_{\kappa\kappa}, F''_{LL}, F''_{\kappa L}$  are calculated in the point  $(\kappa_M, L)$ .

The complicating of the electromagnetic resonant cavity model causes the complicating of electromagnetic resonant processes in it. So, in the case of junction of two cavities, that may be realized in various ways spectral curves split (except of those with zero longitudinal number) and more possibilities for various types of coupling and degeneracy appear. The total picture of diffraction and spectral properties becomes more complicated too. The situation when the solution of system (6) does not satisfy the condition (7) appears. This point is the catastrophe point. In such case the presentation (9) is not valid. In this case it is necessary to carry out the investigation of higher degree terms in expansion (9). But introducing of additional parameters can simplify the problem, because when one of chosen parameters vary even slightly, the catastrophe point break down into finite number of Morce critical points, that satisfy (7) and (8).

The numerous illustrative dates for spectral and diffraction characteristic behavior, eigen mode field configuration, location of Morce critical points, degeneracy e points and their connection with diffraction properties are to be presented and discussed in the report.

1. Sirenko Y. K., Shestopalov V. P., Yashina N. P. U.S.S.R. Comput. Maths. Math. Phys., Vol. 26, No. 2, pp. 142-148, 1986.
2. Pochanina I. E., Shestopalov V. P., Yashina N. P. Radiophysics and Quantum Electronics., Vol. 32, No. 8, pp. 744-752, 1989.
3. Pochanina I. E., Shestopalov V. P., Yashina N. P. Soviet Physics Doklady., Vol. 36, No. 9, pp. 631-633, 1991.

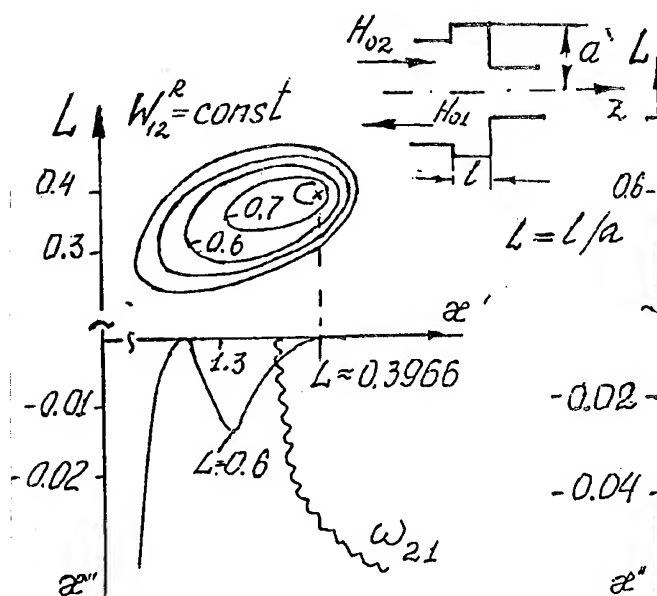


Fig 1.

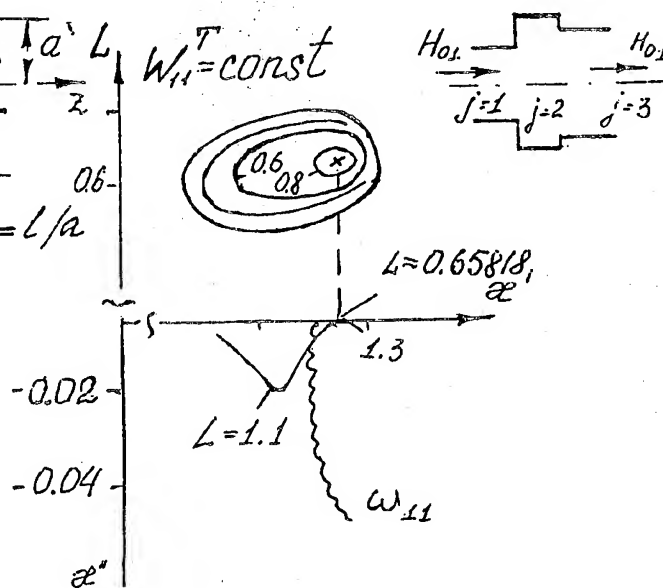


Fig 2.

# RIGOROUS THEORY OF HORN ANTENNAS: ASYMPTOTICAL COMPUTATION OF BACKWARD AND BROADSIDE RADIATION

Tatiana Popkova, Anatoly Slepyan and Gregory Slepyan

Belarus State University for Informatics and Radioelectronics  
P.Brovka st. 6, 220027 Minsk, Belarus

## ABSTRACT

A new rigorous approach to the problem of computation of broadside and backward radiation of horn antennas is suggested. It is based on the theory of dual integral equations associated with Kantorovich-Lebedev integrals.

## INTRODUCTION

Classical theory of horn antennas is based on the asymptotic theory of diffraction (Euygens-Kirchoff's principle). This theory works well in the case of field computation in far zone and 'forward' direction. The present report deals with a rigorous theory of horn antennas which is free of any phenomenological principles and, unlike the classical theory, is valid for field computation in near and transition zones, description of backward and broadside radiation. As an example, we consider two-dimensional  $E$ -plane sectoral horn excited by a line source placed at the vertex. The horn geometry is modelled by a symmetric dihedral angle (see Fig. 1).

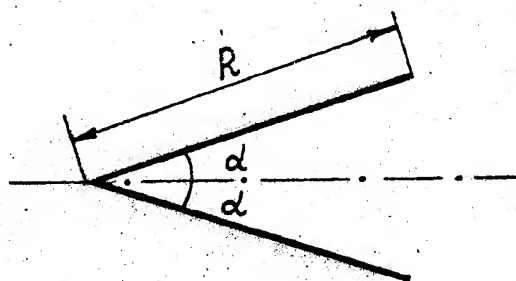


Fig. 1 Geometry of a linear horn

The mathematical statement of the problem in question is to find a solution of the equation

$$(\nabla^2 - \lambda^2)\psi = 0 \quad (1)$$

( $\lambda = jk$ ,  $k$  - wavenumber,  $\psi = H_z$ ) satisfying the boundary condition

$$\left. \frac{\partial \psi}{\partial n} \right|_{\tilde{C}} = 0, \quad (2)$$

where  $\tilde{C}$  is the horn surface.

## METHOD OF ANALYSIS

The first step of our technique is to divide the space into two wedge-shaped partial subareas  $0 < \varphi < \alpha, 0 < r < \infty$  and  $\alpha - \pi < \varphi < 0, 0 < r < \infty$ . Let us present the  $z$ -component of the magnetic field in the first subarea in the form of Kantorovich-Lebedev integral

$$\psi_1 = CK_0(\lambda r) + \int_0^\infty \mathcal{D}(\tau) K_{j\tau}(\lambda r) \cosh[\tau(\varphi - \alpha)] d\tau, \quad (3)$$

where  $\mathcal{D}(\tau)$  is the function sought,  $C$  is the preset constant. The first term in (3) describes the primary field (the field of a linear source placed at the vertex of the horn),  $K_{j\tau}(x)$  - modified Bessel function of the third kind.

The field in the second subarea is presented as

$$\psi_2 = \int_0^\infty \mathcal{B}(\tau) K_{j\tau}(\lambda r) \cosh[\tau(\varphi - \alpha + \pi)] d\tau, \quad (4)$$

where  $\mathcal{B}(\tau)$  is the unknown function to be found.

Using the continuity condition for the tangential component of the electric field at the subareas interface ( $\varphi = 0$ ), we can obtain the following relationship between the unknown functions  $\mathcal{D}(\tau)$  and  $\mathcal{B}(\tau)$ :

$$\mathcal{B}(\tau) = \mathcal{D}(\tau) \frac{\sinh(\tau\alpha)}{\sinh[\tau(\alpha - \pi)]}. \quad (5)$$

Imposing the boundary condition (2) at  $r > R$  and the continuity condition for the tangential component of the magnetic field at the subareas interface  $\psi = 0, r > R$  and using (3)-(5), we obtain the following set of equations for  $\mathcal{D}(\tau)$

$$\int_0^\infty \tau \mathcal{D}(\tau) K_{j\tau}(\lambda r) \sinh(\tau\alpha) d\tau = 0, r < R, \quad (6)$$

$$\int_0^\infty \mathcal{D}(\tau) K_{j\tau}(\lambda r) \frac{\sinh(\tau\pi)}{\sinh[\tau(\alpha - \pi)]} d\tau = CK_0(\lambda r), r > R, \quad (7)$$

Let us introduce new unknown function by the formula

$$d(\tau) = \mathcal{D}(\tau) \frac{\sinh(\tau\pi)}{\sinh[\tau(\alpha - \pi)]}.$$

Then the system (6), (7) can be reduced to the system of dual integral equation including Kantorovich-Lebedev integrals studied by Lebedev and Skal'skaya [1]

$$\int_0^\infty d(\tau) \omega(\tau) K_{j\tau}(\lambda r) d\tau = 0, r < R, \quad (8)$$

$$\int_0^\infty d(\tau) K_{j\tau}(\lambda r) d\tau = cK_0(\lambda r), r > R, \quad (9)$$

where  $\omega(\tau) = \tau \sinh[\tau(\pi - \alpha)] \sinh(\tau\alpha) / \sinh(\tau\pi)$ . The main idea of the solution technique suggested by Lebedev and Skal'skaya is to reduce the system (8), (9) to the Fredholm integral

equation of the second kind for some auxiliary function  $\nu(t)$ . This function is defined by the formula

$$d(\tau) = \frac{2\sqrt{2} \tau \sinh(\tau\pi)}{\pi\sqrt{\pi} \omega(\tau)} \int_R^\infty \nu(t) M(\lambda t, j\tau) dt, \quad (10)$$

where  $M(\lambda t, j\tau) = [K_{1/2+j\tau}(\lambda t) + K_{1/2-j\tau}(\lambda t)]/2$ . Using discontinuous Kantorovich-Lebedev integrals [1], we can show that the function  $d(\tau)$  expressed by the formula (10) identically satisfies the equation (8). Substituting (10) into (9) and performing some transformations, we can obtain the integral equation for  $\nu(t)$

$$\nu(t) + \frac{\lambda}{2\pi} \int_R^\infty \nu(t) K(s, t) ds = f(t), \quad (11)$$

where the kernel  $K(s, t)$  is expressed by the formula

$$K(s, t) = \frac{4}{\pi} \int_0^\infty \Delta(\tau) M(\lambda s, j\tau) M(\lambda t, j\tau) d\tau,$$

where  $\Delta(\tau) = \tau \sinh(\tau\pi)/\omega(\tau) - 2 \cosh(\tau\pi)$ . The free term in (9) is given by the formula

$$f(t) = -\frac{\sqrt{\lambda}}{2\pi} C e^{\lambda t} \frac{d}{dt} \int_t^\infty \frac{e^{\lambda r} K_0(\lambda r) dr}{\sqrt{r-t}}. \quad (12)$$

It is important to note that the integral term in (11) is decreasing with increasing  $|\lambda R|$ . A specific peculiarity of the integral equation (11) is an applicability of the iteration technique for solving (11) at large  $|\lambda|R$  (this case is of the most practical interest). In a first approximation (initial estimate) we have

$$\nu(t) \approx f(t) = -\frac{C\lambda}{\sqrt{2\pi}} K_{1/2}(\lambda t). \quad (13)$$

From Maxwell's equations it follows that

$$E_r|_{\varphi=0} = \frac{j}{\omega\epsilon_0 r} \frac{\partial\psi}{\partial\varphi} \Big|_{\varphi=0} = \frac{j}{\omega\epsilon_0 r} \int_0^\infty d(\tau) \omega(\tau) K_{j\tau}(\lambda r) d\tau. \quad (14)$$

Substituting (10) into (14) and taking into account (13), we obtain

$$E_r|_{\varphi=0} = \frac{j}{2kr} W_0 C e^{jkr} \left( \frac{R}{r-R} \right)^{1/2} \quad (15)$$

The relationship (15) has quite simple and clear form. Note that (15) is applicable for any  $r$  ( $R < r < \infty$ ). This fact can be easily substantiated from the physical point of view: firstly,  $E_r$  expressed by (15) has correct asymptotic behaviour at large  $kr$ ; secondly,  $E_r$  satisfies Meixner condition at the edge  $r = R$ .

Unfortunately, other components and the  $r$ -component of the electric field at arbitrary values of  $\varphi$  cannot be expressed in such simple form as  $E_r$  on the radial extensions of the horn walls. To calculate these components of the electromagnetic field we can use the second Green formula in combination with expression (15). In particular

$$\psi_i(r, \varphi) = \int_R^\infty G_i(r, \varphi | r', 0) \frac{\partial\psi}{\partial\varphi}(r', 0) dr', \quad (16)$$



where  $i = 1, 2$ ,  $G_i$  - Green's functions of the equation (1) for wedge-shaped areas  $0 < \varphi < \alpha$  ( $i = 1$ ) and  $\alpha - \pi < \varphi < 0$  ( $i = 2$ ), satisfying Neumann's boundary condition at  $\varphi = 0, \alpha$  and  $\varphi = \alpha - \pi, 0$  respectively. The expression for  $\partial\psi/\partial\varphi$  at  $\varphi = 0$  results from (15). Various representations of  $G_i$  are given in [2].

Using (16) and Maxwell's equations, one can obtain the expressions for the electromagnetic field in any point of the space. With the aid of (15), (16) we can calculate the fields in near and transition zones, analyse broadside and backward radiation of the linear horns. For such horns the approach suggested seems to be more effective than the incomplete Galerkin method with semiinversion in the boundary conditions [3]. However, the technique [3] can be applied to horns of arbitrary configurations, corrugated horns in particular.

## REFERENCES

- (1) N.N. Lebedev and I.P. Skol'skaya: "Dual integral equations associated with Kantorovich-Lebedev transform", *Applied Mathematics and Mechanics*, (1974), 38, pp. 1090-1097.
- (2) L.B. Felsen and N. Marcuvitz: *Radiation and Scattering of Waves*, Prentice-Hall, New York, 1973.
- (3) A.S. Ilyinsky, G.Ya. Slepyan and A.Ya. Slepyan: *Propagation, Scattering and Dissipation of Electromagnetic Waves* (IEE Electromagnetic Waves series 36), Peter Peregrinus, London, 1993.

# TRANSPARENT BOUNDARIES FOR THE PARABOLIC WAVE EQUATION

Alexei V. Popov

*Institute of Terrestrial Magnetism, Ionosphere and  
Radio Wave Propagation, Russian Academy of Science  
142092 Troitsk, Moscow region, Russia*

(A) The Leontovich-Fock parabolic wave equation (PWE) [1] has many applications to diffraction and wave propagation. It can serve as a powerful computational tool for complicated environments (radio propagation over a curved terrain, in a nonuniform tropospheric duct etc.). A specific difficulty arises when the wave field is to be found in an infinite domain. In order to handle the problem numerically one has to reduce the region to a finite strip (in two dimensions) or to a cylinder (in 3D case) and to transfer the radiation condition posed at infinity onto its border (surface). It is desirable to do that exactly in order to avoid spurious reflections. An exact form of the boundary condition providing full transparency for an arbitrary solution of the PWE in 2D has been found and tested in [2]. An equivalent formula has been published independently in [3]. Here, we discuss this result and make necessary generalization for 3D problems and quasi-stratified environments.

(B) The simplest case is two-dimensional diffraction by a finite dielectric obstacle in the half-space  $z > 0$ . If the dielectric permittivity  $\epsilon(x, z)$  differs not much from unity:  $|\epsilon - 1| \ll 1$ , a paraxial wave beam  $E = u(x, y)e^{ikx}$  can be described by the parabolic equation

$$2ik \frac{\partial u}{\partial x} + \frac{\partial^2 u}{\partial z^2} + k^2(\epsilon - 1)u = 0 \quad (1)$$

Assuming that variation  $\epsilon - 1$  vanishes above the level  $z = a$  we can solve Eq.(1) in the quadrant  $x > 0, z > a$  analytically. So, for a given initial value  $u(0, z) = u_0(z)$  and for an arbitrary boundary value  $u(x, a)$ , the exact solution of Eq.(1) that satisfies the radiation condition can be written in the following form:  $u = v + w$  where

$$v(x, z) = e^{-i\pi/4} \sqrt{k/2\pi x} \left[ \int_{a-z}^{\infty} u_0(z+t) e^{ik \frac{t^2}{2x}} dt - \int_{z-a}^{\infty} u_0(2a-z+t) e^{ik \frac{t^2}{2x}} dt \right] \quad (2)$$

and

$$w(x, z) = - \frac{e^{i\pi/4}}{\sqrt{2\pi k}} \frac{\partial}{\partial z} \int_0^x u(\xi, a) e^{ik \frac{(z-a)^2}{2(x-\xi)}} \frac{d\xi}{\sqrt{x-\xi}} \quad (3)$$

Now we can calculate the normal derivative  $\partial u / \partial z(x, a)$ . Differentiating Eqs.(2)-(3) yields the following relation

$$\frac{\partial u}{\partial z}(x, a) = - e^{-i\pi/4} \sqrt{2k/\pi} \frac{\partial}{\partial x} \int_0^x u(\xi, a) \frac{d\xi}{\sqrt{x-\xi}} + \frac{\partial v}{\partial z}(x, a) \quad (4)$$

It can be considered as a nonlocal generalization of the third-kind boundary condition which enables one to integrate Eq.(1) numerically within the strip  $-a < z < a$ . The finite-difference approximation of Eq.(4) has been examined in [2]. Numerical tests showed full absorption of arbitrary wave packets encountering the interface  $z = a$  from inside of the strip. If the initial function

$u_0(z)$  vanishes for  $z > a$ , the boundary condition (4) takes a homogeneous form

$$-\frac{\partial u}{\partial z}(x, a) = -e^{-i\pi/4} \sqrt{2k} \frac{\partial}{\partial x} u(x, a) \quad (5)$$

that ensues from factorization of the differential operator (1):

$$(2ik \frac{\partial}{\partial x} + \frac{\partial^2}{\partial z^2}) u = (\frac{\partial}{\partial z} + e^{-i\pi/4} \sqrt{2k} \frac{\partial}{\partial x}) (\frac{\partial}{\partial z} - e^{-i\pi/4} \sqrt{2k} \frac{\partial}{\partial x}) u \quad (6)$$

(C) Consider a 3D generalization of the parabolic wave equation

$$2ik \frac{\partial u}{\partial x} + \Delta_{\perp} u + k^2(\epsilon-1) u = 0 \quad (7)$$

assuming that variations  $\epsilon-1$  and the initial value  $u(0, r, \varphi) = u_0(r, \varphi)$  are localized in a vicinity  $r < a$  of the longitudinal axis (a good example is a paraxial wave beam truncated by a finite aperture and propagating through a dielectric quasioptic system). As the PWE (7) can be solved analytically for  $r > a$ , we are able to transfer the radiation condition from infinity to the cylindric boundary  $r = a$ .

Using the Fourier expansion

$$u(x, r, \varphi) = \sum_{m=-\infty}^{\infty} u_m(x, r) e^{im\varphi} \quad (8)$$

and Duhamel principle, one gets an exact expression

$$u(x, r, \varphi) = \frac{1}{2\pi} \frac{\partial}{\partial x} \int_0^x \int_0^{2\pi} u(\xi, a, \psi) d\xi d\psi \sum_{m=-\infty}^{\infty} e^{im(\varphi-\psi)} U_m(x, \xi, r) \quad (9)$$

of the solution  $u(x, r, \varphi)$  outside the cylinder  $r = a$  in terms of its boundary values  $u(x, a, \psi)$ . Here,

$$U_m(x, r) = \frac{1}{2\pi i} \int_{c-i\infty}^{c+i\infty} \frac{H_m^{(1)'}(r\sqrt{2ikp})}{H_m^{(1)'}(a\sqrt{2ikp})} e^{px} \frac{dp}{\sqrt{p}} \quad (10)$$

are partial step functions satisfying the boundary condition

$$U_m(x, a) = \begin{cases} 1, & x > 0 \\ 0, & x < 0. \end{cases} \quad (11)$$

and the radiation condition for  $r \rightarrow \infty$ . Simple calculation yields a perfectly absorbing boundary condition:

$$\frac{\partial u}{\partial r}(x, a, \varphi) = \frac{1}{2\pi} \frac{\partial}{\partial x} \int_0^x \int_0^{2\pi} u(\xi, a, \psi) K(x-\xi, \varphi-\psi) d\xi d\psi \quad (12)$$

with

$$K(x, \varphi) = \frac{e^{-i\pi/4}}{\pi} \sqrt{k/2} \sum_{m=-\infty}^{\infty} e^{im\varphi} \int_{c-i\infty}^{c+i\infty} \frac{H_m^{(1)'}(a\sqrt{2ikp})}{H_m^{(1)'}(a\sqrt{2ikp})} e^{px} \frac{dp}{\sqrt{p}} \quad (13)$$

that enables us to reduce the computation region to the cylinder  $r < a$ .

(D) A parabolic wave equation for UHF propagation in a tropospheric duct has been introduced in [1]

$$2ik \frac{\partial u}{\partial x} + \frac{\partial^2 u}{\partial z^2} + 2k^2 \frac{z}{R^*} \left[ 1 + g(x, z) \right] u = 0 \quad (14)$$

Here, the height-dependent term  $z/R^*$  describes the joint influence of the earth sphericity and barometric refraction ( $R$  is the equivalent earth's radius), and the correction  $g(x, z)$  corresponds to nonuniform variations of the refraction index localized below some reference height  $z=b$ . (similar models comprising a horizontally stratified background and localized perturbations are used in ocean acoustics [4]). Having in mind numerical integration of Eq.(14), we have derived a boundary condition reducing the problem posed in the half-space  $z>0$  to a strip  $0<z<b$ . Omitting details, we just write down the result in dimensionless variables  $\xi=(k/2R^*)^{1/3}x$ ,  $\zeta=(2k^2/R^*)^{1/3}z$ ,  $\beta=(2k^2/R^*)^{1/3}b$ :

$$\frac{\partial u}{\partial \zeta}(\xi, \alpha) = \int_0^\xi \frac{\partial u}{\partial \xi}(\xi', \alpha) K(\xi - \xi') d\xi' \quad (15)$$

Here,

$$K(\xi) = - \frac{1}{2\pi i} \int_{\infty-1c}^{-\infty-1c} e^{it\xi} \frac{w_1'(t-\beta)}{tw_1(t-\beta)} dt \quad (16)$$

and  $w_1(t)$  is Airy-Fock function. It is evident that similar transparent boundary conditions can be obtained for other height-dependent backgrounds.

(E) Our approach to truncation of the computational domain yields a family of special functions being the kernels of integral boundary operators. The simplest 2D example (4) shows that the kernel has a weak singularity at the end of the integration path and some non-local "tail". It is interesting to examine the less trivial examples given above from this point of view.

Consider the 3D parabolic equation (7). In the most interesting axial symmetric case, the boundary condition (12) takes the form

$$\frac{\partial u}{\partial r}(x, a) = \frac{\partial}{\partial x} \int_0^x u(\xi, a) K_0(x - \xi) d\xi \quad (17)$$

with

$$K_0(x) = \frac{e^{-i\pi/4}}{\pi} \sqrt{k/2} \int_{c-1\infty}^{c+1\infty} \frac{H_0^{(1)'}(a\sqrt{2ikp})}{H_0^{(1)}(a\sqrt{2ikp})} e^{px} \frac{dp}{\sqrt{p}} \quad (18)$$

It can be seen that its asymptotic behavior depends on the magnitude of the Fresnel parameter  $q = x/2ka^2$ . For  $q \ll 1$ , substituting the asymptotics  $H_0^{(1)}(z) \sim \sqrt{2/\pi z} e^{i(z-\pi/4)}$  for the Hankel function, one gets

$$K_0(x) \sim -e^{-i\pi/4} \sqrt{2k/\pi x} \quad (19)$$

We see that the boundary operator (17) has the same singularity as its 2D prototype (4) and reduces to the latter for large radii  $a$ . The opposite limiting case  $x \rightarrow \infty$  can be examined by replacing  $H_0^{(1)}(z)$  with its approximation  $2/\pi \log z$  for small  $z$ . It makes possible to

evaluate the integral (18) asymptotically:

$$K_0(x) \sim \int_0^\epsilon e^{-tx} \log \frac{\log(av\sqrt{2k\epsilon}) + i3\pi/4}{\log(av\sqrt{2k\epsilon}) - i\pi/4} dt \approx$$

$$\approx \frac{x}{a} \int_0^\epsilon \frac{e^{-tx}}{\log(av\sqrt{2k\epsilon})} dt \sim -\frac{2}{a \log \frac{x}{2ka^2}} \quad (20)$$

This formula shows that in three dimensions the kernel's tail descends more slowly than  $1/\sqrt{x}$ .

A similar analysis for the PWE (14) in a quasi-stratified medium reveals the same type of singularity:

$$K(\xi) = -\frac{1}{2\pi i} \int_{-\infty-ic}^{\infty-ic} e^{it\xi} \frac{w_1'(t-\beta)}{t w_1(t-\beta)} dt \approx \frac{e^{-i\pi/4}}{\sqrt{\pi\xi}} \quad (21)$$

and a "tail", for large  $\xi$ ,

$$K(\xi) = \frac{w_1'(-b)}{w(-b)} - e^{ibx} \sum_{s=1}^{\infty} \frac{\exp(-t_s \xi e^{-i\pi/6})}{b + t_s e^{i\pi/3}} = \text{Const} + O(e^{-C\xi}) \quad (22)$$

tending exponentially to a constant limit.

This constant does not give nonlocal contribution to the integral boundary operator, therefore, in this case the transparent boundary has extremely short "memory". It is natural because the rays corresponding to the PWE (14) bend upwards and leave the upper boundary  $z = b$  rapidly.

On the contrary, if we write down the analogous boundary condition providing perfect transparency of an arbitrary chosen "bottom" of the nonuniform layer  $a < z < b$ , we will see that the boundary operator has very long "memory". The corresponding kernel

$$K(\xi) = -\frac{1}{2\pi i} \int_{-\infty-ic}^{\infty-ic} e^{it\xi} \frac{v'(t-\alpha)}{t v(t-\alpha)} dt \approx \frac{e^{-i\pi/4}}{\sqrt{\pi\xi}} \quad (21)$$

with  $\alpha = (2k^2/R^*)^{1/3} a$  is closely related to the special function investigated in [5] for the whispering gallery problem.

#### REFERENCES

1. V.A.Fock. Electromagnetic diffraction and propagation problems. Pergamon Press, Oxford, 1965.
2. V.A.Baskakov, A.V.Popov. Implementation of transparent boundaries for numerical solution of the Schrödinger equation. Wave Motion, 14, No 1, 1991, pp.123-128.
3. S.W.Marcus. A generalized impedance method for application of the parabolic approximation to underwater acoustics. J. Acoust. Soc. Am., 90, No 1, pp. 391-398.
4. F.D.Tappert. The parabolic approximation method, in: Lectures Notes in Physics, 70. J.B.Keller, J.S.Papadakis (eds). Wave propagation and underwater acoustics. Springer, New York, 1977.
5. V.M.Babič and V.S.Buldyrev. Short - wavelength diffraction theory (Asymptotic methods). Springer, New York, 1991

# EXCITATION OF THE IMPEDANCE ANTENNA IN THE CIRCULAR WAVEGUIDE

S.D. Priimenko, N.A. Khizhnyak

National Science Center Kharkov Institute of Physics and Technology,  
310108 Kharkov, Ukraine

## ABSTRACT

The equation for an impedance linear antenna in the circular waveguide has been derived. By the averaging method obtained was the solution of the equation for symmetric and antisymmetric current components with taking into account their coupling. The asymptotic expressions being given allow one to describe in the unique form both the resonance and nonresonance cases of excitation. The calculation results for the resonance frequency of the coupled antenna in the waveguide at a frequency above the cutoff are compared with the experimental ones.

## INTRODUCTION

For consideration of loaded waveguiding structures a promising method is of integral equation the macroscopic electrodynamics [1]. For the circular waveguide loaded by the impedance linear antenna this method is developed in [2], [3]. The analogous consideration was applied for the investigation of the linear antenna in [4], [5]. However, the sinusoidal distribution of a current along the linear antenna in [4], and the perfectly conducting uncoupled antenna is considered in [5]. Results from [2], [3] describe the uncoupled impedance antenna and the coupled impedance antenna, which touches the wall of the waveguide by one or two end. The asymptotic expressions for the current describe the real distribution of the current along the antenna.

## ANALITICAL FORMULAS

The symmetric  $J^s$  and antisymmetric  $J^a$  current components being excited in the linear antenna, are described by the system of integrodifferential equation with the small parameter [2], [3]

$$\frac{d^2 J^s(l)}{dl^2} + k^2 J^s(l) = \alpha (i\omega E_0^s(l) + F_0^s[l|J^s] + \bar{F}_0^s[l|J^s] + F^s[l|J^s] + F^s[l|J^a] + (-1)i\omega Z J^s(l)), \quad (1.1)$$

$$\frac{d^2 J^a(l)}{dl^2} + k^2 J^a(l) = \alpha (i\omega E_0^a(l) + F_0^a[l|J^a] + \bar{F}_0^a[l|J^a] + F^a[l|J^a] + F^a[l|J^s] + (-1)i\omega Z J^a(l)), \quad (1.2)$$

where  $\alpha$  is a small parameter,  $E_0^s(l)$ ,  $E_0^a(l)$  are symmetric and antisymmetric components of the intensity of external electric field. In (1.1)  $F_0^s[l|J^s]$ ,  $\bar{F}_0^s[l|J^s]$ ,  $F^s[l|J^s]$  are the functionals dependent on the variable  $l$  and being the symmetrical component of the antenna internal field which depends on the symmetric current component  $J^s(l)$ .  $F_0^s[l|J^s]$  is

determined by the Green function of the Laplace equation  $\frac{1}{R(l,l')}$ ;  $\bar{F}_0^s[l|J^s]$  is determined by the Green function of the

Helmholtz equation  $\frac{e^{ikR(l,l')}}{R(l,l')}$ .  $F^s[l|J^s]$ ,  $F^s[l|J^a]$  is the field of the antenna repeatedly reflected from the waveguide

walls and is determined by the regular Green function.  $F^s[l|J^a]$  is the symmetric component driven by the antisymmetric

current component. The regular tensor Green function  $\hat{G}_e^r(\vec{r}, \vec{r}')$  was obtained in [6] and is related with the Green function of the free space by the relation

$$\hat{G}_e(\vec{r}, \vec{r}') = \hat{I} \frac{ik|\vec{r} - \vec{r}'|}{|\vec{r} - \vec{r}'|} + \hat{G}_e^r(\vec{r}, \vec{r}'), \quad (2)$$

where  $\hat{I}$  is the unit tensor,  $\hat{G}_e(\vec{r}, \vec{r}')$  is the electric tensor Green function for the vector potential of the circular waveguide.

The functionals in (1.2)  $F_0^a[1|I^a]$ ,  $\bar{F}_0^a[1|I^a]$ ,  $F^a[1|I^a]$  are the antisymmetric components of the antenna intrinsic field dependent on the antisymmetric current component;  $F^a[1|I^s]$  is the antisymmetric component of the antenna field reflected from the waveguide and driven by the symmetric current component.

Using the method of averages and introducing the boundary conditions

$$I(-L) = I(+L) = 0, \quad (3)$$

we obtain from the system (1) in the first approximation for  $\alpha$  the resulting current

$$I(l) = \frac{(-1)\alpha \frac{ik}{k}}{\sin 2\bar{k}L - \alpha W^s(ka, 2\bar{k}L) - \alpha W^a(ka, 2\bar{k}L)} (\sin \bar{k}(L-1) \int_{-L}^1 E_0(l') \sin \bar{k}(L+l') dl' + \\ + \sin \bar{k}(L+1) \int_1^L E_0(l') \sin \bar{k}(L-l') dl') \quad (4)$$

and the dispersion equation for the uncoupled impedance antenna

$$\sin 2L(k - \frac{\alpha}{2k} \alpha \ln Z(k)) - \alpha \operatorname{Re} W^s(ka, 2\bar{k}L) - \alpha \operatorname{Re} W^a(ka, 2\bar{k}L) = 0 \quad (5)$$

In (4), (5)

$$W^s(ka, 2\bar{k}L) = \int_{-L}^{+L} (G_{\text{ell}}^s(-L, \xi) + G_{\text{ell}}^s(+L, \xi)) \sin \bar{k}(L - \xi) d\xi, \quad (6.1)$$

$$W^a(ka, 2\bar{k}L) = \int_{-L}^{+L} (G_{\text{ell}}^s(-L, \xi) - G_{\text{ell}}^s(+L, \xi)) \sin \bar{k}(L - \xi) d\xi, \quad (6.2)$$

$\bar{k} = k + \chi$ ,  $\chi = \frac{\alpha}{2k} i\omega Z$ ,  $G_{\text{ell}}^s(l, \xi)$  is the symmetric component of the Green function (2) in the antenna coordinate system.

Solving the system (1), with taking into account the boundary condition

$$\frac{dI(-L)}{dl} = \frac{dI(+L)}{dl} = 0, \quad (7)$$

we obtain for the coupled impedance antenna, the both end of which contact with waveguide walls

$$I(l) = \frac{\alpha \frac{ik}{k}}{\sin 2\bar{k}L - \alpha W^s(ka, 2\bar{k}L) - \alpha W^a(ka, 2\bar{k}L)} (\cos \bar{k}(L-1) \int_{-L}^1 E_0(l') \cos \bar{k}(L+l') dl' + \\ + \cos \bar{k}(L+1) \int_1^L E_0(l') \cos \bar{k}(L-l') dl') \quad (8)$$

where

$$W^s(ka, 2\bar{k}L) = \int_{-L}^{+L} (\frac{1}{k} \frac{d}{d\xi} G_{\text{ell}}^s(-L, l') + (-1) \frac{1}{k} \frac{d}{d\xi} G_{\text{ell}}^s(+L, l')) \cos \bar{k}(L-l') dl', \quad (9.1)$$

$$W^*(ka, 2\bar{k}L) = \int_{-L}^L \left( \frac{1}{k} \frac{d}{d\xi} G_{\omega}(-L, l') + \frac{1}{k} \frac{d}{d\xi} G_{\omega}(+L, l') \right) \cos \bar{k}(L - l') dl' \quad (9.2)$$

The dispersion equation coincides with (5) for the coupled antenna, however in this case  $W^*$ ,  $W^{\#}$  are described by (9.1), (9.2).

The resulting current  $I(l)$  in the coupled antenna, one end of which contacts with the waveguide wall, is the solution of the integrodifferential equation

$$\frac{d^2 J(l)}{dl^2} + k^2 J(l) = \alpha (i\omega E_0(l) + F_0(l|J) + \bar{F}_0(l|J) + F(l|J) + (-1)i\omega ZJ(l)) \quad (10)$$

with the boundary condition

$$I(-L) = \frac{dI(+L)}{dl} = 0 \quad (11)$$

$$I(l) = \frac{(-1)\alpha \frac{i\omega}{k}}{\cos 2\bar{k}L - \alpha W(ka, 2\bar{k}L)} \left( \sin \bar{k}(L + l) \int_{-L}^L E_0(l') \cos \bar{k}(L - l') dl' + (-1) \cos 2\bar{k}L \int_{-L}^L E_0(l') \sin \bar{k}(l - l') dl' \right) \quad (12)$$

The dispersion equation has the form

$$\cos 2\bar{k}L \left( k - \frac{\alpha}{2k} \omega \operatorname{Im} Z(k) \right) - \alpha \operatorname{Re} W(ka, 2\bar{k}L) = 0, \quad (13)$$

where

$$W(ka, 2\bar{k}L) = \int_{-L}^L \left( \sin 2\bar{k}L \frac{1}{k} \frac{d}{d\xi} G_{\text{ell}}(L, l') + G_{\text{ell}}(L, l') \right) \cos \bar{k}(L - l') dl' \quad (14)$$

## NUMERICAL CALCULATION AND EXPERIMENT

The calculation results for the resonance frequency of the coupled antenna in the waveguide at a frequency above the cutoff are compared with the experimental ones. The antenna is oriented by the waveguide radius and is touching to the waveguide

by one end. The ratio resonance frequency  $\frac{f}{f_c}$  ( $f_c$  is the frequency above the cutoff) is calculated as a function of the ratio

length antenna in accordance with (13). The calculation is performed for the perfectly conducting and impedance antenna. The impedance antenna has the form of the rib pivot. The diameter of the perfectly conducting antenna is 1,5 mm; for the impedance antenna, the inner diameter is 1,5 mm, the external diameter is 7,5 mm; the diameter of a waveguide  $D$  is 151 mm. The difference between the calculating and experimental results is about few per cent.

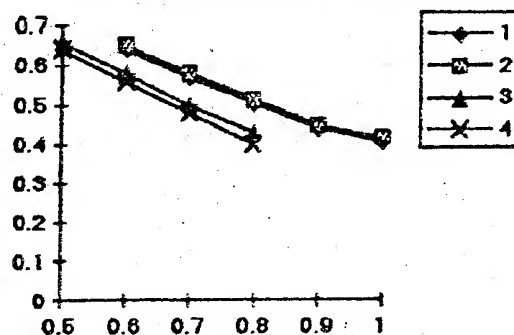


Fig. 1. The ratio resonance frequency  $\frac{f}{f_c}$  ( $f_c$  is the resonance frequency of the antenna)

as a function of the ratio length  $\frac{L}{D}$  ( $L$  is the length of the antenna). The perfectly conducting antenna:

1 - the calculation; 2 - the experiment. The impedance antenna: 3 - the calculation; 4 - the experiment.



## REFERENCES

- (1) N.A.Khizhnyak: "Integral equation of the macroscopic electrodynamics", Kiev: Naukova Dumka, (1986). (In Russian).
- (2) S.D.Prijmenko et. al.: "Impedance linear antenna with the circular cylindrical screen", Preprint KhFTI 92-48, Kharkov, KhFTI (1992). (In Russian).
- (3) S.D.Prijmenko et. al. : "Characteristic resistance of the impedance antenna with the circular cylindrical screen", Preprint KhFTI 93-21, Kharkov, KhFTI (1993).
- (4) Bei-Suo Wang et. al. Acta Electronica Sinica, v.21, №3 (1993), 51.
- (5) J.M.Ifanov: "The scattering of waves by the wire antenna and the small inclusion in the electrodynamics structure". Thesis of Ph. D. in Phys. and Mat., Kharkov, 1990 (In Russian).
- (6) S.D.Prijmenko et. al. : "On the drive of the circular waveguide by the point current source", Preprint KhFTI 91-27. Kharkov: KhFTI, 1991 (In Russian).

# ELECTROMAGNETIC OSCILLATIONS IN A WAVEGUIDE CONJUNCTION WITH MAGNETIZED FERRITE INSERTIONS

*N.I.Pyatak, O.V.Kulakov\**

Radiophysical department of Kharkov State University, Svobody sq., 4 Kharkov 310077 Ukraine  
\*Scientific Centre of Physical Technology, National Academy of Science & Ministry of Education of Ukraine, Novgorodskaya st., 1 Kharkov 310145 Ukraine

## Introduction

Waveguide conjunctions are widely used in super high frequency (SHF) technology [1]. Usually its diffraction properties or natural oscillations are investigated and mainly only isotropic magnetodielectrically-filled systems are considered.

Natural regimes of electromagnetic oscillations in cross-shaped H-plane conjunction of rectangular waveguides with ideally conductive metal walls when one of the waveguides is placed by transversally (along axis  $y$ ) magnetized ferrite insertion (fig.1) are investigated in this work.

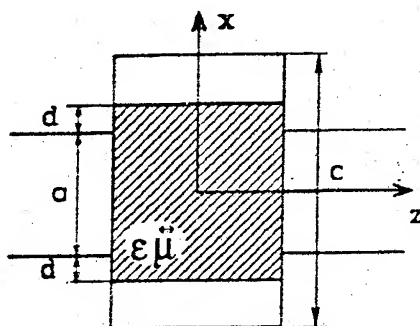


Fig.1

## Statement and solving of the boundary problem

Natural oscillations in the considered system can exist if radiation from every waveguide of conjunction is absent. Oscillations are assumed to be homogenous along axis  $y$  (i.e.  $\frac{\partial}{\partial y} = 0$ ). In this case Maxwell equations turn into two independent systems of equations. One of those systems describes E-oscillations and another- H-oscillations. In the considered system E-oscillations can not exist [2]. Magnetized ferrite can be described by scalar value of electrical permittivity  $\epsilon$  and magnetic permeability tensor  $\mu$  of the standard type [2].

First let us consider an open conjunction with ferrite parallelepiped only in connection region of waveguides ( $d=0, c \rightarrow \infty$ ). Let us perform the solving of the problem using a method of partial regions with the separation of a connection region where field presents itself as a superposition of fields of partial waveguides. Finding the solving of Helmgolz equation for the only different from zero component  $E_y(x,z)$  of electromagnetic field with corresponding boundary conditions and radiation condition, using the continuity condition for tangent components of the field on the partial boundary regions and using the biorthogonality condition

of waves in the transmission line with gyrotropic filling we get a system of linear algebraic equations (SLAE) of the 2-nd kind as to unknown amplitudes. Using existence condition of untrivial solving of the SLAE we can find a disperse equation, which allows to receive natural wavelength  $\lambda$  of the lowest magnetic mode oscillations of the considered structure:

$$\text{Det}\{\delta_{tn} - Q_{tn}\} = 0$$

$$\text{where } \delta_{tn} = \begin{cases} 1 & \text{at } t \neq n, \\ 0 & \text{at } t = n, \end{cases} \quad Q_{tn} = \sum_m P_{tm} S_{nm}.$$

$$P_{tm} = \frac{4tm\pi^2(-1)^{\frac{t+m}{2}}}{ab^2\left[\left(\frac{t\pi}{b}\right)^2 - \Gamma_{ma}^2\right]\left[\Gamma_{tb}\text{tg}\left(\Gamma_{tb}\frac{a}{2}\right) - \gamma_{tb}\mu_{\perp}\right]},$$

$$S_{nm} = \frac{4nm\pi^2(-1)^{\frac{n+m}{2}}}{a^2b\left[\left(\frac{m\pi}{a}\right)^2 - \Gamma_{nb}^2\right]\left[\Gamma_{ma}\text{tg}\left(\Gamma_{ma}\frac{b}{2}\right) - \gamma_{ma}\mu_{\perp}\right]},$$

$$\Gamma_{nb}^2 = \kappa^2\epsilon\mu_{\perp} - \left(\frac{n\pi}{b}\right)^2, \quad \gamma_{nb}^2 = \left(\frac{n\pi}{b}\right)^2 - \kappa^2, \quad \kappa = \frac{2\pi}{\lambda},$$

$\mu_{\perp}$  - effective magnetic permeability,

$a, b$  - dimensions of wide walls of waveguides.

At the great  $t, n$  and  $m$  matrix elements  $Q_{tn}$  behave like  $O\left(\frac{mn}{(m^2+n^2)(m^2+t^2)}\right)$ ,

so the equation received can be applied by the reduction method. Numerical investigations have confirmed that the algorithm convergency rate is quite high.

Having taken off the outside magnetic field ( $\mu_{\perp} \rightarrow \mu$ ) the received disperse equation turns into equation describing natural oscillations  $H_{110}$  of the field of magnetodielectrical parallelepiped in cross-shaped waveguide conjunction [3].

If metal short-circuited planes are installed at the distance  $\frac{c}{2}$  from the symmetry axis of conjunction in a waveguide of width  $b$  then disperse equation should be changed as following:

$$\gamma_{tb}\mu_{\perp} \rightarrow \gamma_{tb}\mu_{\perp} \text{cth}\left[\gamma_{tb}\frac{c-a}{2}\right].$$

If the waveguide of width  $b$  of an open conjunction is completely filled with transversally magnetized ferrite then determinant element  $P_{tm}$  should be changed

as following:

$$P_m = \frac{-4tm\pi^2(-1)^{\frac{l+m}{2}}}{ab^2\left[\left(\frac{t\pi}{b}\right)^2 + \Gamma_{ma}^2\right]\Gamma_{tb}\left[t\left(\Gamma_{tb}\frac{a}{2}\right) + 1\right]}$$

where  $\Gamma_{ma}$  and  $\Gamma_{tb}$  are imaginary values. And, finally, if the waveguide of width  $b$  of open conjunction is placed with magnetized ferrite parallelepiped of finite length ( $0 < d < \infty$ ) then in the last term in the factor  $\left(t\left(\Gamma_{tb}\frac{a}{2}\right) + 1\right)$  should be

$$\frac{\gamma_{tb} \mu_{\perp} \operatorname{cth}(\Gamma_{tb} d) + \Gamma_{tb}}{\Gamma_{tb} \operatorname{cth}(\Gamma_{tb} d) + \gamma_{tb} \mu_{\perp}}$$

instead of the item equal to unity.

Numerical investigations have shown and experimental data confirmed that natural wavelengths of the lowest magnetic type of oscillations of open symmetrical cross-shaped conjunction with ferrite parallelepiped in the connection region of waveguides are situated beyond cutoff range of ferrite-filled segments of waveguides irrespective of external magnetic field quantity. Introducing of lugs  $d$  ( $0 < d < \infty$ ) does not lead to essential changing of natural wavelength quantity when  $\mu_{\perp}$  is fixed.

Presence of the metal short-circuited planes, starting from some value  $\frac{c}{a}$  and asymmetry of the system, starting from some  $\frac{a}{b}$  lead to that ferrite-filled waveguides become not beyond cutoff and resonance volume become restricted by critical sections.

Character of reconstruction of natural wavelength of the lowest magnetic types of oscillations of ferrite-filled cross-shaped waveguide conjunctions of all considered types keeps similar at the changing of external magnetic field value.

Cross-shaped conjunction of rectangular waveguides with magnetized ferrite insertions in natural oscillation regime can be used for creating frequency-selective electrically and (or) mechanically reconstruction devices. It is more expedient, however, to use it as a cell for SHF control and measurement of parameters of magnetized ferrite. Parameters control is based on measuring of natural wavelength of conjunction with tested sample and comparing it with a standard one. Measuring of parameters is carried out by means of the method of two thicknesses. Measurement error is not more than 10%.

## References

1. Резонансное рассеяние волн; в 2-х т. /В.П.Шестопалов, А.А.Кириленко, С.А.Масалов, Ю.К.Сиренко.-Киев:Наукова думка,1986.
2. Гуревич А.Г. Магнитный резонанс в ферритах и антиферромагнетиках. - М.:Наука, 1973. -591с.
3. Коробкин В.А., Осинцев В.В. Собственные резонансы крестообразного разветвления прямоугольных волноводов с магнитодиэлектрическим заполнением. //ЖТФ-1985. -Т. 55. -В. 10. -С. 1907-1912.

# DEVELOPMENT OF TIME-DOMAIN UNIFORM GEOMETRICAL THEORY OF DIFFRACTION AND ITS MODIFICATIONS FOR ANALYZING THE TRANSIENT SCATTERING FROM CURVED WEDGE CONFIGURATIONS

Paul R. Rousseau and Prabhakar H. Pathak  
The Ohio State University ElectroScience Laboratory  
1320 Kinnear Road  
Columbus, Ohio 43212, USA

Tel: (614) 292-7981

Fax: (614) 292-7927

## SUMMARY

Transient electromagnetic (EM) phenomenon are best studied directly in the time-domain (TD). Some transient EM phenomenon of significant interest are those associated with the interaction of natural and man-made EM pulses (such as those due to lightning and explosions) with complex objects (e.g., aircraft and spacecraft), and also those associated with ultra-wideband or transient (or impulse) radars which are being developed for potential use in radar target identification and in radar remote sensing of subsurface targets, etc. Unfortunately, exact analytical solutions in TD are available for only a few simple configurations, whereas brute force numerical solutions in TD lack physical insight and can become inefficient for objects which are large compared to the smallest wavelength present in the frequency content of the exciting pulse. On the other hand, the development of a time-domain (TD) version of the uniform geometrical theory of diffraction (UTD), i.e., TD-UTD, would provide approximate analytical solutions directly for the transient response of pulse excited radiating objects of relatively complex shapes. Furthermore, such a TD-UTD would provide essentially the same physical insight into the radiation and scattering mechanisms as does the frequency domain UTD. Thus, the simple ray picture of the frequency domain UTD transforms into a corresponding progressing wave picture (along time domain rays) in the TD-UTD. Development of a TD-UTD solution is possible by analytically inverting into TD the corresponding UTD solution available in the frequency domain. Since the UTD solution is valid at high frequencies, the corresponding TD-UTD will generally be valid for short to intermediate times with respect to the times of arrivals of each of the different wavefronts (corresponding to various geometrical optics and diffracted rays which arrive at the observation point). The TD-UTD is thus expected to complement (or overlap) with TD numerical methods which are best suited for intermediate to late times. Some previous related work is that due to Veruttipong [1] who obtained a TD-UTD for a perfectly-conducting straight wedge and that due to Heyman and Felsen [2, 3] who developed a spectral theory of transients (STT) for some simple configurations. The work reported in this paper is based on an approach which is different from that in [1]-[3] and it deals with a general curved wedge configuration.

The development of a TD-UTD for a perfectly conducting curved wedge which has been completed recently will be presented. It is obtained by inverting the corresponding frequency domain UTD for edges as developed previously by Kouyoumjian and Pathak [4]; thus, if  $\bar{F}(\omega)$  denotes the UTD frequency domain solution, then the corresponding TD-UTD solution denoted by  $\bar{f}(t)$  can be expressed as

$$\bar{f}(t) = \text{Re} \bar{f}_+(t) \quad ; \quad \text{Im} t = 0$$

where

$$\bar{f}_+(t) = \frac{1}{\pi} \int_0^{\infty} \bar{F}(\omega) e^{-\omega(-jt)} d\omega \quad ; \quad \text{Im} t > 0$$

and  $\omega$  denotes angular frequency (radians/sec) as usual, while  $t$  denotes complex time. Also,

$$\bar{F}(\omega) U(\omega) = \frac{1}{2} \int_{-\infty+j\epsilon}^{\infty+j\epsilon} \bar{f}_+(t) e^{t(-j\omega)} dt$$

in which  $U(\omega)$  represents the Heaviside step function. The use of complex time  $t$  has several advantages over the conventional inversion techniques where  $t$  is always real.

If a UTD ray traverses a line or smooth caustic, then its field undergoes a phase jump described by  $j \text{sgn}(\omega)$ . Normally the  $j \text{sgn}(\omega)$  would be associated with a Hilbert transform operation in the time domain, but with the complex time representation  $\bar{f}_+(t)$  it is simply a constant factor of  $j$ . Such a phase jump may lead to a corresponding TD-UTD which is non-causal. However, it will be shown that time causality for any single TD-UTD ray interaction passing through a line or a smooth caustic can be restored using a recently developed simple rule that is based on an integral representation for TD fields; namely: "causal turn-on time for an otherwise non-causal TD-UTD ray contribution which has passed through a line or smooth caustic = arrival time for the shortest path from source to observer via only that portion of the surface/line source distribution which generates the caustic." This rule indicates how causality must be enforced via "global" considerations. A "local" ray field does not contain all of this required information leading to TD non-causality in the first place!

The inversion of UTD based  $\bar{F}(\omega)$  to arrive at the corresponding  $\bar{f}(t)$  (with  $\text{Im} t = 0$ ) of TD-UTD yields a TD-UTD response to a progressing wavefront illumination which is impulsive in time. Thus, to obtain the response  $\bar{h}(t)$  to some general time dependent incident waveform with time-dependence  $g(t)$  where  $\bar{H}(t) = \text{Re} \bar{h}_+(t)$  and  $g(t) = \text{Re} g_+(t)$ , with  $\text{Im} t = 0$ , one must use the convolution theorem which is expressed below as a complex contour integral.

$$\bar{h}_+(t) = \frac{1}{2} \int_{-\infty+j\epsilon}^{\infty+j\epsilon} \bar{f}_+(t-t') g_+(t') dt' \quad ; \quad \text{Im} t > 0.$$

The above form of the convolution theorem for complex  $t$ , in contrast to the conventional real time convolution, has the advantage that if one expresses the relatively arbitrary input time waveform  $g(t)$  in a set of a few "special" basis functions, then the complex

convolution can be evaluated in closed form (rather than numerically) thus retaining the numerical advantages gained by obtaining an analytical TD-UTD impulse response  $\tilde{f}(t)$ .

While the UTD overcomes the limitations of the conventional geometrical theory of diffraction (GTD) [5] within ray shadow boundary transition regions, the UTD still needs to be patched up in regions of ray caustics, and overlapping shadow boundary and caustic transition regions using the equivalent current method (ECM) (or the incremental theory of diffraction (ITD)) [6]–[8] and the physical theory of diffraction (PTD) [9, 10], respectively. Hence, it is also useful to develop along with TD-UTD, a TD-ECM (or TD-ITD) and TD-PTD for curved wedge configurations. Such a development of TD-ECM and TD-PTD for edged bodies will also be described. Applications of the TD-UTD for edges and its above modifications will be illustrated for curved parabolic strips, circular discs and finite length circular cylinders, as well as for an impulse radiating antenna (IRA) which employs a parabolic reflector (as designed by C. Baum and E. Farr, [11, 12]).

## REFERENCES

- [1] T.W. Veruttipong, "Time-Domain Version of the Uniform GTD," *IEEE Trans. on Antennas and Propagat.*, Vol. AP-38, pp. 1757–1764, 1990.
- [2] E. Heyman and L.B. Felsen, "Weakly Dispersive Spectral Theory of Transients (STT), Part I: Formulation and Interpretation," *IEEE Trans. on Antennas and Propagat.*, Vol. AP-35, pp. 80–86, 1987.
- [3] E. Heyman and L.B. Felsen, "Weakly Dispersive Spectral Theory of Transients (STT), Part II: Evaluation of the Spectral Integral," *IEEE Trans. on Antennas and Propagat.*, Vol. AP-35, pp. 574–580, 1987.
- [4] R.G. Kouyoumjian and P.H. Pathak, "A Uniform Geometrical Theory of Diffraction for an Edge in a Perfectly-Conducting Surface," *Proc. of the IEEE*, Vol. 62, No. 11, pp. 1448–1461, 1974.
- [5] J.B. Keller, "Geometrical Theory of Diffraction," *J. Opt. Soc. Am.*, Vol. 52, pp. 116–130, 1962.
- [6] C.E. Ryan, Jr. and L. Peters, Jr., "Evaluation of Edge Diffracted Fields including Equivalent Currents for Caustic Regions," *IEEE Trans. on Antennas and Propagat.*, Vol. AP-7, pp. 2982–299, 1969.
- [7] E.F. Knott and T.B.A. Senior, "Comparison of Three High-Frequency Diffraction Techniques," *Proc. IEEE*, Vol. 62, No. 11, pp. 1468–1474, 1974.
- [8] R. Tiberio and S. Maci, "An Incremental Theory of Diffraction: Scalar Formulation," *IEEE Trans. on Antennas and Propagat.*, Vol. 42, pp. 600–612, 1994.
- [9] P.Ya. Ufimtsev, "Method of Edge Waves in the Physical Theory of Diffraction," translation from Russian (Izd-Vo. Sov. Radio, pp. 1–243, 1962) prepared by the U.S. Air Force Foreign Technology Division, Wright Laboratories (formerly WPAFB), Ohio, USA; released for public distribution Sept. 7, 1971.



- [10] S.W. Lee, "Comparison of Uniform Asymptotic Theory and Ufimtsev's Theory of EM Edge Diffraction," *IEEE Trans. on Antennas and Propagat.*, Vol. 25, No. 2, pp. 162-170, 1977.
- [11] C.E. Baum, "Aperture Efficiencies for IRAs," *IEEE Antennas and Propagation Society International Symposium*, July 1992, Hyatt Regency, Chicago, Illinois, Vol. III of Symposium Digest, pp. 1228-1231.
- [12] E.G. Farr, "Analysis of the Impulse Radiating Antenna," *IEEE Antennas and Propagation Society International Symposium*, July 1992, Hyatt Regency, Chicago, Illinois, Vol. III of Symposium Digest, pp. 1232-1234.

# ON JUSTIFICATION OF THE METHOD OF DISCRETE SINGULARITIES FOR SOME PROBLEMS OF ELECTRODYNAMICS

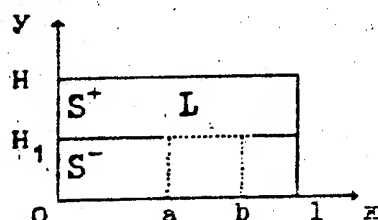
Miroslav Samoilenko

Department of Mechanics and Mathematics  
Kharkov State University  
4, Svobodi sq., Kharkov, 310077, Ukraine

The eigenfrequency problem for rectangular cylindrical waveguide with a slot is considered. This problem is reduced to a characteristic value problem for an integral meromorphic operator-function. An application of the method of discrete singularities to solution of the latter problem is grounded. Besides, some general theorem on convergence is proved and Fourier method is grounded either.

## §1. Statement of the problem

Let us consider the wave propagation process in a cylindrical waveguide with the section



We assume that the areas above and under the slot are filled with isotropic dielectrics whose dielectric permeabilities equal to  $\epsilon^+$  and  $\epsilon^-$  correspondingly, and magnetic permeabilities equal to 1. Considering TM-waves, we arrive at the following set of Gel'mholtz equations

$$\begin{cases} \Delta u^+ + \lambda u^+ = 0, S^+ \cup S^-; \\ u^+ = 0, \partial S^+ \setminus L; \\ u^+ = u^-, L; \\ \frac{1}{\epsilon^+} \frac{\partial u^+}{\partial y} = \frac{1}{\epsilon^-} \frac{\partial u^-}{\partial y}, L. \end{cases} \quad (1.1)$$

We are to find a complex number  $\lambda$  such that (1.1) has a non-trivial solution. As is known this set can be reduced to coupling equation

$$\begin{cases} \sum_{n=1}^{\infty} c_n \sin \frac{\pi n x}{l} = 0, x \in [0, a) \cup (b, 1]; \\ \sum_{n=1}^{\infty} c_n f_n(\lambda) \sin \frac{\pi n x}{l} = 0, x \in (a, b), \end{cases} \quad (1.2)$$

where  $f_n(\lambda)$  are meromorphic functions such that  $f_n(\lambda) = O(n)$

as  $n$  tends to infinity.

Last research of Yu. Gandel allows us to transform (1.2) to the following problem. We are to find a nontrivial function  $u(x) \in L_{2,p}[-1,1]$ , where  $p(x) = \sqrt{1-x^2}$ , and a complex number  $\lambda$  such that

$$\begin{cases} \int_{-1}^1 \frac{u(x)}{x-x_0} \frac{dx}{\sqrt{1-x^2}} + \int_{-1}^1 K(x, x_0; \lambda) u(x) \frac{dx}{\sqrt{1-x^2}} = 0; \\ \int_{-1}^1 u(x) \frac{dx}{\sqrt{1-x^2}} = 0. \end{cases} \quad (1.3)$$

where  $K(x, x_0; \lambda)$  is smooth with respect to  $x$  and  $x_0$ , and meromorphic with respect to  $\lambda$ .

## §2. Theorems on convergence

Thus we arrive at the following problem. We are to find a complex number  $\lambda$  and vector-function  $\varphi(\lambda)$  such that

$$A(\lambda)\varphi(\lambda) \Big|_{\lambda=\lambda_0} = 0, \quad \varphi(\lambda_0) \neq 0,$$

where  $A(\lambda)$  is finite-meromorphic operator-function of Fredholm type. Basic definitions according to operator-functions and the Rouché theorem were represented in (1). Further development of this theory and its application to wave propagation problems were shown in (2).

Define  $[H^{(1)}, H^{(2)}]$  as the set of linear continuous operators acting in the pair of separable Hilbert spaces  $(H^{(1)}, H^{(2)})$ . Let  $K(\lambda)$  be a holomorphic compact-valued operator-function,  $L \in [H^{(1)}, H^{(2)}]$  be an invertible operator. Let all characteristic values of the operator-function  $A(\lambda)$  be normal points. Let  $\{K_n(\lambda)\}_1^\infty$  be a sequence of holomorphic compact-valued operator-functions converged to  $K(\lambda)$  uniformly on any compact set  $F$  in  $\mathbb{C}$ . Under these assumptions the following theorem is valid.

### THEOREM 1 on convergence

In any neighborhood of a characteristic value  $\lambda_0$  of the operator-function  $A(\lambda)$ , beginning with some number, there are so many characteristic values of the operator-function  $A_n(\lambda) = L + K_n(\lambda)$  that the sum of their degrees equals to the degree of  $\lambda_0$ . In terms of the Rouché theorem it can be written as follows:

$$\forall \varepsilon > 0 \exists N \in \mathbb{N} \forall n \geq N : M(A(\lambda); \partial U_\varepsilon(\lambda_0)) = M(A_n(\lambda); \partial U_\varepsilon(\lambda_0))$$

Any convergent sequence of characteristic values of  $A_n(\lambda)$  converges to a characteristic value of  $A(\lambda)$ .

#### COROLLARY

Let operator-functions  $A(\lambda)$  and  $A_n(\lambda)$  be holomorphic in an area  $G$  and satisfy conditions of the theorem on convergence.

Then any convergent sequence of characteristic values of operator-functions  $A_n(\lambda)$  converges either to a characteristic value of  $A(\lambda)$  or to a point on the boundary of  $G$ .

Let there exist two sequences of subspaces  $\{H_n^{(1)}\}_1^\infty$ ,  $\{H_n^{(2)}\}_1^\infty$  such that

$$H_n^{(1)} \subset H_{n+1}^{(1)} \subset H^{(1)}, \quad n \in \mathbb{N}, \quad 1=1,2;$$

$$\forall x \in H^{(1)} \quad \forall \varepsilon > 0 \quad \exists N^{(1)} \in \mathbb{N} \quad \forall n \geq N^{(1)}: \|x - P_n^{(1)}x\| < \varepsilon$$

$$\dim H_n^{(1)} = \dim H_n^{(2)} < \infty,$$

and operator  $L$  be continuously invertible in pairs of spaces  $(H_n^{(1)}, H_n^{(2)})$ . Here  $P_n^{(i)}$  are orthogonal projectors of  $H^{(i)}$  upon  $H_n^{(i)}$ . Let us approximate  $K(\lambda)$  with  $K_n(\lambda) = P_n^{(2)}K(\lambda)P_n^{(1)}$ .

#### THEOREM 2

The sequence  $\{K_n(\lambda)\}$  converges to  $K(\lambda)$  uniformly on any compact set  $F$  in  $\mathbb{C}$ .

Thus operator-functions  $A_n(\lambda) = L + K_n(\lambda)$  and  $A(\lambda)$  satisfy conditions of the theorem on convergence. To calculate characteristic values of  $A_n(\lambda)$  one should choose orthonormal basic sets  $\{e_i\}_1^m$  and  $\{g_i\}_1^m$  in  $H_n^{(1)}$  and  $H_n^{(2)}$  correspondingly, and compare the determinant of the matrix

$$\| \langle Le_i + K(\lambda)e_i, g_j \rangle \|_{i,j=1}^m$$

to zero, where  $\langle \cdot, \cdot \rangle$  is the inner product in  $H^{(2)}$ .

#### §3. Singular integral equations

It is convenient to write (1.1) in the form

$$(\Gamma + K(\lambda))u = 0, \quad (3.1)$$

where  $\Gamma$  is integral operator with Cauchy kernel, and operators  $L$  and  $K_n(\lambda)$  act in the pair of Hilbert spaces  $(L_{2,p}^0[-1,1], L_{2,p}^0[-1,1])$ .

To calculate characteristic values we can use Fourier, or semi-inverting, method. Define  $H_n^{(1)} = \text{Lin}\langle T_1, \dots, T_n \rangle$ ,  $H_n^{(2)} = \text{Lin}\langle U_0, \dots, U_{n-1} \rangle$ , where  $T_k$ ,  $U_k$  are Tchebycheff's polynomials of the first and second types. Thus we are to compare the

determinant of the matrix

$$\|\delta_{ij} + \langle K(\lambda)T_i, U_j \rangle\|_{i=1}^m \quad j=0^{m-1}$$

to zero. This method possesses a defect of computation of double integrals. This fact essentially influences on the speed of calculation.

The method of discrete singularities, which is represented below, is free of this defect. It consists in substituting orthogonal projectors with interpolating ones. Jackson's theorems supply the uniform convergence of approximating operator-functions. Using this method we arrive at the system

$$\begin{cases} \sum_{i=1}^n \frac{u(x_i)}{x_i - x_{0j}} + \sum_{i=1}^{\infty} K(x_i, x_{0j}; \lambda) u(x_i) = 0, & j=1, n-1 \\ \sum_{i=1}^n u(x_i) = 0, & j=n \end{cases} \quad (3.2)$$

where  $\{x_i\}_1^n$  are roots of the polynomial  $T_n$ ,  $\{x_{0j}\}_1^{n-1}$  are roots of the polynomial  $U_{n-1}$ .

Comparing the determinant of the corresponding matrix to zero, we can obtain approximate characteristic values. Numerical experiments have shown the strong convergence of this method.

(1) I.Gohberg, Y.Sigal: "Operator generalization of the theorem on logarithmic residue and the Rouché theorem", Mathematical collection, (1971), vol.84, №4, pp.607-629, (Russian).

(2) A.Iliniski, Yu.Shestopalov: "An application of methods of spectrum theory to wave propagation problems", Moscow, Publishing House of Moscow University, 1989, 184p. (Russian)

(3) Yu.Gandel, T.Polyanskaya, S.Yeremenko: "Mathematical problems of the method of discrete currents", Kharkov, Publishing House of Kharkov University, 1992, 145p. (Russian)

# ELECTROMAGNETIC WAVE SCATTERING BY A LOADED TROUGH ON THE GROUND

Ryoichi SATO \* and Hiroshi SHIRAI

*Department of Electrical and Electronic Engineering  
Faculty of Science and Engineering, Chuo University  
1-13-27 Kasuga, Bunkyo-ku, Tokyo 112 Japan.*

## Abstract

In this paper, plane wave scattering by a loaded rectangular trough has been analyzed using the Nomura and Katsura's method, which can be applied for various mixed boundary problems. This method is based on the characteristics of Weber-Schafheitlin's discontinuous integrals for Bessel functions. It is found that our calculated Radar Cross Section (RCS) results coincide with those obtained by other method. Numerical calculation has been done extensively, and RCS values for loaded trough will be presented.

## 1 Introduction

Electromagnetic wave scattering by a trough on the ground plane has been analyzed by many authors[1-4]. This is due to the fact that this configuration can be a model of many practical objects such as a crack, a pit on the optical disks and a corrugation for antennas. Plane wave scattering by a rectangular empty trough on the perfectly conducting ground has been formulated using the Weber-Schafheitlin's discontinuous integrals[5]. In this paper, the previous analysis for the empty trough case has now been extended for the trough filled by material. Numerical calculation has been done to obtain monostatic radar cross section, which coincides with the result derived from the another method[6]. Scattering far field patterns are also calculated here. Time harmonic factor  $e^{-i\omega t}$  is assumed here and suppressed throughout the context.

## 2 Formulation

As illustrated in Fig.1, H-polarized electromagnetic plane wave:

$$\phi^i (= H_z^i) = \exp[-ik_0(x \cos \theta_0 + y \sin \theta_0)] \quad (1)$$

impinges on the aperture of a perfectly conducting trough of width  $2a$ , and depth  $b$ .  $k_0 (= \omega \sqrt{\epsilon_0 \mu_0})$  denotes free space wavenumber. For later convenience, the total field  $\phi^t$  for the semi-infinite half space ( $y > 0$ ), may be considered as

$$\phi^t = \phi^i + \phi^r + \phi, \quad (2)$$

where  $\phi^r$  is the reflected plane wave:

$$\phi^r = \exp[-ik_0(x \cos \theta_0 - y \sin \theta_0)], \quad (3)$$

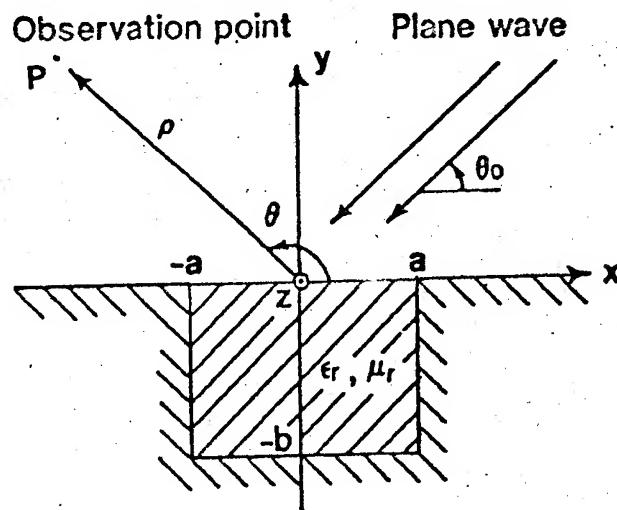


Figure 1: Rectangular trough on a conducting ground.

and  $\phi$  is the scattering contribution due to the existence of the trough, respectively. This contribution  $\phi$  may be written as a spectral integral form:

$$\phi = \sqrt{\frac{\pi u}{2}} \int_0^\infty \sqrt{\xi} \{f(\xi) J_{-1/2}(\xi u) + g(\xi) J_{1/2}(\xi u)\} e^{-\sqrt{\xi^2 - \kappa_0^2} v} d\xi. \quad (4)$$

In the above equation,  $f(\xi)$  and  $g(\xi)$  are arbitrary weighting functions and Cartesian coordinate  $(x, y)$  is normalized by  $a$ , i.e.  $x = au$ ,  $y = av$ ,  $\kappa_0 = k_0 a$ , and  $b = b_0 a$ . By choosing the weighting functions as

$$f(\xi) = \sum_{m=0}^{\infty} A_m \frac{J_{2m}(\xi)}{\sqrt{\xi^2 - \kappa_0^2}}, \quad g(\xi) = \sum_{m=0}^{\infty} B_m \frac{J_{2m+1}(\xi)}{\sqrt{\xi^2 - \kappa_0^2}}, \quad (5)$$

with unknown coefficients  $A_m$  and  $B_m$ , the integral becomes a class of Weber-Schafheitlin's discontinuous integrals. Accordingly, one can automatically satisfy the boundary condition on the ground ( $|x| > a, y = 0$ ).

For a trough region, one can expand the internal field  $\phi^{(II)}$  by waveguide eigen modes as

$$\phi^{(II)} (= H_z^{(II)}) = \sum_{n=0}^{\infty} F_n \cos\left\{\frac{n\pi}{2}(1-u)\right\} [e^{-ih_n v} + e^{ih_n(v+2b_0)}] \quad (6)$$

with the modal propagation constant  $h_n = \{k^2 - (n\pi/2)^2\}^{1/2}$  with respect to the  $y[v]$  direction.  $F_n$  are the modal excitation coefficients to be determined, where  $k (= k_0 \sqrt{\epsilon_r \mu_r})$  is wavenumber for the trough region. By using the continuity condition of the tangential field components at the aperture of the trough ( $|x| \leq a, y = 0$ ), one can determine the unknown coefficients  $A_m$ ,  $B_m$  and  $F_n$ . Following the procedure discussed in Refs.[8,9], one may end up with the simultaneous equations:

$$\sum_{m=0}^{\infty} A_m \{G(2m, 2q) + GN(2m, 2q)\} = -2J_{2q}(\kappa_0 \cos \theta_0), \quad (7)$$

$$\sum_{m=0}^{\infty} B_m \{G(2m+1, 2q+1) + GN(2m+1, 2q+1)\} = 2iJ_{2q+1}(\kappa_0 \cos \theta_0), \quad (8)$$

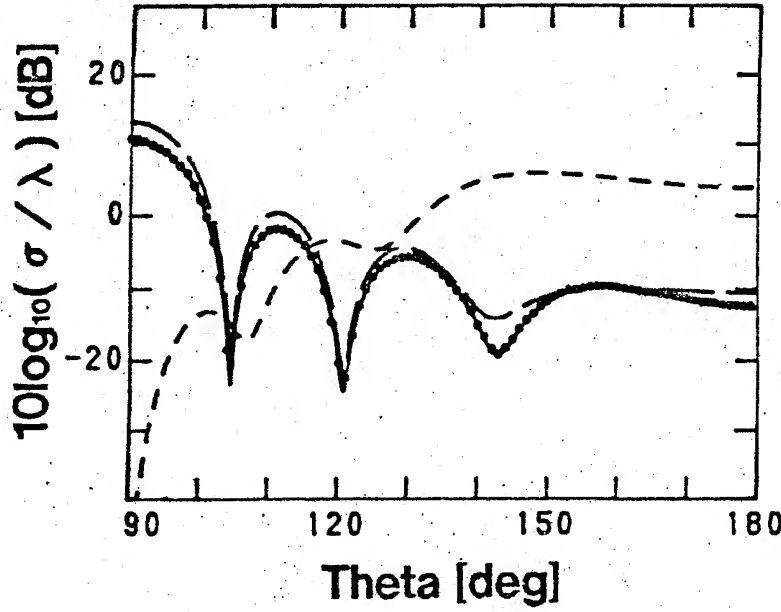


Figure 2: Monostatic RCS calculation from a rectangular trough.  $a = 1.0\lambda$ ,  $b = 0.5\lambda$ , —:  $(\epsilon_r = 2.5 + i0.2, \mu_r = 1.8 + i0.1)$ ; - - -:  $(\epsilon_r = 1.0, \mu_r = 1.0)$ ; ····: Ref.(6), - · - ·:  $(\epsilon_r = 2.5 + i0.2, \mu_r = 1.8 + i0.1, b = 1.0\lambda)$ .

where the function  $G(p, q)$  is given by

$$G(p, q) = \int_0^\infty \frac{J_p(\xi) J_q(\xi)}{\sqrt{\xi^2 - \kappa_0^2}} d\xi, \quad (9)$$

which can be easily computed by a series expansion [7]. Function  $GN(\cdot, \cdot)$  is given by

$$GN(2m, 2q) = -\pi\epsilon_r \sum_{n=0}^{\infty} \frac{J_{2m}(n\pi) J_{2q}(n\pi) (1 + e^{i2h_{2n}ab_0})}{(1 + \delta_{0n})(ih_{2n}a)(1 - e^{i2h_{2n}ab_0})}, \quad (10)$$

$$GN(2m+1, 2q+1) = -\pi\epsilon_r \sum_{n=0}^{\infty} \frac{J_{2m+1}(\frac{2n+1}{2}\pi) J_{2q+1}(\frac{2n+1}{2}\pi) (1 + e^{i2h_{2n+1}ab_0})}{(ih_{2n+1}a)(1 - e^{i2h_{2n+1}ab_0})}, \quad (11)$$

where  $\delta_{ij}$  is the Kronecker's delta.

Introducing the cylindrical coordinate system  $(\rho, \theta)$ , scattering far field  $\phi$  may be obtained from Eq.(4) by the saddle point method, assuming  $k_0\rho \gg 1$ , as

$$\phi = \sqrt{\frac{\pi}{2k_0\rho}} e^{i(k_0\rho + \pi/4)} \sum_{m=0}^{\infty} \{A_m J_{2m}(k_0 a \cos \theta) - iB_m J_{2m+1}(k_0 a \cos \theta)\}. \quad (12)$$

### 3 Numerical Calculation and Discussions

Using the above derived formulation, numerical calculations have been done extensively. First, let us show some numerical calculation of monostatic radar cross section, which may be defined as

$$\sigma(\theta) = \lim_{\rho \rightarrow \infty} 2\pi\rho |\phi(\theta = \theta_0)|^2. \quad (13)$$



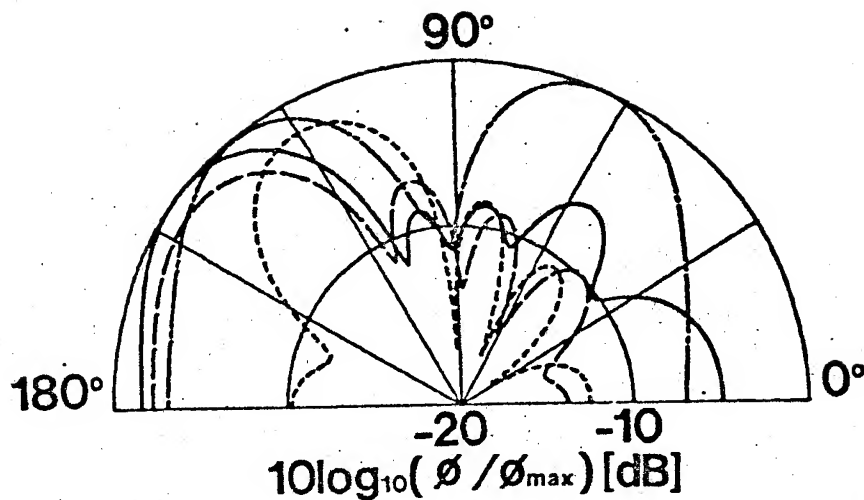


Figure 3: Scattering far field pattern by a rectangular trough.  $a=1.1\lambda$ ,  $b=1.6\lambda$ . —:  $\epsilon_r = 1.0, \mu_r = 1.0, \theta_0 = 30^\circ$ ; ---:  $\epsilon_r = 2.5 + i0.2, \mu_r = 1.8 + i0.1, \theta_0 = 30^\circ$ ; - · -:  $\epsilon_r = 1.0, \mu_r = 1.0, \theta_0 = 60^\circ$ ; ····:  $\epsilon_r = 2.5 + i0.2, \mu_r = 1.8 + i0.1, \theta_0 = 60^\circ$ .

Fig.2 shows the cases for  $2a = 2.0\lambda$ ,  $b = 0.5\lambda, 1.0\lambda$ . In the Figure, we also include a result by Fourier spectral domain method [6]. Good agreement can be seen between two results for all incident angle. Radar cross section seems to have a maximum value at the normal incidence case. Fig.3 shows normalized scattering far field patterns for incidence angle  $\theta_0 = 30^\circ, 60^\circ$ . Comparing with the scattering patterns for the empty trough, it seems that ones for a loaded trough are reduced for almost all direction.

#### References

- (1) T.B.A. Senior, K. Sarabandi, and J.R. Natzke: "Scattering by a narrow gap," IEEE Trans., (1990) AP-38, pp.1102-1110.
- (2) S.D. Gedney and R. Mittra: "A Hybrid method for the solution of the electromagnetic scattering by an inhomogeneously filled trough or slit in a thick conducting screen," 1990 IEEE APS Int'l Symp. Digest, (1990) pp.1736-1733.
- (3) T.M. Wang and H.Ling: "A connection algorithm on the problem of EM scattering from arbitrary cavities," J. Electromag. Waves and Applic., (1991) 5, pp.301-314.
- (4) H. Shirai and K. Hirayama: "Electromagnetic plane wave scattering by a trough on the ground," 1992 Joint Symposia, URSI Radio Science Meeting Digest, (1992), 35.
- (5) H. Shirai and R. Satoh: "Electromagnetic wave scattering by a trough on the ground," 1993 IEEE AP-S Int'l Symposium Digest, (1993) pp.86-89.
- (6) T.J. Park, H.J. Eom and K. Yoshitomi: "An analysis of transverse electric scattering from a rectangular channel in a conducting plane," Radio Science, (1993) 28, pp.663-673.
- (7) Y. Nomura and S. Katsura: "Diffraction of electromagnetic waves by ribbon and slit. I," J. Phys. Soc. Japan, (1957) 12, pp.190-200.
- (8) K. Hongo: "Diffraction of electromagnetic plane waves by infinite slit perforated in a conducting screen with finite thickness," Trans. IECE, (1971) 54-B, 7, pp.419-425.
- (9) K. Hongo and G. Ishii: "Diffraction of an electromagnetic plane wave by a thick slit," Trans. IEEE, (1978) AP-26, 3, pp.494-499.

# SPECTRAL APPROACH TO THE SYNTHESIS OF METAL GRATING ANGULAR AND FREQUENCY FILTERS

Sergei L. Senkevich

Institute of Radiophysics and Electronics of Ukrainian Academy  
of Sciences. 12 Proskura st., Kharkov, 310085, Ukraine

## ABSTRACT

A non-traditional method of synthesis of metal grating angular and frequency band-pass filters based on the analysis of spectrum of complex eigen frequencies of resonators forming a filter is described. Two types of filters, the resonators of which are formed by two infinite metallic strip periodic gratings in H- or E-plane, are considered. It was shown that a filters of the first type has spurious passbands and is more difficult in manufacturing and suggestion method has an advantage over traditional approach in high frequency area.

## INTRODUCTION

Dielectric layers filters with angle-selective properties for sidelobe suppression have a number of disadvantages including excessive weight and cost, dielectric inhomogeneity, polarization sensitivity and so on [1,2]. The obvious remedy for some of this deficiencies is to substitute metallic grids in the place of the dielectric layers.

This paper describes the spectral synthesis, strong analysis and theoretical investigation of a metal strip periodic grating angular (BPAF) and frequency (BFFF) band-pass filters. Two types of filters, the resonators of which are formed by two infinite strip gratings in H- or E-plane of incident wave, are considered (Fig.1). All synthesis and analysis algorithms are based on rigorous mathematical models.

### 1. DIFFRACTION AND SPECTRAL PROBLEMS.

Fig.1. shows a resonator and filter structure for a linearly polarized incident wave and the resonator equivalent circuit. There are period of the all infinite metallic strip grids  $l$ , length resonators  $h/l$ , width strips  $d/l$  and low dielectric constant spacer material  $\epsilon$ . Traditional methods of the filter synthesis are founded on a preliminary design of low-frequency filters taken as prototypes [3]. This is a possibility if we are defining the propagation constant for zero-order Floke-waves as  $\gamma = \chi \cos \phi$ , where  $\chi = l/\lambda$  ( $\lambda$  is wave length in free space). But in high frequency region of the single-wave range this approach have mistakes.

A new approach to the synthesis of manufacturable filters is proposed below. Let us consider filter's section in Fig.1.a as specific open resonator having free eigenmodes damped in time with normalized complex eigenfrequencies  $\gamma = \text{Re} \gamma + i \text{Im} \gamma = \chi \cos \phi$ . The spectral problem consists in a search of those values of the spectral parameter  $\gamma$ , at which the nontrivial solution of the homogeneous boundary value problem with the corresponding boundary and radiation conditions [4] exists. The dispersion equation  $\det((I - RE)(I + RE)) = 0$  was obtained by the moments method. There

$R(\tau)$  is the matrix of the reflection from the resonator boundary. Diagonal matrix  $E(\tau)$  describes the attenuation and phase accumulation on the resonator length  $h$ . The zero-order Floke-waves coefficients in the vicinity of  $\tau_1$  in the single-wave range may be represented similarly [4]

$$S_{00}^{11}(\text{Ret}) = e^{i\xi} \frac{\text{Ret} - \text{Ret}_1}{\text{Ret} - \tau_1} ; S_{00}^{31}(\text{Ret}) = e^{i\xi} \frac{-i\text{Im}\tau_1}{\text{Ret} - \tau_1} ;$$

that corresponds to the pass circuit with the resonant frequency  $\text{Ret}$  and quality factor  $Q = -\text{Ret} / (2\text{Im}\tau_1)$ . For example in the E-polarization case, this expression reduces to the following form

$$S_{00}^{11}(\text{Re}x) = \frac{\text{Re}x - \text{Re}x_1}{\text{Re}x - x_1} ; S_{00}^{31}(\text{Re}x) = \frac{-i\text{Im}x_1}{\text{Re}x - x_1} ; x = l/\lambda = \text{Re}x + i\text{Im}x.$$

for the synthesis in the frequencies domain. For the synthesis in the angle domain  $\varphi = \text{Re}\varphi + i\text{Im}\varphi$  we have

$$S_{00}^{11}(\text{Re}\varphi) = \frac{\text{Re}(\cos\varphi) - i\text{Re}(\cos\varphi_1)}{\text{Re}(\cos\varphi) - \cos\varphi_1} ; S_{00}^{31}(\text{Re}\varphi) = \frac{-i\text{Im}(\cos\varphi_1)}{\text{Re}(\cos\varphi) - \cos\varphi_1}.$$

We have similar expression in H-polarization case, also.

## 2. DIRECT SYNTHESIS METHOD.

The reference planes of the resonator (see Fig.1.a) was selected for  $\arg S_{00}^{11} = 0$ . Resonator was connected with two regular sections with electrical length  $\vartheta/2$ . We will use new variable  $x = (\text{Ret} - \text{Ret}_0)/\text{Ret}_0$ , where  $\text{Ret}_0$  is the parameter value on the central frequency (angle). Then we can obtain

$$S_{00}^{11} = -e^{i\psi} \cos\eta ; S_{00}^{31} = e^{i\psi} i \sin\eta ; \eta = \Pi/2 + 2Qx ; \psi = \eta + \vartheta ; \vartheta = \vartheta_0(1+x) \quad (1)$$

where  $\vartheta$  is the section length on  $\tau = \text{Ret}_0$ .  $\vartheta = \Pi/2$  for filters with quarter-wave coupling on the  $\text{Ret}_0$ . Let us consider resonator with load with reflection coefficient  $K$  on frequency  $\text{Ret}_0$ . Taking into account of  $S_{00}^{11} \ll 1$  in the vicinity of the  $\text{Ret}_0$ , we can obtain from generalized S-matrix technique.

$$\hat{S}_{00}^{11} = S_{00}^{11} - K (S_{00}^{11} S_{00}^{33} - S_{00}^{31} S_{00}^{13}). \quad (2)$$

At the first stage, as usually, due to the given requirement on the filter response and the type of the approximating polynomial (Chebyshev or Butterworth) a number  $N$  of the resonators are determined taking into account the fact that they are coupled by quarter-wave sections in the single-mode range. With (2) we can obtain the reflection coefficient for any number of resonators. For example, for the three-resonator filter we have

$$|\hat{S}_{00}^{11}| = 2\cos\eta_1 \cos(\psi_1 + \psi_2) - \cos\eta_2 = 2x(Q_2 - 2Q_1) + 8Q_1(Q_1 + Q_2 + \Pi/2)^2 x^3.$$

where  $Q = Q_0$  is the quality factor for the outside resonators  $Q_0$  is the quality factor for the central resonator. Contrast this expression with approximating polynomial we obtain simple set of equations for quality factors. For example, for the free-resonator filter we have

$$L = 1/(1 - |\hat{S}_{00}^{11}|^2) \approx 1 + |\hat{S}_{00}^{11}|^2 = 1 + (\mu_3 x^3)^2; \mu_3 = |\hat{S}_{00}^{11}|_{0.5} / x_{0.5}^3;$$

$$Q_2 = 2Q_1; 8Q_1(Q_1 + Q_2 + \pi/2)^2 = \mu_3. \quad (3)$$

There sign 0.5 points to the fact that value is determined under condition  $1/L = 0.5$ . Procedure of resonator synthesis based on the given frequency  $\text{Re}\tau_0$  and quality factor  $Q_1$  reduces as a matter of fact to a search of geometry of the resonator having the eigenfrequency  $\tau = \text{Re}\tau_0 - i\text{Re}\tau_0/2Q_1$ . We consider the dispersion equation, mentioned above, as a system of two non-linear homogeneous equations

$$\text{Re}\{\det[I - A(\text{Re}\tau_0, \text{Im}\tau_0^1, h_1, d_1)]\} = 0; A = (\text{Re}\tau_0)^2; \quad (4)$$

$$\text{Im}\{\det[I - A(\text{Re}\tau_0, \text{Im}\tau_0^1, h_1, d_1)]\} = 0; \text{Im}\tau_0^1 = -\text{Re}\tau_0/2Q_1; i=1+N.$$

solution of which provides the unknown values  $d$  and  $h$ . In computations, the values of the  $d, h$  were obtained from (4) by the Newton method with the accuracy 0.1%. After them one can determine the phase of the reflection coefficient from each resonator by the solution of the diffraction problem and calculate the lengths of the regular sections between resonators. Further on while using the generalized S-matrix technique by known S-matrices of separate filter sections it is easy to restore the characteristics of the whole filter with K-inverters [3].

### 3. NUMERICAL RESULTS OF THE BPAF AND BPFF SYNTHESIS.

As the first example let us consider 2.5% Chebyshev BPFF. Task data were formulated as usually [3] and marked in Fig.2 by triangles. As the results of use of the above described procedure a three-resonator filter was obtained. Calculated insertion loss characteristics  $L$  in dB of the synthesized filters are plotted in Fig.2 by the solid line for H-polarization case and by the dashed line for E-polarization case. Curves practically coincide in all angle range and there are results for  $\varphi=0$ . One can see that the obtained characteristic completely meets the initial task. Diffraction loss (ripple level) in passband is 0.2 dB. In computations five evanescent waves between each pairs of the gratings were taken into account. Resonator lengths are  $h_1 = h_2 = 13.22$  mm,  $h_3 = 12.62$  mm for H-polarization and  $h_1 = h_2 = 11.34$  mm,  $h_3 = 1.99$  mm for E-polarization (period of the all strip grids  $\Lambda = 10$  mm). Width strips are  $d_1 = d_2 = 0.489$  mm,  $d_3 = d_4 = 0.026$  mm for H-polarization and  $d_1 = d_2 = 6.035$  mm,  $d_3 = d_4 = 2.88$  mm for E-polarization. As it is evident from the foregoing filter is more manufacturable in E-case. In this example we used low dielectric constant spacer material with  $\epsilon=1.03$ .

Insertion loss characteristics for three-resonator BPAF are plotted in Fig.3 by the solid line for H-polarization case and by the dashed line for E-polarization case. Task data are marked by triangle. Angular filters were designed with Chebyshev characteristics on frequency  $f=12.15$  GHz. The curves symmetric about  $\varphi=0$ . One can see that input task was completely fulfilled and insertion loss in the passband did not exceed 0.2 dB, but filter in H-polarization case have spurious stopbands in vicinity  $\varphi=80^\circ$ .

Last example is plotted in Fig.4 and conform to  $\chi \cos \varphi = 0.93$ . The dashed line corresponds to traditional approach [3], the solid line corresponds to suggested method. As it is seen from figure in the first case we have inaccuracy results.

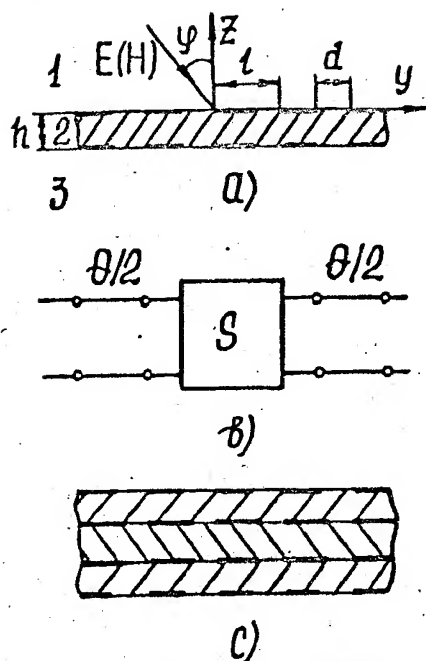


Fig. 1. Geometry of filters

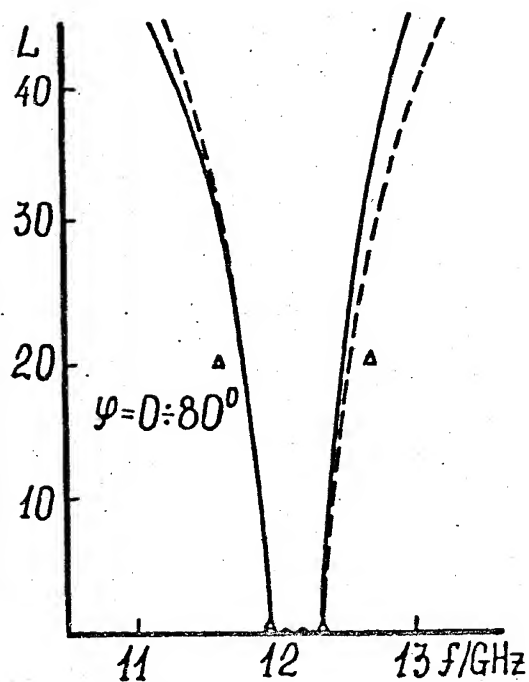


Fig. 2. Characteristics of the frequency-dependent filters.

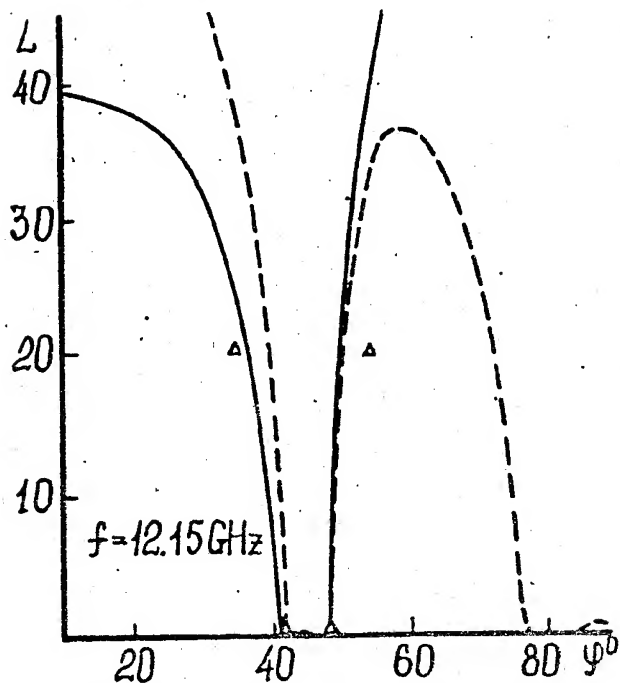


Fig. 3. Characteristics of the angular filters.

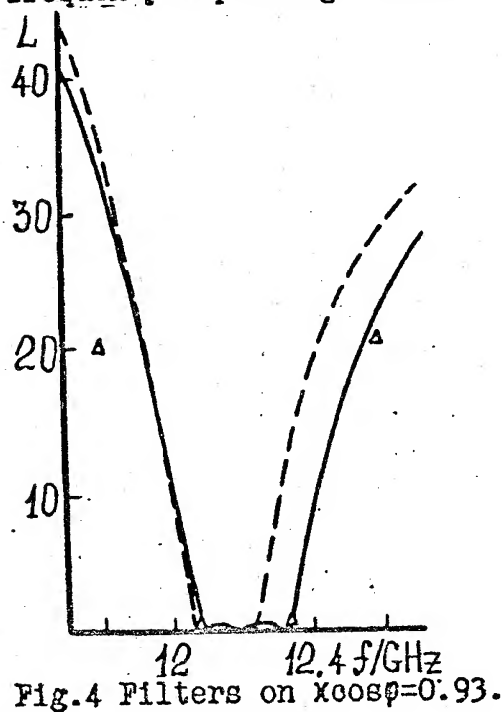


Fig. 4. Filters on  $X\cos\psi = 0.93$ .

#### REFERENCE

- (1) R.J.Mailloux, IEEE Trans., (1976) AP-24, 3, pp.174-181. (2) R.J.Mailloux, K.Zahn, A.Martinez, G.R.Forbes, IEEE Trans. (1979). AP 27, 1, PP.79-83. (3) G.Matthaei, L.Young, E.M.T.Jones, "Microwave Filters, Impedance-Matching Networks and Coupling Structures", New-York:McGraw-Hill, (1964), 486p. (4) V.P.Shestopalov, Yu.K. Sirenko, "Dinamic Theory of Grating", Kiev:Naykova dumka, 1989, 216p.

# METHOD OF TRIAL PULSE RESPONSE IN NONSTATIONARY ELECTRODYNAMICS

Andrey E. Serebryannikov

Radio Astronomy Institute, Ukrainian Academy of Science  
4 Krasnoznamennaya St., 310002 Kharkov, Ukraine

Loudmila V. Vavriv

Research and Engineering Institute "Molniya"  
47 Shevchenko St., 310013 Kharkov, Ukraine

## ABSTRACTS

To solve the time-domain electrodynamic problems the advanced frequency-domain methods in combination with the inverse Fourier transform are widely used. But obvious advantages of this approach often prove to be lost because of low effectiveness of numerical realization. The effective method that allows to increase the velocity of computational algorithms has been suggested.

## 1. INTRODUCTION

Let it is necessary to find the response of an electrodynamic system to a pulse waveform excitation. Consider here that the exciting pulse has a finite duration and it belongs to the class of absolutely integrated signals.

Frequency-domain waveform response is to be found as the discrete function

$$F_r(\omega_j) = G_r(\omega_j)H(\omega_j), \quad \omega \in [0, \omega_b], \quad (1)$$

where both for discrete and continuous functions the following conditions are met:  $g_r \leftrightarrow G_r(\omega)$ ,  $f_r(t) \leftrightarrow F_r(\omega)$ ,  $h(t) \leftrightarrow H(\omega)$ ;  $f_r(t)$  is the waveform response of electrodynamic system being considered;  $g_r(t)$  is the external waveform excitation;  $h(t)$  is the Dirac response of electrodynamic system;  $\omega_b$  is an effective spectrum width.

Number and limits of location of discrete samples whose values are necessary to know for unambiguous restoration of the waveform response in the time domain by samples series are defined by value of TBWP (time-bandwidth product;  $v = T_e \omega_b$ , where  $T_e$  is an external action duration). The value  $v$  defines all sampling parameters.

## 2. GENERAL IDEA

The general idea of the considering approach consists in a following. At the first stage we will find response to a some trial excitation  $g_{tr}(t)$ :

$$F_{tr}(\omega_j) = G_{tr}(\omega_j)H(\omega_j); \quad g_{tr}(t_k) \leftrightarrow G_{tr}(\omega_j), \quad f_{tr}(t_k) \leftrightarrow F_{tr}(\omega_j), \quad t_k = k\Delta t \quad (2)$$

where the time shape of the trial excitation  $g_{tr}(t)$  is picked out so that value of  $v$  realizes smaller value comparing to the case of real waveform excitation. Therefore, we decrease the number of fixed frequencies that require calculation of the function  $H(\omega)$ . Each from the values of  $H(\omega)$  is found in the majority of cases from solution of linear algebraic equations sets. That is why much the time is spent for calculation of discrete values of  $H(\omega)$ , but not for inverse Fourier Transform. As a result, decreasing of TBWP value gives considerable decreasing of a calculation time.

One of the advantages of this approach is a smaller number of samples which is necessary in comparison with a number of samples required for transient response calculation. Other advantage of the method of trial pulse response is a possibility of a priori estimation of sampling parameters which is the necessary condition for correct realization of sampling procedure [1]. Such an estimation is not possible in the case of the use of Dirak-response method.

### 3. WAVEFORM RESPONSE RESTORATION

The transition to the time domain is carried out by FFT algorithms when all samples  $F_r(\omega_j)$  were found. As a result, we have discrete function  $f_r(k\Delta t)$  in the time domain. This function represents the discrete function of trial pulse response. The trial pulse response as continuous function of time is unambiguously restored by samples series

$$u(t) = \sum_{k=-N/2}^{N/2} f_r(t_k) \frac{\sin[\omega_s(t-t_k)]}{\omega_s(t-t_k)} + \varepsilon(t), \quad u(t) = f_r(t) \leftrightarrow F_r(\omega), \quad t_k = k\Delta t, \quad (3)$$

where  $\varepsilon(t)$  is an error caused by the reduction of the infinite spectrum of the trial pulse excitation to the finite one; this error can be estimated using the known methods [2]. As it follows from the eqns. (1,2)

$$F_r(\omega) = F_r(\omega) \frac{G_r(\omega)}{G_r(\omega)} \quad (4)$$

Thus, we have the inverse Fourier Transform for the relationship between spectral densities of the real external action and of the trial action which can be determined analytically as a continuous time function in a case of special form of functions that describe real and trial actions. Then the real waveform time-domain response can be restored as the following convolution

$$w(t) = u(t) \otimes v(t), \quad (5)$$

$$\text{where } v(t) = \frac{1}{2\pi} \int_{-\infty}^{\infty} \frac{G_r^*(\omega)}{G_r(\omega)} e^{i\omega t} d\omega.$$

Here

$g_i(t) \leftrightarrow G_i(\omega)$ ;  $g_p(t) \leftrightarrow G_p(\omega)$ ;  $p = r, tr$ ;  $g_p(t) = g_p^*(t)$  if  $0 \leq t \leq T_s$  and  $g_p(t) = 0$  if  $t \geq T_s$  or  $t \leq 0$ .

### 4. CHOICE OF TRIAL PULSE PARAMETERS

A choice of the time shape of the trial pulse excitation is necessary to perform taking into account physical peculiarities of concrete class of electrodynamic problems. There are two alternative ways which allow to decrease TBWP value. First of them consists in decreasing of the trial excitation duration comparing to the real excitation duration. Other way is concerned with decreasing of an efficient frequency bandwidth of trial action in comparison with the bandwidth of real action. First way is a more universal, because it takes into account the contribution of wide frequency bandwidth. This allows to attribute this way to the methods of broadband analysis.



Second way is oriented to the analysis of the electromagnetic waves interaction with strongly resonancing structures. It attributes to the methods of narrowband analysis.

In a common case the trial pulse excitation  $g_r(t)$  should satisfy the following requirements. The effective width of the trial action spectrum is not to be narrower than the width of the real action spectrum; the relationship between spectral densities of real and trial signals should be met the theorem about the convolution [3] and could be determined analytically (we can assume also that the external action is prescribed analytically). Thus the time domain parameters of the trial action are chosen depending on that of the real action.

For example let us consider the use of trial excitation having shorter pulse duration in comparison with the real one. Let it be given as

$$g_r^*(t) = e^{-\alpha t} - e^{-\beta t}, \quad \alpha \ll \beta.$$

The trial excitation has an analogous structure

$$g_r^*(t) = e^{-\gamma t} - e^{-\delta t}, \quad \gamma < \delta, \quad \text{and besides } \gamma < \beta < \delta.$$

In this case the integral (5) can be calculated analytically and gives

$$v(t) = A e^{-\alpha t} - B e^{-\beta t},$$

$$\text{where } A = -\frac{(\alpha - \gamma)(\alpha - \delta)}{\gamma - \delta}, \quad B = -\frac{(\beta - \gamma)(\beta - \delta)}{\gamma - \delta}.$$

It is not difficult to satisfy oneself that  $\int_{-\infty}^{\infty} |v(t)| dt < \infty$ . Hence, if the function  $u(t)$  is

uniformly continuous and  $\int_{-\infty}^{\infty} |u(t)| dt < \infty$ , then in coincidence with [3]

$$u(t) \otimes v(t) \leftrightarrow F_v(\omega) \frac{G_r^*(\omega)}{G_r(\omega)}.$$

The simplified approach presupposes the replacement of the samples series by a sum of piece-constant functions, so that  $u(t) = f_v(t_k), t \in [k\Delta t, (k+1)\Delta t]$ . In this case is not difficult to obtain the approximate solutions as the series

$$w(t) = \int_0^t f_v(\tau) [A e^{-\alpha(t-\tau)} - B e^{-\beta(t-\tau)}] d\tau = \sum_{k=0}^j f_v(t_k) \int_{t_k}^{t_{k+1}} (A e^{-\alpha t} - B e^{-\beta t}) dt,$$

$$j = \text{Int}(t / \Delta t), \quad t_{j+1} = t.$$

Let us note that terms number don't outnumber the half of a number of samples using for the restoration of the trial pulse response.

In order to exclude an influence of an error caused by transition to the finite spectrum and the error caused by the avoidance of finite duration of the real and trial pulses in the formula (5) it is necessary to compare results of restoration of the function  $w(t)$  in the time domain through the changing limits of trial excitation  $\omega_{b,lr}, T_{s,lr}$ . Besides, it is necessary to provide the validity of the following relationship

$$\max |\sigma(t)| = \left| \int_0^t \varepsilon_1(\tau) v(t-\tau) d\tau \right| \leq |\varepsilon_2(t)|,$$



where  $\varepsilon_2(t)$  is an error of restoration of the function  $f_1(t)$  by samples of  $F_1(\omega)$ ; module  $|\varepsilon_2(t)|$  can be estimated on the basis of the methods given by Gelman etc. [2].

## 5. FIELD OF APPLICATION

The field of application of the approach advanced in this paper refers mainly to the problems on scattering of pulse electromagnetic fields having specific time shape on both the strongly resonant and feebly resonant structures. This approach effectively applies to the cases when exciting action is given by superposition of smooth analytical functions, especially if the derivatives of external excitation varies significantly at the adjacent time intervals. For example, the problems of scattering of the fast transiting LEMPs [4] ( $T_f \ll T_s$ , where  $T_f$  and  $T_s$  are pulse front duration and pulse duration, accordingly) belong to this class of the problems. This approach can be used also in the case of strongly oscillating excitations having  $T_{os} \ll T_s$  (where  $T_{os}$  is a peculiar time scale of oscillations).

The limitation of the method application is connected with the peculiarities of EMP scattering in case of interaction with slow-wave structures, when the significant increase of waveform response duration in comparison with the external action is possible. In this case the preliminary diagnostics of transfer function and of external action in the frequency domain are necessary to provide.

## 6. CONCLUSIONS

Thus, the possibilities of numerical simulation of nonstationary electrodynamic problems can be expanded essentially using the trial pulse excitation that provides a decreasing of TBWP value.

A methodology of the choice of the trial pulse parameters is stipulated by specific peculiarities of concrete class of electrodynamic problems, but it is not at all limited by considered cases. Decreasing of TBWP value is not a far off single criteria of the choice of trial pulse parameters.

The approach advanced in this paper can be interpreted as the generalized method of transient response based on the use of exciting action given by analytical function having special time shape.

## REFERENCES

1. A.A.Molchanov, A.M.Sharadkin, "Discretization of Information Signals" (in Russian), Vyshcha Shkola Press, Kiev, 1991.
2. M.M.Gelman, B.M.Stepanov, V.N.Filinov, "Discretization and Coding of Broadband Signals" (in Russian), Radio i Svyaz' Press, Moscow, 1985.
3. M.A.Evgrafov, "Analytical Functions" (in Russian), Nauka Press, Moscow, 1991.
4. M.A.Uman, E.F.Vance, IEEE Trans. on Electromagn. Compat., Vol.EMC-30, 1, 1988, p.46-52.

# Modes of double core optical fibres with non-identical cores

Victor V. Shevchenko and Aleksey D. Skaballanovich

Institute of Radioengineering and Electronics, Russian Academy of Sciences  
Mokhovaya str. 11, Moscow, 103907, Russia

## Abstract

Modes of double core optical fibres are examined by using the results of a new approximate analytical modal theory of coupled optical dielectric waveguides, which is founded on the shift-formula method.

## Introduction

The shift-formula methods (1) proved to be very effective for examination of nonordinary optical fibres, in particular for calculation of modal parameters and fields of fibres with double cores (2-4). Because the double core fibre modes can be considered as modes of coupled optical dielectric waveguides in (3,4) by the shift-formula  $\alpha$ -method, provided the partial modes of individual waveguide are known, the approximate analytical expressions for modal propagation constants and modal fields of coupled non-identical waveguides are obtained. These are so named quasi even and quasi odd modes. It is shown (4,5) by comparison with the exact numerical results for planar coupled waveguides, that the obtained approximate expressions have sufficiently high accuracy.

In the presented paper some modal parameter dependencies on frequency (dispersion dependencies), on core parameters and on the distance between the cores of double core fibres with non-identical circular cores are given. The results are obtained by using the theory, represented in (3,4). Some results are compared with exact numerical ones, which are got by numerical realization of the shift-formula  $\alpha$ -method (2,6).

## Results

The propagation constants of the quasi even (+) and quasi odd (-) modes can be represented as  $\chi_{\pm} = k n_0 (1 + \Delta_{1,2} B_{\pm})$  where  $k = \omega/c$ ,  $\omega$  is the circular frequency,  $c$  is the velocity of light,  $\Delta_{1,2} = (n_{1,2} - n_0)/n_0$ ,  $n_1, n_2$  and  $n_0$  are the refractive indexes of the cores and cladding,  $B_{\pm}$  are the phase modal parameters, which depend on the core (waveguide) parameter  $V_{1,2} = k R_{1,2} n_0 (2\Delta_{1,2})^{1/2}$ , the distance parameter  $p = (R_1 + R_2)/d$  and the asymmetry parameter  $\sigma = (V_1^2 - V_2^2)/2V_1V_2$ , where  $R_1, R_2$  are radius of the cores,  $d$  is the distance between the core axes.

In Fig 1. the phase modal parameter  $B_{\pm}$  dependences on the waveguides parameter  $V = V_1 = V_2$  (for  $R_1 = R_2 = R$ ,  $\Delta_1 = \Delta_2 = \Delta$ ) are given for different values of the distanced parameter  $p = 2R/d$ . The right curves are for  $d = 2R$ , i.e. the cores touch one another. The dots and broken curves are used for exact results obtained by the shift-formula numerical calculations (2,6). The phase modal parameter dependences on the distance parameter (for  $R_1 = R_2$ ) and on the asymmetry parameter (for  $\Delta_1 = \Delta_2$ ) are given in Fig 2. and Fig 3. The dots show exact numerical results.

The research described in this publication was made possible in part by Grant № MMB000 from the International Science Foundation.

## References

- (1) V.V. Shevchenko : " Shift-formula methods in the theory of dielectric waveguides and optical fibres (review) ", Radiotekhnika i Elektronika, (1986) 31, № 5, pp. 849-864 (Engl. transl. in: Sov. J. Communication Technology and Electronics, (1986) 31, № 9, pp. 28-42).
- (2) Yu. V. Kolesnichenko : " Optical fibres with two noncircular cores", Radiotekhnika i Elektronika, (1989) , № 8, pp. 79-80 (Engl. transl. in: Telecommunications and Radio Engineering, (1984) 44, № 9, pp. 109-111).
- (3) V.V. Shevchenko : " Fundamental modes of double core optical fibres ", Radiotekhnika i Elektronika, (1993) 38, № 3, pp. 557-566.
- (4) V.V. Shevchenko : " On modal theory of coupled optical dielectric waveguides ", Sov. Lightwave Communications, (1993) 3, № 4, pp. 199-211.
- (5) A. D. Skaballanovich, V.V. Shevchenko : " Modes of coupled planar dielectric waveguides with nonequal parameters", Radiotekhnika i Elektronika, (1994) 39, № 5, pp. 785-794.
- (6) Yu. V. Kolesnichenko : " Modes in multicore optical fibre structures ", this issue, (1994), pp.

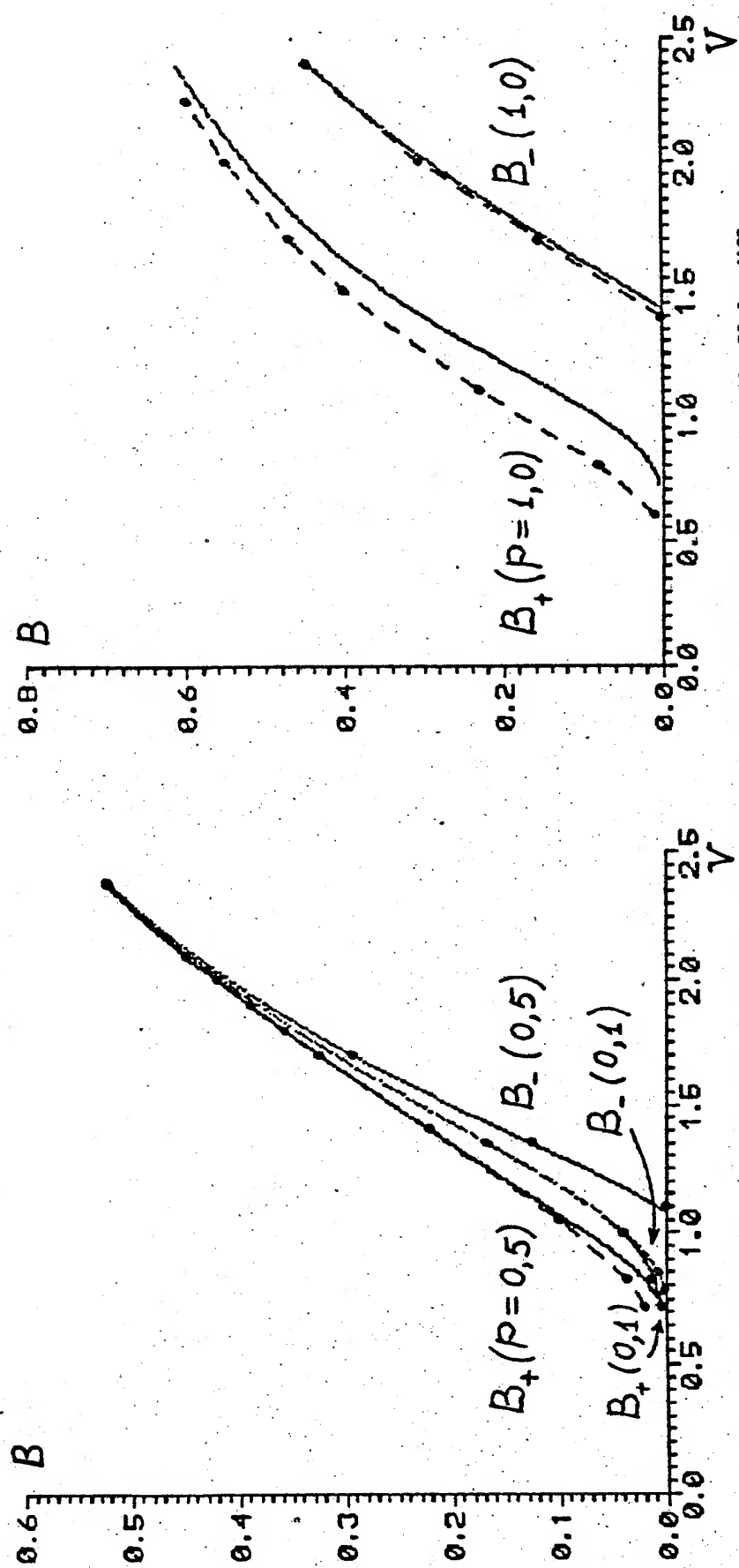


Fig 1. Dependences of the phase modal parameters  $B_+$ ,  $B_-$  on the waveguide parameter  $V = V_1 = V_2$  for different values of the distance parameter  $p = 2R/d$ .

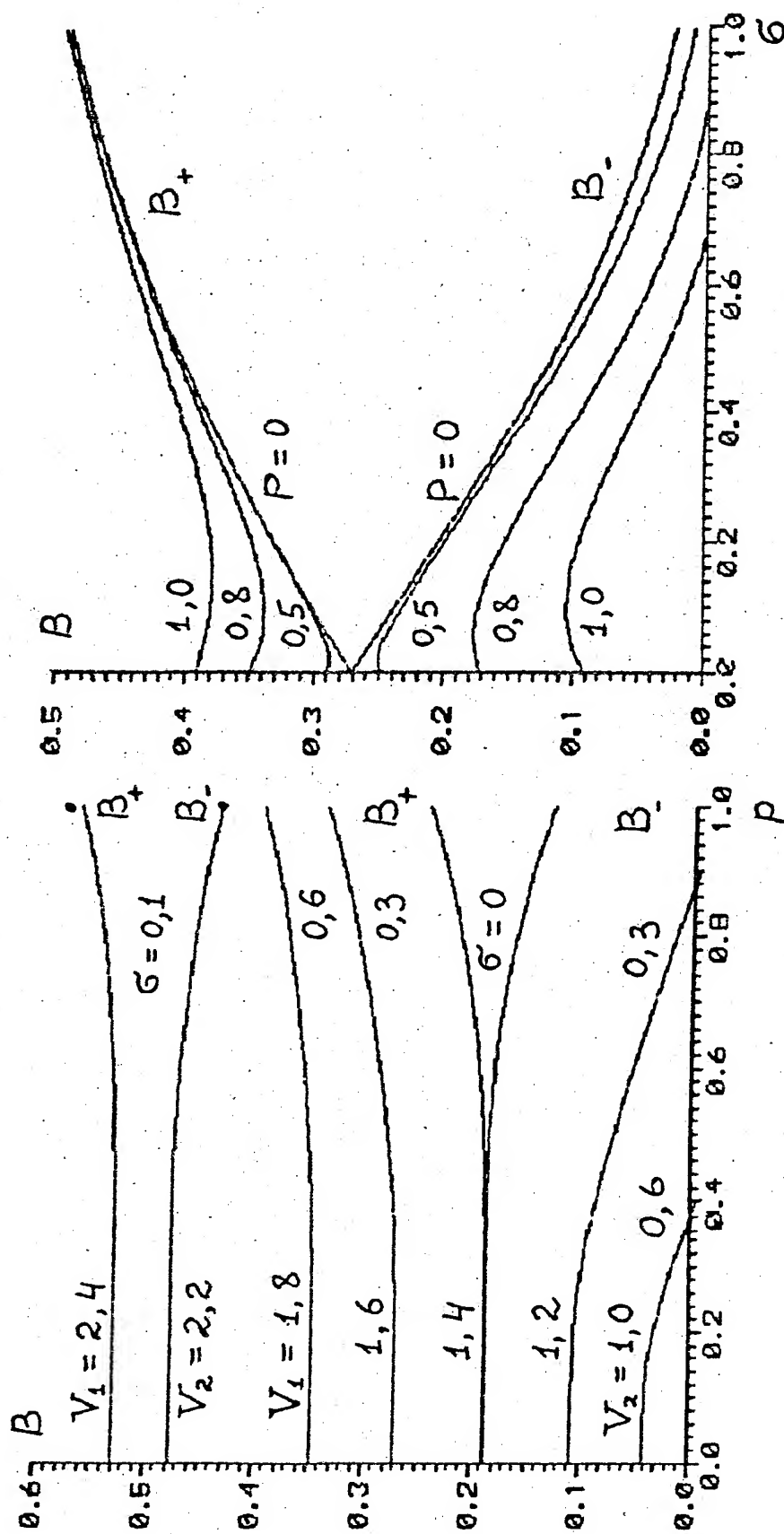


Fig 2. Dependences of the phase modal parameters  $B_+$ ,  $B_-$  on the distance parameter  $p$  for different values of the asymmetry parameter  $\sigma$  and waveguide parameter  $V_1, V_2$ .

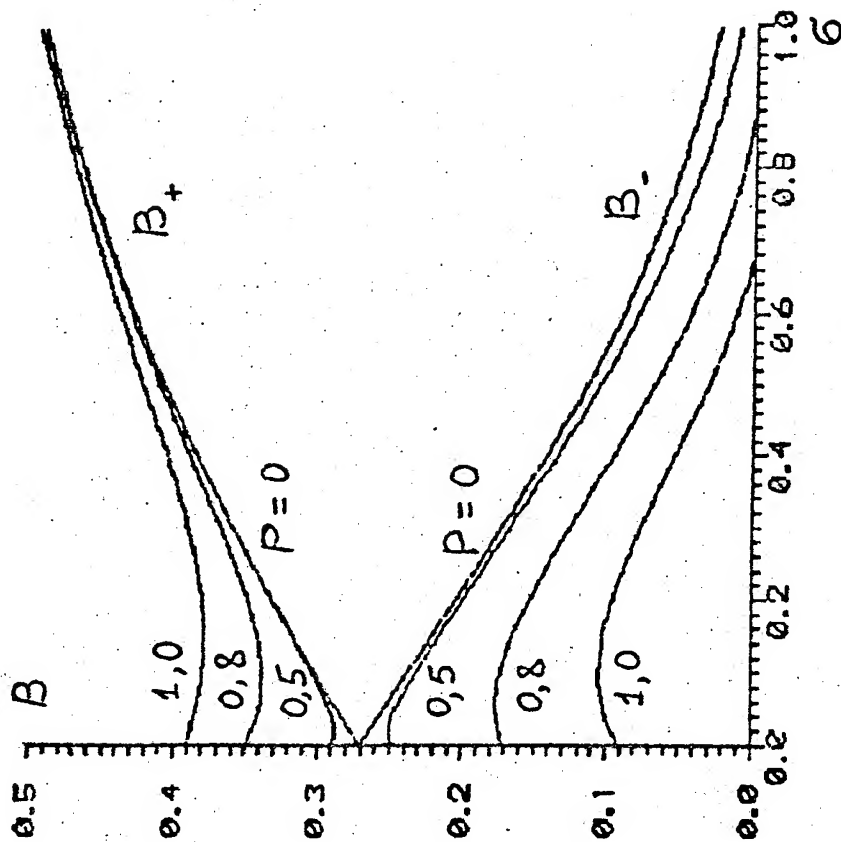


Fig 3. Dependences of the phase modal parameters  $B_+$ ,  $B_-$  on the asymmetry parameter  $\sigma$  for different values of the distance  $p$ :  $V_1 = V_2 = 1.6$  for  $\sigma = 0$ .

# Modes of inhomogeneous anisotropic optical fibres with local diagonal tensor permittivity of a core

Victor V. Shevchenko and Sergey V. Stoyanov

Institute of Radioengineering and Electronics  
Russian Academy of Sciences  
Mokhovaya str.11, Moscow, 103907, Russia

## ABSTRACT

The problem of field formation of guided modes in inhomogeneous anisotropic dielectric optical fibres is under investigation. The goal of the work is to clarify the physical sense of nondiagonal components of the transverse tensor of permittivity and to find the qualitative regularities connecting the functions of tensor nondiagonal components with the parameters and field distributions of guided modes.

## INTRODUCTION

Modes of optical fibres with partially homogeneous and inhomogeneous anisotropic cores are examined by the shift-formula method (1, 2). Particular case of fibres with local diagonal tensor permittivity of core is considered (3, 4). In present paper the dispersion and polarization modal properties of this kind of fibres are analyzed. An attempt was made to distinct clearly the influence each of component of permittivity tensor on polarization properties of fibres. Electromagnetic field distribution figures are presented.

### 1. CONCEPTION OF LOCAL-DIAGONAL PERMITTIVITY TENSOR

Let the tensor nondiagonal components be  $\epsilon_{xy} = \epsilon_{yx} = \text{const}$ . It is possible to show that for such a medium there exists a system of coordinates, we shall designate it  $\tau, \nu$ , in which the tensor will be diagonal. at the same time, axes  $\tau, \nu$  will be rotated relative to axes  $x, y$  by some angle  $\theta$ :

$$\hat{\epsilon} = \begin{bmatrix} \epsilon_x & \epsilon_{xy} \\ \epsilon_{yx} & \epsilon_y \end{bmatrix} \xrightarrow{\theta} \begin{bmatrix} \epsilon_\tau & 0 \\ 0 & \epsilon_\nu \end{bmatrix}, \text{ where}$$

$$\epsilon_\tau = (\epsilon_x + \epsilon_y + [(\epsilon_x - \epsilon_y)^2 + (2\epsilon_{xy})^2]^{1/2})/2$$

$$\epsilon_\nu = (\epsilon_x + \epsilon_y - [(\epsilon_x - \epsilon_y)^2 + (2\epsilon_{xy})^2]^{1/2})/2$$

$$\text{tg}(2\theta) = 2\epsilon_{xy}/(\epsilon_x - \epsilon_y)$$

We introduce for such a medium the notion of a local diagonal tensor of permittivity. Let the parameters of the medium change sufficiently gradually with the variation of the coordinates, and let the medium (structure) be characterized by tensor  $\hat{\epsilon} = \hat{\epsilon}(\rho, \theta)$ . Then it is possible to introduce a local-diagonal permittivity tensor with components  $\epsilon_\tau, \epsilon_\nu$  at any points of this medium.

Such conception allows to predict properties of waveguides taking as a basis the simple models.

## 2. RESULTS

In Model 1 the core of the anisotropic fibre consists as if of two concentric layers, inner and outer, and both the layers are of equal thickness. The profiles of the permittivity tensor components are shown in Fig. 1a. The cladding is taken to be uniform and isotropic, its permittivity being  $\epsilon_0$  and its inner radius  $\rho = R$ . As illustrated in figure, diagonal components  $\epsilon_x, \epsilon_y$  are constants along the whole of the core cross-section. Nondiagonal components  $\epsilon_{xy} = \epsilon_{yx}$  have a drop and change of sign at a radius of  $\rho = R/2$ , and their absolute values are the same in the inner and outer layers. Model 2 which is given in Fig. 1b has a considerable difference, in spite of its outer similarity. The core proper of  $\epsilon_x, \epsilon_y > \epsilon_0$  is limited by the circumference of a  $\rho = R/2$  radius, while in the outer circular layer of  $R/2 < \rho < R$  and in the cladding  $\epsilon_x = \epsilon_y = \epsilon_0$ . Nondiagonal components have the same values as in Model 1 i.e.  $|\epsilon_{xy}| = (\epsilon_x - \epsilon_y)/2$ . Besides this,  $(\epsilon_x - \epsilon_0)/(\epsilon_y - \epsilon_0) = 2$  in the core.

The chosen value is sufficiently great to illustrate vividly the properties typical of inhomogeneous anisotropic fiber waveguides.

Numerical calculations of mode field distributions and propagation parameters were executed by the shift-formula method.

The dispersion curve of fundamental modes are shown in Fig. 3, where  $B = (\gamma^2/k^2 - \epsilon_0)/(\epsilon_x - \epsilon_0)$  is phase parameter,  $V = kR(\epsilon_x - \epsilon_0)^{1/2}$  is normalized frequency,  $\epsilon = (\epsilon_x + \epsilon_y)/2$ ,  $\gamma$  is the propagation constant,  $k = \omega/c$ ,  $\omega$  is circular frequency,  $c$  is the velocity of light. Points (A), (B)...(E) on the dispersion curves correspond to mode field distributions in Fig. 4, 5.

Anisotropy removes the double degeneration of the  $LP_{01}$  fundamental modes. Let the mode with the best propagation conditions be denoted  $LP_{01}'$ , and the other, which has the perpendicular polarization to the first one (at low  $V$ ),  $LP_{01}''$ . The dispersion curve of  $LP_{01}''$  mode goes below that of the  $LP_{01}'$  mode, and for a homogeneous diagonal anisotropic core it would asymptotically tend to become some value  $B'' < 1$ . However, because of the nonuniform dependency of the permittivity tensor nondiagonal components, the  $LP_{01}''$  mode polarization direction changes in such a way that the phase parameters and propagation constants of both these modes tend to become equal with  $V$  grows. (See also Fig. 4, 5.)

Let us consider polarization of the fundamental modes at  $V \rightarrow 0$ . Under such conditions the fundamental modes are almost plane waves which propagate in the limitless cladding and are slightly perturbed by the core of the waveguide. Calculations show that the direction of polarization of the  $LP_{01}'$  principal mode forms an angle of approximately  $11^\circ$  with the X axis for Model 1 and  $28^\circ$  for Model 2.  $LP_{01}''$  mode is polarized orthogonally to the first one.

See Fig. 2.

A simple physical explanation of these results can be

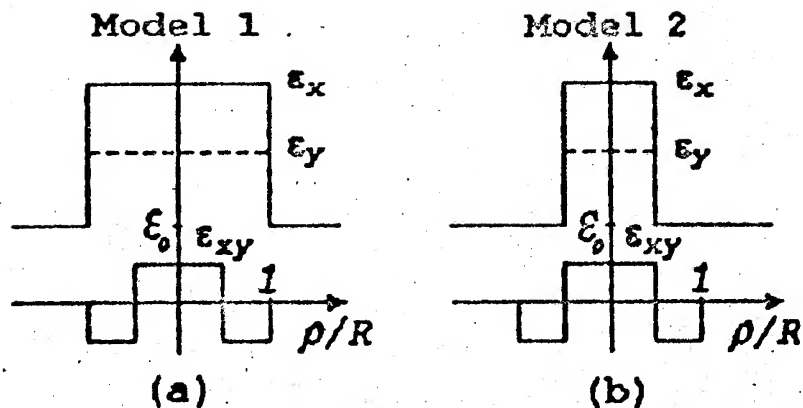


Fig. 1. Components of the permittivity tensor.

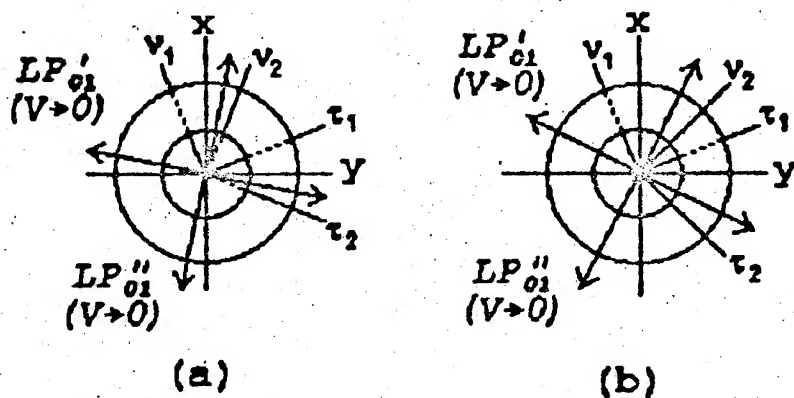


Fig. 2. Local-diagonal coordinate systems

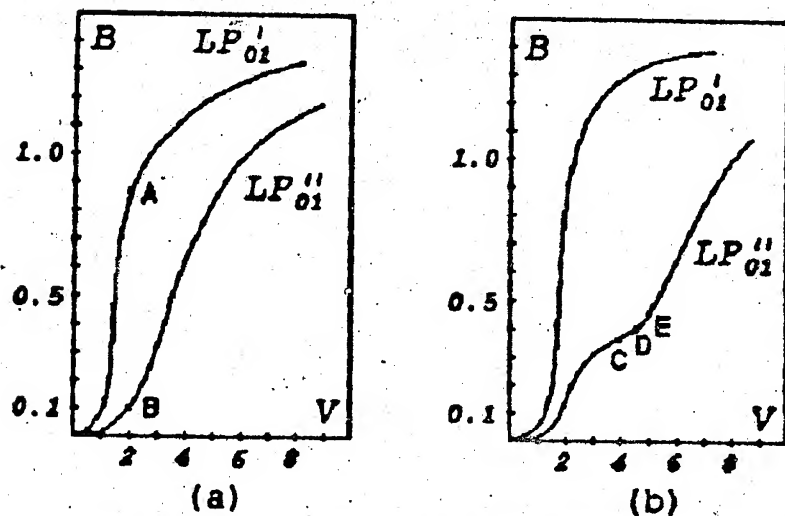
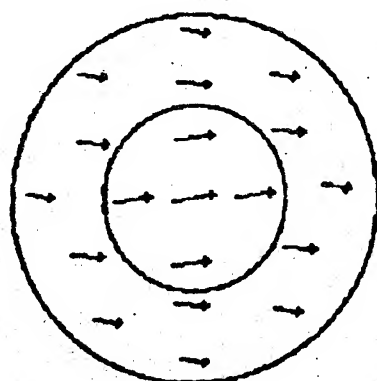
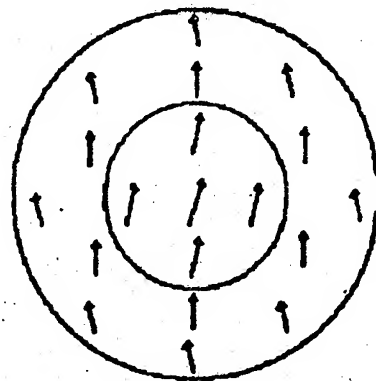


Fig. 3 Dispersion curves of fundamental modes

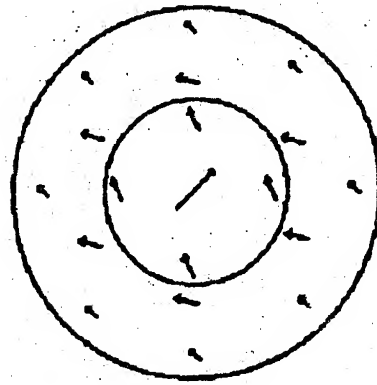
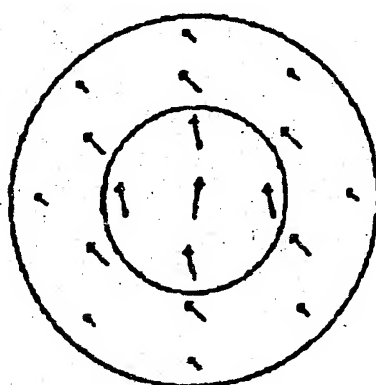


$LP_{01}', V=2, (A)$



$LP_{01}'', V=2, (B)$

Fig.4. The polarization of fundamental modes in Model 1.



$V=4, (C)$   
 $V=4.5, (D)$   
 $V=5, (E)$

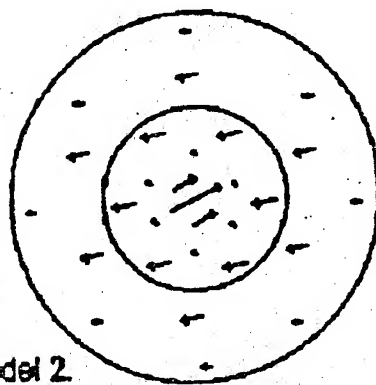


Fig.5. The dynamics of the change of polarization of the  $LP_{01}''$  mode vers normalized frequency  $V$  in Model 2.



proposed. Considering that at  $V \rightarrow 0$  the fundamental mode is almost a plane wave, let us take the field amplitude (or the power density) to be equal along the whole of the core cross-section. Because the area of the inner layer is three times smaller than that of the outer one (at the radial ratio is equal 1/2), its power of the field should be three times less. If we formally average directions  $\tau_1, \tau_2$  with the weights equal to the ratio of the powers, which propagate in the inner and outer circular layers of the core, we shall receive the values that accurately agree with the calculations given above.

Let us consider the dynamics of the change of polarization of the  $LP_{01}'$ ,  $LP_{01}''$  modes vers normalized frequency  $V$ . When  $V$  is increasing, the uniform polarization of these modes is disturbed. In the limiting case of great  $V$  values, the field in the waveguide core tends "to be oriented" in the direction of axis  $\tau$  of the locally diagonal system of coordinates at each point. The said regularities are illustrated in Fig.4,5 where the distributions of the  $LP_{01}'$ ,  $LP_{01}''$  modes in the waveguide cross-section at various  $V$  values are presented. The size of the arrows corresponds to the relative amplitude of the field at the points of arrow origin.

The  $LP_{01}'$  mode (Fig.4.) is less affected by the change of frequency, because its polarization from the very beginning (at  $V \rightarrow 0$ ) was generally oriented towards  $\tau$ , that cannot be said about the polarization of the  $LP_{01}''$  mode, that was mainly oriented towards  $\nu$  (at  $V \rightarrow 0$ ). Consequently, at  $V \rightarrow \infty$ , its polarization is rotated approximately by  $90^\circ$  and tends to be of the same orientation as that of the  $LP_{01}'$  mode. This is vividly illustrated by Model 2 (see Fig.5). At such a big  $V$  values, the field of the fundamental  $LP_{01}''$  mode stops to be like that of the  $LP_{01}''$  mode and starts to remind that of the higher-order  $LP_{02}'$  mode.

The research described in this publication was made possible in part by Grant M2000 from the International Science Foundation.

#### REFERENCES

- (1) V.V. Shevchenko: "Shift-formula methods in the theory of dielectric waveguides and fiber lightguides (review)". Radiotekhnika i Elektronika. (1986) 31, 5, pp. 849-864. (Engl. transl. in: Sov. J. of Communications Technology and Electronics, (1986) 31, 9, pp. 28-42).
- (2) Yu.V. Kolesnichenko, S.V. Stoyanov, V.V. Shevchenko: "Waves in nonordinary optical dielectric waveguides, Electrodynamics of open structures of mm and submm wave bands", Kharkov, IRE AN of Ukraine, (1990), pp. 60-68.
- (3) S. V. Stoyanov, V.V. Shevchenko: "Modes of inhomogeneous anisotropic optical waveguide". Radiotekhnika, 1990, 7, pp. 76-81 (Engl. transl. in: Telecommunications and Radio Engineering, (1990) 45, 8, pp. 118-122).
- (4) S.V. Stoyanov: "Fundamental modes of non-circular inhomogeneous anisotropic waveguide". Radiotekhnika, 1991, 12, pp. 88-87 (Engl. transl. in: Telecommunications and Radio Engineering, (1992) 47, 1, pp. 116-117).

# METHODS OF ANALYSIS OF ANTENNAS WITH NONLINEAR ELEMENTS

Y.S. Shifrin, A.I. Luchaninov

Kharkov State Technical University of Radioelectronics  
Lenin Avenue, 14, Kharkov, 310726, Ukraine

## ABSTRACT

This report deals with the study of the theoretical methods of analysis of nonlinear antenna effects. The main attention is given to the methods based on a state variables conception. Solution of state equations (SE) of antennas with nonlinear elements (ANE) is the key point in this approach. Numerical methods of SE solution in time and frequency domains are analyzed as well as a structural-matrix analytical method of solution of this kind equations is considered.

Advantages and disadvantages of the ANE analysis different methods are indicated as well as expedient areas of application of each of them. The report is mainly based on the results obtained by the authors.

## INTRODUCTION

Research on the nonlinear effects in antennas (NEA) is one of the new trends in modern theory of antennas. The rise and development of this trend is connected firstly with a broad introduction into practice of antennas with nonlinear elements (antenna-mixers, rectennas, frequency multiplication antennas etc.) to solve a number of urgent problems and secondly with the fact that the NEA can cause essential complication of the problem of electromagnetic compatibility (EMC). Both nonlinear elements (NE) specially built into an antenna and parasitic nonlinearities caused either by the antenna design (for example, oxide films of reflector antennas) or by the adverse mode of operation of its active elements (for example in active phase antenna arrays - APAA) can give rise to the NEA. Regardless of nonlinearity the nature its availability in any device is manifested in the appearance of new spectral components in the antenna response and depending on its parameters and the input action nature. Appearance of new spectral components in some cases is useful, as it is the basis for functioning of the new antenna types mentioned above. It is also used in nonlinear radio location systems where the signal of the harmonic frequency of the basic frequency is used as the information signal in the object location. Along with this, appearance of new spectral components is often not wanted, it makes the EMC problem more complicated. This concerns both radiation on the harmonic frequencies of the basic frequency and radiation at combination frequencies.

The fact of antenna characteristics dependence on the nature of the input action is also essentially important in case when the antenna contains the NEs. In cases when the NEA are useful this condition stipulates the necessity to calculate external antenna parameters under different levels of the input action. In addition, in some cases it requires "fitting" of the antenna operation mode taking into account the external conditions for the sake optimization of its output characteristics. The dependence of the antenna characteristics on the level of input action can also manifest in deterioration of its parameters on the basic frequency. Thus if limitation of the signal amplitudes takes place in the amplifiers of receiving APAA this causes main lobe broadening of the radiation pattern (RP) and increase in side lobes level.

It is necessary to emphasize that the degree and peculiarities of manifestation of both useful and adverse NEA depends on specific design of the antenna, interconnection between its elements, the place where the NEs are connected, the nature of input action etc. This equally concerns both the cases when NEA are given rise to either by special NEs in an antenna or by parasitic nonlinearities in it. That is why both indicated types of devices should be considered as a

single class, that is the class of antennas with nonlinear elements (ANE).

1. General characteristic of the ANE theoretical analysis methods. As it follows from the mentioned above the correct analysis of ANE needs complex approach that requires taking into account characteristics and parameters of all the elements included into the ANE as well as its excitation condition. The objective on the analysis is to determine spectral composition of a ANE response depending on the nature of an input action. The ANE response is characterized by the output parameters vector. The vector components must be the values that describe coupling of the antenna with external space and a load or the generators (for receiving or transmitting ANE respectively). Two approaches can be arbitrarily chosen to solve this problem: the structural approach and an approach on the state variables basis.

With the structural approach the antenna is presented as the input action transducer into a response and it is described by some operator  $F$  that converts the vector of the input action  $x(\vec{r}, t) >$  into the output parameters vector

$$y(\vec{r}, t) > = F\{x(\vec{r}, t) >, t\}. \quad (1)$$

The structural approach corresponds directly to the initial statement of the problem, that is determination of the response by the known action. The possibility to use it, is essentially restricted by the fact that with this approach the knowledge of analytical presentation of an  $F$  operator is necessary. This presentation is true on a definite set of input actions of the analyzed ANE. As a rule it results in necessity to make some assumptions idealizations in description of some units and elements of an antenna while constructing  $F$  (for example, neglecting coupling between radiators APAA). Because of this the results obtained on the basis of the structural approach can be useful commonly only to estimate roughly parameters and characteristics of a ANE.

At present an approach on the basis of state variables is the main approach, used to analyze ANE. In this case the device is described by the system of equations in respect to a vector of state variables  $u(\vec{r}, t) >$  and a vector of input actions  $x(\vec{r}, t) >$

$$L\{u(\vec{r}, t) >, x(\vec{r}, t) >, t\} = 0 \quad (2)$$

and a set of functional relations that connect the vectors  $u(\vec{r}, t) >$  and  $x(\vec{r}, t) >$  with the vector of output parameters

$$y(\vec{r}, t) > = y\{u(\vec{r}, t) >, x(\vec{r}, t) >, t\}. \quad (3)$$

The relations (2) are called state equations and the relations (3) are known as output equations.

The form of state equations depends on a choice of state variables. The form of the output equations is dependable on what type of ANE is considered and which parameters or characteristics of the analyzed antenna are chosen as components of the output parameters vector.

Formation of two approaches to analyze ANE - the structural and the state variables ones - is a matter of convention. It is clear from the example when the SE can be solved explicitly. Then it is possible to express  $u(\vec{r}, t) >$  as

$$u(\vec{r}, t) > = L^{-1}\{x(\vec{r}, t) >, t\} \quad (4)$$

for some set of vectors  $x(\vec{r}, t) >$ . Now to obtain a structural model of ANE of a form (1) it is enough to substitute (4) into (3). Such a method is often used to form structural models.

In the process of analysis of ANE by means of the state variables the SE solution is the most labor stage that determines the efficiency of all the methodology as a whole. The methods to solve them can be subdivided into the analytical and numerical ones. Let us consider the numerical methods first. Their ca-

pabilities are higher.

2. Numerical methods to solve SE. These methods can be realized both in time and frequency domain. It is expedient to seek the solution in the time domain when determining a ANE response to an unsteady action (for example its pulse excitation) when ANE works with a super broadband signal (SEBS) etc. The advantages of the time domain method are: the possibility to investigate a transient mode of ANE and its behaviour in all the frequency range at once. Its disadvantages are: the necessity to know the transient responses of all the ANE elements or equivalent circuits of ANE elements with distributed parameters (transmission lines, radiators etc); the necessity to calculate transient process to obtain the characteristics of the state mode; high dimension of the SE system in case of a complex ANE circuit. The listed disadvantages result in a large (sometimes inadmissible) volume of calculations.

That is why the time domain methods are used in case of an ANE operation under purely unsteady conditions. As an example the article /1/ can be mentioned. Characteristics of wire radiator with NE when they are excited with an electromagnetic pulse are investigated in this work. The importance of the ANE analysis in the time domain is increased by the growing interest to SEBS and by the fast rise of capabilities of computers (that can be seen in particular in development and use of the FDTD method).

Nevertheless even taking all this into account in the process of investigation of a state mode of ANE it is obviously preferable to solve SE in the frequency domain.

At present the method of harmonic balance or of modified harmonic balance /2/ is used to solve SE in the frequency domain in the overwhelming majority of cases. The unknown solution, that is time dependence of the state variables (currents or voltages) is presented as Fourier series. In so doing the initial system is transformed into the simpler one of nonlinear equations in respect to amplitudes of harmonic components of currents or voltages that are calculated by some iteration method. The harmonic balance method is used also in the case of ANE excitation by a narrowband signal. In this case the latter can be treated as a harmonic signal with a slowly changing amplitude /3/.

By means of the listed methods the solution of the scattering problems of single dipoles, helix and loop radiators with NE /2/ were obtained, some types of single transmitting ANE were investigated as well as transmitting APAA constructed on their basis /4/. As this takes place in each case a specific own mathematical model of an ANE was used. In particular in /4/ a suggestion was assumed that nonlinearity of active modules characteristics included into APAA, is described by the dependence either a transmission coefficient or an input and output resistance module on a signal amplitude at its input. This situation on the one hand simplified the models essentially and allowed to analyze not only single ANE but also antenna arrays on their basis. Nevertheless on the other hand the assumed proposal means neglecting the process of appearance in a response of new ANE spectral components that are absent from a spectrum of an input action. Thus the accepted model allows to study only NEA at the basic frequency. The other effects (spurious radiation and side reception channels) under such a model cannot be considered and this restricts the fields of application of the results obtained by its means.

A sufficiently general method of the ANE analysis was offered by the authors /5/. The ANE generalized scheme (Fig.1) is initial in this method. According this scheme the ANE is presented as a connection of three linear and nonlinear multiports. The linear multiport LM-1 describes the ANE radiators system and is characterized by the scattering matrix  $S(\omega)$  connecting the vectors of incident  $a''(\omega)$  and reflected  $b''(\omega)$  waves on the radiators system inputs (section  $\beta-\beta$ ) and vector of incident  $u'_n(\omega)$  and reflected  $u'_r(\omega)$  "spherical waves in the free space" /6/.

The linear multiport LM-2 describes the load and is characterized by the scattering matrix  $S_L(\omega)$  connecting the vectors of the incident  $a'(\omega)$  and ref-

lected  $b'(\omega) >$  waves on its inputs (section  $\gamma-\gamma$ ). The vector of the waves  $b_0 >$  excited by the sources in the LM-2 is also shown in the section  $\gamma-\gamma$ .

The linear multiport LM-3 describes the rest of the circuit linear elements (transmitting lines, filtering circuits etc.). It is characterized by the matrix  $Q(\omega)$  giving the coupling between the vectors  $u_\alpha(\omega) >$ ,  $a''(\omega) >$ ,  $a'(\omega) >$  on the one hand and the vector of normalized currents  $i^\alpha(\omega) >$  and the vectors  $b'(\omega) >$ ,  $b'(\omega) > + b_0(\omega) >$  on the other hand:

$$\begin{bmatrix} u^\alpha(\omega) > \\ a''(\omega) > \\ a'(\omega) > \end{bmatrix} = \begin{bmatrix} Q_{\alpha\alpha}(\omega) Q_{\alpha\beta}(\omega) Q_{\alpha\gamma}(\omega) \\ Q_{\beta\alpha}(\omega) Q_{\beta\beta}(\omega) Q_{\beta\gamma}(\omega) \\ Q_{\gamma\alpha}(\omega) Q_{\gamma\beta}(\omega) Q_{\gamma\gamma}(\omega) \end{bmatrix} \begin{bmatrix} i^\alpha(\omega) > \\ b''(\omega) > \\ b'(\omega) > + b_0(\omega) > \end{bmatrix}, \quad (5)$$

The nonlinear multiport is described by the operator  $\mathcal{R}$  transforming the voltages vector  $u_{NL}(t) >$  on its inputs into the currents vectors  $i_{NL}(t) >$ :

$$i_{NL}(t) > = \mathcal{R}\{u_{NL}(t) >\} \quad (6)$$

Definition for concrete ANE parameters (LM-1,2,3, operator  $\mathcal{R}$ , input vectors  $u_{in} >$  and  $b_0 >$ ) constitutes the first stage of ANE analyses. Knowing them we can obtain the SE matching currents and voltages in the section  $\alpha-\alpha$  from the side of the NM and the whole LM (the dashed line, Fig.1).

From now on almost periodic or periodic mode of the ANE operation, i.e. the mode in which the antenna is affected by several signals with different (in general case non multiple) frequencies on the side of the external space  $u_{in}(\omega_k) >$

and (or) from the internal generators  $b_0(\omega_k) >$  ( $k_1, k_2 < k=0, q; q+1$  - the number of different frequencies of the input signals) will be treated. Thus, if we choose the NM input currents as the state variables then the ES for the steady-state conditions will be

$$\sum_{n=-\infty}^{\infty} \delta_n I^\alpha(\nu_n) > e^{j\nu_n t} + \mathcal{R} \left\{ \sum_{n=-\infty}^{\infty} \delta_n Z(\nu_n) I^\alpha(\nu_n) > e^{j\nu_n t} + \mathcal{Z}(t) > \right\} = 0, \quad (7)$$

where  $\delta_n = 1$  for  $\nu_n = 0$  and  $\delta_n = 1/2$  for  $\nu_n \neq 0$ ;  $\nu_n$  - characterize all possible combinations of the input frequencies;  $Z(\nu_n)$  - is the matrix of self and mutual impedance of the LM from the side of the section  $\alpha-\alpha$ ;  $I^\alpha(\nu_n) >$  - is the currents amplitudes vector of the LM inputs on the frequency  $\nu_n$  in the section  $\alpha-\alpha$ ;  $\mathcal{Z}(t) >$  - is result of recalculation to the section  $\alpha-\alpha$  the input vector. The summation in (7) is taken over the whole possible combinations of frequencies of the input signals  $\omega_k$ :

$$\nu_n = m_0 \omega_0 + m_1 \omega_1 + \dots + m_q \omega_q; \quad m_k = 0, \pm 1, \pm 2, \dots \quad (8)$$

The state equations solution (currents identification in  $\alpha-\alpha$  sections) is the first stage of the APAA analysis. The second stage is the definition of the APAA output parameters vector  $\{a'(\nu_n) >, u_r(\nu_n) >\}_T$  with the specified input signals  $b_0(\omega_k) >$ ,  $u_{in}(\omega_k) >$  and already known (found on the stage of the state equations solution) vector  $I^\alpha(\nu_n) >$ . The index  $T$  indicated the transponse operation.



The output parameters vector units in itself, virtually, two vectors - vector  $a'(\nu_n)$  characterizing the link of the antenna with the load and vector  $u_r(\nu_n)$  describing the link with a free space i.e. defining the antenna external parameters. The relations connecting vectors  $a'(\nu_n)$ ,  $u_r(\nu_n)$  on the one hand and vectors  $b_o(\omega_k)$ ,  $u_{in}(\omega_k)$  and  $i^\alpha(\nu_n)$  on the other hand assume the form

$$\begin{bmatrix} a'(\nu_n) \\ u_r(\nu_n) \end{bmatrix} = \begin{bmatrix} \bar{Q}_{\gamma\alpha}(\nu_n) & \bar{Q}_{\gamma\gamma}(\nu_n) & \bar{Q}_{\gamma\delta}(\nu_n) \\ \bar{Q}_{\delta\alpha}(\nu_n) & \bar{Q}_{\delta\gamma}(\nu_n) & \bar{Q}_{\delta\delta}(\nu_n) \end{bmatrix} \begin{bmatrix} i^\alpha(\nu_n) \\ b_o(\omega_k) \\ u_{in}(\omega_k) \end{bmatrix}. \quad (9)$$

In the quoted above expression the blocks  $\bar{Q}_{\gamma\mu}(\nu_n)$  and  $\bar{Q}_{\delta\mu}(\nu_n)$  ( $\mu=\alpha, \beta, \gamma$ ) are defined by the known matrices of the multiports LM-1, LM-2, and LM-3 /5/.

Equation (9) is a matrix representation of the output equations system for the ANE described by the scheme in Fig.1. After computation of  $u_r(\nu_n)$  and  $a'(\nu_n)$  it is possible to define, by the formulas of /6/, all the external parameters of the ANE: its RP, directivity etc.

Because of the availability of a nonlinear element external parameters are to be determined not only at the frequencies of external actions but also at all new frequencies generated by nonlinearities. Parameter values will depend on a level of input action. Since ANE is an non-reciprocity unit the parameters of transmitting and receiving antennas are to be considered separately. The noted circumstances: an appearance of new spectral components in an ANE spectrum, dependence of ANE characteristics on a level of input action, non-reciprocity of ANE predetermines existence of a great number of external antenna parameters.

### 3. Ways to increase efficiency of a solution of SE. Solution of state equa-

tions is the key point in the method of state variables that determines efficiency of the whole approach. With ANE complication, increase of a number of NE in it, a number of harmonics that must be taken into account to obtain correct output results the system dimension grows and this restrict the possibilities to solve it. These possibilities can be essentially extended if NE included into the system are coupled between themselves in different ways. It is for example characteristic of the cases when a NM is a combination of two- or threeport lumped NE (diodes, transistors) that do not couple within this multiport. Under similar conditions, that are rather widely spread in practice, quite an effective algorithm to solve the system (7) can be used; the idea of the algorithm is based on a decomposition conception. Its essence lies in separation of all the NE into groups in such a way that these groups could contain only the so called "strongly coupling" NE, when changing a mode of one of them has an efficient influences on the other NE that belong only to the given group; the influence is insignificant if modes of NE from other groups are considered. This provides a possibility to divide the NM into a number of partial multiports and to form a two-level iteration process to solve the system of equations state variables. Corresponding to each of the partial NM the state variables are determined of the lower iteration level. Their values are defined more exactly at the upper level with taking into account the coupling of NM through the linear parts of the circuit. Such an approach allows to replace a solution of a high dimension problem with a solution of a number of low dimension problems.

Let us consider the peculiarities of the offered algorithm. Let us suppose that  $N$  spectral current components  $i^\alpha(\nu_n)$  are taken into account in the course of the solution. Since the partial NM in the scheme of ANE are not connected the system of equation (7) can be transformed to the following form:

$$\langle \Omega(t) I \rangle_1 + \mathcal{R}_1 \left\{ \langle \Omega(t) \{Z\}_{11} I \rangle_1 + \sum_{\substack{p=1 \\ p \neq 1}}^M \langle \Omega(t) \{Z\}_{1p} I \rangle_p + \mathcal{S}_1(t) \right\} = 0, \quad \forall l=1, M. \quad (10)$$

Here:  $M$  is a number of partial LM in the circuit;  $\langle \Omega(t) \rangle$  is a matrix-row of the form:  $\langle \Omega(t) \rangle = \{ \exp(j\nu_{-N}t), \dots, \exp(j\nu_{-1}t), 2, \exp(j\nu_1t), \dots, \exp(j\nu_Nt) \}$ ;  $\mathcal{R}_1$  is an operator describing coupling between a current and a voltage on the terminals of the 1-st LM;  $I_1 = \{ I_1^{(0)}(\nu_{-N}), \dots, I_1^{(0)}(\nu_{-1}), I_1^{(0)}(0), I_1^{(0)}(\nu_1), \dots, I_1^{(0)}(\nu_N) \}$  is a vector, which components represent complex current amplitudes on linear multiport inputs connected to the 1-st LM;  $\{Z\}_{lp}$  is block-diagonal matrix that has the form:  $\{Z\}_{lp} = \text{diag}\{Z_{lp}(\nu_{-N}), \dots, Z_{lp}(\nu_{-1}), Z_{lp}(\nu_0), Z_{lp}(\nu_1), \dots, Z_{lp}(\nu_N)\}$ ;  $\mathcal{S}_1(t)$  is a value of EMF source of the 1-st LM input.

The system of equations (10) is completely equivalent to the system (7), with being an explicitly derived term  $\sum_{\substack{p=1 \\ p \neq 1}}^M \langle \Omega(t) \{Z\}_{1p} I \rangle_p$  describing connection

between separate "weakly coupling" LM at the basic frequency and at the harmonic frequencies through the LM; the mentioned term is in (10) under the sign of  $\mathcal{R}_1$  operator. Because of this in case the solution of (10) as vectors  $I_l$ ,  $\forall l=1, M$  is known, the next approximation  $I_l^{(k+1)}$  can be determined from the solution of  $M$  independent equations

$$\langle \Omega(t) I \rangle_1^{(k+1)} + \mathcal{R}_1 \left\{ \langle \Omega(t) \{Z\}_{11} I \rangle_1^{(k+1)} + \Delta \mathcal{S}_1^{(k+1)}(t) + \mathcal{S}_1(t) \right\} = 0, \quad \forall l=1, M, \quad (11)$$

where

$$\Delta \mathcal{S}_1^{(k+1)}(t) = \sum_{\substack{p=1 \\ p \neq 1}}^M \langle \Omega(t) \{Z\}_{1p} I \rangle_p^{(k)}. \quad (12)$$

The sequence of the calculations under this algorithm can be presented in the following way.

At the first step of iterations ( $k=1$ )  $I_l^{(0)} = 0$ , ( $l=1, M$ ) is assumed to be an initial value. It means that while determining  $I_l^{(1)}$  the 1-st LM is connected to the corresponding inputs of the linear part of the circuit and all its other inputs are opened. The equations (11) in this case describe  $M$  independent circuits, each of which contains a serial connection of a LM with  $\{Z\}_{11}$  matrix, EMF sources  $\mathcal{S}_1(t)$  and LM, that have  $\mathcal{R}_1$  characteristic. The solution of the equations (11) on a lower level of iterations that is defining of currents  $I_l^{(k)}$  for each of the partial multiport; their mutual coupling being not taken into account. Taking into account of the mutual influences of LM is carried out in the calculations of  $I_l^{(k+1)}$  in the course of the subsequent iterations of the upper level by means of insertion into the circuit of additional EMF sources having  $\Delta \mathcal{S}_1^{(k)}(t)$  voltages.  $\Delta \mathcal{S}_1^{(k)}(t)$  value is determined by the relation (12). Therefore the calculation of the whole circuit at one iteration of the higher level is reduced to subsequent calculation of  $M$  simpler circuits, not only for the first step but also for all the following ones.

It is necessary to note that if high level iterations determined by the relation (11) convergence, they converge to the precise solution of the equation (10). This statement follows from the fact that in case the iteration process

converges  $\|I_1^{(k+1)} - I_1^{(k)}\| \rightarrow 0$  if  $k \rightarrow \infty$ . For  $\Delta x_1^{(k)}(t) >$ , deduced from (12) also  $\|\Delta x_1^{(k+1)}(t) - \Delta x_1^{(k)}(t)\| \rightarrow 0$  when  $k \rightarrow \infty$  if matrix norms  $\{Z\}_{lp}$  are restricted. Thus it is possible to indicate  $\varepsilon_1 \rightarrow 0$  and  $\varepsilon_2 \rightarrow 0$  with  $k \rightarrow \infty$  that if beginning with some  $M_c$  inequality  $\|\Delta x_1^{(k+1)}(t) - \Delta x_1^{(k)}(t)\| < \varepsilon_1$  is true for all  $k \leq M_c$  then in view of continuity of  $x_1$  the inequality

$$\left\| \left\{ \Omega(t) \{Z\}_{ll} I_1^{(k+1)} + \Delta x_1^{(k+1)}(t) \right\} + x_1(t) \right\| -$$

$$\left\| \left\{ \Omega(t) \{Z\}_{ll} I_1^{(k)} + \Delta x_1^{(k)}(t) \right\} + x_1(t) \right\| < \varepsilon_2 \quad (13)$$

is also true. That is why if the sequence  $I_1^{(k)}$  calculated by (11) converges then it converges to the precise solution of the system (10).

Increase in efficiency of the proposed algorithm in comparison with the traditional one is achieved at the expense of the fact that at a low level of an iteration process (11) when an approximate value of a state variable of a partial KM is determined square convergence rate methods are used. It becomes possible since the dimension of the required in this case Jacobi matrix is essentially less than the Jacobi matrix of the system of equations (7). The mentioned required Jacobi matrix dimension depends on the number of frequencies  $\nu_n$  taken into consideration in the process of calculation and on the number of inputs of a partial KM. A convergency rate of a upper level iteration process (11) is linear, nevertheless to ascertain the values of state variables at the expense of coupling between separate "weakly connected" KM one needs only a few iterations that is why time consumption on the upper level of the iteration process is low.

For example it is illustrated by the dependence given on Fig. 2 of a number of iterations of the higher level  $N_{IT}$  on the distance  $d/\lambda$  between radiators, calculated for an array that consists of receiving-rectifying elements of rectennas. For  $d/\lambda < 0,5$ , i.e. when coupling between RE is "strong", to obtain a solution one needs 15...35 iterations. Coupling reduction results in decrease of  $N_{IT}$  and when already  $d/\lambda \geq 2,5$  to achieve the given accuracy of the solution one needs 4...6 iterations of the higher level.

The application of a decomposition idea with the same exactness of the received results allows to analyze the circuits containing as a minimum greater number of RE by several fold that it is possible when one-level iteration method is used.

Besides there exists some more possibilities to increase productivity of the proposed algorithm. One of them is following. Sometimes it may happen that several circuits, analyzed in the course of the iteration process of the lower level, have identical parameters. In this case it is sufficient to obtain a solution only for one of the circuits of this group and not to analyze the rest of them. This results in reduction of the upper iteration process duration and thus the total time consumption of calculations.

Another possibility to increase the algorithm productivity lies in the fact that as a rule an extent of KM coupling by means of the linear part of the circuit appears to be different. It results in a situation when at  $(k+1)$ -th iteration of the upper level the value  $\Delta x_1^{(k+1)}(t) >$  slightly differs from  $\Delta x_1^{(k)}(t) >$ , obtained at the previous stage i.e.

$$\frac{\|\Delta x_1^{(k+1)}(t) - \Delta x_1^{(k)}(t)\|}{\|\Delta x_1^{(k+1)}(t)\|} \ll 1. \quad (14)$$



In this case one does not need to calculate this circuit. Therefore if then instead of analysis of the circuit with the 1-st KM at (k+1)-th stage of the upper level iterations usage of the results of the previous k-th stage of this circuit analysis is sufficient. By doing so general productivity of the algorithm is increased at the expense of reduction of the number of circuits analyzed at the upper level of iteration process.

In conclusion it is necessary to note that the joint usage of the described possibilities of the algorithm productivity increase allow to reduce time consumption of the computer calculations essentially and in its turn broaden the range of the analyzed ANE or provides the possibility of their more accurate research at the expense of taking into account greater number of harmonic terms of currents.

4. Analytical methods to solve SE. So far an analytical solution of state equations was obtained only for a few the simplest problems such as scattering of a plane wave by a linear dipole with one /7/ or a few /8/ NE. The results obtained can be applied only to estimate parameters of these ANE qualitatively since in the course of solution of SE essential simplifying assumptions were made concerning both ANE circuits itself and the parameters of the elements included in it.

Lately the authors developed an analytical method to solve SE that is correct enough for many important cases. It can be called as a structural-matrix method. Such a name is stipulated for the one hand by the fact that in essence the construction of a structural model of ANE is a final result of the proposed method for the other hand - the method itself is based on use of Volterra series in a matrix formulation and many-dimensional scattering matrixes of KM. In this case as initial, also as by numerical solution of SE, a generalized scheme of ANE given in Fig. 1 was chosen. A incident waves vector  $a^{(\omega)}$  in section  $(\alpha-\alpha)$  was chosen as state variables. A system of SE was obtained that connected  $a^{(\omega)}$  with parameters of linear and nonlinear multiports and characteristics of ANE excitation. The system looks like

$$(S_{\alpha\alpha})^{-1} a^{(\omega)} + \hat{a}_0(\omega_k) - \mathcal{J}(a^{(\omega)}) = 0, \quad (15)$$

where  $S_{\alpha\alpha}$  is scattering matrix LM block that characterized it with respect to the section  $(\alpha-\alpha)$ ;  $\hat{a}_0(\omega_k) = (S_{\alpha\alpha})^{-1} (S_{\alpha\delta} u'_{in}(\omega_k) + S_{\alpha\gamma} b_0(\omega_k))$  - vector of external actions on ANE recalculated to section  $(\alpha-\alpha)$ ;  $S_{\alpha\delta}$  и  $S_{\alpha\gamma}$  are blocks of LM scattering matrixes, characterizing coupling between the inputs at the sections  $(\alpha-\delta)$  and  $(\alpha-\gamma)$  respectively;  $\mathcal{J}$  - an operator, characterizing a nonlinear multiport i.e. describing the coupling between the vectors of incident and reflected waves at its inputs. It should be pointed out that unlike a "traditional" scattering matrix, the operator  $\mathcal{J}$  describes also formation of the reflected KM waves in the response with the frequencies different from the frequencies of input signals due to nonlinear characteristics of a multiport.

The system of equation (15) is a system of nonlinear equations from which a solution for a vector of state variables  $a^{(\omega)}$  is determined with known parameters LM (matrixes  $S_{\alpha j}$ ,  $j=\alpha, \delta, \gamma$ ) and KM (the  $\mathcal{J}$  operator) for a given external action, described by the vectors  $u'_{in}(\omega_k)$  and  $b_0(\omega_k)$ . The given system describes the whole ANE as a single nonlinear multiport. Its solution is looked for as an expansion in a matrix Volterra series

$$\hat{a}^\alpha(\omega) = \sum_{n=1}^{\infty} \int \dots \int \hat{S}_n(\nu_1, \dots, \nu_n) \hat{u}_n^\alpha(\nu_1, \dots, \nu_n) \delta(\omega - \nu_1 - \dots - \nu_n) \prod_{i=1}^n d\nu_i \quad (16)$$

In this relation  $\hat{S}_n(\nu_1, \dots, \nu_n)$ , ( $n=1, 2, \dots$ ) are many-dimensional matrixes of ANE and are unknown expansion coefficients of the  $\hat{a}^\alpha(\omega)$  vector into Volterra series. They are to be found from the solution of (15).  $\hat{u}_n(\nu_1, \dots, \nu_n)$  is a vector characterizing external actions on ANE depending only on  $\hat{a}_0(\omega_k)$ .

Hence the solution of (15) lies in finding the  $\hat{S}_n(\nu_1, \dots, \nu_n)$  matrix, i.e. in determination of the coupling between  $\hat{S}_n(\nu_1, \dots, \nu_n)$  on the one hand and the  $\hat{S}_{\alpha\alpha}$  matrix  $\hat{a}_0(\omega_k)$  and the  $\mathcal{V}$  operator on the other hand. As the authors showed for an almost-periodic mode of ANE this coupling has the form

$$\left[ \hat{S}_{\alpha\alpha}^{-1}(\nu_1 + \dots + \nu_n) - \hat{S}_1^{-1}(\nu_1 + \dots + \nu_n) \right] \hat{S}_n(\nu_1, \dots, \nu_n) + \hat{H}_n(\nu_1, \dots, \nu_n) = 0, \quad \forall n=1, 2, \dots \quad (17)$$

In this relation  $\hat{S}_1(\nu_1 + \dots + \nu_n)$  is a low signal scattering matrix of a NM at  $\nu_1 + \dots + \nu_n$  frequency;  $\hat{H}_n(\nu_1, \dots, \nu_n)$  - many-dimensional matrix characterizing signal sources of any of the frequencies present in the ANE response of n-order; the matrix is calculated by the known  $\hat{a}_0(\omega_k)$  vector and by the  $\hat{S}_j(\nu_1, \dots, \nu_n)$  matrixes of the order  $j < n$ . For  $n=1$  this matrix reduces to vector  $\hat{a}_0(\omega_k)$  (this testifies that the external signal sources are the response sources of the first order).

The procedure to calculate  $\hat{S}_n(\nu_1, \dots, \nu_n)$  matrixes lies in their sequential calculation in accordance with the relation (17) for different  $n$  in the order of their increase. It is worth to note that the calculations are of a recursion nature, since in the process of calculation of the many-dimensional matrixes of the  $n$ -th order, in addition to the known scattering matrixes of a LM and the many-dimensional matrixes of a NM, to find  $\hat{H}_n(\nu_1, \dots, \nu_n)$  only many-dimensional scatterings ANE matrixes are needed of the orders less than  $n$ , i.e. the values obtained at the previous stages of calculation are used.

The possibility to describe NE by a short power series is the key point that determines the efficiency of the proposed method. In its turn the latter is determined by the nature of a nonlinearity and the input ANE signal level. As the input signal level is reduced the number of the series members needed to describe NE decreases and the importance of the proposed method grows.

The obtained analytical solution of the SE allowed to expand the range of the analyzed ANE. In particular it is possible to obtain correct results for calculation of a scattering field of APAA on combinative frequencies, its characteristics concerning side reception channels, antenna-mixers parameters etc.

#### REFERENCES

- (1) J.A.Landt et al.: "Time domain modeling of antennas with nonlinear loads", - Trans. IEEE, (1983) AP-31, 1, pp.121-125.
- (2) G.Franceschetti et al.: "Antennas with nonlinear load", in: Nonlinear Electromagnetics, ed. by P.L.E.Uslenghi, (1983) Mir, Moscow, pp.223-249.
- (3) C.Waldi et al.: "Distortion analysis of nonlinearly loaded antennas", in: AP-S Int. Symp. Los-Angeles, Calif., (1981) 2, pp.410-413.
- (4) V.L.Gostyukhin et al.: Designing Active PAA by Computer, Radio i Svyaz, Moscow, 1983.

- (5) Y.S.Shifrin et al.: "Nonlinear effects in active phased arrays", Radiotekhnika i Elektronika, (1994) 39, 7.
- (6) D.M. Sazonov: "Principles of antenna-array matrix theory", in: Collection on Applied Electrodynamics, (1983) Vyssh. Shk., Moscow, 6, pp. 111-162.
- (7) M.Kanda: "Analytical and numerical techniques for analyzing electrically short dipole with nonlinearly load", Trans. IEEE, (1980) AP-28, 1, pp. 71-78.
- (8) T.K.Sarkar et al.: "Analysis of nonlinearly loaded multiport antenna structures an imperfect ground plane using Volterra series method", Trans. IEEE, (1978) EMC-20, 3, pp. 278-288.

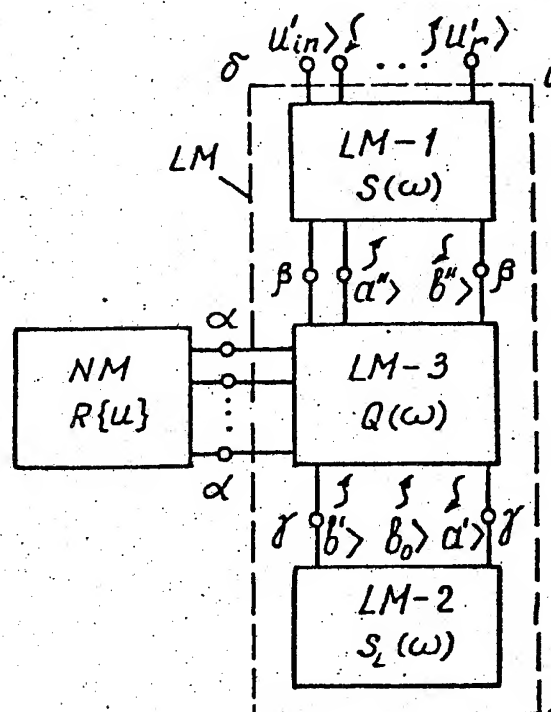


Fig. 1. Generalized scheme of the ANE

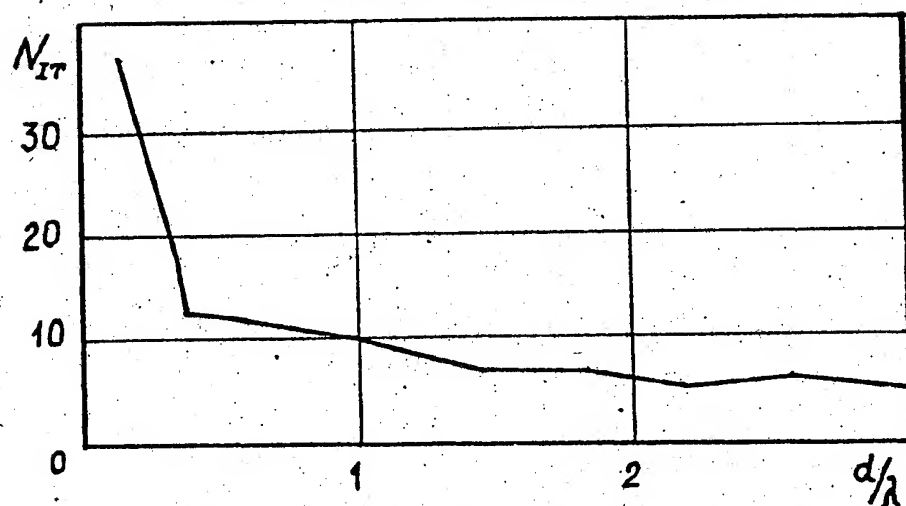


Fig. 2. Dependence of the higher level iterations number on the distance between radiators

# SCATTERING OF ELECTROMAGNETIC WAVES BY SCATTERERS COMPOSED OF CONDUCTING STRIPS

Michinari Shimoda

Dept. of E. Eng. Kumamoto National  
College of Technology  
2659-2 Nishigoushi, Kikuchi-gun,  
Kumamoto-ken, 861-11 Japan

Tokuya Itakura

Dept. of E. E. and C. Sci., Faculty of  
Eng. Kumamoto University  
2-39-1 Kurokami, Kumamoto-shi, 860  
Japan

## ABSTRACT

Two dimensional scattering of electromagnetic waves by the scatterers composed of conducting strips is analyzed by means of the Wiener-Hopf technique together with the formulation using the partition of the scatterers. By using of the concept of the mutual field on the fictitious boundary of the sub-region, the simultaneous Wiener-Hopf equations are obtained, and the numerical solution of scattering by some scatterers are demonstrated.

## I. INTRODUCTION

The electromagnetic wave scattering by scatterers composed of strips has been of much theoretical interest. The problem of scattering by a strip grating made of infinitely conducting strips regularly placed on the same plane was analyzed rigorously by Lüneburg and Westpfahl<sup>(1)</sup> by means of the singular integral equation. The same problem was attacked by Hosono and Hinata<sup>(2)</sup> by the point matching method. The problem of scattering by a parallel strip grating made of infinitely strips oriented in parallel to each other was carried out by Kobayashi et al.<sup>(3)</sup>. The problems of scattering by the finite number of strips are important for engineering and practical cases, however there are very few research reports on those problems. Aoki et al.<sup>(4)</sup> solved the diffraction problem by two strips, placed on the same plane. Using Mathieu functions, Sacrmak<sup>(5)</sup> solved the diffraction problem of two arbitrarily oriented strips.

In the present paper, the problem of two-dimensional scattering of electromagnetic waves by the scatterers composed of conducting strips is analyzed by means of the formulation using the partition of the scatterers<sup>(6)-(7)</sup>. Defining the Fourier transform with respect to each local coordinate which is installed on strips, we investigate the mapping between different complex variables in these Fourier transforms. Consequently, the simultaneous Wiener-Hopf equations are obtained. In order to solve the Wiener-Hopf equations, the evaluation of the integrals along with branch cuts on the complex plane is necessary. In the case of the scatterers composed of a finite number of strips, the saddle point method is used for the evaluation of the integrals. In the case of the gratings in which an infinite number of strips are placed periodically, the sampling function is used to expand the unknown function associated with the field on the strip into a series, and then

the integrals are evaluated by the residue calculus technique. The Wiener-Hopf equations are reduced to a set of simultaneous equations.

The expression of the diffraction patterns in the far-field is obtained for the two arbitrarily oriented strips. The reflection and transmission coefficients of the grating with a periodic structure composed of several arbitrarily oriented conducting strips is obtained. From numerical calculation, the accuracy of the approximate solutions and the validity of the present algorithm are demonstrated. The time factor is assumed to be  $\exp(-i\omega t)$  and suppressed throughout this paper.

## II. FORMULATION

### 2.1 Statement of Problem

Figure 1 shows the scatterers composed of conducting strips and the coordinate system under discussion. The scatterers are uniform in the  $y$ -direction. They consist of perfectly conductors with zero thickness. Consider an incident TE plane wave which is polarized in the  $y$ -direction. In view of the geometry, this is a two-dimensional problem. Let us define the scattered wave  $E$  by

$$E^t(x, z) = E^i(x, z) + E(x, z) \quad (1)$$

where  $E^t$  is the  $y$ -component of the total electric field and  $E^i$  is the incident plane wave in the form

$$E^i(x, z) = \exp(-ikx \sin \theta^i - ikz \cos \theta^i) \quad (2)$$

where  $k(= \omega \sqrt{\epsilon_0 \mu_0})$  is the free space wavenumber. For convenience of analysis, we assume the medium to be slight lossy, i.e.,

$$k = k_1 + ik_2, \quad k_1 \gg k_2 > 0. \quad (3)$$

All scatterers with various structures represented by the position and the width of several strips are composed of three kinds of constituent elements as shown in Figure 2. For the following analysis in this section, we introduce the partition of the scatterers. The scatterers in case of (a) are partitioned at an arbitrary location between two strips. In case of (b), the scatterers are partitioned at the joint point of strips. The scatterers in the case of (c) are partitioned at the joint point of the strip and the extension line of another strip. By the partition of the scatterers, the entire regions is separated into several sub-regions, each of which has only one strip respectively. The boundary of this partition is

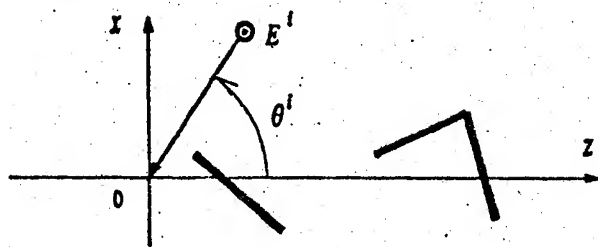


Figure 1: Geometry of scatterers composed of conducting strips.

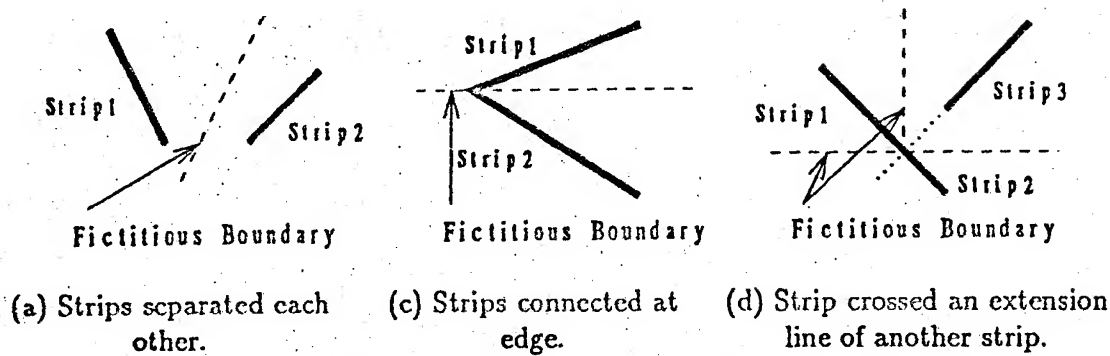


Figure 2: Partition of the scatterers.

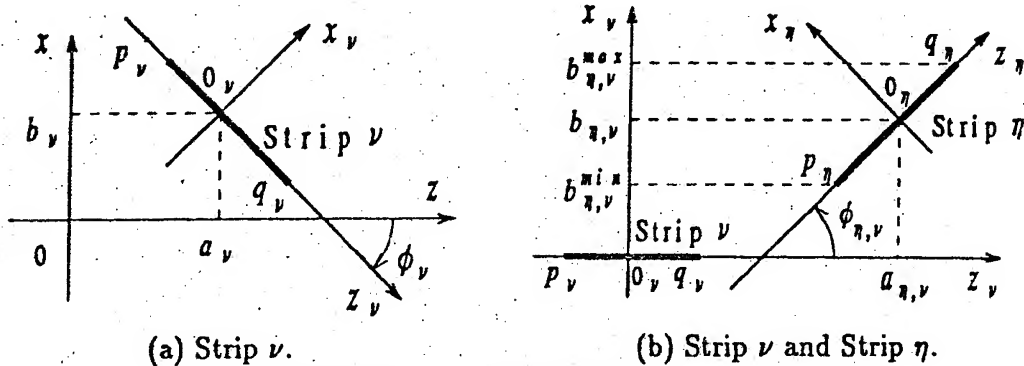


Figure 3: Local coordinate system.

called Fictitious boundary. We use the local coordinate systems  $[x_\nu, z_\nu]$  ( $\nu = 1, 2, \dots$ ) for each strip  $\nu$  as shown in Figure 3(a). Subsequently, the integration path of the Fourier transform with respect to each local coordinate system does not cross other strip in the meaning of separation by the partition of the scatterers. The partitioned strips are expressed as  $\{x_\nu = 0, p_\nu \leq z_\nu \leq q_\nu\}$  for  $\nu = 1, 2, \dots$ . Figure 3(b) shows the coordinate relations between the strip  $\nu$  and the strip  $\eta$  in the position of these strips. In the case of the gratings in which an infinite number of strips are placed periodically, the gratings have the scatterers composed of several strips as shown in Figure 1 in the period. In this case, we use the partition of the scatterers in one period. The partitioned strips are expressed as  $\{x_\nu = 0, -w_\nu \leq w_\nu \leq w_\nu\}$  for  $\nu = 1, 2, \dots$ .

## 2.2 Representation of Scattered Wave

When the number of strips is  $L$  as in Figure 1, the partitioned regions ( $S_1, S_2, \dots, S_L$ ) are separated by the fictitious boundary as shown in Figure 4. The subscript  $\nu, \eta$  of the fictitious boundary  $F_{\nu,\eta}$  shows the boundary between region  $S_\nu$  and  $S_\eta$ . Then, the present scattering problem is reduced to that of deriving the scattered wave  $E$  which satisfies the following conditions:

(a) perfect conductor condition

$$E(x_\nu = 0) = -E^i(x_\nu = 0), \quad p_\nu \leq z_\nu \leq q_\nu, \quad (\nu = 1, 2, \dots, L) \quad (4)$$

(b) radiation condition

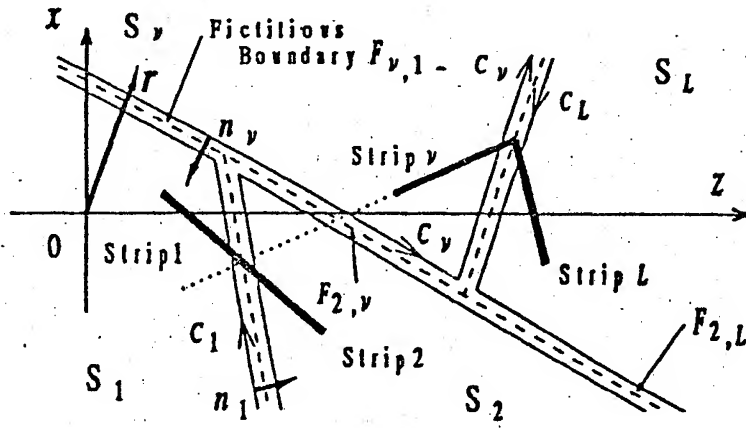


Figure 4: Fictitious boundary.

(c) wave equation.

$$(\partial^2/\partial x^2 + \partial^2/\partial z^2 + k^2)E(x, z) = 0. \quad (5)$$

In the regions  $S_\nu$ , we represent the scattered wave  $E$  as follow:

$$E(x, z) = \sum_{\nu=1}^L E_\nu(r), \quad E_\nu(r) = \begin{cases} E_\nu(r), & r \in S_\nu \\ 0, & r \in \bigcup_{\substack{\eta=1 \\ \eta \neq \nu}}^L S_\eta \end{cases} \quad (6)$$

where  $r$  is the position vector from the origin  $O$ . By applying the Green's theorem to the scattered wave  $E$  and Green's function

$$G(x, z; x', z') = \frac{i}{4} H_0^{(1)}(k \sqrt{(x - x')^2 + (z - z')^2}) \quad (7)$$

which is defined by the Hankel function of the first kind, we have

$$E_\nu(r) = E_\nu^s(r) + E_{M\nu}^i(r), \quad (\nu = 1, 2, \dots, L), \quad (8)$$

$$E_\nu^s(r) = \int_{p_\nu}^{q_\nu} G(x, z; x', z') \Big|_{z'_\nu=0} j_\nu(z'_\nu) dz'_\nu, \quad (9)$$

where  $j_\nu(z'_\nu)$  is the surface current on the strip  $\nu$  and  $E_{M\nu}^i$  is called the mutual field, which is the physical quantity to determine the multiple scattering between the strip  $\nu$  within the region  $S_\nu$  and the other strips outside the region  $S_\nu$ . From the electromagnetic field continuity at the fictitious boundary, we have

$$E_{M\nu}^i(r) = \sum_{\substack{\eta=1 \\ \eta \neq \nu}}^L E_\eta^s(r), \quad r \in S_\nu, \quad (\nu = 1, 2, \dots, L). \quad (10)$$

## 2.3 Simultaneous Wiener-Hopf Equations

We define the Fourier transform  $\mathcal{F}_\nu$  and the Fourier inverse transform  $\mathcal{F}_\nu^{-1}$  ( $\nu = 1, 2, \dots, L$ ) in the coordinate system shown in Figure 3(a) by the following equations:

$$\begin{aligned} F(x_\nu, \alpha_\nu) &= \frac{1}{\sqrt{2\pi}} \int_{-\infty}^{\infty} f(x_\nu, z_\nu) \exp(i\alpha_\nu z_\nu) dz_\nu \\ &= \mathcal{F}_\nu[f(x_\nu, z_\nu) \exp(i\alpha_\nu z_\nu)], \quad (\nu = 1, 2, \dots, L), \end{aligned} \quad (11)$$

$$\begin{aligned} f(x_\nu, z_\nu) &= \frac{1}{\sqrt{2\pi}} \int_{i\tau_{\nu-}}^{i\tau_{\nu+}} F(x_\nu, \alpha_\nu) \exp(-i\alpha_\nu z_\nu) d\alpha_\nu, \\ &= \mathcal{F}_\nu^{-1}[F(x_\nu, \alpha_\nu) \exp(-i\alpha_\nu z_\nu), \tau_{\nu-} < \tau_\nu < \tau_{\nu+}], \\ &\quad (\nu = 1, 2, \dots, L) \end{aligned} \quad (12)$$

where  $\tau_{\nu\pm}$  are constants and the complex number  $\alpha_\nu$  is

$$\alpha_\nu = \sigma_\nu + i\tau_\nu. \quad (13)$$

Substituting Eqs.(8) and (10) into the perfect conductor condition (4), we have the following integral equation with the unknown function  $j_\eta$

$$\begin{aligned} \frac{i}{4} \sum_{\eta=1}^L \left[ \int_{p_\eta}^{q_\eta} H_0^{(1)}(k\sqrt{x_\eta^2 + (z_\eta - z'_\eta)^2}) j_\eta(z'_\eta) dz'_\eta \right]_{x_\nu=0} &= -E^i(x_\nu=0), \\ p_\nu \leq z_\nu \leq q_\nu, \quad (\nu = 1, 2, \dots, L). \end{aligned} \quad (14)$$

Equation(14) is transformed into the extended form, which is valid for  $-\infty < z_\nu < \infty$ . By applying the Fourier transform to the extended form, we have the functional equation which is regular in the strip region  $-k_2 < \tau_\nu < k_2$  on the complex plane  $\alpha_\nu$ . After some rearrangement of the functional equation, by an application of Liouville's theorem and the analytic continuation in the complex plane, we get the simultaneous Wiener-Hopf equations

$$\left. \begin{aligned} Y_{Q\nu-}(\alpha_\nu) + Y_{Q\nu+}(\alpha_\nu) &= -\sqrt{\alpha_\nu + k} [\Phi_{K\nu}^i(\alpha_\nu) + \sum_{\substack{\eta=1 \\ \eta \neq \nu}}^L \Phi_{\eta\nu}(0, \alpha_\nu) \\ &\quad + \frac{Y_{P\nu-}(\alpha_\nu)}{\sqrt{\alpha_\nu - k}} \exp(i\alpha_\nu p_\nu)] \exp(-i\alpha_\nu q_\nu) \\ Y_{P\nu-}(\alpha_\nu) + Y_{P\nu+}(\alpha_\nu) &= -\sqrt{\alpha_\nu - k} [\Phi_{K\nu}^i(\alpha_\nu) + \sum_{\substack{\eta=1 \\ \eta \neq \nu}}^L \Phi_{\eta\nu}(0, \alpha_\nu) \\ &\quad + \frac{Y_{Q\nu+}(\alpha_\nu)}{\sqrt{\alpha_\nu + k}} \exp(i\alpha_\nu q_\nu)] \exp(-i\alpha_\nu p_\nu) \end{aligned} \right\}, \quad -k_2 < \tau_\nu < k_2, (\nu = 1, 2, \dots, L) \quad (15)$$

where

$$\gamma_\nu = \sqrt{\alpha_\nu^2 - k^2}, \quad \text{Re}(\gamma_\nu) \geq 0, \quad (16)$$



$$\Phi_{K\nu}^i(\alpha_\nu) = \frac{1}{\sqrt{2\pi}} \int_{p_\nu}^{q_\nu} E^i(x_\nu = 0) \exp(i\alpha_\nu z_\nu) dz_\nu, \quad (17)$$

$$\Phi_{\eta,\nu}(0, \alpha_\nu) = \mathcal{F}_\nu[E_\eta^s(x_\nu = 0) \exp(i\alpha_\nu z_\nu)]. \quad (18)$$

The  $\Phi_{\eta,\nu}(0, \alpha_\nu)$  on the right hand side of Eq.(15), which is derived by the Fourier transform of the mutual field  $E_{M\nu}^i$ , is the Fourier transform of the scattered field by the strip  $\eta$  at the  $x_\nu = 0$  with respect to the coordinate system  $z_\nu$ . In order to obtain  $\Phi_{\eta,\nu}$ , the mapping between the complex  $\alpha_\eta$ -plane and the complex  $\alpha_\nu$ -plane is investigated. The coordinate transformation from  $[x_\eta, z_\eta]$  into  $[x_\nu, z_\nu]$  and the variable transformation from  $\alpha_\eta$  into  $\alpha_\nu$  are used for the evaluation of Eq.(18). Subsequently, we get

$$\Phi_{\eta,\nu}(0, \alpha_\nu) = \begin{cases} [\sqrt{\alpha_\eta - k} Y_{Q\eta-}(\alpha_\eta) \exp(i\alpha_\eta q_\eta)]|_{\alpha_\eta = \alpha_\nu \cos \phi_{\eta,\nu} + i\gamma_\nu \sin \phi_{\eta,\nu}} \\ \quad \cdot \frac{1}{\gamma_\nu} \exp(-\gamma_\nu b_{\eta,\nu} + i\alpha_\nu a_{\eta,\nu}), & 0 \leq b_{\eta,\nu}^{min} \\ \\ [\sqrt{\alpha_\eta - k} Y_{Q\eta-}(\alpha_\eta) \exp(i\alpha_\eta q_\eta)]|_{\alpha_\eta = \alpha_\nu \cos \phi_{\eta,\nu} - i\gamma_\nu \sin \phi_{\eta,\nu}} \\ \quad \cdot \frac{1}{\gamma_\nu} \exp(\gamma_\nu b_{\eta,\nu} + i\alpha_\nu a_{\eta,\nu}), & 0 \geq b_{\eta,\nu}^{max} \end{cases} \quad (19)$$

where  $b_{\eta,\nu}^{min}$  and  $b_{\eta,\nu}^{max}$  are the coordinates of the edge of the strip  $\eta$  as shown in Figure 3(b). Therefore, the present scattering problem is reduced to that of solving the Wiener-Hopf equation(15) in which Eq.(19) is substituted. We have the representation of the scattered wave:

$$E(x, z) = \sum_{\nu=1}^L \mathcal{F}_\nu^{-1} \left[ \frac{Y_{Q\nu-}(\alpha_\nu)}{\sqrt{\alpha_\nu + k}} \exp(-\gamma_\nu |x_\nu| - i\alpha_\nu(z_\nu - q_\nu)), -k_2 < \tau_\nu < k_2 \right]. \quad (20)$$

Similarly, the formulation using the partition of the scatterers is applied to the analysis of the scattering problem by the grating with a periodic structure composed of infinite strips. In the case that the number of strips in one period is  $L$ , the simultaneous Wiener-Hopf equations is obtained as follow:

$$\left. \begin{aligned} Y_{Q\nu-}(\alpha_\nu) + Y_{Q\nu+}(\alpha_\nu) &= -\sqrt{\alpha_\nu + k} [\Phi_{K\nu}^i(\alpha_\nu) + \Phi_{M\nu}^i(\alpha_\nu) \\ &\quad + \frac{Y_{P\nu-}(\alpha_\nu)}{\sqrt{\alpha_\nu - k}} \exp(-i\alpha_\nu w_\nu)] \exp(-i\alpha_\nu w_\nu) \\ &\quad - Y_{Q\nu-}(\alpha_\nu) \gamma_\nu \sum_{\substack{\mu=-\infty \\ \mu \neq 0}}^{\infty} K_{\nu,\mu}(0, \alpha_\nu), \\ &\quad \tau_{\nu-} < \tau_\nu < k_2 \\ \\ Y_{P\nu-}(\alpha_\nu) + Y_{P\nu+}(\alpha_\nu) &= -\sqrt{\alpha_\nu - k} [\Phi_{K\nu}^i(\alpha_\nu) + \Phi_{M\nu}^i(\alpha_\nu) \\ &\quad + \frac{Y_{Q\nu+}(\alpha_\nu)}{\sqrt{\alpha_\nu + k}} \exp(i\alpha_\nu w_\nu)] \exp(i\alpha_\nu w_\nu) \\ &\quad - Y_{P\nu+}(\alpha_\nu) \gamma_\nu \sum_{\substack{\mu=-\infty \\ \mu \neq 0}}^{\infty} K_{\nu,\mu}(0, \alpha_\nu), \\ &\quad -k_2 < \tau_\nu < \tau_{\nu+} \end{aligned} \right\} \quad (21)$$

where

$$\tau_{\nu-} = k_2 \cos(\theta^i + \phi_\nu), \quad \tau_{\nu+} = k_2 \cos(\theta^i - \phi_\nu) \quad (22)$$

$$K_{\nu,\mu}(x_\nu, \alpha_\nu) = \frac{1}{\gamma_\nu} \exp[-\gamma_\nu |x_\nu - \mu h_\nu| + i\mu(\alpha_\nu d_\nu - k \cos \theta^i d)] \quad (23)$$

$$\begin{aligned} \Phi_{M\nu}^i(\alpha_\nu) = & \frac{1}{\sqrt{2\pi}} \int_{-w_\nu}^{w_\nu} \left[ \sum_{\substack{\eta=1 \\ \eta \neq \nu}}^L \mathcal{F}_\eta^{-1} [\sqrt{\alpha_\eta - k} Y_{Q\eta-}(\alpha_\eta) \exp\{-i\alpha_\eta(z_\nu - w_\eta)\}] \right. \\ & \left. \cdot \sum_{\mu=-\infty}^{\infty} K_{\eta,\mu}(x_\eta, \alpha_\eta), \tau_{\eta-} < \tau_\eta < \tau_{\eta+} \right] \bigg|_{x_\nu=0} \exp(i\alpha_\nu z_\nu) dz_\nu. \end{aligned} \quad (24)$$

where  $d$  is a periodic length and  $h_\nu$  and  $d_\nu$  are the  $x_\nu$  and  $z_\nu$  coordinates of the points, which are placed at a distance by one period from the center of the strip  $\nu$ . We get the scattered wave by the Fourier inverse transform

$$\begin{aligned} E = & \sum_{\nu=1}^L \mathcal{F}_\nu^{-1} [\sqrt{\alpha_\nu - k} Y_{Q\nu-}(\alpha_\nu) \exp(i\alpha_\nu w_\nu) \\ & \cdot \sum_{\mu=-\infty}^{\infty} K_{\nu,\mu}(x_\nu, \alpha_\nu) \exp(-i\alpha_\nu z_\nu), \tau_{\nu-} < \tau_\nu < \tau_{\nu+}]. \end{aligned} \quad (25)$$

### III. SCATTERERS COMPOSED OF ARBITRARY ORIENTED TWO STRIPS

#### 3.1 Solution of the Wiener-Hopf equations

Figure 5 shows the scatterers composed of two strips for numerical calculations. In order to solve the Wiener-Hopf equations(15), the evaluation of the integrals along with branch cuts on the complex plane is necessary. When the distance between the edges of the strips and half plane is no less than a wavelength  $\lambda$ , the saddle point method is used for the evaluation of the integrals. Subsequently, the approximate solutions of the Wiener-Hopf equations are obtained.

#### 3.2 Numerical results

For the far-field calculation, the Fourier inverse transforms(16) is evaluated by the saddle point method similarly. The diffracted far-field is the representation as follow:

$$E^d = D(\theta) R(r), \quad R(r) = \frac{\exp\{i(kr - \pi/4)\}}{\sqrt{r}} \quad (26)$$

where  $D(\theta)$  is the diffraction patterns of the far-field. Being rather lengthy formula, the formulas of the far-field pattern  $D(\theta)$  are cut off. However, it is noteworthy that they are expressed by each term which correspond to the geometrical optics representation.

Figure 6 shows the comparison of the diffraction pattern by the present method, the method of the neglected mutual field and the simple GTD method for the incident angle

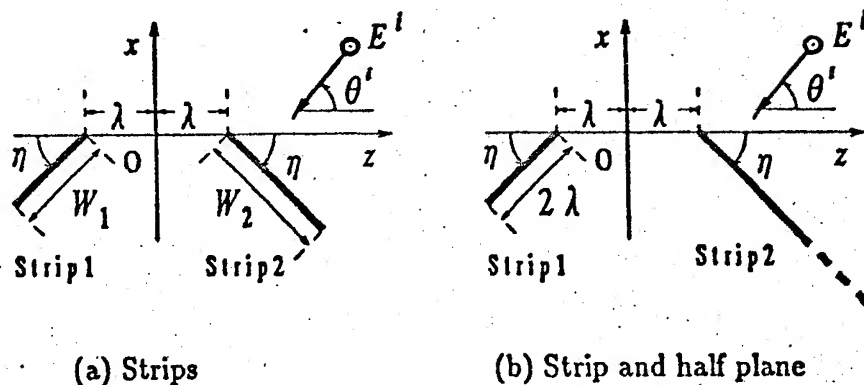


Figure 5: Scatterers for numerical calculation.

$\theta^i = 75^\circ$ . The method of the neglected mutual field is the algorithm which makes the mutual field equal to zero in the present method. Figure 6(a) and 6(b) show the diffraction pattern for two strips of the unequal strip widths ( $W_1 = 2\lambda$ ,  $W_2 = 10\lambda$ ) in Figure 5(a) and, one strip and one half plane in Figure 5(b). There are several discontinuous points for the results by the simple GTD method. these diffraction angles correspond to the shadow boundaries viewed from the edges. They are due to the neglect of multiple scattering between edges.

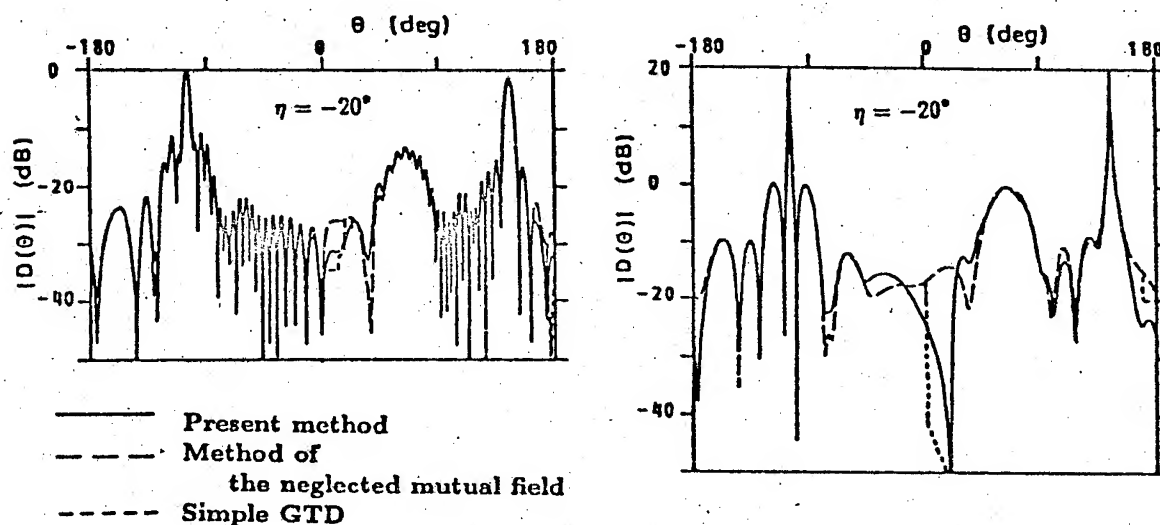


Figure 6: Far-field patterns.

## IV. GRATING COMPOSED OF THE STRIPS

### 4.1 Solution of the Wiener-Hopf equations

From the simultaneous Wiener-Hopf equations(21), we have the following relation:

$$\sqrt{\alpha_\nu - k} Y_{Q\nu-}(\alpha_\nu) \exp(i\alpha_\nu w_\nu) = \sqrt{\alpha_\nu + k} Y_{P\nu+}(\alpha_\nu) \exp(-i\alpha_\nu w_\nu) \equiv \hat{J}_\nu(\alpha_\nu). \quad (27)$$

where  $\hat{J}_\nu(\alpha_\nu)$  becomes the quantity corresponding to Fourier transform of the surface current on the Strip  $\nu$  which compose the gratings. In this section, using the characteristic of the following sampling function:

$$S_\nu(\alpha_\nu - \alpha_{\nu,n}) = \frac{\sin[(\alpha_\nu - \alpha_{\nu,n})w_\nu]}{(\alpha_\nu - \alpha_{\nu,n})w_\nu}, \quad \nu = 1, 2, \dots, L \quad (28)$$

where

$$\alpha_{\nu,n} = k \cos \theta_\nu^i + n\pi/w_\nu, \quad \theta_\nu^i = \begin{cases} \theta^i + \phi_\nu, & -\pi \leq \theta^i \leq \pi - \phi_\nu \\ \theta^i + \phi_\nu - 2\pi, & \pi - \phi_\nu < \theta^i \leq \pi \end{cases}, \quad (29)$$

the function  $\hat{J}_\nu(\alpha_\nu)$  is expressed in terms of the unknown coefficients  $C_{\nu,n}$  as follow:

$$\hat{J}_\nu(\alpha_\nu) = \sum_{n=-N_\nu}^{N_\nu} C_{\nu,n} S_\nu(\alpha_\nu - \alpha_{\nu,n}), \quad \nu = 1, 2, \dots, L \quad (30)$$

where  $N_\nu$  is the large integer. Using the residue calculus technique, the integrals along with branch cuts on the complex plane in the solution of the Wiener-Hopf equations are evaluated by the contributions from infinitely many poles in the integrand. These contributions may be approximated by those from a finite number  $2M+1$  of poles. Consequently, the Wiener-Hopf equations are reduced to a set of the simultaneous equations:

$$\sum_{\nu=1}^L \sum_{n=-N_\nu}^{N_\nu} C_{\nu,n} \hat{D}_{j,n}^{\nu,\mu} = U_j^\mu, \quad (\mu = 1, 2, \dots, L; \quad j = 0, \pm 1, \pm 2, \dots, \pm N_\mu) \quad (31)$$

where

$$\hat{D}_{j,n}^{\nu,\mu} = \sum_{m=-M}^M d_{j,n,m}^{\nu,\mu} - \sum_{l=1}^2 \hat{d}_{j,n,l}^{\nu,\mu}. \quad (32)$$

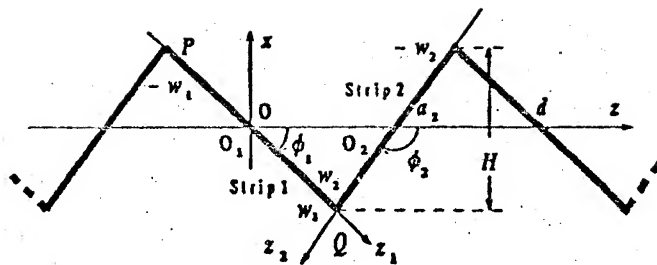
We don't show here  $U_j^\mu$ ,  $d_{j,n,m}^{\nu,\mu}$ , and  $\hat{d}_{j,n,l}^{\nu,\mu}$  as they are rather lengthy formulas.

## 4.2 Numerical Results

Since the space-harmonic coefficients of total electric field in Eq.(1) are calculated by the coefficients  $C_{\nu,n}$  of Eq.(31), the reflection coefficient  $R_m$  and the transmission coefficient  $T_m$  are obtained. The numerical examples for the triangular grating, the strip widths of which are  $w_1 = w_2$  in Figure 7(a), are shown in Figure 7(b). Figure 7(b) shows the power of the  $-1$  order reflection  $|R_{-1}|^2$  versus the normalized depth  $H/d$ . The G1 and G3 are the  $|R_{-1}|^2$  of the gratings with various profiles under a  $-1$ st-order Littrow mounting ( $\cos \theta^i = \lambda/2d$ ). Figure 8(b) shows the  $|R_{-1}|^2$  versus the  $d/\lambda$  for the indented grating in Figure 8(a). By the reciprocity theorem, the  $R_{-1}$  for the the case of  $a/d = 3$  is also equal to that for the case of  $a/d = -2$  in the range  $2/3 < d/\lambda < 4/3$ . Figure 9(a) shows a regular polygonal transmission grating. The  $|T_0|$  versus  $d/\lambda$  is shown in Figure 9(b), where the number  $L$  of strips is a parameter. In the case  $L = \infty$ , the regular  $L$  polygon turns into a circumscribed circle and then the results of the other method shown in Ref.(8) is added to this figure. Figure 10(a) shows a reflection grating with the regular polygonal cavity. The  $|R_0|^2$  versus  $d/\lambda$  is shown in Figure 10(b). The  $|R_0|^2$

(a)

Cross section of the triangular grating composed of two strips, which are connected at edges each other.



(b)

Reflection coefficients  $|R_{-1}|^2$  versus depth  $H/d$ .

( $w_1 = w_2$ ;  $M = 80$ ,  $N_1 = N_2 = 20$ ),

G1 :  $d/\lambda = 1$ ,  
 $\theta^i = \cos^{-1} \lambda/2d$ ,

G2 :  $d/\lambda = 1.5$ ,  $\theta^i = 60^\circ$ ,

G3 :  $d/\lambda = 2$ ,  
 $\theta^i = \cos^{-1} \lambda/2d$ .

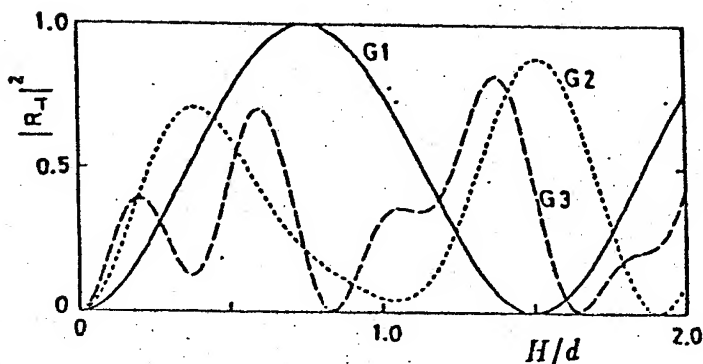
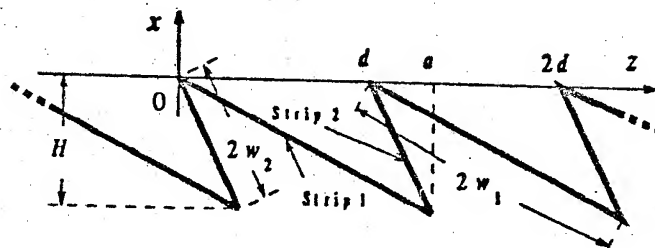


Figure 7: Numerical example for a triangular grating.

(a)

Cross section of an indented grating composed of two strips, which are connected at edges each other.



(b)

Reflection coefficients  $|R_{-1}|^2$  versus  $d/\lambda$ .

( $\theta^i = 60^\circ$ ,  $H/d = 1$ ;  $M = 120$ ,  
 $N_1 = N_2 = 30$ ),

G1 :  $a/d = 3$ ,

G2 :  $a/d = 0.5$ ,

G3 :  $a/d = -2$ .

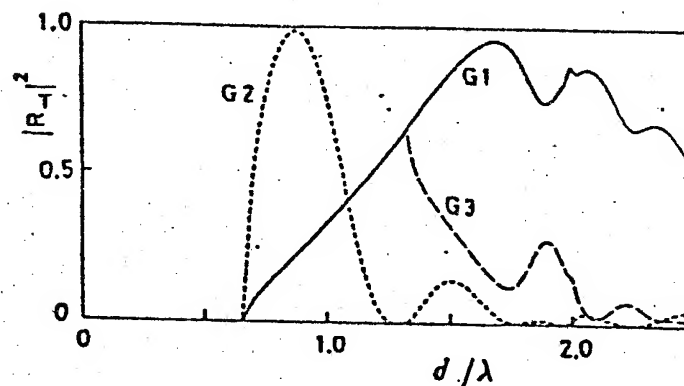
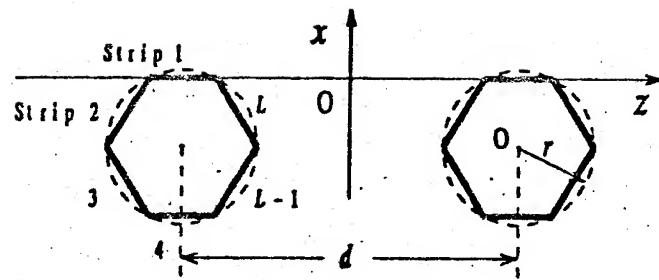


Figure 8: Numerical example for a indented grating.

(a)

Cross section of a regular  $L$  polygonal transmission grating composed of  $L$  strips, which are connected at edges each other.



(b)

Transmission coefficients  $|T_0|$  versus  $d/\lambda$ .

( $\theta^i = 90^\circ$ ;  $r = d/4$ ;  $M = 8N$ ,  
 $N = N_1 = N_2 = \dots = N_L$ ),  
 $G1 : L = 6, N = 10$ ,  
 $G2 : L = 8, N = 8$ ,  
 $G3 : L = 12, N = 5$ ,  
 $G4 : L = \infty$ .

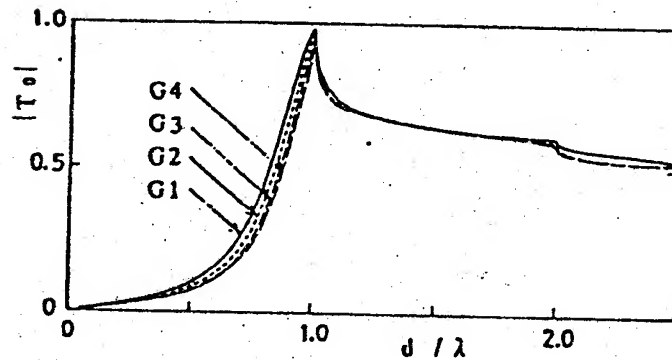
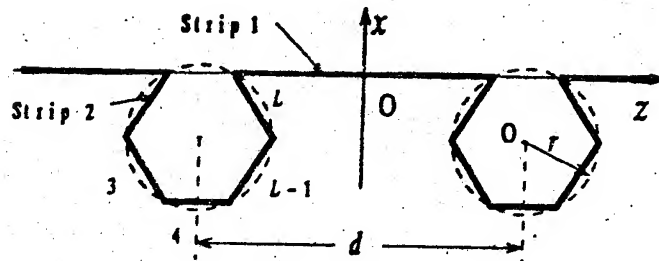


Figure 9: Numerical example for a regular  $L$  polygonal transmission grating.

(a)

Cross section of a reflection grating with the regular  $L$  polygonal cavity composed of  $L$  strips, which are connected at edges each other.



(b)

Reflection coefficients  $|R_0|^2$  versus  $d/\lambda$ .

( $\theta^i = 70^\circ$ ;  $r = d/4$ ;  $M = 8N$ ,  
 $N = N_1 = N_2 = \dots = N_L$ ),  
 $G1 : L = 6, N = 8$ ,  
 $G2 : L = 8, N = 8$ ,  
 $G3 : L = 12, N = 6$ .

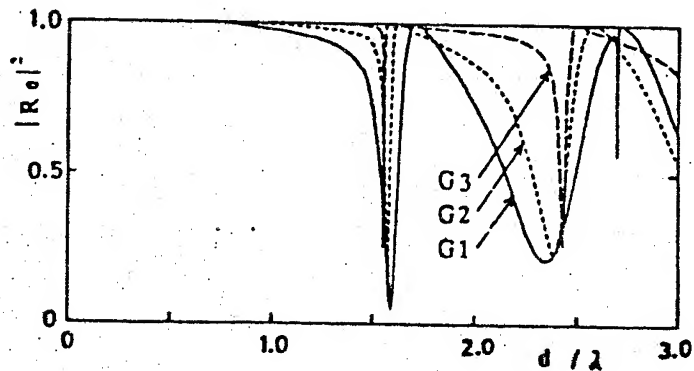


Figure 10: Numerical example for a reflection grating with the regular  $L$  polygonal cavity.

has abrupt changes which are independent of the frequencies corresponding to wood's anomaly (occurring at  $d/\lambda = n/(1 \pm \cos 70^\circ)$ ,  $n = 1, 2, \dots$ ). Physically, this phenomenon is related to the resonance of the cavity composed of the strip 2, 3,  $\dots$  and  $L$ .

## V. CONCLUSION

We have analyzed the diffraction of a plane wave from the scatterers composed of arbitrarily oriented conducting strips by means of the Wiener-Hopf technique together with the formulation using the partition of the scatterers. Our method and numerical results are as follow: (1) Defining the Fourier transform with respect to each coordinate for strips and using of the transformation between complex variables in these Fourier transforms, we derive the extended simultaneous Wiener-Hopf equation. (2) The accuracy of the present method is demonstrated in the cases of the scatterers composed of the finite number of strips and the grating composed of several strips in one period. (3) Since the present method is applicable to the problem of the grating where some strips are connected with others at the edges, it is probable that the scattering problem of electromagnetic waves for the gratings with various profiles represented by the position and the width of strips are analyzed. (4) Some numerical examples of the grating which suggest the characteristics of resonators or frequency selective surface are shown. The last results (4) needs further investigation, and the characteristics of resonators and frequency selective surface will be improved by the dielectric slab loading. we are researching the extended problems.

## REFERENCES

- (1) Lüneburg E. and Westpfahl K.: "Diffraction of plane waves by an infinite strip grating", *Anallen der Physik*, (1971) 27, 3, pp. 257-288.
- (2) Hinata T. Hosono T.: "On the scattering of an electromagnetic wave by plane grating in homogeneous medium-Mathematical foundation of point matching method and numerical analysis", *Trans. IECE*, (1976) J59-B, 12, pp. 571-578.
- (3) Kobayashi K. and Inoue T.: "Diffraction of a plane wave by an inclined parallel plate grating", *IEEE Trans. Antennas & Propag.*, (1988) 36, 10, pp. 1424-1434.
- (4) Aoki K. and Tanaka T.: "Diffraction of a plane wave by two parallel conducting plates", *Trans. IECE*, (1977) J60-B, 11, pp. 836-842.
- (5) Saermark K.: "Scattering of a plane monochromatic wave by a system of strips", *Appl. Sci. Res. B*, (1959) 7, pp. 417-440.
- (6) Shimoda M. and Itakura T.: "Scattering of electromagnetic plane waves by arbitrary oriented two conducting planes", *Trans. IEICE*, (1989) J72-C-1, 1, pp. 1-11.
- (7) Shimoda M. and Itakura T.: "Scattering of electromagnetic plane waves by a grating with several strips arbitrarily oriented in one period", *Trans. IEICE*, (1993) E76-C, 2, pp. 326-337.
- (8) Shestopalov V. P., Kirilenko A. A., Masalov S. A. and Sirenko U. K.: *Resonance scattering of waves, Part 1 - Diffraction gratings*, Naukova Dumka, (1986) p. 68.

# INVERSE BOUNDARY VALUE PROBLEMS IN SCATTERING THEORY: METHODS, RESULTS, OPEN QUESTIONS

Yuriy K. Sirenko and Liudmila G. Velichko

Institute of Radiophysics and Electronics, National Academy of Sciences  
12 Acad. Proskura st., 310085 Kharkov, Ukraine

A modern state of theoretical investigations concerned with solving diagnostics and synthesis problems for perfectly conducting objects is analysed in the review.

A great interest in inverse problems in mathematical diffraction theory arises basically from practical problems: remote sensing, visualization of resonant scatterers in optics, ultrasonic and superhigh-frequency tomography, nondestructive testing, synthesis of selective electromagnetic objects, etc. Above mentioned and others trends determining in many respects scientific and technological progress are supported quite good by research facilities generating given excitation fields and recording secondary scattered fields. The problem is how to interpret the incoming information and to extract the analysed characteristics rather precisely. The only feasible approach is to use computer systems. Analog and numerical methods for solving the inverse scattering problems account for algorithmic maintenance for these systems. The numerical methods are the subject of consideration of this report.

Any direct scattering problem can be described as a problem of determination of some electromagnetic parameters of a structure with a given material and geometric data in a field of monochromatic sources (in a field of plane waves). In inverse problems the parameters of the object and the source are partially or completely unknown and are liable to determination. An amount and a quality of initial information about electromagnetic characteristics specify a class of the inverse problem and determine most acceptable methods and means of a solution. Thus, a problem of existence of the solution does not arise in diagnostics problems when the scattering data are known precisely. In this case the main problems are connected with obtaining an amount of data which will be sufficient for a uniqueness of the solution. However, scattering data are usually obtained experimentally, so they are approximate and not precise. In this case we have additional problems connected with an investigation of existence and stability of the solution. The problem is complicating and becoming ill-posed. For the purpose of regularization it is necessary to revise a notion 'solution' and to restrict substantially the class of functions among which the solution is sought. The problem of solvability is especially important in synthesis problems the ultimate goal of which is creation of the objects having an ability to realize given electromagnetic characteristics. A body of data can be deficient for ensuring the unique solution (if it exists), the most acceptable choice is dictated by practical considerations (a simplicity of making the structure, a convenience of its employment, an additional functional potentialities, etc.). The optimization problems with a few parameters can be classified as inverse problems. In these problems a general type of the object and a source function are given. It is necessary to found a set of particular values



of geometrical or material parameters under which the scattering characteristic minimally distinguishing from required one is implemented. The analysis of such problems is reduced usually to finding local extrema of functionals which form is based completely on the direct problem solution. Similar procedures are used when implementing the analog methods of identification and remote sensing. The effectiveness of both approaches is determined by the effectiveness of solving the direct problems.

The aim of this report is to state the modern condition of theoretical investigations associated with the most urgent diagnostics and synthesis problems arising in electromagnetics, acoustics, geophysics, plasma, scientific instrument-making, optics. Naturally, different problems are solved in different fields, but the mathematical description and, hence, the methods for their solution are practically identical. So, we will confine ourselves without loss of generality to scalar scattering problems for two-dimensional perfectly conducting objects: compact and periodic.

From a great number of the papers devoted to inverse problems we will mention in the report only those ones which are sufficiently general in nature, oriented on solving the principal questions and not restricted in their approaches and techniques to specific (often very interesting) situations, excitation means, a dimensionality, etc., and which enable one to obtain a real result. As is clear from the title, the direct and inverse scattering problems for locally inhomogeneous dielectric objects and the scattering problems in a time domain, which are similar to the problems under discussion by their statements, but sometimes substantially differ from them by methods for solving, remain out of sight. The authors do not touch upon the methods of short-waves band ( $k \gg 1$ ) and physical optics distinguishing in the main from the methods operating in medium-waves and long-waves bands.

A successful investigation of the inverse problems depends to a large extent on efficient (fast and exact) solving the direct problems, therefore, the last ones occupy a sizeable passage of the report.

Then, the results obtained when studying the uniqueness of the inverse problem solution are discussed. It is clear that these results are very important for proper posing the diagnostics problems, for implementing the most general approaches to solving the inverse problems which are based on a construction of regularising operators. It is clear how actual is the problem of accumulation of these results for different objects, characteristics within reach of direct measurements, etc.

In the ideal situation when input data are known exactly and the questions about existence of the solution do not arise, most of the inverse boundary value problems can be solved by means of standard analytic continuation methods. However, their computer (numerical) implementation inevitably leads to errors and, hence, to destruction of the basis which guarantees the existence, uniqueness and stability of the solution with respect to small variations of input data. Inexact and incomplete input data arise in diagnostics and reconstruction problems as a result of not only numerical but also full-scale experiments (measurements). The solutions of synthesis problems are also based on the data which can fall into this category. What problems arise when solving the inverse problems with incomplete or inexact input data? Firstly, it is necessary to define more exactly the term 'solution of the problem' since it can be nonexistent in the habitual sense (the object with geometric parameters which are practically realizable forms the given field). Secondly, the question about uniqueness of the solution defined in a new fashion and its stability with respect to small variations of input

data inevitably arises. A number of possible variants of solving several of these problems is considered using the synthesis problem for a compact or periodic perfectly conducting object as an example.

As regards to the algorithms proper of the inverse problem solutions, they are analysed in the report within the scope of two isolated groups of schemes one of which needs (see, for example, the papers by A. Roger, D. Maystre, W. Tobocman) and the other does not need (see papers by R. Mittra, D. Colton, P. Monk, A. Kirsch, R. Kress) the solution of the corresponding direct problem at intermediate steps. The computational efficiency of algorithms, the validity of principal steps and stages, the correctness of findings and assumptions, the correspondence between the aims and the means used in above mentioned methods are estimated in the report.

The authors of the report put emphasis on the theoretical results being of general importance to the lead on the whole, namely: the scheme using Herglotz wavefunctions (D. Colton and P. Monk), the faithful representation of Fréchet derivatives at Newton-Kantorovitch linearization (A. Roger, D. Maystre), the idea of reformulation of the problem in terms of the Cauchy problem for a hyperbolic equation (P. R. Garabedian), etc.

# ON PHASE CHARACTERISTICS OF SHORT-PERIOD GRATINGS

Alexei N. Sivov, Andrei D. Chuprin and Alexander D. Shatrov

Institute of Radio Engineering and Electronics  
of the Russian Academy of Science  
1 Vvedenskogo sq., Fryazino, Moscow reg.,  
141120 RUSSIA

## ABSTRACT

Thick, conducting gratings were considered in the case with E field parallel to the conductors. It was found that depending on the shape of the conductors the fillfactor of a grating can be chosen such as to ensure the absence of a frequency dependence of the phase of the reflection and transmission coefficients, with the former being equal  $\pi$  and the latter being equal  $\pi/2$ . This phenomenon does not depend on the incidence angle of a plane wave.

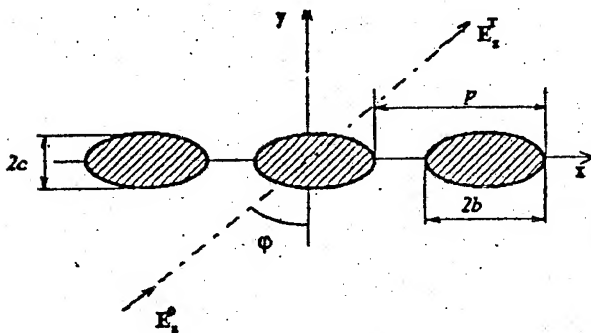


Fig. 1 Geometry of the grating

Consider a problem of diffraction of a plane electromagnetic wave by a grating composed of parallel conductors [1-4]:  $E = \exp(-jk(x \sin \phi + y \cos \phi))$ . (see Fig.1). An  $\exp(j\omega t)$  time dependence is implied but has been suppressed. The problem is two dimensional since there is no  $z$ -dependence. Outside the local waves region, transmitted and reflected fields are presented in the form:

$$E_z^T = T \exp(-jk(x \sin \phi + y \cos \phi)), \quad y > 0 \quad (1)$$

$$E_z^R = R \exp(jk(-x \sin \phi + y \cos \phi)), \quad y < 0 \quad (2)$$

The period of a grating  $p$  is assumed to be small with respect to a wavelength  $\lambda$ . As follows from [1], the reflection coefficient  $R$  and the transmission coefficient  $T$  can be written in the form:

$$R = \exp(j(\psi_2 + \psi_3 + \pi)) \cos(\psi_2 - \psi_3), \quad T = \exp(j(\psi_2 + \psi_3 + \pi/2)) \sin(\psi_2 - \psi_3) \quad (3)$$

where the following notations are used (see [1]):  $\psi_2 = -\arctan(kl_2 \cos \phi)$ ,

$\psi_3 = \arctan(kl_3 \cos \phi)$ ,  $k = 2\pi/\lambda$ ;  $l_2$  and  $l_3$  depend on the grating geometry;  $\phi$  is the incidence angle of a plane wave. The formulae are derived using the conformal transformations method. The cross section of a conductor is assumed to have two axes of symmetry. From (3) it

follows that both the phase of the transmission coefficient  $\psi_T = \psi_2 + \psi_3 + \pi/2$  and the phase of the reflection coefficient  $\psi_R = \psi_2 + \psi_3 + \pi$  are independent of the frequency and the incidence angle when the equation is satisfied:

$$l_2 + l_3 = 0 \quad (4)$$

In other words, by virtue of (4), the phase  $\psi_R$  behaves as well as the phase of a wave reflected from a metal surface placed in the symmetry plane  $y=0$ . The difference of the phases  $\psi_R - \psi_T$  being equal  $\pi/2$  results from the general property of lossless structures with symmetrical geometry:

$$\text{Re}(RT^*) = 0 \quad (5)$$

It should be noted that the magnitudes of  $R$  and  $T$  depend on  $k$  and  $\varphi$ , even if (4) is satisfied.

It is helpful to give several examples of gratings composed of conductors of various cross sections which satisfy (4). In the case of a grating composed of vertical ribbons ( $b=0$ , Fig.1) the formulae for  $l_2$  and  $l_3$  have a simple form [1]:

$$l_2 = -\frac{P}{\pi} \ln \text{ch} \frac{\pi c}{p}, \quad l_3 = -\frac{P}{\pi} \ln \text{sh} \frac{\pi c}{p} \quad (6)$$

The condition (4) is met when

$$\frac{2c}{p} = \frac{1}{\pi} \ln(2 + \sqrt{5}) \approx 0,46 \quad (7)$$

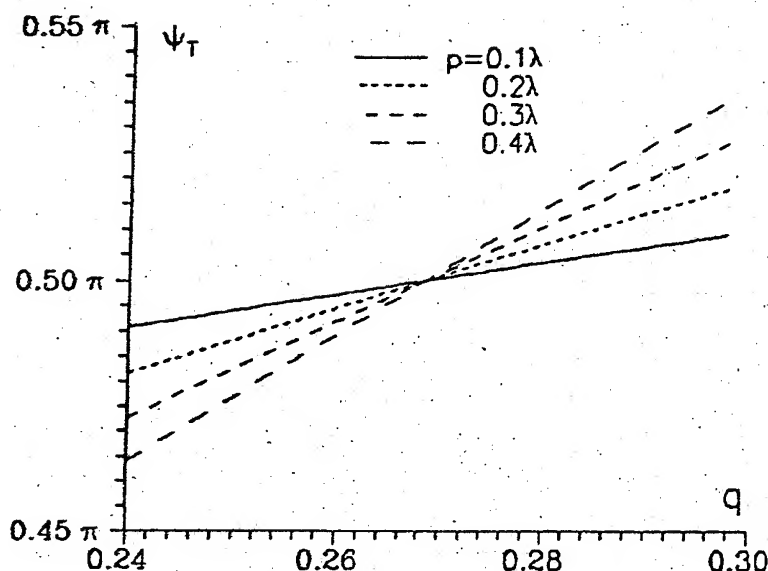


Fig.2 Phase of the transmission coefficient

For the case of a grating composed of circular conductors the parameters  $l_2$  and  $l_3$  are obtained by solving the transcendental equation [1]. Numerical results show that the condition (4) is satisfied when

$$q = \frac{2b}{p} \approx 0,27. \quad \text{The}$$

phase  $\psi_T$  versus the fillfactor  $q$  for various  $p/\lambda$  is illustrated in Figure 2.

For a grating composed of square conductors the phases  $\psi_R$  and  $\psi_T$  become inde-

pendent of frequency when  $q = \frac{2b}{p} = \frac{2c}{p} \approx 0.23$ .

It should be noted that the gratings under consideration have a finite thickness. If the thickness is infinitesimal (a parallel strip-grating,  $c=0$ , Fig.1) the condition (4) is met only when  $q=1$ , i.e., the grating degenerates into a metal surface. This fact results from the

formulae for a parallel strip-grating [1]:  $l_2 = 0$ ,  $l_3 = -\frac{p}{\pi} \ln \sin \frac{\pi q}{2}$

The gratings under consideration may find a use as elements of polarizers. If the grating is used as a window for waveguides and resonators their propagation constant and resonant frequency, respectively, is not perturbed.

The above phenomenon of the frequency independence could be simply interpreted by the full compensation for the "sag" in the electric field through the grating slots towards the region  $y>0$  at the expense of ousting the field from the region  $y<0$  by the conductors of the grating. Thus the plane  $y=0$  is an effective (equivalent) reflection plane, i.e., the phase of the reflection coefficient for the grating under consideration is the same as for the metal plane placed at  $y=0$ , namely it is equal to  $p$ .

It should be noted that the phenomenon of the frequency independence mentioned does not occur for the case with the electric field orthogonal to the conductors.

#### REFERENCES

- (1) Ye. I. Nefedov and A. N. Sivov: "Electrodynamics of periodical structures." Moscow: Nauka Press, 1977 (in Russian)
- (2) L. A. Vainshtein: "On the electrodynamic theory of grids" (in "Electronics of great power,") Moscow: Nauka Press, vol.2, part 1, pp.26-56, part 2, pp.57-74, 1963 (in Russian)
- (3) N. Marcuvitz: "Waveguide Handbook" (M.I.T., Rad. Lab. Ser. New York: McGraw-Hill Book Co., 1951), no 10
- (4) B. Z. Katsenelenbaum and A. N. Sivov (Eds.): "Electrodynamics of antennas with translucent surfaces. Methods of constructive synthesis." Moscow: Nauka Press, 1989 (in Russian)

# SYNTHESIS OF MULTIGRID TRANSMISSION TYPE CONVERTERS OF ELECTROMAGNETIC FIELD POLARIZATION STRUCTURE

Alexei N. Sivov, Andrei D. Chuprin, and Alexander D. Shatrov

Institute of Radio Engineering and Electronics of the Russian Academy of Science  
1 Vvedenskogo sq., Fryazino, Moscow reg., 141120 RUSSIA

## ABSTRACT

A method of synthesis of a multigrid structure is suggested which provides a given polarization transformation without reflection at a specified frequency. The structure is formed by a cascade of arbitrary number of parallel semitransparent screens with anisotropic conductivity. Explicit formulae have been derived that enable screen transparency and screen spacing to be obtained. A three-wire grid circular polarizer has been more fully attacked. The outer grids of the polarizer are mutually rotated by an angle  $\varphi$ , with interior one being composed of the wires perpendicular to the wires of one of the outer grids. All electrical and geometrical parameters of the above structure are expressed in terms of the angle  $\varphi$ . Numerical calculations of the axial ratio and transmission coefficient of the above polarizer have been carried out.

Consider a plane wave normally incident on a cascade of  $M$  parallel translucent (partially-reflecting) surfaces, with every surface being described by the boundary conditions [1]

$$U^+ = U^-, \quad \frac{\partial U^-}{\partial(kN)} - \frac{\partial U^+}{\partial(kN)} = \frac{U}{\rho_m} \quad (1)$$

where  $k=\omega/c$  is a wavenumber,  $N$  is the unit vector normal to the surfaces,  $\rho_m$  is a transparency value (or transparency) of the  $m$ th surface,  $U$  satisfies the Helmholtz equation and means electric field intensity, indices "+" and "-" refer to the opposite sides of the surface.

Translucent surface described by (1) may be realized, e.g., by means of a grid composed of thin conductors parallel to the electric field vector. It should be noted that in this case (when  $\rho$  is independent of coordinates)  $\rho = -1/B$ , where  $B$  is a shunt susceptance used, for example, in [2-4]

It is easy to show that a transmission type resonator formed by two identical translucent surfaces can not only be perfectly matched at a specified frequency  $\omega^0$  but also provide a phase shift  $\alpha^0$  given (i.e., the transmission coefficient  $T = |T| \exp(j\alpha)$  may be presented as  $\exp(j\alpha^0)$ ) if the transparency  $\rho$  and the surface spacing  $a$  are expressed by the formulae<sup>1</sup>

$$\rho = \frac{1}{2} \cot \frac{\alpha^0}{2} \quad (2)$$

<sup>1</sup>If the value of  $\alpha^0$  in (2), (3) is assumed to be  $\pi/2$  one can obtain the well-known results for the two-grid polarizer [3], [4].

$$k_0 \alpha = \frac{\pi + \alpha^0}{2} \quad (3)$$

It will be shown below that the bandwidth of devices based on the phase converters under consideration is determined by the derivative of the transmission coefficient phase  $\alpha$  with respect to frequency (or to  $k$ , that is the same).

$$\left( k \frac{d\alpha}{dk} \right) \Big|_{k=k_0} = - \left[ (\pi + \alpha^0) \tan^2 \frac{\alpha^0}{2} + 2 \tan \frac{\alpha^0}{2} \right] \quad (4)$$

Here we take account of the frequency dependence of the transparency:

$$\rho = \frac{k}{k_0} \rho^0 > 0 \quad (5)$$

It is caused by the inductive nature of the translucent surfaces mentioned.

It is easy to show that merging two translucent surfaces described by (1) with transparency values  $\rho_1$  and  $\rho_2$  forms one with the transparency  $\rho$  defined by the formula:

$$\frac{1}{\rho} = \frac{1}{\rho_1} + \frac{1}{\rho_2} \quad (6)$$

Consider a set of  $n$  two-element transmission type resonators (with a resonant frequency  $\omega^0$ ) placed in series. Let every resonator providing a phase shift  $\alpha_i^0$  ( $i=1,2,\dots,n$ ) be described by the formulae (2)-(4) with proper index " $i$ ." Let us bring the resonators nearer to one another so that the boundaries of neighbor ones coincide with each other. At the frequency  $\omega^0$ , this procedure does not change the total transmission coefficient of the structure. As a result we obtain a cascade of  $n+1$  surfaces, with outer ones having the former transparency values  $\rho_1^0$  and  $\rho_n^0$  and interior surfaces having transparency values calculated by (6) with proper indices. The total phase shift provided by such cascade of surfaces is

$$\alpha^0 = \sum_{i=1}^n \alpha_i^0 \quad (7)$$

The derivative of the transmission coefficient phase for the whole cascade of inductive surfaces is

$$\left( k \frac{d\alpha}{dk} \right) \Big|_{k=k_0} = - \sum_{i=1}^n \left[ (\pi + \alpha_i^0) \tan^2 \frac{\alpha_i^0}{2} + 2 \tan \frac{\alpha_i^0}{2} \right] \quad (8)$$

Let us apply the general technique described above to an important particular case.

Consider a phase shifter composed of  $n$  identical two-grid cells. Assuming  $\alpha_i^0 = \frac{\alpha^0}{n}$  gives

after taking into account (2)-(8)<sup>2</sup>

$$\rho_1^0 = \rho_{n+1}^0 = \frac{1}{2} \cot \frac{\alpha^0}{2n}, \quad \rho_2^0 = \rho_3^0 = \dots = \rho_n^0 = \frac{1}{4} \cot \frac{\alpha^0}{2n} \quad (9)$$

$$k_0 a = \frac{\pi}{2} + \frac{\alpha^0}{2n} \quad (10)$$

$$\left( k \frac{d\alpha}{dk} \right) \Big|_{k=k_0} = - \left[ (n\pi + \alpha^0) \tan^2 \frac{\alpha^0}{2n} + 2n \tan \frac{\alpha^0}{2n} \right] \quad (11)$$

If  $n$  tends towards infinity in (11), the right side of the equation approaches a finite value

$$\left( k \frac{d\alpha}{dk} \right) \Big|_{k=k_0} \rightarrow -\alpha^0 \quad (12)$$

In other words

$$\alpha \rightarrow \frac{k_0}{k} \alpha^0 \quad (13)$$

Such dependence of the phase shift on the frequency is caused by the inductive character of the transparency (see (5)). Thus the bandwidth of a cascade of inductive surfaces cannot increase infinitely at the expense of increasing the number of the surfaces.

Let us apply the above results to constructing polarizers of a plane electromagnetic wave. The translucent surfaces can be realized, for instance, in the form of short-period grids (the period  $p$  is small with respect to a wavelength  $\lambda$ ) composed of parallel conductors with a small fillfactor  $q$ . The electric fields orthogonal to conductors scarcely interact with the grids. Let the angle  $\Theta$  between the electric field vector and a grid

<sup>2</sup>This particular case allows all the optimal solutions of [3] to be obtained when considering

$$\alpha^0 = \frac{\pi}{2}, \quad n = 1, 2, 3.$$



conductor be  $\pi/4$ . To obtain a circular polarizer, it is necessary to equate the phase shift  $\alpha$  to  $\pi/2$ . For a twist polarizer the phase shift  $\alpha$  should be taken equal to  $\pi$ .

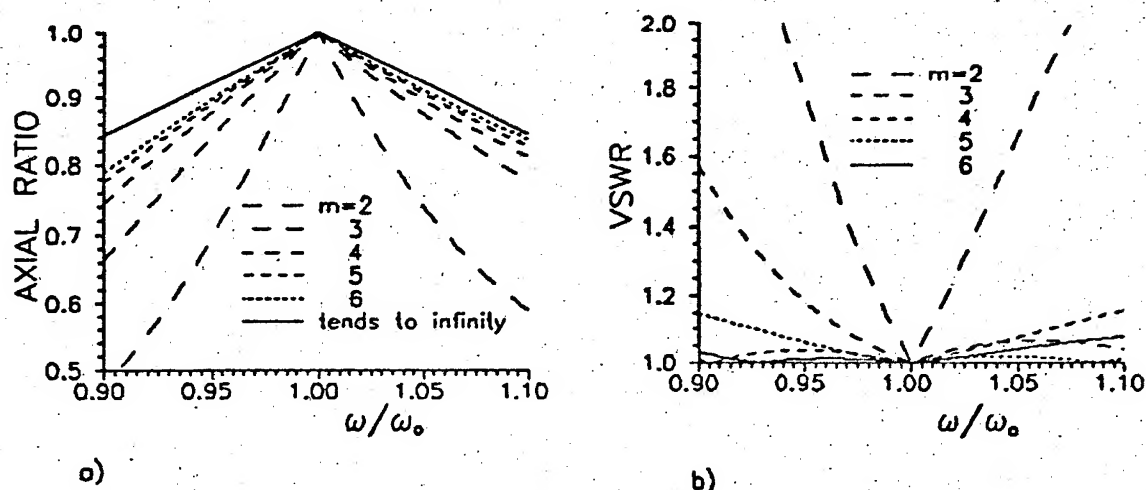


Fig.1 Performance of the polarizers

Fig.1 shows the axial ratio (a) and the transmission coefficient (b) versus the frequency for the circular polarizers constructed on the base of the formulae (9), (10) with various numbers of grids. The behavior of the axial ratio as the number of the grids  $m$  tends towards infinity is pictured by solid lines (see (12)). The formulae (9), (10) give the following parameters of the circular polarizers:  $\rho_1 = \rho_2 = 0.5$ ,  $ka = 3\pi/4$  (for  $m=2$ );  $\rho_1 = \rho_3 = 1.207$ ,  $\rho_2 = 0.604$ ,  $ka = 5\pi/8$  (for  $m=3$ );  $\rho_1 = \rho_4 = 1.866$ ,  $\rho_2 = \rho_3 = 0.933$ ,  $ka = 7\pi/12$  (for  $m=4$ );  $\rho_1 = \rho_5 = 2.514$ ,  $\rho_2 = \rho_3 = \rho_4 = 1.257$ ,  $ka = 9\pi/16$  (for  $m=5$ );  $\rho_1 = \rho_6 = 3.157$ ,  $\rho_2 = \dots = \rho_5 = 1.578$ ,  $ka = 11\pi/20$  (for  $m=6$ ). Analogous results for the twist polarizers are presented in Fig. 2. The same formulae (9), (10) give for these polarizers:  $\rho_1 = \rho_3 = 0.5$ ,  $\rho_2 = 0.25$ ,  $ka = 3\pi/4$  (for  $m=3$ );  $\rho_1 = \rho_4 = 0.866$ ,  $\rho_2 = \rho_3 = 0.433$ ,  $ka = 2\pi/3$  (for  $m=4$ );  $\rho_1 = \rho_5 = 1.207$ ,  $\rho_2 = \rho_3 = \rho_4 = 0.604$ ,  $ka = 5\pi/8$  (for  $m=5$ );  $\rho_1 = \rho_6 = 1.539$ ,  $\rho_2 = \dots = \rho_5 = 0.769$ ,  $ka = 3\pi/5$  (for  $m=6$ ).

#### REFERENCES

- (1) N.N. Voytovich, B.Z. Katsenelenbaum and A.N. Sivov, "The Generalized Method of Characteristic Modes in Diffraction Theory," Nauka Press, Moscow, 1977. (in Russian)
- (2) N. Marcuvitz, "Waveguide Handbook" (M.I.T., Rad. Lab. Ser., McGraw-Hill Book Co., New York, 1951), no 10
- (3) A.J. Lait, "Broadband circular polarizers," The Marconi Review, pp.159-184, Second Quarter 1969.
- (4) L.G. Josefsson, "Wire polarizers for microwave antennas," Ericsson technics, vol.34, no 4, pp. 181-258, 1978.

# ANTISPECULAR EFFECTS IN THE ELECTROMAGNETIC SCATTERING FROM 1D ROUGH SURFACES: CASE OF OBLIQUE INCIDENCE

Diana C. Skigin and Ricardo A. Depine

Dep. de Física, FCEN, Universidad de Buenos Aires  
Pab. I, Ciudad Universitaria, 1428 Buenos Aires, Argentina

## Abstract

A modal theory is applied to calculate the diffracted fields from perfectly conducting 1D rough surfaces in the general case in which the incident wave vector does not lie along the main section of the cylindrical surface. Antispecular effects which appear in finite length surfaces and their relation with the intensification of antispecular orders from deep gratings are analyzed. Numerical examples are shown for  $s$ - and  $p$ - polarization. The close connection between the system under consideration and the corresponding problem in classical mounting is discussed.

## Introduction

The perfectly conducting lamellar profile as a light scatterer has been studied by many authors [1]-[5]. Andrewartha *et al.* [2] and Wirgin and Maradudin [3], for example, studied the diffraction from perfectly conducting gratings in in-plane incidence.

Recently, a modal method has been applied to solve the diffraction problem from perfectly periodic gratings in conical mounting, i.e., when the propagation vector does not lie on the main section of the cylindrical surface [5].

Finite length surfaces of the same shape, i.e., perfectly conducting plane surfaces having a finite number of rectangular grooves, have also been studied when the grooves are equally spaced [6], and when the distance between adjacent grooves is arbitrary [7]. This kind of surfaces is of interest nowadays because they permit us a systematic study of the phenomenon of backscattering enhancement that takes place in such structures. They also make it possible to analyze the relationship between the intensification of antispecular orders from deep gratings and the backscattering peak observed in the angular distribution of intensities from non-periodic surfaces [8]-[9].

A new antispecular effect was predicted by Depine [10] and recently observed by Sant [11] in oblique incidence. This phenomenon consists in the appearing of an enhanced peak in the angular distribution of intensity along the direction opposite to the specular direction. In such a case, the propagation vector does not belong to the plane of incidence, but this effect suggests a connection with the backscattering enhancement of electromagnetic waves in in-plane incidence [10].

The task of this paper is to study the relationship between the intensification of antispecular orders from deep gratings and the "antibackscattering" peak in finite length surfaces, in the general case of oblique incidence.

# 1 Theory

## 1.1 Geometrical Configuration

Let us consider a perfectly conducting one dimensional rough surface. The grooves are along

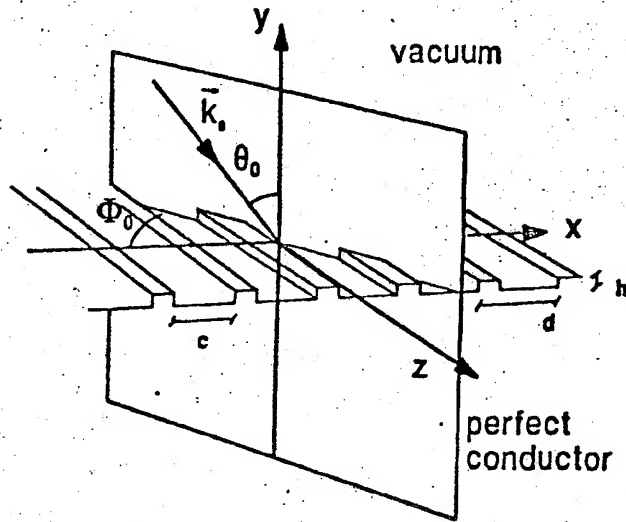


Figure 1: Configuration of the problem

the  $\hat{z}$  direction, and the  $y$ -axis is normal to the mean plane surface. The surface is illuminated from the region  $y > 0$  (see Fig. 1) by an arbitrarily polarized plane wave with wave vector

$$\vec{k}_0 = \alpha_0 \hat{x} - \beta_0 \hat{y} + \gamma_0 \hat{z}, \quad (1)$$

$\alpha_0^2 + \beta_0^2 + \gamma_0^2 = k_0^2$ ,  $k_0 = \omega/c = 2\pi/\lambda$ , where  $\omega$  is the frequency and  $\lambda$  is the wavelength of the incident wave. We express the components of  $\vec{k}_0$  in terms of the incidence angles  $\theta_0$  and  $\phi_0$ :

$$\begin{aligned} \alpha_0 &= k_0 \sin \theta_0 \cos \phi_0, \\ \beta_0 &= k_0 \cos \theta_0, \\ \gamma_0 &= k_0 \sin \theta_0 \sin \phi_0, \end{aligned} \quad (2)$$

where  $\theta_0$  measures the angle between the direction of incidence ( $\vec{k}_0$ ) and the normal to the surface ( $\hat{y}$ ), and  $\phi_0$  measures the angle between the plane of incidence and the  $x$ -axis (see Fig. 1). For classical mounting  $\phi_0 = 0, \pi$  ( $\gamma_0 = 0$ ), and  $\theta_0$  becomes the usual angle of incidence.

In order to determine the polarization of the incident electric field, we define two unit vectors perpendicular to  $\vec{k}_0$ :  $\hat{e}^\perp$  (perpendicular to the plane of incidence), and  $\hat{e}^\parallel$  (in the plane of incidence):

$$\begin{aligned} \hat{e}^\perp &= \cos \phi_0 \hat{z} - \sin \phi_0 \hat{x} \\ \hat{e}^\parallel &= -\cos \theta_0 \cos \phi_0 \hat{x} - \sin \theta_0 \hat{y} - \cos \theta_0 \sin \phi_0 \hat{z} \end{aligned} \quad (3)$$

## 1.2 Field Decomposition

The incident electric field is assumed to have the form

$$\vec{E}^i(x, y, z) = \vec{E}^i(x, y) \exp(i\gamma_0 z) , \quad (4)$$

where a time dependence in the form  $e^{-i\omega t}$  has been dropped. As the problem is invariant when infinitesimal translations along the  $\hat{z}$  direction are performed, the fields have everywhere the same propagation constant  $\gamma_0$  as that of the incident fields. This fact, and a property from the theory of waveguides [13] led us to write the fields everywhere as:

$$\vec{E}(x, y, z) = [\vec{E}_T(x, y) + \hat{z}E_z(x, y)] \exp(i\gamma_0 z) , \quad (5)$$

$$\vec{H}(x, y, z) = [\vec{H}_T(x, y) + \hat{z}H_z(x, y)] \exp(i\gamma_0 z) , \quad (6)$$

where the subscript T denotes the field component transverse to the  $\hat{z}$  direction. The transverse components can be written in terms of  $\vec{E}_z$  and  $H_z$  [12] [13]:

$$\begin{aligned} \vec{H}_T &= \frac{i}{(k_0^2 - \gamma_0^2)} (\gamma_0 \vec{\nabla}_T H_z + k_0 \hat{z} \times \vec{\nabla}_T E_z) , \\ \vec{E}_T &= \frac{i}{(k_0^2 - \gamma_0^2)} (\gamma_0 \vec{\nabla}_T E_z - k_0 \hat{z} \times \vec{\nabla}_T H_z) , \end{aligned} \quad (7)$$

where  $\vec{\nabla}_T = \vec{\nabla} - \hat{z}\partial/\partial z$ .

It is important to remark that although the general case of oblique incidence involves a vectorial treatment and polarization mixing, when we are dealing with a perfectly conducting material, the boundary conditions do not couple the  $z$ -components of the electric and the magnetic fields. This fact simplifies the numerical treatment and allows us a solution of the conical diffraction problem in terms of the solutions of two scalar problems corresponding to the fundamental modes of polarization in in-plane incidence [14].

## 1.3 Incident and Diffracted Fields

Let us consider that the surface is illuminated by a plane wave

$$\vec{E}^i(x, y, z) = \vec{A}^i \exp[i(\alpha_0 x - \beta_0 y + \gamma_0 z)] , \quad (8)$$

$$\vec{H}^i(x, y, z) = \frac{\vec{k}_0}{k_0} \times \vec{E}^i(x, y, z) , \quad (9)$$

where  $\vec{A}^i$  is a vector with complex components  $A_s^i$  and  $A_p^i$  along  $\hat{c}^s$  and  $\hat{c}^p$  respectively. Decomposition of  $\vec{A}^i$  into its cartesian components gives:

$$\begin{aligned} A_x^i &= -A_s^i \sin \phi_0 - A_p^i \cos \theta_0 \cos \phi_0 \\ A_y^i &= -A_p^i \sin \theta_0 \\ A_z^i &= A_s^i \cos \phi_0 - A_p^i \cos \theta_0 \sin \phi_0 \end{aligned} \quad (10)$$

As it was stated above, the electric and the magnetic fields are completely determined if the  $z$ -components  $E_z$  and  $H_z$  are known. The solution for the  $z$ -components of the diffracted fields in

the upper region, depend on the type of surface we are considering (infinitely periodic or finite):

### Infinite gratings

We consider a perfectly conducting grating of rectangular profile and period  $d$ , width of the grooves  $c$  and height  $h$ . In this case, a Rayleigh expansion is appropriate to describe the  $z$ -components of the fields:

$$E_z^{diff}(x, y, z) = \sum_{n=-\infty}^{\infty} R_n \exp[i\vec{k}_n \cdot \vec{r}] = \sum_{n=-\infty}^{\infty} R_n \exp[i(\alpha_n x + \beta_n y + \gamma_0 z)] , \quad (11)$$

$$H_z^{diff}(x, y, z) = \sum_{n=-\infty}^{\infty} S_n \exp[i\vec{k}_n \cdot \vec{r}] = \sum_{n=-\infty}^{\infty} S_n \exp[i(\alpha_n x + \beta_n y + \gamma_0 z)] , \quad (12)$$

where

$$\alpha_n = \alpha_0 + \frac{2\pi}{d}n , \quad (13)$$

$$\beta_n = \begin{cases} \sqrt{k^2 - \gamma_0^2 - \alpha_n^2} & \text{if } k^2 - \gamma_0^2 > \alpha_n^2 \\ i\sqrt{\alpha_n^2 - k^2 + \gamma_0^2} & \text{if } k^2 - \gamma_0^2 < \alpha_n^2 \end{cases} \quad (14)$$

$n$  refers to the diffracted orders and  $R_n$  and  $S_n$  are complex amplitudes. Making use of eqs. 7, the total diffracted fields become

$$\vec{E}^{diff} = \sum_{n=-\infty}^{\infty} \left\{ \frac{1}{k_0^2 - \gamma_0^2} [-(\gamma_0 \alpha_n R_n + k_0 \beta_n S_n) \hat{x} + (k_0 \alpha_n S_n - \gamma_0 \beta_n R_n) \hat{y}] + R_n \hat{z} \right\} \times \exp[i(\alpha_n x + \beta_n y + \gamma_0 z)] , \quad (15)$$

$$\vec{H}^{diff} = \sum_{n=-\infty}^{\infty} \left\{ \frac{1}{k_0^2 - \gamma_0^2} [(k_0 \beta_n R_n - \alpha_n \gamma_0 S_n) \hat{x} - (\gamma_0 \beta_n S_n + k_0 \alpha_n R_n) \hat{y}] + S_n \hat{z} \right\} \times \exp[i(\alpha_n x + \beta_n y + \gamma_0 z)] . \quad (16)$$

The time-averaged power per unit area of the  $n$ - order that crosses any plane parallel to the  $y = 0$  plane is given by:

$$\left\langle \frac{dP^j}{da} \right\rangle = \frac{c}{8\pi} \operatorname{Re} [ \hat{y} (\vec{E}_n^j \times \vec{H}_n^{j*}) ] , \quad j = s, p \quad (17)$$

where the asterisk denotes complex conjugate. Then, the total efficiency of the  $n$ - order is  $e_n$ :

$$e_n = \frac{\operatorname{Re}(\beta_n)}{\beta_0} \frac{k_0^2}{k_0^2 - \gamma_0^2} \left\{ |A_z^i|^2 |R_n|^2 + \left| \frac{\alpha_0 A_y^i + \beta_0 A_x^i}{k_0} \right|^2 |S_n|^2 \right\} . \quad (18)$$

As shown in [14], the Rayleigh amplitudes  $R_n$  ( $S_n$ ) correspond to the solution of classical problems for  $s$ - ( $p$ )- polarization and unit amplitude incident electric (magnetic) field. These

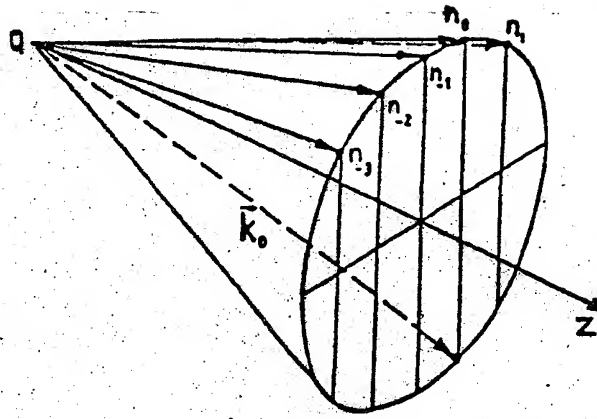


Figure 2: Conical diffraction

classical problems correspond to another wavelength  $\lambda^{eq}$ , which is related with the original wavelength  $\lambda$  through:

$$\lambda^{eq} = \frac{\lambda}{\sqrt{1 - \sin^2 \theta_0 \sin^2 \phi_0}} = \frac{\lambda}{\cos \phi'_0} \quad (19)$$

$\phi'_0$  being the angle between  $\vec{k}_0$  and its projection on the  $(x, y)$ -plane. It should be noticed that if we vary  $\theta_0$  for a fixed  $\phi_0$ , the value of  $\lambda^{eq}$  is different for each angle of incidence. But we can describe the problem in terms of another pair of angles  $\theta'$  (between the projection of  $\vec{k}_0$  on the  $(x, y)$ -plane and the  $y$ -axis) and  $\phi'$ , which are related with  $\theta$  and  $\phi$  by:

$$\cos \theta' = \frac{\cos \theta}{\sqrt{1 - \sin^2 \theta \sin^2 \phi}} \quad (20)$$

$$\cos \phi' = \sqrt{1 - \sin^2 \theta \sin^2 \phi} \quad (21)$$

Then varying  $\theta'_0$  and keeping  $\phi'_0$  fixed, the equivalent wavelength is maintained for every  $\theta'_0$ . This change of variables will make it easier the comparison between the conical and classical mounting curves.

### Finite length surfaces

In this case we consider a plane surface having a finite number of rectangular grooves of width  $c$  and height  $h$ , in which the distance between adjacent grooves can be chosen arbitrarily. The solution for the  $z$ -components of the fields in the upper region can be written as:

$$E_z^{scat}(x, y, z) = \int_{-\infty}^{\infty} R(\alpha) e^{i(\alpha x + \beta y + \gamma z)} d\alpha \quad (22)$$

$$H_z^{scat}(x, y, z) = \int_{-\infty}^{\infty} S(\alpha) e^{i(\alpha x + \beta y + \gamma z)} d\alpha \quad (23)$$

where

$$\beta = \begin{cases} \sqrt{k^2 - \gamma_0^2 - \alpha^2} & \text{if } k^2 - \gamma_0^2 > \alpha^2 \\ i\sqrt{\alpha^2 - k^2 + \gamma_0^2} & \text{if } k^2 - \gamma_0^2 < \alpha^2 \end{cases} \quad (24)$$

Replacing 22 and 23 in 7, we obtain the expressions for the total diffracted fields:

$$\vec{E}^{diff} = \int_{-\infty}^{\infty} \left\{ \frac{1}{k_0^2 - \gamma_0^2} [-(\gamma_0 \alpha R(\alpha) + k_0 \beta S(\alpha))\hat{x} + (k_0 \alpha S(\alpha - \gamma_0 \beta R(\alpha))\hat{y}) + R(\alpha)\hat{z}] \right\} \times \exp[i(\alpha x + \beta y + \gamma_0 z)] \quad (25)$$

$$\vec{H}^{diff} = \int_{-\infty}^{\infty} \left\{ \frac{1}{k_0^2 - \gamma_0^2} [(k_0 \beta R(\alpha) - \alpha \gamma_0 S(\alpha))\hat{x} - (\gamma_0 \beta S(\alpha + k_0 \alpha R(\alpha))\hat{y}) + S(\alpha)\hat{z}] \right\} \times \exp[i(\alpha x + \beta y + \gamma_0 z)] \quad (26)$$

The time-averaged power per unit area that crosses any plane parallel to the  $y = 0$  plane is given by 17, replacing  $E_n^j$  and  $H_n^j$  by  $E^j(\alpha)$  and  $H^j(\alpha)$  respectively.

## 2 Results

In figure 3 we show curves of efficiency of a diffracted order vs. the angle of incidence  $\theta_0$  keeping  $\phi_0$  fixed, for a perfectly conducting grating with  $c/d = 0.9$ ,  $\lambda/d = 0.31$ ,  $\phi_0 = 5^\circ$  and for two values of  $h/d$ . It is remarkable that for  $\phi_0 = 5^\circ$  (a small  $\phi_0$  so that the problem does not differ too much from the classical one), an increase in  $h/d$  produces an intensification in the  $n$ -efficiency when the  $n$ -order propagates in the antispecular direction for both polarizations. This behavior was found to happen for all the diffracted orders. If we compare the plots in Fig. 3 and the corresponding curves for in-plane incidence, we can notice a great degree of similarity between curves (see Fig. 4), as it should be expected because of the small value of  $\phi_0$  taken. To better appreciate the effects caused by the conical mounting in the diffracted light, we increased the value of  $\phi_0$  and made curves similar to those of Figure 3. In Figure 5 we show curves of -1 efficiency vs.  $\theta'_0$  for greater values of  $\phi'_0$ .  $\lambda$  and  $\phi'_0$  have been chosen so that  $\lambda^{eq}$  remains the same for all the cases considered. It can be observed that the curves resemble the classical ones (see Figs. 4a and 4c). This feature is related to the fact that values of  $\theta_0$  belonging to the interval  $[0, 90^\circ]$  correspond to a variation of  $\alpha_0/k$  in  $[0, 1]$  for in-plane incidence, and to a variation of  $\alpha_0/k$  in  $[0, 1/\cos \phi'_0]$  in oblique incidence. Another important fact to remark is that in all cases the peak is located at the value of  $\theta'_0$  at which the curves in classical mounting have their maximum (antispecular direction for in-plane incidence), but not in the "antispecular" direction for oblique incidence (AS), that is:

$$\frac{\alpha^{peak}}{k} = -\frac{n \lambda^{eq}}{2 d} = -\frac{n \lambda}{2 d \cos \phi'_0}$$

$$\frac{\alpha^{AS}}{k} = -\frac{n \lambda}{2 d}$$

This result is in agreement with the prediction made in [10].

We turn now to show some examples for finite length surfaces. In Figure 6 curves of intensity as a function of the observation angle are shown, for a surface having three grooves of width  $c/d = 0.9$  and  $h/d = 1.5$ . It can be observed in Figure 6 that the scattered intensity has a peak

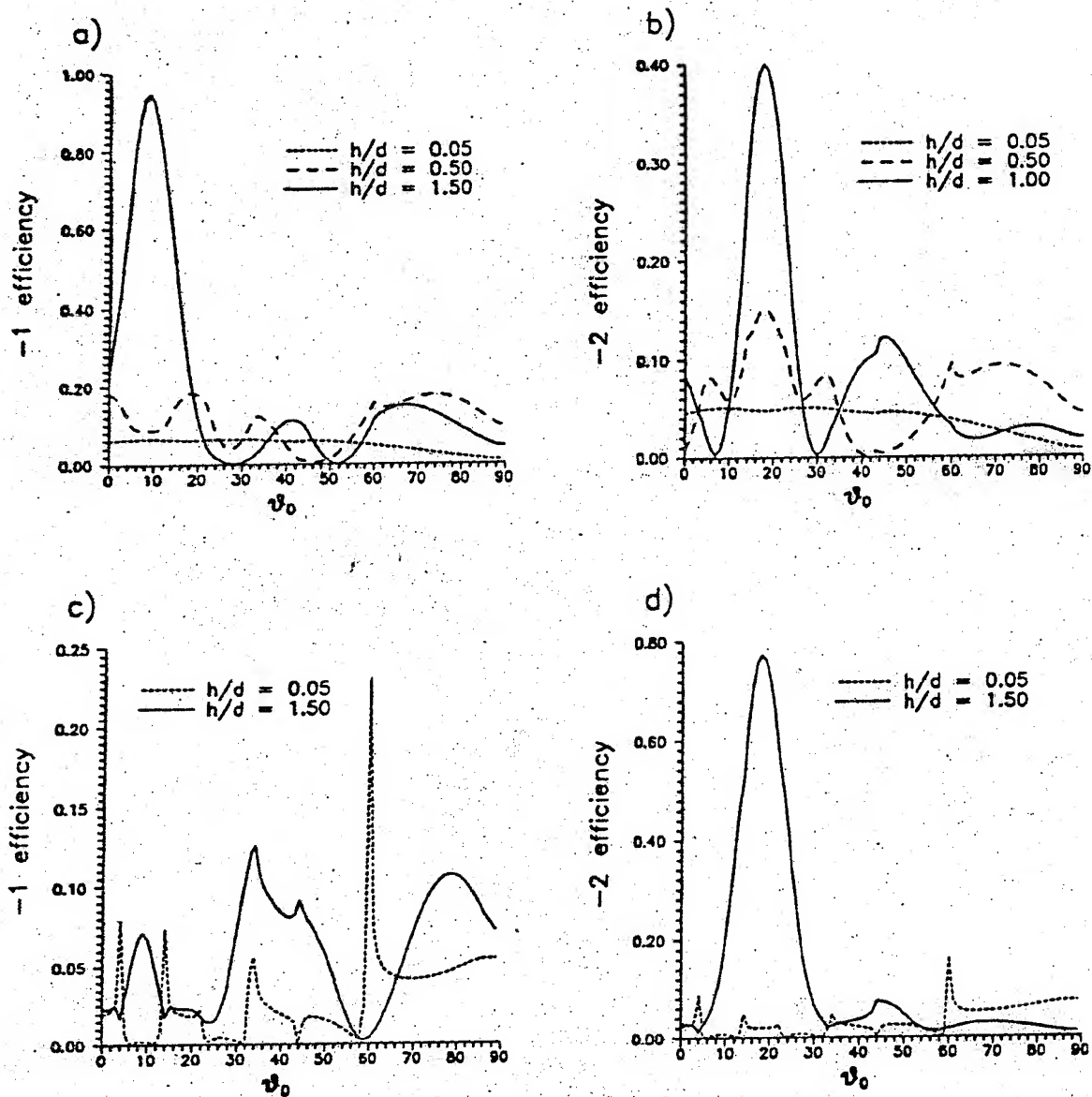


Figure 3: Efficiency vs.  $\theta_0$  for a grating with  $c/d = 0.9$ ,  $\lambda/d = 0.31$  and  $\phi_0 = 5^\circ$ . a) -1 efficiency for  $\delta = 90^\circ$  (s-pol.); b) -2 efficiency for  $\delta = 90^\circ$  (s-pol.); c) -1 efficiency for  $\delta = 0^\circ$  (p-pol.); d) -2 efficiency for  $\delta = 0^\circ$  (p-pol.).



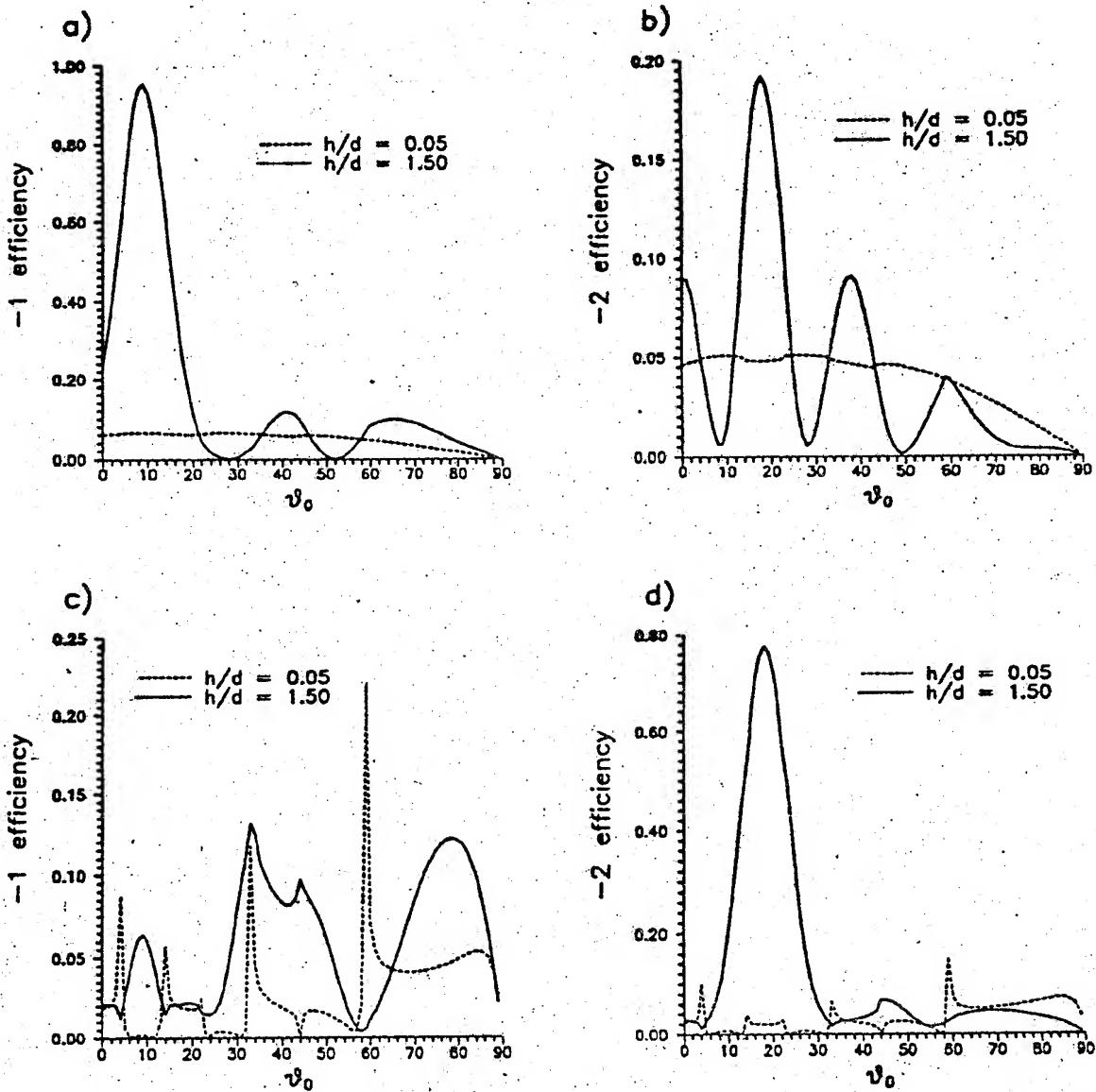


Figure 4: Efficiency vs.  $\theta_0$  for a grating with  $c/d = 0.9$  and  $\lambda/d = 0.31$  in classical mounting ( $\phi_0 = 0^\circ$ ). a) -1 efficiency for incident s-pol.; b) -2 efficiency for incident s-pol.; c) -1 efficiency for incident p-pol.; d) -2 efficiency for incident v-pol.

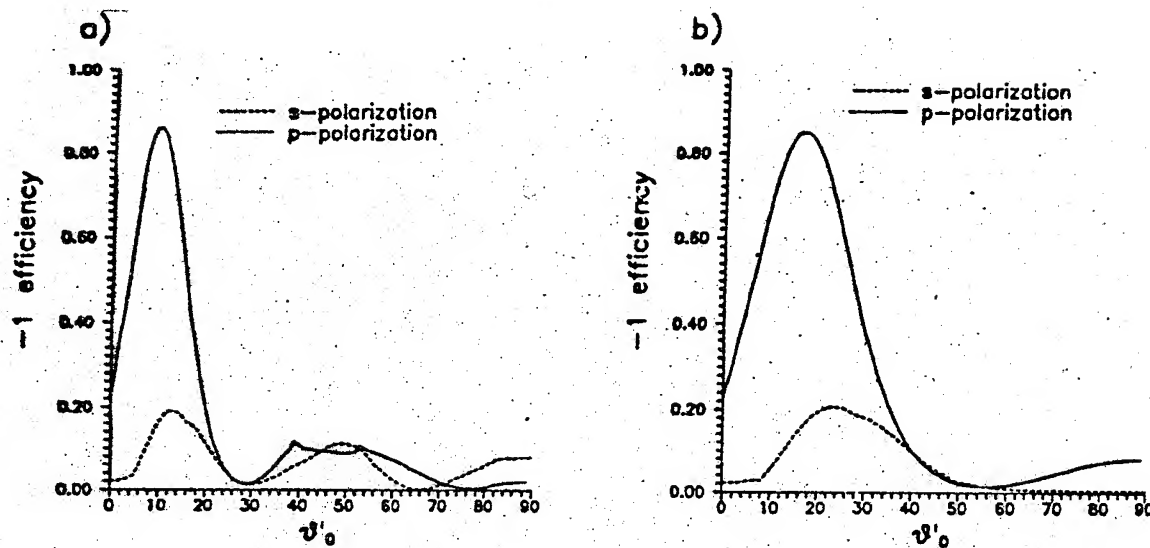


Figure 5: -1 efficiency vs.  $\theta'_0$  for a grating with  $c/d = 0.9$  and  $h/d = 1.5$ . a)  $\phi'_0 = 30^\circ$ ,  $\lambda/d = 0.268$ ; b)  $\phi'_0 = 60^\circ$ ,  $\lambda/d = 0.155$ .

in the antibackscatter direction only for a low value of  $\phi_0$  when the surface is illuminated by  $s$ -polarized light, which agrees with the curves shown for the infinite periodic grating. On the other hand, the opposite behavior is observed for incident  $p$ -polarization (see Figure 7). Then it is derived that this kind of surfaces keep some features of the infinite gratings. If we change the distance between adjacent grooves but keeping the length of the corrugation fixed, the scattering pattern does not change significantly, and the peaks remain located at the same directions of observation.

### 3 Conclusion

The scattering problem from rectangularly shaped and perfectly conducting surfaces was solved in the case of oblique incidence. A rigorous modal theory was applied to the infinite gratings as well as to the finite length surfaces. As it was predicted [10], it was found that for small deviations from the classical mounting, the efficiency curves exhibit their maximum at the antispecular direction, which is coincident with the antispecular direction in in-plane incidence. On the other hand, as the value of  $\phi_0$  is increased, the antispecular direction in oblique incidence ceases to be the same as the corresponding to classical mounting, thus showing its peak in the direction at which the diffracted order is antispecular for in-plane incidence. Concerning the finite surfaces, the results were found to agree with those obtained for the infinite periodic grating.

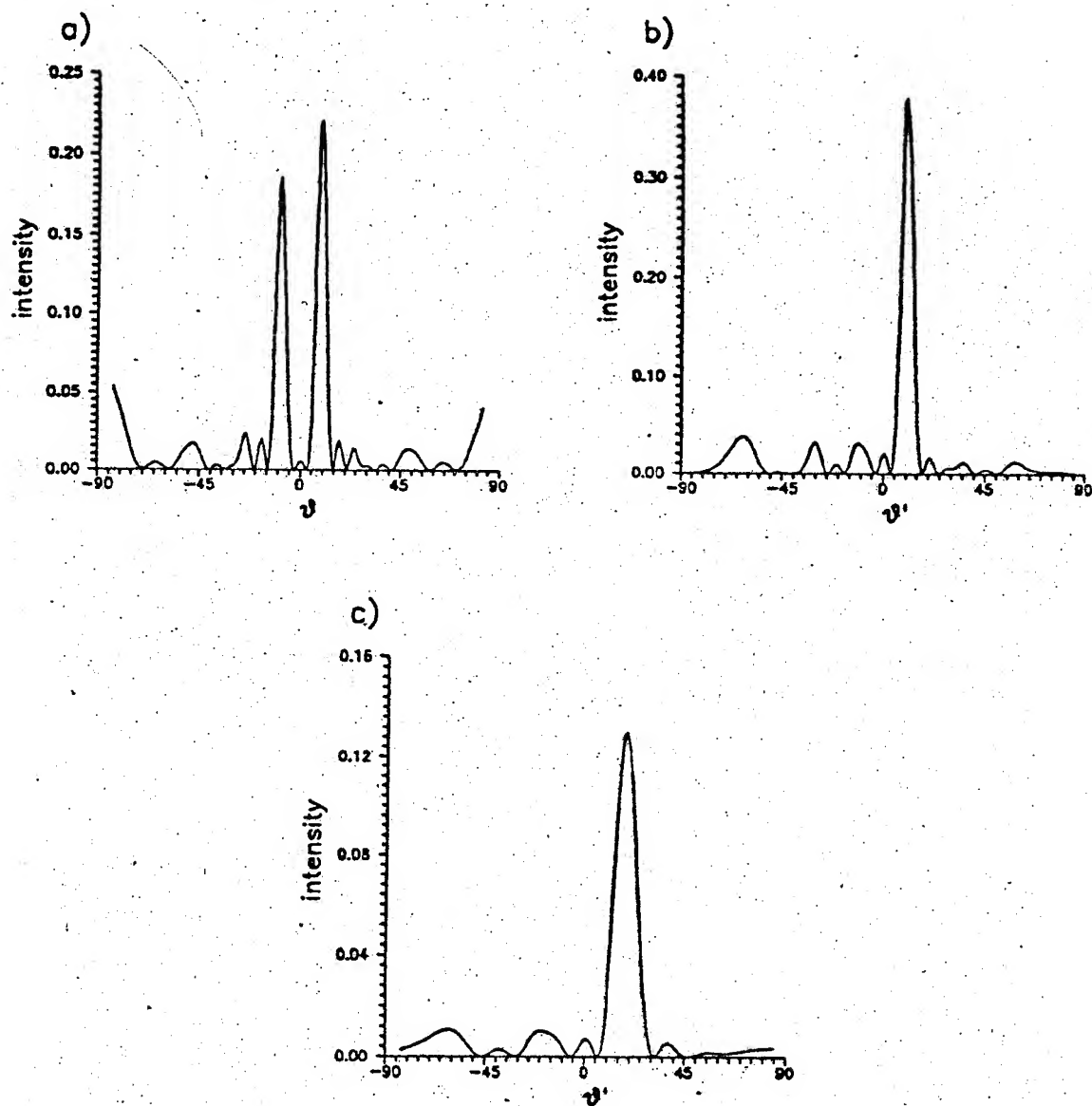


Figure 6: Intensity vs.  $\theta_{ob}$ , for s-polarized light incident upon a surface having 3 grooves of width  $c/d \geq 0.9$  and height  $h/d \geq 1.5$ . a)  $\phi_0 = 5^\circ$ ,  $\lambda/d \geq 0.31$ ; b)  $\phi'_0 = 30^\circ$ ,  $\lambda/d \geq 0.268$ ; c)  $\phi'_0 = 60^\circ$ ,  $\lambda/d \geq 0.155$ .

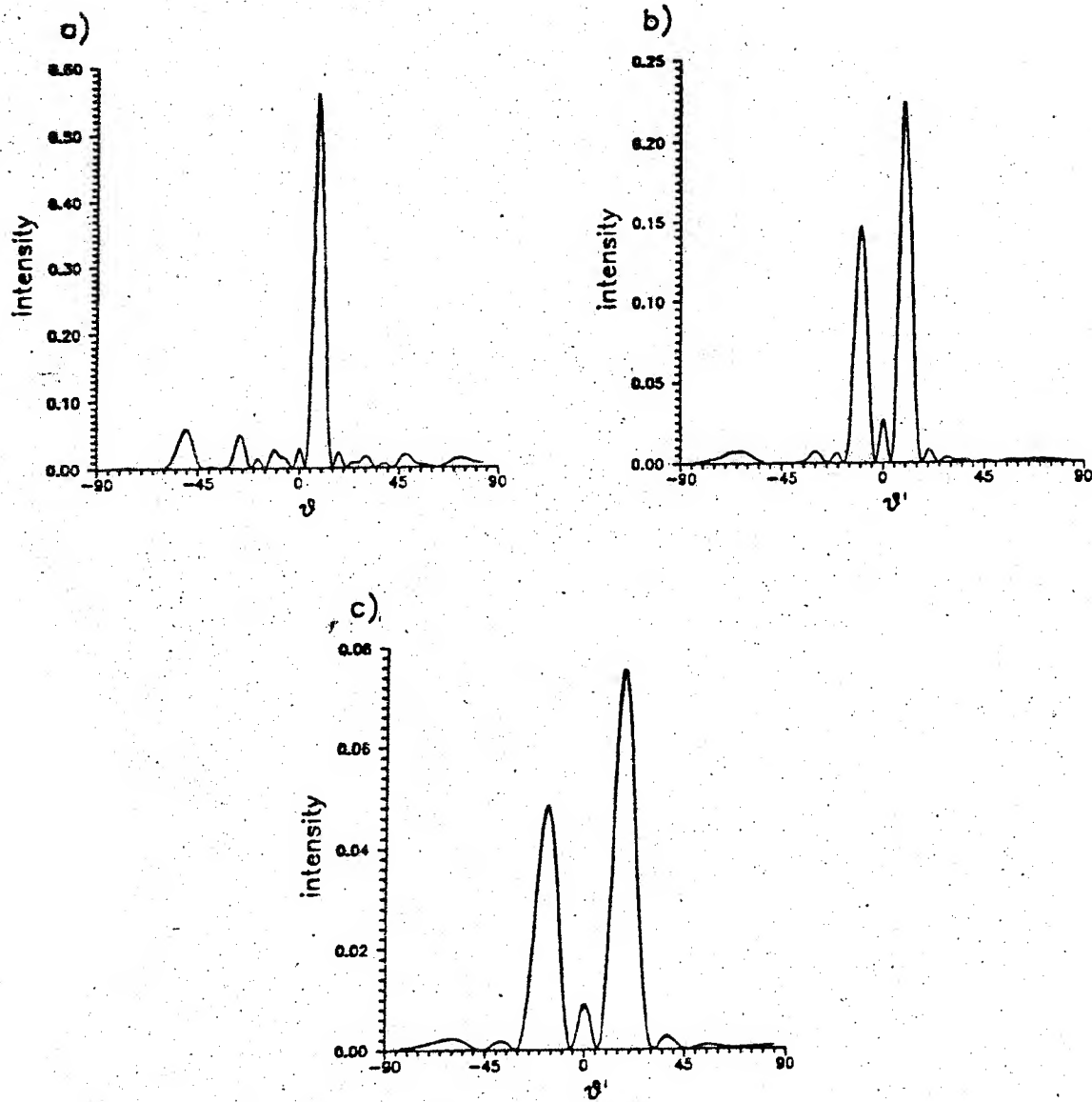


Figure 7: Intensity vs.  $\theta_{obs}$ , for  $p$ -polarized light incident upon a surface having 3 grooves of width  $c/d = 0.9$  and height  $h/d = 1.5$ . a)  $\phi_0 = 5^\circ$ ,  $\lambda/d = 0.31$ ; b)  $\phi'_0 = 30^\circ$ ,  $\lambda/d = 0.268$ ; c)  $\phi'_0 = 60^\circ$ ,  $\lambda/d = 0.155$ .

## Acknowledgements

This work was supported by grants of CONICET, Fundación Antorchas and UBA.

### \*References

- [1] R. Petit, C. r. hebd. Seanc. Acad. Sci., Paris, 260, 4454 (1965).
- [2] J. R. Andrewartha, J. R. Fox and I. J. Wilson, "Resonance anomalies in the lamellar grating", *Optica Acta*, **26**, 69-89 (1977).
- [3] A. Wirgin and A. A. Maradudin, "Resonant enhancement of the electric field in the grooves of bare metallic gratings exposed to S-polarized light", *Phys. Rev. B*, **31**, 5573-5576 (1985).
- [4] E. G. Loewen, M. Nevière and D. Maystre, "Efficiency optimization of rectangular groove gratings for use in the visible and IR regions", *Appl. Opt.* **18**, 2262-2266 (1979).
- [5] L. Li, "A modal analysis of lamellar diffraction gratings in conical mountings", *J. Mod. Optics* **40**, 553-573 (1993).
- [6] T. J. Park, H. J. Eom and K. Yoshitomi, "Analysis of TM scattering from finite rectangular grooves in a conducting plane", *J. Opt. Soc. Am. A* **10**, 905-911 (1993).
- [7] R. A. Depine and D. C. Skigin, "Scattering from metallic surfaces having a finite number of rectangular grooves", *J. Opt. Soc. Am. A*, 1993 (submitted).
- [8] D. C. Skigin and R. A. Depine, "Backscattering enhancement in metallic random gratings", *Proceedings of the XXIV URSI GA, Japan*, 1993.
- [9] E. R. Méndez and K. A. O'Donnell, "Observation of Depolarization and Backscattering enhancement in light scattering from gaussian rough surfaces", *Opt. Commun.* **61**, 91-95 (1987).
- [10] R. A. Depine, "Scattering of light from one dimensional random rough surfaces: a new antispecular effect in oblique incidences", *J. Opt. Soc. Am. A*, **9**, 920-927 (1993).
- [11] M. Sant, "Enhanced Backscattering of light from randomly rough diffusers", PhD thesis, Imperial College, University of London, 1991.
- [12] J. A. Stratton, "Electromagnetic Theory", Mc. Graw-Hill, New York, p.365 (1941).
- [13] J. D. Jackson, "Classical Electrodynamics", 2nd. ed., Wiley, New York (1975).
- [14] R. Petit, "Electromagnetic theory of gratings", Springer-Verlag New York, 1980.

# VECTOR PSEUDODIFFERENTIAL EQUATIONS IN ELECTROMAGNETIC DIFFRACTION PROBLEM ON ARBITRARY SCREEN

Youri B. Smirnov

Penza State Technical University, Dept. of Mathematics,  
Krasnaya st., 40, Penza 440017, Russia.

## 1. STATEMENT OF THE PROBLEM.

In the following we study electrodynamic scattering problem on the bounded screen. The surface of the screen is assumed to be infinitely thin and perfectly conducted. Let  $\Omega$  be the two-dimensional bounded surface in  $\mathbb{R}^3$  with the smooth boundary  $\partial\Omega$  outside a finite set of singular points. Consider boundary value problem for Maxwell equations

$$(1) \quad \operatorname{rot} E = ikH, \quad \operatorname{rot} H = -ikE \quad \text{in } \mathbb{R}^3 \setminus \bar{\Omega}, \quad \operatorname{Im} k \geq 0, \quad k \neq 0$$

$$(2) \quad E_t + E_t^0 = 0 \quad \text{on } \Omega$$

$$(3) \quad r \left[ \frac{\partial E}{\partial r} - ikE \right] \rightarrow 0, \quad r \left[ \frac{\partial H}{\partial r} - ikH \right] \rightarrow 0 \quad \text{as } r = |x| \rightarrow \infty$$

$$(4) \quad E, H \in L_{loc}^2(\mathbb{R}^3)$$

where  $E_t^0$  are the tangential electric components of the incident electromagnetic field  $E^0, H^0$ . It is supposed that the sources of the incident field lie away from the screen  $\Omega$  and, hence  $E_t^0|_{\Omega} \in C^\infty(\bar{\Omega})$ .

For the functions  $E, H$  it is required that  $E, H \in C^2(\mathbb{R}^3 \setminus \bar{\Omega}), E_t \in C(\mathbb{R}^3 \setminus \partial\Omega)$ . The static case  $k = 0$  is not considered because it leads to the well elaborating Dirichlet or Neumann scalar problems for the Laplacian [1].

One can mention that it is not generally possible to use the classical methods of layer potentials in screen problems. For closed surfaces the problem is reduced to the Fredholm integral equations of the second kind by these methods. Unlike closed surfaces the screens have two sides and the jump-theorems for layer potentials yield the different values on the different sides of the screen what leads to contradiction with the

continuity of the incident field.

The uniqueness of the solution to (1)-(4) follows from Lemma 1. For  $\text{Im } k \geq 0, k \neq 0$  the homogeneous problem (1)-(4) (with  $E_t^0|_\Omega = 0$ ) has at most the trivial solution.

The problem (1) - (4) can be reduced to the integro-differential equation

$$(5) \quad (\text{Grad } A (\text{div } u) + k^2 Au)|_t = f, \quad x \in \Omega$$

where  $A$  denotes the integral operator

$$(6) \quad Au = \int_{\Omega} \frac{\exp(ik|x-y|)}{|x-y|} u(y) dS, \quad f = 4\pi ik E_t^0|_\Omega \quad \text{and}$$

$\text{div}$  is the tangential divergence on  $\Omega$ .

Here the tangential vector  $u$  is the so-called current density on  $\Omega$ . In this case the fields  $E, H \in C^\infty(\mathbb{R}^3 \setminus \Omega)$  are obtained by the formula

$$E = ik^{-1} \left[ \text{Grad } A_1 (\text{div } u) + k^2 A_1 u \right], \quad H = \text{Rot } A_1 u, \quad k \neq 0,$$

$$A_1 u = \frac{1}{4\pi} \int_{\Omega} \frac{\exp(ik|x-y|)}{|x-y|} u(y) dS, \quad x = (x_1, x_2, x_3)$$

The purpose of this work is to extend the method of pseudodifferential equations to the electrodynamic screen problem.

## 2. PSEUDODIFFERENTIAL EQUATIONS FOR SCREEN PROBLEM

Taking (6) into account the equation (5) can be rewritten as the vector pseudodifferential equation on manifold  $\Omega$  [2]

$$(7) \quad (\text{Grad } \Delta^{-1/2} (\text{div } u) + k^2 \Delta^{-1/2} u)|_t = f$$

Note that the principal symbol of the equation (7) is degenerated.

In order to study the equation (7) the Sobolev space  $W$  is introduced in accordance with the asymptotic behaviour of the solution  $u$  near the edge  $\partial\Omega$ . Define the space of distributions  $W$  as the closure of  $C_0^\infty(\Omega)$  in the norm

$$\|u\|_W^2 = \|u\|_{-1/2}^2 + \|\text{div } u\|_{-1/2}^2$$

with the inner product

$$(u, v)_W = (u, v)_{-1/2} + (\text{div } u, \text{div } v)_{-1/2}.$$

Corollary 1.

$$W = \left\{ u \in \tilde{H}^{-\frac{1}{2}}(\bar{\Omega}) : \operatorname{div} u \in \tilde{H}^{-\frac{1}{2}}(\bar{\Omega}) \right\}, \text{ where}$$

the Sobolev spaces  $\tilde{H}^s(\bar{\Omega})$  is denoted in the usual way [3].

The space  $W$  has the following important property. Let  $W_1$  and  $W_2$  be the subspaces of  $W$  such that

$$W_1 := \left\{ u \in W : \operatorname{div} u = 0 \right\},$$

$$W_2 := \left\{ u \in W : \operatorname{rot} u = 0 \right\},$$

where  $\operatorname{div}$  and  $\operatorname{rot}$  are the tangential divergence and rotor on  $\Omega$ .

Corollary 2. The space  $W$  may be decomposed into the direct sum of the closed subspaces  $W_1$  and  $W_2$ :  $W = W_1 \oplus W_2$ .

Now one can write

$$Lu := (\operatorname{grad} A(\operatorname{div} u) + k^2 Au)|_t$$

and treat (7) as pseudodifferential equation

$$(8) \quad Lu = f, \quad u \in W, \quad f \in C^\infty(\bar{\Omega}).$$

Here (8) is interpreted in the sense of distributions.

By using the method of quadratic forms one can show that it is possible to consider  $L$  as the bounded operator  $L: W \rightarrow W'$ , where  $W'$  denotes antidual space for  $W$ :

$$W' = \left\{ u|_{\bar{\Omega}} : u \in H^{-1/2}(M), \operatorname{rot} u \in H^{-1/2}(M) \right\},$$

where  $M$  is the closed surface such that  $\bar{\Omega} \in M$ .

The operator  $L$  is well-defined on the space  $C_0^\infty(\Omega)$ . Then it is extended onto  $W$  by the continuity. Furthermore, the decomposition of operator  $L$  into the spaces  $W_1$  and  $W_2$  yields the result which is important in different applications!

Theorem 1. For  $\operatorname{Im} k \geq 0$ ,  $k \neq 0$  there exists exactly one solution of the equation (7) (or (8)):

$$(9) \quad L(k)u = f, \quad u \in W, \quad f \in W'$$

Moreover, it is established the limiting absorption principle. Let  $\operatorname{Im} k \geq 0$ ,  $k \neq 0$ . Then the bounded operator-function  $L^{-1}(k): W' \rightarrow W$  exists and depends analytically with respect to  $k$  in the neighbourhood of every real point  $k_0 \neq 0$ . This implies

Theorem 2. Let  $\operatorname{Im} k > 0$ ,  $\operatorname{Im} k_0 = 0$ ,  $k_0 \neq 0$  and  $f(k) \xrightarrow{W'} f(k_0)$  weakly as  $k \rightarrow k_0$ . Then  $u(k) \xrightarrow{W} u(k_0)$  strongly as  $k \rightarrow k_0$ , where  $u(k)$  and  $u(k_0)$  solve the problems  $L(k)u(k) = f(k)$ ,  $L(k_0)u(k_0) = f(k_0)$ .



### 3. THE BEHAVIOUR OF THE FIELDS NEAR A CORNER.

Consider a singular point  $P \in \partial\Omega$ , where  $\partial\Omega$  consists of two arcs of two smooth curves intersecting transversally at the singular point. If  $\alpha(P)$  denotes the interior angle of the tangent cone to  $\Omega$  at  $P \in \partial\Omega$  then  $\alpha(P) = \pi$  iff  $P$  is a regular point and  $0 < \alpha(P) < 2\pi$ ,  $\alpha(P) \neq \pi$  for singular points.

Let  $f \in C^\infty(\bar{\Omega})$ . Represent  $f$  in the form

$$f = f^1 + f^2, \quad f^1, f^2 \in C^\infty(\bar{\Omega}), \quad \operatorname{div} f^1 = 0, \quad \operatorname{rot} f^2 = 0.$$

In this case two equations from (7) are obtained

$$(10) \quad k^2 \Delta^{-1/2} u^1 = \tilde{f}^1, \quad u^1 \in W_1$$

$$(11) \quad \Delta^{1/2} u^2 = \tilde{f}^2, \quad u^2 \in W_2$$

The regularity theory for the equations (10), (11) is sufficiently well elaborated in [3,4]. The application of these results yields the values of the critical exponent  $\beta$  for the singularities of the fields  $|E|, |H| \leq Cr^{-\beta}$  near the corner point  $P$ , where  $r$  is the distance to the point  $P$ :

$\alpha/\pi$	0. (+0)	0.125	0.250	0.375	0.500	0.625	0.750	0.875	1.000
$\beta$	1.0	.8317	.7820	.7384	.6956	.6517	.6057	.5561	.5000

$\alpha/\pi$	1.125	1.250	1.375	1.500	1.625	1.750	1.875	2. (-0)
$\beta$	.4448	.3799	.3073	.2277	.1444	.0702	.0281	0

#### REFERENCES

1. Stephan E. Boundary integral equations for screen problems in  $\mathbb{R}^3$ . Integral Equations and Operator Theory 10, pp. 236-257 (1987).
2. Smirnov Yu.G. On the solvability of vector integro-differential equations in electromagnetic diffraction problem on arbitrary screen. Comp. Math. Phys., Vol. 34, No. 8 (1994).
3. Paivarinta L., Rempel S. A deconvolution problem with the kernel  $1/|x|$  on the plane. Appl. Anal. 26, pp. 105-128 (1987).
4. Paivarinta L., Rempel S. Corner singularities of solutions to  $\pm 1/2$   
 $\Delta u = f$  in two dimensions. Asymptotic Analysis. Vol. 5, pp. 429-460 (1992).

# THE DIFFRACTION ON THE THICK DIPOLE

A.V. Sochilin, S.I. Eminov

Novgorod, B.S.-Peterbyrgskaia 41, Novgorod St. University

Let the arbitrary electro-magnetic wave falls on the dipole. As a result, the surface electric currents are directed on the surface of the dipole. These current have density

$$\vec{j} = \vec{t}_z j_z(z, \varphi) + \vec{t}_\varphi j_\varphi(z, \varphi) \quad (1)$$

The system [1] is formed for the definition of the current

$$\left\{ \begin{aligned} \int_S \left[ j_z \left( -\frac{\partial^2 G}{\partial z \partial z'} + k^2 G \right) + j_\varphi \left( -\frac{\partial^2 G}{a \partial z \partial \varphi'} \right) \right] a d\varphi' dz' &= -i \sqrt{\frac{\epsilon}{\mu}} E_z^0 \\ \int_S \left[ j_z \left( -\frac{\partial^2 G}{\partial z' \partial \varphi'} \right) + j_\varphi \left( -\frac{\partial^2 G}{a^2 \partial \varphi \partial \varphi'} + k^2 \cos(\varphi - \varphi') G \right) \right] a d\varphi' dz' &= \\ &= -i \sqrt{\frac{\epsilon}{\mu}} E_\varphi^0 \end{aligned} \right. \quad (2)$$

where  $G = G(z, z', \varphi, \varphi') = \sum_{m=-\infty}^{+\infty} e^{-im(\varphi - \varphi')} S_m(z, z')$

$$S_m(z, z') = \frac{1}{2\pi^2} \int_0^\infty \cos[kx(z-z')] I_m \left( \sqrt{x^2 - 1} ka \right) K_m \left( \sqrt{x^2 - 1} ka \right) dx$$

Expand function  $j_z$ ,  $j_\varphi$ ,  $E_z^0$ ,  $E_\varphi^0$  in to series of the Fourier's type:

$$j_z(z, \varphi) = \frac{1}{2\pi a} \sum_{m=-\infty}^{+\infty} I_z^m(z) e^{-im\varphi}, \quad \int_0^{2\pi} j_z(z', \varphi') e^{im\varphi'} a d\varphi' = I_z^m(z')$$

and bring the system (2) to the independent systems

$$\left\{ \begin{aligned} & \int_{-1}^1 \left[ I_z^m \left( \frac{-1}{\hat{1}} \frac{\partial^2 S_m}{\partial \tau \partial t} + \hat{1} S_m \right) + I_\varphi^m \left( \frac{-im}{\hat{a}} \frac{\partial S_m}{\partial \tau} \right) \right] dt = -\frac{1}{k} \sqrt{\frac{\epsilon}{\mu}} E_z^0 \\ & \int_{-1}^1 \left[ I_z^m \left( \frac{-im}{\hat{a}} \frac{\partial S_m}{\partial t} \right) + I_\varphi^m \left( \frac{-m^2 \hat{1}}{\hat{a}^2} S_m + \hat{1} \frac{S_{m-1} + S_{m+1}}{2} \right) \right]_2 dt = \\ & \qquad \qquad \qquad -\infty \leq m \leq +\infty \end{aligned} \right. = -\frac{1}{k} \sqrt{\frac{\epsilon}{\mu}} E_\varphi^0 \quad (4)$$

where  $z=lt$ ,  $z'=lt'$ ,  $\hat{1}=kl$ ,  $\hat{a}=ka$ .

Turn from function  $I_z^m(l\tau)$ ,  $I_\varphi^m(l\tau)$  to news

$$I_z^m(l\tau) = \rho_2(\tau) u(\tau), \quad I_\varphi^m(l\tau) = \rho_1(\tau) v(\tau) \quad (5)$$

Choose the spaces in which system (4) is investigated. We'll find function  $u(\tau)$  in the gilbert space  $L_{2,\rho_2}[-1,1]$  with basis

$$\psi_n(\tau) = \frac{1}{\rho_2(\tau)} \sqrt{\frac{2}{\pi}} \sin(n \arccos \tau), \quad n = 1, 2, \dots \quad (6)$$

and function  $v(\tau)$  in the space  $L_{2,\rho_1}[-1,1]$  with basis

$$\varphi_n(\tau) = \begin{cases} \sqrt{1/\pi}, & n=1; \\ \sqrt{2/\pi} \cos[(n-1) \arccos \tau], & n \geq 2. \end{cases} \quad (7)$$

The following theorem is proved

**THEOREM.** The system (4) is equivalent of the infinite system of Fredholm of the second kind

$$(I + M)x = y, \quad (8)$$

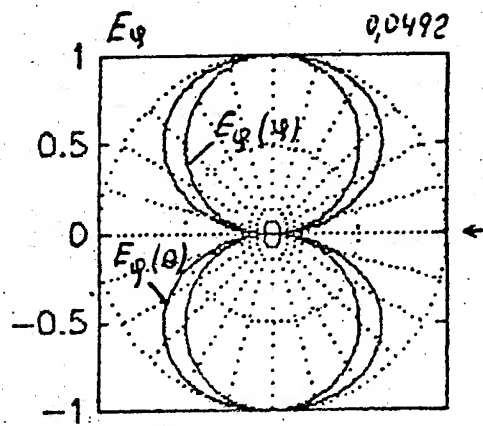
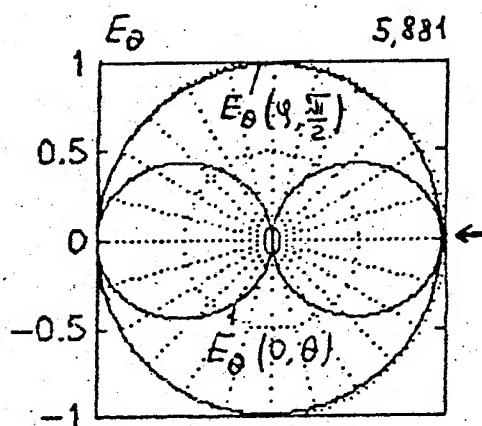
where  $I, M: l_2 \oplus l_2 \rightarrow l_2 \oplus l_2$

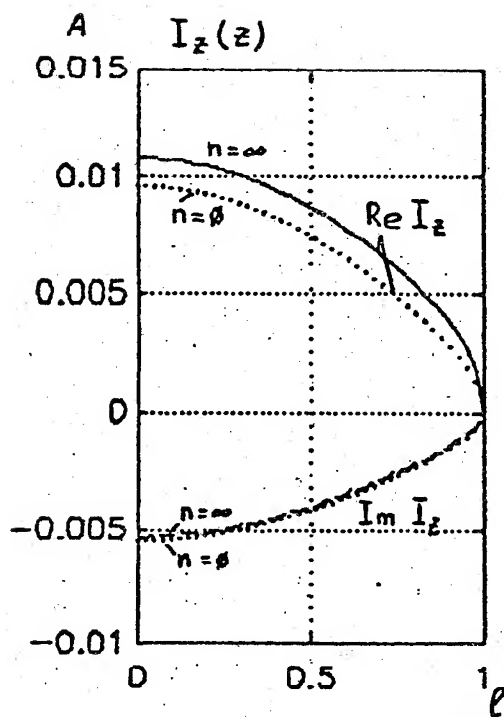
System (8) is solved by method of the truncation. The series of the calculation were carried out for the case of incidence of the plane cylindrical wave on the dipole.

In this case the two problems is solved. At first, it is investigation of the effectiveness of the method. By the definition of the currents the stability comes when the 3 - 4 basic function in the wide diapason by the changes of the entrance parameters are taken into account. The effectiveness is as in the standart problems of diffraction of E and H - polarizations on the band. At second, it's the investigation of the currents and the diagrams of diffusions depending on the radius and lenght of the dipole. Something of this calculation are shown on the figures.

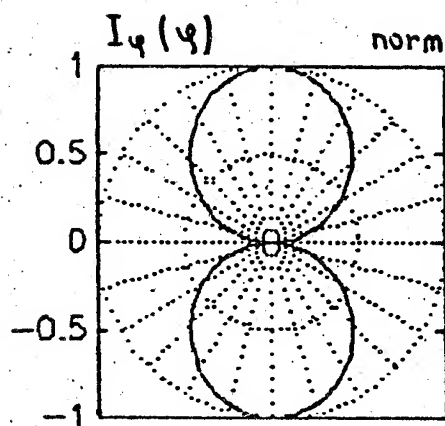
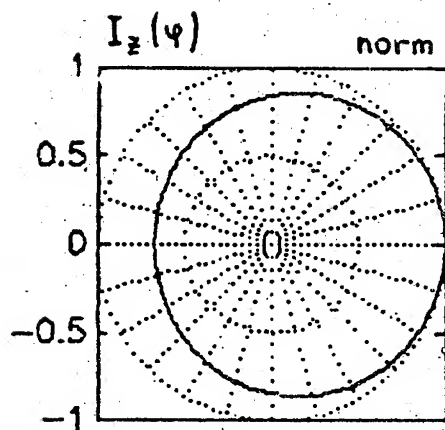
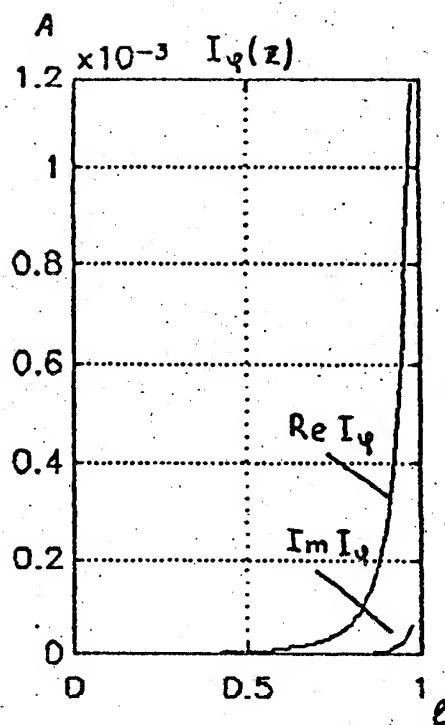
#### References:

1. Сочилин А.В., Эминов С.И. Теория системы интегро - дифференциальных уравнения вибратора = [The ory of system of the integro - differential equation of dipole]// Дел. В ВИНТИ, N 2678 - В93 ОТ 28.10.93 - 17 с. рус.





$$l = 0,25 \lambda_0$$



## WAVE ATTENUATION IN RECTANGLE-GROOVE GUIDES

Alexander Ye. Svezhentsev

Institute of Radiophysics & Electronics  
Kharkov 310085, Ukraine

Groove guides are low-loss single-mode waveguides at millimeter wavelengths [1]. The proposed centrally symmetric rectangle-groove guides are of interest because only one of the geometry parameters, namely, a groove depth, is fixed. This makes possible retunability of such a guide by a simple plane-parallel shift of the walls. The disadvantage is that for low propagation loss to be achieved, the guide transverse overall dimension is to be impractically large. The problem is to find the balance between practicable dimensions and minimum loss.

### The Problem Formulation

The boundary-value problem of finding the cut-off frequencies for an axially symmetric rectangle groove guide (ASG) (Fig.1a) and centrally symmetric rectangle-groove guide (CSG) (Fig.2a) is considered. The analysis is based on a moment method solution of the spectral problem. Expanding the trigonometrical function series in terms of Gegenbauer polynomials [2] one can reduce the solution to the system of linear coupled algebraic equations (SLAE) which yields the cut-off frequencies and natural wave fields.

### Design Algorithm

The design algorithm is starting from specifying the  $L/c$  value and the field attenuation  $q$  over waveguide arm distance. Then the normalized resonant frequency can be approximated by the formula  $k_0 = (\pi/2) \sqrt{1 - (2 \ln q / \pi D)^2}$ , where  $D = L/c$ . Once  $g/c$  has been given, the guide normalized overall transverse dimension

$G/c=2\pi(g/c+D)$  is known. From the SLAE one finds groove depth  $a/c$  and then the attenuation factor normalized  $\hat{\alpha}$ . Specifying  $c$  one finds the attenuation factor  $\alpha$ .

### Results

The outlined algorithm was used in designing ASG. Transverse overall dimension  $G/c$  as a function of attenuation factor  $\hat{\alpha}$  was calculated for  $L/c$  from 4 to 5 (Fig.1,c). The optimum dimensions of ASG given in [1] are:  $g/c=0.4$ ;  $a/c=0.6$ . For  $g=100$ ,  $L/c$  is to be 5.

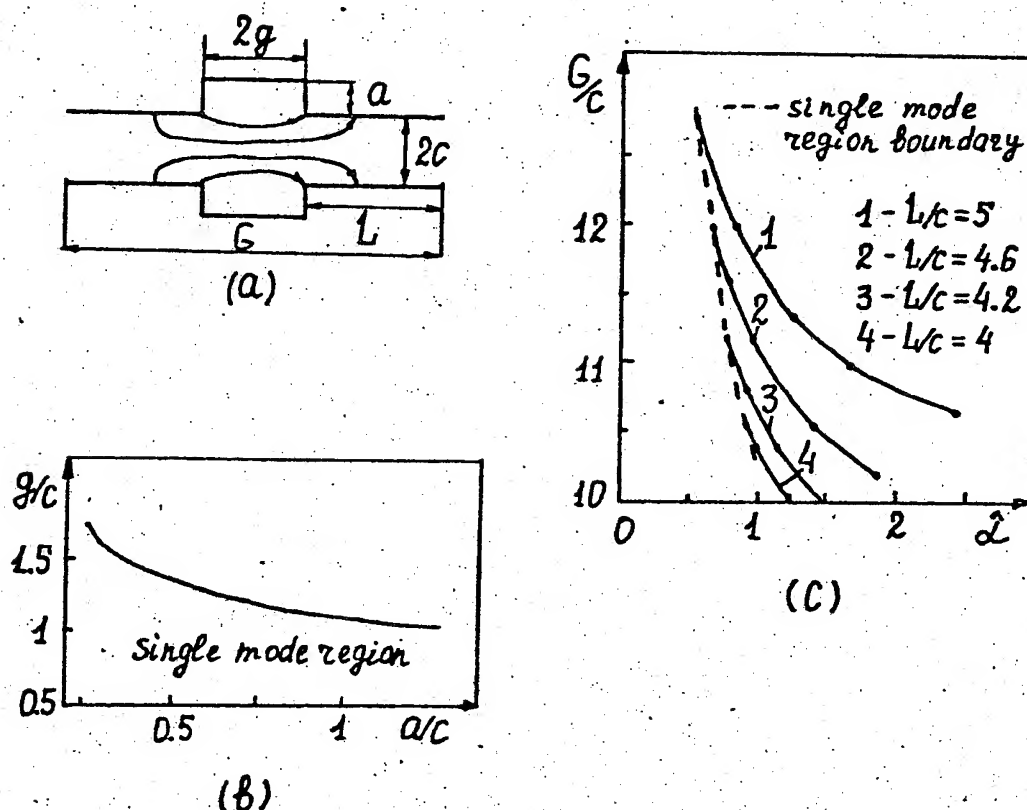


Fig.1. (a) geometry of axially symmetric rectangle-groove guide; (b) normalized groove dimension  $g/c$  of the guide versus groove depth  $a/c$  at the second mode critical condition; (c) normalized overall dimension  $G/c$  as a function of normalized attenuation factor  $\hat{\alpha} = \alpha \cdot (2c)^{3/2} \cdot 10^{-4}$ , where  $\alpha$  is the attenuation factor in DB/M.

The obtained results show that at the  $L/c$  decrease one can achieve falling attenuation factor with the transverse overall dimension unchanged. In so doing  $g/c$  increases. In this case the optimum  $g/c$  is near a threshold value corresponding to the critical condition for the next order mode propagation.

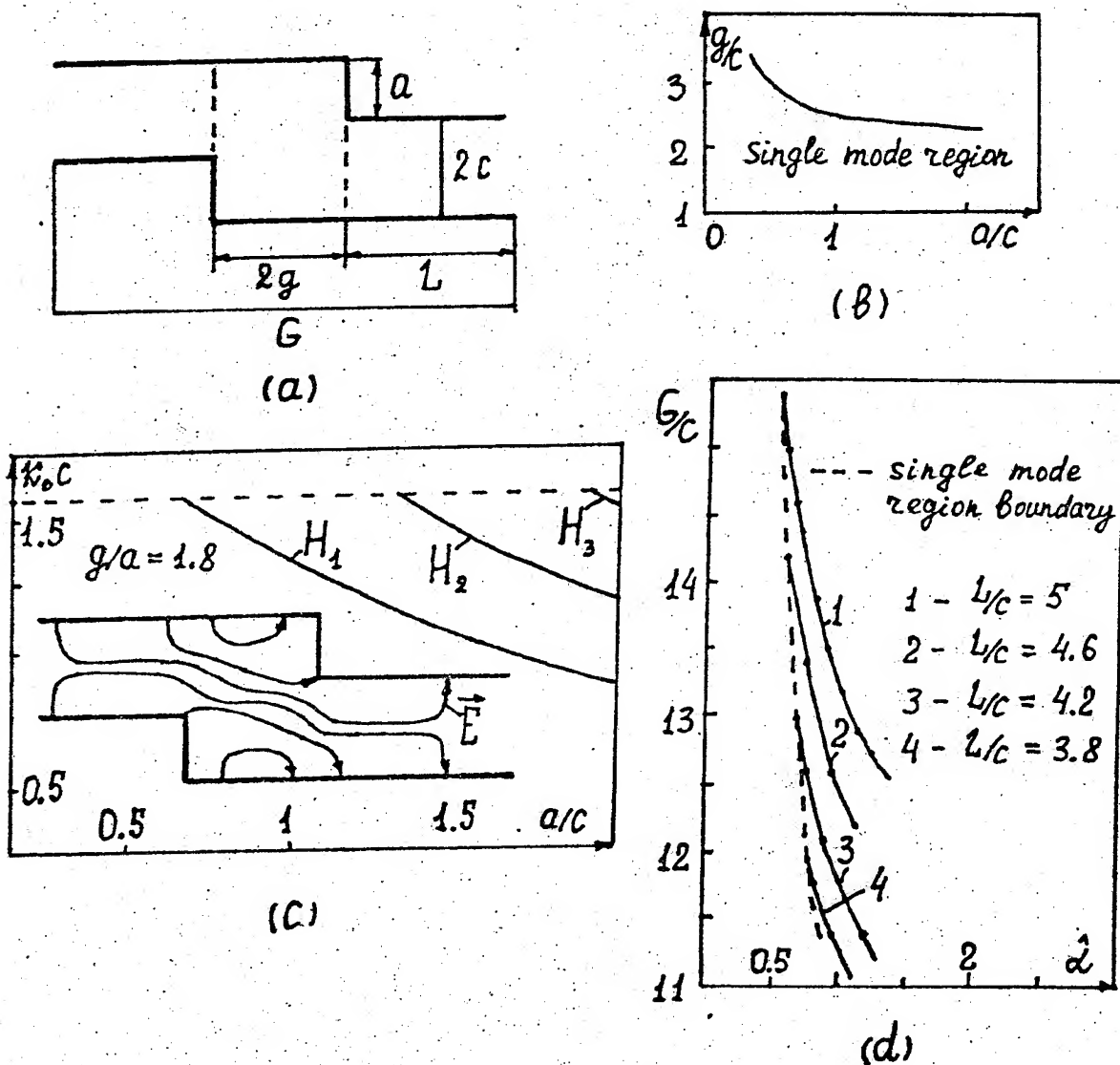


Fig.2 (a) geometry of centrally symmetric rectangle-groove guide; (b) normalized groove dimension  $g/c$  versus groove depth  $a/c$  at the second mode critical condition; (c) normalized cut-off frequencies  $k_0 c$  as functions of normalized height  $a/c$  of the guide step; (d) normalized overall dimension  $G/c$  versus normalized attenuation factor  $\alpha$ .



In this connection for the second order mode the critical values of  $g/c$  were calculated depending on  $a/c$ . A basic guideline in deciding which value of  $g/c$  is optimal is waveguide single-mode requirement (Fig.1,b).

With the devised design algorithm the CSG cut-off frequencies  $k_c c$  of three lower order modes versus normalized height  $a/c$  of the guide step were calculated and the lower mode field distribution are mapped (Fig.2c). As seen, the lower order H<sub>1</sub> mode is of interest.

In Fig.2,d CSG transverse overall dimension  $G/c$  is plotted as a function of attenuation factor  $\alpha$  for lower order mode for some values  $L/c$ . It was shown that the optimum dimensions may be determined using dependences of critical values of  $g/c$  and  $a/c$  for the second propagation mode (Fig.2b).

### Conclusions

A new type groove guide, namely, centrally symmetric rectangle-groove guide was proposed and examined.

With the proposed design algorithm the optimum relations between transverse overall dimensions and ohmic loss for both centrally symmetric rectangle-groove guide and axially symmetric one were first calculated.

### References

1. T.K.Ho and D.J.Harris. Millimetre Wave Groove Guide With V-Shaped Grooves. Electronic Letters, 1984, vol.19, No.19, pp.777-778.
2. G.F.Zargano, V.P.Lapin, V.S.Michalevski et al. Waveguides of Complex Cross-Section. Moscow, Radio and Communication, 1986 (In Russian).

# Propagation of Super-Wideband Signals through Waveguides

Oleg. A Tretyakov

Dept. Radiophysics, Kharkov University, 310077 Kharkov, the Ukraine

Fax 7-0572-476506

The background of present theory is a new approach which we have advanced recently to solve EM field boundary-value problems in time domain [1]. The vectors of the desired EM field can be presented as a sum of 2-D projections to waveguide cross-section plane, and one-component vectors directed along waveguide axis  $Oz$ , namely

$$\vec{E} = \vec{E}_{tr} + \vec{z}_0 E_z, \quad \vec{H} = \vec{H}_{tr} + \vec{z}_0 H_z \quad (1)$$

In a particular case of TM-modes these components can be written as

$$\vec{H}_{tr} = \nabla_{tr} \Psi(\vec{r}) \frac{\partial}{\partial z} F(z, t), \quad \vec{E}_{tr} = [\vec{z}_0 \times \nabla_{tr} \Psi(\vec{r})] \frac{\partial}{\partial t} F(z, t) \quad (2)$$

$$H_z = \kappa^2 \Psi(\vec{r}) F(z, t), \quad E_z = 0 \quad (3)$$

where  $\vec{r}$  is 2-D position vector in cross-section  $S$  bounded by contour  $L$ ,  $\nabla_{tr}$  is transversal nabla-operator. Scalar function  $\Psi(\vec{r})$  is a Neumann-type eigenfunction satisfying a problem

$$(\nabla_{tr}^2 + \kappa^2) \Psi(\vec{r}) = 0, \quad \frac{\partial}{\partial n} \Psi|_L = 0; \quad \kappa \equiv \kappa_m \quad (m = 1, 2, 3 \dots) \quad (4)$$

Another scalar function of (2) is solving the Klein-Gordon hyperbolic equation as

$$\left( \frac{1}{c^2} \frac{\partial^2}{\partial t^2} - \frac{\partial^2}{\partial z^2} + \kappa^2 \right) F(z, t) = 0 \quad (5)$$

The group theory enables one to separate variables, based on 11 2-nd order symmetric operators which yield 11 new pairs of variables [2]. As an example we give only one of the variety of solutions

$$F(z, t) = A \left( \frac{ct - z}{ct + z} \right)^{\nu/2} J_\nu[\kappa(c^2 t^2 - z^2)^{1/2}], \quad ct \geq |z|; \quad F(z, t) = 0, \quad ct < |z| \quad (6)$$

where  $A$  is a constant,  $\nu$  is the parameter of variables separation,  $J_\nu(\cdot)$  is the Bessel function. Applying the Fourier transform to (6) one obtains

$$F(z, \omega) = B \frac{\exp[i(\omega^2 - \omega_c^2)^{1/2}|z|/c]}{(\omega^2 - \omega_c^2)^{1/2}} \left[ \frac{i\omega_c}{\omega + (\omega^2 - \omega_c^2)^{1/2}} \right]^\nu \quad (7)$$

where  $B$  is a constant,  $\omega$  is the frequency,  $\omega_c = \kappa_c$  is cutoff frequency. This equation demonstrates that the solution (6) is itself a signal of remarkably wide band. Besides of it, a whole variety of super-wideband signals can be obtained as linear combinations of (6).

[1] O.A. Tretyakov, Essentials of Nonstationary and Nonlinear EM Field Theory, in M. Hashimoto, M. Idemen, O.A. Tretyakov (Eds.), *Analytical and Numerical Methods in EM Wave Theory*, Tokyo: Science House, 1993, 123-145.

[2] W. Miller, *Symmetry and Separation of Variables*, Massach.: Addison-Wesley, 1977.

# ANALYTICAL REGULARIZATION OF SURFACE- INTEGRAL AND INTEGRO-DIFFERENTIAL EQUATIONS IN DIFFRACTION THEORY

Yu. A. Tuchkin

Institute of Radiophysics and Electronics  
of the Ukrainian Academy of Sciences  
12, ac. Proskura st., Kharkov, 310085, Ukraine  
(Tel: (7-0572)-44-85-56; FAX: (7-0572)-79-11-11)

The general methodological principles of numerical solution of the wide range of boundary value problems (BVP) of diffraction theory are discussed here. The described procedure of analytical regularization reduces equivalently (in mathematical terms) an initial BVP to the equation  $(I + H)x = b$  of the second kind with compact operator  $H$  in the Hilbert space  $l_2$ . As is known, such an equation is solvable with any preassigned accuracy by the truncation method. The solution procedure for truncated to the reasonable dimension algebraic systems is numerically stable and offers certain advantages over many other techniques such as method of moments, finite differences method, etc.

1. The regularization term is used here in traditional sense of functional analysis. Let an operator  $A$  be given in a pair of functional spaces. It is required to solve the equation of the first kind  $Az = b$ , where  $b$  and  $z$  are, respectively, known and unknown elements of these spaces. Take the pair of operators  $L_0, R_0$  (being a two-sided regularizer) in the form  $L_0 A R_0 = I + H$ , where  $I$  and  $H$  are, respectively, identity and compact operators. Then, under relevant assumptions, the initial equation of the first kind is equivalent to the equation of the second kind  $(I + H)x = L_0 b$ , where  $x = R_0^{-1} z$  is the new unknown element of the corresponding space.

By the term of analytical regularization (AR) we mean the constructive development of the operators  $L_0$  and  $R_0$  as well as the adequate BVP formulation including the proper choice of the relevant pair of the functional spaces. By the simplest example we illustrate below the central ideas of the approach which are complicated with BVP complexity. Being limited by the abstract volume, we shall resort to rather informal presentation style.

2. Let the Green's function  $G(q, p)$  of the Helmholtz equation be given in a two-dimensional (maybe unbounded) domain  $\Omega$  so that  $G(q, p)$  satisfies both in  $q$  and  $p$  the equations

$$(\Delta_q + k^2)G(q, p) = (\Delta_p + k^2)G(q, p) = \delta(q - p), \quad q, p \in \Omega, \quad (1)$$

where  $\delta(q - p)$  is the delta function. Besides,  $G(q, p)$  satisfies in  $q$  and  $p$  the boundary conditions of the first, or second, or third kind, or - for an unbounded domain - the corresponding radiation condition of Sommerfeld or Reichardt, etc.

Let a contour  $L \subset \Omega$  be a one-bounded piece of a smooth, simple, closed contour  $S$ , i.e.  $L \subset S$ ,  $S \subset \Omega$ ,  $S \cup \partial\Omega = \emptyset$  (maybe  $L = S$ ). The  $2\pi$ -periodically smooth parametrization  $\eta(\theta) \equiv (x(\theta), y(\theta))$ ,  $\theta \in [-\pi, \pi]$  of the contour  $S$  is supposed to be given, and the vector-function  $\eta(\theta)$ ,  $\theta \in [-d, d]$  parametrizes the contour  $L$  for the certain  $d \in (0, \pi]$ ;  $x(\theta), y(\theta)$  are the Cartesian coordinates of a point  $\eta(\theta) \in S$  for any  $\theta \in [-\pi, \pi]$ , and  $l(\theta) = \{[x'(\theta)]^2 + [y'(\theta)]^2\}^{1/2} > 0$ ,  $\theta \in [-\pi, \pi]$ .

For any "not-too-much-singular" function  $\mu(p)$ ,  $p \in L$ , we define, in the ordinary way, single and double-layer potentials as

$$[P_\mu](q) = \int_L \mu(p) G(q, p) dl_p, \quad q \in \Omega; \quad (2)$$

$$[Q_\mu](q) = \int_L \mu(p) \frac{\partial G(q, p)}{\partial n_p} dl_p, \quad q \in \Omega \setminus S, \quad (3)$$

where  $n_p$  is the outward unit normal to the contour  $S$  at a point  $p \in S$ . In the sufficiently small vicinity of the contour  $S$  the normal and tangential derivatives of these potentials are

$$[\partial_n P_\mu](q), [\partial_n Q_\mu], [\partial_t P_\mu](q), [\partial_t Q_\mu]. \quad (4)$$

Direct and limiting values (if any) of a function  $f(q)$ ,  $q \in S$  on the contour  $S$  are denoted as

$$\bar{f}(q) = f(q), \quad q \in S; \quad f^\pm(q) = \lim_{h \rightarrow 0} f(q \pm hn_q), \quad q \in S. \quad (5)$$

Direct and limiting values of integral transformations (2)-(4) are denoted similarly.

3. Let a function  $U^i(q)$ ,  $q \in \Omega$  be the incident field. It is required to find in the relevant functional space the scattered field  $U^s(q)$  which satisfies the homogeneous Helmholtz equation in  $\Omega$ , the boundary condition which the function  $G(q, p)Q_n \partial \Omega$  satisfies, and, finally, the corresponding boundary condition at the contour  $L$  (see [1]-[4]).

We start with the simplest Dirichlet problem  $U^{s(\pm)}(q) = -U^i(q)$ ,  $q \in L$  resulting (see [1]-[4]) in the integral equation

$$[\bar{P}Z_D(q)] = -U^i(q), \quad q \in L; \quad Z_D(p) = \frac{\partial U^{s(+)}(p)}{\partial n} - \frac{\partial U^{s(-)}(p)}{\partial n}, \quad p \in L \quad (6)$$

in the unknown function  $Z_D(p)$ . It is easy to prove that

$$G(\eta(\theta), \eta(\tau)) = \frac{1}{2\pi} \left\{ \ln \left| 2 \sin \frac{\theta - \tau}{2} \right| + P^{(1)}(\theta, \tau) \right\}, \quad \theta, \tau \in [-\pi, \pi], \quad (7)$$

where  $P^{(1)}(\theta, \tau)$  is a  $2\pi$ -periodically continuous, together with its first derivatives, function. Its second derivatives have only logarithmic singularities when  $\theta = \tau \pmod{2\pi}$ . Eq.(6) is equivalently reduced to the integral equation of the first kind

$$\frac{1}{2\pi} \int_{-d}^d z(\tau) \left\{ \ln \left| 2 \sin \frac{\theta - \tau}{2} \right| + P^{(1)}(\theta, \tau) \right\} d\tau = -U^i(\eta(\theta)), \quad \theta \in [-d, d], \quad (8)$$

where  $z(\tau) = l(\tau)Z_D(\eta(\tau))$  is the unknown function. Expand the functions  $z(\tau)$ ,  $P^{(1)}(\theta, \tau)$ ,  $\theta, \tau \in [-\pi, \pi]$  in the Fourier series

$$z(\tau) = \sum_{n=-\infty}^{\infty} z_n e^{in\tau}; \quad P^{(1)}(\theta, \tau) = \sum_{s=-\infty}^{\infty} \sum_{n=-\infty}^{\infty} p_{s,n} e^{i(s\theta + n\tau)}. \quad (9)$$

For simplicity, consider the case  $L = S$  (i.e.  $d = \pi$ ). Putting (9) into (8) and using the orthogonality of the system  $e^{in\tau}$  in  $[-\pi, \pi]$  we obtain the infinite algebraic system of the first kind [4]

$$(1 - \delta_{s0})\tau_s^{-2}z_s - 2 \sum_{n=-\infty}^{\infty} p_{s,-n} z_n = g_s, \quad s = 0, \pm 1, \pm 2, \dots, \quad (10)$$

where  $\delta$  is the Kronecker delta,  $g_s$  is, within a constant factor, the  $s$ th Fourier coefficient of the function  $U^i(\eta(\theta))$ ,  $\theta \in [-\pi, \pi]$ , and  $\tau_s = \max(1, |s|^{1/2})$ . By changing the unknowns  $\hat{z}_s = \tau_s^{-1}z_s$  and multiplying (10) by  $\tau_s$  we obtain in  $l_2$  the equation

$$(I + H)\hat{z} = \hat{g}, \quad \hat{z}, \hat{g} \in l_2, \quad (11)$$

with, respectively, the unknown and known vector-columns  $z = \{\hat{z}_n\}_{n=-\infty}^{\infty}$  and  $\hat{g} = \{\tau_n g_n\}_{n=-\infty}^{\infty}$ , and the matrix operator

$$H = \{h_{s,n}\}_{s,n=-\infty}^{\infty}, \quad h_{s,n} = -[2p_{s,-n} + \delta_{s0}\delta_{n0}]\tau_s\tau_n. \quad (12)$$

It may be shown that the conditions  $\hat{z}, \hat{g} \in l_2$  are relevant to the rigorous Dirichlet formulation, the operator  $H$  is compact, and moreover

$$\sum_{s=-\infty}^{\infty} \sum_{n=-\infty}^{\infty} (1 + |n|)(1 + |s|)|h_{sn}|^2 < \infty. \quad (13)$$

Thus in  $I_2$  the initial BVP is reduced to the equation of the second kind of the form (11), (13). This equation solution is a relatively simple problem provided that eq.(11) has a unique solution. This is valid when the initial BVP has this property and eq.(11) is equivalent to this BVP. In the considered case  $L = S$  the initial BVP falls into two ones: for the domain  $\text{int}(S)$  enclosed by the contour  $S$ , and for the domain  $\text{ext}(S) = \Omega \setminus (S \cup \text{int}(S))$ . It is well known that eqs.(6) and, consequently, (11) are not equivalent to the initial BVP within the domain  $\text{ext}(S)$  if  $L = S$ , and the  $k$  value coincides with the domain  $\text{int}(S)$  resonance [5]. This drawback is easily overcome by replacing the function  $G(q, p)$  for the relevant Green's function dissipative in  $\text{int}(S)$  [5].

When  $L = S$ , the two-sided regularizer is easily constructed when going from (10) to (11):  $L_0 = R_0 = T$ , where the operator  $T = \{\delta_{nn}\}_{n=-\infty}^{\infty}$  is diagonal. In the less trivial case  $L \neq S$  (and  $d < \pi$ ) eq.(8) is reduced [1-4] to the special dual series equations which AR method is described in [6],[7]. Then the initial BVP (with  $L \neq S$ ) results in the equivalent equation of the type (11) (see [1]-[3]).

4. For the Neumann boundary condition  $\frac{\partial U^{(\pm)}(q)}{\partial n} = -\frac{\partial U^i(q)}{\partial n_q}$ ,  $q \in L$ , instead of (6) we have the equation

$$[Q^{(-)}Z_N](q) = -\frac{\partial U^i(q)}{\partial n_q}, \quad q \in L; \quad Z_N(p) = U^{(-)}(p) - U^{(+)}(p), \quad p \in L. \quad (14)$$

It can be shown [8] that this equation is equivalent to the integro-differential equation of the form

$$\frac{1}{2\pi} \frac{d^2}{d\theta^2} \int_{-d}^d z_N(\tau) \ln \left| 2 \sin \frac{\theta - \tau}{2} \right| d\tau + \int_{-d}^d z_N(\tau) Q^{(1)}(\theta, \tau) d\tau = -l(\theta) \left[ \frac{\partial U^i(q)}{\partial n_q} \right]_{q=\eta(\theta)}, \quad \theta \in (-d, d), \quad (15)$$

where  $z_N(\tau) = Z_N(\eta(\tau))$ ;  $\tau \in [-d, d]$  is the unknown function, and the function  $Q^{(1)}(\theta, \tau)$  has only logarithmic singularities if and only if  $\theta = \tau \pmod{2\pi}$ . In the both cases  $L = S$  and  $L \neq S$ , the AR methods for eq.(15) are actually the same as for eq.(8). The obtained equation of the second kind exhibits in  $I_2$  the qualitative properties identical with those of eq.(11).

5. Let consider in the domain  $\text{ext}(S)$  the diffraction BVP of the third kind

$$\alpha(q)kU^{(+)}(q) + \beta(q)[\partial U^{(+)}(q)/\partial n] = F_0(q), \quad q \in S, \quad (16)$$

where  $F_0(q)$ ,  $\alpha(q)$ ,  $\beta(q)$  are smooth given functions;  $|\alpha(q)| + |\beta(q)| \neq 0$ ,  $q \in S$ . Using (2)-(4) the integral representations of the functions  $W(q) = U^{(+)}(q)$  and  $V(q) = \partial U^{(+)}(q)/\partial n_q$  may be constructed. Putting these representations into (16) we obtain

$$k\alpha(-\bar{Q}W + \bar{P}V) + \beta(-\partial_n Q^{(+)}W + \partial_n \bar{P}V) = \frac{1}{2}F_0, \quad (17)$$

where the argument  $q \in S$  is omitted. Eqs.(16),(17) may be regarded as a system of equations in the unknown functions  $W(q)$  and  $V(q)$ . In the regular case  $|\beta(q)| > 0$ ,  $q \in S$ , using (16) one can eliminate the unknown function  $V(q)$  from (17). Then

$$[\partial_n Q^{(+)}W](q) + [RW](q) = F_1(q), \quad q \in S, \quad (18)$$

where  $F_1(q)$  is known function,  $R$  is integral operator with the rather smooth kernel. The AR procedure for eq.(14) can be easily generalized for eq.(18), and this is the way to reduce (18) to the equation of the type (11) with estimate (13). In the case  $|\alpha(q)| > 0$ ,  $q \in S$  the analogous equation in the unknown function  $V(q)$  is easily obtained. But when  $\epsilon(q) = |\beta(q)/k\alpha(q)| \ll 1$ , both the initial BVP and the last equation are

singularly perturbed in reference to the Dirichlet problem with  $\beta(q) \equiv 0$ . The main part of this singular perturbation we managed to reduce to the ordinary singular differential equation of the second order - with a small factor of the senior derivative - for the standard solution approach including analysis of the solution asymptotics with  $\epsilon \rightarrow 0$  to be employed. As a result, the initial BVP was reduced to the equation of the type (11) with the compact operator  $H$  regular when  $\max|c(q)| \rightarrow 0$ , the perturbation theory series in powers of  $\epsilon$  was constructed.

6. Take the contour  $S$  as the interface between two media with different dielectric and/or magnetic constants and, consequently, different wave numbers:  $k = k^i$  for  $\text{int}(S)$  and  $k = k^e$  for  $\text{ext}(S)$ . The scattered field  $U^s(q)$  must satisfy homogeneous Helmholtz equation in the both domains with the corresponding  $k$ . The boundary conditions at  $S$  are of the form

$$\alpha^e[U^{s(+)}(q) + F(q)] = \alpha^i U^{s(-)}(q), \quad q \in S; \quad (19)$$

$$\beta \left[ \frac{\partial U^{s(+)}}{\partial n}(q) + G(q) \right] = \beta^i \frac{\partial U^{s(-)}}{\partial n}(q), \quad q \in S, \quad (20)$$

where  $\alpha^e, \alpha^i, \beta^e, \beta^i$  are the constants determined by the media parameters,  $F(q), G(q)$  are known functions determined by the incident field. The AR procedure is based on the above-stated ideas. The values (2)-(4) can be individually deduced for  $\text{int}(S)$  and  $\text{ext}(S)$  domains with  $k = k^i$  and  $k = k^e$ , respectively (see (1)). The substitution of the above-mentioned integral representations of  $U^{s(\pm)}$  and  $\partial U^{s(\pm)}/\partial n$  into (19), (20) yields two equations of the type (17). The elimination of  $U^{s(+)}$  and  $\partial U^{s(+)}/\partial n$  using (19), (20) gives the coupled system of integral and integro-differential equations. If  $\lambda = \alpha^i \beta^e + \alpha^e \beta^i \neq 0$ , these equations have actually the same main singularities that eqs.(6) and (14), respectively. The constraint  $\lambda \neq 0$  is adequate to the physical formulation of the problem. Then we result in the equation of the (11) type with estimate (13) (this equation is more conveniently written in the space  $l_2 \oplus l_2$ ).

Let conditions (19),(20) be given at  $S \setminus L$ , and the Dirichlet or Neumann condition at  $L$  as if a portion of  $S$  be of metal. Then the AR procedure seeks to discover the additional unknown function on  $L$ . With this function we obtain the coupled system of equations of the type (17) on the contour  $S$  and the equation of the type (6) or (14) on  $L$ . The regularization of the obtained equations is realized using the combination of the above-stated methods to yield the equation of the kind (11) in  $l_2 \oplus l_2 \oplus l_2$ .

7. If we deal with a single-periodicity system of the contours  $\{S_j\}_{j=-\infty}^{\infty}$  such that  $S_j \cap S_{j+1} = \emptyset$ , then for all the above-described boundary conditions, a BVP is translated to the corresponding BVP for a single contour  $S = S_0$  in the certain domain  $\Omega_0$ . The regularization procedure is carried out as before but with a quasiperiodic Green's function (see [9]). If  $S$  is a smooth infinite single-periodicity contour, that any one of the above-considered BVPs is translated to the corresponding BVP for a single period of the contour  $S$ . Note, the unknown functions and kernels of integral transformations (2)-(4) are not periodic. This presents additional difficulties which can be overcome with the method described in [10],[11]. As a result, all the considered BVPs are reduced to the equation of (11) type with estimate (13).

8. It is possible to think of all the above-mentioned structures as the *roy*-cross-sectional views of the corresponding cylindrical (uniform in  $z$ ) structures which may be considered as open or volume waveguides extended along the  $z$ -axis and investigate the spectrum of normal waves dependent on  $z$  like  $e^{ihz}$ . Properly speaking, these problems are the subject of "spectral theory". For dielectric and metal-dielectric structures these problems correspond to more complicated boundary conditions describing the polarizations coupling and involving not only normal but tangential derivatives of the scattered fields too. We have constructed the AR procedures for the spectral problems for all the above-described structures. As a result, these spectral problems are equivalently reduced to the homogeneous equations of the type (11) where  $H$  is compact analytic operator-function of  $k$  and  $h$  which belong to the corresponding Riemann surfaces. This forms the efficient basis for numerical solving and investigation of the qualitative features of these spectral problems (see [12],[13]).

9. Numerical experiments demonstrate high efficiency of the presented methods. For this see [3], [9], [11], [13] - [17].

## References

1. Yu.A. Tuchkin, DAN SSSR, 1985, v.285, N6, pp. 1370-1373.
2. Yu.A. Tuchkin, Ibidem, 1987, v.293, N2, pp. 343-345.
3. Yu.A. Tuchkin, International School-Seminar "Mathematical Methods in Electromagnetic Theory-90", Gurzuf, USSR, 1990.
4. Yu.A. Tuchkin and V.P. Shestopalov, DAN SSSR, 1990, v.310, N5, pp. 1100-1104.
5. D. Colton and R. Kress. "Integral Equation Methods in Scattering Theory". New-York: Wiley, 1983.
6. Yu.A. Tuchkin and V.P. Shestopalov, Differential equations, 1982, v.18, N4, pp. 663-673.
7. Yu.A. Tuchkin, DAN USSR, Ser. A, 1987, N5, pp. 24-27.
8. Yu.A. Tuchkin, Ibidem, 1987, N4, pp. 21-25.
9. Yu.I. Krutin', Yu.A. Tuchkin, and V.P. Shestopalov, Zhurnal vychislit. matematiki i matem. fiziki, 1991, v.31, N6, pp.864-876.
10. Yu.A. Tuchkin and V.P. Shestopalov, DAN SSSR, 1990, v.311, N6, pp. 1355-1359.
11. Yu.I. Krutin', Yu.A. Tuchkin, and V.P. Shestopalov, Radiotekhnika i elektronika, 1992, v.37, N2, pp. 202-210.
12. A.Ye. Poyedinchuk, Yu.A. Tuchkin, and V.P. Shestopalov, DAN SSSR, 1987, v.295, N6, pp. 1358-1362.
13. Yu.A. Tuchkin, E.V. Shepel'skaya, and V.P. Shestopalov, DAN USSR, Ser. A, 1989, N10, pp. 76-79.
14. V.V. Veremey, A.Ye. Poyedinchuk, and Yu.A. Tuchkin, IEEE APS Symposium Digest, Chicago, USA, July 19-25, 1992, pp. 1869-1872.
15. V.V. Veremey, A.Ye. Poyedinchuk, and Yu.A. Tuchkin, IEEE APS-URSI Symp. Digest, Chicago, USA, July 19-25, 1992, pp. 1869-1872.
16. V.V. Veremey, Yu.A. Tuchkin, and V.G. Dudka, Journees Internationales de Nice sur les Antennes, JINA'92, 12-14 Novebre, Nice, France, 1992, pp. 309-312.
17. V.V. Veremey, Yu.A. Tuchkin, Yu.V. Svishev, and V.G. Dudka, Conference Proceedings of the 10th Annual Review of Progress in Applied Computational Electromagnetics (ACES- 94), Monterey, CA, March 21-26, 1994. pp. 150-154.

# TWO-DIMENSIONAL BOUNDARY PROBLEM FOR UNIFORM DIELECTRIC STRUCTURES

Alexander Tyzhnenko

Kharkov Engineering Economic Institute  
Lenin ave. 9A, 310002, Kharkov, Ukraine

## ABSTRACT

*The scattering of electromagnetic E-polarized waves by an arbitrary dielectric scatterer is described by two-dimensional Fredholm equation of the second kind with weak singularity. A method of decreasing the dimension of the Fredholm equation is proposed. The boundary conditions satisfaction leads to Fredholm's equation of the 1-st kind on the whole real axis or to a system of those equations. It depends on the scatterer's form.*

The Maxwell equations are formulated as an integral equation [1]:

$$E(\vec{\rho}) = E_0(\vec{\rho}) + \lambda \theta(\vec{\rho}) \int H_0^{(2)}(k_0 |\vec{\rho} - \vec{\rho}'|) E(\vec{\rho}') d\vec{\rho}'. \quad (1)$$

where

$E(\vec{\rho}) = \theta(\vec{\rho}) E_0(\vec{\rho})$ ,  $E_0(\vec{\rho}) = \theta(\vec{\rho}) E_0(\vec{\rho})$ ,  $k_0^2 = \omega^2 \epsilon_0 / c^2$ ,  $\lambda = k_0^2 \delta / 4i$ ,  $\delta = (\epsilon - \epsilon_0)$ .  $\epsilon(\epsilon_0)$  is an outside(inside) permittivity,  $E_0(\vec{\rho})$  is an incident wave and  $\mu = \mu_0 = 1$ . In this equation  $\theta(\vec{\rho})$  is denoted the characteristic function of the scatterer, with is one inside D and zero outside one. In order to simplify notation the integration ranges will be omitted in all cases, where the range is  $R_1$  or  $R_2$ .

Equation (1) belongs to a class of integral equations with translation kernels. Solving conditions where discussed in [2] for the one-dimensional case.

But in the two-dimensional case the integral operator  $I - \lambda H$  has the infinite-dimensional null-space and equation  $1 - 2\pi\lambda h(\vec{x}) = 0$  has the uncountable set of solutions. Here the Fourier transform is denoted by small letters. For Hankel function  $h(\vec{x})$  is well known. The set of solutions of the equation

$$x^2 = k_0^2 \epsilon \quad (k_1^2 = k_0^2 \epsilon)$$

may be defined as  $x_1 = \xi$ ,  $x_2 = \pm(k_1^2 - \xi^2)^{1/2}$  and  $x_1 = \pm(k_1^2 - \xi^2)^{1/2}$ ,  $x_2 = \xi$  because of the eigenfunctions set of the integral operator may be written as

$$\psi_{1,2}(\vec{\rho}) = \int A_{1,2}(\xi) \exp(-i\xi y \pm (k_1^2 - \xi^2)^{1/2} z) d\xi \quad (2)$$

$$\psi_{3,4}(\vec{\rho}) = \int A_{3,4}(\xi) \exp(\pm(k_1^2 - \xi^2)^{1/2} y - i\xi z) d\xi.$$



It is impossible to receive unique solution of the equation (2) in the whole space  $R_2$ . But because of the constancy of the  $\theta(\vec{\rho})$  inside  $D$  it is possible to perform the solution for  $\vec{\rho} \in D$  as the sum of the regular solution  $R(\vec{\rho})$  and a system of eigenfunctions (2):

$$E(\vec{\rho}) = R(\vec{\rho}) + \sum \psi_i(\vec{\rho}). \quad (3)$$

The unknown functions  $A_i(\xi)$  are defined from boundary conditions. Every set of functions  $\psi_i(\vec{\rho} \in \Gamma)$  is dense in  $L_2$  because of the solvability in  $L_2$  of the integral equation of the 1-st kind such as

$$\int A_i(\xi) \exp(-i\xi y - i(k_1^2 - \xi^2)^{1/2} z) d\xi = f(\vec{\rho}), \vec{\rho} \in \Gamma \quad (4)$$

with the bounded continuous kernel and the continuous right side. That is why it is possible to satisfy any boundary conditions with help of functions such as (2). It is easy to prove that this functions satisfy the Maxwell's equations inside  $D$ .

The regular solution inside  $D$  in the class  $L_2$  is founded by Fourier representation:

$$R(\vec{\rho}) = E_0(\vec{\rho}) + \lambda \int H_0^{(2)}(k_1 |\vec{\rho} - \vec{\rho}'|) E_0(\vec{\rho}') d\vec{\rho}'. \quad (5)$$

It is necessary to remark that if the boundary has only non-singular points then regular solution may be omitted. In the opposite case the regular solution will give so call "edge wave".

Outside the scatterer the electric field is defined by

$$E_{\text{ext}}(\vec{\rho}) = E_0(\vec{\rho}) + \lambda \int H_0^{(2)}(k_0 |\vec{\rho} - \vec{\rho}'|) E_{\text{int}}(\vec{\rho}') d\vec{\rho}'. \quad (6)$$

where  $E_{\text{int}}(\vec{\rho})$  is obtained from (3). Unknown functions  $A_i(\xi)$  are defined from the boundary condition

$$E_{\text{ext}}(\vec{\rho}) = E_{\text{int}}(\vec{\rho}), \vec{\rho} \in \Gamma \quad (7)$$

One of the important applications of the above described method is the scattering of an arbitrary wave by a semispace  $z \geq z(y)$  with a smooth boundary. In this case the electric field inside  $D$  may be represented as

$$E_{\text{int}}(\vec{\rho}) = \psi_1(\vec{\rho})$$

and its substitution into the boundary condition leads to the integral equation for  $A_1(\xi)$ :

$$\int K(y, \xi) A_1(\xi) d\xi = E_0(y, z(y)), \quad (8)$$

where

$$K(y, \xi) = (1 - \lambda Q(y, \xi)) \exp(-i\xi y - i(k_1^2 - \xi^2)^{1/2} z(y))$$

and

$$Q(y, \xi) = \int d\tau_1 \int_{z(y+\tau_1)-z(y)} H_1^{(2)}(k_0 \tau) \exp(-i\xi \tau_1 - i(k_1^2 - \xi^2)^{1/2} \tau_2) d\tau_2,$$

$$\tau = (\tau_1^2 + \tau_2^2)^{1/2}.$$

For the plane boundary ( $z \geq 0$ ) the equation (8) may be solved analytically in the class  $L_2$ . Electric field inside D is defined by

$$E_{int}(\vec{\rho}) = \sqrt{2/\pi} \int \frac{(k_0^2 - \xi^2)^{1/2} f(\xi)}{(k_0^2 - \xi^2)^{1/2} + (k_1^2 - \xi^2)^{1/2}} \exp(-i\xi y - i(k_1^2 - \xi^2)^{1/2} z) d\xi$$

where  $f(\xi) = F(E_0(y, 0))$  is the Fourier transform of  $E_0(y, 0)$ .

It is important to remark that the error problem of the approximate solution of the Fredholm equation of the 1-st kind is reduced because of the functions  $A_1(\xi)$  are integrated further on in the final expressions.

#### REFERENCES

- (1) N.A. Khizhnyak: "Green's function of the Maxwell equations for inhomogeneous media", Journal of Technical Physics, (1958), 28, 7, pp. 1592-1609.
- (2) L.S. Rakovshtchik: "To the theory of certain convolution equations", Uspekhy Matematicheskikh Nauk (in Russian), (1963), 18, 4, pp. 171-177.

A HYBRID APPROACH: THE INTEGRAL EQUATIONS METHOD  
AND THE PHYSICAL THEORY OF DIFFRACTION

Evgeniy Vasil'ev and Vyacheslav Solodukhov

Moscow Power Engineering Institute  
Krasnokazarmennaja 14, 111250, Moscow, Russia

Abstract

The physical theory of diffraction (PTD) is based on the analytical solution of some canonical problems, the number of which is very limited. The integral equation (IE) method has been used for solving a very large class of new canonical problems, such as dielectric, multilayered, partially coated and other objects, including the structures with surface waves. It permits us to considerably extend the field of application of PTD. The technique is developed and applied to a variety of two- and three- dimensional objects in order to illustrate the PTD + IE approach and its validity.

I. Introduction.

This report is devoted to the development and application of a hybrid approach where the possibilities of both numerical and asymptotic methods are combined to solve a wide range of new problems of electromagnetic wave diffraction. As it is well known, the numerical methods are in most common use in the resonance frequency domain where the characteristic dimensions of a scatterer is of the order of a wavelength. In principle, the methods applied to arbitrary shape bodies can be developed. Indeed, it is not difficult to reduce a boundary value problem, for example, to the integral equation (IE). This equation can be solved numerically by means of reducing it to the system of linear algebraic equations (SLAE).

While considering the radar cross-sections, the high frequency domain is more interesting. The application of numerical methods developed for the resonance domain is not effective here because the computational difficulties (computer time and memory) increase as the sixth power of the frequency. The special high-frequency asymptotic techniques have to be used when the scatterer is large compared to the wavelength. The physical theory of diffraction (PTD) [1,2] and the geometrical theory of diffraction (GTD) [3] are widely used. Both of these theories are not closed. They need some additional information from the solution of canonical problems, describing the most important properties of the diffraction processes in the vicinity of surface irregularities. Practically, PTD and GTD are based on the solution of the same canonical problem of diffraction by a perfectly conducting straight wedge. But they employ different information out of the canonical problem solution, and have different forms and different potentialities. GTD use only the ray asymptotic ("diffraction coefficients") and has some wellknown restrictions in its application. However, in PTD, the distribution of surface currents (first of all, "nonuniform" components) on the wedge surface is taken from the solution of the canonical problem. Since the current is a source of the scattered field, PTD allows one to calculate the fields everywhere.

Unfortunately, the number of canonical problems which can be solved analytically is very limited. The only way to considerably extend the catalogue of canonical problems is the application of numerical methods.

A numerical approach based on the IE method is used for solving a very large class of new canonical problems [4]. As we know, it was the first publication [5], where the numerical approach was combined

with the asymptotical theories. Rather a complete review of more recent works one can find in [6].

## II. Irregularities of an edge type in the absence of guided wave structures.

As an example of such irregularities we shall consider a semi-infinite dielectric slab with losses. It can be treated as a cylinder of arbitrary cross-section whose generator is parallel to the  $z$ -axis of some coordinate system (Fig. 1a). All the fields and currents is represented as the Fourier integrals along this axis. Using the orthogonalities of the Fourier harmonics it is not difficult to show that the

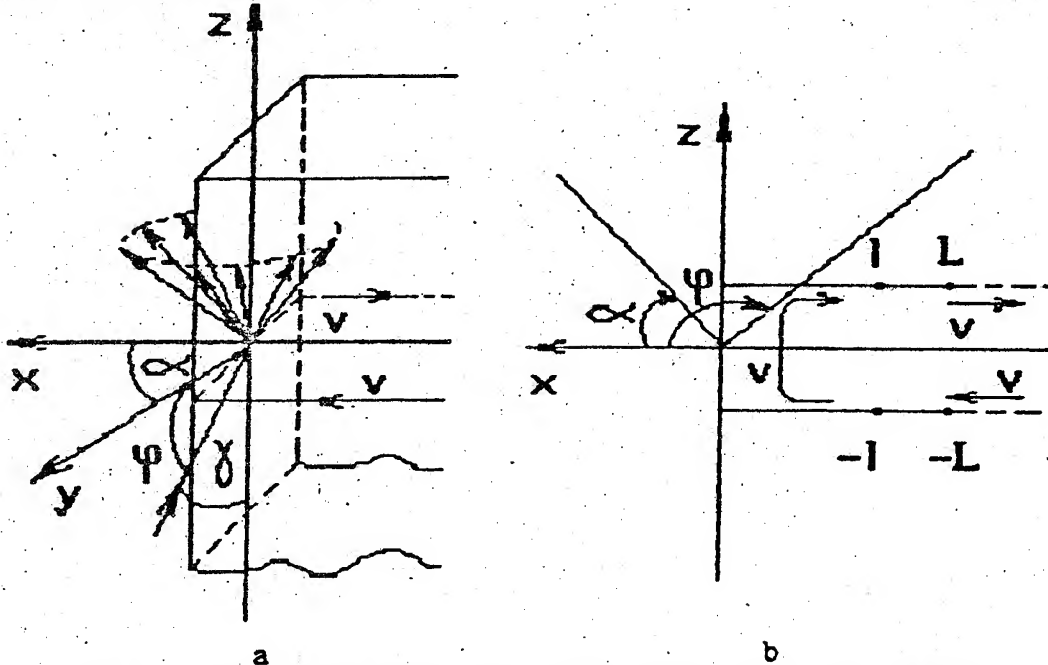


Fig.1. Diffraction by a semi-infinite dielectric slab.

$z$ -dependence of all these fields and currents will be identical to that of the incident plane wave. The problem of electromagnetic wave diffraction by such a cylinder can be reduced to the system of four Fredholm IEs of the second kind relative to a Fourier transform of the equivalent electric and magnetic current densities. In matrix notation the system has the form [10,11]

$$I(v) + 0.5 \int_v P(v, v') I(v') dv' = I^i(v), \quad (1)$$

where the column vectors of the desired  $I(v)$  and primary (incident)  $I^i(v)$  current densities have four components each:

$$I(v) = \{J_v, J_z, M_v, M_z\}; \quad I^i(v) = \{J_v^i, J_z^i, M_v^i, M_z^i\};$$

$\bar{J} = [\bar{n}, \bar{H}]$ ,  $\bar{M} = [\bar{E}, \bar{n}]$ ,  $\bar{n}$  is a unit vector for the external normal. The matrix kernel  $P(v, v')$  consists of sixteen elements  $P_{mn}(v, v')$ , which depend on the positions  $v$  and  $v'$  of the field and source points, and are expressed in terms of Hankel function [10]. The integration in (1) is carried out over the contour of the body cross section (the coordinate  $v$ , Fig. 1b).

All the canonical bodies have infinite cross-section contour lengths, and the direct application of numerical methods is impossible. We have overcome this difficulty in the following

manner. Unknown surface currents can be represented as a sum of "uniform" and "nonuniform" components [3,8,9]

$$I(v) = I^u(v) + I^{nu}(v). \quad (2)$$

The former may be calculated according to the laws of geometric optics and may, in this sense, be assumed as known

$$I^u(v) = I_{go}^u(v). \quad (3)$$

Obviously, unknown additional currents - the "nonuniform" components  $I^{nu}(v)$ , - which are associated with the presence of the edge, decrease rapidly with distance and become negligibly small in comparison with  $I^u(v)$  far from the edge of the slab (as a rule, it is enough to have a distance of about  $l = (2+3)$  wavelengths).

Substituting (2), (3) into (1) and neglecting  $I^{nu}(v)$  for  $|v| \geq l$ , we obtain the following system of IEs

$$I(v) + 0.5 \int_{-l}^l P(v, v') I(v') dv' = I^u(v) - 0.5 \Delta I(v), \quad (4)$$

where

$$\Delta I(v) = \int_{-l}^l P(v, v') I_{go}^u(v') dv' + \int_l^\infty P(v, v') I_{go}^u(v') dv'. \quad (5)$$

This system of IEs can be solved numerically.

The additional term (5) are integrals of the products of the IE kernels and the uniform currents, which are fields of a plane wave. All integrals in (4) can be expressed in terms of the functions

$$N_\nu(\lambda, x, \xi_0, \eta_0) = \int_0^\infty e^{-i\lambda\xi} \rho^{-\nu} H_\nu^{(2)}(x\rho) d\xi, \quad (6)$$

where  $\rho = [(\xi + \xi_0)^2 + \eta_0^2]^{1/2}$ ,  $\lambda, \xi_0, \eta_0$  are real numbers and  $x$  is a coefficient of refraction,  $\nu = 0, 1$ . The method which was used to calculate these integral is given in [9].

Any standard procedure can be used to solve the IE (4). Necessary details of our solution one can find in [9,13]. It is worth to note, that the symmetry of the slab permits the equivalent matrix order to be reduced by a half. In addition, this matrix has a large Toeplitz block (it is clear from the geometry of the slab). The use of these two facts leads to the essential economy in computer memory and time.

Solution of the system of IE gives the total surface currents. In order to calculate the patterns for scattering of electromagnetic waves we represent the scattered fields as a sum of two components, the first of which is caused by the currents on the finite segment  $|v| \leq l$ , while the second is caused by the currents on the semi-infinite intervals  $(-\infty, -l)$  and  $(l, \infty)$ . The integrals in the first component are performed numerically. The method of stationary phase is used for the second component. Both of them take part in the formation of the cylindrical wave. The stationary point contribution corresponds to the plane waves reflected (transmitted) by the semi-infinite plane parts of the body. By the way, if the incident plane wave has a unit amplitude, the scattered field represents a diffraction coefficient which can be used at once in generalized GTD.

As an example, let us consider a plane wave diffraction by a semi-infinite lossy dielectric slab. The distribution of the modulus of the magnetic surface currents are shown in Fig.2 (the behavior of the electric currents is analogous). The wave number is perpendicular to the edge ( $\gamma = 90^\circ$ ), so TE- and TM-polarizations are

independent. Because of the losses, the current amplitudes are very different on the illuminated ( $v > 0$ ) and shadow ( $v < 0$ ) sides of the slab, and the surface waves arisen on the edge decrease rapidly.

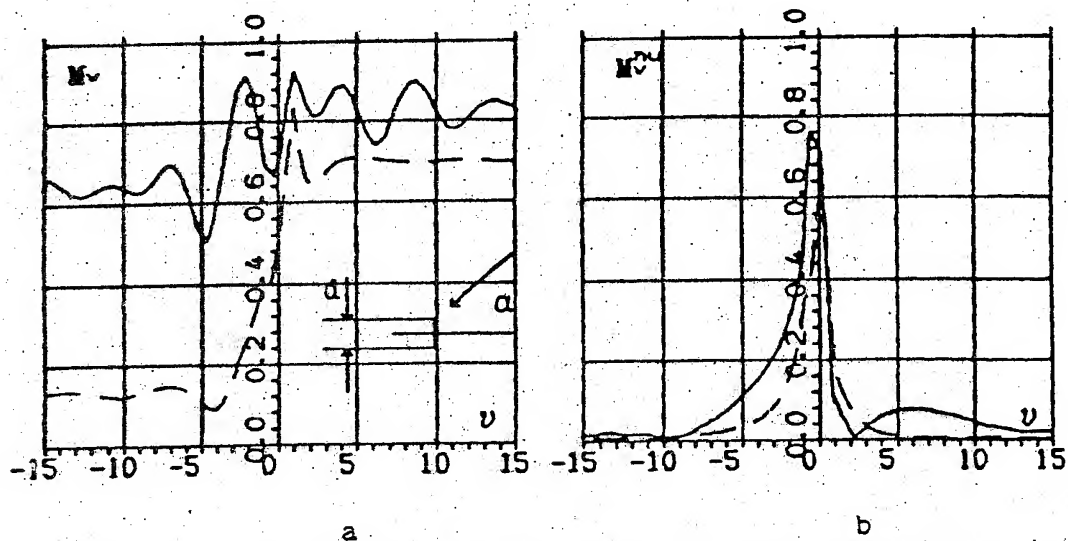


Fig.2. Distribution of the total (a) and nonuniform (b) magnetic currents on the surface of a dielectric slab. TM - polarization;  $k d = 2$ ,  $\alpha = 90^\circ$ ;  $x = 1.7 - 10.2$ ;  $x = 1.7 - 11.0$ .

The numerical solution of the canonical problems may be used at once to construct PTD - solutions for more complex objects. Practically, the far fields produced by nonuniform currents of the corresponding canonical problem have to be added to the ordinary physical optics approach. The far fields can be calculated numerically by integrating over the region occupied by the nonuniform currents.

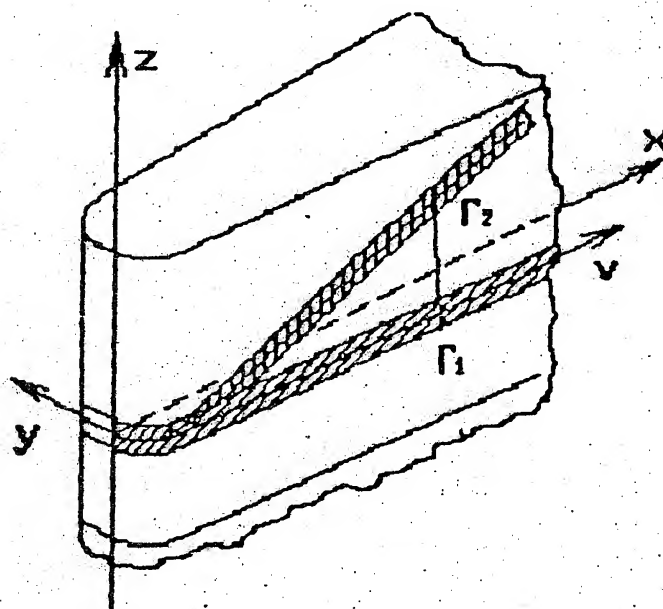


Fig.3. Element of a tangential straight rounded wedge.

This procedure meets additional difficulties if we have to deal with a curved edge. The conception of elementary edge waves (EEWs) can be successfully used in such a situation. This conception was developed in recent publication [2] as a basis of a more general and rigorous form of the PTE. Unfortunately, this theory deals only with perfectly conducting bodies. Nevertheless, our hybrid approach allows us to considerably extend the field of application of this theory.

At any point of a curved wedge with a general configuration (for example, a wedge with a rounded edge, Fig.3) we introduce the straight tangential wedge and separate out an infinitely narrow strip. This strip is directed along the line of intersection of the wedge with a plane, whose slope is determined by a ray cone (contour  $\Gamma_1$  in Fig.3). A numerical solution of the appropriate canonical problem provides the total and nonuniform surface currents in the plane  $z = 0$  (contour  $\Gamma_2$ ). In order to find the desired currents on the strip  $\Gamma_1$  it is enough to multiply the solution by a phase factor which is proportional to  $\cot \gamma$ . An example of the practical use of this approach will be considered in Sec.V.

### III. Irregularities of an edge type in the presence of guided wave structures.

Here we consider again a semi-infinite slab but now it is assumed that dielectric is lossless [13].

The existence of the surface waves which are excited on the edge of the slab and are travelling along it is the principal difference of this problem from the one considered above. The equivalent surface currents connected with these waves do not decrease at all, or decrease very slightly, with distance from the edge. Additionally, the direction of any surface wave propagation (or their phase velocities in the  $x$ -direction) and their amplitudes have to be determined. The former can be determined without solving the IE. In fact, the phase velocity of all these waves in  $z$ -direction should be the same and depends upon the angle  $\gamma$  of the plane wave incidence (Fig.1a). Their phase velocities  $v_{sn}$  in the direction of propagation are different and wellknown (they are determined by the thickness of the slab and the dielectric slab parameters). Because of this, far from the edge the equivalent currents of the  $n$ -th surface wave can be written in the form

$$I_n^{sv}(x, z) = A_n B_n \exp(i k_x x + i k_z z), \quad (7)$$

$$\text{where } k_z = k_0 \cot \gamma, \quad k_x = k_0 \left[ (c/v_{sn})^2 - \cos^2 \gamma \right]^{1/2},$$

$A_n$  is the unknown amplitudes,  $B_n$  is a vector with four components (it determines the correlation between the current components of the  $n$ -th surface wave, its structure is similar to  $I$  in (1),  $c$  is the velocity of light,  $k_0$  is the wave number of the free space.

Let us include the surface currents (7) into the uniform components of the currents (2). Now we have

$$I^u(v) = I_{go}^u(v) + \sum_{m=1}^M A_m I_m^{sv}(v), \quad (8)$$

where  $I_{go}^u$  is the uniform component defined by the geometrical optics fields,  $M$  is the number of the surface waves (modes) which can exist in the slab. Again, we use the IE (4) with additional terms (5), completed by



$$\Delta I^{sv}(v) = \sum_{m=1}^{\infty} A_m \left[ \int_{-\infty}^{-l} P(v, v') I_m^{sv}(v') dv' + \int_l^{\infty} P(v, v') I_m^{sv}(v') dv' \right]. \quad (9)$$

In order to calculate the unknown coefficients  $A_m$  the additional intervals  $(-L, -l)$  and  $(l, L)$  in Fig.1b are included into the contour of integration in (4), and in (9) the "l" has to be changed by "L". On these intervals the nonuniform components of the currents are negligibly small and the distribution of total currents has a form of "standing" wave, which is the result of interference of the plane wave  $I_{go}^{sv}$  and the surface waves. We use the iteration procedure to determine  $A_m$ . In the initial step, we suppose all the coefficients  $A_m^{(0)} = 0$ . After solving the SLAE, we apply a least-mean-square method on the intervals  $(-L, -l)$  and  $(l, L)$  to determine the first approach of  $A_m^{(1)}$ , and so on. As a rule, the necessary accuracy can be achieved after 3-5 iterations.

Some numerical results concerning to scattering of a plane wave by a semi-infinite dielectric slab ( $\gamma = 90^\circ$ ) are shown in Fig.4. The total and nonuniform magnetic currents ( $M_z$  for TE-waves and  $M_y$  for TM-waves) are plotted there.

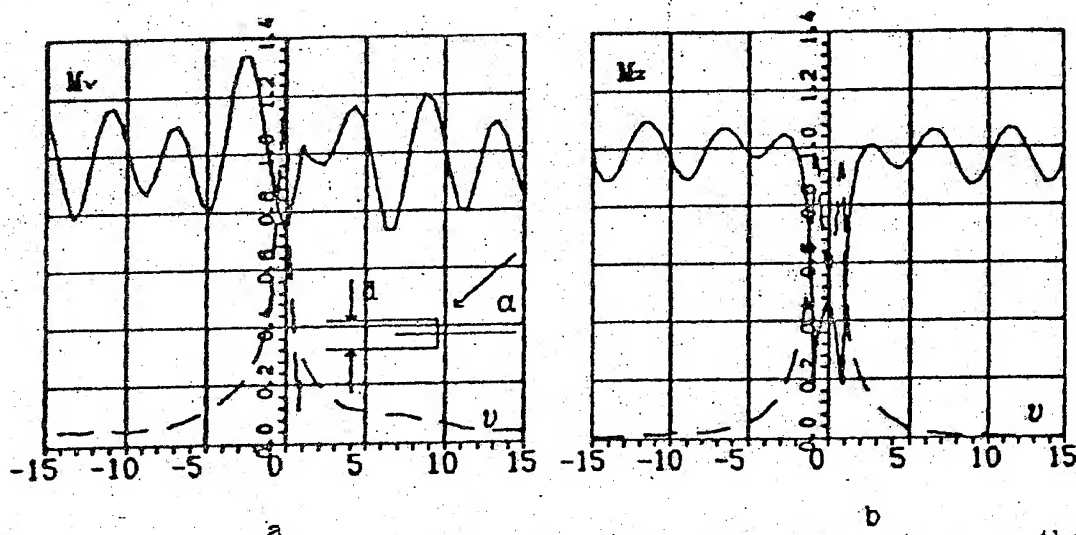


Fig.4. Distribution of the magnetic currents on the surface of a dielectric slab. Plane wave incidence ( $\alpha = 90^\circ$ ).  $\epsilon = 1.7$ ,  $kd = 2$ ; TM - (a) and TE - (b) polarization; — total current; --- nonuniform current.

One can see, that the nonuniform components are decreasing with the distance from the edge and at the distances amounting to  $(2+2.5)$  wavelengths they become negligibly small (it confirms our initial assumptions which our approach based on). The surface waves are formed in the vicinity of the edge. Besides, the edge space waves corresponding to Keller's rays, can be seen in this region, but their amplitudes are small in comparison with surface wave ones.

Let us consider one more aspect of the problem. As a matter of fact, in any real case the dielectric slab (or any other obstacle) is not infinite, and the surface wave excited on one edge will reach another edge. The part of its energy will be radiated (the ray cone will arise) and another part will be reflected and transformed into another types of surface waves. In order to investigate these



phenomena, it is necessary to solve one more canonical problem - the surface wave incidence on the edge of a semi-infinite dielectric slab. The method of IEs can be used again [14]. The results of the solution is illustrated by Fig.5.

The practical use of the canonical problem solutions involves some difficulties if the object under consideration supports surface waves. They are connected with curved edges (there are no serious additional problems if the edges are straight: such an example will be considered in Sec.IV).

As a consequence, we have restricted ourselves to application of GTD to achieve the result. Again, the numerical solutions of the canonical problems are used. In order to apply the GTD in such a generalized form, it is necessary to describe the following physical processes:

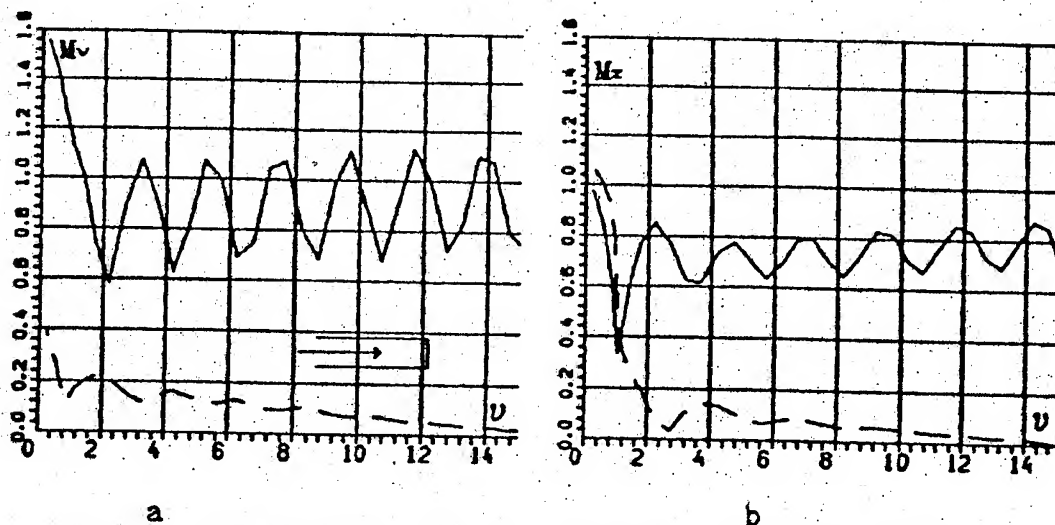


Fig.5. Distribution of the magnetic currents on the surface of a dielectric slab. Surface wave incidence.  $\epsilon = 1.7$ ,  $k d = 2$ ; TM - (a) and TE - (b) polarization; ——— total current; - - - - nonuniform current.

the incidence of the rays of TE - and TM - waves ( $E_{TE}^i$  and  $E_{TM}^i$ ) and arising the ray cones in the free space ( $E_{TE}^s$  and  $E_{TM}^s$ ) and some surface waves in the dielectric slab ( $E_{sv1}^s, E_{sv2}^s, \dots, E_{svM}^s$ );

the incidence of the surface wave ray of  $\kappa$  - type ( $E_{sv\kappa}^i$ ) and arising of two ray cones in the free space and the reflected and transformed surface waves in the slab.

The connection between these amplitudes can be written with the help of the generalized matrix diffraction coefficient in the form

$$\begin{aligned} E_{TE}^s &= D_{11} E_{TE}^i + D_{12} E_{TM}^i + D_{13} E_{sv1}^i + \dots + D_{1,M+2} E_{svM}^i \\ E_{TM}^s &= D_{21} E_{TE}^i + D_{22} E_{TM}^i + D_{23} E_{sv1}^i + \dots + D_{2,M+2} E_{svM}^i \\ &\dots \end{aligned} \quad (10)$$

$$E_{svM}^s = D_{M+2,1} E_{TE}^i + D_{M+2,2} E_{TM}^i + \dots + D_{M+2,M+2} E_{svM}^i$$

where  $M$  - is the number of surface waves which can exist in the slab. As an example of this approach, the diffraction of a plane wave by a dielectric disk will be considered in Sec.V.

#### IV. Some numerical results.

The IE method and the technique described above have been applied to solve some new diffraction problems, such as diffraction by the homogeneous dielectric wedge [9] and the perfectly conducting wedge with a multilayered coating [15], by the same wedge with a partial coating near its edge and along one side of the wedge [16], by the mentioned above dielectric slab [13,14] and the different combinations of dielectric absorbing layers with perfectly conducting planes [17,18]. They all can be used as canonical problems for PTD and GTD.

The behavior of nonuniform current and their contribution to scattering patterns is of prime interest for applications. Detailed investigation of these phenomena one can find in [9,15].

Now let us consider the plane wave scattering by a dielectric slab of finite width as a simple example which can illustrate the application of the numerical solution of canonical problems. In order to construct a PTD solution of the problem it is necessary to take into account that the scattered fields are determined by the following factors:

1. the surface currents which correspond to the plane wave incidence on a infinite dielectric slab (the ordinary physical optics approach). This field can be calculated in usual manner ( $\gamma = \pi/2$ ,  $E_z = E_0$ ) and shown dashed in Fig.6a,b;

2. the surface currents which correspond to the surface wave excited by the edges of our slab (their amplitudes are determined from the problem considered in Sec.III). In our example these amplitudes are:  $1.78e^{i1.33}$  for  $\alpha = 90^\circ$ , and  $0.306e^{i1.41}$ ,  $0.112e^{i1.18}$  for  $\alpha = 60^\circ$  (for the left and right edges, respectively);

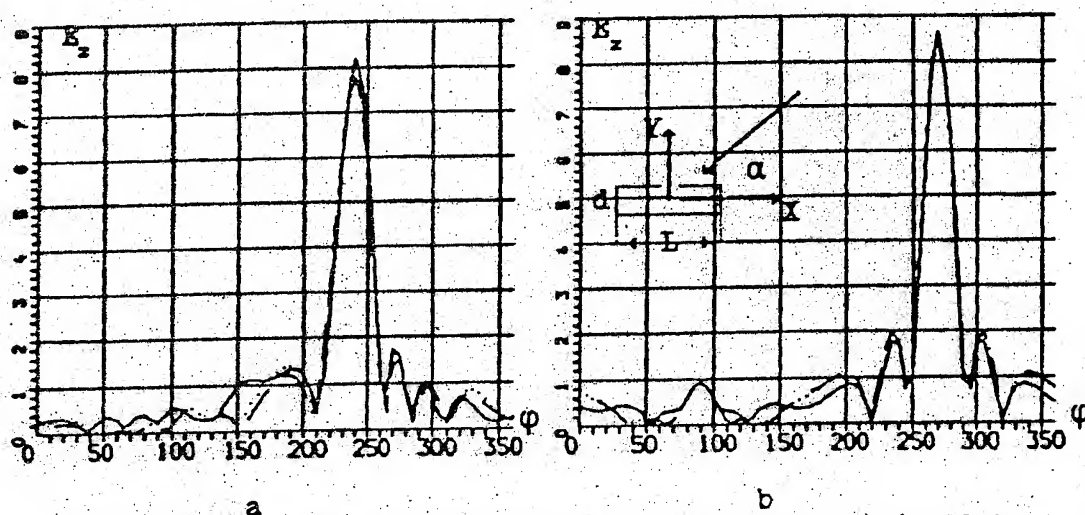


Fig.6. Scattering patterns for a finite dielectric slab.  
TM - polarization;  $kL = 16.4$ ,  $k d = 2$ ;  
 $\alpha = 60^\circ$  - (a),  $\alpha = 90^\circ$  - (b).

3. the surface currents which correspond to the surface waves of the second order: the surface wave excited by the left edge, travelled along the slab and diffracted by the right edge, and vice versa. The coefficient of reflection is determined from the problem considered in Sec.III. It does not depend upon the angle of the plane wave incidence and is equal to  $0.231e^{i0.05}$  in our case. The scattering patterns caused by these three factors are shown short

dashed in Fig.6;

4. the contribution of the third and more high order diffraction of the surface waves and the secondary diffraction of the space cylindrical waves is too small and we neglect it;

5. the contribution of the nonuniform currents can be calculated as it was described in Sec.II. After adding it, we obtain the PTD solution which practically coincides with the exact solution plotted in Fig.6 with the solid line. (The exact numerical solution was obtained by the direct application of IE (1) to the slab).

The technique developed here may be successfully used to construct PTD solutions of three-dimensional problems. We illustrate it by considering a plane wave incidence on a lossy dielectric disk (Fig.7a).

Let the incident wave is, for example, TM polarized. The main contribution in the scattered field will give the ordinary physical optics approximation (the field of surface currents corresponding to the incident, reflected and transmitted waves). The result is shown dashed in Fig.7b.

Then we need to calculate the fields of the nonuniform currents. For this purpose, we have to do the following steps:

1. representation of the incident wave as a sum of TE- and TM-waves at any point of the disk's edge;

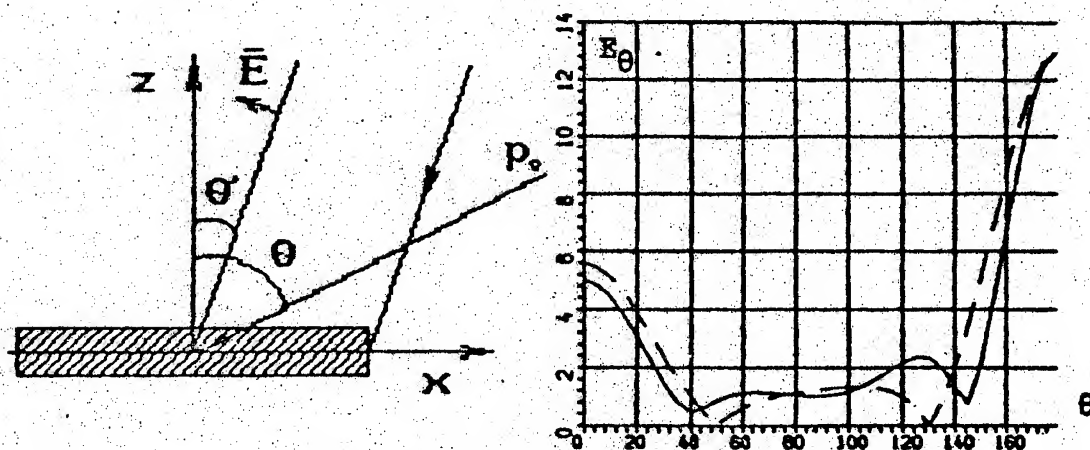


Fig.7. Diffraction by a dielectric disk.  
Coordinate system and geometry (a).  
Scattering pattern for a lossy disk (b);  
 $k_0 a = 5$ ,  $k_0 d = 2$ ,  $\alpha = 2.0 - i1.0$ .

2. solving the canonical problems for both polarizations and calculation of the elementary edge currents as it was described above;

3. calculation of EEW by integrating along the narrow strips;

4. calculation of the fields, provided by all the elementary edge currents with the help of integrating of them over the disk's edge.

The result (the total scattering pattern) is shown in Fig.7b. One can see that the contribution of the nonuniform currents is not too essential in this case. There is no depolarization in the plane of observation for our simplest example ( $\varphi = 90^\circ$ ).

Let us now consider the plane wave diffraction by a lossless dielectric disk. The most attention will be concentrated on the scattering by the disk edge. In addition there are two more beams of rays, corresponding to the reflected and transmitted fields. But

these beams are the delta-functions of the angle coordinates in the far zone and will not be taken into account. Suppose that the disk thickness is as small as only two surface waves exist.

As it was mentioned above, the application of PTD meets some additional difficulties, connected with surface waves, which we have not yet overcome. The next example will demonstrate the application of our hybrid approach to extend the possibilities of the classical GTD by the use of the numerical solution of new canonical problems. By analogy with classical GTD, the diffraction coefficients are determined from the solution of the canonical problem about the semi-infinite dielectric slab, which edge is tangential to the disk in the incident ray point  $P$  (Fig.8).

The mechanism of scattering is the following. The incident wave ray falls on the edge (point  $P$ ) and it generates the ray cone in the free space and two surface waves - in the dielectric. The cone angle is determined by the incident angle, and the direction of the surface waves - by the formula (7) (the trajectory of the only one wave is shown in Fig.8a). The ray of surface wave falling on the edge in the point  $Q$  initiates the ray cone in the free space. Its angle is determined by the same formula (7). In addition, the reflected and, may be, the surface waves of the other types are generated. These waves fall on the edge again and the process will be repeated.

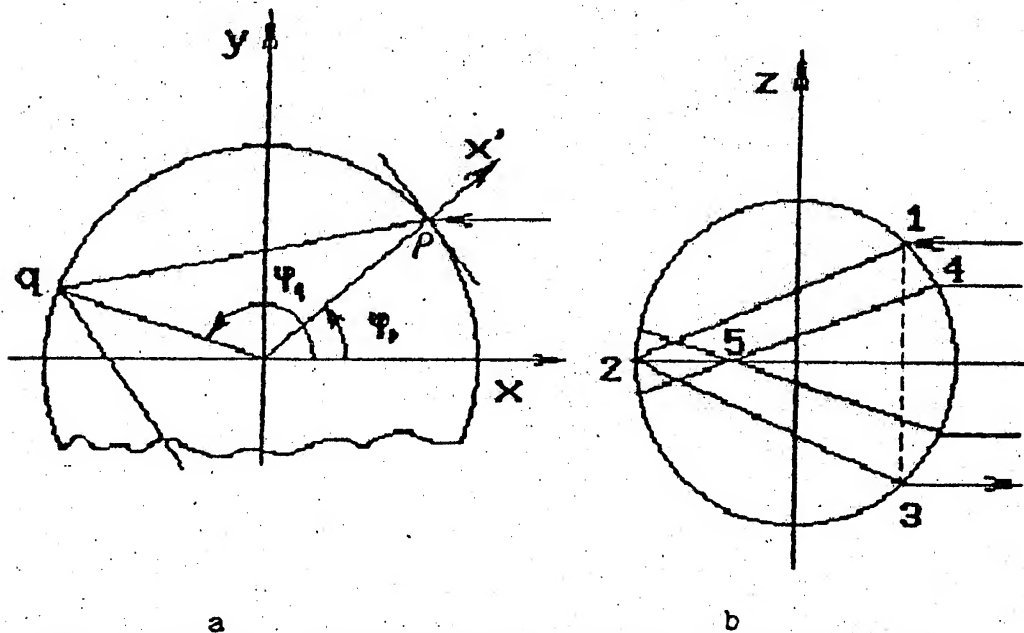


Fig.8. The ray pictures for a lossless dielectric disk.

Now let us consider this problem in detail. Suppose that the plane TM wave incidents on the disk at an angle of  $\theta^i$  and the observation points are located in the plane  $xOz$ . In this plane the scattered field is mainly formed by two rays, fallen on the points  $\varphi_p = 0, \pi$ . Firstly, these rays generate two radial beams (the ray cones are degenerated into disks) with the amplitudes determined by the element  $D_{22}$  of the diffraction coefficients (12). Secondly, the incident rays generate two surface waves coming from the opposite points. Their amplitudes are determined by the element  $D_{32}$  of the same matrix. As in the corresponding canonical problem the wave vector of the incident plane wave is perpendicular to the edge of

the semi-infinite slab the only surface wave is excited. As the disk edge is curved, it is necessary to take into account the variation of the ray tube cross-section while the surface wave propagation. Also it is necessary to evaluate the possibility of multiray generation.

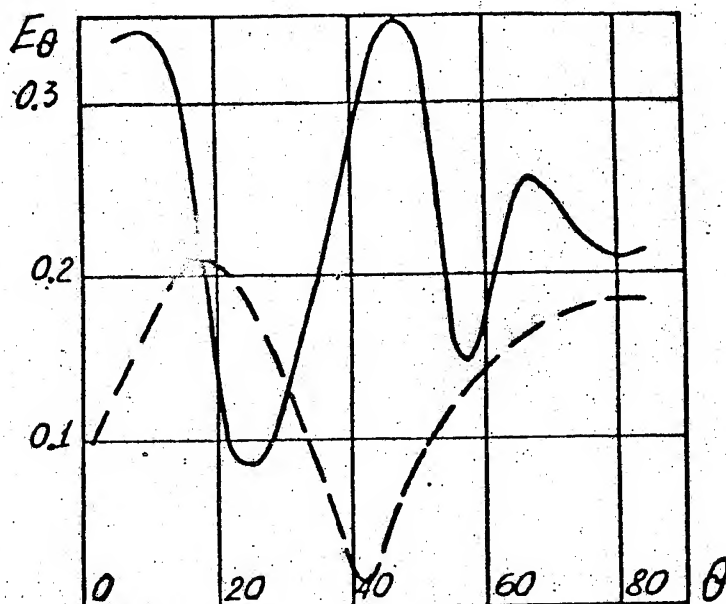


Fig.9. Scattering patterns for a lossless dielectric disk. Angle of incidence  $30^\circ$ ;  $\epsilon = 1.7$ ,  $k d = 2$ ;  
 $k_0 a = 6.28$ ; - - - -  $k_0 a = 9.42$ .

The analysis of the process shows that if  $t = \sin^2(\theta/c/v_{sn})^{-1} < 0.5$ , only the rays appeared in points 2 and 4 (Fig.8b) exist. If  $t > 0.5$ , at least 4 rays: 1-2-3, 3-2-1 and two similar rays of the second surface wave are added. But the main contribution to the scattering field belongs to the rays scattered in the points 2 and 4 (Fig.8b) because of the significant losses in the processes of transformation and reflection for the peripheral rays. For example, the scattering pattern was calculated as a function of the angle of observation (Fig.9). Considerable change in the level of field is explained by the existence of the two scattering centers, and the field of both ones weakly depend on the angle.

#### V. Conclusion.

The short conclusions on this paper may be formulated in the following way.

1. A numerical approach based on the method of IEs is developed and used to solve a very large class of diffraction problems for semi-infinite structures rather an arbitrary nature (dielectric, multilayered, partially coated and so on).
2. These solutions are used as new canonical problems for the PTD.
3. A hybrid technique combining the method of IE and PTD has considerably extended the field of application of the PTD (in particular, dielectric objects and some structures with surface waves can be investigated now).
4. The basis of the hybrid approach is the solution of canonical problems. In addition to the two-dimensional problems, some three-dimensional ones are solved now [19,4].
5. Some simple examples of the PTD + IE technique application are given in this report to illustrate its possibilities and accuracy.



6. The nearest problem which has to be solved is the extension of the EEWs conception to the complex bodies with curved edges and surface waves. This problem is under consideration now.

#### Reference

- (1) P.Ufimtsev: "Method of edge waves in the physical theory of diffraction," Moscow: Sov.radio (1962).
- (2) P.Ufimtsev: "Elementary edge waves and the physical theory of diffraction," *Electromagnetics* (1991), 11, n°2, pp. 125-160.
- (3) J.Keller: "Geometrical theory of diffraction," *J.Opt. Soc. Amer.* (1962), 52, n°2, pp 116-130.
- (4) E.Vasil'ev, V.Solodukhov, A.Fedorenko: "The integral equation method in the problem of electromagnetic wave diffraction by complex bodies," *Electromagnetics* (1991), 11, n°2, pp. 161-182.
- (5) E.Vasil'ev, V.Solodukhov: "On diffraction coefficients for dielectric wedge," *Trudy 6 Vses. Symp. difr. i raspr. voln* (1973), 1, pp.238-242, Moscow-Erevan.
- (6) L.Medgyesi-Mitschang, D.Wang: "Hybrid methods for analysis of complex scatterers," *Proc. IEEE* (1989), 77, n°5, pp.770-779.
- (7) E.Vasil'ev: "Excitation of bodies of revolution," Moscow: Radio i Svyaz (1987), 272p.
- (8) E.Vasil'ev, V.Solodukhov: "Numerical solution of the problem of electromagnetic waves diffraction by a dielectric wedge," *Symp. on Electromagnetic Wave Theory, URSI* (1971), pp. 512-517, Tbilisi.
- (9) E.Vasil'ev, V.Solodukhov: "Diffraction of electromagnetic wave by a dielectric wedge," *Izv. VUZ, Radiofizika* (1974), 17, n°10, pp.1518-1528. (Translation into English: *Radiophysics and Quantum Electronics* (1976), 17, n°10, pp.1161-1169).
- (10) V.Solodukhov, E.Vasil'ev: "Diffraction of a plane electromagnetic wave by a dielectric cylinder of arbitrary cross section," *Zh. Tekh. Fiz.* (1970), 40, n°1, pp. 47-53. (Translation into English: *Sov. Phys.-Tech. Phys.* (1970), 15, n°1).
- (11) E.Vasil'ev, V.Solodukhov: "Oblique incidence of electromagnetic wave on a dielectric cylinder with arbitrary cross section shape," *Vichisl. Metody i Progr.* (1973), 20, pp. 144-157, Moscow: Izd.MGU.
- (12) J.Bach Andersen, V.Solodukhov: "Field behavior near a dielectric wedge," *IEEE Trans. Antennas and Prop.* (1978), 26, n°4, pp. 598-602.
- (13) E.Vasil'ev, A.Polynkin, V.Solodukhov: "Diffraction of electromagnetic wave by the end of a planar semi-infinite dielectric waveguide," *Izv. VUZ, Radiofizika* (1981), 24, n°8, pp. 1022-1027.
- (14) E.Vasil'ev, A.Polynkin, V.Solodukhov: "Diffraction of a surface wave by the end of a planar semi-infinite dielectric waveguide," *Radiotek. i Elektr.* (1980), 25, n°9, pp. 1862-1872.
- (15) E.Vasil'ev, V.Solodukhov: "Diffraction of electromagnetic wave by a wedge with a multi-layer absorbing covering," *Izv. VUZ, Radiofizika* (1977), 20, n°2, pp. 280-289.
- (16) E.Vasil'ev, A.Fedorenko: "Diffraction by the perfectly conducting wedge with a dielectric coating on one side of the wedge," *Izv. VUZ, Radiofizika* (1983), 26, n°3, pp. 351-356.
- (17) E.Vasil'ev, A.Fedorenko: "Scattering of electromagnetic wave by the end of a semi-infinite dielectric slab buried into perfectly conducting semi-space," *Izv. VUZ, Radiofizika* (1983), 26, n°7, pp. 860-866.
- (18) E.Vasil'ev, A.Fedorenko: "Scattering of electromagnetic wave on a slot in dielectric layer on a perfectly conducting plane," *Izv. VUZ, Radioelektronika* (1982), 25, n°2, pp. 66-70.
- (19) E.Vasil'ev, V.Nasochevsky: "Diffraction of a plane electromagnetic wave by a semi-infinite cylinder of arbitrary cross section shape," *DAN SSSR* (1989), 305, n°1, pp. 68-70.

# APPLICATION OF A SUCCESSIVE APPROXIMATIONS SCHEME TO SCATTERING FROM A PERFECTLY CONDUCTING SURFACE, ROUGH IN ONE DIMENSION

Christos N. Vazouras, Panayotis G. Cottis and John D. Kanellopoulos

Department of Electrical and Computer Engineering  
National Technical University of Athens, 9 Iroon Polytechniou Str., Zografou 15773, Athens, Greece  
Tel.: (+3) 01 3691355, Fax: (+1) 01 3647704, e-mail: chvazour@alexander.ntua.gr

## ABSTRACT

A successive approximations approach in the wavenumber space is proposed to treat scattering from conducting rough surfaces, based on the extinction theorem formulation. It is shown that this approach can lead to the derivation of the general term of the perturbation series, and it correctly reduces to the Kirchhoff and first-order perturbation approximations in the appropriate limit. Preliminary numerical results are presented for the simple case of a sinusoid.

## INTRODUCTION

Integral equation formulations are very commonly used to treat scattering by rough surfaces. A classical formulation of the problem is based on the well-known pair of the electric and magnetic field integral equations [1]. In the case of a perfectly conducting surface, the two equations decouple and either of them can (in principle) be alternatively used.

On the other hand, iterative methods have been quite widely used to treat problems formulated by means of integral equations [2]. In the case of the above mentioned electric and/or magnetic field integral equations, since they have the form of the second kind, the so-called method of successive approximations has been applied [3-5]. However, in analytic studies, higher order terms appear too complicated to be practically useful [3]. Furthermore, it is difficult to relate higher order iterations to certain surface characteristics [4].

An alternative formulation of the rough surface scattering problem is based on the extended boundary condition (EBC) [6], or, equivalently, the so-called extinction theorem. When combined with an underlying generalized function interpretation, this method leads to a somewhat simpler integral equation. But, since this has the form of the first kind, no application of the successive approximations method has, to our knowledge, been carried out so far. In this work, such an application will be attempted, by means of a representation of the unknown source function in terms of distributions in the wavenumber variable and a subsequent reformulation of the integral equation of the problem.

## SUCCESSIVE APPROXIMATIONS

Let us consider a perfectly conducting surface, rough in one dimension, described by the profile function

$$z = \zeta(x) \quad (1)$$

which, of course, must be continuous and bounded. We will not deal here with the problem of singularities in any derivative of the profile function; however, we explicitly assume at least the existence of a normal at any point (i.e. continuity of the first derivative) in order to define the source function; the problem of an edge point requires a separate treatment. We assume a plane incident wave of horizontal polarization

$$\psi_i(\mathbf{r}) = \exp(jkx \sin \theta - jkz \cos \theta) \quad (2)$$

where  $k$  is the free-space wavenumber,  $\theta$  is the incidence angle with respect to the vertical ( $z$ ) direction and the letter  $\psi$  throughout the text denotes the  $y$ -component of the electric field. A harmonic time dependence  $\exp(-j\omega t)$  is assumed and suppressed in the following.

Starting from the EBC [6] applied for any location  $z < \min\{\zeta(x)\}$ , introducing the plane wave expansion of the two-dimensional free-space Green's function and using the Dirichlet boundary condition, we come up with the following integral equation

$$\int d\lambda \frac{\exp[j\lambda x - jv(\lambda)z]}{4\pi v(\lambda)} \int dx' \exp[j\lambda x' - jv(\lambda)\zeta(x')] f(x') = \psi_i(\mathbf{r}) \quad (3)$$

where the limits of integration are  $-\infty$  and  $+\infty$  (and will be omitted hereafter for simplicity), and the function  $v(\lambda)$  is defined in the usual way

$$v(\lambda) = \begin{cases} \sqrt{k^2 - \lambda^2} & , \quad |\lambda| \leq k \\ j\sqrt{\lambda^2 - k^2} & , \quad |\lambda| > k \end{cases} \quad (4)$$

so that the radiation conditions hold. The source function  $f(x')$  is related to the unknown boundary value  $\partial\psi/\partial n$  on the rough surface through

$$f(x') = j \hat{n} \cdot \nabla' \psi(r') \sqrt{1 + \left[ \frac{d\zeta(x')}{dx'} \right]^2} \quad (5)$$

It is convenient to so choose the coordinate system that  $\zeta(x) \geq 0$  for all  $x'$ , and the  $z$  of Eq. (3) be less than zero. Under these circumstances, the function  $\exp[j\lambda x - jv(\lambda)z]/4\pi v(\lambda)$  will certainly be of rapid descent (i.e. it will decrease faster than any power of  $\lambda$ , as  $|\lambda| \rightarrow +\infty$ ) and infinitely smooth at all points but  $\lambda = \pm k$ .

In Eq. (3), an interchange of the order of integration is implicit, which is performed by means of a distributional interpretation of the inner integral over  $x'$ . In view of the above considerations, such an interpretation will have a sense if the integral over  $x'$  represents a distribution of slow growth whose support does not contain the points  $\lambda = \pm k$ . (Since the support of a distribution is a closed set, this implies that the distribution will equal zero over a neighborhood of each of these points). Hence, a sufficient condition for (3) to hold is

$$\int f(x) \exp[-j\lambda x + jv(\lambda)\zeta(x)] dx = 4\pi v(\lambda_0) \delta(\lambda - \lambda_0) \quad (6)$$

since the delta distribution satisfies both the above constraints, except in the extreme case  $\lambda_0 = k$ . In (6), we have dropped the primed notation and set

$$\lambda_0 = k \sin \theta \quad (7)$$

The EBC formulation can also yield an expression for the scattered field (which essentially constitutes no more than an application of the Helmholtz-Kirchhoff integral). In this work, however, we are concerned with the evaluation of the source function on the surface.

At this point, we adopt the following Ansatz for the unknown source function

$$f(x) = \int \varphi(\mu) \exp[j\mu x - jv(\mu)\zeta(x)] d\mu \quad (8)$$

with

$$v(\mu) = \begin{cases} v(\mu) & , \quad |\mu| \leq k \\ 0 & , \quad |\mu| > k \end{cases} \quad (9)$$

Notice that the right-hand side of (8) will have a meaning for  $\varphi(\mu)$  subject to conditions looser than those previously stated. In fact, it suffices that  $\varphi(\mu)$  be a distribution of slow growth such that, in some neighborhood of  $\mu = k - k$

$$\left| \int \varphi(\mu) \chi(\mu) d\mu \right| \leq C \sup |\chi(\mu)| \quad (10)$$

for every testing function  $\chi(\mu)$  whose support is contained in this neighborhood (see e.g. the arguments in Reference [9], Sec. 3.4). Eq. (8) defines a mapping of the set of distributions described above into that of distributions in the space variable  $x$  (which, in general, contains the unknown source function).

The particular form of the above Ansatz (8) expresses  $f(x)$  in terms of downgoing propagating plane waves; of course, there is no implication concerning the fields above the boundary surface. It is analogous to the discrete plane harmonics expansion adopted in [6], as far as the "propagating part" of the angular spectrum is concerned; as a matter of fact, spectral contributions around the point  $\mu = \lambda_0$  appear to be important for the effectivity of the solution.

Introducing (8) into (6), one can derive an operatorial equation of the form

$$T\varphi = 2v(\lambda_0) \delta(\lambda - \lambda_0) \quad (11)$$

where the operator  $T$  consists in first applying (8) to the unknown  $\varphi$  and then performing the integration of the left-hand side of (6), in the distributional sense; a factor of  $1/2\pi$  has also been incorporated for reasons of formal convenience, as it will be seen in the following. Eq. (11) is viewed as an operatorial one because both the unknown  $\varphi$  and the right-hand side of (11) belong to the same space of distributions in the wavenumber variable.

At this point, one can apply to (11) the Neumann iterative procedure [2]. A prerequisite for this is that the operator  $T$  maps a distribution  $\varphi$  of the kind described above (i.e. of slow growth and having the property given by (10)) to another distribution of the same kind, so that (8) has a sense at each successive iteration. This, of course, is expected to impose certain restrictions on the profile function  $\zeta(x)$ . A way to formally describe the procedure is to rewrite (11) as

$$\varphi + (T - I)\varphi = 2v(\lambda_0) \delta(\lambda - \lambda_0) \quad (12)$$

with  $I$  the unit operator, and then apply the customary method of successive approximations, with the right-hand side of (12) as initial guess. The result is

$$\varphi = \sum_{n=0}^{+\infty} \varphi_n \quad (13)$$

$$\begin{aligned} \varphi_0 &= 2v(\lambda_0) \delta(\lambda - \lambda_0) \\ \varphi_n &= (I - T)^n \varphi_0, \quad n > 0 \end{aligned} \quad (14)$$

The key point to proceed is the implementation of the operator  $T$ .



## RESULTS AND DISCUSSION

Let us suppose that, in the definition of the T operator, the order of integrations can be interchanged. This would mean that the expression

$$F(\lambda, \mu) = \int \exp[j(\mu - \lambda)x] \left\{ \exp[j(u(\lambda) - v(\mu))\zeta(x)] - 1 \right\} dx \quad (15)$$

possesses a sense as a generalized function with respect to  $\mu$  and  $\lambda$ , and the general term of the successive approximation series can be written down as

$$\varphi_n(\lambda) = 2v(\lambda_0) \frac{(-1)^n}{(2\pi)^n} \int \dots \int d\lambda_{n-1} \dots d\lambda_1 F(\lambda, \lambda_{n-1}) \dots F(\lambda_2, \lambda_1) F(\lambda_1, \lambda_0) \quad (16)$$

the repeated integrations meaning successive application of the distributions involved.

If, furthermore, the power series corresponding to the exponential inside the brackets in (15) is convergent in the distributional sense, one has

$$\begin{aligned} \varphi_n(\lambda) = 2v(\lambda_0) \frac{(-1)^n}{(2\pi)^n} \int \dots \int d\lambda_{n-1} \dots d\lambda_1 \sum_{m_0=1}^{+\infty} \dots \sum_{m_{n-1}=1}^{+\infty} \frac{j^{m_0+\dots+m_{n-1}}}{m_0! \dots m_{n-1}!} [v(\lambda) - v(\lambda_{n-1})]^{m_{n-1}} \dots \\ \dots [v(\lambda_2) - v(\lambda_1)]^{m_1} [v(\lambda_1) - v(\lambda_0)]^{m_0} Z_{m_{n-1}}(\lambda_{n-1} - \lambda) \dots Z_{m_1}(\lambda_1 - \lambda_2) Z_{m_0}(\lambda_0 - \lambda_1) \end{aligned} \quad (17)$$

where  $Z_m$  denotes the Fourier transform of the  $m$ -th power  $\zeta^m(x)$  of the profile function.

Eq. (17), even if viewed as a purely formal expression, can yield an interesting result, namely a systematic way to derive the general term of the perturbation series for the problem under consideration. To this end, we insert (17) into (8), expand the exponential and apply Fourier transformation; the result is an expression containing one more sum (i.e. multiple summation with respect to  $m_0, \dots, m_n$ ). Observing that the aforesaid general (say  $m$ -th) term should be of order  $m$  with respect to  $\zeta(x)$ , we rearrange the multiple series obtained and collect together all terms with

$$m_0 + \dots + m_n = m$$

The result is an expression which, after a straightforward simplification process, reduces to the expression reported in [8] and independently shown there to satisfy the recursion relation which characterizes the general term of the perturbation series. It is interesting to notice that, according to the above procedure, the  $m$ -th perturbative term will be contained in the first  $(m+1)$  successive approximations (up to the  $m$  order one).

Another interesting result is obtained if, under the assumption of narrow bandwidth of the Fourier transforms  $Z_m$ , one expands the multivariable function

$$v^{m_n}(\lambda_n) [v(\lambda_n) - v(\lambda_{n-1})]^{m_{n-1}} \dots [v(\lambda_2) - v(\lambda_1)]^{m_1} [v(\lambda_1) - v(\lambda_0)]^{m_0}$$

which arises after combining (17) with (8) and Fourier transforming, into a Taylor series with respect to the variables  $\lambda_1, \dots, \lambda_n$  around the point  $(\lambda_0, \dots, \lambda_0)$ . The terms of order 1 will yield, after Fourier inversion, terms proportional to the derivative  $d\zeta(x)/dx$ ; higher order terms yield contributions proportional to  $[d\zeta(x)/dx]^2$  or  $d^2\zeta(x)/dx^2$ , and so on. The  $m$ -th successive approximation contains terms of order  $m$  or higher. Hence, the terms of order up to 1 are contained in the first two (0 and 1) approximations, and it is easily shown that they recover the Kirchhoff approximation for the surface under consideration. As it has been seen, they also contain the first perturbation term; therefore, the present approach appears to interpolate between the first-order perturbation and Kirchhoff theory, correctly recovering each of them in the appropriate limit.

At this point, it can be observed that the Ansatz (8) could be replaced by other expansions, and the same procedure followed. One possible (and perhaps conceptually simpler) alternative would be the Fourier transform of the unknown source function  $f(x)$ . As some calculation would show, the general perturbative term could also be derived in that case by means of the procedure described above; however, the series would no more exhibit the interpolating behavior previously mentioned.

As a preliminary numerical check, we have applied the proposed procedure to a sinusoidal surface described by

$$\zeta(x) = b[1 - \cos(2\pi x/d)]$$

The sinusoidal profile function is quite convenient for comparison because it is simple and infinitely smooth; moreover, various well established methods exist, giving reliable numerical results. We have chosen the so-called Masel, Merrill and Miller (MMM) method (see e.g. [10]), restricted the values of the surface parameters well within its region of validity and checked conservation of energy up to 6 decimal digits; thus, we consider the results obtained as exact for our purpose.

In Figs 1-2 those results are compared with the results of the present successive approximations (SA) approach, the Kirchhoff approximation (KA) and the phase perturbation technique (PPT) [8,11]; results from the customary perturbation technique (PT) (see e.g. [12]) are also included. All three (SA, PPT and PT) techniques have been restricted to first order. To avoid large phase variations, we have plotted the modulus and phase of the function

$$f_s(x) = f(x) \exp(-jkx \sin \theta)$$

In Figs. 1a-b, a surface of small spatial period  $d$  and not great corrugation height is examined; perturbative techniques appear to give better results than the KA, due to the fact that the curvature of the surface may take appreciable values.

Figs. 2a-b refer to the case of a surface of larger  $d$  and smaller curvature values; the PT is unsatisfactory, whereas the KA and PPT are quite effective. In both cases, the SA approach proposed here is at least as efficient as the PPT, with the additional advantage of a general term known in closed form.

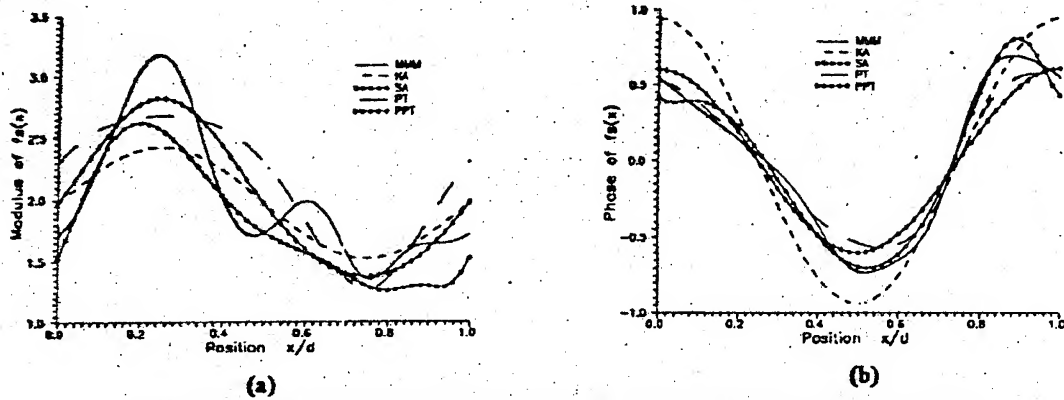


Fig. 1: (a) Modulus and (b) phase of  $f_s(x)$  for a sinusoid with  $kd=10$ ,  $kb=1$ ,  $\theta=20^\circ$ .

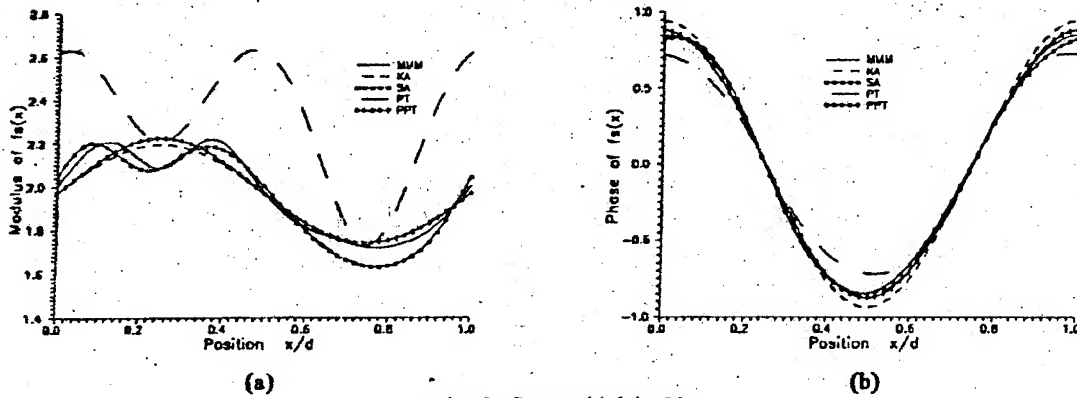


Fig. 2: Same with  $kd=20$ .

#### REFERENCES

- [1] A.W. Maue, "On the formulation of a general scattering problem by means of an integral equation", Z. Phys. (1949), 126, 7, pp.601-608.
- [2] R.E. Kleinman and P.M. van den Berg, "Iterative methods for solving integral equations", Radio Sci. (1991), 26, 1, pp.175-181.
- [3] Z. Li and A.K. Fung, "A reformulation of the surface field integral equation", Jour. Electromagn. Waves Appl. (1991), 5, 2, pp.195-203.
- [4] G.S. Brown, "Application of the integral equation method of smoothing to random surface scattering", IEEE Trans. Antennas Propagat. (1984), AP-32, 12, pp.1308-1312.
- [5] G.S. Brown, "Simplifications in the stochastic Fourier transform approach to random surface scattering", IEEE Trans. Antennas Propagat. (1985), AP-33, 1, pp.48-55.
- [6] P.C. Waterman, "Scattering by periodic surfaces", J. Acoust. Soc. Am. (1975), 57, 4, pp.791-802.
- [7] D. Winebrenner and A. Ishimaru, "Investigation of a surface field phase perturbation technique for scattering from rough surfaces", Radio Sci. (1985), 20, 2, pp.161-170.
- [8] C.N. Vazouras, P.G. Cottis and J.D. Kanellopoulos, "Scattering from conducting rough surfaces: A general perturbative solution", IEEE Trans. Antennas Propagat. (1993), AP-41, 9, pp. 1232-1241.
- [9] A.H. Zemanian, "Distribution theory and transform analysis", Dover publications, New York, 1987.
- [10] S.L. Chuang and J.A. Kong, "Scattering of waves from periodic surfaces", Proc. IEEE (1981), 69, 9, pp.1132-1144.
- [11] J. Shen and A.A. Maradudin, "Multiple scattering of waves from random rough surfaces", Phys. Rev. B (1980), 22, 9, pp.4234-4240.
- [12] M. Nieto-Vesperinas and N. Garcia, "A detailed study of the scattering of scalar waves from random rough surfaces", Opt. Acta (1981), 28, 12, pp.1651-1672.

# TWO-DIMENSIONAL SCATTERING FROM A THIN SCREEN IN THE VICINITY OF THE INTERFACE BETWEEN TWO MEDIA

Natalia Veremey and Vladimir Veremey

Institute of Radiophysics and Electronics Ukrainian Academy of  
Sciences, 12, ac. Proskura st., Kharkov, 310085, Ukraine.  
(Tel. (7-0572)-44-85-43; FAX: (7-0572)-79-11-11)

The two-dimensional problem is solved for determining the field scattered by a perfectly conducting thin cylindrical screen located near the planar interface separating two homogeneous half-spaces of different electromagnetic properties. The initial boundary value problem was reduced to the infinite system of linear algebraic equations of the second kind by the generalized method of the Riemann-Hilbert problem. It is shown that the proposed solution of the problem is the rigorous one. The more general situation of a metal thin screen in the vicinity of diffraction gratings has been considered.

## Introduction.

Diffraction solution for plane wave or local sources incidence of various reflector in the vicinity of material bodies or some extent domain are needed in many antenna applications. Most simple vibrator antennas near an impedance plane, stratified dielectrics and in the absorbing space have been examined in [1]. Description of more complicated antennas forming the direct radiation as a rule are limited by the case of antenna excitation in the free space. Thus the subsurface influence on the scattering field was not taken into account in reflector antenna calculations. It may be explained apparently that approximate methods are not capable enough to give far field values in all directions and the rigorous method technique has not been developed for complicated electromagnetic structures. Some interesting results have been obtained in [2] where the diffraction wave problem on the cylinders with various cross-sections near the planar interface is solved.

In this work the rigorous solution of the diffraction problem for an unclosed perfectly conductive cylinder near an impedance plane is presented and used to analyze the reflector antenna radiation transformed by inserting the plane in the antenna near zone.

## 1. Diffraction Problem

The two-dimensional problem of a line magnetic current field or TE-polarized plane wave field scattering by a circular cylindrical perfectly conductive unclosed reflector near a planar interface between two media is solved.

The total field in this structure is given as the superposition of the scattered field by the reflector ( $H^r$ ), by the plane ( $H^p$ ) and the field of the source ( $H^i$ ) and has to satisfy the wave equation in the free space, Sommerfeld radiation condition, Meixner condition on the reflector edges and the boundary conditions on the surfaces of the reflector and impedance plane.

The Z-component of the total field may be written as

$$H_z = H_z^i + H_z^r + H_z^p. \quad (1)$$

Assume an incident TE wave  $H^i(\vec{r})$  to excite the screen in the presence of a plane interface is given in Fig.1. We shall consider two cases: the plane wave and line magnetic current excitation.

$$\begin{aligned} 1) \quad H_z^i &= e^{ikx \cos \varphi_{inc} - iky \sin \varphi_{inc}}; \\ 2) \quad H_z^i(\vec{r}) &= H_0^{(1)}(k|\vec{r} - \vec{r}_0|); \end{aligned} \quad (2)$$

$H_0^{(1)}$  - is the Hankel function of the first kind.

Here  $H_z^i(\vec{r})$  is the incident field of the line magnetic feed situating in the point  $\vec{r}_0(r_0 = \sqrt{x_0^2 + y_0^2}, \varphi_0)$ ,  $k = 2\pi/\lambda$ ,  $\lambda$  is the wave length.

The time dependence  $e^{-i\omega t}$  ( $\omega = 2\pi c/\lambda$ ,  $c$  is the speed of light) as a common multiplier in (1) is omitted here and later.

Assuming that  $x(\tau), y(\tau)$  are the parametrization functions of the screen's contour ( $\tau \in [-\alpha, \alpha]$ ,  $\alpha \leq \pi$ ) the field scattered by the isolated cylindrical screen can be represented in the following potential form:

$$H_z^s(x, y) = \frac{i}{4} \int_{-\alpha}^{\alpha} \mu(\tau) \frac{\partial}{\partial \bar{n}_\tau} H_0^{(1)}(k \sqrt{(x - x(\tau))^2 + (y - y(\tau))^2}) l(\tau) d\tau, \quad (3)$$

where  $l(\tau) = \sqrt{(\frac{dx(\tau)}{d\tau})^2 + (\frac{dy(\tau)}{d\tau})^2}$ ,  $\bar{n}_\tau$  is the normal to the reflector surface  $L$ ,  $\mu(\tau)$  is the unknown function which is proportional to the surface current density on the screen.

Let the function  $\mu(\tau)$  is equal 0 if  $\tau \in [-\pi, \pi] \setminus (-\alpha, \alpha)$ . Thus the function  $\mu(\tau)$  determined on the interval  $[-\pi, \pi]$  may be expanded in the Fourier series:

$$\mu(\tau) = \sum_{n=-\infty}^{\infty} \mu_n e^{in\tau} = \begin{cases} \mu(\tau), & \tau \in [-\alpha, \alpha] \\ 0, & \tau \in [-\pi, \pi] \setminus (-\alpha, \alpha) \end{cases} \quad (4)$$

Using the integral representation of the Hankel function:

$$H_0^{(1)}(k \sqrt{(x - x(\tau))^2 + (y - y(\tau))^2}) = \frac{1}{\pi} \int_{i\infty}^{\pi - i\infty} e^{ikx \cos t - iky \sin t} e^{-ikx(\tau) \cos t + iky(\tau) \sin t} dt, \quad y < y(\tau), \quad (5)$$

(3) can be rewritten in the region under the cylinder as

$$H_z^s(x, y) = \frac{i}{4\pi} \int_{i\infty}^{\pi - i\infty} \sum_{n=-\infty}^{\infty} \mu_n \Lambda_n(t) e^{ikx \cos t - iky \sin t} dt, \quad (6)$$

where

$$\Lambda_n(t) = \int_{-\pi}^{\pi} e^{in\tau} \frac{\partial}{\partial \bar{n}_\tau} e^{-ikx(\tau) \cos t + iky(\tau) \sin t} l(\tau) d\tau.$$

It was shown that in the case of the screen near an interface between two different media and in more general case of the screen in the vicinity of an infinite diffraction grating the field scattered by an interface or grating can be represented as

$$H_z^R(x, y) = \frac{1}{\pi} \int_{i\infty}^{\pi - i\infty} \Psi^R(t, x, y) dt, \quad (7)$$

where  $\Psi^R(t, x, y)$  is the unknown function which satisfies the Floquet condition:

$$\Psi^R(t, x + l, y) = e^{ikl \cos t} \Psi^R(t, x, y), \quad (8)$$

$l$  is the period of the grating.

The similar representation was proposed by Skurlov [3]. Another approach to the problem of the point source excitation of a periodical structure was suggested by Il'inski [4]. The field scattered by the grating was represented in the following form:

$$H_z^R(x, y) = \frac{1}{2\pi} \int_0^{2\pi} U(t, x, y) dt \quad (9)$$

where  $U(t, x, y)$  satisfies the Floquet condition. This approach allows to use an interesting mathematical method considered in [5]. The Skurlov's approach was also used in [6].

Taking into account (9) one can write when the screen is near a grating:

$$\Psi^R(t, x, y) = \sum_{n=-\infty}^{\infty} \begin{cases} a_n(t) e^{i\gamma_n(y+b)}, & y > -b \\ b_n(t) e^{-i\gamma_n(y+b)}, & y < -b \end{cases} e^{ih_n x}, \quad (10)$$

Here  $\{a_n(t), b_n(t)\}_{n=-\infty}^{\infty}$  are known Fourier coefficients of the field scattered by a grating in the case of the plane wave incidence:  $\{H_z^{inc} = e^{ikx \cos t - iky \sin t}, \quad t \in C, \quad \} h_n = k \cos t + \frac{2\pi n}{l}, \gamma_n = \sqrt{k^2 - h_n^2}$  ( $Re \gamma_n > 0$ , if  $Re \gamma_n = 0$  then  $Im \gamma_n > 0$ ). There are  $a_n(t) = b_n(t) = 0, (n \neq 0)$  when the screen is near an interface between two media.

Therefore

$$H_z^R = \frac{1}{\pi} \int_{i\infty}^{\pi-i\infty} A(t) e^{ikb \sin t} \sum_{n=-\infty}^{\infty} a_n(t) e^{i\gamma_n y} e^{ih_n x} e^{i\gamma_n b} dt, \quad y > -b, \quad (11)$$

where

$$A(t) = F^i(t) + \frac{i}{4} \sum_{n=-\infty}^{\infty} \mu_n \Lambda_n(t),$$

$$F^i(t) = \begin{cases} e^{-ik h_0 \cos(\varphi_0 + t)} & \text{for a line magnetic current} \\ \pi \delta(t - \varphi_{inc}) & \text{for a plane wave} \end{cases}$$

The field scattered by the interface between two media characterized by  $\varepsilon_1$  and  $\varepsilon_2$  can be represented in the upper half-space as:

$$H_z^s = \frac{1}{\pi} \int_{i\infty}^{\pi-i\infty} A(t) \hat{R}(t) \hat{A} e^{ikx \cos t + iky \sin t} dt, \quad (12)$$

$$\hat{R}(t) = \hat{A} \frac{\varepsilon_2 \sin t - \sqrt{\varepsilon_1 \varepsilon_2 - \varepsilon_1^2 \cos^2 t}}{\varepsilon_2 \sin t + \sqrt{\varepsilon_1 \varepsilon_2 - \varepsilon_1^2 \cos^2 t}}, \quad \hat{A} = e^{ikb \sin t}, \quad k = \frac{2\pi}{\lambda} \sqrt{\varepsilon_1}; \quad (13)$$

Using the Neumann boundary conditions on the reflector surface and extracting the singular term of the Hankel function the integral equation can be obtained:

$$-\frac{1}{2\pi} \frac{\partial^2}{\partial \theta^2} \int_{-\alpha}^{\alpha} \mu(\tau) \ln \left| 2 \frac{\tau - \theta}{2} \right| d\tau + \frac{1}{2\pi} \int_{-\alpha}^{\alpha} \mu(\tau) H(\theta, \tau) d\tau = g(\theta), \quad \theta \in [-\alpha, \alpha], \quad (14)$$

where

$$g(\theta) = l(\theta) \frac{\partial H_z^i(x, y)}{\partial \bar{n}_\theta} \Big|_{x, y \in L} + l(\theta) \frac{1}{\pi} \int_{i\infty}^{\pi-i\infty} F^i(t) \hat{A} \sum_{n=-\infty}^{\infty} a_n(t) \frac{\partial}{\partial \bar{n}_\theta} e^{i\gamma_n y(\theta) + ih_n x(\theta)} e^{i\gamma_n b} dt +$$

$$+ l(\theta) \sum_{m=-\infty}^{\infty} \mu_m \frac{i}{4\pi} \int_{i\infty}^{\pi-i\infty} \Lambda_m(t) \hat{A} \sum_{n=-\infty}^{\infty} a_n(t) \frac{\partial}{\partial \bar{n}_\theta} e^{i\gamma_n y(\theta) + ih_n x(\theta)} e^{i\gamma_n b} dt =$$

$$= \sum_{n=-\infty}^{\infty} g_n e^{in\theta} + \sum_{n=-\infty}^{\infty} g_n^{(1)} e^{in\theta} + \sum_{n=-\infty}^{\infty} \sum_{m=-\infty}^{\infty} \mu_m g_{nm}^{(2)} e^{in\theta}$$

This equation is reformulated in the terms of Dual Series Equations with trigonometrical kernel. The idea of the reformulation was suggested in [7].

$$\left\{ \begin{aligned} & \frac{1}{2} \sum_{n \neq 0} \mu_n |n| e^{in\theta} - \sum_{n=-\infty}^{\infty} \sum_{m=-\infty}^{\infty} \mu_m h_{n,-m} e^{in\theta} = \sum_{n=-\infty}^{\infty} (g_n + g_n^{(1)}) e^{in\theta} + \\ & + \sum_{n=-\infty}^{\infty} \sum_{m=-\infty}^{\infty} \mu_m g_{n,m}^{(2)} e^{in\theta} \quad \theta \in [-\alpha, \alpha] \\ & \sum_{n=-\infty}^{\infty} \mu_n e^{in\theta} = 0, \quad \theta \in [-\pi, \pi] \setminus (-\alpha, \alpha) \end{aligned} \right. \quad (15)$$

where  $H(\theta, \tau) = \sum_{n=-\infty}^{\infty} \sum_{m=-\infty}^{\infty} h_{nm} e^{in\theta + im\tau}$ .

Using the solution of the Riemann-Hilbert Problem — the problem of restore of an analytical function of a complex variable in the complex space with an arc slit  $L$ , when the sum of the boundary values of this function on the  $L$  is known — the Dual Series Equations reduced to the  $N$  systems of linear algebraic equations of the second kind.

$$\mu_n = \sum_{m=-\infty}^{\infty} C_{nm} \mu_m + b_n$$

where

$$C_{nm} = 2 \sum_{p=-\infty}^{\infty} (h_{p,-m} + g_{pm}^{(2)}) \frac{V_{n-1}^{p-1}(\cos \alpha)}{n}$$

$$b_n = 2 \sum_{m=-\infty}^{\infty} (g_m + g_m^{(1)}) \frac{V_{n-1}^{m-1}(\cos \alpha)}{n}, \quad \frac{V_{n-1}^{m-1}}{n} \Big|_{n=0} = W_m$$

$V_{n-1}^{p-1}, W_p$  are defined by the Legendre polynomials [8].

It can be proved following by [9] that the condition number of the obtained system does not increased with increasing of the truncation parameter and the obtained solution is efficient for analysis of scattering from thin sections of arbitrary cross-sections in the vicinity both diffraction gratings and a planar interface between two media.

The obtained solution is very efficient one and allows to carry out the detailed analysis of the near field at various frequencies for different parameters of the slotted cylinder. The cylindrical screen may be considered as the model of the two-dimensional antenna reflector. An analysis of transformations of far field patterns caused by the changing of the orientation of the reflector with regard to the interface can be carried out.

## REFERENCES

1. King R, Smith G. Antennas in Media, v.1. Moscow, Mir, 1984.
2. X.-B. Xu, C.M. Butler. IEEE Trans. Antennas and Propagation, AP-34, 7, p.880-890, 1986.
3. Skurlöv V. M. Radiotekhnika, Kharkov Univ. Ed. 1965, n.1, pp. 69-79.
4. Il'inski A. S. Numerical Methods and Programming. v. 24, Moscow Univ. 1975 pp. 220-230
5. Titchmarsh E.C. Eigenfunction expansions associated with second - order differential equations. Part II Moscow, 1961, Appendix VIII by Lidskii V. B. p.529
6. Nosich A.I. Dopovidi Ukrainian AS, ser A, 1985, n.3, pp.23-25
7. Tuchkin Yu. Doklady Akademii Nauk SSSR, 1987, v. 293, n. 2.
8. Shestopalov V. P. Method of the Riemann - Hilbert Problem in the Theory of Diffraction and Propagation of waves, Kharkov, Univ. Ed. 1973
9. Poyedinchuk A. Ye. , Tuchkin Yu. A. , Shestopalov V. P. Trans. IEE Japan, 1993, v.113-A, n.3, pp.139-146.

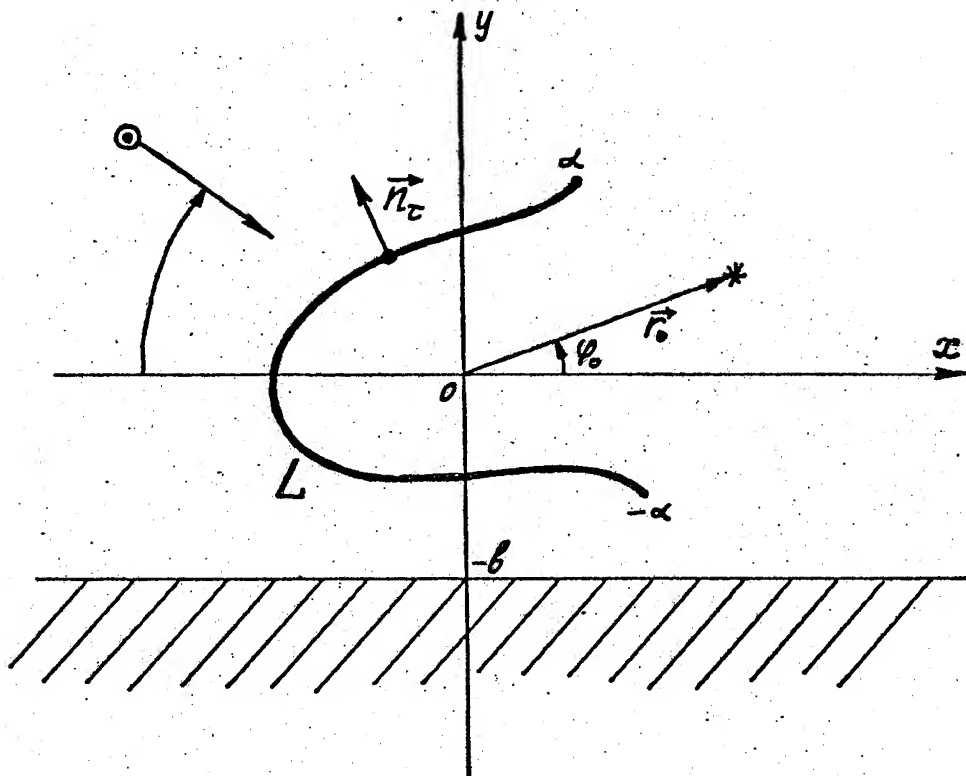


Fig. 1

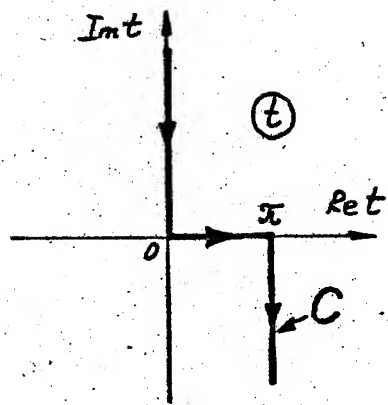


Fig. 2

# MM-Waves Reflection and Transmission by Leaves

A.Vertiy<sup>(1)</sup>, İ.H.Batum<sup>(1)</sup>, Ş.Aydınlık<sup>(1)</sup>, A.Chuklantsev<sup>(2)</sup>, A.H.Serbest<sup>(1,2)</sup>

(1) Department of Space Sciences

Marmara Research Center

TÜBİTAK, Gebze, Kocaeli, Turkey

(2) Department of Electrical and Electronics Engineering

Çukurova University, 01330 Balcalı, Adana, Turkey (Fax: +(322)3386326)

The possibilities of remote sensing of vegetation in mm-band are now under investigation of many researches. Since the brightness temperature or the backscattering coefficient of vegetation canopy is determined in great extent by the scattering and extinction properties of a single canopy element (leaf or stem) it is important to study these properties and their relation with biophysical parameters, for example, moisture content.

To measure transmission and reflection of leaves in mm-band ( $f=53-78$  GHz) the experimental set has been designed. It includes the oscillator, the quasi-optical beam waveguides, the precise attenuator, the cell with investigated sample, and detector section. The moisture content of sample is determined by its weighting under the wet and dry conditions. The transmission and reflection coefficients are determined by the compensation method with the help of precise attenuator. To avoid rereflections the sample is placed in the gap between waveguides at a certain angle with respect to the beam direction. It is found that in the range of gravimetric moisture from 0.2 to 0.6 the transmission coefficient changes approximately linearly from 0.7 to 0.3, and the reflection coefficient changes from 0.02 to 0.25 but with strong nonlinear dependence. The dependence of absorption coefficient calculated from measured data on the moisture content has a maximum at certain value of leaf moisture condition. The significant influence of the leaf structure change during the drying process on the result of measurements is also observed. The results of experiment are discussed and compared with the results of calculations of transmission and reflection for infinite dielectric layer.

The data obtained may be useful for calculation the radiative parameters of vegetation canopies in mm-band and for understanding the relation of these parameters with the canopy state.



# THE USING OF TWO-DIMENSIONAL SOLUTIONS IN THREE-DIMENSIONAL PROBLEMS FOR SCATTERERS OF ARBITRARY PROPERTIES

M.V.Vesnik

Institute of Radioengineering and Electronics  
Russian Academy of Sciences,  
6 Mokhovaya St., Moscow, 103907, Russia

## ABSTRACT

The technique of using the two-dimensional (2D) solutions in three-dimensional (3D) problems for the case of arbitrary shaped 2D scatterers and arbitrary boundary conditions is developed. It is previously supposed that one can find the analytical expression of 2D solution separately on each side of a rectilinear segments bounding contour surrounding the two-dimensional scatterer. Then the 3D solution may be received easily by substituting special simple-found parameters (in general case each of them may represent a complex number) into the analytical 2D solution instead of real angles of observation. In the practically important case of a large polygonal flat 3D scatterer (the corresponding 2D solution is a half-plane with arbitrary boundary conditions) the technique transforms to the simple substitution of the special parameter ("complex angle") into the previously obtained 2D analytical expression for a separated rectilinear segment of the bounding contour[10].

## INTRODUCTION

Recently several diffraction techniques related to the EM scattering by complex objects have been widely developed. The techniques are: Ufimtsev's method of edge waves in physical theory of diffraction (PTD) (new formulation) [1,2], method of equivalent currents (MEC) [3] and scattered field formulation in terms of incremental length diffraction coefficients (ILDC) [4-7]. All these methods are based on the concept of the PTD [8] and may be converted one into the other [9]. The methods allow to use two-dimensional (2D) solutions in three-dimensional (3D) problems. The solutions mentioned above are applicable mainly to perfectly conducting 2D scatterers that consist of planar surfaces and to the impedance wedge. The solution developed in [6] often leads to the wrong result. In this paper a method of using the 2D solution in 3D problems is generalized for the scatterers of arbitrary properties.

## 1. STATEMENT OF THE PROBLEM

When scattering of the electromagnetic wave on the body of a finite electric size (time dependence is  $\exp(-i\omega t)$ ) the solutions for the complex amplitude vectors of the electric and magnetic fields are:

$$\begin{aligned}\vec{E} &= -\frac{1}{ik}(\text{grad div} \vec{A}^e + k^2 \vec{A}^e) - \text{rot} \vec{A}^m, \\ \vec{H} &= -\frac{1}{ik}(\text{grad div} \vec{A}^m + k^2 \vec{A}^m) - \text{rot} \vec{A}^e,\end{aligned}\quad (1)$$

where

$$\vec{A}^e(\vec{R}) = \frac{1}{c} \iint_S \frac{\exp(ikr)}{r} \vec{j}^e ds, \quad \vec{A}^m(\vec{R}) = \frac{1}{c} \iint_S \frac{\exp(ikr)}{r} \vec{j}^m ds, \quad (2)$$

$\vec{A}^e$  и  $\vec{A}^m$  are the electric and magnetic vector potentials,  $\vec{j}^e$  и  $\vec{j}^m$  are the electric and magnetic surface currents,  $S$  is the surface of the scatterer,  $r=|\vec{R}-\vec{\rho}|$  is the distance from a point on the scatterer surface which position vector is  $\vec{\rho}=(\xi, \eta, \zeta)$  to the observation point which position vector is  $\vec{R}=\vec{n}^*R=(n_x^*R, n_y^*R, n_z^*R)$ ,  $\vec{n}^*$  is the unit vector of the observation direction,  $R$  is the distance from the coordinate center to the point of observation,  $k=2\pi/\lambda$  is the wavenumber of the incident wave,  $c$  is the velocity of light,  $i$  is the imaginary unit.

## 2. INFINITE CYLINDER

Consider integrals (2) for the infinite cylindric edge of an arbitrary shape which cylinder axis coincides with the  $X$  axis. The excitation is made by the plane wave:

$$\vec{E}^{(i)} = \vec{E}_0 \exp\{ik(\vec{n}', \vec{r})\}, \quad (3)$$

where  $\vec{E}_0$  is the complex amplitude, and  $\vec{n}'$  is the plane wave directing vector;  $\vec{r}=(x, y, z)$  is the position vector of an arbitrary point of the space. The equations (2) may be written in a number of scalar equations for any scalar component  $A^*$  of the electric or magnetic vector-potential.

Let us divide the vector  $\vec{\rho}$  into two parts:

$$\vec{\rho} = \vec{e}_x \xi + \vec{\rho}_0, \quad (4)$$

where  $\vec{\rho}_0$  is the component of  $\vec{\rho}$  vector in the plane  $YOZ$  which contains the cylindric surface bounding contour  $C$ ,  $\vec{e}_x$  is the unit vector along the  $X$  axis. The currents on the infinite cylindric surface satisfy the same equation as the incident field:

$$J(\vec{\rho}) = J(\vec{\rho}_0) \exp\{ik\xi n_x'\} \quad (5)$$

## 3. FAR ZONE CONDITION

For the body of finite size in far zone ( $r \geq 2D^2/\lambda$ ), where  $D$  is the size of the object, the following equation exist for 3D case

$$r \approx R - (\vec{n}^*, \vec{\rho}), \quad (6)$$

and for 2D case (6) becomes [10]:

$$r_{yz} \approx R_{yz} - (\vec{n}_{yz}^* / |\vec{n}_{yz}^*|, \vec{\rho}_0) \quad (7)$$

Index  $yz$  means the projection of the object without the index on the plane  $YOZ$ . From this one can see that  $\vec{\rho}_0 = \vec{\rho}_{yz}$ . Vector  $\vec{n}_{yz}^* / |\vec{n}_{yz}^*|$  is the unit vector in the plane  $YOZ$ , directed just as the vector  $\vec{n}_{yz}^*$ . Further we will suppose that (6) and (7) are satisfied.

## 4. A RECTILINEAR SEGMENTS BOUNDING CONTOUR

Let the contour  $C$  consist of  $N$  rectilinear segments  $C_k$ . Then

in force of transformation linearity for  $A^*$  и  $A^a$  will be:

$$A = \sum_{k=1}^N A_k. \quad (8)$$

Denoting:

$$\vec{\rho}_0 = \vec{\rho}_{k1} + \vec{\rho}_{k\tau}, \quad (9)$$

where  $\vec{\rho}_{k1}$  is the initial position vector of the  $\vec{\rho}_0$  on the segment  $C_k$ ,  $\vec{\rho}_{k\tau}$  is the vector directed along the rectilinear segment  $C_k$ . Taking into account (8) and (9) one can get from (2) and (7) for the infinite cylindrical surface [10]:

$$A_k^* = \frac{\exp\{ikn_x^* R n_x^* + ik_1 R_{yz}\}}{c} \sqrt{\frac{2\pi l}{k_1 R_{yz}}} I_k^*. \quad (10)$$

$$I_k^* = \exp\{-ik_1 (\vec{n}_{yz}^* / |\vec{n}_{yz}^*|, \vec{\rho}_{k1})\} \int_{C_k} j(\vec{\rho}_0) \exp\{-ik_1 (\vec{n}_{yz}^* / |\vec{n}_{yz}^*|, \vec{\rho}_{k\tau})\} dl. \quad (11)$$

Following the PTD we will consider the currents on a finite fragment of the cylindrical surface the same as on the infinite surface, and for this fragment we get from (2) and (6) [10]:

$$A_k^a = \frac{1}{c} \frac{\exp\{ikR\}}{R} \frac{\exp\{ikb(n_x' - n_x^a)\} - \exp\{ika(n_x' - n_x^a)\}}{ik(n_x' - n_x^a)} I_k^a. \quad (12)$$

$$I_k^a = \exp\{-ik(\vec{n}^a, \vec{\rho}_{k1})\} \int_{C_k} j(\vec{\rho}_0) \exp\{-ik(\vec{n}^a, \vec{\rho}_{k\tau})\} dl. \quad (13)$$

Here  $a$  and  $b$  are the coordinates of the fragment end points on the  $X$  axis,  $\vec{n}^a$  is the arbitrary direction to the point of observation, generally not lying on the diffraction cone (by contrast to  $\vec{n}^*$ ). So the solutions of (12) generally do not contain the solutions of (14).

Suppose we know separate analytical equations for all the  $A_k^*$  and  $I_k^*$ . This condition may be fulfilled when we use numerical methods to find the 2D solution or when our 2D problem is a half-plane or the wedge [3,7]. It is the same as if we know the analytical expressions of the integrals from (11). It may be shown [10] that if the angle  $\varphi_k^*$  presents as a parameter in the analytical expressions for  $I_k^*$  from (18) then a formal substitution into these expressions such  $\varphi_k^*$  (it may be a complex number) that:

$$\cos \varphi_k^* = \frac{(\vec{n}^a, \vec{\rho}_{k\tau})}{\rho_{k\tau} \sqrt{1 - (n_x')^2}} = \frac{\sqrt{1 - (n_x^a)^2}}{\sqrt{1 - (n_x')^2}} \cos \varphi_k^a, \quad (14)$$

where  $\varphi_k^*$  and  $\varphi_k^a$  are the angles between the vectors  $\vec{\rho}_{k\tau}$  and the

vectors  $\vec{n}_{yz}$  and  $\vec{n}_{yz}^a$  correspondingly, will bring to the situation when in the exponents inside the integrals in (11) and (13):

$$k_1(\vec{n}_{yz}/|\vec{n}_{yz}|, \vec{\rho}_{k\tau}) = k(\vec{n}^a, \vec{\rho}_{k\tau}) \quad (15)$$

along all the rectilinear segment  $C_k$  of the contour  $C$  and thus because the currents  $j(\vec{\rho}_0)$  in (11) and in (13) are the same (PTD):

$$I_k^* \exp(ik_1(\vec{n}_{yz}/|\vec{n}_{yz}|, \vec{\rho}_{k1})) = I_k^a \exp(ik(\vec{n}^a, \vec{\rho}_{k1})). \quad (16)$$

If one has  $I_k^*$  from (11) then it is possible to receive from (11) with the help of (14) the analytical expression for (13) without the direct integration.

The results of this paper may be wholly used in ILDC technique, but this paper we intentionally avoided the ILDS terminology in order not to limitate the generity of the approach. So the equations (14) are similar to the ones from [3,6-7]. But the "direct substitution" of the parameter  $\phi_k^*$  into the 2D equations in order to get the solution for the corresponding 3D scatterer may often lead to the wrong result because in the case of the diffracted field representation in the form of equivalent currents integration over some surface this surface must surround the singularities of the field [11].

#### REFERENCES

- [1] D.I. Butorin, N.A. Martynov, P.Ya. Ufimtsev, "Asymptotic Expressions for Elementary Edge Waves", Radiotekhnika i Electronica, vol.32, No.9, pp.1818-1828, 1987, (in Russian)
- [2] P.Ya. Ufimtsev, "Elementary Edge Waves and the Physical Theory of Diffraction", Electromagnetics, vol.11, No.2, pp.125-160, 1991
- [3] A. Michaeli, "Equivalent Edge Currents for Arbitrary Aspects of Observation", IEEE Trans. A&P, vol.AP-32, pp.252-258, Mar. 1984
- [4] K.M. Mitzner, "Incremental Length Diffraction Coefficients", Tech. Rep. AFAL-TR-73-296, Northrop Corp., Aircr. Div., Apr. 1974
- [5] R.A. Shore and A.D. Yaghjian, "Incremental Diffraction Coefficients for Planar Surfaces", IEEE Trans. A&P, vol.AP-36, No.1, pp.55-70, Jan. 1988
- [6] T.B. Hansen and A.D. Yaghjian, "Incremental Diffraction Coefficients for Cylinders of Arbitrary Cross Section: Application to Diffraction from Ridges and Channels in Perfectly Conducting Surfaces", Digest of A&P Society Symp., vol.2, pp.794-797, June 24-28, the University of Western Ontario, London, Canada, 1991
- [7] G. Pelosi, S. Maci, R. Tiberio and A. Michaeli, "Incremental Length Diffraction Coefficients for an Impedance Wedge", IEEE Trans. A&P, vol.AP-40, No.10, pp. 1201-1210, Oct. 1992
- [8] P.Ya. Ufimtsev, "Method of Edge Waves in the Physical Theory of Diffraction", 1962 (in Russian), translation prepared by the U.S. Air Force Foreign Technology Division, Wright-Patterson AFB, OH, released for distribution Sept. 7, 1971
- [9] E.F. Knott, "The Relationship Between Mitzner's ILDS and Michaeli's Equivalent Currents", IEEE Trans. A&P, vol.AP-33, No.1, pp.112-114, Jan. 1985
- [10] M.V. Vesnik, "The Using of Two-Dimensional Solutions in Three-Dimensional Problems", Radiotekhnika i Electronica, vol.38, No.8, pp.1416-1423, 1993 (in Russian)
- [11] Apeltsin V.F., A.G. Kyurkchan, "The analytical properties of the wave fields", Moscow, 1990 (in Russian)

# THE WAVE SCATTERING BY SPHEROIDAL SHELLS

Ye.D. Vinogradova

Institute of Radiophysics and Electronics Ukrainian Academy of  
Sciences, 12, ac. Proskura st., Kharkov, 310085, Ukraine  
(Tel. (7-0572)-44-85-43; FAX: (7-0572)-79-11-11)

## Introduction

In the presented paper the well-known approach [1] with the partial inversion of Helmholtz operator is generalized to the boundary value electromagnetic problems for a new class of thin nonclosed spheroidal and toroidal screens. In due time this approach was devised for spherical screens and did not do with spheroidal screens, since when applied to the Helmholtz equation in spheroidal coordinates, the Fourier method yields the angle functions  $S_{ml}(c, \eta)$  dependent not only of the angle parameter  $\eta = \cos \nu$  but the wave parameter  $c = kd/2$  too. Therefore the regularization procedure was inviting further development for spheroidal screens in order to perform the partial inversion of the Helmholtz operator for both the radial and angular parts. In so doing, the knowledge of the operator Laplace properties was required. The solved for this purpose boundary value potential problems on distribution of the electrostatic fields about charged nonclosed spheroidal conductors (Fig.1) have, in addition, their own significance and practical application.

The boundary value diffraction problems for the same geometry conductors require the investigations of dual (or higher) series equations with not understood kernels involving spheroidal angle functions. Resting on the solution to the corresponding boundary value potential problem and using the Abel's integral transform procedure adapted for the similar diffraction problem for nonclosed spherical screens [2],[3], we reduce the dual series equations of the new type to the known ones. In order to separate the static and dynamic parts of the Helmholtz operator, the spheroidal angle functions are expanded in the series in associated Legendre functions (Jacoby polynomials). The resulting equations are solved by the method outlined in [2],[3].

Now let consider the sequence of problems solved by the proposed method to illustrate its efficiency.

1. Rigorous solution to the potential problems on distribution of the electrostatic fields generated by nonclosed spheroidal shells (Fig.1) charged to a constant potential has been constructed. With no restriction on geometrical parameters, the developed methodics is used for calculations of capacitances, charges, and electrostatic field distributions about conductors of this kind. The calculation methodics for much used capacitance coefficients has also been considered. As a numerical example, the  $xy$  cross sectional views of electrostatic fields distribution about charged ( $U=1$ ) nonclosed spheroids (Fig.1) are shown in Fig.2 (for prolate spheroids with  $a/b = 0.2, \beta_0 = 60^\circ$ ) and Fig.3 (for oblate spheroids,  $a/b = 2.0, \beta_0 = 30^\circ$ ).

2. Proceed to the problem of a plane acoustic wave scattering by an ideally stiff spheroidal shell with a circular hole shown in Fig.4. The incidence and the  $oz$  axis direction are coinciding, the potential velocity is

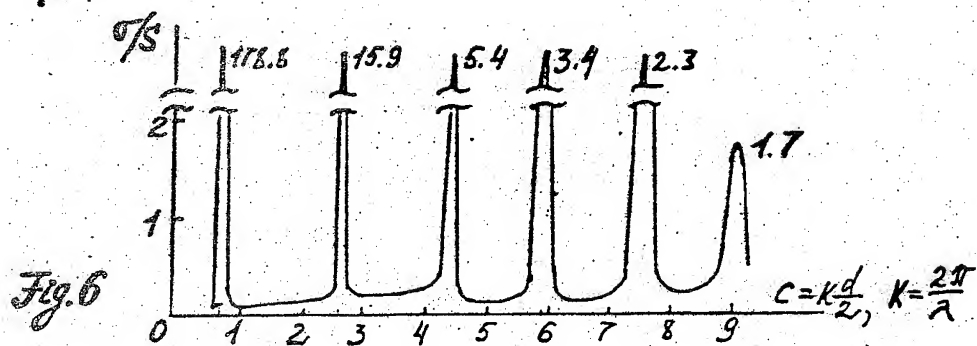
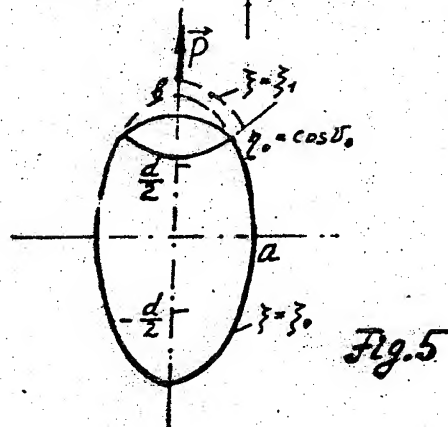
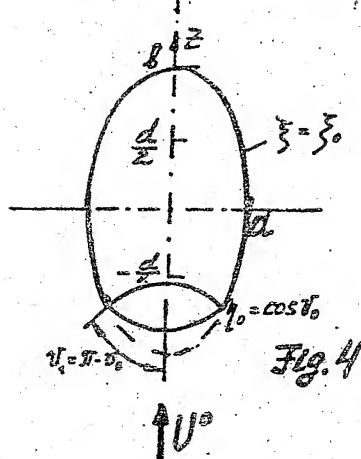
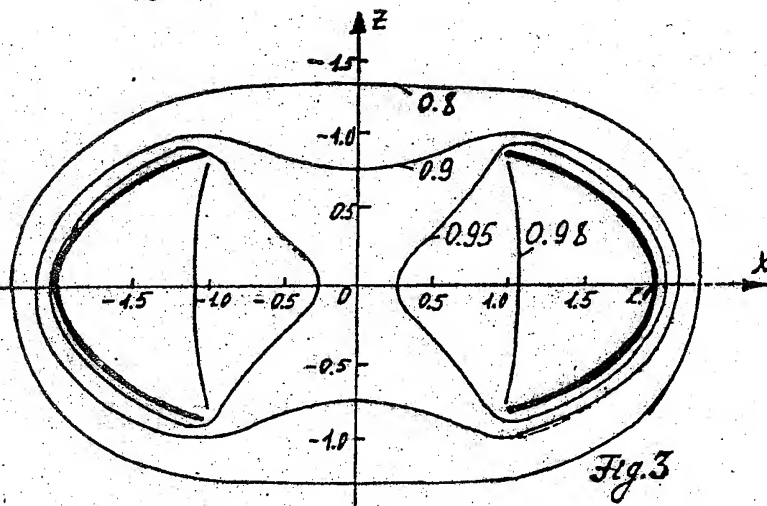
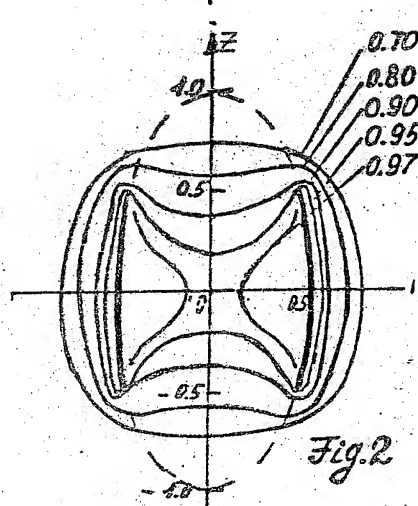
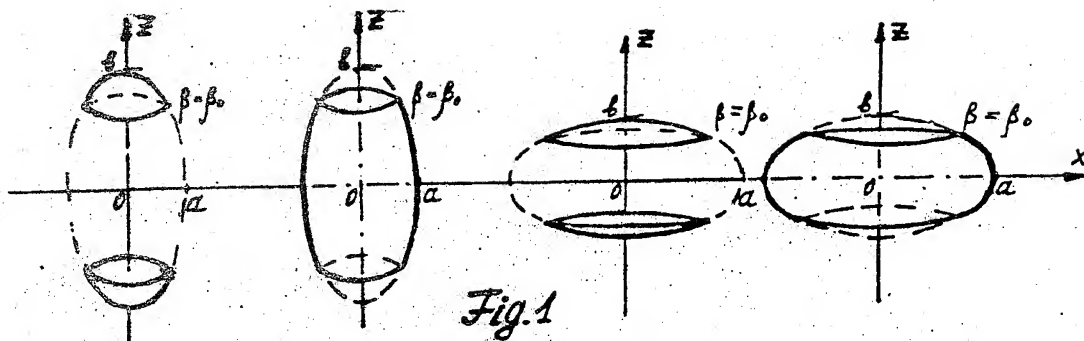
$$U^0 = \exp(i\eta\xi) \cdot \exp(-i\omega t). \quad (1)$$

The time dependence  $\exp(-i\omega t)$  is neglected.

Implying the Dirichlet boundary condition, we arrive at the dual series equations with the kernels of prolate spheroidal angle functions (PSAF). With the representation

$$S_{0l}(c, \eta) = d_l^{0l}(c) \cdot \left\{ P_l(\eta) + \sum_{r=0,1}^{\infty} d_r^{0l}(c) / d_l^{0l}(c) \cdot P_r(\eta) \right\} \quad (2)$$

the deduced equations are transformable to the equations with Legendre polynomials as the kernels. These equations are solved with traditional scheme to yield the infinite system of linear algebraic equations of the





Fredholm type. The resulting frequency dependences of the total scattering cross-section are exemplified for  $a/b = 0.2$ ,  $\nu_1 = 30^\circ$  in Fig. 6.

3. The rigorously formulated problem for the field generated by a concentrated electric source in the vertical dipole form and scattered by a thin perfectly conducted spheroidal shell with a circular hole (Fig. 5) has been solved. The dipole position is varying along the antenna axis. As before, this problem is reduced to the equations with PSAF of the first kind as the kernels

$$\sum_{l=1}^{\infty} \frac{A_l}{[(\xi_0^2 - 1)^{1/2} \cdot R_{1l}^{(3)}(c, \xi_0)]'} S_{1l}(c, \eta) = 0, \quad \eta \in (1, \eta_0) \quad (3)$$

$$\sum_{l=1}^{\infty} A_l [(\xi_0^2 - 1)^{1/2} R_{1l}^{(1)}(c, \xi_0)]' \cdot S_{1l}(c, \eta) = \sum_{l=1}^{\infty} \alpha_l S_{1l}(c, \eta), \quad \eta \in (\eta_0, -1). \quad (4)$$

Introducing an infinitesimally small parameter of the form

$$\epsilon_l = 1 + ic(\xi_0^2 - 1)^{1/2} \frac{2l+1}{l(l+1)} [(\xi_0^2 - 1)^{1/2} R_{1l}^{(1)}(c, \xi_0)]' \cdot [(\xi_0^2 - 1)^{1/2} R_{1l}^{(3)}(c, \xi_0)]', \quad (5)$$

representing PSAF as

$$S_{1l}(c, \eta) = d_{l-1}^{1l}(c) \left\{ P_l^1(\eta) + \sum_{r=0,1}^{\infty} d_r^{1l}(c) / d_{l-1}^{1l}(c) \cdot P_{r+1}^1(\eta) \right\} \quad (6)$$

and using the Abel's integral transform procedure, we reduce dual series equations (3), (4) to the infinite system of linear algebraic equations of the second kind.

By the similar way, the vectorial problem on a plane wave diffraction may be attacked. Unlike the foregoing problems, the vectorial problem is reduced to the two coupled dual series equations. The coupling between these series equations is due to the interaction between electric and magnetic types of waves arising when a circular hole is cut from a thin spheroidal shell. Resting on the outlined method, we solve equations of this kind in accordance with [4].

1. V.P. Shestopalov, The Riemann-Hilbert Problem Method in The Theory of Diffraction and Electromagnetic Wave Propagation. Kharkov: Kharkov University, 1971.
2. S.S. Vinogradov, Yu.A. Tuchkin, and V.P. Shestopalov, Investigation of Dual Series Equations Involving Jacoby Polynomials, DAN SSSR, 1980, v.253, N11, pp.318-321 (the English translation is in the Soviet Physics Doklady, The USA).
3. V.P. Shestopalov, Dual Series Equations in Contemporary Diffraction Theory. Kiev: Naukova dumka, 1983.
4. S.S. Vinogradov and V.P. Shestopalov, Solution of Vectorial Scattering Problem for a Sphere with a Hole, DAN SSSR, 1977, v.237, N1, pp.60-63.

Electromagnetic Wave Diffraction by Finite-Element  
Microstrip Structure. Comparison of Full-Wave Spectral  
and Approximate Methods.

Serge N. Vorob'ev

Institute of Radio Astronomy Academy of Sciences of Ukraine  
#4, Chervonopraporna Str., Kharkiv 310002, Ukraine  
FAX: 7-0572-476-506 Telex: 311039 SPACE SU  
E-mail: raiXira.kharkov.ua@relay.ussr.eu.net

As it's well-known the method of semi-inverting of the electromagnetic wave diffraction problem operator is used successfully. There exists the effective variant of this method in which the original boundary value problem operator undergoes decomposition that leads to the extraction of diffraction problem operator of the single element of structure with following analytical inverting of its singular static part using the full-wave spectral method (currents on strips are represented in terms of Chebyshev polynomials expansion with appropriate weight function, i.e. entire orthogonal basis which accounts for field singularities in the neighbourhood of each element edges analytically rigorously). Such approach had allowed to solve rigorously problems of wave diffraction by periodical [1, 2] and finite extent non-equidistant [2-4] strip structures as well as by strip which is spaced arbitrary with respect to plane interface of two magnetic-dielectrics [5]; it permits to obtain rigorous solutions of problems of wave scattering by structure consisting of finite number of strips non-equidistantly spaced in a stratified magnetic-dielectric medium and by a finite-element microstrip structure.

In the latter case an excitation by electromagnetic wave of the structure consisting of the finite number of non-equidistant metal strips placed on a magnetic-dielectric layer with a metal screen is considered. The electromagnetic field inside and outside of mentioned layer has the Fourier-integral form. After boundary conditions on the screen and on the layer-free space are obeyed the operator connecting a Fourier-amplitude of currents on strips with a Fourier-amplitude of tangential field component over the structure will be obtained. Thus the electrical field is expressed in terms of Fourier-amplitudes of currents on all strips. So this approach is based on the application of the Green function of magnetic-dielectric layer with the metal screen and the superposition principle. Using the full-wave spectral method with Chebyshev polynomials as basic and probe functions one can obtain the system of linear algebraic equations for unknown coefficients of the expansion of currents on strips at last.

Matrix elements of this system are, using the known literature term, mutual and own resistances of strips for some current harmonics. The recurrent relationship for matrix elements calculations was constructed that has decreased the time of computing essentially. Some transformations were done to increase the convergence of the integral describing own resistances which has the infinite upper limit, namely, the singular statical part of the Green function was separated and the integral of it was expressed in analytical form. Thus the obtained system of linear algebraic equations was reduced to the system of the second kind with the Fredholm-type matrix operator [6]. Formulas for mutual resistances allowing to calculate a value of the integral analytically with given accuracy in the case when the argument is great were built, the residual part of this integral was expressed as the integral in finite terms and was computed using Gauss quadrature methodic.



When surface waves in the magnetic-dielectric layer can propagate it leads to the presence of simple pole type singularities in matrix elements kernels, these poles are roots of the dispersion equation for surface waves. Formulas in which mentioned above singularities are excluded analytically from integrating expressions were constructed. The generalized criteria of the accuracy of computing is the energy law.

As a result of the detailed numerical analysis physical characteristics of scattered fields were investigated (in the case of the plane wave incidence). Features of mutual coupling of strips and their interaction on the main and higher current harmonics have been studied. The given problem has been solved approximately also with currents on strips approximation by chosen constants and results obtained have been compared with the rigorous ones. Limitations of this approximate approach have been determined, its validity and accuracy of calculations have been estimated.

Fig.1 and fig.2 present the distribution of the scattered E-field amplitude in the far-field zone over the equidistant strip structure consisting of 2 strips (upper side of figures) and of 7 strips (low side of figures). Continuous curves show results of the rigorous spectral method, interrupted lines show ones of approximate approach when currents on strips are set as chosen constants. The width of each strip equals to the wavelength in the magnetic-dielectric layer and the distance between neighbour strip edges equals to the strip width. The relative permeability equals to unity and the thickness of the layer is chosen rather small, so that surface waves in layer can't propagate. Other parameters are: for fig.1 the relative permittivity is 2,55 and normal incidence of the exciting wave, for fig.2 the relative permittivity is 4,5 and the angle of incidence equals to 30 degree.

First of all one can see that approximate approach doesn't give right results (for this parameters). The best its result describes the main beam for seven-element structure at fig.1 but this result is obvious because it is defined by the superposition of main diffractive harmonics with corresponding phase shifts from fields of all elements. Higher diffractive harmonics (which exist in periodical gratings [1,2]) are present in patterns obtained by the rigorous method in the form of diffraction beams. But in approximate scattering patterns they are either almost absent (fig.1) or don't correct neither by the amplitude nor by the direction (fig.2). This is the consequence of the essential irregularity in the current distribution on the each strip and, hence, of the impossibility to approximate in a right way the real complex current distribution using constants only irrespective of the number of strips consisting the structure. In such cases the solution can be obtained by the rigorous electrodynamical theory only.

- [1]- Vorob'ev S.N., Litvinenko L.N., Prosvirnin S.L. Zhurnal vychislitelnoi matematiki i matematicheskoi fiziki, 1986, v.26, No.6, pp.894-905.
- [2]- Vorob'ev S.N., Prosvirnin S.L. Zhurnal tekhnicheskoi fiziki, 1988, v.58, No.3, pp.458-468.
- [3]- Vorob'ev S.N. Radiotekhnika i elektronika, 1987, v.32, No.4, pp.687-695.
- [4]- Vorob'ev S.N. Izvestiya vysshikh uchebnykh zavedenii seriya radiofizika, 1990, v.33, No.4, pp.517-520.
- [5]- Vorob'ev S.N., Litvinenko D.L. Doklady Akademii Nauk UkrSSR seriya A, 1990, No.12, pp.38-42.
- [6]- Vorob'ev S.N., Nechaev U.B., Prosvirnin S.L. Izvestiya vysshikh uchebnykh zavedenii seriya radiofizika, 1992, v.35, No.8, pp.688-701. (in Russian)..

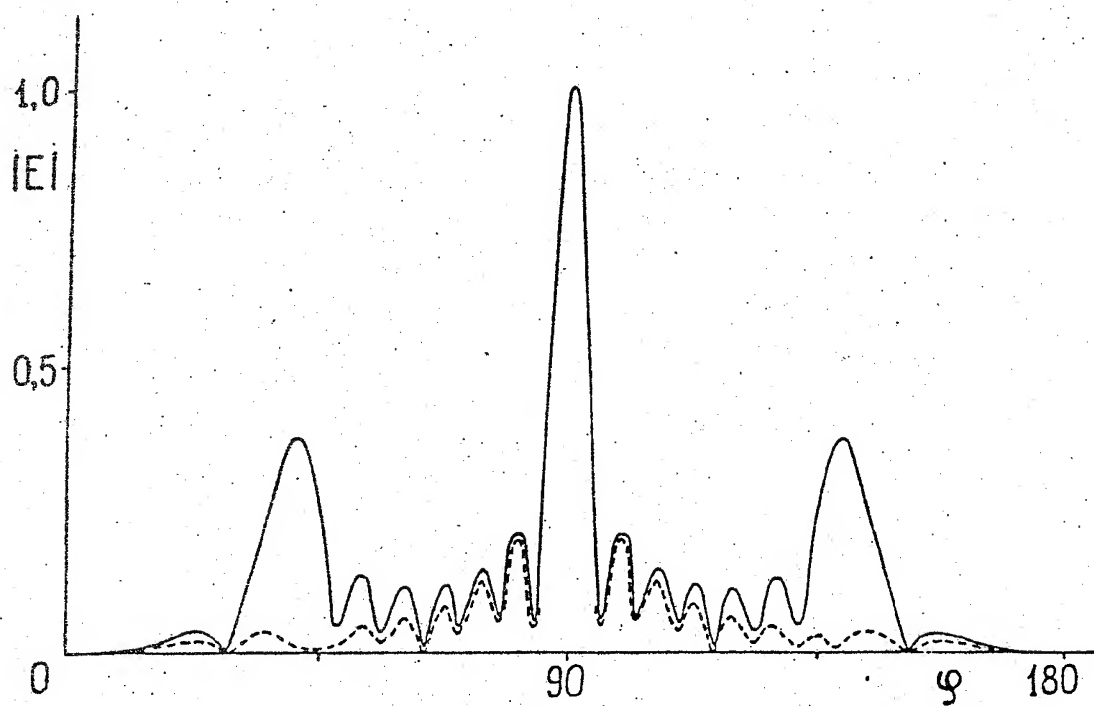
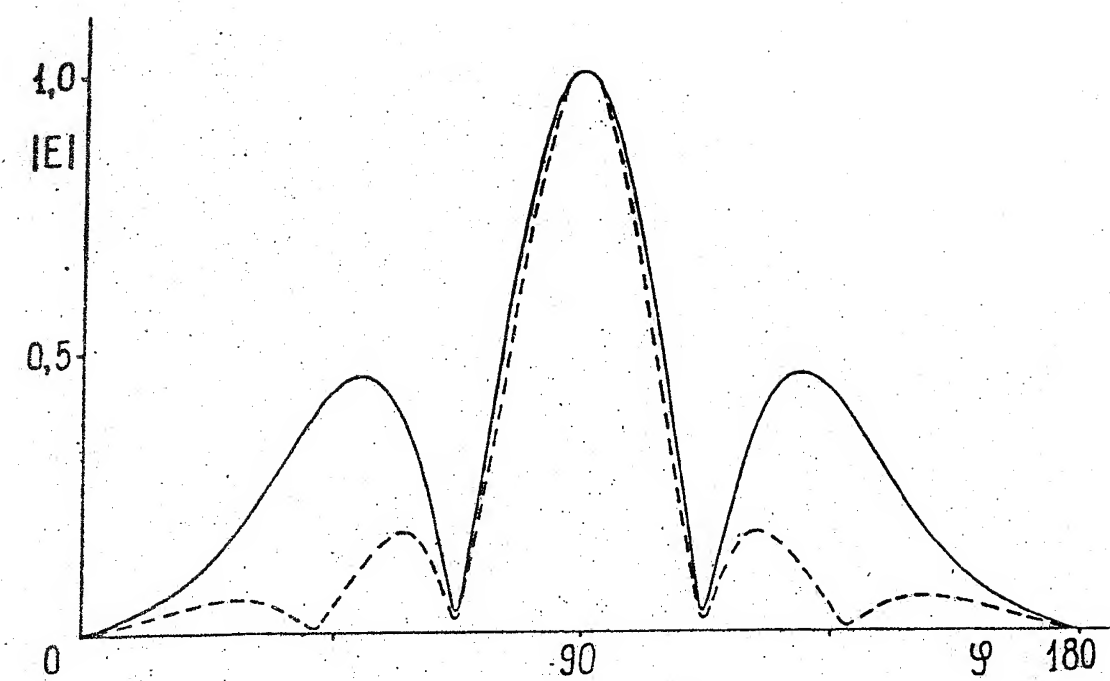


Fig. 1

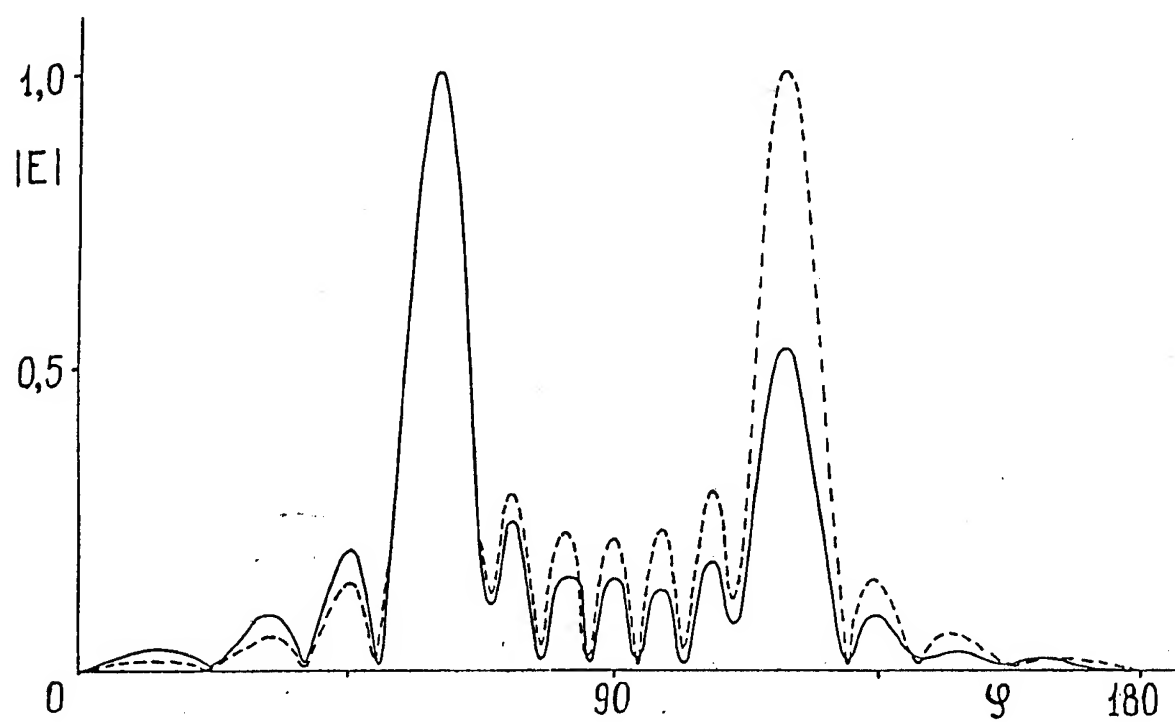
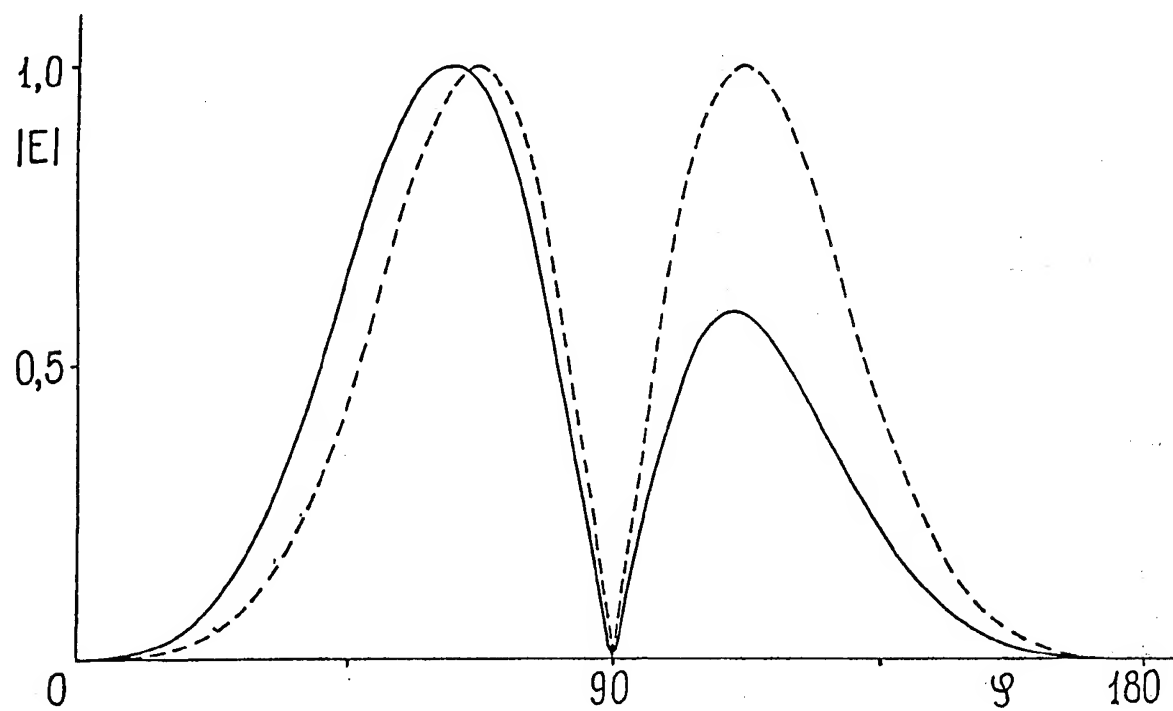


Fig. 2

# THE SCATTERING OF ELECTROMAGNETIC WAVES BY PERIODIC MAGNETODIELECTRIC LAYER.

VLADIMIR V. YACHIN AND NIKOLAY A. KHIZNYAK

Institute of Radio Astronomy  
of Ukrainian Academy of Sciences,  
4, Krasnoznamennaya st., Kharkov, 310002, Ukraine

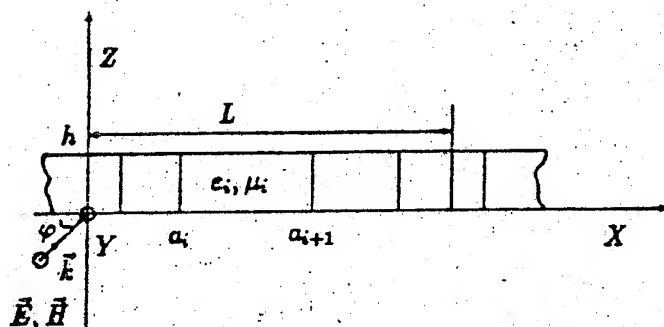


Fig. 1 Frequency selective surface composed of periodic magnetodielectric rods .

## ABSTRACT

The scattering of electromagnetic waves by periodic magnetodielectric layer was solved by the new method based on the rigorous integral equations of macroscopic electrodynamics. The general moments of the solution was given. The computer program for the numerical solution of the proposed scattering problem was created. The effect of moving of the maximum transmitting coefficient with changing of  $\epsilon$  modulation depth have been observed.

## METHODS AND RESULTS

The use of periodic magnetodielectric structures as elements of microwave engineering such as tunable selective filters, polarizes, varied types of shields as well as accelerating structure of laser accelerators makes the study of the problem of electromagnetic waves scattering by periodic magnetodielectric layers very interesting for practical purposes. At this point, of particular practical interest are the structures with controlled  $\epsilon$  and  $\mu$  of the layer. The solving of these problems has been carried out advantageously by the new method submitted here.

The solution of the problem of scattering H- and E- polarized waves by periodic multisegment magnetodielectric layer (Fig.1) and algorithm for the calculations of the scattered field characteristics have been obtained. Initial expressions for solving this problem are the rigorous integral relations of macroscopic electrodynamics which are equivalent to the Maxwell's equations [1/. These equations satisfy the boundary conditions, quasiperiodic conditions, the law of energy conservation, condition of energy limitation in any finite spatial volume and describe the field in every point of space.

The application of this method permits to find the scattered field characteristics in wide frequency range, in particular in resonance region [2/. The problem for the integral equations

can be reduced to the linear differential equations of the first degree with constant coefficients in functionals by entering the limited integral operator. In this manner it can be shown that scattered fields can be obtained through functionals mentioned above which contained complete information on geometric and physical field properties of one segment of layer.

The general vector problem was divided with two scalar problems (for H- and E- polarization). For the structure formed by periodic magnetodielectric rods the solution has been built for any polarization ( for example for H- polarization ). And the solution for E- polarization has been formed by formal substitutions : changing H and E components on E and H components accordingly and  $\epsilon$  on  $\mu$ ,  $\mu$  on  $\epsilon$ ,  $k$  on  $-k$ .

The integral functional can be written as :

$$C_{x,s}^i(\psi, z) = \sum_m 1/L(\epsilon_i - 1) \int_{mL+a_i}^{mL+a_{i+1}} E_{x,s}(x', z) e^{-ix'\psi} dx'$$

$$G_y^i(\psi, z) = \sum_m 1/L(\epsilon_i - 1) \int_{mL+a_i}^{mL+a_{i+1}} H_y(x', z) e^{-ix'\psi} dx';$$

and the limited integral operator as :

$$\hat{A}_n^i = \int_{2\pi/Ln}^{2\pi/L(n+1)} dv_n e^{iv_n} \sum_{m=-\infty}^{+\infty} \int_{mL+a_i}^{mL+a_{i+1}} dx e^{-ixv_n}.$$

Solving the obtained system of differential equation for the unknown functionals  $C_{x,s}$ ,  $G_y$  and substituting the obtained solutions into expressions for the scattered fields we can write transmitted fields for the H- polarization as :

$$H_y^tr = H_{0y} + k/4 \sum_s \frac{e^{is\psi} e^{is\chi_s} e^{-i\lambda\chi_s}}{\chi_s} \left( \sum_{n=1}^N a_n e^{\lambda\lambda_n} (\lambda + i\chi_s) [kW_6 - \psi, W_2 + \chi_s, W_3] + i(\chi_s - k_s) e^{i\lambda\lambda_s} P_s \right).$$

Here  $a_n$  defining spatial harmonic amplitudes and  $\lambda_n$  are the roots of the dispersion equation.

As an example we have considered the case of multisegment magnetodielectric layer. As a size of one layer segment shown in (Fig.1) tend to zero, a layer becomes holographic with a smooth changing of  $\epsilon$  along the X axis. By this means we can studied the model of acoustooptic grating, accompanied by the exploration of the effect of maximal transmitting coefficient movement with changing of an  $\epsilon$  modulation depth on incident angle. The solution for case of enclosed magnetodielectric grating has been also built [3/].

For H- polarization dispersive equation of the structure described above can be written in the following manner :

$$\left( \int_0^1 \frac{1}{\epsilon(x)} e^{v_n x} dx \right)^{-1} \left( \Psi \left( \int_0^1 \epsilon(x) e^{v_n x} dx \right)^{-1} \Psi + \int_0^1 \mu(x) e^{v_n x} dx \right) + \lambda^2 = 0$$

Where

$$v_n = 2i\pi/L(s - n), \quad \Psi = (k_s + 2\pi/Ln)I, \quad X^2 = k^2 I - \Psi^2$$

The integrals can be calculated as shown in [4/].

One of the aspects of holographic layers consideration is to obtain of frequency resonances of the structure when layer are acoustooptical element.

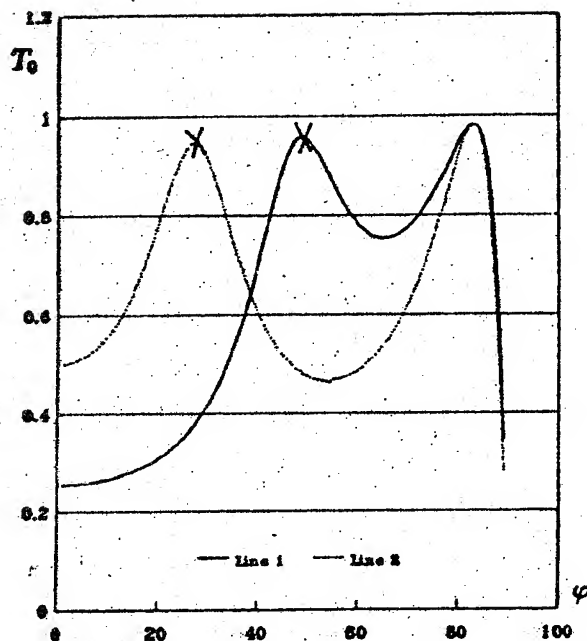


Fig.2 The transmitting coefficient  $T_0$  as a function of an incident wave angle .

In (Fig.2) displacement of marked with cross resonance when  $\epsilon$  depth have been varied is clearly visible. Here the dashed curve is for  $\epsilon = 69$  the solid curve is for  $\epsilon = 69 - 7 * \cos(2\pi/Lx)$

This investigation demonstrates a possibility of mechanical change of structure selective properties, what can be used for microwave device design.

The convergence and accuracy of the method were checked by a conservation of power criterion and by comparison with other published data, for example with /5/.

## REFERENCES

- (1) Khizhnyak N. A. et al "The Integral Equation of Macroscopic Electrodynamics", Naukova Dumka, Kiev, 1986. (in Russian)
- (2) Gamulya O.G., Yachin V.V., Borovski I.V., Math.Meth. in the Electromagnetic Theory, TPRS DI "Test - Radio", Alushta, 1991, 292-293
- (3) Yachin V.V., Khizhnyak N.A. International Symposium "Physics and Engineering of Millimeter and Submillimeter Waves", Kharkov, 1994, v.1
- (4) Naeimark B. et al " About the More Sophisticated Procedure of the Calculation of the Fourier Integral", Teor. i Vychisl. Geofizika 1974, n2, pp.50-54 (in Russian)
- (5) Bertoni, H.L., Li H.S.Cheo and T.Tamir "Frequency selective reflection and transmission by a periodic dielectric layer" Trans. Antennas Propagat. IEEE, V.37, 78-83, 1989.

# EXCITATION PROBLEM OF THE PLANAR SPIRAL IN THREE LAYER DIELECTRIC

K.P.Yatzuk, R.R.Shvelidze

Kharkov State University, High Freq. Dept.  
Svoboda sq., 4, Kharkov, 310077, Ukraine

## ABSTRACT

The excitation of a planar spiral placed in the three-layer dielectric medium in asymmetric wave regime has been analysed using the integral representation method. Numerical computations of the patterns, polarization and power characteristics have been carried out for various geometrical and physical parameters. A great influence of the system geometry and outer medium permittivity on radiated field characteristics has been shown.

## INTRODUCTION

In an earlier publication the contact planar spiral radiator of an alive organism was proposed. But a real radiator consists of spiral with substrate and superstrate layers and dielectric halfspace (a model of alive organism). In [1] the model of above mentioned system and the method of its investigation for symmetric waves was suggested. The radical changes of the radiation characteristics in the presence of dielectric medium were shown. The investigation of an asymmetric excitation of such system is of interest.

## PROBLEM SOLUTION

The system under consideration consists of planar spiral with substrate and superstrate layers and halfspace medium. We use the cylindrical coordinate system  $\rho, \varphi, z$  and consider three regions:

I -  $d < z < \infty$ ,  $\epsilon = \epsilon_1$ ; II -  $0 < z < d$ ,  $\epsilon = \epsilon_2$ ; III -  $-a < z < 0$ ,  $\epsilon = \epsilon_3$ , where  $\epsilon_1, \epsilon_2, \epsilon_3$  are permittivities. The spiral described by the curve

$\rho = \rho_0 \exp(\varphi/\mu)$ , where  $\mu$  is the spiral constant, is located in the plane  $z = 0$  and excited by the system of voltage sources located at the ring of small radius  $\rho = \rho_0$ . The source field is

$E = k_0 \delta(\rho - \rho_0) e^{in\varphi}$ , where  $\delta(\rho - \rho_0)$  is the Dirac delta function,  $U_0$  is the input amplitude. The grounded plane is located in the plane  $z = -a$ .

The electric and magnetic fields for each region are obtained from electric  $\vec{\Pi}_j^e$  and magnetic  $\vec{\Pi}_j^m$  Hertz vectors, oriented along the  $z$  axis

$$\vec{\Pi}_j^{e,m} = \sum_n e^{in\varphi} \int_0^\infty [A_{nj}^{e,m}(\delta) e^{ip_j z} + B_{nj}^{e,m}(\delta) e^{-ip_j z}] J_n(\delta \rho) \delta \delta \cdot \vec{z}_0, \quad (1)$$

where  $\rho_j = \sqrt{k^2 \epsilon_j - \gamma^2}$ ,  $k = 2\pi/\lambda$  is the free space wave number,  $\lambda$  is the free space wavelength,  $j$  is the region number,

$A_{nj}^{e,m}(\delta)$ ,  $B_{nj}^{e,m}(\delta)$  are the coefficients to be found.

For the first region ( $j=1$ )  $A_{n1}^{c,m}(\chi) = 0$ . That is why the fields for one asymmetric wave (number  $n$ ) may be represented as

$$E_{\varphi 1} = e^{in\varphi} \left[ \int_0^\infty \frac{\eta p_1}{p} B_{e1}(\chi) J_n(\chi p) e^{-ip_1 z} \chi d\chi + \right. \\ \left. + i\kappa \int_0^\infty B_{m1}(\chi) J_n'(\chi p) e^{-ip_1 z} \chi^2 d\chi \right], \quad (2)$$

where symbol " ' " is argument derivative.

Using the conventional boundary conditions on the dielectric boundaries and metal screen and the approximation of an anisotropic-conducting plane for the spiral, a set of 10 integral equations for unknown functions has been obtained. These integral equations are transformed by means of inverse Hankel formula to two coupled differential equations for two unknown functions and algebraic expressions for other ones.

It is convenient to express the far fields in spherical coordinates  $R, \theta, \varphi$ . Then  $\rho = R \sin \theta$ ,  $z = R \cos \theta$ . For  $R \rightarrow \infty$  the first term in (2) may be neglected, because  $1/p |_{R \rightarrow \infty} \rightarrow 0$ . Using the recurrency relation between the Bessel functions and asymptotics for large arguments one can use stationary phase method for integral (2) calculation. The stationary point in our case is

$\chi_{st} = \kappa \sqrt{\epsilon_1} \sin \theta$  and the expressions for far fields  $E_{\varphi 1}, E_{\theta 1}$  are

$$\begin{aligned} E_{\varphi 1} &= \left\{ B_{m1}(\chi_{st}) e^{i(n+1)\pi/2} \right\} \frac{R^3 \sin^2 \theta}{2R} e^{-i[\kappa \sqrt{\epsilon_1} R - n\varphi]} \\ E_{\theta 1} &= \left\{ B_{e1}(\chi_{st}) e^{i(n-1)\pi/2} \right\} \frac{R^3 \sin^2 \theta}{2R} e^{-i[\kappa \sqrt{\epsilon_1} R - n\varphi]} \end{aligned} \quad (3)$$

Using the algebraic relations between the coefficients, it was found, that

$$\begin{aligned} B_{m1}(\chi) &= B_{m2}(\chi) 2\epsilon_2 p_2 e^{-ip_2 d} / (\epsilon_1 p_2 + \epsilon_2 p_1), \\ B_{e1}(\chi) &= B_{e2}(\chi) 2p_2 e^{-ip_2 d} / (p_1 + p_2). \end{aligned} \quad (4)$$

Thus the problem is reduced to a solution of two coupled differential equations for unknown functions

$$\begin{aligned} \frac{d}{d\chi} [A_1(\chi) B_{e2}(\chi) + B_1(\chi) B_{m2}(\chi)] + C_1(\chi) B_{m2}(\chi) + D_1(\chi) B_{e2}(\chi) &= U_s, \\ \frac{d}{d\chi} [A_2(\chi) B_{e2}(\chi) + B_2(\chi) B_{m2}(\chi)] + C_2(\chi) B_{m2}(\chi) + D_2(\chi) B_{e2}(\chi) &= 0, \end{aligned} \quad (5)$$

where  $A_{1,2}(\chi), B_{1,2}(\chi), C_{1,2}(\chi), D_{1,2}(\chi)$  are the known functions of  $\chi, R, u, a, d, \epsilon_j$ ,  $U_s = -k_0 \chi^2 p_0^3 (1+u^2)^{1/2}$  is the source function. The system (5) was transformed to the normal form according to [2]. It was also established that the expressions for  $E_{\varphi 1}, E_{\theta 1}$  in (3) are to be multiplied by  $1/\exp(\epsilon_1 \kappa \tan \delta / \sin \theta)$ , if there are the losses in halfspace medium.



## NUMERICAL RESULTS

The computations were carried for the regime of  $n=1$  and a set of parameters  $\alpha, \mu, \epsilon_1, \epsilon_2, \epsilon_3, \kappa$ . It was established that for  $\epsilon_1 = \epsilon_2 = \epsilon_3 = 1$ ,  $\alpha = (2S+1)\lambda / (4\sqrt{\epsilon_3})$ , where  $S=1, 2, \dots$ , and various  $\mu$  the patterns were smooth and have maximum in the normal direction. The increase of  $\mu$  leads to the decrease of  $E_\theta$  amplitudes. In the case of  $\epsilon_1 = \epsilon_2 = \epsilon_3 = \epsilon > 1$  the pattern's smoothness does not vary, but the increase of  $\epsilon$  causes the growth of the radiated power and narrowing of lobe width. Fig. 1a, b show the amplitudes of  $E_\theta$  in halfspace medium ( $j=1$ ) as the function of the angle  $\theta$  for  $\mu = 1 \text{ cm}^{-1}$ ,  $\alpha = \frac{\lambda}{4}$ ,  $d = 0.2 \text{ cm}$ ,  $\epsilon_2 = \epsilon_3 = 1$ . The dashed curves are given for  $\epsilon_1 = 1$ ,  $\epsilon_2 = \epsilon_3 = \epsilon$ , the solid curves above and below the dashed ones are given for  $\epsilon_1 > 1$ ,  $\epsilon_2 = \epsilon_3 = \epsilon$  and  $\epsilon_1 > 1$ ,  $\epsilon_2 = \epsilon_3 = 0.3$  accordingly. Fig. 1a is for  $\mu = 10$ , Fig. 1b is for  $\mu = 2$ . From Fig. 1a, b one can see that if a permittivity of halfspace medium  $\epsilon_1$  is greater than the permittivity of supersstrate  $\epsilon_2$ , the side lobes (SL) in the patterns appear. The increase of  $\epsilon_1$  brings about the rising of SL amplitudes and SL shift to the main lobe. For some  $\epsilon_1 = \epsilon_2$  the SL merges with the main lobe and after that the increase of  $\epsilon_1$  causes the narrowing of the main lobe and the appearing of the second lobe. Fig. 1a, b show that for large  $\mu$  ( $\approx 10$ ) the spread of this process is more fast than for small  $\mu$  ( $\approx 1-2$ ). It is also observed that for small  $\mu$  the field amplitude is bigger than for great  $\mu$  for the same permittivity. In addition, pattern does not reach the normal to the spiral for small  $\mu$  but the lobe widths decrease with the increase of  $\epsilon_1$ .

In the case of small separation between spiral and screen ( $\alpha = 0.2 \text{ mm}$ ) we have the similar behaviour but with smaller amplitudes. The presence of the losses in halfspace medium causes the decrease of  $E_\theta$  amplitudes. For the given losses the increase of  $\epsilon_1$  results in the amplitude decrease for  $\mu \approx 10$ , but for  $\mu = 1-2$  the amplitudes pass through the maximum. In the vicinity of this maximum the field amplitude may be equal to the field amplitude in a lossless medium. But patterns in lossy medium are conical while they are axial in a lossless system.

Fig. 2 shows the axial ratio  $|Z|$  as function of  $\theta$  for parameters mentioned in Fig. 1a. It is clear that the increase of  $\epsilon_1$  gives rise to the variation of the polarization from the circular to linear in the direction normal to the spiral, but for some  $\alpha$  the  $|Z|$  may be equal to 0.6 - 0.8.

## REFERENCES

- (1) N.E. Ivanova et al.: "The electrodynamic properties of plain logarithmic helixes in three layer dielectric", Radiotek. i Electr., (1993), v. 38, N11. pp. 2010-2013.
- (2) K.P. Yatzuk et al.: "Calculation and experimental investigation of the radiation characteristics of a coupled logarithmic spirals with screen", Izv. VUS, Radioelectronica, (1978), v. 21, N8, pp. 3-9.

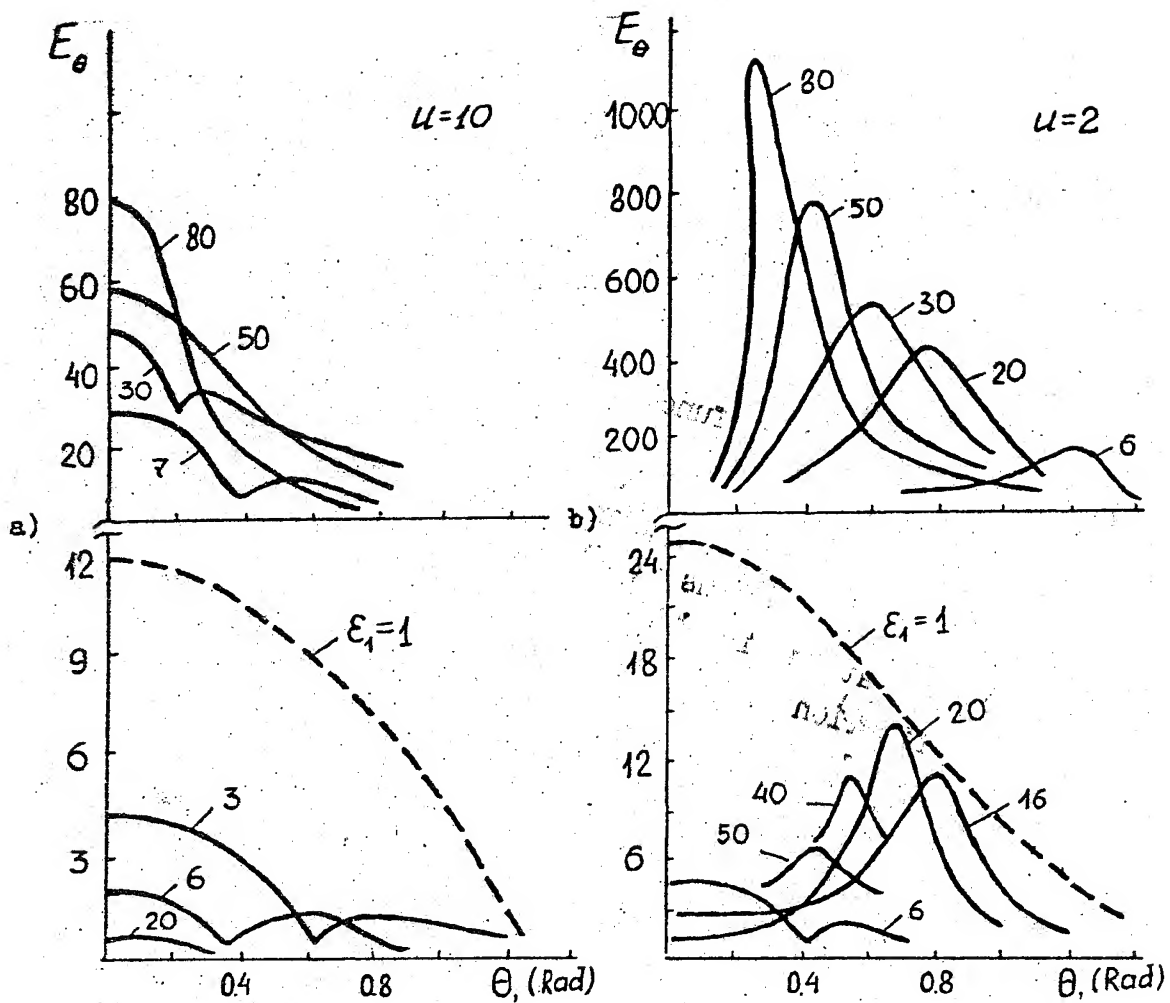


Fig.1 The amplitudes  $E_\theta$  in halfspace for various  $\epsilon_1$ .

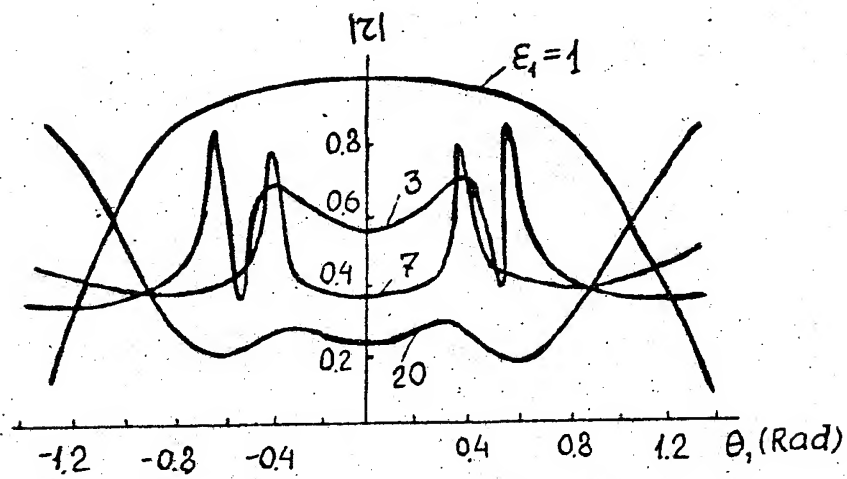


Fig.2 Axial ratio  $|z|$  for various  $\epsilon_1$ .

# CALCULATION OF ELECTRIC AND MAGNETIC FIELDS FOR THE DENSE LAMINAR ELECTRON BEAM FORMING

L. V. Yurchenko

Institute of Radiophysics and Electronics  
of Ukrainian Academy of Sciences, Kharkov 310085, Ukraine

Electron beams have usually a rather complicated structure due to a number of reasons, both the intrinsic (the influence of electron space charge) and the outer ones depending on the method of the beam focusing. In general case, electron motion is nonlaminar that is very undesirable. This paper presents the analysis which answers to the question whether or not such an Electron Optical System (EOS) could be synthesized that a strictly laminar high-power electron beam with any desired electrical and geometrical characteristics would be formed, and what kinds of restrictions take place in this case. As opposed to the previous investigations, the problem has been formulated in most general terms, that is, first, the conditions ensuring the forming of the given laminar high-power electron beam with the finite width have been found, without any approximation or restriction on the method of the beam focusing, and, second, the Dirichlet or Neumann boundary value problem for the Poisson equation has been considered, instead of an ill-posed Cauchy problem.

Suppose a dense axial electron beam is to be formed, with electron trajectories given by the equation

$$r = r(r_c, z) = \frac{1}{2} r_c \left[ (1 - \alpha) \cos \left[ \frac{\pi}{2} \left( 1 - \cos \frac{\pi z}{L} \right) \right] + (1 + \alpha) \right] \quad (1)$$

and the trajectory density distribution at the input end being as follows

$$P_c(r_c) = \begin{cases} \frac{1}{2} P_\infty (\cos(\pi r_c / R_c) + 1) & \text{if } r_c \leq R_c; \\ 0 & \text{if } r_c > R_c. \end{cases} \quad (2)$$

where  $L$  is the length of EOS section ( $0 \leq z \leq L$ ),  $R$  is its maximum radius ( $0 \leq r \leq R$ ),  $z$  and  $r$  are the longitudinal and radial coordinates, respectively,  $r_c$  is the parameter determining the specific trajectory of the beam passing the point  $(r, z)$ , namely, the radial coordinate of the initial point,  $P_\infty$  is the axial density of trajectories,  $R_c$  is the input radius of the beam ( $R_c = 0.5R$ ),  $R_A = \alpha R_c$  is the output radius,  $\alpha \leq 1$  is the coefficient of beam compression.

To determine the fields forming the given beam, it is necessary to solve the set of equations which consists of the motion equation for the charged particles in the axial electric and magnetic fields,

$$\frac{d^2 r}{dz^2} = \left( \frac{\partial Q}{\partial r} - \frac{\partial Q}{\partial z} \frac{\partial r}{\partial z} \right) \left[ 1 + \left( \frac{\partial r}{\partial z} \right)^2 \right] \frac{1}{2Q} \quad (3)$$

and the Poisson equation

$$\frac{\partial^2 U}{\partial r^2} + \frac{1}{r} \frac{\partial U}{\partial r} + \frac{\partial^2 U}{\partial z^2} = -\frac{\rho}{\epsilon_0} \quad (4)$$

where  $Q = Q(r, z) = U + \eta(\psi - \psi_c)^2/r^2$  is the unknown equivalent potential of the general force,  $U(r, z)$  is the electric potential,  $\psi(r, z)$  is the magnetic flux connected with the circuit of the radius  $r$ ,  $\psi_c$  is the value of  $\psi$  at the initial point of trajectory,  $\eta = e^2/8\pi^2 m$ ,  $e$  and  $m$  are the charge and the mass of electron respectively,  $\epsilon_0$  is the absolute dielectric coefficient,  $\rho(r, z)$  is the electron charge density which determines the electron concentration in the beam. The electron concentration depends on both the trajectory density cross-sectional distribution and the longitudinal component of the electron velocity  $V$  at the point with coordinates  $(r, z)$ , so it depends on the solution of the equation (3) as far as  $V(r, z) = \sqrt{-2eQ/m(1 + d^2r/dz^2)}$ .

Thus, we see that the problem considered in the most general and accurate formulation can be solved by determining the equivalent potential  $Q$  from the equation (3) and then electric potential  $U$  from the equation (4). The equipotential surfaces  $U = \text{const}$  yield the form of the possible EOS electrodes as well as their potentials. Using these potentials and the definition of  $Q$  presented in (3), the function  $\psi(r, z)$  and the current density in the EOS windings can be calculated from the corresponding Maxwell equation. Such a problem can be solved only numerically.

The set of the equations (3) and (4) must be completed by the boundary conditions. Since the equation (3) is the partial differential equation of the first order, it could be solved, in general, by the method of characteristics. In this case, the boundary condition is given by setting the value of the function  $Q$  along some curve which is not a characteristic of this equation. The analysis shows it is advisable to set the function on  $z$ -axis, i.e. at  $r = 0$ . The form of this function has essential influence on the further solution of the problem, and, in particular, on the electron velocity distribution and the current density in the beam. The Dormand-Prince method with automatic choice of integration step, as well as accuracy checking of obtained solution is used for solving this equation. The Poisson equation (4) has been solved by Stone's strongly implicit procedure. In order to apply this method, the rectangular domain of calculation ought to be considered and the boundary conditions at all the sides of it should be formulated. The most common and convenient conditions may be such ones when the values of the potential  $U$  are equal to the equivalent potential  $Q$  calculated on the previous stage of the solution at all the parts of the boundary. Thus, the Dirichlet boundary-value problem for the Poisson equation arises

$$U|_s = Q|_s \quad (5)$$

where  $s$  is the closed boundary of the rectangular domain of calculation. Under these conditions the relation

$$\psi(r_s, z_s) = \psi_c(r_s, z_s) \quad (6)$$

takes place at all the points of the boundary. In the plane  $z = 0$  this relation must be satisfied by definition. Therefore, the condition  $U = Q$  is obligatory at the boundary  $z = 0$ . The potential  $U$  can be given arbitrarily at the boundaries  $z = L$  and  $r = R$ . It means that, in general, the magnetic fluxes are not connected by the relation (6). In

this work we, however, consider only the case when  $U = Q$  at these boundaries. As for the condition to which the potential on the axis of the EOS have to satisfy, this one is reduced to requirement of the absence of the radial field component (this is due to the axial symmetry of the problem and the finiteness of current density at the axis), namely,

$$\frac{\partial U}{\partial r} = 0, \quad \text{for } r = 0. \quad (7)$$

For the potential  $Q$  the equation  $\partial Q/\partial r = 0$  is valid too, because  $dr/dz = 0$  and  $d^2r/dz^2 = 0$  at the axis. Since the magnetic field does not tend to infinity, the magnetic flux  $\psi$  decays rapidly with decreasing  $r$  ( $\psi \sim r^2$  for  $r \rightarrow 0$ ) and the equation  $\partial Q/\partial r = 0$  is in good agreement with the condition (7). Moreover, since  $\psi = \psi_c = 0$  at  $r = 0$ , the equation  $U = Q$  is valid at the axis  $z$  too. This equation can be used as the boundary condition at this part of the boundary. However, keeping in mind the possible errors arising under numerical simulations we used (7) at  $r = 0$  and the condition (5) at the rest three parts of the boundary ( $z = 0, z = L$  and  $r = R$ ).

Note, that functions  $U$  and  $Q$  differ from each other only in the presence of magnetic field, such that  $\psi(r, z) \neq \psi_c(r_c)$  in the inner points of the domain of calculation. It means that, in general, the arbitrary laminar electron beam cannot be formed only by electric field without magnetic one. The choice between different solutions under the given configuration of the beam depends on formulation of different boundary conditions to the equations (3), (4). Thus, it is connected with arbitrary choice of the four functions: electric potentials  $U(R, z)$  and  $U(r, L)$  along generatrix  $r = R$  and at the EOS output cross-section  $z = L$ , respectively; the magnetic flux  $\psi_c(r_c)$  at the input cross-section  $z = 0$  and the equivalent potential  $Q(0, z)$  at the axis  $r = 0$  (in the last case, if the velocity of electrons at the beam axis was not given beforehand). According to the boundary conditions chosen above, this paper considers basically the influence on the electron beam of the two functions out of four, namely,  $Q(0, z)$  and  $\psi_c(r_c)$ .

The different kind of beams were considered including the cases of transverse, longitudinal and simultaneous transverse-longitudinal compression as well as the uniform cylindrical beam. The distributions of electric and magnetic fields for the most general situation when both the transverse and longitudinal compression of the beam takes place are shown in Fig.1. Here  $\alpha = 0.5$  and the dependence  $Q_0(z)$  is given as

$$Q_0(z) = Q_c \exp(-z^2/l^2), \quad (8)$$

where  $Q_c$  is the potential at the EOS input end,  $l$  is the characteristic length of the  $Q$  variation, such that  $Q_0(0)/Q_0(L) = 4$ . Fig.1a shows that the electrodes creating the electric potential must have the shape of rotation surfaces coinciding with some of the calculated equipotential surfaces (thin curves) and have a corresponding value of potential. In this case, for example, we can chose the surfaces determined by thick curves 1-3 in Fig.1a. Thus, in the situation considered we arrive at the three electrode scheme of EOS. Note that the solution obtained has some interesting features which consist in the fact that the inner electrode (the second in Fig.1a) has not repulsive but attractive potential with respect to the both electrodes 1 and 3. The latter enables one to balance better the focusing action of magnetic field, which is greater for exterior trajectories than for interior ones. Such a balance provides the necessary laminar structure of the beam with a uniform thickening of trajectories and without their intersection. Fig.1b shows that magnetic flux

distribution needed to create the given beam has a complicated form, but it can be simplified considerably if the values of  $\psi_c(r_c)$  are changed. The required distribution of  $\psi_c(r, z)$  can be always created by the corresponding distribution of azimuthal currents calculated from the Maxwell equations.

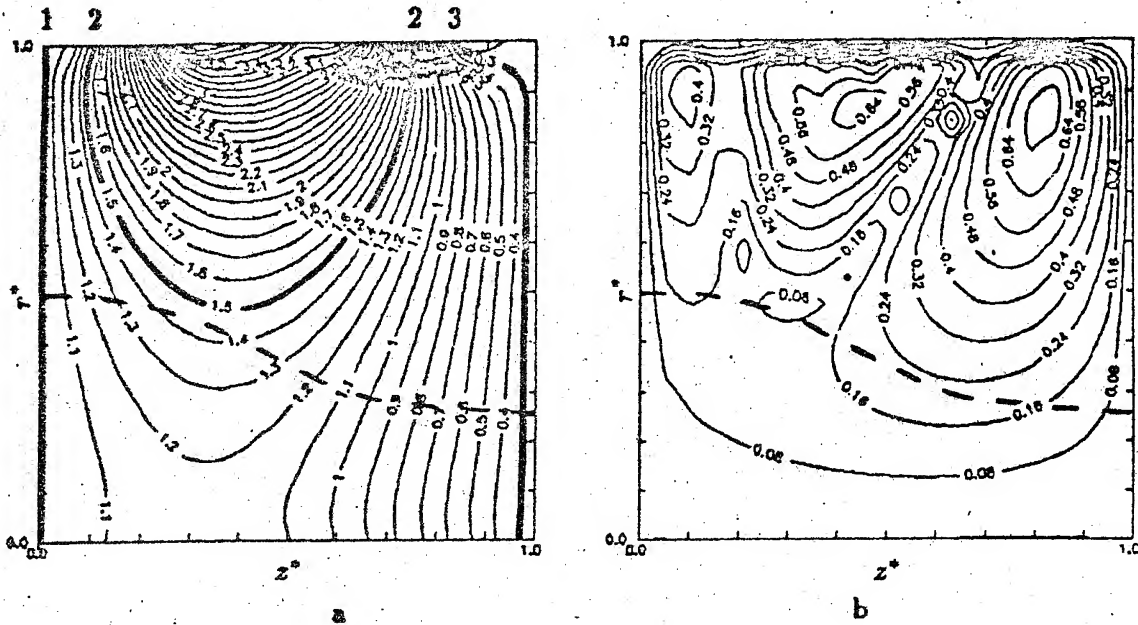


Fig.1. Spatial distribution of (a) the electric potential  $U^*$  and (b) the magnetic flux  $\psi^*$  in the relative units ( $U = c_U U^*$ ,  $\psi = c_\psi \psi^*$ ,  $r = c_L r^*$ ,  $z = c_L z^*$ , where  $c_U$  and  $c_L$  are the scaling factors,  $c_\psi = 4\pi(2e/m)^{-1/2} c_U^{1/2} c_L$ ). The dashed line depicts the edge of the electron beam.

Thus, the general possibilities and the conditions for creating dense laminar axial electron beams with arbitrary configuration and any kind of beam compression have been studied. The problem of calculating electric and magnetic fields forming the given beam was reduced to successive solution of the linear partial differential equation of the first order (the equation for the equivalent potential  $Q$  with variable coefficients), and the second order one (the Poisson equation with the charge density dependent on  $Q$ ), under the suitable conditions at the boundaries. If both the spatial beam structure (the form of the trajectories and their spatial distribution) and the axial electron velocity are given, then, under the given choice of electric potential at the EOS boundaries and the magnetic flux in the input cross-section of the beam, the solution of the problem always exists and is unique. A number of numerical solutions, for a set of qualitatively different physical situations being of the practice interest has been obtained. Since the formulation of the boundary conditions for this problem (the choice of values of magnetic flux and potentials on the boundaries) is arbitrary, to a great extent, then the solutions of the problem may be different, i.e. the beam with the given parameters can be created by essentially different electric and magnetic fields.

# SPACE-TIME CONCENTRATION of WAVE PROCESSES

D.Zanevskiy, S.Nefedov, Ph.Petrosian

Minsk Higher Military Engineering college

220057 Minsk-57 MHMEC

## ABSTRACT

The work deals with the method of radiation energy concentration in the fixed volume of space in far zone. It was investigated a radiation field structure of lineal and double - dimensional multi-frequency arrays (MFA) with the lineal law of frequency alteration by means of analytic and numerical methods. It was described a way of creation of electric and guided sectors of radiation energy concentration in compliance with the situation and dimensions.

The work comprises the results of numerical modulation of radiation field for different amplitude and frequency distribution on aerial array and different amplitude and frequency of elements, the comparative analysis of their energetical characteristics between themselves and with energetics of one - frequency array as well as the question of radiation field stability relative to an error of aerial production, phasing arrange, heterogeneity of distribution way, frequency unstability and so on. The work deals with questions of practical realizations of multi - frequency arrays.

## INTRODUCTION

The problem of wave processes concentration has two major applications: transmission of energy without using guiding equipment or localization of energy in the fixed volume of space.

The conventional methods of energy concentration such as: using collimated beams or their superposition (energy channelling) and focusing of radiation at point (energy localization) are usually used at the present time.

The essential disadvantage of the traditional methods of energy concentration is a limitation of the action radius by dimensions of Frienele zone and this fact limits a sphere of its application. This disadvantage may be solved by expansion the radiation signal spectrum. Using the nonsinus signals



[1] determines the complicated technical realization.

Therefore, it is very interesting to find the decision of this problem by means of multi-frequency arrays, which each of elements radiates harmonious signal.

#### SPACE-TIME CONCENTRATION of WAVE PROCESSES by MEANS of MFA

Using the multi-frequency excitation of aerial arrays in contrast to conventional one-frequency arrays gives the additional extension in time coordinate that results the specific space-time structure of radiation field for this array. This structure depends on geometry of radiation aperture, number of elements, amplitude and frequency distribution (AFD) of radiation signal. The numerical aerial array model was created to analyze the field space-time structure.

It was studied the dependence of radiation field space distribution as function of radiational elements frequencies location on aperture with uniform amplitude distribution. It was considered linear frequency distribution along aperture coordinates, superposition of linear, square and arbitrary nonlinear distributions. Sometimes it can be gained analytical expressions for radiation field that are described in the report.

Field distribution for linear aerial array with linear-increasing FD  $f=f_0+nf_n$  is described by expression:

$$F(\theta, r) = \frac{\sin(\frac{N\Phi}{2})}{\sin(\frac{\Phi}{2})}, \quad \Phi = -k_0 d \sin\theta + k_n r - \Omega t. \quad (1)$$

This expression is differed from well-known expression for one-frequency array by addition argument  $\Phi$  items, which give to field a new properties. The radiation field at fixed time moment has evident maximum if the frequency dependence of element coordinates is linear. This maximum moves along angle coordinate in limits of radiation pattern width with changing a range of observed point. All picture moves along propagation axis with speed of this wave if time  $t$  is alternating. Disadvantage of such AFD is redistribution of average power density during the period that becomes uniform in limits of element radiation pattern width.

Field distribution for linear array with linear-changing symmetric FD  $f=f_0+nf_n$  is described by expression:



$$F(\theta, r) = 2 \frac{\cos \frac{N-1}{2} \alpha \cos \frac{N+1}{2} \beta - \cos \frac{N+1}{2} \alpha \cos \frac{N-1}{2} \beta}{\cos \beta - \cos \alpha} \quad \beta = -k_0 d \sin \theta$$

$$\alpha = k_n r - \Omega t \quad (2)$$

In normal direction is formed space field pulse, which exceed the field in other directions by 3-8 dB.

It was determined that linear MFA are not able to solve a energy concentration task because of approximately uniform redistribution of average power density during the period.

More best space field distribution is provided by use rectangular or hexagonal aerial aperture. The analyze of results shows that the most optimal case is superposition both linear-increase and linear-decrease frequency distributions in dependence on the elements number. In this case partial fields in fixed space of volume is summed with the same phase, but in other space - with casual phase. It results to additional power gain. The field distribution of such array is a space pulse sequence, which is formed in sectors where took place the condition of sinphase summing of partial fields of elements and move with the period, which is inverse proportional to modulate frequency. Elements number increase results to increasing pulse field intensity with it simultaneous shorting in the time and decrease of relative level of field outside space-time length.

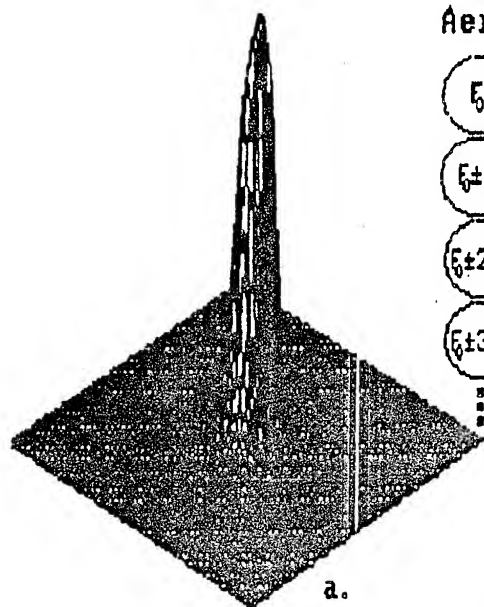
Kind of amplitude distribution insignificantly changes field structure, but it promotes increase the degree of reciprocal compensation of spectral components outside the fixed local volume and provides redistribution of this power part.

The creation of electric-guided sectors of radiation energy concentration in compliance with the situation and dimensions may be reached by means of the aerial radiation time strobing. Distribution of average density of power flow during the period of the considered field is represented in fig.1 (a - space distribution, b - aerial structure, c - projection of space distribution).

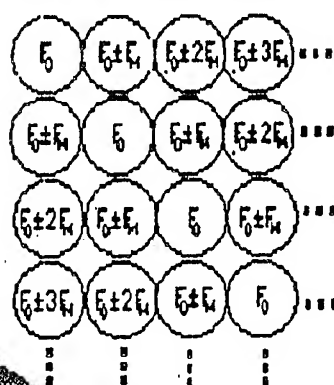
The analyse of fig.1 shows that average radiation energy during the period is concentrated in the fixed volume of space.

It was studied the question of radiation field stability relative to different destability factors (errors of aerial production, phasing arrange, heterogeneity of distribution way,

## Middle density of power flow



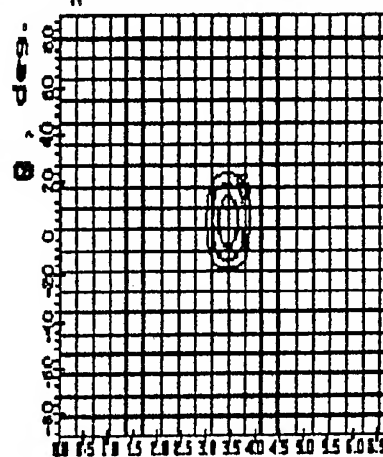
## Aerial structure



b.

## Field projection

$N=81$ ,  $f_0=0.01\text{ MHz}$ ,  
 $f_N=0.05\text{ kHz}$ ,  $d=1.5\text{ cm}$



c.

fig.1

frequency instability and so on). The analysis of results show that radiation field structure has good stability relative to influence of different destability factors and it was almost not changed by the influence of root-mean-square deviation frequency not over  $10^{-4}$ , phase -  $40^\circ$ , amplitude - 30%.

The work deals with the questions of practical realizations of scientific reaserchers, such as: using cross-concentrating field in purpose to create the ionization volume of atmosphere for its application in radiocommunication re-transmitter; using multifrequency ultrasound devices in purpose to increase quality of medical image and increase safety measures medical reaserches, using MFA in purpose to increase secrecy and vitality of radars and radiocommunication devices.

## CONCLUSION

Therefore, the field concentration method with use of MFA allows to expand the capabilities of existente technical devices considerably and reach new properties, which are not realized by means of conventional devices.

## REFERENTS

1. R.W.Ziolkowski "Electromagnetic or other directed energy pulse launcher" US patent 4.959.559, H01Q3/26.

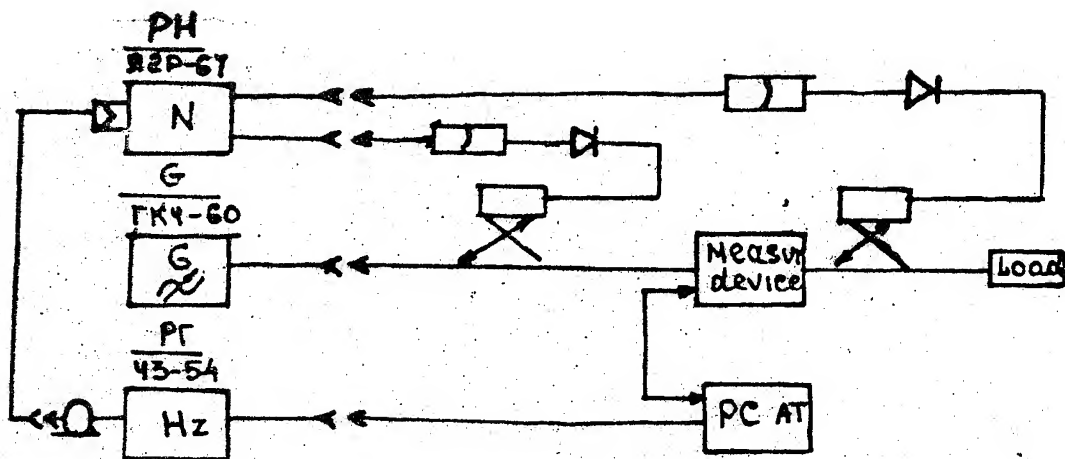
# HIGH-ACCURACY METHOD FOR NON-DESTRUCTIVE LOCAL PARAMETER MICROWAVE MEASUREMENTS OF MATERIALS

Dr.sc. ZVYAGINTSEV A.A., Dr.sc. STRIZHACHENKO A.V.

University, Kharkov, Ukraine

Modern methods of measurement allow to determine with a high degree of exactness dielectric electric parameters. However, the overwhelming majority of existing measuring instruments made on the basis of those methods are actually destructive measuring means, allowing to measure only integral characteristics of materials. Modern technological process demands a basically new approach to this problems: manufacturing new high  $Q$  and highly expensive materials (leucosapphires, artificial rubins, a number of ferrite marks, etc.) and also goods on their basis (stripline bases and microwave integral schemes, dielectric waveguides and resonators, etc.) supposes materials characteristics measurements without ruining them. From this point of view nondestructive methods of measurement possess obvious advantages. Nevertheless, the existing non-destructive measuring means mostly have a not very high exactness of measurement of dielectric permittivity, magnetic permeability and material losses and also have low sensitivity to their changes. On the basis of our analysis, an automated complex, allowing to measure samples measurability with high degree of exactness, effectively and without destructing them, has been constructed. An original part of the complex is a measuring device on the basis of a waveguide junction of cylindrical and radial waveguides. The necessary condition of natural modes presence in such a structure is out-off of all junction-forming waveguides at resonant frequencies. In such a case an electromagnetic field of resonating modes appears to be concentrated in the region of waveguide junction and its characteristics (resonant frequency,  $Q$ -factor) are determined by the region sizes and the parameters of that volume of the sample being tested, which is to be found in the above-mentioned region. The coupling of a measuring resonator with the plumbing of the automatic VSWR and attenuation meter (a measuring complex block-diagram is shown in Fig.1) is achieved by waveguide-to-coaxial adapters ending in excitation elements and a waveguide channels selector. A test sample of flat form and arbitrary configuration in the perimeter (a substrata, a disk, etc.) is fixed on a frame with divisions on it. The frame is moved on the guides so that the sample part successively get into each resonant region.

After a measuring section is made, there is no need in special tuning of any kind. The integration of a frequency meter and personal computer, allowing to introduce data from the frequency meter directly in the process of measurements, allows to essentially improve the effectiveness of measurements. The measuring complex includes PC AT 286/287, due to which the



average time of one  $\varepsilon$ ,  $\mu$  and  $\text{tg}\delta$  measurement with the error of not more than 0.5% ( $\varepsilon, \mu$ ) and 3% ( $\text{tg}\delta$ ), is 5-10 sec. The symmetrical  $H_{011}$  mode and non-symmetrical

## CONCLUSION

## **MANUSCRIPTS**

received after the deadline

# THE GENERALIZE SOLUTIONS OF BESSEL EQUATIONS

Alexander Khapalyuk

Applied Physical Problems Research Institute  
7 Kurchatov Str., Minsk 220064, Belarus

Let's apply to Bessel equation [1]

$$x^2 \frac{d^2 \hat{z}_\nu(x)}{dx^2} + x \frac{d\hat{z}_\nu(x)}{dx} + (x^2 - \nu^2) \hat{z}_\nu(x) = 0 \quad (1)$$

Fourier transformation and get new equation

$$(\xi^2 - 1) \frac{d^2 \check{z}_\nu(\xi)}{d\xi^2} + 3\xi \frac{d\check{z}_\nu(\xi)}{d\xi} + (1 - \nu^2) \check{z}_\nu(\xi) = 0 \quad (2)$$

In this case the solutions of equation (1) (Bessel function) are interpreted as the original and those of equation (2) - as the transformant. Those the one-to-one correspondence between solutions of this equations is established via Fourier integrals

$$\check{z}_\nu(\xi) = \int_{-\infty}^{\infty} \hat{z}_\nu(x) e^{ix\xi} dx, \quad \hat{z}_\nu(x) = \frac{1}{2\pi} \int_{-\infty}^{\infty} \check{z}_\nu(\xi) e^{-ix\xi} d\xi. \quad (3)$$

This give possibilities to present the comparative complex solutions of Bessel equations as inverse Fourier transformations of very simple solutions of equation (2) that promote the investigation of it's properties substantially. Further instead equations (3) we will use reduced form:  $\hat{z}_\nu(x) \rightarrow \check{z}_\nu(\xi)$ .

The solutions of equation (2) may be written as:

$$\check{z}_\nu(\xi) = \frac{(1\xi + \sqrt{1-\xi^2})^\nu}{\sqrt{1-\xi^2}}, \quad \check{z}_{-\nu}(\xi) = \frac{(1\xi + \sqrt{1-\xi^2})^{-\nu}}{\sqrt{1-\xi^2}} = \frac{(-1\xi + \sqrt{1-\xi^2})^\nu}{\sqrt{1-\xi^2}}. \quad (4)$$

It is necessary to calculate the inverse Fourier transformations

of functions (4) and hence to found the solutions of Bessel equations. But there are difficulty on this way: when  $\xi = \pm 1$  the branch points exist and Fourier integrals converge not for all  $\nu$ . It is necessary to examine the particular case of integer value of  $\gamma$  ( $\gamma = m, m = 0, \pm 1, \pm 2, \dots$ ).

For integer order the solutions of equation (2) better to write in different forms that are linear combinations of solutions (4):

$$\frac{T_m(\xi)}{\sqrt{1-\xi^2}}, \quad U_m(\xi), \quad (5)$$

where  $T_m(\xi)$  and  $U_m(\xi)$  are Chebyshev polynomials of first and second order that are defined here by identity:

$$(\xi + i\sqrt{1-\xi^2})^m = T_m(\xi) + i\sqrt{1-\xi^2} U_m(\xi). \quad (6)$$

The first expression in (5) has two branch points. It is not difficult to see that for different selection of branches we get different solutions. The investigation shows that the branch selection gives three linear independent solutions. When to take the branch selection into account the solutions (5) may be written as next four independent variants:

$$\begin{aligned} \check{z}_m^{(1)}(\xi) &= T_m(\xi) \begin{pmatrix} 0 \\ 1 \\ \sqrt{1-\xi^2} \\ 0 \end{pmatrix}, & \check{z}_m^{(2)}(\xi) &= T_m(\xi) \begin{pmatrix} 1 \\ \sqrt{\xi^2-1} \\ 0 \\ 1 \\ \sqrt{\xi^2-1} \end{pmatrix}, \\ \check{z}_m^{(3)}(\xi) &= T_m(\xi) \begin{pmatrix} 1 \\ \sqrt{\xi^2-1} \\ 0 \\ -1 \\ \sqrt{\xi^2-1} \end{pmatrix}, & \check{z}_m^{(4)}(\xi) &= U_m(\xi). \end{aligned} \quad (7)$$

Here and in the next the upper line define the solution when  $\xi > 1$ , the middle line - when  $|\xi| < 1$  and below line - when



integer order. The Fourier integrals for first solution converge in usual sense for all  $m$  and they are in literature [2]. But we use different method that is applicable in more complicated cases:

$$\begin{aligned}\hat{z}_m^{(1)}(x) &= \frac{1}{2\pi} \int_{-1}^1 \frac{T_m(\xi)}{\sqrt{1-\xi^2}} e^{-ix\xi} d\xi = T_m\left(i\frac{d}{dx}\right) \frac{1}{2\pi} \int_{-1}^1 \frac{e^{-ix\xi}}{\sqrt{1-\xi^2}} d\xi = \\ &= \frac{i}{2} T_m\left(i\frac{d}{dx}\right) J_0(x),\end{aligned}\quad (8)$$

where  $J_0(x)$  - usual Bessel function of first kind zero order. The polynomial  $T_m(\xi)$  is considered here as multiplier [2] that can be factored outside the integral sign. Then change the variable of integration on operator of differentiation with respect to  $x$  ( $\xi \rightarrow i d/dx$ ). This is known method in theory of generalize function of L.Schwartz and it is applicable in particular to calculation of some integrals that not convergent in usual sense including Fourier integrals for remain three solutions (7). All four solutions are easy get with this method and they may be written in view of standart normalization as:

$$\begin{aligned}J_m(x) &= 2i^m \hat{z}_m^{(1)}(x) = i^m T_m\left(i\frac{d}{dx}\right) J_0(x), \\ 2i^m \hat{z}_m^{(2)}(x) &= i^m T_m\left(i\frac{d}{dx}\right) Y_0(|x|), \\ 2i^m \hat{z}_m^{(3)}(x) &= i^m T_m\left(i\frac{d}{dx}\right) [J_0(|x|) \operatorname{sgn} x], \\ i^m \hat{z}_m^{(4)}(x) &= i^{m-1} U_m\left(i\frac{d}{dx}\right) \delta(x),\end{aligned}\quad (9)$$

where  $Y_0(|x|)$  - Bessel function of second kind,  $\delta(x)$  - Dirac



function. The solutions are generalize functions of L. Schwartz and hence all derivatives in (9) exist and practically can be founded easy.

It is obviously that all four equations are linearly independent and they identically satisfy Bessel equation. First of this solutions fully coincide with known Bessel function of first kind, second solutions differ from known Bessel function of second kind, third and fourth solutions are new. The fourth solution of zero order don't define on formula (7) and (9) and can be written as [2]:

$$\hat{z}_0^{(4)}(x) = Y_0(|x|) \operatorname{sgn} x - \frac{4}{\pi} \left\{ \frac{\ln(\xi - \sqrt{\xi^2 - 1})}{-i\sqrt{\xi^2 - 1}} + \frac{\ln(i\xi + \sqrt{1 - \xi^2})}{\sqrt{1 - \xi^2}} + \frac{\ln(-\xi - \sqrt{\xi^2 - 1})}{i\sqrt{\xi^2 - 1}} \right\} \quad (10)$$

Turn to solutions (4) for common case. For different selection of branches it is possible to get rather few different particular solutions, but only four from their will be linearly independent. For definiteness taken next four sufficient simple solutions (let us call their as b-solutions).

$$\begin{aligned} \delta_v^{(1)}(\xi) &= \begin{cases} e^{i\nu\frac{\pi}{2}} \frac{(\xi - \sqrt{\xi^2 - 1})^\nu}{-i\sqrt{\xi^2 - 1}} \\ e^{i\nu\frac{\pi}{2}} \frac{(\xi - i\sqrt{1 - \xi^2})^\nu}{\sqrt{1 - \xi^2}} \end{cases}, & \delta_v^{(2)}(\xi) &= \begin{cases} e^{-i\nu\frac{\pi}{2}} \frac{(\xi - \sqrt{\xi^2 - 1})^\nu}{i\sqrt{\xi^2 - 1}} \\ e^{-i\nu\frac{\pi}{2}} \frac{(\xi + i\sqrt{1 - \xi^2})^\nu}{\sqrt{1 - \xi^2}} \end{cases}, \\ & \begin{cases} e^{-i\nu\frac{\pi}{2}} \frac{(-\xi - \sqrt{\xi^2 - 1})^\nu}{i\sqrt{\xi^2 - 1}} \\ e^{i\nu\frac{\pi}{2}} \frac{(-\xi - \sqrt{\xi^2 - 1})^\nu}{-i\sqrt{\xi^2 - 1}} \end{cases} \end{aligned} \quad (11)$$

$$\delta_{\nu}^{(3)}(\xi) = \begin{cases} e^{-i\nu\frac{\pi}{2}} \frac{(\xi + \sqrt{\xi^2 - 1})^{\nu}}{-i\sqrt{\xi^2 - 1}} \\ e^{i\nu\frac{\pi}{2}} \frac{(\xi + i\sqrt{1 - \xi^2})^{\nu}}{\sqrt{1 - \xi^2}} \\ e^{i\nu\frac{\pi}{2}} \frac{(-\xi + \sqrt{\xi^2 - 1})^{\nu}}{i\sqrt{\xi^2 - 1}} \end{cases}, \quad \delta_{\nu}^{(4)}(\xi) = \begin{cases} e^{i\nu\frac{\pi}{2}} \frac{(\xi + \sqrt{\xi^2 - 1})^{\nu}}{i\sqrt{\xi^2 - 1}} \\ e^{i\nu\frac{\pi}{2}} \frac{(\xi - i\sqrt{1 - \xi^2})^{\nu}}{\sqrt{1 - \xi^2}} \\ e^{-i\nu\frac{\pi}{2}} \frac{(-\xi + \sqrt{\xi^2 - 1})^{\nu}}{-i\sqrt{\xi^2 - 1}} \end{cases}.$$

That are linearly independent solutions for fractional  $\nu$  and for integer  $\nu$  only three solutions stay linearly independent but fourth solution is easy founded additionally. The solutions (11) are reliable base for investigation of all space of solutions of Bessel equation.

It is seen from (11) that b-solutions satisfy to conditions:

$$\delta_{\nu}^{(2)}(\xi) = \delta_{\nu}^{(1)*}(\xi), \quad \delta_{\nu}^{(3)}(\xi) = \delta_{-\nu}^{(1)}(\xi), \quad \delta_{\nu}^{(4)}(\xi) = \delta_{-\nu}^{(1)*}(\xi), \quad (12)$$

that after inverse Fourier transformation go to next conditions for b-solution of Bessel equation:

$$\delta_{\nu}^{(2)}(x) = \delta_{\nu}^{(1)*}(-x), \quad \delta_{\nu}^{(3)}(x) = b_{-\nu}^{(1)}(x), \quad \delta_{\nu}^{(4)}(x) = b_{\nu}^{(1)*}(-x). \quad (13)$$

The Fourier integrals for function (11) converge in usual sense and meet in literature, for example, ones [2] have next values of Fourier integrals:

$$J_{\nu}(|x|) \rightarrow \delta_{\nu}^{(1)}(\xi) + b_{\nu}^{(2)}(\xi), \quad \nu > -1,$$

$$J_{\nu}(|x|)\operatorname{sgn} x \rightarrow \delta_{\nu}^{(1)}(\xi) - b_{\nu}^{(2)}(\xi), \quad \nu > -2, \quad (14)$$

$$Y_{\nu}(|x|) \rightarrow \operatorname{ctg} \nu \pi [\delta_{\nu}^{(1)}(\xi) + b_{\nu}^{(2)}(\xi)] - \operatorname{cosec} \nu \pi [b_{\nu}^{(3)}(\xi) + b_{\nu}^{(4)}(\xi)], \quad |\nu| < 1$$

$$Y_{\nu}(|x|)\operatorname{sgn} x \rightarrow \operatorname{ctg} \nu \pi [b_{\nu}^{(1)}(\xi) - b_{\nu}^{(2)}(\xi)] - \operatorname{cosec} \nu \pi [b_{\nu}^{(3)}(\xi) - b_{\nu}^{(4)}(\xi)], \quad |\nu| < 2$$

This formulae define all four linear independent solutions for  $|\nu| < 1$ . As seen they are close to classic one's the difference is that  $|x|$  is argument but not  $x$  and from one classic solutions we get two generalige solutions - even and odd. From (14) it is easy to get the b-solutions:

$$\begin{aligned} \delta_\nu^{(1)}(x) &= \frac{1}{2} [J_\nu(|x|) + J_\nu(|x|) \operatorname{sgn} x] = J_\nu(x_+), \\ \delta_\nu^{(2)}(x) &= \frac{1}{2} [J_\nu(|x|) - J_\nu(|x|) \operatorname{sgn} x] = J_\nu(x_-), \\ \delta_\nu^{(3)}(x) &= \cos \nu \pi J_\nu(x_+) - \sin \nu \pi Y_\nu(x_+) = J_{-\nu}(x_+), \\ \delta_\nu^{(4)}(x) &= \cos \nu \pi J_\nu(x_-) - \sin \nu \pi Y_\nu(x_-) = J_{-\nu}(x_-), \end{aligned} \quad \begin{array}{l} \nu > -1 \\ (15) \\ |\nu| < 1, \end{array}$$

where notations  $f(x_\pm) = f(|x|)h(\pm x)$  and  $h$  - Hevicide function are used.

It is need to remove the limitation on value  $\nu$  in (14)-(15) and find the solution for arbitrary value of  $\nu$ . But when  $\nu$  is arbitrary Fourier integrals and their solutions (11) don't converge in usual sence and their calculation is hindered. Use the idea that was applied for definition the solutions for integer value of  $\nu$ . For large integer value of  $\nu$  the deriving of results of calculations of correspuding Fourier integrals reduce in correspondence to (9) to differentiation of solutions of zero order. Analogous with that we try to get the solutions for arbitrary value of  $\nu$  from known solutions (14)-(15) for  $|\nu| < 1$ .

Get  $\nu = m + \lambda$ , where  $m$  is some integer positive or negative number and write the solutions (11) as

$$\begin{aligned} \delta_\nu^{(1)}(\xi) &= t^m T_m(\xi) b_\lambda^{(1)}(\xi) + t^{m-1} U_m(\xi) v_\lambda^{(1)}(\xi), \\ \delta_\nu^{(2)}(\xi) &= (-t)^m T_m(\xi) b_\lambda^{(2)}(\xi) + (-t)^{m-1} U_m(\xi) v_\lambda^{(2)}(\xi), \\ b_\nu^{(3)}(\xi) &= (-t)^m T_m(\xi) b_\lambda^{(3)}(\xi) + (-t)^{m-1} U_m(\xi) v_\lambda^{(3)}(\xi), \\ b_\nu^{(4)}(\xi) &= t^m T_m(\xi) b_\lambda^{(4)}(\xi) + t^{m-1} U_m(\xi) v_\lambda^{(4)}(\xi), \end{aligned} \quad (16)$$

where next notations are introduced:

$$\begin{aligned}
 V^{(1)}(\xi) &= \begin{cases} (i\xi - i\sqrt{\xi^2 - 1})^\lambda \\ (i\xi + \sqrt{1 - \xi^2})^\lambda \\ (i\xi + i\sqrt{\xi^2 - 1})^\lambda \end{cases}, & V^{(2)}(\xi) &= \begin{cases} (-i\xi + i\sqrt{\xi^2 - 1})^\lambda \\ (-i\xi + \sqrt{1 - \xi^2})^\lambda \\ (-i\xi - i\sqrt{\xi^2 - 1})^\lambda \end{cases}, \\
 V^{(3)}(\xi) &= \begin{cases} (-i\xi - i\sqrt{\xi^2 - 1})^\lambda \\ (-i\xi + \sqrt{1 - \xi^2})^\lambda \\ (-i\xi + i\sqrt{\xi^2 - 1})^\lambda \end{cases}, & V^{(4)}(\xi) &= \begin{cases} (i\xi + i\sqrt{\xi^2 - 1})^\lambda \\ (i\xi + \sqrt{1 - \xi^2})^\lambda \\ (i\xi - i\sqrt{\xi^2 - 1})^\lambda \end{cases}
 \end{aligned} \tag{17}$$

When Fourier integrals are calculated with functions of (16) the Chebyshev's polynomials may be considered as multipliers that may be taken outside the integral sign and it is need to change  $\xi$  on  $i d/dx$ . This procedure reduce the calculations of Fourier integrals for  $b_\nu$  - solutions to calculations integrals for  $b_\lambda$  - and  $V_\lambda$  - solutions. The solutions for  $b_\lambda$  are already known and it is stay to find inverse Fourier transformations of functions (17). Consider the first function from (17) and will be start from identity

$$\hat{V}_\lambda^{(1)}(\xi) = \int_{-\infty}^{\infty} \hat{V}_\lambda^{(1)}(x) e^{i x \xi} dx, \tag{18}$$

where tranformate  $\hat{V}_\lambda^{(1)}(\xi)$  known and original  $\hat{V}_\lambda^{(1)}(x)$  is desired functions. To differentiate this identity on  $\xi$

$$\frac{d\hat{V}_\lambda^{(1)}(\xi)}{d\xi} = i\lambda \hat{b}_\lambda^{(1)}(\xi) = i \int_{-\infty}^{\infty} x \hat{V}_\lambda^{(1)}(x) e^{i x \xi} dx. \tag{19}$$

It is seen that the derivative of function  $\hat{V}_\lambda^{(1)}(\xi)$  is transformate of Fourier function  $\hat{b}_\lambda^{(1)}(x)$  up to a factor  $i\lambda$  and this gives next eguativity:

$$\hat{V}_\lambda^{(1)}(x) = \lambda \frac{\hat{b}_\lambda^{(1)}(x)}{x} \rightarrow \hat{V}_x^{(1)}(\xi) \tag{20}$$

The next functions are calculated analogously:

$$\begin{aligned} \hat{\nu}_\lambda^{(2)}(x) &= -\lambda \frac{\delta_\lambda^{(2)}(x)}{x}, & \hat{\nu}_\lambda^{(3)}(x) &= -\lambda \frac{\delta_\lambda^{(3)}(x)}{x}, \\ \hat{\nu}_\lambda^{(4)}(x) &= \lambda \frac{\delta_\lambda^{(4)}(x)}{x}. \end{aligned} \quad (21)$$

Now the b - solutions of Bessel equations (inverse Fourier transformations) of function (16) may be written in form:

$$\begin{aligned} \delta_\nu^{(1)}(x) &= t^{mT_m} \left[ t \frac{d}{dx} \delta_\lambda^{(1)}(x) + \lambda t^{m-1} U_m \left[ t \frac{d}{dx} \right] \frac{1}{x} \delta_\lambda^{(1)}(x) \right], \\ \delta_\nu^{(2)}(x) &= (-t)^{mT_m} \left[ t \frac{d}{dx} \delta_\lambda^{(2)}(x) - \lambda (-t)^{m-1} U_m \left[ t \frac{d}{dx} \right] \frac{1}{x} \delta_\lambda^{(2)}(x) \right], \\ \delta_\nu^{(3)}(x) &= (-t)^{mT_m} \left[ t \frac{d}{dx} \delta_\lambda^{(3)}(x) - \lambda (-t)^{m-1} U_m \left[ t \frac{d}{dx} \right] \frac{1}{x} \delta_\lambda^{(3)}(x) \right], \\ \delta_\nu^{(4)}(x) &= t^{mT_m} \left[ t \frac{d}{dx} \delta_\lambda^{(4)}(x) + \lambda t^{m-1} U_m \left[ t \frac{d}{dx} \right] \frac{1}{x} \delta_\lambda^{(4)}(x) \right]. \end{aligned} \quad (22)$$

It should be noted that b-solutions (22) differ rather from classical solutions. To get more close solutions it is necessary to take corresponding linear combinations of b-solutions. The two functions that defined by first and second formulae in (14) can be considered as generalized Bessel function of first order for anyone negative and positive  $\nu$ .

The third and fourth formulae in (14) can be considered as Bessel functions of second order for  $|\nu| < 1$ . But this formulae are not usable for  $|\nu| \geq 1$ .

It is known that Bessel functions widely use and new functions open new possibilities to solution of new problems of mathematical physics.

#### REFERENCE

1. Watson G.N. A Treatise on the Theory of Bessel Functions. - Cambridge: Cambridge Univ. Press, 1958.
2. Bremermann H. Distributions, Complex Variable and Fourier Transforms. Addison-Wesley Publishing Company, Inc. 1965.

# Modeling with Integral Equations in Computational Electromagnetics

Donald R. Wilton

Department of Electrical and Computer Engineering  
University of Houston  
Houston, TX 77204-4793  
USA

## ABSTRACT

It is often a complex and time-consuming task to model three-dimensional electromagnetic scattering and radiation problems. The task is made somewhat easier, however, by developing a flexible computational paradigm and associated software to handle each of the subtasks involved in a typical problem. This requires that one take an abstract view of computational electromagnetics, and identify the unifying elements of various subtasks in both formulation and algorithm implementation. This paper explores one useful paradigm for formulating and solving two- and three-dimensional electromagnetics problems using integral equations and the method of moments. The approaches used are selected for their generality and simplicity.

## INTRODUCTION

For any frequency domain electromagnetics problem to be solved using integral equations and the method of moments, the basic steps in the solution process are the following:

- Formulate the problem as an integral equation involving equivalent sources as the unknowns to be determined.
- Define a numerical specification for the problem geometry and other problem parameters. Determine what auxiliary tables are needed to automate the filling of the moment matrix.
- Develop a scheme for assembling the moment matrix. This step is at the heart of the computational procedure and involves the specification of the elements (subdomains), basis and testing functions, Green's functions, symmetries, types of source currents, and boundary conditions to be satisfied. In a general purpose program, one should have a number of useful choices available with regard to each of these problem parameters.
- Assemble the right hand side forcing function. This involves modeling the excitation by various sources such as plane waves, point or line sources, apertures, or terminal voltages. In determining certain waveguide or cavity parameters, no forcing function is specified.
- Solve the resulting system of equations for actual or equivalent sources. In problems for which no forcing function is specified, usually the system determinant is searched for zeros as a function of guide wavenumber or excitation frequency.
- Compute desired figures of merit (patterns, gain, impedance, etc.) from the sources or from the fields they produce.

- Display or print problem input and computed data.

While the steps above apply to all moment method problems regardless of dimensionality, the increased complexity of three-dimensional problems often makes it particularly difficult to develop the necessary software for specific problems. Following a trend in the finite element community, (c.f. [1]), we find that it is possible to systematically develop canonical numerical field representations which lead to well-structured software to carry out the associated numerical algorithms. The algorithms apply regardless of the problem's dimensionality and are sufficiently independent and general that a user often can, by selecting appropriate modules, quickly construct a moment method program for a problem of interest. Particularly useful have been concepts developed by the finite element community to efficiently aid in assembling the matrix and to model, organize, and display geometry descriptions and output data. However, a maturation of the discipline in the following areas of electromagnetics has also been crucial in permitting such algorithms to be developed:

- Robust and efficient formulations for conducting objects have been developed and successfully applied to a number of problems with different dimensionalities and symmetries. Though somewhat less well-developed, formulations have also been developed for problems involving both piecewise homogeneous and inhomogeneous dielectric materials. In a few cases, anisotropic materials have also been considered.
- General methods for modeling the geometries of arbitrarily-shaped surfaces for use with integral equations have been developed. These approaches apply to one-, two-, or three-dimensional problems.
- Representations for surface tangent vector unknowns in one, two, or three dimensions and for various subdomain shapes have been developed and applied successfully. Higher order versions of such representations are also becoming available.
- Numerically efficient Green's function representations have been developed which parallel the mixed potential representations of homogeneous regions. Thus programs written to treat scattering or radiation by objects in homogeneous media may be easily extended to objects in multi-layered media, for example.
- Methods have been developed to automate the use of reflection, discrete rotational, and discrete translational (periodic) symmetry in the numerical solution of integral equations. Rectangular waveguides and cavities may also be treated by combining different forms of these symmetries.
- Static potential integrals have been found in closed form for constant and linear source densities on a number of commonly occurring subdomain shapes. Such integrals are of direct use in solving static and time-domain integral equations, but are also used to regularize the integrands of time-harmonic potential integrals when an observation point is near the source region.

Algorithms developed on a paradigm employing these concepts must rely on a standardized numerical representation for electromagnetic field quantities. In the following sections, we discuss various aspects of this representation.

## GEOMETRY MODELING

The geometry of an electromagnetic boundary value problem is defined by specifying the spatial dependence and electrical parameters of all materials involved. For problems involving piecewise homogeneous media, one need only specify the interfaces between various homogeneous regions; for continuously varying media, material parameters must be specified or interpolated.  $B_n$  may be shrunk to a point, resulting in adjacent line segments used to model a curve ( $\mathcal{D} = \mathcal{C}$ ).

In homogeneous, isotropic, source-free material regions, all fields may be computed from equivalent electric and/or magnetic surface currents on the region's boundaries. Inhomogeneous regions may be represented via equivalent volume electric and magnetic polarization currents radiating in a homogeneous background medium. Once these currents, which are the unknowns in an integral equation formulation, are known, any electromagnetic fields of interest may be computed from them. Thus, we are led to consider the fields due to electric currents  $J_{\mathcal{D}}$  and magnetic currents  $M_{\mathcal{D}}$  representing line, surface, or volume currents for  $\mathcal{D} = \mathcal{C}, \mathcal{S}$ , or  $\mathcal{V}$ , respectively, and radiating in an infinite homogeneous medium. These fields are conveniently expressed in terms of magnetic vector, electric scalar, electric vector, and magnetic scalar potentials  $A$ ,  $\Phi$ ,  $F$ , and  $\Psi$ , respectively, as

$$E = -j\omega A - \nabla\Phi - \frac{1}{\epsilon} \nabla \times F \quad (1)$$

$$H = -j\omega F - \nabla\Psi + \frac{1}{\mu} \nabla \times A \quad (2)$$

where

$$A(\mathbf{r}) = \mu \int_{\mathcal{D}} J_{\mathcal{D}}(\mathbf{r}') \frac{e^{-jkR}}{4\pi R} d\mathcal{D}' = -\frac{1}{j\omega} \nabla_{\mathcal{D}} \cdot J_{\mathcal{D}} \quad (3)$$

$$m_{\mathcal{D}} = -\frac{1}{j\omega} \nabla_{\mathcal{D}} \cdot M_{\mathcal{D}}, \quad (4)$$

where appropriate extensions of the divergence operator are assumed to apply to currents on curves or surfaces. Any electric or magnetic currents present may be approximated by means of a linear combination of known *basis or expansion functions*  $\Lambda_n^{\mathcal{D}}$ . For the electric current, for example,

$$J_{\mathcal{D}}(\mathbf{r}) = \sum_{n=1}^N J_n \Lambda_n^{\mathcal{D}}(\mathbf{r}), \quad (5)$$

where the constants  $J_n$  represent the current crossing the boundary  $B_n$  between adjacent elements and the current is assumed to be directed from the element  $\Delta\mathcal{D}_{n+}$  to  $\Delta\mathcal{D}_{n-}$ . A so-called *generalized triangular basis function*  $\Lambda_n^{\mathcal{D}}$  is associated with each  $B_n$  and is defined as follows:

$$\Lambda_n^{\mathcal{D}}(\mathbf{r}) = \begin{cases} \frac{\rho_{n\pm}}{h_{n\pm}} & , \mathbf{r} \text{ in } \Delta\mathcal{D}_{n\pm} \\ 0 & \text{otherwise,} \end{cases} \quad (6)$$

and  $\rho_{n\pm}$  is a vector beginning or ending at a vertex, edge, or face opposite  $B_n$ , and  $h_{n\pm}$  is a distance which normalizes the basis so that its flux density at  $B_n$  is unity. An important



observation is that  $\Lambda_n^{\mathcal{D}}$  can be represented as a linear combination of vectors of constant direction and linearly varying amplitude as,

$$\frac{\rho_{n\pm}}{h_{n\pm}} = \frac{1}{h_{n\pm}} \sum_{i,j=1}^{I_{n\pm}} \alpha_{n\pm}^{ij} \xi_{n\pm}^i \ell_{n\pm}^j, \quad (7)$$

where  $\ell_{n\pm}^j$  is the  $j$ -th edge vector of  $\Delta\mathcal{D}_{n\pm}$  not belonging to  $B_n$ , and the  $\xi_{n\pm}^i$  are normalized coordinates varying linearly across  $\Delta\mathcal{D}_{n\pm}$ . The number,  $I_{n\pm}$ , and the coefficients  $\alpha_{n\pm}^{ij}$  have the values 0, 1, -1 depending on the element shape and dimension. A number of important properties of these basis functions are summarized in [3,4]; the set includes the familiar triangle, rooftop, and edge-based basis functions.

Substituting  $J_{\mathcal{D}}$  from (5) into (3) yields

$$A(\mathbf{r}) = \mu \sum_{n=1}^N J_n \int_{\Delta\mathcal{D}} \Lambda_n^{\mathcal{D}}(\mathbf{r}') \frac{e^{-jkR}}{4\pi R} d\mathcal{D}'. \quad (8)$$

and substituting (6) and (7) into (8) yields

$$A(\mathbf{r}) = \mu \sum_{n=1}^N J_n \left[ \sum_{i,j=1}^{I_{n+}} \frac{\alpha_{n+}^{ij} \ell_{n+}^j}{h_{n+}} \psi_i^{\Delta\mathcal{D}_{n+}}(\mathbf{r}) + \sum_{i,j=1}^{I_{n-}} \frac{\alpha_{n-}^{ij} \ell_{n-}^j}{h_{n-}} \psi_i^{\Delta\mathcal{D}_{n-}}(\mathbf{r}) \right], \quad (9)$$

where

$$\psi_i^{\Delta\mathcal{D}_{n\pm}}(\mathbf{r}) = \int_{\Delta\mathcal{D}_{n\pm}} \xi_{n\pm}^i \frac{e^{-jkR}}{4\pi R} d\mathcal{D}' \quad (10)$$

is the potential produced by a scalar source of linearly varying source density on  $\Delta\mathcal{D}_{n\pm}$ .

To compute the scalar potential from the current, the charge is needed. It, in turn, requires the divergence of the basis functions:

$$\begin{aligned} \nabla_{\mathcal{D}} \cdot \Lambda_n^{\mathcal{D}} &= \begin{cases} \pm \frac{\sigma_{n\pm}}{h_{n\pm}}, & \mathbf{r} \text{ in } \Delta\mathcal{D}_{n\pm} \\ 0 & \text{otherwise} \end{cases} \\ &= \frac{\sigma_{n+}}{h_{n+}} \Pi_{n+}^{\mathcal{D}}(\mathbf{r}) - \frac{\sigma_{n-}}{h_{n-}} \Pi_{n-}^{\mathcal{D}}(\mathbf{r}), \end{aligned} \quad (11)$$

where  $\Pi_{n\pm}^{\mathcal{D}}(\mathbf{r})$  is a unit pulse function in  $\Delta\mathcal{D}_{n\pm}$ . The quantity  $\sigma_{n\pm}$  is defined as

$$\sigma_{n\pm} = \begin{cases} \dim(\Delta\mathcal{D}_{n\pm}), & \text{on simplex domains,} \\ 1 & \text{on rectangular or hexahedral domains,} \\ 1 & \text{if } B_n \text{ is a rectangular face of a pentahedral domain,} \\ 2 & \text{if } B_n \text{ is a triangular face of a pentahedral domain,} \end{cases} \quad (12)$$

and  $\dim(\Delta\mathcal{D}_{n\pm})$  is the spatial dimension of  $\Delta\mathcal{D}_{n\pm}$  ( $= 1, 2$ , or  $3$  for  $\mathcal{D} = \mathcal{C}, \mathcal{S}$ , or  $\mathcal{V}$ , respectively). Thus charge distributions are approximated as piecewise constant. We have from (1), (2), (5), and (11)

$$\Phi(\mathbf{r}) = \frac{-1}{j\omega\epsilon} \sum_{n=1}^N J_n \left[ \frac{\sigma_{n+}}{h_{n+}} \psi^{\Delta\mathcal{D}_{n+}}(\mathbf{r}) - \frac{\sigma_{n-}}{h_{n-}} \psi^{\Delta\mathcal{D}_{n-}}(\mathbf{r}) \right] \quad (13)$$

where  $\psi^{\Delta\mathcal{D},\pm}$  is defined below. From (9) we obtain

$$\nabla \times A(\mathbf{r}) = \mu \sum_{n=1}^N J_n \left[ \sum_{i,j=1}^{I_{n+}} \frac{\alpha_{n+}^{ij}}{h_{n+}} \nabla \psi_i^{\Delta\mathcal{D},+}(\mathbf{r}) \times \ell_{n+}^j + \sum_{i,j=1}^{I_{n-}} \frac{\alpha_{n-}^{ij}}{h_{n-}} \nabla \psi_i^{\Delta\mathcal{D},-}(\mathbf{r}) \times \ell_{n-}^j \right] \quad (14)$$

and from (13),

$$\nabla \Phi(\mathbf{r}) = \frac{-1}{j\omega\epsilon} \sum_{n=1}^N J_n \left[ \frac{\sigma_{n+}}{h_{n+}} \nabla \psi^{\Delta\mathcal{D},+} - \frac{\sigma_{n-}}{h_{n-}} \nabla \psi^{\Delta\mathcal{D},-} \right]. \quad (15)$$

Using (9), (14), and (15) in (1) and (2), we can compute  $E$  and  $H$  for electric current sources. By duality, similar expressions are obtained for the fields due to magnetic sources. A key observation is that the problem of computing the fields is thus reduced to the evaluation of scalar potential integrals due to linear and constant source density distributions,

$$\psi_i^{\Delta\mathcal{D},\pm}(\mathbf{r}) = \int_{\Delta\mathcal{D}} \xi_{n\pm}^i \frac{e^{-jkR}}{4\pi R} d\mathcal{D}' \quad (16)$$

and

$$\psi^{\Delta\mathcal{D},\pm}(\mathbf{r}) = \int_{\Delta\mathcal{D}} \frac{e^{-jkR}}{4\pi R} d\mathcal{D}', \quad (17)$$

and their gradients. One also observes that  $\psi_i^{\Delta\mathcal{D},\pm}$ ,  $\psi^{\Delta\mathcal{D},\pm}$ , and their gradients may be evaluated simultaneously for numerical efficiency.

A collection of subprograms have been developed to compute both static and time-harmonic scalar potential integrals for linear and constant source densities over the following domains [5]:

- Wire segments
- Strip segments
- Conical frusta with  $e^{jm\phi}$  circumferential variation
- Rectangular patches
- Triangular patches
- Tetrahedral cells
- Pentahedral cells
- Hexahedral cells

In order to model surface vertex junctions, the potential due to a  $1/\rho$  distribution on a triangular patch is also available. The static forms of most of these potential integrals may be written in closed form [6] and aid in the near field and source region evaluation of the time-harmonic potentials.

Lorenz gauge condition, may be written as

$$-j\omega\epsilon\Phi() = \int_S \hat{\mathbf{z}} \cdot (') K^{\Phi}(k; |') dS' + \int_S \hat{\mathbf{z}} \cdot (') \psi(k; |') dS'. \quad (18)$$

Eqs. (5) and (18) are not only found to be efficient from a numerical point of view, but also allow the mixed potential approach to be extended from the free space formulation to a wide variety of problems. Slightly different approaches are used when dealing with periodic or non-periodic problems; these are discussed independently below.

### Periodic Multi-Layered Media

Montgomery [8] has shown that the periodic layered-media Green's function can be written in the highly convergent form

$$\begin{aligned} G(k; l') = & \sum_{p=-\infty}^{\infty} \sum_{q=-\infty}^{\infty} (\tilde{G}_{pq}(k; l') - \mathcal{I} \tilde{G}_{pq}^0(-ju; l')) \\ & - \sum_i \Gamma_i \tilde{G}_{pq}^0(-ju; l'_i) \\ & + \sum_{r=-\infty}^{\infty} \sum_{s=-\infty}^{\infty} (\mathcal{I} G_{rs}^0(-ju; l') + \sum_i \Gamma_i G_{rs}^0(-ju; l'_i)) \end{aligned} \quad (19)$$

involving both spatial and spectral domain representations. The series in the first integral represents a spectral form of the Green's function with the smoothed spectra of the homogeneous medium and dominant quasi-image terms removed. Smoothing is simply accomplished by replacing the medium wavenumber  $k$  with the imaginary wavenumber  $(-ju)$  [9]. The kernel of the second integral is just the spatial domain representation of the terms removed from the first integral. A similar representation applies to the kernels of the scalar potentials  $K^\Phi(k; l')$  and  $\psi(k; l')$  in (18). When basis functions  $\Lambda_n()$  are used to represent the current in (5) and (18), integrals equivalent to Fourier transforms of the element shapes arise, and these may be expressed in closed form [8,10,11].

### Non-Periodic Multi-Layered Media

The spectral domain Green's function for a single point source in a multi-layered medium is merely a continuous spectral version of the periodic media spectral representation, the summations over spectral components becoming integrals over the spectral wavenumbers. Terms in the Green's function representing periodic arrays of point sources in a homogeneous medium, reduce to a single point source radiating in a homogeneous medium, and this contribution may be extracted directly from the superposition integral; no spectral smoothing is needed in this case, but a few dominant quasi-image and surface wave terms may be extracted from the spectral integral to improve convergence. The remaining integral is a Sommerfeld-like integral which may be efficiently evaluated by shifting the path of integration into the complex plane [12], and by applying the method of averages to evaluate any remaining oscillatory integrals [13]. When source and observation points are in the same layer, the Sommerfeld integral may also be replaced by a series of complex images, dramatically speeding up the computation of the Green's function.

## GEOMETRICAL SYMMETRIES

The presence of geometrical symmetry in a problem often provides significant opportunity

for reducing the computational labor by providing a partial decoupling of components of the problem. The benefits of symmetry may be exploited even when the excitation does not excite a structure symmetrically by decomposing both the excitation and the induced equivalent currents into their (uncoupled) *symmetrical components*.

Bodies with continuous symmetry, like bodies of revolution, are usually treated by analytically constructing their Green's functions. Discrete symmetries, such as those of  $N$ -fold rotational or of reflection symmetries, are probably most easily treated by numerically handling the rotations or reflections. The symmetrical components of these problems involve discrete reflections or rotations coupled with discrete Fourier transform (DFT) weightings. These may also be automated in a straightforward manner [14,15,16].

## TESTING PROCEDURES AND APPLICATION OF BOUNDARY CONDITIONS

For the mixed potential field representations and subdomain-based basis functions described above, Galerkin's method, in which the testing functions are the same as the basis functions, is usually used to form the moment matrix. The functions  $\Lambda_n()$  are sufficiently differentiable to allow at least one of the tangential derivatives in the field representation to be transferred onto the testing function by integration by parts. This procedure is important since it reduces the differentiability requirements on the original basis functions. Thus for an electric field representation of the form

$$E(.) = -j\omega A - \nabla\Phi - \frac{1}{\epsilon}\nabla \times F, \quad (20)$$

testing with testing functions  $\Lambda_m()$  yields

$$\langle \Lambda_m, E(.) \rangle = -j\omega \langle \Lambda_m, A \rangle + \langle \nabla \cdot \Lambda_m, \Phi \rangle - \frac{1}{\epsilon} \langle \Lambda_m, \nabla \times F \rangle, \quad (21)$$

where the symmetric product for vector quantities  $A()$  and  $()$  is defined as

$$\langle A, \rangle = \int_D A() \cdot () dD,$$

and where the gradient derivative has been transferred onto  $\Lambda_m$  by integration by parts. A similar expression results from testing the magnetic field, (2). The above approach leads to the following types of integrals to be evaluated:

$$\int_D \int_D \Lambda_m() \cdot \Lambda_n()$$

Electric field is proportional to magnetic fields (impedance boundary condition).

Electric field is proportional to the discontinuity in magnetic field (thin shell impedance boundary condition).

Electric and magnetic fields are continuous across an interface (bulk material interface boundary conditions).

Linear combination of electric and magnetic fields vanish on the side of an interface opposite to that of the region in which fields are represented (combined field boundary conditions for conductors or dielectrics).

The application of these boundary conditions can be automated in a computer program which selects appropriate potentials and their gradients, and constructs the tested fields needed to model designated boundary conditions at the observation point. The appropriate potential combinations are then assembled in the moment matrix.

## SUMMARY AND CONCLUSIONS

It is possible to automate the most common tasks in the solution of electromagnetic scattering and radiation problems by the method of moments. For example, we have developed a set of subroutines to read in data describing discretized contours, surfaces, and volumes in a standardized format. For contours, provisions are made for simultaneously specifying several segment attributes (e.g., wire radii, segment radius of curvature, or surface impedance), and node attributes (e.g., voltage sources or lumped loading impedances). Similar provisions are made for specifying vertex, edge, face, and cell attributes for surfaces and volumes. To aid in the matrix assembly, subprograms can be developed to identify and tag contour and surface junctions, and to set up tables mapping potential integral contributions from source and observation point pairs defined on nodes, edges, faces, or cells, to appropriate moment matrix locations. Other mapping tables, such as for defining trees and loops for the decomposition of basis functions into divergence- and curl-free parts, can also be constructed.

A set of subprograms has been developed to evaluate potential integrals and their gradients for uniform and linearly varying source distributions defined on simply shaped domains. Such domains include linear wire and cylinder segments, triangular and rectangular planar surfaces, conical segments with  $\exp(jm\phi)$  phase variation, prisms of rectangular or triangular cross section and of infinite or finite extent, and tetrahedral cells. Practically all electromagnetic field quantities of interest can be expressed in terms of these integrals.

The availability of subprograms such as those described free the code developer from being overly concerned with the details of the method of moments, leaving him to concentrate on the analytical and numerical formulation of a problem. The flexibility also allows him to experiment with alternative numerical approaches. And while it must be admitted that codes based on general purpose subroutines cannot be optimal for specific problems, they can serve as developmental platforms and validation tools for more problem-specific codes.

## REFERENCES

- [1] J. E. Akin, *Application and Implementation of Finite Element Methods*, Orlando: Academic Press, 1984.
- [2] P. Silvester, "High-Order Polynomial Finite Elements for Potential Problems," *Int. J. Eng. Sci.*, vol. 7, 8, pp. 849-861, 1969.
- [3] S. M. Rao, D. R. Wilton, and A. W. Glisson, "Electromagnetic Scattering by Surfaces of Arbitrary Shape," *IEEE Trans. Antennas Propagat.*, vol. AP-30, 3, pp. 409-418, 1982.
- [4] D. H. Schaubert, D.R. Wilton, and A. W. Glisson, "A Tetrahedral Modeling Method of Electromagnetic Scattering by Arbitrarily Shaped Inhomogeneous Dielectric Bodies," *IEEE*

*Trans. Antennas Propagat.*, vol. AP-32, 1, pp. 77-85, 1984.

[5] S. V. Yesantharao, "EMPAC—A Software Toolbox of Potential Integrals for Computational Electromagnetics," master's thesis, Univ. Houston, Houston, TX, 1989.

[6] D. R. Wilton, S. M. Rao, A. W. Glisson, D. H. Schaubert, O. M. Al-Bundak, and C. M. Butler, "Potential Integrals for Uniform and Linear Source Distributions on Polygonal and Polyhedral Domains," *IEEE Trans. Antennas Propagat.*, vol. AP-32, 3, pp. 276-281, 1984.

[7] K. A. Michalski and D. Zheng, "Electromagnetic Scattering and Radiation by Surfaces of Arbitrary Shape in Layered Media, Part I: Theory," *IEEE Trans. Antennas Propagat.*, vol. AP-38, 3, pp. 335-344, 1990.

[8] N. W. Montgomery, "Periodic Structures in Stratified Media—A Mixed Potential Formulation," Ph.D. dissertation, Univ. Houston, Houston, TX, 1991.

[9] S. Singh, W. F. Richards, J. Zinecker, and D. R. Wilton, "Accelerating the Convergence of Series Representing the Free Space Periodic Green's Function," *IEEE Trans. Antennas Propagat.*, vol. AP-38, 12, pp. 1958-1962, 1990.

[10] N. W. Montgomery and D. R. Wilton, "Analysis of Arbitrary Conducting Periodic Structures Embedded in Layered Media," *1991 IEEE AP-S Symposium*, London, Ontario, June 1991.

[11] K. McInturff and P. S. Simon, "The Fourier Transform of Linearly Varying Functions with Polynomial Support," *IEEE Trans. Antennas Propagat.*, vol. AP-39, 9, pp. 1441-1444, 1991.

[12] E. H. Newman and D. Forrai, "Scattering From a Microstrip Patch," *IEEE Trans. Antennas Propagat.*, vol. AP-35, 3, pp. 245-251, 1987.

[13] J. R. Mosig and F. E. Gardiol, "A Dynamical Radiation Model for Microstrip Structures," *Adv. Electron. Electron Phys.*, (P.W. Hawkes, ed.), New York: Academic Press, vol. 59, pp. 139-237, 1982.

[14] L. L. Tsai, D. G. Dudley, and D. R. Wilton, "Electromagnetic Scattering by a Three-Dimensional Conducting Rectangular Box," *J. Appl. Phys.*, vol. 45, 10, pp. 4393-4400, 1974.

[15] R. M. Sharpe, "Electromagnetic Scattering and Radiation by Discrete Bodies of Revolution," master's thesis, Univ. Houston, Houston, TX, 1987.

[16] J. T. Williams, N. Champagne, D. R. Wilton and D. R. Jackson, "Numerical Modeling of Planar Antennas and Scatterers Embedded in Layered Media," Rept. No. 91-11, Applied Electromagnetics Laboratory, Univ. Houston, Houston, TX, 1991.

# ATOMIC FUNCTIONS BASED MATHEMATICAL METHODS OF SIGNAL PROCESSING AND IMAGE RECONSTRUCTION

V. F. Kravchenko, V. A. Rvachev, V. L. Rvachev

Several problems of signal processing and image reconstruction from mathematical point of view can be reduced to finding the best approximation in the sense of certain norm of given function  $f(x)$  by finite functions with given support. The norms in question frequently are expressed more naturally in terms of  $Ff(x)$  - the Fourier transform of  $f(x)$ . Such are problems of FIR filter synthesis, deconvolution finite windows for blurred image reconstruction, spectral density estimation, construction of finite windows for Fourier analysis of signals, signal interpolation etc. If we choose to approximate  $f(x)$  by means of linear combinations of particular finite function  $g(x)$  and its derivatives, then in frequency domain we encounter familiar problem of best approximation by algebraic polynomials. The  $g(x)$  function should satisfy certain conditions to provide for both reasonable degree of approximation and simplicity of computing procedures. Yet another approach is to use shifts (translations) instead of derivatives, which brings us in frequency domain to no less classical trigonometric polynomial approximation. In either case atomic functions are among much promising candidates to the  $g(x)$  role.

Atomic functions are finite solutions of ordinary linear functional differential equations with constant coefficients and linear transformations of independent variable. The Fourier transforms of atomic functions are known in the explicit form of infinite product of quasipolynomials or alternatively trigonometric polynomials. The simplest example of an atomic function is the  $up(x)$  function which satisfies the equation

$$y'(x) = 2y(2x+1) - 2y(2x-1)$$

and has support  $[-1, 1]$ . Its Fourier transform is the product



factors of  $\sin(t/2\pi k)/(t/2\pi k)$  .

Atomic functions proved to be helpful in such fields as approximation theory of functions, in generalized Taylor series expansion in orthogonal systems of the "wavelet" type. [1]

Atomic function  $u_p(x)$  has been applied to construction of windows for Fourier analysis [2,3], atomic function  $h(x)$  has been used for obtaining deconvolution windows for image restoration [3], atomic functions for filter synthesis were considered in [4,5].

The atomic function based wavelet systems recently have also been applied to signal processing, time series analysis in economy and image restoration.

#### References

1. Rvachev V. A. Soviet Math. Surveys, 1990, v. 45, N 1, p. 77-103.
2. Kravchenko V. F., Rvachev V. A., Rvachev V. L., Sov. Math. Doklady, 1989, v. 306, N 1, p. 78-81.
3. Afanasiev V. A., Kravchenko V. F., Rvachev V. A., Rvachev V. L., Sov. Math. Dokl. 1991, v. 321, N 5, p. 938-940.
4. Gorshkov A. S., V. F. Kravchenko, Rvachev V. A., Rvachev V. L., ibid. 1991, v. 321, N 5, p. 914-918.
5. Gorshkov A. S., Kravchenko V. F., Rvachev V. A., Rvachev V. L., ibid. 1991, v. 321, N 4, p. 697-700.
6. Afanasiev V. A., Kravchenko V. F., Rvachev V. A., Rvachev V. L., ibid. 1992, v. 322, N 3, p. 498-500.



# WAVE-GUIDE PROPERTIES OF ONE-DIRECTIONAL PERIODICAL THREE-DIMENSIONAL TRANSPARENT AND NON-TRANSPARENT STRUCTURES.

*Sergey V. Sukhinin  
Natalya G. Shevchenko*

## Abstract

The qualitative features of waves propagated near one-directional periodical structure of transparent and non-transparent obstacles in three dimensional case are studied.

**Formulation of problem.** Let  $\Omega_1$  and  $\Omega_2$  not be intersection regions in  $R^3$  with Cartesian coordinates  $(x, y, z)$ . It is assumed that  $\Omega_1$  and  $\Omega_2$  are periodical along the  $z$  axis, with a period of  $2\pi/N$  and have the common boundary  $\Gamma$  and complement each other in the space  $R^3 = \Gamma \cup \Omega_1 \cup \Omega_2$  where  $\Omega_2$  models the external medium,  $\Omega_1$  is the one-directional periodical structure of another medium. The obstacles may be either connected or not connected (see Fig.1).

The steady-state oscillations are described by functions

$$\operatorname{Re}[u_1(x, y, z) \exp(-i\omega t)] \text{ and } \operatorname{Re}[u_2(x, y, z) \exp(-i\omega t)].$$

Here  $\omega$  is the angular frequency of oscillations. The functions  $u_1$  and  $u_2$  must satisfy to the equation describing steady-state vibrations in  $\Omega_1$  and  $\Omega_2$ , respectively.

$$\begin{cases} (\Delta + \lambda^2 \kappa^2) u_1 = 0, & \text{in } \Omega_1 \\ (\Delta + \lambda^2) u_2 = f, & \text{in } \Omega_2 \end{cases} \quad (1)$$

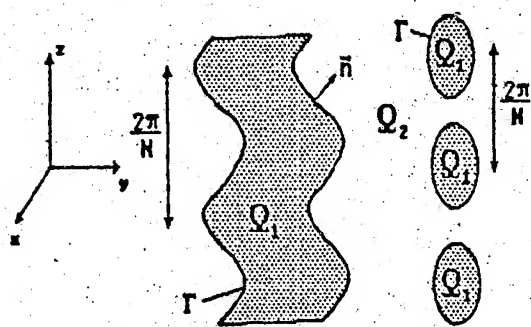


Fig. 1

Function  $f(x, y, z) \exp(-i\omega t)$  describes the sources of oscillation. It is assumed that the sources are situated in  $\Omega_2$ , and positioned periodically along  $z$  axis with a period of  $2\pi$ , and localized about the internal structure.

This means that  $f(x, y, z) \equiv 0$  with increasing the distance from the barrier.

At the boundary of contact between the media the conditions of conjugation must be satisfied:

$$\begin{cases} u_1 = \sigma u_2 \\ \frac{\partial u_1}{\partial \vec{n}} = \tau \frac{\partial u_2}{\partial \vec{n}} \end{cases} \quad (2)$$

where  $\lambda$  is the complex parameter,  $\kappa > 0, \sigma > 0, \tau > 0$  are real, whose physical meaning is determined by the content of the effect investigated, and  $\vec{n}$  is normal to  $\Gamma$ .

Since the sources  $f(x, y, z)$  and the boundary of contact between the media are  $2\pi$ -periodical along the  $z$  axis, the functions  $u_1$  and  $u_2$  will also be  $2\pi$ -periodical along the  $z$  axis. The solution of Eqs.(1) must satisfy the radiation condition

$$u_2 = \sum_{n=-\infty}^{+\infty} \sum_{m=-\infty}^{+\infty} c_{mn} H_m^{(1)}(\sqrt{\lambda^2 - n^2} \rho) e^{im\theta} e^{inz} \quad (3)$$

( $n, m$  are integer numbers,  $i$  is the imaginary unity,  $c_{mn}$  are certain complex numbers,  $H_m^{(1)}$  are Hankel functions,  $(\rho, \theta, z)$  are cylindrical coordinates)

Radiation condition (3) represents of solution with increasing the distance from the barriers, that is  $\sqrt{x^2 + y^2} > C$ , where  $C$  is the quite large positive number.

The dependence of the complex number  $\lambda$  in expression of the shape (3) is assumed to be analytical on the Riemann surface  $\Lambda$ . The Riemann surface is built by analytical continuation and possesses the following properties:

- 1) the Riemann surface is infinite-sheeted;
- 2) points  $\lambda = n$  for all integers  $n$  are logarithmic branching points.

For the formulated problem the following theorem is valid

**Theorem 1.** *The solution of problem (1), (2), (3) is a single one, provided that  $\text{Im}\lambda > 0$  and  $\text{Im}\sqrt{\lambda^2 - n^2} > 0$  for all integers  $n$ .*

**Proof.** Reductio ad absurdum. Let there exist a nontrivial solution of the corresponding uniform problem. If we multiply similar relationships (1) by the complex conjugate to  $u_1$  and  $u_2$  the functions  $u_1$  and  $u_2$

integrate over  $\Omega_1$  and  $\Omega_2$ , then using of the Green's theorem we can derive relationships:

$$\begin{aligned} 0 &= \int_{\Omega_1} (\Delta + \lambda^2 \kappa^2) u_1 \bar{u}_1 d\Omega_1 = \int_{\Omega_1} (\operatorname{div}(\bar{u}_1 \nabla u_1) - |\nabla u_1|^2 + \lambda^2 \kappa^2 |u_1|^2) d\Omega_1 = \\ &= \int_{\Omega_1} (\lambda^2 \kappa^2 |u_1|^2 - |\nabla u_1|^2) d\Omega_1 + \int_{\Gamma} \bar{u}_1 \frac{\partial u_1}{\partial \vec{n}} d\Gamma \\ 0 &= \int_{\Omega_2} (\lambda^2 |u_2|^2 - |\nabla u_2|^2) d\Omega_2 + \int_{\Gamma} \bar{u}_2 \frac{\partial u_2}{\partial \vec{n}} d\Gamma \end{aligned}$$

Integrals over boundaries  $z = 0$  and  $z = 2\pi$  equal to zero by virtue of periodic conditions, integral over too remote boundary tends to zero, because the solution attenuation is assumed.

After multiplying the second of the relationships by  $\tau$  and combining the first and the second equation, with consideration for the conditions of conjugation (2), we can obtain identity

$$0 = \int_{\Omega_2} (\lambda^2 \tau |u_2|^2 - \tau |\nabla u_2|^2) d\Omega_2 + \int_{\Omega_1} (\lambda^2 \kappa^2 |u_1|^2 - |\nabla u_1|^2) d\Omega_1$$

It follows that

$$\operatorname{Im} \lambda^2 \left( \int_{\Omega_1} \kappa^2 |u_1|^2 d\Omega_1 + \tau \int_{\Omega_2} |u_2|^2 d\Omega_2 \right) = 0$$

Since  $\operatorname{Im}(\lambda^2) \neq 0 \implies u_1 \equiv 0, u_2 \equiv 0$ .

Theorem is proved.

**Operator equation.**

**Lemma 1.** Function  $\Phi(x, y, z, x_0, y_0, z_0, \lambda)$  of the shape

$$\Phi = -\frac{i}{8\pi} \sum_{n=-\infty}^{+\infty} H_0^{(1)}(\sqrt{\lambda^2 - n^2} \sqrt{(x - x_0)^2 + (y - y_0)^2}) e^{in(z - z_0)}$$

is the fundamental solution of the Helmholtz equation with parameter  $\lambda$  and satisfies  $2\pi$ -periodicity in  $z$ , radiation condition (3).

**Proof.**  $\Phi(x, y, z, x_0, y_0, z_0, \lambda)$  must satisfy the relationship

$$(\Delta + \lambda^2)\Phi(x, y, z, x_0, y_0, z_0, \lambda) = \sum_{k=-\infty}^{+\infty} \delta(x - x_0)\delta(y - y_0)\delta(z - z_0 + 2\pi k).$$

Since the right side of this relationship is periodic in  $z$ , then  $\Phi$  may be represented in view of the Fourier series.

$$(\Delta + \lambda^2) \sum_{n=-\infty}^{+\infty} \Phi_n(x - x_0, y - y_0) e^{ik(z - z_0)} = \frac{1}{2\pi} \delta(x - x_0) \delta(y - y_0) \sum_{k=-\infty}^{+\infty} e^{ik(z - z_0)},$$

where  $\Phi_n$  are coefficients of the Fourier series for the function  $\Phi$ .

Hence

$$(\Delta + \lambda^2 - n^2)\Phi_n(x, y, x_0, y_0) = \frac{1}{2\pi} \delta(x - x_0) \delta(y - y_0).$$

Considering the radiation condition, one can obtain the expression

$$\Phi_n(x, y, x_0, y_0, \lambda) = -\frac{i}{8\pi} H_0^{(1)}(\sqrt{\lambda^2 - n^2} \sqrt{(x - x_0)^2 + (y - y_0)^2}),$$

whence the statement of lemma follows. Lemma is proved.

In order to use the potential method, it is necessary

**Lemma 2.** Fundamental solution  $\Phi(\vec{x}, \vec{x}_0, \lambda)$  under condition

$$r = |\vec{x} - \vec{x}_0| = \sqrt{(x - x_0)^2 + (y - y_0)^2 + (z - z_0)^2} \rightarrow 0$$

has a feature as for the fundamental solution of the Helmholtz equation in  $R^3$ .

**Proof.** We separate the main feature in  $x, y, z$  of the series

$$-\frac{i}{8\pi} \sum_{n=-\infty}^{+\infty} H_0^{(1)}(\sqrt{\lambda^2 - n^2} \sqrt{(x - x_0)^2 + (y - y_0)^2}) e^{in(z - z_0)}$$

For sufficient large numbers  $|n|$  and fixed  $\lambda, \lambda \in \Lambda$ , the estimate holds

$$\sqrt{\lambda^2 - n^2} = i|n|(1 + o(\lambda^2/n^2)).$$

Then the series can be rewritten

$$-\frac{i}{8\pi} \sum_{n=-\infty}^{+\infty} H_0^{(1)}(i|n|\sqrt{(x - x_0)^2 + (y - y_0)^2}) e^{in(z - z_0)} + q(x, y, z, x_0, y_0, z_0, \lambda)$$

the function  $q$  continuously depends on variables  $x, y, z, x_0, y_0, z_0, \lambda$ .

$$\begin{aligned} & -\frac{i}{8\pi} \sum_{n=-\infty}^{+\infty} H_0^{(1)}(i|n|\sqrt{(x-x_0)^2 + (y-y_0)^2}) e^{in(z-z_0)} = \\ & = -\frac{1}{4\pi^2} \sum_{n=-\infty}^{+\infty} K_0(i|n|\sqrt{(x-x_0)^2 + (y-y_0)^2}) e^{in(z-z_0)} = \\ & = -\frac{1}{4\pi^2} \int_0^\infty \frac{\text{sh}(\sqrt{(x-x_0)^2 + (y-y_0)^2} \text{ch}\xi) d\xi}{\text{ch}(\sqrt{(x-x_0)^2 + (y-y_0)^2} \text{ch}\xi) - \cos(z-z_0)}, \end{aligned}$$

where  $K_0$  is the McDonald function. Using the Taylor expansion of trigonometric functions, we obtain the investigated series having the feature  $\frac{1}{r}$ . Lemma is proved.

Let  $\phi = f * \Phi$  (\* denotes convolution). When substituting  $v = u - \phi$ , where  $u = u_1$  if  $(x, y, z) \in \Omega_1$ ,  $u = u_2$  if  $(x, y, z) \in \Omega_2$ , we reduce the equations (1), (2) to the system of relationships

$$\begin{cases} (\Delta + \lambda^2)v_1 = \lambda^2(1 - \kappa^2)(v_1 + \phi), & \text{in } \Omega_1 \\ (\Delta + \lambda^2)v_2 = 0, & \text{in } \Omega_2 \end{cases} \quad (4)$$

At the boundary of the media  $\Gamma$  the conjugation conditions are rewritten:

$$\begin{cases} v_1 = v_2 \\ \delta \frac{\partial v_1}{\partial \vec{n}} = \frac{\partial v_2}{\partial \vec{n}} + (1 - \delta) \frac{\partial \phi}{\partial \vec{n}}, \delta = \sigma/\tau \end{cases} \quad (5)$$

Since  $\phi, u_1, u_2$  satisfy the periodicity and radiation conditions, then  $v$  will also satisfy these conditions.

The solution satisfying the relationships (4), (5), will found as the sum of the volumetric potential and the potential of a simple layer with densities  $\rho$  and  $\nu$ , respectively,  $\rho$  and  $\nu$  satisfy  $2\pi$ -periodic condition in  $z$ ,  $\rho$  is localized in  $\Omega_1$ ,  $\nu$  is determined on  $\Gamma$ , the function  $v(x, y, z)$  can be presented in the form

$$v(\vec{x}) = \int_{\Gamma_0} \nu(\vec{x}_0) \Phi(\vec{x}, \vec{x}_0, \lambda) d\Gamma_0 + \int_{\Omega_0} \rho(\vec{x}_0^1) \Phi(\vec{x}, \vec{x}_0^1, \lambda) d\Omega_0, \quad (6)$$

where  $\Omega_0 = \{0 \leq z \leq 2\pi\} \cap \Omega_1$ ,  $\Gamma_0 = \{0 \leq z \leq 2\pi\} \cap \Gamma$ ,  $\vec{x}_0 \in \Gamma_0$ ,  $\vec{x}_0^1 \in \Omega_0$ ,  $\vec{x} \in \mathbb{R}^3 \setminus \Gamma$ .

The following is valid

**Lemma 3.** The volumetric potential and the potential of a simple layer of the fundamental solution  $\Phi$  for the Helmholtz equation are decreasing on moving away from the obstacles.

The following equations, in the light of (4), (5), are valid for the unknown functions  $\nu$  and  $\rho$ :

$$\begin{cases} \nu = \frac{2(1-\delta)}{\delta+1} \left[ \int_{\Gamma_0} \nu \frac{\partial \Phi}{\partial \bar{n}} d\Gamma_0 + \int_{\Omega_0} \rho \frac{\partial \Phi}{\partial \bar{n}} d\Omega_0 + \frac{\partial \phi}{\partial \bar{n}} \right] \\ \rho = \lambda^2(1-\kappa^2) \left[ \int_{\Gamma_0} \nu \Phi d\Gamma_0 + \int_{\Omega_0} \rho \Phi d\Omega_0 + \phi \right] \end{cases} \quad (7)$$

The relationships (7) will be written as  $\vec{X} = T\vec{X} + \vec{F}$ , where  $\vec{X} = (\nu, \rho)$ ,  $\vec{F} = (\frac{\partial \phi}{\partial \bar{n}}, \phi)$ .

Here  $T$  is the linear operator in the Hilbert space  $L = L^2(\Gamma_0) \times L^2(\Omega_0)$ .

Operator  $T : L \rightarrow L$ , defined in (7), is compact, and analytically depends on the parameter  $\lambda$ ,  $\lambda \in \Lambda$ , and continuously depends on the real parameters  $\tau$  and  $\kappa$ ,  $0 \leq \tau < 1$ ,  $\kappa^2 \neq 1$ .

For the operator equation (7) is valid

**Theorem 2.** The solution of the operator equation (7) is a single one, provided that  $\text{Im} \lambda > 0$  and  $\text{Im} \sqrt{\lambda^2 - n^2} > 0$  for all integers  $n$ .

Proof is the same as given in [1].

The proof of following lemma methodologically coincides with that for an analogous lemma in [2].

**Lemma 4.**  $\nu$  и  $\rho$ ,  $(\nu, \rho) \in L$ , are solutions of (7) if and only if  $v$  of shape (6) is the solution of the problem (4), (5).

Then, as a consequence of the above considerations on the Fredholm alternative, for any given  $\vec{F} \in L$  there arises  $\vec{X} \in L$  satisfying (7). There exists an element  $\lambda$  of the Riemann surface  $\Lambda$  for which the solution of (7) exists singly for all values of the parameters  $\tau$  and  $\kappa$ ,  $0 \leq \tau < 1$ ,  $\kappa^2 \neq 1$ .

**Eigenvalues and eigenwaves.**

**Definition.** The quasioeigenvalue of the scattering problem is that the element  $\lambda_*$  of the Riemann surface  $\Lambda$ , for which the solution of this problem is not single-valued or that there exists a nontrivial solution of

the uniform problem. The eigenvalue here is such a quasioeigenvalue of  $\lambda_*$ , for which the relationships  $(\operatorname{Re} \lambda_*)(\operatorname{Re} \sqrt{\lambda_*^2 - n^2}) \geq 0$  are satisfied for all integers  $n$ , given that  $c_{mn} \neq 0$  under the radiation condition (3).

For  $T$  the analytical Fredholm theorem has been satisfied, therefore the following is valid.

**Theorem 3.** The set of the quasioeigenvalues  $\Lambda_c$ ,  $\Lambda_c \subset \Lambda$ , of problems (1), (2), (3) is discrete on the Riemann surface in its topology. Each quasioeigenvalue possesses a finite multiplicity. Resolvent  $(I - T(\lambda, \tau, \kappa))^{-1}$  of the operator value function  $T$  is meromorphic on the Riemann surface  $\Lambda$ .

In physical applications it is often useful to know the evolution of the poles of  $(I - T(\lambda, \tau))^{-1}$  on the Riemann surface as a function of  $\tau$ . It is valid.

**Theorem 4.** If  $\tau$  tends to zero ( $\tau \rightarrow 0$ ), then for sufficiently small  $\tau$  the quasioeigenvalues of  $\lambda_*(\tau)$  of the problem (1), (2), (3) exist and converge in the topology of the Riemann surface  $\Lambda$  either toward  $\nu_*$ , if  $\nu_*^2 \kappa^2$  is the eigenvalue of the Laplace operator in region  $\Omega_1$ , for functions satisfying the conditions of  $2\pi$ -periodicity along the  $z$  axis and the uniform Neumann conditions at the boundary  $\Gamma$ , of this region or to the quasioeigenvalues  $\mu_*$  of the Dirichlet problem for the Helmholtz equation in region  $\Omega_2$ .

Proof is the same as given in [1].

Let the investigated permeable structure  $\Omega_1$  with boundary  $\Gamma$  has a period  $2\pi/N$  along the  $z$  axis. Moreover, the structure has a periodicity about rotation and shift around this axis with periods  $2\pi/L$  and  $2\pi/LN$ , respectively, where the natural numbers  $N$ ,  $L$  are greater than unity. In this case, if  $u_*(\rho, \theta, z)$  is a quasioeigenfunction of the problem (1), (2), (3), then  $u_*(\rho, \theta + 2\pi j/L, z + 2\pi k/LN)$  will also be a quasioeigenfunction of the problem for all natural numbers  $j$ ,  $k$ .

Let  $u(\rho, \theta, z)$  be  $2\pi$ -periodic function in  $z$  and  $\theta$ , whose expansion into a Fourier series for any natural numbers  $N$ ,  $L$  can be written as follows

$$\begin{aligned} u(\rho, \theta, z) &= \sum_{n=-\infty}^{+\infty} \sum_{m=-\infty}^{+\infty} a_{mn} \exp(i(nz + m\theta)) = \\ &= \sum_{k=1}^{LN} \sum_{j=1}^L \sum_{n=-\infty}^{+\infty} \sum_{m=-\infty}^{+\infty} a_{j+mL, k+nN} \exp(i[(k+nNL)z + (j+mL)\theta]) = \end{aligned}$$



$$= \sum_{k=1}^{LN} \sum_{j=1}^L u_{jk}(\rho, \theta, z)$$

According to the definition, the functions  $u_{jk}$  satisfy conditions of quasiperiodicity

$$u_{jk}(\rho, \theta + 2\pi j/L, z + 2\pi k/LN) = u_{jk}(\rho, \theta, z) \exp(2\pi i[j/L + k/LN]) \quad (8)$$

Let  $u_{jk}(\rho, \theta, z)$  be solution of problem (1), (2), (3) for which the conditions of quasiperiodicity (8) are valid, then radiation condition has the form

$$u_{jk} = \sum_{n=-\infty}^{+\infty} \sum_{m=-\infty}^{+\infty} a_{mn} H_{j+mL}^{(1)}(\sigma_{nk}\rho) \exp(i[(k+nLN)z + (k+mL)\theta]) \quad (9)$$

$$\sigma_{nk} = \sqrt{(\lambda^2 - (k+nLN)^2)}$$

Functions of  $\lambda$  such as (9) are analytical on the Riemann surface  $\Lambda_{jk}$  of their analytical continuation. The branching points of  $\Lambda_{jk}$  are numbers  $(k+nLN)$  for all integers  $n$ . Let  $\Lambda_{jk}^0$  be such a sheet of the Riemann surface  $\Lambda_{jk}$  with sections  $(-\infty, -\min\{k, LN-k\})$  and  $[\min\{k, LN-k\}, +\infty)$ , where the inequalities for all integers  $n$  are satisfied  $\text{Im}\sqrt{\lambda^2 - (k+nLN)^2} > 0$ . From the stand point of application the following is essential.

**Theorem 5.** *If the quasieigenfunction  $u_*$  of the problem (1), (2), (3) satisfies the conditions of quasiperiodicity in (8) and the corresponding quasieigenvalue  $\lambda_*$  is found on the shape  $\Lambda_{jk}^0$  of the Riemann surface  $\Lambda_{jk}$ , then  $u_*(\rho, \theta, z, \lambda_*)$  diminishes with increasing a distance from the barrier and is an eigenfunction, while  $\lambda_*$  is a real eigenvalue of the problem (1), (2), (3).*

Proof is the same as given in [3].

**Conclusion.** For problem of scattering at a permeable structure in unbounded regions the theorem of uniqueness is proved. Equivalent formulation of the problem in the form the operator equation is obtained. It is shown that the respective operator is Fredholm one and its resolvent is meromorphic on the Riemann surface. The existence of real eigenvalues



is proved and the type of associated eigenwaves is investigated. The essential distinction of the three-dimensional case is that the investigated solution may possess a helical symmetry, under condition where the structure satisfies this type of symmetry.

### REFERENCE

1. E. Sanchez-Palencia, Non-Homogeneous Media and Vibration Theory [Russian translation], Mir, Moscow (1984).
2. S.V. Sukhinin, "Qualitative problems in the theory of scattering at periodic penetrable barriers," in: the Dynamics of continuous Media [in Russian], Inst. Gidrodin. Sib. Otd. Akad. Nauk SSSR, Novosibirsk (1988), No 86.
3. S.V. Sukhinin, "The waveguide effect in a one-dimensional periodically penetrable structure," Zh. Prikl. Mekh. Tekh Fiz., No 4 (1990).
4. A.F. Nikiforov, V.B. Uvarov, The special functions of mathematical physics [in Russian], Nauka, Moscow (1978).
5. M. Reed, B. Simon, Methods of Modern Mathematical Physics [Russian translation], vol.1, Mir, Moscow (1977).
6. E. Jahnke, F. Emde, and F. Loesch, Special Functions [Russian translation], Nauka, Moscow (1964).

© foreword, composition by E. I. Veliev, 1994

PROCEEDINGS  
of the  
International Conference  
on  
MATHEMATICAL METHODS  
in  
ELECTROMAGNETIC THEORY

Editor-in-Chief E. I. Veliev

Co-editors A. I. Nosich and V. N. Vavilov

Technical editors A. V. Zharkov and A. G. Kleva

Computer editing V. M. Kobelev

Designer V. V. Veremey

---

Поліграфічна фірма «Прінтал». Зам. 1739. Тир. 120. 1994 р.